UNCONVENTIONAL OIL AND GAS RESOURCES EXPLOITATION AND DEVELOPMENT

EDITED BY
USMAN AHMED AND
D. NATHAN MEEHAN, PhD, PE
WITH A FOREWORD BY PROFESSOR STEPHEN A. HOLDITCH

BAKER HUGHES

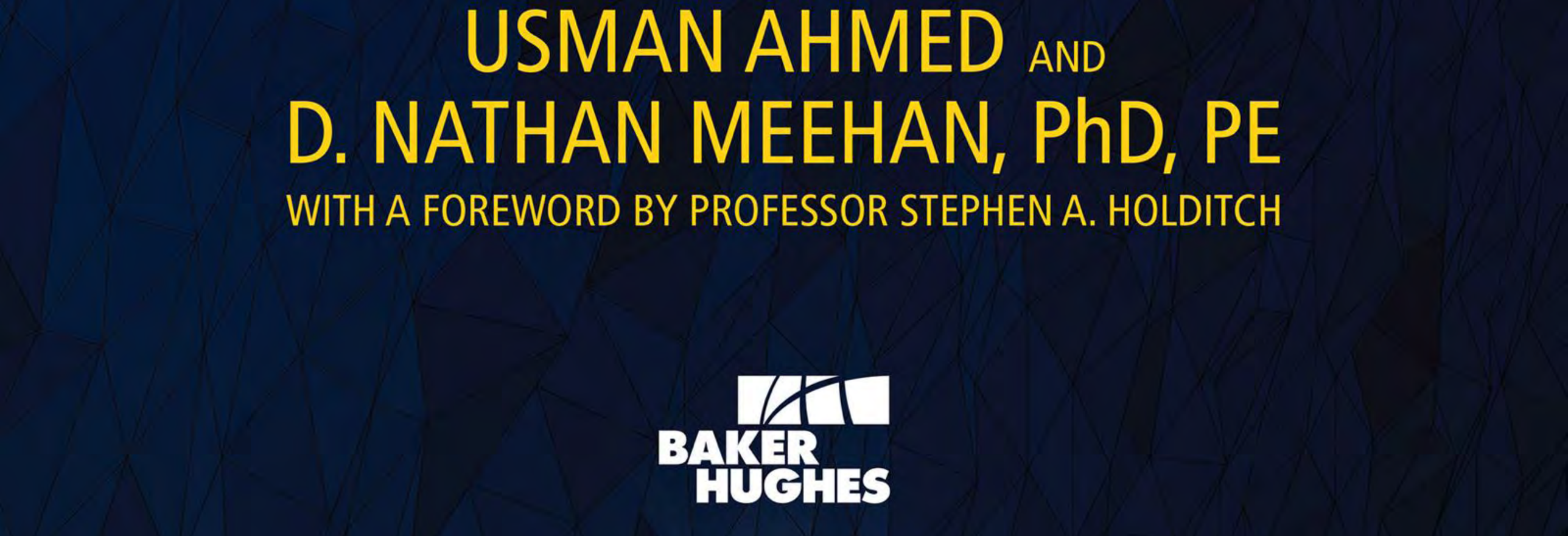

CRC Press
Taylor & Francis Group

UNCONVENTIONAL OIL AND GAS RESOURCES EXPLOITATION AND DEVELOPMENT

Emerging Trends and Technologies in Petroleum Engineering

Series Editor
Abhijit Y. Dandekar

PUBLISHED TITLES:

Unconventional Oil and Gas Resources: Exploitation and Development,
Usman Ahmed and D. Nathan Meehan

Hydraulic Fracturing, *Michael Berry Smith and Carl Montgomery*

Wax Deposition: Experimental Characterizations, Theoretical Modeling, and Field Practices,
Zhenyu Huang, Sheng Zheng, H. Scott Fogler

UNCONVENTIONAL OIL AND GAS RESOURCES EXPLOITATION AND DEVELOPMENT

USMAN AHMED AND
D. NATHAN MEEHAN, PhD, PE

WITH A FOREWORD BY PROFESSOR STEPHEN A. HOLDITCH

CRC Press
Taylor & Francis Group
Boca Raton London New York

CRC Press is an imprint of the
Taylor & Francis Group, an **informa** business

CRC Press
Taylor & Francis Group
6000 Broken Sound Parkway NW, Suite 300
Boca Raton, FL 33487-2742

Version Date: 20160329

International Standard Book Number-13: 978-1-4987-5941-0 (eBook - PDF)

Contents

Chapter 5:
Unconventional Resources Workflow—Exploitation and Development 5-1

William Knecht and Shanna Sambol-Koseoglu

Chapter 16:
Multistage Completion Systems for Unconventionals 16-1

William (Aaron) Burton

Chapter 21:
Rejuvenating Unconventional Resources 21-1

Robert Kennedy, Iman Oraki Kohshour, and Usman Ahmed

This page intentionally left blank

Emerging Trends and Technologies in Petroleum Engineering Series Preface

This petroleum engineering book series includes works on all aspects of petroleum science and engineering, but with special focus on emerging trends and technologies that pertain to the paradigm shift in the petroleum engineering field. It deals with the increased exploitation of technically challenged and atypical hydrocarbon resources that are receiving a lot of attention from today's petroleum industry, as well as the potential use of advanced nontraditional or nonconventional technologies such as nanotechnology in diverse petroleum engineering applications. These areas have assumed a position of prominence in today's petroleum engineering field. However, although scientific literature exists on these emerging areas in the form of various publications, much of it is scattered and highly specific. The purpose of this book series is to provide a centralized and comprehensive collection of reference books and textbooks covering fundamentals but paying close attention to these emerging trends and technologies from the standpoint of the main disciplines of drilling engineering, production engineering, and reservoir engineering.

Given the dwindling supply of easy to produce conventional oil, rapidly climbing energy demands, the sustained ~$100/bbl oil price, and technological advances, the petroleum industry is increasingly in pursuit of E & P of atypical or unconventional and technically challenged oil and gas resources, which may eventually become the future of the petroleum industry. Unconventional resources typically include (1) coal bed methane or CBM gas; (2) tight sands gas in ultra low permeability formations; (3) shale gas and shale oil in very low permeability shales; (4) oil shales; (5) heavy and viscous oils; (6) tar sands; and (7) methane hydrates. Compared to the world's proven conventional natural gas reserves of 6600+ trillion cubic feet (TCF), the combined CBM, shale gas, tight sands gas, and methane hydrate resource estimates are in excess of 730,000 TCF.[1-3] Similarly, out of the world's total 9 to 13 trillion barrels of oil resources, the conventional (light and medium oil) is only 30%, whereas heavy oil, extra heavy oil, tar sands, and bitumen combined make up the remaining 70%.[4] In addition shale-based oil resources worldwide are estimated to be between 6 and 8 trillion barrels.[5] As a case in point, shale-based oil production in North Dakota has increased from a mere 3000 barrels/d in 2005 to a whopping 400,000+ barrels/d in 2011.[6] Even the most conservative technical and economic recovery estimates of the unconventional resources represent a very substantial future energy portfolio that dwarfs the conventional gas and oil reserves. However, to a large extent these particular resources, unlike the conventional ones, do not fit the typical profile and are to some extent in the stages of infancy, thus needing a different and unique approach from the drilling, production, and reservoir engineering perspective.

The petroleum engineering academic and industry community also is aggressively pursuing nanotechnology with the hope of identifying innovative solutions for problems faced in the overall process of oil and gas recovery. In particular, a big spurt in this area in the last decade or so is evident from the significant activities in terms of research publications, meetings, formation of different consortia, workshops, and dedicated sessions in petroleum engineering conferences. A simple literature search for a keyword ***nanotechnology*** on www.onepetro.org, managed by the Society of Petroleum Engineers (SPE), returns over 250 publications dating from 2001 onward with the bulk of them in the last 5 or 6 years. Since 2008, SPE also organized three different applied technology workshops specifically focused on nanotechnology in the E & P industry. An Advanced Energy Consortium (AEC) with sponsorships from some major operators and service companies also was formed in 2007 with the mission of facilitating research in "micro and nanotechnology materials and sensors having the potential to create a positive and disruptive change in the recovery of petroleum and gas from new and existing reservoirs." Companies such as Saudi Aramco have taken the lead in taking the first strides in evaluating the potential of employing nanotechnology in the E & P industry. Their trademarked Resbots™ are designed for deployment with the injection fluids for in-situ reservoir sensing (temperature, pressure, and fluid type) and intervention, eventually leading to more accurate reservoir characterization once fully developed. Following successful laboratory core flood tests, they conducted the industry's first field trial of reservoir nanoagents.[7]

The foregoing is clearly a statement of the new wave in the petroleum engineering field that is being created by emerging trends in unconventional resources and new technologies. The publisher and its series editor are fully aware of the rapidly evolving nature of these key areas and their long-lasting influence on the current state and future of the petroleum industry. The series is envisioned to have a very broad scope that includes but is not limited to analytical, experimental, and numerical studies and methods and field cases, thus delivering readers in both academia and industry an authoritative information source of trends and technologies that have shaped and will continue to impact the petroleum industry.

Abhijit Dandekar
University of Alaska—Fairbanks

References

1. http://www.eia.gov/analysis/studies/worldshalegas/

2. Kawata, Y. and Fujita, K., Some Predictions of Possible Unconventional Hydrocarbons Availability until 2100, Society of Petroleum Engineers (SPE) paper number 68755.

3. http://www.netl.doe.gov/kmd/cds/disk10/collett.pdf

4. https://www.slb.com/~/media/Files/resources/oilfield_review/ors06/sum06/heavy_oil.ashx

5. Biglarbigi, K., Crawford, P., Carolus, M. and Dean, C., Rethinking World Oil-Shale Resource Estimates, Society of Petroleum Engineers (SPE) paper number 135453.

6. Mason, J., http://www.sbpipeline.com/images/pdf/Mason_Oil%20Production%20Potential%20of%20the%20North%20Dakota%20Bakken_OGJ%20Article_10%20February%202012.pdf

7. Kanj, M.Y., Rashid, M.H., and Giannelis, E.P., Industry First Field Trial of Reservoir Nanoagents, Society of Petroleum Engineers (SPE) paper number 142592.

1

Foreword

Steve Holditch, Texas A&M University

This page intentionally left blank

Chapter 1: Foreword

1.1 The Shale Revolution

Question: Who would have predicted it 20 or 30 years ago?

Answer: No one.

1.1.1 Background

In August 1970, I published a Master of Science Thesis entitled "Low Permeability Gas Reservoir Production Using Large Hydraulic Fractures." I had no idea that I would still be working on this issue in 2014, much less reading articles every day in the media about "Fracking." It is astonishing if not bizarre.

Certain groups opposed to the oil and gas industry who are trying to shut down drilling have determined that if they can demonize hydraulic fracturing, they might be able to slow down or prevent drilling. Thus, instead of calling it hydraulic fracturing, they coined the word "Fracking," so it would sound vulgar to some.

These groups first tried to say fracturing would pollute the drinking aquifers. That has proven not to be true so now they are concentrating their efforts on emissions and community disruption. However, the oil and gas industry is addressing all of these concerns to minimize the impact of our operations on the environment.

So my entire professional life, since finishing my master's degree in 1970, I have been involved in drilling, evaluating, completing, fracture treating, and then doing the post-fracture treatment evaluation of the production and pressures of unconventional reservoirs. It has been fascinating and rewarding.

The shale revolution will continue because it is providing the energy needed by the world to sustain economic growth and improve the standard of living for many parts of the world. The shale revolution also provides jobs and many other benefits such as increased tax revenue that can be used for infrastructure, education, and other worthy causes.

The shale revolution will also continue because the leaders of the oil and gas industry realize there is a Social License to Operate (SLO) that requires companies to conduct business in a safe and environmentally responsible manner. The oil and gas industry has developed best practices that are being routinely adopted by operators.

Finally, the shale revolution will continue because of technology improvements. By improvements, I mean new, breakthrough technologies and properly applying existing technologies through training and publishing. A lot of improvement can be expected by just applying state-of-the-art methods now.

This book is an important asset to fostering the continuation of the shale revolution. The authors and editors have compiled the best information on "everything you need to know" to develop an unconventional reservoir. Practicing engineers and geoscientists need to know what is in this book, use the information, improve the methods going forward, and keep learning.

1.1.2 The Resource Triangle

So what is an "unconventional reservoir"? The best way to explain the concept is to review the resource triangle shown in **Fig. 1.1**. John Masters, who was the founder of Canadian Hunter in Calgary in the 1970s, published the concept of the resource triangle. Canadian Hunter found tight gas in the deep basin in Alberta using the resource triangle concept. While searching for tight gas, they also found gas in the high-permeability Falher conglomerate, which is actually in the conventional portion of resource triangle. The lesson from the Canadian Hunter experience is that when exploring in a basin, you should expect to encounter both conventional and unconventional reservoirs. Even in the unconventional reservoirs, there are sweet spots that provide most of the production.

The concept is that all natural resources are distributed log-normally in nature. Everything is distributed long log-normally, from gold, silver, copper, iron, and, yes, oil and gas also. The conventional resources (such as a pure vein of gold) are hard to find, but are high quality and easy to extract after they are discovered. As you go deeper into the resource triangle, you need either higher product prices or better technology or both to extract the resource economically. For example, vertical wells with hydraulic fracturing helped unlock resources in tight gas sands and coal seams in the 1980s.

However, it takes long horizontal wells with multistage hydraulic fracturing to economically produce gas shales or oil in low-permeability rocks, like shales. For other resources, like heavy oil, horizontal wells and heat must be applied.

At the bottom of the resource triangle, the industry is still working on the technology breakthroughs that will unlock gas hydrates and oil shale.

The upside in moving down into the resource triangle is that the resource volumes are enormous. There is ample evidence in the literature on the enormous volumes of natural gas in shales, oil in shales, and heavy oil to easily confirm that the resource triangle is a useful and accurate description of the energy potential in virtually every oil and gas basin in the world.

The shale revolution we have seen in North America can be reproduced in other basins outside of North America. In any basin around the world that has produced large volumes of oil and gas from conventional reservoirs, one would expect there to be even larger volumes of oil and gas in unconventional reservoirs. However, to economically produce unconventional reservoirs outside of North America, there are a number of actions that must be taken by both the industry and the governmental entities. The industry will need rigs, trucks, people, pipelines, markets, and oil and gas prices that are high enough to justify the expenditures. The governments must provide contract law and legal systems so that political risks are manageable.

The impact of the shale revolution was not predictable in the 1990s, but it is very much a reality in the late 2000s and early 2010s. It is here to stay for the rest of this century, although the activity level will vary as the prices of oil and gas oscillate and the industry continues to develop technology.

But the unconventional reservoir revolution is more than shale; it is tight sands, coal seams, and much more. For a given level of technology, the drilling activity will be directly impacted by the oil and gas prices. However, as implied in the concept of the resource triangle, you can dip deeper into the triangle as technology improves. Technology breakthroughs can be a game changer and are to be expected.

1.1.3 How Large Is the Resource?

The volume of original gas or oil in place is a constant and the industry refers to that volume as the resource. The technically recoverable resource (TRR) is the amount of oil and gas that can be produced in a given formation assuming a specified level of technology. The TRR can be computed using a reservoir simulator given the appropriate input data.

Oil and gas prices affect the amount of oil or gas that can be produced in a given formation using a given level of technology. Thus, we also have to compute the economically

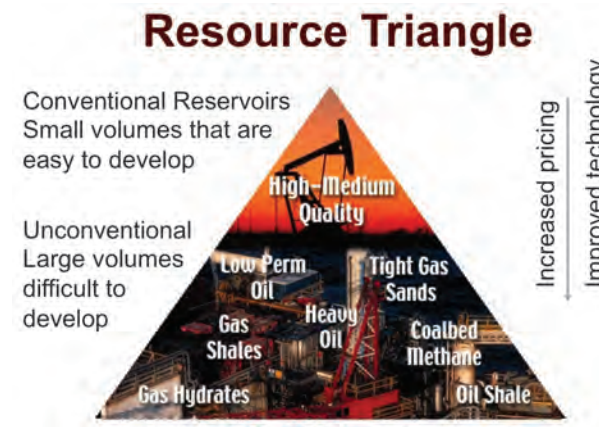

Figure 1.1—The Resource Triangle.

recoverable resource (ERR) using the results from the estimate of TRR and an economic model. ERR is a continuum that is a function of both the finding and development costs and the oil and gas prices.

We have published studies at Texas A&M University on shale gas that implies that there is enough natural gas to supply the world for this century and beyond. Although we have not done similar calculations for oil in tight formations or heavy oil, it is clear that the same conclusion should be true of crude oil, i.e., we will not run out of crude oil any time soon.

Table 1.1 is from a dissertation at Texas A&M University.

The work by Dr. Zhenzhen Dong has also been published in peer-reviewed journals. The journal articles and several other articles are in the references at the end of this chapter. Table 1.1 presents the median estimates of original gas in place and technically recoverable gas for seven regions in the world. These regions are, in general, Asia Pacific, North America, Russia and Eastern Europe, Latin and South America, Middle East, Western Europe, and Africa. Dr. Dong used region boundaries that had been defined in prior work by others. For more detail, the reader should refer to her dissertation.

Table 1.2 illustrates the potential supply of natural gas using the values from Table 1.1. Currently, North America uses about 32 Tcf of gas per year, so there is over 250 years of technically recoverable gas remaining. The world uses around 118 Tcf per year, so we have over 400 years of technically recoverable gas supply for the world. We are referring to TRR and not ERR. A lot of moving parts have to converge to convert even one-half of the technically recoverable resource to economically recoverable resource. Even though we believe the natural gas is there in each region and can be technically recovered with

Table 1.1—Estimation of median values of original gas in place and technically recoverable gas in seven regions in the world.

Texas A&M Study Results
from Zhenzhen Dong dissertation—August 2012

Region	OGIP (P50), Tcf				OGIP (P50), Tcf			
	CBM	Tight gas	Shale gas	Total	CBM	Tight gas	Shale gas	Total
AAO	1,348	6,253	2,690	10,291	483	3,783	676	4,942
NAM	1,629	10,784	5,905	18,318	584	6,525	1,505	8,614
CIS	859	28,604	15,880	45,343	308	17,307	3,924	21,539
LAM	13	3,366	3,742	7,122	5	2,037	964	3,006
MET	9	15,447	15,416	30,872	3	9,346	4,000	13,349
EUP	176	3,525	2,149	5,895	63	2,133	561	2,757
AFR	18	4,000	3,882	7,901	7	2,420	1,007	3,434
World	4,052	71,981	49,709	125,742	1,453	43,551	12,637	57,641

Table 1.2—Estimate of gas supply using values of technically recoverable gas and current gas use in North America and the world.

Area	OGIP	TRR	USE	Supply
	(Tcf)	(Tcf)	(Tcf)	(years)
North America	18,318	8,614	32	269
World	125,742	57,641	118	488

existing technology, only 20-50% of this TRR gas will be economically recoverable because of lack of infrastructure, markets and governmental policy. But the natural gas is there if the people and governments in the world want it.

1.2 Industry Image

The oil and gas industry should be praised for providing abundant, affordable energy to support a high standard of living in most countries in the world. Some countries, such as the US and Canada, and much of Western Europe have very high standards of living that can be correlated directly to the amount of energy used per capita.

However, there are still many underdeveloped nations that need to improve the standard of living in their countries. In addition, the earth will have several billion more inhabitants in the coming century. Clearly, the world will need more energy to improve the standard of living in many countries. The needed energy can only come from hydrocarbons, although it can be supplemented with some renewables. To provide the energy the world will require and to keep the oil and gas industry's license to operate, the industry will have to continue to improve its activities to protect the environment, work with local communities, governments, and do so in a safe manner

The leaders of the oil and gas industry are aware of the environmental and political pressures to operate safely and in an environmentally responsible manner. The topics of shale development and hydraulic fracturing are in the news constantly. The industry must develop the unconventional resources properly. There is clear evidence that much progress is being made in "doing it right" and this is exemplified in this textbook.

1.3 Summary

To summarize my thoughts on the future, I offer the following:

1. The oil and gas industry uses some of the most sophisticated technology of any industry. The industry is high-tech, which should be attractive to the next generation of engineers and geoscientists.

2. We are not going to run out of oil or natural gas this century. In fact, oil and gas supply and demand are both increasing, so this is a growing industry with no end to the growth in sight. The oil and gas industry will not be substantially replaced by wind, solar, or biofuels in the coming decades based on markets and associated technology.

3. However, the populace could make an emotional decision to ban drilling and hydraulic fracturing. A widespread ban could disrupt the progress the industry has made in the past few decades. As such, the industry must strive to be good citizens, take care of the environment, and keep the public and the government bodies informed on what it is doing.

4. As it continues, the shale revolution will provide abundant, affordable energy, jobs, tax revenues to governments, royalties to mineral owners, and hope for the future.

1.4 References

Dong, Z. 2012. A New Global Unconventional Natural Gas Resource Assessment. PhD Dissertation. Texas A&M University, College Station, Texas. (August 2012).

Dong, Z., Holditch, S.A., and McVay, D.A. 2013. Resource Evaluation for Shale Gas Reservoirs. *SPE Economics & Management Journal*, **5**: 5–16, January.

Dong, Z., Holditch, S.A., McVay, D. A., and Ayers, W.B. 2012. Global Unconventional Gas Resource Assessment, *SPE Economics & Management Journal*, **4**: 222–234. October.

Holditch, S.A. 1970. Low Permeability Gas Reservoir Production Using Large Hydraulic Fractures. MS thesis. Texas A&M University, College Station, Texas. (August 1970).

Holditch, S.A. 2006. Tight Gas Reservoirs. Distinguished Author Article, *Journal of Petroleum Technology*, 84-90. June.

Holditch, S.A. and HusamAdDeen, M. 2010. Global Conventional Gas–It Is There, But Is It Profitable? *Journal of Petroleum Technology*, 42–49, December.

Makogon, Y.F. and Holditch, S.A. 2007. Natural Gas Hydrates–A Potential Energy Source for the 21st Century. *Journal of Petroleum Science and Engineering*, **56** (1–3): 14–31.

Masters, J.A. 1979. Deep Basin Gas Trap, Western Canada, *AAPG Bulletin*, **63** (2): 152.

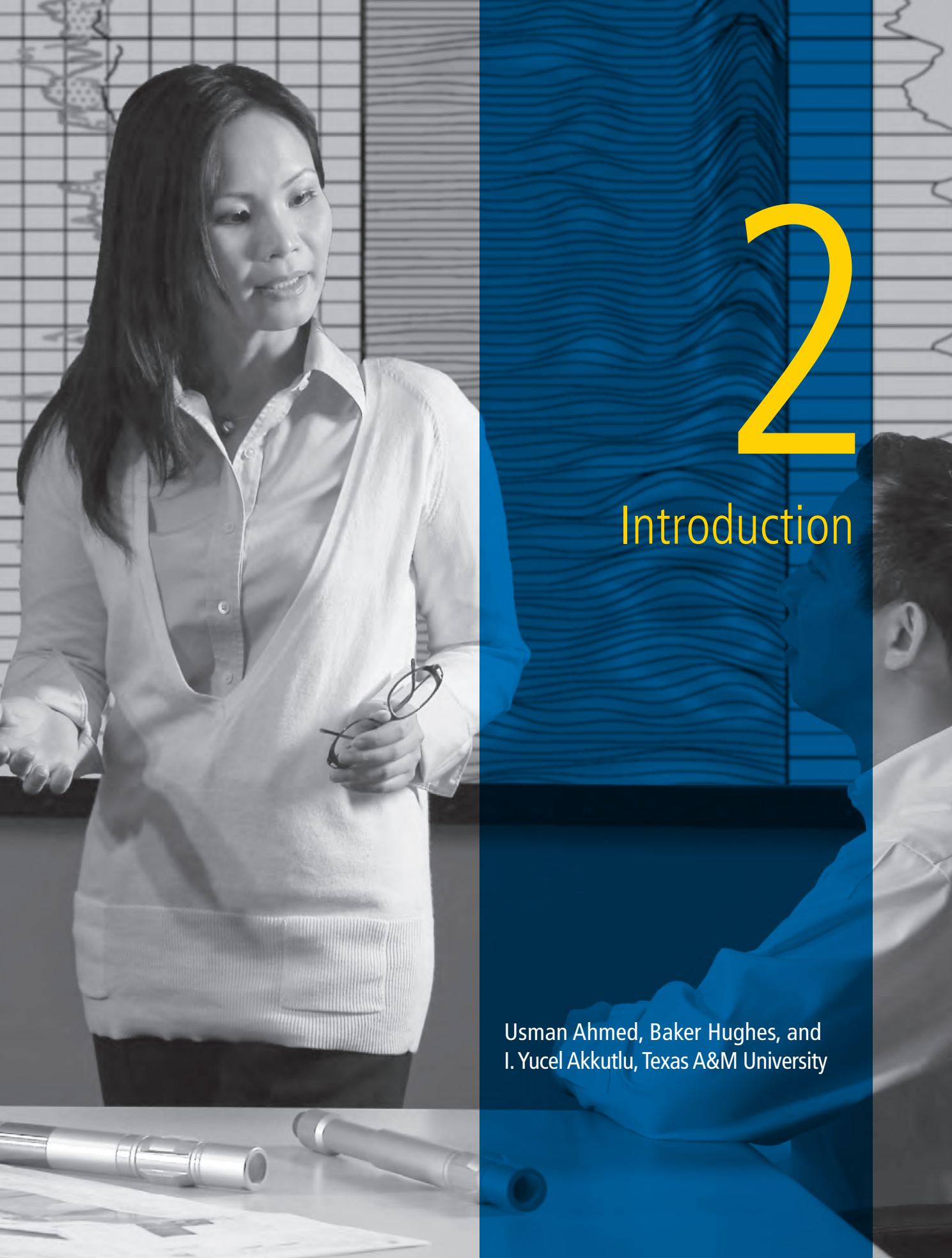

2 Introduction

Usman Ahmed, Baker Hughes, and
I. Yucel Akkutlu, Texas A&M University

This page intentionally left blank

Chapter 2: Introduction

2.1 Setting the Stage

A Brief Conversation with Henry Carey of Philadelphia

"This hard work will always be done by one kind of man; not by scheming speculators, nor by soldiers, nor professors, nor readers of Tennyson; but by man of endurance—deep-chested, long-winded, tough, slow and sure, and timely."

Ralph Waldo Emerson,
"The Man with the Hoe,"
29 September 1858

The science and engineering of oil and gas production has experienced a fast evolution since the early years. Not only have the number and kinds of tools used for research changed dramatically but also has interest in resources. What is the dominant factor that has driven this resourceresearch duality change?

Consider the American farmer in the 1830s when he increased the wheat yield fivefold thanks to the introduction of tile drainage that European migrants advocated. In "Society and Solitude," Ralph Waldo Emerson referred to this success: "See what the farmer accomplishes by a cart load of tiles." The farmer dug down to subsoil and found that another Concord existed under the current town of Concord. This soil yielded the best crops. Massachusetts has a lower level that is more valuable and promises to pay a return greater than the entire superstructure.

The use of tiles generated a discussion among the elite, some of whom announced the arrival of a better era with more bread. The dogma that men breed too fast for the powers of soil and the concept of diminishing returns seemed to be obsolete. Earlier concerns of political economists Thomas Malthus and David Ricardo, who stated that population would outstrip the yield capacity of cropland, were distant. The premise was that because the first comer takes up the best lands and the next the second best inevitably drives each succeeding generation to poorer conditions. The notion that the plight of every new generation is worse than that of the foregoing turned out to be an empty proposition.

Cultivating these lands in the best manner, however, requires science and a large population with a certain moral quality. The discussion in "Society and Solitude" is short of explicit definitions of this required morality. Perhaps this is tied to Emerson's ideal farmer, the man of endurance. These words cannot explain convincingly how the global population at the time managed to grow to approximately one billion people and that the earth could barely sustain if humans were using only local resources such as wood, peat, and crops as energy sources. Nor are they likely to explain how the accumulation of the last billion humans, adding up to a fifth billion, took only a dozen years, with the population reaching that mark by the end of the twentieth century.

Scientific endeavor and technical achievements such as tile drainage were present, and ethics arguably has been at the center of our communities. However, an earlier discovery approximately 900 years ago led to Carey's unconscious optimism. Humankind discovered a new source of fuel other than wood: fossil fuel. First in the form of coal, the new fuel reduced the reliance on forestland and enabled the farmer to convert it into cropland to become less dependent on trees for heating. In "The Last Hours of Ancient Sunlight," Thom Hartmann refers to this discovery below the surface of the earth as "a critical moment in human history."

Until the early nineteenth century, coal was the primary fuel supporting human growth beyond the levels that Earth could sustain by simply making more croplands available. Later, during the twentieth century, and on a much larger scale, oil and natural gas were abundant and were used widely. This time they were used within a much closer proximity to advancements in medicine, science, and technology at a head-spinning rate, driving a machine- and chemistry-based agriculture along with a hydrocarbon-based economy. Fuel availability in the form of coal, oil, and, more recently, natural gas led to a dense population that is heavily dependent on it in nearly every aspect.

Much like the land's capacity to yield crops, however, Earth has a certain, and often seen as limited, amount of fossil fuels. Consequently, the media echoes the words of Malthus and Ricardo, predicting how much fuel is left and when the fuel will run out. These often note that the easily accessible and vast pools of oil and gas have been discovered and thus it is going to become harder for succeeding generations to discover new fields of "ancient sunlight." Some argue that it is going to be more difficult or more costly to extract from the remaining fields.

Recent reports show that the world's fossil fuel resource base remains sufficient to support growing levels of production. For a decade or so, we have projected remaining global

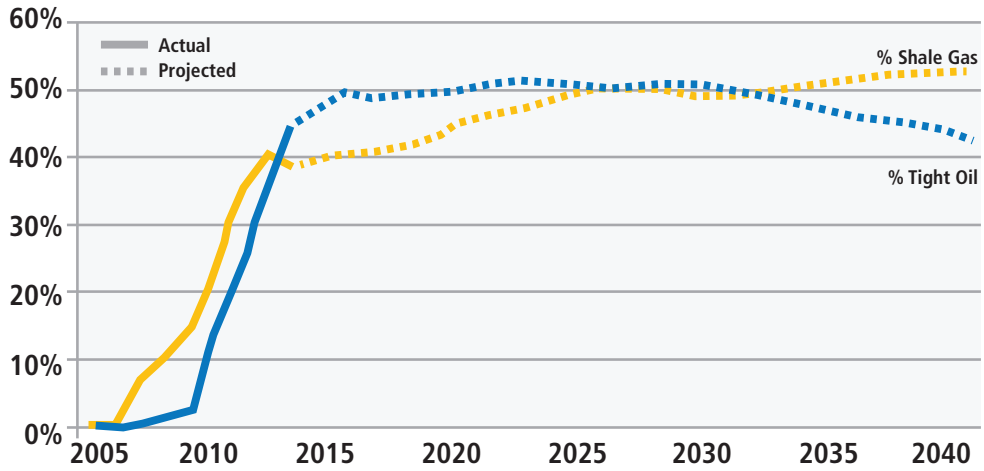

Fig. 2.1—Growth of the tight oil and shale gas production in terms of the percentage of the total US production. Prior to 2007, the Energy Information Administration did not report tight oil and shale gas data.

oil reserves of 50 years. Today, despite the current growth in consumption above the last 10-year average, the same expectation is valid. We have enough oil for the next 50 years. We have proven natural gas reserves for another 60 years and coal reserves for 130 years.

Is the rapid development of unconventional oil and gas in North America not another example of the basement story that is more valuable than the entire superstructure? Are the recent advances in horizontal drilling and hydraulic fracturing not the hard work done by the man of endurance—deep chested, long-winded, tough, slow and sure, and timely? Is cultivating the unconventional resources not requiring science and great numbers with a certain moral quality?

However, fuel resource reports cite a tight balance of supply and demand, putting issues such as water resources, energy security, and trade at the forefront of international politics. We have pushed exploration and production into more difficult and deeper environments. Have we reached a catastrophic ratio of man to fuel usage? Have we already discovered Concord underneath the town of Concord?

The Concord story can be a concept symbolizing the fruits of an infinitely awarding nature that we are allowed to access within the current bounds of our potential. The potential is the science and the great numbers with a certain morality and the idea that we may not have to worry because we came from the land, and the farmer is the ancestor of us all.

2.2 Mission and Scope

The unconventional resources exploitation and development, especially in conjunction with shale resource, have risen sharply since 2006 to 2007. The US and Canada have experienced a resurgence in oil and gas production, mainly driven by technology improvements associated with multi-stage hydraulic fracturing and horizontal and lateral well drilling that were developed for natural gas, condensate, oil production from shale and tight formations. Application of these technologies enables natural gas to be economically produced from shale and other unconventional formations and have contributed significantly to the US becoming the world's largest natural gas producer in 2009. Ratner and Teiman note that use of these technologies has contributed to the rise in US oil production over the last few years. In 2009, annual oil production increased over 2008, the first annual rise since 1991, and has increased each year since. Between October 2007 and October 2013, US monthly crude oil production rose by 2.7 million barrels per day, with about 92% of the increase from shale and related tight oil formations in Texas and North Dakota. Other tight oil plays are being developed and will help raise the prospect of energy independence, particularly for North America.

Fig. 2.1 illustrates the growth pattern for gas and oil production.

Independent oil and gas companies dominated most of these activities in the US. Independents performed thousands of horizontal wells and hundreds of thousands of hydraulic fracturing stages and now several major national and international oil companies are involved. Most

of the activity has been based statistically, and the use of knowledge, technology, and experience has been varied and involved certain levels of inconsistency. The mission and overall scope of this textbook is to present the knowledge, applied technology, and experience in a coherent fashion for the day-to-day user and developer of unconventional resources and, in particular, shale.

2.2.1 The Intended Audience

As the shale revolution continues in North America, emerging markets are opening up in all continents. In the next eight to ten years, more than 100,000 wells and one to two million hydraulic fracturing stages could be executed and lead to an industry-spending level close to one trillion dollars. Such level of activity requires knowledgeable professionals in all aspects of exploitation and development. The present demand for shale resource exploitation and development has prompted thousands of oil and gas professionals experienced in conventional oil and gas development to adapt to this new environment. Hence, the intended audience for this textbook is advanced university students and practitioners of shale resource exploitation and development.

This book covers all aspects of the exploitation and development. The 25 chapters start with a basic understanding of the unconventional resources and go to an in-depth coverage of sub-surface measurements (geological, geophysical, petrophysical, geochemical, and geomechanical) and associated interpretation plus all disciplines associated with drilling, completion, stimulation, production, production, reservoir, monitoring techniques, the associated software, and the overall unconventional resource development workflow. There are chapters on emerging technology like data mining and future areas of technological development. The textbook, thus, addresses the needs of the geologist, geophysicist, petrophysicist, geomechanic specialist, and drilling, completion, stimulation, production, and reservoir engineers.

2.2.2 Comprehensive Reference Material

Any professional wanting to further research the exploitation and development of shale resource will find this textbook to be thorough, comprehensive reference material. If one wants to conduct an in-depth research in a particular area, for example microseismic measurement uniqueness, this textbook is a good starting point and allows the researcher to get more details from the references cited.

2.3 Defining Unconventional Resources

2.3.1 The Classic Definition

The classic definition of the unconventional resources has evolved over time and is expected to continue the evolution as new hydrocarbon sources are identified. A decade ago the term "oil and gas from shale" was virtually non-existent. The term source rock meaning shale oil and gas has been in the literature for decades; however, commercial production from such source rock was not envisaged until the last decade.

Unconventional oil and gas is defined as petroleum produced or extracted using techniques other than the conventional oil and gas well methods. This, of course, is a very broad definition.

According to the Energy Information Administration (EIA) report in 2001, unconventional oil and gas includes shale oil and gas, oil sands-based synthetic crudes, and derivative products like heavy oil, coal-based liquid supplies, biobased liquid supplies, and gas to liquid from the chemical processing of gas.

In the IEA's 2011 World Energy Outlook report, "[u] nconventional oil include[d] extra-heavy oil, natural bitumen (oil sands), kerogen oil, liquids and gases arising from chemical processing of natural gas (GTL), coal-to-liquids (CTL), and additives."

On their webpage jointly published with the Organization for Economic Co-operation and Development (OECD), the EIA observed that as technologies and economies change, definitions for unconventional and conventional oils also change.

The EIA and OECD joint publication states that conventional oil is a category that includes crude oil and natural gas and its condensates. Crude oil production in 2011 stood at approximately 70 million barrels per day. Unconventional oil consists of a wider variety of liquid sources including oil sands, extra heavy oil, gas to liquids, and other liquids. In general, conventional is easier and less expensive to produce than unconventional oil. However, the conventional and unconventional categories are not fixed. As economic and technological conditions evolve, resources previously considered unconventional can migrate into the conventional category. The US Department of Energy (DOE) echoes this by stating unconventional oils have yet to be strictly defined.

The National Petroleum Council (NPC) notes that unconventional oil and gas cannot be produced unless the well is stimulated by a large hydraulic fracture treatment, a horizontal wellbore, or by using multilateral wellbores or some other techniques to expose more of the reservoir to the wellbore.

The Society of Petroleum Engineers (SPE) echoes the NPC and the Canadian Association of Petroleum Producers (CAPP) reiterates the NPC comment and further states that unconventional oil and gas reservoirs include tight oil and gas, coalbed methane, gas hydrates, and shale oil and gas.

At IHS, unconventional is used as an umbrella term referring to hydrocarbon resources that cannot be produced at economic flow rates or that do not produce economic volumes without artificial stimuli and special recovery processes and technologies. Their definition and choice of words are in **Table 2.1**.

2.3.2 Definitions Used

In summarizing the classic definitions, the unconventional category can be simplified to include shale oil and gas, tight oil and gas (typically sedimentary rocks), coalbed methane (CBM), which also is referred to as coal seam gas (CSG), gas hydrates, oil shale, and heavy oil.

The exploitation and development process and methodology for shale oil and gas, tight oil and gas, and CBM are similar as compared to the process and methodology for gas hydrates, oil shale, and heavy oil. Hence, this textbook's focus is on shale oil and gas, tight oil and gas, CBM, and, more specifically, shale oil and gas. **Fig. 2.2** illustrates the transition from conventional sandstone to the unconventional grouping of shale oil and gas, tight oil and gas, and CBM as used in this textbook.

2.3.2.1 Introducing Shale

Shale is the central theme of this textbook. Chapter 3 examines the details of what makes up shale, tight oil and gas, and coalbed methane, which is also known as coal seam gas. In classic petroleum geology, source rock refers to rocks from which hydrocarbons have been generated or are capable of being generated under certain conditions. They are organic-rich sediments that have been deposited in a variety of environments including deep-water marine, lacustrine, and deltaic and form one of the necessary elements of a working petroleum system. Subsurface source rock mapping methodologies make it possible to identify

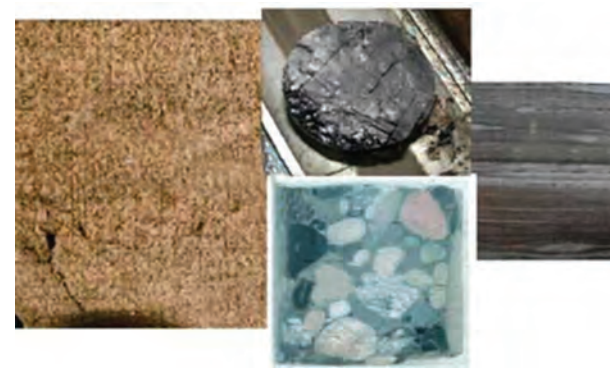

Fig. 2.2—Moving from conventional sandstone to the unconventional grouping of shale, tight sandstone, and CBM. (From Canadian Petroleum Institute.)

Table 2.1—IHS List of the Unconventional Group.

List A	List B
1. Oil Shale	1. Shale Oil
2. Tight Oil Shale	2. Tight Oil Shale
3. Gas Shale	3. Shale Gas
4. Oil Sands	4. Extra Heavy Oils
5. Tight Gas Sands	5. Tight Sands Gas
6. Coalbed Methane	6. Coal Gas
7. Coal Mine Methane	7. Coal Mine Gas
8. Syngas Coal	8. Syngas
9. Natural Gas Hydrates	9. Hydrates Gas
10. Dissolved Gas	10. Dissolved Gas
11. Unspecified	11. Unspecified

likely zones of petroleum occurrence in sedimentary basins and shale gas plays.

Source rocks are classified from the types of kerogen that they contain. Kerogen is a mixture of organic chemical compounds that make up a portion of the organic matter in sedimentary rocks. Kerogen governs the type of hydrocarbons that potentially will be generated such as:

- Type 1 source rocks are formed from algal remains deposited under anoxic (areas of sea water, fresh water, or groundwater that are depleted of dissolved oxygen) conditions in deep lakes. They tend to generate waxy crude oils when submitted to thermal stress during deep burial.
- Type 2 source rocks are formed from marine planktonic and bacterial remains preserved under anoxic conditions in

marine environments. These source rocks can produce both oil and gas when thermally cracked during deep burial.

- Type 3 source rocks are formed from terrestrial plant material that has been decomposed by bacteria and fungi under oxic or sub-oxic conditions. These types of source rocks tend to generate mostly gas with associated light oils when thermally cracked during deep burial. Most coals and coaly shales are Type 3 source rocks.

Kerogen Type 1 signifies potential presence of oil whereas Type 3 signifies mostly gas and in some cases condensate. Type 2 is the transitional zone between oil and gas, and both phases could be present including condensate.

2.3.2.2 Unconventional Resource Basins

Chapter 4 focuses on this subject in detail. The resource basins are spread throughout the globe. However, development of such resources are dependent on the specific country policies, involved exploration and production companies and their priorities, and service providers and their capabilities today and in the near future.

It is the opinion of the authors that outside North America and Australia, where citizens potentially can own mineral and hydrocarbon rights, the local governments and the associated national oil companies will significantly influence the shale resources development. In the western hemisphere forward-looking countries include Argentina, Colombia, and Mexico as the first tier and followed by Venezuela, Ecuador, and Brazil. In the eastern hemisphere the forward-looking countries include Russia, Ukraine, Saudi Arabia, Oman, Kuwait, Turkey, Algeria, Tunisia, South Africa, and China. European countries like the UK, France, and Poland are positively addressing the environmental issues and could commence commercial development in the near future. Countries like India, Pakistan, and Indonesia, where there is lot of shale potential, appear to be moving slowly in awarding acreage and in the development process.

Emerging markets outside North America are not expected to exceed more than 10% of the overall wells and hydraulic fracturing stages planned for the next five to seven years, approximately 100,000-plus wells and one to two million hydraulic fracturing stages. North America will continue to be the dominant place for shale resource development. A change in the development paradigm could alter the scenario.

2.4 Chapter Summary

The following is a brief summary of the chapters.

Chapter 3: Characteristics of Unconventional Oil and Gas Resources

The chapter discusses the unconventional resource triangle and where the shale, tight oil, and gas, and CBM resource falls within that resource triangle. The aspects that make shale resource different from conventional resource are discussed in detail. Because the focus of this textbook is on shale resource exploitation and development, special considerations regarding CBM and tight oil and gas are discussed in separate sections.

Chapter 4: The Unconventional Basins and Plays—North America, the Rest of the World, and Emerging Basins

This chapter discusses the major North American shale basins, the EIA 2-11 study, the 2013 worldwide total recoverable resource, average statistics, and the US model for shale development. This discussion is followed by detailed outlining and maps of the major oil and gas plays in the US and Canada. The chapter discusses the emerging shale plays throughout the rest of the world and in particular Latin America, Mexico, Europe, Russia, the Middle East, north and south Africa, China, and Australia.

Chapter 5: Unconventional Resources Workflow—Exploitation the Development, and Energying Basins

The workflow centers on a life-cycle approach to shale resource exploitation and development. The life-cycle approach calls for a circular workflow path connecting all the stages. Each of the stages has a linear or circular workflow path depending on the required outcome. The first stage looks into identifying and evaluating the resource base for an optimized field development plan starting with the pilot. The process is flexible enough to make changes as lessons are learned. What follows next involves determining interval selection for optimal horizontal well placement and the associated drilling precision and navigation. Integration of completion and stimulation strategy is a key part of the workflow as well as the effectiveness evaluation of these treatments for continuous production and most effective recovery by in-fill drilling and re-fracturing or a combination. Managing the water cycle throughout the workflow process is included.

Chapter 6: Seismic Reservoir Characterization Applications for Unconventional Resources

The chapter focuses on surface seismic utilization in unconventional plays during exploration, appraisal, and development phases. It discusses the seismic survey design and acquisition considerations particularly for unconventional reservoirs and associated processing and interpretation methods and techniques leading to effective seismic reservoir characterization. Seismic attribute analysis and interpretation addresses mapping sweet spots, preferential drilling direction, aid in effective completion strategy, and avoidance of hazards. A section focuses on validation techniques where calibration is done to wireline and image logs, core, and cuttings measurements and microseismic delineation.

Chapter 7: Pilot Projects in Unconventional Resources Development

This chapter discusses the need for pilot wells, which should be considered for an effective pilot program, and how the pilot program is dependent on the type of unconventional resource information and data. This chapter provides the process and methodology to transition from the pilot program to a full field-development program. Uncertainty analysis is discussed as part of the pilot project. The authors use field case studies to illustrate the design criteria and the success of a pilot project to conceptual field development considerations.

Chapter 8: Formation Evaluation and Reservoir Characterization of Source Rock Reservoirs

The introduction and overview of Chapter 8 point out that formation evaluation and reservoir characterization of source rock is performed via various sources that include wireline and logging while drilling logging technologies, core and laboratory core analyses, wellsite evaluation methodologies, and geophysical (seismic) techniques.

This chapter focuses on wireline and logging while drilling logging technologies and the associated interpretation techniques. This chapter also presents methods and process that integrate all formation evaluation related data including seismic and laboratory data. The focus on petrophysical methodology concentrates on but is not limited to lithology and mineralogy determination; organic content characterization; porosity, permeability, and saturation determinations; and geological and geomechanical characterization. The chapter addresses using formation evaluation results to optimize lateral well placement and stimulation program design.

Chapter 9: Role of Geomechanical Engineering in Unconventional Resources Developments

Chapter 9 explains the need for geomechanical data as an integral part of formation evaluation and provides geomechanics details as pertaining to an unconventional shale reservoir. The chapter identifies the geomechanical properties that are most critical for shale reservoirs and how micromechanical stress-strain modeling helps shale anisotropy characterization. Comments are made regarding the differences in geomechanical related to the understanding required for the shale and CBM environment. Specific topics are addressed such as in-situ stress and pore pressure characterization, wellbore stability, geomechanical considerations in shale stimulation, and geomechanical considerations in CBM.

Chapter 10: Laboratory Tests and Considerations to Complement the Overall Reservoir Understanding

The chapter covers laboratory analysis objectives and provides an overview of the sample types used, unconventional rock types, and core preservation. Know-how of rock and sample types is critical to the subsequent testing type decision. Also covered is the main body of laboratory analysis and the techniques and the associated interpretation for sedimentology (which includes detailed fracture analysis), porosity, permeability, fluid saturations, mineralogy, elemental compositions by X-ray fluorescence, wettability, measurements, thin-section petrography, scanning electron microscopy, fluid compatibility testing, mechanical rock properties, geochemistry, canister gas and adsorption isotherms, and fracture conductivity. The authors explain how each of these individual measurements can impact the overall shale source exploitation and development process.

Chapter 11: Reservoir Engineering Aspects of Unconventional Oil and Gas

The chapter introduces the conventional approach only to illustrate how it contrasts to unconventional. The authors characterize the common reservoir properties in a mechanical earth model and evaluate economic optimization of development scenarios using reservoir simulation studies. The chapter focuses on understanding development of unconventional oil and gas resources and some of the most important properties in the development of unconventional resources. The authors present some of the main reservoir engineering dilemmas such as storage, flow mechanism, well-to-well variations, fracture characteristics, and drainage volume. The chapter addresses

other issues and how the proper strategy in well design and artificial lift methods can increase the economic life of the unconventional oil and gas wells.

Chapter 12: The Art of Data Mining and Its Impact on Unconventional Reservoir Development

Chapter 12 outlines the importance of data mining in unconventional reservoirs by discussing the fundamental reservoir quality drivers in unconventional reservoirs, variability of key geomechanical properties, and the impact of time dependence of well architecture, completion, and stimulation trends. The authors explain the evolution of the data mining techniques leading to the present-day use of multivariate statistics combined with geographical information systems. The key to useful data-mining outcome is dependent on sources and availability of data, data quality control, and analysis methods. The chapter presents case studies from the Barnett shale, Bakken play, and Eagle Ford shale.

Chapter 13: Unconventional Reserves Accounting and Booking

Chapter 13 addresses the difference between reserves and resources and why it is important to exploration and production companies, regulators, governments, and national companies. The terms ***reserves*** and ***resources*** are defined including the types of reserves (proved, probable possible, 1P, 2P, and 3P) and resources (contingent, prospective). Reporting methodologies for Petroleum Resources Management System (PRMS) framework (the basis for most corporate planning), and the US Securities and Exchange Commission (SEC) revised regulations including the Financial Accounting Standards Board (FASB) are addressed.

Additional reserves accounting guidelines are discussed including aggregation methods. Details are provided for assessing reserves and resources in unconventional reservoirs. They include but are not limited to types of unconventional resources (shale gas, shale oil, CBM, tight gas and oil, etc.) with a focus on shale gas, what has been discovered, how far from a discovery can be considered reserves, contingent resources, and how to categorize reserves. The authors state how to estimate and incorporate forecasts of future recovery and discuss potential pitfalls or red-flag issues for regulators.

Chapter 14: Production Evaluation and Forecasting

The chapter outlines potential expectations and pitfalls associated with evaluating and forecasting production in unconventional reservoirs while considering the impact of completion strategy, hydraulic fracture design, and well spacing. Several sections describe and discuss applications of various production evaluation and forecasting models. The models of interest include statistical methods (evaluation only). Other analytical models are decline-curve analysis (DCA); type curves rate transient analysis (RTA), and pressure transient analysis (PTA); and numerical models such as hydraulic fracture models, reservoir simulation models, integrating hydraulic fracture models, and reservoir simulation. Model applications have a significant effect on the completion optimization and field development in unconventional reservoirs. This process impacts workflows used and model calibration requirements. The chapter discusses the aspects of model calibration requirements including integrating microseismic, tilt-meter, and other far-field fracture diagnostics; integrating production logs, radioactive tracers, and other near wellbore measurements; production data, PTA, and history matching; and offset well data. The ultimate goal is optimizing stage spacing (horizontal wells), hydraulic fracture design, and well spacing. The chapter includes examples and case studies.

Chapter 15: Drilling Systems for Unconventionals

Chapter 15 summarizes the development of unconventional drilling and what led to the recognition of important parameters associated with optimized drilling of unconventionals like reservoir understanding, well architecture, rigs, cementing, and current drilling challenges. Starting with drilling systems, the section covers deflection tools such as conventional motors, rotary steerable systems, measurement while drilling systems, and other enabling technologies like bits and fluid.

The author discusses the changing needs associated with the need for efficiency; common pitfalls; data-driven approach; reservoir navigation such as advanced mud logging techniques and logging while drilling; use of image logs; completion optimization using logging while drilling logs; modern cementing technologies and drilling optimization; and remote drilling technology. Case studies are used to illustrate the methodologies.

Chapter 16: Multistage Completion Systems for Unconventionals

This chapter discusses the basics of unconventional wellbore completions with items such as liners; float shoes and collars; openhole versus cemented liner, and early methods of completing unconventionals including single-stage massive hydraulic fracturing; slotted and pre-perforated liner; intervention isolation; and evolutionary nature of completion design. The chapter focuses on completion systems details including plug-and-perf completions, ball-activated completions, and coiled tubing-activated completion systems and the pros and cons of each system. The operational comparison of each completion system is presented with emphasis on multiple entry versus selective entry, long laterals, increased number of stages, low number of stages, shortage of supplies for fracturing, appraisal and exploration phase of the asset life-cycle, and development stage of the asset life-cycle. The chapter concludes with how the completion system can interact effectively with drilling and stimulation systems to optimize the overall development process.

Chapter 17: Stimulation of Unconventional Reservoirs

The chapter explains the evolution of hydraulic fracturing and how the process defines what needs to be addressed to accommodate the technology for unconventional resource development. The chapter then focuses on fracture treatment design and the associated new data requirements. Having discussed the data from logging and core measurements, additional data are required. This leads to a discussion about diagnostics, including mini-fracture and diagnostic fracture injection tests. Hydraulic fracture design models and the use of relevant data from logs, cores, and dynamic tests are discussed. Special emphasis is placed on using discrete fracture network modeling as an inclusive part of the fracture design model. For shale resource development, various types of fractured design systems are used. They include nonstop, simo-fracs, zipper fractures, and computed tomography fracturing. Field case studies illustrate the application of hydraulic fracture design and the implications for the observed production results.

Chapter 18: Flow Assurance

The chapter identifies key issues associated with production assurance in the unconventional arena and implications on cost, operations, and what needs to be addressed for prevention, mitigation, and remediation. The chapter discusses details of the proper avenues to avoid thus addressing optimized flow assurance. The author identifies the key flow assurance detractors and their impact on operations and provides recommendations to overcome the flow derailment. The key flow assurance detractors discussed include inorganic scale, paraffin, asphaltene, gas hydrates, corrosion, and bacteria. Other flow impediments include hydrogen sulfide gas and solids and fines. The chapter focuses on the planning related issues to prevent production assurance that address the design for expectations, preventative measures, monitoring, and adapting. The planning involves operational aspects such as ascertaining production assurance indicators, perform analysis, cost benefit, mitigation, and needed fixes. A section on specialty chemicals addresses diversified fluid systems needed for shale formation production. The chapter concludes with field examples illustrating major flow assurance issues with scale, paraffin, asphaltene, and gas hydrates.

Chapter 19: Artificial Lift Technology

Chapter 19 covers unconventional oil plays and associated issues in reference to the operator's production strategy and how that impacts technical strategies for artificial lift in unconventional oil plays. The chapter focuses on challenges related to fluid; sand and abrasives such as fracture sand; gas; scale and other depositions; temperature; well depth; and production decline or depletion. The author explains the challenges via oil producing unconventional plays in the US-ESP experience. They include the following:

- Bakken and Three Forks: Bakken geology and ESP case studies in the Bakken shale
- Niobrara: Geology and ESP case study
- Mid-continent: Unconventional plays including geology and the fracture design model
- Permian Basin: Unconventional plays, Permian Basin geology
- Permian Basin: Unconventional ESP experience
- Eagle Ford shale: Eagle Ford geology and case study
- West coast: Unconventional plays.

The author takes a futuristic look at the technology requirements and evolution.

Chapter 20: Monitoring Technologies—Microseismic, Fiber Optic, and Tracers

This chapter discusses hydraulic fracturing monitoring technologies and focuses on microseismic (borehole and surface), fiber optic, and tracers. Production logging is an important monitoring technique; however, the methodology and interpretation aspects are similar to conventional

resource analysis and as such are not covered. The microseismic section starts with seismology concepts and addresses data acquisition requirements for optimal results. The data processing and interpretation section addresses important aspects of velocity modeling and the relevance of all events leading to location methodologies and the overall microseismic cloud. This section illustrates the methodology via case studies and addressing future needs.

The section on fiber optics introduces distributed temperature sensing and distributed acoustic sensing and how they can be used to evaluate hydraulic fracturing results and support production logging. The tracer section focuses on the permanent downhole inflow tracer monitoring technology, introducing the concept of tracer surveillance. This is followed by discussion on inflow tracer interpretation methodologies and what such interpretation can deliver.

Deliverables can include quantitative interpretation, steady state monitoring, water breakthrough predictions, well integrity monitoring and alarms, and chemical sensors all tied to simulation models. The section covers the laboratory flow loop system used to validate simulation models. The section presents a case study addressing multistage fracturing. The chapter concludes by discussing the inter-relationship of the monitoring technologies.

Chapter 21: Rejuvenating Unconventional Resources

Restimulation (refracturing) is currently the most effective method of rejuvenation to restore productivity to declining shale wells, while enhanced shale oil recovery (ESOR) is the emerging technology that is only being studied in a couple of basins. North America is the only market mature enough to experience the need for refracturing and potential emerging ESOR. This chapter discusses both the refracturing and the ESOR technology.

The refracturing process addresses the need to create additional reservoir rock surface area and/or reopen existing hydraulic fracture. The authors address the types of refracturing that need to be considered and the associated procedure, design, and operation including required equipment. Criteria for refracturing candidate selection are outlined while ensuring that the economics are embedded in the process. The authors illustrate the concept with field case studies and derive conclusions in terms of recommendations for future application of refracturing technology.

The ESOR discussion is also primarily focused on the US. A growing body of research examines the potential application of injecting CO_2 as an EOR agent in liquid-rich shale formations to evaluate changes in recovery rates. The refracturing technique and the ESOR method both provide a common platform for rejuvenating shale assets, even though they are principally and operationally different. They can both be applied to arrest production decline in oil wells and maximize oil recovery in a given play, while ESOR has the potential to additionally increase the recovery factor by sweeping the by-passed oil. In the ESOR section, the authors review the technology and present a case study to illustrate the present industry status.

Chapter 22: Environmental Issues in Unconventional Oil and Gas Resource Development

Environmental issues in unconventional oil and gas resource development begin with the license to operate in the most appropriate manner and paying attention to the environment while harnessing the needed energy for the bettering of human life. This leads to the discussion of the greenhouse gas issue. The chapter identifies the key elements that may manifest as an environmental issue and encompasses a range of topics from noise to hydraulic fracturing. Discussions are presented on how each of these can be addressed and mitigated while following the required regulatory issues. The chapter focuses on the current outlook based on developments associated with federal initiatives like the EPA Hydraulic Fracture Study, the Clean Air Act, and toxic substance control. Issues related to water management challenges, sourcing, and innovations plus cleaner and greener fluids and chemicals are discussed as the way forward.

Chapter 23: Case Studies, Accessing JewelSuite™ Software and Data

This chapter presents case studies from three major unconventional plays in the US and how different fracture treatment and completion strategies can affect the outcome of the reservoir development studies. Readers must request access via email to get a login to the software, access to the case studies, and to see the models and the impact of any adjustments to configuration of hydraulic fractures and reservoir properties.

Chapter 24: New Considerations and Future Trends in Reservoir Technologies for Unconventional Resources Development

This chapter includes current and future research directions in shale resource assessment. It introduces shale as a rock with multiple-scale pore structure: large and stress-sensitive inorganic pores and micro-fractures, and small (nano-scale) organic pores. The chapter considers distribution of hydrocarbons in the pore space as free gas, adsorbed phase, capillary condensed phase, liquid, and super critical phases. Challenges in hydrocarbon in-place calculations are discussed, and a state-of-the-art permeability model is introduced.

Chapter 25: Epilogue

This textbook is one of the first of its kind addressing the downstream technical aspects associated with unconventional resources. Hence, there is potential skepticism associated with the way forward and the chapter addresses the topic head on. Some of the critical aspects that have the potential of causing a paradigm shift in our thinking include the nature of matrix-fracture flow duality, reservoir uncertainties, and anomalies leading to a potential crisis in the reservoir engineering discipline. When compounded with the impact of the required operational efficiency of the unconventional resources development, a paradigm shift appears to be in the cards.

2.5 The Way Forward

The authors and co-authors thank the readers for using this textbook and hope it is a valuable tool. We would like to hear from you regarding any constructive comments you may have.

2.6 References

Canadian Association of Petroleum Producers (CAPP), http://www.capp.ca/canadaIndustry/naturalGas/Conventional–Unconventional/Pages/default.aspx (accessed 2 July 2014).

EIA. 2001. World Energy Outlook 2001: Assessing Today's Supplies to Fuel Tomorrow's Growth, http://www.worldenergyoutlook.org/media/weowebsite/2008-1994/weo2001.pdf (accessed July 2014).

EIA. 2011. World Energy Outlook 2011, http://www.iea.org/publications/freepublications/publication/WEO2011_WEB.pdf (accessed July 2014).

EIA. 2013. About Us, ***IEA*** (International Energy Agency/OECD). (accessed 28 December 2013).

EIA. 2014. Annual Energy Outlook 2014, http://www.eia.gov/oiaf/aeo/tablebrowser (accessed July 2014).

Gordon, D. 2012. Understanding Unconventional Oil, Washington, DC: Carnegie Endowment for International Peace. http://carnegieendowment.org/files/unconventional_oil.pdf (accessed July 2014).

HIS. 2013. Global Unconventional Resources: Some Examples from the IHS Unconventional Play Database. October 2013, http://64be6584f53 5e2968ea8-7b17ad3adbc87099ad3f7b89f2b60a7a.r38.d2.rackcdn.com/1HS%20Unconventional%20oil%20and%20gas%20resource_v2.pdf (accessed July 2014).

Ratner, M. and Tieman, M. 2014. An Overview of Unconventional Oil and Natural Gas: Resources and Federal Actions. Congressional Research Services Report R43148 (January 2014).

SPE PRMS Report 2011. Guidelines for Application of the Petroleum Resources Management System. http://www.spe.org/industry/docs/PRMS_Guidelines_November (accessed 22 August 2014).

3

Characteristics of Unconventional Oil and Gas Resources

Usman Ahmed and
D. Nathan Meehan, Baker Hughes

This page intentionally left blank

Chapter 3: Characteristics of Unconventional Oil and Gas Resources

"The pessimist complains about the wind. The optimist expects it to change. The leader adjusts the sails."

John Maxwell

Foreword

The adjustments to the unconventional resource exploitation and development sail starts here.

Chapter 2 discussed the difference between unconventional resources and conventional resources. Here, discussions are presented to characterize unconventional oil and gas resources. We start the discussion by reviewing the unconventional resources in general, followed by addressing the unconventional resource triangle, which then leads us to discuss the shale resources. This is followed by an overview of tight oil and gas and coalbed methane (also referred to as coal seam gas, or CSG, in Australia).

3.1 Introduction to Unconventional Resources

Some definitions change with time. The depths that correspond to deep water for oil and gas have increased over time as technologies and capabilities have been enhanced. Similarly, the definition of tight oil has changed, as has the meaning of unconventional in relation to reservoirs. For our purposes, we often describe reservoirs as shales, when they may be, in fact, a combination of marls, mudstones, or even carbonates. This chapter presumes the reader has some familiarity with both conventional and tight oil and gas principles as we discuss unconventional reservoirs. For this purpose we can use practical and approximate definitions based on the types of wells and completions required.

- Conventional reservoirs can be developed with vertical wells and do not need large hydraulic fracture stimulation treatments. If used, a conventional well's hydraulic fracturing treatment is typically less than a 100-ft. wing length and has a cost that is less than 10% of total well costs. Using horizontal wells in conventional reservoirs may significantly improve performance if the reservoir is naturally fractured, is thin, or has important gravity features such as a gas-oil or water-hydrocarbon contact. Transient flow behavior in such wells is often a practical approach for characterizing the reservoir.
- Tight reservoirs require large hydraulic fracture stimulation treatments whose half-wing length is hundreds of feet, which can cost a significant portion of total well costs. Tight reservoirs produce at negligible to uneconomical rates without stimulation. Horizontal wells with multiple hydraulic fracture stages may improve production; however, operators rarely use dozens of such stages in typical tight reservoirs. Transient flow periods in such wells may be over many months.
- Unconventional reservoirs require long (3,000 to 10,000 ft.) horizontal wells with dozens of hydraulic fracture stages for commercial production. The proximity of the fracture stages results in stress interference and some degree of improvement in the aggregate matrix permeability. This arises from multiple mechanisms that can include slippage of critically stressed fractures, movement along slowly slipping faults, and complex hydraulic fracture geometry. Transient flow behavior in such wells is highly complex. Diffusion may ultimately be an important contributor to production.

3.1.1 Shale Reservoirs as Unconventional Plays

According to the US Geological Survey, production from unconventional reservoirs exists in geographically extensive accumulations (USGS report). Unconventional reservoir deposits generally lack well-defined hydrocarbon/water contacts and include coalbed methane, some tight sandstone reservoirs, chalks, and self-sourced oil and gas in shale accumulations. The assessment methodology and production practices for unconventional reservoirs vary from those used for conventional resources. General categories of unconventional petroleum include:

- Deep gas
- Shallow biogenic gas
- Heavy oil and/or natural bitumen
- Shale gas and oil
- Gas hydrates
- Coalbed methane

While the level of maturity of these unconventional resources varies, oil and gas production from shale reservoirs is growing at a phenomenal rate. The type of shale production being discussed is generally conventional oil or gas produced from relatively deeply buried shales that are produced in a manner

roughly similar to conventional wells. We refer to this as shale oil and shale gas. The term ***oil shale*** is widely applied to petroleum extracted from shallow rocks with very high kerogen content. Many of the rocks referred to as oil shales are not shales and theses rocks are often physically mined rather than having the hydrocarbons produced through wellbores. Oil shales typically contain solid or ultraviscous hydrocarbon material in their pores. While some oil shales can be burned directly, most require some sort of extractive process, coupled with upgrading, to yield oil like hydrocarbons. Oil shales are not discussed in this book.

3.1.2 So, What Is a Shale Anyway?

Shales are the most abundant types and volumes of rocks in sedimentary basins worldwide. Shales are the most abundant sources of hydrocarbons for oil and gas fields and due to their low permeabilities form the hydrocarbon seal for many fields. A conventional oil or gas field needs a source, a reservoir (usually porous sandstones or carbonates such as limestone or dolomite), a trap (such as a structural closure, sealing fault, or pinchout), and a seal. The source is necessary for hydrocarbons to exist and some pathway is necessary for these hydrocarbons to migrate. The reservoir porosity was usually water filled at the time of deposition, allowing the hydrocarbons to migrate through the porosity due to having lower density than the water. The trap and seal are necessary to prevent continued migration (to keep the hydrocarbons in place) and to allow the reservoir to accumulate and store oil or gas. As a result, geologists and geochemists have studied shales extensively with most of their historical effort focused on shale's source rock potential. The fact that many shales still contain significant amounts of natural gas is no surprise to drillers and geologists. It is routine to observe natural gas "shows" while drilling through shales, occasionally in significant volumes. But while it may be clear to most readers what porous sandstone or carbonate rock is like (the rocks that form most oil and gas reservoirs), shales remain somewhat of a mystery.

There are multiple definitions of what constitutes shale. A geologist once mentioned that the way to differentiate between siltstone and shale was to put it in your mouth. If it tastes gritty, it is a siltstone. If it tastes smooth or oily, it is shale. For the record, the authors do not recommend putting any rocks in your mouth!

Shales are sedimentary rocks composed of clastics (portions of older rocks) comprised of silts, muds, and clays. Geological definitions of shales typically reference their grain size as being clay-like (less than 1/256th mm diameter particles). Silts are also defined based on grain sizes (between 1/16th and 1/256th mm) and are positioned between clays and sands. Very fine silts can be primarily composed of quartzitic materials that are lacking in typical clay minerals. Clay minerals often include kaolinite, montmorillonite-smectite, illite, and chlorite. There are dozens of pure clays, with most clays being mixtures of multiple pure clays. One important clay type in oilfield operations is bentonite, a typical weighting component of drilling mud. Another physical property often used in defining shales is their tendency to split into thin sheets or slabs (fissility). Muds are simply mixtures of water and very fine silt, clay, and soil particles. Mudstones are hardened muds that may not show fissility unless desiccated. While most shales are clastics, significant carbonate components can be present in shales. The formations we refer to as ***shale gas*** or ***shale oil plays*** are often layers of shales and layers of silts and/or carbonates.

The depositional environment of shales that are resource plays is typically a low-energy one that allows very fine-grained particles that will constitute future shales to be deposited. High-energy deposits such as channel sands and turbidites will also lead to shale deposition. The low depositional environments associated with marine shales means that their geological and petrophysical properties change relatively slowly over large distances compared with the higher levels of heterogeneities in many sandstones and carbonates. Petrophysicists take advantage of this when analyzing logs of varying vintages and from varying suppliers by normalizing log responses in marine shales.

Very fine-grained, organic material (usually from plant materials) is often deposited concurrently with the silt, mud, and clay matter that will eventually form shales. Total organic carbon (TOC) is the weight-percent of organic carbon in the shale (and does not include carbon from carbonates for example). Because many shales have relatively high organic carbon content, under certain heat and temperature conditions, shales can serve as source rocks for oil and gas reservoirs. The organic content originated with living material, ultimately from plant, animal, and bacterial matter such as algae, plankton, or decomposed plant materials. After death, the materials decompose, and the decomposition products can form new polymers to form kerogen. Diagenesis is controlled primarily by biological and chemical activity associated with mineralogy and redox conditions. Complex thermal transformations characterize subsequent kerogen transformation.

The word kerogen was originated by Professor Crum Brown (of the University of Edinburgh, Scotland) and referred specifically "…to the carbonaceous matter in shale that gives rise to crude oil in distillation" (Brown 1979). Kerogen now refers more broadly to all of the solid organic material in sedimentary rocks; kerogen is generally insoluble in water or organic solvents due to their high molecular weights. Bitumen refers to the insoluble portion.

Kerogen may be formed under various circumstances from this organic matter, which can be broken down into lighter organic materials under heat and pressure. Most oil and gas produced originated with such shales as sources with a few exceptions.

Shales generally have extremely low permeability due to their very fine grain size. Permeabilities are so low in most shales that excellent seals for oil and gas fields can be formed by shales. Drillers and mud loggers have long known that many shales contain significant quantities of natural gas, because natural gas discoveries are commonplace during drilling through shales. While some shales are rich in heavy hydrocarbons (oil shales), this discussion focuses on shales that are likely to contain natural gas or oil.

It is important to note that the type of shale production being discussed here is generally conventional oils or gas produced from relatively deeply buried shales that are produced in a manner roughly similar to conventional wells. We refer to this as shale oil and shale gas. The term ***oil shale*** is widely applied to petroleum extracted from shallow rocks with very high kerogen content. Many of the rocks referred to as oil shales are not actually shales—these rocks are often physically mined rather than having the hydrocarbons produced through wellbores. Oil shales contain typically solid or ultraviscous hydrocarbon material in their pores. While some oil shales can be burned directly, most require some sort of extractive process coupled with upgrading to yield oil like hydrocarbons. Oil shales are not discussed here.

Shale gas production has been recorded for over a century in the Devonian age formations in the Appalachian basin. More than 20,000 wells have been drilled in these shallow shales. Older (and deeper) Devonian shales include the Marcellus formation, which is now a major focal point for the application of advanced technology. Because we have known about these shales and their hydrocarbon potential for decades, if not more than a century, why has it taken so long to produce them? The answer is clear: the technology to drill, evaluate, complete, and produce these shale plays has only been available for a decade (at best), and many advances have been made in just the last few years.

3.1.3 Shales as Resource Plays

A resource play is a relatively large hydrocarbon accumulation that occurs over a broad geological area. In a resource play, the geological risk of encountering the hydrocarbon bearing strata is nearly certain within the play area. A resource play may nonetheless have wide variability in well performance; however it is often the case that such variability cannot easily be predicted in advance or even correlated to conventional measurements (e.g., porosity, thickness). Resource plays have alternately been described as statistical plays, in which an operator must drill a large number of wells and can expect fairly repeatable results if enough wells are drilled.

Tier one criteria used in defining resource plays include the following characteristics taken from the Society of Petroleum Evaluation Engineers (SPEE) Monograph 2011:

1. Exhibits a repeatable statistical distribution of estimated ultimate recoveries (EURs).

2. Offset well performance is not a reliable predictor of undeveloped location performance.

3. Continuous hydrocarbon system that is regional in extent.

4. Free hydrocarbons (non-sorbed) are not held in place by hydrodynamics.

The SPEE provides certain statistical guidelines for the evaluation of resource plays that require each of the prior criteria to be met. Many shale gas reservoirs are considered to be resource plays, with both geological and engineering data supporting the criteria. It cannot be proven that a given area is a resource play until a significant number of wells have been drilled—and enough performance data is analyzed—to justify the conclusion. From those criteria, the most important criterion is the first one, which is the repeatable statistical distribution of EURs. Having a statistical distribution of EURs is characteristic of many reservoirs. If the mean measurement (and other measures of the statistical distributions) varies significantly spatially, especially if the variance is, in some way, correlated to readily identifiable geological data (such as TOCs, thickness, etc.), the play is unlikely to be a true resource play.

The second criterion implies heterogeneity in well performance. This is true of many non-resource plays, including many carbonate reservoirs, so it is not sufficient. The importance is that reasonably obtainable measurements (such as kh) do not predict well performance changes. This truly complicates matters when operators assume the second

criterion is "true" and decide not to go to the expense of obtaining well logs. As we will see in Chapter 8, formation evaluation tools for shale gas wells are available that can produce detailed geological and mineralogical information including clay types, TOC, silica content, etc. Such data might be highly predictive of well performance and could even indicate ways to improve well completions and future drill site selections. If such logs are not run and analyzed, the operator will conclude that there is no way to explain variability other than the "statistical" nature of the play.

The third and fourth criteria are generally present in all productive shale gas plays. Tier two criteria (the next tier of criteria) include:

5. Requires extensive stimulation to produce at economic rates.

6. Produces little in-situ water (except for coalbed methane and tight oil reservoirs).

7. Does not exhibit an obvious seal or trap.

8. Low permeability (< 0.1 md) shale bulk permeabilities are typically less than 0.001 md.

Shale gas plays generally satisfy each of these criteria easily. As the plays form seals for conventional reservoirs, they do not have to have a separate trap. Thus, a syncline may easily be as productive as an anticline in shale. The permeabilities of shale gas reservoirs are often well below 0.01 md and generally require stimulation. Shale gas reservoirs have such low permeabilities that free water production is rare; highly fractured shales could allow water from deeper zones to be produced.

3.1.4 Shale as Reservoirs?

While shales are known to be the principal sources for conventional hydrocarbon plays as well as seals, shales can also be the reservoir and trap. Most of the gas created in such reservoirs would be thermogenic in origin, although some shales (e.g., the Antrim) have significant quantities of biogenic gas. Gas is stored in shales either as free gas in the pore spaces or adsorbed onto the organic material or surface walls in the shale.

Thermogenic methane was formed when organic matter was compressed at very high pressures for a very long time. Just as in oil formation, thermogenic methane is a cracking process that transforms organic particles carried in the clastic material, which then forms the origin of shales. The nature of the organic material and time and pressure dictate what is formed in thermogenic processes. Thermogenic gas can contain significant quantities of heavier hydrocarbons.

Biogenic methane can be formed by microorganisms that chemically break down organic matter. Biogenic methane is generally formed at shallow depths in anoxic environments. While most of this methane escapes to the atmosphere, some can be trapped and buried at depth. Modern landfills can also form biogenic methane. Biogenic methane is essentially unrelated to the processes that form oil—biogenic gas primarily contains methane with very few heavier hydrocarbons. A standard measure of whether a gas is thermogenic or biogenic can be determined by gas geochemistry. Thermogenic gas has less carbon 13 compared to the predominant carbon 12 than do biogenic gases.

3.1.5 Role of Geochemistry

Many tools are used to analyze and study shales. The total organic carbon (TOC) is typically determined by calculating the difference between total organic carbon and the carbonate carbon concentration. While both of the latter measurements are generally made with cuttings or core samples, petrophysical estimates of TOC can provide excellent and continuous estimates of TOC.

Pyrolysis of organic matter in shales involves heating samples to extract volatile hydrocarbons (referred to as S1), thermogenic hydrocarbons (S2), and the carbon dioxide released up to a fixed temperature (S3). The methodology to make these measurements involves pulverizing a small sample of rock and heating it to increasing temperatures. These values (S1 through S3) are used in calculating several common geochemical values including the hydrogen and oxygen indices (HI and OI). The temperature above which no further hydrocarbons are released by pyrolysis is referred to as T_{max} and provides a common measure of organic matter. The indices are defined as follows:

$$HI = (100S\_2)/TOC$$

with units of milligrams hydrocarbons per gram of organic carbon and

$$OI = (100S\_3)/TOC$$

with units of milligrams CO_2/gram organic carbon.

Geochemists use these values to assess the shale's source rock potential along with the hydrocarbon generation potential and also to describe the types of kerogen. The authors of Chapter

8 point out the value of the S_1/TOC ratio and demonstrate that values in excess of 100 milligrams hydrocarbons/gram of organic carbon are very positive for the production potential of shale oil and shale gas.

Vitrinite reflectance is another widely used measurement associated with shales. Plants take in CO_2 and water to generate carbohydrates and polymers that form plant material such as cellulose and lignins. It is this plant material that (with time, temperature, and pressure) ultimately creates oil or natural gas. Vitrinite is a shiny material formed by the thermal alteration of such organic matter; it is present in most kerogens and coals. Vitrinite reflectance is often used to describe the maturity of coals. For example, lignite is a coal with low thermal maturity and reflectance, and anthracite is a highly reflective and more mature coal. Coalification of peat is strongly analogous chemically and physically to the maturation of kerogen. Vitrinite reflectance can be used in conjunction with TOC values, pyrolysis data, etc. Vitrinite reflectivity is typically measured with an oil-immersion microscope and a device for measuring reflected light. Comparisons are made with reference standards to define the reflectance in oil, R_0. While R_0 is a measure of thermal maturity, its significance is a function of the type of kerogen being analyzed. Nonetheless, low values of R_0 indicate immature kerogen. As R_0 increases, the indicated maturity levels suggest oil generation, gas generation with condensates (wet gases), and, ultimately, dry gases at high levels of thermal maturity. At such levels, sufficient time and temperature will have cracked heavier organic molecules.

Different types of kerogen are usually described based on their relative amounts of hydrogen, carbon, and oxygen. Each type of kerogen has varying tendencies to form oil, gas, and coal. The reasons for the different chemical compositions include the type of organic material present (including plankton, algae, spores, pollen, diatoms, etc.) and the chemical processes to which the material was exposed.

While not as routinely used in shale oil and shale gas evaluations, geoscientists often make use of the organic carbon isotope ratios, and atomic carbon nitrogen ratios, to analyze shale depositional histories and in related studies. Geochemistry can be a powerful tool for reservoir engineers in many areas besides the analysis of unconventional reservoirs.

3.2 Workflow to Address Unconventional Resource Development

As we have noted, classical unconventional resource definitions include coalbed methane (CBM), tight oil and gas reservoirs, and shale oil and gas. Sometimes heavy oil development is lumped with unconventional resources. We choose to place heavy oil in a different category, because the others, as a group, have a lot of similarity in the technology and development requirements that heavy oil does not.

Cost-effective development of the three unconventional resources (listed previously) can follow a certain life-cycle approach, which is a six-step, phased approach that addresses exploration, appraisal, development, production, rejuvenation, and abandonment phases. In the life-cycle approach, we acknowledge the subtle differences between the three groups of unconventional resources and how these factors affect the overall understanding of the reservoir. From this, we can extrapolate the exploitation strategy (placement of wells and stimulation locations and all aspects associated with the process followed by a rejuvenation phase). Field case studies suggest that using such a process can positively affect the recovery factor, while the increased operational efficiency garnered from the process can reduce cost, depending on the scale and scope of the project. Finally, well-thought-out field understanding and development design alone is not good enough without a continued commitment of resources (people, tools, and software). Of these resource commitments, typically the hardest one to meet is securing the proper unconventional resources expertise. Over the last decade, an increased understanding about unconventional resource development has come about in North America, which is now prime to be potentially disseminated as long as we take the time to understand the difference of the new basin and its associated challenges (Ahmed 2014).

There are subtle differences between the three unconventional resources, even though they still follow a similar workflow process as illustrated in **Fig. 3.1** (an entire chapter on workflow is dedicated within Chapter 5). Therefore, as we illustrate the resource triangle, we will then follow with a detailed characterization of the shale oil and gas. Then, we dedicate sections to tight oil and gas and CBM to illustrate the subtle differences in the characterization of both, even though the workflow and development process remain unchanged.

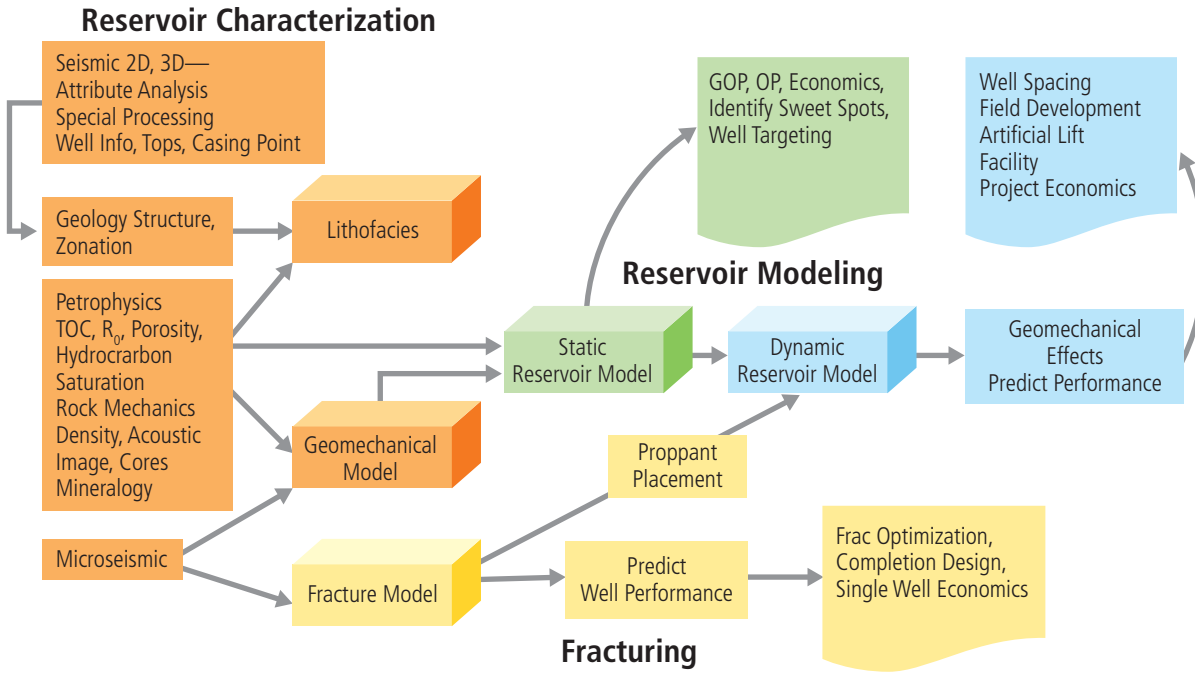

Fig. 3.1—Workflow process and outline for unconventional resources exploitation and development. (From Vassilellis et al. 2011.)

3.3 The Unconventional Resource Triangle

The resource triangle concept was used by Masters (1979) as a method to find large gas fields and build a company in the 1970s. **Fig. 3.2** illustrates the principle of the resource triangle. In the resource triangle, conventional gas is located at the top with better reservoir characteristics and quality, is associated with conventional technology and ease of development, but exists in small volumes (Holditch 2006). As we navigate further down the triangle, past tight gas and coalbed methane (CBM), shale gas (and gas hydrates) are found at the bottom of the triangle. Progression to the bottom of the triangle is associated with permeability and reservoir quality decreasing, the technology needed to develop increasing (i.e., becoming more complex), and difficulty of development increasing; however large volumes of these resources can be found. The concept of the resource triangle applies to every hydrocarbon-producing basin in the world. Martin et al. (2008) validated the resource triangle concept using a computer program, database, and software they developed. They also expanded the resource triangle to include liquid and solid hydrocarbons adding heavy oil and oil shale, and referencing work from Gray (1977). Shale resource development is at the bottom left signifying that the resource base is huge (documented in Chapter 4) with decreasing reservoir quality requiring deployment of increasing and demanding technology.

3.4 Characteristics of Shale Oil and Gas

In addition to Section 3.1, in this section we will use the work done by others to characterize shale oil and gas as an unconventional reservoir contained in fine-grained, organic rich, sedimentary rocks, including shale, but composed of mud containing other minerals like quartz and calcite (US DOE 2009; Warlick 2010; US EIA 2011). A number of formations broadly referred to by industry as ***shale***, may contain very little shale lithology and/or mineralogy, but are considered to be shale by grain size only. Passey et al. (2010) describes shale as extremely fine-grained particles, typically less than 4 microns in diameter, but that may contain variable amounts of silt-sized particles (up to 62.5 microns). No two shales are alike and they vary areally and vertically within a trend and even along horizontal wellbores (King 2010). Not only will shales vary from basin to basin, but also within the same field (Economides and Martin 2007). These reservoirs are continuous hydrocarbon accumulations that persist over very large geographic areas. Shale hydrocarbon accumulations can range from dry gas to wet gas to condensate, and to all oil phases as seen in the Eagle Ford development. The challenge in developing shale resources is not just to find oil and gas, but to also find the best areas, or sweet spots, that can result in the best production and recovery (Jenkins and Boyer 2008).

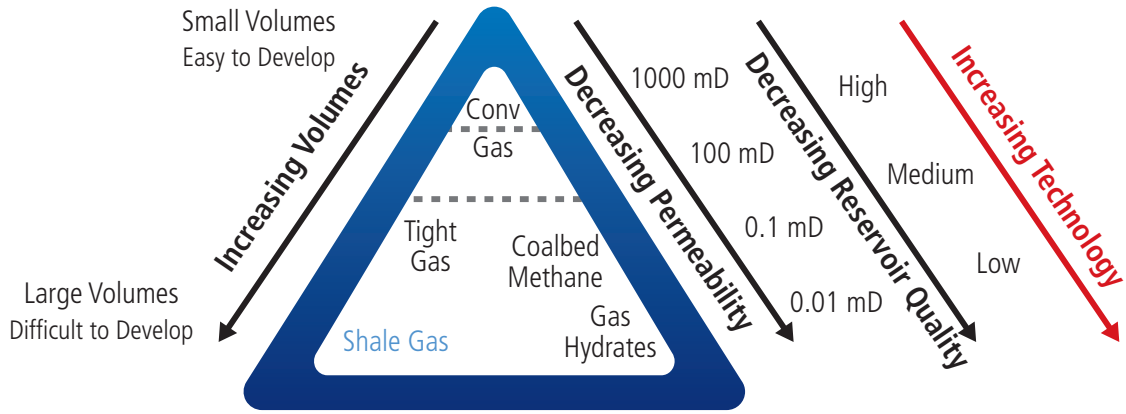

Fig. 3.2—The Unconventional Resource Triangle: The concept of the resource triangle applies to every hydrocarbon-producing basin in the world. (Holditch 2006 after Masters 1979 and Gray 1977.)

Shale reservoirs have no trap like conventional gas reservoirs, and do not contain a gas and/or water contact. Shales are the source rock, which also now acts as the reservoir, where the total or partial volume of oil and gas (hydrocarbon) remains. Shales are the source rock for most of the hydrocarbons. The key to success with shale is to find the shale plays where the remaining hydrocarbons were not expulsed and did not migrate into conventional formations and are now economically viable for development. A note of caution: not all shales are source rocks and not all shale source rocks still hold the accumulated hydrocarbon.

In terms of the flow behavior, we have already mentioned in the coalbed methane section that shale has more similarity with coalbed methane than tight sedimentary rocks and is illustrated further below.

Natural matrix permeability in shales is extremely low, often in the nano-darcy range. Measurement of shale permeability is difficult and the results are probably inaccurate. In this extreme low-permeability environment, gas (hydrocarbon) flow through the matrix is extremely limited and insufficient for commercial production. Various authors have estimated that a gas molecule will move no more than 10 to 50 feet per year through shale matrix rock. Shale porosities are also relatively low ranging from less than 5 to 12%. Shale reservoirs require hydraulic fracturing to produce commercial amounts of gas. Shale reservoirs with oil resources tend to have relatively higher permeability and porosity, yet still very low. The porosity is still fairly low; therefore, hydraulic fracturing is still required in this type of shale reservoir to create a path for the oil to flow.

A number of different reservoir parameters that are not necessarily deemed important for conventional gas are still significant for assessing economic viability, development, and well completion techniques for shale production. This includes the following parameters that we must now consider for shale reservoirs:

- Total organic carbon (TOC) content, kerogen type, and thermal maturity (also referred to as, and measured as, vitrinite reflectance, R_0)
- Mineralogy/lithology, brittleness, existence of natural fractures, and stress regime
- Multiple locations and types of oil and gas storage in the reservoir
- Thermogenic or biogenic systems
- Depositional environment, thickness, porosity, and pressure

Though not a parameter, the characteristic steep production decline profile is an important aspect here.

The discussion, next, briefly covers each of these parameters along with the unique aspects of shale, to provide an understanding of the parameters' significance in play analysis and development.

Organic materials, microorganism fossils, and plant matter provide the required carbon, oxygen, and hydrogen atoms needed to create natural gas and oil. TOC is the amount of material available to convert into hydrocarbons (depending on kerogen type) and represents a qualitative measure of source rock potential (Jarvie et al. 2007). This measure is commonly expressed as a ***percent by weight***, but it is also sometimes expressed as ***percent by volume*** (volume % approximately twice that of weight %). Oil and gas

Table 3.1—Types of kerogen and the hydrocarbon potential by environment, type, and origin. (From Holditch 2011.)

Types of Kerogen and Their Hydrocarbon Potential				
Environment	Kerogen Type	Kerogen Form	Origin	HC Potential
Aquatic	I	Alginite	Algal bodies	Oil
			Structureless debris of algal origin	
	II	Amorphous Kerogen	Structureless planktonic material, primarily of marine origin	
Terrestrial		Exinite	Skins of spores and pollen, cuticles of leaves, and herbaceous plants	
	III	Vitrinite	Fibrous and woody plant fragments and structureless colloidal humic matter	Gas, some oil
				Mainly gas
	IV	Inertinite	Oxidized, recycled woody debris	None

source rocks typically have greater than 1.0% TOC. TOC richness can range from poor at < 1%, to fair at 1 to 2%, to good-to-excellent at 2 to 10% (PESGB 2008). TOC is not the same as kerogen content, because TOC includes both kerogen and bitumen. TOC measurements in shale are determined from wireline logs and by direct measurement from cores and drill cuttings. Kerogen is a solid mixture of organic chemical compounds that make up a portion of the organic matter in sedimentary rocks. Kerogen is insoluble in normal organic solvents because of the huge molecular weight of its component compounds. The soluble portion is known as bitumen. There are basically four types of kerogen, three of which can generate hydrocarbons. Type I generates oil, Type II wet gas, and Type III dry gas (Holditch 2011). Understanding the kerogen type helps to predict the hydrocarbon type in a play. **Table 3.1** shows the types of kerogen and their hydrocarbon generating potential.

Thermal maturity measures the degree to which a formation has been exposed to high heat needed to break down organic matter in hydrocarbons. As temperature increases with the increasing depth in the earth's crust, heat causes generation of hydrocarbons and can ultimately destroy them. Typical temperature ranges at which oil and gas are generated are shown on **Fig. 3.3**. The oil window is 60 to 175°C (140-to-350°F) and the gas window is 100 to 300°C (212 to 570°F). The position of oil and gas windows within a basin is dependent on the type of organic matter and heating rate. Thermal maturity is a function of both time and temperature (Holditch 2011). Understanding the level of thermal maturity, or indeed whether the shale is thermally mature at all, is key to understanding shale resource

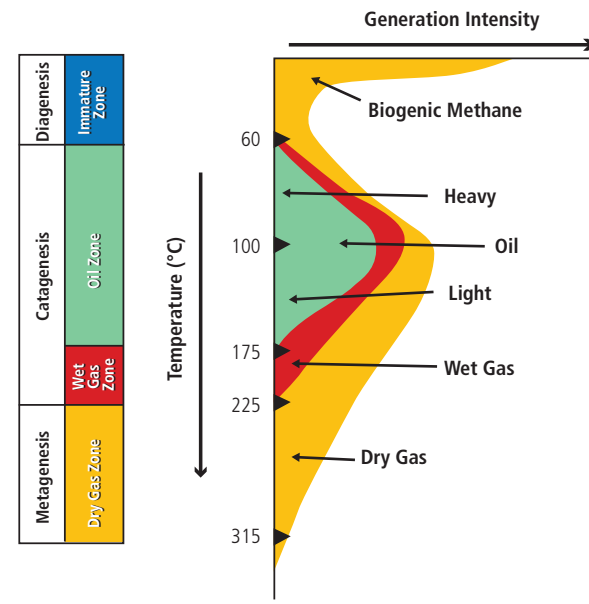

Fig. 3.3—Typical temperature range at which oil and gas are generated. (From Holditch 2011.)

potential (PESGB 2008). Also, higher thermal maturity leads to the presence of nanopores, which contribute to additional porosity in the shale matrix rock (Kuuskra et al. 2011).

Vitrinite reflectance, R_0%, the most commonly used technique for source rock thermal maturity determination, measures the intensity of the reflected light from polished vitrinite particles (a maceral group formed by lignified, higher-land plant tissues, such as leaves, stems, and roots) in shale under a reflecting microscope. Increased reflectance is caused by aromatization of kerogen and loss of hydrogen (Jarvie et al. 2007). **Fig. 3.4** is the thermal maturation scale. Dry gas occurs when R_0 is greater than 1.0%, wet gas when R_0 is between 0.5 and 1.0%, and oil when R_0 is between 0.5 and 1.3% (Kuuskraa et al. 2011).

Mineralogy and lithology are important for:

1. Quantifying TOC.
2. Reducing porosity uncertainty.
3. Identifying shale lithofacies.
4. Indicating variations in mechanical rock properties including brittleness.
5. Assisting in planning well hydraulic fracturing and completion designs.

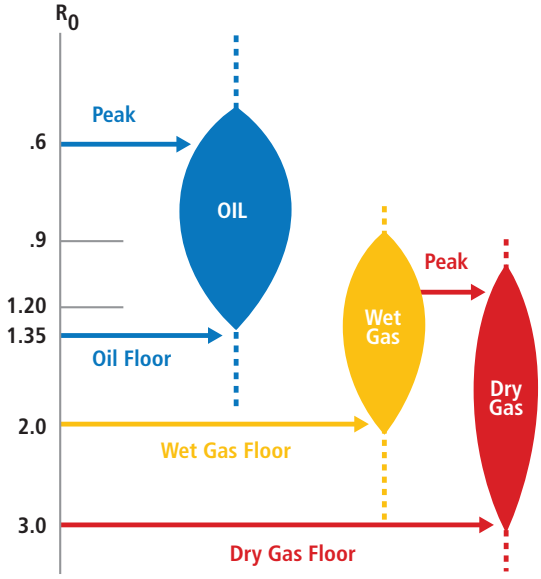

Fig. 3.4—Thermal maturation scale. (From Kuuskra et al. 2011.)

Most shale reservoirs can be chemostratigraphically classified into three primary lithofacies—siliceous mudstone (such as the Barnett), calcareous mudstone lithofacies, and organic mudstone lithofacies. Additional lithofacies have been identified in some reservoirs based on their unique characteristics. Lithology and mineralogy information is obtained from conventional and pulsed neuron log responses, laboratory analysis of cores and cuttings, and mineral spectroscopy analyses. TOC is quantified by the amount and vertical distribution of kerogen, kerogen type, level of maturity, and mineral spectroscopy plus core analysis. Log-derived and computed geomechanical properties include minimum horizontal stress (SH_{Min}), Poisson's ratio, Young's modulus, fracture migration, and static mechanical properties. Brittleness indicators that are used for identifying best interval to initiate a fracture and location at the vertical from which to drill horizontal laterals are computed from mineralogy and geomechanical brittleness and hardness (Jacobi et al. 2009; LeCompte et al. 2009; Pemper et al. 2009; Mitra et al. 2010).

Geomechanics considerations are significant in the development of unconventional resources in general, not just shale resources. Comments here are also applicable to coalbed methane and tight gas and oil formations. The stress regime in a basin must be considered during well drilling, fracturing, and production. Well orientation is dictated by in-situ stress systems and wellbore stability during drilling. In general, initiating a fracture depends on the stresses around the wellbore—both from the geologically produced tectonic effects and from changes in stresses produced by the fracture growth. Fractures are difficult to initiate where total rock stresses are very high. A major consideration during shale production is the stress evolution accompanying drawdown and depletion activity. It is now well established that reservoir pressure changes have an effect on both the stress magnitudes and direction in the sub-surface (Addis and Yassir 2010; King 2010).

Presence, location, and orientation of natural fractures in shale are significant with respect to the hydraulic fracturing process. In these naturally fractured reservoirs, well placement for initial development is dictated by two sub-surface factors:

1. Location and orientation of natural fracture sets, orientation of the most conductive natural fracture set, and in-situ stress magnitudes and directions
2. Propagation direction of hydraulic fractures from the wellbore and the intersection of natural fracture system (Addis and Yassir 2010)

Table 3.2—Free gas, sorbed gas, and dissolved gas storage methods.

Shale Gas Type →	Free Gas	Sorbed Gas	Dissolved Gas
↓ Storage Method →	In the rock matrix porosity	Adsorbed (chemically bound) to the organic matter (kerogen) and mineral surfaces within the natural fractures	In the hydrocarbon liquids present in the bitumen
	In the natural fractures	Absorbed (physically bound) to the organic matter (kerogen) and mineral surfaces within the matrix rock	

One purpose of hydraulic fracturing is to connect the existing natural fractures to create a complex network of pathways that enable hydrocarbons to enter the wellbore (King 2010; Jenkins and Boyer 2008). For shale gas, the gas (free and sorbed) is stored in three ways in a shale reservoir, as described in **Table 3.2**.

To obtain the total amount of gas in place (GIP), free gas, sorbed gas, and dissolved gas must be added together. Free gas is the ***initial flush*** production that occurs early, during the first few years of the life of a well. The absorbed gas volume is often significantly more than the free gas stored in the matrix porosity. Gas contents can exceed apparent free gas-filled porosity by 6 to 8 times where organic content is high (Warlick 2010). However, sorbed gas is produced by diffusion or desorption and does not occur until later in the field life after the reservoir pressure has declined. It is generally accepted that sorbed gas does not have an appreciable effect on shale field economics (because it is not produced early in well life), but sorbed gas can constitute a significant part of GIP in some shale reservoirs. Dissolved gas is only a small part of GIP in most shale reservoirs.

Most shale gas wells produce only dry gas (90% methane) and essentially little water. A notable exception to this is the Eagle Ford where part of the play produces dry gas, part wet gas, and another part produces shale oil. It is understood, based on operator experience, that the emerging Utica shale basin is similar to the Eagle Ford with dry gas, wet gas, and oil areas. The Antrim and New Albany shale do produce formation water. Concerns about water production handling, treating, re-use, or disposal due to flowback water from fracturing is discussed in Chapter 17.

Shale gas and oil wells display a rather unique decline profile character. Shale gas wells typically exhibit gas storage and flow characteristics uniquely tied to geology and physics (Rushing et al. 2008). Initial production rates are relatively low, in the 2-10+ MMcfd range (horizontal wells), and these rates decline rather rapidly.

However, it seems that a well producing around less than 100 Mcfd would be approaching the economic limit. Shale oil wells have exhibited initial productivity rates in the range of 250 to 2,000 BOPD. Some examples of typical decline type curves are shown as **Fig. 3.5** for Barnett shale gas, in **Fig. 3.6** for Eagle Ford shale gas, in **Fig. 3.7** for Bakken shale oil, and in **Fig. 3.8** for Eagle Ford shale oil.

Shale natural gas is either ***biogenic*** in origin, formed by the action of biologic organisms breaking down organic material within the shale, or of ***thermogenic*** origin formed at depth and high temperatures. Relatively few biogenic gas systems are producing economic gas within the United States. The Antrim shale in Michigan is one of those systems. Another is the New Albany shale of Illinois and Indiana. Wells producing from the biogenic Antrim and New Albany shales have relatively low production rates, e.g., 135 Mcfd; however, they will produce for a long time: 20+ years. In many cases large quantities of water are produced before, or as, any gas is produced. Gas production is closely tied to dewatering the system (like coalbed methane) to gain economic production. Geochemistrical analysis indicates that the water is usually fairly fresh.

The majority of producing shale gas reservoirs in the US are thermogenic systems. Thermogenic gas occurs as a result of primary thermal cracking of the organic matter into a gaseous phase. Secondary thermal cracking of remaining liquids also occurs. Thermal maturity in these reservoirs determines the type of hydrocarbon that will be generated. Gas produced in a thermogenic environment will be relatively dry (Economides and Martin 2007). Reservoir pressure is one of the key parameters to how well conventional gas (and oil) reservoirs perform. Pressure controls production rates and is used along with boundary conditions to predict recovery. Shale reservoirs range from normally pressured to highly overpressured. The higher pressured shale reservoirs, like the Haynesville, have higher initial production (IP) and higher recovery than others. Higher reservoir pressures do have an effect on the hydraulic fracturing designs; especially selection of appropriate proppants, as higher reservoir pressure can crush some types of proppants.

Depositional environment of shale is important, particularly whether it is marine or non-marine. Marine-deposited shale tends to have lower clay content and be high in brittle materials, such as quartz, feldspar, and carbonates. Because of

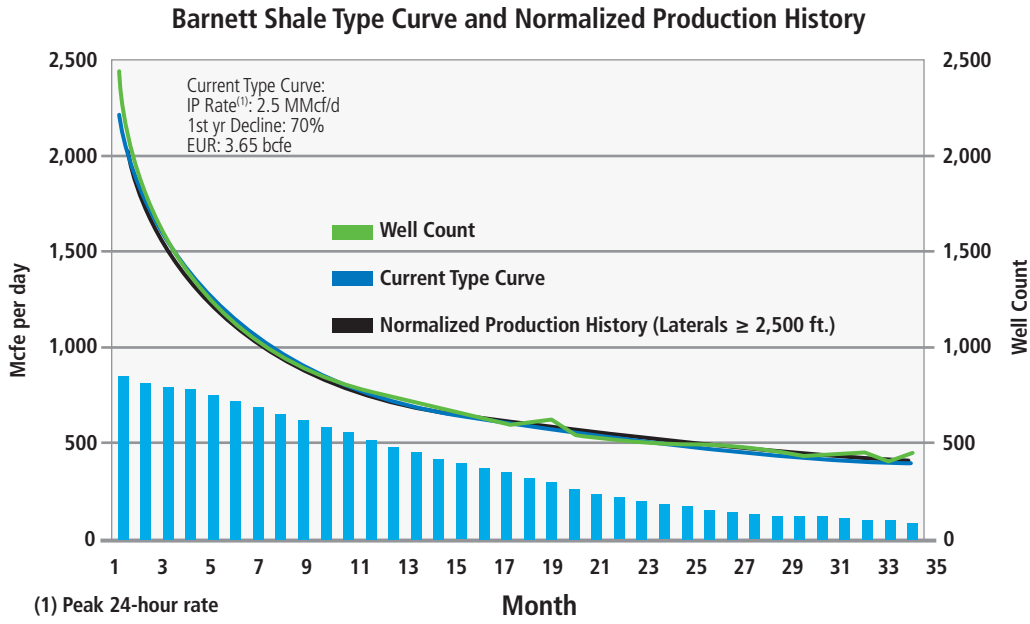

Fig. 3.5—Barnett shale gas. (From EIA 2011.)

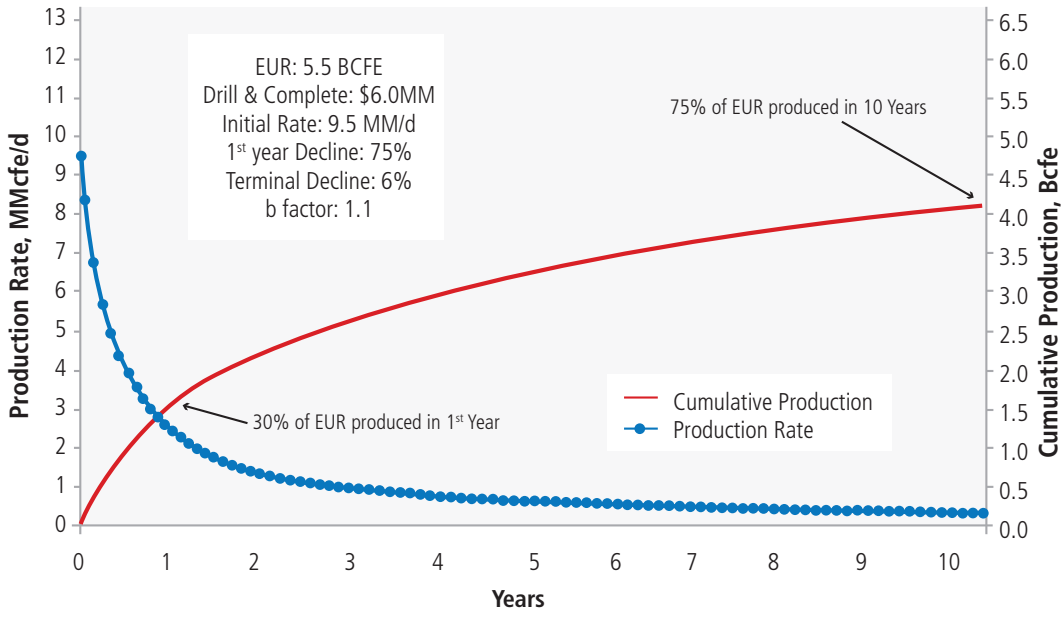

Fig. 3.6—Eagle Ford shale gas. (From EIA 2011.)

this mineralogy, marine-deposited shales respond favorably to hydraulic fracturing. Non-marine deposited shale, i.e., lacustrine and fluvial, tend to be higher in clay, more ductile, and less responsive to hydraulic fracturing. Transgressive systems (also called onlap systems, due to a transgression) are characterized by higher TOC and quartz and less clay. Shale deposited during transgressive systems not only responds favorably to hydraulic fracturing, but also can have higher hydrocarbon recoveries. Alternatively, regressive systems are characterized by lower TOC and quartz and higher clay content. Shales deposited during regression are less responsive to hydraulic fracturing and have lower hydrocarbon recoveries. Thus, depositional environment for shale can be important along with thickness and reservoir pressure.

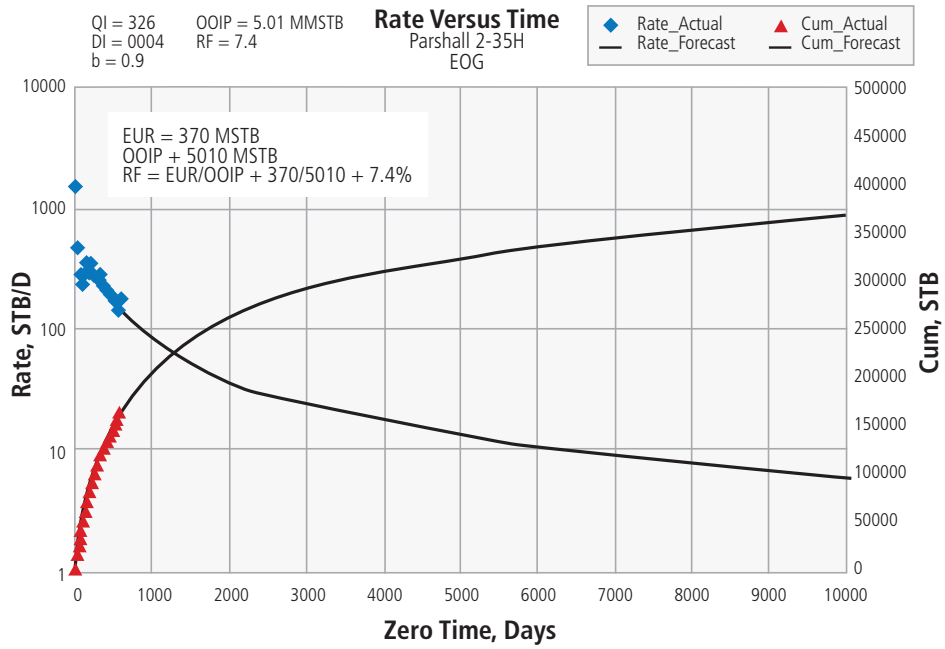

Fig. 3.7—Bakken shale oil. (From Aaron 2009.)

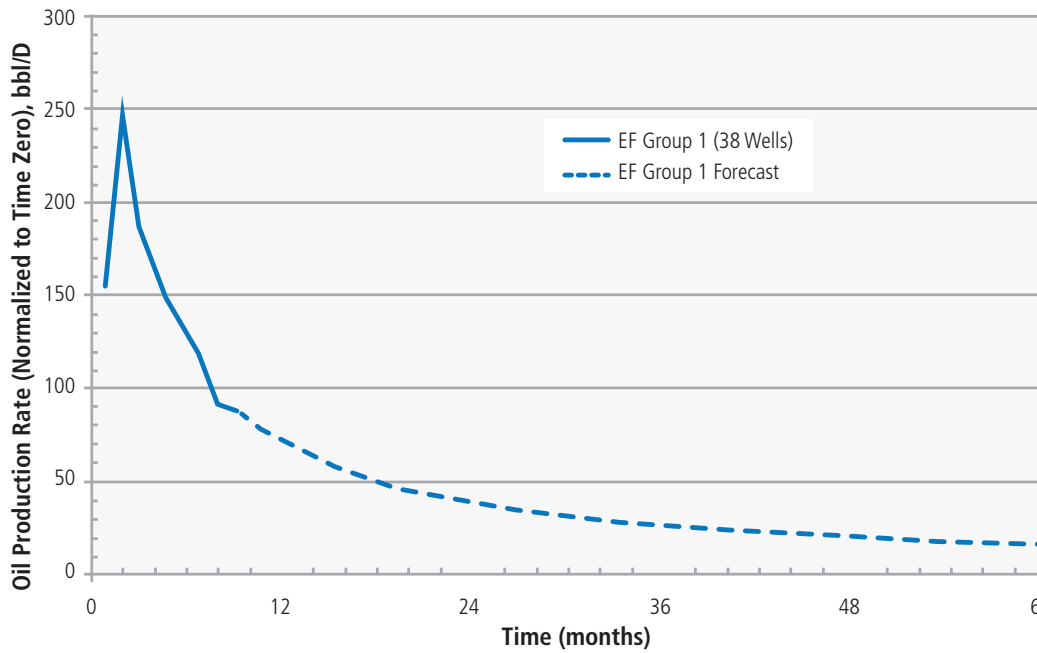

Fig. 3.8—Eagle Ford shale oil. (From Martin et al. 2011.)

3.5 Specific Considerations for Tight Oil and Gas

"In the 1970s the US government decided that the definition of a tight gas reservoir is one in which the expected value of permeability to gas flow would be less than 0.1 md. This definition was a political definition that has been used to determine which wells would receive federal and/or state tax credits for producing gas from tight reservoirs," (Holditch 2006). Holditch wrote that the tight gas definition is a function of a number of physical and economic factors.

Another definition of a tight gas reservoir is "a reservoir that cannot be produced at economic flow rates nor

recover economic volumes of natural gas unless the well is stimulated by a large hydraulic fracture treatment or produced by the use of a horizontal wellbore or multilateral wellbores," (Holditch 2006; Shrivastava and Lusatia 2011). Other authors say that flow rate—rather than permeability—should be the measure of what is termed a tight gas reservoir. Certainly that approach has merit, since some reservoirs with 10+md permeability are being fractured and the flow rate is being increased.

There are no "typical" tight oil and gas reservoirs. They can be:

- Deep or shallow
- High-pressure or low-pressure
- High-temperature or low-temperature
- Blanket or lenticular
- Stratigraphic, structural, and channel-influenced
- Homogeneous or naturally fractured
- Single layer or multiple layers
- Sandstone or carbonate
- Shale oil and gas—at times defined as tight oil and gas

Additionally, coal seam gas (CSG)—also referred to as coalbed methane—can be included in this category.

Unlike shale gas and coalbed methane, the hydrocarbons found in tight reservoirs are sourced in another formation, migrate, and then are trapped (like conventional gas) in the formation where they are found. Discrete gas and water contacts are usually absent, but wells may produce water. Microscopic study of pore and permeability relationships indicates the existence of two varieties of tight oil and gas reservoirs. One variety is ***tight*** because of the fine grain size of the rock. The second variety is ***tight*** because the rock is relatively tightly cemented, diagnetically altered, and has pores that are poorly connected by small pore throats and capillaries. What have we learned about the tight oil and gas development in the US? Based on our observations and available statistics from a number of sources, the following conclusions can be drawn and information gathered:

- Tight gas wells must be fracture-stimulated to produce commercially.
- Average well spacing is now (following several field development iterations) 5 to 10 acres in the lenticular formations (Pinedale Anticline, and Piceance).
- Formation thickness ranges from 600 to 6,000 ft.
- Formation depth ranges from 4,700 to 20,000 ft.
- Multiwells pads contain wells that are S-shaped, directional, or vertical (Pinedale Anticline and Piceance).
- Some wells are horizontal and multilateral (Texas Panhandle, Anadarko basin).
- Well IPs range from < 3 to 20 MMcfd.
- Production is dry gas, wet gas, and water.
- Tight gas formations producing water require deliquification (also called dewatering), in particular for coalbed methane.
- Wells exhibit high decline rates in the first few years of production.
- A high number of wells are required to develop shale (low per well EUR).

The four tight gas basins that produce most of the US tight gas are the Pinedale Anticline, Anadarko, Piceance, and Deep Bossier. Step-by-step procedures to effectively develop these tight oil and gas fields have been documented by Ahmed and Jones (1981); Abou-Sayed and Ahmed (1984); Ahmed and Cannon (1985). **Table 3.3** is a comparison of these US tight gas basins.

All tight wells, gas in particular, display the unique decline curve profile similar to shale but not as drastic. **Fig. 3.9** shows several modeled production profiles of various tight gas well scenarios compared to the profile for a conventional gas well plotted from actual measurements obtained from a productive field. Plots show that the initial rates and EUR per well are significantly less than those for conventional gas wells.

Table 3.3—Comparison of the four significant US tight basins. (Source from Warlick 2010.)

BASIN	Depth, ft.	Thickness, ft.	IP, MMcfd	EUR/Well, Bcf	Production	Well Spacing, ac	Formation	Well Cost, $MM	TRR, Tcf
Pinedale Anticline	7,000–14,000	5,000–6,000	9	6.5	Gas + Water	5	Lenticular, Stacked	3	73
Piceance	6,500–9,000	1,500–4,500	3	3–8	Dry Gas + Water	10 (fr 160)	Lenticular, Stacked	1.5–4.0	7
Anadarko	4,700–13,000	3,500–3,600	10–15	7.0	Wet Gas	80	Granite Washes	7.0–8.5	6
Deep Bossier	16,300	600	15–20	1.5–2.0	Dry Gas, No Water	20	Lenticular	7.6–11.0	6

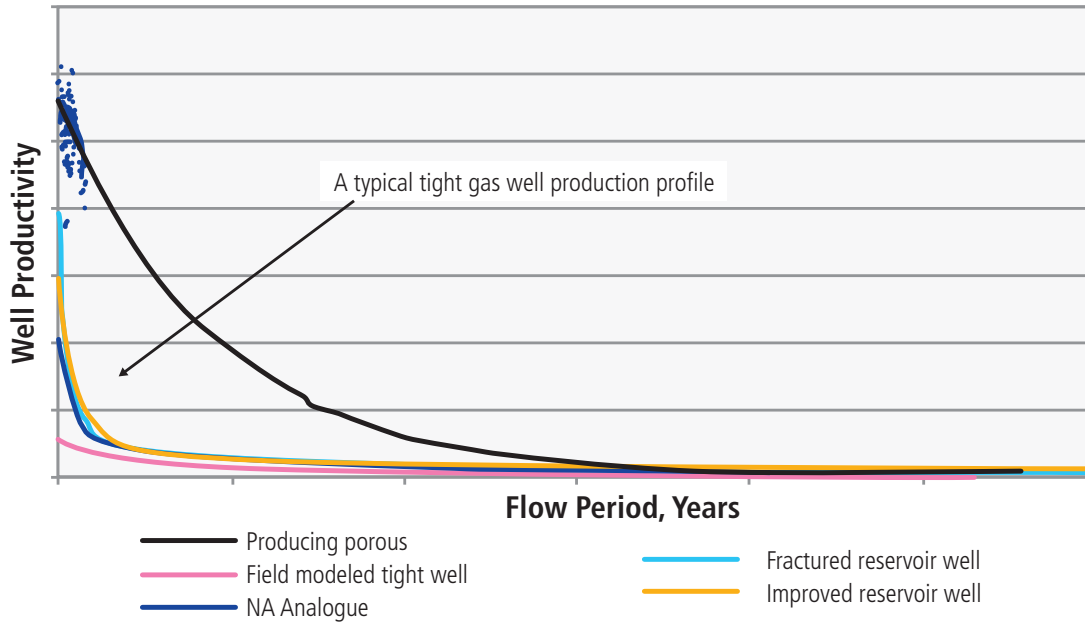

Fig. 3.9—Modeled typical tight gas production profiles compare to a conventional gas well. (Al Kindi et al. 2011.)

3.6 Specific Considerations for Coalbed Methane

The flow and production mechanism within coalbed methane has more similarity to shale oil and gas than to the production of oil or gas associated with tight sedimentary rocks. The initial flow is dictated by the stored gas and water in the fracture network (both the orthogonal butt and face cleats as illustrated in **Fig. 3.10**). Subsequent long-term production is controlled by desorption of the gas from the coal matrix as reservoir pressure drops due to long-term water production.

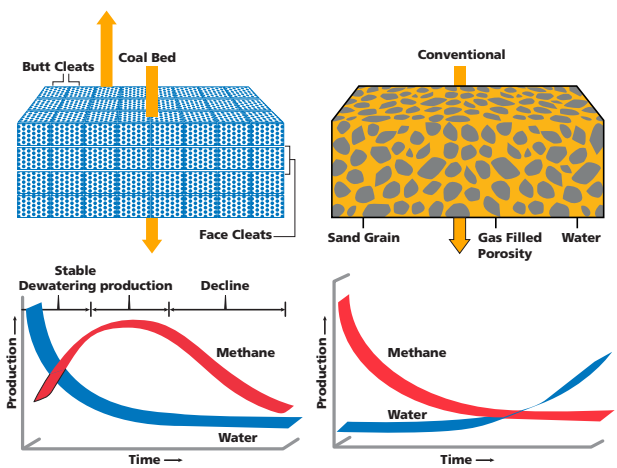

Fig. 3.10 —The flow channels (cleat system) and the production mechanism via dewatering. (From Brown 2002.)

The rate of desorption on the other hand is controlled by macerals (the microscopically recognizable components of coal, analogous to minerals in inorganic rocks), which, in turn, can define the percentage of vitrinite. Vitrinite reflectance values indicate when the coal has reached the gas-generating phase (**Fig. 3.11**), and a rank of class A, a high-volatile bituminous coal (**Table 3.4** for coal rank classes).

Other relevant parameters for further detailed understanding include *cation exchange capacity* (to detect and quantify hydratable clay fractions), *petrographic analysis* (to define pore or flow that channels like the butt and face cleats) and *geophysical logging* (to measure in-situ inferences) allow the estimation of almost all the above parameters in italics as discussed in detail by Ahmed and Newberry (1988). **Fig. 3.12** illustrates a desorption isotherm suggesting the potential production rate and ultimate recovery over a certain pressure and temperature regime while **Fig. 3.13** illustrates the various items that define the adsorption Isotherm (the amount of gas that the coal in question can adsorb as stored methane gas.

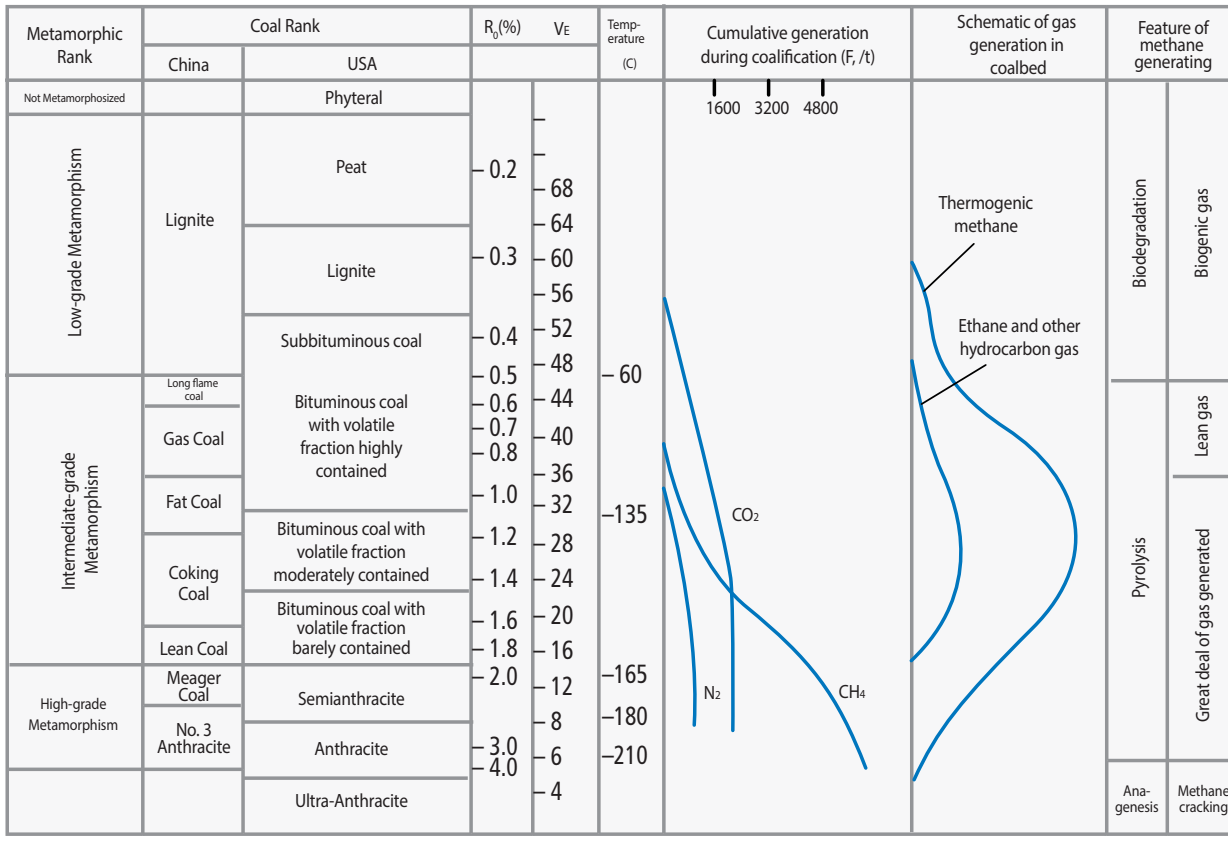

Fig. 3.11—Coal rank and hydrocarbon generation potential (after Qin and Zeng 1995 in Unconventional Petroleum Geology).

Table 3.4—Vitrinite reflectance limits (in oil) and A, S, T, and M coal rank classes.

Rank	Maximum Reflectance %
Sub-Bituminous	Less than 0.47
High Volatile Bituminous C	0.47-0.57
High Volatile Bituminous B	.057-0.71
High Volatile Bituminous A	0.71-1.10
Medium Volatile Bituminous	1.10-1.50
Low Volatile Bituminous	1.50-2.05
Semi-Anthracite	2.05-3.00 (approx.)
Anthracite	Greater than 3.00

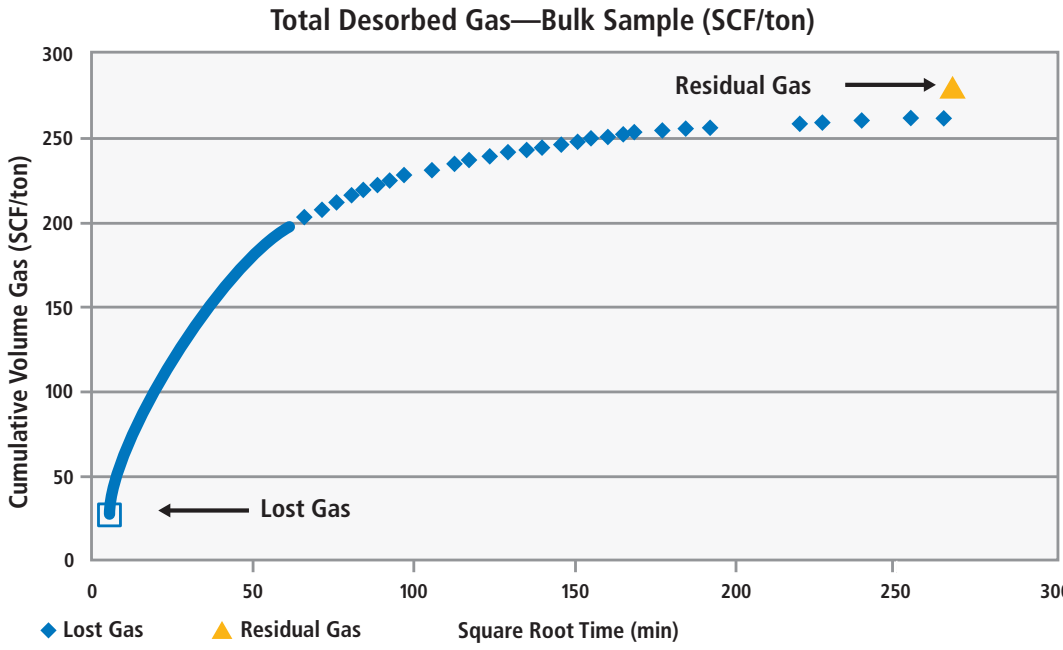

Fig. 3.12—Example of a desorption isotherm as measured in the laboratory environment. (From Waechter et al. 2004.)

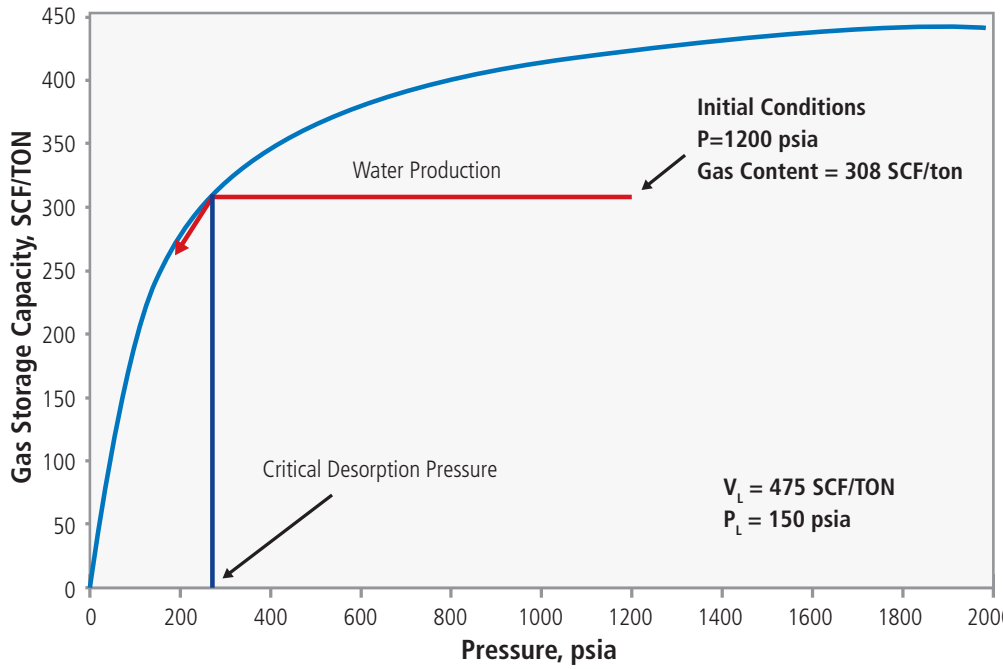

Fig 3.13—A typical adsorbtion isotherm. (From Aminian, West Virginia University.)

3.7 References

Aaron, J.C. 2009. Determination of Recovery Factor in the Bakken Formation, Mountrail County, ND. Paper SPE 133719 presented at the SPE Annual Technical Conference and Exhibition. New Orleans, Louisiana. 4–7 October. http://dx.doi.org/10.2118/133719-STU.

Abou-Sayed A., Ahmed U., and Jones, A. 1982. A Step-by-Step Procedure to Hydraulic Fracture Treatment Design, Implementation and Analysis for Tight Gas Sands. Paper SPE 10829 presented at the SPE Unconventional Gas Recovery Symposium. Pittsburgh, Pennsylvania. 16–18 May. http://dx.doi.org/10.2118/10829-MS.

Addis, M.A. and Yassir, M., 2010. An Overview of Geomechanical Engineering Aspects of Tight Gas Sand Developments, Paper SPE 136919, presented at the 2010 SPE/DGS Annual Technical Symposium and Exhibition. Al-Khabor, Saudi Arabia. 4–7 April.

Ahmed, U. 2014. Optimized Shale Resource Development: Balance between Technology and Economic Considerations. Paper SPE 169984 presented at the SPE Energy Resources Conference. Trinidad and Tobago. 9–11 June. http://dx.doi.org/10.2118/169984-MS.

Ahmed, U., Abou-Sayed, A., and Jones, A. 1981. Systematic Approach to Massive Hydraulic Fracture Treatment Design. Society of Petroleum Engineers, DOE.

Ahmed, U., Johnston, D., and Colson, L. 1991. An Advanced and Integrated Approach to Coal Formation Evaluation. Paper SPE Paper 22736 presented at the SPE Annual Technical Conference and Exhibition. Dallas, Texas. 6–9 October. http://dx.doi.org/10.2118/22736-MS.

Ahmed, U., Newberry, B., and Cannon, D. 1985. Hydraulic Fracture Treatment Design of Wells with Multiple Zones. Paper SPE 13857 presented at the SPE/DOE Low Permeability Gas Reservoirs Symposium. Denver, Colorado. 19–22 March. http://dx.doi.org/10.2118/13857-MS.

Ahmed, U., Schatz, J.F., Holland, M.T., et al. 1982. State-of-the-Art Hydraulic Fracture Stimulation Treatment for Western Tight Sand Reservoir. Paper SPE 11184 presented at the SPE Annual Technical Conference and Exhibition. New Orleans, Louisiana. 26–29 September. http://dx.doi.org/10.2118/11184-MS.

Al Kindi, S., Weissenback, M., Mahruqi, S., et al. 2011. Appraisal Strategy for a Tight Gas Discovery. Paper SPE 142735 presented at the SPE Middle East Unconventional Gas Conference and Exhibition. Muscat, Oman. 30 January–2 February. http://dx.doi.org/10.2118/142735-MS.

Aminian, K. 2007. Coalbed Methane–Fundamental Concepts, West Virginia University, WVU edu publishers.

Brown, A.C. F.R.S. 1906. The Oil Shales of the Lothians. In Memoirs of the Geological Society, Scotland, 2nd edition. In Crain, E.R. ***Crain's Petrophysical Handbook***, http://spec2000.net/17-speccbm.htm (accessed August 2014).

Brown, W.T. 2002. Developing CBM in the Powder River Basin. In proceedings, Coalbed Methane Development in the Intermountain West, Natural Resources Law Center at the University of Colorado School of Law.

Cainneng, Z. 2012. Unconventional Petroleum Geology. Elsevier.

Economides, M.J. and Martin, T., 2007. Modern Fracturing Enhancing Natural Gas Production, BJ Services Company: Houston, Texas, 2007.

EIA—Energy Information Administration, 2011. Review of Emerging Resources: U.S. Shale Gas and Shale Oil Plays, prepared by INTEK Inc. for the EIA, U.S. Department of Energy, Washington, DC. http://www.eia.gov/analysis/studies/usshalegas/pdf/usshaleplays.pdf (accessed August 2014).

Gray, J. K. 1977. Future Gas Reserve Potential Western Canadian Sedimentary Basin: 3d Natl. Tech. Conf. Canadian Gas Assoc.

Holditch, S.A. 2006. Tight gas sands. ***J Pet Tech***, **58** (6): 86–93. SPE 103356-JPT. http://dx.doi.org/10.2118/103356-JPT.

Holditch, S.A. 2011. Unconventional Oil and Gas go for the Source, presentation, Texas A&M University, http://energyengineering.org/media/73700/stephen%20holditch%20unconventional%20oil%20and%20gas%20go%20for%20the%20source_eei.pdf (accessed August 2014).

King, G.E. 2010. Thirty Years of Gas Shale Fracturing: What Have We learned? Paper SPE 133456 presented at the SPE Annual Technical Conference and Exhibition. Florence, Italy. 19–22 September. http://dx.doi.org/10.2118/133456-MS.

Jarvie, D.M., Hill, R.J., Ruble, T.E., and Pollastro, R.M., 2007. Unconventional Shale Gas Systems: The Mississippian Barnett Shale of North-Central Texas as One Model for Thermogenic Shale-Gas Assessment, the American Association of Petroleum Geologists, *AAPG Bulletin*, **91** (4): 475–499.

Jacobi, D., Breig, J., LeCompte, B., et al. 2009. Effective Geochemical and Geomechanical Characteristics of Shale Gas Reservoirs from the Wellbore Environment: Caney and Woodford Shale. Paper SPE 124231 presented at the SPE Annual Technical Conference and Exhibition. New Orleans, Louisiana. 4–7 October. http://dx.doi.org/10.2118/124231-MS.

Jenkins, C.D. and Boyer, C.M. 2008. Coalbed- and Shale-Gas Reservoirs *J Pet Tech*, **60** (2): 92–99. SPE 103514-PA. http://dx.doi.org/10.2118/103514-PA.

Kennedy, R.L., Knecht, W.N., and Georgi. D.T. 2012. Comparison and Contrasts of Shale Gas and Tight Gas Development, North American Experience and Trends. Paper SPE 160855 presented at the SPE Saudi Arabia Section Technical Symposium and Exhibition. Al-Khobar, Saudi Arabia. 8–11 April. http://dx.doi.org/10.2118/160855-MS.

Kuuskraa, V., Stevens, S., Van Leeuwen, T., et al. 2011. World Shale Gas Resources: An Initial Assessment of 14 Regions Outside the United States, prepared by Advanced Resources International Inc. (February 17, 2011) for the U.S. Energy Information Administration, U.S. Department of Energy, Washington, DC (April 2011).

LeCompte, B., Franquet, J.A., and Jacobi, D. 2009. Evaluation of Haynesville Shale Vertical Well Completions with a Mineralogy Based Approach to Reservoir Geomechanics. Paper SPE 124227 presented at SPE Annual Technical Conference and Exhibition. New Orleans, Louisiana. 4–7 October. http://dx.doi.org/10.2118/124227-MS.

Martin, R., Baihly, J.D., Malpani. R., et al. 2011. Understanding Production from Eagle Ford-Austin Chalk System. Paper SPE 145117 presented at the SPE Annual Technical Conference and Exhibition. Denver, Colorado. 30 October–2 November. http://dx.doi.org/10.2118/145117-MS.

Martin, S.O., Holditch, S.A., Ayers, W.B., et al. 2008. PRISE: Petroleum Resource Investigation Summary and Evaluation. Paper SPE 117703 presented at the SPE Eastern Regional/ AAPG Eastern Section Joint Meeting. Pittsburgh, Pennsylvania. 11–15 October. http://dx.doi.org/10.2118/117703-MS.

Masters, J. A. 1979. Deep Basin Gas Trap, Western Canada. *AAPG Bulletin*, **63** (2): 152.

Mitra, A., Warington, D., and Sommer, A. 2010. Application of Lithofacies Models to Characterize Unconventional Shale Gas Reservoirs and Identify Optimal Completion Intervals Paper SPE 132513 presented at the SPE Western Regional Meeting. Anaheim, California. 27–29 May. http://dx.doi.org/10.2118/132513-MS.

Nome, S. and Jonston, P. 2008. From Shale to Shining Shale: A Primer on North American Shale Gas Plays, Deutsch Bank (July 22, 2008), http://www.renewwisconsin.org/pdf/shaletoshiningshale.pdf (accessed August 2014).

Passey, Q.R., Bohacs, K.M., Esch, W.L., et al. 2010. From Oil-Prone Source Rock to Gas-Producing Shale Reservoir–Geologic and Petrophysical Characterization of Unconventional Shale Gas Reservoirs. Paper SPE131350 presented at CPS/SPE International Oil & Gas Conference Exhibition. Beijing, China. 8–10 June. http://dx.doi.org/10.2118/131350-MS.

Pemper, R., Han, X., Mendez, F., et al. 2009. The Direct Measurement of Carbon in Wells Containing Oil and Natural Gas Using Pulsed Neutron Mineralogy Tool. Paper SPE 124234 presented at SPE Annual Technical Conference and Exhibition. New Orleans, Louisiana. 4–7 October. http://dx.doi.org/10.2118/124234-MS.

Petroleum Exploration Society of Great Britain. 2008. Exploration and Production in a Mature Basin: North Sea Petroleum Geology, presentation, Aberdeen, Scotland, April.

Qin, Y. and Zeng, Y. 1995. Evaluation of Coalbed Methane Reservoirs and Production Technology (in Chinese). China University of Mining and Engineering Press: Xuzhou.

Rushing, J.A., Newsham, K.E., and Blasingame, T.A. 2008. Rock Typing—Keys to understanding Productivity in Tight Gas Sands. Paper SPE 114164, presented at the SPE Unconventional Reservoirs Conference. Keystone, Colorado. 10–12 February. http://dx.doi.org/10.2118/114164-MS.

Shrivastava, C. and Lawatia, R. 2011. Tight Gas Reservoirs: Geological Evaluation of the Building Blocks Paper SPE 142713 presented at the SPE Middle East Unconventional Gas Conference, and Exhibition. Muscat, Oman. 31 January–2 February. http://dx.doi.org/10.2118/142713-MS.

Society of Petroleum Evaluation Engineers, Monograph 3, 2011. Guidelines for the Evaluation of Resource Plays.

USGS, Unconventional (Continuous) Petroleum Sources, http://energy.cr.usgs.gov/oilgas/addoilgas/unconventional.html (accessed August 2014).

U.S. Department of Energy, 2009. Modern shale gas development in the United States: A primer. Prepared by Ground Water Protection Council and ALL Consulting, Inc., for the U.S. Department of Energy, Office of Fossil Energy and National Energy Technology Laboratory, 2009,Tulsa, Oklahoma. http://energy.gov/sites/prod/files/2013/03/f0/ShaleGasPrimer_Online_4-2009.pdf (accessed August 2014).

Vassilellis, G.D., Li, C., Bust, V.K., et al. 2011. Shale Engineering Application: The MAL-145 Project in West Virginia, Paper CSUG and SPE 146912 presented at the Canadian Unconventional Resources Conference, Calgary, Alberta, Canada. 15–17 November. http://dx.doi.org/10.2118/146912-MS.

Waechter, N.B., Hampton, G.L., and Ships, J.C. 2004. Overview of Coal and Shale Gas Measurement: Field and Laboratory Procedures. ***Proceedings of the 2004 International Coalbed Methane Symposium***, May 2004, Alabama.

Warlick International. 2010. Warlick International, North American Unconventional Gas Market Report 2010, Edition 1 of 2, http://www.scribd.com/doc/20603184/Unconventional-Gas-Report-Edition-1-Special-Sample (accessed August 2014).

This page intentionally left blank

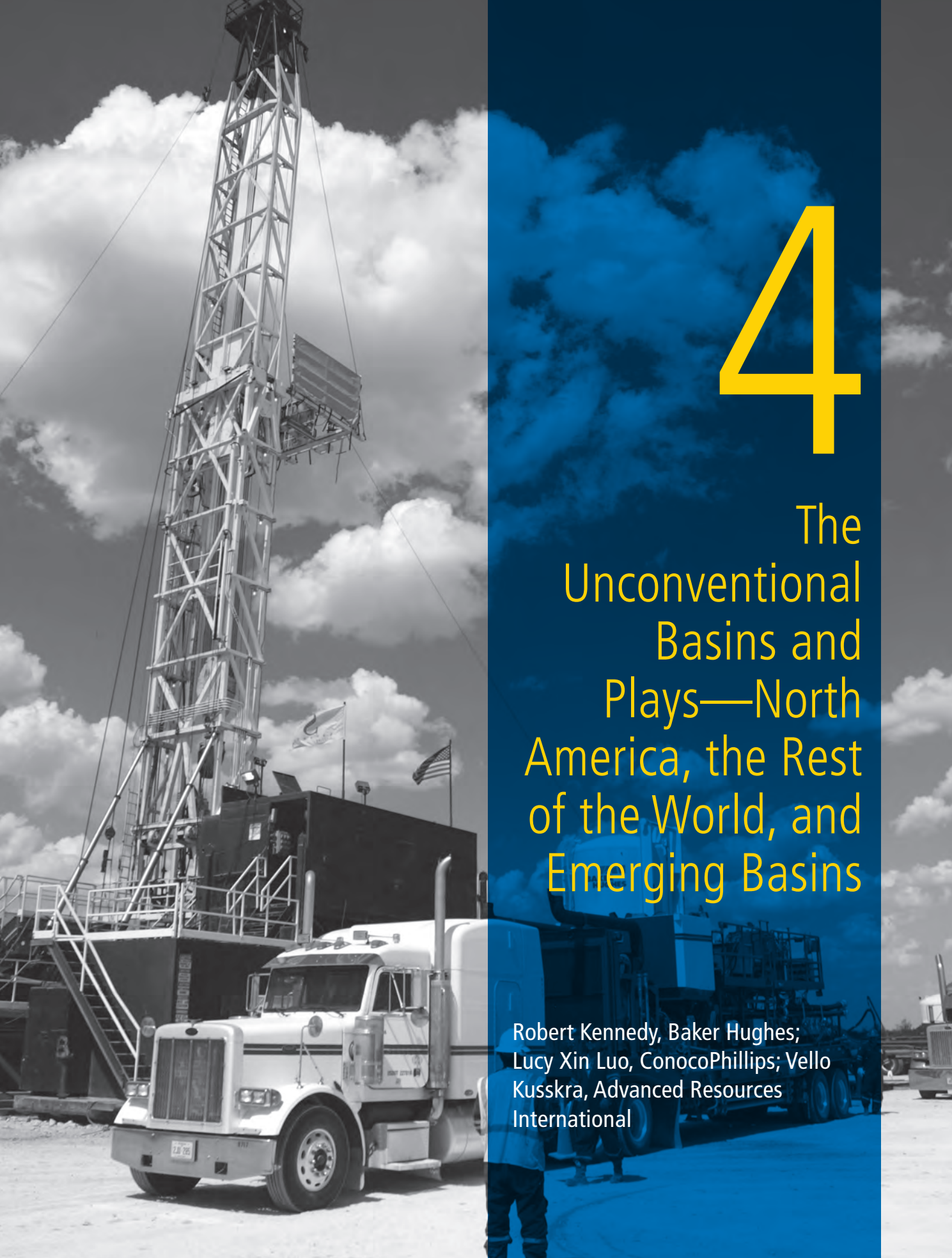

4

The Unconventional Basins and Plays—North America, the Rest of the World, and Emerging Basins

Robert Kennedy, Baker Hughes; Lucy Xin Luo, ConocoPhillips; Vello Kusskra, Advanced Resources International

This page intentionally left blank

Chapter 4:
The Unconventional Basins—North America, the Rest of the World, and Emerging Basins

4.1 Introduction

According to the US Energy Information Administration (EIA) Report (2013), 7,299 trillion cubic feet (Tcf) of shale gas technically recoverable resources (TRR) and 345 billion barrels (bbl) of shale oil TRR exist in the world. The EIA covered the most prospective shale formations in 41 countries that demonstrated some level of relatively near-term promise and that had a sufficient amount of geologic data for a resource assessment (**Fig. 4.1**).

In Fig. 4.1, the red areas represent the basins with shale formations for which estimates of natural gas in-place and technically recovered resources were provided. The tan areas represent the basins that were reviewed but shale resource estimates were not provided because of lack of data necessary to conduct an assessment. The white areas were not assessed, and include significant omissions, including Saudi Arabia.

Using data from the EIA Report, we constructed the bar chart; **Fig. 4.2** shows the top ten countries with shale gas TRR. **Fig. 4.3** shows the top ten countries with shale oil TRR (EIA 2013).

Fig. 4.2 was created using data from the EIA report and shows the top 10 countries with shale gas TRR. Fig. 4.3 shows the top 10 countries with shale oil TRR.

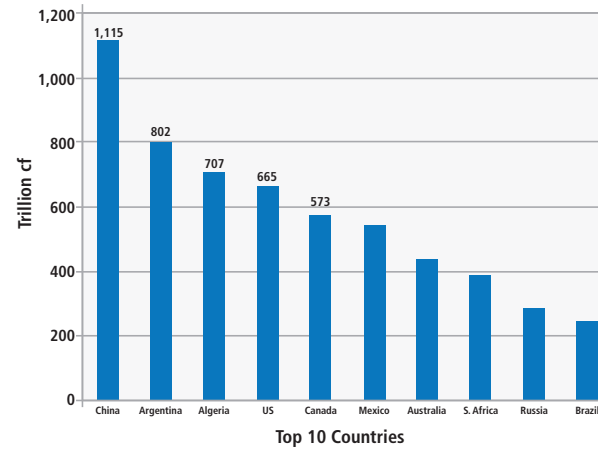

Fig. 4.2—World shale gas TRR, Tcf. (Source: EIA Report 2013.)

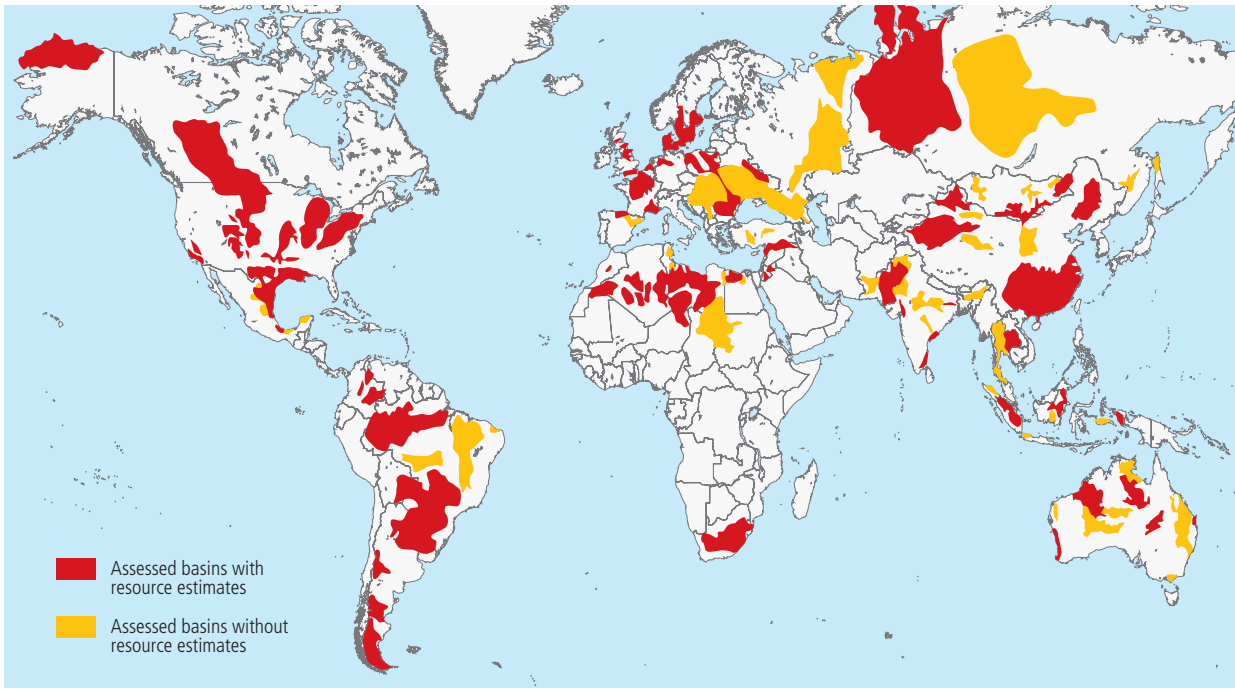

Fig. 4.1—Map of basins with assessed shale oil and shale gas formations as of May 2013. (Source for US basin: EIA Report 2013; other basins: ARI 2013.)

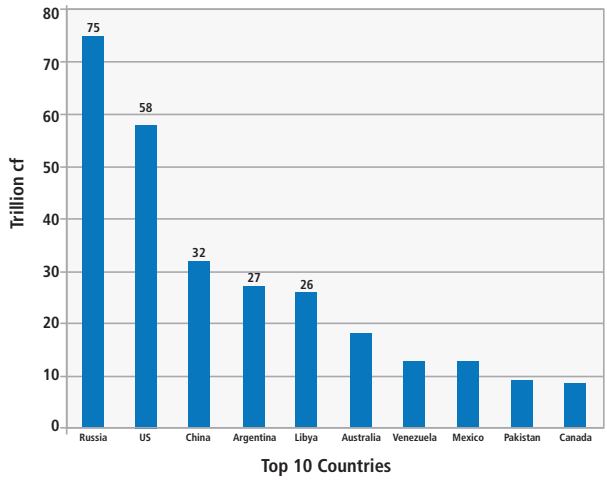

Fig. 4.3—World shale oil TRR, bbl. (Source: EIA Report 2013.)

4.2 US Shale Gas, Oil Plays, and Basins

Approximately 180,000 producing shale wells exist in the US, and 18,000 new wells are drilled each year (Drilling Information Database 2014). Currently, in the US 665 Tcf of technically recoverable resources shale gas and 58 bbl of TRR shale oil exist. In this book, the six major shale gas and the six major shale oil plays in the US are discussed in detail (**Fig. 4.4**). Three major shale plays in Canada and major shale oil and shale gas basins in the rest of the world will be briefly covered.

Table 4.1, a listing of the US shale and play well counts (oil and gas) and rig counts (oil and gas directed), is a summary and reflects information available as of end 3Q14. Data on some plots shown later in this chapter will not necessarily agree, as they were prepared earlier in 2014. Source of data in Table 4.1 for well counts is from IHS, and rig counts are from Baker Hughes.

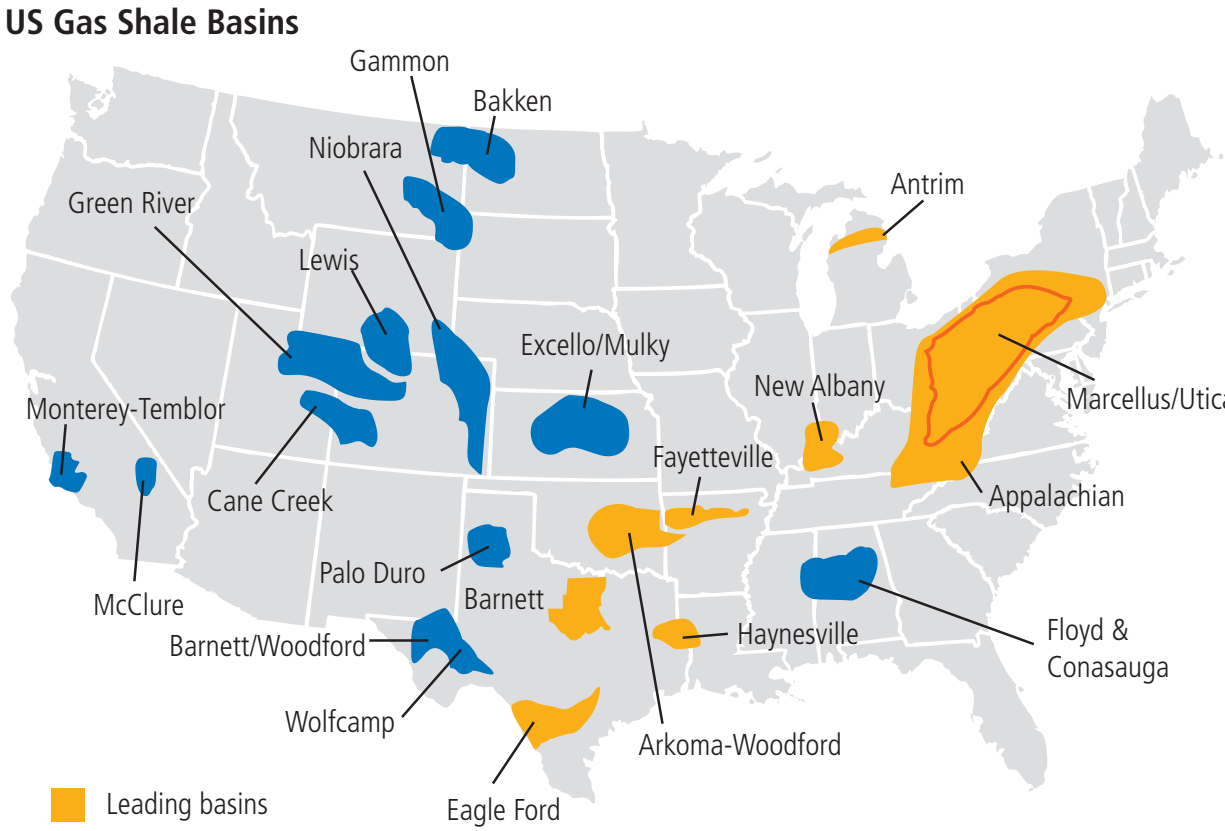

Fig. 4.4—The 23 significant US shale gas basins and plays in the US. (Kennedy et al. 2012; EIA 2012; and Warlick International.)

Table 4.1—US shale play well counts and rigs running.

Shale Play	Vertical Well	Horizontal Wells		Total Wells	Rigs Running	
		Gas	Oil		Gas Dir	Oil Dir
Barnett	5,005	14,199	0	19,204	11	11
Marcellus	2,462	6,999	10	9,471	81	0
Fayetteville	65	5,405	0	5,470	9	0
Woodford	304	1,565	748	2,617	6	6
Haynesville	75	3,278	0	3,353	39	1
Bakken	248	0	10,336	10,584	0	192
Eagle Ford	56	3,487	7,173	10,716	10	206
Niobrara	1,969	0	3,594	5,563	16	46
Utica	107	291	179	577	27	22
Wolfcamp	148	368	2,224	2,606	1	243
Monterey	451 oil	0	29	480	45	0
Total US land rigs running					313	1,539

4.2.1 Barnett Shale

The first modern commercial shale play in the US was the Barnett shale, discovered in 1981 (**Fig. 4.5, Table 4.2**). This Mississippian-age shale was deposited in a deep, NW-SE trending marine basin (Fort Worth basin) and formed as a result of the Ouachita-Marathon orogeny. The areal extent of the resulting productive shale is up to 7,000 square miles with 4,065 square miles currently active. The depth is 6,500 to 8,500 ft. with the gross thickness increasing from 100 to 600 ft. west to east.

Barnett lithology includes two sections, the Upper and Lower Barnett, separated by the Forestburg limestone.
The Lower Barnett is considerably thicker and contributes "about 70 to 80%" of the production in most wells. Overlying the Barnett is the Marble Falls, which is a barrier to hydraulic fractures' growth. The lower Barnett boundary is either the Viola or the Ellenburger limestone. While the Viola can contain good reservoir characteristics, the Ellenburger often contains water. Well trajectories and hydraulic fractures are designed to avoid the Ellenburger. Lithology is a siliceous shale with +/- 40% silica, +/-13% carbonate, and +/-23% clay. This composition makes formation brittle and thus prone to being hydraulically fractured.

Fig. 4.6 shows Barnett shale with vertical wells drilled by Mitchell Exploration and the 30-plus year drilling learning curve. The vertical axis indicates individual well gas production, and the horizontal axis is time. Vertical wells are depicted by blue triangles, horizontal wells by red squares, and deviated wells by green diamonds. Vertical wells were used to develop the Barnett from discovery until 2003. Small energized fractures and cross-linked massive hydraulic fractures were tried in 1983 and 1987, respectively. Slickwater fractures came along in 1995. In 1991 the first horizontal well was drilled; production rate was not any better than from vertical wells. In 1998 the second horizontal well was drilled; again, production was not any better than from vertical wells. In 2003, horizontal wells with multistage hydraulic fracturing unlocked the key to effective Barnett shale development. Some of the horizontal wells, however, are not producing any better than vertical wells. Some operators recognize that individual well productivity depends on reservoir quality along the horizontal lateral and on effective hydraulic fracturing stages. Optimized placement of well and hydraulic fracture stages is being recognized as a key element.

Until 2012 when replaced by the Marcellus, the Barnett shale was the largest onshore shale gas basin in the world

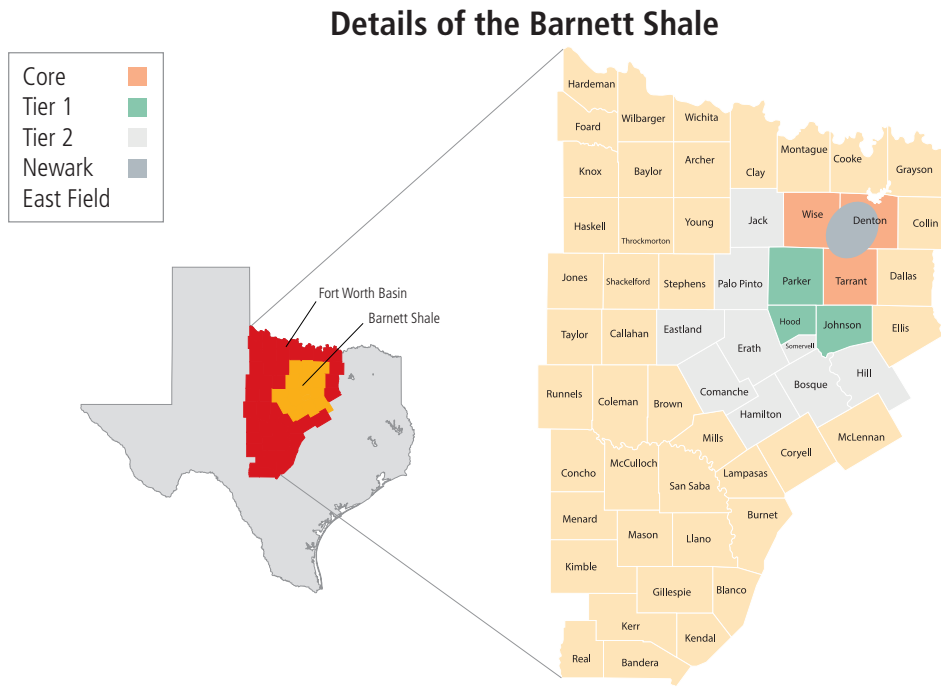

Fig. 4.5—Barnett shale map. (Modified from Warlick International.)

attaining a daily production rate of near 5.6 billion cubic feet per day (Bcfd) (**Fig. 4.7**). More than 15,000 shale wells have been completed in the Barnett. Rig activity has dropped from a high of 80 to the current (2015) 11 gas-directed rigs (Fig. 4.7). This trend is being experienced by all the other US dry gas shale plays. However, 13 oil-directed rigs are working in the Barnett.

The Barnett success established the US model for shale development. The US industry found the key to shale development with a model with two key elements: multistage hydraulic fracturing and horizontal wells (**Fig. 4.8**). This scenario, combined with slickwater fracturing fluid, maximized reservoir contact and allowed induced fracturing to intersect the national formation fractures along the wellbore and away into the reservoir.

4.2.2 Marcellus Shale

After the Barnett, it was not until 2005 when the next commercial shale gas play, the Marcellus (**Fig. 4.9**, **Fig. 4.10**, **Table 4.3**), came on production. The Marcellus, an extensive (95,000 mi^2 area) shale gas play with 410 Tcf of TRR, eclipsed the Barnett and is the largest US onshore shale gas play in the world.

Table 4.2—Barnett shale information. (From various sources.)

Barnett Shale	
Geologic Age	Late Mississippian
Area Size, mi.^{2}	5,400 (4,065 active)
Depth, ft.	6,500–8,500
Thickness, ft.	100–600
TOC, %	4–5
Thermal Maturity, R_0 %	1.3–2.1
Porosity, %	4–8
Well Avg. IP, MMcfd	2.5
Horizontal Lateral, ft.	3,950–4,350
TRR, Tcf	43
EUR/Well, Bcf	1.6
Pressure Gradient, psi/ft	0.43–0.45
Well Spacing, Ac	116
First Production	1981
■ Largest onshore gas shale basin in the world until 2012 ■ Proving ground for shale technology: slickwater fractures	

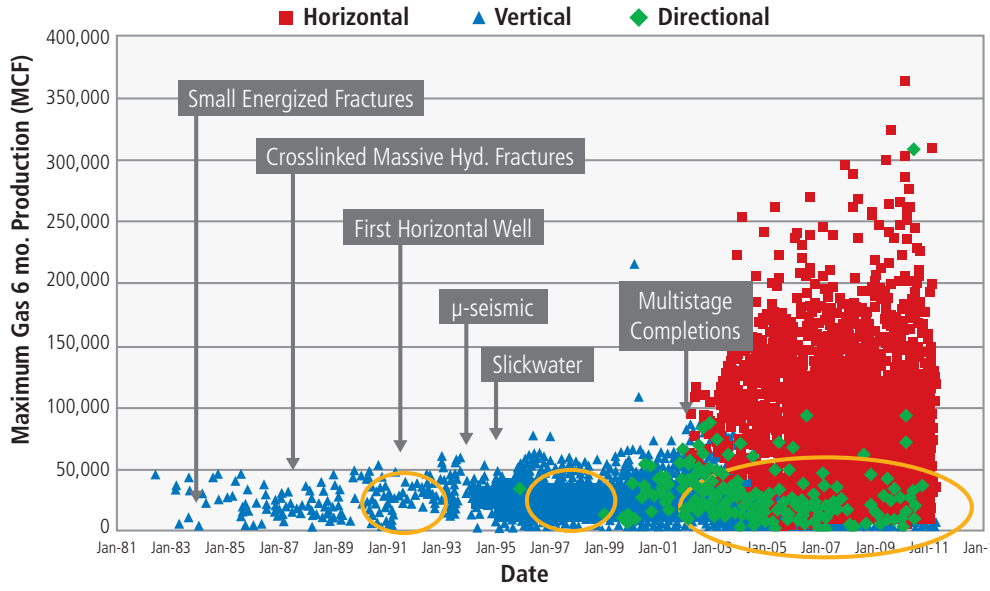

Fig. 4.6—Barnett shale development learning curve. (Modified from LaFollette et al. 2012.)

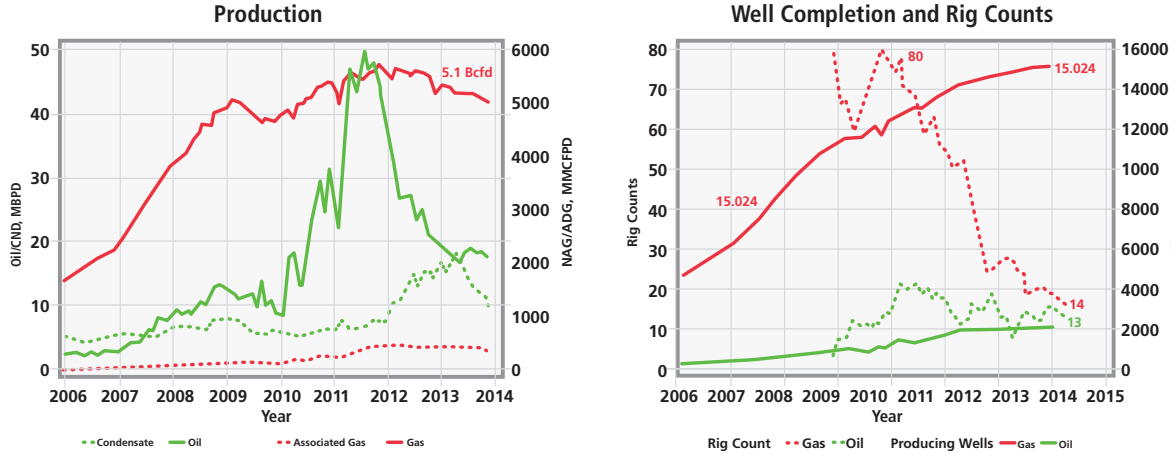

Fig. 4.7—Barnett shale production, wells, and rigs. (Baker Hughes rig counts; Drilling Information Database.)

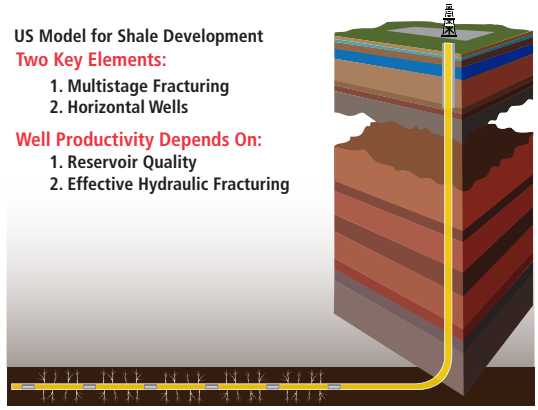

Fig. 4.8—The US model for shale development.

As of 2014, in the Marcellus, 5,400 wells are completed with a total production rate of 10.1 Bcfd (Table 4.3). Approximately 78 gas-directed rigs were running in the Marcellus as of 2014; some areas with wet gas production and the initial production are higher than the Barnett and Fayetteville, and are equal to the Woodford.

The Devonian age shale of the Marcellus was the producing formation of the first natural gas well drilled in the US in 1821. In 1826, the first shale gas well in the US also was drilled in a Devonian age shale, the Dunkirk shale in Fredonia, New York. The Marcellus (Fig. 4.9) extends from its northern extent in west central New York on a northeast southwest trend into Pennsylvania, Ohio, and West Virginia. Smaller parts of the eastern side of shale extend into Maryland and Virginia.

Fig. 4.9—Marcellus shale map. (Warlick International.)

Table 4.3—Marcellus shale information. (From various sources.)

Marcellus Shale	
Geologic Age	Devonian
Area Size, mi.^{2}	95,000
Depth, ft.	4,000–8,500
Thickness, ft.	50–200
TOC, %	2–8
Thermal Maturity, R_0 %	1.3–2.4
Porosity, %	4–8
Well Avg. IP, MMcfd	3.5
Horizontal Lateral, ft.	4,200–4,900
TRR, Tcf	410
EUR/Well, Bcf	4.5
Pressure Gradient, psi/ft.	0.60–0.70
Well Spacing, Ac	80
First Production	2005
■ Extensive play ■ Currently largest US gas resource	

The Marcellus is a highly organic, black shale deposited in a shallow marine environment of the Appalachian basin of the northeast US. Directly overlying the Marcellus is the Middle and Upper Devonian Hamilton Group, a thick section of siltstones and shales that act as a barrier to upper migration of any fluids. Lithology of the Marcellus, which generally is termed a siliceous shale, consists of 10 to 60% silica, 3 to 50% carbonate, and 10 to 35% clay; which makes for a brittle formation prone to hydraulic fracturing.

4.2.3 Fayetteville Shale

In 2006, production began from the Fayetteville (**Fig. 4.11**, **Fig. 4.12**, **Table 4.4**) and the Woodford shale plays. The Fayetteville is a dry gas play similar to the Barnett, but first production was not established until a year after the Marcellus. As rig activity moved toward shale liquid plays, by late 2014, only nine rigs were running, down from the high of 45 rigs (Fig. 4.12).

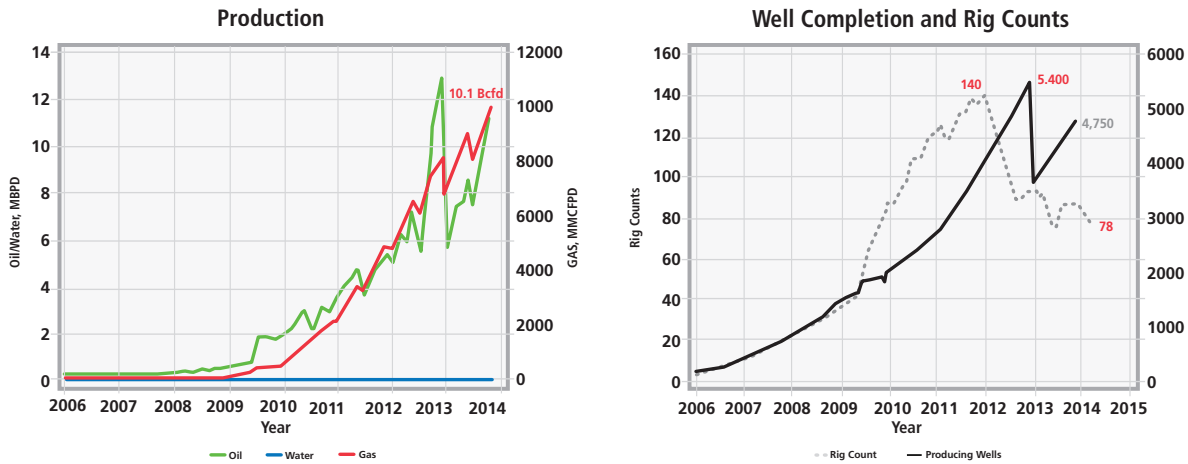

Fig. 4.10—Marcellus shale production, well completion, and rig count. (Sources: Baker Hughes rig counts; Drilling Information Database.)

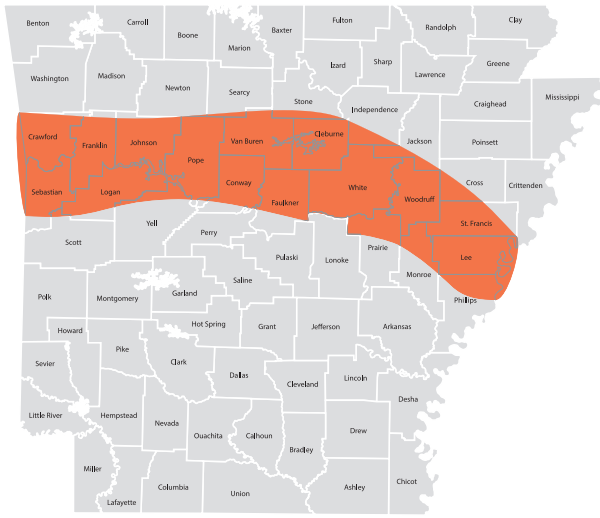

Fig. 4.11—Fayetteville shale map. (Warlick International.)

Table 4.4—Fayetteville shale information. (From various sources.)

Fayetteville Shale	
Geologic Age	Late Mississippian
Area Size, mi.^{2}	9,000
Depth, ft.	1,000–7,000
Thickness, ft.	20–200
TOC, %	4–9.8
Thermal Maturity, R_0 %	1.5–4.0
Porosity, %	4–5
Well Avg. IP, MMcfd	2.8
Horizontal Lateral, ft.	4,700–5,500
TRR, Tcf	32
EUR/Well, Bcf	2.1
Pressure Gradient, psi/ft	0.38–0.45
Well Spacing, Ac	80
First Production	2006
■ First land grab after the Barnett was proven	

The Fayetteville shale is a black, organic-rich rock of Mississippian age that underlies much of northern Arkansas. It is located on the Arkansas side of the Arkoma basin. The Fayetteville is geologically equivalent to the Barnett shale characteristics. Lithology of the Fayetteville is termed as siliceous shale, consisting of 20 to 60% silica, with very little carbonate and clay. This makes for a fairly brittle formation prone to hydraulic fracture treatment.

4.2.4 Woodford Shale

The Woodford shale (**Fig. 4.13, Table 4.5**) is not a typical dry gas play as it has some liquids. It sits in southeastern Oklahoma and western Arkansas in the complex formations of the Ardmore and Arkoma basins. The Woodford is present in the Permian Basin of west Texas and southeastern New Mexico. In western Kansas the

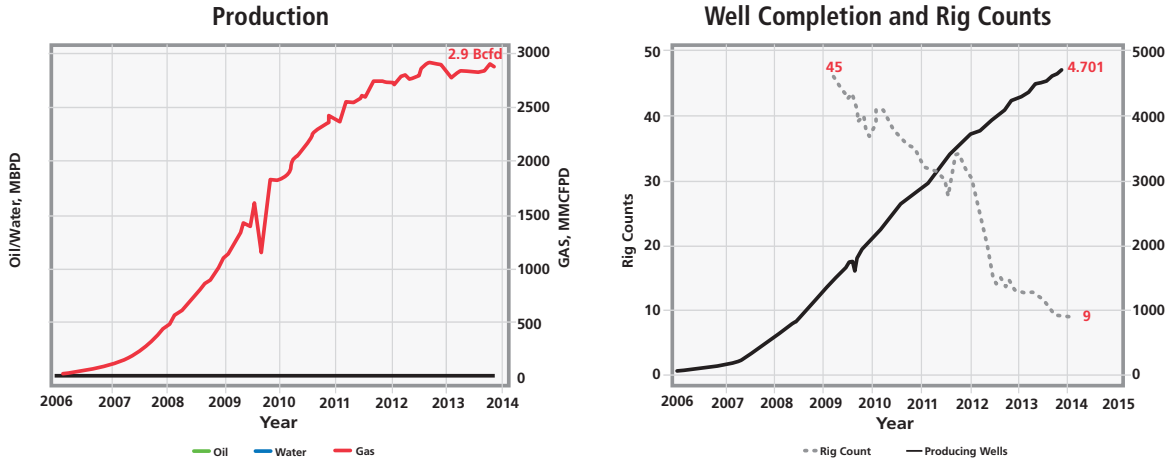

Fig. 4.12—Fayetteville shale production, well completion, and rig count. (Sources: Baker Hughes rig counts; Drilling Information Database.)

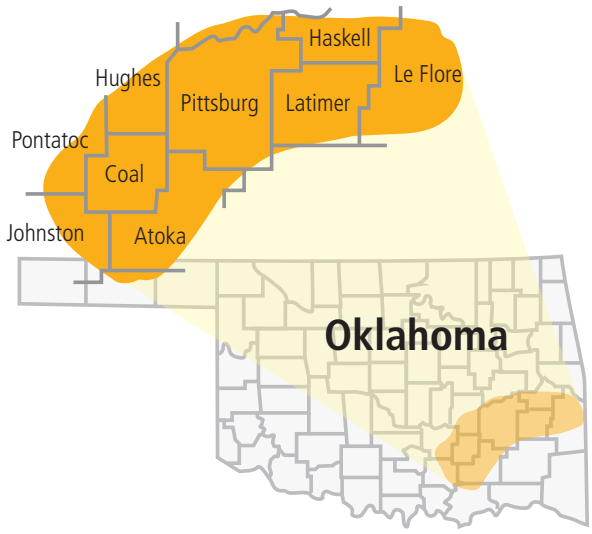

Fig. 4.13—Woodford shale map. (Warlick International.)

Table 4.5—Woodford shale information. (From various sources.)

Woodford Shale	
Geologic Age	U. Devonian/L. Mississippian
Area Size, mi.^{2}	11,000
Depth, ft.	5,000–9,500
Thickness, ft.	15–250
TOC, %	4–8
Thermal Maturity, R_0 %	1.2–2.8
Porosity, %	5–6
Well Avg. IP, MMcfd	3.6
Horizontal Lateral, ft.	2,500–5,000
TRR, Tcf	22
EUR/Well, Bcf	2.1
Pressure Gradient, psi/ft	0.50–0.55
Well Spacing, Ac	160
First Production	2006
■ Relatively complex structure ■ Reservoir navigation and well placement are critical.	

equivalent is the Chattanooga shale. A dark gray to black shale, it has a high organic content with TOC up to 9.8%. Lithology of the Woodford consists of 50 to 65% silica, 5 to 10% carbonate, and 30 to 35% clay. This makes for a fairly brittle formation. Presently (in late 2015), only 9 gas-directed rigs from a high of 81 are operating, but 38 oil-directed rigs are operating (**Fig 4.14**).

4.2.5 Haynesville Shale

In 2008, two years after the Fayetteville and Woodford plays began production, the Haynesville play with significant resources of 75 TRR attracted operators. Haynesville was deeper, hotter, and higher porosity than the previous gas plays (**Fig. 4.15**, **Fig. 4.16**, and **Table 4.6**). The overpressured

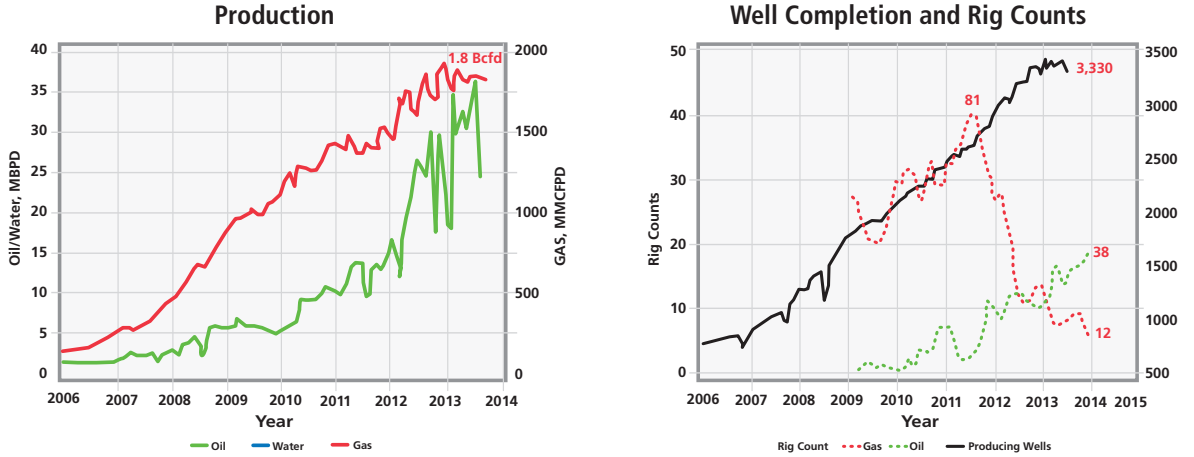

Fig. 4.14—Woodford shale production, well completion, and rig count. (Sources: Baker Hughes rig counts; Drilling Information Database.)

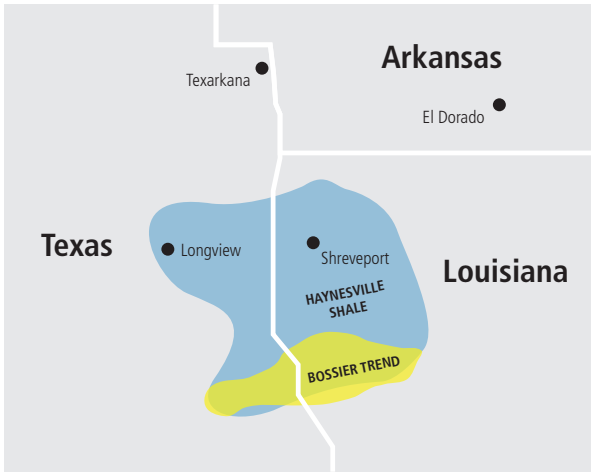

Area Straddles NW Louisiana and East Texas Border

Fig. 4.15—Haynesville shale map. (From Warlick International.)

Table 4.6—Haynesville shale information. (From various sources.)

Haynesville Shale	
Geologic Age	Upper Jurassic
Area Size, mi.^{2}	9,000
Depth, ft.	10,500–13,500
Thickness, ft.	200–300
TOC, %	0.5–4
Thermal Maturity, R_0 %	1.7–2.8
Porosity, %	7–10+
Well Avg. IP, MMcfd	14+
Horizontal Lateral, ft.	4,400–4,700
TRR, Tcf	75
EUR/Well, Bcf	6.5
Pressure Gradient, psi/ft	0.7–0.9
Well Spacing, Ac	80
First Production	2008
■ Deep, hot, overpressured ■ High IPs and recovery	

formation delivered higher initial production (14+ MMcfd) and greater recoveries, 6.5 Bcf per well, than the four earlier shale gas plays. The Haynesville had significant growth since first production with a peak production rate of 7.5 Bcfd compared to the Barnett and Marcellus peaks of 5.7 and 10.1 Bcfd, respectively. It has declined to 4.4 Bcfd as the rig count has dropped from 210 down to 50 in late 2014. A relatively higher rig count than the other four shale gas plays today reflects the higher initial productions and recoveries.

Some geologists think the Haynesville and Bossier shales are equivalent, but the Bossier occurs more frequently as a separate section above the Haynesville.

Lithology of the Haynesville shale, generally termed a siliceous marl, consists of 25 to 45% silica, 15 to 40% carbonate, and 30 to 45% clay, which makes it a more ductile formation and not as prone to hydraulic fracture treatment.

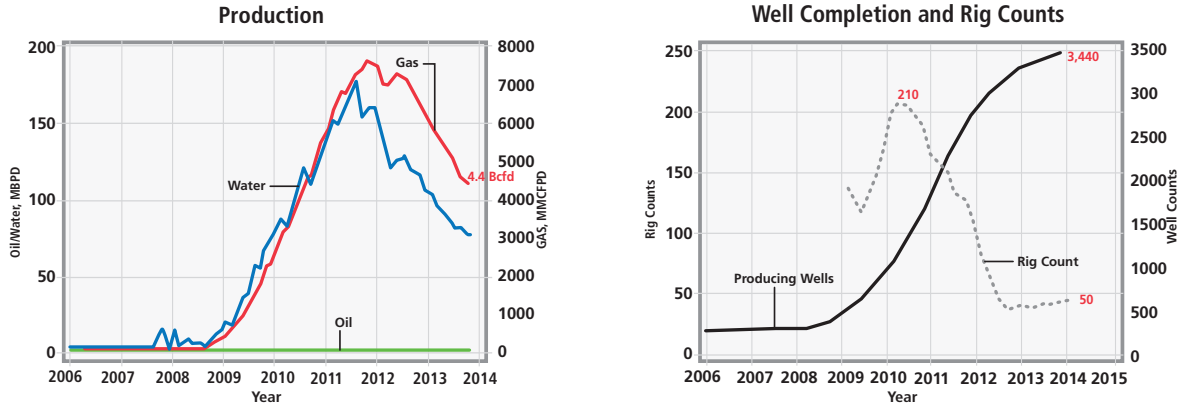

Fig. 4.16—Haynesville shale production, well completion, and rig count. (Sources: Baker Hughes rig counts; Drilling Information Database.)

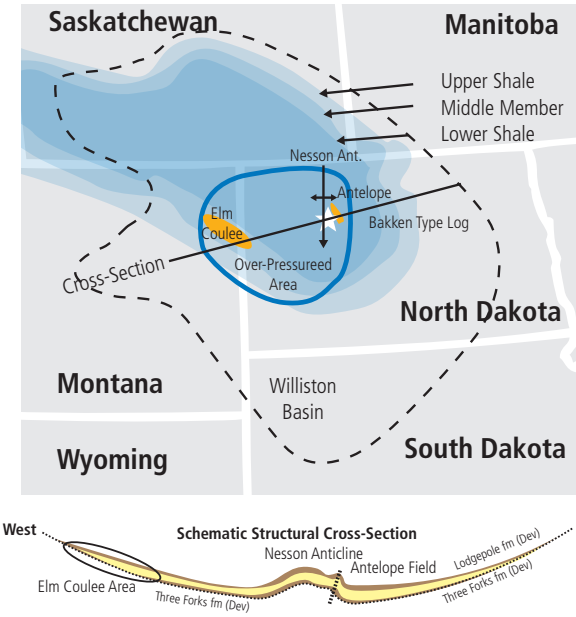

Fig. 4.17—Bakken map. (Modified after Meissner 1978.)

4.2.6 Bakken Tight Oil

The first of the liquids plays, the Bakken (**Fig. 4.17**), came on in 2008, with first oil production. The Bakken is not a shale but a true tight-oil play. Early in the 1950s, the Upper and Lower Bakken shale formation, which were the source rocks for the Middle Bakken formation, produced at rates of less than 100 barrels of oil per day (BOPD) of shale oil. Major production and all of the current activity now centers on the Middle Bakken tight oil formation (**Fig. 4.18**).

Although the literature and the industry call the Bakken a shale oil play, wells in this tight oil have a production decline pattern similar to a conventional oil formation, unlike the steep decline in other shale plays. Lithology consists of siltstones, sandstones, limestones, dolomite, and some shale. Initial production ranges from 200 to 1,800 BOPD The total field average is close to 400 BOPD. Recovery per well averages near 700 MBO. Horizontal laterals average about 10,000 ft., which is nearly twice as long as the average horizontal laterals for shale gas wells, with some as long as 13,000 ft. (**Table 4.7**). As of early 2014, , the Bakken's 7,630 wells are producing at a total rate of 906 MBOPD with 1.0 Bcfd of associated gas (**Fig. 4.19**). Rig count peaked in mid-2012 to 220 and by early 2014, it had dropped to 181.

4.2.7 Eagle Ford Shale

In 2009, the prolific Eagle Ford shale, with dry gas, wet gas, and oil windows, began first production (**Fig. 4.20**, **Fig. 4.21**, **Fig. 4.22**, and **Table 4.8**). The Eagle Ford along with the first five significant shale gas plays (Barnett, Marcellus, Fayetteville, Woodford, and Haynesville) are known as the Big Six. When the first and largest Canadian shale, the Horn River, was added to the group, they became known as North America's Magnificent Seven.

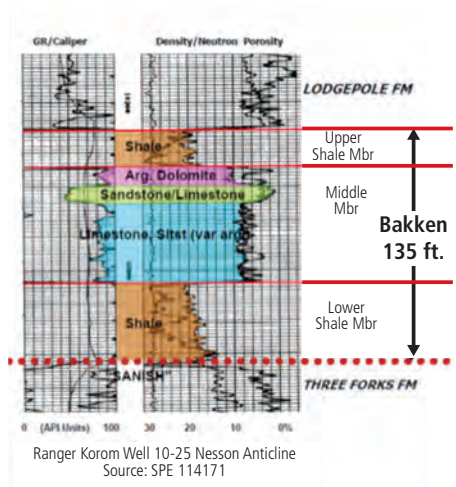

Upper
- Black shale, silty, calcareous, pyrite
- TOC = High to 20%
- Thickness = 15 ft.
- Well IP = 86 BOPD, EUR = 145 MBOE

Middle
- Late Devonian to Early Mississippian
- Basin Area = 200,000 mi²
- Depth = 9,600-10,400 ft.
- Thickness = 40-75 ft.
- Horizontal Lateral = 10,000+ ft.
- Permeability = Nano-Microdarcy
- Porosity = 4-10%
- Overpressured, 0.50 to 0.60 psi/ft.
- Well IP = 200 to 2,000 BOPD (44° API)
- EUR/Well = 700 MBO
- Minimal Water Production
- Initially Flow, then put on Artificial Lift
- Shaley siltstones, Sandstones, Limestones, and Dolomite (Not Shale)

Lower
- Geology similar to Upper Bakken
- TOC = High to 12%
- Thickness = 30 ft.

Fig. 4.18—Three parts of Bakken formation, log, and information. (Source: Walker et al. 2006.)

Table 4.7—Bakken tight oil information. (From various sources.)

Bakken Tight Oil	
Geologic Age	Late Devonian/Early Mississippian
Area Size, mi.^{2}	200,000
Depth, ft.	9,600–10,400
Thickness, ft.	40–75
(U & L Shales)–TOC, %	9+
Thermal Maturity, R_0 %	0.6–1.0
Porosity, %	8–12
Well Avg. IP, BOPD	200–1,800
Horizontal Lateral, ft.	8,700–10,000
TRR, BBO	7.4 (Ind. est. 24)
EUR/Well, MBO	700
Pressure Gradient, psi/ft.	0.50–0.60
Well Spacing, Ac	160
First Production	2008 (Middle Bakken)
■ Tight oil: Initial flow plus water, then artificial lift ■ Shaly siltstone, sandstone, limestone, dolomite	

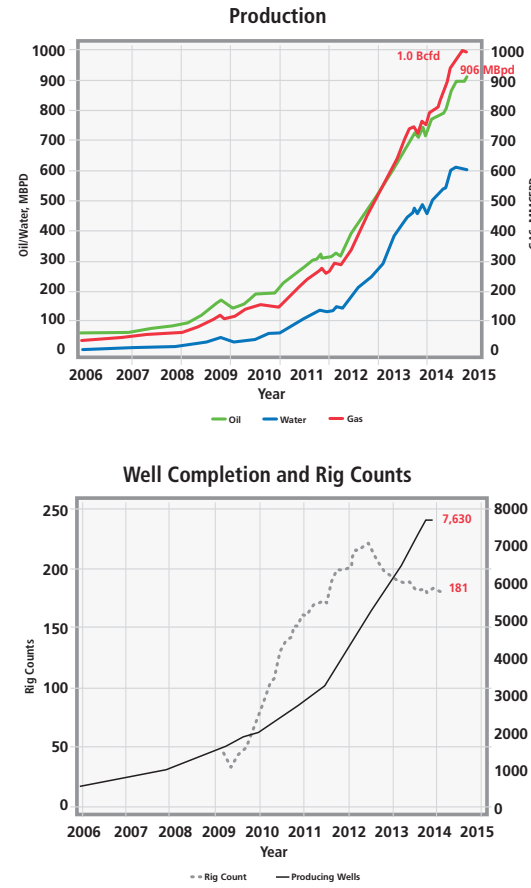

Fig. 4.19—Bakken tight oil production, well completion, and rig count. (Sources: Baker Hughes rig counts; Drilling Information Database.)

The Eagle Ford covers 24 counties in the south Texas Maverick basin and has its three hydrocarbon windows extending across the border into Mexico's Burgos basin. The Eagle Ford formation is considered to be the source rock for hydrocarbons in the Austin Chalk and Edwards formation, which also lie above the Eagle Ford shale. It is located deeper, down to 12,000 ft. plus, and is thicker, up to 475 ft., than the other major shale plays. Lithology of the Eagle Ford consists of 10 to 25% silica, 60 to 80% carbonate, and 10 to 20% clay, which makes for a brittle formation and prone to hydraulic fracture treatment.

From late 2010 to 2012 the trend shifted with the number of oil-directed rigs increasing to 188 in early 2014; the gas-directed rig number dropped from a high of 85 to 35 in early 2014. This is a respectable number as operators still are drilling in the wet gas window. Initial production of gas wells ranges up to 8 MMcfd plus condensate. Oil well initial production can run as high as 2,500 BOPD. Estimated ultimate recovery (EUR) for both oil and gas wells remains high compared to other plays. The Eagle Ford continues to be one of the most active US shale plays with more rigs running than any other shale play except for the Wolfcamp shale in the Permian.

4.2.8 Niobrara Shale

First production began in the Niobrara shale in 2006; however, it is considered an emerging shale liquids play. Located in the Denver-Julesburg basin, conventional oil and gas reservoirs have produced for a number of years, some as early as 1846 (**Fig. 4.23**, **Table 4.9**). The Niobrara core area is the old Wattenberg Field, where 17,000 vertical wells had been completed in conventional reservoirs. During the past few years horizontal drilling has been successful in the unconventional part of the Wattenberg. Drilling has expanded out of the Wattenberg, with operators having good success to the north and east. Geologic complexity and its location in the tectonic area of the Rocky Mountains have presented challenges to operators trying to understand the Niobrara and locate the sweet spots to develop. Currently,

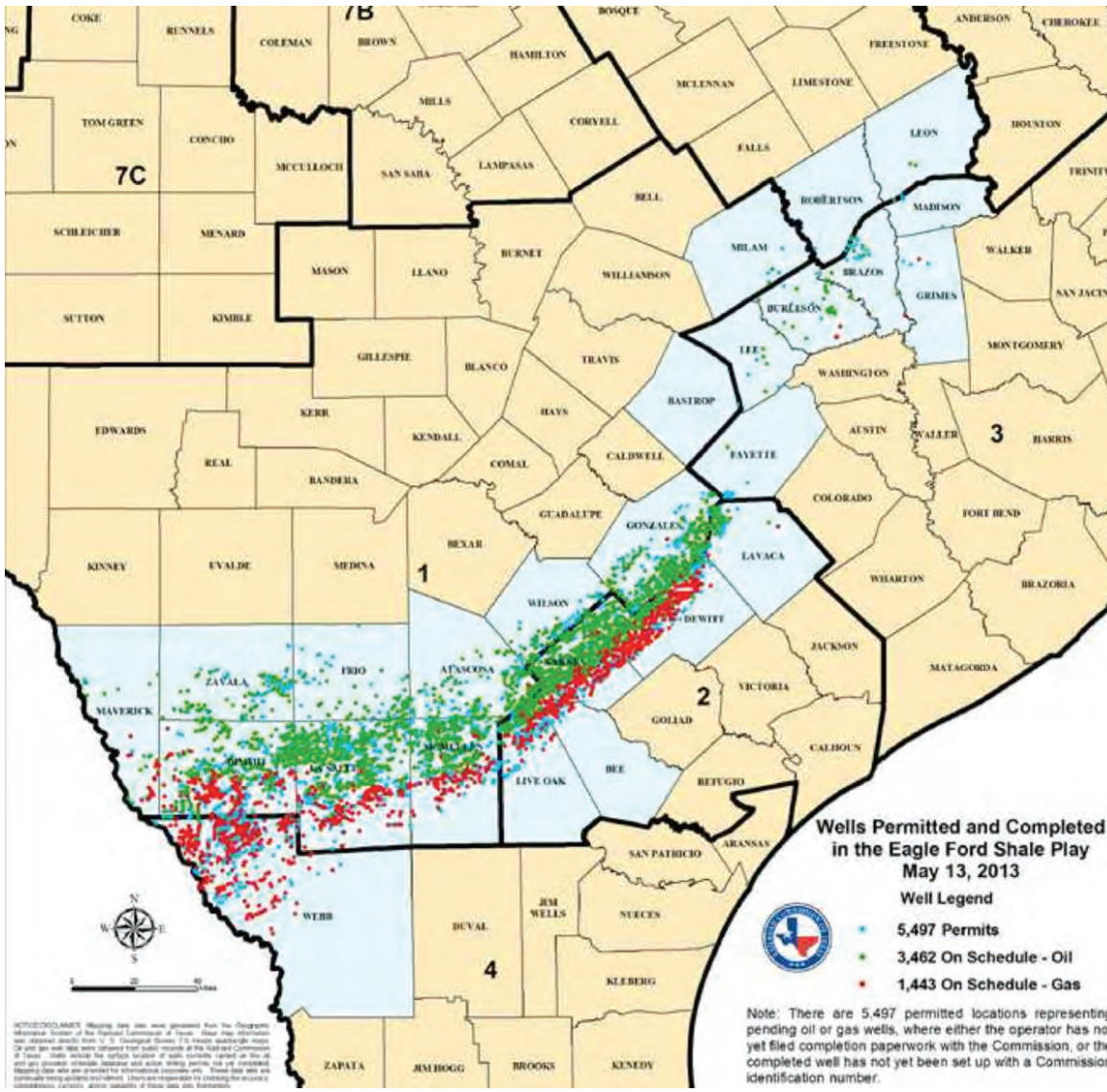

Fig. 4.20—Eagle Ford shale map. (Source: Texas Railroad Commission.)

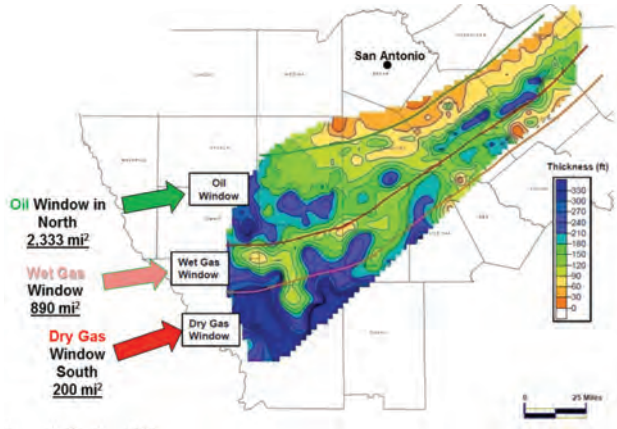

Fig. 4.21—Eagle Ford shale phase windows. (Source: Modified from EOG Resources.)

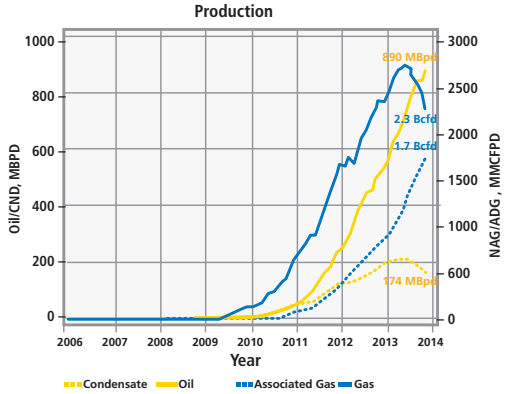

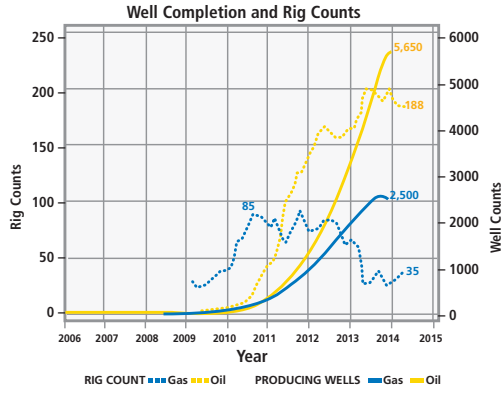

Fig. 4.22—Eagle Ford shale production, well completion, and rig count. (Sources: Baker Hughes rig counts; Drilling Information Database.)

Table 4.8—Eagle Ford shale information. (From various sources.)

Eagle Ford shale	
Geologic Age	Lower Cretaceous
Area Size, mi.^{2}	3,320 (Active)
Depth, ft.	7,000–12,000
Thickness, ft.	100–475
TOC, %	4–8
Thermal Maturity, R_0 %	0.7–1.8
Porosity, %	4–10
Well Avg. IP, MMcfd	8.0 + Cond.
Well Avg. IP, BOPD	340–2,500 (41.5 °API)
(41.5 °API)	7.4 (Ind. est. 24)
Horizontal Lateral, Gas, ft.	5,000–5,300
Horizontal Lateral, Oil, ft.	6,000–7,000
TRR, Tcf	22
TRR, BBO	8.0
EUR/Well, Bcf	5.0
EUR/Well, MBO	600
Pressure Gradient, psi/ft.	0.5–0.75
Well Spacing, Ac	40–80
First Production	2006

- Dry gas, wet gas, and oil windows
- Overpressured and high BHT in Live Oak County

the Niobrara has 870 completions and 54 rigs running; production is near 60 MBOPD and 290 MMcfd of associated gas (**Fig. 4.24**).

4.2.9 Utica Shale

The Appalachian basin is another emerging shale play located in the northeast US. Underlying part of the giant Marcellus is the Utica shale (**Fig. 4.25**). With three hydrocarbon windows, like the Eagle Ford, the Utica has attracted operators because of the liquids content. This led operators to move rigs from the dry gas Marcellus to the liquids-rich Utica. Early in 2014, 36 oil-directed rigs were running with 350 completed wells. Total production reported was less than 500 BOPD and 13 MMcfd. Pennsylvania requires operators to report only every six months production rates and well completions, so these are well behind the current numbers (**Table 4.10**). Average well IP production ranges between 200 and 1500 BOPD and 4.5 to 17.0 MMcfd. EUR per well ranges between 500 to 900 MBD and 3.6 to 5.4 BGF.

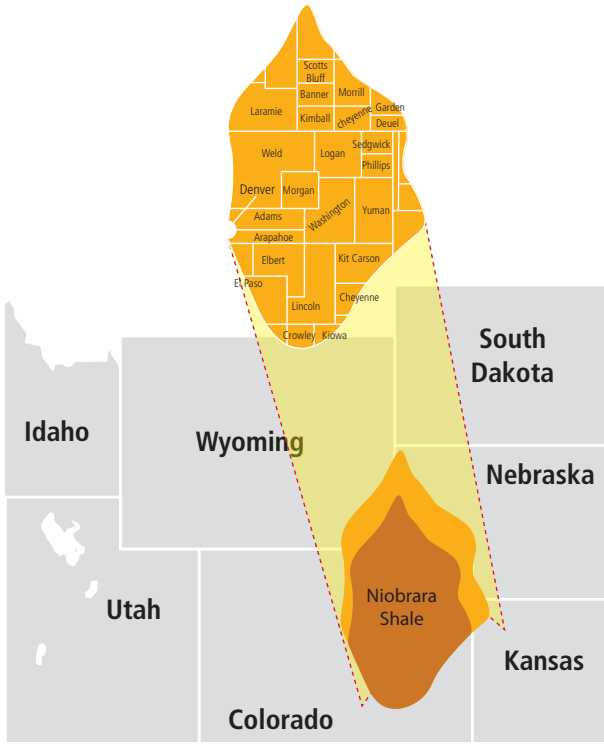

Fig. 4.23—Niobrara shale map.
(Source: Oil & Gas Financial Journal.)

Table 4.9—Niobrara shale information. (From various sources.)

Niobrara Shale	
Geologic Age	Upper Cretaceous
Area Size, mi.^{2}	14,000
Depth, ft.	3,000–14,000
Thickness, ft.	50–300 (to 1,500)
TOC, %	3.0
Thermal Maturity, R_0 %	0.5–1.4+ (Uneven Cooking)
Porosity, %	7–12
Well Avg. IP, BOPD	400–500
Horizontal Lateral, ft.	4,050–5,100 (Extend Lat to 10,000)
TRR, BBO	1.5
EUR/Well, MBO	350–750 (Norm-Extend Lat)
Pressure Gradient, psi/ft.	0.42- 0.60
Well Spacing, Ac	160 (D/S to 40)
First Production	2006

- Emerging: highly fractured, complex structure.
- Old Wattenberg field is core area.

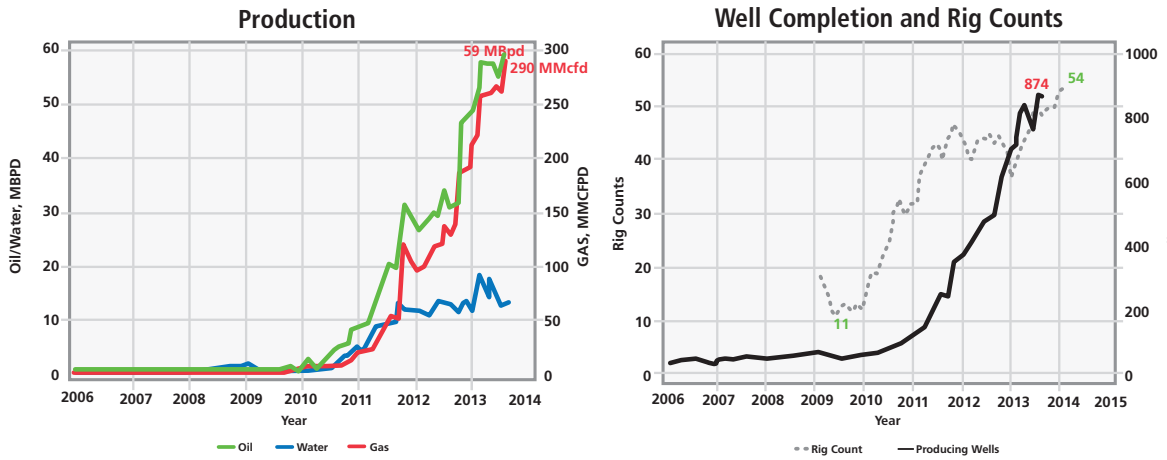

Fig. 4.24—Niobrara shale production, well completion, and rig count. (Sources: Baker Hughes rig counts; Drilling Information Database.)

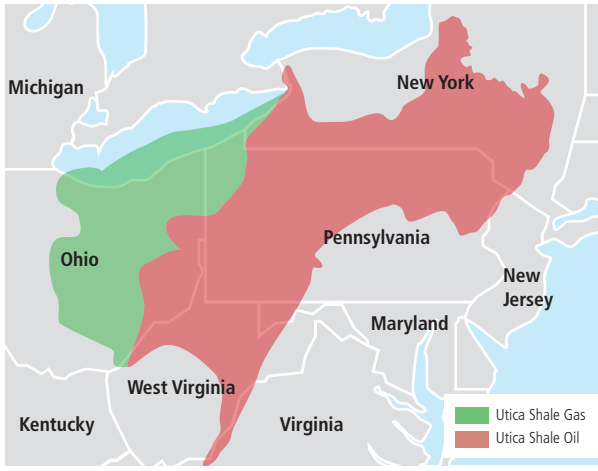

Fig. 4.25—Utica shale map. (From USGS.)

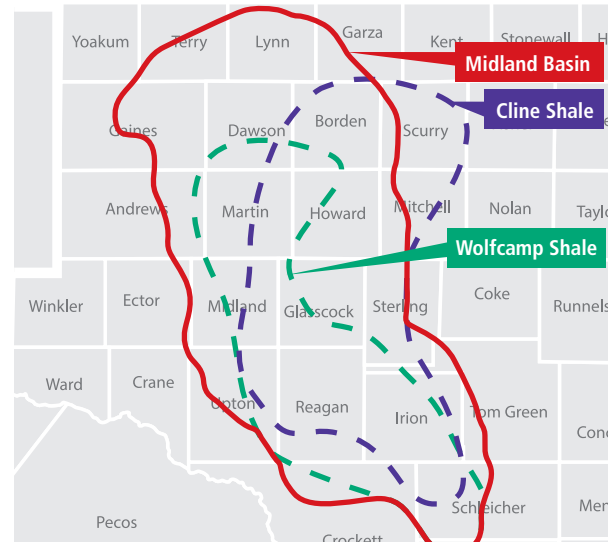

Fig. 4.26—Wolfcamp shale map. (Courtesy of Apache.)

4.2.10 Wolfcamp Shale

One of the most active, emerging shale liquids play areas is in the Wolfcamp shale located in the Permian basin of west Texas (**Fig. 4.26**). The Permian basin encompasses a huge swath of west Texas and southeast New Mexico covering 86,000 square miles and includes 52 counties. The Permian includes three sub-basins: the Midland, Central Platform, and Delaware. The Wolfcamp shale is primarily located within the Midland sub-basin on the eastern side of three sub-basins. The Permian includes numerous conventional formations and several unconventional shale plays with the Wolfcamp currently the most active. As late as 2013, operators were completing or re-completing vertical wells into the Wolfcamp. Some were and still are dually completing wells with the Wolfcamp in the horizontal and with other conventional formations in the vertical part of the well.

Table 4.10—Utica shale information. (From various sources.)

Utica Shale	
Geologic Age	Middle Ordovician
Area Size, mi.^{2}	170,000
Depth, ft.	2,000–14,000 (avg. 8,300)
Thickness, ft.	70–750
TOC, %	0.3–2.5
Thermal Maturity, R_o %	1.1–4.0
Porosity, %	6–12
Well Avg. IP, MMcfd	4.5–17
Well Avg. IP, BOPD	200–1,500
Horizontal Lateral, ft.	4,700–6,200
TRR, Tcf & BBO	3.8 & 1.3 to 15.7 & 5.5 (Ohio)
TRR	est. 38 Tcf (entire play)
EUR/Well, Bcf	3.6–5.4
EUR/Well, MBO	500–900
Pressure Gradient, psi/ft	0.6
Well Spacing, Ac	160
First Production	2011
■ Dry gas, wet gas, and oil windows (like Eagle Ford) ■ An emerging gassy, liquids play	

In early 2014, 24% of oil production of the Permian basins came from shale wells. Based on mid-2014 data, there are 470 rigs running in the Permian, which is more than any other basin in the US. The number of rigs in the US during the same period is about 1,800. Of those, approximately 215 rigs run in the Wolfcamp; about half of those are drilling horizontal wells (**Fig. 4.27**). More than 6,100 are completed wells, and total production is 132 MBOPD. The Wolfcamp and Permian are some of the most active shale plays today (late 2014) in the US.

Average initial productions are near 1,000 BOPD, and EURs are projected to be in the 650 to 750 MBO range. According to industry experts, TRR for the Wolfcamp can approach 30 to 50 bbl of oil (**Table 4.11**).

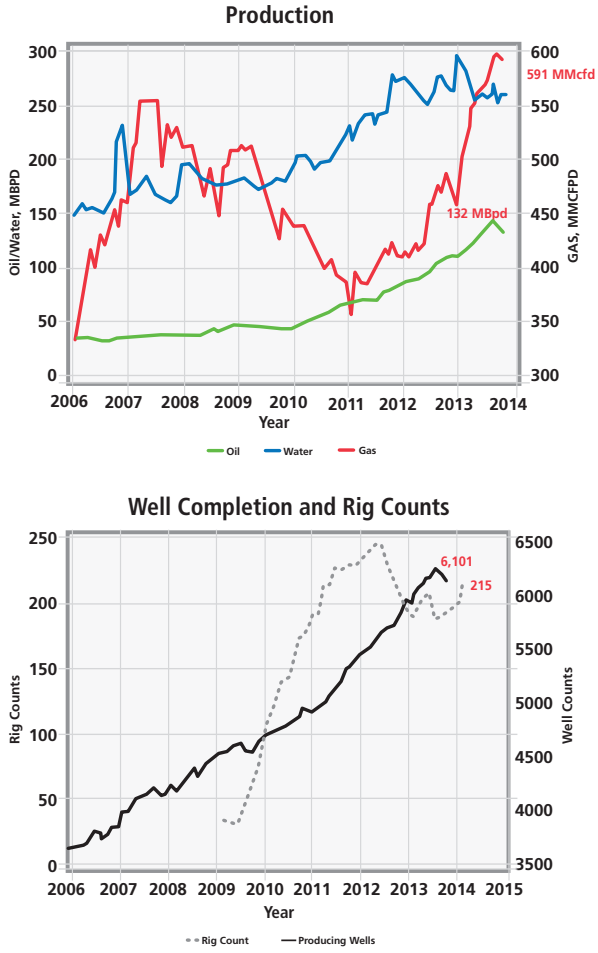

Fig. 4.27—Wolfcamp shale production, well completion, and rig count. (Source: Drilling Information Database.)

4.2.11 Monterey Shale

The Monterey in California (**Fig. 4.28**) is an emerging shale oil play and has been the most challenging to operators. This Miocene-age shale is much younger than the other US shales. As a result of the San Andreas Fault, the geologic layers of the Monterey-are folded like an accordion and not stacked on top of each other like other formations. The shale has been cracked naturally by these folds. The Monterey is the source rock for much of California's conventional producing reservoirs. With the massive folding, the solution of horizontal drilled wells does not work in the Monterey, and hydraulic fracturing has not been effective due to the unique lithology and mineralogy. Although TRR of the Monterey was assessed at 15 bbl of oil by the US EIA, operators have not solved the problem of how to recover the resource. The two major operators in the Monterey,

Table 4.11—Wolfcamp shale information. (From various sources.)

Wolfcamp Shale	
Geologic Age	Permian
Area Size, mi^2	9,800
Depth, ft.	5,500–11,000
Thickness, ft.	1,500–2,600
TOC, %	2–6
Thermal Maturity, R_o %	0.8
Porosity, %	2–10
Well Avg. IP, BOPD	1,050
Horizontal Lateral, ft.	4,550–6,700
TRR, BBO	30 (Ind. est. is 50)
EUR/Well, MBO	650–750
Pressure Gradient, psi/ft	0.55–0.70
Well Spacing, Ac	80
First Production	2011

- Located in Permian Basin.
- More rigs in Permian than any other US area.

Venoco, and Occidental, have dialed back exploration after approximately 50 wells. The data in **Table 4.12** are what Venoco planned to accomplish in the Monterey and they are awaiting implementation of optimum development techniques.

Fig. 4.28—Monterey shale map. (AAPG Explorer 2012.)

Table 4.12—Monterey shale information. (From various sources.)

Monterey Shale	
Geologic Age	Miocene
Area Size, mi.^{2}	1,750
Depth, ft.	8,000–14,000
Thickness, ft.	1,000–3,000 (gross)
TOC, %	5.0
Thermal Maturity, R_0 %	0.6–1.0 (est.)
Porosity, %	13–29
Well Avg. IP, BOPD	350–700 (Venoco)
Horizontal Lateral, ft.	Not Determined
TRR, BBO, and Tcf	15.4 and 1.5 to 2.0
EUR/Well, MBO	230–800
Pressure Gradient, psi/ft.	Normal
Well Spacing, Ac	160
First Production	1980s initially (limited)

- Much younger age than other US shales.
- Complex lithology and mineralogy geology, highly folded.
- Vertical wells, acidized some horizontal, fractured.
- Operators have not determined optimum development techniques.

4.2.12 US Shales Summary

Each US shale gas play has its unique lithology, mineralogy, and reservoir characteristics. With a few exceptions like the Eagle Ford and Haynesville, these shales tend to be similar in depth (6,500 to 8,500 ft.), thickness (50 to 500 ft.), production rates (IP 2.5 to 3.5 MMcfd or 500 to 1,500 BOPD), and recoveries (2.0 to 3.5 Bcf or 500 to 900 MBO) (**Table 4.13**). As a result, average horizontal lateral lengths tend to be similar (3,000 to 5,000 ft. for gas plays and 6,000 to 10,000 ft. for oil plays). However, each shale requires a specific hydraulic fracturing treatment, pumping schedule, and stage placement to attain the highest production rates and recoveries.

Each US shale oil play also has its unique lithology, mineralogy, and reservoir characteristics. These shales tend be somewhat similar in depth (8,000 to 12,000 ft.), thickness range is wider (14 to 600 to 2,600 ft.), production rates vary (IP 500 to 1,500 BOPD), and recoveries (500 to 900 MBO) (**Table 4.14**). Average horizontal lateral lengths tend to range wider (6,000 to 8,000 to 10,000 ft.). However, like gas shales each requires a specific hydraulic fracturing treatment, pumping schedule, and stage placement to attain the highest production rates and recoveries. As can be seen in Table 4.14, significant differences appear when Eagle Ford, Niobrara, Utica, and Wolfcamp, the true shale oil plays, are compared. If the Monterey were added, its uniqueness would further enhance the differences within the shale oils.

Fig. 4.29 shows the number of existing wells in the six major US shale gas plays and the total number of wells required to develop the TRR. This is based on EUR per well (EIA 2011) for each play using the typical number of 200 to 300 wells needed to recover one Tcf of gas. Most plays have not yet approached the required number of wells. It will take again, many more wells to develop all the shale gas resources in the major US plays.

Fig. 4.30 shows the number of existing wells in the five major US shale oil plays and the total number of wells required to develop the TRR from each play. Using the typical number of 1,700 wells required to recover one bbl of oil, most plays have not yet approached the required number of wells. Again, many more wells will be needed to develop all the shale oil resources in the major US plays.

Table 4.13—US shale gas plays comparison of well data.

Play	Barnett	Fayetteville	Woodford	Eagle Ford	Haynesville	Marcellus
Area, Mi^2	4,075	9,000	3,700	1,100	9,000	95,000
Depth, Ft	6,500–8,500	1,000–7,000	5,000–9,500	10,500–11,300	10,500–13,500	4,000–8,500
Thickness, Ft	100–600	20–200	150–250	180–375	200–300	50–200
Cond Ratio, B/MMcf IP Rate, MMcfd	2.5	2.8	3.6	50-200 7.0 + Cond	14+	3.5
Eur/Well, Bcf	1.6	2.1	3.0	5.0	6.5	3.5
Avg Lateral, Ft	3,950–4,350	4,700–5,500	3,000–5,000	5,000–5,300	4,400–4,700	4,200–4,900
Well Spacing, Acres	116	80	160	160	80	80
TRR, Tcf	43	32	22	21	75	410
Well Cost, $MM	2.8	3.0	5–6	6–9	7.5	3.7

Table 4.14—US shale oil plays comparison of well data. (Source: EIA 2011.)

Play	Bakken	Eagle Ford	Niobrara	Utica	Wolfcamp
Area, Mi^2	200,000	1,100	14,000	170,000	98,000
Depth, Ft	8,500–10,000	4,000–12,000	6,000–8,000	2,000–14,000	5,500–11,000
Thickness, Ft	8 -14	300–475	150–300	70–750	1,500–2,600
Cond Ratio, B/MMcf IP Rate, MMcfd	200–1,800	250–1,500	400–500	4,5–17 MMcfd 200–1,500 Bcpd	1,050
EUR/Well, MBO	700	600	250–450	3.6–5.4 Bcf 500–900	650 -750
Avg Lateral, Ft	8,700–10,000	6,000–7,000	4,050–5,100	4,700–6,200	4,550–6,700
Well Spacing, Acres	160	40–80	160 (D/S 40)	160	80
TRR, BBO	4.5 (20)	7–10	1.5	3.0 (5.5)	30 (Ind. est.)
Well Cost, $MM	8.5–9.0+	6.0–9.0	3.5–5.5	6.0–8.0	7.0–8.0

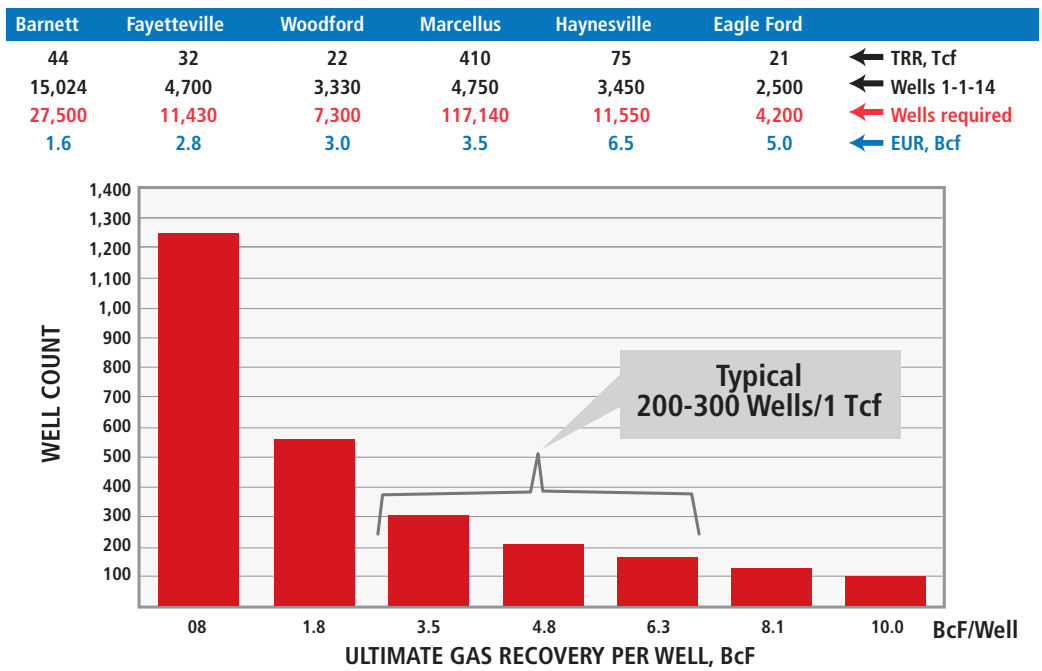

Fig. 4.29—Number of wells required to develop US shale gas. (Updated from Kennedy et al. 2012.)

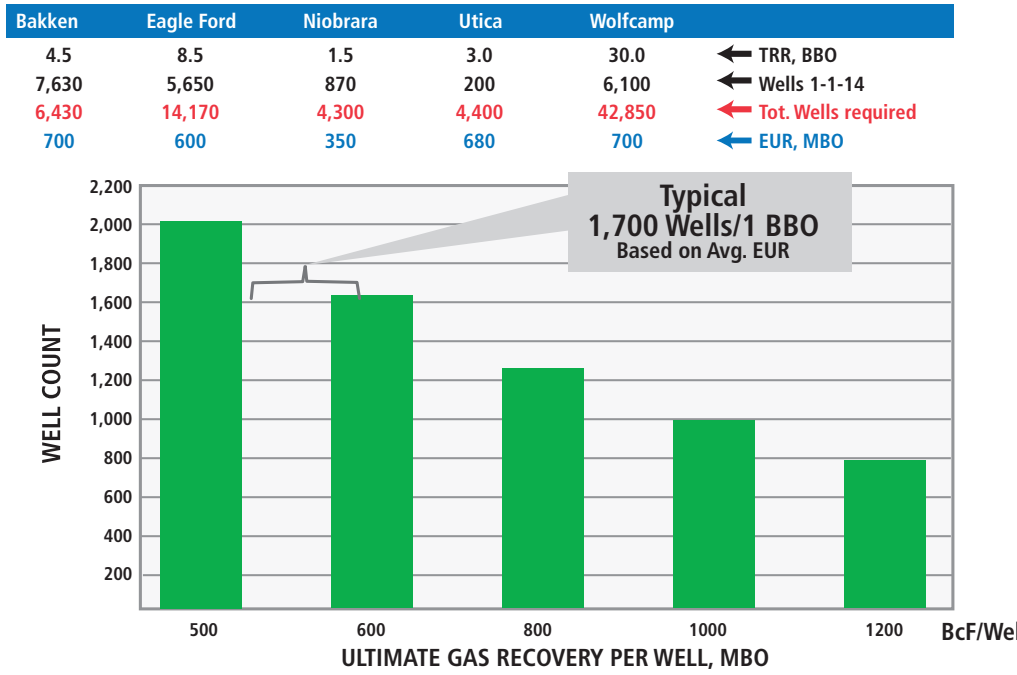

Fig. 4.30—Number of wells required to develop one BBL of oil. (Kennedy and Knecht, Baker Hughes.)

4.3 Canada Shale Oil and Shale Gas Basins

Canadian shale gas has been somewhat slower in developing than in the US. **Fig. 4.31** shows the five significant shale gas Canadian basins and plays: Horn River, Montney, and Colorado Group in western Canada and the Utica and Horton Bluff Group in eastern Canada. The emerging Duvernay is in west-central Alberta. Total Canadian shale oil and shale gas TRR are 573 Tcf of gas and 9 bbl of oil. The Bakken tight oil play is also located

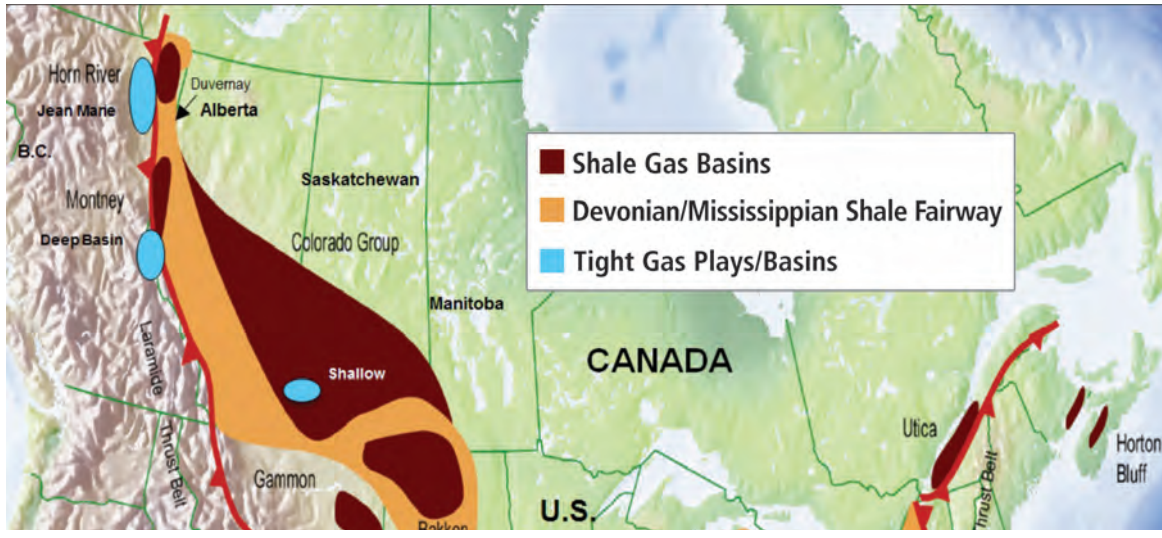

Fig. 4.31—Map of Canada shows the five significant shale gas basins: Horn River, Montney, Colorado Group and emerging Duvernay in western Canada, and Utica and Horton Bluff in eastern Canada. (Modified from NEB—Canada 2009.)

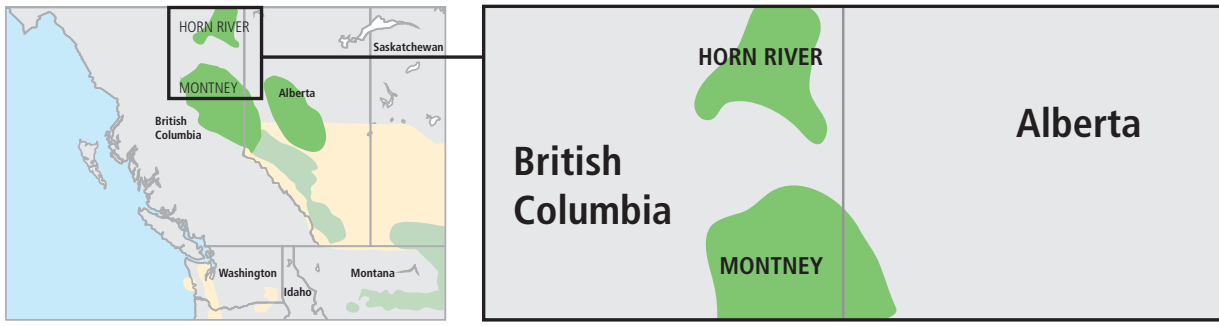

Fig. 4.32—Horn River shale map.

in Canada and was discussed earlier. Only the more active Horn River, Montney, and emerging Duvernay Canadian shales are discussed here.

4.3.1 Horn River Shale

The Horn River Shale, of middle Devonian age, is located in the far north British Columbia Province in Canada (**Fig. 4.32**). The remoteness of the area with limited infrastructure and higher well costs of USD 16 to 22 million per well caused the slower development of Canadian shales (EIA 2014). This thermally mature (in the gas window) shale exhibits high temperature of 300 to 350°F and high pressure up to 0.75 psi/ft. and, unlike the US shale gas plays, contains up to 12% CO_2 and traces of H_2S (**Table 4.15**). Prior to entry into the sales pipeline, this sour gas must be treated, which adds to the operating cost. With 55% silica, it is very brittle and prone to favorable hydraulic fracturing. Horn River TRR of 100 Tcf (marketable) make it the largest shale gas play in Canada and exceeds the size of most US shale gas plays. High initial well production from 10 to 30 MMcfd and EUR from 15 to 35 Bcf per well also exceeds those of typical US shales. Total Horn River gas production is currently 360 MMcfd from 225 producing wells, and 135 rigs (as of mid-2014) running. Most wells are drilled from 20 to 24 well pads with a fully centralized operation with dedicated processing, water source, and water disposal wells.

4.3.2 Montney Shale

Located south of the Horn River in the Canadian provinces of British Columbia and Alberta (partly) is the Montney shale (**Fig. 4.33**). The Early Triassic-age Montney is a tight gas-shale gas hybrid reservoir. It is a complex play that has different lithologies varying from fine-grained sandstones and siltstones in the east to very fine-grained siltstones and shales to the west. The formation has produced conventionally from areas with high-quality reservoir properties. Significantly variable characteristics (**Table 4.16**) include depth ranges from 4,900 to 11,500 ft., thickness varying from 150 to 1,000 ft., and from dry gas to rich wet gas. Restricted production has been enforced until additional processing (condensate separation) facilities are built. Condensate is currently trucked out. As of mid-2014, total Montney production is 2.4 Bcfd from 2,650 producing wells.

Table 4.15—Horn River shale information. (From various sources.)

Horn River Shale	
Geologic Age	Middle Devonian
Area Size, mi.^{2}	5,000
Depth, ft.	6,500–9,000
Thickness, ft.	125–450
TOC, %	1–6
Thermal Maturity, R_0 %	2.2–2.8
Porosity, %	4–8
Well Avg. IP, MMcfd	10–30 (up to 12% CO2, Tr. H2S)
Horizontal Lateral, ft.	5,000–6,550
TRR, Tcf	165 (100 marketable)
EUR/Well, Bcf	15–35
Pressure Gradient, psi/ft.	0.55–0.75 (local pressure differences)
Well Spacing, Ac	
First Production	2005
■ Largest shale gas field in Canada; limited infrastructure ■ 55% silica content, brittle and hydraulic fracture prone ■ High BHT (300—350°F at 8,500 ft.)	

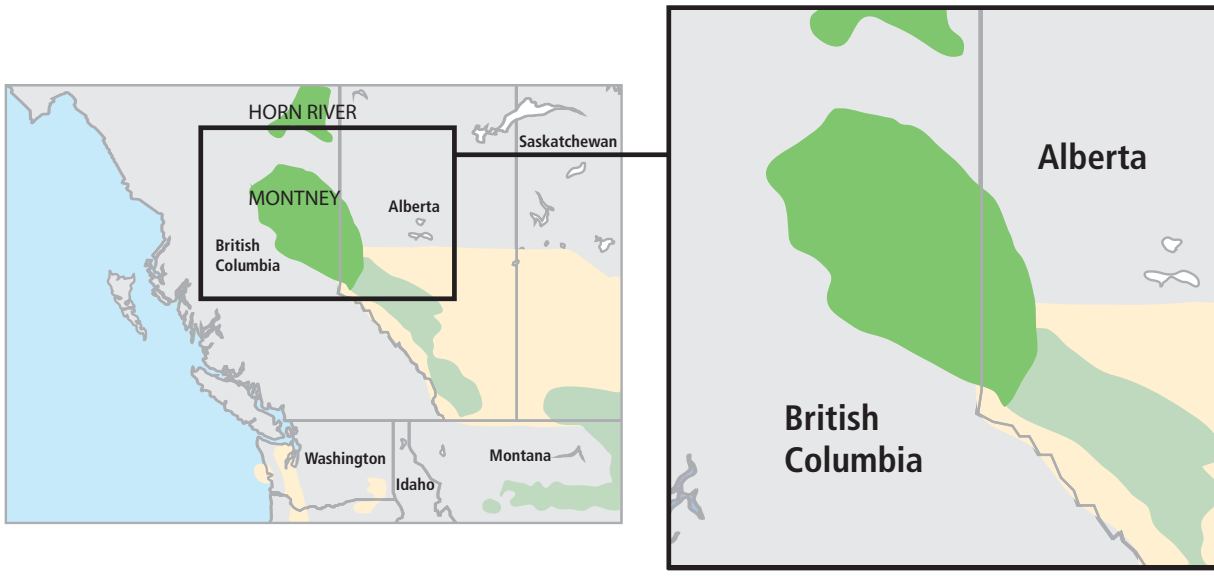

Fig. 4.33—Montney shale map. (www.naturalgasintel.com/shalemap.)

Table 4.16—Montney shale information. (From various sources.)

Montney Shale	
Geologic Age	Early Triassic
Area Size, mi.^{2}	1,150
Depth, ft.	4,900–11,500
Thickness, ft.	150–1,000
TOC, %	0.4–4.0
Thermal Maturity, R_o %	0.8–2.5
Porosity, %	2–9
Well Avg. IP, MMcfd, BCPD	3.0–4.0 and 575
Horizontal Lateral, ft.	4,700–5,700
Shale TRR, Tcf and BB Cond	49 and 1.1
Tight Gas TRR, Tcf	230
EUR/Well, Bcf	4.0–5.0
Pressure Gradient, psi/ft.	0.48
Well Spacing, Ac	
First Production	Before 2000
■ Hybrid shale gas and tight gas reservoir ■ Complex lithology across play ■ To 60% silica plus to 20% calcite, brittle and hydraulic facture prone	

4.3.3 Duvernay Shale

The Devonian age Duvernay shale is located generally in the same area as the Horn River and Montney but concentrated mostly in Alberta Province, which is east of British Columbia, (**Fig. 4.34**). Reservoir lithology consists of 50% to 70% silica, 10% to 30% carbonate, and 15% to 30% clay. This provides for a very brittle formation prone to hydraulic fracturing. It is overpressured and depths exceeding more than 13,000 ft. (deeper than the Montney and Horn River) have resulted in

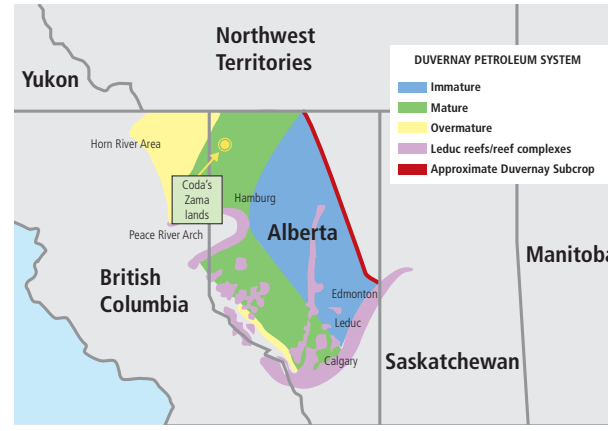

Fig. 4.34—Duvernay shale map. (Mooncor Oil and Gas Corporation.)

Table 4.17—Duvernay shale information. (From various sources.)

Duvernay Shale	
Geologic Age	Upper Devonian
Area Size, mi.^{2}	3,900
Depth, ft.	8,200–13,100
Thickness, ft.	65–230
TOC, %	1–20
Thermal Maturity, R_0 %	0.6–2.9
Porosity, %	3–8
Well Avg. IP, MMcfd	3.0–8.5 + Condensate
Well Avg. Cond Ratio, bbl/MMcf	60–700
Horizontal Lateral, ft.	6,000–7,000
TRR, Tcf, and BBO	440 and 62
EUR/Well, Bcf	
Pressure Gradient, psi/ft.	0.72–0.96
First Production	2012
■ Like Eagle Ford has dry gas, wet gas, and oil windows. ■ Brittle lithology, very fracable. ■ Emerging – Only 120 wells drilled to date.	

higher drilling costs (**Table 4.17**). The Duvernay has been compared to the Eagle Ford in the US because of similar reservoir properties and the three hydrocarbon windows of dry gas, wet gas, and oil. Although in the early stage of development, an expected total resource recovery (440 Tcf and estimated 6.2 bbl of oil) is high compared to the other Canadian plays and the US. As of early 2014, 120 wells produce 254 MMcfd with 91 rigs running.

4.4 Major Shale Oil and Shale Gas Basins in the Rest of the World

This section introduces the major shale basins in the world that are either under refined resource evaluation phases or being considered for practical application of the technology. Today, shale wells have been tested and hydraulically fractured in countries such as United Kingdom, Australia, China, Mexico, and Argentina with the possibility of commercial production under way.

4.4.1 Northern South America

Northern South America has prospective shale gas and shale oil potential within marine-deposited Cretaceous shale

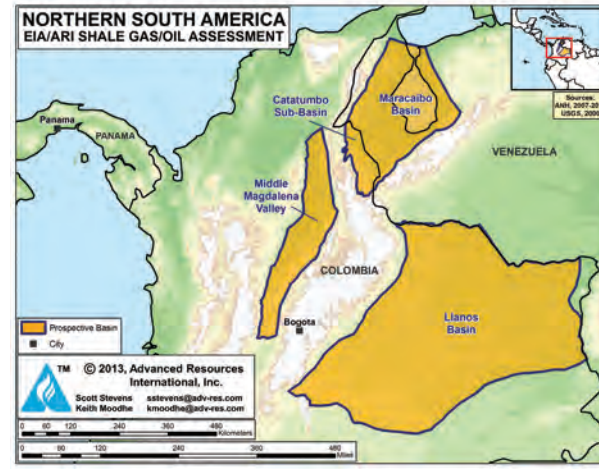

Fig. 4.35—Prospective shale basins of northern South America. (Source: ARI 2013.)

formations in three main basins: the Middle Magdalena Valley and Llanos basins of Colombia and the Maracaibo-Catatumbo basins of Venezuela and Colombia (**Fig. 4.35**). The organic-rich Cretaceous shales (La Luna, Capacho, and Gacheta) sourced much of the conventional gas and oil produced in Colombia and western Venezuela and are similar in age to the Eagle Ford and Niobrara shale plays in the US. Ecopetrol, ConocoPhillips, ExxonMobil, Shell, and other companies have initiated shale exploration in Colombia. Colombia's petroleum fiscal regime is attractive to foreign investment.

For the current EIA and ARI assessment, the Maracaibo-Catatumbo basin was re-evaluated while new shale resource assessments were undertaken in the Middle Magdalena Valley and Llano basins. TRR of shale gas and shale oil in northern South America are estimated at approximately 222 Tcf and 20.2 bbl.

Colombia accounts for 6.8 bbl and 55 Tcf of risked TRR, while western Venezuela has 13.4 bbl and 167 Tcf. Eastern Venezuela may have additional potential but has not been assessed due to lack of data.

Colombia's first publicly disclosed shale well logged 230 ft. of over-pressured La Luna shale with average 14% porosity. More typically, the black shales within the La Luna and Capacho formations total about 500 ft. thick, 10,000 ft. deep, calcareous, and average 2 to 5% TOC. Thermal maturity comprises oil, wet-gas, and dry-gas windows (R_0 0.7-1.5%). Shale formations in the Llanos and Maracaibo-Catatumbo basins have not yet been tested but also have good shale oil and gas potential.

For the complete details on northern South America, refer to the US EIA/ARI 2013 report.

4.4.2 Argentina

Argentina has world-class shale gas and shale oil potential, primarily within the Neuquen Basin, possibly the most prospective outside of North America. Additional shale resource potential exists in three other untested sedimentary basins (**Fig. 4.36**).

Significant exploration programs and early-stage commercial production are under way in the Neuquen Basin by Apache, EOG, ExxonMobil, TOTAL, YPF, and other smaller companies. Thick, organic-rich, marine-deposited black shales in the Los Molles and Vaca Muerta formations have been tested in 50 wells as of mid-2014, with mostly good results. Vertical shale wells are producing at initial rates of 180 to 600 BOPD following typically 5-stage hydraulic fracture stimulation. Horizontal wells are also being tested although initial results have not been uniformly encouraging possibly due to the massive formation thickness.

Fig. 4.36—Prospective shale basins of Argentina. (Source: ARI 2013.)

Cretaceous shales in the Golfo San Jorge and Austral basins in southern Argentina also have good potential although higher clay content may pose a risk in these lake-formed deposits. Marine-deposited Devonian shales in the Parana basin are considered prospective in a limited area of northeast Argentina.

Argentina has an estimated 802 Tcf of risked, shale gas in-place out of 3,244 Tcf of risked, technically recoverable shale gas resources. In-place risked shale oil resources are estimated at 480 bbl, of which about 27 bbl of shale oil may be technically recoverable.

For the complete details on Argentina, refer to the US EIA/ARI 2013 report.

4.4.3 Brazil

While Brazil's most prolific petroleum basins lie offshore, the country has 18 mostly undeveloped and lightly explored sedimentary basins onshore (**Fig. 4.37**). Three of these basins, the Paraná in the south and the Solimões and Amazonas in the north, produce significant conventional oil and gas from demonstrated source rock systems. These three basins have sufficient geologic data to be assessed for shale gas and shale oil potential.

The main shale target is the Devonian (Frasnian) marine black shale, which is extensively developed in the three structurally simple basins but has relatively modest TOC from 2 to 2.5%. Several other basins in Brazil may have shale oil and shale gas potential but lack of proven source

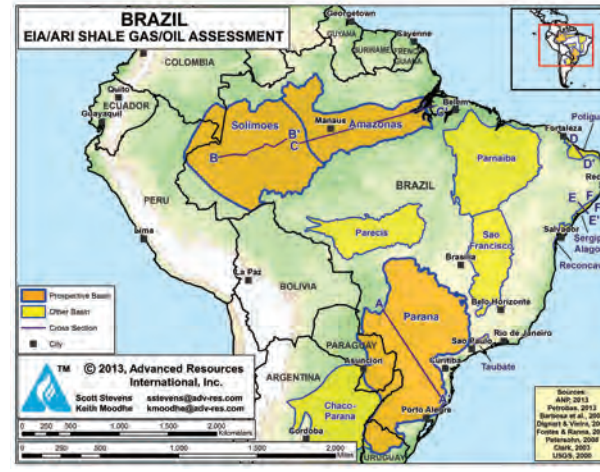

Fig. 4.37—Prospective shale basins of Brazil. (Source: ARI 2013.)

rock systems, thermal immaturity, and insufficient public data prevent further assessment.

Brazil's risked, technically recoverable shale gas and shale oil resources in the Paraná, Solimões, and Amazonas basins are estimated at 245 Tcf and 5.4 bbl. Risked, in-place shale resources are estimated to be 1,279 Tcf of shale gas and 134 bbl of shale oil. No shale-focused exploration leasing or drilling has been announced to date (as of late 2014) in Brazil.

For the complete details on Brazil, refer to the US EIA/ARI 2013 report.

4.4.4 Other South American Countries

Bolivia, Chile, Paraguay, and Uruguay in South America have prospective shale gas and shale oil potential within marine-deposited Cretaceous and Devonian shale formations in three large basins: the Paraná basin in Paraguay and Uruguay; the Chaco basin in Bolivia and Paraguay; and the Magallanes basin in Chile (**Fig. 4.38**). Extensions of these basins within neighboring Argentina and Brazil were assessed earlier in the chapter.

Fig. 4.38—Prospective shale gas and shale oil resources in Bolivia, Chile, Paraguay, and Uruguay. (Source: ARI 2013.)

Risked, technically recoverable shale oil and shale gas resources in these four South American countries are estimated at 162 Tcf and 7.2 bbl. The geologic setting of this region generally is favorably simple, with mostly gentle structural dip and relatively few faults or igneous intrusions apart from surface basalt flows. Technically recoverable shale resources by country are: Bolivia (36 Tcf, 0.6 bbl); Chile (49 Tcf, 2.4 bbl); Paraguay (75 Tcf, 3.7 bbl); and Uruguay (2 Tcf, 0.6 bbl). Initial shale-related leasing and evaluation has been reported in Paraguay and Uruguay within existing conventional petroleum license areas.

For the complete details on other South American basins, refer to the US EIA/ARI 2013 report.

4.4.5 China

China has abundant shale oil and shale gas potential in seven prospective basins: Sichuan, Tarim, Junggar, Songliao, the Yangtze Platform, Jianghan, and Subei (**Fig. 4.39**).

China has an estimated 1,115 Tcf of risked, technically recoverable shale gas, mainly in marine- and lacustrine-deposited source rock shales of the Sichuan (626 Tcf), Tarim (216 Tcf), Junggar (36 Tcf), and Songliao (16 Tcf) basins. Additional risked, technically recoverable shale gas resources totaling 222 Tcf exist in the smaller, structurally more

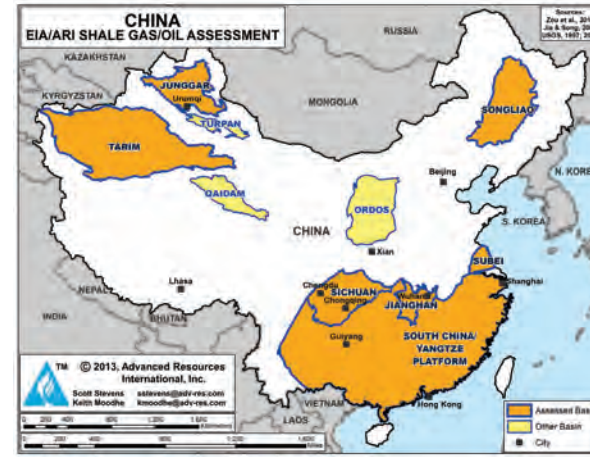

Fig. 4.39—China's seven most prospective shale oil and shale gas basins are the Jianghan, Junggar, Sichuan, Songliao, Subei, Tarim, and Yangtze platform. (Source: ARI 2013.)

complex Yangtze Platform, Jianghan, and Subei basins. The risked shale gas in-place for China is estimated at 4,746 Tcf.

China has considerable shale oil potential that is geologically less defined. Risked, technically recoverable shale oil resources in the Junggar, Tarim, and Songliao basins are estimated at 32.2 bbl, out of 643 bbl of risked, prospective shale oil in place. However, China's shale oil resources tend to be waxy and are stored mostly in lacustrine-deposited shales, which may be clay-rich and less favorable for hydraulic stimulation.

The shale gas and shale oil resource assessment for China represents a major upgrade from the 2011 EIA/ARI shale gas assessment. Importantly, this update assessment incorporates significant new information from ARI's proprietary database of geologic data extracted from recent drilling data and about 600 published technical articles that are primarily in Chinese.

Shale gas leasing and exploration drilling are under way in China and are focused in the Sichuan basin and Yangtze platform areas and led by PetroChina, Sinopec, and Shell. The government has set an ambitious target for shale gas production of 5.8 to 9.7 bcfd by 2020.

For the complete details on China, refer to the US EIA/ARI 2013 report.

4.4.6 Mexico

Mexico has excellent potential for developing its shale oil and shale gas resources stored in marine-deposited, source-rock shales distributed along the onshore Gulf of Mexico region (**Fig. 4.40**).

Technically recoverable shale resources, estimated at 545 Tcf of natural gas and 13.1 bbl of oil and condensate, are potentially larger than the country's proven conventional reserves. The best-documented play is the Eagle Ford shale of the Burgos basin. Here oil- and gas-prone windows extend south from Texas into northern Mexico and have an estimated 343 Tcf and 6.3 bbl of risked, technically recoverable shale gas and shale oil resource potential.

Further to the south and east in Mexico, the shale geology of the onshore Gulf of Mexico basin becomes structurally more complex and the shale development potential is less certain. The Sabinas basin has an estimated 124 Tcf of risked, technically recoverable shale gas resources within the Eagle Ford and La Casita shales, but the basin is faulted and

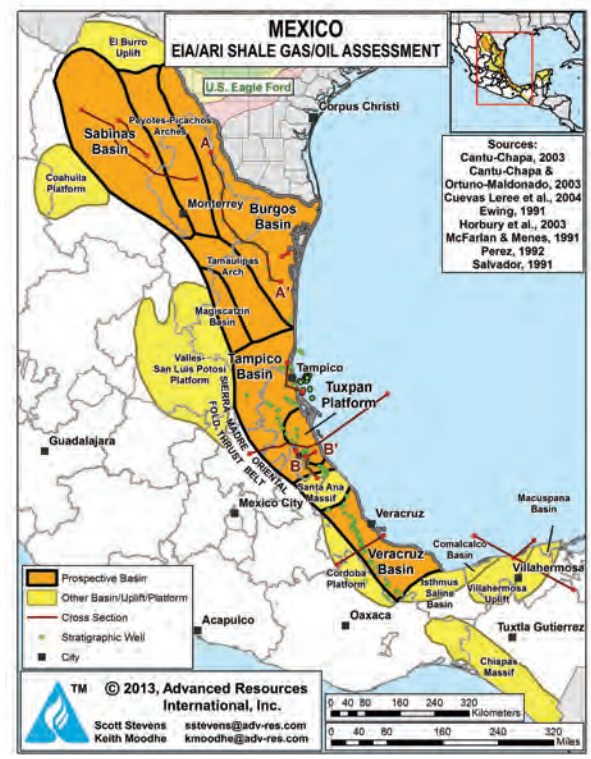

Fig. 4.40—Onshore shale oil and shale gas basins of eastern Mexico's Gulf of Mexico basins. (Source: ARI 2013.)

folded. The structurally more favorable Tampico, Tuxpan, and Veracruz basins add another 28 Tcf and 6.8 bbl of risked, technically recoverable shale oil and shale gas potential from Cretaceous and Jurassic marine shales. These shales are prolific source rocks for Mexico's conventional onshore and offshore fields in this area. As of mid 2015, shale drilling has been planned and the first drilling pad is in progress in these southern basins.

PEMEX envisions commercial shale gas production being initiated in 2015 and increasing to around 2 bcfd by 2025, with the company potentially investing USD one billion to drill 750 wells (EIA 2014). However, PEMEX's initial shale exploration wells have been costly at USD 20 to 25 million per well and have provided only modest initial gas flow rates at approximately 3 MMcfd per well with steep decline. Mexico's potential development of its shale gas and shale oil resources could be constrained by several factors including potential limits on upstream investment, the nascent capabilities of the local shale service sector, and public security concerns in many shale areas.

For the complete details on Mexico, refer to the US EIA/ARI 2013 report.

4.4.7 Northern and Western Europe

Numerous shale gas basins and formations exist in northern and western Europe. Five of the more prominent of these shale basins and formations are the Paris and South-East basins in France, the Lower Saxony basin in Germany, the West Netherland basin in the Netherlands, and the Alum shales underlying Scandinavia (**Fig. 4.41**).

The risked shale gas in-place for the five northern and western European shale basins addressed by this study may be 1,165 Tcf, with 221 Tcf as the risked, technically recoverable shale gas resource. These five shale basins may contain 190 bbl of risked shale oil in-place, with 8.3 bbl as the risked, technically recoverable shale oil resource (**Table 4.18**).

For the complete details on northern and western Europe, refer to the US EIA/ARI 2013 report.

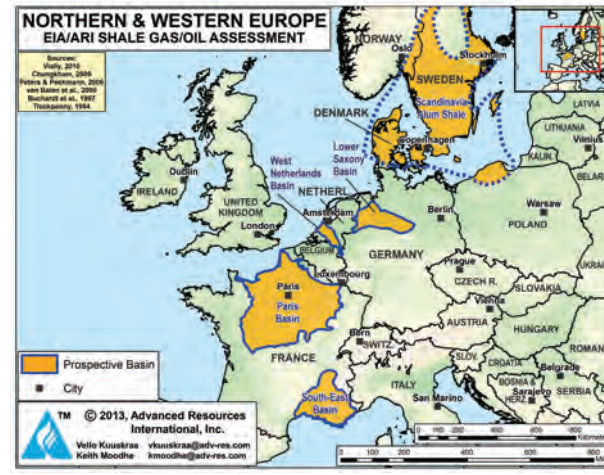

Fig. 4.41—Prospective shale basins of northern and western Europe. (Source: ARI 2013.)

4.4.8 Poland

Poland has some of Europe's most favorable infrastructure and public support for shale development. The Baltic basin in northern Poland remains the most prospective region with a relatively simple structural setting. The Podlasie and Lublin basins have potential but are structurally complex, with closely spaced faults that may limit horizontal shale drilling. The

Table 4.18—Shale gas and shale oil resources of northern and western Europe. (ARI 2013.)

	Risked Shale Gas Resources		Risked Shale Oil Resources	
Basin/Formation	**In-Place (Tcf)**	**Technically Recoverable (Tcf)**	**In-Place (B bbl)**	**Technically Recoverable (B bbl)**
Paris Basin (France)				
• L. Jurassic Lias	23.8	1.9	38.0	1.52
• Permian-Carboniferous	666.1	127.3	79.5	3.18
Total	689.9	129.3	117.5	4.70
South-East Basin (France)				
• L. Jurassic Lias	37.0	7.4	0.0	0.00
Total	37.0	7.4	0.0	0.00
Lower Saxony Basin (Germany)				
• Toarcian Posidonia	77.7	16.9	10.6	0.53
• Wealden	1.8	0.1	3.2	0.13
Total	79.5	17.0	13.8	0.66
West Netherlands Basin (Netherlands)				
• Namurian Epen	93.7	14.8	47.1	2.35
• Namurian Geverik	50.6	10.1	6.3	0.32
• Toarcian Posidonia	6.8	1.0	5.4	0.27
Total	151.1	25.9	58.8	2.94
Alum Shale				
• Denmark	158.6	31.7	0.0	0.00
• Sweden	48.9	9.8	0.0	0.00
Total	207.5	41.5	0.0	0.00
Total	**1,165.1**	**221.0**	**190.0**	**8.29**

Fig. 4.42—Location of assessed shale basins in Poland. (Source: EIA/ARI 2013, modified from San Leon Energy 2012.)

Fore-Sudetic Monocline in southwest Poland is less recognized but has non-marine coaly shale potential similar to Australia's Cooper basin (**Fig. 4.42**).

Poland's risked, technically recoverable shale resources are estimated at 146 Tcf of shale gas and 1.8 bbl of shale oil in four assessed basins. Lithuania adds 0.4 Tcf and 0.3 bbl of risked, technically recoverable shale oil and shale gas resources. Kaliningrad adds 2.0 Tcf and 1.2 bbl of risked, technically recoverable shale oil and shale gas resources. Initial exploration confirmed the shale resource potential but suggests that reservoir conditions are more challenging than originally anticipated. New data collected since the 2011 resource assessment resulted in a 20% reduction in the EIA/ARI estimate of Poland's shale resources, on an energy-equivalent basis.

For the complete details on Poland, refer to the US EIA/ARI 2013 report.

4.4.9 United Kingdom

The United Kingdom has substantial volumes of prospective shale oil and shale gas resources within Carboniferous- and Jurassic-age shale formations distributed broadly in the northern, central, and southern parts of the country.

The risked, technically recoverable shale resources of the UK are estimated at 26 Tcf of shale gas and 0.7 bbl of shale oil and condensate in two assessed regions. This is based on the much larger, unrisked estimates of 623 Tcf of shale gas in-place (134 Tcf, risked) and 54 bbl of shale oil in-place (17 bbl, risked). These estimates reflect only the higher TOC portions of the Carboniferous and Jurassic shale intervals.

Initial exploration drilling confirmed the presence of thick, gas-bearing shale deposits in the Bowland sub-basin in the western part of the Pennine basin of northwest England. However, production testing has not occurred yet, and the other shale regions remain undrilled. EIA/ARI's current estimate of the UK's shale gas resources is about 10% higher than the initial 2011 assessment, while new shale oil potential has been added.

Compared with North America, the shale geology of the UK is considerably more complex, while drilling and completion costs for shale wells are substantially higher. The Pennine basin, one of the country's most prospective areas, has been tested with five vertical wells that cored the Carboniferous Bowland shale. Other prospective areas include the rest of the North UK Carboniferous shale region and the liquids-rich Jurassic shale region of southern England in the Wessex and Weald basins (**Fig. 4.43**).

Shale testing is at an early phase in the UK; flow testing and horizontal shale drilling have not been attempted. In

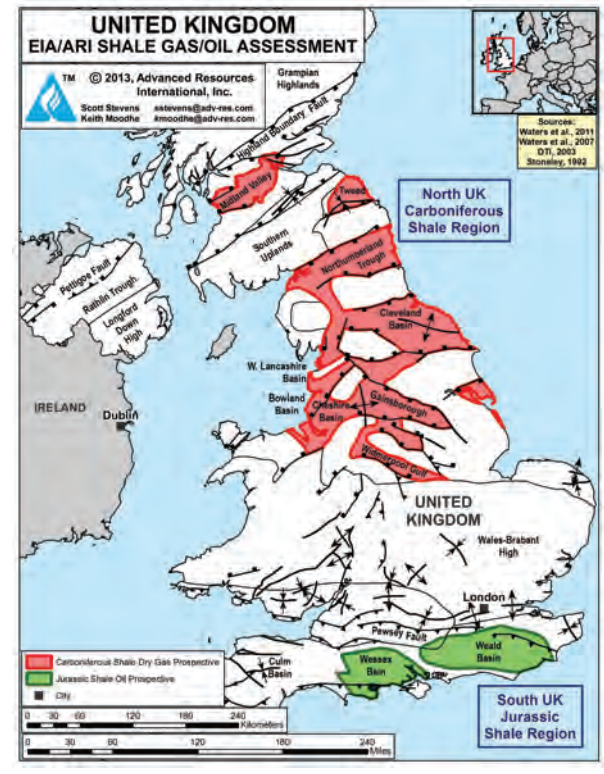

Fig. 4.43—Shale basins in the United Kingdom. (Source: Ari 2013.)

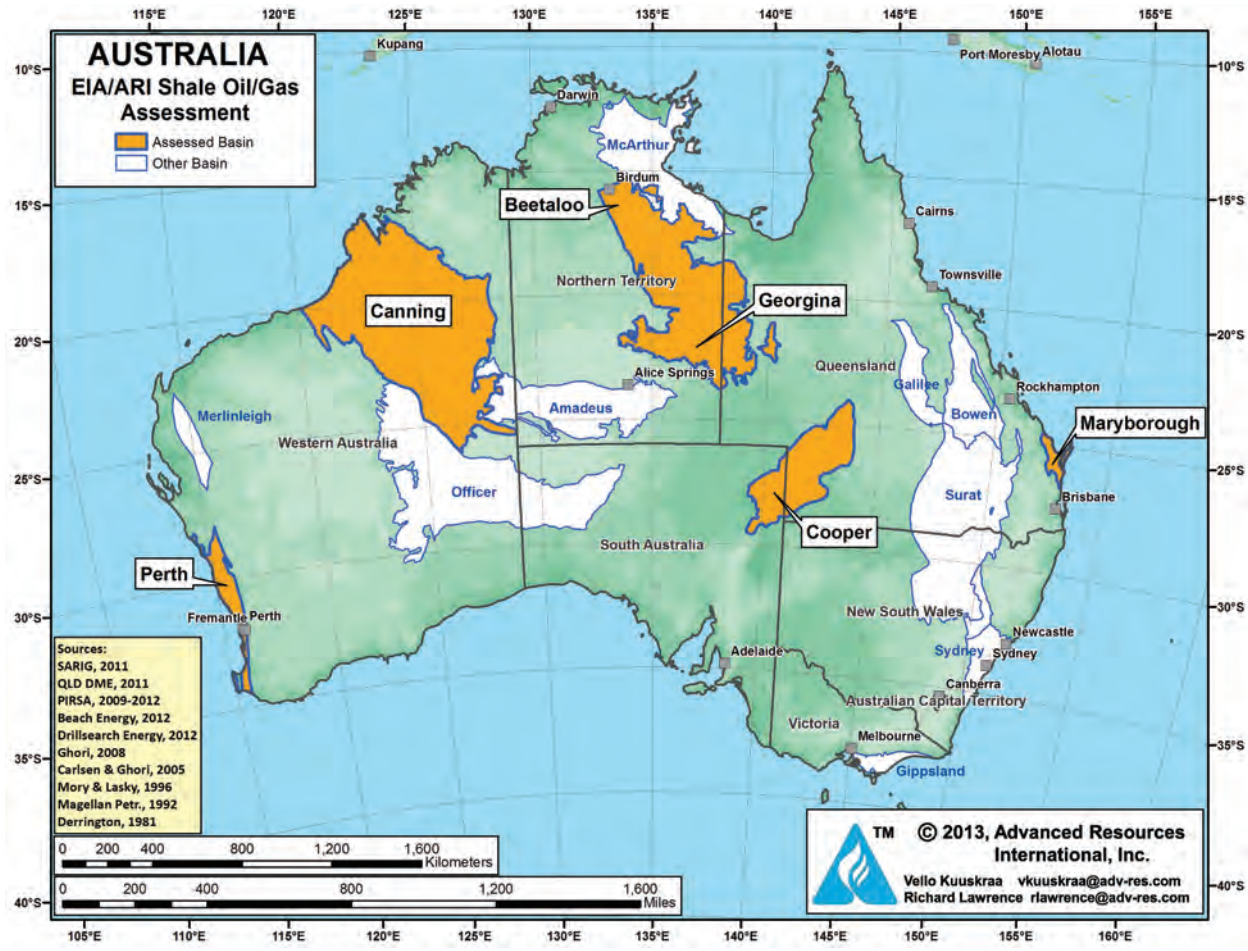

Fig. 4.44—Australia's assessed prospective shale oil and shale gas basins. (Source: Ari 2013.)

a temporary setback, the first shale well to be hydraulically stimulated triggered a series of minor earthquakes related to a nearby fault. Following an 18-month moratorium, the government concluded that the environmental risks of shale exploration are small and manageable. Shale drilling was allowed to resume in December 2012, albeit with stricter monitoring controls. Current shale operators include Cuadrilla Resources, IGAS, Dart Energy, and others.

For the complete details on the United Kingdom, refer to the US EIA/ARI 2013 report.

4.4.10 Australia

With geologic and industry conditions resembling those of US and Canada, Australia has the potential to be one of the next countries with commercially viable shale oil and shale gas production. As in the US, small independents have led the way, assembling the geological data and exploring the high potential shale basins of Australia (**Fig. 4.44**). International majors now are entering these plays by forming joint venture (JV) partnerships with these smaller independents and bring capital investment to the table. However, with the remoteness of many of Australia's shale oil and shale gas basins, development probably will proceed at a moderate pace.

Here, we assess the shale oil and shale gas potential in six major Australian sedimentary basins that have sufficient geologic data for a quantitative assessment. Additional potential probably exists in other basins but is not yet assessed.

The six assessed shale oil and shale gas basins of Australia hold an estimated 2,046 Tcf of risked shale gas in-place, with 437 Tcf as the risked, technically recoverable shale gas resource. These six basins hold an estimated 403 bbl of risked shale oil in-place, with 17.5 bbl as risked, technically recoverable shale oil resource.

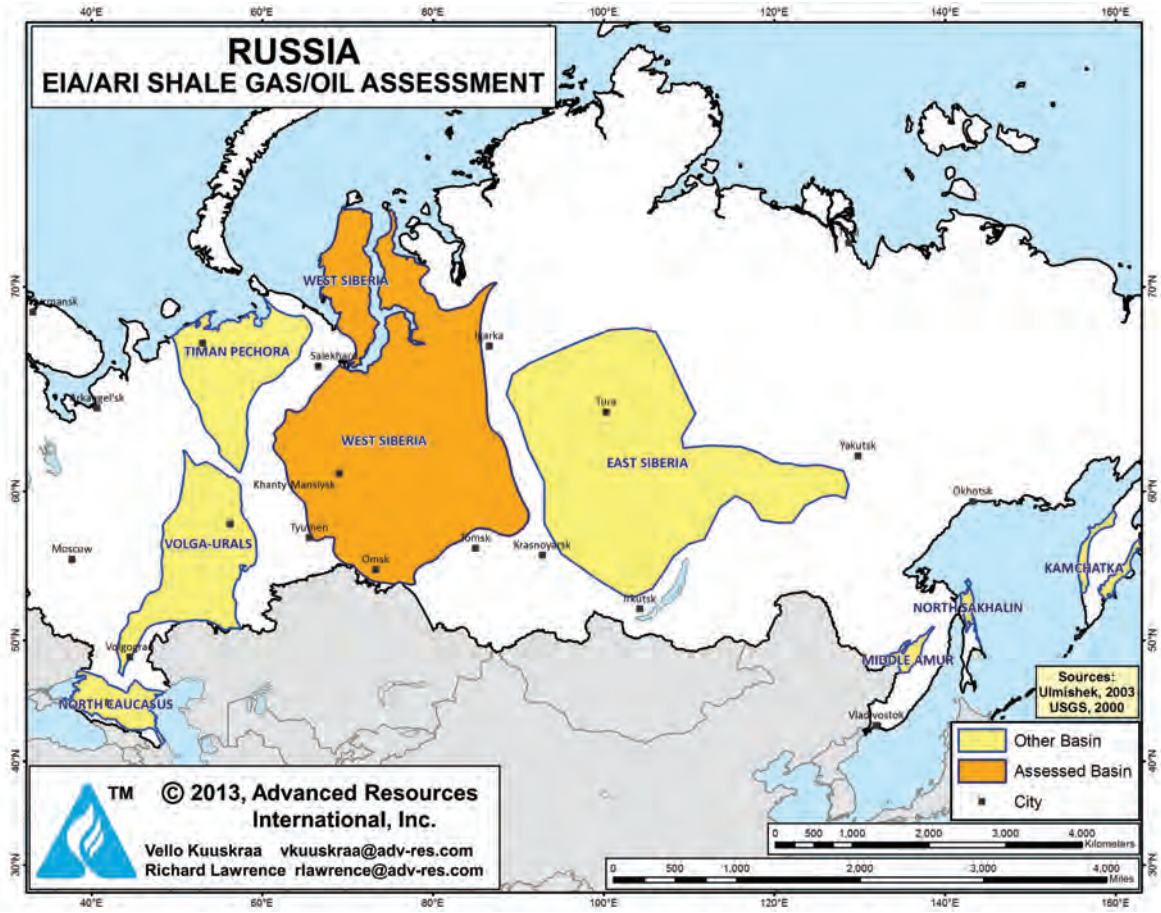

Fig. 4.45—Prospective shale oil and shale gas basins of Russia. (Source: ARI 2013.)

Of the six assessed basins, the Cooper basin, Australia's main onshore gas-producing basin, with its existing gas processing facilities and transportation infrastructure, could be the first commercial source of shale hydrocarbons. The basin's Permian-age shales have non-marine (lacustrine) deposition, and the shale gas appears to have elevated carbon dioxide content. Both factors add risk to these shale oil and shale gas plays. Santos, Beach Energy, and Senex Energy are testing the shale reservoirs in the Cooper basin. Initial results,as of mid 2015, from vertical production test wells provide encouragement for further delineation into horizontal lateral placement.

The other prospective Australian shale basins addressed here include the small, scarcely explored Maryborough basin in coastal Queensland. This basin contains prospective Cretaceous-age marine shales thought to be over-pressured and gas saturated. The Perth basin in western Australia, undergoing initial testing by AWE and Norwest Energy, has prospective marine shale targets of Triassic and Permian age. The large Canning basin in western Australia has deep, Ordovician-age marine shales that are roughly correlative with the Bakken shale in the Williston basin. In Northern Territory, the Pre-Cambrian shales in the Beetaloo basin and the Middle Cambrian shale in the Georgina Basin have reported oil and gas shows in shale exploration wells. If proved commercial, these two shale oil and shale gas basins would be some of the oldest producing hydrocarbon source rocks in the world.

For the complete details on Australia, refer to the US EIA/ARI 2013 report.

4.4.11 Russia

Our shale gas and shale oil resources assessment for Russia addresses the Upper Jurassic Bazhenov shale in the West Siberian basin (**Fig 4.45**). This organically rich, siliceous shale is the principal source rock for the conventional gas and oil produced from the West Siberian basin. We examined

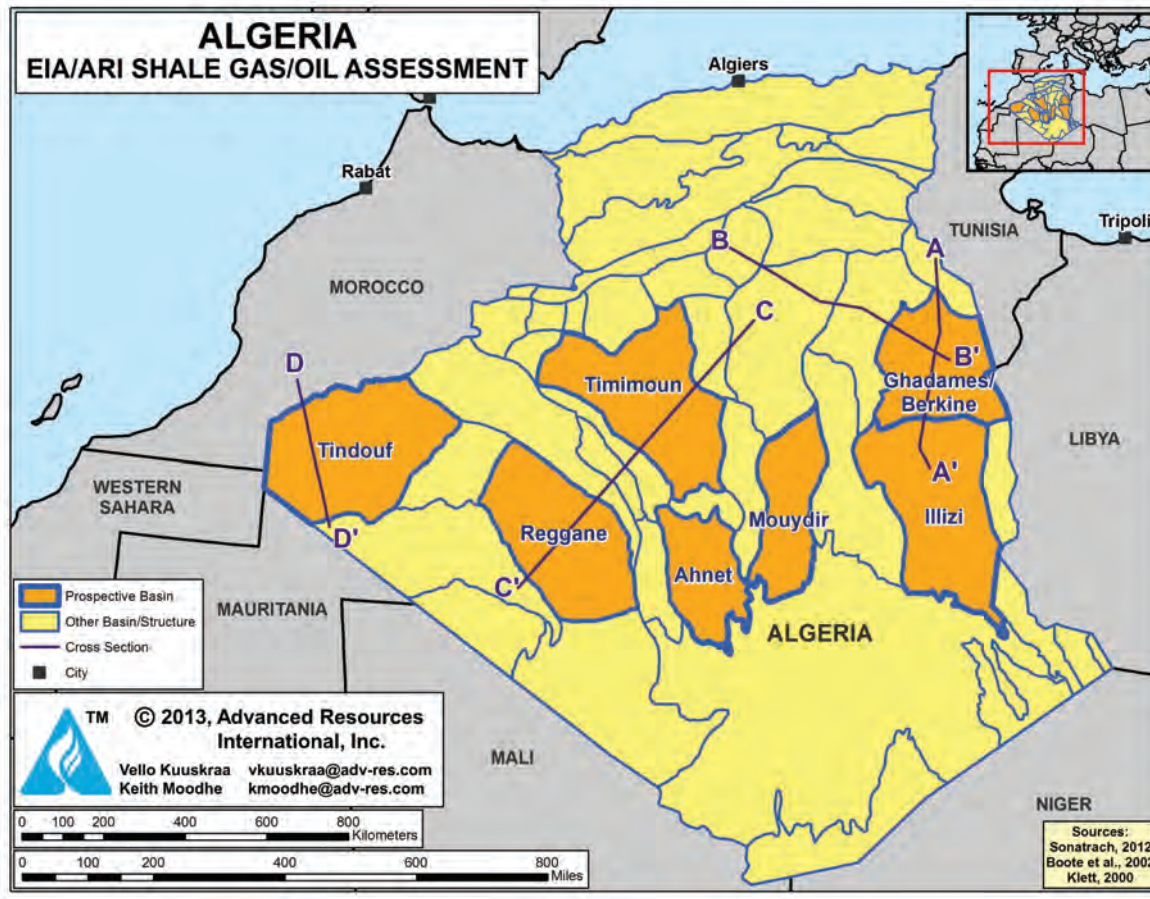

Fig. 4.46—Shale oil and shale gas basins of Algeria. (Source: ARI 2013.)

other shale basins such as the Timan-Pechora but were not able to assemble sufficient, publicly available data for a quantitative resource assessment.

For the Bazhenov shale, we estimate 1,243 bbl of risked shale oil in-place, with 74.6 bbl as the risked, technically recoverable shale oil resource. In addition, we estimate 1,920 Tcf of risked shale gas in-place, with 285 Tcf as the risked, technically recoverable shale gas resource.

For the complete details on Russia, refer to the US EIA/ARI 2013 report.

4.4.12 Algeria

Algeria's hydrocarbon basins hold two significant shale oil and shale gas formations, the Silurian Tannezuft shale and the Devonian Frasnian shale. This study examines seven of these shale oil and shale gas basins: the Ghadames (Berkine) and Illizi basins in eastern Algeria; the Timimoun, Ahnet, and Mouydir basins in central Algeria; and the Reggane and Tindouf basins in southwestern Algeria (**Fig. 4.46**).

The seven basins contain approximately 3,419 Tcf of risked shale gas in place, with 707 Tcf as the risked, technically recoverable shale gas resource. Six of these basins hold 121 bbl of risked shale oil and condensate in place, with 5.7 bbl as the risked, technically recoverable shale oil resource.

For the complete details on Algeria, refer to the US EIA/ARI 2013 report.

4.4.13 Tunisia

Tunisia has two significant formations with potential for shale oil and shale gas: the Silurian Tannezuft hot shale and the Upper Devonian Frasnian shale. These shale formations are in the Ghadames basin, of southern Tunisia. Additional

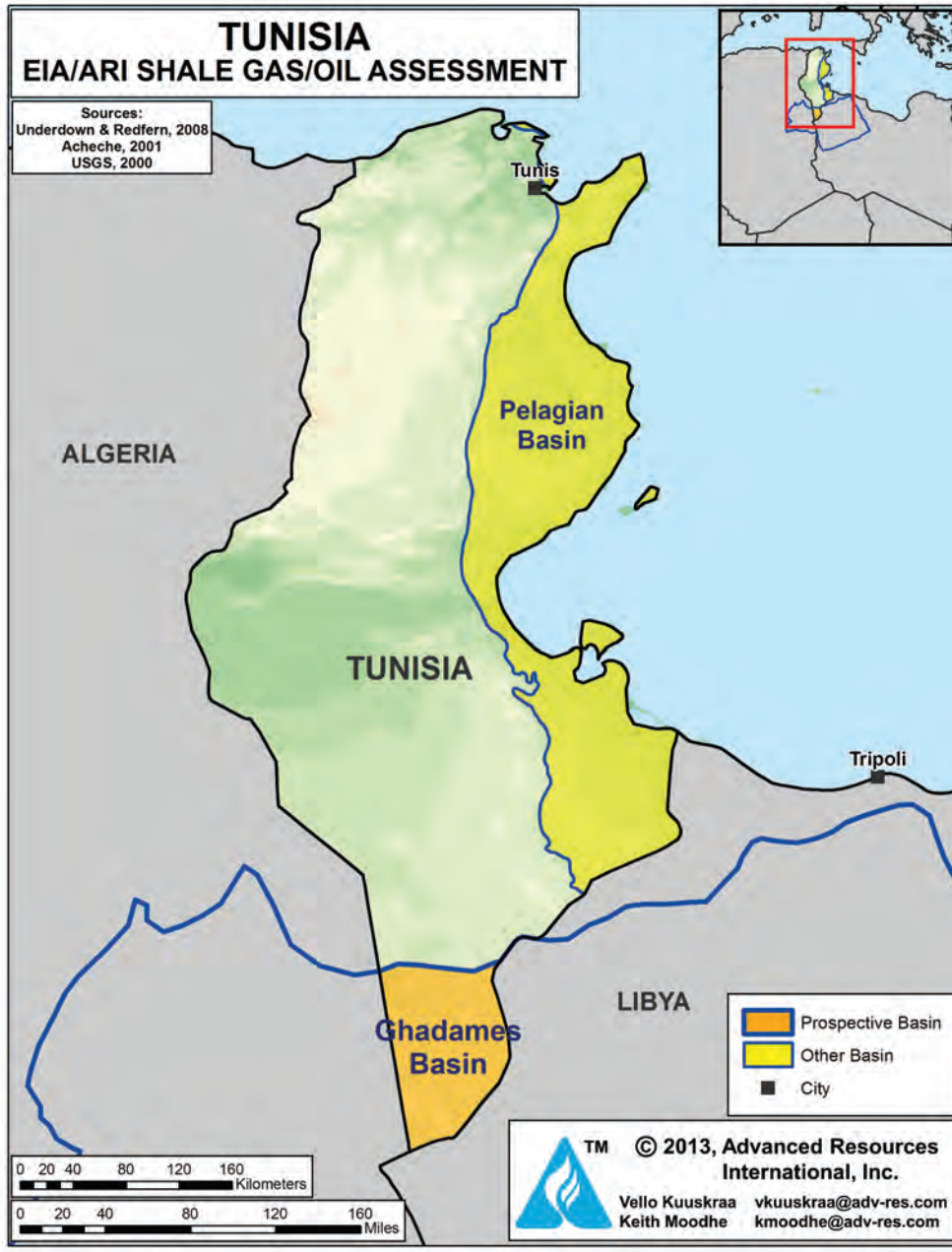

Fig. 4.47—Tunisia's shale oil and shale gas basins. (ARI 2013.)

shale oil and shale gas potential may exist in the Jurassic-Cretaceous and Tertiary petroleum systems in the Pelagian basin of eastern Tunisia (**Fig. 4.47**).

Our assessment is that the Tannezuft and Frasnian shale formations in the Ghadames basin contain 114 Tcf of risked shale gas in-place, with 23 Tcf as the risked, technically recoverable shale gas resource. These two shale formations contain 29 bbl of risked shale oil in place, with 1.5 bbl as the risked, technically recoverable shale oil resource.

For the complete details on Tunisia, refer to the US EIA/ARI 2013 report.

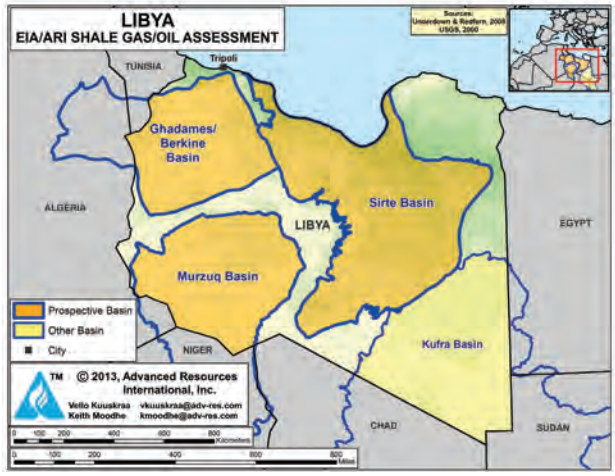

Fig. 4.48—Shale oil and shale gas basins of Libya. (Source: ARI 2013.)

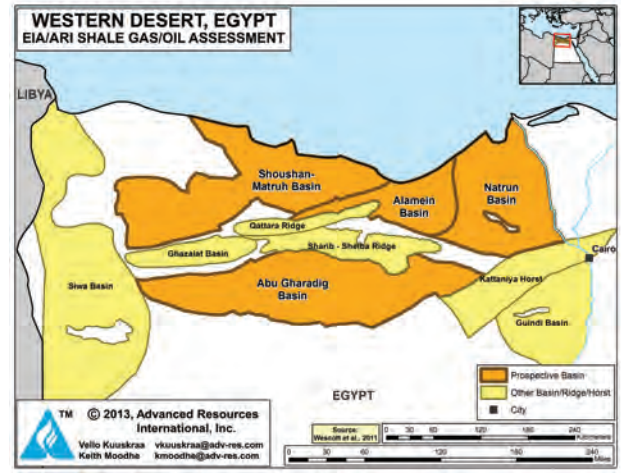

Fig. 4.49—Hydrocarbon basins of the Western Desert in Egypt. (Source: ARI 2013.)

4.4.14 Libya

This shale gas and shale oil resource assessment addresses three of Libya's major hydrocarbon basins: the Ghadames (Berkine) basin in the west, the Sirte basin in the center, and the Murzuq basin in the southwest of the country (**Fig. 4.48**). The Kufra basin in the southeast is not assessed quantitatively due to the speculative and limited nature of the available data.

The three basins in Libya contain approximately 942 Tcf of risked shale gas in-place, with 122 Tcf as the risked, technically recoverable shale gas resource. The shale formations in these three basins also contain 613 bbl of risked shale oil and condensate in place, with 26.1 bbl as the risked, technically recoverable shale oil resource.

For the complete chapter on Libya, refer to the US EIA/ARI 2013 report.

4.4.15 Egypt

Egypt has four basins in the Western Desert with potential for shale gas and shale oil: Abu Gharadig, Alamein, Natrun, and Shoushan-Matruh (**Fig. 4.49**). The target horizon is the organic-rich Khatatba shale, also called the Kabrit shale or Safa shale, and is within the larger Middle Jurassic Khatatba formation.

The Khatatba shale contains approximately 535 Tcf of risked shale gas in place, with 100 Tcf of risked, technically recoverable shale gas resources. The Khatatba shale contains about 114 bbl of risked shale oil in-place, with 4.6 bbl of risked, technically recoverable shale oil resources.

For the complete chapter on Egypt, refer to the US EIA/ARI 2013 report.

4.4.16 Middle East

The US EIA/ARI 2013 report did not include some countries, most notably those in the Middle East. Therefore, another reference (Hart Energy Research Group, 2011) provided this information. The Middle East has some of the most prolific petroleum basins in the world and, within them are rich source rocks, many of which could be developed into high-quality shale gas plays. These major petroleum basins in the Middle East with shale gas potential are shown on the map (**Fig. 4.50**).

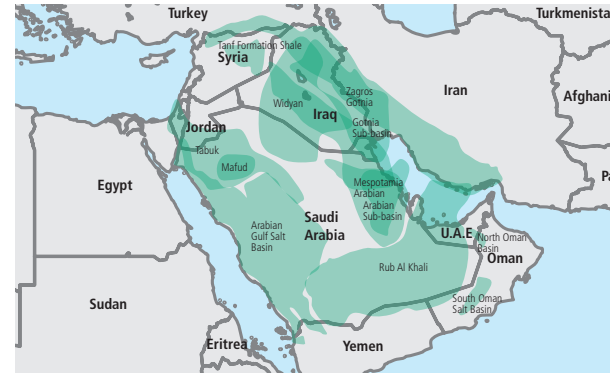

Fig. 4.50—Petroleum basins with shale gas resources in the Middle East. (Source: Hart Energy Research Group, 2011.)

These petroleum systems are found in the Greater Arabian Gulf basin, the Zagros Fold Belt, the Mesopotamian Foredeep, the Rub Al Khali, and Widyan basins. Smaller sub-basins are located in Oman, Syria, Iran, and Iraq. Major source rocks were deposited in the Silurian, Triassic-Jurassic, and Cretaceous periods. Although the Hart Report includes a detailed discussion of geology and geochemistry, it does not attempt to assess or assign TRR to any of the Middle East basins or countries.

For the complete report, refer to Global Shale Gas Study by the Hart Energy Research Group, HARTENERGY.

4.4.17 Other Basins

For the complete report, including additional basins such as in Spain, Eastern Europe, Morocco, South Africa, Mongolia, India, Pakistan, Indonesia, Jordan, Thailand, and Turkey, among others, see the US EIA/ARI 2013 report.

It appears that the unconventional resources technology in North America can be applied globally with some exceptions as needed to accommodate the local requirements and any divergence of rock properties.

4.5 References

AAPG Explorer. November 2012.

Advanced Resources International Inc. (ARI) 2013. EIA/ARI World Shale Gas and Shale Oil Resource Assessment. http://www.adv-res.com/pdf/A_EIA_ARI_2013 World Shale Gas and Shale Oil Resource Assessment.pdf (accessed June 2014).

Baker Hughes http://eo2.commpartners.com/users/spe/downloads/131009_Presentation_Slides.pdf

Drilling Information Database. http://info.drillinginfo.com (accessed July 2014).

EIA. 2011. Review of Emerging Resources: U.S. Shale Gas and Shale Oil Plays, July 2011. http://www.eia.gov/analysis/studies/usshalegas/pdf/usshaleplays.pdf (accessed July 2014).

EIA. 2013. Technically Recoverable Shale Oil and Shale Gas Resources: An Assessment of 137 Shale Formations in 41 Countries Outside the United States. http://www.eia.gov/analysis/studies/worldshalegas/pdf/fullreport.pdf (accessed June 2014).

EIA. 2013. EIA/ARI World Shale Gas and Shale Oil Resource Assessment, http://www.eia.gov/analysis/studies/worldshalegas/pdf/fullreport.pdf?zscb=84859470 (accessed July 2014).

Harper, J. 2008. The Marcellus shale–An old new gas reservoir in Pennsylvania. ***Pennsylvania Geology*** (special issue) **38** (1): 2–13.

Hart Energy Research Group, 2011. Global Shale Gas Study, http://www.hartenergy.com/Upstream/Research-And-Consulting/Global-Shale-Gas-Study/GSGS_TOC_detailed.pdf (accessed July 2014).

Kennedy, R.L., Knecht, W.N., and Georgi, D.T. 2012. Comparisons and Contrasts of Shale Gas and Tight Gas Developments, North American Experience and Trends. Paper SPE 160855 presented at the Saudi Arabia Section Technical Symposium and Exhibition. 8–11 April. Al-Khobar, Saudi Arabia. http://dx.doi.org/10.2118/160855-MS.

Lafollette, R., Holcomb, W.D. and Aragon, J. 2012. Practical Data Mining: Analysis of Barnett Shale Production Results with Emphasis on Well Completion and Fracture Stimulation. Paper SPE 152531 presented at the SPE Hydraulic Fracturing Technology Conference. 6–8 February. The Woodlands, Texas. DOI: http://dx.doi.org/10.2118/152531-MS.

Meissner, F.F. 1978. Petroleum Geology of the Bakken Formation, Williston Basin, North Dakota and Montana. In D. Rehig, (ed.), The economic geology of the Williston Basin: Proceedings of the Montana Geological Society, 24th Annual Conference. p. 207–227.

National Energy Board Canada. 2009. ***A Primer for Understanding Canadian Shale Gas Plays***. Calgary, Alberta, Canada. November.

Natural Gas Intelligence. http://www.naturalgasintel.com/shalemap.

Oil and Gas Finance Journal website. http://www.ogfj.com/unconventional/niobrara-play-map.html (accessed June 2014).

Rowan, E.L. 2006. Burial and thermal history of the central Appalachian basin, based on three 2-D models of Ohio, Pennsylvania, and West Virginia: U.S. Geological Survey. *Open File Report* 2009–1019, 35.

San Leon Energy, 2012. Annual Records and Accounts. http://www.sanleonenergy.com/media/631659/san-leon-ar12.pdf (accessed July 2014).

Walker, B., Powell, A., Rollins, D., et al. 2006. Elm Coulee Field Middle Bakken Member (Lower Mississippian/Upper Devonian) Richland County, Montana. Search and Discovery Article 20041 adapted from presentation at the 2006 AAPG Rocky Mountain Section meeting. 11–13 June. Billings, Montana.

Warlick International 2009. North American Unconventional Gas Market Report. Edition 1 of 2. http://www.scribd.com/doc/20603184/Unconventional-Gas-Report-Edition-1-Special-Sample (accessed June 2014).

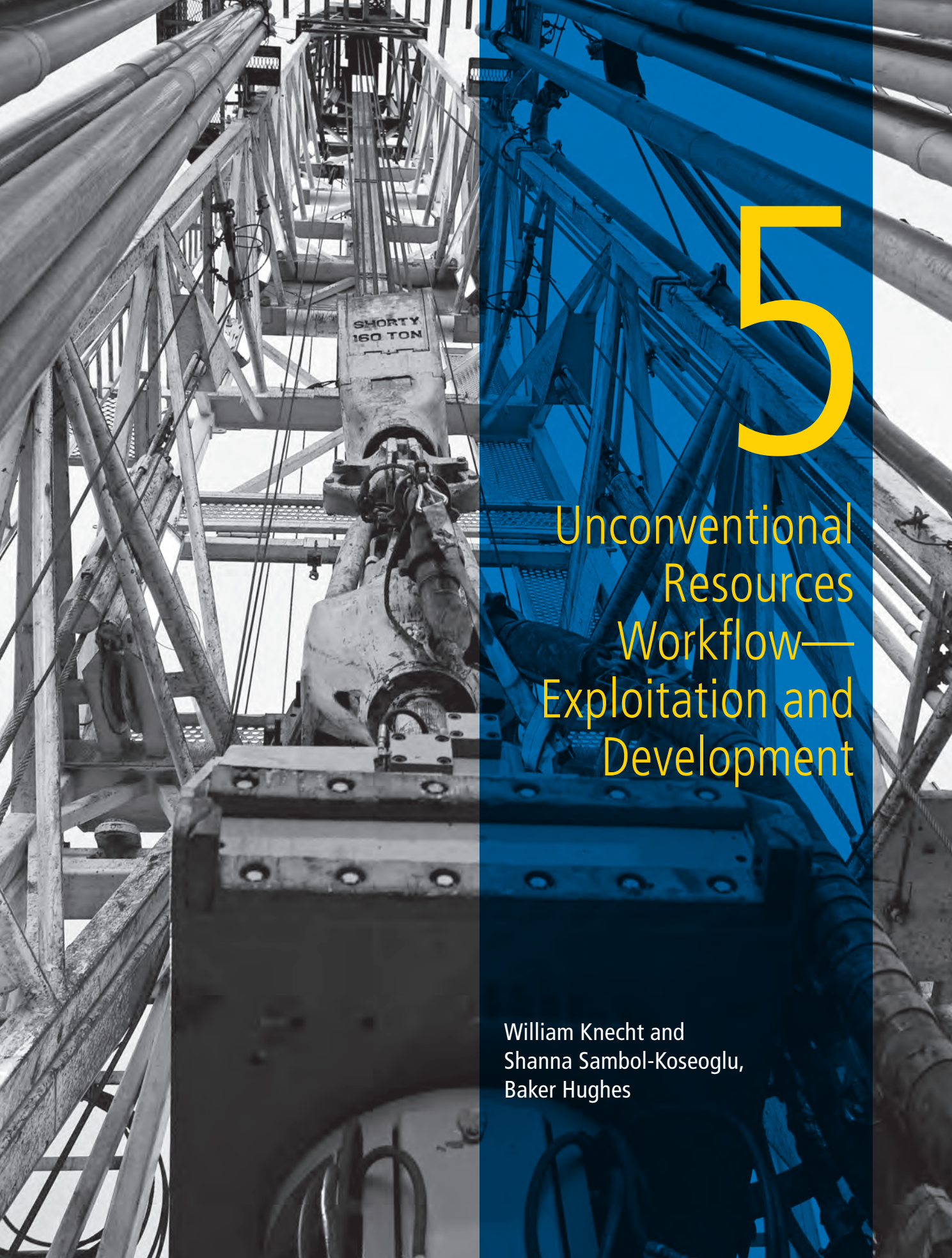

5

Unconventional Resources Workflow—Exploitation and Development

William Knecht and
Shanna Sambol-Koseoglu,
Baker Hughes

This page intentionally left blank

Chapter 5: Unconventional Resources Workflow—Exploitation and Development

Foreword

This chapter is a compilation of work by the Baker Hughes Center of Reservoir Excellence (CORE) team during the development of the data-driven approach to informed solutions.

5.1 Introduction

Over the past decade, significant supplies of natural gas, natural gas liquids, and oil have been discovered in unconventional reservoirs. During this time, the industry has developed technology that has provided the capability to drill longer laterals and complete more stages during the development of these reservoirs in onshore US sedimentary basins. Although the development of new technologies has driven down the cost of extraction, pursuing hydrocarbons in unconventional reservoirs continues to be risky and capital intensive.

Applying a data-driven, life-cycle workflow approach that encompasses upfront reservoir evaluation with well planning can provide more complete understanding of the reservoir. That insight can help operators to align engineering imperatives with project objectives across each phase of development. This approach can help operators to ensure they are using the most effective techniques with only the technology required to engage in continuous performance.

This chapter will discuss this approach in detail and outline the challenges of unconventional resource development, provide some solutions to address those challenges, and highlight the value the solutions contribute to unconventional resource development while they balance efficiency with effectiveness.

5.2 Workflows in Unconventional Resource Development

Unconventional resource development is capital intensive, mainly due to the large number of wells required to develop the oil and gas reserves. Development requires input from many disciplines and the application of the right technology. What ties all of this together? It is the workflow that integrates people, processes, and technologies, by combining and describing all the parts that are included in any activity Most workflows indicate the types of tasks needed to reach the goal, list the inputs that are required, describe any decision points, and provide the outputs that are expected, for example. Larger workflows can also incorporate smaller ancillary workflows as a way to manage and understand discrete activities, like services that are related to, or necessary for, the main workflow.

5.3 Challenges and Background

There are many challenges to be overcome in unconventional resource exploration and development from North America to international locations. Geology differs radically just within single play areas, and international locations are no different. In both areas, determining and understanding subsurface conditions before development begins is a main predictor of success during the exploitation and development of the shale oil and gas fields, no matter the location.

5.3.1 North American Challenges

In North America, the geological, geomechanical, geochemical, and petrophysical characteristics in shale vary considerably across short distances—both vertically and laterally. The variability of mineralogy, total organic content, thermal maturity, porosity, stress orientations and the presence of natural fractures have a direct affect on the ultimate resource recovery. Often, very little emphasis is placed on reducing subsurface uncertainty. Instead of gathering pertinent reservoir data for well control, operators rely heavily on offset data to economically appraise prospect-drilling locations, determine horizontal well placement and design fracture operations. This strategy has proven to be only partially effective.

Recent studies (Welling and Company 2012; Hart Energy E & P Magazine 2012) of US shale plays reported that as much as 60% of fracture stages that are developed contribute to production, with the remaining 40% of the fracture stages contributing little, if any, production at all. Accordingly, 73% of operators admitted they didn't know enough about the subsurface to develop an effective fracture design.

Unconventional resource development is capital intensive and, as a result, operators need to have immediate cash flow. Many operators are already hard-pressed for time and money as they ramp up for a well-intensive development

program. A pilot program to obtain much needed reservoir data takes time, and the required technologies can increase initial capital expenditures.

A common practice is to avoid logging altogether and rely instead on "statistical drilling" (placing a horizontal well every 200 to 300 feet regardless of vertical and lateral heterogeneity) and "geometric fracturing" (evenly spacing stages along the lateral). In fact, less than 10% of the 15,000 horizontal wells drilled annually in the US are logged (SPE Applied Technology Workshop 2012). Statistical drilling practices have led to many wells being placed and completed in reservoir intervals with unfavorable mineralogy, rock properties producibility—contributing to lower-than-expected production performance and unnecessary costs related to excessive stage placement, horsepower, and proppant. These practices can lead to production that is inconsistent or lower than expected.

Could inconsistent production be a direct result of poorly placed wells and fracture design? Is it possible to reduce commercial and technical risk by gaining a better understanding of shale's unique reservoir properties? If it is possible, can we predict and offset the factors that can prevent profitability?

5.3.2 International Challenges

Shale gas and tight oil development is becoming a more significant part of the global energy exploration and development mix. Many operators that are entering the global arena face many more complications than just higher development costs. In some countries, mineral rights are owned by the state. To develop shale plays in these locations, operators must navigate foreign governments' rules and regulations for buying, selling, or trading the land used for development. Operators also have to face the possibility of entering into a mandatory "partnership" with a state-owned enterprise, if the operator is to be allowed to develop at all. Add scarce subsurface data, difficult terrain, and limited experience, and you can see how international shale development could be very challenging for the unprepared.

Conditions in North American exploration and development are somewhat simpler. Mineral resources in the US are mostly owned privately by individuals or corporations, which means that mineral rights are often leasable from non-government entities, and terms and conditions for use of those mineral rights can be negotiated. Leases on offshore and onshore US federal lands tend to be by fixed lease secured by a competitive bidding process. In Canada, the Canadian Crown land is government owned, but there is still much freehold acreage in Canada. Globally, difficult terrains, such as mountains and deserts, are more the norm, as is development in densely populated areas. These factors alone can increase the level of difficulty, but significant risks are involved as well, due to lack of data about the reservoirs of interest. In underdeveloped fields where reservoir properties are not well defined, acquiring sufficient reservoir data is imperative to identify commercially viable prospects. In addition, effective exploration requires seismic acquisition and a number of wells to prove the existence of hydrocarbons. This is the best way to determine if the hydrocarbons are recoverable in a way that is economical.

To meet these challenges, assessing geological, geomechanical, petrophysical, and geochemical properties on a regional level and near the wellbore to identify sweet spots can help to determine economic value and higher production potential. This can save operators considerable amount of unnecessary time and investment.

Additional wells are also required to establish an effective combination of engineering techniques. Operators look to integrated service providers who are capable of transferring the knowledge and experience acquired developing these plays, as well as those who understand the technologies and techniques needed to increase productivity while driving down operational cost and maximizing efficiency.

5.4 The Common Solution

5.4.1 Oversimplified Approach

Production performance is highly dependent on accurately placing horizontal wells and fracture stages in reservoir intervals that have quality rock properties and good production potential. However, because many operators don't characterize the reservoir, they drill and stimulate blindly. Many don't understand the reservoir's fracture capability (shale brittleness, stress, and clay content) or if their wells were placed in organic-rich (high total organic content or hydrocarbons) zones. Without evaluating the reservoir, operators can't place wellbores in the most productive zones, selectively fracture the zones with the most production potential. These practices inhibit building an effective design for stimulation treatment that can prevent costly fracture-related consequences like higher-than-normal treatment pressure, screen-outs, and fracturing into offset wells and hazards. Additionally, without reservoir evaluation, there is no opportunity to improve stimulation effectiveness in real time and for future wells. The result is a higher cost for completions, lower initial production and recovery, and drilling more wells than necessary to penetrate enough sweet spots to make the development economic.

5.4.2. Reservoir Characterization during Exploration and Appraisal

Characterizing the reservoir takes time. The required services (geoscience analysis) and technologies (logging and coring applications) increase initial capital expenditures, so operators rely heavily on 2D seismic plus any available offset logging and coring data to identify prospective drilling locations.

Without proper reservoir data, operators depend on "statistical drilling" (placing a horizontal well every 100 to 120 acres regardless of vertical and lateral heterogeneity) and "geometric fracturing" (evenly spacing stages along the lateral).

5.4.3 Horizontal Drilling and Evaluation

Operators choose to drill with mud motors because they are cheaper than rotary steerable systems (RSS). In the Welling Report Worldwide Survey of the Market for Rotary Steerable Systems, 2012 edition, price was mentioned by 97% of respondents as a factor preventing them from using rotary steerable systems. Although mud motors are cheaper, a RSS drills a smooth, quality borehole in less time, which can reduce the long-term cost. Using an RSS also makes it easier to run casing and wireline logs, as well as intelligent completions, by reducing tortuosity (typically caused by mud motors). Less time drilling is more money in the operator's pocket.

About one-third (33%) of the world's largest oil and gas companies agree that an integrated drilling system provides a higher level of performance for more precise wellbore positioning, improved safety performance, reduced drilling risks, and enhanced rate of penetration (ROP). However, several independent operators piecemeal these technologies from multiple service providers, which results in lower accountability and performance issues (compatibility and execution).

5.4.4 Determining Shale Mineralogy and Rock Quality

Shales diverge considerably vertically and laterally across very short distances. During the development phase, there is little effort to characterize the reservoir with an integrated petrophysical approach to determine optimal interval and orientation for horizontal wellbore and fracture stage placement. In most cases, gamma rays are used to geosteer. Use mud logging for fracture stage placement.

5.4.5 Fracturing by Brute Force

Many operators use a brute-force approach to fracturing that relies more on pumping rate plus larger volumes of water and proppant, versus a stimulation design, which many perceive as unnecessary. The stimulation design approach is based on sound geologic and engineering principles and practices. Without characterizing the reservoir along the lateral for mineralogy, natural fractures, stress magnitude, and orientation, operators using the brute-force approach cannot fracture the zones selectively to choose those with the most production potential. Not only that, but they are also unable to effectively design a stimulation treatment that prevents costly fracture-related consequences like higher-than-normal treatment pressure, screen-outs, and fracturing into offset wells and geohazards.

5.4.6 Is Using Multiple Suppliers a Good Idea?

Most operators believe it weakens their bargaining power if they work exclusively with a single supplier. Instead, they piece together services to get the best price. We see very little if any project coordination or cooperation between suppliers. Some try to manage everything from within but often lack the expertise, or even the time, to operate efficiently and effectively.

Multi-vendor buying can hinder the seamless communication and workflows, dilute quality, and affect reliable delivery, which can lead to needless non-productive time. The lack of project coordination between service suppliers causes unintended consequences. Operators suffer from the lack of accountability between vendors and increased safety and regulatory compliance risks. Without coordination, administration costs usually are higher and operators lose the economies of scale that can be achieved with a coordinated approach.

5.5 The Ideal Solution

Production performance is highly dependent on accurately placing horizontal wells and fracture stages in reservoir intervals with favorable mineralogy, total organic content, and stress. Adequately characterizing the lateral provides insight into these reservoir properties.

Data acquisition is an iterative process. At certain stages of development, critical datasets should be acquired (vertical science wells and horizontal laterals). This data can be used to refine reservoir and fracture models that support operational decisions for creating optimal development plans, fracture designs, and predictable production performance.

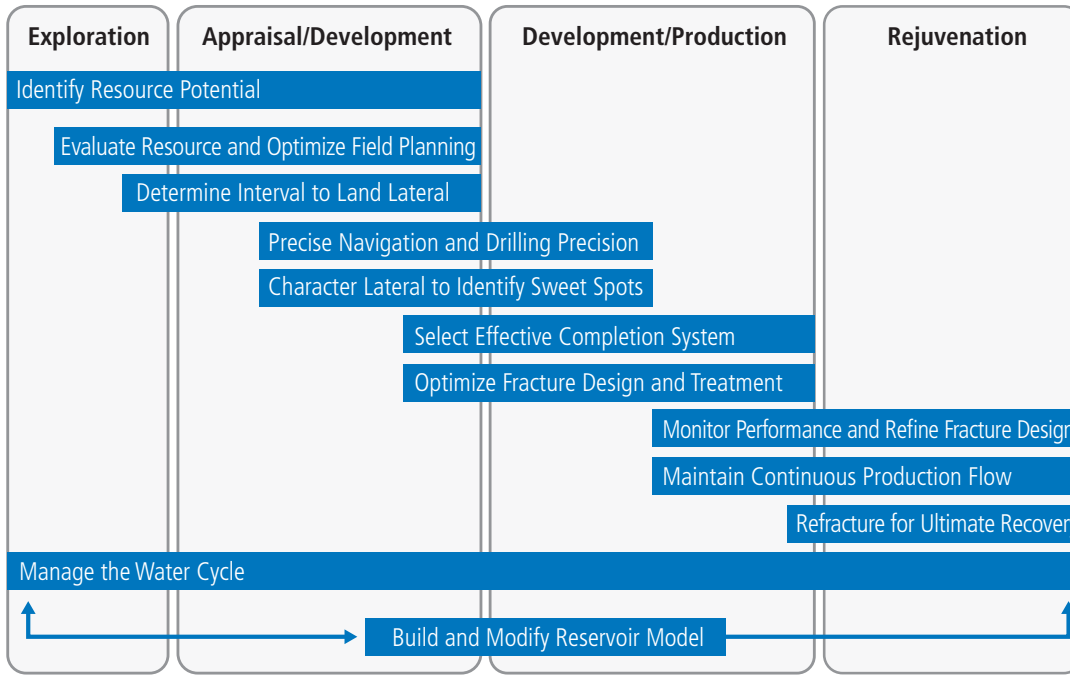

Fig. 5.1—Data driven approach: 12 steps to success.

Drawing on best practices captured from thousands of wells across North America's lucrative shale plays, Baker Hughes has established a data-driven approach (**Fig. 5.1**) that combines the knowledge, technology, and technique necessary to:

- Assess and invest in economically viable acreage.
- Identify sweet spots and determine best intervals for stimulation.
- Construct quality wellbores quickly and effectively.
- Generate fractures that yield greater returns.
- Extend the productive life of the well.

The result is a robust baseline for field development that reduces technical and commercial risk and establishes repeatable, more profitable recovery.

Subsurface knowledge is the foundation to balancing the effectiveness and efficiency of an asset across the asset's life-cycle. Good data is the basis for operational decisions that impact production effectiveness, such as:

- Targeting the sweet spots
- Identifying the ideal reservoir interval
- Optimizing stage placement and spacing
- Designing an effective fracture treatment

Making data-driven decisions can optimize development by allowing operators to focus their drilling and completion efforts in areas with greater production potential. Data also allows them to map large-scale horizontal well orientations for optimal pad placement and field planning. Each of the data-driven solutions, listed next, has a direct impact on production as a whole—and each solution influences the success of the others.

This knowledge helps operators keep costs down by:

- Eliminating unnecessary infrastructure and wells
- Decreasing rig time and rig moves
- Avoiding unwarranted completion stages
- Reducing stimulation footprint, horsepower, and proppant

This data-driven, life-cycle-based approach provides the operator with enough insight about the reservoir to make confident decisions that can result in cost-effective field planning, optimal well placement, completion quality, and increased production and recovery.

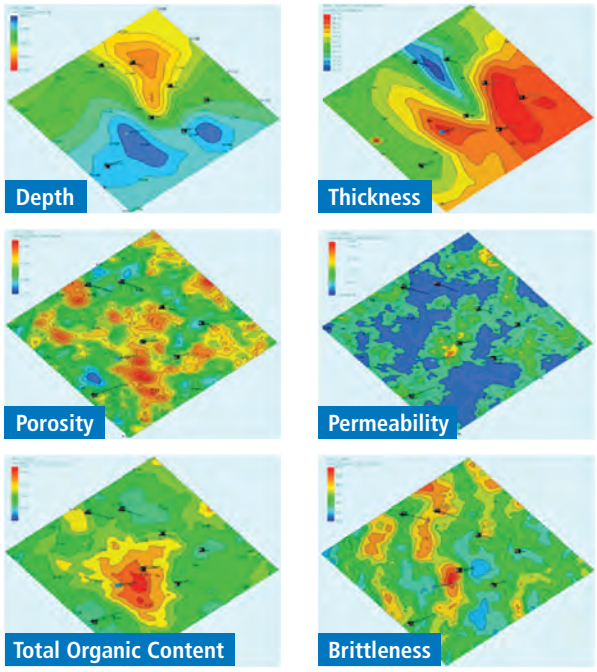

Fig. 5.2—Identify and evaluate resource potential with depth, thickness, porosity, permeability, total, and brittleness.

5.6 Identify and Evaluate Resource Potential

Many operators are considering, or have already secured, a solid acreage position in these rapidly developing plays, but determining where to invest, or even where to begin drilling, can be challenging with hundreds of thousands of acres under lease. Exploration begins with a basin screening, where data for existing geology, seismic, well data, core measurements, basin studies, and outcrops are gathered for a regional estimation of commercial viability. Ideal information used to determine viability includes organic total organic carbon, maturity level, mineralogy, thickness, natural fractures, porosity, and water saturation (**Fig. 5.2**).

Data for the region may be limited, but preliminary evaluation can help eliminate plays that fail to meet minimum subsurface requirements. Piecing together and standardizing the various sources of data can take a considerable amount of time and effort.

Engineers and geoscientists correlate these properties with previous studies, actual results, or available source-rock samples to identify commercially successful analogs. Through the Baker Hughes' Shale Science Alliance with CGG, we can seamlessly integrate seismic acquisition, processing, interpretation, and inversion into the exploration program. Our geoscientists work quickly to organize, reprocess, and merge raw data in a consistent manner for reliable interpretation of subsurface properties. These attributes are then mapped in a fully integrated reservoir model and simulated using the JewelSuite™ reservoir modeling software to identify regions with higher production potential.

5.6.1 Challenge

- Stitching together all existing data for an initial understanding of subsurface variation across the area and field
- Targeting areas with preferred rock and mechanical properties
- Estimating resources in place and determining whether they can be produced economically
- Determining which factors have the greatest influence on productivity
- Prioritizing exploratory and appraisal well locations

5.6.2 Value

- Estimate the resource potential and producibility to reduce commercial risk and identify regions with higher production potential.
- Determine an initial resource potential gross estimate.
- Identify the potential sweet spots to develop.
- Create an initial field development plan or pilot plan and initial economics.
- Reduce the commercial risk.

5.6.3 Solution

- Analyze existing data.
- Find, organize, and reconcile pre-existing well data, including geological data and maps, 2D and 3D seismic, logs, cores, public data, and analogs.
- Analyze geological, geochemical, geomechanical, geophysical, and petrophysical data to gain an initial understanding of variations across the area.
- Interpret existing seismic.
- Understand the subsurface at the regional level.
- Identify areas of highest total organic content.
- Estimate geomechanical properties and in-situ stress.
- Calibrate the seismic with well control to identify core areas for drilling and completion.
- Construct the reservoir model.
- Estimate hydrocarbons in place.
- Investigate recoverability.
- Determine risk factors and uncertainties that have the greatest influence on productivity.

5.7 Build and Modify Reservoir Models

The proactive approach to unconventional resource development includes reservoir modeling as illustrated in **Fig. 5.3**. Data acquired in the exploration and pilot phase of development is used to populate the model. According to Vassilellis et al. (2010), conventional reservoir engineering tools are inadequate to use with the change in reservoir characteristics after hydraulically fracturing "shale" well. This complex, newly altered reservoir (after fracturing) must be described and properly modeled in order to reliably predict long-term production and recovery. Vassilellis and his co-authors introduced a multidisciplinary integrated approach called "shale engineering."

Shale engineering, which integrates geology, geomechanics, geochemistry, petrophysics, and seismology, is a holistic approach to understanding and analyzing shale reservoirs. The underlying premise is the necessity to understand the complexities of the reservoir and then use that understanding to optimize and prioritize operations. Complete reservoir simulation models are constructed using geologic and engineering data to develop a more reliable prediction about how the reservoir will perform.

5.7.1 Challenge

- Reservoir heterogeneity and low quality
- Validating hydrocarbons in place and ultimate recovery
- Determining prospective development locations, well spacing, orientation, and lateral length
- Determining optimal location to place wells and prioritizing drilling locations

5.7.2 Value

- Get a field-level look at rock properties and structural complexity for more confident investment decisions.
- Identify core areas to commence exploratory drilling.
- Characterize the reservoir to identify and prioritize prospective development locations.
- Determine optimal well placement, spacing, orientation, and lateral length.
- Identify fracture barriers and geohazards.
- Validate hydrocarbons in place and determine whether the resource warrants proceeding to appraisal.
- Optimize field development plan and economics.

5.7.3 Solution

- Understand the subsurface at regional level.
- Identify the areas of highest total organic content.
- Estimate the geomechanical properties and in-situ stress.
- Calibrate the seismic information with existing wireline data to refine the initial reservoir model and identify core areas to begin exploratory drilling.
- Determine the porosity, fluid saturation, and fluid type.
- Determine the hydrocarbons in place and verify total organic content.
- Acquire the geochemical log to characterize lithology and mineralogy.
- Quantify the amount of total organic content.
- Calibrate the logging measurements with core samples to validate permeability, porosity, mineralogy, saturation, and lithology.
- Detect the vertical fractures to determine optimal horizontal placement and trajectory.
- Characterize the rock mechanical properties and stress regime to determine optimal fracture strike direction.
- Determine the geomechanical issues, fracture closure pressures, and in-situ stress.
- Validate the hydrocarbons in place and recoverability and ability to produce.
- Refine the predictive reservoir models and economics.
- Optimize the field development plan.

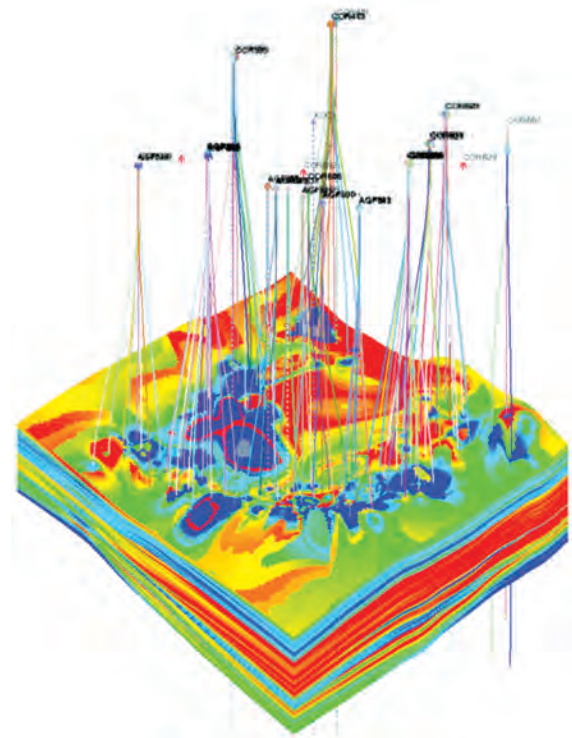

Fig. 5.3—Reservoir modeling.

5.8 Refine Resource Evaluation and Generate a Field Development Plan

5.8.1 Redefining the Field Development Plan

More wells are drilled during the appraisal phase than in the exploration phase; therefore, data from these additional wells can continue to be used to further characterize the reservoir. The recommended practice is to drill vertical wells to be used for data collection. Horizontal appraisal wells can be drilled to test hydraulic fracturing and mechanical wellbore completion designs, which can then be used to obtain estimates of production potential from the designs.

Information from horizontal wells will also assist you to determine initial lateral length, and to begin early drilling optimization. This information can then be incorporated into the reservoir models. The "refined" versions of the models can validate hydrocarbons in place and expected ultimate recovery, and help you to generate better scenarios and more accurately predict results. These include well lateral lengths, number, and spacing of fracture stages, and perforation clusters for economically producing at higher IPs and recoveries.

Internationally, it has been observed that NOC operators plan to take the approach of conducting a pilot program before full-field development. In these virgin areas with very few wells or any offset wells to observe, this approach certainly makes economic sense. Pilot programs are useful for proving commerciality, or for defining the best possible technology and development plan. After conducting the pilot program, international operators will stop to evaluate the results before making the decision to proceed with full-field development. A recommended practice is to consider implementing a pilot program in the US if you are developing in a new basin or entering a new area of an existing productive shale basin.

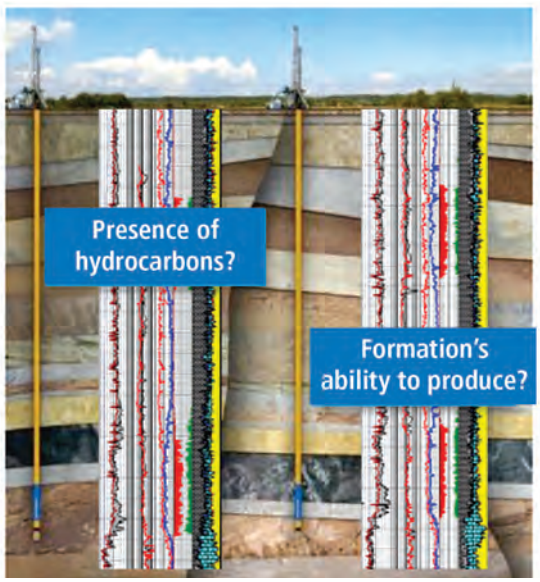

Fig. 5.4—Hydrocarbons and formation producibility.

Field development plans for shale reservoirs should include (as a recommended practice) the well type, placement, attitude, direction, and spacing. Drilling wells in the direction of minimum principal horizontal stress maximizes access to existing natural fractures when perpendicular and transverse-trending hydraulic fractures intersect these natural fractures (as previously discussed). This is why it is important to understand the stress regime in the field. Usually a full FDP also includes completion and fracturing designs.

When implementing a field development plan that includes a large number of wells, the operator is cautioned not to become complacent and to allow the rig schedule to totally determine the plan. Interim analyses should be undertaken to ensure that drilling and completion programs are delivering wells with the expected IP producing rates.

5.8.2 Challenge

- Characterizing reservoir heterogeneity and quality
- Refining estimates of hydrocarbons in place and estimated ultimate recovery of hydrocarbon
- Optimizing development locations, well spacing, orientation and refining lateral length

5.8.3 Value

- Validate hydrocarbons in place and characterize the ultimate recovery.
- Identify sweet spots for development.
- Generate the field development plan and determine economics.

5.8.4 Solution

- Use appraisal wells and implement a pilot program to characterize the reservoir and test completion design illustrated in **Fig. 5.4**.
- Determine lithology and mineralogy and total organic content.
- Determine porosity and permeability and fluid saturations.
- Understand rock mechanics and stress regime.
- Identify vertical fractures.
- Drill vertical wells for reservoir characterization.

- Develop horizontal wells to test the wellbore and fracture completion designs.
- Generate a field development plan.
- Determine well type and the initial completion design.
- Estimate the well spacing for the number of development wells required.

5.9 Determine the Optimal Horizontal Well Placement

In unconventional reservoirs, vertical and lateral heterogeneity varies considerably from basin to basin and well to well. For many regions where subsurface data may be scarce, history matching alone is often ineffective and fails to deliver reliable predictions. Acquiring additional data can provide the insight necessary to optimize operational decisions, reduce uncertainty, and increase economic success. Through the Baker Hughes alliance with CGG, it is possible to integrate seismic acquisition, processing, interpretation, and inversion seamlessly into the exploration program.

5.9.1 Horizontal Well Placement in a Potential Zone

Seismic is typically "shot" over a prospective area for basin-wide and field-level evaluation of hydrocarbon indicators, rock properties, and structural complexity. Calibrating the seismic information with existing wireline data refines the initial subsurface model, enabling our experts to identify primary locations to begin exploratory drilling (**Fig. 5.5**). Early exploratory wells can be widely spaced across a target area and designed for intensive data collection. These wells typically consist of a logging and coring program to acquire the critical performance data required to identify sweet spots, prioritize drilling locations, and then determine the best intervals for stimulation. Quality core samples and analysis are also required to calibrate qualitative interpretations from wireline logs. The Baker Hughes' Formation Evaluation Suite™ of logging and coring services can be customized to meet data requirements. Services also include access to geoscience expertise, and captured analyses from other known plays and core laboratories that are experienced in handling and testing ultra-low permeability rocks. The acquired reservoir properties are then used to further refine predictive reservoir models in order to validate hydrocarbons in place and determine whether the resource warrants proceeding to appraisal. What you may not realize is that variable mineralogy, total organic content, thermal maturity, porosity, stress orientations, and the presence of natural fractures have a direct effect on your ultimate recovery.

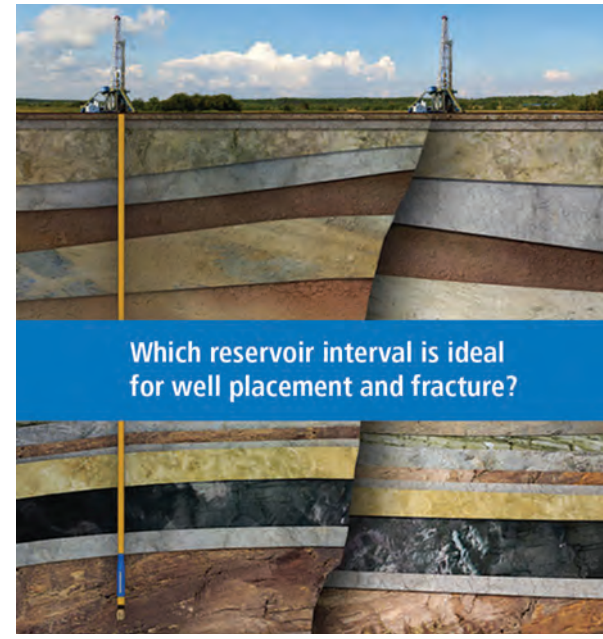

Fig. 5.5—Ideal reservoir intervals for targeting well placement and fractures.

By acquiring these wireline logging measurements and calibrating them with core samples from vertical pilot wells, you can:

- Identify reservoir intervals ideal for well placement and fracture stimulation.
- Determine optimal well spacing, orientation, and lateral length.

This data can be used to refine your reservoir model in order to reduce commercial risk by helping you to:

- Validate hydrocarbons in place
- Determine the formation's ability to produce
- Optimize field development plans and project economics

5.9.2 Challenge

- Characterizing reservoir vertical and azimuthal heterogeneity, facies, and quality
- Identifying reservoir intervals ideal for well placement and fracture stimulation

5.9.3 Value

- Identify the optimal interval in reservoir for lateral placement and lateral length.
- Refine a field development plan for optimized well placement.

5.9.4 Solution

- Analyze complete dataset (all appraisal and early development wells) for determination of lithology, mineralogy, total organic content, porosity, permeability, and fluid saturations. This is detailed in Chapter 8.
- Analyze complete dataset (all appraisal and early development wells) for determination of rock mechanics, stress regime, natural fractures, fracture barriers (containment) and vertical fractures
- Identify the reservoir intervals ideal for well placement and fracture stimulation.
- Best reservoir quality based on logs, cores, and surveys to yield highest producing rates.
- Best rock quality for achieving the most effective fracture stimulation.
- Places where the two, reservoir and rock quality, coincide is an ideal location for well placement.
- Refine reservoir model with new well information.

5.10 Achieve Drilling Precision and Efficiency

The unique reservoir characteristics found in these formations present challenges that can impact the overarching goal of optimizing costs and performance. Applying a total systems approach that integrates application engineering, drilling systems, drill bits, and drilling fluids provides the directional control and stability you need to drill through these complex formations quickly and effectively, while optimizing reservoir contact, surface area exposure, and environmental compliance.

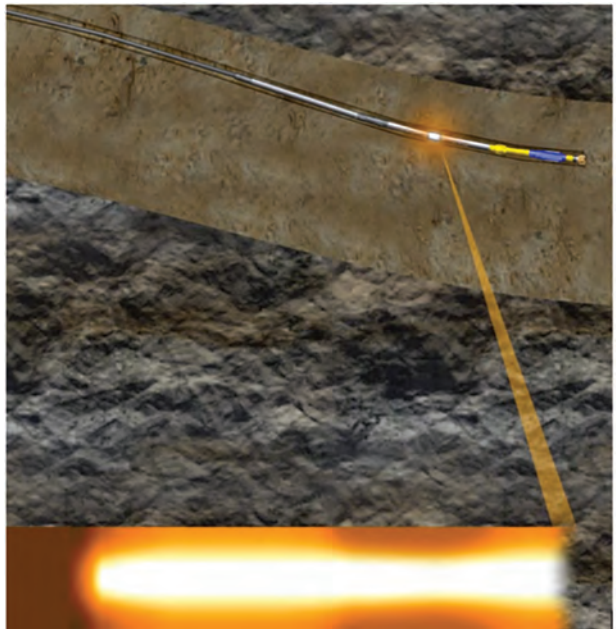

Fig. 5.6—Reservoir navigation with AziTrak™.

- Plan down to the details for your well. Planning quality affects drilling expenditure—and ultimate recovery. Using reservoir analytics, geosciences, knowledge-based systems, and downhole conditions to plan the details of your well can reduce risk. From modeling optimal well paths and pore-pressure trends to pairing the most effective tool string with a compatible drilling fluid, purpose-built systems may be designed that support drilling performance and enhance precision to total depth.
- Maintain placement within the targeted interval. The AziTrak™ deep azimuthal resistivity measurement tool delivers a 360° peripheral of approaching bed boundaries to ensure precise placement in the prospective interval for maximum reservoir exposure (**Fig. 5.6**). Acquired measurements can also be used to identify faults and areas drilled out of zone to eliminate unnecessary fracture stage placement.
- Drill a straight, smooth wellbore in less time. Drill the curve and lateral in one run using Autotrak™ rotary steerable systems. In addition to delivering precise steering control and near-bit inclination measurements, rotary steerable systems reduce tortuosity (typically caused by mud motors) making it easier to run casing, characterize the lateral, and install intelligent completion systems—which are pertinent technologies used to enhance completion and fracture performance. When paired with our premium PDC bit technology, you optimize performance using a custom-fit, aggressive cutting structure that maximizes penetration rates and minimizes trips.
- Stabilize boreholes in reactive formations. Drilling through high-pressure, high-temperature formations with an invert-emulsion drilling fluid combined with optimum mud-weight-window determination and drilling practices, can help you maintain wellbore stability, prevent formation damage, and reduce lost circulation. With the onset of stringent environmental regulations, high performance water-based fluids, such as the TERRA-MAX™ drilling fluid system, can deliver the performance of an invert emulsion while minimizing environmental impact.
- Drilling systems and reservoir navigation can affect wellbore quality, reservoir contact, and the completion method. The quality of the wellbore determines if the completion system can be run to the intended depth, and if annular isolation can be achieved. An out-of-gauge hole can make it difficult to achieve annular isolation with cement or openhole packers, particularly openhole packers, because they are designed to seal in certain size holes. A wellbore full of

ledges, sharp bends, and tortuosity makes it difficult to get a completion system to the intended depth. This is especially true for systems that require completion tools that have a larger diameter than the liner and increase the stiffness of the liner string. In addition, how fast the curve is built, and the stiffness and diameter of the completion string affect the system getting to the intended depth.

5.10.1 Challenge

- Landing the lateral within the prospective interval
- Maintaining placement within the prospective interval
- Increase drilling efficiency

5.10.2 Value

- Maintain optimal reservoir contact within the prospective interval.
- Drill a straight and smooth wellbore in less time.
- Stabilize boreholes in reactive formation.

5.10.3 Solution

- Real-time directional, azimuthal gamma ray, and azimuthal resistivity deliver 360° peripheral of approaching bed boundaries to ensure precise placement in prospective interval.
- Identify faults and areas drilled out of zone to eliminate unnecessary stage placement.
- Drill the curve and the lateral in less time.
- Achieve precise steering control and near-bit inclination measurements.
- Reduce tortuosity (typically caused by mud motors) making it easier to run casing and wireline logs, as well as intelligent completions.
- Get a solution that is optimized for one-run curve and lateral drilling.
- Improve cutting efficiency and evacuation.
- Improve durability and reliability in longer laterals.
- Maintain wellbore stability, prevent formation damage, and reduce lost circulation.
- Enhance resolution of the high definition image log.
- Deliver the performance of an invert emulsion while minimizing environmental impact.
- A total systems approach integrates directional drilling, reservoir navigation, bits, and fluids to ensure you can drill effectively and navigate precisely through the zone of interest while maintaining low drilling costs.

5.11 Characterize the Lateral for Fracture Stage Placement

Production performance is highly dependent on the fracture stage placement and treatment. Studies show that geometric fracturing techniques can result in stimulated reservoir intervals with unfavorable rock properties and producibility, and that these factors contribute to lower production performance. This can also lead to unnecessary cost related to excessive stage placement, horsepower, and fluids. By understanding the distribution of critical properties along the lateral, you can target productive zones, determine optimal stage placement, and design effective stimulation treatments that optimize reservoir contact, conductivity, and productivity (**Fig. 5.7**). There are three types of data required to characterize the horizontal lateral:

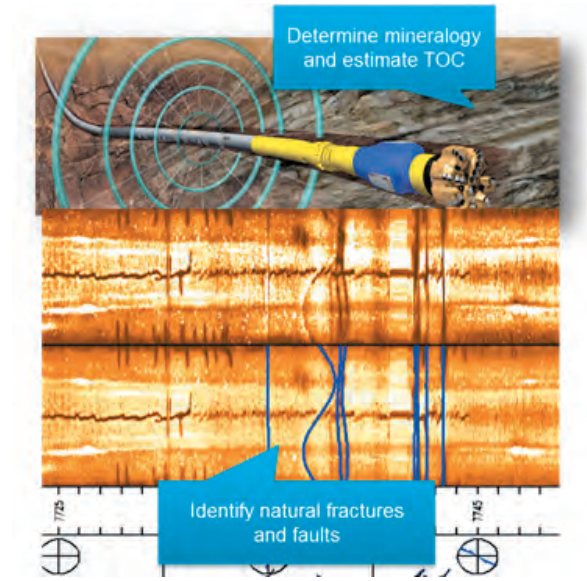

Fig. 5.7—Depicting the LWD HD resistivity imaging tool and log.

1. Information about the natural fractures (their location, prevalence, direction, and conductibility) is available using the Baker Hughes StarTrak™ LWD system.

2. Stress profile data (used in fracture design to initiate and propagate fractures), which is usually obtained from vertical pilot wells as the horizontal well, will be landed in the pay zone only intersecting the non-prospective formation above the target with no possible characterization of the formation below the pay zone. Logging tools, such as the Baker Hughes XMAC–F1™ acoustic log, can provide information detailing stresses along the lateral, but very few operators opt for this risky approach.

3. Reservoir, geological, and geochemical data (mineralogy, brittleness, total organic content levels, porosity) from well site cuttings analysis systems like the Baker Hughes RoqSCAN™ and Pyrolysis.

5.11.1 Challenge

- Determining intervals along the lateral for optimum fracture stimulation
- Identifying these optimum fracture intervals, and most natural fractures, plus the low stress profile
- Evaluating the best reservoir quality indicators, such as brittle mineralogy, highest total organic content, and good porosity

5.11.2 Value

- Avoid stage placement in areas drilled out of zone.
- Zero in on zones with greater production potential.
- Measure horizontal stress profiles and identify high flow-capacity natural fracture systems.
- Simulate fracture geometry, conductivity, and interactivity.
- Design an effective fracture treatment to improve proppant distribution and stimulated reservoir volume.

5.11.3 Solution

- Review azimuthal gamma ray and the azimuthal resistivity measurements logged while drilling so you can avoid stage placement in the areas that were drilled outside of the zone.
- Identify faults and areas drilled out of zone to eliminate unnecessary stage placement.
- Analyze lateral lithology, mineralogy, total organic content, and porosity along the lateral.
- Measure horizontal stress differentiation and magnitude to determine orientation and width of the fracture network.
- Integrate vertical stress profile to identify any barriers and determine height.
- Characterize the horizontal rock's mechanical properties to determine zones with low stress and high brittleness.
- Acquire high-definition borehole imaging to identify natural fractures, faults, and geohazards.

5.12 Determine the Optimal Horizontal Wall Hydraulic Fracture Stage Placement

Each completion type has benefits and considerations. There is no single solution for every application in unconventional reservoirs. Each application has its own challenges that require analysis from the economic, operational, and practicality standpoints. In addition, to have a fully optimized wellbore, the drilling, completion, and stimulation plans have to be coordinated with each other so that one aspect of the well does not cause limitations to another. As these techniques and knowledge of these formations continue to grow in North America and across the globe, work with these types of plays will continue to drastically shape the oil and gas markets, as well as the global economy. Each of these completion types has proven to be efficient and effective in unconventional reservoirs that require multistage hydraulic fracturing. However, there are applications where certain systems have advantages over the other ones, as described in the following paragraphs.

5.12.1 PNP (Plug-and-Perforate Systems)

"The flexibility of stage placement can be a huge benefit if stage placement is unknown immediately after the well is drilled. As soon as the well is drilled, the rig can run and cement the liner string completion and move on to the next location. Operators can then analyze any additional data obtained while drilling, or run additional logs to characterize the lateral and place the stages in the optimal location. In addition, any real-time monitoring of the fracture job, such as microseismic, could influence where the stages are placed. The capability to move the perforations enables the stage placement to be adjusted on the fly, and to place the stages in the optimal location." (Burton 2013a.)

"These completions might prove to be more cost efficient in applications where the days on location cannot be reduced by the type of completion system, such as wells with a shortage of fracture components or a low number of stages." (Burton 2013b).

5.12.2 BACS (Ball-Activated Completion Systems)

The combination of improved logistics, nonstop fracturing, and no need for through-tubing operations are the big advantages with this type of completion system. The only service required on location for the fracture job is pressure pumping, which will simplify the logistics before, during, and after the fracture job. The nonstop fracturing and the lack of through-tubing operations affect overall efficiency during the fracture process. The efficiency gains are more prevalent in wells with an increased number of stages. In these applications the BACS can reduce the amount of pumping time from weeks to days. In addition, using no-no-through-tubing operations to either fracture, or to put the well on production, helps lower the risks associated with extended-reach laterals (Burton 2013b).

5.12.3 CTACS (Coiled Tubing-Activated Completion Systems)

The key advantages for this system are having coiled tubing (CT) in the hole while fracturing and fracturing out of a single-injection point. If a screen-out does occur, the CT is at the same depth as the problem, and the CT tool assembly is capable of circulating and recovering from the screen-out. This drastically reduces the amount of nonproductive time because a CT unit does not have to be mobilized and run in the hole, making this a very efficient solution in formations that frequently have screen-out. Fracturing out of a single-injection point enables better height containment in applications where it is critical to stay in the zone, where there is a lack of natural fracture barriers. In addition, changing a well from multiple-injection-points-per-stage to a single-injection-point-per-stage can reduce the amount of hydraulic horsepower needed, and can potentially reduce the amount of space needed on location (Burton 2013b) as illustrated in **Fig. 5.8**.

There is also a variety of applications where all three-completion systems are viable options from an operational and practicality standpoint, so an economic analysis must be performed to determine the best completion. Because there is no dominant differentiator from a reservoir perspective, the most effective and efficient completions must be determined from an application viewpoint.

5.12.4 Challenge

- Determining an effective completion system specific to the application
- Connecting to the reservoir and effectively stimulating the target reservoir
- Managing or recovering from screen-out
- Efficiency and reliability and reducing NPT while fracturing
- Limiting the fracture design
- Multiple services and logistics

5.12.5 Value

- Maximizes the efficiency and productivity of plug and perforation completion and pressure pumping operations
- Increases efficiency and effectiveness in longer laterals
- Optimizes height containment and improves proppant distribution in the intended zone

5.12.6 Solution

- Offers flexibility and ease of use
- Provides virtually unlimited number of stages

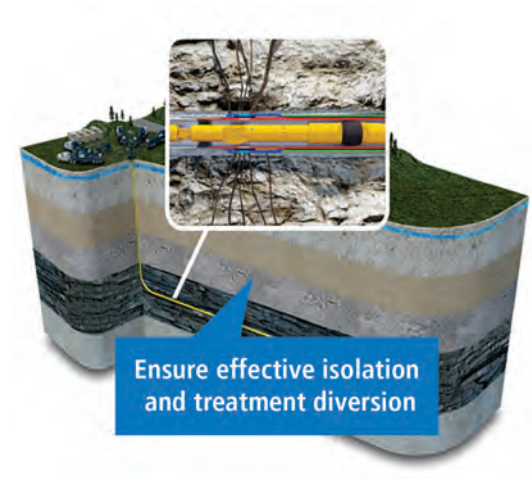

Fig. 5.8—Wellbore completion schematic for OptiPort™ depicted.

- Offers flexibility because placement of the stage is not final until the perforations are fired; this gives you time to analyze data obtained while drilling or logged along the lateral to determine optimal stage placement and spacing
- Builds in time to gather and analyze microseismic data for adjustments during the fracture job
- Saves time and adds compatibility; integrated service combines project management, design, logistics, completions, pressure pumping, and post-fracture milling to avoid mixing and matching components from multiple service providers, and the resulting downtime due to incompatibility; avoid non-collaboration that can result in operational missteps and operational inefficiency, unnecessary costs, and unproductive stages
- Reduces risk, because a "no-through-tubing" intervention eliminates through-tubing wireline or a coiled-tubing trip to fracture the well
- Eliminates down time between stages with continuous and non-stop fracturing, which can reduce cycle time from weeks to days
- Eliminates post-fracture milling requirements because you can produce through the ball seats
- Gets you simplified logistics because pressure pumping is the only service required on location
- Optimizes proppant distribution and height containment by stimulating through a single point of entry; delivers optimal proppant and fluid placement to intended stages
- Reduces the impact of screen-outs with coiled tubing already down hole; immediate clean-out reduces NPT and gets operators back online faster
- Monitors the downhole pressures in real time for early warning signs to take preventative measures against screen-outs
- Reduces hydraulic horsepower needs

5.13 Design a Fracture Program and Treatment

5.13.1 Fracture Design

In situ permeability is so low in shale reservoirs that little-to-no well production can occur without first breaking the rock with some kind of fracturing process. Fracturing the rock and propping the induced fractures open create high-permeability pathways, allowing the formation to produce at much higher flow rates than it could naturally. This process dramatically increases hydrocarbon production and makes the well profitable, which it would not have been without fracturing. The more the fracturing process can penetrate the rock the more successful the fracture will be to allow hydrocarbons to move into the reservoir and then into the wellbore. As opposed to traditional vertical wells, horizontal wells with multiple hydraulic fractures provide significantly more surface contact area with the reservoir rock. And, this holistic view is critical to accurately model and simulate fracture geometry, orientation, conductivity, and interactivity between fractures. **Fig. 5.9** illustrates two industry-used 3D fracture simulation and modeling technologies. We can refine the fracture model further by monitoring fracture activity in order to optimize fracture designs on future wells.

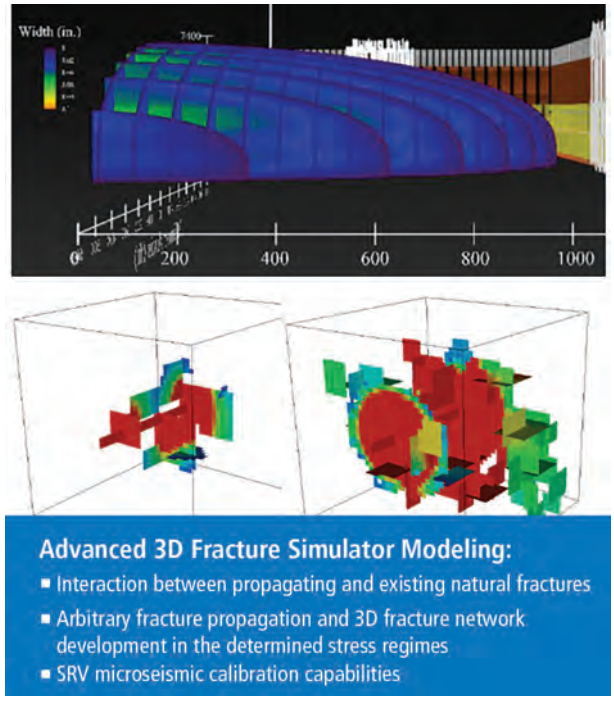

Fig. 5.9—Advanced 3D fracture simulation and modeling (top Baker Hughes' MShale™, bottom Lawrence Livermore Natural Laboratories, Steven R. Bohlen).

5.13.2 Challenge

- Poor conductivity, proppant distribution, and/or reservoir contact
- Uncertainty in production results

5.13.3 Value

- Simulate fracture geometry, conductivity, and interactivity.
- Design an effective fracture treatment to improve proppant distribution and stimulated reservoir volume.
- Predict well performance.
- Reduce environmental impact.
- Refine the field development plan.

5.13.4 Solution

- Calibrate the reservoir and geomechanical characteristics to help to estimate fracture geometry and conductivity, and to compare various treatment scenarios, and, finally, to optimize economics.
- Simulate the fluid volume and proppant mass at different injection points so you can predict fracture dimensions and conductivity.
- Determine the effective pump rate, proppant concentration, and hydraulic horsepower requirements.
- Compare the various treatment scenarios, forecast net present value, and determine return on investment for each stimulated well, which can result in more effective planning and better economics.
- Predict the post-fracture well performance (with cross-disciplinary modeling).
- Protect the well from microbial attack, improve fluid recovery, stabilize the formation, support fracture height containment, and reduce hydraulic horsepower—as well as environmental footprint.
- Monitor fracture performance and refine the fracturing program.

5.14 Microseismic Fracture Monitoring Services

With microseismic fracture monitoring services, you can learn how the current perforation pattern and fracture design affect the fracture propagation. This insight into the most effective fracture spacing, height, and length for maximum drainage is invaluable, because it allows you to adjust geometry, proppant concentration, fluid volume, and pumping requirements for future fracture designs. Microseismic monitoring services can also help to prevent breaching into unwanted zones by allowing you to evaluate and control fracture dimensions during the stimulation

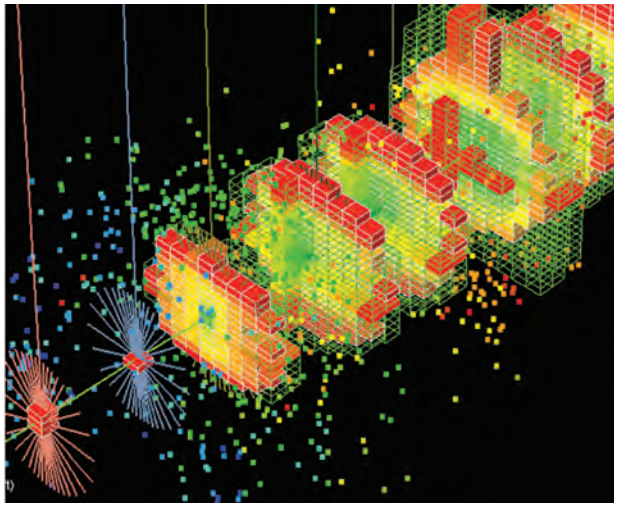

Fig. 5.10—Microseismic overlay with fracture pressure modeled for multistage fracture. From Vassilellis et al. (2011).

process (**Fig. 5.10**). By monitoring the actual performance versus the designed fracture performance, you can determine the effectiveness of the various fractures, and get a better estimate of each fracture's stimulated rock volume. You also gain insight about how the current perforation pattern and fracture design has affected fracture propagation. This way, you can determine any needed refinements in length and spacing, proppant and fluids, and pumping operations on planned horizontal wells—in order to maximize reservoir contact and drainage.

5.14.1 Challenge

- Estimating stimulated reservoir volume
- Understanding how the fractures are propagated
- Understanding the fracture interactions
- Determining stage production contribution

5.14.2 Value

- Determine effective fracture spacing, height, and length for maximum drainage.
- Adjust geometry, proppant concentration, fluid volume, and pumping requirements.
- Evaluate and control fracture dimensions during the stimulation.
- Identify refracturing candidates.

5.14.3 Solution

- Evaluate in real-time and control fracture dimensions during the stimulation treatment.
- Evaluate and control fracture dimensions during the stimulation treatment.
- Prevent breaching into unwanted zones.
- Estimate stimulated reservoir volume to refine and optimize future fracture design.
- Understand how the current perforation pattern and fracture design affect fracture propagation.
- Determine the most effective spacing, height and length, proppant and fluid concentrations, and pumping operations for maximum drainage on future fracture design.
- Simulate fracture geometry and conductivity of planned horizontal wells.
- Refine the fracture model.
- Maintain continuous production flow.

5.15 Optimize Production Flow

You can counter steep decline curves by taking the necessary steps to maintain and optimize production flow. Predict potential threats early to prevent costly intervention. Using reservoir data and offset well experiences, petroleum engineers predict post-stimulation problems to prevent post-fracture intervention costs related to scale, organic deposition, bacteria, and corrosion. By pumping long-term inhibitors deep into the reservoir with a system such as the STIMPLUS™ chemical system from Baker Hughes, you can ensure formation fluids are treated before they can cause production flow problems. Automation technologies can also ensure chemicals are applied optimally throughout late life production. Enhance production lift per stage. The FLEX™ series pump increases lift per stage, allowing for more drawdown with a shorter system that improves uptime by reducing cyclic shutdowns (**Fig. 5.11**). Higher lift per stage also lowers motor temperatures for increased run life and superior overall system efficiency. Combined with WellLink VISION™ downhole monitoring software, you can

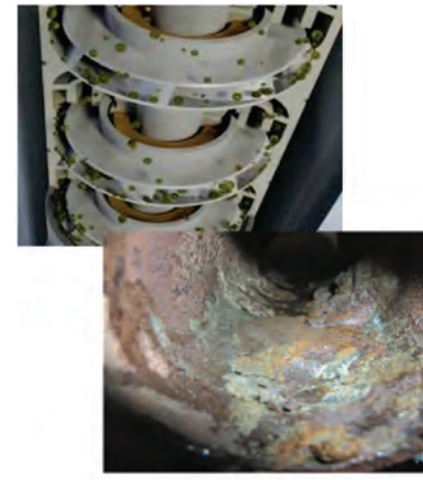

Fig. 5.11—Flow assurance (FLEX™ series pump, scale buildup).

avoid production shut-ins by monitoring bacteria cultures, scale inhibitor residuals, and other deposits, plus corrosion that can affect wellbore integrity and production flow.

5.15.1 Challenge

- Managing the well flowback
- Maintaining and optimizing the production flow
- Determining any artificial lift requirements
- Protecting the wells and facilities from corrosion, scale, bacteria, paraffin

5.15.2 Value

- Artificial lift restores production and extends well life.
- Reduce well shut-in time (flow assurance).
- Arrest premature well-production decline.
- Help identify refract candidates.

5.15.3 Solution

- Manages well flowback
- Real-time monitoring with electric submersible pump systems and other artificial lift systems
- Achieve long-term flow assurance and balanced production chemicals
- Remediation services available
- Wellbore remediation and cleanout available

5.16 Refracture to Improve Ultimate Recovery

Baker Hughes supports restimulation (refracturing) as the most effective method of rejuvenation to restore productivity to declining shale wells. Although the refracture concept and practice has been around for some time (ever since the first fracture job in 1947), this section's focus is on refracturing in modern North American (primarily in the US) horizontal shale wells (**Fig. 5.12**).

Current refracturing potential in the US includes about 180,000 completed shale wells. In addition, the industry is drilling an additional 16,000 shale wells per year. The majority of US shale gas wells (as well as the liquids play wells in the Eagle Ford, and emerging Utica) have been completed using the cased hole, plug-and-perforation method of completion. Operators are very familiar with this method, because it is a carryover from fracturing earlier vertical tight gas wells in the US Rocky Mountains. The plug-and-perforation method has flexibility, allows multiple perforation clusters as fracture entry points, and involves minimum downhole wellbore equipment. Shale gas wells in major plays with plug-and-perforation completions are numbered at 15,024 (with an estimated

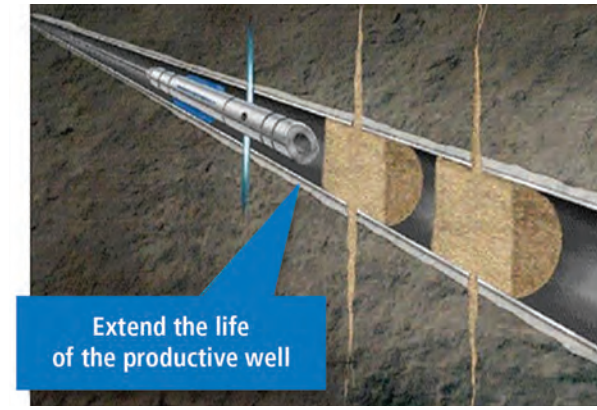

Fig. 5.12—Refracturing schematic.

9,000 of those being horizontal wells) in the Barnett, 4,700 in the Fayetteville, 3,300 in the Woodford, 4,750 in the Marcellus, and 3,450 in the Haynesville.

There are 5,650 oil wells in the Eagle Ford and essentially all have been completed using the plug-and-perforation method. There are 7,600 oil wells in the Bakken, all of which have been completed with some form of open-hole wellbore completions; i.e., packers and fracture sleeves, like Baker's FracPoint™. There are some operators in the Bakken that are going back to the cased-hole, plug-and-perforation completion method. Currently, there are 870 completed oil wells in the Niobrara, and the predominant completion method is non-cemented fracturing sleeves and packers. The emerging Utica has about 220 oil wells, primarily completed with plug-and-perforation. Coil tubing activated methods of completion are relatively new in the US, and a limited number of shale wells have been completed using these systems.

Refracturing methods for the completion types used in the Bakken and Niobrara will certainly be more complex than cased-hole (plug-and-perforation) wells refracturing. However, the first Baker Expandable Liner (cladding) job is in the Niobrara; others are scheduled in the Eagle Ford and Fayetteville (which will be discussed later). The results of these jobs may prove that the cladding isolation method of refracturing is the most viable option for the Bakken and Niobrara wells completed with openhole completion methods. The typical refracturing method used with the cladding isolation method is plug and perforation.

In the US today, there are only a few wells being refractured. Vincent (2010 and 2011), Craig et al. (2012), Martin and Rylance (2010), Cipolla (2005), and King (2010) all discuss the topic of refracturing in their papers, but certainly Vincent has studied refractures more extensively than others.

In general, refracture can:

- Re-establish good connectivity with the reservoir
- Bypass near-wellbore damage
- Restore and increase production rates
- Flatten the original decline profile
- Extend productive life of the well
- Increase net present value and accelerate cash flow

The two refracture isolation methods close to being available, or already in the market, are the expandable liner method and the multi-set packer with diverters.

- Operator and customer economics for refracturing shale oil wells are favorable for the expandable liner and the multi-set packer with diverters.
- Operator and customer economics for refracturing shale gas wells are not favorable for any refracturing method (primarily due to low gas price).

5.16.1 Recommendations for Refracturing

- Use a selection criteria that uses different types of refracture equipment and procedures for different reservoir pays.
- Use the four-step refracturing procedure.
- Select the applicable refracture type and equipment and procedure:
  - Use the expandable liner on refractures requiring isolation of existing perforations.
  - Use the multi-set packer with diverter system on refractures of plug-and-perforate completions.
- Determine the best, most effective casing hole logs to run to evaluate the horizontal wellbore for each refracture case (such as RPM™ and Star™).
- Use the Baker Hughes xFractor (MFrac™ and MShale™ Fracture Simulators) simulator to design refracture treatment.
- Use coil tubing services for cleanouts and TeleCoil™ where applicable.
- Use a shale value model to calculate operator economics for a particular refracturing case.
- Use pressure pumping services and wireline services to refracture the well.

5.16.2 Challenge

- Poor well conductivity and wellbore damage
- Production declines
- Ineffective initial fracture treatment and placement
- Determining refracture candidates
- Selecting an appropriate refracture method

5.16.3 Value

- Re-establish good connectivity with the reservoir.
- Bypass near-wellbore damage.
- Restore and increase production rates.
- Flatten the original decline profile.
- Extend productive life of the well.
- Increase net present value and accelerate cash flow.

5.16.4 Solution

- Performing the well cleanout before refracturing.
- Using coil tubing where indicated.
- Inspecting the casing as needed.
- Keeping a casing inspection log.
- Identifying zones to refracture and determine treatment.
- Operating with production logging systems like the XMAC-F1™ and RPM™.
- Using isolation and refracture methods.
- Implementing multi-set packers with diverters (LitePlug™) and refracturing using plug-and-perforate methods.
- Using an expandable liner (cladding) and refracturing using plug-and-perforate methods.
- Refracturing using FracPoint™ (in special cases).
- Managing the water cycle.

5.17 Holistic Approach to Water Management

On average, the oilfield industry produces three-to-five barrels of water for every barrel of oil. And, the industry spends billions of dollars every year to source, treat, reuse, store, transport, and dispose of that water. Cost-effectively managing produced and flowback water can mean the difference between economic success and failure in many oilfield operations (**Fig. 5.13**). This is particularly critical in unconventional plays. Using specialized water management services can provide solutions for technical, economic, and regulatory issues related to oilfield water. Baker Hughes developed their H2prO™ water management services to address all of these reasons. Baker Hughes designs effective water management strategies to meet an operator's production objectives and lower the operating expenses associated with water sourcing and disposal. It is important to use an integrated approach to overcoming surface water management challenges that incorporates the specific reservoir and wellbore characteristics and hydraulic fracture design. Look for experts who can ensure the appropriate solution is produced and deployed from a comprehensive suite of water management technologies that supports reusing flowback waters safely and effectively.

5.17.1 Challenge

- Conserving and reducing water consumption
- Treating water for reuse in hydraulic fracturing fluids and drilling fluids
- Reducing transportation, handling, storage, recovery, and disposal costs
- Ensuring compliance with regulations

5.17.2 Value

- Recycles produced or flowback water for fracturing and drilling fluids
- Reduces cost and risk
- Reduces the environmental impact

5.17.3 Solution

- Create and use effective water sourcing, transportation, storage, treatment, recovery, and disposal strategies.
- Leverage expert water management services like Baker Hughes' H2prO™ Water Management Services.
- Run pre- and post-treatment water analysis (fit-for-purpose solution).
- Develop a full portfolio of treatment options so you can manage oilfield water effectively for both flowback and produced categories.
- Utilize mobile field treatment units.
- Consider Baker Hughes' electrical submersible pump systems for lifting water source wells.

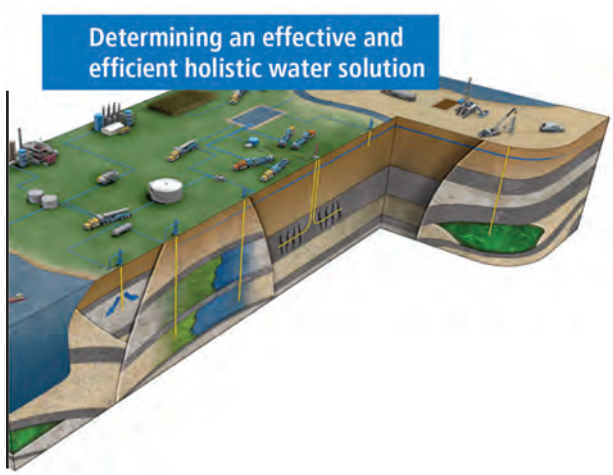

Fig. 5.13—Determining an effective and efficient holistic water management solution.

5.18 Conclusion

So what are the foundational ideas in this chapter? In summary, acquiring subsurface knowledge supports making better decisions about orientation, interval selection, stage placement, and fracture design for unconventional exploitation and development. Conversely, using only generic offset data will most likely prevent recovering the reservoir's full potential.

Effective well construction and stimulation programs require something that generic data can't provide: a clear understanding of the reservoir—from seismic through simulation and production.

Maximizing production from shale reservoirs requires optimal lateral and fracture placement as well as an effective stimulation program. If you're using only offset data to make these decisions, you can't achieve the reservoir's full potential. However, the right formation evaluation technologies can give you the data needed to make the most informed, most profitable decisions. The result: fracture performance and optimized recovery.

A data-driven, asset life-cycle approach also encompasses the necessary steps to maximize production flow by preventing costly intervention, monitoring production levels, automating chemical treatments, and enhancing recovery solutions to extend the producing life of your shale wells.

In the years ahead, we will see increasing challenges for the oil and gas industry. As energy demand rises and easily accessed sources dwindle, the industry—and the world in general—can no longer afford to leave oil and gas fields underutilized. Integrating people, technology, and processes through workflows will help to improve the operational efficiency as well as completion effectiveness in unconventional reservoirs.

5.19 Acknowledgments

The following members of the CORE Team collaborated in the writing of this chapter: Robert L. Kennedy, Aaron Burton, Rajdeep Gupta, Sergey Kotov, Marie Meyet, Matt Bratovich, and Javier Franquet.

5.20 References

Burton, W.A. 2013a. Unconventional Completions: Which One is Right for Your Application. Paper SPE 166431 presented at the SPE Annual Technical Conference and Exhibition, New Orleans, Louisiana. 30 September–2 October. http://dx.doi.org/10.2118/166431-MS.

Burton, W.A. 2013b, Unconventional Completions – An Operational Comparison. Paper SPE 167030 presented at the SPE Unconventional Resources Conference and Exhibition. Brisbane, Queensland, Australia, 11–13 November. http://dx.doi.org/10.2118/167030-MS.

Castro, L., Watkins, T., Bedore, B., et al. 2012. Reducing Operational Time, Fluid Usage, Hydraulic Horsepower, Risk and Downtime: Targeted Fracs Using CT-Enabled Frac Sleeves, Paper SPE 154391 presented at the SPE and ICoTA Coiled Tubing and Well Intervention Conference and Exhibition. The Woodlands, Texas. 27–28 March. http://dx.doi.org/10.2118/154391-MS.

Cipolla, C.L. 2005. The Truth about Hydraulic Fracturing–It's More Complicated Than We Would Like to Admit, Paper SPE 108817 SPE Distinguished Lecture Series, 2005–2006. http://dx.doi.org/10.2118/22334-PA.

Presley, J. 2012. Production 2012-a year in review. Hart E&P December 2012 issue.

King, G.E. 2010. Thirty Years of Gas Shale Fracturing: What Have We Learned? Paper SPE 133456 presented at the SPE Annual Technical Conference and Exhibition. Florence, Italy. 19–22 September. http://dx.doi.org/10.2118/133456-MS.

Martin, A.N., and Rylance, M. 2010. Hydraulic Fracturing Makes the Difference: New Life for Old Fields. Paper SPE 127743 presented at the North Africa Technical Conference and Exhibition. Cairo, Egypt. 14–17 February. http://dx.doi.org/10.2118/127743-MS.

Maxwell, S., Pirogov, A., Bass, C., et al. 2013. A Comparison of Proppant Placement, Well Performance, and Estimated Ultimate Recovery between Horizontal Wells Completed with Multi-Cluster Plug & Perf and Hydraulically Activated Fracture Ports in a Tight Reservoir. Paper SPE 163820 presented at the SPE Hydraulic Fracturing Technology Conference. The Woodlands, Texas. 4–6 February. http://dx.doi.org/10.2118/163820-MS.

Meehan, Nathan D. 2014. Risks and Opportunities Associated with Shale Plays as Unconventional Projects as Projects Go Global, Baker Hughes Reservoir Blog, 5 January 2014. http:// blogs.bakerhughes.com/reservoir/2014/01/05/risks-andopportunities-associated-with-shale-plays-as-unconventionalprojects-go-global-part-55. (accessed August 6, 2014).

Paneitz, J., Johnson, C.C., White, M., et al. 2012. Advancements in Openhole Completion Technology Increases Efficiencies and Production in the Williston Basin. Paper SPE 159586 presented at the SPE Annual Technical Conference and Exhibition. San Antonio, Texas. 8–10 October. http://dx.doi.org/10.2118/159586-MS.

SPE Applied Technology Workshop. 2012. Petroleum Resources Management System, Panag, Malaysia.Prague, Czech Republic. 24 October, http://www.spe.org/ events/12aprg/pages/about/index.php (accessed July 2014).

SPE Applied Technology Workshop. 2012. Shale as a Reservoir: Leveraging Formation Characteristics, Well Placement and Unique Completions to Improve Multistage Stimulation. Prague, Czech Republic. 24 October, http://www.spe.org/events/12aprg/pages/about/index.php (accessed July 2014).

Vassilellis, G.D., Li, C., Bust, V.K., et al. 2011. Shale Engineering Application: The MAL-145 Project in West Virginia, Paper CSUG and SPE 146912 presented at the Canadian Unconventional Resources Conference, Calgary, Alberta, Canada. 15–17 November. http://dx.doi.org/10.2118/146912-MS.

Vassilellis, G.D., Li, C., Seager, R., and Moos, D. 2010. Investigating the Expected Long-Term Production Performance of Shale Reservoirs. Paper CSUG and SPE 138134 presented at the Canadian Unconventional Resources & International Petroleum Conference, Calgary, Alberta, Canada, 19–21 October. http://dx.doi.org/10.2118/138134-MS.

Vincent, M.C. 2010. Refracs–Why Do They Work, and Why Do They Fail? In 100 Published Field Studies. Paper SPE 134330 presented at the SPE Annual Technical Conference and Exhibition. Florence, Italy. 19–22 September. http://dx.doi.org/10.2118/134330-MS.

Vincent, M.C. 2011. Restimulation of Unconventional Reservoirs: When Are Refracs Beneficial? ***J.Cdn. Pet. Tech.***, **50** (5): 36-52. SPE 136757. http://dx.doi.org/10.2118/136757-PA.

Welling & Company. 2012. Market Research on the Success of Shale Wells in the U.S. Welling & Company, Market Research Studies Repost, November 2012.

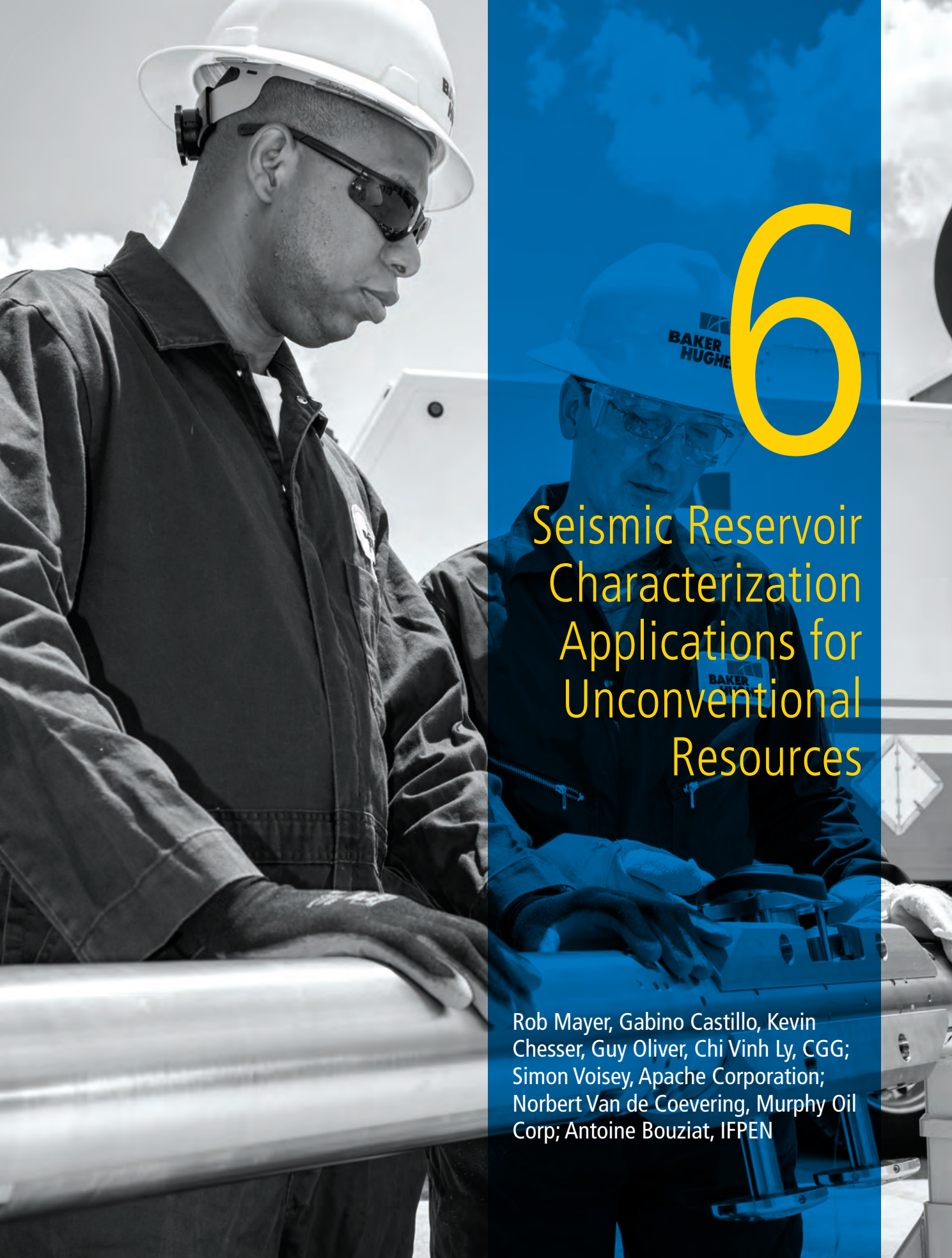

6

Seismic Reservoir Characterization Applications for Unconventional Resources

Rob Mayer, Gabino Castillo, Kevin Chesser, Guy Oliver, Chi Vinh Ly, CGG; Simon Voisey, Apache Corporation; Norbert Van de Coevering, Murphy Oil Corp; Antoine Bouziat, IFPEN

This page intentionally left blank

Chapter 6: Seismic Reservoir Characterization Applications for Unconventional Resources

Introduction

Several examples of technological paradigm shifts in the oil and gas industry resulted in significant changes to the strategies, plans, and economics of energy companies. In the 1990s, improvements in computer hardware and geoscience desktop applications, along with the acquisition of large regional exploration-oriented 3D seismic data volumes, improved exploration efficiency and effectiveness. Explorationists were, for the first time, able to see 3D geologic interpretations of the subsurface. This enabled a radical enhancement in their ability to pick optimal locations for leases, wells, and even production facilities. Seismic, however, is not a perfect model of the subsurface, and in early 3D seismic interpretation there were many inaccuracies. As a simple example, seismic data is measured in time and can be erroneous when converted to depth. As understandings matured, new technologies were released and improved techniques were implemented, and the overall exploration success rates increased significantly.

Fast forwarding to unconventional shale resource development, 3D seismic initially proved helpful but not conclusive for operators. The use of 3D seismic in shale plays was limited to estimating the depth, thickness, and geologic structure for well locations. Areas known to be highly faulted or discontinuous were avoided as drilling and completion hazards. While the initial use of seismic was helpful in these unconventional shale plays, the true value of seismic is only now beginning to reach its full potential. Recent advances in seismic processing technology and workflows along with advanced seismic analysis indicate that important rock properties related to production potential can be derived from the seismic data. Reservoir quality, organic content, rock strength, pore pressure, and in situ stress are all measurements that are being used and calibrated to production to locate sweet spots, which can provide a much more precise and successful approach to drilling and completion in shales.

In this chapter, we will review the current issues, techniques, and ongoing research for using seismic to increase production and to reduce the costs and environmental risks associated with operating in shale plays. We address survey design and acquisition parameters to ensure the resulting seismic is optimal for shale analysis. Seismic processing that enhances the seismic signal and enables stress analysis will be reviewed. Seismic reservoir characterization will be addressed in detail with a focus on seismic inversion techniques, and post inversion processing for rock property attributes. Finally, calibration and validation of these techniques will be examined with an emphasis on direct calibrations for mineralogy and production predictions. The final section of this chapter is a case study where these technologies and techniques were used in the Haynesville shale to characterize reservoir properties and develop an optimal drilling and completion program.

6.1 Overview of Surface Seismic Utilization in Unconventional Plays

Utilization of surface seismic in unconventional plays requires that one recognizes the contrast in the structural and geomechanical characteristics present in the conventional and unconventional resources. Such recognition may help differentiate the use of 2D and 3D seismic data in the exploration and appraisal phases of reservoir characterization of unconventional plays from that of conventional plays. This is illustrated further.

6.1.1 2D Seismic—Exploration

In conventional plays, the primary value for seismic data is found in the exploration and delineation phase of a project. The ability to determine the structural framework to ascertain the structural position, reservoir extent, and trap mechanism are all key issues in assigning risk to an exploration well. Once the well is drilled, the operator has the go or no-go decision for the well completion and production phase. Correlation of the well to the initial seismic model through the use of synthetic seismograms to confirm reservoir thickness and structural position are critical activities in this decision-making process.

For unconventional wells the value and utilization of seismic is quite different. As the shale serves as source, reservoir and trap, the structural aspects of the proposed location are different. Wells will produce whether they are structurally high or low. The volume of hydrocarbons recovered is more closely related to subtle stratigraphic heterogeneities in the shale and the effectiveness of the completion strategy. These subtle stratigraphic variations can be difficult to recognize and validate from seismic in early stages of development. Careful correlation of wireline, core, and production data

requires a sufficient number of well data points and are the focus of this chapter and the value of seismic in shale plays.

In early exploration stages of shale play development, some of the key values for seismic data are related to, providing a structural predrill model to determine where to land the well, and how to drill horizontally in the shale. Shale thickness and structural complexity are key criteria that can be gained from the seismic in this exploration stage. The well should be placed in a section of shale such that the energy from the hydraulic fracture stays within the target shale. Fracturing out of zone wastes valuable resources at a minimum, and potentially can degrade the viability of the well if the fracture extends into a saline aquifer. For this reason, careful analysis of the structural characterization of the well plan should be considered from the seismic. Well planners should avoid areas that are faulted or karsted.

6.1.2 3D Seismic Appraisal—Development

In conventional plays, the focus and value of seismic data move to attribute analysis in the appraisal and development phase of the project. Extraction of amplitude based attributes, including those obtained by pre-stack and post-stack inversion can help with the analysis of reservoir quality away from the discovery well. Acoustic properties of fluids can be seismically modeled at the well bore, assisting the geoscientist in locating phase changes for gas, oil, and water contacts. Additional spatial attributes may assist in locating small faults or other discontinuities to determine reservoir compartmentalization.

For unconventional plays, the importance of seismic attributes is also apparent in the appraisal and development phase. Very slight and subtle changes in the rock fabric, organic content, or stress can result in drilling programs that deliver substantially different production results. It is in this stage of shale development that seismic can add tremendous value in determination of sweet spots and assist operators with information that can be economically valuable for effective completion strategy.

The key seismic reservoir characterization technologies and workflows in the development and appraisal stage of a shale program are related to seismic inversion. Pre-stack seismic inversion provides two key and critically important responses for us to analyze: acoustic impedance and shear impedance. Carefully correlated and calibrated to wireline, core, and drill cuttings, a three-dimensional seismic model of key rock and geomechanical properties can be estimated. These include but are not limited to mineralogy, lithofacies, porosity, water saturation, volume of organic content, geomechanical estimates of brittleness and rock strength, and in situ stress. All of these attributes are useful tools in the prediction of properties away from the wells shale plays. Each shale play has a unique set of geologic properties and conditions governing production performance. Additionally, a substantial amount of heterogeneity exists within individual shale plays. No single attribute can be used as a prediction of success or failure in these plays. However, statistical approaches that correlate production values to multiple well and seismic rock property attributes are demonstrating potential as a tool to determine sweet spots and assist with drilling and completion strategies.

Even though thousands of wells are being drilled annually in many of the North American shale plays most operators agree that their overall knowledge of these plays and how to effectively produce them is still growing. Seismic data and analysis will play an increasingly important role in this knowledge base as this is currently the only viable method of predicting properties away from the well bore. In the coming years we will see the growing importance of some key technologies. Multicomponent seismic data utilizes three component geophones and directly measures P-wave and mode converted S-wave responses. Inversion of this data can yield more reliable predictions of bulk density, a key attribute that is often estimated from pre-stack P-wave inversion. Additional analysis of multicomponent data can provide validation of azimuthal anistopy, and associate in situ stress fields. Time lapse seismic, or 4D, is used extensively in some geologic scenarios to map production effects over time. Although successful land-based 4D surveys seem to be limited to analysis of production and steam fronts in heavy oil operations, further analysis of seismic anisotropy could assist with the determination and mapping of stress fields that have been influenced by drilling and hydraulic fracturing, therefore assisting in the determination of optimal well and fracturing stage spacing. Microseismic monitoring has been used sparingly in shale production operations. These surveys provide a qualitative measure of the effectiveness and extent of where the stress field has been affected; however, they cannot be used to accurately predict the behavior of the proppant and therefore production. More research and analysis are needed to accurately predict the stimulated rock volume from microseismicity. Calibration to surface seismic attribute measurements may lead to improved interpretation and prediction of production.

6.2 Seismic Survey Design and Acquisition Considerations

Before conducting a seismic survey and arranging the equipment needed for a seismic survey acquisition, feasibility studies must be carefully designed and performed to ensure that the information acquired through the use of seismic data will be accurate and robust based on the target geologic features.

6.2.1 Feasibility Studies

The ultimate design and execution of a seismic acquisition program should be done in such a manner that the final processed survey is precisely tuned to extract the most pertinent geologic information leading to a successful development program. It is therefore surprising how often survey design requests from operators are based only on historical experience or cost minimization strategies. As the earth model and geologic success criterion change from play to play, a seismic feasibility study can be critical to overall success of the seismic program. A seismic feasibility study will utilize the basic structural framework of the location and depth, thickness, and acoustic and elastic properties of the target and surrounding rock. Forward seismic modeling from logs can lead to the understanding of the seismic sensitivity to subtle changes in lithology, fluid, stress, and fractures. Once understood, a fit for purpose survey design process can begin.

6.2.2 Seismic Survey Acquisition Techniques and Equipment

Land seismic programs are designed to obtain information about the earth's subsurface by examining the energy reflected to the surface from an induced source. Depending on surface conditions, the seismic source is either dynamite or vibroseis trucks that are designed to shake the surface for several seconds. Geophones are placed at the surface and capture the returning signal.

Recent advances in seismic acquisition techniques are adding tremendous value to the ultimate usability and interpretation of seismic data for shale plays. High channel count systems are allowing for survey design that utilizes long offset and full-azimuthal coverage, the importance of which will be covered later in this chapter. These systems also enable excellent spatial coverage of the reservoir both laterally and vertically. Improvements in vibroseis technology are leading to enhancements of the seismic signature bandwidth. Wider frequency bandwidth content recovered, particularly the low frequency, can yield valuable reservoir information, not obtainable from older vintage seismic surveys.

6.3 Seismic Processing

The raw unprocessed seismic responses recorded at the geophone must be digitally processed to create an accurate seismic image. The processing of a seismic survey is an interactive and interpretative process that is both time and computer intensive. Many decisions must be made in the process and an understanding of the ultimate interpretation goal by the processor is of critical importance to the project success. The number and combination of digital processes that potentially can be applied are too numerous and detailed for the scope of this primer. However, a generalized overview of the process and a few key workflows that are important for seismic analysis of shale are detailed below.

From a simplistic standpoint, seismic processing can be thought of as having three main components, with potentially dozens of steps or workflows to be applied depending on the particular challenge. Initially, the seismic must be quality control checked and organized properly. Unexpected problems that happen in the field during acquisition are numerous and varied and must be corrected in the processing stage. Source and geophone locations need to be confirmed or corrected. Near surface geology, geophone, and source elevation corrections must be applied. Surface conditions such as passing trucks, weather phenomena, or wildlife or livestock disturbing equipment in the field may cause bad traces and need to be edited or removed.

6.3.1 Migration

Due to the physics of the seismic wave propagation in the subsurface and the geometry of the earth, subsurface seismic reflectors must be migrated, or repositioned, to place the reflectors in their proper X, Y, time, or depth location in the earth. To accomplish this migration the processing geophysicist must create an accurate velocity model over the seismic survey to determine ray path geometries. While many different approaches and methods have been applied over the years, current industry standards organize into two types of approaches, pre-stack time migration (PSTM) and pre-stack depth migration (PSDM).

As with any seismic processing procedure, there are trade-offs as to whether PSTM or PSDM is the more appropriate methodology for a project. PSDM has one obvious advantage in that it delivers a 3d volume of data in the depth domain. Migration is never perfect, and errors will occur in the depth volume predicted by PSDM compared to the true 3D earth model. In general, PSDM produces a better overall structural depiction of the earth and will enhance the interpreter's

ability to recognize subtle structural features. Conversely, PSTM generally is a better process for amplitude preservation. The importance of this will become apparent in the seismic inversion and attributes section, and for this reason, PSTM tends to be the migration method of choice in shale plays.

Both PSTM and PSDM approaches rely on complex velocity profiles and volumes created by the processing geophysicist. Both PSTM and PSDM velocity profiles take into account vertical anisotropy otherwise known as vertical transverse isotropy (VTI). Simply described, VTI is a variation of the seismic velocity as the wave field moves through bedding planes at different angles. Horizontal transverse isotropy (HTI) measures the anisotropy in the velocity field as seismic waves move through the earth at different horizontal azimuths. This effect is caused by vertically aligned fractures in the rock, which when correctly interpreted can be of critical assistance to a full understanding of our earth model for shale play exploitation. Orthorhombic PSTM is a migration technique which accounts for both VTI and HTI and ultimately benefits the fracture and stress analysis attributes that will be described later.

6.3.2 Techniques for Signal Improvement

A critical processing step needed for shale analysis is related to signal improvement. In this stage, signal is enhanced, and random and non-random noise is attenuated to compensate for poor signal, multiples, dispersion, gaps, or holes in source or receiver locations. A variety of digital filters, signal enhancements, and interpolation techniques can be applied.

Irregularly sampled seismic acquisitions due to surface topography, gaps, or holes in permitting, or manmade obstacles such as towns, factories, highway systems, etc., are responsible for gaps in the seismic response. These interruptions give rise to ambiguous images for the interpreter, or worse, misinterpretation of the earth model. One of the many signal improving processing techniques used by processing geophysicists that has shown strong value for shale play analysis, is 5D interpolation of pre-stack data. 5D interpolation is based on a Fourier reconstruction of super-sampled seismic dataset (what is desired) from under-sampled data that is recorded in the field. The algorithm will simultaneously interpolate samples from inline, xline, source-receiver offset distance, source-receiver azimuth, and time.

As pre-stack seismic data is used for pre-stack time migration (PSTM), pre-stack depth migration (PSDM), and orthorhombic PSTM migration, use of 5D interpolation improves the confidence in the final migration. **Fig. 6.1** shows a picture of a surface mine over which a 3D survey was acquired and processed. Due to the steep slopes and water filled pit, no receivers or sources were able to be placed at this location. **Fig. 6.2** shows seismic line from the PSTM 3D volume prior to 5D interpolation. Although reflectors do exist under the mine, there is substantial risk in the interpretation of the earth model due to incomplete data. **Fig. 6.3** shows resulting migrated data after 5D interpolation. Shallow reflectors under the mine now demonstrate a higher level of continuity, while many other deeper reflectors that would not have been as adversely effected by the mine, remain relatively unchanged.

Equally important for shale exploitation, 5D interpolation will regularize the amplitude responses along the pre-stack seismic gather improving very important pre-stack amplitude attributes used in shale characterization projects. **Fig. 6.4** shows seismic gathers before and after 5D interpolation has been applied. The resulting amplitude continuity and improvement of signal is obvious in the interpolated gather. **Fig. 6.5** shows a resulting AVO amplitude based on seismic attribute. The second map, generated from the 5D interpolation volume appears cleaner and more geologically feasible. Channel geometries running northwest to southeast (light green) are expected based on the geologic framework and appear to be more pronounced on the interpolated volume map.

6.3.3 Seismic Reservoir Characterization

Seismic reservoir characterization is the process of describing important reservoir properties from the pre-stack and post-stack seismic data volumes. It integrates geological measurements such as wireline logs and

Fig. 6.1—A surface mine location target for 3D seismic survey.

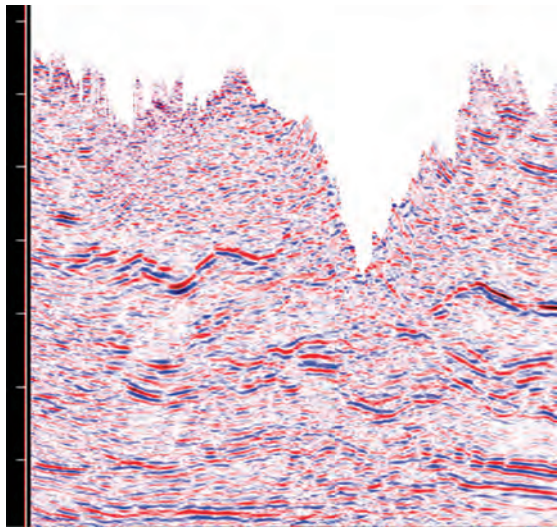

Fig. 6.2—Seismic lines from PSTM before 5D interpolation.

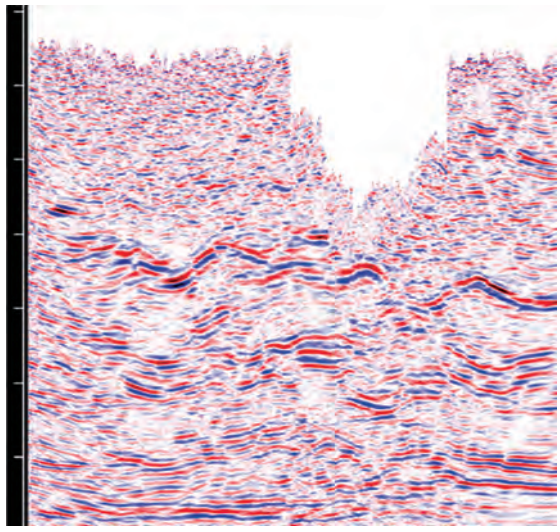

Fig. 6.3—Seismic lines from PSTM after 5D interpolation.

estimates from cores and cuttings with different seismic attributes extracted from pre-stack and post-stack seismic volumes. In conventional plays the focus of reservoir characterization is generally on a few key attributes such as porosity, water saturation, and volume of shale. With unconventional shale analysis, the picture is not quite so clear. There are potentially dozens of geologic attributes that can be important to the characterization of producing shale. These attributes generally fall into one of three major groups, all of which are analyzed in the seismic reservoir characterization process of shales.

Rock property attributes, such as mineral percentage, total organic carbon (TOC), porosity, and lithofaces, can all be

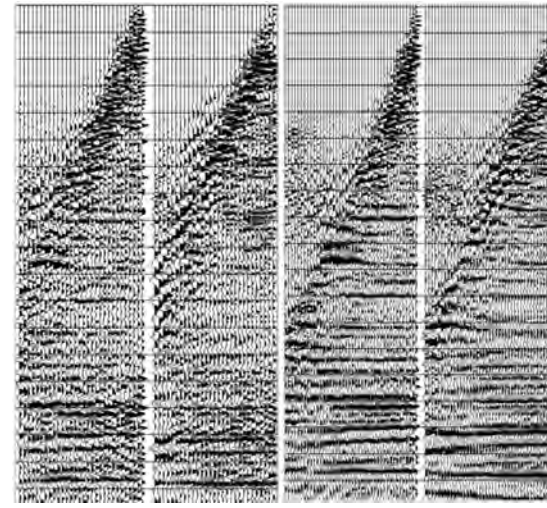

Fig. 6.4—Seismic gathers before (left) and after (right) 5D interpolation.

estimated with post inversion geological calibration. These attributes help in the understanding of some of the key productivity drivers for the reservoir.

Geomechanical property attributes, such as Young's modulus, Poisson's ratio, and resulting estimates of rock brittleness, are also estimated from geologic calibration of pre-stack inversion results. These attributes can be used to understand whether the shale is ductile or brittle and subsequently how it will behave when hydraulically stimulated.

Fracture and stress attributes, such as differential horizontal stress ratio and stress orientation, are calculated from azimuthal analysis of the seismic data and can assist in the interpretation of in situ horizontal stress and orientation. This information can be calibrated to image logs and provide value when determining optimal drilling direction and a hydraulic fracture strategy.

6.3.4 Seismic Inversion

Sheriff (2002) defines seismic inversion as deriving from field data, a model to describe the subsurface that is consistent with the data. The forward seismic model is simple and can be created from any well with a sonic and density log. Unfortunately, however, the inverse model is a bit more complicated. When seismic data is acquired, the earth filters the original seismic source, removing both low and high frequency from the original signal. **Fig. 6.6** demonstrates this effect in the earth filter in the frequency domain. Notice how the original earth reflectivity spectrum

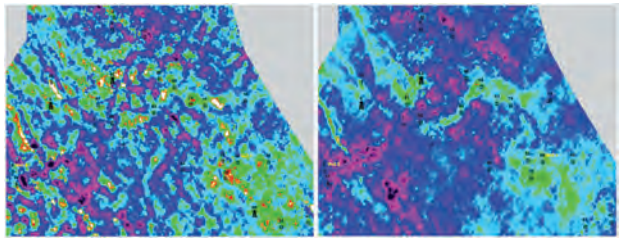

Fig. 6.5—Resulting AVO amplitude based on seismic attribute.

is filtered by the wavelet spectrum (earth filter). The effect on the resulting seismic trace spectrum is the removal of high and low frequencies.

In the inversion process, the geoscientist must provide a reasonable initial model of impedance along with an estimate of the wavelet, which can be extracted using well ties. This additional information combined with judicious constraints on the inverse model will lead to reasonable impedance models (**Fig. 6.7**).

There are many different approaches to seismic inversion. Some work on post-stack seismic data with the intention of describing the acoustic impedance of the subsurface. Pre-stack seismic inversion creates an earth model of acoustic impedance, shear impedance, and density utilizing the relationships defined in the Zoeppritz equations (Zoeppritz 1919). These relationships describe how seismic energy is partitioned at a geological boundary. Both pre-stack and post-stack inversions can utilize a deterministic or stochastic approach. A deterministic inversion finds the single best earth model that can describe the seismic response. Stochastic inversion creates a number of high-resolution earth models of impedance, using geostatistical techniques. Each realization is equally probable allowing geoscientists to measure probability and uncertainty in the impedance prediction.

6.3.4.1 Post-Stack Seismic Inversion

Post-stack inversion is essentially a processing technique that creates a broadband acoustic impedance response from every seismic trace. To accomplish this, key well logs containing velocity log information are converted from the depth to time domain. Well logs are correlated to the seismic data through the use of a synthetic seismogram. A wavelet or series of wavelets is then extracted from the seismic data to maximize the correlation of the synthetic to seismic section. This wavelet will be used later to deconvolve the seismic trace. The acoustic impedance logs from the wells are interpolated, honoring the interpreted geologic structure. This low-frequency model contains information that the

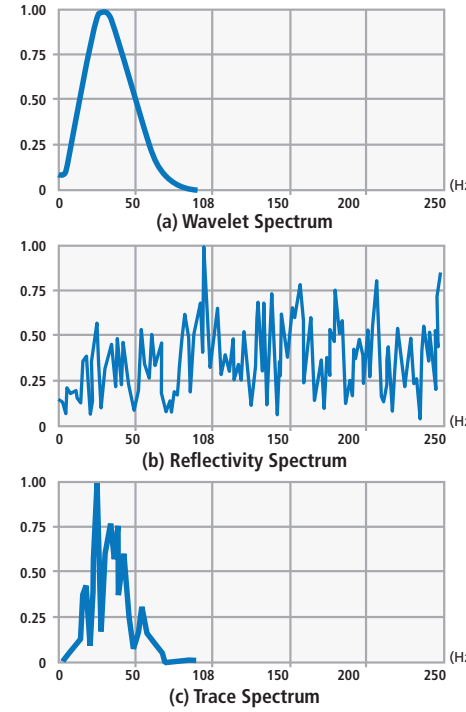

Fig. 6.6—Effect of earth filter in the frequency domain.

earth has filtered and will be added back to properly bias the acoustic impedance trace.

- **Sparse-Spike Inversion:** The sparse-spike algorithm seeks the simplest possible reflectivity model that when convolved with a wavelet produces a synthetic seismogram trace that matches the original input seismic. As with recursive inversion, the final acoustic impedance inversion result is biased with a well log derived low-frequency background model.
- **Model Based Inversion:** In model-based inversion the low-frequency well log derived background model serves as a starting point. Using the model, a synthetic seismogram is created at each trace and compared to the original seismic trace. The acoustic impedance model is modified to minimize the error between the synthetic and seismic trace.
- For shale reservoir characterization, a post-stack acoustic impedance inversion can provide interpreters with a very quick result. Although a comprehensive shale seismic reservoir characterization requires much more thorough analysis, post-stack inversion gives geoscientists some quick wins in interpretation. To begin with, all seismic traces are transformed to acoustic impedance logs removing side lobes and enhancing the ability to correlate seismic stratigraphy with log data. Some reservoir properties may

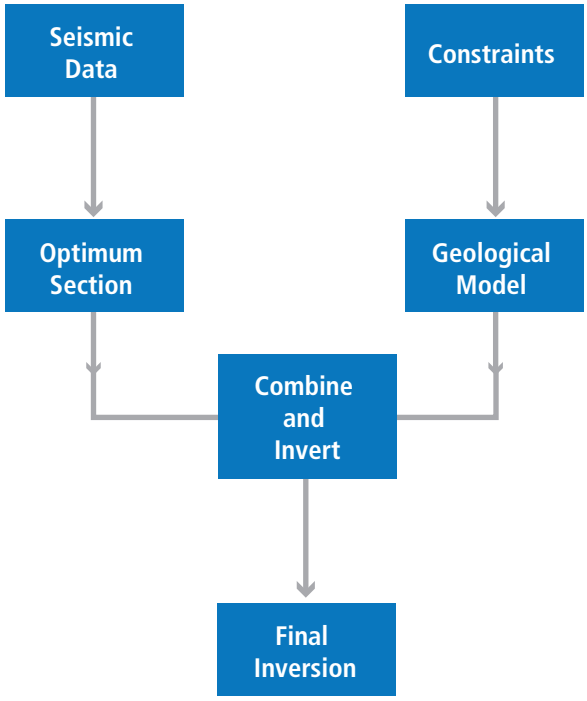

Fig. 6.7—Use of constraints together with the seismic data to derive the final inversion model.

show a positive correlation with the impedance, allowing for precursory reservoir descriptions. The knowledge gained in seismic conditioning, well ties, wavelet extraction, and construction of the low-frequency model can assist the geoscientist with more complicated and laborious stochastic and pre-stack inversions.

6.3.4.2 Pre-Stack Simultaneous Inversion

Similar to post-stack inversion, pre-stack inversion will create an earth model of impedance. This requires conditioning of the seismic data, proper well correlation in time to the seismic trace, extraction of wavelets over the zone of interest for deconvolution, and a low-frequency model to be the creation of the missing frequency content from the seismic bandwidth. Pre-stack inversion, however, is designed to invert seismic data of PSTM angle gathers or multiple angle stacks, creating an earth model of acoustic impedance, shear impedance, and density. This is done using seismic transmission-reflectivity relationships defined in the Karl Zoeppritz equations. Zoeppritz (1919) defined a set of equations describing how seismic energy behaves at bed boundaries in the earth (**Fig. 6.8**). At each geologic interface, incident P-wave energy is transmitted and reflected. Although, only recorded with multicomponent acquisition equipment and processing techniques, mode conversion at these boundaries and reflecting and transmitting S-wave energy as well. The relationship of incident P-wave energy to reflective P-wave energy at different angles can give rise to the changes in VP, VS, and density between bed boundaries and is the basis for pre-stack inversion.

Several linearized approximations simplify the original Zoeppritz equations. The Aki–Richards equation (Aki and Richards 1980) is written in a more intuitive sense and is the basis for AVO and prestack inversion methods. The equation defines that the total reflectivity and any angle can be calculated as the weighted sum of the acoustic impedance, shear impedance, and density reflectivities. Acoustic impedance and shear impedance models are well constrained and a common output from all pre-stack inversions. Density, however, is only truly obtained in a pre-stack inversion with clean high-angle seismic gathers. These criteria rarely are obtained with onshore shale oriented seismic surveys; thus, density must often be estimated with other procedures.

6.3.4.3 Pre-Stack Azimuthal Analysis

Many of the attributes acquired in seismic reservoir characterization for shales describe mineralogical, geomechanical, or lithofacies properties of the reservoir. Pre-stack azimuthal analysis techniques illuminate how some key seismic attributes behave when the data is interrogated azimuthally. This information can be used to predict the orientation and magnitude of fractures in the reservoir.

The technique for analyzing horizontally transverse isotropic media using amplitude variations with angle and azimuth was proposed by Rüger (1996). To begin, we assume a single set of vertical or near vertically aligned fractures left open due to local horizontal stress. **Fig. 6.9** simply illustrates that seismic waves propagate slower when the travel path is normal to the fracture orientation, encountering more fluid filled voids in the rock that alters both the velocity of the seismic wave and amplitude response of the reflected events as the wave moves through the earth at different azimuths.

Changes in the amplitude versus angle azimuthal (AVAz) response provide the reflectivity estimate of both orientation and magnitude of stress based on reflectivity. We can extend this analysis to pre-stack azimuthal inversion for more interpretive layer base estimates of stress and fracture density and orientation (**Fig. 6.10**).

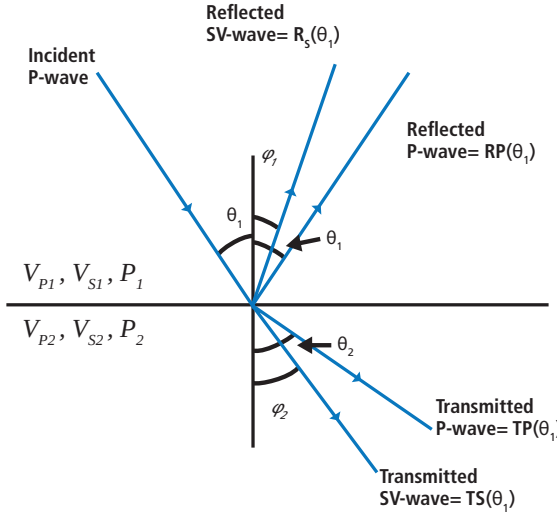

Fig. 6.8—Model conversion of an incident P-wave on the boundary between two elastic layers. (Russell et al. 2006.)

6.3.5 Post-Inversion Processing

The seismic inversion process provides acoustic impedance, shear impedance, and density as data volumes for our analysis

$$R(\theta) = aR_{VP} + bR_{VS} + cR_D \qquad \textbf{(Eq. 6.1)}$$

where:

$$R_{VP} = \frac{\Delta V_P}{2\overline{V}_P}, \; R_{VS} = \frac{\Delta V_S}{2\overline{V}_S}, \; R_D = \frac{\Delta \rho}{2\overline{\rho}},$$

$$a = 1 + \tan^2\theta, \; b = -8K\sin^2\theta,$$

$$c = 1 - 4K\sin^2\theta, \text{ and}$$

$$K = \left(\frac{\overline{V}_S}{\overline{V}_P}\right)^2$$

of the shale reservoir. With some simple algebraic expressions, we can convert these impedance volumes to key rock property estimates. Typically a geoscientist may convert inversion volumes to the Lamé parameters of Lamda-Rho and Mu-Rho and dynamic geomechanical estimates of Young's modulus and Poisson's ratio. These estimates of rock property values can be calibrated with the wells and extrapolated throughout the extent of the seismic volume. Additional volume attributes derived from seismic are numerous and are calculated from a variety of transforms. Fourier analysis of individual seismic yield a variety of amplitude, phase and frequency based attributes. Spatial analysis of the volume can lead to curvature, semblance, and continuity volumes.

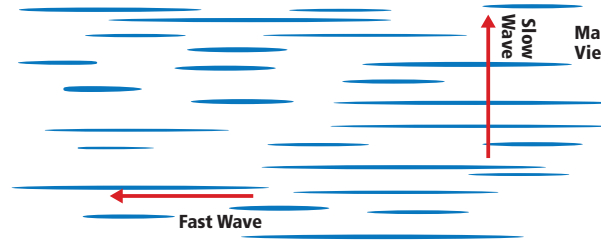

Fig. 6.9—Seismic waves propagate more slowly when the travel path is normal to the fracture orientation.

6.3.5.1 Multiple Attribute Analysis for Rock Property Volumes

The utilization of multiple seismic attributes to estimate log and reservoir properties away from wells in a seismic volume was proposed by Schultz et al. (1994) in a series of three articles in *The Leading Edge*. Hampson et al. (2001) describe a statistical methodology that essentially trains a set of seismic attributes to predict reservoir properties using multilinear and neural network transforms. In the simplified display in **Fig. 6.11**, a single point on a well log can be described by using a variety of weighted seismic amplitudes. With potentially dozens of seismic attributes, multivariate geostatistical processes can be employed to predict meaningful reservoir properties, such as mineral percentage volumetrics, TOC, porosity, and water saturation away from the well bore. **Fig. 6.12** shows a specific example where this process was employed on a project in the Haynesville shale. The black log curve is the Vshale calculated from the well logs. The red curve is the predicted Vshale using multivariant analysis from the seismic. Once the relationship is validated, it can be applied to the full seismic volume, essentially creating a full volume of that particular log property. In the display, this process was repeated for a variety of reservoir properties.

Quantitative estimation of reservoir properties is a powerful predictive tool. However, the predictive ability of this type of process relies on sufficient well log coverage within a certain geographic extent. These processes should be validated judiciously and updated as new wells become available. Consistency in log processing and seismic signal are key in the creation of a meaningful predictive attribute.

6.3.5.2 Bayesian Classification for Lithofacies Probability Volumes

In the previous section we explored the use of multi-variant analysis in the prediction of rock property volumes from key seismic attributes. The correlation coefficient between well log and seismically derived rock property can easily

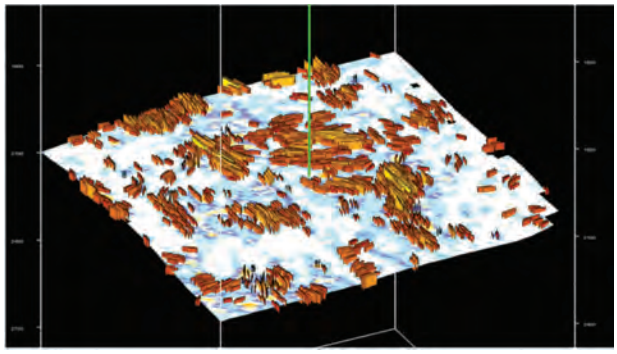

Fig. 6.10—Predicted fracture intensity and direction displayed by color-coded platelets. (From CGG 2014.)

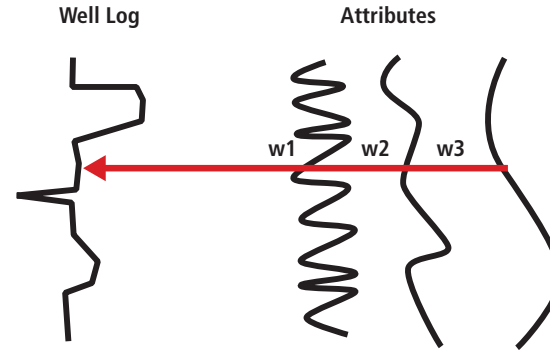

Fig. 6.11—Weighted seismic amplitudes.

be calculated at the well locations. One way to quantify the uncertainty in rock property and lithofacies predictions from seismic is through the use of a supervised Bayesian classification. In the equation below, we predict the probability of any class ***c***.

where:

- c is a class (e.g., sand).
- X is a seismic attributes vector (e.g., X = (Zp, Vp/Vs)).
- $p(c)$ is the a priori probability for class ***c*** (e.g., probability of getting sand in general).
- $p(X \mid c)$ is the probability of attributes X knowing we are in class c (e.g., distribution of (Zp, Vp/Vs) in sand).
- $p(X)$ is the probability of attributes X.

The schematic diagram (**Fig. 6.14**) demonstrates the process. Multiple rock properties are extracted from both well logs (the training dataset) and from seismic inversions (the input data). Cross plotting and analysis of the training dataset leads to the calculation of multivariate probability functions. The probability of any particular class and the determination of the most likely class can now be determined. If acceptable for the training data, the probability function can be applied to seismic volumes, creating volumes of lithofacies probability and most likely class.

The application of this process is demonstrated in the case study below. For successful predictions, careful consideration should be given to the creation of the lithofacies training dataset and specifically the ability to separate distinct attributes in multidimensional cross plot space.

6.4 Seismic Attribute Interpretation

$$p(c \mid X) = \frac{p(c) \cdot p(X \mid c)}{p(X)} \qquad \textbf{(Eq. 6.2)}$$

In previous sections, we explored the calculations of multiple attributes from seismic inversions, Fourier and spatial analysis, and seismic anisotropy. Multiple attributes were combined in statistical analysis and classification schemes to create rock property and lithofacies probability volumes. Alone, some of these volumes can be quite useful. A TOC seismic volume should be useful in the measurement of gas in place. Geomechnical estimates of Young's modulus and Poisson's ratio yield an understanding of rock strength and how the rock may behave when hydraulically stimulated. Anisotropy volumes and the associated interpretation of stress and fractures may also help predict how fractures will propagate under hydraulic stimulation.

6.4.1 Utilization of Attributes in Hazard Avoidance

One of the most fundamental applications of seismic data in shale well development relates to geologic structures. Seismic can be crucial for the well planning stage in determination of bed thickness, dip, faults, fractures, and karsts. Pre-stack time migrated (PSTM) data is often sufficient with simple structural interpretation. The value of pre-stack depth migrated (PSDM) data increases with the structural complexity of the reservoir.

PSTM stack seismic data can be used to help land a well in the reservoir with lateral well design, either avoiding or steering though faults and ensuring the well stays in the zone. Faults fractures and karst are hazardous to both drilling and completion stages of a well and should be identified predrill. Several seismic attributes prove useful in

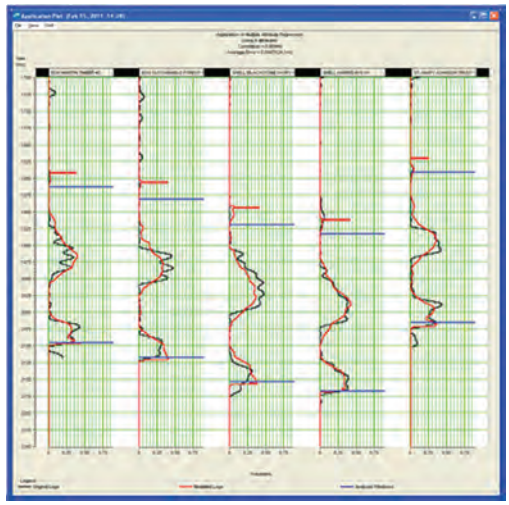

Fig. 6.12—Seismic characterization analysis.

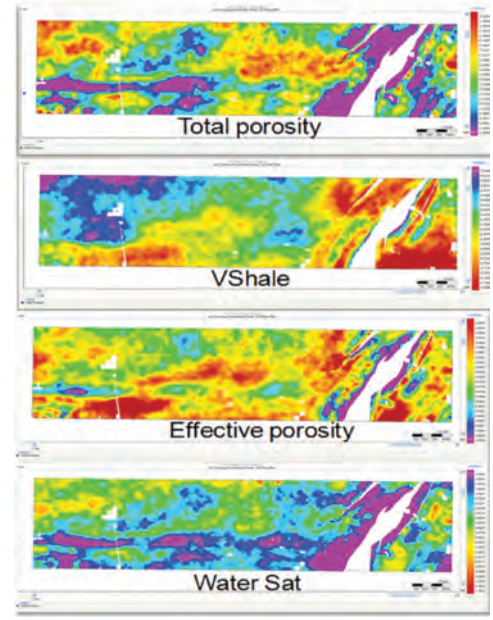

Fig. 6.13—Seismic characterization analysis.

this effort: geospatial attributes such as curvature, continuity, and seismic anisotropy. In **Fig. 6.15** stress is estimated from seismic anisotropy analysis and may help in the identification of faults and other hazards not resolvable in the stack seismic data.

6.4.2 Seismic Attribute Correlation with Production Information

A high degree of heterogeneity within many shale plays leaves the task of finding sweet spots, determining preferential drilling direction, and optimal completion strategy challenging. Seismic reservoir characterization has created dozens of seismic attributes that may be directly or indirectly related to production. Finding the sweet spots or preferential drilling locations within a field, may require the use of several attributes in combination. A high TOC content may point to an area with superior source rocks, potentially degraded by a lower silica content, leaving the rock less brittle and harder to fracture. There is no single silver bullet attribute. However, careful statistical calibration to production information may illuminate a combination of attributes valuable for prediction.

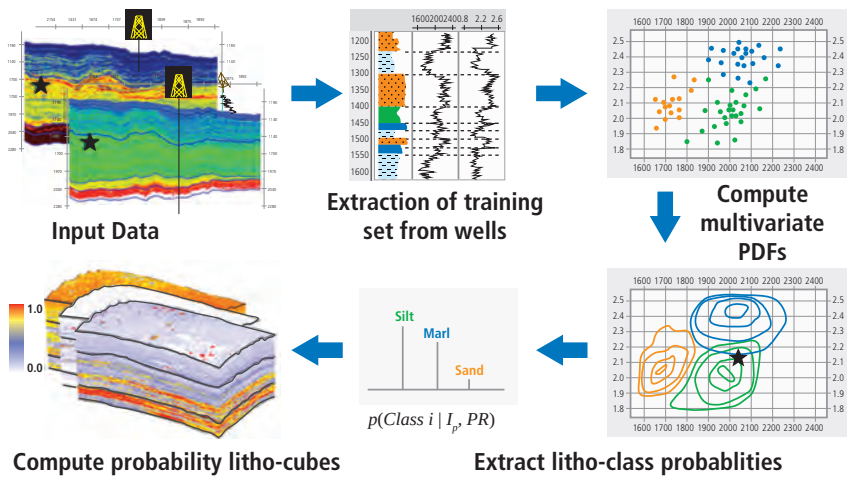

Fig. 6.14—Typical workflow for probability computation of litho-cubes. (CGG 2012.)

6.4.2.1 Mapping Sweet Spots

Earlier, we explored the use of multiple attribute analysis of seismic data in the creation of rock property volumes such as TOC and mineralogy. The process used multivariate statistics to determine the best combination of known seismic attributes in the prediction of a target curve originating from the well control. We can exploit a similar technique to map the sweet spots within an area.

The process can be simplified to predict production values from mapped locations. **Fig. 6.16** demonstrates the multi-attribute map transform approach where weights are computed and applied to multiple attribute slices from the reservoir volume to predict production values from multiple wells. Well production values must be carefully conditioned and normalized to take into account the length of the lateral, the production strategy, length of time producing, and possibly variations in completion strategy.

In **Fig. 6.17**, the well value to be predicted are kriged. Four seismic attributes are determined to be predictive of the production values, shown in **Fig. 6.18** and **Fig. 6.19** shows the predicted production or sweet spot map to be used as an aid in the placement of wells.

6.4.2.2 Preferential Drilling Direction

Shale wells are typically drilled perpendicular to the maximum principal horizontal stress to optimize the benefit from hydraulic fracturing. Naturally occurring fractures in the rock and those induced by the hydraulic fracturing process normally will be aligned with the stress field, thus creating a maximum amount of fractures and production. Analysis of the seismic anisotropy can illuminate the orientation and magnitude of the stress for placement and orientation decisions. In **Fig. 6.20**, the map base color represents Young's modulus. Higher values of Young's modulus are considered to be brittle. The stress field appears to vary in orientation and magnitude as indicated on the platelet display, originating from the seismic anisotropy analysis.

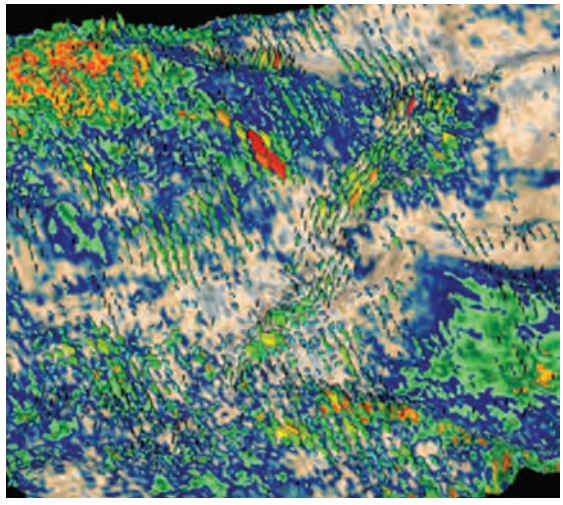

Fig. 6.15—An example of shale gas sweet spot detection via inversion (rock properties) and fracture analysis combined. (Delbecq et al. 2013.)

6.4.2.3 Completion Strategy

It is well understood by the industry that not all fracture stages contribute to production. Cipolla et al. (2010) show the results from a production log study demonstrating the discrepancy in production between perforation clusters caused by reservoir heterogeneity. In **Fig. 6.21**, a substantial number of stages contribute no production at all. Careful analysis of the rock properties predicted by seismic along the lateral should illuminate the areas most likely to produce. Again, a variety of attributes can be considered in this analysis: TOC, mineralogical volumetrics, geomechanical properties, and in-situ stress. In the section on mapping sweet spots, a combination of attributes was statistically determined and validated as a predictor of production. Upon closer inspection, these attributes show heterogeneity along the length of the lateral well planned and drilled. **Fig. 6.22** is an enlarged version of the same style productivity map. The log display shows mineralogical information extracted from the well. The fractured wing displays suggest a strategic completion approach as opposed to a geometric approach to completion.

6.5 Validation Techniques

Our shale earth model probably will change with each additional well. As new information becomes available in terms of logs, core, cuttings, microseismic surveys, and production, we can validate and recalibrate the model. New production information is relatively simple to add in the 2D multivariate analysis described above. Two additional techniques described here and employed in the case study below are calibration to mineralogy and calibration to microseismic.

6.5.1 Calibration to Mineralogy

Mineralogy prediction from seismic was achieved above by using pre-stack seismic inversion, generating acoustic impedance, shear impedance, and density volumes. These volumes then transform to different reservoir properties

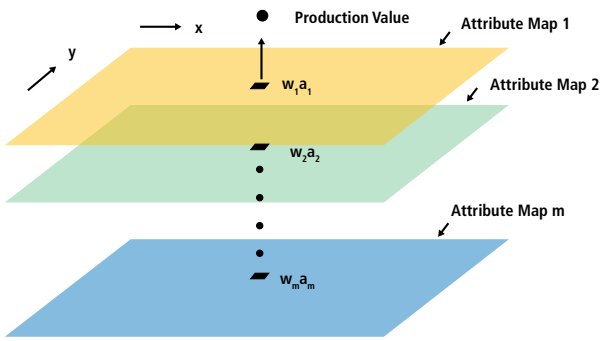

Fig. 6.16—Multi-attribute map transform approach in predicting production values from multiple wells. (CGG 2008.)

including mineralogical volumetric percentages through the use of multivariate analysis. Drill cuttings sampled from both the vertical and lateral portions of the well can be calibrated for mineralogy porosity and compared to seismic predrill models.

6.5.2 Calibration to Microseismic

Microseismic monitoring of pressure pumping operations can give operators a qualitative idea as to the fracture intensity and complexity by stage. Studies have shown that stress, brittleness, and geologic hazards all influence the effectiveness of the hydraulic fracture treatment and often can be measured by the size and orientation of the microseismic volume. **Fig. 6.24** shows the extent of microseismic events from one well. The map color represents Young's modulus from the shale seismic reservoir characterization process. In **Fig. 6.25**, we cross plot the size of area affected by microseismic (stimulate rock volume) for 87 microseismic stages, with the corresponding Young's modulus value captured within each stage. The relationship appears clear that larger values of Young's modulus generate larger stimulated rock volumes.

6.6 Case Study

A case study was conducted on the Lower Haynesville section of the Haynesville shale play located in northwest Louisiana to identify sweet spot locations and determine well placement using a 3D seismic reservoir characterization workflow integrating reservoir and geomechanical properties. The study emphasizes the importance of examining multiple measurements from different sources in improving drilling and completion strategies. This section presents the details and discusses results of that study integrating surface seismic, microseismic, rock properties, and mineralogy in the Haynesville shale play.

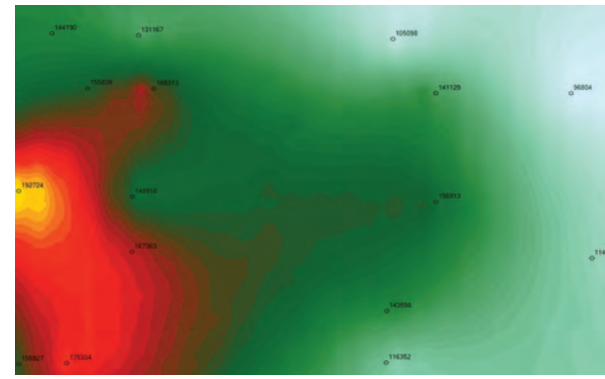

Fig. 6.17—Well value to be predicted.

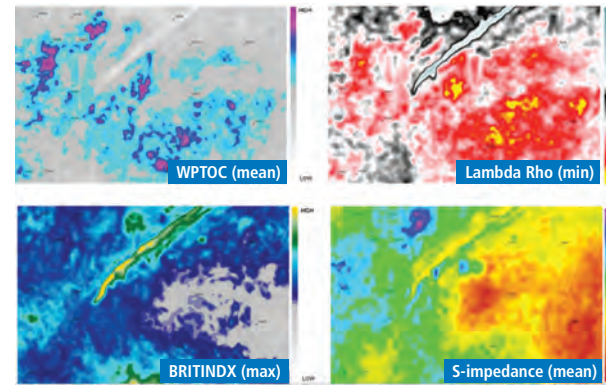

Fig. 6.18—Four seismic attributes are determined to be predictive of the production values.

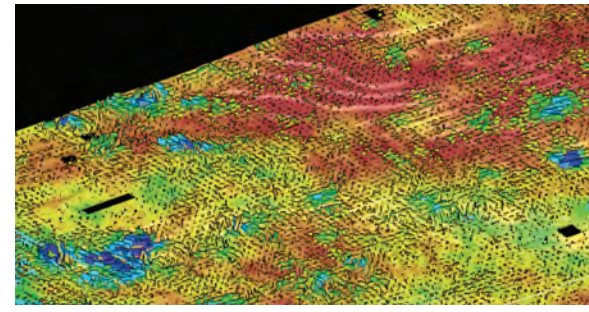

Fig. 6.19—Map of the sweet spot locations for drilling.

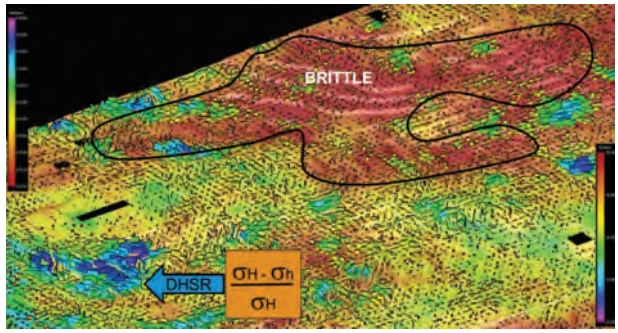

Fig. 6.20—Stress direction and derived Young's modulus generated from seismic anisotropic study. (From Hampson-Russell, a CGG Company.)

6.6.1 Integrating Surface Seismic, Microseismic, Rock Properties, and Mineralogy in the Haynesville Shale Play

Although drilling has slowed substantially from its peak in 2010, steadily improving natural gas prices coupled with the promise of demand from liquefied natural gas and gas to liquids facilities have renewed interest in the prolific Haynesville shale gas play in northwest Louisiana. A consensus of opinion among operators in the field will agree that only a fraction of the Haynesville potential has been developed.

As is the case in most shale plays, production from wells has been highly variable, leading to the use of 3D seismic reservoir characterization studies for the determination of sweet spots, well placement, and completion strategies where seismic anisotropy has been proven to be an important factor in understanding the shale plays.

This chapter illustrates a workflow (**Fig. 6.26**), integrating reservoir and geomechanical properties obtained from pre-stack seismic inversion and incorporating stress and fracture information extracted from azimuthal analysis of the seismic data. Eight area wells targeting the Haynesville and Mid-Bossier reservoirs were used for calibration of surface seismic measurements of reservoir and geomechanical properties. A variety of seismically derived attributes are used to estimate production potential in the field. This paper shows the application of global azimuthal inversion, a technology for extracting the azimuthal anisotropy. Above all, the workflow makes quantitative use of microseismic and scanning electron microscope-derived mineralogy data to validate the seismic-derived attributes.

Although the Mid-Bossier formation proved successful in certain wells in the study area (**Fig. 6.27**), the Lower Haynesville is the main target for shale gas production for this study. Geological structure in the area can be complex with numerous faults bisecting the study area. Generally, wells are positioned on the plateaus of the geological structures and between major faults. Laterals are generally oriented north-south perpendicular with the regional stress field.

6.6.2 Rock Properties from Seismic

Well log data provides calibration for all subsequent seismic analysis, including interpretation of elastic properties, HTI anisotropy and stress analysis. The study integrates eight wells targeting the Haynesville and Mid-Bossier reservoirs. Information from core (**Fig. 6.28**), cuttings and diagnostic fracture injection test (DFIT) analysis complements the well, surface, seismic, and microseismic data.

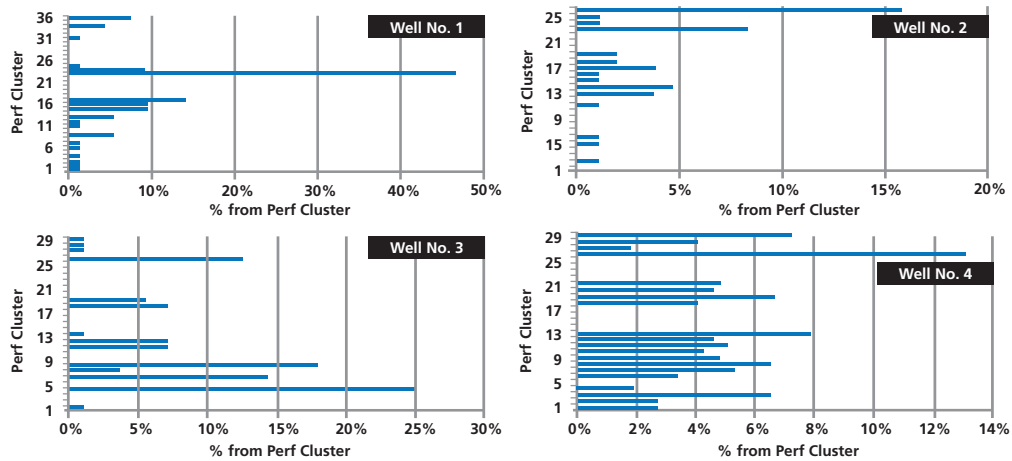

Fig. 6.21–Uneven production contribution from each perforation cluster. (Cipolla et al. 2010.)

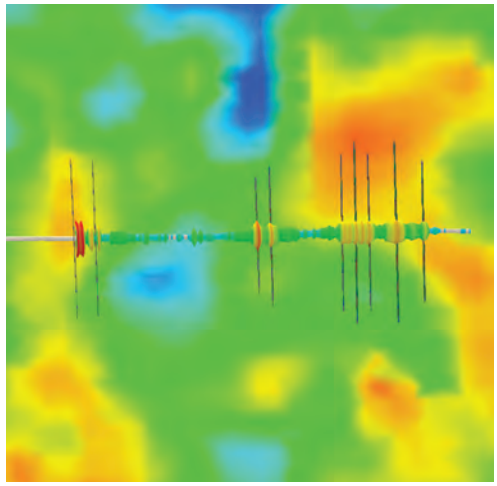

Fig. 6.22—Strategic completion approach resulted from production log analysis.

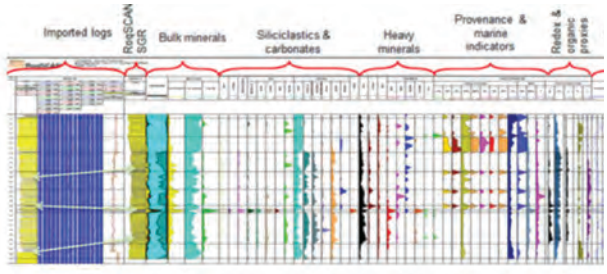

Fig. 6.23—A vertical RoqSCAN data summary log showing calibration of mineralogy data. (From Robertson, a CGG company.)

Properties associated with gas-bearing rocks in the Haynesville and Mid-Bossier (free gas mingled with absorbed gas and TOC are similar to those associated with free gas in conventional reservoirs, including correlation of increasing gas volume with decreasing Poisson's ratio and Lambda-Rho. In the target intervals, subtle contrasts attributed to gas are somewhat larger than those attributed to minor lithology variation but smaller than contrasts observed between different zones marked by dramatic changes in lithology and porosity (Fig. 6.28), such as the transition from lower Haynesville to Smackover.

In this study, pre-stack simultaneous inversion was applied to conditioned angle gathers to derive P-impedance, S-impedance, and density. Commonly used descriptive reservoir attributes, such as mineral volumetrics, TOC, porosity, water saturation, and lithofacies, were estimated with multilinear regression prediction techniques. This analysis suggests P-impedance is mainly inversely related to porosity. Density and TOC also have an inverse relationship.

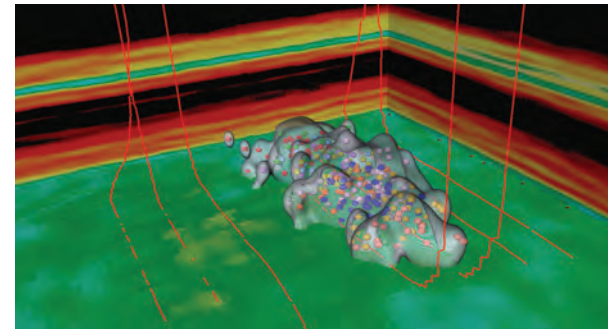

Fig. 6.24—Extent of microseismic events from one well. (CGG.)

Additionally, Lambda-Rho (product of Lamé's parameter and bulk density) appears to be directly related to Haynesville zones with high gas volumes that are estimated from log data (**Fig. 6.29**).

Rocks with higher clay content are more ductile and difficult to fracture. Zones with high quartz volumes are stiffer and more likely to fracture when under hydraulic stress. Mineral fractions of quartz, calcite, and clay were used in conjunction with Young's modulus (the ability to maintain a fracture) and Poisson's ratio (the ability of the rock to resist failure under stress) to provide insight into how brittle or ductile the rock may be.

Petrophysically derived lithofacies were created and applied to each well in the study. A supervised Bayesian classification methodology was applied with well control to generate probability cubes of lithofacies. This analysis is based on probability distribution functions associated with classes of pay (red), marginal gas-bearing zones (yellow), transitional "shoulder" facies (gray), and carbonate (cyan) (Fig. 6.29). The resulting seismic volumes of most-probable lithofacies (**Fig. 6.30a**) and probability of each lithofacies class (**Fig. 6.30b**) provided encouraging results for mapping. Indicative attributes in the identification of sweet spots could be compared directly and analyzed based on probabilities.

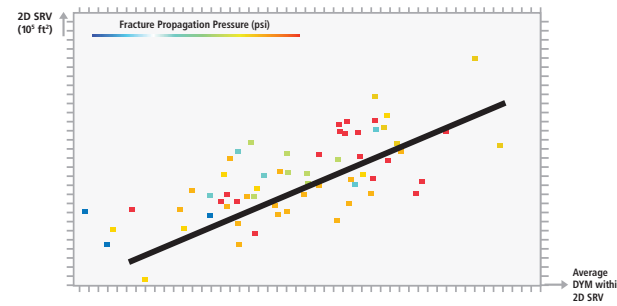

Fig. 6.25—2D SRV correlation with dynamic Young's modulus. (Castillo et al. 2014.)

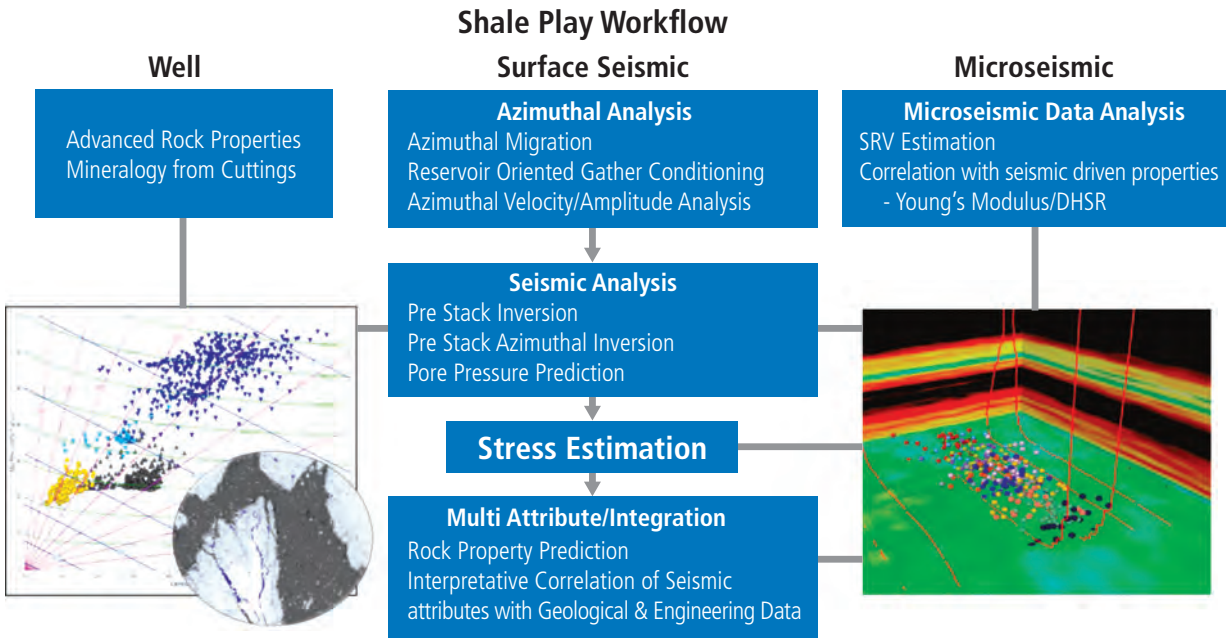

Fig. 6.26—Integrated geoscience workflow for a shale play, incorporating numerous disciplines to high grade the survey area to identify sweet spots and optimize drilling locations and completions.

6.6.3 Azimuthal Inversion: Stress Estimation from Seismic

In-situ stress, present in the earth prior to drilling, affects propagation of induced fractures and the long-term productivity of wells. Therefore, understanding the stress regime in the subsurface is important when planning the orientation of laterals. Further inspection of the seismic gathers illuminates the amount of HTI anisotropy in the data and azimuthal AVO and azimuthal elastic inversion (Castillo and Van de Coevering 2013) techniques give insights into in-situ stress and fracture parameters in the area. In this study, the stress state was estimated by employing a global inversion of pre-stack azimuthal seismic data using Fourier coefficients (Downton and Roure 2010) to derive fracture properties and eventually local in-situ stress fields. **Fig. 6.31** shows the resulting azimuthal anisotropy plates generated from attribute volumes: direction and height plus color. Direction, in this example, is the isotropy plane (orthogonal to symmetry axis) while height and color represent the magnitude of differential horizontal stress ratio (DHSR), calculated using azimuthal inversion. DHSR gives information about fracture orientation and style. The data slice (color of base horizon) is Young's modulus (approximates the ability to maintain a fracture).

Fig. 6.27—Location of the study area, northwest Louisiana. (Map and seismic data courtesy of CGG Land Multi-Client Data Library.)

Minimum (σh) and maximum (σH) horizontal stress can be viewed and interpreted independently; σh, or closure stress, represents the minimum amount of stress required to maintain open fractures. DHSR is the normalized difference between σh and σH and is an indicator of the stress regime.

In the Haynesville it has been suggested that with respect to hydraulic fracturing, low DHSR favors fractures with random orientation, while high DHSR favors fractures that are more aligned (Sena et al. 2011). Therefore, in this example, low DHSR may be more desirable if natural, open fractures are absent,

because the area stimulated (and hence production) can be maximized when the induced fracture pattern is more random.

Estimation of maximum vertical stress (σV) and σh is derived from pore pressure estimation using Eaton's equation (Eaton1975) modified for unconventional reservoirs. All elements of pore pressure prediction are verified by independent measurements that include DFIT tests and mud weights used while drilling. Additionally, σH is taken from tri-axial measurements of oriented core plugs. Conventional pore pressure methods assume low P-wave velocity in shale occurs whenever pore pressure is greater than hydrostatic pressure. Because high gas content and TOC can mimic pressure changes, this assumption was tested by running parallel calculations based on S-wave velocity and Mu-Rho. Where calibration data is available, P-wave velocity gives results closest to known pressures in the Mid-Bossier and Haynesville.

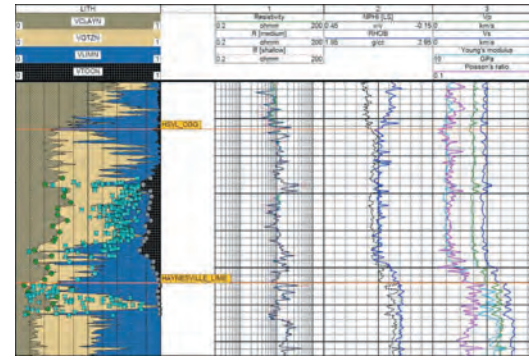

Fig. 6.28—Haynesville section with well log lithology fractions matched to up-scaled and normalized carbonate fraction/ volume–mineralogy from cuttings (left track: cross shapes) and up-scaled XRD (left track: round shapes).

6.6.4 Mapping Sweet Spots

The previous mention of rock property attributes alluded to manipulation of pre-stack inversion volumes through regression techniques. Multi-attribute linear regression finds

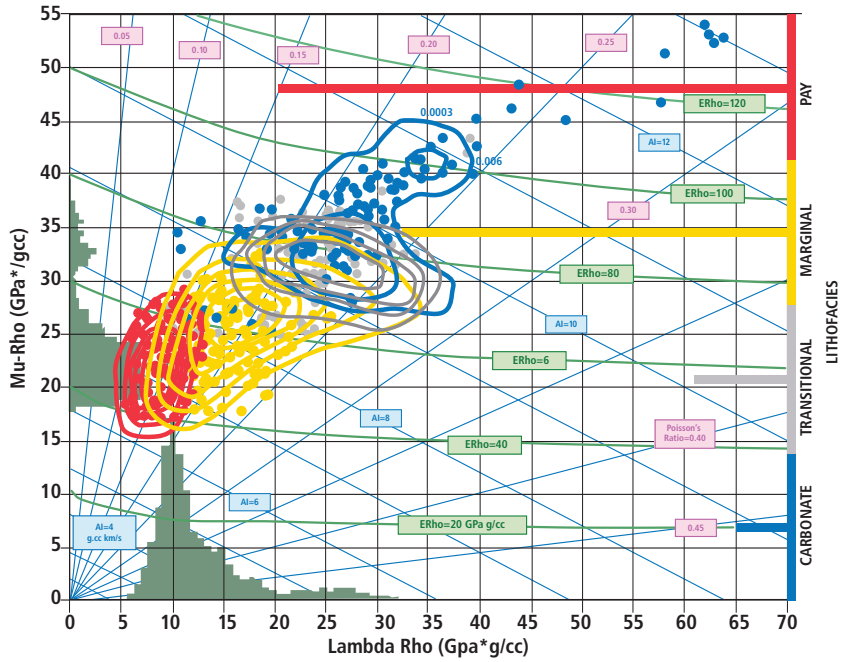

Fig. 6.29—Scatter of lithofacies data from multiple wells in the Haynesville. Red and yellow samples have <30% total carbonate; red samples have >70% gas saturation, while yellow samples have <70% gas saturation. Blue points have >40% carbonate by volume. Gray points, which do not fall into any of these classes, are transitional between lithofacies. The gas-rich (red) lithofacies are associated with high levels of TOC. Contours represent probability distribution functions for each lithofacies. Horizontal bar lengths give relative frequency of each lithofacies. Additionally, LRM cross plot space shows constant lines of acoustic impedance (AI = blue), Poisson's ratio (PR = magenta), and product of Young's modulus*density (ERho = green).

a relationship among attributes in multidimensional space leading to a best-fit seismic volume of a given target attribute. Target attributes tend to be volumetric well logs, such as total porosity, mineralogy, or water saturation. The process creates links between multiple seismic attributes and petrophysical data in three dimensions (x, y, and time or depth).

In this study, multi-attribute linear regression was applied to generate a 2D map of productivity index or a sweet spot map. The link is built between production data and maps extracted from the seismic attributes at the target level (**Fig. 6.32**).

Multi-attribute analysis is statistically driven; the method has no prior information or biases regarding which attributes are best. The optimal number of attributes and rank of each is determined during the analysis by validating the prediction at each production sample using the remaining control points. In our case, the closure stress has the highest correlation with the production index.

6.6.5 Integrating Microseismic

As shown, elastic and geomechanical attributes derived from surface seismic reflection data have proven to be very useful in shale gas reservoir management by delineating reservoir sweet spots where formation properties make the rock matrix more fracture-prone under hydraulic stimulation and predicting reservoir stress anisotropy, which may affect the orientation of hydraulic fractures. The impact of rock properties and spatial stress distribution on the success of hydraulic fracturing treatments may be evaluated by integrating data from hydraulically induced microseismic events. Spatial correlation of microseismic events with specific seismic attributes implies that both are governed by the same in-situ properties of the rock.

The study reveals physically meaningful statistical correlations between microseismic event density with estimates of Young's modulus and DHSR from azimuthal analysis (**Fig. 6.33a** and **6.33c**). The size of the stimulated reservoir volume (SRV) and stimulated reservoir area (SRA, i.e., 2D SRV) is directly proportional to average Young's modulus and inversely proportional to DHSR, implying SRV and SRA are maximized in areas of high Young's modulus and low differential horizontal stress. It is recognized that SRV derived from transcent pressure tests and production data may reveal a smaller volume.

Fig. 6.33b shows SRA with Young's modulus (color axis). The time evolution of the SRA was calculated to gain insight into the fracture growth process and to better understand the spatial and temporal correlation of microseismic events with the spatial distribution of seismic-derived

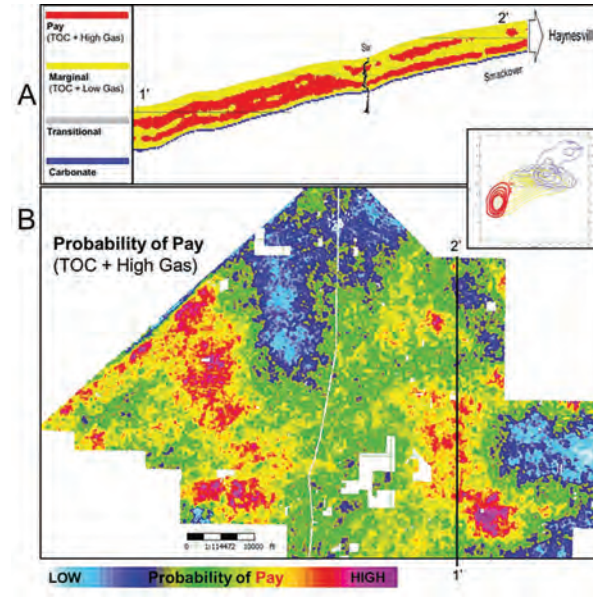

Fig. 6.30—Most probable lithofacies section (A) and (B) pay probability map at lower Haynesville level based on Lambda-Rho versus Mu-Rho (LMR) crossplot. The probability distribution functions that are applied to inverted seismic volumes honor the distribution of well log data in the LMR crossplot space (Fig. 6.29).

rock properties. The seismic to microseismic correlation is enhanced by relating the calculated size of the SRA with seismic attributes spatially averaged over the computed SRA for each stage.

6.6.6 Integrating Scanning Electron Microscope Mineralogy

Macro-effects sensed by surface seismic and microseismic observations span a much broader area than the relatively small volumes of rock sensed by well logs, yet both are ultimately controlled by the rock fabric at scales beyond even the well log measurements. To access this scale, cuttings and core chippings were analyzed at high resolution (in both vertical and lateral wells) using a scanning electron microscope (SEM) fitted with energy-dispersive X-ray detectors. This provides measured quantitative data on elemental and mineralogical composition, rock texture, porosity, and pore aspect ratio (Ashton et al. 2013). The dataset complements older, but less extensive, X-ray diffraction (XRD) data. Scanning electron microscope data is consistent with X-ray diffraction results for mineral fractions such as total carbonate and also match lithology estimates from conventional well logs (**Fig. 6.28**).

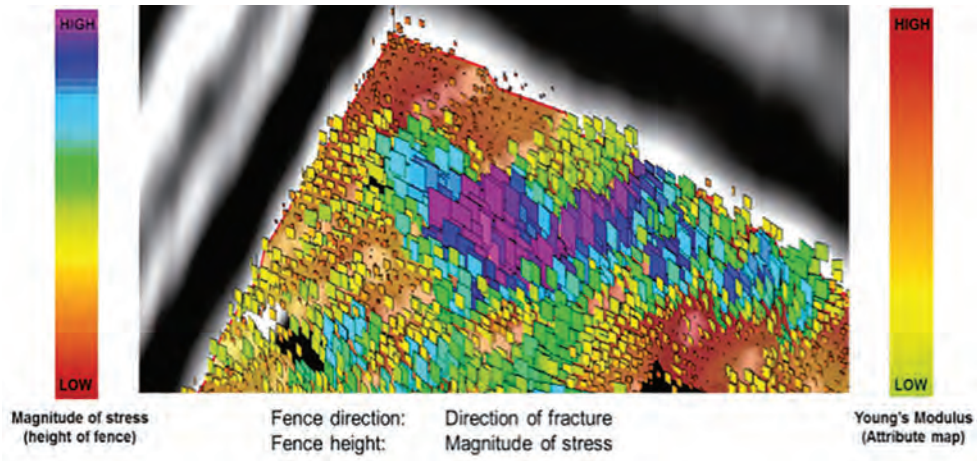

Fig. 6.31—Azimuthal inversion results—surface showing DHSR overlaying Young's modulus (ability to maintain the fractures) for the Haynesville shale. The background color indicates Young's modulus. Plate orientation represents the direction of maximum horizontal stress. Plate height represents DHSR (derived from the azimuthal inversion). Seismic stack is shown in density display (black and white).

Textural and mineralogical data are combined to produce a brittleness/ductility estimate as well as other indices useful for characterization of well completions. Although qualitative, microseismic amplitude appears to be directly correlated with factors such as pore aspect ratio and number of pores larger than 200 microns. This is significant in that data shown in **Fig. 6.34** is collected from 172 cuttings samples from a horizontal well in which no conventional well logs or core data were acquired. The only other source of information about this particular lateral comes from pre-stack seismic inversion and azimuthal inversion analysis. **Fig. 6.35** suggests there is a strong correlation between the brittleness index from mineralogy/cuttings and the estimated Young's modulus from pre-stack seismic inversion. The brittleness index log was not used in the inversion process for validation purposes.

6.7 Conclusion

In this chapter, we discuss a workflow process which integrates petrophysical well log analyses and seismically derived rock properties such as pore pressure and azimuthal stress-field analysis to produce maps and volumes of predicted pay. Geomechanical properties such as Young's modulus provide estimates of relative brittleness/stiffness or ductility, which is important for completions and fracture stimulation designs. These estimates are related to lithology, TOC, and rock texture.

The stress state is determined by the spatial distribution of elastic properties and strength properties, the structural and pore pressure, in addition to tectonic stresses acting in the subsurface. Observations of azimuthal variations of velocity and reflection coefficients were used to estimate the principal stresses.

To finalize the workflow, mineralogical and elemental data together with microseismic data have been integrated and used to validate the results of the seismically derived properties. Interesting and perhaps significant correlations between the size of the stimulated area and key properties such as Young's modulus and DHSR exist. Low DHSR and high Young's modulus, taken together, correlate with wide zones of microseismic activity. Low horizontal stresses and

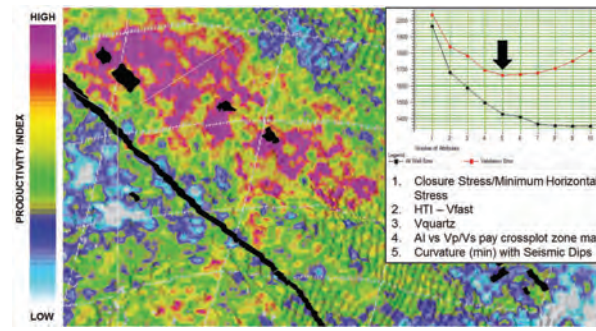

Fig. 6.32—Productivity index. The result utilizes multi-attribute analysis to build a relationship between seismic attribute maps and production data from producing wells in the survey area. The graph shows that the validation error (red curve) is minimized with the five attributes listed, ranked in order of contribution to the overall correlation.

low stress bias represent one possible path to creating a wide network of induced fractures. However, a variety of combinations of stress state and existing fracture patterns allow the creation of a wide network (shear slip on pre-existing fractures). In addition, correlations are apparent between Young's modulus and brittleness/ductility estimate derived from cuttings-based mineralogy. This is important on long laterals where only limited well log data is available.

Technology is continually being enhanced to improve exploitation of shale plays, in part by quantitatively integrating and interpreting data from wells, surface seismic, and microseismic. Integration of disciplines and data types and sources including at different scales is a key element in efforts to improve drilling and completion strategies, by examining how these relate to well production. No single attribute by itself is conclusive; multi-attribute analysis is required to derive physically meaningful correlations.

6.8 Acknowledgments

The authors would like to acknowledge Exco Resources and BG Group (Bill Reinhart, Rick Borkowski) and CGG Data Library (Mike Bertness) for permission to use and publish this chapter and for providing access to their expertise and high-quality data.

We would like to thank Jon Downton, Benjamin Roure (Fourier coefficients and azimuthal inversion), Philippe Doyen, Remi Moyen, Cedric Godefroy, and Thomas Bardainne (correlating reservoir attributes with microseismic data and SRV computation), and Lucy Plant (RoqSCAN X-ray mineralogy) for their technical contributions. We also thank Roger Taylor, Neil Peake, King Banerjee, Sara Pink-Zerling, and Lucia Levato for reviewing the manuscript and providing constructive comments.

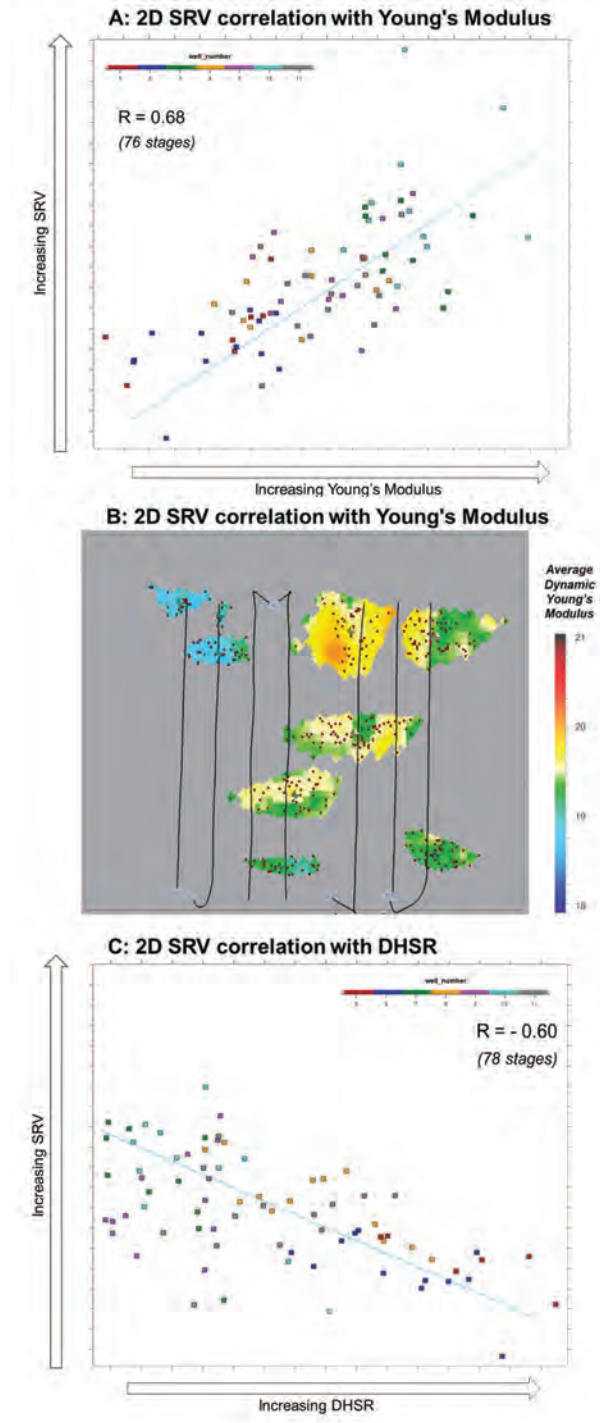

Fig. 6.33—2D SRV (SRA) correlation with Young's modulus (positive slope) (A). Map view (B). SRA associated with hydraulic fracturing stages, Young's modulus is shown in color inside the associated 2D SRV; black lines are the horizontal well paths, (C) 2D SRV correlation with DHSR (negative slope). Note: 2D SRV (stimulated reservoir volume) = SRA (stimulated reservoir area).

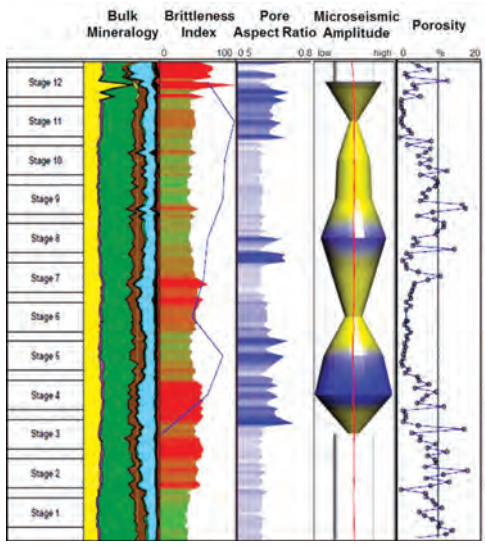

Fig. 6.34—Scanning electron microscope X-ray analysis of mineralogy from cuttings, brittleness index, pore aspect ratio and porosity, shown with amplitude of microseismic events and fracturing stages (stages 1 and 2 planned but not executed) in a lateral well. The displays show correlations among variables.

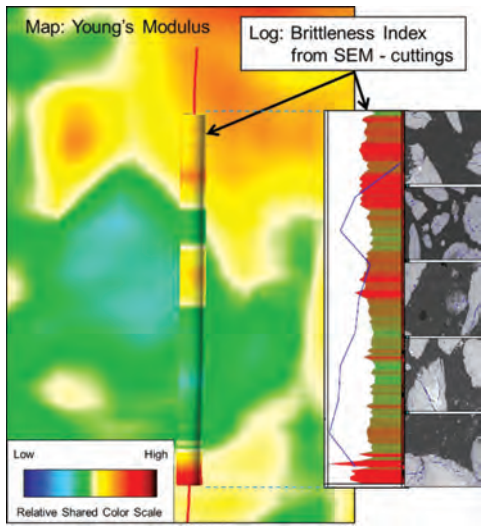

Fig. 6.35—Validation in a horizontal well. Correlation between dynamic Young's modulus from seismic inversion (map view) and brittleness index from SEM data.

6.9 References

Aki, K. and Richards, P.G. 1980. ***Quantitative Seismology: Theory and Methods***. San Francisco: W.H. Freeman.

Ashton, T., Ly, C.V., Spence, G., and Oliver, G. 2013. Drilling completion and beyond, RoqSCAN case study from the Barnett/Chester Play. ***Oilfield Technology***, **6** (4): 63.

Castillo, G. and Van de Coevering, N. .2013. Global azimuthal seismic inversion using fourier coefficients providing unambiguity and detail in fracture parameters for shale gas characterization. ***SEG Workshop, Unconventional Resources, the Role of Geophysics***, Pittsburg.

Castillo, G., Voiser, S., Chesser, K., et al. 2014. Integrating surface seismic, microseismic, rock properties and mineralogy in the Haynesville shale play. ***First Break***, **32**: 71–77.

CGG. 2008. EMERGE for Maps in ISMap. http://www.cgg.com/default.aspx?cid=4-3609-2124-2327-2432 (accessed 26 June 2014).

CGG. 2012. Defining Uncertainty. http://www.cgg.com/data//1/rec_docs/2233_Final_OT_LithoSeis_article_May_2012.pdf (accessed 26 June 2014).

CGG. 2014. New Software Targets Unconventional Resources. Paris, France. http://www.cgg.com/default.aspx?cid=8818&lang=1 (accessed 26 June 2014).

CGG. 2014. Shale Science Report: Optimizing Production & Maximizing Recovery. http://www.cgg.com/default.aspx?cid=8464&lang=1 (accessed 26 June 2014).

Cipolla, C., Mack, M., and Maxwell, S. 2010. Reducing Exploration and Appraisal Risk in Low Permeability Reservoirs Using Microseismic Fracture Mapping. Paper SPE 138103 presented at the SPE Latin American and Caribbean Petroleum Engineering Conference, 1–3 December, Lima, Peru. http://dx.doi.org/10.2118/138103-MS.

Delbecq, F., Downton, J., and Letizia, M. 2013. A math-free look at azimuthal surface seismic techniques. ***CSEG Recorder*** **38**: 20–31.

Downton, J. and Roure, B. 2010, Azimuthal simultaneous elastic inversion for fracture detection: 80th Annual International Meeting, SEG, Expanded Abstracts, 263–267.

Eaton, B.A. 1975. The equation for geopressure prediction well logs. Paper SPE 5544 Presented at Fall Meeting of the SEG of AIME, 28 September–1 October. Dallas, Texas. http://dx.doi.org/10.2118/5544-MS.

Gray, D. .2012. Estimation of stress and geomechanical properties using 3D seismic data. *First Break*, **30** (3): 59–68. http://dx.doi.org/10.3997/1365-2397.2011042.

Hampson, D.P., Schuelke J.S., and Quirein, J.A. 2001. Use of multiattribute transforms to predict log properties from seismic data: *Geophysics*, **66** (1): 220–236. http://dx.doi.org/10.1190/1.1444899.

Hampson-Russell, A CGG Company. Targeted shale play development: Searching & calibrating the "silver bullet." Presented by Adrian Smith, http://www.cgg.com/data//1/rec_docs/2596_5_Shale_Science.pdf (accessed 26 June 2014).

Ikelle, L.T. 1996. Amplitude variations with azimuths (AVAZ) inversion based on linearized inversion of common azimuth sections. In: *Seismic Anisotropy*, (eds E. Fjaer, R. Holt, and J.S. Rathore) 601–644. Tulsa, Oklahoma.

Roberston, a CGG Company. RoqScan Data Outputs. http://www.robertson-cgg.com/roqscan/data-outputs (accessed 26 June 2014).

Rüger, A. 1996. Reflection Coefficients and Azimuthal AVO Analysis in Anisotropic Media, PhD dissertation, Center for Wave Phenomena, Colorado School of Mines.

Rüger, A. and Tsvankin, I. 1997. Using AVO for fracture detection: Analytic basis and practical solutions. *The Leading Edge* **10**: 1429–1434.

Russell, B., Hampson, D., and Bankhead, B. 2006. An inversion primer. *CSEG RECORDER*, **31** (10): 101–108.

Schoenberg, M. and Sayers, C. 1995. Seismic anisotropy of fractured rock. *Geophysics*, **60**: 204–211. http://dx.doi.org/10.1190/1.144374.

Schultz, P.S., Ronen, S., Hattori, M., et al. 1994. Seismic guided estimation of log properties, parts 1, 2, and 3. *The Leading Edge*, **13**: 305–310, 674–678, 770–776.

Sena, A., Castillo, G., Chesser, K., et al. 2011. Seismic reservoir characterization in resource shale plays: Stress analysis and sweet spot discrimination. *The Leading Edge*. 30 (7): 758–764.

Sheriff, R.E. 2002. *Encyclopedic Dictionary of Applied Geophysics*. 4th Edition, Geophysical References Series 13, Society of Exploration Geophysicists.

Zoeppritz, Karl. 1919. About reflection and passage of seismic waves by surfaces of discontinuity (Erdbebenwellen VII. VIIb. Über Reflexion und Durchgang seismischer Wellen durch Unstetigkeitsflächen), trans. News from the Royal Society of Sciences in Göttingen, Mathematics and physics class. 66–84.

6.10 Case Study

The following section is from *First Break*, Volume 32, February 2014.

Integrating surface seismic, microseismic, rock properties and mineralogy in the Haynesville shale play

Gabino Castillo[1*], Simon Voisey[1], Kevin Chesser[1], Norbert van de Coevering[1], Antoine Bouziat[1], Guy Oliver[1], Chi Vinh Ly[1] and Lih Kuo[2] illustrate a workflow integrating reservoir and geomechanical properties obtained from pre-stack seismic inversion and incorporating stress and fracture information extracted from azimuthal analysis of the seismic data.

Although drilling has slowed substantially from its peak in 2010, steadily improving natural gas prices coupled with the promise of demand from liquefied natural gas and gas to liquids facilities have renewed interest in the prolific Haynesville shale gas play in NW Louisiana. A consensus of opinion among operators in the field will agree that only a fraction of the Haynesville potential has been developed to date.

As is the case in most shale plays, production from wells has been highly variable, leading to the use of 3D seismic reservoir characterization studies for the determination of sweet spots, well placement and completion strategies where seismic anisotropy has been proven to be an important factor in understanding the shale plays.

This paper illustrates a workflow (Figure 1) integrating reservoir and geomechanical properties obtained from pre-stack seismic inversion and incorporating stress and fracture information extracted from azimuthal analysis of the seismic data. Eight wells in the area targeting the Haynesville and Mid-Bossier reservoirs were used for calibration of surface seismic measurements of reservoir and geomechanical properties. A variety of seismically derived attributes are used to estimate production potential in the field. This paper shows the application of global azimuthal inversion, a technology for extracting the azimuthal anisotropy. Above all, the workflow makes quantitative use of microseismic and SEM (Scanning Electron Microscope) derived mineralogy data to validate the seismic-derived attributes.

Study area

The area of study (Figure 2) is located in northwest Louisiana. The Haynesville Formation is an organic-rich Upper Jurassic shale overlying the Smackover Formation and overlain by the Cotton Valley Group. The Haynesville is dominated by calcareous and micro-laminated, argillaceous mudstones. Organic-rich and siliceous lithofacies, which favour gas-recovery, contain both quartz and calcite in excess of 20–30%.

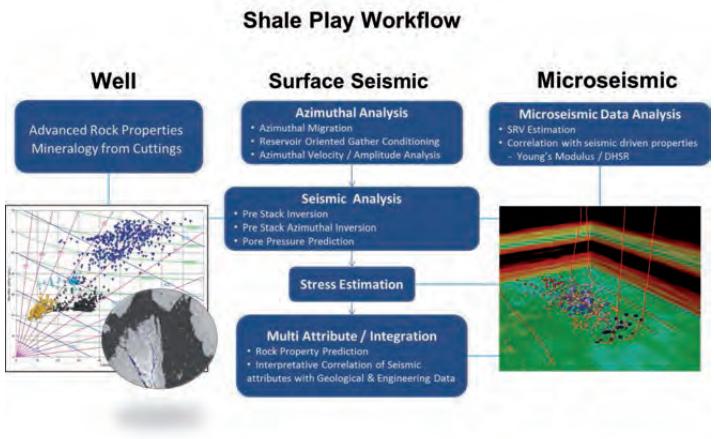

Figure 1 *Integrated geoscience workflow for a shale play, incorporating numerous disciplines to high-grade the survey area to identify 'sweet spots' and optimize drilling locations and completions.*

[1] *CGG.*
[2] *ex Exco Resources.*
[*] *Corresponding Author, E-mail: gabino.castillo@cgg.com*

Although the Mid-Bossier Formation proved successful in certain wells in the study area, the Lower Haynesville is the main target for shale gas production for this study. Geological structure in the area can be complex with numerous faults bisecting the study area. Generally, wells are positioned on the plateaus of the geological structures and between major faults. Laterals are generally oriented North-South perpendicular with the regional stress field.

Rock properties from seismic

Well log data provides calibration for all subsequent seismic analysis, including interpretation of elastic properties, HTI anisotropy and stress analysis. The study integrates eight wells targeting the Haynesville and Mid-Bossier reservoirs. Information from core (Figure 3), cuttings, and DFIT (Diagnostic Fracture Injection Test) analysis complements the well, surface, seismic and microseismic data.

Properties associated with gas-bearing rocks in the Haynesville and Mid-Bossier (free gas mingled with absorbed gas and TOC – Total Organic Carbon) are similar to those associated with free gas in conventional reservoirs, including correlation of increasing gas volume with decreasing Poisson's ratio and Lambda-Rho. In the target intervals, subtle contrasts attributed to gas are somewhat larger than those attributed to minor lithology variation, but smaller than contrasts observed between different zones marked by dramatic changes in lithology and porosity (Figure 3), such as the transition from lower Haynesville to Smackover.

In this study, pre-stack simultaneous inversion was applied to conditioned angle gathers to derive P-impedance, S-impedance and density. Commonly used descriptive reservoir attributes (i.e., mineral volumetrics, TOC, porosity, water saturation and lithofacies) were estimated with multi-linear regression prediction techniques. This analysis suggests P-impedance is mainly inversely related to porosity. Density

Figure 2 *Location of the study area, northwest Louisiana. Map and seismic data courtesy of CGG Land Multi-Client Data Library.*

and TOC also have an inverse relationship. Additionally, Lambda-Rho (product of Lamé's parameter and bulk density) appears to be directly related to Haynesville zones with high volumes of gas that are estimated from log data (Figure 4).

Rocks with higher clay content have been demonstrated to be more ductile and difficult to frac. Zones with high quartz volumes are stiffer and more likely to fracture when under hydraulic stress. Mineral fractions of quartz, calcite and clay were used in conjunction with Young's modulus (the ability to maintain a fracture) and Poisson's ratio (the ability of the rock to resist failure under stress) to provide insight into how brittle or ductile the rock may be.

Petrophysically-derived lithofacies were created and applied to each well in the study. A supervised Bayesian classification methodology was applied with well control to generate probability cubes of lithofacies. This analysis is based on Probability Distribution Functions (PDFs) associ-

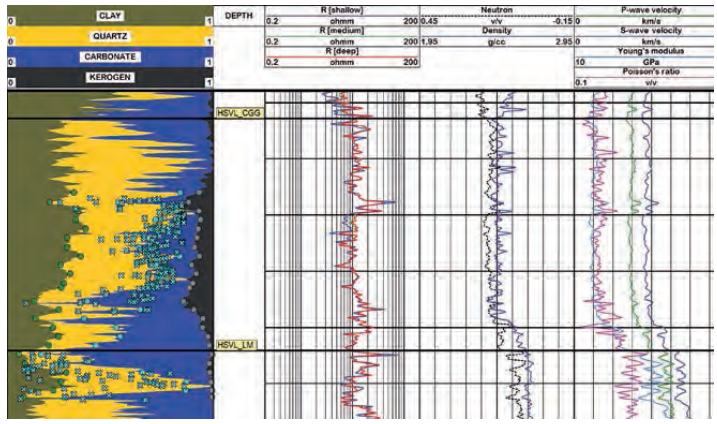

Figure 3 *Haynesville section with well log lithology fractions matched to up-scaled and normalized carbonate fraction / volume – mineralogy from cuttings (left track; cross shapes) and up-scaled XRD (X-ray diffraction) core data (left track; round shapes).*

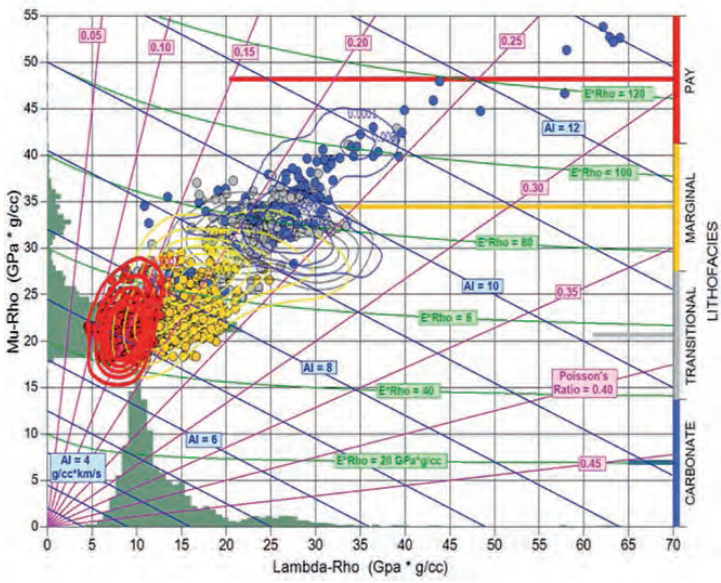

Figure 4 *Scatter of lithofacies data from multiple wells in the Haynesville. Red and yellow samples have < 30% total carbonate; red samples have > 70% gas saturation, while yellow samples have < 70% gas saturation. Blue points have > 40% carbonate by volume. Grey points, which do not fall into any of these classes, are transitional between lithofacies. The gas-rich (red) lithofacies is associated with high levels of TOC. Contours represent probability distribution functions for each lithofacies. Horizontal bar lengths give relative frequency of each lithofacies. Additionally, LRM crossplot space shows constant lines of acoustic impedance (AI = blue), Poisson's ratio (PR = magenta), and product of Young's modulus*density (ERho = green).*

ated with classes of pay (red), marginal gas-bearing zones (yellow), transitional 'shoulder' facies (grey), and carbonate (cyan) (Figure 4). The resulting seismic volumes of most probable lithofacies (Figure 5a) and probability of each lithofacies class (Figure 5b) provided encouraging results for mapping. Indicative attributes in the identification of sweet spots could be compared directly and analyzed based on probabilities.

Azimuthal inversion – stress estimation from seismic

In-situ stress, present in the earth prior to drilling, affects propagation of induced fractures and the long-term productivity of wells. Therefore, understanding the stress regime in the subsurface is important when planning the orientation of laterals. Further inspection of the seismic gathers will illuminate the amount of HTI anisotropy in the data and Azimuthal AVO and Azimuthal elastic inversion (Castillo and Van de Coevering, 2013) techniques will give insights into in-situ stress and fracture parameters in the area.

In this study, the stress state was estimated by employing a global inversion of pre-stack 'azimuthal' seismic data using Fourier Coefficients (Downton and Roure, 2010) to derive fracture properties and eventually local in-situ stress fields. Figure 6 shows the resulting azimuthal anisotropy plates generated from attribute volumes; (i) direction and (ii) height plus colour. Direction, in this example, is the isotropy plane (orthogonal to symmetry axis) while height and colour represent the magnitude of Differential Horizontal Stress Ratio (DHSR), calculated using azimuthal inversion. DHSR gives information about fracture orientation and style. The data slice (colour of base horizon) is Young's modulus (approximates the ability to maintain a fracture).

Minimum (σh) and maximum (σH) horizontal stress can be viewed and interpreted independently; σh, or closure stress, represents the minimum amount of stress required to maintain open fractures. DHSR is the normalized difference between σh and σH and is an indicator of the stress regime.

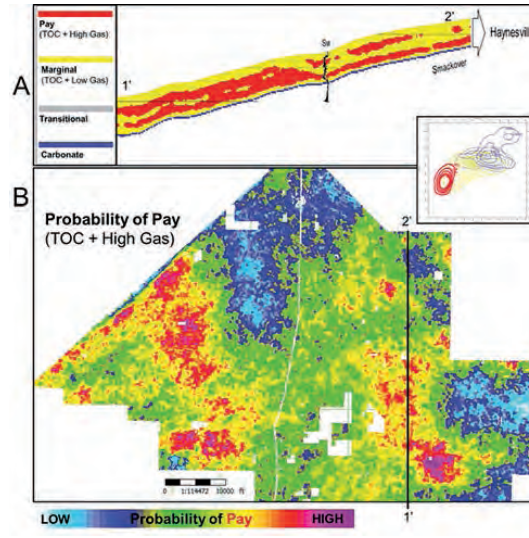

Figure 5 *a) Most Probable Lithofacies Section and b) Pay Probability Map at Lower Haynesville level based on Lambda-Rho vs. Mu-Rho (LMR) crossplot. The PDF's which are applied to inverted seismic volumes honour the distribution of well log data in the LMR crossplot space (Figure 4).*

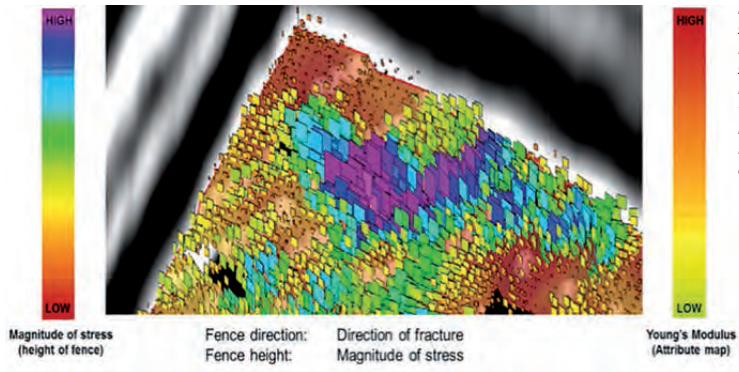

Figure 6 *Azimuthal Inversion results – surface showing DHSR overlaying Young's Modulus (ability to maintain the fractures) for the Haynesville shale. The background colour indicates Young's modulus. Plate orientation represents the direction of maximum horizontal stress. Plate height represents DHSR (derived from the azimuthal inversion). Seismic stack is also shown in density display (B&W).*

In the Haynesville it has been suggested that with respect to hydraulic fracturing, low DHSR favours fractures with random orientation, while high DHSR favours fractures that are more aligned (Sena et al., 2011). Therefore, in this example, low DHSR may be more desirable if natural, open fractures are absent, because the area stimulated (and hence production) can be maximized when the induced fracture pattern is more random.

Estimation of maximum vertical stress (σV) and σh is derived from pore pressure estimation using Eaton's equation (Eaton, 1975) modified for unconventional reservoirs. All elements of pore pressure prediction are verified by independent measurements which include DFIT tests and mud weights used while drilling. Additionally, σH is taken from tri-axial measurements of oriented core plugs. Conventional pore pressure methods assume low P-wave velocity in shale occurs whenever pore pressure is greater than hydrostatic pressure. Because high gas content and TOC can mimic pressure changes, this assumption was tested by running parallel calculations based on S-wave velocity and Mu-Rho. Where calibration data is available, P-wave velocity gives results closest to known pressures in the Mid-Bossier and Haynesville.

Mapping sweet spots

The previous mention of rock property attributes alluded to manipulation of pre-stack inversion volumes through regression techniques. Multi-attribute linear regression finds a relationship among attributes in multi-dimensional space leading to a 'best-fit' seismic volume of a given target attribute. Target attributes tend to be volumetric well logs, such as total porosity, mineralogy or water saturation. The process creates links between multiple seismic attributes and petrophysical data, in three dimensions (x, y, and time or depth).

In this study, multi-attribute linear regression was applied to generate a 2D map of productivity index or a 'sweet spot' map. The link is built between production data and maps extracted from the seismic attributes at the target level (Figure 7).

Multi-attribute analysis is statistically driven; the method has no prior information or biases regarding which attributes are 'best'. The optimal number of attributes and rank of each is determined during the analysis by validating the prediction at each production sample using the remaining control points. In our case, the closure stress has the highest correlation with the production index.

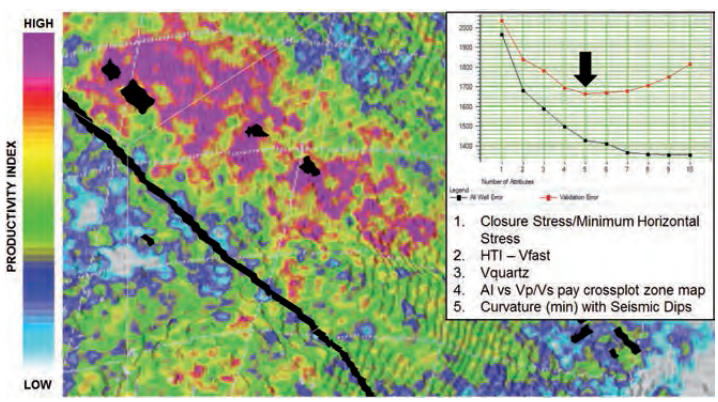

Figure 7 *Productivity Index. The result utilizes multi-attribute analysis to build a relationship between seismic attribute maps and production data from producing wells in the survey area. The graph shows that the 'validation error' (red curve) is minimized with the five attributes listed, ranked in order of contribution to the overall correlation.*

Integrating microseismic

As shown, elastic and geomechanical attributes derived from surface seismic reflection data have proven to be very useful in shale gas reservoir management by (1) delineating reservoir sweet spots where formation properties make the rock matrix more fracture-prone under hydraulic stimulation and (2) predicting reservoir stress anisotropy which may affect the orientation of hydraulic fractures. The impact of rock properties and spatial stress distribution on the success of hydraulic fracturing treatments may be evaluated by integrating data from hydraulically-induced microseismic events. Spatial correlation of microseismic events with specific seismic attributes implies that both are governed by the same in-situ properties of the rock.

The study reveals physically meaningful statistical correlations between microseismic event density with estimates of Young's modulus and DHSR from azimuthal analysis (Figures 8a and 8c). The size of the Stimulated Reservoir Volume (SRV) and Stimulated Reservoir Area (SRA, i.e., 2D SRV) is directly proportional to average Young's Modulus and inversely proportional to DHSR, implying SRV and SRA are maximized in areas of high Young's modulus and low differential horizontal stress.

Figure 8b shows SRA with Young's modulus (colour axis). The time-evolution of the SRA was also calculated to gain insight into the fracture growth process and to better understand the spatial and temporal correlation of microseismic events with the spatial distribution of seismic-derived rock properties. The seismic-to-microseismic correlation is enhanced by relating the calculated size of the SRA with seismic attributes spatially averaged over the computed SRA for each stage.

Integrating scanning electron microscope mineralogy

Macro-effects sensed by surface seismic and microseismic observations span a much broader area than the relatively small volumes of rock sensed by well logs, yet both are ultimately controlled by the rock fabric at scales beyond even the well log measurements. To access this scale, cuttings and core chippings were analyzed at high resolution (in both vertical and lateral wells) using a Scanning Electron Microscope (SEM) fitted with energy-dispersive X-ray detectors. This provides measured quantitative data on elemental and mineralogical composition, rock texture, porosity and pore aspect ratio (Ashton et al., 2013). The dataset complements older, but less extensive, X-ray diffraction (XRD) data. SEM data is consistent with XRD results for mineral fractions (such as 'total carbonate') and also match lithology estimates from conventional well logs (Figure 3).

Textural and mineralogical data are combined to produce a brittleness/ductility estimate as well as other indices useful for characterization of well completions.

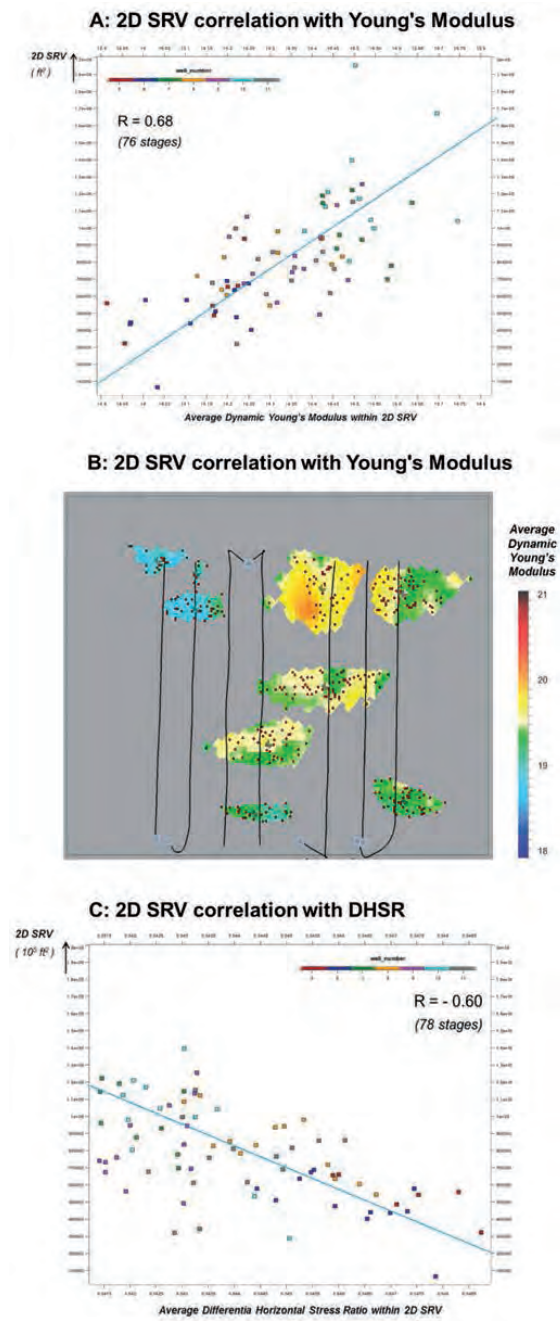

Figure 8 a) 2D SRV (SRA) correlation with Young's Modulus (positive slope), b) Map view. SRA associated with hydraulic fracturing stages, Young's Modulus is shown in colour inside the associated 2D SRV, black lines are the horizontal well paths, c) 2D SRV correlation with DHSR (negative slope). Note: 2D SRV (Stimulated Reservoir Volume) = SRA (Stimulated Reservoir Area).

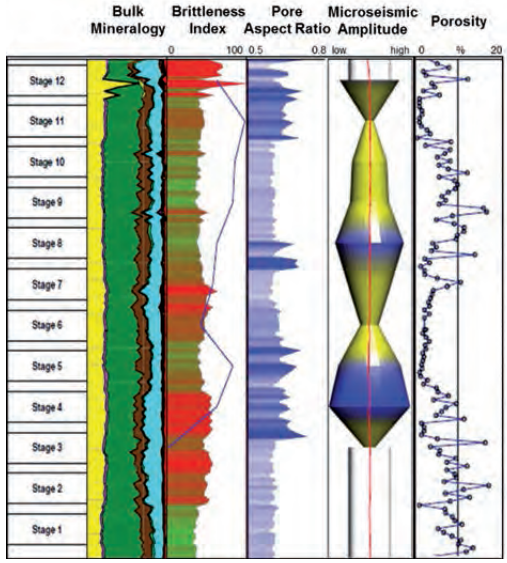

Figure 9 *Scanning Electron Microscope X-ray analysis of mineralogy from cuttings, brittleness index, pore aspect ratio and porosity, shown with amplitude of microseismic events and frac stages (stages 1 and 2 planned but not executed) in a lateral well. The displays show correlations among variables, as detailed in the text.*

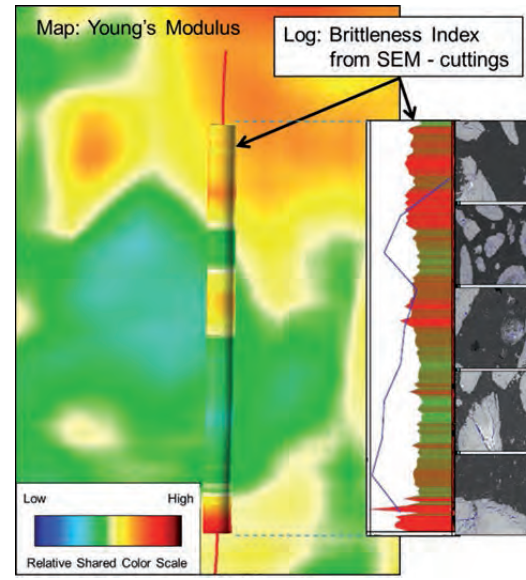

Figure 10 *Validation in a horizontal well. Correlation between dynamic Young's Modulus from seismic inversion (map view) and Brittleness Index from SEM data.*

Figure 9 shows several of these indices plotted with microseismic 'fracture amplitude' in the fourth track. Although qualitative, microseismic amplitude appears to be directly correlated with factors such as pore aspect ratio and number of pores larger than 200 microns. This is significant in that data shown in Figure 9 is collected from 172 cuttings samples from a horizontal well in which no conventional well logs or core data was acquired. The only other source of information about this particular lateral comes from pre-stack seismic inversion and azimuthal inversion analysis. Figure 10 suggests there is a strong correlation between the brittleness index from mineralogy/cuttings and the estimated Young's Modulus from pre-stack seismic inversion. The brittleness index log was not used in the inversion process for validation purposes.

Conclusion

In this paper, we discuss a workflow which integrates petrophysical well log analyses and seismically derived rock properties such as pore pressure and azimuthal stress-field analysis to produce maps and volumes of predicted pay. Geomechanical properties such as Young's Modulus provide estimates of relative brittleness/stiffness or ductility, which is important for completions and fracture stimulation designs. These estimates are clearly related to lithology, TOC, and rock texture.

The stress state is determined by the spatial distribution of elastic properties and strength properties, the structural framework and pore pressure, in addition to tectonic stresses acting in the subsurface. Observations of azimuthal variations of velocity and reflection coefficients were used to estimate the principal stresses.

To finalize the workflow, mineralogical and elemental data together with microseismic data have been integrated and used to validate the results of the seismically-derived properties. Interesting and perhaps significant correlations between the size of the stimulated area and key properties such as Young's modulus and DHSR exist. Low DHSR and high Young's Modulus, taken together, correlate with wide zones of microseismic activity. Low horizontal stresses and low stress bias represent one possible path to creating a wide network of induced fractures. However, a variety of combinations of stress state and existing fracture patterns allow the creation of a wide network (shear slip on pre-existing fractures). In addition, correlations between Young's modulus and brittleness/ductility estimate derived from cuttings-based mineralogy are apparent. This is important on long laterals where only limited well log data is available.

Technology is continually being enhanced to improve exploitation of shale plays, in part by quantitatively integrating and interpreting data from wells, surface seismic, and microseismic. Integration of disciplines and data types and sources (including at different scales) is a key element in efforts to improve drilling and completion strategies, by examining how these relate to well production. No single

attribute by itself is conclusive; multi-attribute analysis is required to derive physically meaningful correlations.

Acknowledgements

The authors would like to acknowledge Exco Resources and BG Group (Bill Reinhart, Rick Borkowski), and CGG Data Library (Mike Bertness) for permission to use and publish this paper and for providing access to their expertise and high-quality data.

We would like to thank Jon Downton, Benjamin Roure, (Fourier Coefficients and Azimuthal Inversion), Philippe Doyen, Remi Moyen, Cedric Godefroy and Thomas Bardainne (correlating reservoir attributes with microseismic data and SRV computation) and Lucy Plant (RoqSCAN X-ray mineralogy) for their technical contributions.

We would also like to thank Rob Mayer, Roger Taylor, Neil Peake, King Banerjee, Sara Pink-Zerling and Lucia Levato for reviewing the manuscript and providing constructive comments.

References

Ashton, T., Ly, C.V., Spence, G. and Oliver, G. [2013] Drilling completion and beyond, RoqSCAN case study from the Barnett/Chester Play. *Oilfield Technology*, **6**(4).

Castillo, G. and Van de Coevering, N. [2013] Global azimuthal seismic inversion using fourier coefficients providing unambiguity and detail in fracture parameters for shale gas characterization. *SEG Workshop, Unconventional Resources, the Role of Geophysics*, Pittsburg.

Downton, J. and Roure, B. [2010] Azimuthal simultaneous elastic inversion for fracture detection. SEG, Expanded Abstracts, 29, 263.

Eaton, B.A. [1975] The equation for geopressure prediction well logs. Presented at Fall Meeting of the SEG of AIME, Paper SPE 5544.

Gray, D. [2012] Estimation of stress and geomechanical properties using 3D seismic data. *First Break*, **30**(3).

Rüger, A. and Tsvankin, I. [1997] Using AVO for fracture detection: Analytic basis and practical solutions. *The Leading Edge*, **10**, 1429–1434.

Ikelle, L.T. [1996] Amplitude variations with azimuths (AVAZ) inversion based on linearized inversion of common azimuth sections. In: *Seismic Anisotropy*, (eds E. Fjaer, R. Holt and J.S. Rathore), pp. 601–644. SEG, Tulsa.

Schoenberg, M. and Sayers, C. [1995] Seismic anisotropy of fractured rock. *Geophysics*, **60**, 204–211.

Sena, A., Castillo, G., Chesser, K., Voisey, S., Estrada, J., Carcuz, J. *et al.* [2011] Seismic reservoir characterization in resource shale plays: Stress analysis and sweet spot discrimination. *The Leading Edge*, 30(7), 758–764.

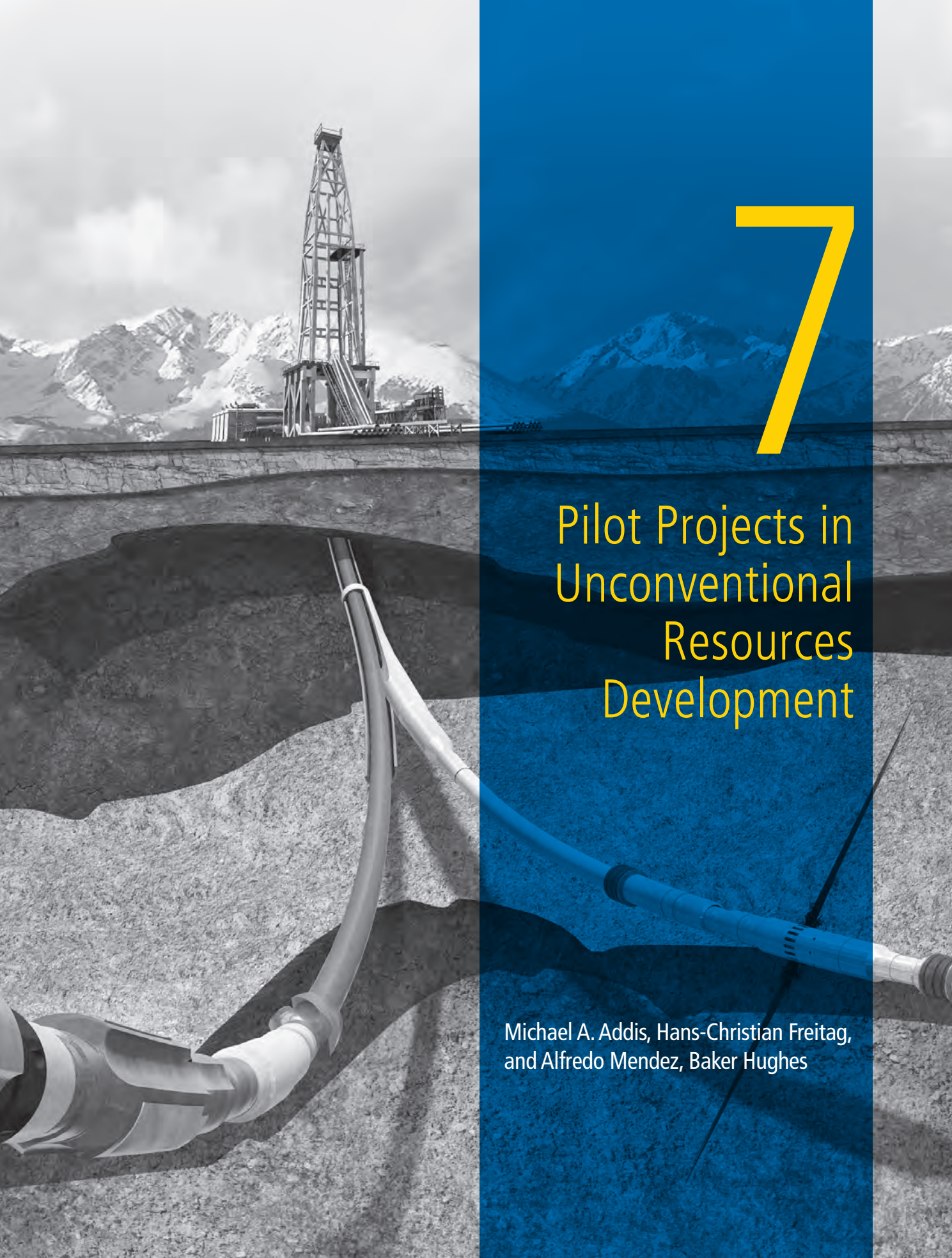

7

Pilot Projects in Unconventional Resources Development

Michael A. Addis, Hans-Christian Freitag, and Alfredo Mendez, Baker Hughes

This page intentionally left blank

Chapter 7:
Pilot Projects in Unconventional Resources Development

7.1 Introduction

The development of unconventional resources, whether shale gas and oil or tight gas and oil, involves the challenge of producing hydrocarbons from formations with very low porosities and permeabilities. The absence of a significant natural permeability in unconventional resources has economic consequences that affect the method by which these resources are assessed and developed. Conventional field development relies upon both well production tools and dynamic reservoir models to estimate the production from wells of specific geometries. The estimates are based on pressures, fluid properties, matrix or gross permeabilities, as well as the porosity, water saturations, relative permeabilities and net to gross lithology estimations of the formation. These reservoir models are used to predict the expected production profile for wells, the plateau production, and production decline for specific development scenarios. The well production forecasts are, in turn, used to generate revenue projections that are used in the field development economics to evaluate the project attractiveness and viability.

In sharp contrast, the development of unconventional resources in practice is less reliant on well production models and dynamic reservoir models. Production from these tight formations relies not only upon Darcy flow but also on diffusion and desorption from the matrix and two-phase flow along the fractures as detailed in Chapter 11 and Chapter 14. Models with this additional complexity are not well developed, and much of the required input data (such as the desorption isotherms, and the hydraulic fracture and natural fracture geometries and conductivities) are absent during the early development stages.

Consequently, conventional reservoir models are not commonly used, because:

- The physics underlying the production from the in-place volumes is not well known.
- The natural fracture system is not well understood.
- There is a lack of consensus about the mechanisms controlling the production decline.
- The flow is not directly related to the pressure difference and material balance for such systems.

Before a pilot study or development is undertaken, the formation pressures, fluid properties, and permeability systems are poorly defined or unknown, which results in large subsurface uncertainties. These shortcomings exacerbate the challenge of building a reliable model of the production at the exploration or appraisal stage, and can lead the operator to depend on poorly defined geological analogs on which to base the initial production estimates and potential production declines for assets in these tight formations.

Subsurface uncertainties for conventional plays are managed routinely through probabilistic analysis. In addition, for more advanced simulations, these uncertainties can be evaluated using experimental design techniques, with many of the uncertainties characterized through their magnitudes and probability functions or distributions.

In unconventional plays, subsurface uncertainties are significant, and less well understood than in conventional plays. These uncertainties include the geological setting at the time of deposition, the permeability, and, notably, the induced permeability system, the connectivity between the induced permeability system and the natural or geological permeability, pressure distributions across the play, lateral and vertical variations in the fluid properties (including maturity variations), TOC, porosity, brittleness, and hydrocarbon maturity.

These uncertainties manifest themselves in the large variations in well productivity and in the large range of estimated ultimate recovery (EUR) per well, which are characteristic of plays in North America. Typically, one to two orders of magnitude differences in EUR are observed for wells in a particular play (Giles 2012). This broad range of estimated EURs reflects the large number of subsurface uncertainties (Ahmed 2014), as well as completion and stimulation variations, resulting in the need for large numbers of wells to properly evaluate a play, even in well-characterized and mature areas such as North America. Martin and Eid (2011) have quoted operators' experience that it takes at least 10 wells to optimize a completion in a new shale gas play in North America.

Consequently, subsurface managers and asset and project managers who are planning unconventional resources developments face the challenges of having limited confidence in the production predictions, considerable subsurface uncertainty, and the prospect of committing to a large number of wells—and costs—to assess and develop the resource.

Clearly, an approach is required where the production potential for an unconventional resource is evaluated through a multiwell commitment, while limiting the risk and cost exposure for the operating company.

The approach most commonly adopted to optimize developments and to reduce the risk exposure of new unconventional resource developments is a modification of the stage-gate process, which is commonly used for controlling conventional field developments by the inclusion of a structured pilot project.

7.2. Pilot Projects

A pilot project has a place as a distinct stage in the development of an unconventional resource. This is similar to pilot projects in either enhanced oil recovery (EOR) and improved oil recovery (IOR), or heavy oil developments where the resource is evaluated, production is demonstrated, and the commerciality is established before an operating company commits to a full field development.

The aim of the pilot project is to validate a development concept by demonstrating optimized production and, to the extent possible, showing cost effectiveness of the well construction by moving down the learning curve, to assist the operator in optimizing the unit's technical costs (cost per mscf, or cost per BOE) for the pilot stage.

The timing and scope of pilot projects can vary significantly depending upon the operating company and the operating environment. However, for an initial field development, this stage is a risk-reduction exercise that should be completed before development concepts are approved. In addition, the pilot project provides a "proof of commerciality." As such, a pilot project generally follows the appraisal stage of a potential development, and constitutes, to a lesser or greater extent, the concept-selection stage. Additional pilot projects can be used to refine concepts and well designs further. Together, these pilots can precede the detailed design stage of a development. Unconventional play developments in North America use pilot projects in mature production areas to reduce drilling costs and optimize completion designs and stimulation practices, as well as to increase production and recovery through decreased well spacing.

This initial pilot project stage is becoming increasingly important as a project development stage as unconventional resource assessment grows in the international arena with the associated elevated cost structures and greater subsurface uncertainty, compared to the developments in North America.

7.2.1 The Role and Timing of Pilot Projects within a Project Delivery Process

The project delivery process is a commonly used platform for conventional field developments, outlining at a high level (**Fig. 7.1**) the different stages, and major decision points for a field development or project. Numerous national oil companies (NOCs) and integrated oil companies (IOCs) have adopted this approach to use with project control and field development management with various refinements of the project deliverables and criteria for different stages. This stage-gate approach is the basis for a decision-based project rather than an activity-based project, placing the focus on development control and the need to satisfy project targets by addressing economic, commercial, technical, and organizational criteria—before the development is allowed to continue.

Within this project delivery process, smaller sub-projects are accommodated, with similar or identical stage gates, for example, with an exploration or an appraisal program.

The small and independent operating companies have not formally adopted such a project delivery approach in the early unconventional resources developments in North America. However, IOCs and NOCs operating within North America and internationally are adopting this approach to risk and investment management in a modified form, for application to unconventional resource developments (**Fig. 7.2**).

The decisions during the planning stages, or front-end engineering design (FEED), of a field development project (the stages before project execution) occur at the end

Fig. 7.1—Illustration of elements of a stage gate process for project management of conventional field developments.

of each of the stage gates, and for the development of unconventional resources are likely to require the following:

- **Identify and assess:** Proving the tight and unconventional resource exists. This is validated by performing a review and analysis of earlier drilling of conventional plays, or through drilling dedicated vertical exploration wells.
- **Feasibility and appraisal:** Demonstrating materiality and productivity. This is proved by stimulation of vertical exploration and appraisal wells, and through dedicated staged stimulations of laterals, or horizontal sections. Limited production tests are performed.
- **Concept selection and pilot:** Establishing the commercial productivity of the play. This is achieved through a dedicated multiwell program of laterals with multistaged fracture stimulations, to establish the range of initial productivities and production decline curves, through extended well production tests. This may be concluded with the development of a field development plan (FDP).
- **Define:** Ensure field and asset development plans, monitoring and surveillance plan, and project execution plans are in place, with supporting documentation [e.g., basis of design (BoD) documents] and well specifications for a full development, to satisfy a final investment decision (FID).

The timing of a pilot project within an unconventional resource development will vary with the development maturity. However, for the development of new plays, the pilot project is focused on establishing a development concept with acceptable project criteria, including a UTC, and proving the commercial productivity for the development. These activities are required before moving to a detailed design stage leading to an FID.

The pilot project in a new unconventional resource development constitutes a predominantly field-based concept selection stage, rather than the largely office-based FEED stage typical of conventional field developments. This move from office to field for the concept selection results from the poorly developed production modeling tools that are available for unconventional resource developments, the large areal extent of these resources, the subsurface uncertainty, and (commonly) a lack of subsurface data input for models.

At this stage of the development, establishing the commercial viability using a pilot project and identifying improvements in the detailed design stage is only the start of the commercial optimization of the play. Continual drilling and exploration is a characteristic of extensive unconventional resource play development, and optimization of both the production and well construction is an ongoing process as the development continues, with the establishment of well-defined learning curves.

Later in the life of the play additional pilot projects may be required to further optimize and target specific optimization requiring multiwell pilots. These technology pilot project trials have included drilling and well spacing as mentioned earlier, as well as refracturing trials, zipper fracture trials, and simultaneous fracturing trials of adjacent laterals in thin shale formations, in order to induce a stimulated zone of the play, where the reservoir, based on the natural fracture system and minimum and maximum horizontal stress contrast are conducive to developing a stimulated reservoir volume (SRV) (Cipolla and Wallace, 2014), rather than relying on classical bi-wing hydraulic fractures.

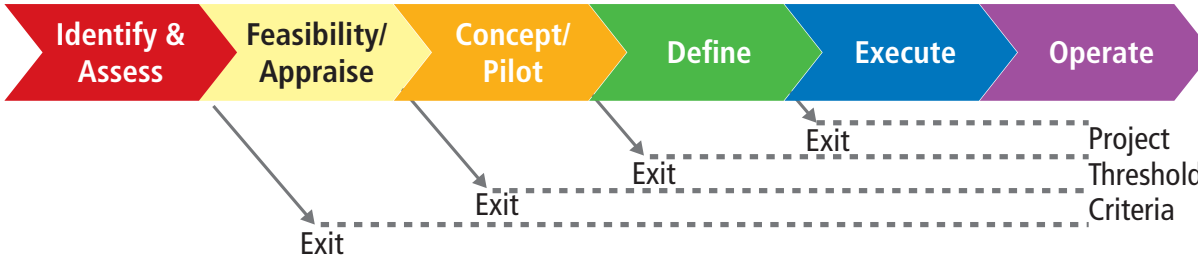

Fig. 7.2—Illustration of elements of an unconventional stage gate process, including the pilot project stage. (Modified from Giles et al. 2012.)

7.2.2 Information Required to Move to a Pilot Project

Pilot projects are considered once the unconventional resource has been identified, either through evidence from drilling of conventional reservoirs, or through dedicated unconventional resources vertical exploration wells.

These pilot projects are normally preceded by appraisal wells and involve a multiwell commitment to establish the potential of a development. The appraisal wells may be vertical, if the resource is thick, as in the basin centered gas plays west of the Rockies, or in the Bowland shale, in the UK; however most involve drilling horizontal lateral well sections, through thin shale sections, typically 10 to 50 m thick. The appraisal wells drilled into these thin shale sequences, may comprise a vertical pilot hole section, before the well is plugged back and a lateral sidetrack drilled, from the vertical section. The pilot hole in the vertical sections of these appraisal wells are used to core, log, and characterize the vertical sequence through the resource, and identify the depths of the formations in which to place the lateral sidetrack.

Appraisal wells should be stimulated and commonly comprise multistage fractures at different locations (stages) along the appraisal well. Lateral wells with staged transverse fracture—i.e., hydraulic fractures oriented perpendicular to the wellbores, are the normal well design for shale gas and shale oil developments in relatively thin shales sections. Lateral appraisal wells are used to confirm the optimum well azimuth to drill these wells to ensure transverse hydraulic fractures are generated (**Fig. 7.3**).

The well azimuth should be parallel to the minimum horizontal stress direction. Varying from this well azimuth orientation is likely to lead to near wellbore tortuosity of the hydraulic fractures, with an increased risk of proppant screen-out and lower initial production from the wells. The impact of tortuosity is well known in the hydraulic fracturing community and that tortuous transverse fractures have a poor connection to the wellbore leading to elevated fracture initiation and breakdown pressures and propagation pressures. When the well is put on production the transverse fractures result in convergent flow radially into the horizontal borehole causing a high-pressure drop similar to a choke in the fluid flow.

The confirmation of the correct well azimuth is achieved through the use of downhole or surface microseismic measurements, through which the geometry, orientation, and distribution of the hydraulic fractures along the lateral well can be observed, confirming that they are transverse and oriented perpendicular to the wellbore azimuth.

The design of horizontal appraisal wells for tight gas sands in Oman has been described by Rylance et al. 2011, where the wells were designed to maximize the learning on each well and applying the lessons learned to the remainder of the appraisal program. The planning of these wells included a technology plan, fracturing technology optimization, operational equipment and readiness assessment, treatment integrity, and QA and QC.

Recently, a practice that involves a design where several fracturing fluid systems, such as crosslinked, hybrid, and slickwater, are used for different stages along the horizontal lateral has been adopted for appraisal wells outside of North America. This was done to compare production results and microseismic events for a better understanding of which fluid and design is better suited for the reservoir in question.

The production data obtained from these appraisal wells during short term tests are significant for the approval of a pilot project, while the logging, monitoring, and surveillance of the appraisal wells provide information to optimize well and completion design to help the project advance to the pilot project stage. **Fig. 7.4** is a proposed post-stimulation surveillance plan for appraisal wells for unconventional resources proposed by Barree et al. (2002), later by Rylance (2013), and most recently Ahmed et al. (2015).

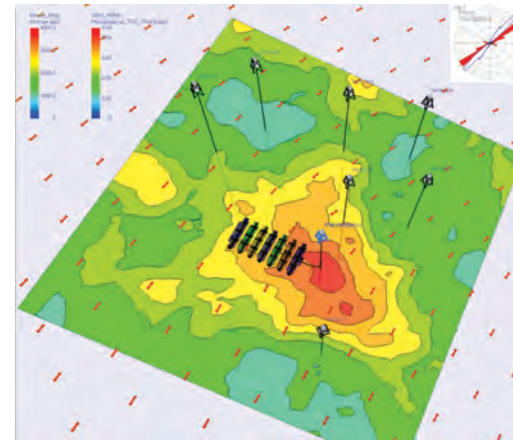

Fig. 7.3—Illustration of a stimulated appraisal well oriented parallel to the minimum horizontal stress direction to generate transverse hydraulic fractures.

Desired in Appraisal Well		Appraisal		Will Determine	Ability to Estimate						
Helpful in Appraisal Well		Vertical	Horiz.	May Determine	Length	Height	Width	Azimuth	Dip	Volume	Con.
Not Required/Not Attainable				Cannot Determine							
Group	**Diagnostic**			**Appraisal-Pad Comments**							
Indirect	Net Pressure Analysis			Key in the Vertical Well to Calibrate the Model							
	Well Testing			Need for the foundation of Development Economics							
	Production Analysis			Need Accurate Permeability and Pressure							
Direct Near-Wellbore	Radioactive Tracers			Combined with other Diagnostics for height							
	Temperature Logging			Combined with other Diagnostics for height							
	Continuous DST or DAT			Not easily reconciled with Cased-Hole (Development)							
	HIT			Probably not applicable to most operations							
	Production Logging			May reconcile experimentation in Horizontal							
	Chemical Tracing			Cheap effective PLT, should always be used							
	Borehole Imager Logging			Not applicable to cased-hole operations							
	Downhole Video			More intervention activities (fishing)							
	Caliper Logging			Not applicable to cased-hole operations							
Direct Far Field	Surface Tilt Mapping			Resolution Decreases with depth							
	DH Offset Tilt Mapping			Resolution decreases with offset well Distance							
	Microseismic Mapping			Availability of Vertical well for Horizontal is key							
	Treatment Well Tiltmeters			A very useful Vertical well option if required							

Fig. 7.4—An example of a proposed surveillance program for vertical and horizontal appraisal wells. (From Barree 2002; Rylance 2013.)

The data available before the sanction of a multiwell pilot project, is likely to comprise seismic data, interpretation, and attribute analysis, log (wireline or LWD) data from the exploration and appraisal wells, both through the vertical section and along any lateral sections, core data normally obtained from vertical well sections, and monitoring and surveillance data from the early fracture stages and well test production.

Core analysis is important at this stage because fluid sampling taken before hydraulic fracturing is impossible to obtain in nanodarcy permeability environments, and to provide suitable calibration of log data. Low TOC and adsorbed and absorbed hydrocarbons in the source rock have almost no affect on log data, which presents challenges to estimating gas and water saturation data from the logs. Accurate estimates of rock mechanical properties used in hydraulic fracturing design also require calibration with core lab tests.

The data gathered during the exploration and appraisal stages should be sufficient to stop a development, recommend additional data gathering, or enable the pilot project to proceed at the end of the Feasibility and Appraise stage gate.

The exact data required at this stage will vary by play, and according to specific company policies and project threshold criteria, most notably the financial criteria for a project to move to a pilot project and de-risking stage.

The technical data might reasonably be expected to include:

- 3D (or 2D) seismic interpretations, for hydrocarbon indicators, stress, and brittleness
- Mineralogy, including clay volume and type
- Geological setting
- Facies identification
- Total organic carbon (TOC)
- Permeability
- Porosity
- Saturation
- Estimated gas or oil in place
- Elastic mechanical properties
- Core-to-log calibration
- Pore pressures
- Stress regime and fracture gradient
- Microseismic interpretations
- Production analysis, including initial production

This information is sufficient to establish the extent of the resource and the initial indications of the deliverability, or productive potential of the formation.

The role and timing of appraisal well drilling and testing may overlap the pilot project and concept selection stage of a project, depending upon the size of the play. The definition and separation of the appraisal and pilot and concept selection stage may also vary with the operator's internal procedures.

7.2.3 Uncertainty and Pilot Project Design

The goal of the pilot project is to de-risk the resource, from one which has the potential for delivering hydrocarbons, to a resource which can produce hydrocarbons commercially, with the correct well, completion, stimulation designs, and operational procedures.

Following the appraisal stage, a number of subsurface uncertainties and broader project risks will be evident. These risks and uncertainties captured in a project-wide risk register enable the critical risks to the potential development to be identified by the asset team. These risks, and specifically the subsurface, well construction, completion, and stimulation risks and uncertainties, are the focus for the pilot project, lowering the risk for these elements of the development, or more certainty and confidence around the unknowns.

Approximately 80% of unconventional resource development costs in North America can be attributed to well construction, completion, and stimulation costs (EIA, 2014). This is likely to be a smaller percentage of the total development costs in international developments, but will still remain a very significant project cost element, which can be addressed with the pilot project. This is in addition to the primary purpose, which is to optimize the production and revenue stream for any development.

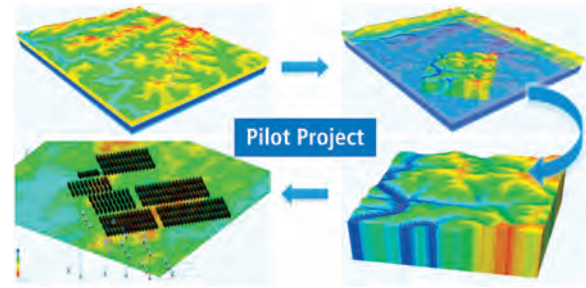

Fig. 7.5a—Pilot project location, prospectivity identification, and optimizing the project's success.

Before the start of any large development, one or more pilot projects may be initiated on the play. Pilot projects can help to assess the lateral variability of the play, and to evaluate whether more prospective areas can be identified from the preliminary subsurface static model generated from the 3D seismic and appraisal data.

Identifying areas with high prospectivity for appraisal and pilot project locations is a primary focus for companies embarking on unconventional resources development (**Fig. 7.5a** and **Fig. 7.5b**). These areas have the potential to be sweet spot areas for any development. To date, finding sweet spot areas of higher initial productivity in shale gas and oil plays in North America is the result of production analysis primarily. These areas have rarely been correlated to a particular set of unique

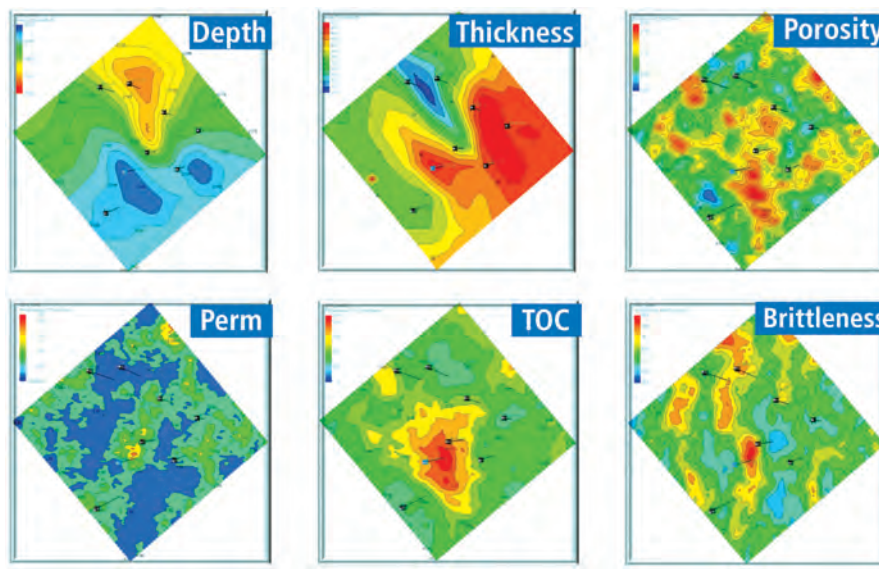

Fig. 7.5b—Depth, thickness, porosity, permeability, TOC, and brittleness factors.

subsurface characteristics, though recent work has correlated high productive areas in the Barnett to the product of porosity and thickness (Browning et al. 2013). In contrast, cutoffs have been identified in North American plays where low productivity predominates and have been attributed to specific geological features. Sondergeld et al. (2010) compiled most of the shale gas attributes commonly used by operators. Highlights of the attributes considered to be critical in defining an unconventional system taken from Sondergeld et al. (2010) and adding the oil window on vitrinite reflectance (%R_0) is shown next:

- Bulk Volume Gas, > 2%
- Mineralogy, > 40% quartz or carbonates and < 30% clays
- Permeability, >100 nanodarcy
- Poisson's Ratio (static), < 0.25
- Pressure, > 0.5 psi/ft
- Thermal maturity, dry gas > 1.4% R_0 and for oil > 0.6%
- Total organic carbon, > 2%
- Thickness, > 30 m

Even if specific subsurface characteristics constraining a sweet spot cannot be uniquely defined, the identification of pilot project locations should be approached as a risk-reduction exercise, with the aim of maximizing the probabilities of success through the use of 3D seismic, geological, petrophysical and geomechanical appraisal well data (**Figs. 7.5a** and **Fig. 7.5b**). If successful, the extent of the productive play acreage still needs to be assessed, during either subsequent pilot projects or during the development of the play.

The pilot project would optimally be located close to an existing exploration or appraisal well. Placing the pilot well in close proximity will enable this offset well to act as a microseismic monitoring observation point for the pilot project wells. The pilot project wells can be comprised of individual well sites, though more recent developments utilize drilling pads with 6 to 12 lateral wells per pad with the wells aligned with the minimum stress direction in order to generate transverse hydraulic fractures from each stage of the well (Fig. 7.5a, Fig. 7.5b, and **Fig. 7.6**).

One of the main uncertainties associated with the development of unconventional resources concerns the well placement and particularly the spacing or offset between horizontal wells. The use of microseismic measurements to monitor the zone of influence associated with a hydraulic fracturing stimulation is one approach to deciding on the initial spacing between the laterals.

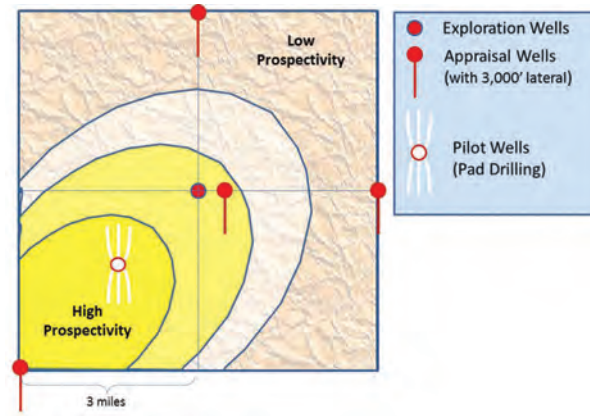

Fig. 7.6—Illustration of potential exploration, appraisal, and pilot wells, driven by sub-surface characterization.

In North America the lateral spacing between wells has been set by acreage, well commitment considerations, or previous experience on a play, which has been subsequently refined based on experience from infill drilling. In the Eagle Ford play one operator has moved from initial spacings of 130 acres per well (1,000 ft. between laterals) to 65 acres (500 ft. spacing) to 40 acres (300 ft. spacing) over a period of 3 years, with observed increases in productivity and estimated EUR per well. The spacing between wells should ideally be related to the size of the hydraulic fracture treatments and the expected length of the fracture stimulations. Appropriate monitoring and surveillance during the pilot project phase should aim to address such key design considerations.

The adoption of microseismic, tracer, and fiber optic monitoring during the pilot project stage also provides information about the interaction of either the hydraulic fracturing stages in a single well or between laterals. At the risk-management (i.e., lowering risk) stage of the project, microseismic measurements once interpreted can be used to provide recommendations on fracture stage spacings in laterals and identify whether any fracture containment issues exist.

The pilot project in the development delivery process is the principal opportunity to de-risk a development and establish its commerciality, in the absence of model-based concept selection. The data gathered during the pilot project stage needs to address the main project uncertainties and may include, for a typical shale gas or oil development comprised of horizontal wells (**Fig. 7.7**):

- Lateral lengths for the wells.
- Spacing between laterals.

- Fracture stages per lateral, distance between stages, geometrical or bespoke.
- If cluster stages are used, length of clusters, distance between clusters.
- Wellbore connectivity: perforations, abrasive jetting, and sliding sleeves.
- Completion design: plug and perforate, ball-drop systems, CT-sliding sleeve systems.
- Perforation cleanup.
- Stimulation design: gel fractures, slickwater fractures, and seawater versus freshwater designs, waterless fractures. This includes fluid selection, proppant selection, and concentration; pump rates, breaker selection, cleanup practices, and production bean-up procedures.

On the cost control side, well construction optimization is achieved through the following:

- Well design, casing design, cementing
- Batch and pad drilling
- Well stability and reduction of NPT
- Drilling mechanics optimization, vibration, BHA design, bit selection
- Drilling fluid selection and hole cleaning
- Drilling practices, including simultaneous operations (Simops)

To optimize production and well construction, additional data is gathered to address key challenges and to assess relative performance (benchmark) for any ongoing development.

With a large number of wells used in the pilot project stage, development issues associated with logistics for supplying drilling fluids, fracturing fluids, and proppant along with any reuse, recycling, and disposal become significant considerations during a full development. This stage of a pilot project can be used to assess the broader issues, which will affect the commerciality of a development. Foremost among these is water and fluid management.

7.2.4 Water and Fluid Management

- Full disclosure of fracturing fluids formulations
- Water and fluid cycle management plan
- Operations fully compliant with environmental standards, as a minimum requirement, and where possible, operations exceed requirements

The goal is to be proactive with the external stakeholders, including local communities and regulatory bodies, which demonstrates responsible operational procedures and processes.

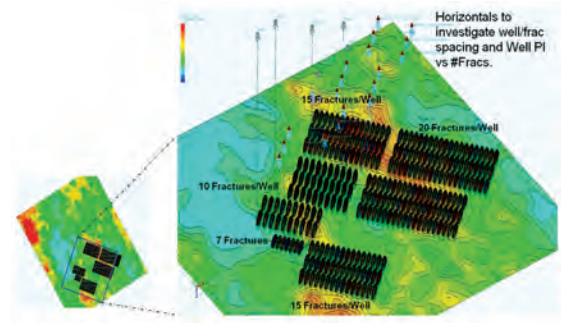

Fig. 7.7—Illustration of a pilot project to evaluate optimum well lateral length and hydraulic fracture stages.

In the United States in 2011, it is estimated that 0.4 billion gallons of water per day were used for hydraulic fracturing (EIA, 2014). The volume of flowback water can be zero, but typically primary flowback water is in the range of 30% to 70% of the injected fluid, which requires up to 0.3 billion gallons of water per day to be managed for the development of these unconventional resources. The flowback water typically has a high total dissolved solids (TDS) content, commonly in the range of 80,000 to 350,000 mg/l.

Compliance with local and national standards or regulations will be used to define a considerable portion of any water management plan. In addition, best practices and recommended practices can be evaluated at this stage of the pilot before upscaling to a full-scale development. This assessment of different water and fluid management options mirrors the approaches used for the appraisal and pilot stages for the completion and stimulation selection.

International guidelines specify that water should be managed in an integrated manner (Bickle et al. 2012):

- Techniques and operational practices should be implemented to minimize water use and avoid abstracting water from supplies that may be under stress.
- Wastewater should be recycled and reused where possible.
- Options for treating and disposing of wastes should be planned from the outset. The construction, regulation, and siting of any future onshore disposal wells need to be investigated.
- Flowback water is categorized in some jurisdictions (e.g., European regulations) as radioactive waste, and may require the appropriate licenses for any disposal.

Water disposal from fracturing fluids and flowback, or back-produced water in North America is a significant cost consideration for the overall economics of an

unconventional shale play, and as such evaluating the water management options, including reuse and recycling during a pilot project phase will help improve the robustness of project economics and reduce potential environmental incidents and unexpected project risks. Internationally, many unconventional resource plays are located in arid regions, with limited water resources. Consequently, water management is likely to play a more significant role in project viability and attractiveness in these areas.

Alternatives to freshwater sources for drilling and hydraulic fracturing fluids are available and may enhance the project success, through the use of seawater, brines, or non-aqueous fluid systems. Evaluating these alternatives would be appropriate at the pilot project stage along with any constraints on the reuse, recycle, and disposal of these alternatives.

To detect groundwater contamination, Bickle et al. (2012) recommends the following:

- The national environmental regulators should work with the relevant geological, mining, or licensing authorities to carry out comprehensive national baseline surveys of methane and other contaminants in groundwater.
- Operators should carry out site-specific monitoring of methane and other contaminants in groundwater before, during, and after shale gas operations.
- Arrangements for monitoring abandoned wells need to be developed. Funding of this monitoring and any remediation work needs to be addressed.
- The data collected by operators should be submitted to the appropriate regulator.

Specific details around the frequency and duration of monitoring should be sufficient to ensure any affect to the environment and any operational risks can be reduced to as low as reasonably practical (ALARP). This water and fluid management plan will be a component of a more extensive environmental impact assessment and environmental due diligence.

7.2.5 Environmental Impact Assessments

Environmental impact assessments (EIA) and environmental risk assessments (ERA) for any pilot project are precursors to establishing a sustainable and commercial development. In the stage-gate delivery of a project, the technical issues, as well as the commercial aspects of a project, are reviewed in technical reviews and value assurance reviews, and must comply with regulatory and company criteria before any decision gate approval in order to advance a project to the next phase of development.

Much of the focus has been on water and fluid management for shale gas and shale oil development. However, as the level of industry activity increases, more issues are becoming important, and need to be addressed in any health safety and environment (HSE) plan and environmental impact assessment. Details of the environmental issues are addressed in Chapter 22. Here we only point out specifics as they apply to pilot studies.

These issues include anti-flaring policies, potential air pollution through flaring, release of carbon dioxide and methane, the presence of heavy metals, and increasingly, the presence of naturally occurring radioactive materials (NORMs) in the production stream. The presence of NORMs has implications for the production, handling, transportation, and disposal of these materials, which can contain elements such as radium, thorium, and uranium. These issues need to be addressed in any HSE plan and environmental impact assessment.

Managing these radioactive substances—or any other hazardous components involved in the development of shale gas or oil resources—should be accounted for through a tracking or auditing system that includes a disposal plan for the responsible management of these materials. The disposal sites should meet strict environmental standards for radioactive materials including transportation, handling, and storage by approved and licensed disposal companies with a fully monitored site.

Bickle et al. (2012) and Smith (2014) recommend that environmental due diligence by the operator is achieved through mandatory environmental risk assessments or environmental impact assessments for all shale gas (or shale oil) operations, involving the participation of local communities at the earliest possible opportunity. The significant increase in the drilling and fracturing activity during the pilot project, which is commonly restricted to a small area such as a well pad, would be the appropriate juncture in the development to implement these recommendations. The environmental risk assessment should assess risks across the entire life-cycle of the development through to disposal and well abandonment, and include subsurface induced and natural seismic risks. This approach is consistent with assessing the full life-cycle costs and establishing the commerciality of a development during the pilot project stage.

7.2.6 Data Gathering, Monitoring, and Surveillance Plan

During the pilot project, the primary data gathered should include measurements while drilling, completing, and stimulating the reservoir. This data can provide improved

reservoir characterization of the subsurface and distinguish between subsurface reservoir factors and the completion design, stimulation design, and operational factors for differences in the production performance.

These parameters are already discussed as a part of the earlier appraisal well evaluation and stimulation assessment and include:

- Gamma ray and azimuthal resistivity. Reservoir navigation for horizontal laterals.
- Spectral gamma ray. Lithology and mineralogy, TOC, porosity, brittleness.
- Array acoustic (dipole) logging. Geomechanical parameters, stress and brittleness, pore pressure, and deep shear imaging.
- Pulsed neutron logging. Mineralogy and brittleness.
- Magnetic resonance logging. Porosity, fluid typing, TOC.
- Image logging. Lateral characterization: fracture and fault detection and characterization.
- Mud logging. Real time geochemistry and rock cuttings analysis.

Further details can be found in Chapter 8. Many of these measurements should be obtained while drilling, using LWD tools. The completion and stimulation performance should include measurements of surface and downhole pressures, flow rates, slurry rates and concentrations, and the normal range of measurements measured during a fracture stimulation job. In addition, in a selected number of wells, in the pilot study, or in pads located in new parts of the shale play, microseismic monitoring during the fracture stimulations would be recommended, to assess the following:

- Fracture height and containment
- Fracture orientation
- Fracture geometry, which is whether a planar bi-wing fracture or a stimulated zone is generated

All of the above factors will aid in the optimization of subsequent well planning and fracture treatments. For the initial well pads and a pilot project, dedicated vertical wells can be included in the well pad design to obtain additional wireline data or cores to further characterize the reservoir at the pad location and to locate microseismic geophones for monitoring the stimulation treatments on the pad, where feasible.

Prestimulation data fractures, or the more commonly used diagnostic fracture injection tests (DFITs), should be included in any stimulation program. Details of DFITs can be found in Chapter 17. A monitoring and surveillance plan should be a part of any pilot study or a new pad location, as this will enable characterization of the fracture location for both stress magnitudes and pore pressures. The monitoring time for DFITs should not be compromised to ensure sufficient data is obtained to characterize the wells and pilot location. DFITs are commonly performed during the first stage of a multistage fracture treatment; however valuable data can be obtained from performing DFITs in a number of different stages across a single lateral, to assess the change in the conditions along the horizontal well (**Fig. 7.8**), and to optimize the fracture stage spacing and design.

In a new prospective area of a play, if the horizontal stresses are expected to be high, and either high strength formations (>50 MPa unconfined compressive strength) are expected, or high net pressures are observed during fracture treatments and DFITs, then it is recommended step-down tests be performed to assess the cause of the high net pressures and any fracture tortuosity. This surveillance technique can be a valuable addition to completion and stimulation optimization.

The stimulation, well cleanup, and long-term production performance of the wells should be assessed through a focused monitoring and surveillance plan, which could include the following:

- Production logging
- Permanent downhole pressure gauges
- Tracers, chemical tracers, and radioactive tracers, in the fracture fluids and proppant
- Temperature measurements
- DTS, DAS fiber optic measurements
- Microseismic monitoring

These measurements, when combined with the characterization of the laterals that were discussed earlier, enable the variations in the well production to be apportioned as a result of subsurface factors or completion, stimulation, and operational procedures. The production data will be available from well specific in-line production meters, or preferably from dedicated extended well tests of the pilot project wells, and pads.

These well measurements allow improvements to the well construction and production operations. The monitoring and surveillance plan should also address surface and environmental surveillance requirements, including appropriate benchmarking measurements before operational start-up. Typically, operating companies start measurements for benchmarking in the pilot development areas at least one year before the start of operations so they can capture seasonal variations.

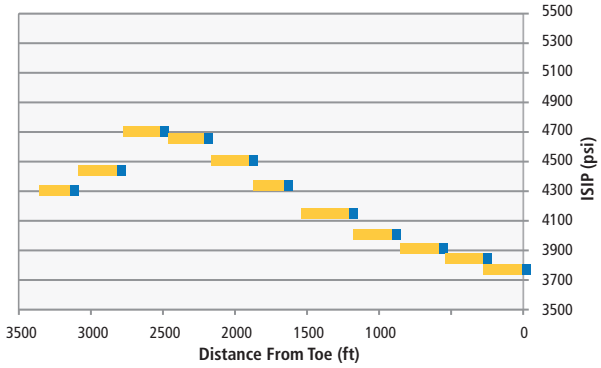

Fig. 7.8—Variation of ISIP across a lateral from the work of Vermylen (2011), and Vermylen and Zoback (2011).

The complete data gathered and the monitoring and surveillance plan should provide information to improve the operation, economically and environmentally, to ensure a sustainable and responsible approach is pursued in development stage.

7.2.7 Well Testing

The purpose of the pilot project is to prove commerciality of the prospect, which requires optimizing the production in addition to controlling costs. The production optimization requires extended tests of the wells to establish initial peak production and the decline rate, but, in practice, these tests are often constrained by operational considerations, such as flaring limitations, a company's zero flaring policies, or regulated limitations for flaring.

Well production tests in conventional reservoirs are used to assess and verify the reservoir characteristics, and reduce production-related subsurface uncertainties, which, as well as the rock and fluid properties, may include drainage radius, drainage boundaries, and well connectivity.

The low permeabilities of the tight and source rock formations comprising unconventional plays require production tests with long durations typically requiring many months of production. Consequently, production well tests are not commonly adopted in these plays.

It is well documented that hydrocarbon production from unconventional reservoirs decline rate is steep ~65-75% per year in the first year. This is thought to be due to transient effects, pressure depletion, and stress effects, or a number of other different mechanisms. Early production rates are high due to initial flow through fractures, but these decrease drastically and become stabilized when controlled by the longer-term supply of gas from the matrix to the fracture system.

Production from shale gas and oil wells is normally defined by monthly average production. During the first year of production, peak production is achieved and commonly quoted as either a monthly or a three-month average production value. The subsequent decline is also quoted using monthly or three-monthly average values. As such, to understand how an individual well is going to perform may take several years of production, especially if the decline curve characteristics and the estimated ultimate recovery (EUR) per well are to be established. Production forecasting is further detailed and discussed in Chapter 14.

Consequently, well testing to obtain reservoir parameters such as reservoir pressure, permeability, and fluid viscosity, as well as the fracture closure stress, which are used for the design of hydraulic fractures, rely on small volume DFIT tests run prior to the main hydraulic fracture.

This test, however, does not provide information about the drainage radius or connectivity that underpins well spacing decisions in either the pilot or the development stage.

7.2.8 Technology Plan

The viability and success of unconventional resource developments (shale gas and oil and tight gas and oil) in North America has been the result of two key technologies, horizontal drilling in low permeability formations, and multistage fracturing. As such, unconventional resource development is regarded as a "technology play" in the industry, as the resources have become unlocked through the application of appropriate technology.

As a part of any pilot project, the aim of establishing the commerciality involves well drilling optimization and production optimization. This involves identifying operational efficiencies as well as adopting beneficial new technology.

Pilot project planning, specifically, data acquisition requirements and monitoring and surveillance needs, will be guided by the asset project risk register, identification of key uncertainties, and key risks to the project. The identification and application of new technologies should be focused on these challenges, with the aim of ensuring project success.

Companies perform technology mapping exercises to align new available technologies to the development challenges, which are then included in the pilot project. It is good practice to incorporate new technology implementation as a part of the early pilot and development, in order to accelerate the adoption of lessons-learned and efficiencies

to improve project commerciality.

One-off technology trials (e.g., one well trials) should be avoided, as these have a track record of not securing the potential benefits of new technology deployment. A technology program based on multiwell trials should be formulated and applied during the pilot project stage and early development stage of these unconventional resource developments.

7.3 Pilot Project Design and Review to Capture Improvements

The role of pilot wells is to establish commerciality and reduce uncertainty. Targeted specific improvements should be pursued in a structured manner, i.e., not try to improve everything at the same time: focusing on the uncertainties with the largest potential impact on the pilot project and the development.

The lessons learned from the pilot project should be captured and assessed quantitatively in a post-pilot project analysis and review. The review should identify both the trials that worked as well as those that were unsuccessful, and provide lessons that should underpin the basis of design (BoD) or concept selection for the future development of the unconventional resource. The goals at this pilot stage are to characterize the reservoir to determine prospect viability, start the knowledge sharing between key stakeholders, and to continue the ongoing appraisal to reduce uncertainty for optimal well placement, completion design, and field development.

The post-pilot project development will build on the successes identified in the review and may also form the basis for commercial models for the play, which may include competitively tendering out all aspects, versus single allocation or source, with or without performance elements.

7.4 Concluding Remarks and Future Trends

The development of a large play does not need to be limited to one pilot project. Pilot projects may be replicated at a number of high prospectivity locations around the play in order to assess the lateral extent and variations of the unconventional resource.

If commercially successful, and if supported by subsurface characterization, the pilot project locations can be used as the basis for a phased start for the full-field development, which can be achieved by drilling well pads adjacent to the pilot project pads to form production clusters across the play (**Fig. 7.9**). The expansion and further optimization of these pilot project-based clusters can then form the basis for the larger field development.

7.5 References

Ahmed, U., Roux, P.F., Leung, E., and Gill, C. 2015. Hydraulic Fracturing Monitoring Technologies: Microseismic, Fiber Optic, and Tracers and their Interpretation. ***HFJ***, 2 (1): 40–60.

Ahmed, U. 2014. Optimized Shale Resource Development: Balance between Technology and Economic Considerations. Paper SPE 169984 presented at the SPE Energy Resources Conference. Trinidad and Tobago. 9–11 June. http://dx.doi.org/10.2118/169984-MS.

Barree, R.D., Fisher, M.K., and Woodroof, R.A. 2002. A Practical Guide to Hydraulic Fracture Diagnostic Technologies. SPE 77442.

Bickle, M., Goodman, D., Mair, R., et al. 2012. *Shale Gas Extraction in the UK: A Review of Hydraulic Fracturing*. The Royal Society and the Royal Academy of Engineering. London, England.

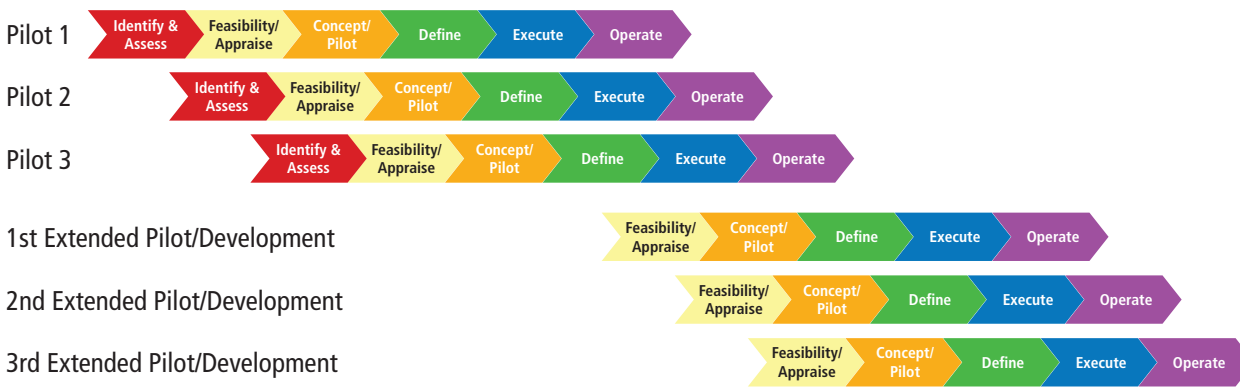

Fig. 7.9—The transition from pilot projects to a cluster-based field development for an unconventional reservoir.

Browning, J., Tinker, S.W., Ikonnikova, S., et al. 2013. Barnett Shale Model–1. *Oil and Gas Journal*. **5**.

Cipolla, C. and Wallace, J. 2014. Stimulated Reservoir Volume: A Misapplied Concept. Paper SPE 168596.

Giles, M.R., Nevin, D., Johnston, B., and Hollanders, M. 2012. Understanding Volumes, Economics and Risk Mitigation in Unconventional Gas Projects. Paper SPE 151906.

Martin. A. N. and Eid, R. 2011. The Potential Pitfalls of Using North American Tight Gas and Shale Gas Development Techniques in the North African and Middle Eastern Environments. Paper SPE 141104.

Rylance, M. 2013. Optimizing Remote Unconventional Gas Exploration. Paper SPE 163987.

Rylance, M., Nicolaysen, A., Ishteiwy, O., Judd, T., et al. 2011. Hydraulic Fracturing: Key to Effective Khazzan-Makarem Tight Gas Appraisal. Paper SPE 142783.

Smith. A. 2014. Environmental and Community Due Diligence Impact on Shale Gas Projects. Presentation at the 4th Shale Gas Southern Africa Summit. 25 March.

Sondergeld, C.H., Newsham, K.E., Cominsky, J.T., et al. 2010. Petrophysical Considerations in Evaluating and Producing Shale Gas Resources. Paper SPE 131768.

Vermylen, J.P. 2011. Geomechanical Studies of the Barnett Shale, Texas, Ph.D. Thesis, Stanford University.

Vermylen, J.P. and Zoback, M.D. 2011. Hydraulic Fracturing, Microseismic Magnitudes, and Stress Evolution in the Barnett Shale, Texas, U.S.A. SPE 140507. SPE Hydraulic Fracturing Technology Conference and Exhibition, Woodlands, Texas, 24–28 January.

This page intentionally left blank

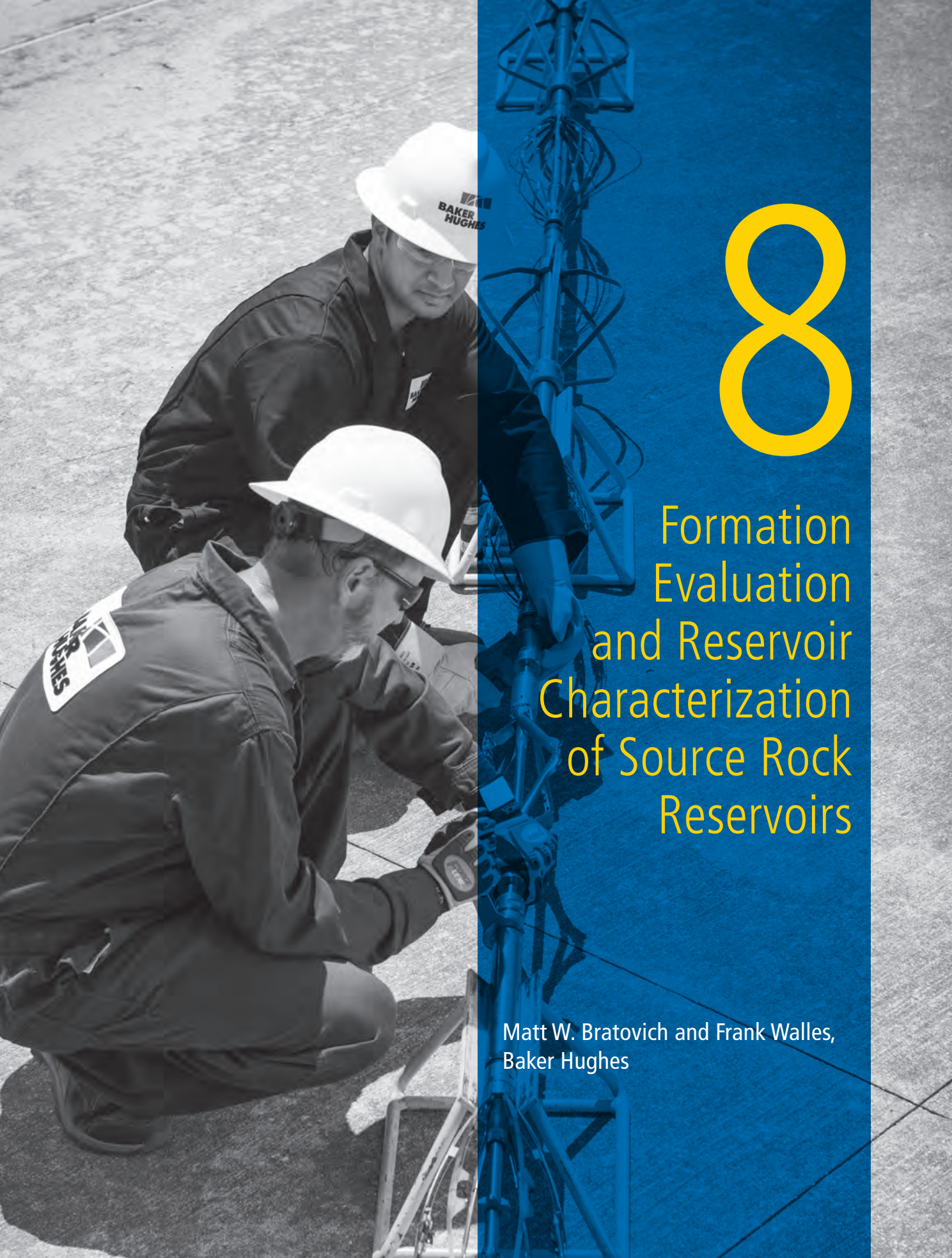

8

Formation Evaluation and Reservoir Characterization of Source Rock Reservoirs

Matt W. Bratovich and Frank Walles,
Baker Hughes

This page intentionally left blank

Chapter 8: Formation Evaluation and Reservoir Characterization of Source Rock Reservoirs

Unconventional source rock reservoirs, commonly referred to as unconventional gas or oil shale reservoirs, are geologically and petrophysically complex, organic rich, fine-grained mudrocks that must be hydraulically fracture-stimulated to produce gas or oil at economic rates. Increasingly these hydrocarbon reservoirs are being developed and produced using horizontal laterals. The dominant clay matrix particle size of these source rock reservoirs include heterogeneous compositional components that may include varying amounts of extrabasinal (terringenous fluid or airborne origin) clastics (quartz, feldspars, clays, and reworked rock fragments that include carbonate, igneous and metamorphic and volcanic rock fragments), and intrabasinal sedimentary particles (biologic origin silica, and calcite and preserved and altered kerogens), and diagenetically or chemically altered origin chert, dolomite, siderite, clays, and pyrite. These complex reservoirs possess complex pore systems that are dominantly nanoscale (extremely small-sized) inorganic, and organic interparticle, inter-crystalline and intraparticle pores (Loucks et al. 2012). In order for these reservoirs to produce hydrocarbons, the reservoir must exhibit very high hydrocarbon saturations (oil saturation, abbreviated, as So, or gas saturation, abbreviated as Sg) and very low (irreducible to sub-irreducible) water saturations abbreviated, as Sw. Natural fracture systems can also occur, either sub-vertical (of tectonic origin) or horizontal (of petroleum system origin). Permeability is extremely low, often in the nanodarcy range. Movable hydrocarbons may be present within the pores (identified as free gas) but are also present as adsorbed or absorbed hydrocarbons to the kerogen and clay surfaces (identified as adsorbed gas). These very complex and nanoscale varying reservoir characteristics pose significant formation evaluation challenges. Successful formation evaluation of reservoir characterization requires the acquisition and analysis of high-definition, first-order technical data from many sources.

8.1 Overview of Formation Evaluation Objectives for Reservoir Characterization of Source Rock Reservoirs

Compared to conventional reservoirs unconventional source rock reservoirs often extend across large portions of a basin. Consequently, reservoir characterization across the entire basin may be required to identify the higher potential areas. This step involves quantifying a variety of petrophysical, geological, geophysical, engineering, geomechanical, and geochemical properties of the fluids and rock. We can group source rock reservoir characteristics into categories to help us identify what specific rock or fluid property or parameters are required and how that property can be measured. **Fig. 8.1** illustrates these reservoir characteristic categories.

8.1.1 Rock Composition Quantification

Reservoir characterization of unconventional shale gas and oil reservoirs starts with quantifying the lithology and mineral composition of the formation. Mineral composition

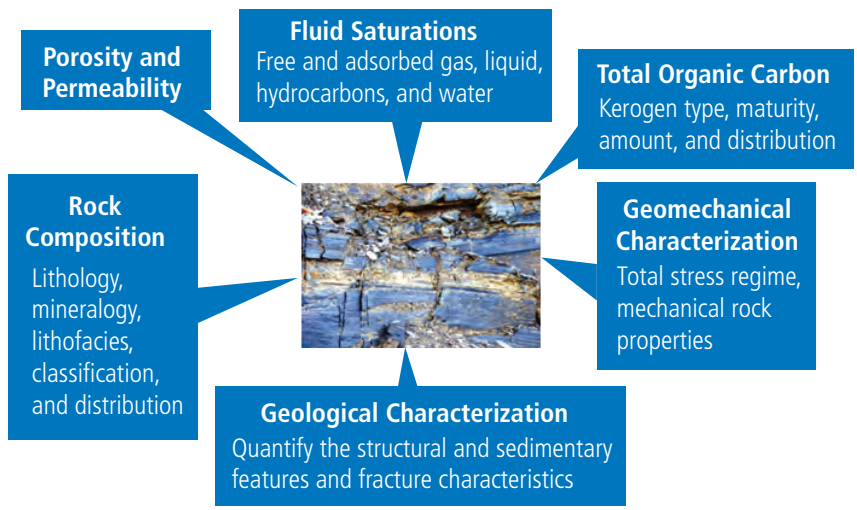

Fig. 8.1—Categories of source rock reservoir characteristics required for petrophysical evaluation.

of shale reservoirs is the property that can have the most impact on reservoir productivity, good or bad (Walles et al. 2009). When dealing with source rock reservoirs the term ***shale*** is used to describe fine-grained organic rich sedimentary rocks composed of primarily clay-sized particles with some silt sized. It includes rock that may possess a laminar or fissile structure and rock that does not.

While grain size is generally similar in most shale plays, mineralogy varies significantly, both vertically and areally within a single shale reservoir and between shale plays. The reservoir may have variable amounts of clay, kerogen, and also varying amounts of quartz, feldspars, calcite, dolomite, and other mineral particles. These inorganic minerals may be detritral or biologic in origin. Variations in mineralogy indicate variations in the mechanical properties of the rock. In each wellbore the lithology and mineral composition would be quantified using data from wireline or logging while drilling (LWD), core analyses, and mud log cuttings examination. After this determination is made, a set of lithofacies representative of that reservoir would be developed. Each shale reservoir contains a variety of lithofacies, or zones of rock with similar mineral composition, organic content, and geomechanical properties. Accurate lithology and mineralogy allows more accurate porosity determination and as well as providing input for planning stimulation and completion design and horizontal lateral placement.

8.1.2 Geological Characterization

Geological characterization objectives include understanding the tectonic and structural history of the basin and of the source rock formation. The major structural features should be identified. Establish and map the organic-rich shale formation top and base true vertical depths and thickness. Determine and understand the stratigraphic framework of the formation, sequence stratigraphy, and depositional environments that occur within the shale reservoir and correlate and map their distribution. Unconventional shale gas and oil reservoirs exhibit variations in organic content, mineral composition, and mechanical rock properties which are a function of variations in the depositional environment and each unit's sequence stratigraphic position (Passey et al. 2010; Lash and Engelder 2011).

Natural fracture systems are present in most source rock reservoirs. These natural fractures can have a positive factor on shale productivity by connecting with the hydraulic fracturing stimulation, intersecting them in a complex network of pathways to the wellbore (King 2010; Jenkins and Boyer 2008). They may, however, be a negative factor if the hydraulic fracturing stimulation intersects natural fractures that extend out of the source rock reservoir into porous and permeable water-bearing formations (Jacobi et al. 2008). A thorough description of these systems, which includes identifying the depth of fractures seen in the wellbores, the orientation of those fractures (dip and azimuth), and total number of fractures observed with subdivisions of those partially open or mineralized should be performed. The Marcellus shale reservoir has multiple joint systems that impact well productivity (Engelder et al. 2009). **Fig. 8.2** shows the relationship of the J1 and J2 joint systems in the Oatka Creek member of the Marcellus shale exposed in a quarry in central Pennsylvania.

Fig. 8.2—J1 and J2 joint systems in the Oatka Creek member of the Marcellus shale.

8.1.3 Total Organic Carbon Quantification

The most obvious characteristic of a source rock is that it contains a high amount of total organic carbon (TOC). In the industry the terms ***TOC*** and ***kerogen*** are often used interchangeably but they are not the same. TOC has

three components: the gas or oil that is already present in the rock, the kerogen that represents the available carbon that could be generated, and residual carbon that has no potential to generate hydrocarbons (Jarvie 1991). Hydrocarbon is formed (sourced) within the source rock from kerogen, a solid mixture of organic chemical compounds that is insoluble in normal organic solvents because of the huge molecular weight of its component compounds and bitumen, when they are subjected to increasing temperature and pressure. In a typical source rock some of the hydrocarbon is expelled and migrates into traps to become conventional reservoirs. In source rocks that are unconventional shale gas or oil reservoirs a substantial volume of the generated hydrocarbon is not expelled and the source rock itself becomes the reservoir. Many characteristics about the TOC and kerogen must be quantified, these include:

- How much weight percentage of TOC is present in each wellbore and across the reservoir? Experience has shown that for a shale gas/oil reservoir to be capable of economic production of gas or oil a minimum weight percentage of TOC must be present.
- How is the TOC weight percentage distributed both vertically and areally in the reservoir? Some shale reservoir plays such as the Haynesville shale produce only gas. But several producing shale plays, including the Eagle Ford shale in south Texas and the Vaca Muerta shale in Argentina, produce gas and oil from different areas within the play. Some types of kerogen are prone to produce oil while others are prone to produce gas, so another objective is:
- Determine what types of kerogen are present and how each type is distributed areally across the reservoir. The type of hydrocarbon that is produced is also dependent on the thermal maturity of the kerogen, which is what levels of temperature and pressure the kerogen has been exposed to since the deposition of the sediment.
- Determine the thermal maturity of the kerogen across the reservoir.

Productive potential of each mudrock and shale reservoir also depends on how much potential still exists in the kerogen to generate hydrocarbon, the TR, or transformation ratio. Rock pyrolysis analyses can provide that parameter. **Fig. 8.3** shows the distribution of kerogen type, thermal maturity, and the TR for the Vaca Muerta shale in Argentina.

8.1.4 Porosity and Permeability Quantification

Shale reservoirs possess complex pore systems composed of extremely small interparticle and intraparticle, inorganic and organic pores. Often, natural fractures also are present (Loucks et al. 2012). Typical total shale porosities are also low, in the range of 5 to 12%. Porosity determination for shale reservoirs using conventional log responses is complicated due to the variable amount of TOC and the heterogeneous mixture of inorganic mineral components present. The use of elemental spectroscopy and nuclear magnetic resonance logging technologies can reduce some uncertainty. Core measured porosity data should be obtained to calibrate and verify the log-derived porosities. Standard laboratory methods for porosity and permeability determination are unsuitable in shale reservoirs. Several types of laboratory porosity analysis are used that include MICP, GRI-standard crushed porosity, and SEM-FIB tomography.

Permeability in shale gas and or oil reservoir rock is extremely low, often in the nanodarcy range. Estimations of rock permeability must be based on core analysis measurements. A sufficient number of analyses must be taken to allow permeability estimates based on log responses to be calibrated. Laboratory methods utilized for permeability determination include pressure decay, pressure pulse decay, and MICP (Passey et al. 2010; Sondergeld et al. 2010).

8.1.5 Fluid Saturation Quantification

In conventional reservoirs hydrocarbons are stored only in the pores (porosity) of the matrix. The hydrocarbon saturations are calculated from laboratory analyses or from wireline or LWD log measurements of resistivity and porosity. In mudrock and shale gas and oil reservoirs, hydrocarbons are stored as:

- Free gas and oil in the matrix inorganic and organic pores and natural fractures
- Sorbed gas and oil either adsorbed (chemically bound) to the organic matter (kerogen) and mineral surfaces within the natural fractures or absorbed (physically bound) to the organic matter (kerogen) and mineral surfaces within the matrix rock
- Dissolved gas, in the hydrocarbon liquids present in the bitumen

In mudrock and shale gas or oil reservoirs, a combination of laboratory analyses is the primary method used to determine gas or oil saturations and volumes. Dean Stark and/or preferably Step Wise Retort analyses are conducted to determine free gas and oil saturation on crushed rock samples. Adsorption and desorption isotherm analyses are utilized in gas shale reservoirs to calculate both total gas volumes and adsorbed gas volumes (Bustin et al. 2009). Most

Vaca Muerta Source Rock (Late Jurassic)
Kerogen Type and Total General Potential

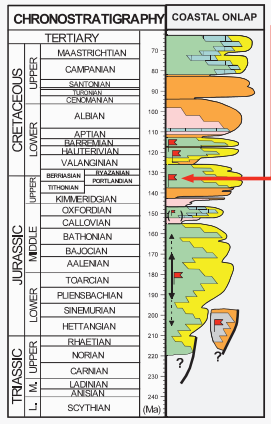

(Villar et al., 1998; Legarreta et al., 1999)

Vaca Merta FM: Organic-rich shales deposited in a marine setting under anoxic water conditions and locally euxinic

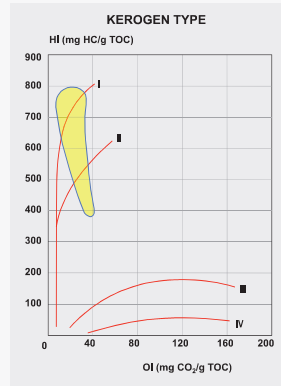

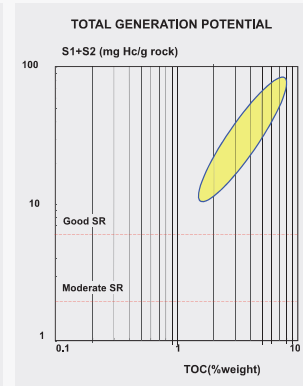

Kerogen Type: Type I-II dominantly amorphous marine. Locally Type IIS (South Dorsal)
Source Rock Quality: Very high organic matter content (TOC: 3-8%). Main source rock of the basin and four oil types were identified

Vaca Muerta Source Rock (Late Jurassic)

Evolution of the Transformation Ratio (%) and Present-Day Maturity Level

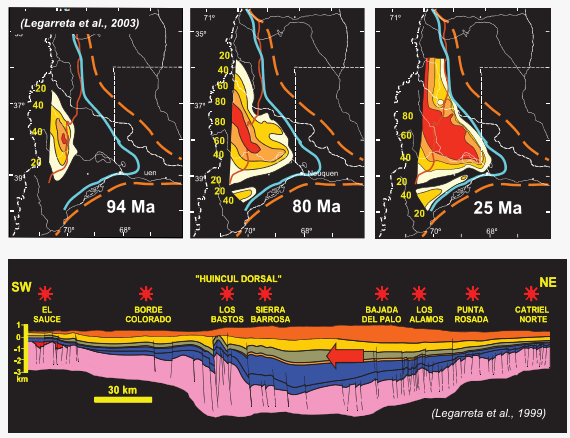

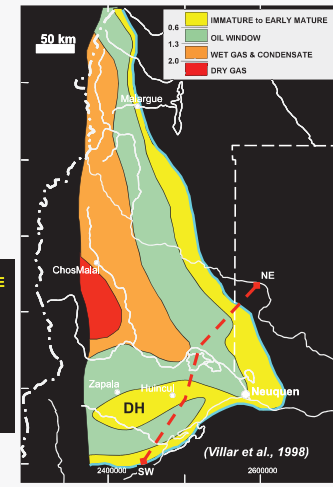

A relatively widespread area remains within the mid to late oil-window. The Dorsal High (DH) is still immature.

Fig. 8.3—Distribution of kerogen and TOC properties in the Vaca Muerta shale, Argentina. (Modified from Legaretta and Villar 2012.)

mudrock and shale reservoirs produce little free water and the water saturation in the pores has been determined to be at irreducible or sub-irreducible values. Water saturation is often estimated from resistivity and porosity log measurements using either an Archie equation or shaly reservoir methodology as are done for conventional reservoirs. However, there is more uncertainty in these estimations as the accuracy of many of the required parameter values including formation water salinity and appropriate electrical parameters may be suspect. Sufficient core-measured-saturation control must be used to validate these log-derived fluid saturations. Details of the laboratory testing can be found in Chapter 10.

8.1.6 Geomechanical Characterization

Exploitation of unconventional shale gas/oil reservoirs depends on successful horizontal drilling and multistage hydraulic fracturing results. This requires understanding the in-situ stress state and natural fracture distribution in each shale reservoir. Stress states and natural fracture patterns can vary between and even within shale reservoir plays. These variations affect the shape and character of the stimulated rock volumes, the requirements for safe drilling, and the optimal directions to drill to exploit natural fractures. The in-situ stress analysis should include determination of the in-situ stress orientations, magnitudes, pore pressure, effective rock strength, fracture patterns, and rock structure (LeCompte et al. 2009). The geomechanical characterization should also include determination of the rock static and dynamic mechanical properties, anisotropy, rock brittleness, and hardness.

Details of the geomechanical laboratory testing can be found in Chapter 9.

8.2 Technologies Utilized for Formation Evaluation and Reservoir Characterization of Source Rock Reservoirs

Evaluating mudrock and shale reservoirs involves quantifying a variety of petrophysical, geological, engineering, geomechanical, and geochemical properties of the fluids and rock. Technical data will need to be acquired from many sources. Wireline and LWD log measurements are two of the most frequently used data sources, but a robust reservoir characterization of an unconventional mudrock and shale reservoir requires careful analysis and examination and study of actual reservoir rock.

Table 8.1 lists the technologies most commonly used to quantify shale reservoir and fluid properties.

8.2.1 Elemental Spectroscopy Logging

Elemental spectroscopy logging is being utilized extensively to quantify the mineral composition in unconventional shale oil and gas reservoirs. Elemental spectroscopy logging instruments utilize gamma ray spectroscopy to quantify the weight fractions of various elements in the rock. Neutrons are emitted from a chemical or pulsed neutron source and interact with elements in the rock causing gamma rays to be emitted from both the capture and inelastic energy spectra.

A spectral gamma ray instrument is also run in combination with the instrument to measure responses in the natural gamma ray spectrum. These gamma rays are measured by a scintillation detector and processed to obtain elemental yields and those are converted to elemental weight fractions (Pemper et al. 2006). Corrections are made to account for the borehole environment and chemical composition of the mud. The specific methodologies utilized by individual service companies to convert from elemental yields to dry elemental weight fractions vary. **Table 8.2** lists the four spectroscopy instruments currently commercially available. **Table 8.3** compares the elements measured by the commercially available spectroscopy instruments.

All instruments measure essentially the same elements in the capture energy spectrum. The advantage of a pulsed neutron instrument is the ability to measure additional elements in the inelastic spectrum, particularly carbon. While some elements such as aluminum and magnesium are detectable in the capture spectrum they are difficult to quantify. The additional presence of those elements in the inelastic spectrum allows for a more robust determination for both (Pemper et al. 2006). The methods used by petrophysicists and the service companies to use the elemental weight fractions to determine mineral composition vary and will be discussed in the lithology and mineralogy section of this chapter.

8.2.2 Core and Fluid Laboratory Core Analyses

The necessity of quantifying the mineralogy, porosity, permeability, fluid properties, and the properties of the organic material present in these source rock reservoirs requires obtaining specialized laboratory analyses. The extremely low permeability and small pore sizes also require modifications of conventional laboratory measurement procedures of those properties. **Table 8.4** lists the analyses performed related to mineral composition, TOC, kerogen

Table 8.1—Source rock reservoir evaluation wireline and LWD technology applications.

Source Rock Reservoir Evaluation Wireline and LWD Technology Applications			
Generic Tool Technology	Baker Hughes Wireline Tool	Baker Hughes LWD Tool	Evaluation Application
Resistivity	HDIL™	OnTrak™/AziTrak™	Fluid saturations, TOC determinations
Compensated Density Compensated Neutron	ZDL™/CN™	LithoTrak™	Total porosity, lithology, and TOC determination
Cross Dipole Acoustic	XMAC™-F1	SoundTrak™	Acoustic slownesses, mechnical properties, geomechanical stress determinations, fracture identification
Gamma Ray Spectral Gamma Ray	GR™ Spectralog™	GR Included with LWD resistivity service	Lithology, mineralogy, and TOC determination
NMR	MReX™	MagTrak™	Porosity, TOC, fluid volumes and type determination, permeability estimation
Elemental Spectroscopy	FLeX™		Lithology, mineralogy, and TOC determination
Resistivity Imaging	STAR™ (WBM) GeoXplorer™ (OBM)	StarTrak™ (WBM)	Geologic structure and sedimentary analysis, in-situ stress determination, fracture identification
Acoustic Imaging	CBIL™ UltrasonicXplorer™		Geologic structure and sedimentary analysis, in-situ stress determination, fracture identification
Fluid and Pressure Testing	RCI™ Straddle Packer Micro-Frac™		In-situ stress measurements. Real-time pressure decline analysis to determine formation breakdown, fracture closure, and fracture re-opening pressures.
Rotary Cores	PowerCOR™ MaxCOR™		Obtain core samples suitable for laboratory analysis
Production Logging	POLARIS™		Characterize production profiles post stimulation
Cased Hole Pulsed Neutron	RPM™-C		Lithology, mineralogy, and porosity determination in a cased hole

Table 8.2—Commercially available spectroscopy logging instruments.

Elemental Spectroscopy Wireline Logging Instruments			
Service Company	Tool Name	Neutron Source	Spectra Measured
Baker Hughes	FLeX™	Pulsed Neutron (14 MeV)	Capture + Inelastic
Halliburton	GEM™	Chemical Americium-Beryllium (AmBe) (600 keV-8 MeV)	Capture
Schlumberger	ECS™	Chemical Americium-Beryllium (AmBe) (600 keV-8 MeV)	Capture
Schlumberger	LithoScanner™	Pulsed Neutron (14 MeV)	Capture + Inelastic

and bitumen characterization, total gas content, porosity, permeability, and fluid saturations. Analyses related to geomechanical properties will be discussed in Chapter 9.

Rock and fluid analyses results are critical for the determination of reservoir quality in these reservoirs but many of these analyses require significant amounts of time to complete. Due to the large number of unconventional shale wells drilled each year in North America, commercial core analyses laboratories are often backlogged, resulting in additional delays in obtaining results.

8.2.3 Wellsite Evaluation Technologies

Typical wellsite evaluation technologies used in North American onshore exploration or appraisal of unconventional vertical wells are usually limited to open and cased hole wireline logging with occasional use of MWD or LWD logging

Table 8.3—Elements measured by commercially available spectroscopy logging instruments.

Capture Spectrum	Baker Hughes FLeX™	Halliburton GEM™	Schlumberger ECS™	Schlumberger LithoScanner™	Inelastic Spectrum	Baker Hughes FLeX™	Schlumberger LithoScanner™
Al	X	X		X	Al	X	X
Ba				X	Ba		X
Ca	X	X	X	X	Ca	X	X
				X	C	X	X
Cl	X	X	X	X			
Cu				X			
H	X	X	X	X			
Fe	X	X	X	X	Fe	X	X
Gd	X	X	X	X			
Mg	X	X		X	Mg	X	X
Mn				X			
					O	X	X
Ni				X			
K	X	X	X	X	K	X	
Si	X	X	X	X	Si	X	X
Na	X	X		X			
S	X	X	X	X	S	X	X
Ti	X	X	X	X	Ti	X	X
Natural Spectrum							
K	X	X	X	X			
Th	X	X	X	X			
U	X	X	X	X			

instruments. Basic mud logging services including monitoring of drilling and mud parameters, gas chromatography (C1–C5), used to evaluate hydrocarbon shows and geological description of drill cuttings may also be acquired.

The extensive use of horizontal lateral wells in development drilling and the need to improve stimulation performance and increase well productivities in unconventional shale wells is slowly increasing the use of additional wellsite evaluation services that were previously only available in a laboratory environment. Due to high cost and risk associated with obtaining reservoir information in horizontal wells from wireline or LWD logging, the majority of wells drilled may have only a MWD GR curve to characterize the reservoir section. Service companies have been introducing ruggedized equipment to acquire organic and inorganic chemistry analyses, mineralogy, TOC, fluid, and gas characterization, quantification of permeable, or natural fractured intervals and other rock and fluid properties in a wellsite environment. These advanced cuttings analyses and advanced gas analyses can obtain high-quality reservoir characterization measurements at a relatively lost cost and low risk when compared to traditional logging methods. An additional benefit is that the lengthy delays often encountered with completing laboratory analyses are avoided by conducting the analyses at the wellsite. The application of these services for lateral characterization is covered in detail later in this chapter. **Table 8.5** is a listing of wellsite analytical services currently available.

8.2.4 Overview of Petrophysical Evaluation Workflow Approaches for Unconventional Source Rock Reservoirs

Several reservoir parameters must be quantified for unconventional source rock reservoirs requiring a variety of logging, mud logging, and geophysical technologies and the acquisition and laboratory analyses of mudrock and shale rock and reservoir fluid samples. The evaluation workflow

Table 8.4—Source rock reservoir evaluation core and fluid laboratory analyses.

Source Rock Reservoir Evaluation Core and Fluid Laboratory Analysis		
Reservoir Rock Property: Mineral Composition/Sedimentology and Stratigraphy	Analysis Name	Analysis Result
XRF	X-Ray Fluorescence	Elemental Composition
ICP-OES	Inductively Coupled Plasma - Optical Emission Spectroscopy	Elemental Composition
LIBS	Laser-induced Breakdown Spectroscopy	Elemental Composition
XRD	X-Ray Diffraction	Mineral Composition
FTIR	Fourier Transform Infrared Spectroscopy	Mineral Composition
NIR	Near Infrared Spectroscopy	Clay Identification, Thermal Maturity
CL	Cathodoluminescence	Mineral Composition
PLM	Polarized Light Microscopy	Mineral Composition
Core CT	Whole Core X-Ray Computed Tomography	Sedimentary, Structural Characterization, and Fracture Geometry
Micro CT	Core Plug X-Ray Computed Tomography	Small Scale Sedimentary Features, Microfracture Characterization
Reservoir Rock Property: Mineral Composition/Rock Texture and Pore Systems	Analysis Name	Analysis Result
Qemscan/RoqSCAN	Scanning Electron Microscopy with EDXRF	Mineral Composition Texture & Pore Image
FIBSEM	Focused Ion Beam Scanning Electron Microscopy	Mineral Composition Texture & 3D Pore Image
Reservoir Rock Property: Total Organic Carbon Characterization	Analysis Name	Analysis Result
Ro	Vitrinite Reflectance	Kerogen Thermal Maturity
CAI	Conodont Alteration Index	Kerogen Thermal Maturity
TAI	Thermal Alteration Index	Kerogen Thermal Maturity
Rock-Eval	Rock-Eval Pyrolysis	Kerogen Type, Thermal Maturity, HC Fluid Type, Wt% TOC
Leco TOC	Leco Carbon Analyzer	Wt% TOC
C12/C13 Isotopes	Carbon Isotope Analysis	Gas Type, Maturity
SAM	Scanning Acoustic Microscopy	Impedance Microstructure, Texture, Kerogen Maturity
Reservoir Rock Property: Total Gas Quantification	Analysis Name	Analysis Result
GC/MS	Gas Chromatography/Mass Spectrometry	Gas Composition C1-C10+
C12/C13 Isotopes	Carbon Isotope Analysis	Gas Type, Maturity
Adsorption/Desorption Isotherms	Canister Desorption & Langmuir Adsoprtion Analyses	Total Gas Content

Table 8.4, continued.

Reservoir Rock Property: Porosity and Permeability	Analysis Name	Analysis Result
MICP	Mercury Injection Capillary Pressure	Porosity, Permeability
PPD	Pulse Pressure Decay	Permeability
PD	Pressure Decay	Permeability
GRI Permeability	Gas Research Institute Methodology - Permeability	Crushed Sample Permeability
NMR	Laboratory Nuclear Magnetic Resonance	Porosity, Permeability
GRI Porosity	Gas Research Institute Methodology - Porosity	Porosity
Reservoir Rock Property: Fluid Saturations	Analysis Name	Analysis Result
GRI Saturation	Gas Research Institute Methodology - Saturations	Crushed Sample Fluid Saturations
GRI Porosity	Gas Research Institute Methodology - Porosity	Crushed Sample Porosity
GRI Saturation	Gas Research Institute Methodology - Saturations	Crushed Sample Fluid Saturations
Reservoir Rock Property: Fluid Sensitivity	Analysis Name	Analysis Result
CST	Capillary Suction Time	Fluid Sensitivity

approaches commonly used can be separated into two broad categories: deterministic and probabilistic. Each approach has advantages and disadvantages with neither clearly superior for all shale petrophysical evaluations.

8.2.4.1 Deterministic Workflow Approaches

A deterministic workflow is typically a sequential approach that solves for one reservoir parameter at a time. These workflows may utilize empirical relationships that were developed from extensive log and core/fluid sample analyses from one or more basins such as the Passey Delta R technique or may be specific to one individual well or limited geographic portion of one shale play. Core/fluid analyses are utilized to validate or calibrate the log calculated values to each parameter. These calibration processes may vary from simple linear regressions to more sophisticated multiple linear or non-linear regressions or neural networks. Deterministic approaches can be used for simple datasets with only conventional logging measurements such as formation density, resistivity, acoustic compressional slowness, and gamma ray or one that includes more sophisticated logging technologies such as elemental spectroscopy or nuclear magnetic resonance instruments. The amount and types of core and fluid analyses available for use has a significant impact on how representative or realistic the derived parameter or parameters may be.

8.2.4.2 Probabilistic Workflow Approaches

A probabilistic workflow is one where a mathematical least squares error minimization solver is used to obtain simultaneously all the required reservoir parameters such as lithology/mineralogy (including TOC volumetric percent), porosity, and fluid saturations. The solvers perform best when the number of the mineral and fluid components to be solved by the model is greater than the number of log and core inputs. Endpoints of each component modeled must be selected for each log and core input curve utilized along with uncertainty or error ranges and curve weighting values for each. The software performs inversions based on an initial estimate of volumes for each component and forward modeling computes the theoretical log input responses for those volumes that are then compared to the input curve measurements. This process is iterated until the amount of incoherence, or error, between the actual and theoretical values is optimized. The optimized solution from

Table 8.5—Source rock reservoir evaluation core and fluid wellsite analyses.

Source Rock Reservoir Evaluation Core and Fluid Laboratory Analysis		
Reservoir Rock Property: Mineral Composition/Sedimentology and Stratigraphy	Analysis Name	Analysis Result
XRF	X-Ray Fluorescence	Elemental Composition
LIBS	Laser-induced Breakdown Spectroscopy	Elemental Composition
XRD	X-Ray Diffraction	Mineral Composition
NIR	Near Infrared Spectroscopy	Clay Identification, Thermal Maturity
FTIR	Fourier Transform Infrared Spectroscopy	Mineral Composition
HRDM/PLM	High Resolution Digital Microscope/ Polarized Light Microscopy	Mineral Composition
CL	Cathodoluminescence	Mineral Composition
Reservoir Rock Property: Mineral Composition/Rock Texture and Pore Systems	Analysis Name	Analysis Result
RoqSCAN	Scanning Electron Microscopy with EDXRF	Mineral Composition Texture & Pore Image
Reservoir Rock Property: Total Organic Carbon Characterization	Analysis Name	Analysis Result
Rock-Eval	Rock-Eval Pyrolysis	Kerogen Type, Thermal Maturity, HC Fluid Type, Wt% TOC
Reservoir Rock Property: Total Gas Quantification	Analysis Name	Analysis Result
GC/MS	Gas Chromatography/Mass Spectrometry	Gas Composition C1-C10+

these solvers is not unique and is impacted by the weight factors and uncertainty range used in the model (Peeters and Visser 1991). As was the case for deterministic approaches, probabilistic approaches can be utilized with very basic conventional log datasets as well as more sophisticated datasets that may include elemental spectroscopy and nuclear magnetic resonance measurements.

Numerous solvers are available to the petrophysicist from logging service and petrophysical software companies. A partial list of some commonly used solvers includes STATMIN (CGG Powerlog™ software), Multimin (Paradigm Geolog™ software), Mineral Solver (Senergy IPTM software), and Quanti.ELAN (Schlumberger TechLog™ software).

8.2.4.3 Hybrid Workflow Approaches

Workflow methodology used is often a combination of deterministic and probabilistic types. One reason for this is the variability in the number and types of log measurements acquired and or the amount of core analyses available for an individual well or for a specific shale play. Both deterministic and probabilistic workflows may group similar minerals in the model to reduce the number of variables.

There is no standard workflow for either the deterministic or probabilistic approaches. Each reservoir parameter is discussed in the following sections. Some of the variations in the calculation of each parameter by both the approaches are discussed.

8.3 Organic Carbon Quantification

8.3.1 Objectives of Organic Content Characterization

Hydrocarbon producibility of unconventional resource play targets is initially controlled through the fundamental original deposition components of the mudrock target system (**Fig. 8.4**).

These include the deposited mineral suite, its internal texture, the original clay types, the organic matter (or TOC original), and the heterogeneity of how these components have been layered.

Organic matter, however, plays a dominant role within the overlying petroleum system processes that develop the capacity to produce and store hydrocarbons.

Within the most productive unconventional resource plays, organic matter kerogen-based nanoscale interconnected porosity systems play a significant producibility and HC deliverability role. Nanoscale porosity systems within unconventional resource plays can include either a singular or combination of intra-kerogen, interparticle/inter-crystalline, or intraparticle porosity systems (**Fig. 8.5**). An important reservoir quality factor within unconventional resource liquids-rich or gas plays is to confirm that it contains a sufficient amount and quality (kerogen-suite type) of organic carbon that can develop both the specific desired producible hydrocarbon(s) within an interconnected nanoscale porosity system.

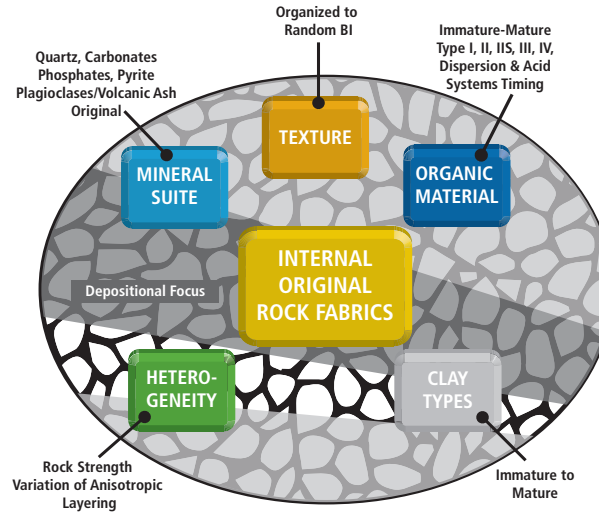

Fig. 8.4—Fundamental original deposition controlled components of a mudrock target system.

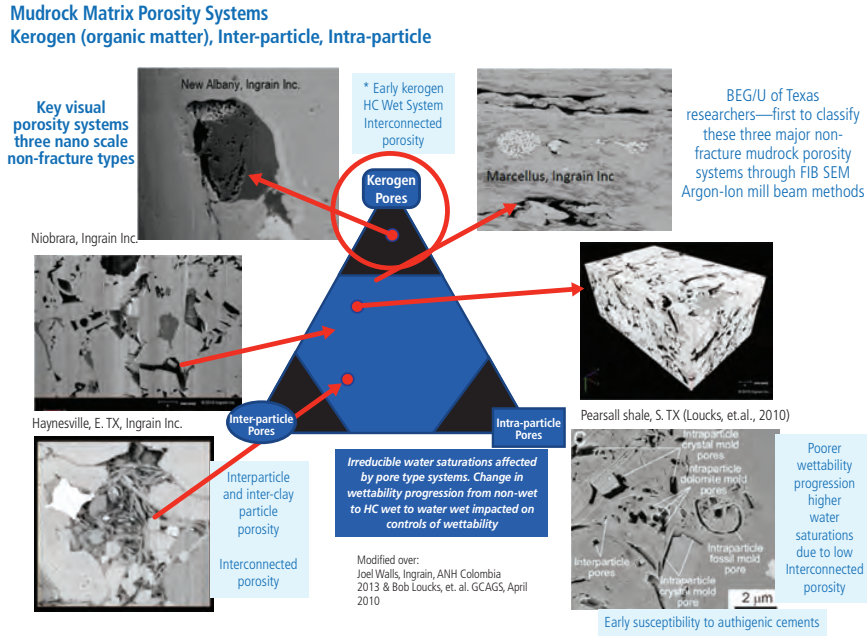

Fig. 8.5—Nanoscale porosity systems (with example FIB SEM images) of unconventional mudrocks. (Modified over Walls 2013, Loucks et al. 2010.)

Organic carbon or matter is a general catchall industry term to describe the total non-mineral carbon within a rock sample. This can include soluble (within organic solvents) transitional high molecular weight portions known as bitumens. Organic carbon, within the petroleum industry, is referred to by the general term of total organic carbon (TOC). TOC is the amount of material available to convert into hydrocarbons (depending on kerogen type) and represents a qualitative measure of source rock potential (Jarvie et al. 2007).

Organic carbon characterization along with specific nanoscale developed porosity systems based upon transformation ratio and organic matter type has been an evolving science of understanding. Much of the early characterization of organic materials focused on understanding coals and coal bed methane gas systems and their complex maceral storage and delivery suites dominated by structured kerogens that were gas prone (methane). The field of kerogen description still includes many aspects of the maceral typing terminology of the coal industry (Okeefe 2013). Within coal systems, co-occurrence or sapropelic (oil prone alginate maceral, or microorganism, kerogens) and humic coals (gas prone structural maceral kerogens) led to recognition of differential components within TOC that contributed to gas and/or liquid hydrocarbons.

However, original TOC volumes within the marine or transitional marine dominant depositional systems of typical unconventional resource plays are at most ~ 20%. This compares to the type and compositional differential kerogen systems of coals where kerogen volume percentages are as high as 90+%. Earlier assumption models of TOC origination within the marine systems included extrabasinal, transport models of terrestrial origin coal maceral materials into these environments. This extrabasinal transport assumption model has been shown to be generally incorrect within most unconventional resource play mudrock systems (Milliken and Reed 2009).

TOC is normally reported as a rock weight percent, not a volume percent. Volume percent is approximately twice that of weight percent. TOC can be a kerogen suite mixture of both original reactive and/or non-reactive kerogens and can be oxidized and/or fully transformed recycled.

Oil and gas source rocks typically have greater than 1.0% TOC. TOC richness can range from Poor: <1%; Fair: 1 to 2%; and Good to Excellent: 2 to 10% (PESGB 2008). TOC is not the same as kerogen content, as TOC is made up of both kerogen and bitumen. Measurement of TOC in shale is determined from wireline logs and by direct measurement from cores and drill cuttings using pyrolysis.

Kerogen definitions (Lewis et al. 2013) include that the material is insoluble organic matter that is primarily composed of carbon and hydrogen with lesser amounts of oxygen, sulfur, and nitrogen. Importantly the hydrogen content decreases with thermal maturity. Kerogens typically exhibit a low grain density (1.1 to 1.4 g/cm3) that also increases with maturity. Kerogens are rarely quantified in standard core analyses, as compared to TOC that is a common core analysis. Another important organic component is bitumen, a soluble organic matter that is considered a lower oil window thermal maturity product, which is non-producible at typical reservoir temperatures. Bitumens can also occur in the form of pyrobitumens that are considered a high thermal dry gas window product.

Measured total organic carbon (TOCpd) within the subsurface occurs within the form of transformed kerogen types and bitumens that can be best described as a mixture (suite) of kerogens (organic derived and preserved high molecular weight carbon based organic chemical compounds). This suite of present day (PD) transformed kerogens have or may have had a past or current capacity to generate and/or expel specific hydrocarbons and non-hydrocarbons, organic acids and inorganic acids, specific nanoscale surface wetting agents, as well as the ability to develop unconventional kerogen-based nanoscale porosity systems.

However, volumes of TOC present day are not volumes of TOC original due to the transformative processes that change the physical properties and volumes of the transforming defined type(s) of kerogens. Current advanced formation evaluation approaches (wireline/LWD based) utilize a number of methods to determine present-day total organic carbon (TOCpd), but not TOC original.

Dominant kerogen type of organic carbon (TOC original) within an unconventional resource play significantly impacts reservoir quality and resulting producibility. Specific kerogen types (especially I,IS, II, & IIS) develop the sequential fluids and gases leading to pore level high hydrocarbon saturations and irreducible or sub-irreducible water saturations. This occurs through association to the thermal transformation of these original kerogen compositional suites.

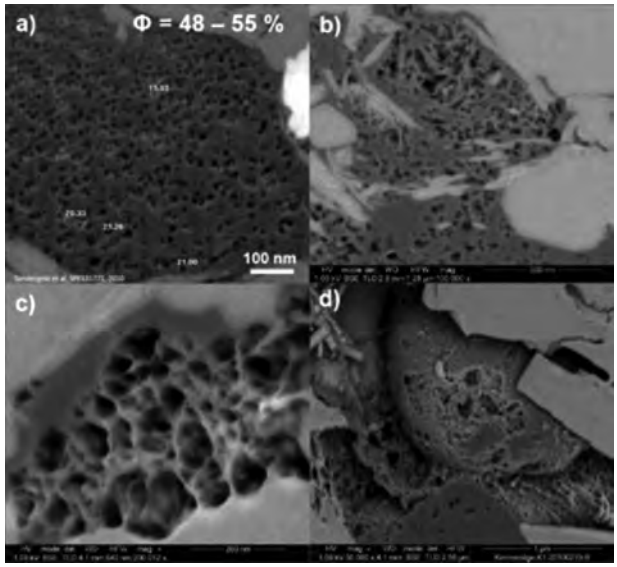

Fig. 8.6—Kerogen organic porosity. (From Curtis et al. 2011.)

These can include:

- Interconnected nanoscale kerogen reservoir porosity system (**Fig. 8.6)** resulting from the thermal and pressure maturity volatization within the specific kerogens, as well as within the nanoscale porosity within resulting bitumens and pyrobitumens.
- The volume of hydrocarbons present within a free phase and an adsorbed phase (adsorption is defined as the accumulation of the hydrocarbon molecular species on kerogen surfaces rather than within the bulk of the solid kerogen).
- The development of specific hydrocarbon (HC) composition fractions of hydrocarbon solids, liquids, and gases. These can include early maturity phase fractions of bitumens, and intermediate maturity phase fractions of asphaltenes and resins, as well as hydrocarbon liquids including pore system wetting organic acids as well as polar hydrocarbons. Hydrocarbon gases can include important fractions of carbon dioxide (CO_2), hydrogen sulfide (H_2S), as well as inerts (NO_2).
- Petroleum system sequential thermal maturity generation and expulsion inefficiency processes including elevated hydrocarbon generated geopressures from internal mudrock characteristics as well as system developed adjacent seals, directly affect the extent of reservoir pore HC phase and porosity system saturations (HC and water).
- Interconnected nanoscale inorganic reservoir porosity systems that can result from dissolution and re-precipitation

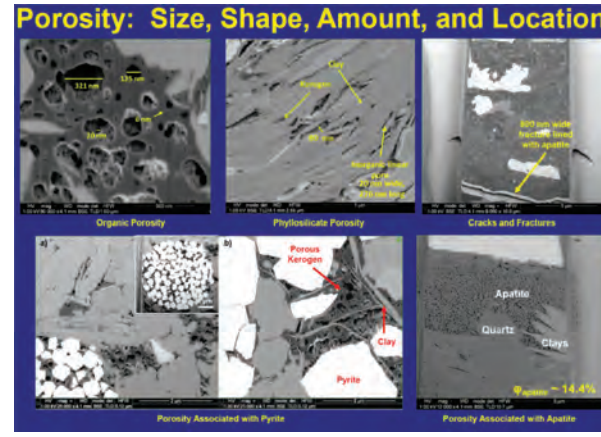

Fig. 8.7—Nanoscale porosity systems. (From Mark Curtis 2011.)

of susceptible mineralogical compositional components through in-situ kerogen generated:

- Weak organic acids including carboxylic and bi-carboxylic acids that have an increased propensity to degrade system plagioclase constituents and clays as well as enhancing hydrocarbon wetness of pore surfaces (kerogen and mineral).
- Weak inorganic acids including carbonic acid, as developed from the interaction of devolved CO_2 gas with pore and clay waters within pore systems. Carbonic acids have a capacity to diagenetically alter carbonate components and redistribute cement fabrics.

Nanoscale interparticle, inter-crystalline, and intraparticle porosity systems can be associated porosity to specific mineralogical components (i.e., mineralogically more stable silica and high magnesium calcite) of adjacent biologic tests/particles/crystalline minerals, that may also be resistant to compaction and burial history alteration processes, as well as with the interaction from these kerogen-derived fluids and gases.

Nanoscale interparticle porosity can also be associated with specific clay mineralogical transformations, such as smectite, and mixed layer (water-layered) clays that develop through clay maturity and compaction induced mineralogical processes (loss of clay-bound and intramolecular water) to illite. These additional nanoscale mudrock porosity systems may develop in parallel corresponding to thermal and compaction processes but separately from nanoscale kerogen-origin processes of kerogen transformation to hydrocarbons (**Fig. 8.7**).

Pore occlusion diagenetic cementation processes related to specific fluid-based basin burial, tectonic and thermal history controlled processes must also be considered within

a formation reservoir characterization program. Differential timing and spatial distribution of these basin pore occlusion process include fluid re-distribution associated rate of burial, compaction, uplift, and tectonic processes (system strain).

These parallel processes should be incorporated with hydrocarbon generation and expulsion efficiency process understanding (related to kerogen transformation and system seal development). Of note, these adjacent HC source rock associated cementation processes may also be critical in developing top, lateral, and basal specific molecular gas level seal systems that control system hydrocarbon and water saturations within an expanded target system that may include hybrid (tight conventional and unconventional) reservoir systems.

An unconventional resource play (URP) layered processes system illustration (**Fig. 8.8**) assists in defining the overlapping petroleum system layered processes that influences unconventional resource play producibility.

The composition of the organic matter influences, identified by the brown radiating arrow lines, is a foundation component of the developed petroleum system. The influences of the organic matter type include the developed gas and fluid types, the influence on the HC source generation type, the HC storage (kerogen based), and the seal type induced based upon the associated developed fluids and gases. The organic matter composition can also influence the in-situ stress and pressures related to compaction and the tectonic natural fracture systems and the specific progression of pore system oil and water wettability and the pore level efficiency expulsion process, which is related to the pore system geopressure distribution.

Therefore, the distribution of an unconventional resource play system total organic carbon (TOC original), which is comprised of original organic facies suites of kerogens, can significantly influence the variability of reservoir properties and producibility of a target mudrock system. An overriding problem and issue in kerogen characterization is that the TOCpd (present day) kerogens have had subsurface transformation processes that have altered its original characteristics.

TOC original type strongly influences the overlapping petroleum system layered processes through the generation of specific fluids and gases and specific potential kerogen porosity systems related to kerogen de-volatilization due to kerogen-specific activation energies. These petroleum system processes include overlapping clay transformation reactions (especially smectite and mixed layer clays) that liberate water and are coincident thermal and compaction related (clay types in Fig. 8.8).

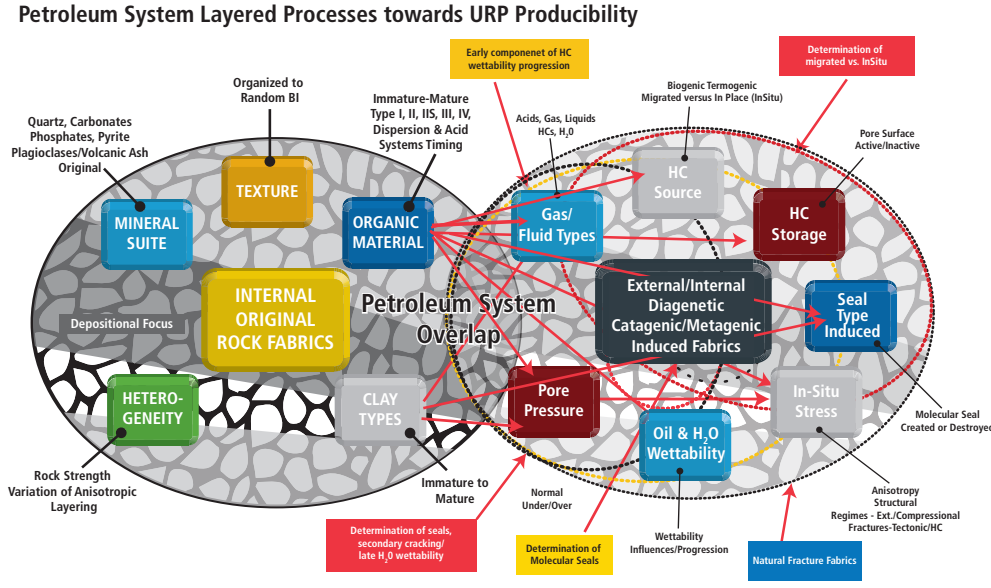

Fig. 8.8—Unconventional resource play process model foundation characterization components.

To better understand what TOCpd signifies, as computed from wellsite wireline and/or LWD logging measurements, we need to integrate the underlying properties of target system kerogens in relationship to their present-day extent of generation (transformation) related to potential nanoscale porosity and permeability networks; their level of generation of appropriate hydrocarbon fluid(s) and gas(s); and their indicated capacity to contribute associated fluids to enhance hydrocarbon saturation and irreducible to sub-irreducible water saturation.

Integration of indicated original kerogen details can significantly influence the determination of the spatial reservoir characterization properties within a target system. An investigative approach that better defines original kerogen suite distribution may assist in the understanding of producibility and or zonation within an unconventional resource play target system.

These investigations may include:

- What is the vertical and areal distribution of TOCo, kerogen suites, or facies across the play? How is it related to TOCpd. How does this influence hydrocarbon and water saturations and storage (nanopores free and adsorbed)?
- What is the maximum generated kerogen porosity related to the kerogen suites with progressive kerogen transformation TOCgen (generated) to hydrocarbon fluids and gases?
- What is the spatial (vertical and horizontal) distribution of thermal maturities affecting the transformation of each kerogen suite (activation energy) type?
- What is the transformation ratio relating to remaining hydrocarbon generation potential by spatial kerogen suite and what is current nanoscale porosity system characterization and wetness?

A series of cores, cuttings, and gas laboratory analyses may be conducted and integrated with derived parameters of wireline and/or LWD logging measurements to help define these investigations. Integrative kerogen transformation techniques can be utilized to determine TOCo. These methods may include measured spatial detailed hydrocarbon composition (including carbon and hydrogen isotopes) and concentrations, specific associated fluids and gases (organic and inorganic acids, gases, and inerts), as well as detailed kerogen or bitumens analyses including kerogen slides, FIB SEM, and other laboratory techniques. Mudrock reservoir characterization protocols for organic kerogen characterization, including that of wellsite and laboratory analyses, should be consulted.

Wellsite surface logging systems (SLS) advanced technology can now be utilized to characterize well cuttings and drilling mud fluids and gases to better define kerogen type systems, kerogen type generation capacity, transformation levels, and specific types of diagenetic alteration fabrics and developed mineralogy. A highly defined characterization level of analysis, near commercial laboratory level standards, can be applied through advanced fluids and gases and cuttings wellsite technologies. These additional reservoir quality and completion quality characterization technologies can supplement or enhance the ability to better design (stage width, cluster spacing, proppant design, fluid volumes, need fluid rates, sequential fluid types) geologically or engineer-driven lateral completions.

Quantitative characterization of fluids and gases can be completed through advanced gas mud trap configurations, as well analytical devices (high speed gas chromatography and or mass spectrometry) for extended range molecular specific HC characterization. Organic kerogens can also be characterized through advanced wellsite pyrolysis (SRA, HAWK™ technologies). Measured impact on inorganic mineralogy and elemental core/cuttings characterization (XRD, XRF, NIR, and LIBS) can also be made available at the wellsite, to equivalent laboratory standards.

8.3.2 Characteristics of Kerogen

8.3.2.1 Kerogen Types

From an unconventional resource play reservoir quality perspective, three first-order petroleum system processes are significantly controlled by the quality and type of the TOCo kerogen maceral suite (**Table 8.6**) and include the following:

- Increased volume and quality of hydrocarbon fluids, associated non-hydrocarbon fluids, and gases correspond to high hydrogen content, amorphous structure, sapropelic, and lipid-rich kerogens. These kerogens exhibit high original hydrogen index (HI) and a low original oxygen index (OI). Kerogens that develop primarily methane gas exhibit a high level of structured land plant kerogens that are defined by low original hydrogen index and high original OI. Extensive ring and aromatic systems incorporating oxygen atoms within structured kerogens result in lower hydrogen content and diminished capacity to produce complex hydrocarbons. This is an important reason why structured kerogens are poorly capable of generating longer chain hydrocarbons, unless the kerogen suite contains the previous amorphous kerogen components.

Table 8.6—Source rock reservoir kerogen characteristics.

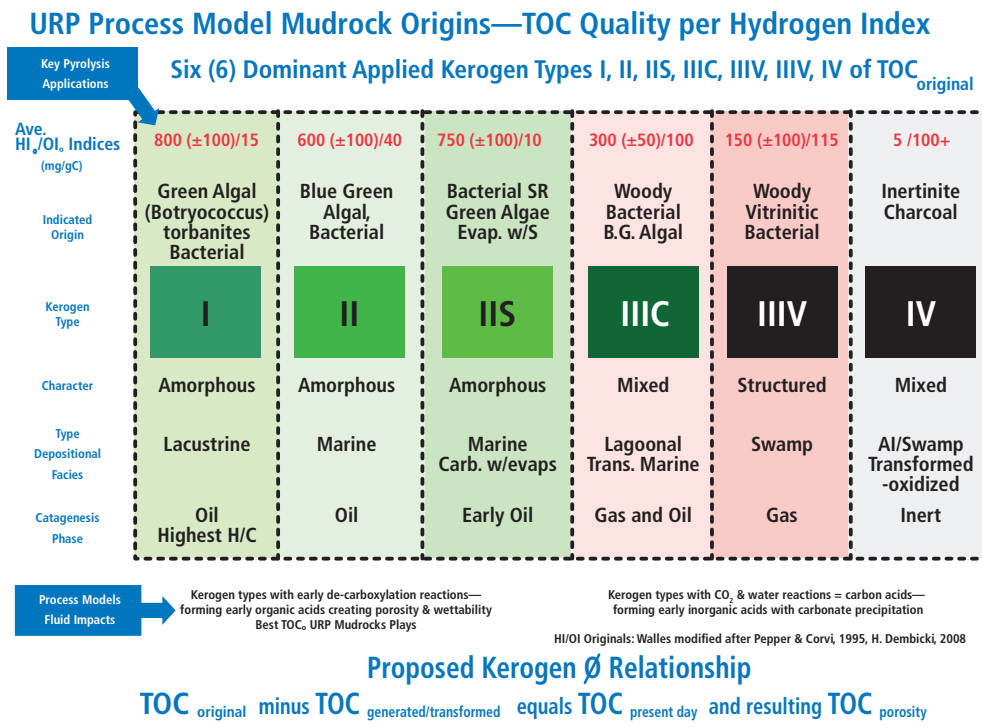

- An interconnected (permeable) kerogen nanoscale porosity system is a function of both kerogen transformation generated transformable kerogen composition and its degree of thermal transformation. Higher hydrogen quality, original amorphous sapropelic, lipid-rich kerogen suites systems are associated with developed nanoscale kerogen porosity (FIB–SEM studies). Increasing nanoscale pore throat size has also been attributed to increased thermal transformation (dry gas level). HC liquids producibility is also related to kerogen quality (hydrogen content) and to the specific kerogen suite activation energy levels and corresponding transformation ratio (thermal maturity).
- Irreducible to sub-irreducible water saturation and high hydrocarbon saturation processes include progressive nanoscale pore wetness changes that modify pore surface energy properties that restructure pore fluid positioning of generated water and hydrocarbons. Early transformation phase kerogen specific pore surficial hydrocarbon wetting agents can include polar hydrocarbons (alcohols) and organic acids that help displace pore waters toward the center of developed pore systems, allowing preferential expulsion. These kerogen developed HC wetting fluids in conjunction with compaction processes can enhance the ability to expel pore and clay derived waters within a developing nanoscale porosity system. In addition, this ability to expel water may be enhanced through later inorganic sulfur oxidation processes within the elevated thermal and pressure dry gas secondary cracking window, where pore system wetness may reach molecular level water wetness.

Within a sixteen component reservoir/completion quality model for unconventional reservoirs, the organic matter component is a high-level characterization component that impacts producibility (**Fig. 8.9**) Critical indices or sidebars include the characterization of the kerogen suite/TOC original, the preservation, environment of deposition, biostratigraphy, the microbial systems, and the original level of preserved hydrogen. Kerogens have genetic origins related to water-based marine/transitional marine to terrestrial life organisms or plants. Within preserved intrabasinal and extrabasinal input geologic depositional systems, including marine and transitional marine systems, the preserved organic kerogens are dominantly microbial in origin. Within preserved depositional environments/sections that can contain extrabasinal-derived organics dependent upon geologic age, the preserved kerogens can often have a dominant component of preserved or recycled land plant derived structured kerogens (coal type maceral suites).

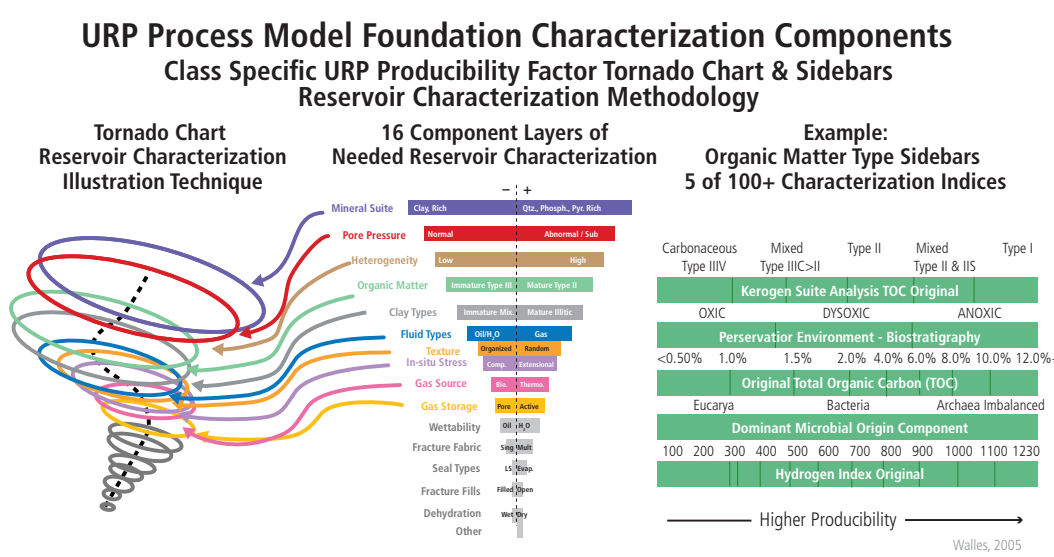

Tornado charts and sidebars are a comprehensive layered reservoir characterization methodology
towards assessing petroleum system processes through a comparisoin of layerd 1st order indices

Fig. 8.9—Unconventional resource play process model foundation characterization components including organic matter sidebars.

Kerogen quality with respect to hydrocarbon fluid and gas generation is a function of the microorganisms and plant materials from which the preserved detritus is derived. Advanced kerogen slide studies of kerogen materials within identified hydrocarbon source rock intervals within laboratory TOC studies help to determine gas-prone versus oil-prone kerogen percentages. This physical appearance approach of separated present-day kerogen (from the host rock) samples is commonly done through the microscopic identification and volume measurement of total structured or gas prone kerogens from amorphous or oil prone kerogens.

Within intrabasinal (Milliken 2010) marine or transitional marine organic materials are most often microbial—bacteria, algal, planktonic, or benthic—microorganisms that are composed of extensive phylum (52) or large numbers of microorganism species (10 million to 1 billion estimated) illustrated in **Fig. 8.10**, of the three dominant trees of life: the Archaea, the Bacterial, and the Eucarya. This recognition of an extraordinary volume and type of microorganisms within the industry definition of TOC makes the typing of the kerogen types much more difficult and challenging. However, from a hydrocarbon generation perspective, these preserved, decomposed, and petroleum system transformed remains of microorganisms can best be defined by a definition of original hydrogen content or original hydrogen index and original oxygen content or oxygen index along with total organic sulfur content.

Fig. 8.10 further illustrates the size range of these microorganisms with respect to the nanoscale size of the pore throat systems of the multiple types (Fig. 8.5) of unconventional resources play targets. An understanding that the target pore systems are submicrobial to subvirus to even subprotein level in diameter allows for a better understanding of the origin and capacity of generation of biogenic and hydrocarbon gases with geologic burial and compaction processes.

Due to these extremely narrow subprotein level, pore-throat size distributions within unconventional resource plays, the ability to generate bacterial methane gases in the subsurface is basically limited by the burial history processes and is most often limited to shallow burial depths. Due to these extremely small pore systems (typically occurring within the kerogens) the hydrocarbons generated within these system targets are directly related to in-situ thermal alteration kerogen transformation processes and not to active biological processes occurring within the deeper subsurface.

To better define kerogen types, it is important to understand the relationships within the original microbial system suites present within the original deposition environmental system. Within the microbial life model (Fig. 8.10 and **Fig. 8.11**) of competing and symbiotic microbial systems present within original water-based environments, most systems should tend to fully recycle or precipitate carbon and silica into stable (non-food) mineral forms. Carbon enters the system

Improved measurement/characterization of controls of microbial component w/prediction of Kerogen HI, OI variance

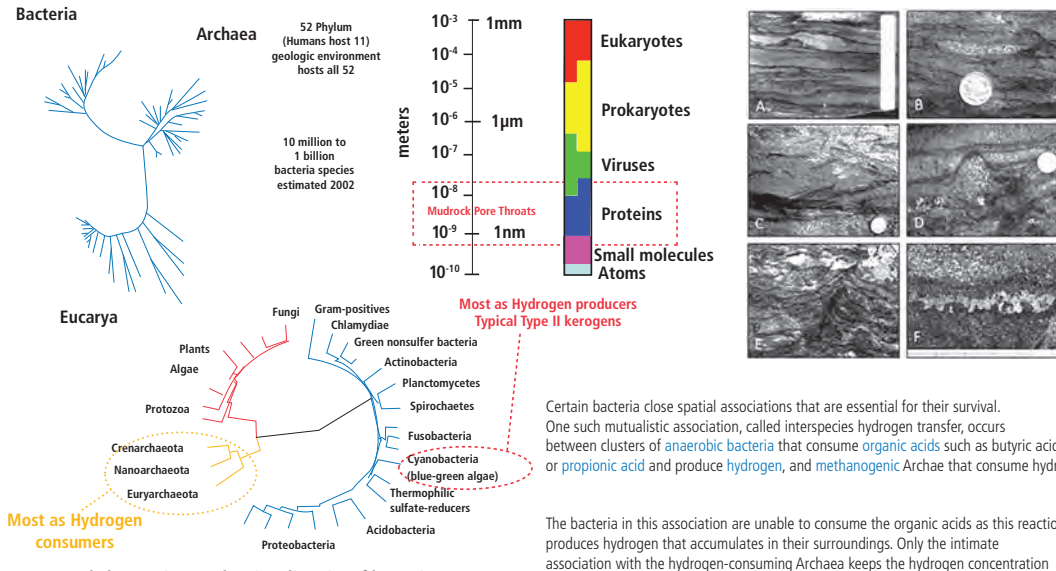

Phylogenetic Tree showing diversity of bacteria. Eukaryotes are colored red, archea green, and bacteria blue. The archaea and eukaryotes are more closely related to each other than either is to the bacteria.

Certain bacteria close spatial associations that are essential for their survival. One such mutualistic association, called interspecies hydrogen transfer, occurs between clusters of anaerobic bacteria that consume organic acids such as butyric acid or propionic acid and produce hydrogen, and methanogenic Archae that consume hydrogen.

The bacteria in this association are unable to consume the organic acids as this reaction produces hydrogen that accumulates in their surroundings. Only the intimate association with the hydrogen-consuming Archaea keeps the hydrogen concentration low enough to allow the bacteria to grow.

Disruptions of these microbial populations/relationships can occur with introduction/existence of specific metals into the depositional system. Dissolved, diagenetically altered, volcanic ashes can provide both system level nutrients and "disrupters."

Fig. 8.10—Unconventional resource play process model mudrock origins—families of life hydrogen enrichment of TOCo. (From Walles 2012.)

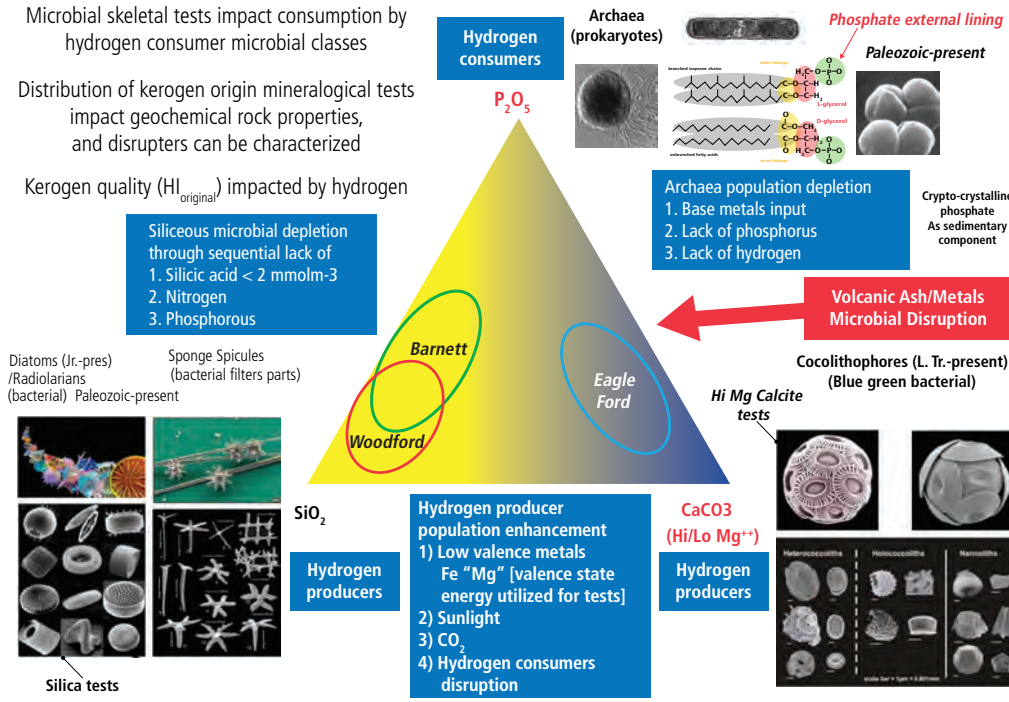

Fig. 8.11—Unconventional resource play process model mudrock origins—hydrogen enrichment of TOCo. (From Walles 2011.)

most often in the original form of CO_2, or weak inorganic acids such as HCO_3-. Many microorganisms can utilize this carbon input for their molecular organic components and ultimately where this carbon is preserved into the subsurface as a sink of more stable mineral carbonates.

Hydrogen is concentrated and developed within these systems through specific microorganisms that can be broadly termed hydrogen producers. They can utilize as an energy source, either or both sunlight and low valence metals (i.e., Fe++) inputs, to concentrate hydrogen and carbon in the form of lipids and other hydrogen-rich compounds. Fig. 8.11 illustrates how these microbial population systems may utilize system energy and system elemental components to develop calcium carbonate, silica, and even phosphate in the form of microorganism tests.

Hydrogen is also consumed within the system through hydrogen consumers, most often of the Archaea-type microorganisms. Of significance of the Archaea-type microorganisms are their phosphate external linings, where with significant blooms may often be preserved in the target system as cryptocrystalline apatite. These microbial symbiotic hydrogen systems allow for the continuous recycling and/or consumption of hydrogen within preserved depositional systems (Fig. 8.10 and Fig. 8.11).

Kerogen type within the hydrocarbon industry is currently classified into at least six primary types as illustrated in Table 8.6 (seven if Type IS is included). These broad types are based upon the dominant kerogen character (structured, mixed, amorphous), indicated origin (general framework depositional environment), and organic sulfur content (kerogen organic molecular S integration). These broad kerogen types have been the result of efforts to tie kerogen quality to broad depositional environments. However much of this typing did not take into account the full knowledge of the degree of microbial input, controls to these microbial organisms productivity (nutrient systems), disruption to microorganism populations and the actual preservation processes of these organic components.

Each industry type or subtype has layered defining characteristics. Table 8.6 defines the current industry-recognized characteristics of these primary industry types of kerogens. The table is organized to include average representative HI original and OI original (mg/g C) indices, indicated organic type origin (microorganism dominant type or plant materials), the assigned industry kerogen type, the prepared kerogen slide (kerogen separation slide) organic matter character, a designated type depositional system, and the catagenesis stage maturity HC product type.

Type I kerogens are defined as having the highest hydrogen and lowest oxygen original content from an original microorganism source of blue green/green algal microorganisms. The Type I kerogen depositional environment model has been generally assigned to lacustrine. Industry Type II and IIS (sulfur rich) kerogens are also characterized as being hydrogen rich and oxygen poor, with an assigned deposition environment of anoxic marine. Type II/IIS kerogens are defined as including mixtures of blue and green algal material along with structured kerogen plant materials. Generally an assigned marine/transitional marine depositional environment is associated with this kerogen suite . Both Type I and Type II (as well as Type IS and Type IIS) kerogens are recognized as very prone to generate liquid hydrocarbons and are associated with liquid-rich unconventional resource plays and oil source rock systems. The integration of sulfur into the kerogens (Types IS, IIS) requires either a lack of available iron within the depositional and preservation system, and/or an overload of sulfur within the system. Sulfur reduction bacteria are an important system mechanism related to this sulfur capture.

Type III (IIIC, IIIV) and Type IV kerogens are defined as having structured woody plant origin debris materials that were originally deposited within terrestrial-to-transitional marine environments such as swamps, delta complexes, or shallow lagoons. These kerogen types exhibit much lower original hydrogen content and higher oxygen content. Type IIIC kerogens are most often assigned to a transitional marine depositional system where lipid-rich (hydrogen-rich) algal microorganisms have been preserved. Type IIIV is defined as dominantly structured plant vitrain macerals that are most often gas (methane) prone. Type IV kerogens, are incapable of generating hydrocarbons. These kerogens are either fully transformed kerogens (reworked and/or oxidized) or are charcoal materials that are often assigned as burnt plant materials.

These assigned kerogen types are illustrated within the modified Van Krevelen plot (**Fig. 8.12**). This plot includes the defined relationship of rock pyrolysis originated hydrogen index (HI) versus oxygen index (OI) to original TOCo (TOCoriginal). This plot is also useful in defining the transformation of specific kerogen types with greater maturity. The maturity arrow illustrates how these kerogens change types (as defined by hydrogen and oxygen content). This helps explain how present day TOC (TOCpd) may be very different than original TOC. Four of the six primary kerogen types are quickly assessed in this plot of HI versus OI. This is due to the ease of utilizing HI and OI values derived from Rock-Eval pyrolysis analyses, which are less expensive and quicker to obtain than the atomic H/C versus O/C analysis (Tissot and Welte 1978; Peters and Casaa 1994).

Original kerogen suite composition determinations require an integrated characterization of the composition and structure of the observed kerogens along with the observed and defined relationships of generated hydrocarbons, fluids, and gases. To more fully predict and correlate kerogen system porosity, permeability, pore surficial characteristics, and expected developed hydrocarbons, comprehensive laboratory analyses are often required (i.e., FIB SEM nanoscale level). To fully interpret these laboratory analyses requires a thorough understanding of the specific molecular level compositional components of kerogen suites and their inferred relationships to expected potential depositional environments. This is an ongoing developing field of study with the integration of recognition of extensive microorganism suites that are responsible for the characteristics of the industry kerogen types (Type I, Type II, Type IS, Type IIS, and Type IIIC).

Fig 8.12 and **Fig. 8.13** illustrate the kerogen typing issue related to maturity transformation reactions of kerogens. Fig 8.12 illustrates a cross plot of hydrogen index versus oxygen index as defined by pyrolysis data of rock samples. Fig. 8.13 illustrates a cross plot of remaining hydrocarbon potential (mg HC/g Rock) versus total organic carbon (TOC, weight percentage).

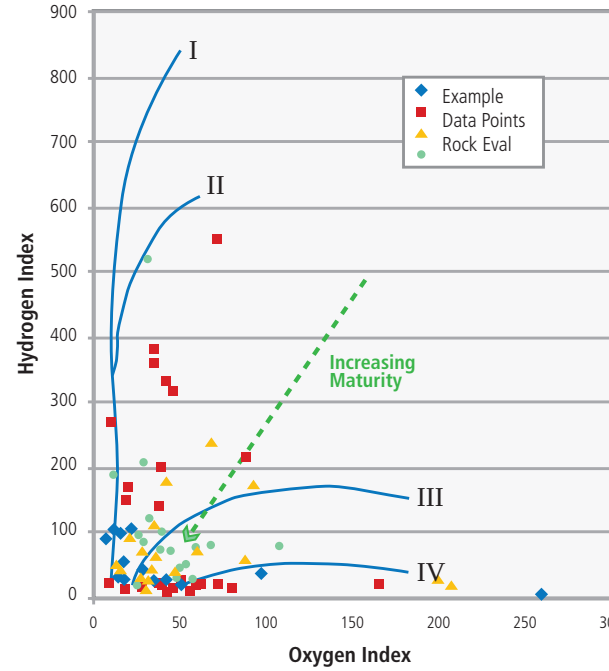

Fig. 8.12—Modified Van Krevelen plot identification of kerogen type.

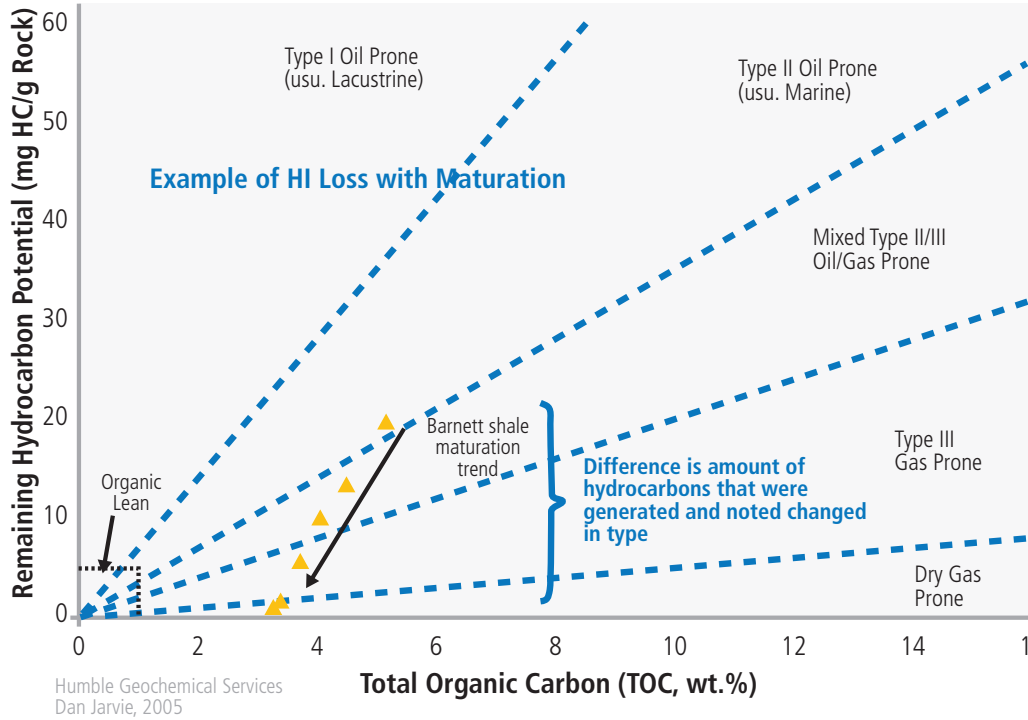

Fig. 8.13—Remaining hydrocarbon potential (mg HC/g rock) versus TOC, weight percentage. (Modified over Jarvie 2005.)

These time-, temperature-, and pressure-related maturity transformation reactions result in a reduction of hydrogen indexes, alteration, and/or reduction of oxygen indexes and changes in sulfur content. The combined effect changes the HI and OI, so that with increasing maturity, the HI and OI descend approximately in parallel, depending upon the original kerogen present. Determination of original kerogen type of present-day TOC, therefore, requires additional investigational processes that go beyond present-day hydrogen index, oxygen index, and organic sulfur content.

High hydrogen content, amorphous structure, sapropelic, and lipid-rich kerogens have a high propensity to develop liquid hydrocarbons' and non-hydrocarbons' organic components. A high hydrogen level kerogen capacity supports nanoscale porosity development through the full transformation process which includes thermal catagenesis transformation reactions of volatization or decarboxylation of kerogen components into bitumens, bitumens into hydrocarbon liquids and gases. This is subsequently followed by thermal alteration (metagenesis) of these HC liquids into thermally stable HC gases (propane, ethane, and methane). These thermally stable HC gases, created through higher temperature or pressure processes, is termed secondary cracking. This process may further alter these thermally stable gases into pure methane gas.

Kerogens, either structured or original kerogens with associated reduced hydrogen content and higher oxygen content, exhibit only poorly developed and poorly interconnected intra-kerogen porosities. This porosity character can be attributed to a lack of liquid hydrocarbon generation capacity. The lower original hydrogen levels and higher oxygen levels in the kerogen define a lack of capacity for bitumen and resulting hydrocarbon liquid generation.

TOC original values that can be determined from an integrated organic carbon investigation perspective that can include:

- TOCpd (TOC present day): HIpd–hydrogen index present day (a Rock-Eval measurement of source potential) measured at present-day thermal maturity.
- TOCo (TOC original): HIo–total organic carbon; hydrogen index at original conditions as measured from immature sediments or in the case of TOC_0, which can be back-calculated using Rock-Eval data after Claypool (Peters et al. 2006). The TOC_0 calculation requires a HIo value, but that may not be straightforward enough for selection, in that it requires correlation to a prediction of the original value through inferences from the original depositional environment, which is often inaccurate.
- TOCgen (TOC generated) equals TOC_0-TOCpd: a measure of the amount of carbon taken up in hydrocarbon generation of both oil and gas that is expelled and retained.
- TOCgen can be related to maximum generated kerogen porosity, depending upon the kerogen suite.

Specific kerogen components may contribute specific surface hydrocarbon wetting polar hydrocarbons and non-hydrocarbons (such as alcohols, phenols, and sterols) and organic acids (such as carboxylic and bi-carboxylic). Decarboxylation of kerogen components may often develop high acid oils with increased organic acid components. Specific kerogen high organic acid transformation sources may include algal, cyst-rich kerogen materials (usually assigned as Type II). Increased capacities for polar hydrocarbons and non-hydrocarbons (including NSOs, alcohols) are often associated with sulfur rich kerogens (Type IS, Type IIS).

Maturation processes for kerogens occur through a time and thermal maturity process that can include system-limited hydrocarbon expulsion processes related to system diagenesis that develop pore plugging authigenic cement fabrics. This is often a critical system process that can define the spatial distribution of mudrock reservoir quality and hydrocarbon producibility. This is reviewed within the next section.

In summary, the specific type of organic carbon (TOC) within unconventional resource plays does impact the reservoir quality and its producibility through multiple overlapping petroleum system process pathways (associated with its kerogen compositional suite components). It is important to understand how the integration of kerogen transformation determines the TOC original and its comparison to the TOC present-day kerogen typing.

Kerogen-related reservoir quality components of unconventional resource play targets can include:

- The interconnected nanoscale intra-kerogen reservoir porosity system resulting from the thermal and pressure maturity volatization and decarboxylation processes occurring within the specific kerogens, as well as within the resulting nanoscale porosity system at higher thermal maturity levels within resulting bitumens and pyrobitumens.
- The volume of hydrocarbons present within a free phase and an adsorbed phase (adsorption is defined as the accumulation of the hydrocarbon molecular species on kerogen surfaces rather than within the bulk of the solid kerogen).

- The development of hydrocarbon composition fractions of hydrocarbon solids, liquids, and gases. These can include early maturity phase fractions of bitumens, and intermediate maturity phase fractions of asphaltenes and resins, as well as hydrocarbon liquids, including pore system wetting organic acids, polar hydrocarbons, and hydrocarbon gases (carbon dioxide, hydrogen sulfide (H_2S), and NO_2). These products of sequential and GRathermal maturity petroleum system generation and expulsion inefficiency processes (including elevated hydrocarbon generated geopressures) directly affect the extent of reservoir pore HC phase and saturations (HC and water).
- The interconnected nanoscale inorganic reservoir porosity system results from the dissolution and re-precipitation of susceptible mineralogical compositional components through generated in-situ system acids, which are kerogen-specific inorganic (carbonic) and organic acids (especially carboxylic and bi-carboxylic).

To better understand how kerogen suites affect producibility (TOC present day versus TOC original) through the maturity or transformation level related to the specific kerogen suite. This development will be defined within the next section.

8.3.2.2 Maturation Process and Thermal Maturity

Thermal maturity indices help to measure and define the degree to which a formation or a specific kerogen suite has been exposed to a specific level of subsurface thermal heat flow, pressure and time. A combined rate (time) dependent thermal heat flow with generated and retained geopressure will affect the petroleum system expulsion process within the transformation of specific spatial kerogen suites. Industry Type I, Type IS, Type II, and Type IIS dominant kerogen suites transform into liquid hydrocarbons within a phase that is termed catagenesis. Through attaining the required activation energy levels, these kerogen types develop gases and an intermediate liquid hydrocarbon phase that is termed bitumen. Bitumen then transforms (also within catagenesis) into liquid petroleum hydrocarbons (fluids and gases). With higher levels of time, pressure, and temperature, the metagenesis phase involves cracking these generated liquid hydrocarbons and gases into thermally stable hydrocarbon gases of propane, ethane, and methane. With even higher levels of time, temperature, and pressure, the secondary cracking phase will even transform these thermally stable gas types into methane gas.

However, not all kerogen suite types (industry Type IIIC, Type IIIV) will transform from kerogen to bitumen, to liquid hydrocarbons, and finally into gaseous hydrocarbons within the catagenesis to metagenesis phases. Early methane gas and minor amounts of hydrocarbon fluids and gases (if lipid materials are present) and then finally to pure methane gas is the primary hydrocarbon generation sequence.

Within most hydrocarbon source rock formations, their kerogen suite facies will vary spatially within a basin. When this spatial distribution is integrated with the specific basin position burial history (burial, uplift, reburial, and resulting thermal and pressure tectonic overprint processes) the resulting kerogen transformation levels may be spatially highly variable. Multiple tectonic and process-related thermal events within a basin, through time, may also result in overprinted thermal indices from differential stress and resulting strain-related fluid and pressure conditions. To reduce the geologic risk associated with thermal maturity assessment, layered independent method thermal maturity indices are utilized, including that of the inorganic mineral suites, the organic materials, and an integrated assessment of the observed quantitative (composition and concentration) hydrocarbon fluids and gases.

Kerogen to hydrocarbon transformation and petroleum system overlap processes contribute to the development of the critical unconventional resource play reservoir quality properties. An unconventional resource play petroleum-system-overlap process model (**Fig. 8.14**) stipulates that specific chemical processes coupled with expulsion inefficiency mechanisms during catagenesis and metagenesis, within specific source rock systems, can develop high hydrocarbon saturations (SHC) and very low water saturations (SW) at or below irreducible levels (Walles 2007).

Within a general basement origin thermal heat flow model, where temperatures gradually increase (Fig. 8.14) with increasing depth of burial, the early kerogen and source rock transformative processes (diagenesis) initially involves a subsurface fluid expulsion system dominantly related to compaction and sediment lithification and can include clay maturity transformations and the flow of early diagenetic fluids and biogenic gases resulting in the generation of early authigenic cement fabrics. This early diagenesis phase is followed by catagenesis (time and temperature levels appropriate to the generation of hydrocarbons from kerogens) and then metagenesis (levels transforming liquid hydrocarbons to condensate and gas (propane, ethane, and methane). Within higher geopressure and temperature conditions, a secondary cracking phase can occur toward pure methane gas as derived from thermally stable C3 (propane) and C2 (ethane) hydrocarbon gases. At even higher levels of thermal maturity, such as from low-grade to high-grade

URP Process Model

An unconventional resource play (URP) requires specific progressive petroleum system inorganic and organic geochemical processes that develop appropriate reservoir and seal fabrics

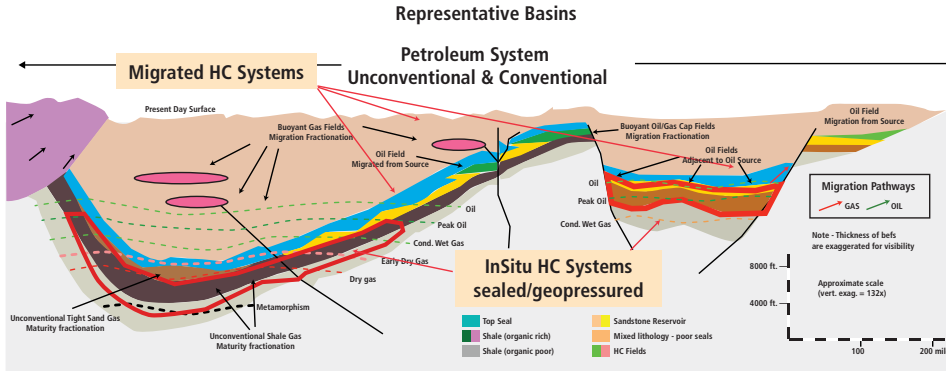

Critical URP observation:

Specific chemical processes coupled with expulsion inefficiency mechanisms for catagenic and metagenic HCs, within specific source rock systems, can develop high HC saturations and low water saturations (S_w) at or below irreducible levels.

Layered process models allow teams to spatially predict HC producibility drivers of these critical reservoir properties through integrative reservoir characterization indices.

Fig. 8.14—Unconventional resource play layered process models that include thermal alteration processes within a basin.

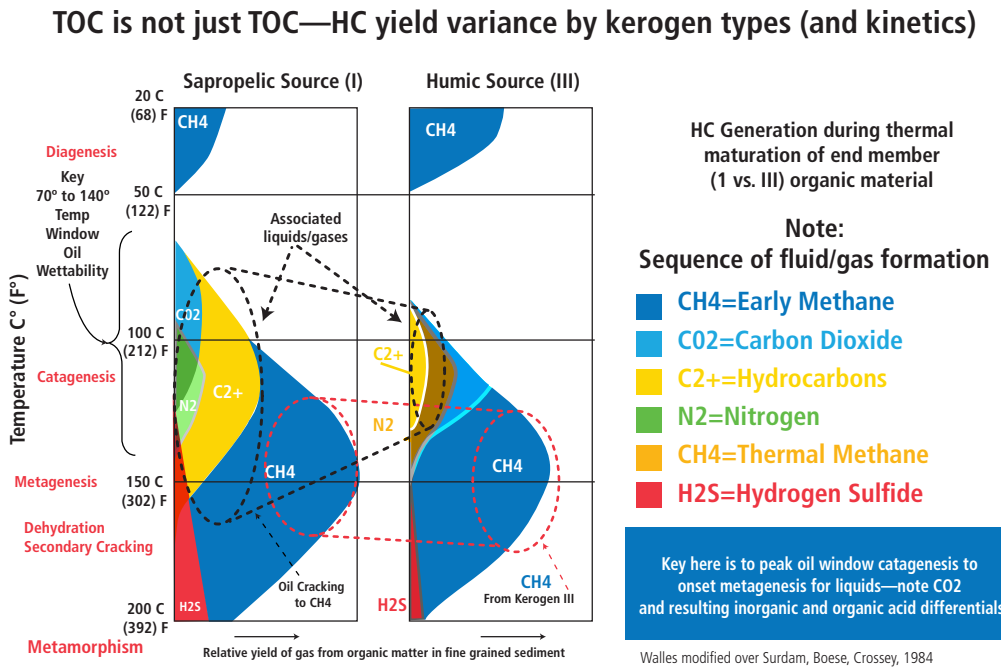

Differential Fluids and Gases by stage: 1. Diagenisis, 2. Catagenisus, 3. Metagenesis, 4. Secondary Cracking

Fig. 8.15—Diagenesis, catagenesis, metagenesis, dehydration secondary cracking and metamorphism fluids and gases of sapropelic (Type I) versus humic (Type IIIV). (Modified over Surdam et al. 1984.)

The utility of layered rock maturity data—Multiple indice integration to layered process models defining hydrocarbon prducibility within mudrocks

Industry Correlation Chart of HC events to Coal Rank $\%R_{O(mean)}$ CAI, TAI, Litinite fluorescence

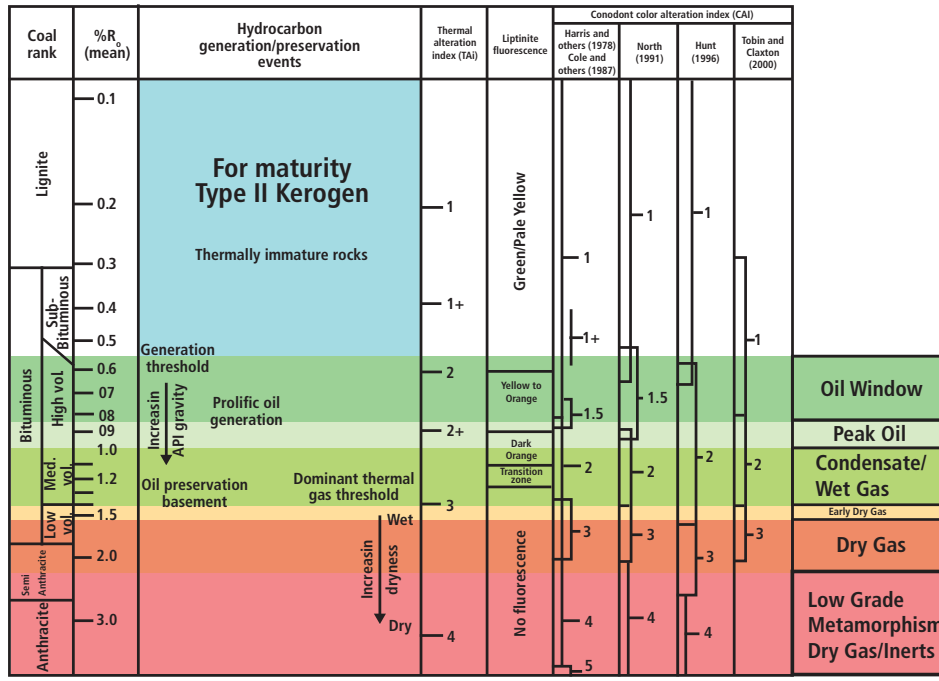

Fig. 8.16—Utility of layered rock maturity data relation among various thermal maturity indicators (including CAI and %Ro) and associated zones of HC generation. (Modified after Stach et al. 1975; Dow 1977; Harris et al. 1978; Cole et al. 1987; Noth 1991; Hunt 1996; Tobin and Claxton 2000). The CAI 1+ was introduced by Repetski (Repetski et al. 2008; overlay of Jarvie 2008 by Walles 2010.)

metamorphism, additional diagenetic changes of the host rock inorganic mineralogy can coincide with additional destruction of the developed nanoscale level kerogen and matrix porosity and permeability systems as well as the thermally stable methane (**Fig. 8.15**).

Defined temperature ranges at which oil and gas are generated are illustrated within Fig. 8.15. Depending on the activation energies and kinetics of the specific kerogen suite, the liquid HC window can be within the range of 60° to 175°C (140° to 302°F) and the gas window can be 100° to 300°C (212° to 570°F). The spatial position of oil and gas windows within a basin is very dependent on the time temperature heating rate and the type of organic matter with their associated kerogen suite activation energies. Thermal maturity is a function of both time and temperature (Holditch 2011, Lopatin, 1971). Advanced methodologies that incorporate a quantitative time component into kerogen transformation algorithms were developed by Lopatin (1971). His work along with that of Waples (1980) and Wood (1988) better defines the influence of time into the kerogen maturity transformation basis for determining net transformation ratios that also incorporate reaction kinetics of specific kerogen suites. These algorithm-defined approaches are the foundation for many petroleum system basin modeling software programs.

Characterizing and measuring thermal maturity processes within subsurface formations is a high-interest scientific field that is extensively written about. Many scientific investigations have generated independent maturity measurement techniques that have resulted in the availability of multilayered approaches to evaluating thermal maturity. These include measurements related to the current kerogen state (maceral degradation such as vitrinite reflectance R0%, Rock-Eval pyrolysis datasets, TAI, CAI, coal rank), hydrocarbon fluids and gases (SARA full range concentrations, compositions, GOR, CGR, isomers, isotopes, diamondoids) as well as inorganic matrix mineralogical changes (due to clay type transformations), and diagenesis origin authigenic cement fabrics. These maturity index approaches can include fission track annealing of radioactive trace components within cements and/or apatite grains. A summary of the most prevalent industry maturity index is included in **Fig. 8.16**. Those indices most often utilized within unconventional targets are defined in **Fig. 8.17**.

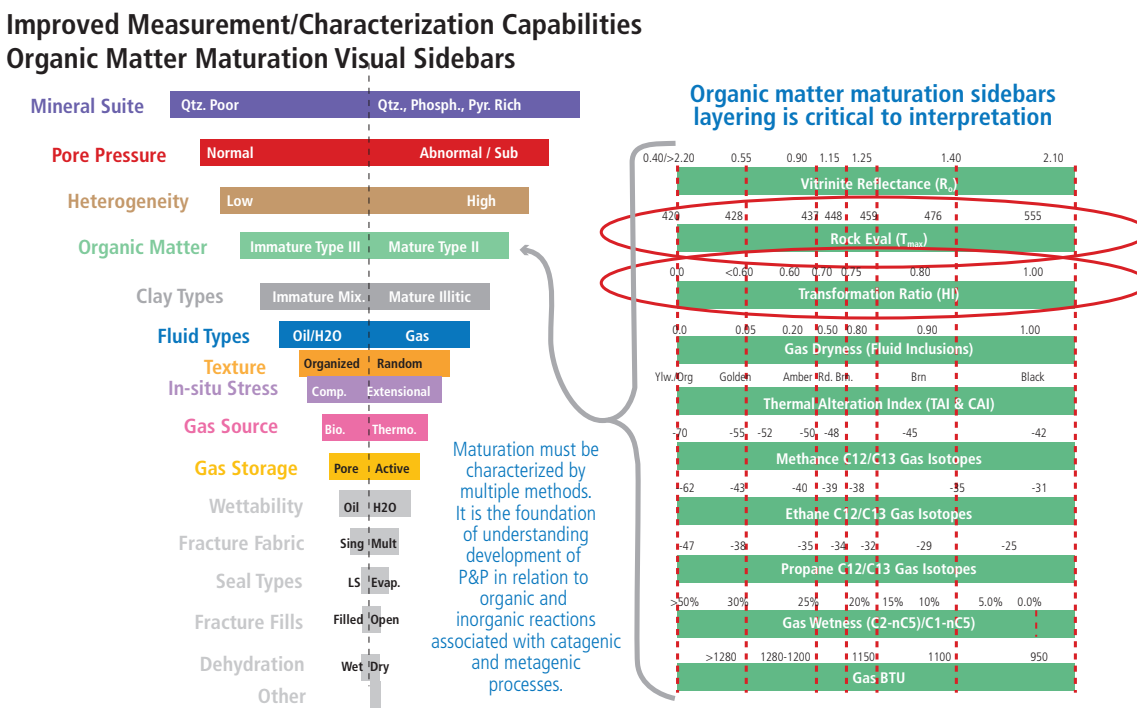

Fig. 8.17—Sidebars illustration of Type II kerogen organic matter maturation indices often utilized within unconventional resource plays. (From Walles and Cameron 2005.)

The specific level of thermal maturity is critical to unconventional mudrock resource potential with respect to hydrocarbon content (oil, condensates, gas types) (PESGB 2008) and to the degree of developed nanoscale kerogen porosity into an interlinked permeability system. Elevated thermal maturity can also be associated with pore destruction as to diagenetic (authigenic cement filling) degradation and compaction related processes of accompanying nanoscale interparticle, intercrystalline, and intraparticle porosity. Specific levels of thermal maturity can lead to the presence of specific degrees of nanopores within specific kerogen suites, which then contribute to the critical producible (interlinked) porosity in the shale matrix rock (Kuuskraa et al. 2011). The reservoir quality characterization of unconventional resource plays is the subject of much ongoing industry work within the field of nanoscale characterization using FIB SEM and other advanced equipment techniques of kerogen suites and associated thermal maturity levels.

Early within the industry evaluation of unconventional resource plays, the application of the maturity index of vitrinite reflectance. R0 percent was utilized as the most common technique for source rock thermal maturity determination. However, this application proved problematic in its application because it measured a kerogen (structural Type IIIV) component that often did not exist within the original depositional environment of most intrabasinal unconventional resource plays (which are identified as many of the current most economic producible plays). In addition, these measurements were often made on the wrong particles (especially bitumens or pyrobitumens) within the rock samples resulting in erroneous maturity conclusions. With these limitations, the industry has still found the vitrinite reflectance scale a useful reference point for maturity level. This scale is for a Type II kerogen suite and not for any of the other kerogen suite types.

The vitrinite reflectance technique measures the intensity of the reflected light from polished vitrinite particles (a maceral group formed by lignified, higher-land plant tissues such as leaves, stems, and roots) of mudrocks under a reflecting microscope. Increased reflectance is caused by aromatization of kerogen and loss of hydrogen (Jarvie et al. 2007). Fig. 8.16 includes the type II kerogen vitrinite reflectance thermal maturation scale. Dry gas occurs when R_0 ranges from 1.0 to 3.0%; wet gas when R_0 ranges between 1.0 and 3.0%; and oil when R_0 is between 0.6 and 1.0% (Kuuskraa et al. 2011). An R_0 of less than 0.6% is considered immature and will not produce any hydrocarbon. An R_0 greater than 3.0% is over-cooked, and results in pure carbon.

Multiple issues with interpretation have been attributed to vitrinite reflectance datasets, such as incorrect particle measurement, filtering, and non-statistically valid measurement techniques, including selection of preferred representative particles by specific operators, resulting in non-repeatability by different laboratories. Geologic condition processes include vitrinite suppression by geopressure processes, as well as fluid, origin, and oxidation issues. To reduce the risk associated with maturity assessment, the industry has chosen to utilize multiple layered indices within unconventional targets (Fig. 8.17).

These methods listed in Fig. 8.17 include data derived from core and/or cuttings samples providing indices such as HI and T_{max} data as derived from Rock-Eval pyrolysis laboratory methods or well site application methods. These advanced well site technology solutions, such as Rock-Eval equipment, include the Hawk and Source Rock Analyzer (SRA).

Thermal alteration index (TAI) of plant spores and conodont alteration index (CAI) of Paleozoic-dominant, aged conodonts are especially useful within the appropriate geologic age formations. Advanced fluid inclusion analyses of hydrocarbon phase and composition within fluid inclusions inside fracture or pore filling cements can also be very useful in reconstructing the petroleum system. Analyses of Carbon δ C13 isotopes of hydrocarbon gases C1, C2, C3, C4+ (methane, ethane, propane, butane +) are especially appropriate for measurement of maturities of free gas and adsorbed gas systems and can be calibrated to specific kerogen suites through gold tube pyrolysis maturation analyses. Produced gas wetness, produced gas BTU values, as well as produced gas Carbon δ C13 isotopes of hydrocarbon gases, are also appropriate maturity indices that may lower the geologic risk associated with inferred kerogen transformation and the resulting prediction of reservoir hydrocarbon yield and phase.

Each of these methods has important quality and interpretation limitation components that may require consultation with respective industry specialists and interpreters. The scope of this section is not designed to develop and document these issues.

From a rock sample (the first-order dataset) based approach, repeatable high-quality analyses can best be developed by the industry from applying commercial laboratory level approaches to the circled indices in Fig. 8.17. Wellsite and/or fast track laboratory Rock-Eval approaches for developing HI,OI, and T_{max} data are especially applicable for rapid kerogen characterization.

For maturity confirmation, gas carbon and hydrogen isotope methodologies can also provide high-quality (repeatable) high-value data. With respect to transformation yields for hydrocarbon liquids (volatile oils and condensates), the concentration and compositional characteristics of saturates, aromatics, resins, and asphaltenes (SARA) fractions are useful. Applying diamondoid concentration and compositional analyses that include methyl adamantine (MAI) and methyl diamantine ratios (MDI) can also be useful maturity indices, especially for determining extent of metagenic alteration.

Integrating the composition of produced hydrocarbons may be problematic for inferred kerogen transformation and maturity determination due to the specific producibility limits associated with specific hydrocarbon molecular nanopore throat size limits, including their associated surficial charge level and resulting wetness to specific fluids (including water) and gases. However, applying layered characterization approaches may help to decrease the geologic risk associated with the inferred kerogen suite and its associated spatial transformation level. An applied layered index approach can be very useful in identifying data quality and or petroleum system issue identification and characterization issues related to unconventional reservoir producibility. These issues may include bitumen plugging of nanopore throat systems, inappropriate wettability progression related to incomplete water expulsion, pyrobitumens and hydrocarbon charge types, including that of H_2S and other specific detrimental gaseous compositional components such as CO_2 and/or mercury components.

Because maturity indices are applicable to specific kerogen suites, an applied industry methodology was developed to integrate specific kerogen suite transformation relationships into their expected hydrocarbon yields. Nanoscale intra-kerogen porosity expectation by kerogen volatization and decarboxylation processes is defined through the expected and/or determined transformation ratio. One such method is defined in **Fig. 8.18** (Walles et al. 2008; Walles 2006, 2008, 2009, 2010, 2013, 2014) of the transformation ratios of kerogens to HC phases. The transformation gates are used to define specific hydrocarbon phases with a specific layered series of thermal indices that define those gates within that specific kerogen suite activation energy profile.

These components can be defined by additional hydrocarbon characterization methodologies as defined within the gas and fluid thermal indices (Fig. 8.17) such as vitrinite suppression, and gas carbon isotopes.

Included within the summary example in (Fig. 8.18) are secondary cracking components that can be associated to

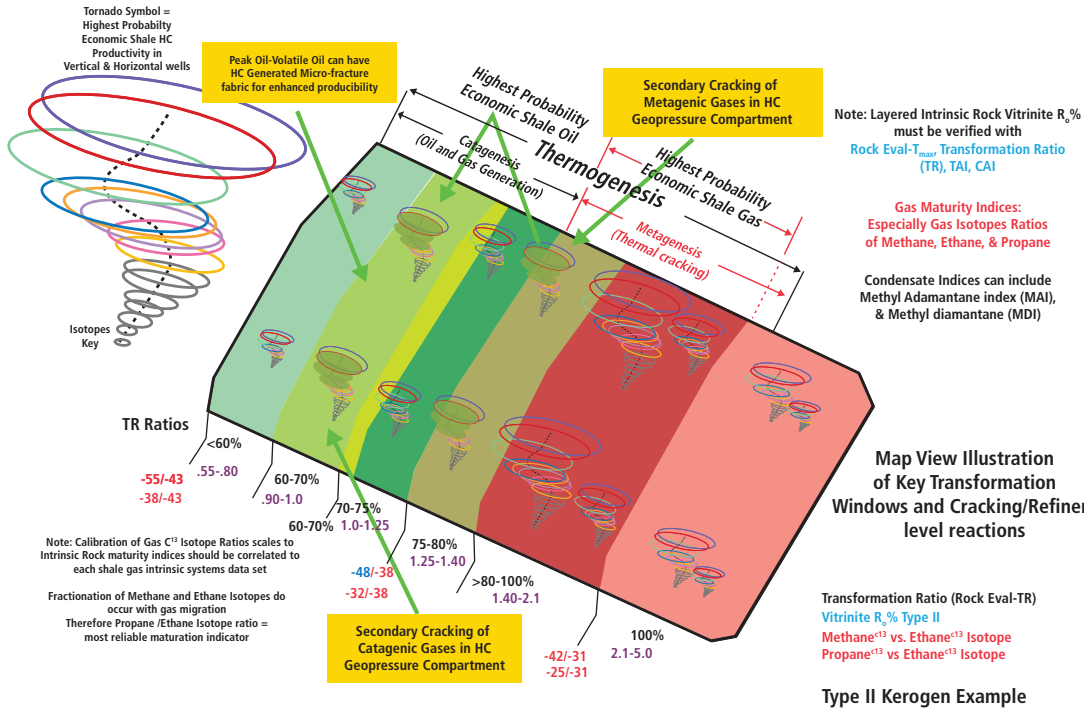

Layered Integrative Gateway Methodology of Transformation Rations to HC Phases

Fig. 8.18—Gateway transformation ratio integration to HC phases of specific kerogen suites. (Walles 2014.)

higher geopressure compartments that improve hydrocarbon producibility within an unconventional resource play. Expulsion inefficiency is often related to reservoir properties and resource play system seals.

To better illustrate how thermal maturation levels or indices compare to kerogen transformation level (0 to 100%) and as directly related to the specific kerogen suite, **Fig. 8.19** better defines these specific relationships. This cross plot of transformation ratio versus the index of vitrinite reflectance (%R_0) defines the hydrocarbon compositional gates or windows of activation energies of kerogen suites as related to the inferred standard vitrinite reflectance value. Each of the colored curves represents an activation energy profile related to that industry defined kerogen type (specific HI, OI, kerogen-sulfur relationships).

As example, the blue line on Fig. 8.19 illustrates a vitrinite reflectance value of 0.97% R_0. Following this value vertically on the cross plot illustrates the full range of dry gas generation to onset oil generation to peak oil generation to oil stability to condensate/wet gas generation dependent upon the specific kerogen suite.

Fig. 8.19 also illustrates that an industry rule of thumb value of pursuing a typical liquids window inferred onset oil generation value to a 0.75% R_0 vitrinite reflectance value could result in gas to bitumens to onset oil to peak oil and to increasing gas-to-oil ratio (GOR) oil. These relationships help illustrate that hydrocarbon phase can easily change along horizontal wells simply because of changes in kerogen suite dominance and or types.

Realizing these relationships provides an industry need to carefully characterize system hydrocarbons along lateral wells. Issues of liquid loading, need of artificial lift in portions of laterals may often be related to changes within kerogen suites within unconventional resource play wells.

Integration of analyses of kerogen components and specific kerogen transformation relationships related to kerogen suite activation energies allows a geochemical specialist to better predict maximum expected nanoscale kerogen porosity systems and infer changes in reservoir quality as well as expected producible hydrocarbon types within an unconventional resource play.

Ongoing investigations into specific kerogen types and specific pore throat sizes and geometries of kerogen

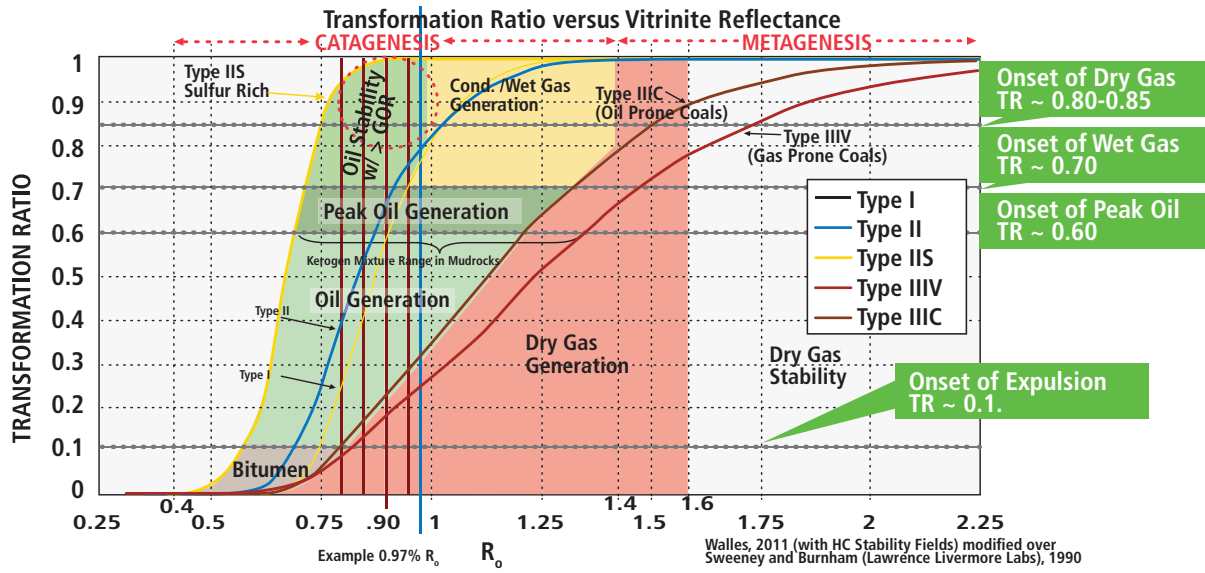

Layered indices critical (a single R_o% data point can have different kerogen porosity and HC phase)

Fig. 8.19—Transformation of kerogen types: Thermal maturity process integration (TR versus R_o% and HC stability fields. (Walles 2011 modified over Sweeny and Burnham 1990.)

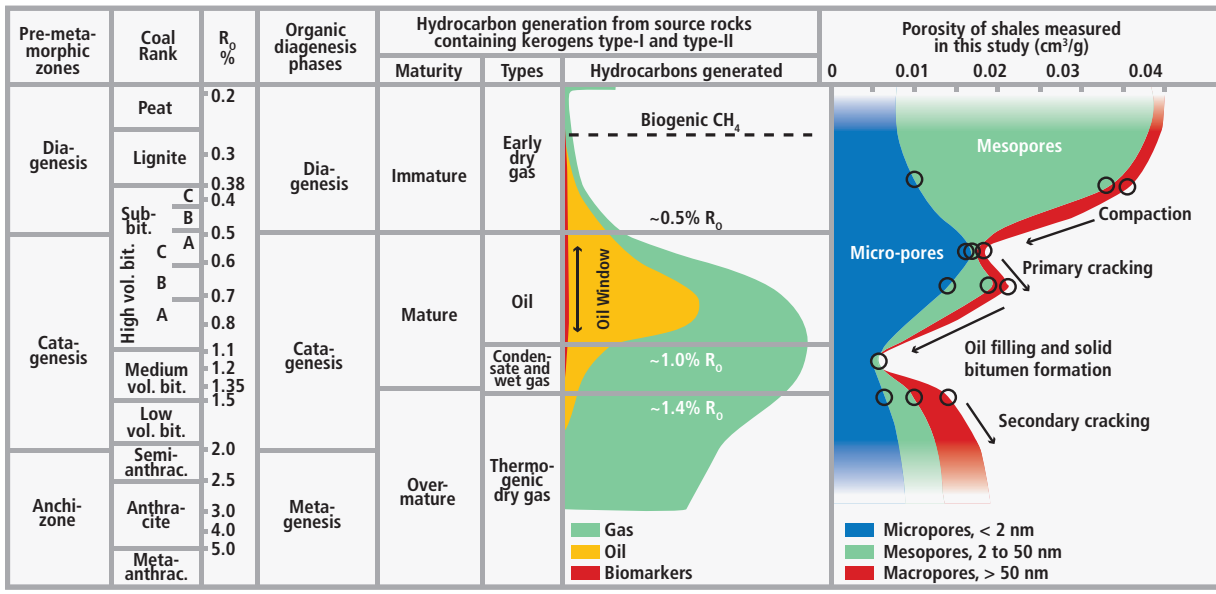

Fig. 8.20—Porosity of coal and shale: insights from gas adsorption and SANS/USANS technique. (From Mastalerz et al. 2012.)

transformation developed nanoscale porosity systems, includes such studies as from Mastalerz et al. 2012 (**Fig. 8.20**) and Walls 2013 (**Fig. 8.21**).

Within Mastalerz et al. 2012 (Fig. 8.20) the distribution of nanoscale pore throat sizes from micropores (< 2 nanometers) to mesopores (2 to 50 nanometers) to macropores (> 50 nanometers) within a relationship to diagenesis, catagenesis to metagenesis includes diagenetic pore filling processes to bitumen and solid hydrocarbon filling processes and renewed porosity development with secondary cracking processes related to expulsion inefficiencies resulting in hydrocarbon generated geopressures.

The specific geometries of the nanopores systems can change from pendular (bubble) in oil window maturity systems to

spongy within gas level maturity systems. These nanoscale pore geometries can affect the resulting pore level physics and resulting capillary pressures. Within both oil and gas windows where hydrocarbon geopressures are developed there is documentation of fracture type nanoscale kerogen systems.

Kerogen types also have a significant influence on the geometry of the expected pore systems. The figure has been modified to include inferences of expected pore surface energies related to hydrocarbon and water wetness. These surficial properties, as a result of the system chemistries, help define specific hydrocarbon producibility, the potential formation damage component related to completion fluids, and the preferred completion fluids within horizontal lateral wells to match system wetness within newly induced mineral and kerogen face fracture sets.

Nanoscale pore system chemistry and physics related to these complex nanoscale pore geometries and surficial energies are actively being investigated within research teams in ongoing studies and are expected to result in additional applied knowledge that is important to recognizing reservoir quality variability within the hydrocarbon deliverability of respective kerogen suites and their maturity levels.

Kerogen investigations can provide insights of adsorbed hydrocarbon storage capacity. Unconventional reservoirs are complex systems where hydrocarbon storage occurs within the kerogens and intrakerogen porosity system, whereas in comparison, within conventional reservoirs hydrocarbons are stored dominantly within the pores (porosity) associated between matrix particle components. In the mudrock unconventional reservoir, the hydrocarbons can be stored in multiple ways including:

- Free gas
  - In the rock matrix porosity
  - In the natural fractures
- Adsorbed gas
  - Adsorbed (chemically bound) to the organic matter (kerogen) and mineral surfaces within the natural fractures
  - Absorbed gas (physically bound) within the organic matter (kerogen) and mineral surfaces within the matrix rock
- Dissolved gas within the hydrocarbon liquids or water or within the bitumen

To obtain the total amount of gas in place (GIP), free gas, sorbed gas, and dissolved gas must be added together. Free gas is the dominant production that occurs early, with the greatest rates during the first few years of the life of a well. The absorbed gas volume is often significantly more than the free gas stored in the matrix porosity itself and may or may not be produced. Gas contents can exceed apparent free gas-filled porosity by six-to-eight times where organic content is high (Warlick 2010). However, sorbed gas may be produced by diffusion or desorption and often does not occur until later in the field life after the reservoir pressure has declined. It is generally accepted that sorbed gas does

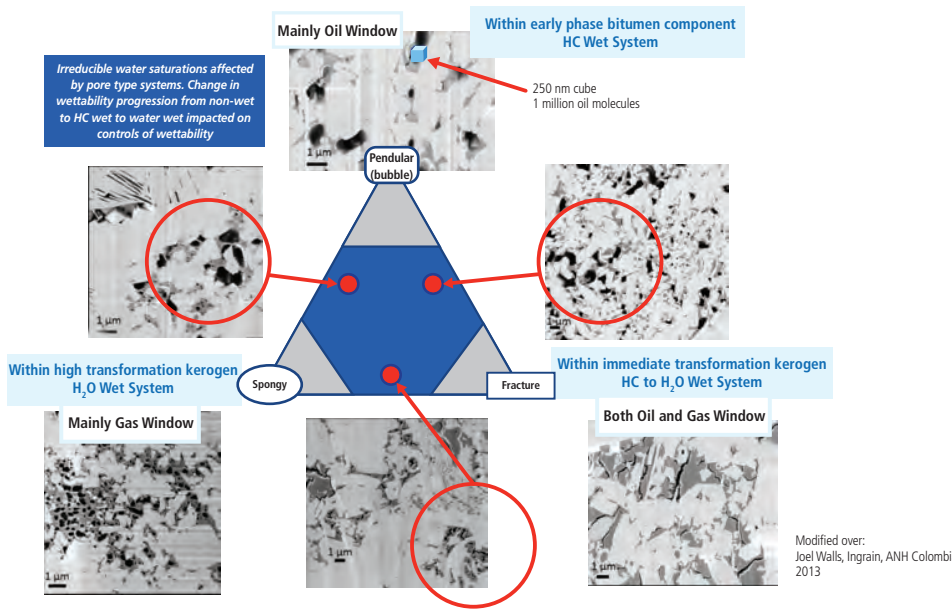

Fig. 8.21—Remaining hydrocarbon potential (mg HC/g rock) versus total organic carbon (TOC, weight percentage). (Modified over Walls 2013.)

not have an appreciable effect on unconventional mudrock field economics because it is not produced within the high productivity life position within the well production history. However, sorbed gas can constitute a significant part of GIP within most mudrock reservoirs. Usually dissolved gas is also only a small part of GIP within most mudrock reservoirs.

Maturation and maturity relationships affect the progression of pore system fluid types and inorganic chemical oxidation processes related to nanoscale pore throat surficial energies. Resulting wettability to hydrocarbons and water will and can also affect adsorbed and free hydrocarbon systems and their nanoscale productivity relationships. Applications including atomic force spectroscopy (AFS) are being utilized to better understand these nanoscale surficial energy relationships within nanoscale pores in relation to both free and adsorbed hydrocarbons. Gas isotopic characterization (carbon and hydrogen) of these specific hydrocarbon systems is another approach that can provide additional insights as to prediction of well EUR and production management issues.

8.3.3 Utilization of Core and Geochemistry Core Analyses in Organic Content Characterization

8.3.3.1 Pyrolysis Analyses (LECO and Rock-Eval Pyrolysis)

The early-accepted industry standard laboratory equipment for total organic carbon (TOCpresent day or pd) is the LECO TOC pyrolysis equipment. This methodology had been originally used by the steel industry for determining carbon levels within steel. TOCpd can also be measured by Rock-Eval equipment, as well as the SRA and Hawk™ instruments. These advanced, later-generation equipment methods are now considered as likely higher-standard quality analyses of TOCpd for mudrock resource plays (slightly higher TOC results), although some users prefer the LECO method results for comparison to prior industry datasets.

The LECO application requires decarbonation of the sample, then combustion at about 900°C for one minute.

The LECO Carbon Analyzer (LECO TOC pyrolysis equipment) utilizes a small rock sample that is combusted in an oxygen atmosphere where the carbon present is converted to CO_2. The sample gas flows into a non-dispersive infrared (NDIR) detection cell. The NDIR measures the mass of CO_2 present. The mass is converted to percent carbon based on the dry sample weight. The total organic carbon content is subtracted from the total carbon content to determine the total inorganic carbon content of a given sample.

Additional techniques such as the Carmhograph Wosthoff apparatus (Katz 1988) can derive elemental (C, H, O, and N) compositions of isolated kerogens to determine the H/C and O/C ratios. These techniques can be difficult to obtain in comparison to rapid Rock-Eval analysis approaches.

Rock-Eval pyrolysis equipment (Rock-Eval models from 1 to 6) oxidizes the sample after pyrolysis at about 580°C (S_4 in mg carbon/g of rock). The analysis combines carbon after oxidation with carbon in S_1 and S_2.

where:

$$TOC = 0.083 (S_1+S_2) + 0.10 (S_4) \quad \textbf{(Eq. 8.1)}$$

(The hydrocarbons in S_1 and S_2 are assumed to be about 83%.)

The pyrogram generated from the Rock-Eval apparatus (**Fig. 8.22**) illustrates the relationship of time (minutes) with the temperature trace (non-isothermal at 25°C/min) and the volumes of the derived gas (CO_2) associated with temperature levels (T_{max}) (Tissot and Welte 1984) where:

- S_1 is correlated to the free oil that volatizes at 300°C. It is equal to the amount of free hydrocarbons (gas and oil) in the sample (in milligrams of hydrocarbon per gram of rock). If $S_1 > 1$ mg/g, it may be indicative of an oil show. S_1 normally increases with depth. Contamination of samples by drilling fluids (OBM) and mud can give an abnormally high value for S_1.
- S_2 is correlated to the organic matter that pyrolyzes (cracks) between 300 to 600°C. It is equal to the amount of hydrocarbons generated through thermal cracking of nonvolatile organic matter. S_2 is an indication of the quantity of hydrocarbons that the rock has the potential of producing should burial and maturation continue.
- S_3 is correlated organic carbon dioxide from kerogen and is equal to the amount of CO_2 (in milligrams CO_2) produced during pyrolysis of kerogen. S_3 is an indication of the amount of oxygen in the kerogen and is used to calculate the OI or oxygen Index. Contamination of the samples should be suspected if abnormally high S3 values are obtained. High concentrations of carbonates that break down at temperatures lower than 390°C will also cause higher S_3 values than expected.
- T_{max} is the temperature at maximum evolution of S_2 peak or can be defined as the temperature at which the maximum release of hydrocarbons from cracking of kerogen occurs during pyrolysis (top of S_2 peak). T_{max} is often utilized as an indication of the stage of maturation of the organic matter. Care must be utilized with this value in that with changing

kerogen suites, changes in T_{max} values will occur. So organic kerogen facies dependent T_{max} values will occur (Espitalie et al. 1985; Delvaux et al. 1990). Mixtures of dominant type kerogen suites can also impact the results and develop additional or flat peaks where T_{max} is difficult to distinguish. High transformation of the kerogens will also result in a difficult to distinguish flat top value.

- S_4 is often not reported, but it is the oxidation of residual carbon when Rock-Eval TOC is utilized.

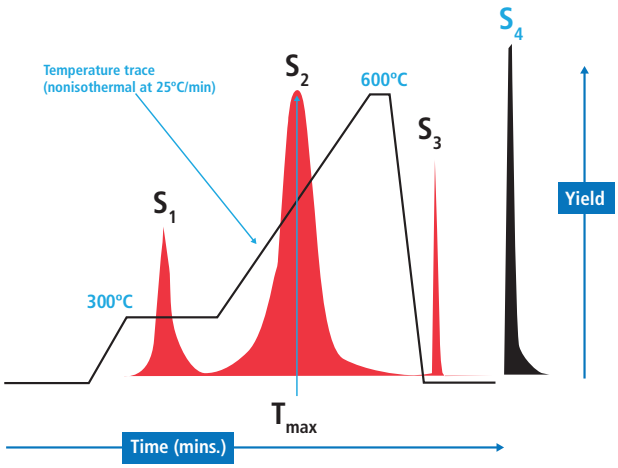

Fig. 8.22—Rock-Eval pyrogram illustrating S1, S2, S3, S4, and T_{max} with temperature trace of pyrolysis. (Walles et al. 2008.)

Each of these indices can be a quite useful index for maturation and kerogen transformation calculations for a specific kerogen organic suite for the expected hydrocarbon phase within the spatial position within an in-situ generated petroleum system or for the specific time migrated hydrocarbons associated to a specific plumbing or charge system of a petroleum accumulation. An illustration (Fig. 8.23) of the experimental conversion of an in-situ source rock exhibits the expected pyrogram curves of the S_2 peak with kerogen transformation (maturity). The listed values illustrate the progression of T_{max} values with transformation, the TOCpd, the S_2 volume levels, and the calculated HI. Within this case example, utilizing these progressive maturation curves, a TOC original can be back calculated from the high maturity samples.

The type and maturity of organic matter in petroleum source rocks can be characterized from Rock-Eval pyrolysis data. These results can be calculated into the following indices by utilizing the quantitative pyrogram data results from the pyrolysis including S_1, S_2, S_3, S_4, and T_{max}:

HI = hydrogen index (HI = [100 x S_2]/TOC). **(Eq. 8.2)**

Hydrogen index is a parameter used to characterize the origin and present-day hydrogen content of organic matter. Hydrogen-rich marine microorganisms (including algae, in general) are composed of lipid- and protein-rich organic matter, where the ratio of H to C is higher than in the carbohydrate-rich constituents of land plants. HI pd typically ranges from ~100 to 600, but can be as high as 900+ with a maximum of 1230, in geological samples dependent upon the maturity state and original kerogen type. See the prior section on kerogen types for a more complete discussion.

OI = oxygen index (OI = [100 x S_3]/TOC). **(Eq. 8.3)**

OI is a parameter that correlates with the ratio of O to C, which is high for polysaccharides-rich remains of land plants and inert organic material (residual organic matter encountered as background in marine sediments). OI values range from near 0 to ~150. See the prior section on kerogen types for a more complete discussion.

PI = production index (PI = S_1/[S_1 + S_2]). **(Eq. 8.4)**

Production index (PI) is used to characterize the evolution level of the organic matter. At certain levels of transformation (up to peak oil transformation) it can be used as a kerogen transformation ratio. However, this ratio will lower within the level of transformation that corresponds to higher levels of transformation beyond peak hydrocarbon generation (lower associated PI values).

PC = pyrolyzable carbon (PC = 0.083 x [S_1 + S_2]). **(Eq. 8.5)**

Pyrolyzable carbon (PC) corresponds to carbon content of hydrocarbons volatilized and pyrolyzed during the analysis. This can be used as an index for organic system carbon (Katz 1988).

TR = transformation ratio (S_1/(S_1 + S_2). **(Eq. 8.6)**

Transformation ratio is a useful index for determining the degree of transformation of the kerogens. This analysis is especially useful if based upon high-quality S_1 and S_2 data. Unfortunately S_1 data quality can be variable or undependable if oil-based mud contamination is present. Alternative methods for determining transformation ratio can be completed through utilizing HI original to HI present-day values.

8.3.3.2 Pyrolysis Analyses (SRA and HAWK Pyrolysis)

With the development of portable and wellsite pyrolysis instruments, applicable for both active and previously drilled wells, a variety of applications are possible. In non-

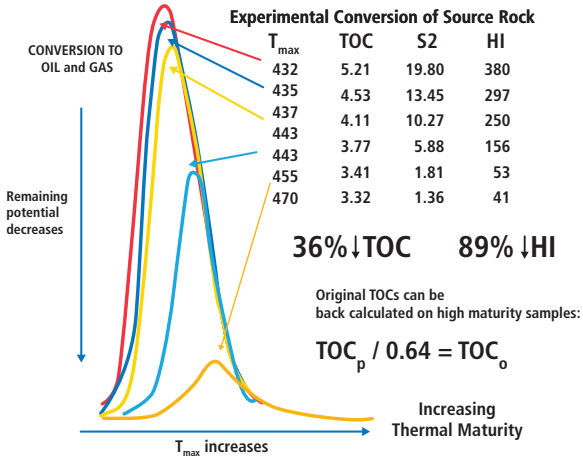

Fig. 8.23—S2 Portion pyrogram illustrating T_{max} change with progressive transformation of kerogens. (Walles et al. 2008.)

contaminated samples or non-oil based muds (OBM), high value applications include identifying potential net liquids pay (high free oil) zones (by elevated S_1) and bypassed (high free oil) pay (by elevated S_1) is also possible.

The methods listed in Fig. 8.23 include kerogen indices from core or cuttings samples measuring components of S_1, S_2, S_3, S_4 and T_{max} data derived from Rock-Eval pyrolysis, as well as from laboratory level Rock-Eval equipment to the wellsite and laboratory Source Rock Analyzer (SRA) (TOC, S_1, S_2, T_{max}) and the wellsite and laboratory advanced Hawk equipment (TOC, S_1, S_2, S_3,T_{max}).

The source rock analyzer (SRA) pyrolyzes rock samples to deliver accurate source rock and reservoir data, such as total organic carbon (TOC), thermal maturity (T_{max}), free oil content (S_1), and source potential carbon (S_2). The SRA calculations include deriving:

S_1 – the amount of free hydrocarbons (oil)

S_2 – the amount of hydrocarbons generated through thermal cracking of nonvolatile organic matter, such as kerogen

S_3 – the amount of CO_2 produced during pyrolysis of kerogen

T_{max} – the temperature at which the maximum release of hydrocarbons from kerogen cracking occurs during pyrolysis

TOC – total organic content

HI – hydrogen index

OI – oxygen index

PI – production index

SI/TOC – oil or contamination indication **(Eq. 8.7)**

These methods listed in Fig. 8.23 include data that was derived from core and/or cuttings samples with indices such as HI and T_{max} data as derived from rock evaluation pyrolysis laboratory methods or wellsite application methods. This advanced wellsite technology Rock-Evaluation equipment includes the HAWK (Hydrocarbon Analyzer with Kinetics) and the Source Rock Analyzer instruments the (SRA –TPH SRA – TPH/TOC or SRA –TPH/Kinetics).

The HAWK Workstation is utilized to assess kerogen maturity, quality, TOCpd, TOC original inference, and inferred kerogen porosity. This instrument measures all the classical pyrolysis parameters (S_1, S_2, S_3, and T_{max}) together with TOC using a small ground rock sample. In addition inorganic carbon is defined where an inorganic carbonate carbon content of the sample can be assigned. Acid preparation of samples for TOC analysis is not required, resulting in minimal loss of carbon through sample preparation.

This instrumentation also provides a capability of processing kinetics data, utilizing internal advanced software. An application is for defining the specific mudrock HC source rock organofacies. A kerogen suite kinetics determination assists with predicting matrix HC phases (specific composition changes of liquids, condensate, and gas content).

8.3.3.3 Additional TOC Weight Percentage Analyses (XRF Description of Method)

Due to the significant advances occurring within development of wellsite or core laboratory processes, rapid elemental and mineralogical analytical instruments including XRF and XRD approaches are now available. With the kerogen and microbial systems advancing knowledge developed within earlier sections, elemental relationships to resulting preserved kerogen quality are being developed.

Elemental components, especially non-ferrous base metals such as nickel, copper, silver, gold, lead, zinc, tin, tungsten, molybdenum, tantalum, cobalt, bismuth, cadmium, titanium, zirconium, antimony, manganese, beryllium, chromium, germanium, vanadium, gallium, hafnium, indium, niobium, rhenium, and thallium can exhibit significant biological disruption components to specific families of life and species of microbial organisms. Many of these microbial organisms

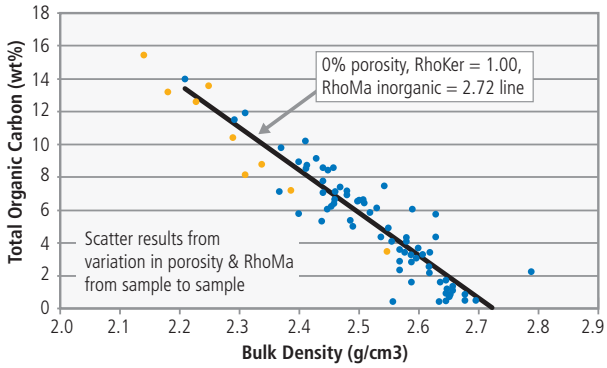

Fig. 8.24—Density versus TOC weight percentage New Albany shale. (Modified from Cluff 2011.)

are responsible for system processing of hydrogen, oxygen, and sulfur species that directly impact resulting and preserved (through millions of years of burial processes within the subsurface) kerogen quality. Many of these elemental species include enrichment factors associated with marine system depletion of oxygen levels from oxia to dysoxia to anoxia (Walles 2009, 2010, 2011, 2012, 2013, 2014).

The relationship to the enrichment of these components can occur within marine environments that have both external controls as extrabasinal fluid transport (non-marine into marine, including volcanic ash or immature igneous and metamorphic materials transport) and/or air transport from volcanic ash systems (Walles 2009, 2010, 2011, 2012, 2013, 2014).

These preserved, diagenetically altered and clay transformed, and/or bioturbated volcanic ash systems are dominant compositional components within many unconventional resource plays. Very thin (millimeters to centimeters) volcanic ash beds, either preserved or altered, are often below the resolution of most wireline and LWD tools. However, these non-ferrous elemental metal components, dependent upon the specific mudrock system biologic age and depositional environment often exhibit close correlation to TOC enrichment. Due to the biologic and system TOC preservation response, the levels of specific non-ferrous elemental components that become available within a marine system biologic system can be good indicators of TOC original levels.

These components can be displayed within a log basis with respect to environmental conditions of oxia and to biologic disruption capacity and preservation of organic matter. This is useful for an indication of distribution of the potential kerogen component prior to thermal alteration and maturation processes.

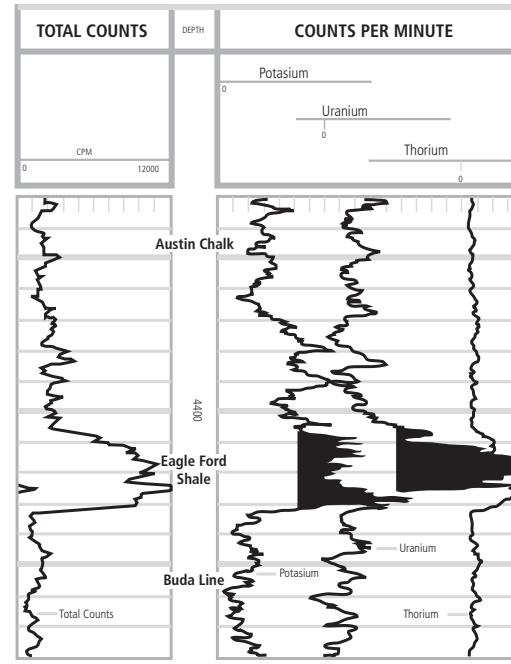

Log response over Austin chalk, Eagle Ford shale, and Buda limestone in Cretaceous carbonate trend, Caldwell County, TX. Eagle Ford section exhibits typical organic-rich shale response (>K, > >U, Th) which can be applied to source-rock potential determinations.

Fig. 8.25—Spectral gamma ray response across the Eagle Ford shale. (From Fertl and Reike 1980.)

8.3.4 TOC Weight Percentage Determination from Conventional Log Measurements

Basic techniques to estimate TOC weight percent from conventional wireline log responses today were first developed in the late 1970s to mid 1980s. Linear empirical relationships between core pyrolysis TOC weight percentage and a variety of individual conventional log measurements were developed on an individual formation or basin basis. The three log measurements most commonly used in this manner today are the compensated formation density (**Fig. 8.24**), the gamma ray, and the spectral GR uranium curves (**Fig. 8.25**).

In 1979 Schmoker developed a relationship between formation density and TOC for the Devonian Appalachian shales in Ohio and West Virginia. He expanded this concept in the same shales and utilized the gamma ray response in a similar manner. He confirmed that a relationship between formation density and TOC weight percent would work in other areas by developing one for the Bakken Formation in the Williston basin (Schmoker 1979, 1981; Schmoker and Hester 1983). This generic relationship can be stated as the following:

$$TOC = (A / \rho) - B$$

where:

TOC = weight percent total organic carbon

ρ = formation density gm/cc

B = constants specific to a formation or area

(Eq. 8.8)

These relationships worked because of the low matrix density value of the organic material, which in these cases was 1.0 to 1.01 gm/cc and the relatively constant inorganic matrix density values of the shale formations, which were in the 2.68 to 2.72 gm/cc range.

All density versus TOC relationships have additional constraints. They assume a constant kerogen density, a constant ratio of organic content between kerogen and total organic carbon, a constant inorganic matrix density, and the assumption that all decreases in measured formation density are due to increased amounts of organic carbon not variations in total porosity. Many source rock reservoirs contain minor amounts of heavy minerals such as pyrite, apatite, or anhydrite. If the weight percentages of these minerals increase, the calculated TOC weight percent from the relationships will be in error. These relationships are empirical and will vary between basins and even across a single basin. Many shale plays have variations in kerogen maturity such that portions are dry gas productive and some condensate or liquid productive. Multiple sets of relationships would be needed in these cases. Log data must also be normalized when using data from multiple service companies or dealing with various generations of tools.

Organic rich shale intervals typically exhibit a linear relationship of increasing gamma ray response with increasing TOC weight percent (**Fig. 8.26**). The increase in radioactivity of the organic-rich shales is related to the anoxic marine depositional environment of many of these shale formations. Under these conditions uranium forms insoluble compounds that sorb to clays, organic material, and organogenic phosphate particulates. While the marine depositional environment is common for many source rock reservoirs, it is not the only type. In a more oxidizing lacustrine environment, uranium may occur in more soluble forms and be flushed from the formation precluding the increase in radioactivity associated with organic material (Jacobi et al. 2008).

The conventional gamma ray response is primarily the combined gamma ray emissions from potassium-40 (K^{40}), the uranium series nuclide bismuth-214 (Bi^{214}), and the thorium series nuclide thallium-208 (Tl^{208}) (Fertl and Reike 1980).

A linear empirical relationship can also be constructed using the uranium concentration plotted against TOC weight percent. All of these GR and spectral GR relationships are also empirical and will vary between basins and even across a single basin. Multiple sets of relationships may be required. The GR and spectral GR responses need to be environmentally corrected before plotting. Log data must also be normalized when using data from multiple service companies or dealing with various generations of tools. Uranium may also be sorbed to apatite, a calcium phosphate ($Ca_5(PO_4)_3F$) mineral which occurs in many source rock shale reservoirs (Jacobi et al. 2008). Both GR and spectral GR data should be corrected for the presence of apatite prior to plotting against TOC weight percentage.

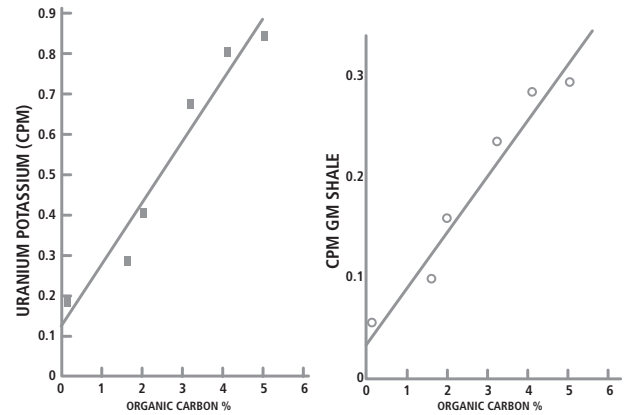

Fig. 8.26—Crossplots of organic carbon weight percent versus uranium/potassium and uranium responses for the New Albany shale. (From Fertl and Reike 1980.)

8.3.4.1 Passey Delta Log R Method

The Passey Delta Log R method is a graphical porosity–resistivity overlay technique developed in 1990 that is still widely used. It was originally developed using the acoustic compressional slowness (Δt in usec/ft.) but also works with density or compensated neutron measurements. The technique allows the organic rich intervals to be identified and the TOC weight percentage calculated if the level of maturity (LOM) of the kerogen is known or can be estimated. The LOM could be calculated from T_{max}, vitrinite reflectance R_0 measurements, or other kerogen maturity indicators (Passey et al. 1990). While not as frequently used, the approach also allows the S_2 Rock-Eval pyrolysis value to be estimated.

8.3.4.2 Methodology

A deep resistivity curve is plotted on a logarithmic grid and a porosity curve, such as the compressional acoustic slowness, Δt, is plotted on a linear grid such that 50 usec/ft. corresponds to one decade of resistivity on the logarithmic scale. The acoustic curve is shifted until the acoustic and resistivity curves overlay each other in an inorganic shale interval. In organic shale intervals, the separation between the shifted acoustic curve position and the resistivity curve is the Δ log R.

where:

$$\Delta \log R = \log_{10}(R/R_{baseline}) + 0.02 \times (\Delta t - \Delta t_{baseline})$$

R = resistivity value in ohm-m

$R_{baseline}$ = baseline resistivity value in ohm-m

Δt = acoustic slowness value in usec/ft.

$\Delta t_{baseline}$ = baseline acoustic slowness value in usec/ft.

(Eq. 8.9)

The LOM was then estimated or obtained from other analyses such that the TOC weight percentage could be calculated using the relationship:

where:

$$TOC = (\Delta \log R) \times 10^{(2.297 - 0.1688 \times LOM)}$$

TOC = weight percentage TOC

LOM = kerogen level of maturity **(Eq. 8.10)**

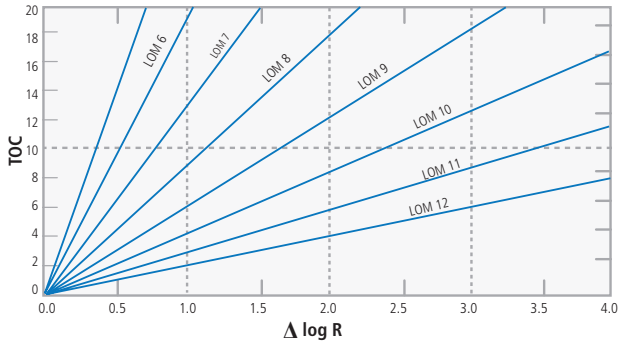

Fig. 8.27—Relationship of Δ log R values, TOC weight percentage and LOM. (Modified from Passey et al. 1990.)

The 1990 paper included a chart that showed the relationships between the Δ log R values, LOM, and TOC weight percentage. **Fig. 8.27** shows the 1990 published relationship between Δ log R values, TOC weight percentage, and kerogen level of maturity.

This chart could also be used to calculate the kerogen LOM in a specific well by plotting core LECO pyrolysis results and the Δ log R values. **Fig. 8.28** illustrates the use of the overlay.

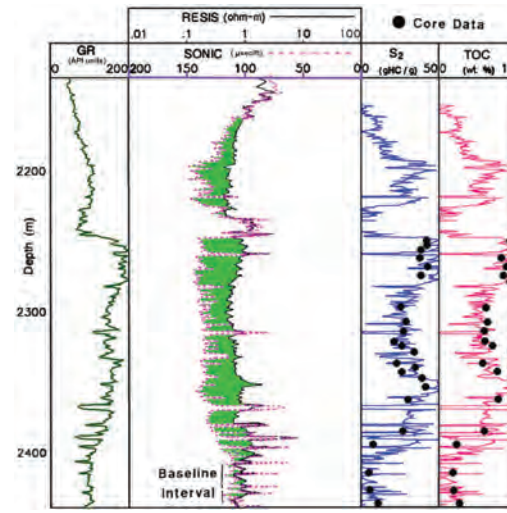

Fig. 8.28—Example use of Δ log R overlay technique. (Modified from Passey 2011.)

8.3.4.3 Factors to Remember

In addition to identifying organic rich intervals by the Δ log R separation, note that separation may occur for other reasons. Zones with very low porosities, such as salt, anhydrite, or some carbonates, have high formation resistivities and will exhibit separation on the plot. Conventional oil or gas reservoirs will also exhibit separation due to their increased resistivity values. If intervals of the borehole are enlarged or rugose the porosity curve selected may require correction or editing before calculation of the TOC weight percentage. At very high kerogen maturities, >> R_0 3, the resistivity of the organic-rich intervals may be significantly reduced and impact the estimation of the TOC weight percentage present.

The original calibration in the 1990 paper was based on samples mostly in the oil maturity window (R_0 = 0.5-0.9 or LOM 6 to 10.5). The chart values for shales with LOMs >10.5 were just extrapolated. By 2010 a large number of R_0 measurements with values in the gas maturity window were acquired from gas productive unconventional shales. Study of

those samples indicated that use of the original relationships for R_0 values >0.9 would underestimate the TOC weight percentage and published revised calculation guidelines (Passey et al. 2010). The recommendation is to use the LOM limit line for all sale gas reservoirs with kerogen maturities > R_0 0.9. **Fig. 8.29** shows the revised relationship between Δ log R values, TOC weight percentage, and maturity.

Passey was not the only researcher revisiting the 1990 equation. A modification to Passey's original empirical equation for mature gas shales was proposed where a variable multiplier, with a value greater than one, was added:

$$TOC = (\Delta \log R) \times 10^{(2.297 - 0.1688 \times LOM)} \times C$$

(Eq. 8.11)

The value of the correction variable is based on matching the calculated TOC weight 5 with core measured core TOC weight percentage (Sondergeld et al. 2010). Vitrinite reflectance

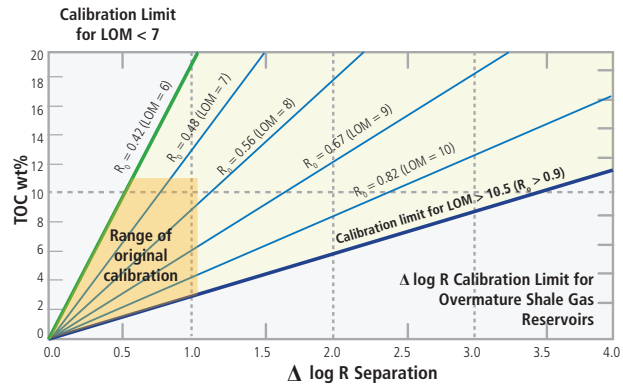

Fig. 8.29—Revised relation of Δ log R to TOC weight percentage for high kerogen maturity shales. (Modified from Passey 2011.)

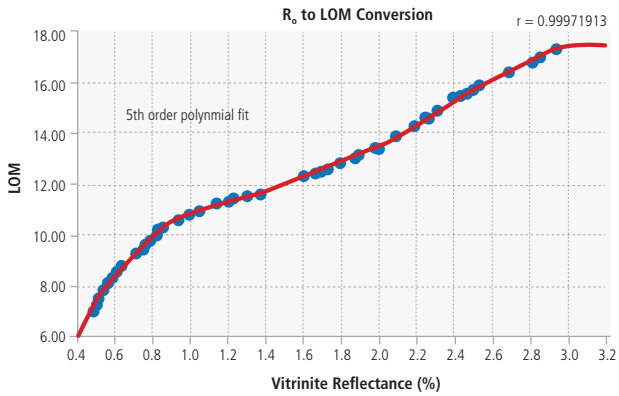

Fig. 8.30—Relationship between vitrinite reflectance R_o values and LOM. (Modified from Cluff and Miller 2010.)

maturities, R_0, can also be used to calculate LOM values. **Fig. 8.30** shows the relationship between LOM and vitrinite reflectance R_0 values.

8.3.5 TOC Weight Percentage Determination Utilizing Pulsed Neutron Elemental Spectroscopy

The addition of elemental spectroscopy logs to a conventional log and core dataset provides additional options to determine TOC weight percentage.

Pulsed neutron spectroscopy instruments measure elemental concentrations in both the capture and inelastic energy spectra and this gives them an advantage over chemical source instruments as chemical neutron source elemental spectroscopy instruments effectively measure only from the capture gamma ray spectrum. Carbon is an element that can only be measured and quantified from the inelastic spectrum.

Methodologies have been developed to determine from the total carbon weight percentage measured by the instruments the weight percentage of inorganic carbon and the weight percentage of organic carbon. Currently two open hole pulsed neutron elemental spectroscopy instruments are commercially available: the Baker Hughes FLeX™ and the Schlumberger Litho Scanner™. Each service company has developed a methodology. While the principles in both methodologies are similar, some variations exist. Details relating to the Schlumberger Litho Scanner methodology can be found in Craddock et al. 2013.

8.3.5.1 TOC Percentage Determination Methodology for the Baker Hughes FLeX and Spectralog Logging Sondes

Carbon is an element that can only be quantified from the gamma ray inelastic spectrum. After corrections to the elemental yields are made to account for borehole geometry and mud composition the Baker Hughes pulsed neutron spectroscopy instrument (FLeX) uses the measured elemental weight percentages to calculate the mineral composition of the formation. A sequential deterministic expert system, RockView™, applies geologic constraints to compute the most probable mineralogical solution in an underdetermined system (Pemper et al. 2006, Jacobi et al. 2007, 2008, Pemper et al. 2009). A more complete description of the RockView expert system will be presented in the lithology and mineralogy section. The elemental weight fractions are combined into mineral weight percentages honoring the principles of mass balance and mineral stoichiometry. The amount of carbon

required for the weight percentage of each of the inorganic minerals containing carbon computed by the expert system, primarily calcite, dolomite, and siderite, is subtracted from the total elemental weight percent of carbon the instrument measured. The remaining elemental carbon is classified as excess carbon, which may exist as kerogen (or bitumen), coal, or liquid hydrocarbon (Jacobi et al. 2008, Pemper et al. 2009). The excess carbon is classified as kerogen based on differences in trace element concentrations, such as increased uranium concentration, while lithology differences are used to separate coal from liquid hydrocarbons (Jacobi et al. 2008, Pemper et al. 2009). **Fig. 8.31** illustrates the workflow used to compute reservoir mineralogy and TOC weight percentages.

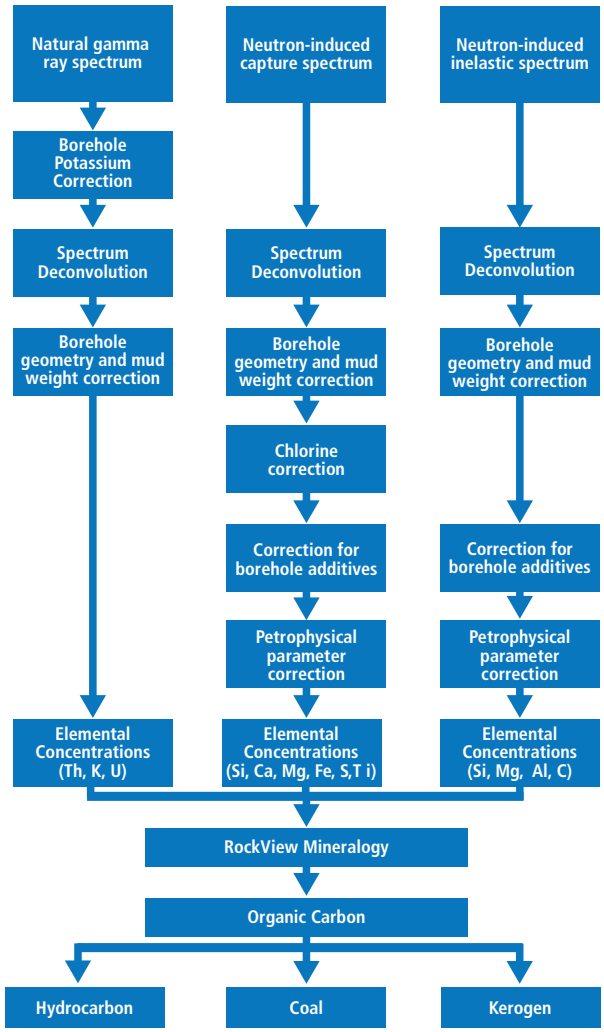

Fig. 8.31—FLeX and Spectralog workflow for determination of mineralogy and organic carbon weight percentages. (From Pemper et al. 2009.)

$$TOC = [C_{total} - C_{calcite} - C_{Dolomite} - C_{Siderite}] \quad \textbf{(Eq. 8.12)}$$

Fig. 8.32 shows an example RockView mineralogy plot across the organic-rich Eagle Ford shale and the underlying Buda Limestone. The mineralogy components are presented in weight percent as opposed to volumetric percentage. While both of these formations contain a high percentage of carbonate minerals, particularly calcite, TOC is only occurring in the Eagle Ford shale formation. Notice that the uranium concentration is noticeably higher (magenta curve Track 7 from the left) in the Eagle Ford shale formation than in the Buda Limestone.

This approach has been utilized to determine both mineralogy and organic carbon content in more than 600 wells in unconventional shale plays around the world. The computed TOC weight percentage has been confirmed by comparison to core measured TOC values in numerous gas and liquid productive shale formations but it is not necessary to have core measured TOC weight percentage to calibrate the computation of TOC from the spectroscopy instrument.

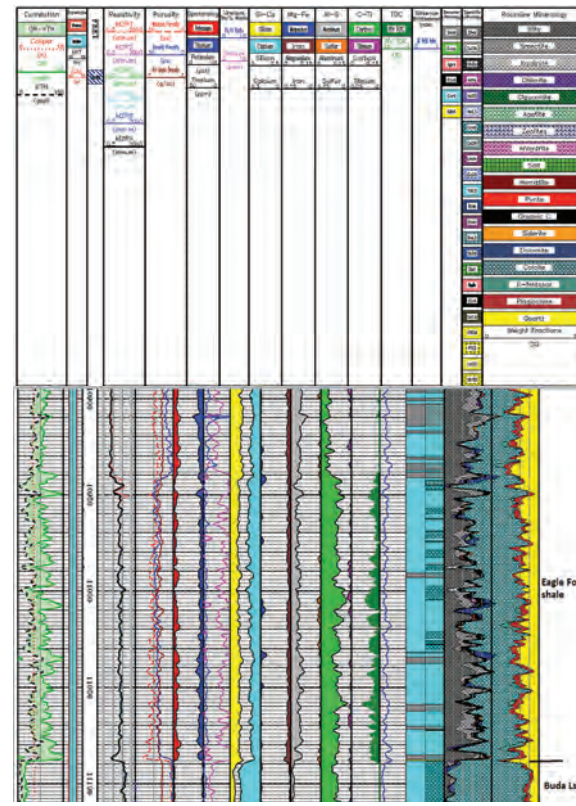

Fig. 8.32—RockView mineralogy plot across the organic rich Eagle Ford shale and underlying Buda Limestone in Texas.

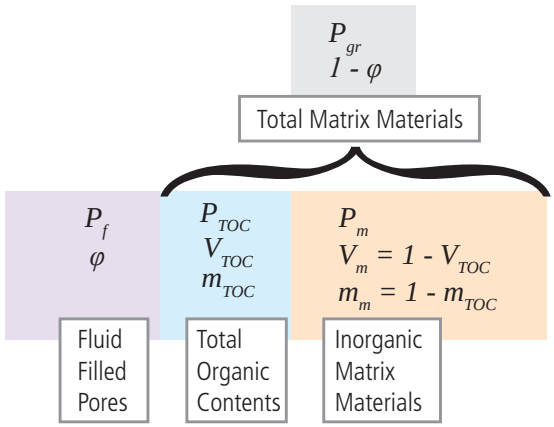

1. Total Grain Density $$P_{gr} = \frac{\rho_b - \rho_{fluid}\varphi}{(1 - \varphi)}$$

2. TOC Volume Fraction $$V_{TOC} = \frac{\rho_m - \rho_{gr}}{\rho_m - \rho_{TOC}}$$

3. TOC Weight Fraction $$m_{TOC} = \frac{\rho_{TOC}}{\rho_{gr}} V_{TOC}$$

where:

ρ_b is the bulk density

ρ_{gr} is the total grain density including inorganic and organic matrix constituents

ϕ is the NMR total porosity

ρ_{fluid} is the density of pore filling fluid, determined from NMR fluid typing

V_{TOC} is the volume fraction of organic matrix components

m_{TOC} is the mass fraction of organic matrix components

ρ_{TOC} is the density of organic matrix components, determined from core and/or Rockview TOC calibration

ρ_m is the density of inorganic matrix components, determined using mineralogy from geochemical logs

(Eq. 8.13)

8.3.5.2 TOC Weight Percentage Determined from Nuclear Magnetic Resonance Measurements

Schmoker confirmed that TOC weight percentages could be estimated by correlation to the bulk density of the organic shale formation (Schmoker 1979, 1981, Schmoker and Hester 1983). However, scatter in these empirical relationships exists because of several factors including variations in the inorganic matrix density of the formation, variations in the shale total porosity and variations in the bulk density of the kerogen. Kerogen has a low bulk density, typically ranging from 1.0 to 1.8 gm/cc. The density of kerogen has been shown to increase with increasing thermal maturity (Ward 2010). The kerogen density can be computed in a mass balance equation that includes all rock components. The individual terms in the equation can be obtained from either core analyses or log measurements as detailed in **Table 8.7** (LeCompte and Hursan 2010).

$$\rho_b = \varphi \cdot \rho_{fl} + (1 - \varphi - V_k) \cdot \rho_{io} + V_k \cdot \rho_k$$

$$V_k = 1 - \varphi - \frac{\rho_b(1 - W_k) - \varphi \cdot \rho_{fl}}{\rho_{io}}$$

$$\rho_k \quad W_k \times \frac{\rho / \rho_b}{V_k}$$

(Eq. 8.14)

Table 8.7—Methods to measure kerogen density. (From LeCompte and Hursan 2010.)

Methods to Measure Kerogen Density		
	CORE	**LOG**
Porosity, Φ	**GRI Method**	**NMR/Multi-Mineral**
Bulk Density, ρ_b	**As-Received**	**RHOB log**
Kerogen, V_k, W_k	**LECO/Rock-Eval**	**TOC log/Uranium/RHOB**
Inorganic density, ρ_{io}	**XRD**	**Mineralogy Log**
Fluid density, ρ_{fl}	**Dean-Stark**	**Sw Log**

A second independent determination of TOC weight percent can be made by combining the results of the RockView mineralogy, the bulk density response, and the nuclear magnetic resonance (NMR) total porosity. An inorganic matrix density can be computed every .25 ft. from the RockView derived inorganic mineralogy. The NMR total porosity measurement does not respond to the composition of the rock matrix but rather the volume of movable fluids in the pores. The density-calculated porosity responds to the whole rock, the pore fluids, and the total composition of the matrix, which includes the kerogen weight percent (Jacobi et al. 2008, 2009).

A total grain density using the NMR total porosity and the bulk density measurement is compared to the inorganic grain density

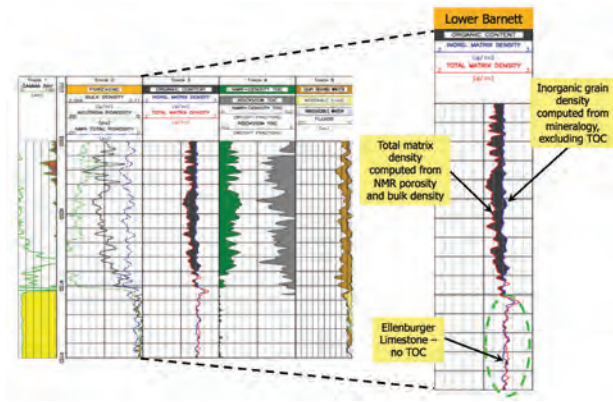

Fig. 8.33—NMR density and RockView mineralogy derived TOC weight percentages, Barnett shale example. (Jacobi et al. 2008.)

calculated from the RockView mineralogy using the following relationships illustrated in **Fig. 8.33** (Jacobi et al. 2009).

Both calculated TOC weight percentages have been validated with LECO core analyses TOC measurements in numerous shale plays including the Barnett, Haynesville, Woodford, and Marcellus shales. **Fig. 8.34** shows the comparison of both TOC determinations with core analyses TOC weight percent, a comparison of NMR total porosity with core measured porosity, and the mineralogy derived inorganic grain density compared to the core inorganic matrix density and the total matrix density, which includes the organic carbon for Woodford shale (Jacobi et al. 2009).

In shale dry gas productive reservoirs TOC weight percentages from both methods are generally in good agreement. Excess carbon is classified as kerogen based upon an elevated uranium concentration cutoff, which can be varied from play to play. This methodology was validated in several dry gas productive shales including the Barnett, Haynesville, Woodford, and Marcellus shales. As exploration expanded into liquid producing shale plays such as the Eagle Ford, Niobrara, and Bakken we observed that the calculated TOC weight percentage from the RockView elemental carbon method were often consistently larger than the TOC weight percentage calculated from the NMR/density/mineralogy method.

The higher TOC weight percentage calculated from the excess carbon method is the result of the FLeX instrument and RockView expert system responding to not only the carbon in the kerogen, but also to the liquid hydrocarbons in both the organic and inorganic pore systems. Core TOC weight percentage in these liquid productive shale wells agreed more closely to the NMR, density-neutron, and mineralogy derived TOC weight percentage. The conclusion is obvious that the assumption that all excess carbon is kerogen in liquid productive shales is incorrect. However, this discrepancy can be leveraged to identify potential liquid productive intervals by the differences in computed values between the two methods. Core measured TOC weight percentage and RockEval pyrolysis analyses should be obtained to validate liquid productive intervals.

8.4 Lithology and Mineralogy Determination

Common practice when discussing these reservoirs is to group organic mudrocks of widely different mineral composition and fabric together and refer to them collectively as unconventional shale reservoirs. These differences in mineral composition and fabric can reflect significant differences in the ability to effectively fracture stimulate an individual well or reservoir and consequently the potential productivity of that reservoir. One primary evaluation objective then is to accurately determine that mineral composition. This can be accomplished using a combination of conventional wireline or LWD logging technologies, a variety of petrological and inorganic geochemistry core and cuttings analyses, and wireline elemental spectroscopy logging.

The matrix composition of these organic mudstone reservoirs is typically heterogeneous containing varying amounts of clays, kerogen, clastics (quartz, feldspars, and micas), carbonates (calcite, dolomite, and siderite), pyrite, and minor occurrences of additional minerals.

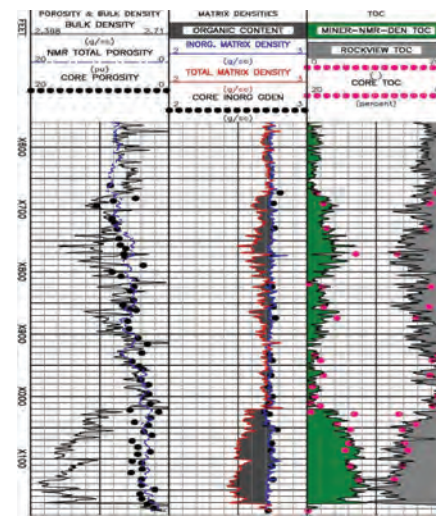

Fig. 8.34—A Woodford shale example comparing the excess carbon-derived TOC weight percentage to the NMR density mineralogy TOC weight percentages, inorganic, total and core analyses grain densities and NMR total porosity, core total porosity, and bulk density. (Modified from Jacobi et al. 2009.)

8.4.1 Lithology and Mineralogy Determination Utilizing Conventional Log Measurements

Lithology and mineral composition can be determined using only conventional log inputs supplemented by varying amounts of core analyses. Both deterministic and hybrid workflows, which contain deterministic steps and the use of mathematical solvers, are often utilized. The input for kerogen weight percentages and volume percentages is most likely obtained from deterministic regressions of core TOC weight fractions and conventional log measurements such as density, uranium, GR, or the Passey Δ log R method. A simplified lithology/mineralogy determination can be made by estimating the shale volume and cross plotting multiple porosity responses, as is done for determination in conventional reservoirs. However, the amount of kerogen needs to be determined prior to that process to remove the impact of the kerogen on the log responses (Cluff 2011).

Conventional log measurements of resistivity, density, neutron and acoustic, and gamma ray or spectral gamma ray including thorium and uranium concentrations can be input into a least squares error minimization solver. If available the selection of minerals to be input into the model is guided by study of the XRD analyses for that individual well or XRD data from other wells in the same shale play reservoir. Some grouping of minerals is required to reduce the number of output parameters that must be solved (Ramirez et al. 2011).

8.4.2 Lithology and Mineralogy Determination Utilizing Elemental Spectroscopy Log Measurements

Varying methods are employed by petrophysicists and the service companies to utilize the elemental weight fractions obtained from individual spectroscopy instruments to estimate formation mineralogy. Deriving mineralogy from logging geochemical instruments has been difficult without a priori knowledge of the minerals present for several reasons.

Elemental spectroscopy logging tools directly measure formation elements from induced gamma rays generated by formation and borehole nuclei collision interactions in one or both the capture and inelastic spectra. Each element is characterized by a unique spectral signature. A conversion for spectral deconvolution or inversion of the recorded gamma ray spectra is applied to obtain relative elemental yields, which typically include Al, C, Ca, Fe, Gd, H, K, Mg, Mn, Na, O, S, and Si. Capture and inelastic gamma ray diffusion and absorption are not proportional to the elemental concentration, but instead dependent upon the capture cross section (**Table 8.8**). Neutron capture cross sections of elements such as Mg and Na are small and can be difficult to identify. The capture cross section for Gd is very large and must be included to ensure the accuracy of least squares deconvolution, although the concentration of Gd is low (ppm) compared to major oxides.

Table 8.8—Neutron capture cross section values for selected elements. (Source of values Sears 1992.)

Element		Neutron Capture Cross Section (Barns)
Aluminum	Al	0.231
Calcium	Ca	0.42
Chlorine	Cl	33.5
Iron	Fe	2.56
Magnesium	Mg	0.063
Potassium	K	2.1
Silicon	Si	0.171
Sodium	Na	.53
Titanium	Ti	6.09

Neutron interactions generate gamma ray emissions not just from the formation, but also from the borehole. A second challenge is to isolate the elemental yields from the formation from the contribution of elements from the borehole, cement, or other sources. Models to correct for borehole geometry, mud compositions, and other conditions must be considered before final yield-to-weight conversions are calculated (**Fig. 8.35**).

The solution is generally an under-determined one as the number of elements measured is generally less than the amount required (Harvey et al. 1992) especially with low neutron capture cross section elements (e.g., Al, Mg). The traditional approach continues to be to input the geochemical data as well as additional log inputs from conventional logs into a least squares error minimization solver. However, these approaches are challenged by colinearity between minerals (Chakrabarty and Longo 1997; Jacobi et al. 2007).

The chemical composition of sedimentary rocks must relate to the constituent rock forming mineralogy. Estimating the presence and proportion of minerals from elemental data presents a non-unique solution where multiple combinations of minerals can be estimated from elemental data. Determining quantitative mineralogy in sedimentary rocks is particularly challenging due to the variability in

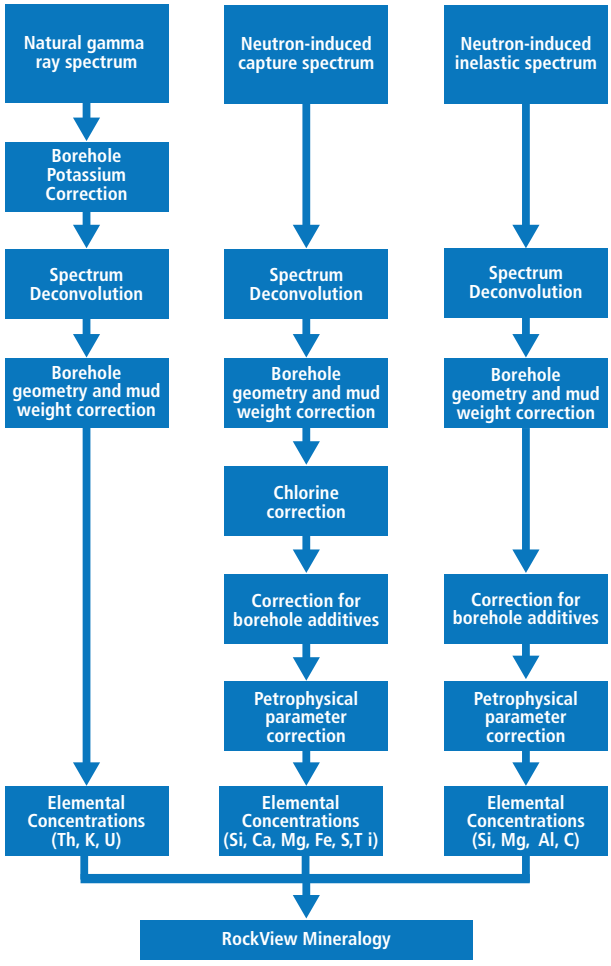

Fig. 8.35—Processing scheme for natural gamma ray, neutron induced capture and inelastic spectra for input into mineralogy estimation used in processing Baker Hughes FLeX and Spectralog data. (From Han et al. 2009.)

the composition of common clay mineral phases. The compositions of kaolin group phyllosilicates are normally constrained, but substitution of Fe^{3+} can occur. Smectite, illite, and chlorite group minerals can vary considerably in Ca, Na, K, Fe, and Mg concentrations.

Workflows that incorporate elemental weight fractions usually, but not always, are hybrid in nature. They incorporate a mathematical solver for some parameters and use deterministic empirical relationships involving calibration to core analyses results for others. If available the determination of the elemental weights should be compared to core XRF or ICP-MS core analyses.

8.4.2.1 Lithology and Mineralogy Determination Using Chemical Source Elemental Spectroscopy Logging Instruments

Chemical source elemental spectroscopy tools measure primarily in the capture gamma ray spectrum and consequently cannot directly measure carbon. The elemental weight fractions for Si, Ca, K, Mg, Al, Fe, and S may be input along with U, Th, and K from spectral gamma ray instruments and conventional log measurements of resistivity, density, neutron, and acoustic into a least squares error minimization solver. If available the selection of minerals to be input into the model is guided by study of XRD analyses for that individual well or XRD data from other wells in the same shale play reservoir. Some grouping of minerals is often used to reduce the number of output parameters that must be solved. The input for kerogen volume is obtained from basic regressions of core TOC weight fractions and conventional log measurements such as density, uranium, GR, or the Passey Δ log R method (Ramirez et al. 2011). **Fig. 8.36** illustrates the basic elemental spectroscopy probabilistic workflow.

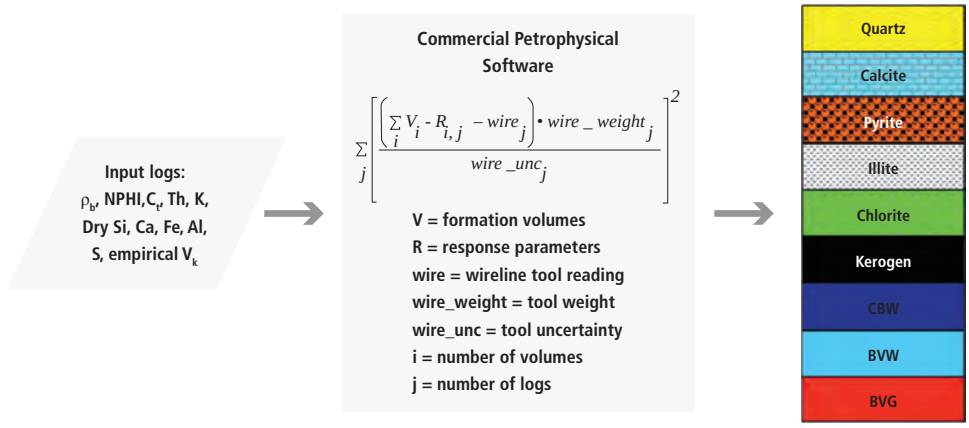

Fig. 8.36—Typical elemental spectroscopy probabilistic workflow. (From Ramirez et al. 2011.)

An alternative approach utilizes a deterministic suite of regression equations developed from an extensive core database of mineralogy and chemistry measurements to process the elemental weight percentages from Si, Ca, Fe, and S to solve for mineral volumes of pyrite, siderite, total carbonate (calcite + dolomite), total clay, and QFM (quartz + feldspar_ mica). Another regression equation is then used to determine the inorganic matrix grain density (Herron and Herron 2000, Herron et al. 2002). A mathematical solver is then used to determine kerogen volume, mineral volumes, porosity, and fluid saturations.

8.4.2.2 Lithology and Mineralogy Determination Methodology for the Baker Hughes FLeX and Spectralog Logging Sondes

The Baker Hughes pulsed neutron spectroscopy instrument, FLeX, uses a sequential deterministic Expert System, RockView™, to convert the measured elemental weight percentages to the most probable mineral weight percentage composition of the formation (Pemper et al. 2006, Jacobi et al. 2007, 2008, Pemper et al. 2009). This system uses a series of algorithms formulated from numerous ternary, hybrid ternary, and bivariate diagrams of the normalized oxides and ratios between oxides of the elements measured by the FLeX and Spectralog instruments (Pemper et al. 2006, 2009; Jacobi et al. 2007) to determine the general and specific lithology. **Fig 8.37** illustrates the processing workflow.

8.4.2.3 General Lithology

The RockView expert system applies the elemental algorithms in a three-step sequential manner to apply geologic constraints at each step to obtain the most probable mineral composition for each recorded data increment. First a general lithology is derived for each data increment using multiple ternary plots and elemental ratios. **Fig. 8.38** illustrates how major individual lithologies can be identified using a CaO, MgO, and SiO_2 ternary diagram.

Common sedimentary lithologies can be identified by the concentrations of MgO, CaO, and SiO_2 when plotted in a ternary diagram. The location of each lithology with respect to MgO, CaO, and SiO_2 provides a general indication to guide the RockView expert system. Carbonate and siliciclastic sediments are separated by the respective CaO and SiO_2 apexes. Dolomite is distinguished from limestone by the presence of MgO. Clay-rich shale lies along the SiO_2-MgO axes and is identified from quartz-rich sandstones by the increasing proportion of Mg-bearing clay minerals. The presence of calcite cement can be identified as clastic sediment plotting along the CaO-SiO_2 axis. Mixtures of rock types plot between the dolomite, limestone, sandstone, and shale endmembers. **Fig. 8.39** illustrates the RockView expert system workflow to derive a general lithology.

Additional general lithologies are identified using element ratios and other discriminant diagrams. Coal is identified by concentrations of C. High concentrations of K_2O and Th are used to identify the presence of igneous rocks. If an incremental data point is classified as none, it implies erroneous data in many cases due to wellbore conditions.

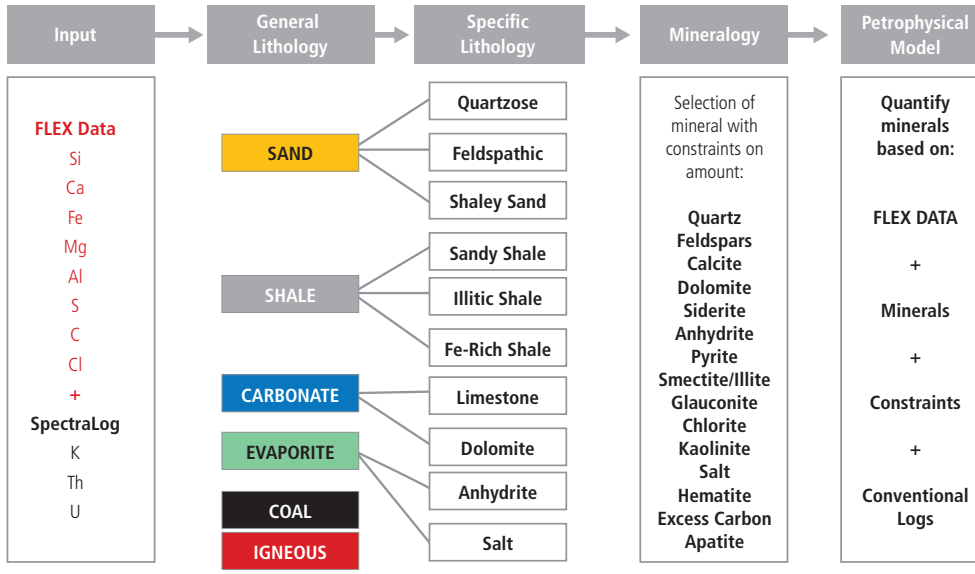

Fig. 8.37—The RockView Expert system workflow.

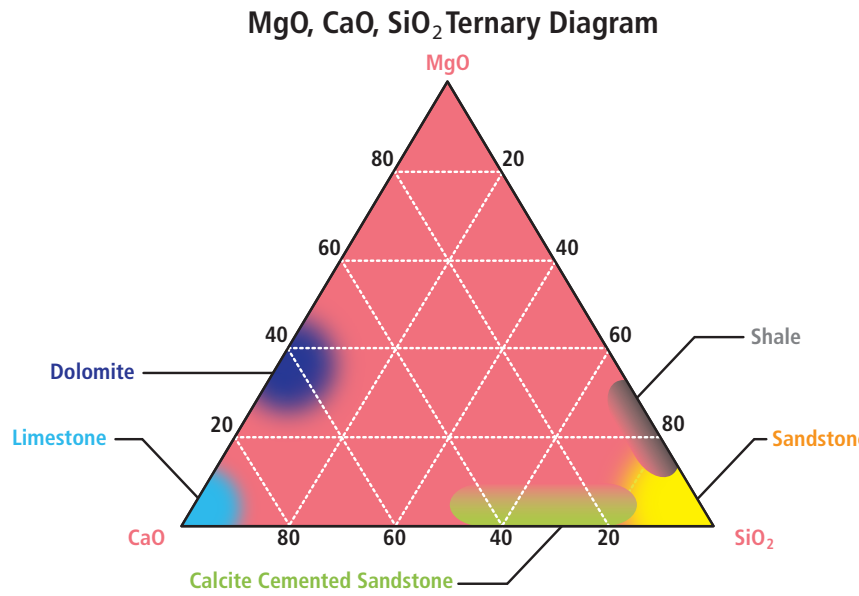

Fig. 8.38—Lithologies discriminated using an oxide ternary diagram. (From Pemper et al. 2006.)

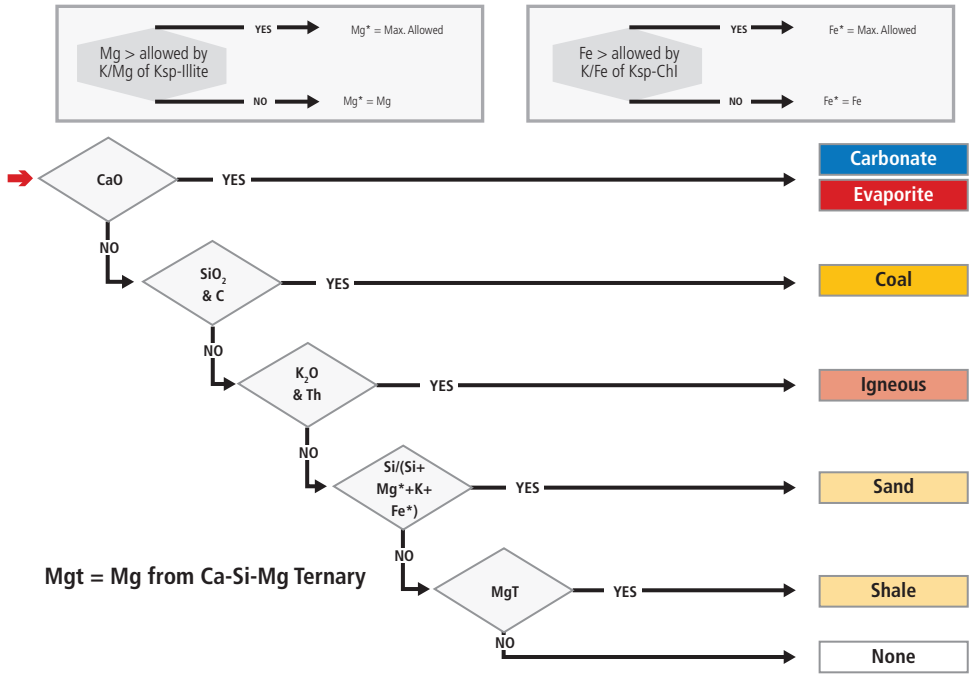

Fig. 8.39—Expert system workflow for derivation of general lithologies.

8.4.2.4 Specific Lithology

Hybrid ternary diagrams are utilized in the derivation of specific lithologies. Hybrid ternary diagrams differ from standard ternary plots in that they maintain the ratio of two oxides in the base but the vertical scale varies with the maximum of that component. The actual amount of the third component is plotted. **Fig. 8.40** illustrates the hybrid ternary plots used in the RockView expert system workflow. The K-Mg-Ca or K-Fe-Ca diagrams are the most useful to distinguish the non-carbonate or evaporite content. These six modified ternary diagrams are particularly useful because they provide guidance for many of the rules used to define the specific lithologies of sands and shales.

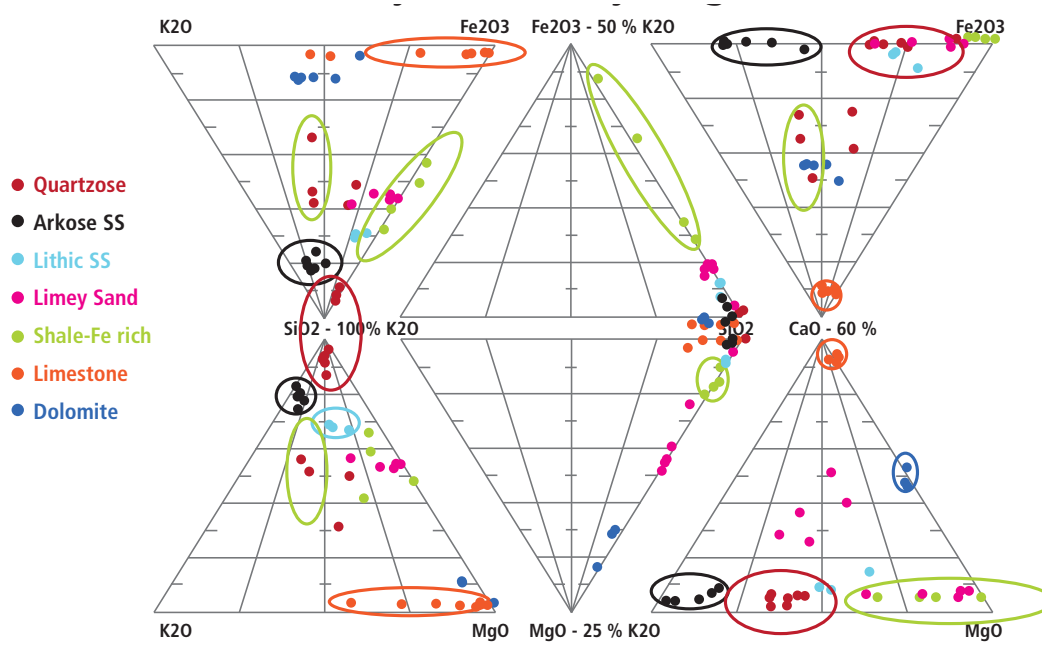

Fig. 8.40—Hybrid ternary plots used to derive specific lithologies.

Arkosic sandstones are generally formed from the chemical weathering of feldspar-rich protoliths primarily composed of quartz and feldspar that can be distinguished from quartzose sandstones composed primarily of quartz. Shales are further separated by the proportions of Fe-K-Si-Mg. Plots of Ca-S-Mg are used to separate carbonates and anhydrites.

A unique workflow is employed for each general lithology category to derive a specific lithology. **Fig. 8.41** illustrates the specific workflow for the sand general lithology category.

8.4.2.5 Mineralogy

Mineral composition is derived for each data increment starting from the derived specific lithology. Input from the Spectralog instrument that provides elemental data for potassium, thorium, and uranium measured in the natural gamma ray spectrum is also utilized in the expert system. Mineral identification using the potassium (K) and thorium (Th) relationships is shown in **Fig. 8.42**.

At each interval the elemental weight fractions of each element measured by the FleX and Spectralog instrument are allocated in a specific order honoring the principles of mass balance and mineral stoichiometry. **Fig. 8.43** shows the mineral derivation sequence used in the expert system. First K_2O is allocated to orthoclase feldspar, illite, or glauconite. The remaining elements (CaO, $Al2O_3$, Fe_2O_3, MgO, SiO_2, S) are then adjusted to preserve a mass balance. The expert system continues to allocate elements in a limiting order to determine the proportion of pyrite, anhydrite, calcite, dolomite, chlorite, hematite, siderite, plagioclase, kaolinite, and quartz. The resulting mineral composition and input elemental weight fractions are compared, if available, to XRD and XRF or ICP-MS core analyses. Significant differences are investigated including a review of input mud composition data. The elemental concentrations input for the minerals would be checked against any available data for that formation and basin to investigate if a variation in one or more mineral's elemental composition differed from that utilized in the initial processing. If needed the processing would be modified and rerun.

8.2.4.6 Volumes

The ending point of the workflow is a derived mineral weight percent composition. Combining these mineral weight percentages with total porosity values allows them to be converted to volumetric percentages for inclusion into traditional petrophysical models. **Fig. 8.44** shows the equations used to perform the conversion of mineral weight fractions into mineral volumetric fractions.

In this conversion the mineral volumes computed for minerals with a lower grain density will increase over their derived mineral weight percent. The volume percentage for TOC with a grain density ranging from 1.0 to 1.5 gms/cc

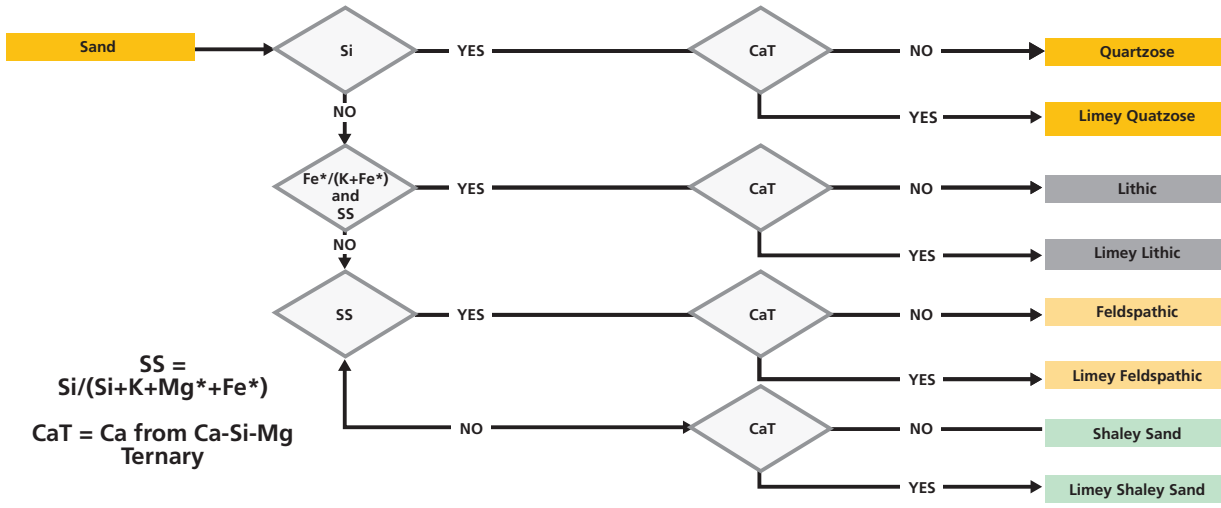

Fig. 8.41—Expert system workflow for derivation of sand specific lithologies.

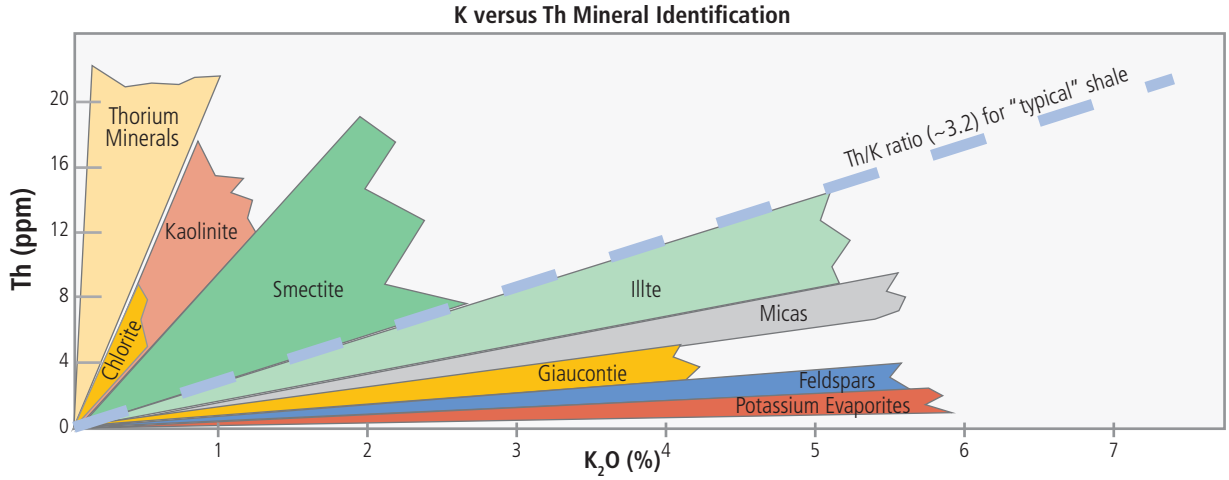

Fig. 8.42—Mineral identification utilizing Spectralog potassium and thorium responses.

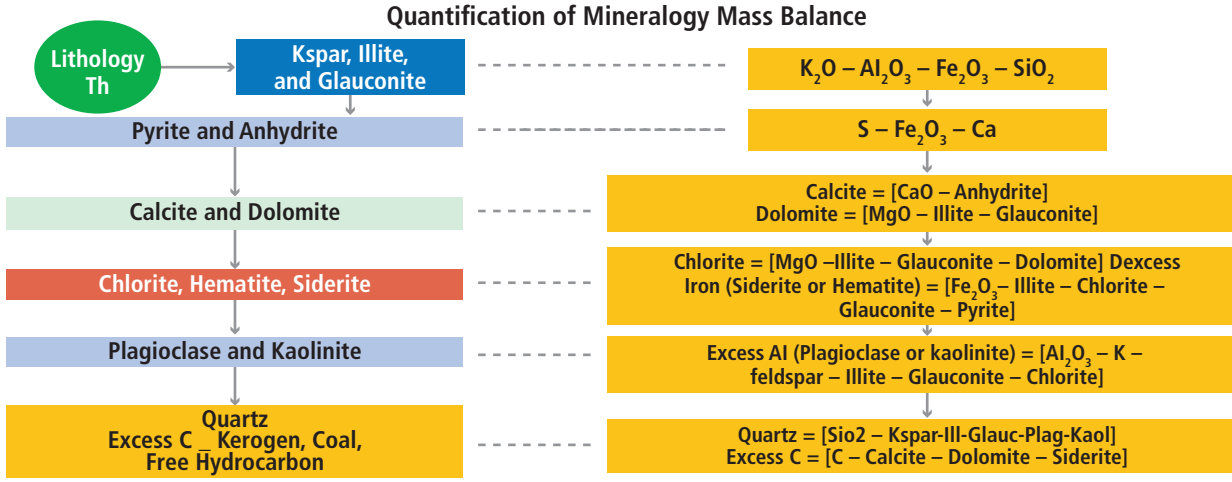

Fig. 8.43—Expert system mineralogy derivation sequence.

Converting mineral weight fractions to volumetric fractions

$$V_{rock} = \sum\left(\frac{Qtz}{2.65} + \frac{Calc}{2.71} + \frac{Dolo}{2.87} + \ldots + \frac{Mineral}{Density}\right)$$

$$\varphi = \frac{V_{fluid}}{V_{total}} = \frac{V_{fluid}}{V_{rock} + V_{fluid}}$$

$$V_{fluid} = \frac{V_{rock} * \varphi}{1 - \varphi}$$

$$V_{total} = \sum\left(\frac{Qtz}{2.65} + \frac{Calc}{2.71} + \frac{Dolo}{2.87} + \ldots + \frac{Mineral}{Density}\right) + \frac{\sum\left(\frac{Qtz}{2.65} + \frac{Calc}{2.71} + \frac{Dolo}{2.87} + \ldots + \frac{Mineral}{Density}\right) * \varphi}{1 - \varphi}$$

$$V_{QTZ} = \frac{Qtz}{2.65 * V_{total}} \ldots$$

$$V_{CALC} = \frac{Calc}{2.71 * V_{total}} \ldots$$

$$V_{MINERAL} = \frac{MINERAL}{DENSITY * V_{total}} \ldots$$

$$V_{fluid} = V_{fluid}$$

$$V_{QTZ} + V_{CALC} + V_{MINERAL} + \varphi = 1$$

Fig. 8.44—Methodology for conversion of RockView mineral weight fractions to mineral volumetric fractions.

will essentially double. The volume percentages for those minerals with a grain density in the range of 2.6 to 2.7 gm/cc will remain essentially the same while the heavy minerals such as pyrite, hematite, siderite, and apatite compute lower volume percentages than their derived mineral weight percentages.

The expert system is unique in that it derives mineralogy directly from the geochemistry measurements of the FLeX and Spectralog instruments without the requirement of additional logging response inputs. The number of minerals that can be derived is not limited to a specific number as is the case when using least squares error minimization solvers. This allows minerals that are present in small amounts but that may provide valuable insight into stratigraphic or depositional characteristics to be identified along with the major mineral constituents. **Fig. 8.45** shows the standard colors and patterns used to identify the general and specific lithologies and mineralogy derived from the expert system.

Fig. 8.46 is an example of a standard RockView mineralogy deliverable for unconventional shale reservoirs from the Woodford shale in Oklahoma. The plot presents the measured elemental weight percentages from the FLeX instrument (Track 8, Track 9, Track 10, and Track 11), the total GR and KTH corrected GR (Track 1), potassium and thorium weight percentages (Track 6), and the uranium ppm measurement (Track 7) from the Spectralog instrument. The general and specific lithologies are presented in Track 14 and Track 15 and the derived mineralogy in Track 16. Note the variation in the excess carbon weight percentage (Track 12), which in this well has been classified as the TOC weight percentage. To improve interpretation of this reservoir conventional log measurements of the caliper (Track 2), resistivity (Track 4), density and compensated neutron porosities, and the inorganic grain density computed from the RockView expert system mineralogy (Track 5) are included. A brittleness indicator based on variation in the mineral composition is also included in

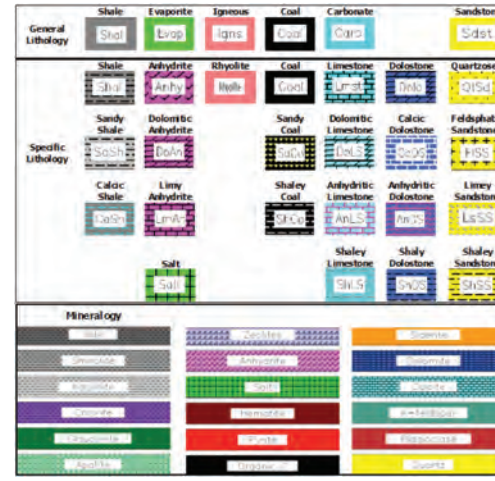

Fig. 8.45—Standard colors and patterns for general and specific lithologies and minerals for output plots of RockView product deliverables.

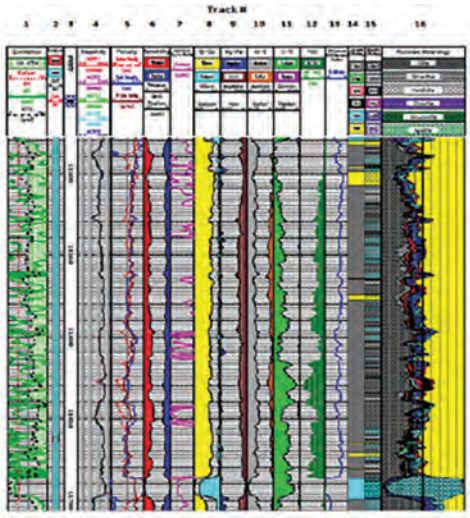

Fig. 8.46—Woodford shale example of standard RockView plot deliverable for unconventional shale reservoirs.

Track 13. This type of indicator can be computed using various combinations of minerals. In this well the customer requested one where the total weight percentage of quartz plus feldspars was divided by the total of all minerals plus organic carbon. Twelve mineral components have been derived in this Woodford shale interval.

8.4.3 Lithology and Mineralogy Characteristics of Unconventional Source Rock Reservoirs

Fig. 8.47 contrasts the mineral composition between three North American shale plays, as defined from pulsed neutron elemental spectroscopy log measurements.

Unconventional mudstone reservoirs exhibit a high level of variability in mineralogical composition, organic carbon content, fabric, and texture both vertically and laterally reflecting depositional environment changes which occur in stacked parasequences related to eustatic sea level fluctuation. These transgressive-regressive sequences reflect alternating deposition occurring between shallow/oxic and deeper/anoxic environments. Many of these observed variations are directly related to their position in these parasequences (Slatt et al. 2008; Passey et al. 2010). The variations are also a function of the proportion of biogenic versus detrital sediment input to the basin (Walles 2013; May and Anderson 2014). Mudrock systems can be classified into those intrabasinal, which are composed of biologic dominated sediments generated near in-place and below storm base levels, and those extrabasinal, which are dominated by external sourced fine-grained components with specific flow regimes (Walles 2013) (**Fig. 8.48**).

This variability in mineral composition, organic carbon richness, fabric, and texture as well as the depositional environments results in variation in mechanical properties and pore structure within the mudrock both of which impact reservoir productivity. Intervals that exhibit the most favorable mechanical properties are often those with a load-bearing brittle framework. Higher biologic silica content shown in several plays, the Barnett, Woodford, and Marcellus, provide a more brittle lithofacies fabric. This is more conducive to hydraulic fracture initiation and development of a more complex fracture network associated with higher productivity than detrital silica (Jacobi et al. 2008, 2009; Blood et al. 2013).

To determine those most favorable to hydraulic fracture stimulation, an integrated study must be conducted to understand and map the vertical and areal distribution of variations in mineral composition, TOC richness, fabric, and texture, i.e., lithofacies, and the mechanical properties of each. This study requires a careful description of whole core and outcrops and associated core analyses to identify the stratigraphic cycles existing in the play and to construct a methodology to accurately delineate those lithofacies and parasequences using well log and seismic responses in uncored wells and areas lacking any well control. Intervals that exhibit the most favorable mechanical properties are often those with a load-bearing brittle framework. In extrabasinal reservoirs that are dominated by detrital sediment input, the more favorable intervals are frequently third-order highstand

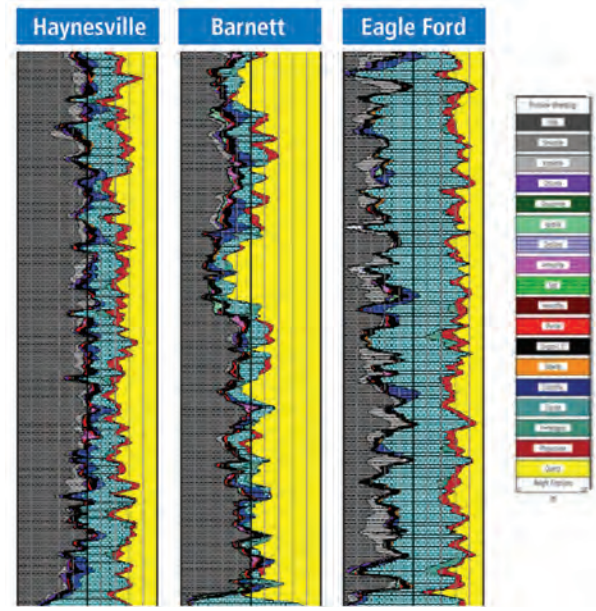

Fig. 8.47—Variation in mineral composition for three North American shale plays.

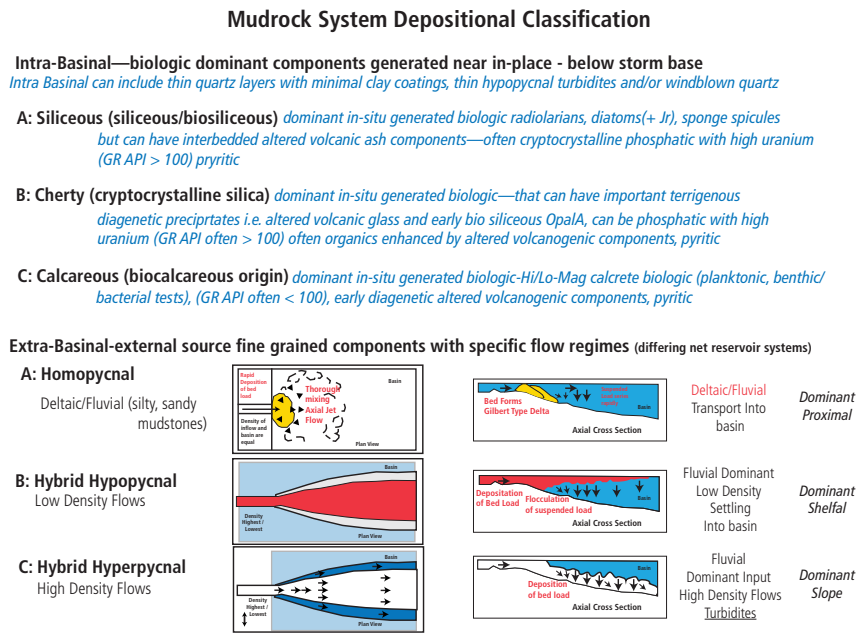

Fig. 8.48—Mudrock system depositional classification characteristics. (Modified from Walles 2013.)

or lowstand with silica influx, composed of detrital clay, and silt or highstand carbonate influx, from the platform margin, or lowstand carbonate influx (from eroded terrain). The more favorable intervals in intrabasinal plays where the input is dominantly biologic are frequently high frequency, third-order condensed sections with high TOC and lower clay composition (May and Anderson 2014).

A variety of core analysis measurements and well log responses can be utilized to identify the parasequence features. One approach is organic carbon richness that can be quantified with core analyses as well as well log responses. Organic matter is preserved when deposited in anoxic environments. The thorium/uranium (TH/U) ratio from spectral gamma ray instruments can be used as a chemostratigraphic method to identify organic-rich intervals and the elevated uranium content associated with it deposited in anoxic (marine depositional) conditions. This is opposed to a leaching continental depositional environment where the uranium would be flushed from the system. Plotting the uranium content along with the TH/U ratio allows the stratigraphic identification of regression and transgressive cycles as the high spike of uranium indicates a change from a transgressive to regressive sequence (Jacobi et al. 2009) (**Fig. 8.49**). The amount of uranium concentration is only indirectly related to the TOC richness. This relationship appears to be more reliable in intrabasinal plays as opposed to extrabasinal depositional environments.

In intrabasinal plays such as the Eagle Ford, significant increases in TOC content often occur in condensed sections (**Fig. 8.50**).

XRF and ICP-OES/MS bulk elemental concentrations are utilized in the determination of lithofacies and stratigraphic characterization in a variety of ways. They can reflect lithological changes, identify intervals with increased detrital composition, identify oxic dysoxic and anoxic paleoenvironments (**Fig. 8.51**), and TOC richness. Elevated levels of Mo, V, and U are utilized to identify intervals where significant organic accumulation occurred under anoxic conditions. Trace elemental concentrations of Ni and U can be related to TOC weight percentage (Martinez-Kulikowski et al. 2013).

Elemental ratios are utilized for correlation and indicators of terrigeneous and detrital quartz composition. Among these controls the Th/Al ratio can be related to clay mineral changes. The Zr/Al ratio serves as a proxy for zircon content, which is used as a proxy for terrigeneous, detrital quartz input. A positive increase in Zr concentration with increasing quartz (SiO_2) concentration is indicative of a terrestrial source for the quartz. A decrease in Zr with increasing quartz is indicative of a biogenic quartz origin (**Fig. 8.52**) (Wright et al. 2010).

The relative hydrocarbon potential (RHP) is a computed parameter from Rock-Eval pyrolysis (S_1+S_2)/TOC. This has been used to identify transgressive and regressive

parasequences related to fluctuations in sea level. **Fig. 8.53** Illustrates reasonable agreement of the interpretation of RHP methodology to a core derived sequence stratigraphy and relative sea level fluctuation interpretation for the Barnett shale. Of important note, S1–which is directly proportional to current hydrocarbon saturation, and S2– which is directly proportional to remaining hydrocarbon potential–are representative of the kerogen types and the maturity state (transformation ratio) of those kerogens. Relating these relationships to sea level changes assumes first-order relationships, which may not be representative of the actual controlling conditions of the organic productivity, organic preservation, and the levels of kerogen transformation.

8.4.3.1 Lithofacies Identification

Unconventional shale reservoirs can be roughly grouped into three types: siliceous mudrocks, calcareous mudrocks, and argillaceous mudrocks. Ternary plots of the total weight percentage of clay, total amount of carbonate, and the total

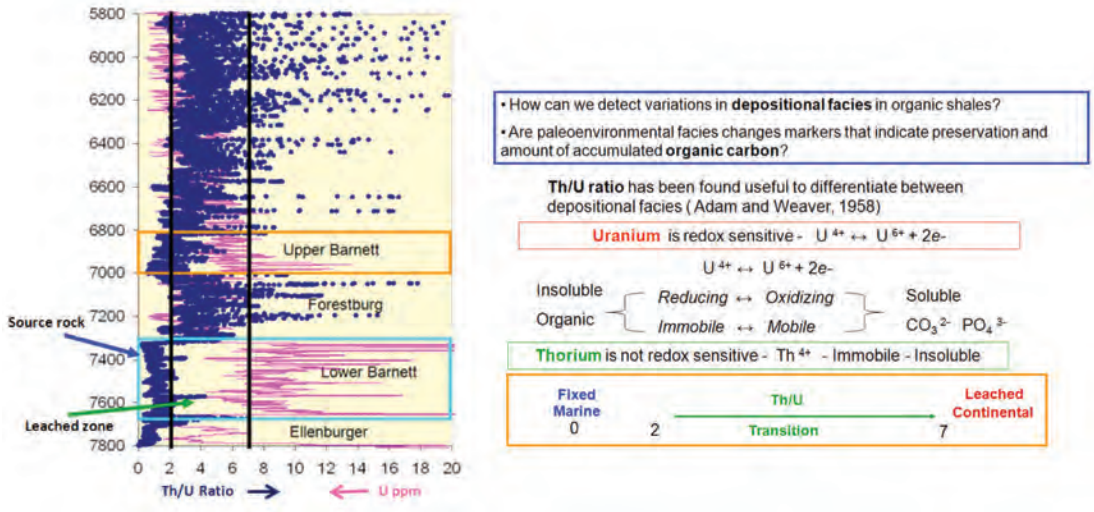

Fig. 8.49—Plot of the Th/U ratio versus uranium concentration in a Barnett shale well identifying the organic rich intervals and delineation of sequence stratigraphic features.

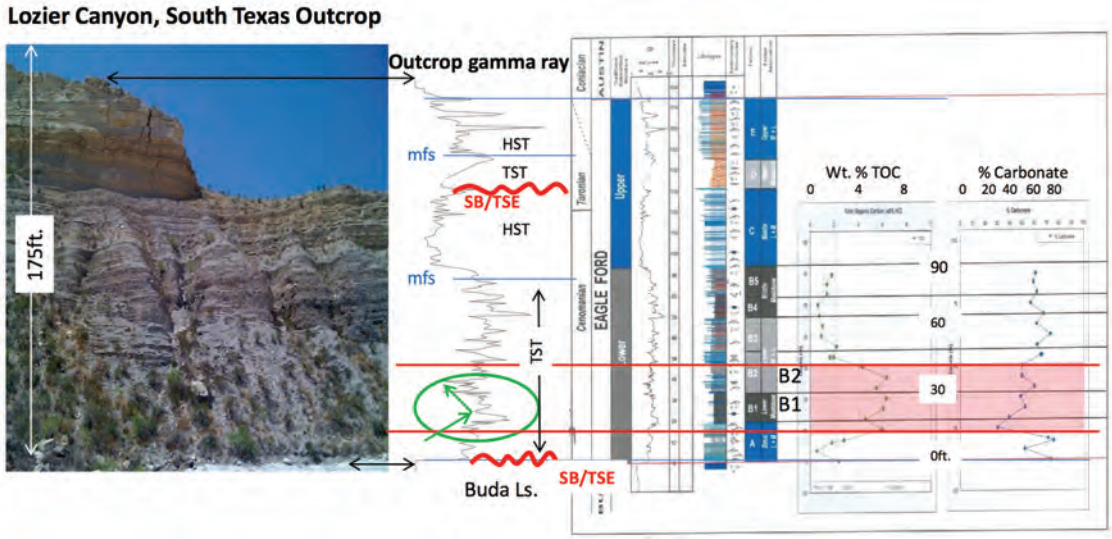

Fig. 8.50—Increased TOC weight percentages observed in a condensed section interval within the Eagle Ford shale. (Modified from Slatt et al. 2012.)

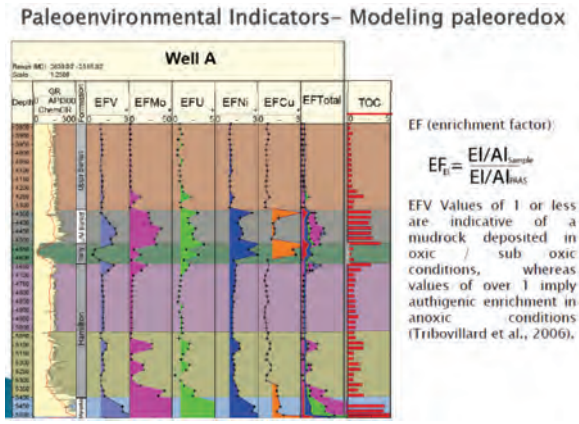

Fig. 8.51—Plot of XRF or ICP-OES/MS elemental enrichment factors in the Marcellus shale for identification of TOC weight percentages and paleoenvironments indicators. (Modified from Martinezz-Kulikowski et al. 2013.)

amount of quartz and feldspars are used to examine the variation in mineral composition between or within a given shale reservoir (**Fig. 8.54**).

Researchers have noted that variations in mineralogy in source rock reservoirs often reflect dissimilarity in mechanical properties. For many North American shale plays, several authors or core consortium groups have developed multiple lithofacies schemes. A representative set of lithofacies can be developed for each shale play using the available conventional log measurements, elemental spectroscopy, TOC weight percent from either LECO core analyses, regression from log responses or pulsed neutron elemental spectroscopy, core or cuttings derived XRD, and description of whole core and thin sections. Each adopted lithofacies should exhibit a similar mineral composition and organic carbon richness and be identifiable in multiple wells. A variety of approaches have been used to define lithofacies in certain shale plays. Some focus more heavily on core examination and analyses, some use more limited amounts of core combined with conventional logging responses, elementary spectroscopy data as well as seismic data (Wang and Carr 2013) (**Fig. 8.55**). The selection of which approach to use and how detailed the system can be predicated on the amount and types of core, core analyses, and log information available. As a starting point, a thorough review and comparison of any existing classifications should be conducted.

Fig. 8.56 shows the mineral composition distribution of a lithofacies scheme and the associated workflow from a relatively simplistic scheme developed for the Haynesville shale. The simplistic scheme was used because the data available for this study was primarily pulsed neutron elemental spectroscopy derived mineral with a small amount of XRD core analyses.

After the mineral variation has been examined and a tentative lithofacies classification organized a statistical study of a variety of mechanical rock properties is performed for each lithofacies type. Mechanical properties examined would include Young's modulus, Poisson's ratio, unconfined compressive strength, and minimum horizontal stress. The specifics of this step are covered in a later section of this chapter.

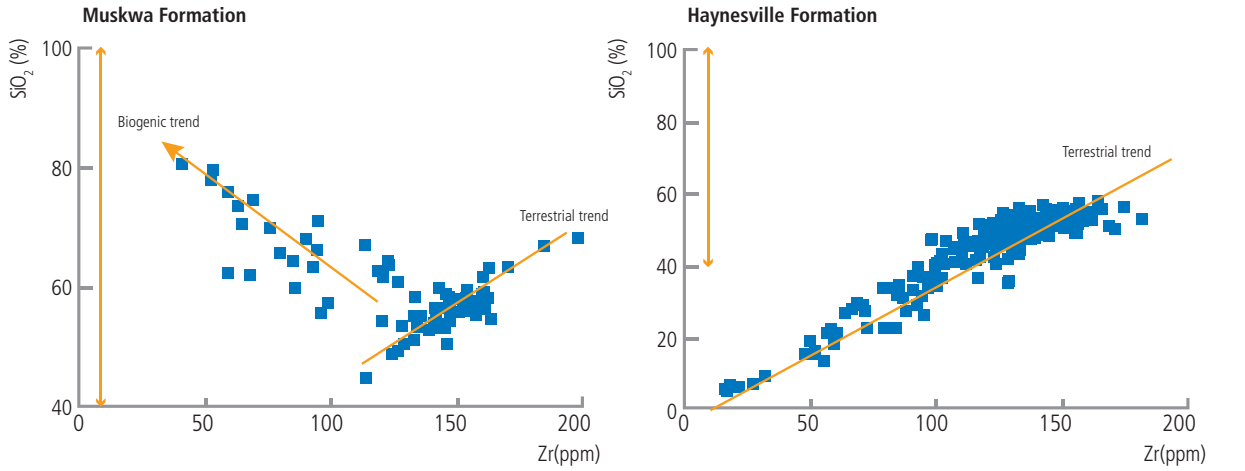

Fig. 8.52—Crossplots of the Zr versus SiO_2 concentration from two North American shale plays indicative of a detrital or biogenic quartz origin. (Modified from Wright et al. 2010.)

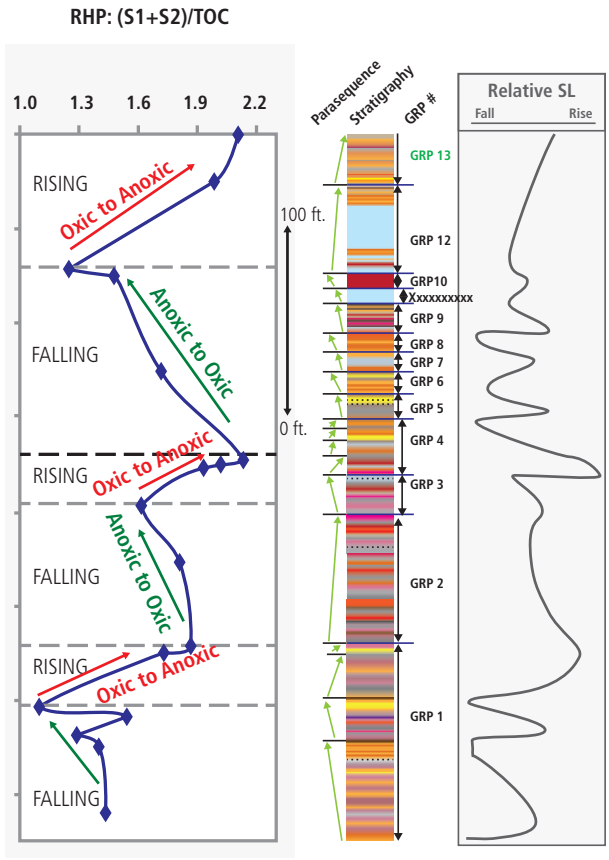

Fig. 8.53—Comparison of transgressive and regressive sequence patterns in the Barnett shale between RHP results and a core-derived sequence stratigraphic interpretation. (Modified from Slatt et al. 2008.)

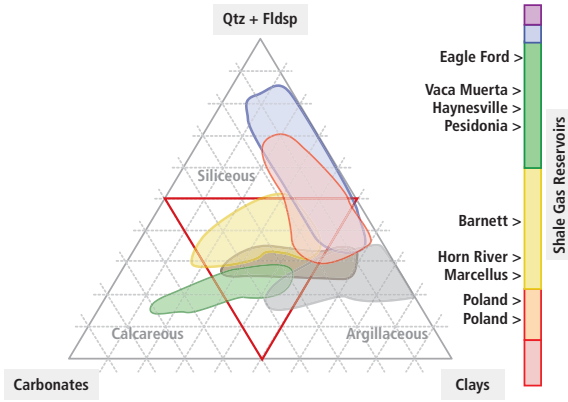

Fig. 8.54—Varying mineral composition for selected North American and international shale reservoirs ranging from siliceous to calcareous and argillaceous. (Modified from Passey et al. 2012.)

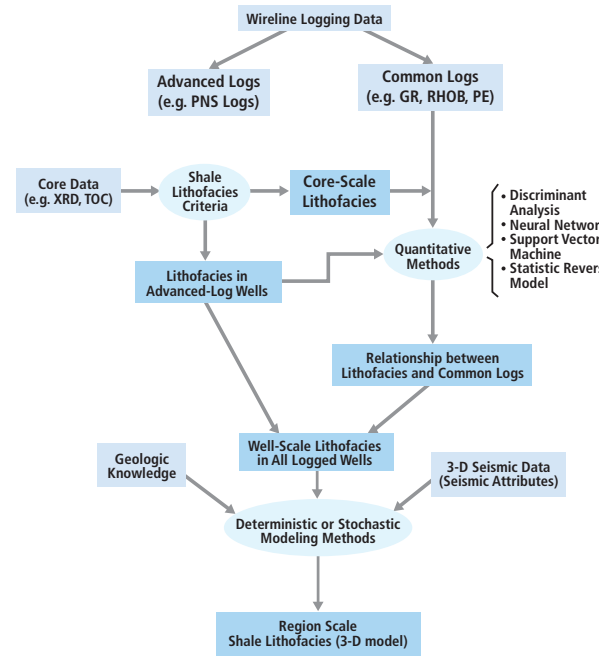

Fig. 8.55—Lithofacies determination workflow used to define the Marcellus shale. (From Wang and Carr 2013.)

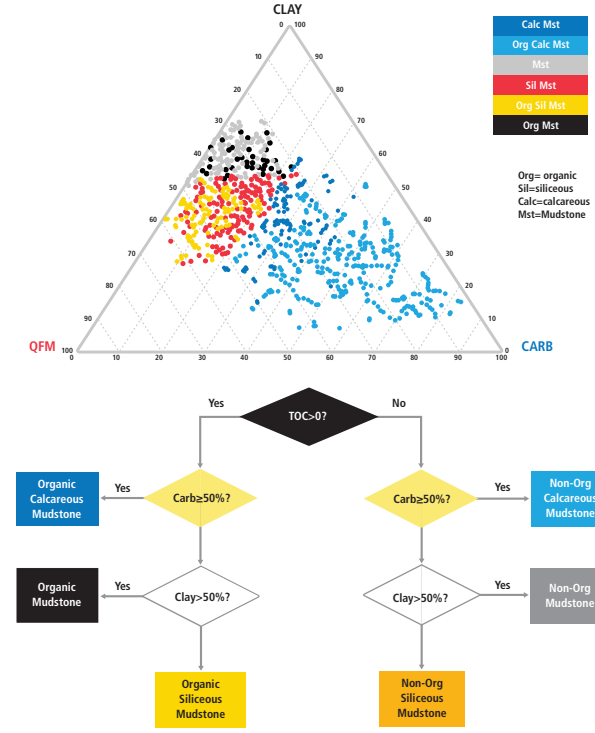

Fig. 8.56—Lithofacies determination workflow used to characterize the Haynesville shale.

8.5 Porosity Determination

8.5.1 Characteristics of the Porosity Systems in Unconventional Source Rock Reservoirs

Mudrock porosity systems have been poorly understood within the literature and within the hydrocarbon industry for many years. Accepted geologic models proposed complete porosity destruction due to the prevailing accepted understanding of clay compaction and clay diagenesis processes. This was reinforced by available petrologic imaging (thin sections to SEM technologies upon rough surfaces), which exhibited little to no porosity observation (**Fig. 8.57**).

Mudrocks were, with general industry acceptance termed shales, considered to be compositionally homogenous, deposited within a low-energy depositional setting with a dominantly detrital (extra-basinal) clay origin composition (as a prevailing siliclastic delta model system). This shales model is still a prevailing model within the general population and large portions of industry.

Due to the historical lack of productivity, mudrocks were not specifically characterized for detailed porosity characterization or evaluated properly as to origin and composition due to lack of applicable technology. The accepted industry model began to change with the HC production associated with the early successful unconventional resource plays, especially the Barnett shale.

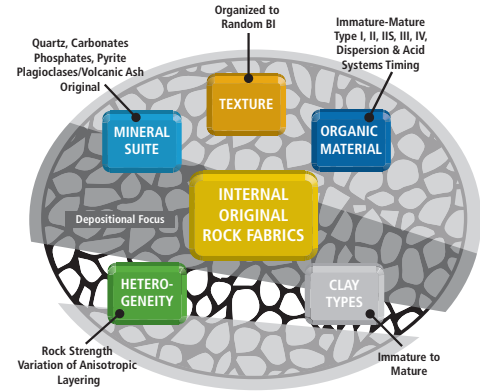

Fig. 8.57—Original-defining components of mudrocks. (From Walles 2013.)

Hydrocarbon source rock systems were also very poorly understood due to the lack of associated production, except in the presence of tectonic fractured systems. In addition, the understanding and imaging at a pore scale of the physical processes associated with the transformation of organic kerogens was also limited. Appropriate imaging technologies were also not available until the early 2000s.

Mudrock porosity destruction processes have been documented through the literature to begin very early just post deposition with diagenesis and cementation related to the often initial mudrock composition state of 70% + water and the other fine materials. Near surface- to deep-subsurface clay alteration/ transformation processes were shown to be dominant. Most

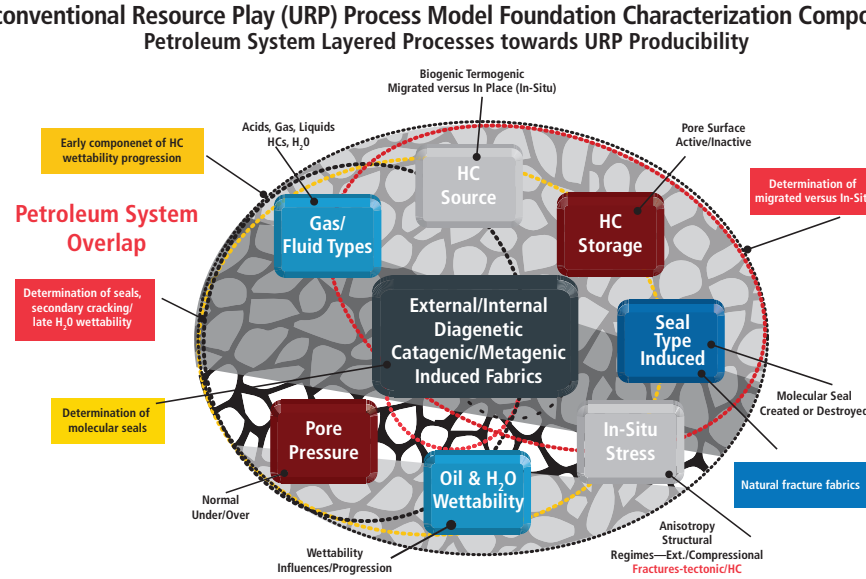

Fig. 8.58—Petroleum system overprint processes of mudrocks. (From Walles 2013.)

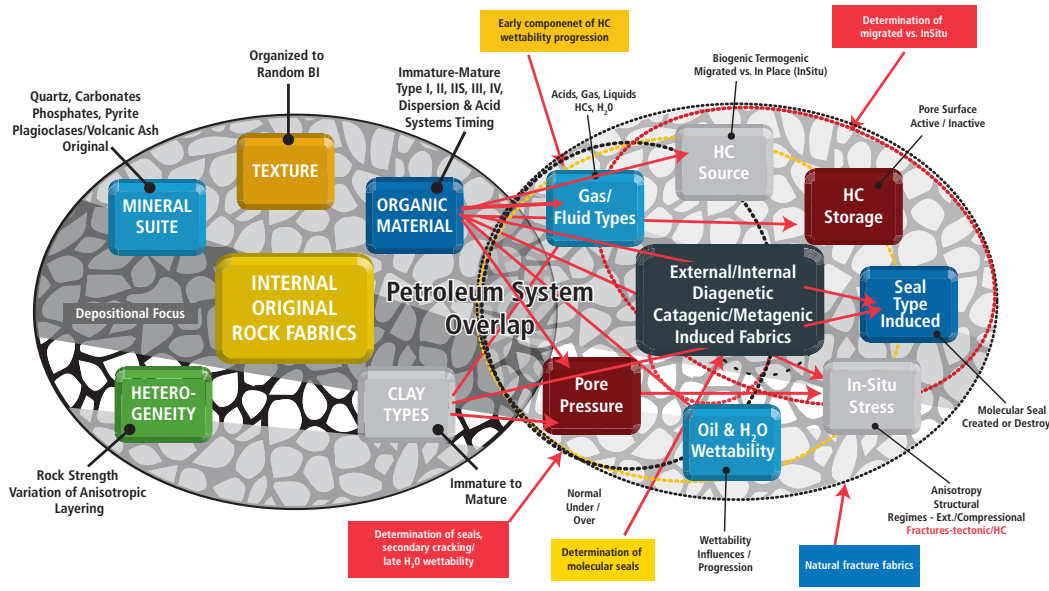

Fig. 8.59—Original mudrock components with petroleum system overprint processes of mudrocks. (From Walles 2013.)

of the post-depositional alteration processes of fluid loss with compaction were shown to destroy the majority of porosity. Early organic and inorganic acids resulting from thermal-burial diagenesis to deep-burial diagenesis were also proposed to be involved in available porosity destruction.

Geopressured shales were encountered while drilling within the subsurface. Accepted geopressure models indicated that the dominant geopressured origins are related to under-compaction associated with either rapid burial and inefficiency of water expulsion related to the transformation of mixed layered clays to ordered clays (illite—as from montmorillinite/ mixed layered clay to illite transformation).

Deeper geopressured shales were encountered below these clay transformation boundary regions. However, geopressure origins were either assigned to under-compaction due to high-water content or to hydrocarbon expulsion inefficiency within the petroleum systems. No matrix porosity systems were considered to be present.

Modern-day investigations have significantly changed the understanding of mudrock reservoirs systems. These understandings include fundamental process understanding changes related to mudrock system classifications to mudrock origin(s), energy systems, matrix porosity systems and types, microbiologic inputs and controls, compositional variances, kerogen variances and controls, petroleum system components and controls including seals, system mixing, and pressure controls (**Fig. 8.58**).

The industry has realized that many separate geologic processes impact mudrock porosity generation and destruction within mudrock reservoirs.

The reservoir defining components occurring within a mudrock reservoir begins with the foundation mudrock components as determined by the associated depositional processes. These include the original mineral suite, the kerogens, the clay types, the texture (ordered/mixed), and heterogeneity (sequences). Those of special significance include the non-clay constituents (elemental and mineralogical) as well as defining the biologic system components.

Defining geologic processes that control mudrock porosity generation are generally processes that are dominantly part of what is defined as petroleum system overlap geologic processes (**Fig. 8.59**).

The petroleum system processes that overlap and define porosity and hydrocarbon producibility within mudrock unconventional play reservoir systems include controls such as: the specific kerogen type (activation energies and structure) transformation as an HC source; the HC storage as either in situ or migrated; the fluids, inorganic/organic processes affecting the ability to displace water within nanoscale pore systems to irreducible/ sub-irreducible levels as defined through wettability influences and progression; the specific gas and fluid types, including inorganic acids and organic acids affecting porosity genesis and diagenesis; the induced pressure system(s) through time including expulsion inefficiency by matrix, secondary cracking processes and micro fracturing with associated (diagenetic) sealed or unsealed nature within and defining the petroleum system(s); the spatial distribution of developed high-quality (specific HC transmission opaque) top, bottom, and lateral seals including the capacity for specific mixing of the petroleum system(s); and the in-situ stress systems as defined by the full basin paleotectonic history (uplift, compression, extension, transpression) developing fluid induced fracture systems as well as impacts on the thermal system (including thermal conductivity of formation sequences) affecting kerogen rate transformation.

Unconventional resource play (URP) mudrock porosity systems have been poorly characterized. This is in large part due to the previous physical (petrologic imaging method) inability to characterize and measure the most significant nanoscale porosity variance of complex porosity systems. This especially is relevant when including organic kerogens (as well as mixed hydrogen quality types from amorphous to structural fabric types). These complex kerogen systems may include kerogen-derived bitumen, which can also exhibit its own separate porosity system.

Another poorly understood component has been the characterization of free and adsorbed hydrocarbons (HCs) within these complex kerogen systems. Advances in the understanding of adsorbed and free gas systems from coalbed methane system characterization (a Type III structured kerogen type endmember) has been part of the advances needed for the characterization of these molecular scale storage component systems within multiple kerogen components.

Advanced applied reservoir characterization technologies are required to characterize these complex reservoirs systems, due to the multiple overlapping porosity generation and destruction processes, as well as the nanoscale size nature of these systems.

Hydrocarbon productive porosity systems of unconventional resource plays, within source rock—mudrock reservoirs—exhibit a combination of up to four dominant types of nanoscale inter-connected porosity reservoir systems. Dominant observed pore sizes range from 0.5 nanometer (nm) to 100 nanometers (nm) but can range as large as 1 micrometer (μm). Inter-connected pore throats can often be even smaller with throat sizes often less than 50 nanometers (nm). The observation, as well as the direct measurement, of these dominant associated nanoscale porosity systems is a reservoir distinction that contributes significantly to hydrocarbon producibility of unconventional resource plays.

Within these nanoscale reservoir porosity systems, hydrocarbon transport, as well as both free and adsorbed hydrocarbon components, interact within molecular level relationships. These fluid and gas transport relationships, as well as the advanced characterization of each nanoscale structure porosity system within each mudrock target system, are under ongoing extensive investigation by research scientists of industry, government, and universities.

In severely confined settings such as less than < 50 nanometer pore size, the oil and gas phases can be in a metastable state, which can suppress the bubble-point pressure in oil or enhance the dew-point pressure in gas condensate reservoirs. Nanoscale pore throats and their net diameter size distribution may also have a hydrocarbon composition fractionation impact on deliverability within the unconventional resource play.

The flow of fluids may not follow the conventional Darcy's law due to the relatively higher impact of molecular diffusion as the mean-free path of the molecules approaches these nanometer-sized pore throats.

Through the application of advanced technologies, specifically argon ion beam milling for 2D SEM sample preparation and FIB-SEM for 3D image volumes, these nanoscale porosity systems can be visualized and quantified. Nanoscale pore throats, especially less than eight nanometers, may limit transport to the hydrocarbon saturates (C5 to C7). These small pore throats can cause filtration of the larger molecules, thus leading to osmotic pressure differences. Net nanoscale pore volume relationships related to net pore throat size distributions may impact the net composition of the produced hydrocarbons and may not be directly related to system maturity.

8.5.1.1 Nanoscale Porosity Systems

Nanoscale porosity systems within mudrocks are not capable of being visualized in an unaided advanced technology setting. **Fig. 8.60** illustrates that these systems are at a pore size distribution between viruses and proteins.

Through the application of advanced technologies, specifically the focused ion argon mill beam (FIB) sample preparation technique in combination with advanced SEM technology (FIB SEM), these nanoscale porosity systems can now be imaged. Advances within FIB SEM technology are occurring and include instrumentation and ion mill beam advances that are providing imaging to the 1 nm scales and smaller. This allows the characterization of extensive porosity systems within the 1-to-2 nm size range.

Observed nanoscale scale mudrock porosity systems can be specifically defined as intrakerogen (organic); interparticle (inorganic dominant); intraparticle (inorganic dominant), and fractures–tectonic (external stresses) or hydrocarbon related–genesis or degradation related (internal stresses). Many mudrock URPs exhibit mixed components of these porosity type systems.

The three critical non-fracture type matrix-level porosity systems observed within a mudrock URP can be spatially displayed within a ternary display plot as a net distribution spatial point of these porosity types. See an example with red points in **Fig. 8.61**. These three major subtypes include kerogen pores, interparticle pores, and intraparticle pores. Specific URP target reservoir level pore systems can be dominated by one type.

Ongoing FIB SEM investigations of multiple unconventional resource plays, of their nanoscale microstructure fabrics of the mineral matrix, organic matter distribution, and pore networks, has determined that the organic matter (kerogen) system most often exhibits the dominant portion of the net interconnected porosity system. Mudrock from unconventional resource play reservoir systems often includes substantial nanoscale porosity systems within the kerogen, as well as within interparticle (often clays and clay types) and intraparticle fabrics (**Fig. 8.62**).

Each of these complex reservoir systems exhibits differential pore throat geometries, roughness, wettability, interconnectability characteristics, and adsorption to fluids (hydrocarbons and water) and gases.

This observation of correlation of mudrock producibility contribution to kerogen porosity systems continues to focus on the extensive characterization efforts toward the kerogen system of understanding of mudrock reservoirs.

Hydrocarbon flow within nanoscale porosity systems that exhibit < 50 nanometer pore sizes can be in the meta-stable state. This may suppress the bubble-point pressure in oil or may enhance the dew point in gas condensate reservoirs. The variation of surface chemistry of the rocks has been shown to

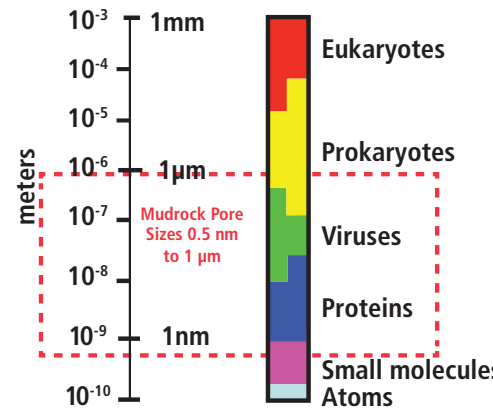

Fig. 8.60—Scale comparison of mudrock reservoir system pore sizes (.5 nm to 1 to 2 µm) to original kerogen origin microbial cells scale (original 200+ nm to 1mm). (Modified over Vickers and Vasconcellos 2006.)

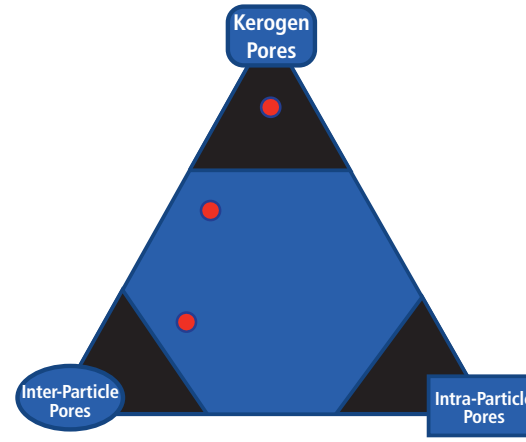

Fig. 8.61—Three mudrock non-fracture HC storage porosity systems. (From Loucks et al. 2010.)

affect molecular scale surface wettabilities of subsurface fluids. The flow of fluids within these porosity systems may not follow the conventional Darcy's law due to relatively higher impact of the molecular diffusion and as the mean-free path of the molecules as they approach the nanometer-sized pore throats.

Characterizing the types/subtypes and spatial distribution of porosity systems is a foundation for the prediction of spatial reservoir characteristics for the appropriate horizontal lateral well vertical positioning as well as the site-specific completion design program. Each type of reservoir quality/type/subtype system is expected to have a distinct set of production characteristics and optimum methods for an effective reach.

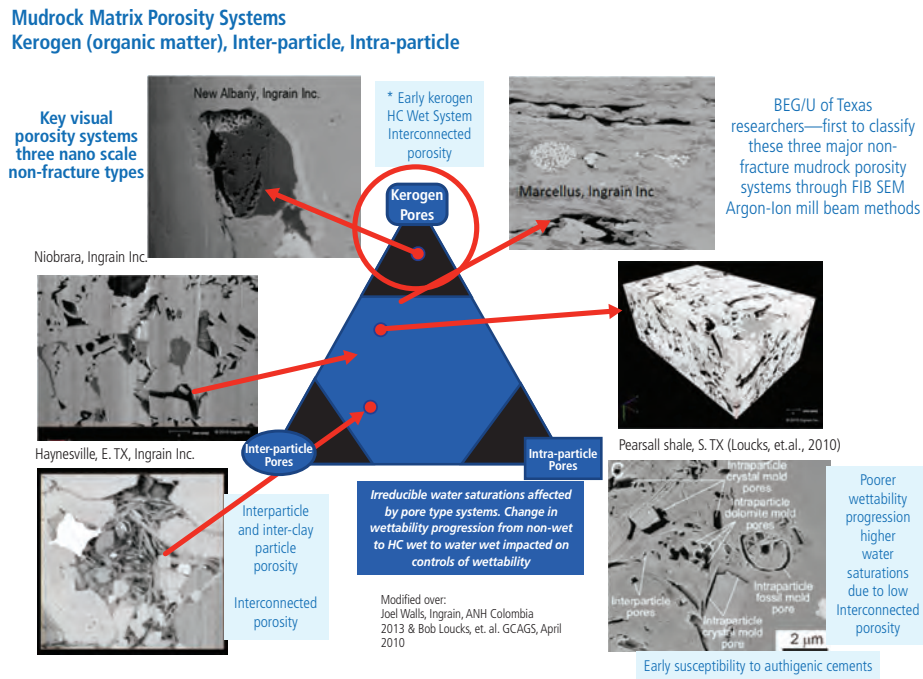

Fig. 8.62—Three non-fracture HC storage porosity systems. (Walls 2013; Loucks et al. 2010.)

Kerogen porosity systems have an origin tied to the transformation of the kerogens to bitumens and hydrocarbons. However, within mudrock reservoirs there can be extensive variation within kerogen types related to their origin (**Fig. 8.63**). The origin can be a specific microbial component family of life or from an original structured organic plant component. There can also be extensive mixing of kerogen types where activation energies associated with transformation to hydrocarbon liquids and gases can be highly varied.

Organic kerogen characterization is a critical field for the determination of the upscaling of spatial characterization of organic, as well as inter- and intraporosity within mudrock reservoirs. Specific organic kerogens also provide specific organic acids and the basis for specific inorganic acids that are involved in either the enhancement or destruction of mineral components and resulting inter- and intraparticle mudrock porosity fabrics within each of these systems.

Porosity type systems can vary both vertically and laterally. This variation depends on the original mudrock system constituents and fabrics including microbial or structured kerogen) types and mudrock system origin—biologic or external dominant components, as well as from the post-depositional system processes (near surface to subsurface depth compaction and hydrologic, to deeper subsurface petroleum and tectonic processes).

Kerogen porosity systems (**Fig. 8.64**) include three observed major subtypes:

- Pendular (bubble) porosity systems often related to the catagenic oil window with associated early phase bitumens.
- Spongy character systems often associated with the gas window (metagenic transformation level).
- Intrakerogen fracture system found in both the catagenic and metagenic transformation levels and or kerogen types.

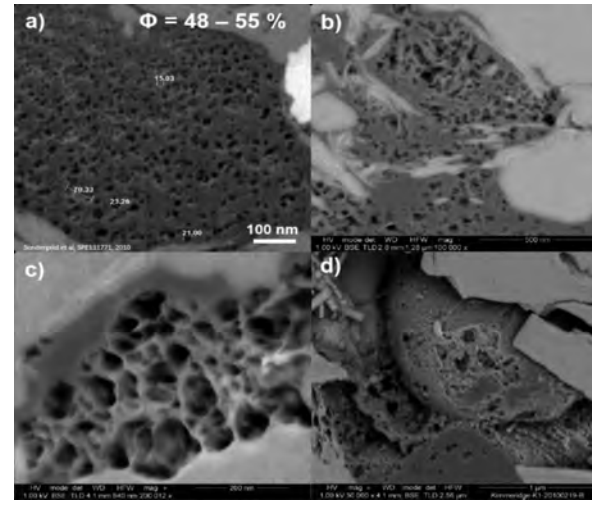

Fig. 8.63—Example nanoscale structure porosity fabric systems within kerogen from FIB SEM imaging. (From Curtis et al. 2011.)

An example (**Fig. 8.65**) of pendular (bubble) subtype kerogen porosity illustrates a porosity character that is often found within the liquid kerogen transformation oil window (black oil to volatile oil phase). Kerogen types have significant impact in transformation to hydrocarbons and the resulting volatization/transformation remaining space.

Fig. 8.66 illustrates an example of spongy subtype kerogen porosity often associated with wet to dry gas window high-level kerogen transformation. Kerogen types again have significant impact in transformation to hydrocarbons and resulting volatization/transformation remaining space.

Fig. 8.67 shows an example of fracture subtype kerogen porosity that can be associated with the full range of kerogen transformation from oil to dry gas window. Kerogen types do have a significant impact in transformation to hydrocarbons and the resulting volatization/transformation remaining space. Kerogen porosity subtypes may be important in the interconnection and resulting permeability within the system.

Researchers have identified at least three subtypes of kerogen porosity systems, and some are associated with specific oil window transformation (pendular subtype). This interconnection within these porosity systems for hydrocarbon producibility may be functions of a combination of these subtype systems. Within source rock systems, a major efficiency consideration has been the determination of hydrocarbon expulsion efficiency. Different kerogen types and resulting kerogen porosity subtype systems may be an important component of the retention processes related to hydrocarbon fluid and gas and water saturations. These considerations may be important, both vertically and lateral spatially, with respect to producibility variances tied to kerogen porosity systems within specific mudrock systems.

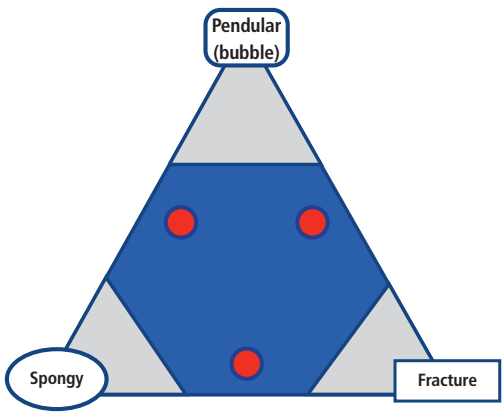

Fig. 8.64—Three major kerogen porosity systems. (Modified over Walls et al. 2013.)

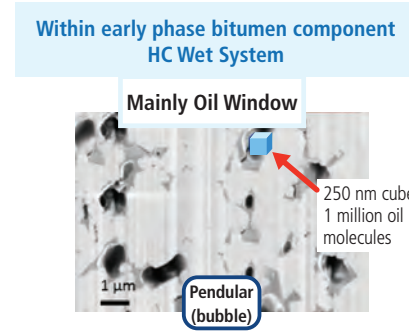

Fig. 8.65—Pendular (bubble) subtype kerogen porosity associated with early phase bitumen component HC wet system, possible type IIS kerogen example. (Modified over Walls et al. 2013.)

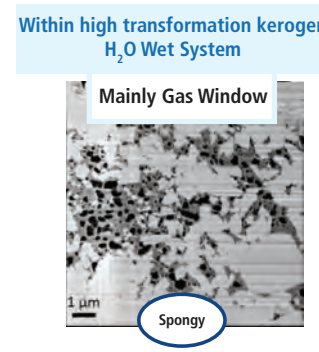

Fig. 8.66—Spongy subtype kerogen porosity often associated with wet to dry gas window high-level kerogen transformation, possible Type II kerogen example. (Modified over Walls et al. 2013.)

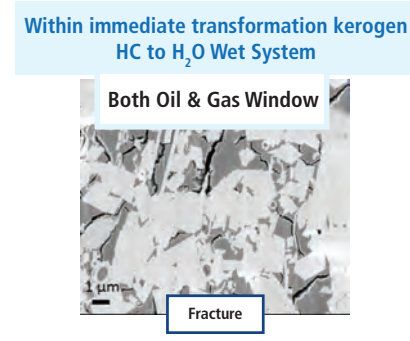

Fig. 8.67—Fracture kerogen porosity often associated with oil and gas window level kerogen transformation. (Modified over Walls et al. 2013.)

Active ongoing investigation in characterizing organic kerogen systems with regard to kerogen types (Type I, Type IS, Type II, Type IIS, Type IIIc, Type IIIv, and Type IV) with resulting kerogen porosity subtypes corresponding to varying transformation ratio levels (10 – 95 + percentage) is developing a better porosity characterization knowledge of kerogen specific transformation within catagenesis (kerogen to HCs) and metagenesis processes (alteration of HCs).

Mudrock porosity systems can often have specific porosity type dominance (**Fig. 8.68**) related to the specific mudrock facies related to formation age, biota (microbial to non-microbial), and depositional facies.

Interparticle porosity systems are normally associated with specific mineral components within mudrock systems. These particles can include biologic skeletal components (siliceous, carbonate, phosphatic); inorganic extrabasinal sand/silt grains (often windblown or volcanic ash materials related); and or clays (mixed layer clays, illites, kaolinite, chlorite, or other complex mineral materials. These systems can exhibit ranges of surficial properties that can directly affect hydrocarbon deliverability and recovery.

A FIB SEM example (**Fig. 8.69**) of interparticle and inter-clay particle porosity highlights the complexity (pore throat size distribution/interconnectivity) that can be associated with these systems.

Intraparticle porosity within mudrock systems can be significant. However, this type of porosity is often considered to have limited interconnection and or associated reservoir permeability. Due to their lack of observed isolated pore connections, these pores may very often exhibit poorer hydrocarbon saturations due in part to their inability to displace prior pore fluids such as water. Surface wetness properties may be poorly developed due to the non-connection to the system pore fluids and gases. **Fig. 8.70** illustrates such a dominant pore type system from the Pearsall shale in south Texas.

Many Paleozoic-age unconventional resource play target systems such as the Barnett and Woodford can have 90 to 95% dominant kerogen porosity systems. Other unconventional resource play systems such as the Eagle Ford often have variances of 30 to 50% kerogen porosity systems, 30 to 70% interparticle systems, and 10 to 30% intraparticle systems. **Fig. 8.71** shows the range of the pore system types within a series of representative FIB SEM images of nine unconventional resource play mudrock systems.

The characterization of the porosity, including pore size, pore throat sizes, smoothness, geometry, and inter- or intraparticle components and their distribution requires advanced nanoscale characterization technologies such as focused ion beam (FIB)/scanning electron microscopy (SEM).

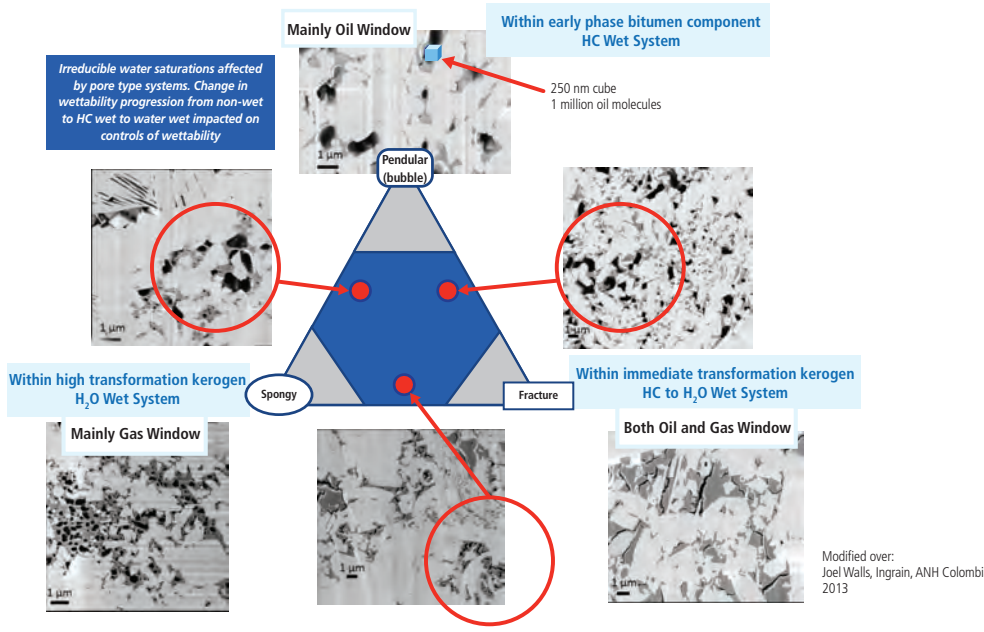

Fig. 8.68—Three major kerogen porosity systems. (Modified over Walls et al. 2013.)

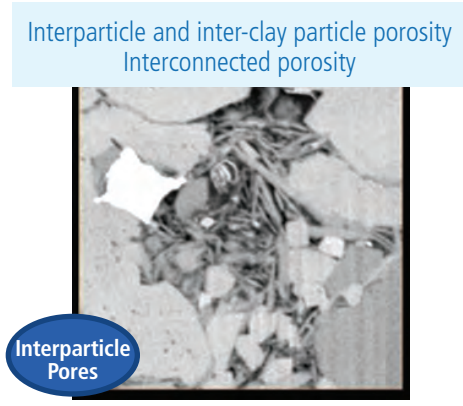

Haynesville, E. TX, Ingrain Inc.

Fig. 8.69—Example Haynesville shale interparticle and inter-clay particle porosity. (From Walls et al. 2013; Loucks et al. 2010.)

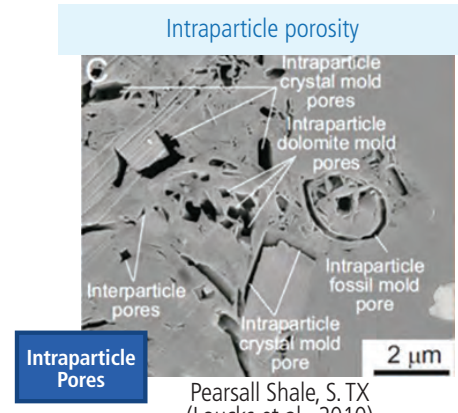

Pearsall Shale, S. TX
(Loucks et.al., 2010)

Fig. 8.70—Example Pearsall Shale, south Texas intraparticle porosity. (From Loucks et al. 2010.)

Advanced nanoscale porosity characterization methodologies, including 3D FIB SEM, have further defined interconnected nanoscale porosity systems of mudrock reservoirs. This work illustrated that the degree of interconnection of the pore systems can also be highly variant. In addition, the size of the pore throats can often be much smaller than the pores. An example of this advanced characterization of the degree of pore interconnectivity (**Fig. 8.72**) illustrates the significant potential of lack of interconnectivity and resulting permeability.

Within commercial laboratories 3D FIB SEM evaluation streams are now able to mathematically calculate porosity volumes as well as system permeability based upon the specific representative sample. Critical limitations are the volume of area of investigation and the number of samples representing a net formation contribution. However, with considerations of assumptions, estimates can be made that have a greater degree of confidence and data support.

In addition to this interconnectivity challenge there is also a net reduction of pore size to pore throat size distribution (**Fig. 8.73**). Issues related to pore size and pore throat sizes, and net interconnectivity of the pore system are also impacted by larger hydrocarbon molecular sizes (length and width), especially aromatics, resins, and asphaltenes.

Within these nanoscale pore system reservoir systems, complex overprinting fracture systems have been documented. As illustrated above, evidence indicates a kerogen nanoscale fracture type even within the kerogens.

Two dominant fracture type/origin porosity systems are observed within mudrock unconventional resource plays.

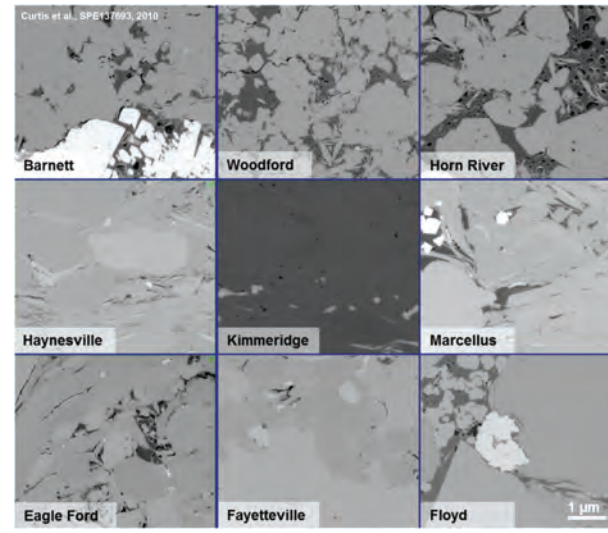

Fig. 8.71—Example of FIB SEM 2D slices of nanoscale porosity system of various formation mudrock target systems. (From Curtis 2011.)

These include subvertical/vertical fracture porosity systems caused by the tectonic/external system stress that can often have a significant pressured fluid origin and horizontal/sub-horizontal hydrocarbon geopressured (exceeding overburden vertical pressure) origin fracture systems (**Fig. 8.74**).

A combination of these fracture system major types can also occur, as example, where within regional compressional systems, the horizontal hydrocarbon geopressured fracture systems exhibit weak surficial properties and can often become the horizontal slippage tectonic induced décollment surface.

Fracture systems occur from macroscale to microscale and even the nanoscale and can exhibit open, closed, and partially open-system properties. These fractures can have a combination of origins and orientations that are related to tectonic stresses (3D stresses including overburden, as well as horizontal). They also can have bedding parallel (**Fig. 8.75**) that can be in-situ hydrocarbon generation (catagenesis of kerogens and bitumens) as well as degradation of hydrocarbons (metagenesis of existing hydrocarbons) related.

Fracture systems most often do not exhibit significant hydrocarbon/fluid storage capacity, most often at best 0.5% or at most 1.0%, but they are believed to have a likely impact on porosity system interconnectivity within a mudrock reservoir porosity system (often 2 to 6% net porosity).

The net fracture network (fabric) of the natural fracture systems of these two dominant process origin systems will define:

- Subvertical macrofractures corresponding to a tectonic fluid based origin related to tectonic forces that are $\sigma 1$ and $\sigma 2$ dominant with stress system Modes I extensional, Mode II compressional, and or Mode III trans-pressional/trans-extensional out-of-plane shear.
- Horizontal microfractures, often bedding parallel/anastomosing to the kerogen/bitumen distribution (**Fig. 8.76**), within a dominant in situ generated active/paleo hydrocarbon generated overpressure system exceeding overburden stress ($\sigma 3$). Expulsion inefficiency within a high-quality level (gas-level quality seals) sealed system enhances the extent of these types of horizontal microfracture fabrics.

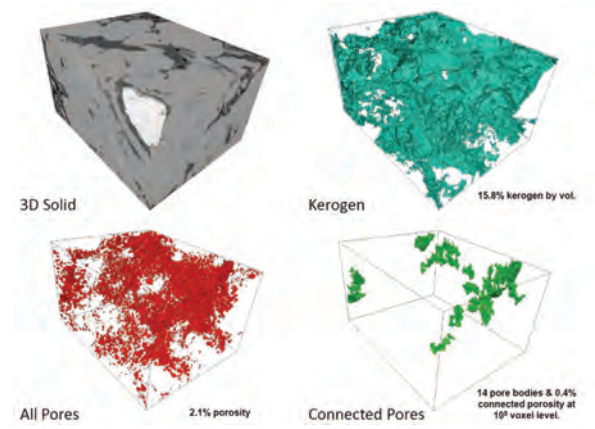

Fig. 8.72—3D FIB-SEM of example pore system interconnectivity. (From Curtis 2011.)

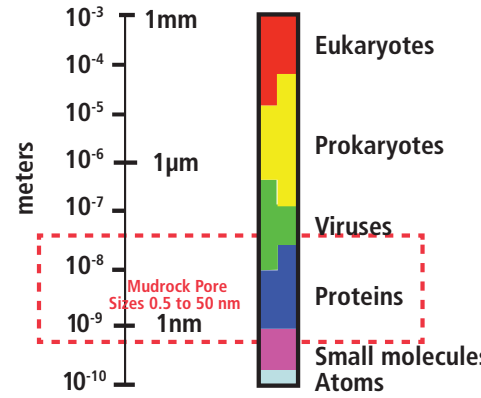

Fig. 8.73—Range of mudrock pore throat sizes. (Walles modified over Vickers and Vasconcellos 2006.)

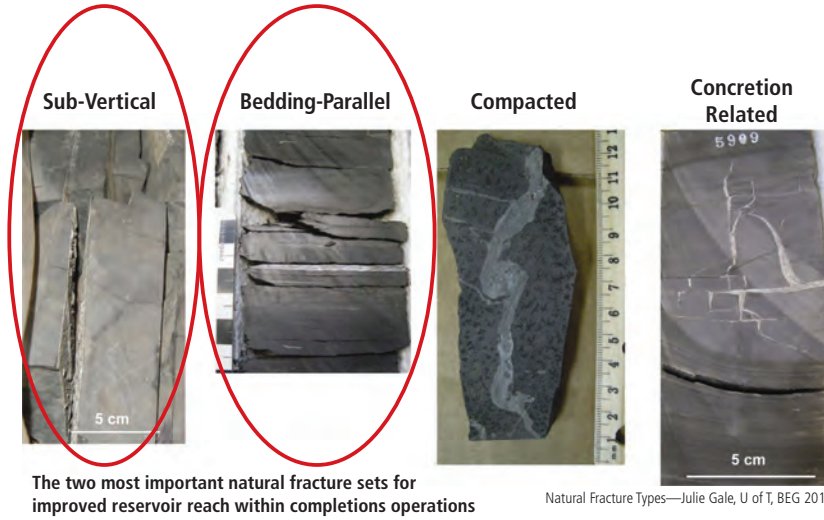

Fig. 8.74—Four natural fracture types with two most important to completion operations. (Gale 2013.)

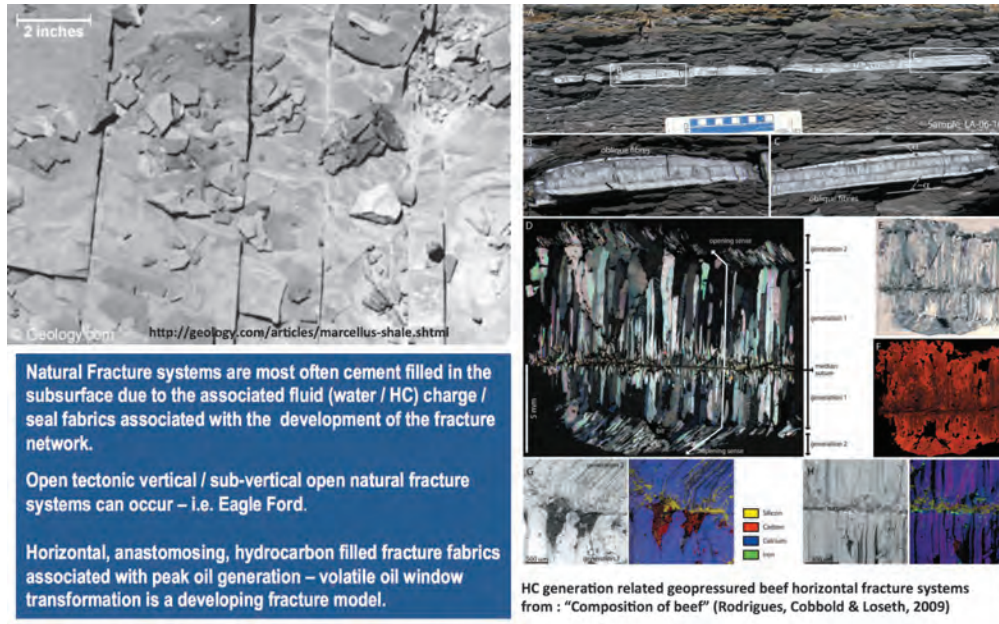

Fig. 8.75—Two major dominant types of natural fracture systems and origins–tectonic and hydrocarbon generated. HC generation-related geopressured beef horizontal fracture systems from: Composition of beef. (Rodrigues et al. 2009.)

Fracture porosity systems and their influence on producibility within mudrock systems have been a source of significant debate within the mudrock reservoir characterization community. Much effort has been spent in developing discrete fracture network (DFN) fracture models for reservoir simulation models, as well as for completion models. A higher-quality DFN model can be developed with the proper integration of cores, wireline and wireline image tools, LWD, and LWD image tools tied to wellsite analytic datasets, especially quantitative fluids and gases in relationship to rate of penetration that illustrate fracture sets.

Awareness and identification of these outlined fracture types is of critical importance within ramp-up and development stage programs. Understanding fracture cement fills and genesis can also have design considerations of completion approaches and target selection.

Fracture porosity system characterization tools encompass a range of technologies including wireline and LWD imaging advances, CT core scanning, micro CT scanning of cores (**Fig 8.77**), and various core sample petrographic thin section techniques including methods utilizing fluorescence technologies. These methodologies are most often utilized within whole core evaluation/investigation projects particularly in the pilot and ramp-up phase evaluations within mudrock systems.

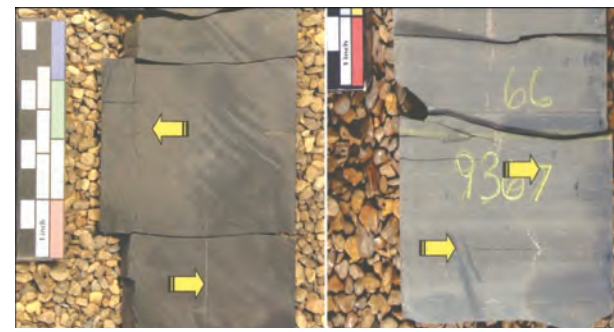

Fig. 8.76—Bakken example of hydrocarbon generation related microfracture fabrics exhibiting horizontal anastomosing fabrics. (From Pollastro et al. 2008.)

8.5.1.2 Core Analyses to Determine Pore Types

Multiscale reservoir characterization (outcrop, wireline, LWD, cuttings, cores) that utilizes technologies from advanced microscopy to CT to SEM to FIBSEM integration requires relational observation methods for well or field scale integration (Huang 2013). High imaging magnifications of nanoscale pores within mudrock pore systems is a further narrowing of investigation area, in comparison to micro to macro investigation scales. Mosaic image processing techniques of linking multiple images may assist in improving this limitation of representative investigation areas.

Imaging analyses to determine the characteristics and geometries of the three dominant mudrock pore types (kerogen, interparticle, and intraparticle) require investigative characterization tools that can specifically image pores from 1 nanometer to 200 nanometers.

For this imaging to be possible, surfaces such as rock mineral and organic kerogen must be prepared. They must be perfectly flat at this scale with no artifact of surface processing processes imparted on the sample investigation surface. All prior techniques of thin-section preparation with abrasive materials and or fluids created large volumes of sample preparation artifacts within mudrocks.

The available advanced technology tool of choice to prepare these surfaces is argon or gallium ion mill beaming equipment. Most instruments use liquid-metal ion sources (LMIS) and often gallium ion sources. FEI and Zeiss are two significant equipment manufacturers of this type of equipment and accompanying software that allows the preparation of surfaces through ion beam ablation. This equipment has been incrementally derived from the application of the advanced manufacturing of nanoscale electronic circuitry within silicon chips.

Focused ion argon/gallium mill beam (FIB) sample preparation technique in combination with advanced scanning electron microscopy (SEM) technology (FIB SEM) to image these nanoscale porosity systems was effectively championed to industry in the 2000s by R. Reed, K. Milliken, and S. Ruppel, research scientists with The University of Texas Jackson School of Geosciences/Bureau of Economic Geology. This technology is now utilized in many of the commercial, industry, and university laboratories that determine characteristics of mudrock organic and mineral relationship related nano porosity systems.

The application of focused argon/gallium ion mill beam has the critical advantage in that it allows the preparation of perfectly flat sample surfaces with minimal artifacts of porosity related to sample preparation. This includes delicate clay fabrics of mineral interparticle porosity as well as intraparticle mineral porosity. The ability to incrementally slice surfaces with none of these artifacts allows the generation of 3D imaging of mudrock porosity systems.

Focused ion-beam scanning electron microscopy uses a focused (gallium or argon) ion beam (FIB) to cut parallel, evenly spaced slices in combination with SEM imaging. This allows for the development of 3D datasets (**Fig. 8.78**). Depending upon equipment, slice thickness can be as low as 3 nm. Currently, 10 nm thicknesses is the standard for mudrock sample analyses.

FIB SEM imaging can have an artifact called curtaining, or laminations in the cross section shown as vertical bands in the SEM image. This is due to the different material removal rates of these heterogeneous materials under the ion beam.

Mudrock surfaces tend to be prone to extreme surface charging under the electron beam of the SEM that can complicate image acquisition. Traditional SEM methods to mitigate charging, such as coating a sample with a conductive layer (such as gold), cannot be used in that it can obscure and fill in the features of interest (porosity). Image artifacts can occur by SEM surface settings for image acquisition as a byproduct effect of accelerating voltage on the source of imaged electrons.

Advanced equipment designs utilizing low-accelerating voltages help prevent charge buildup that result in images without compromising resolution or contrast.

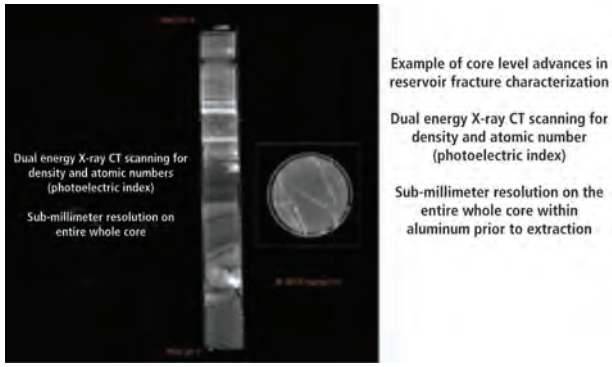

Fig. 8.77—Micro X-ray CT scanning for core fracture systems. (From Walls 2010; Walls and Armbruster 2012.)

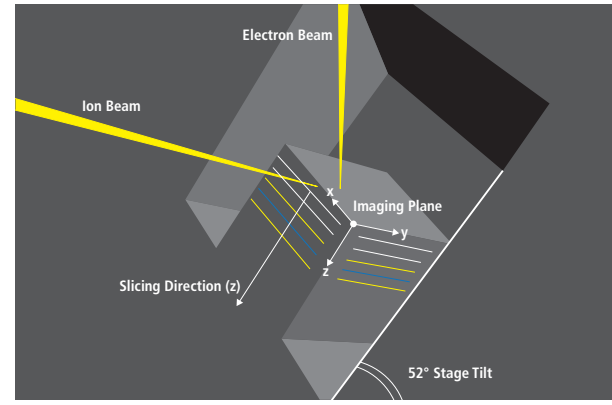

Fig. 8.78—Schematic relationships of the imaging plane with the dual beams of electron and ion beams. (From Holzer et al. 2004.)

Active technical advances within the FIB SEM technology, including SEM and ion mill beam advances, can provide imaging within the 1 nm scale.

Small volume area FIB-SEM datasets are often selected using full-core x-ray computed tomographic (CT) datasets to integrate the formation/core spatial positioning of the data (Walls and Sinclair 2011). Within a 1-in. core plug, a limited number of SEM images are often obtained to decide the important features for analysis, which is often only 1% of total area.

With higher resolution characterization of mudrock reservoir characteristics (SEM and FIB SEM), many important characteristics of the reservoir can be missed including the fabric heterogeneity and structural association (fluid diagenesis components). Tiling and stitching SEM images into mosaics may enable pore-scale resolution of the entire core plug surface into one image. This can also be useful prior to selecting the location of the FIB SEM spatial analysis position.

8.5.2 Core Analyses Utilized for Porosity Determination

Measurement of reservoir-relevant rock properties including that of pore characterization from wireline, LWD, core, and cuttings is especially challenging when handling very low-permeability nanoscale porosity (IUPAC classification for pore sizes) (Sing et. al. 1985) mudrock formations that exhibit micro, meso, and macro pore size distribution. This range of pore sizes, both within inorganic mineral matrixes and organic (kerogen), requires a combination of techniques to characterize the pore structures.

Laboratory measurement techniques include that of measuring radiation interferences and penetration of fluids and gases of subsurface derived samples for the determination of basic reservoir properties such as porosity. Many of these methods on mudrocks have been improved upon from previously developed special core analysis (including SCAL) of conventional tight gas sands and/or coals of coalbed methane (CBM) sample analysis procedures.

Many commercial labs are still developing applied experience and protocol techniques for unconventional mudrock reservoir characterization. Industry wants reliable, routine, and nondestructive techniques to characterize the pores to provide estimates of hydrocarbon in place and permeability. However, each of the current methods has limitations including time, cost, accuracy, and sample testing conditions.

Often, these procedures are still being done at surface state conditions (including altered states of pressure, temperature, oxidation, saturations, fluid inputs, etc.), rather than within applicable subsurface state conditions. Proper methods are in development for the appropriate conditions and methods of sample measurement.

Even storage conditions issues of handling samples (i.e., time, freezing, humid, arid, non-inert gas) can impart indicated erroneous reservoir artifacts. Many unconventional resource play whole cores can have at best a storage shelf half-life of less than three months for accurate fluid saturations, porosity, and permeability measurements.

A unconventional resource play reservoir includes a process-based definition of reservoir properties where water saturations have attained at or near irreducible saturation. Because this irreducible water saturation state can be reversible, especially at surface conditions, appropriate sample handling of subsurface samples as well as appropriate laboratory analytical conditions must be considered.

Within the industry focus toward HC liquid-rich (black oil/volatile oil phase) mudrocks, sample and pore alteration have been recognized due to volume changes of kerogen materials in the presence of specific hydrocarbons. Fluid/gas saturations and permeability measurements are especially susceptible to error from altered state surface samples.

Scaling methods of integrating subsurface derived samples (core or cuttings) of basic reservoir characterization (porosity, permeability, fluid and gas saturations) to subsurface reservoir characterization (including wireline and or LWD based approaches) can be especially difficult. The integration of multiple-layered method mudrock analysis datasets often requires the inclusion of trained professionals knowledgeable of the full series of specific reservoir (i.e., porosity) characterization techniques.

8.5.2.1 Helium Porosity on Core Plugs

Conventional methods of porosimetry, such as liquid saturation in vacuum or summation of fluids from conventional retort, fall short when applied to the very small pores and nanometer-scale interconnected pore throats found in mudrocks. Issues include that there may be considerable non-connected nanoscale porosity systems within the pore systems of mudrocks including intrakerogen.

Helium is a small molecule (D ~ 2.5 Å; Van der Waals b = 0.0237 L/mol) and can pass through ultra-small pore

throats that may not be accessible to larger molecules such as methane (D ~ 4.3 Å; Van der Waals b = 0.04278 L/mol). Molecular size of helium is < 60% that of methane.

Helium determined porosity is potentially greater than the effective methane porosity (Bustin et al. 2006). This may be analogous to total porosity versus effective porosity in log analysis.

Core porosity is determined through Boyle's law using helium as the penetrant gas. Samples are crushed and sieved to reduce the diameter of the particles that helium has to penetrate for valid porosity measurements. The effect of the irregular particle surfaces on the measured porosity is considered small.

Gas is stored as both a free gas phase and as an adsorbed phase on kerogen or clays. To determine effective porosity using helium, one must subtract helium porosity from a total sorption isotherm to determine the partitioning between free and adsorbed gas. Because helium is a much smaller molecule than methane, the helium porosity is certainly greater than the pore space available to methane and consequently the adsorbed fraction will be underestimated and porosity overestimated.

8.5.2.2 Helium Porosity on Crushed Samples (GRI Technique)

The industry consensus currently seems to favor the use of Boyle's law helium porosimetry on crushed samples, which is a "Quick Look Laboratory" analysis adhering roughly to the procedure outlined as follows:

- Measure bulk volume by mercury displacement method (immersion in mercury and measurement of displaced volume). Mercury is non-wetting and will not fill pore volume. In the GRI method, bulk density is measured by mercury immersion using Archimedes' principle on a large (~300 g) block of intact untreated core material.
- Crush sample. Many labs may include a step of sieving to a given mesh size. The sample is crushed to accelerate the extraction and pretreatment stages and also to facilitate complete invasion of helium in the pore space during the subsequent grain volume measurement.
- Connect sample to pressurized cell containing known volume of helium. For single-cell technique, hold the sample in a seal-fitting elastomer container. For dual-cell technique, hold the sample in a chamber of known volume.
- Observe change in pressure in helium cell. Displaced volume (i.e., pore volume of sample) can be inferred by Boyle's law from change in pressure.
- The crushed sample is solvent extracted with hot toluene using the Dean Stark method, and then dried in an oven at 200°C. Grain volume of the crushed material is measured by helium pycnometry (Boyle's law).
- Divide pore volume by bulk volume to obtain porosity. Pore volume can be calculated using the difference between bulk volume and grain volume.

Most major labs utilize some variation of this technique, although consistent differences are observed in measurements between them on similar formations. For instance, some labs appear to consistently report higher values for porosity than other labs (Karastathis 2007; Passey et al. 2010; Sondergeld et al. 2010; Spears et al. 2011).

Due to the proprietary nature of each lab's techniques, it is unclear what accounts for these differences. Variation in crushing technique and resultant particle size is a strong candidate to explain a portion of the observed bias. Clay-bearing and kerogen-bearing rocks also have high hydration potentials and abundant nanoscale porosity making them sensitive to changes in the relative humidity (RH) of the environment. Alteration of nanoscale surface energy properties (wettability properties) through oxidation with core storage time is likely part of this problem.

For the full-suite rock fluid analysis for integrated studies the effective porosity, Klinkenberg-corrected air and liquid permeability and fluid saturation should be measured on selected core plug samples under net confining stress (NCS) for validation of crushed sample analysis.

8.5.2.3 High Pressure Mercury Injection Capillary Pressure

Within tight formations (typically cemented tight sand or siltstone reservoirs), mercury injection capillary pressure (MICP) has been traditionally the preferred method for characterizing the pore (actually the pore throat structure). The MCIP technique may prove feasible for tight sands or carbonates but is often too slow or destructive to the small pores within mudrocks. This includes the non-wetness properties of mercury to nanoscale pore systems, which can hinder and impact accurate measurements.

Comisky et al. (2011) provide an excellent summary of MICP procedures, considerations, and potential errors of MICP application to mudrocks.

Within mudrocks, a significant pore volume is too small to be accessed by MCIP. Current instruments can only go up to 414 MPa (60,000 psi), corresponding to a theoretical limit on

the smallest pores that can be measured of diameter 3.6 nm. However, this level is unlikely to be reached for many important reasons such as heating and compression of mercury and the rock structure, particle deformation, and the opening of closed pores.

MICP on core plugs and crushed mudrock samples does not represent true capillary pressure characteristic. However, they can be referenced to other layered analysis approaches (Honapour 2012). The strength of the crushed sample approach is faster analysis time due to faster equilibration (in comparison to core plugs), but it does not honor heterogeneities and is sample destructive.

Many important papers discuss surface area and pore size distribution within mudrocks with the utilization of low pressure N_2 and CO_2 gas adsorption, mercury injection capillary pressure (MICP) (Chalmers and Bustin, 2007a, 2007b; Ross and Bustin 2009; Mastalerz et al. 2012; Kuila and Prasad 2013; Schmitt et al. 2013).

8.5.2.4 USANS/SANS

Properties at dimensions around the micron level for derived porosity (void structure) and particle size can be understood with approaches including small angle and ultra-small angle neutron scattering (USANS/SANS). This application is used to obtain microstructural information of pores and particles typically between 0.01 to 10 microns (**Fig. 8.79**). Within crystallography, atomic structures can be studied by applying diffraction techniques using neutrons, X-rays, and electrons, the USANS/SANS utilizes neutrons.

Utilizing neutrons as a probe for the study of structure includes the following advantages:

- Neutrons scatter from nuclei (as compared to X-rays from the electron distribution in the atoms) so neutrons see hydrogen atoms, as well as isotopic compositions of samples.
- Cause minimal radiation damage.
- Possess a magnetic moment (magnetic properties can be investigated).
- Possess a high bulk penetrating power.
- Only small absorption for most elements.

Microstructures of porous media show length scales ranging from 10 Å to 1,000 Å (10-3 to 0.1 μm) that can be probed by small-angle scattering (bulk samples) and reflectivity measurements using neutrons (SANS).

Small angle neutron scattering (SANS) is a technique that can provide quantitative information about the structure and geometry of the pore network at length scales (1 nm

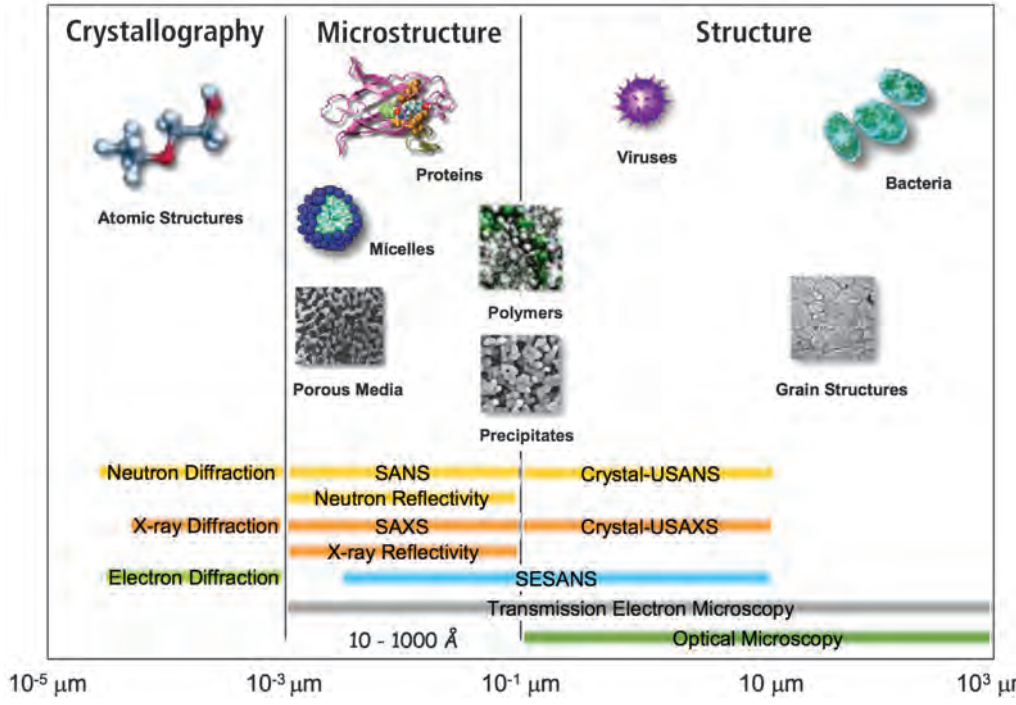

Fig. 8.79—Size scales by various techniques (10-3 μm = 1 nanometer). (From Rehm 2007.)

to 0.3 μm) inaccessible by other techniques such as X-ray computed tomography.

The volume and surface roughness of submicron pores can be measured using SANS in geologic materials. When a beam of neutrons is transmitted through a sample, some of the neutrons are effectively scattered by interfaces between phases of contrasting scattering length density. Minerals have similar values of scattering length density that are very different than the value of pores; therefore, in rocks neutrons scatter from interfaces between pores and minerals.

The intensity of scattered neutrons, I(Q), with Q being the scattering vector, gives information about the number and volume of scattering objects (pores), their arrangement in the sample, and the chemical and physical composition of the scattering objects. The slope of the scattering data when plotted as log Q versus log I(Q) provides information about the surface or mass fractality of the sample and related fractal dimensions.

USANS allow investigating large-scale structures of, e.g., grains (a few tens of μm). USANS has the capability of studying porosity as well as particle size but differs from conventional techniques in measuring closed and open pores.

USANS is designed for the study of hierarchical structures in natural materials. An advanced version of the classical Bonse–Hart double-crystal diffractometer (DCD), in contrast with its single-wavelength reactor-based analog, will operate with the discrete multiwavelength spectrum of Bragg reflections (**Fig. 8.80**).

TOC content and Rock-Eval pyrolysis data evaluate source richness, source quality, kerogen type, and thermal maturity.

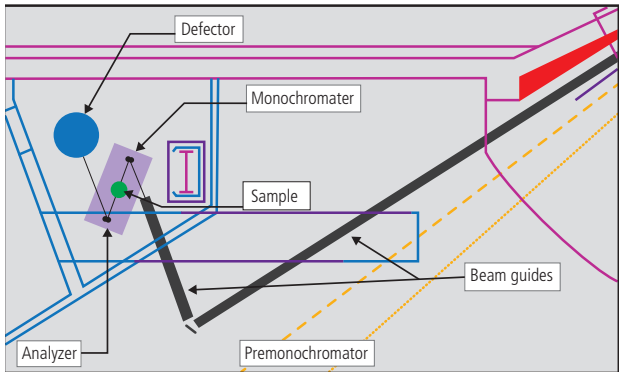

Fig. 8.80—Size example schematic of USANS technique. (Courtesy of Oak Ridge National Laboratory, US Department of Energy, USANS 2014.)

Within mudrocks SANS/USANS technology is especially useful when combined with these measurements, in that it can detect the presence of generated bitumen in pores that are pore-size specific.

The presence of bitumen in the small pores (up to 0.1 μm) detected by SANS indicates the onset of hydrocarbon generation, whereas the presence of bitumen in the largest pores detected by USANS (about 10 μm) indicates a significant saturation and the onset of hydrocarbon expulsion.

Important papers that describe in detail the small angle and ultra-small angle neutron scattering (SANS/USANS) techniques within mudrocks include Clarkson et al. 2012a and Mastalerz et al. 2012.

8.5.2.5 Subcritical Nitrogen Gas Adsorption

Surface area and pore size distribution can be obtained by low-pressure N_2 and CO_2 gas adsorption. Low-pressure adsorption is a non-destructive and relatively inexpensive technique compared with MICP. **Fig. 8.81** compares the pore size range for various porosity analyses methods.

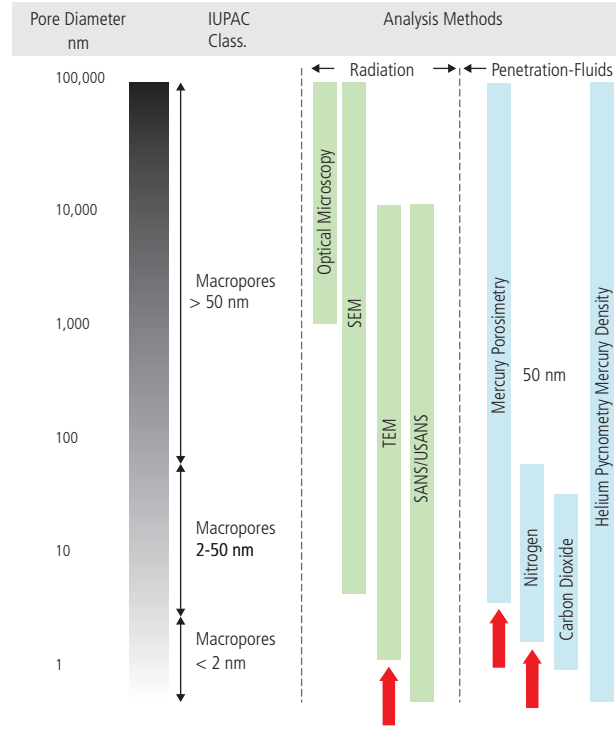

Fig. 8.81—Methods used to estimate porosity. (From Clarkson et al. 2012; modified from Bustin et al. 2008 with IUPAC classification for pore sizes; From Sing et al. 1985).

Utilizing core plugs for low-pressure adsorption analysis instead of the more usual crushed-rock analysis allows for the better comparison to additional core-plug porosity as well as permeability measurements. Analysis times will be much longer than for crushed samples, but comparison datasets for accuracy determinations will be available.

For low pressure N_2 the isotherms of adsorption and desorption of N_2 at liquid nitrogen temperature (-195.5°C) are utilized.

The isotherm obtained from N_2 adsorption, when applied over a wide range of relative pressures (p/po), can provide information on the surface area, pore volume, and pore size distribution (Kuila and Prasad 2013).

The saturation vapor pressure (po) is obtained by using a nitrogen vapor pressure thermometer. The relative pressure (p/po) ranges from 0.011 to 0.995 and an equilibration time of 10 s is normally applied during a typical analysis (Hui Tian et al. 2013).

Specific surface areas are best calculated from the adsorption isotherms and utilize the Brunauer–Emmett–Teller (BET) equation (rather than BJH method) and t-plot method (Hui Tian et al. 2013). The BJH method (Greg and Sing 1982), the traditional method, had been the preferred method for deriving pore-size distributions, but their simple models for gas desorption and pore structure are not considered robust. Of insight interest, the specific surface areas are mainly determined by smaller pores, and the pore volumes are mainly controlled by the larger pores (Hui Tian et al. 2013).

8.5.2.6 Nuclear Magnetic Resonance Core Porosity

Nuclear magnetic resonance (NMR) techniques have been effectively applied for fluid and reservoir properties within conventional reservoirs. In these reservoirs NMR has the capacity to sense fluids in the pore space independent of lithology (Sondergeld et al. 2010b).

Utilizing T2 and T1 relaxation time measurements one can distinguish fluids and estimate viscosities of the fluids. The number of hydrogen atoms present is directly proportional to the NMR signal, which in conventional reservoirs is related to direct porosity measurement in brine saturated (water = H_2O) rocks.

Due to the observed very weak signal strength within mudrocks, a mudrock plug may need as many as 10,000 scans in comparison to the 24 scans of a fully saturated Berea Sandstone plug (Sondergeld et al. 2010b). In addition, the nanoscale pore sizes of mudrocks equates for fast T2 relaxation time.

Within **Fig. 8.82**, most of the T2 signal occurs below the 3 ms cutoff (red vertical line) for clay-bound water. Applying a surface relaxivity of 0.05 μm/ms, the left most distribution maps into pore body sizes of 3 nm to 100 nm with a peak near 25 nm, which is very consistent with typical shale SEM observations.

Applied research is ongoing to utilize the NMR response of mudrocks to defining specific porosity and fluid/gas relationships.

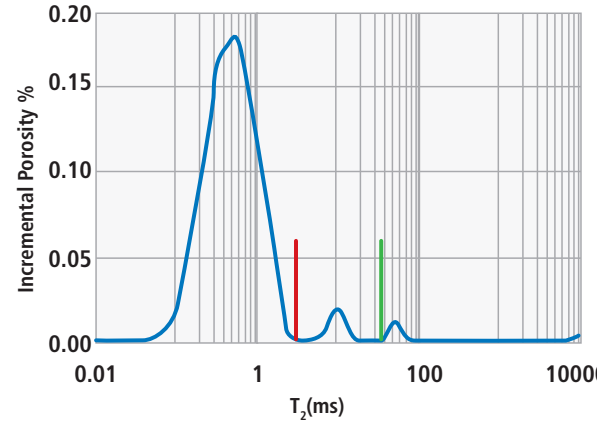

Fig. 8.82—Typical T2 relaxation spectrum for a gas shale (10,000 scans, porosity = 7.1%). (From Sondergeld et al. 2010.)

8.6 Permeability Determination

Measurement of reservoir-relevant rock properties from core becomes especially challenging when handling very low-permeability formations such as gas/liquid-bearing mudrocks with permeability in the nanodarcy to picodarcy ranges. Laboratory measurement techniques for basic properties of shale samples are based on the methods used for conventional tight gas sand or CBM analysis and in most labs are not specifically developed for unconventional shale samples. Whereas steady-state methods of flow measurement and permeability determination are feasible for higher permeability within conventional reservoirs, mudrocks require the use of transient flow measurements. These can generally be divided into pressure-decay and pulse-decay measurement techniques. Mercury injection capillary pressure techniques have also been used. However, within mudrocks, there is significant pore volume that is too small to be accessed by MCIP. The technique is often too time consuming or destructive to the small pores within mudrocks. Comisky et al. (2011) provide an excellent summary of MICP procedures, considerations, and potential errors of MICP application to mudrocks.

Advanced nanoscale characterization of porosity and resulting calculated permeability analyses of mudrocks have been developed through industry, government, and university labs and their associated consortiums. Industry and university labs have now developed additional advanced instrumentation, resulting in 3D imaging of nanoscale pore throat structures. This imaging is performed utilizing focused ion beam (FIB) scanning electron microscopy (SEM) or FESEM (field emission scanning electron microscopy) of ultra-smooth argon-ion milled surfaces (**Fig. 8.83**). A major issue continues to be the scaling of these measured observations from the sample, to the core, to the logs, and to the spatial properties of the objective formation, due to the very small amount of material that is sampled.

Additional applications for permeability inference and analysis include "Quick Look Laboratory" approaches of methane carbon gas isotope separation through proxies of adsorbed gas (geojars) and free gases (isotubes) and advanced interpretative methodologies, which are being developed using nuclear magnetic resonance techniques.

There is often considerable variation in permeability and fluid saturation measurement results from differing laboratories (Sondergeld et al. 2010). The quality of these analyses is affected by several factors. One significant factor relates to differing procedures used for core acquisition, core retrieval, and core surface handling. A recognized issue is the rate of core retrieval. The presence of extensive partings (e.g., poker chipping) on some cores has been of high concern. For canister desorption analysis, the large surface area developed by extensive poker-chipping and coring induced fracturing results in large amounts of loss gas during tripping, decreasing the reliability of the desorption measurements. The large induced surface area also enhances the drill-fluid invasion, causing changes in pore fluid saturations. Poker-chipping and extensive coring-induced fracturing creates serious problems for obtaining high-quality samples for laboratory testing. In cases of severe fracturing, it may not be possible to collect any samples, except those used for crushed rock analysis. When conducting numerical modeling of pore pressure diffusion during coring and unloading it has been found that coring practices and core size are the most dominant conditions defining core integrity. Cores from the same region of the same play, cut by different operators, and retrieved at the same rates, can exhibit substantial differences in their integrity.

Clearly some coring companies are better than others in their coring practices. Numerical simulations suggest that

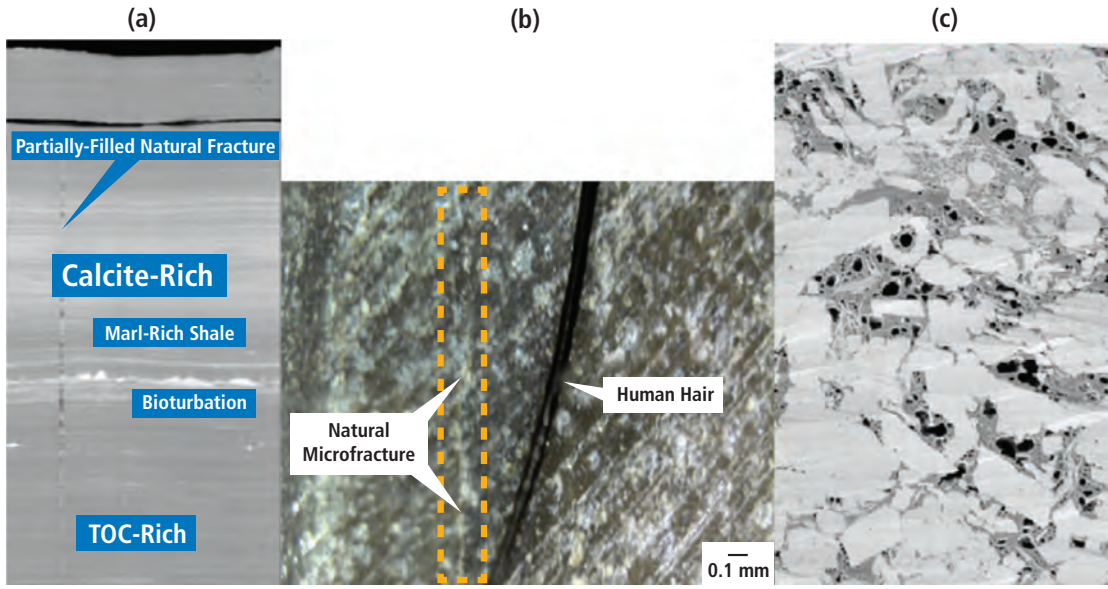

Fig. 8.83—(a) Core CT image, variation of CT density related to porosity, mineralogy, and TOC at millimeter scale; (b) Calcite- and TOC-rich laminations; microfractures with air permeability of 0.0016 mD and 0.0007 mD @1500 & 3,000 psi NCS, respectively, at submillimeter-scale; human hair is shown for comparison; (c) Focused Ion Beam/SEM showing the nano and subnanoscale pore network at nanometer scale. (From Honarpour et al. 2012.)

most partings occur at stress concentrations associated with the core-rock interface and due to flexure instabilities. This means that most partings can occur during the coring process. The analysis also indicates that the time scale for pore pressure diffusion and prevention of overpressure during core retrieval scales with permeability. The required retrieval time for a core with 10 times lower permeability is 10 times longer. Given the nanodarcy scale permeability of tight mudrocks, changes in retrieval times should be of 100 to 1000 times longer, to make any significant difference.

Consider a larger diameter core over smaller diameter core and using coring companies with strong experience with tight mudrocks with a good track record of core quality.

As previously stated laboratory measurement techniques for basic properties of shale samples are based on the methods used for conventional tight gas sand or CBM analysis and in most labs are not specifically developed for unconventional shale samples. Laboratories worked to develop techniques specifically for shale measurements and to protect their research many of the techniques developed remain proprietary in nature. In addition to differing measurement techniques, service companies' labs differentiate their services by carrying out techniques with varying, often proprietary, combinations of parameters: crushed-sample sieve mesh size, for instance. An important reference paper describing the issue of permeability measurement variance through the utilization of the crushed sample GRI methodology is SPE 152257 "Advances in Measurement Standards and Flow Properties Measurements for Tight Rocks such as Shales" by S. Sinha, E.M. Braun, Q.R. Passey. S.A. Leonardi, A.C. Wood III, J.A. Boros, and R.A. Kudva at the 2012 SPE/EAGE Vienna Conference, March 2012.

Permeabilities resulting from these analyses are usually plotted versus core-measured porosities. Wireline or LWD log porosity measurements, corrected for TOC as necessary, can then be used to derive permeability estimates.

8.6.1 Pressure-Decay and Pulse-Decay Measurement Techniques for Permeability Estimation

In pressure-decay permeameters, used by many labs, a sample is subjected to an induced pressure at one end. The transient pressure response as a function of time and distance from the pressure source is measured in the sample and the effective permeability is inferred.

Pulse-decay permeameters work under similar principles. However, the entire sample is held at a given confining pressure and a small increment pressure pulse is applied at one end. This allows for measurements to be taken on samples whose pressure states more closely approximate in-situ conditions, which may help account for error due to, for instance, compressibility of pore throats.

In practice pulse-decay measurements require prohibitive amounts of time to carry out for shale core, so the industry consensus currently favors the use of pressure-decay measurements. These methods can be carried out on whole core. However, this can result in erroneously high values due to the presence of fractures induced by the coring process and other artifacts.

The crushed-sample technique of mudrock pressure decay permeability measurement was developed in the early 1990s through the Gas Research Institute (GRI) on Appalachian (Devonian) shale gas core samples. A summary reference of this procedure is in the Society of Petroleum Engineers JPT, November 1992, by D.L. Luffel and F.K Guidry, titled "New Core Analysis Methods for Measuring Reservoir Rock Properties of Devonian Shale."

Labs carry out shale permeability analysis on crushed core samples. Unfortunately there is no consensus on the degree to which the sample should be crushed and then sieved. It appears that variations in the ranges of permeability reported for similar samples between laboratories may at least partially result from differences in crushed-particle size. A coarser sample particle size may be more reflective of the expected in-situ flow in the shale matrix within and around silt-sized constituent particles. A somewhat finer sample, particle size, silt-sized to sub-silt sized, may be reflective of permeability within (intraparticle porosity), but not between (interparticle porosity). Differences in the amount of effort to homogenize the sample particle size may result in problematic repeatability of measured permeabilities.

In addition to variations due to crushed-particle size, no crushed-sample measurement can account for permeability due to natural fractures, whether they come in the form of hydrocarbon generation-induced microfractures or larger-scale tectonically or dissolution-created systems. For this reason, system permeability calculated from injection testing (mini-fracturing) may be preferable for a target formation, especially if natural fracturing is believed to be prevalent.

8.6.2 Advanced Nanoscale Characterization of Porosity and Resulting Calculated Permeability Analyses

Digital rock physics models (DRP) are developed from 3D imaging of nanoscale pore throat structures obtained from focused ion beam (FIB), scanning electron microscopy (SEM), or FESEM (field emission scanning electron microscopy) of ultra-smooth argon-ion milled surfaces. Images resulting from this technique can provide better resolution of the mineral, organic carbon, and pore systems than a standard SEM image (**Fig. 8.84**).

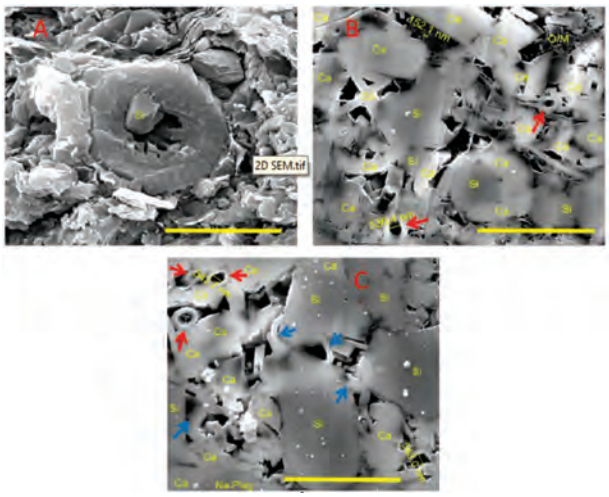

Fig. 8.84—Differences in resolution of grain-related, organic matter and pore types and distribution that can be identified from ion milled SEM samples (b, c) compared to a standard SEM image for an Eagle Ford shale sample. (From Driskill et al. 2013.)

This dual procedure of continuous milling while simultaneously imaging (photographing) the milled surface provides a 3D image of the porosity systems (intrakerogen, dissolution porosity trails, intra/intercrystalline, intra/interparticles, clay slots, and interclay). Net percentages of porosity associated with each of these porosity systems can be developed and the sample can be classified accordingly. Connected and non-connected porosity volumes can be generated. From the connected pore system, permeability can be computed (Tolke, et. al, 2010) along three orthogonal axes using Lattice–Boltzmann fluid flow simulation (**Fig. 8.85**).

Variations in the relative proportions of the various pore networks will be reflected in differing porosity versus permeability responses. **Fig. 8.86** illustrates this variation in permeability in a Brazilian shale play.

Within liquid-rich systems, kerogen porosities may be affected by swelling of kerogens in contact with liquid HCs. Studies are ongoing within consortiums to understand HC interaction to kerogen developed porosities within specific kerogen transformational window and pressure and/or temperature conditions.

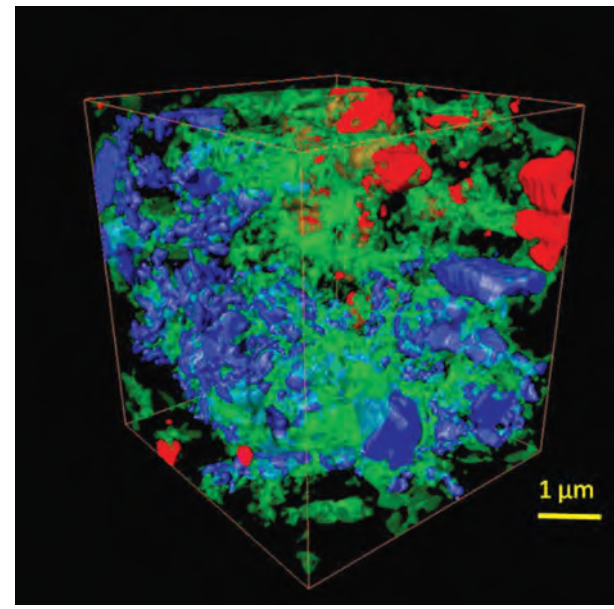

Fig. 8.85—Example of a segmented 3D FIB-SEM volume of a Lower Eagle Ford sample from well SE. Connected porosity is blue; disconnected porosity is red; organic material is green; and framework minerals are transparent. Total porosity was 11.5%, and absolute permeability was 1034 nD. (From Driskill et al. 2013.)

8.7 Fluid Saturation Determination

As stated in the introduction to this chapter we stated that a combination of laboratory analyses is the primary method used to determine gas/oil saturations and volumes. Dean Stark or Retort analyses are conducted to determine free gas and oil saturation on crushed rock samples. Adsorption and desorption isotherm analyses are utilized in gas shale reservoirs to calculate both total gas volumes and adsorbed gas volumes (Bustin et al. 2009). Most shale reservoirs produce little free water and the water saturation in the pores is believed to be at irreducible values. Water saturation is often estimated from resistivity and porosity log measurements using either an Archie equation or shaly sand equation methodologies as is done for conventional reservoirs. However, there is more uncertainty in these estimations as the accuracy of many of the required parameter values including formation water salinity and appropriate electrical parameters may be suspect.

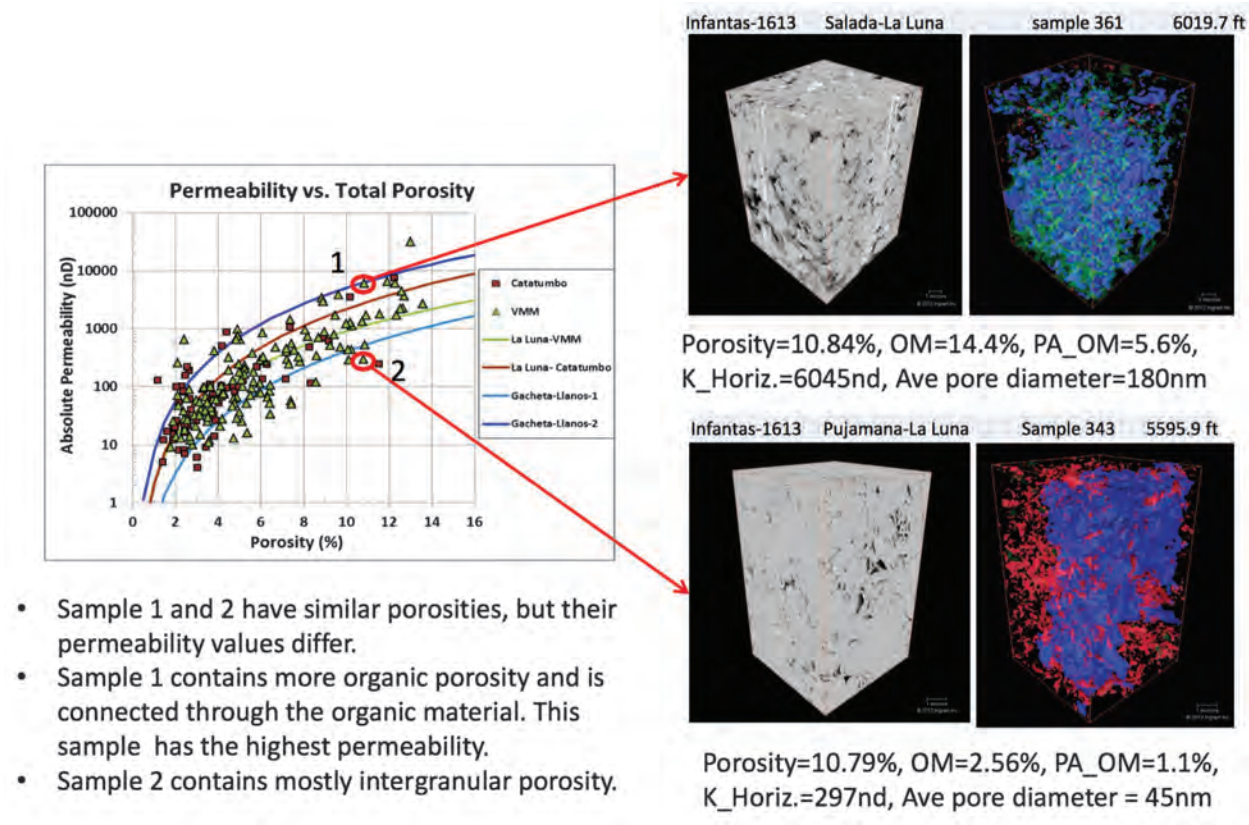

Fig. 8.86—Example illustrating differences in permeability related to pore type and size. (From Walls and Diaz, 2014.)

While sometimes criticized for ignoring the complexities of this type of reservoir, in many situations the limited data available provides few options. Obtain sufficient laboratory saturation analyses to calibrate the parameters required in this approach to yield reasonable results. Examples of this approach include Ramirez et al. 2011; Jacobi et al. 2009; Glorioso and Rattia, 2012; Quirein et al. 2009.

8.7.1 Core Analyses for Determination of Free Fluid Saturations

Two core analyses methods of saturation determination are commonly used on crushed samples: the Dean–Stark distillation method and a retort method. Given current laboratory reporting procedures it is difficult to determine from Dean–Stark analysis if the extracted water volume describes free fluid saturations with a limited amount of capillary bound water or if some amount of clay bound water volumes have been included. Comparisons of lab derived water saturations from Dean–Stark and retort methodologies found significantly higher water saturations from the Dean–Stark samples (Sondergeld et al. 2010). Currently the majority of labs have adopted the retort processes for measurement of water and hydrocarbon saturations from shale core. Unfortunately, the specifics of the process vary from provider to provider, resulting in systematic differences in measured values.

These differences include the use of a single-stage retort process versus a multistage process as well as variations in the single retort protocols between laboratories. An additional factor in this difference may be the storage humidity conditions of each group's laboratory. The major laboratory companies have labs globally in areas with variable amounts of humidity. Because shale gas (mudrock) producibility is associated with levels of pore water saturation at irreducible to sub-irreducible conditions—surface humidity, oxidation (changes in wettability), fluid evaporation, and handling conditions (fluid imbibition) can have dramatic impacts on these measurements.

Age of core material is critical in all of these physical measurements where degradation or enhancement of these physical properties occurs. An industry rule of thumb is that cores older than six months do not provide accurate porosity, permeability, and saturation data.

Fluid saturation measurements (of water, oil, and gas) and some fluid sensitivity laboratory tests can be altered by drilling fluid invasion and contamination. The extremely low permeability of unconventional reservoirs usually limits fluid invasion. Proper sampling, processing, and analysis minimize drilling fluid invasion effects. On large diameter cores, the invasion may be seen as a thick halo around the external core surface, which can be easily discriminated to avoid influencing saturation measurements. On small diameter cores, the invasion may reach the center of the core. Given that tight mudrocks are organic rich, normally with dual organic and inorganic porosity systems, imbibition cannot be fully prevented. The organic kerogens within the core can also swell (adsorb) with the condensed HCs and the saturation measurements, especially within liquid-rich mudrocks, can be affected. However, drilling fluid imbibition, especially of oil-based muds (OBM), can be high, such that the measured saturations are significantly altered from the native state in the formation. Forensic methods may be required to detect the extent to which fluid imbibition has occurred. Field samples of the OBM are required. As an example, at the end of a 90-ft. coring effort, the upper section of the core was exposed to the coring fluid for approximately 4 to 6 hours, which can lead to significant fluid invasion in the upper section. Incorporating the position of core sample with respect to the coring operation can be an integral component regarding data quality assessment.

8.7.2 Determination of Kerogen Contained Fluid Saturations

$$V_{free}\,(scf/ton) = (32.0368/B_g)\,(Ø \times ((1 - Sw)/\rho_b) -$$

$$1.318 \times 10^{-6} \times (M/\rho_s) \times (V_L \times P)/(P_L + P) \qquad \textbf{(Eq. 8.15)}$$

The nature of storage and transport of hydrocarbon gases and liquids within unconventional resource play mudrock reservoirs continues to be an active area of investigation. A better understanding of the variation of kerogen systems/facies and their storage and delivery systems needs to be established to define their capacity to hold and release hydrocarbons. Molecular level scale to nanoscale porosity and non-darcy transport systems, with ranges of molecular scale pore throats, accompanied by diffusion processes within kerogen and bitumen components, are being considered within the free and adsorbed systems within unconventional resource play mudrock systems. Developing advanced models for molecularly active kerogen adsorption surfaces with varying adsorption capacities for both hydrocarbon gases and liquids, within free and adsorbed hydrocarbon systems is an important area of investigation.

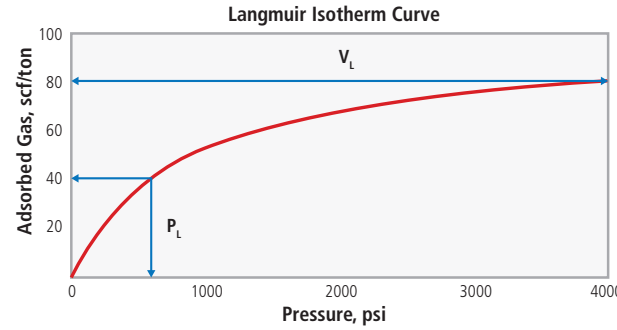

Fig. 8.87—Langmuir isotherm. (Das et al. 2012.)

Research groups have approached the understanding of these free and adsorbed hydrocarbon components through progressive advances in model approaches including coalbed methane molecular diffusion model(s) approaches for gas quantification through desorption and adsorption studies (Xu et al. 2012; Ren et al. 2013). Mudrock gas systems (shale gas) approaches have similarly involved gas (methane) diffusion models that have been based upon canister desorption and adsorption laboratory studies. Hydrocarbon liquid-rich mudrock resource plays are currently the least understood with respect to these complex transport mechanisms and adsorption systems. Current approaches (Shabro et al. 2012) include developing new numerical algorithms that simultaneously take into account gas diffusion in kerogen, slip flow, Knudson diffusion, and Langmuir desorption.

8.7.2.1 Adsorption

Adsorption in unconventional mudrock gas reservoirs is currently expressed by the Langmuir isotherm, which is the capacity of the rock matrix to adsorb gas at any given temperature (**Fig. 8.87**). This laboratory determined that Langmuir isotherm is developed with crushed rock samples. However, within the presence of CO_2 with CH_4 (methane) in the free gas state, the desorption measurement and behavior becomes more complex due to the differential molecular forces (van der Waals) present between specific molecules (such as CO_2 being greater, with an increased capacity toward displacement adsorption).

In addition, sorption experimental procedures can be laboratory variant and can provide a wide range of results (Das et al. 2012). These challenges in data variability in sorption measurement can significantly impact estimated ultimate recovery (EUR) and gas in place (GIP) related to TOC inferences. Because TOC can have a variable kerogen facies component with differential hydrocarbon adsorption

capacities, accurate inferences can be difficult, unless spatial kerogen facies is well known.

Langmuir Isotherm

The Langmuir isotherm, or adsorption isotherm (Bumb and McKee 1988), describes the dependency of adsorbed gas volume on pressure at constant temperature:

$$V = \frac{V_L P}{(P_L + p)} \quad \textbf{(Eq. 8.16)}$$

where V (scf/ton) is the amount of gas adsorbed at pressure p (psia). V_L is the Langmuir volume (the maximum adsorption capacity at a given temperature, scf/ton), and P_L is the Langmuir pressure (the pressure at which the adsorbed gas content is equal to $V_L/2$ psi) for a particular gas component.

For multicomponent adsorption, an extended Langmuir isotherm is commonly used (Leahy-Dios et al. 2011). Two methodologies are now used for gas in place calculations for unconventional mudrock gas reservoirs.

8.7.2.1.1 Free and Adsorbed Gas Calculation

The free gas component and the Gibbs excess (adsorbed) gas volume of the mudrock system is considered to be the OGIP present in the mudrock gas. The governing equation (Ambrose et al. 2010) for this calculation is:

$$V_{free}\,(scf/ton) = 32.0368 \times Ø \times (1\text{-}Sw)/(\rho_b \times B_g) \quad \textbf{(Eq. 8.17)}$$

$$V_{adsorbed} = V_L\,((P)/\,(P + P_L)) \quad \textbf{(Eq. 8.18)}$$

where VL (scf/ton) and PL (psi) are Langmuir volume and pressure, and P (psi) is the reservoir pressure.

Free + Adsorbed Gas: Adsorbed Volume Calculation

The free-gas volume is adjusted by subtracting the volume occupied by the adsorbed gas on the surface. The governing equation (Ambrose et al. 2010) for this calculation is:

$$V_{GIP} = V_{free} + V_{adsorbed} \quad \textbf{(Eq. 8.19)}$$

where ρs is the adsorbed gas density; $V_{adsorbed}$ in this method was calculated from **Eq. 8.18** and OGIP by **Eq. 8.19**.

8.7.2.2 Desorption

Desorption studies are commonly completed on cores and or sidewall core materials collected within sealed canisters at the wellsite. Hydrocarbon type, composition, and volumes can be measured within standard laboratory protocol procedures. Within these calculations, a lost-gas calculation must be included with respect to the time, temperature, and pressure change that have occurred with the recovery of the samples. These corrections can be significant and may infer a margin of error that may be unacceptable. However, desorption measurements are a critical component in assessing the need for multicomponent adsorption studies. Adsorption studies completed under controlled conditions are considered a methodology to reduce the uncertainty with respect to adsorption capacity of the target intervals.

8.8 Geological and Geomechanical Characterization

Geological characterization involves understanding as much as possible the structural and stratigraphic characteristics of the unconventional source rock reservoir and any natural fracture systems that may be present. The starting point to accomplish this is careful detailed study of outcrops of the formation. If that is not possible, identify an analog shale play and examine outcrops of that formation. The role of seismic and microseismic technologies in geological characterization is significant and is addressed in other chapters. This section focuses on the role of resistivity and acoustic imaging instruments and wireline cross dipole acoustic technology.

Geomechanical characterization of unconventional source rock reservoirs is a particularly critical objective as economic exploitation of these reservoirs depends on successful horizontal drilling and multistage hydraulic fracturing results. This requires understanding the in-situ stress state and natural fracture distribution in each shale reservoir. Stress states and natural fracture patterns can vary widely between and even within shale reservoir plays. These variations affect the shape and character of the stimulated rock volumes, the requirements for safe drilling, and the optimal directions to drill to exploit natural fractures. Geomechanical characterization also requires determination of the rock static and dynamic mechanical properties, anisotropy, rock brittleness, and hardness. Variations in the mechanical

properties of these mudstone reservoirs are related to changes to the mineral composition and amount of organic material present. Detailed technical discussion of the role of geomechanics in the exploration and development of unconventional shale gas and oil reservoirs is in Chapter 9.

8.8.1 Application of Borehole Resistivity and Acoustic Imaging Technologies in Unconventional Source Rock Reservoirs

Interpretation of borehole acoustic and resistivity imaging and examination of whole core enables us to recognize in a wellbore structural, stratigraphic, and sedimentological features observed in the shale outcrops. Two types of measurement technologies are utilized for wireline imaging instruments: resistivity and acoustic. Wireline resistivity imaging instruments are designed to operate in either conductive (water-based) mud systems or non-conductive (oil-based) mud systems. LWD resistivity instruments are available which operate in conductive mud systems. Wireline acoustic imagers operate in both types of mud systems. While image maps of additional LWD measurements of formation density and gamma ray are available, interpretation of structural and stratigraphic features is based primarily on the LWD resistivity imaging responses. Wireline and LWD imaging instruments can be used in both vertical exploration or pilot holes and horizontal laterals in unconventional source rock reservoirs to provide:

- Structural analysis of the shale formation
- Characterization of the natural fracture systems
- Description of the in-situ stress regime
- Stratigraphic analysis of the formation

8.8.1.1 Structural Analysis of the Shale Formation

Structural analysis includes identification, classification, and interpretation of the structural dips and azimuths of structural features or boundaries intersected by the wellbore such as faults, folds, and unconformities. The impact of faulting on shale reservoir performance can be varied such that it might be a positive factor in some plays and a negative factor in others where faulting could be considered a geohazard. Hydraulic fracturing stimulation treatment design generally attempts to avoid fault zones as these zones may divert a significant portion of the fracturing fluid and energy and reduce the effectiveness of the stimulation treatment. In the Barnett shale lateral well placement and hydraulic fracture stimulation design are both planned to avoid faulting related to the paleokarsting in the underlying Ellenburger group, which if reactivated can provide a pathway for water production from the Ellenburger. This could significantly reduce the ultimate gas production from that lateral (Gale et al. 2007). **Fig. 8.88** illustrates the resistivity image of faulting in a vertical and horizontal shale gas reservoir well and lists some identification criteria.

8.8.1.2 Characterization of the Natural Fracture Systems

Natural fractures are classified into three general categories and identified based on their resistivity or acoustic responses, open (conductive), partially open (mixed), or mineralized (resistive). **Fig. 8.89** illustrates the response of different fracture types in vertical and horizontal unconventional shale reservoirs. **Fig. 8.90** is an example of a finalized fracture characterization plot that describes the dip and azimuths of the identified bedding, faults, and fractures, and the spatial frequencies for each fracture category.

Natural fracture networks are almost always present in productive unconventional shale gas and oil reservoirs but the extent of fracturing and their impact on well productivity varies. The Antrim shale is a shallow biogenic gas play, which is highly fractured with a significant amount of open natural fractures as seen in **Fig. 8.91**.

Fracture systems can still positively impact well productivity when the natural fractures are mineralized or partially open. The natural fractures in the Barnett shale are primarily mineralized or partially open but still play an important role in the shale productivity as they are reactivated during hydraulic fracture stimulation and combine with the hydraulically stimulated fractures to form a complex fracture network (Gale et al. 2007). Gas productivity is enhanced in the Marcellus shale play by two regional joint sets, the J1 and J2 (**Fig. 8.92**), which contain both open (or unhealed) and mineralized joints (Engelder et al. 2009). The orientation of natural fracture networks reflects the direction of the maximum horizontal stress (SH_{max}) at the time the fractures were formed which may not coincide with the present-day stress regime orientation. The natural fracture network seen in the Barnett shale is oriented in a northwesterly direction while the orientation of present-day SH_{max} is NE-SW (Gale et al. 2007).

8.8.1.3 Description of the In-Situ Stress Regime

Borehole resistivity and acoustic imaging instruments provide a reliable method for characterizing the in-situ stress magnitudes and their orientations by observing the stress induced compressional (breakouts) and tensile (drilling induced tensile fractures) in wellbores. Stress configuration plays a critical role in hydraulic fracture stimulation design.

Fault Indicators

- Change of dip direction and angle over large intervals
- Deformation of bedding due to fault-related drag folds
- Discordant lithology changes
- Higher fracture density (natural fractures) around faults
- Brecciation or mineralized fractures
- Modifications of the regional stress field or drilling-induced fractures that change orientation.

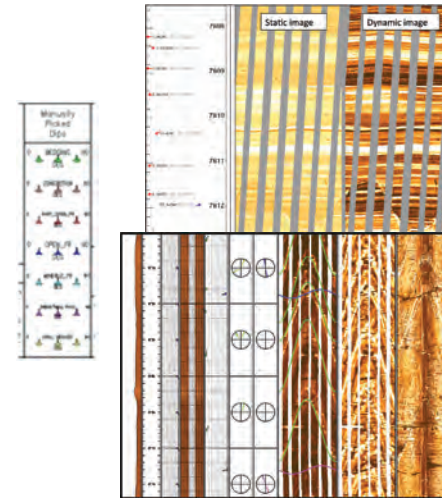

Fig. 8.88—Borehole imaging examples of faults intersecting the wellbore in vertical and horizontal wellbores. (Zarian 2010.)

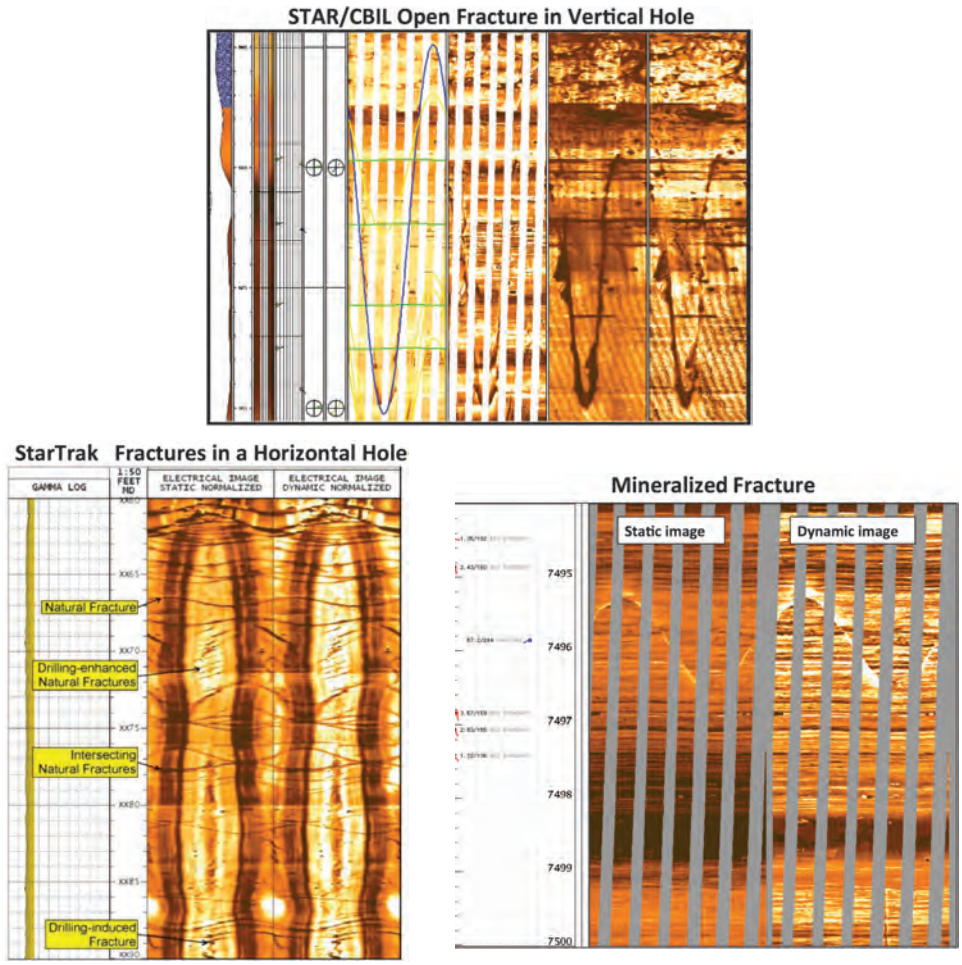

Fig. 8.89—Borehole imaging examples of fracture types intersecting the wellbore in vertical and horizontal wellbores. (Zarian 2010; Sadykov et al. 2012.)

The orientation of the maximum and minimum stresses varies for normal, thrust, and strike slip faulting environments with the direction of the maximum and minimum stresses controlling the fracture orientation, the magnitude of the stresses determining the injection pressures required, and the stress contrast controlling fracture geometry. Borehole breakouts are shear failure features oriented in the direction of the minimum horizontal stress (S_{Hmin}) in vertical wells. Drilling-induced fractures and fractures from hydraulic stimulation propagate in the direction of the maximum horizontal stress (S_{Hmax}) (**Fig. 8.93**).

Depending on the orientation of the wellbore to the stress regime DITF fracturing may also be inclined rather than vertical and exhibit spalling at the tip of the fracture with a J- or S-shaped morphology (blue circles). They may also exhibit an en echelon morphology with a vertical offset between fracture pairs (green arrows) (**Fig. 8.94**).

8.8.1.4 Stratigraphic Analysis of the Formation

Shale reservoirs are very heterogeneous and composed of a variety of lithofacies that can be recognized by their mineral composition, fabric, texture, and biota (Loucks and Ruppel 2007). Examples of this variation include the occurrence of phosphatic or carbonate concretions or nodules (**Fig. 8.95**), skeletal debris, pyrite framboids, lenses, or thin laminar pyrite, bioturbated, or debris flow depositional textures (**Fig. 8.96**).

Lithofacies can be developed for each shale play by integration of log-derived mineral composition with whole core description and various core analyses including thin sections, XRD, FTIR, cathodoluminescence, and SEM measurements. A range of sedimentary image fabrics and features can be identified from borehole resistivity images, which can be incorporated with the lithofacies classification to achieve additional insight into reservoir depositional environments and sequence stratigraphy. One simplistic example is that borehole resistivity images often exhibit a correlation to increasing TOC weight percentage. The color of the displayed image is a function of the interval resistivity with lower resistivities being darker and higher resistivities lighter. The increasing resistivity in these shale formations is associated with increasing kerogen content (Passey et al. 2010). **Fig. 8.97** compares a resistivity image section from a Marcellus shale well and the TOC weight percentage derived from the excess carbon measurement from the Baker Hughes FLeX™ instrument.

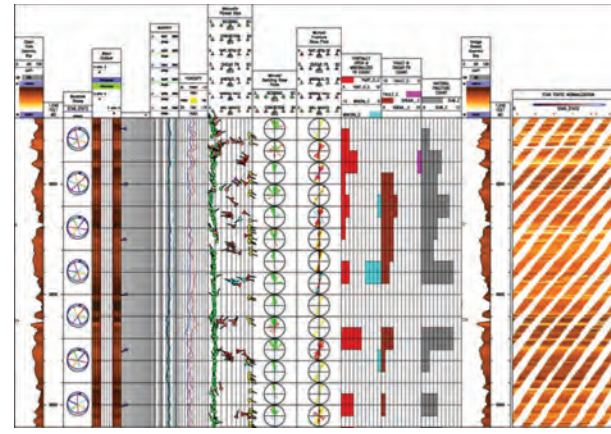

Fig. 8.90—Baker Hughes final fracture characterization plot.

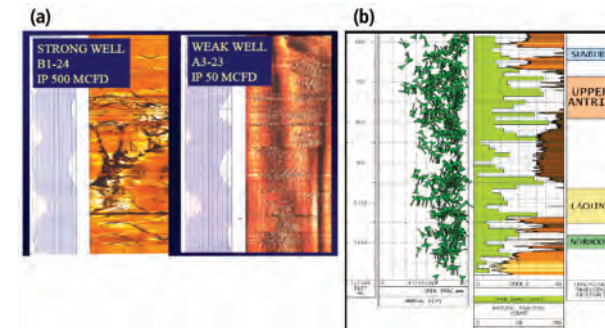

Fig. 8.91—Antrim shale wireline acoustic images contrasting production from two wells with and without open fractures. (From Manger et al.1991; Moss 2005.)

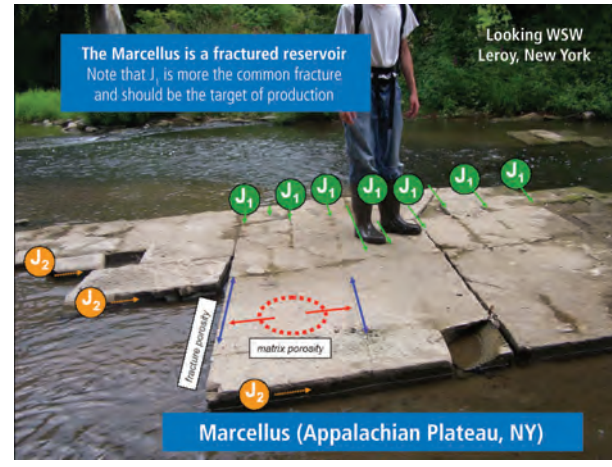

Fig. 8.92—Crosscutting J1and J2 joints in the Marcellus black shale. (Modified from Engelder et al. 2009.)

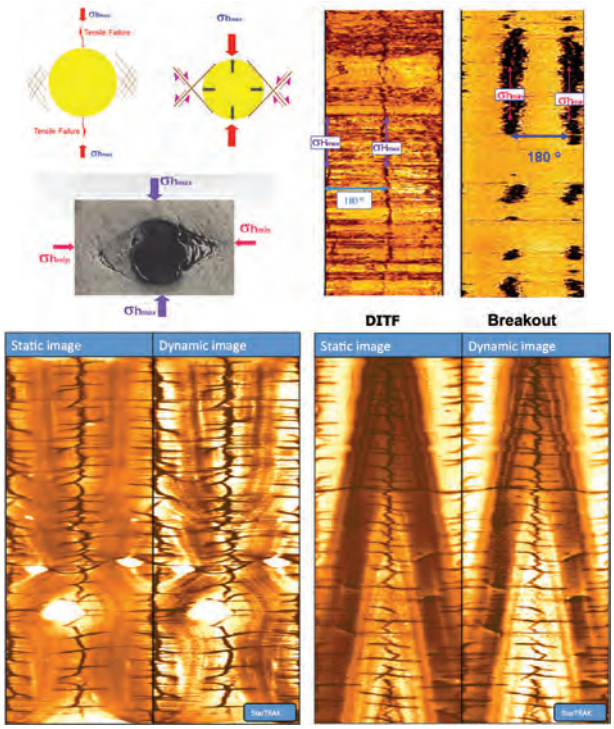

Fig. 8.93—Acoustic imaging characteristics of drilling-induced tensile fractures and borehole breakouts.

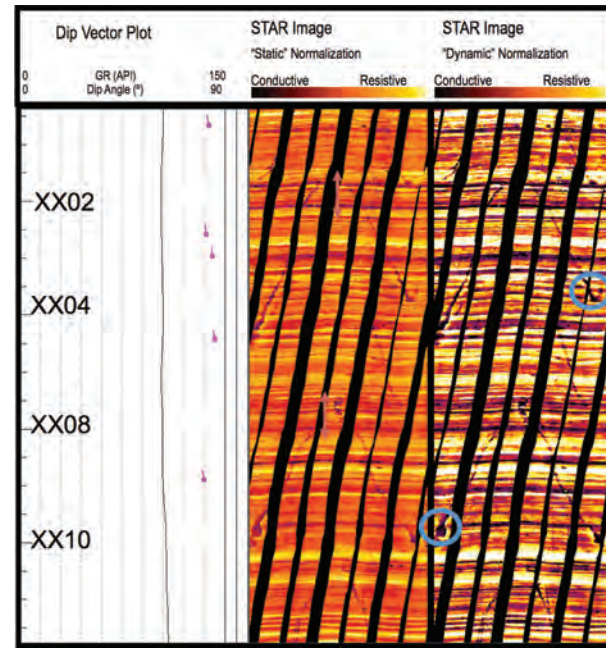

Fig. 8.94—Resistivity imaging characteristics of inclined drilling induced tensile fractures.

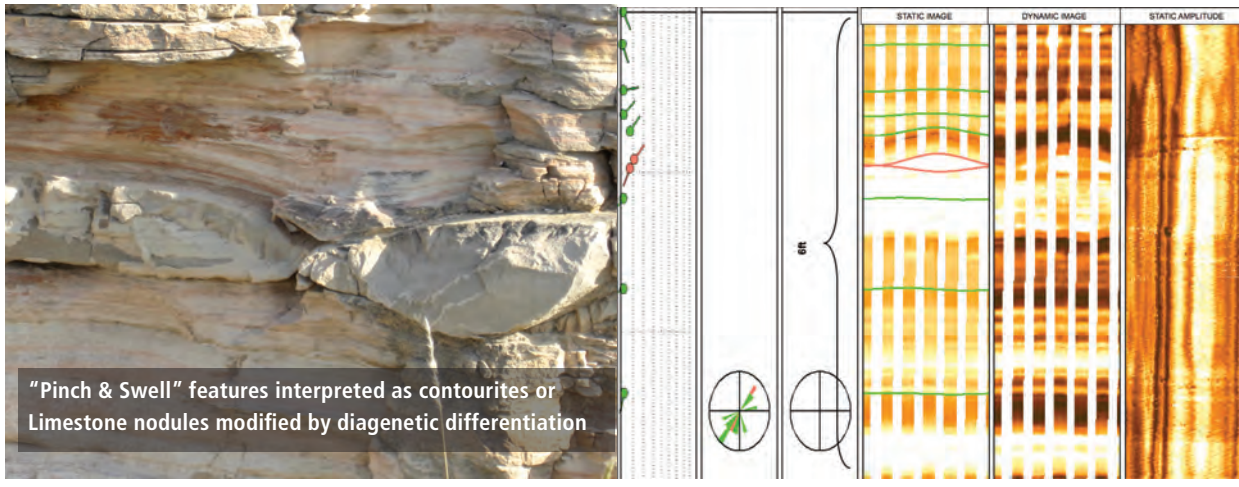

Fig. 8.95—Resistivity imaging characteristics of carbonate nodules observed on an Eagle Ford shale outcrop. (From Palmer and Guidry 2013.)

8.8.2 Applications of Wireline Cross Dipole Acoustic Technology

8.8.2.1 Shear Wave Azimuthal Anisotropy Analysis

In addition to borehole resistivity and acoustic imaging shear wave azimuthal anisotropy analysis using cross dipole acoustic responses provides another technique to determine the direction of the maximum horizontal stress (in vertical wells). A detailed technical description of this topic that is based on the identification of fast and slow shear velocities is covered in Chapter 9. Shear wave anisotropy can be caused by the magnitude of the difference between the maximum and minimum horizontal stresses, intrinsic structural anisotropy due to dipping bedding intersecting the wellbore, or the presence of near wellbore microfractures either natural or drilling induced (Franquet et al. 2011). See **Fig. 8.98**.

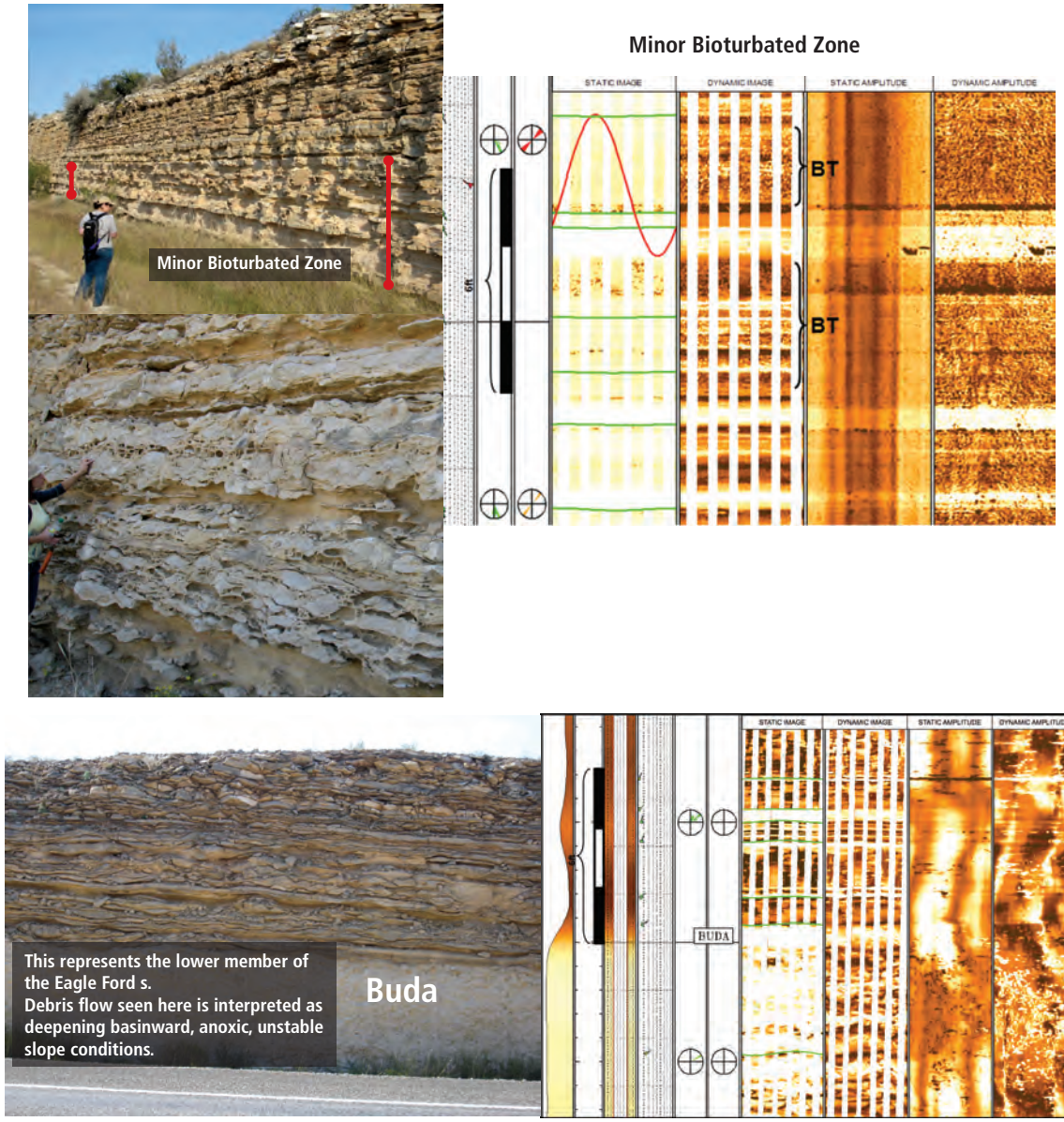

Fig. 8.96—Eagle Ford shale outcrop photos of a bioturbated interval (upper photo) and the contact of the Buda Limestone with a debris flow depositional interval at the base of the Eagle Ford shale (lower photo) and their equivalent resistivity imaging characteristics. (From Palmer and Guidry 2013.)

8.8.2.2 Deep Shear Wave Imaging: Identification of Geologic Hazards or Fractures away from the Wellbore

Deep shear wave imaging consists of using shear body waves generated by a co-located X and Y polarized dipole source that radiate away from the borehole. In the presence of geologic structures with shear impedance contrast, these shear waves can be reflected back to the borehole, enabling the structure to be imaged. The dipole's azimuthal sensitivity, along with the four-component analysis, enables the determination of the reflector's azimuth. This principle has been used to trace anhydrite beds into salt dome structures (Patterson 2008; Tang 2009) and natural fractures in unconventional shale plays (Patterson 2011; Franquet 2011; Bolshakov 2011). Deep shear wave imaging not only characterizes strike and dip angle of reflectors that intersect the wellbore but also can image structures that do not intersect the wellbore trajectory up to 60 ft. away (**Fig. 8.99**).

The shear wave radiation is zero along the dipole source polarization direction because the particle motion is pure compressional in that direction, while the radiation is stronger perpendicular to the dipole source polarization, as shown in **Fig. 8.100**. Tang and Patterson 2009 demonstrated the horizontal polarized shear wave radiation pattern (SH wave) has the best coverage for imaging structures into the formation. Most significantly, they also developed an inversion algorithm to solve for the strike of the acoustic reflector using both in-line (XX and YY) and cross components (XY and YX) recorded by a dipole tool.

Dipole shear wave imaging not only enables deeper investigation into the formation due to lower signal attenuation at lower frequencies (2 to 3 kHz for a dipole signal versus 10 to 15 kHz for a monopole signal) but also allows the calculation of the azimuthal direction of the reflectors (strike).

The directional aspect of P-wave produced by a dipole acoustic transmitter to determine a reflector's azimuth (strike) was studied by Tang (2004). However, that investigation showed that it can only be applicable to slow formations that produce enough P-wave energy from a dipole tool, hence the importance of getting the strike of geological features (discontinuities, beddings, or natural fractures) in fast formations from shear waves generated by cross-dipole logging devices.

Fig. 8.101 shows the comparison among fracture reflectivity imaging from dipole vertical (SV) polarized shear wave, dipole horizontal (SH) polarized shear wave, and monopole

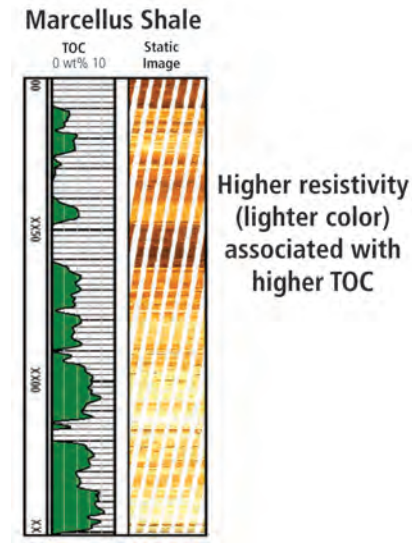

Fig. 8.97—Resistivity imaging characteristics reflecting varying TOC weight percents.

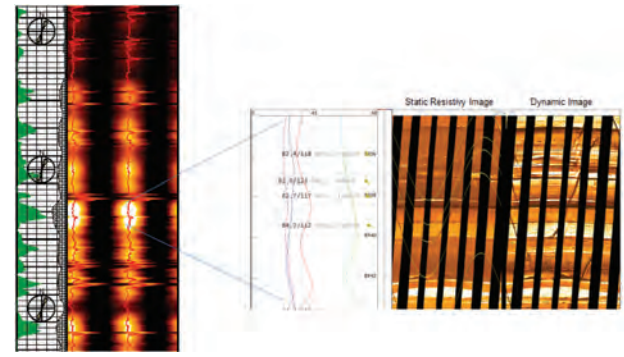

Fig. 8.98—Cross dipole acoustic azimuthal anisotropy associated with near wellbore drilling-induced fractures in the Barnett shale. (Franquet, Patterson, and Moos 2011.)

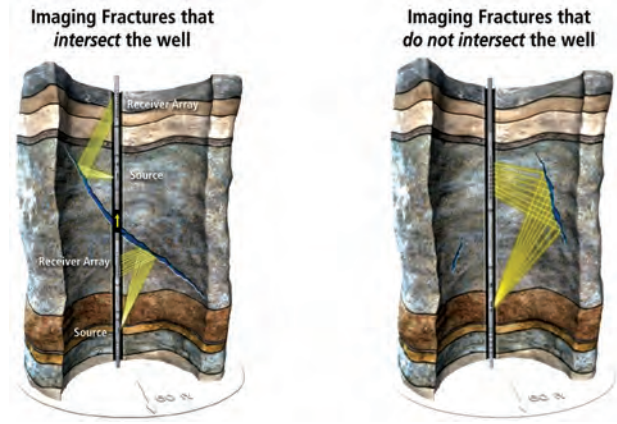

Fig. 8.99—Illustration of deep shear wave imaging characterizing natural fractures.

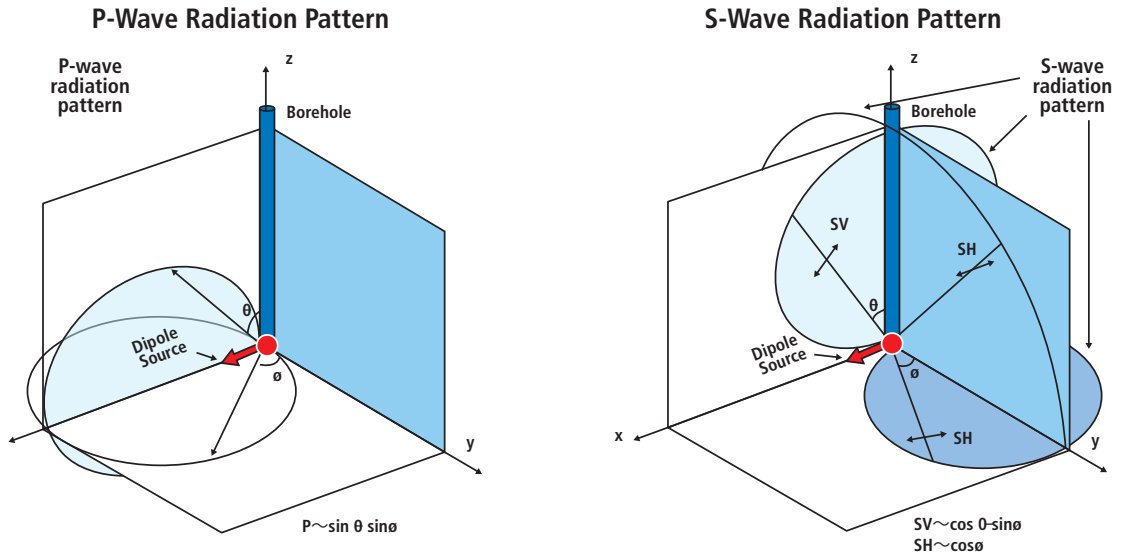

Fig. 8.100—Comparison between P-wave and S-wave radiation patterns of a dipole source.

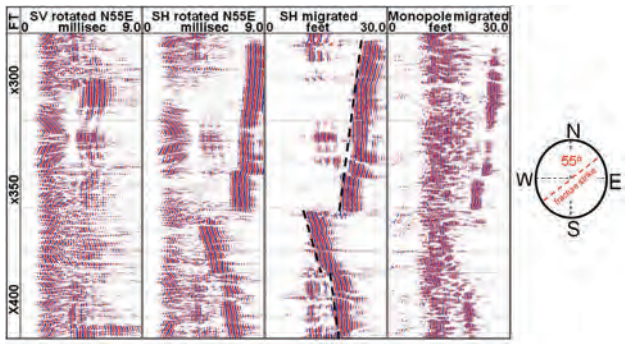

Fig. 8.101—Comparison between vertical and horizontal polarized dipole shear waves azimuthally rotated in the N55E direction and comparison between horizontal polarized dipole shear wave and monopole full-wave forms migrated to radial distance.

full-wave forms acquired on a vertical well drilled in the Haynesville shale (Bolshakov et al. 2011). The dipole SH-wave produces better fracture imaging than the monopole and vertical polarized dipole shear wave. The first two tracks from left to right in Fig. 8.101 correspond to the SV and SH azimuthally rotated dipole waves polarized to N55E direction mapped in the travel-time domain; while, the other two tracks illustrate the SH dipole and monopole waves migrated to radial distance. It is obvious that the SH dipole imaging data have a much better signal-to-noise ratio (SNR) and provide a clear continuous image of fractures located 10 to 27 ft. away from the wellbore than the SV dipole and monopole borehole acoustic reflectivity data.

The deep shear wave imaging consisted of three acoustic borehole data processing stages: shear wave reflection enhancements, reflector strike azimuthal direction inversion, and time-to-radial-distance full-wave data migration.

Shear wave reflection enhancements of the dipole data involve a series of full-wave processes starting from data filtering of direct wave modes, up-going and down-going wave separation, reflected signal stacking, and finally deconvolution to enhance signal-to-noise-ratio. These borehole reflectivity data enhancement techniques can be used separately or in combination to improve the reflected wave imaging (Bolshakov et al. 2011).

- Data filtering of direct wave modes from dipole data
  - Borehole-guided flexural dipole (DTS)
  - Refracted compressional wave (DTC Leaky-P wave)
  - Borehole-guided Stoneley wave (DTST)
- Up-going and down-going wave separation (Tang et al. 2007)
  - Receiver array (below reflector)
  - Transmitter array (above reflector)
- Reflected-signal stacking
  - Common midpoint stacking CMP for reflectors parallel to the borehole
  - Dip move out stacking DMO for reflector with diverse angles respect to the borehole
- Enhancing signal to noise ratio of the reflections
  - Deconvolution

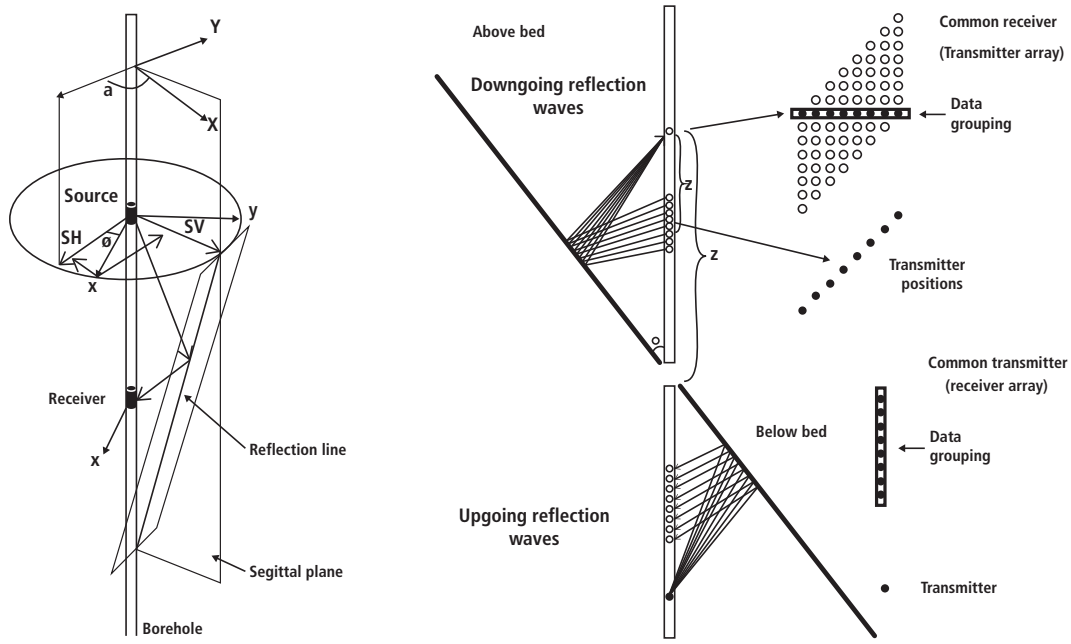

Fig. 8.102—(Left) SV and SH reflections acquired from an inclined reflector using a 4-component cross-dipole tool. (Right) Down-going reflection waves from transmitter array above the reflector and up-going reflection waves from receiver array below the reflector, vertical, and horizontal polarized dipole shear waves azimuthally. (Tang and Patterson 2009.)

The inversion technique to obtain the azimuthal direction of the reflector strike was developed by Tang and Patterson (2009) using the azimuthal sensitivity of the SH and SV waves generated by a dipole source (**Fig. 8.102**). Because the XY and YX cross-components vanish when the dipole source is parallel or perpendicular to the strike of the reflector, a minimization of those components in amplitude or energy can be used to determine the azimuthal angle of the reflector strike.

The borehole data migration from travel time to radial distance is done using the near-field slowness to obtain the final image of the structures around the wellbore.

Fig. 8.103 shows a clear non-intersecting 50 ft. natural fracture striking N75E and detected at 30 ft. away from a vertical well drilled in the Haynesville shale. This large natural fracture has no effect in the near-wellbore cross-dipole anisotropy that is plotted side-by-side with the deep shear wave imaging including both up-going and down-going reflection waves. This fracture is also vertically bounded by lithology changes clearly observed by spikes in the GR curve. Another wellbore drilled vertically in the Haynesville shale (**Fig. 8.104**) also detected many reflectors with varying dip angles after the deep shear wave imaging processing of the cross-dipole borehole acoustic data. These imaging results indicated different structural and mechanical stratigraphic layers within the shale play. The identification of these features is considered important for wellbore completion, reservoir stimulation operations, and future horizontal well placements.

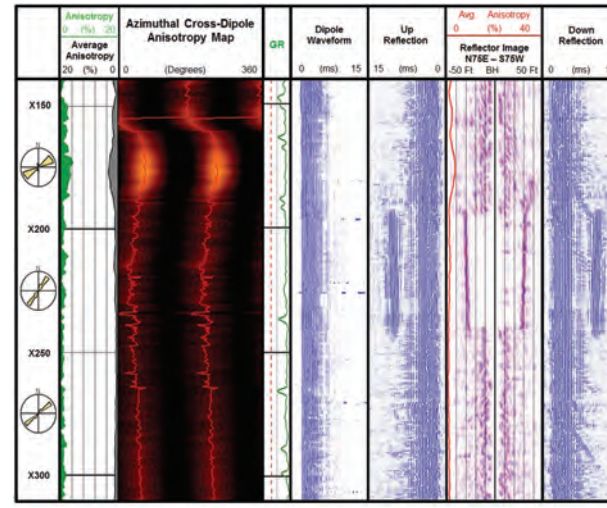

Fig. 8.103—Clear vertical fracture captured by dipole deep shear wave imaging on a vertical wellbore drilled in the Haynesville shale.

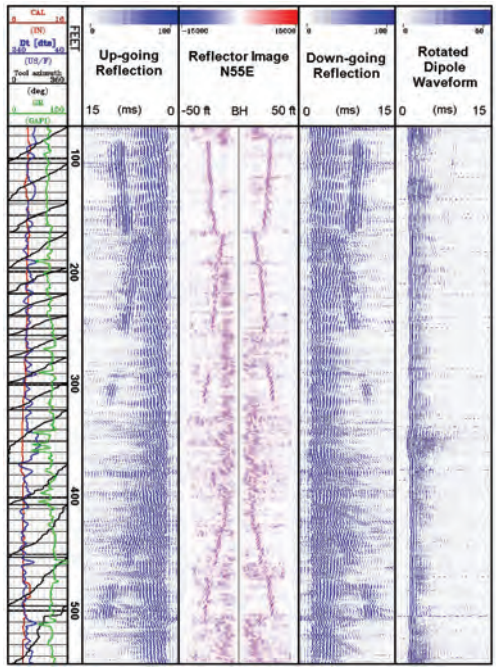

Fig. 8.104—Several dipping natural fractures identified from deep shear wave imaging on a vertical wellbore drilled in the Haynesville shale.

8.8.3 Geomechanical Characterization

The role of geomechanics in unconventional resource development relates to the design and modeling of hydraulic fracturing stimulation, safe and efficient drilling of both vertical and horizontal wellbores, and identification and characterization of sweet spots within the reservoir. In-situ stress analysis includes determination of the in-situ stress orientations, magnitudes, pore pressure, effective rock strength, fracture patterns, and rock structure of the reservoir and surrounding formations (LeCompte et al. 2009). In this section we examine the use of wireline and LWD log measurements to investigate properties of the reservoir that impact the effectiveness of a hydraulic stimulation program and well productivity. This includes determination of the static and dynamic mechanical properties of the reservoir, anisotropy, rock brittleness, hardness, and characterization of any natural fracture networks. The specifics related to the calculation of these parameters, explanation of the related laboratory analyses methodology, and interpretation is covered in detail in Chapter 9.

In the Baker Hughes shale evaluation approach a variety of log-derived mechanical properties and geomechanical analyses are routinely computed for each well (**Fig. 8.105**).

As previously discussed, unconventional shale reservoirs exhibit variability in mineral composition, organic carbon richness, fabric, texture, and depositional environments, which result in variation in mechanical properties of the rock. A representative set of lithofacies can be developed for each shale play using the available conventional log measurements, elemental spectroscopy, TOC weight percent, from either LECO core analyses, regression from log responses or pulsed neutron elemental spectroscopy, core or cuttings derived XRD and description of whole core and thin sections. Each lithofacies adopted should exhibit a similar mineral composition and organic carbon richness and be identifiable in multiple wells. After the mineral variation has been examined and a tentative lithofacies classification organized a statistical study of a variety of mechanical rock properties is performed for each lithofacies type.

Previously in this chapter, we briefly discussed a set of lithofacies developed for the Haynesville shale. **Fig. 8.106** shows the mineral composition variations for each facies.

The lithofacies methodology was applied to each well in a project area in the Haynesville shale. Dynamic and static elastic properties, minimum horizontal stress (SH_{min}), unconfined compressive strength (UCS) a hardness indicator, and two brittleness indexes were computed for each well.

This plot of a Haynesville shale well shows the mineral distribution through the upper, middle, and lower Haynesville shale intervals and a small portion of the underlying Smackover Limestone (**Fig. 8.107**).

- Track 1 is the total GR and THK corrected GR and Haynesville shale interval measured depth tops.
- Track 2 is the measured depth in feet for this vertical well.
- Track 3 shows the compensated neutron porosity (LS units) and the compensated bulk density. The total porosity from the MReX wireline magnetic resonance instrument is in Track 4.
- Track 5, Track 6, and Track 7 contain the weight percentage total clay, total QFM, and total carbonate as plotted on the ternary diagram.
- Track 8, Track 9, and Track 10 display the distribution of anhydrite and pyrite as well as the weight percentage of TOC each on a scale of 0 to 10%. Note that with the exception of only a few feet the middle Haynesville shale, this well contains no organic carbon. That is true for the other wells in this study.
- Track 11 displays the Th/U ratio (blue curve) and the uranium concentration. When the Th/U ratio is two or lower, which is indicative of anoxic deposition, it is shaded gray.

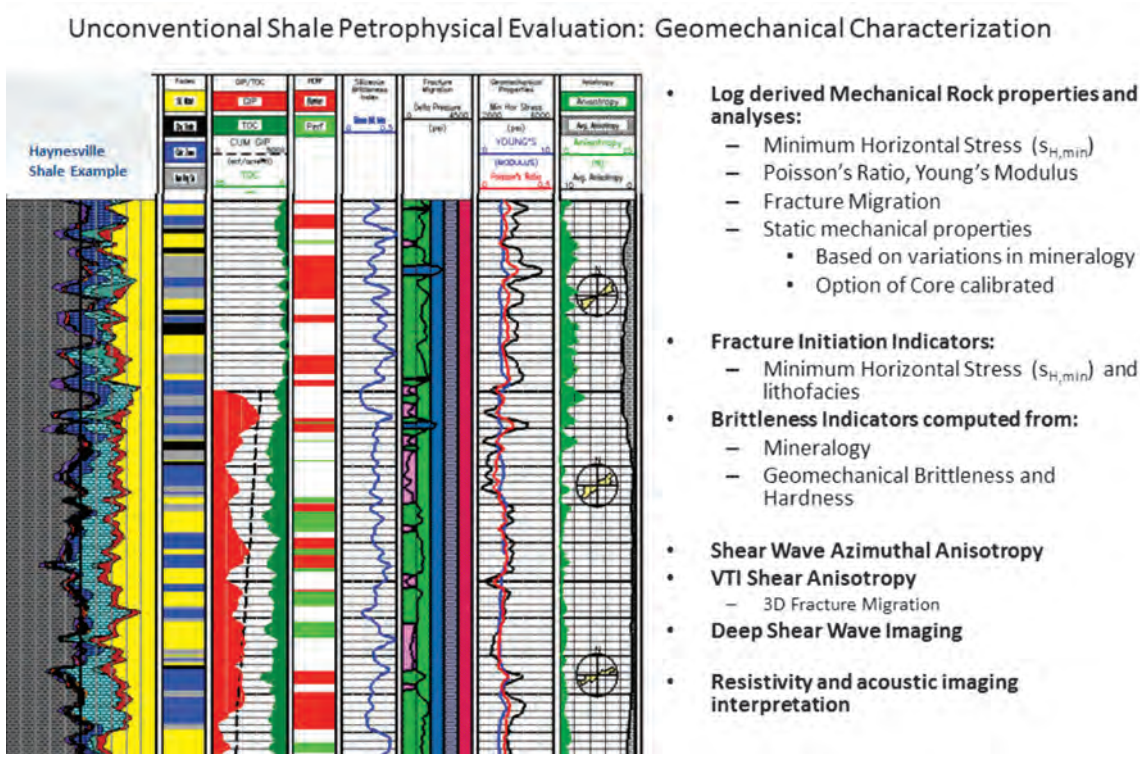

Fig. 8.105—Log plot illustrating some of the routine analyses used in geomechanical characterization of shale reservoirs.

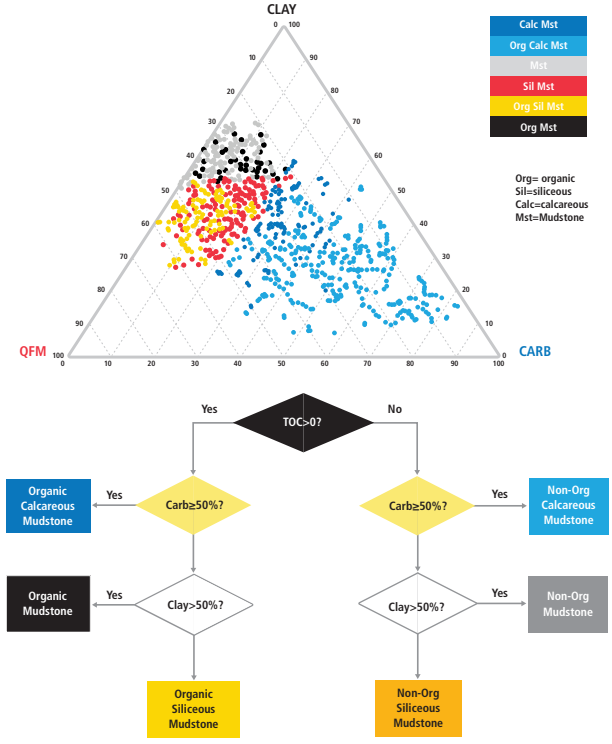

Fig. 8.106—Ternary diagram illustrating mineral composition of Haynesville shale lithofacies.

- Track 12 contains the unconfined compressive strength derived in our geomechanical characterization presented on a scale of 2,000 to 7,000 psi increasing from left to right. The computed minimum horizontal stress (S_{Hmin}) plotted on a scale of 9,000 to 12,000 psi is in Track 14.
- Track 15 displays the lithofacies that were determined. The lithofacies colors are the same as on the ternary diagram with the exception of the non-organic siliceous mudstone, which is orange on the ternary diagram. The crossplot is a pale yellow with a dotted black overlay on the log plot.
- Track 16 contains the computed mineralogy in weight percentage from the Baker Hughes Rock-View expert system which uses the FLeX pulsed neutron elemental spectroscopy and Spectralog spectral gamma ray wireline logging instruments.

The objective of this study was to identify the specific lithofacies that is more conducive to hydraulic fracture initiation and development of a more complex fracture network (Jacobi et al. 2008; Mitra et al. 2010). Often the preferred lithofacies exhibits the most favorable mechanical properties and has a fabric that provides a load-bearing brittle framework (May and Anderson 2013). These intervals would have lower values of minimum horizontal stress, lower values of unconfined compressive strength and Poisson's ratio, and higher values of Young's modulus.

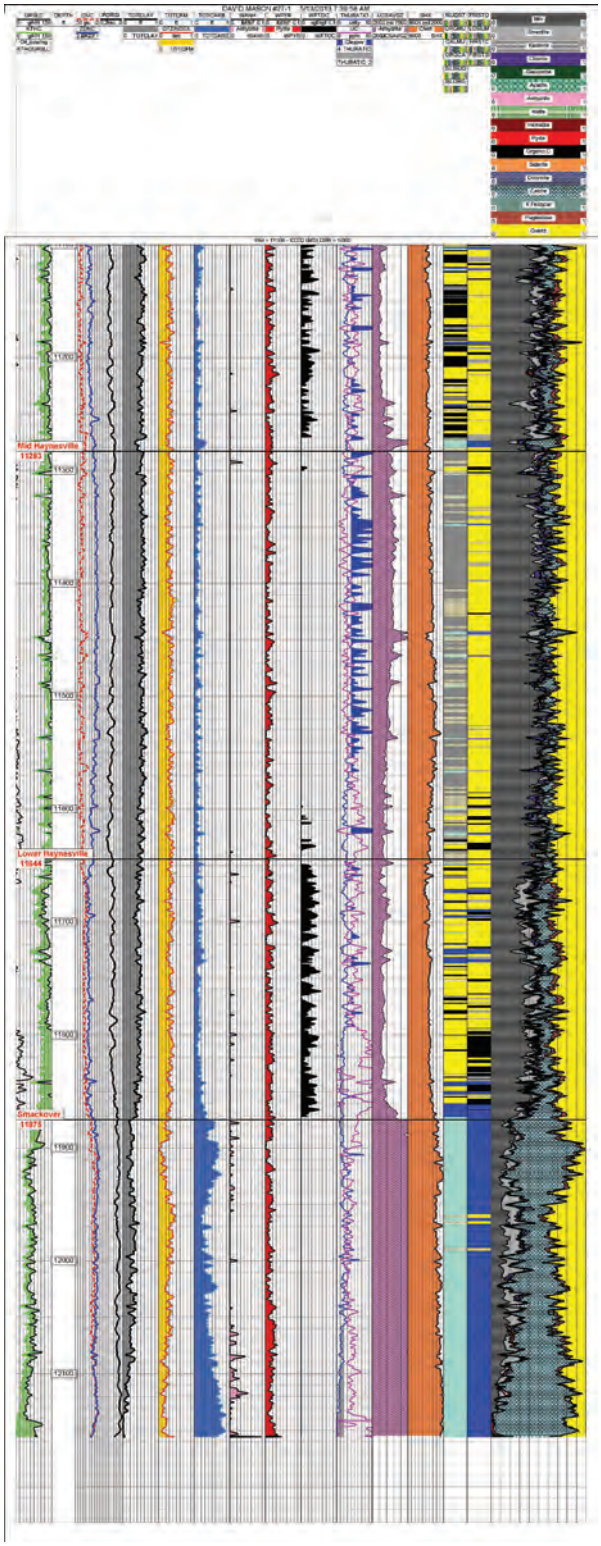

Fig. 8.107—Mineral distribution through the upper, middle, and lower Haynesville shale intervals and a small portion of the underlying Smackover Limestone.

In the Baker Hughes approach, brittleness is computed in two ways. One brittleness index is computed from the Young's modulus and Poisson's ratio. A second brittleness indicator is derived from the mineral composition of the rock. Several versions of mineralogy-based brittleness indicators have been published.

The BIM indicator (brittleness indicator from mineralogy) is calculated by:

$$\frac{\text{Quartz} + \text{Feldspars} + \text{Calcite} + \text{Dolomite}}{\text{Quartz} + \text{Feldspars} + \text{Calcite} + \text{Dolomite} + \text{Siderite} + \text{TOC}}$$

A hardness indicator was also calculated based on a linear relationship between Brinell hardness and the static Young's modulus. The properties of each lithofacies were examined across the gas productive upper and lower Haynesville shale intervals as well as the nonorganic middle Haynesville interval.

Fig. 8.108 compares the mineralogy-derived brittleness index to the unconfined compressive strength for one well in the study. Unconfined compressive strength is one gauge of the tensile strength of the rock. The plot identifies the organic siliceous mudstone facies as having a high brittleness and favorable UCS properties compared to the remaining lithofacies.

Additional histograms and crossplots were examined that identified the organic siliceous mudstone facies as the preferred lithofacies for this Haynesville study area. In **Fig. 8.109** the organic siliceous mudstone facies (yellow)

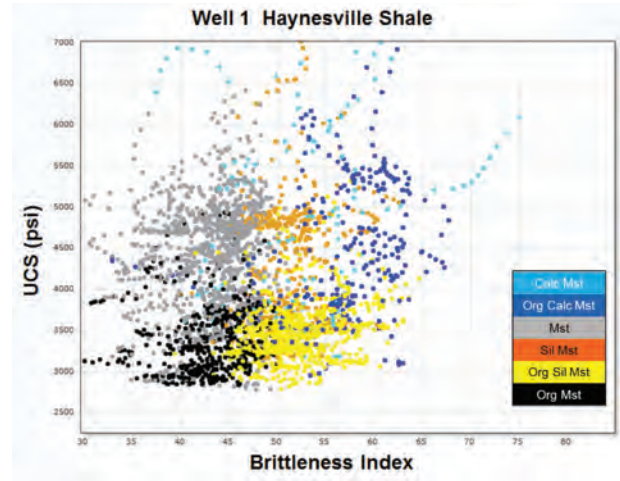

Fig. 8.108—Crossplot of a Haynesville shale illustrating the variation in UCS and brittleness characteristics of a lithofacies scheme.

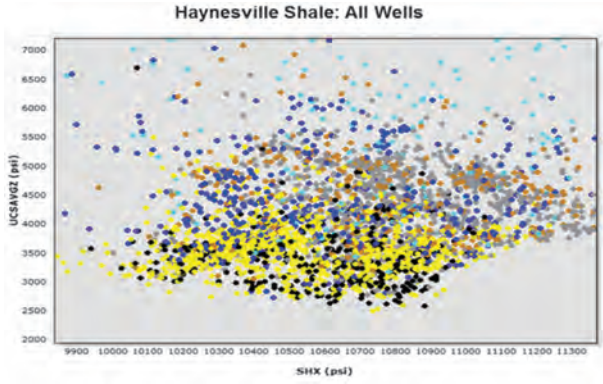

Fig. 8.109—Relationship of S_{Hmin} to UCS for each Haynesville shale lithofacies in the study area.

exhibit lower S_{Hmin} and UCS characteristics than the remaining facies. The plot shows the response for all wells in the study for the complete Haynesville shale section that has a gross thickness of approximately 800 ft.

Fig. 8.110 compares the variation in the computed geomechanical properties for the study wells between the upper, middle, and lower Haynesville shale intervals. The increase in Poisson's ratio and SH_{min} in the middle Haynesville interval is clearly evidenced.

8.9 Utilization of Formation Evaluation Results to Optimize Lateral Well Placement and Lateral Characterization for Stimulation Program Design

Previously we identified the properties of the rock and fluids found in unconventional shale gas and oil reservoirs that must be quantified as part of the petrophysical analysis (**Fig. 8.111**).

The petrophysical analysis results are then used to provide input to the design of the hydraulic fracturing stimulation program by identifying the reservoir zones in each wellbore that are more conducive to hydraulic fracture initiation and development of a more complex fracture network (Jacobi et al. 2008; Mitra et al. 2010). The spatial relationship of these preferred intervals can then be examined to provide input as to the selection of the optimal interval for horizontal lateral placement. **Fig. 8.112** illustrates this process in a Barnett shale well.

The integrated petrophysical analysis plot of this vertical Barnett shale well displays the total porosity from the MReX NMR wireline instrument (Track 5); the calculated free gas saturation (Track 6); TOC weight percentages from two methods in Track 7; total gas in place (Track 8); and two computed geomechanical parameters, unconfined compressive strength and SH minimum stress (Track 9). A set of lithofacies representative of the Barnett shale had been developed and the siliceous mudstone lithofacies (yellow) identified as the preferred lithofacies. A set of

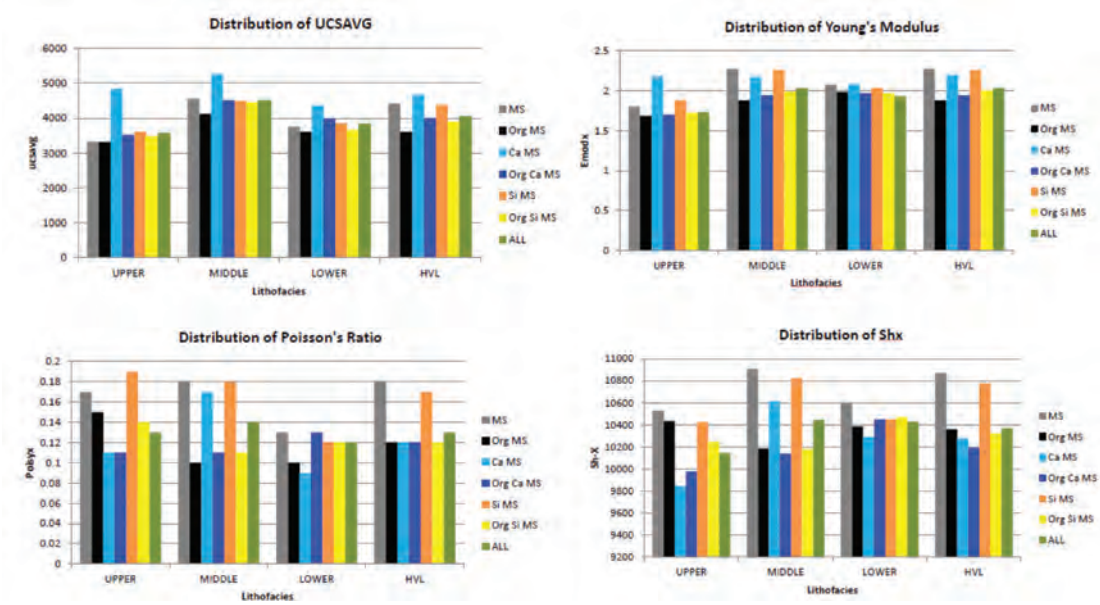

Fig. 8.110—Comparison of the responses by Haynesville shale interval for selected geomechanical properties from the study area wells.

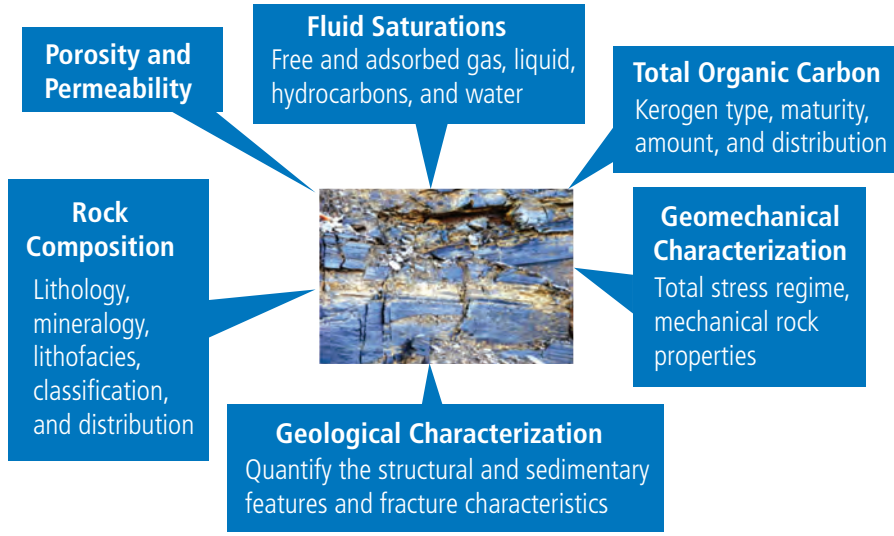

Fig. 8.111—Categories of source rock reservoir characteristics required for petrophysical evaluation.

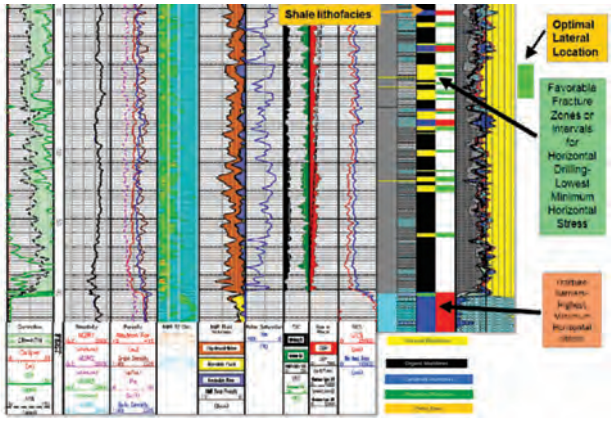

Fig. 8.112—Identification of optimal horizontal lateral interval from an integrated petrophysical analysis.

stoplight indicators were also developed that satisfied the criteria for the computed lithofacies in conjunction with the TOC content, mineralogy, total porosity, and computed geomechanical properties. Intervals were flagged that could act as possible barriers to fracture propagation (red) that had high values of S_{Hmin} and UCS. Intervals identified as the preferred siliceous mudstone lithofacies that had low SH_{min} and UCS values were flagged as being favorable for fracturing (green). The spatial distribution of the thickness of the siliceous mudstone lithofacies flagged as green was examined and an interval of approximately 30 ft. composed almost entirely of the preferred lithofacies with preferred geomechanical properties was identified and was selected by the operator to place the horizontal lateral well.

Detailed petrophysical analyses can also contribute to improved lateral well placement and orientation by integrating the results with 3D seismic datasets to develop a set of improved multicomponent attributes to examine reservoir properties across areas without well control. This was done for the Haynesville well study and was presented previously in this chapter. The detailed results from the petrophysical study including TOC content, mineral composition, porosity, fast and slow dipole acoustic slownesses, and other parameters were used with the 3D seismic data to develop and map a range of reservoir properties including a Brittleness Index and TOC distribution across the interwell areas of the study area (**Fig. 8.113**).

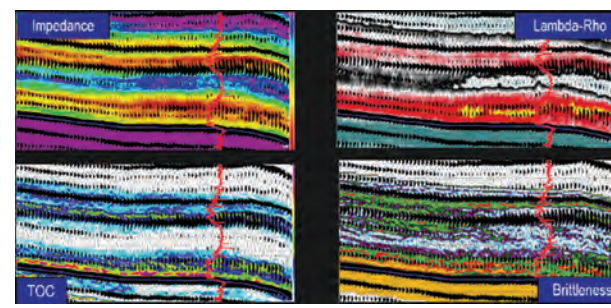

Fig. 8.113—Distribution of reservoir properties including TOC content and brittleness developed from a multi-attribute analysis of Haynesville shale wells.

8.9.1 Integration of Components and Role in Lateral Placement and Completions

8.9.1.1 Stimulation Design

As illustrated in the previous sections, Baker Hughes has industry-competitive wireline, LWD, testing tools, fluids technologies, completion/stimulation technology applications, and now is also developing advanced technology within surface logging systems (SLS).

From an advanced reservoir and completions characterization perspective toward optimal landing of horizontal wells and geologically/engineered driven completions, many specialized datasets provide valuable first-order datasets that can be correlated toward improved reservoir characterization (reservoir and completions quality).

Recommended petrophysical wireline and LWD measurements, rock sample characterization from cores to samples (cuttings and rotary or percussion cores) including operational handling and stabilization procedures, surface logging systems techniques, and recommended laboratory sequence of analyses including core storage and preservation procedures protocols must be defined early within a reservoir characterization program.

Due to the more operationally difficult bottom hole environment in horizontal laterals, as well as the extended horizontal scale of completion zones, LWD, and advanced surface logging systems technologies that do not interfere with operations can assist in cost effectively defining reservoir and completion quality for geologically engineered-driven completions and stimulation.

Advanced technology within surface logging systems that provide differential insight characterization may include rapid quantitative extended hydrocarbon gases and fluid analyses, kerogen characterization, and elemental and mineralogical approaches for predicting kerogen component porosity and completion quality properties. These unconventional resource target reservoir and completion quality attributes, that an interpreter needs to be aware of in these advancing technology fields, can assist in reducing geologic risk, costs, and improving net present value of these industry investments. In addition, the purpose of wellsite analytics is to provide rapid rig time, cost effective, reservoir characterization data for vertical zone placement within exploitation wells and to facilitate custom zone completion decisions within laterals. For custom completion design, lateral reservoir characterization must include reservoir matrix variations of potential HC deliverability, open and closed stressed fracture fabrics, and calculated reach considerations (rock mechanical system).

Defining reservoir and completion quality variability with respect to production results and linking to local spatial reservoir heterogeneity is a critical component of the need of the geologically proper spatial location of completion approach pilots. Most often within unconventional resource plays, "all correlations are local," in that pilot projects apply to their local area only, because of geological, geochemical, and geomechanical variability. That is a significant reason that site-specific reservoir characterization is so important to maximizing the value (NPV) of the asset.

Reservoir integration component approaches within unconventional reservoir lateral placement and lateral completions and stimulation design can be most effectively focused through the characterization of two major component areas: reservoir quality and completions quality.

Project protocols must be established on the acquisition of fit for purpose reservoir characterization datasets for drilling operation programs of unconventional resource plays for exploration and exploitation vertical pilot wells. Reservoir characterization within unconventional reservoirs includes both the evaluation of reservoir quality, which includes measures of the producible hydrocarbon in place which is a function of hydrocarbon viscosity, matrix permeability and pore pressure, and completion quality, which is a function of hydraulic fracture surface area, conductivity, and containment. These components appear to be easy to characterize. However, in practice within the high degree of heterogeneity and variability within nanoscale pore system reservoirs, these are quite difficult to accurately spatially assess.

The optimized recipe requires rock-based calibrated datasets that encourage evaluation of unconventional resource play opportunities (exploration wells) plus their specific hydrocarbon compositional yields and producibility variances (exploitation pilot wells), and the most cost effective and fit for purpose effective completion design methods for improved reservoir reach and reduction of operational costs (D&C) and incremental NPV. Integration of these exploration and exploitation pilot well rock and fluid and gas datasets are required for the reservoir reach and operational improvements for the subsequent high-capital, intensive lateral exploitation wells program. A resulting dynamic spatial rock/fluid/gas data reservoir model that is integrated with completion data/productivity data and geophysical data (3D and microseismic), should be the

basis for geologically engineer-driven lateral completions and improved treatment (completion design) approaches within the development program.

Framework protocol procedural sequence of analyses can be high graded and developed fit for purpose, dependent upon the reservoir characterization producibility constraint components. Additional specialized reservoir characterization protocols may be required within liquids-rich and or gas-rich zones or spatial regions of the unconventional reservoir target(s) dependent upon the fit for purpose need.

Unconventional reservoir characterization is currently considered to have at least sixteen layers of reservoir characterization for reservoir and completion quality. Extensive reservoir characterization indices include developing and improving direct rock-based including geomechanical completion quality and inversion of geophysical data with interpretational approaches that are unconventional reservoir target specific. Critical subsurface reservoir and completion quality risks and uncertainties can be assessed quantitatively, or semiquantitatively, to evaluate the impact of the variation of reservoir characterization on production performance. An example approach to identify measurable reservoir characterization layers is through the tornado plots example (**Fig. 8.114**).

Baker Hughes has recognized that up to sixteen layers of reservoir characterization may be required for unconventional resource play targets. Within each of these layers, multiple characterization sidebars can be developed to characterize each layer component of that unconventional resource play target within a spatial environment. Multiple-layered index sidebars can also increase the confidence and lower the reservoir and completion quality characterization risk associated with each reservoir characterization layer component.

A play or zone-specific recommended unconventional reservoir characterization protocol, for the pad-based exploitation lateral well program, should be the result of this exploration and exploitation pilot well reservoir characterization protocol. A developed lateral exploitation reservoir characterization program should include geosteering reservoir components protocols, drill pipe conveyed characterization tools, minimum wellsite analytics protocols, and spatial geophysical data (3D) integration with processing advances.

These unconventional play or zone specific reservoir characterization protocols should result in well-specific custom completion recommendations for maximum reservoir reach. Protocols should include microseismic monitoring of

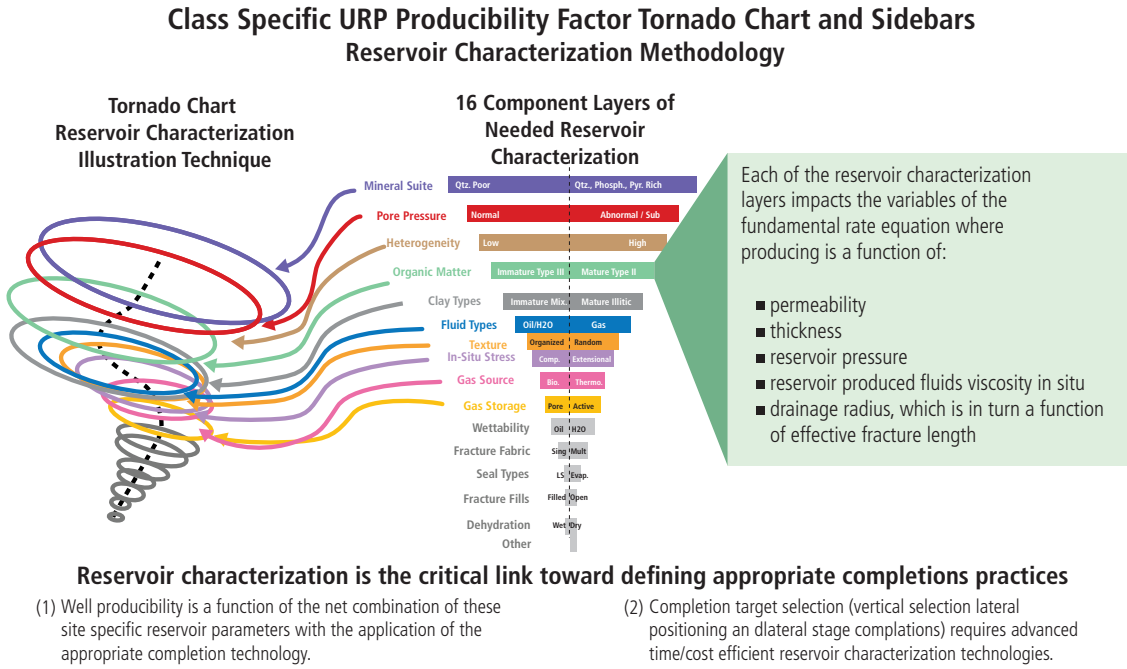

Fig. 8.114—Class-specific URP producibility factor tornado chart and sidebar. (Walles 2014.)

completions, and rock and expected discrete fracture system (DFN) type geologic engineering-driven completions designs regarding specific completion fluids, type (strength and size) of proppant variation during completion fluid placement, width of specific stages, perforation clusters, and post completion production logging (PLT practices).

URP geophysical protocols, with respect to microseismic applications for lateral reach characterization during completion operations, are part of the resulting play-specific document described above (pad exploitation lateral wells protocols). Prior to and within unconventional drilling operations programs, 2D and 3D seismic processing and interpretation protocols are also important.

8.10 References

Ambrose, R.J., Hartman, R.C., Diaz-Campos, M., et al. 2010. New Pore-Scale Considerations for Shale Gas in Place Calculations. Paper SPE 131772 presented at the SPE Unconventional Gas Conference, Pittsburg, Pennsylvania, 23–25 February. http://dx.doi.org/10.2118/131772-MS.

Blood, R., Lash, G. and Bridges, L. 2013. Biogenic Silica in the Devonian Shale Succession of the Appalachian Basin, USA. AAPG Search and Discovery Article 50864 presented at the 2013 Annual Convention and Exhibition, Pittsburgh, Pennsylvania, 19–22 May.

Bolshakov, A., Patterson, D., and Lan. C. 2011. Deep Fracture Imaging around the Wellbore Using Dipole Acoustic Logging. Paper SPE 146769 presented at the SPE Annual Technical Conference and Exhibition, Denver, Colorado, 30 October –2 November. http://dx.doi.org/10.2118/146769-MS.

Bumb, A. C. and McKee, C.R. 1988. Gas-Well Testing in the Presence of Desorption for Coalbed Methane and Devonian Shale. ***SPE Form Eval***, **3** (1): 179–185. SPE 15227-PA. http://dx.doi.org/10.2118/15227-PA.

Bust, V.K., Majid, A.A., Oletu, J.U., et al. 2011. The Petrophysics of Shale Reservoirs: Technical Challenges and Pragmatic Solutions. Paper, IPTC 14631 presented at the International Petroleum Technology Conference, Bangkok, Thailand. 15–17 November. http://dx.doi.org/10.2523/166297-MS.

Bustin, R.M., Bustin, A., Cui, X., et al. 2008. Impact of Shale Properties on Pore Structure and Storage Characteristics. Paper SPE 119892 presented at the SPE Shale Gas Production Conference, Fort Worth, Texas. 16–18 November. http://dx.doi.org/10.2523/119892-MS.

Bustin, R.M., Bustin, A., Ross, D., et al. 2006. Rethinking Methodologies of Characterizing Gas in Place in Gas Shales (Abstract). AAPG Annual Meeting, Houston, Texas.

Bustin, R.M., Bustin, A., Ross, D., et al. 2009. Shale Gas Opportunities and Challenges. AAPG Search and Discovery Article 40382, February.

Chakrabarty, T. and Longo, J.M. 1997. A New Method for Mineral Quantification to Aid in Hydrocarbon Exploration and Exploitation. ***J. Cdn. Pet. Tech.***, **36**: 15–20.

Chalmers, G.R.L. and Bustin, R.M. 2007a. On the Effects of Petrographic Composition on Coalbed Methane Sorption. *International Journal of Coal Geology*, **69**: 288–304.

Chalmers, G.R.L. and Bustin, R.M., 2007b. The Organic Matter Distribution and Methane Capacity of the Lower Cretaceous Strata of Northeastern British Columbia, Canada. *International Journal of Coal Geology*, **70**: 223–339.

Clarkson, C.R., Freeman, M., He, L., et al. 2012a. Characterization of Tight Gas Reservoir Pore Structure Using USANS/SANS and Gas Adsorption Analysis. ***Fuel***, **95**: 371–385.

Clarkson, C.R., Wood, J., Burgis, S., et al. 2012. Nanopore-Structure Analysis and Permeability Predictions for a Tight Gas Siltstone Reservoir by Use of Low-Pressure Adsorption and Mercury-Intrusion Techniques. ***SPE Res Eval & Eng*** **15** (6): 648661. SPE 15537-PA. http://dx.doi.org/10.2118/15537-PA.

Cluff, R. 2011. Approaches to Shale Gas Log Evaluation–A Petrophysicist's Perspective. Presentation during Denver SPE chapter, December 2011.

Cluff, B. and Miller M. 2010. Log Evaluation of Gas Shales: a 35-Year Perspective. Presented at the Denver Well Logging Society (DWLS), SPE, http://dwls.spwla.org/2010-04-Newsletter.htm (accessed 12 October 2014).

Cole, G.A., Drozd, R.J., Sedivy, R.A., et al. 1987, Organic Geochemistry and Oil-Source Correlations, Paleozoic of Ohio. *AAPG Bulletin*, **71** (7): 788–809.

Comisky, J.T., Santiago, M., McCollom, B., et al. 2011. Sample Size Effects on the Application of Mercury Injection Capillary Pressure for Determining the Storage Capacity of Tight Gas and Oil Shales. Paper SPE 149432 presented at the Canadian Unconventional Resources Conference, Alberta, Canada. 15–17 November. http://dx.doi.org/10.2118/149432-MS.

Craddock, P., Herron, S.L., and Badri, R. 2013. Hydrocarbon Saturation from Total Organic Carbon Logs Derived from Inelastic and Capture Nuclear Spectroscopy. Paper SPE 166297 presented at the SPE Annual Technical Conference and Exhibition, New Orleans, Louisiana, 30 September–2 October. http://dx.doi.org/10.2118/166297-MS.

Curtis, M., Ambrose, R., Sondergeld, C., et al. 2011. Investigating the Microstructure of Gas Shales by FIB/SEM Tomography & STEM Imaging. University of Oklahoma, 2011.

Das, M., Jonk, R., and Schelble, R. 2012. Effect Of Multicomponent Adsorption/Desorption Behavior on Gas-In-Place (GIP) and Estimated Ultimate Recovery (EUR) in Shale Gas Systems. Paper SPE 159558 presented at the SPE Annual Technical Conference and Exhibition, San Antonio, Texas. 8–10 October. http://dx.doi.org/10.2118/159558-MS.

Dow, W.G. 1977. Kerogen Studies and Geochemical Interpretations. *Journal of Geochemical Exploration*, **7**: 7999.

Driskill, B., Walls, J., Sinclair, S.W., et al. 2013. Applications of SEM Imaging to Reservoir Characterization in the Eagle Ford Shale, South Texas, U.S.A., in W. Camp, E. Diaz, and B. Wawak, eds., *Electron Microscopy of Shale Hydrocarbon Reservoirs. AAPG Memoir*, **102**: 115–136.

Engelder, T., Lash, G.G., and Uzcategal, R.S. 2009. Joint Sets that Enhance Production from Middle and Upper Devonian Gas Shales of the Appalachian Basin. E&P Note, *AAPG Bulletin*, **93** (7): 857–889.

Franquet, J.A., Mitra, A., Warrington, D.S., et al. 2011. Integrated Acoustic, Mineralogy and Geomechanics Characterization of the Huron Shale. Paper, CSUG/SPE 148411 presented at the Canadian Unconventional Resources Conference, Alberta, Canada. 15–17 November. http://dx.doi.org/10.2118/148411-MS.

Franquet, J.A., Patterson, D., and D. Moos. 2011. Advanced Dipole Borehole Acoustic Processing–Rock Physics and Geomechanics Applications. Paper presented at the SEG International Exposition and 81st Annual Meeting, San Antonio, Texas, 19–23 September.

Fertl, W.H. and Rieke, H.H. 1980. Gamma Ray Spectral Evaluation Techniques Identify Fractured Shale Reservoirs and Source–Rock Characteristics. *J. Pet Tech*, November, 2053–2062.

Gale, J.F.W. 2013. Natural Fractures and Their Relevance for Completions in Shales. Presented at the SPE Industry Workshop–Horizontal Well Completions in North American Shales, June 2013.

Gale, J.F.W., Reed, R.M., and Holder, J. 2007. Natural Fractures in the Barnett Shale and Their Importance for Hydraulic Fracture Treatments. *AAPG Bulletin*, **91** (4) 603–622.

Glorioso, J.C. and Rattia, A. 2012. Basic Petrophysical Concepts for Shale Gas. Paper SPE 153004 presented at the SPE/EAGE European Unconventional Resources Conference and Exhibition, Vienna, Austria. 20–22 March. http://dx.doi.org/10.2118/153004-MS.

Gregg S.J. and Sing, K.S.W. 1982. *Adsorption, Surface Area, and Porosity*, second edition, London; Academic Press, 1982.

Hammes, U. 2009. Sequence Stratigraphy, Depositional Environments and Extent of the Haynesville Shale, East Texas. Presentation during Houston Geological Society Mudstone Conference, February, 2009.

Harris, A.G., Harris, L.D., and Epstein, J.B. 1978, Oil and gas data from Paleozoic rocks in the Appalachian basin: Maps for assessing hydrocarbon potential and thermal maturity (conodont color alteration isograds and overburden isopachs). U.S. Geological Survey Miscellaneous Investigations Series Map I-917-E, 4 sheets, scale 1:2,500,000.

Harvey, P.K., Lofts, J.C., and Lovell, M.A. 1992. Mineralogy Logs: Element to Mineral Transforms and Compositional Collinearity in Sediments. Transactions, SPWLA 33rd Annual Logging Symposium.

Herron, M.M., Herron, S.L., Grau, J.A., et al. 2002. Real-Time Petrophysical Analysis in Siliclastics from the Integration of Spectroscopy and Triple-Combo Logging. Paper SPE 77631 presented at the SPE Annual Technical Conference and Exhibition, San Antonio, Texas. 29 September–2 October. http://dx.doi.org/10.2118/77631-MS.

Herron, S.L. and Herron, M.M. 2000. Application of Nuclear Spectroscopy Logs to the Derivation of Formation Matrix Density. Paper SPWLA-2000-JJ presented at the SPWLA Logging Symposium Dallas, Texas, 4–7 June.

Holzer, L., Indutnyi, F., Gasser, P.H., et al. 2004. Three-Dimensional Analysis of Porous BaTiO3 Ceramics Using FIB Nanotomography. *Journal of Microscopy*, **216** (Pt 1): 84–95.

Honarpour, M.M., Nagarajan, N.R., Orangi, A., et al. 2012. Characterization of Critical Fluid, Rock, and Rock-Fluid Properties-Impact on Reservoir Performance of Liquid-Rich Shales. Paper SPE 158042 presented at SPE Annual Technical Conference and Exhibition, San Antonio, Texas. 8–10 October. http://dx.doi.org/10.2118/158042-MS.

Huang, J., Cavanaugh, T., and Nur, B. 2013. An Introduction to SEM Operational Principles and Geologic Applications for Shale Hydrocarbon Reservoirs, in W. Camp, E. Diaz, and B. Wawak, eds., *Electron Microscopy of Shale Hydrocarbon Reservoirs. AAPG Memoir*, **102**: 1–6.

Hui Tian, H., Pan, L., Xiao, X., et al. 2013. A Preliminary Study on the Pore Characterization of Lower Silurian Black Shales in the Chuandong Thrust Fold Belt, Southwestern China Using Low Pressure N2 Adsorption and FE-SEM Methods. *Marine and Petroleum Geology*, **48**: 8–19.

Hunt, J. M., 1996. *Petroleum Geochemistry and Geology*. W. H. Freeman and Co., New York, 743 p.

Jacobi, D., Brieg, J., LeCompte, B., et al. 2009. Effective Geochemical Characterization of Shale Gas Reservoirs from the Wellbore Environment: Caney and the Woodford Shale. Paper SPE 124231 presented at the SPE Annual Technical Conference and Exhibition, New Orleans, Louisiana. 4–7 October. http://dx.doi.org/10.2118/124231-MS.

Jacobi, D., Gladkikh, M., LeCompte, B., et al. 2008. Integrated Petrophysical Evaluation of Shale Gas Reservoirs. Paper SPE-114925 presented at the CIPC/SPE Gas Technology Symposium 2008 Joint Conference, Calgary, Alberta, Canada. 16–19 June. http://dx.doi.org/10.2118/114925-MS.

Jacobi, D., Longo, J., Sommer, A., et al. 2007. A Chemistry-Based Expert System for Mineral Quantification of Sandstones. Paper PETROTECH-2007 presented at the 7th, International oil & gas conference; PETROTECH-2007; 45, New Delhi, India.

Jarvie, D.M. 1991. Total Organic Carbon (TOC) Analysis, in Merill, R.K.ed., *Treatise of Petroleum Geology: Handbook of Petroleum Geology, Source and Migration Processes and Evaluation Techniques, AAPG*: 113–118.

Jenkins, C.D. and Boyer, C.M. 2008. Coalbed- and Shale-Gas Reservoirs. Distinguished Author Series, *J. Pet Tech*, 60 (2): 9299. SPE 103514-JPT. http://dx.doi.org/10.2118/103514-JPT.

Karastathis, A. 2007. Petrophysical Measurements on Tight Gas Shales. MS thesis University of Oklahoman, (2007).

King, G.E. 2010. Thirty Years of Gas Shale Fracturing: What Have We Learned? Paper SPE 133456 presented at the SPE Annual Technical Conference and Exhibition, Florence, Italy. 19–22 September. http://dx.doi.org/10.2118/1334561-MS.

Kuila, U. and Prasad, M. 2013. Specific Surface Area and Pore-Size Distribution in Clays and Shales. *Geophysical Prospecting*, **61**: 341–362.

Lash, G.G. and Engelder, T. 2011. Thickness Trends and Sequence Stratigraphy of the Middle Marcellus Formation, Appalachian Basin: Implications for Acadian Foreland Basin Evolution. *AAPG Bulletin*, **95** (1): 61–103.

Leahy-Dios, A., Das, M., Agarwal, M., et al. 2011. Modeling of Transport Phenomena and Multicomponent Sorption for Shale Gas and Coalbed Methane in an Unstructured Grid Simulatord. Paper SPE 147352 presented at the SPE Annual Technical Conference and Exhibition, 30 October–2 November, Denver, Colorado. http://dx.doi.org/10.2118/147352-MS.

LeCompte, B. and Hursan, G. 2010. Quantifying Source Rock Maturity from Logs: How to Get More than TOC from Delta Log R. Paper SPE-133128 presented at the SPE Annual Technical Conference and Exhibition, Florence, Italy. 19–22 September. http://dx.doi.org/10.2118/133128-MS.

LeCompte, B., Franquet, J.A., and Jacobi, D. 2009. Evaluation of Haynesville Shale Vertical Well Completions with a Mineralogy Based Approach to Reservoir Geomechanics. Paper SPE-124227 presented at the SPE Annual Technical Conference and Exhibition, New Orleans, Louisiana. 4–7 October. http://dx.doi.org/10.2118/1242271-MS.

Legaretta, L. and Villar, H.J. 2012. Discussing the Maturity of the Source Rock in Neuquén Basin to Determine which Specific Areas Will Produce Gas and Oil, American Business Conference: Shale Gas and Oil. American Business Conference: Shale Gas and Tight Oil Production, Buenos Aires, 24–26 January.

Lemmens, H. and Richards, D. 2013. Multiscale Imaging of Shale Samples in the Scanning Electron Microscope in W. Camp, E. Diaz, and B. Wawak, eds., *Electron Microscopy of Shale Hydrocarbon Reservoirs. AAPG Memoir*, **102**: 27–35.

Lewis, R., Singer, P., Jiang, T., et al. 2013. NMR T2 Distributions in the Eagle Ford Shale: Reflections on Pore Size. Paper SPE 164554 presented at the SPE Unconventional Resources Conference, The Woodlands, Texas, 10–12 April. http://dx.doi.org/10.2118/164554-MS.

Loucks, R.G., Reed, R.M., Ruppel S.C., et al. 2010. Preliminary Classification of Matrix Pores in Mudrocks. Presented to Gulf Coast Association of Geological Societies (GCAGS), April 2010.

Loucks, R.G., Reed, R.M., Ruppel S.C., et al. 2012. Spectrum of Pore Types and Networks in Mudrocks and a Descriptive Classification for Matrix-Related Mudrock Pores. *AAPG Bulletin*, **96** (6): 1071–1078.

Loucks, R.G. and Ruppel S.C. 2006. Mississippian Barnett Shale in the Fort Worth Basin: Lithofacies and Depositional Setting of a Deep-Water Shale-Gas Succession. Presentation during Barnett Shale-Gas Play of the Fort Worth Basin Seminar, Bureau of Economic Geology and Texas Region Petroleum Technology Transfer Council.

Loucks, R.G. and Ruppel S.C. 2007. Mississippian Barnett Shale: Lithofacies and Depositional Setting of a Deep-Water Shale-Gas Succession in the Fort Worth Basin, Texas. *AAPG Bulletin*, **91** (4): 579–601.

Luffel, D.L. and Guidry, F.K. 1992. New Core Analysis Methods for Measuring Reservoir Rock Properties of Devonian Shale. *J. Pet Tech*, **44** (11): SPE 20571-PA. http://dx.doi.org/10.2118/20571-PA.

Manger, K.C., Oliver, S.J.P., Curtis, J.B., et al. 1991. Geologic Influences on the Location and Production of Antrim Shale Gas, Michigan Basin. Paper SPE 21854 presented at the Low Permeability Reservoirs Symposium, Denver, Colorado. 15–17 April. http://dx.doi.org/10.2118/21854-MS.

Martinez-Kuliowski, N., Wright, M., and Reynolds, A. 2013. Effective Application of Inorganic Geochemical Data in Shale Resource Plays: A Case Study from the Appalachian Basin. AAPG Search and Discovery Articles 10556, presented at the AAPG Annual Convention and Exhibition, Pittsburgh, Pennsylvania, 19–22 May.

Mastalerz, M., He, L., Melnichenko, Y.B., et al. 2012. Porosity of Coal and Shale: Insights from Gas Adsorption and SANS/USANS Techniques. *Energy & Fuels*, **26**: 5109–5120.

May, J.A. and Anderson, D.S. 2013. Mudrock Reservoirs–Why Depositional Fabric and Sequence Stratigraphic Framework Matter. AAPG Search and Discovery Article 80338 adapted from AAPG Distinguished Lecture, 2012–13 Lecture Series.

Michael, G.E., Packwood, J., and Holba, A. 2014. Determination of In-Situ Hydrocarbon Volumes in Liquid Rich Shale Plays. AAPG Search and Discovery Articles 80365a adapted from oral presentation given at Geoscience Technology Workshop, Hydrocarbon Charge Considerations in Liquid-Rich Unconventional Petroleum Systems, Vancouver, BC, Canada, 5 November 2013.

Mitra, A., Warrington, D., and Sommer, A. 2010. Application of Lithofacies Models to Characterize Unconventional Shale Gas Reservoirs and Identify Optimal Completion Intervals. Paper SPE 132513 presented at the SPE Western Regional Meeting, Anaheim, California. 27–29 May. http://dx.doi.org/10.2118/132513-MS.

Moss, K. 2005. Antrim Shale Fracture Frequency Analysis, presentation, Baker Hughes internal presentation.

Nöth S. 1991. Die Conodontendiagenese als Inkohlungsparameter und ein Vergleich unterschiedlich sensitiver Diageneseindikatoren am Beispiel von Triassedimenten Nord– und Mitteldeutschlands, (German), *Boch Geol Geotech Arb*, 37: 1–169.

Passey, Q.R. 2011. Source Rock Analysis from Well Logs, presented at the topical conference, Society of Petrophysicists and Well Log Analysts.

Passey, Q.R., Bohacs, K.M., Esch, W.L., et al. 2010. From Oil-Prone Source Rock to Gas-Producing Shale Reservoir–Geologic and Petrophysical Characterization of Unconventional Shale-Gas Reservoirs. Paper SPE 131350 presented at the International Oil and Gas Conference and Exhibition in China, Beijing, China. 8–10 June.

Passey, Q.R., Bohas, K.M., Esch, W.L., et al. 2012. My Source Rock Is Now My Reservoir–Geologic and Petrophysical Characterization of Shale–Gas Reservoirs. ***Search and Discovery*** Article 80231.

Passey, Q.R., Creaney, J.B., Kulla, F., et al. 1990. A Practical Model for Organic Richness from Porosity and Resistivity Logs. ***AAPG Bulletin***, **74** (12): 1777–1794.

Patterson, D., Mekic, N., Bolshakov, A., et al. 2011. Unconventional Reservoir Fracture Evaluation Utilizing Deep Shear-Wave Imaging. Paper presented at 52nd SPWLA Annual Logging Symposium, Colorado Spring, Colorado. 14–18 May.

Patterson, D., Tang, X.M., and Ratigan, J. 2008, Mapping Structural Geology from Solution-Mined Storage Cavern Wellbores for Selecting Casing Shoe and Leaching String Depths. Paper presented at the SMRI Solution Mining Research Institute Technical Conference, Galveston, Texas, October 13–14.

Pemper, R., Han, X., Mendez, F., Jacobi, D., et al. 2009. The Direct Measurement of Carbon in Wells Containing Oil and Natural Gas Using a Pulsed Neutron Mineralogy Tool. Paper SPE 124234 presented at the SPE Annual Technical Conference and Exhibition, New Orleans. 4–7 October. http://dx.doi.org/10.2118/124234-MS.

Pemper, R., Sommer, A., Guo, P., et al. 2006. A New Pulsed Neutron Sonde for Derivation of Formation Lithology and Mineralogy. Paper SPE 102770 presented at the SPE Annual Technical Conference and Exhibition, San Antonio, Texas. 24–27 September. http://dx.doi.org/10.2118/102770MS.

Peeters, M. and Visser, R. 1991. A Comparison of Petrophysical Evaluation Packages: LOGIC, FLAME, ELAN, OPTIMA and ULTRA. ***SPWLA The Log Analyst***: 350–357, July–August.

Peters, K.E. and Cassa, M.R. 1994. Applied Source Rock Geochemistry. In L.B. Magoon and W.G. Dow, eds., ***The Petroleum System–From Source to Trap. AAPG Memoir***, **60**: 93–120.

Pollastrano, R.M., Roberts, L.N.R., Cook, T.A., et al. 2008. US Geological Survey, Assessment of Undiscovered Technically Recoverable Oil and Gas Resources of the Bakken Formation, Williston Basin, Montana and North Dakota, http://pubs.usgs.gov/fs/2008/3021/pdf/FS08-3021_508.pdf (accessed 12 November 2014).

Quirein, J.A., Galford, J.A., Shannon, S., et al. 2009. Field Test Results of a New Neutron Induced Gamma Ray Spectroscopy Geochemical Logging Tool. Paper SPE 123992 presented at the SPE Annual Technical Conference and Exhibition, 4-7 October, New Orleans, Louisiana. http://dx.doi.org/10.2118/123992.

Radlinski A.P., Edwards, D.S., Hinde, A.L., et al. 2007. Hydrocarbon Generation and Expulsion from Early Cretaceous Source Rocks in the Browse Basin, North West Shelf, Australia: A Small Angle Neutron Scattering and Pyrolysis Study, Geoscience Australia Record 2007/04, ISBN 9781921236273.

Ramirez, T.R., Klein, J.D., Bonnie, J.M., et al. 2011. Comparative Study of Formation Evaluation Methods for Unconventional Shale-Gas Reservoirs: Application to the Haynesville Shale (Texas). Paper SPE 144062 presented at the North American Unconventional Gas Conference and Exhibition, The Woodlands, Texas, 14–16 June. http://dx.doi.org/10.2118/144062-MS.

Rehm, C., ed. 2007. Pushing Small-Angle Neutron Scattering at OPAL to Smaller Q. Workshop report, ***Australian Nuclear Science and Technology***, 15–16 November.

ResTech Houston, Inc. 1996. Development of Laboratory and Petrophysical Techniques for Evaluating Shale Reservoirs: Gas Research Institute final report GRI 95/0496, 286.

Rodrigues, N., Cobbold, P.R., Løseth, H., et al. 2009. HC generation related geopressured beef horizontal fracture systems from: Composition of beef. Widespread bedding-parallel veins of fibrous calcite ("beef") in a mature source rock (Vaca Muerta Fm, Neuquén Basin, Argentina): evidence for overpressure and horizontal compression. ***Journal of the Geological Society***, London, **166** (4): 695–709. http://dx.doi.org/10.1144/0016-76492008-111.

Sadykov, S., Collamore, A., Guidry, M., et al. 2012. North American Analogues and Strategies for Success in Developing Shale Gas Plays in Europe. Search and Discovery Article #80298, AAPG GTW presented at the 2013 Annual Convention and Exhibition, Pittsburgh, Pennsylvania, 19-21 May.

Schmitt, M., Fernandes, C.P., da Cunha Neto, J.A.B., et al. 2013. Characterization of Pore Systems in Seal Rocks Using Nitrogen Gas Adsorption Combined with Mercury Injection Capillary Pressure Techniques. *Marine and Petroleum Geology*, **39**: 138–149.

Schmoker, J. 1979. Determination of Organic Content of Appalachian Devonian Shales from Formation-Density Logs. *AAPG Bulletin* **63** (9): 1504–1537.

Schmoker, J. 1981. Determination of Organic-Matter Content of Appalachian Devonian Shales from Gamma-Ray Logs. United States Geological Survey, March 1981.

Schmoker, J. and Hester, T. 1983. Organic Carbon in Bakken Formation, United States Portion of Williston Basin. *AAPG Bulletin*, **67** (12): 2165–2174

Sing, K.S., Everett, D.H., Haul, R.A.W., et al. 1985. Reporting Physisorption Data for Gas/Solid Systems with Special Reference to the Determination of Surface Area and Porosity. *Pure Appl. Chem.*, **57** (4): 603–619.

Sinha, S., Braun, E.M., Passey. Q.R., et al. 2012. Advances in Measurement Standards and Flow Properties Measurements for Tight Rocks such as Shales. Paper SPE SPE 152257 presented at the SPE/EAGE Vienna Conference, March. http://dx.doi.org/10.2118/1522571-MS.

Slatt, R.M., Molinares-Blanco, C., Amorocho, J.D. et al. 2014. Sequence Stratigraphy, Geomechanics, Microseismicity and Geochemistry Relationships in Unconventional Resource Shales Paper URTeC 1934195 presented at the SPE/AAPG/SEG Unconventional Resources Technology Conference, Denver, Colorado. 25–27 August. http://dx.doi.org/10.15530/urtec-2014-1934195.

Slatt, R.M., Singh, P., Philip, R.P., et al. 2008. Workflow for Stratigraphic Characterization of Unconventional Gas Shales. Paper SPE 119891 presented at the SPE Shale Gas Production Conference, Fort Worth, Texas. 16–18 November. http://dx.doi.org/10.2118/119891-MS.

Sondergeld, C.H., Newsham, K.E., Comisky, J.T., et al. 2010. Petrophysical Considerations in Evaluating and Producing Shale Gas Resources. Paper SPE 131768 presented at the SPE Unconventional Gas Conference, Pittsburgh, Pennsylvania. 23–25 February. http://dx.doi.org/10.2118/131768-MS.

Sondergeld, C.H., Rai, C.S., and Moncrief, J. 2010. Micro-Structural Studies of Gas Shales. Paper SPE 131771 presented at the SPE Unconventional Gas Conference, Pittsburgh, Pennsylvania. 23–25 February. http://dx.doi.org/10.2118/131771-MS.

Stach, E., Mackowsky, M.T., Teichmuller, M., et al. 1975. *Stach's Textbook of Coal Petrology*. Gebruder Bornttraeger, Berlin, Germany, 428.

Surdam, R.C., Boese, S. and Crossey, L. J. 1984. The Chemistry of Secondary Porosity. In Mcdonald, D.A. and Surdam, R.C. (eds), *Clastic Diagenesis*. *AAPG Memoir*. **37**: 127–151.

Tang, X.M. 2004. Imaging Near-Borehole Structure Using Directional Acoustic-Wave Measurement. *Geophysics*, **69**: 1378–1386.

Tang, X.M. and Patterson, D.J. 2009. Single-Well S-wave Imaging Using Multicomponent Dipole Acoustic-log Data. *Geophysics*, **74** (6): WCA211–WCA223. http://dx.doi.org/10.1190/1.3227150.

Tang, X.M., Patterson, D., and Ratigan, J. 2009. Mapping Structural Geology from Solution-Mined Storage Cavern Wellbores Using Single-Well Acoustic Imaging. *Oilfield Technology*, **2**: 35–39.

Tang X.M., Zheng Y., and Patterson D. 2007. Processing Array Acoustic-Logging Data to Image Near-Borehole Geologic Structures. *Geophysics*, **72**: E87–E97.

Tobin, R.C. and Claxton, B.L. 2000. Multidisciplinary Thermal Maturity Studies Using Vitrinite Reflectance and Fluid Inclusion Microthermometry: A New Calibration of Old Techniques. *AAPG Bulletin*, **84** (10): 1647–1665.

Tolke, J., Baldwin, C. Mu, Y., Derzhi, N. Fian, Q. Grader, A. and Dvorkin, J. (2010). Computer Simulations of Fluid Flow in Sediment; From Images to Permeability. *The Leading Edge*, 29(1), 68-74.

USANS 2014. Oak Ridge National Laboratory Neutron Sciences, http://neutrons.ornl.gov/usans/ (accessed 12 October 2014).

Vickers, T. and Vasconcellos, F. 2006. Relative Scales of Eukaryotes, Prokaryotes, Viruses, Proteins and Atoms, 27 November. http://common.wikipedia.org/wiki/File:Relative scale.svg (accessed 12 November 2014).

Walles, F. 2007. A New Method to Help Identify Unconventional Targets for Exploration and Development through Integrative Analysis of Clastic Rock Property Fields. 2007 Bulletin Corpus Christi Geologic Society & Coastal Bend Geophysical Society November 2007: 21–35 ISSN 0739- http://www.ccgeo.org/bulletin/November2007.pdf (accessed 12 November 2014).

Walles, F., Cameron, M., and Jarvie, D. 2008. Unconventional Resources: Quantification of Thermal Maturity Indices with Relationships to Predicted Shale Gas Producibility "Gateway" Visualization & Attribute Technique, presented at the, Houston Geological Society, and AAPG Convention poster, February.

Walles, F. 2010. What Makes a Shale System–Gas Producible? How/Why May Producibility Vary? Presented at the AAPG Annual Convention ACE, New Orleans, Louisiana, April 2010.

Walles, F. 2012. Layered Process Models towards Sweetspot Identification of Unconventional Resource Reservoirs. Presented during The Statoil Research Summit, 15 October 2012, Trondheim, Norway.

Walles, F. 2012. Layered Process Models towards Sweetspot Identification of Unconventional Resource Reservoirs. Presented at the Sonatrach/Talisman Summit, October 2012.

Walles, F. 2013. Unconventional Integrating Layered Petroleum System Process Model Approaches towards Unconventional Reservoir Assessment and Optimization. Presented at Baker Hughes Innovation Forum 2013 Distinguished Lecture Series, April 2013.

Walles, F. 2014. Could Vertical and Horizontal Unconventional Petroleum System Based Reservoir Characterization Approaches form a Basis towards Improved Reservoir Reach and Recovery? Presented at the SPE Horizontal Well Completions in North American Unconventionals ATW. June 9–12, Huntington Beach, California.

Walles F.E. 2004. A New Method to Help Identify Unconventional Targets for Exploration and Development through Integrative Analysis of Clastic Rock Property Fields. Presented at the Petroleum Technology Transfer Council (PTTC) Unconventional Reservoirs Symposium, Ellison Mills Geotechnology Institute-Dallas, Texas. 3 November 2004.

Walles, F.E. 2004. A New Method to Help Identify Unconventional Targets for Exploration and Development through Integrative Analysis of Clastic Rock Property Fields. Presented at the Houston Geological Society Bulletin, Paper illustrates authored Clastic Graphic Synthesis Model (CGSM) approach, October. http://www.hgs.org/en/articles/printview.asp?250.

Walles F.E. 2009. Framework for Potential Performance Classification of Gas Shales. Presented at the Unconventional Reservoirs Workshop, University of Oklahoma Mewbourne School of Petroleum and Geological Engineering, Norman, Oklahoma. August.

Walles F.E. 2009. Matrix Assessment of Thermal Maturity. Presented at the Shale Resource Workshop, Energy Institute at TCU, Ft. Worth, Texas, January.

Walles F.E. 2013. Layered Process Model Approaches in Understanding Geological Drivers for Production and Productivity of Unconventional Reservoirs. Presented at the SPE ATW Understanding Well Performance and Optimizing Completions in the Bakken, San Diego, CA. 10–12 December.

Walles F.E. 2013. Integrating Layered Petroleum System Process Model Approaches towards Unconventional Reservoir Assessment and Optimization. Presented at the SPE ATW Horizontal Well Completions in North American Shales, Keystone, Colorado.

Walles F.E. and Cameron, M.S., 2009. Evaluation of Unconventional Gas Reservoirs: Tornado Charts and Sidebars. Poster presented at the AAPG 2009 Annual Convention.

Walls, J. 2010. Micro X-Ray CT Scanning for Core Fracture Systems. *InGrain*.

Walls, J., Anderson, E.D., and Ceron, M.R. 2013. Results and Methodology from ANH (Colombia) Unconventional Resources Core Project, Search and Discovery Article 80346.Walles F.E. 2006. Applying the "Geo" into Organic Geochemistry of Shale Gas Systems. Presented at the SPE ATW Unconventional Gas Reservoirs, Keystone, Colorado. April 2006.

Walls, J. and Armbruster, M. 2012. Shale Reservoir Evaluation Improved by Dual Energy X-Ray CT Imaging. *J Pet Tech*, **64** (11): 28–32.

Walls, J. and Diaz, E. 2014. Comparison of Reservoir Quality from the LaLuna, Gacheta and US Shale Formations. *AAPG Search and Discovery* Article #41396.

Walls, J. and Sinclair, S.W. 2011. Eagle Ford Shale Reservoir Properties from Digital Rock Physics: European Association of Geoscientists and Engineers. *First Break*, **29**: 97–101.

Wang, G. and Carr, T.R. 2013. Organic-rich Marcellus Shale Lithofacies Modeling and Distribution Pattern Analysis in the Appalachian Basin. *AAPG Bulletin*, **97** (12): 2205.

Ward, J.A. 2010. Kerogen Density in the Marcellus Shale. Paper SPE 131767 presented at the SPE Unconventional Gas Conference, Pittsburgh, Pennsylvania, 23–25 February. http://dx.doi.org/10.2118/137946-MS.

Wright, A.M., Spain, D., and Ratcliffe, K.T. 2010. Application of Inorganic Whole Rock Geochemistry to Shale Resource Plays. Paper CSUG/SPE 137946 presented at the Canadian Unconventional Resources and International Petroleum Conference, Calgary, Alberta, Canada. 19–21 October. http://dx.doi.org/10.2118/137946-MS.

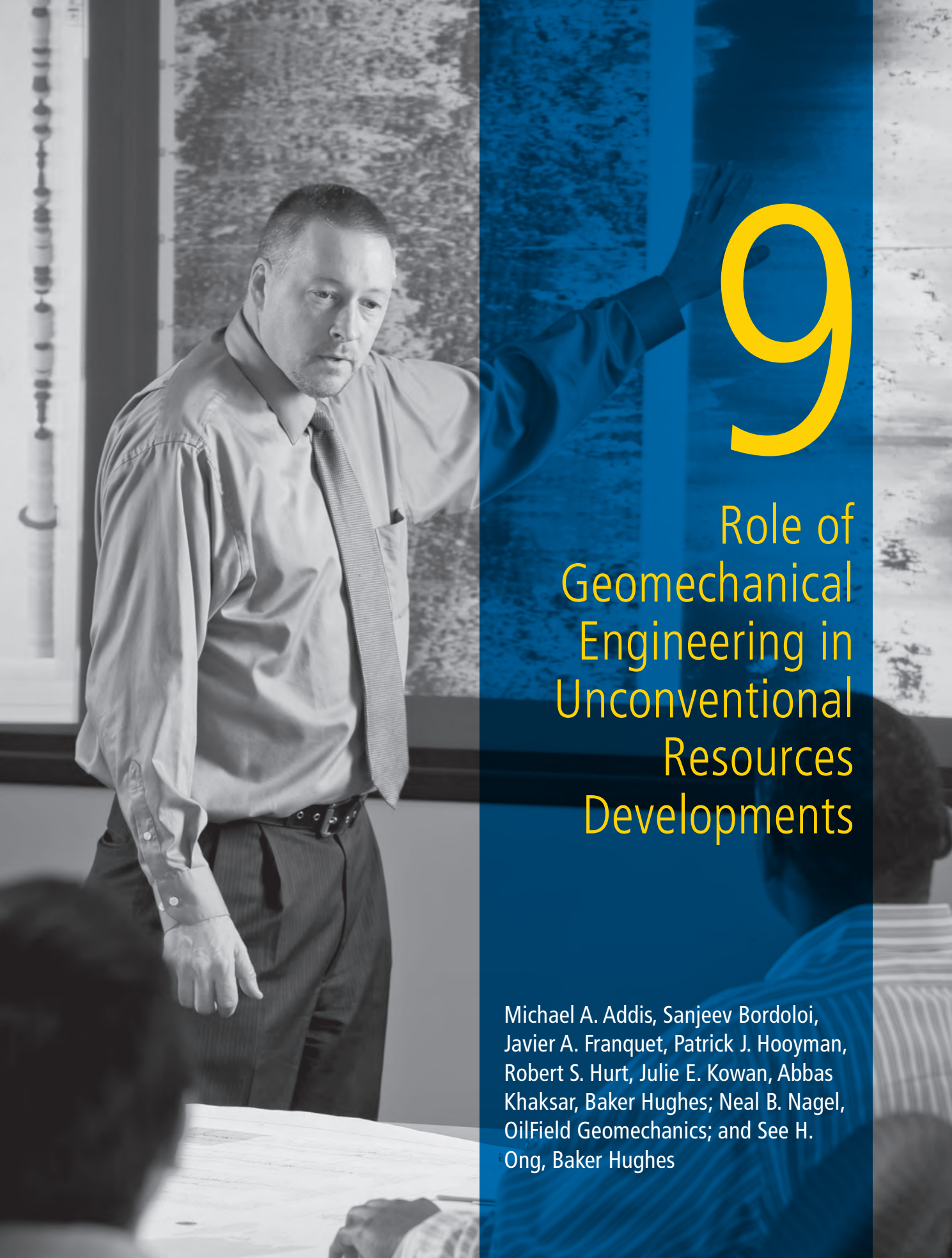

9

Role of Geomechanical Engineering in Unconventional Resources Developments

Michael A. Addis, Sanjeev Bordoloi, Javier A. Franquet, Patrick J. Hooyman, Robert S. Hurt, Julie E. Kowan, Abbas Khaksar, Baker Hughes; Neal B. Nagel, OilField Geomechanics; and See H. Ong, Baker Hughes

This page intentionally left blank

Chapter 9: Role of Geomechanical Engineering in Unconventional Resources Developments

9.1 Introduction

The development of unconventional resources, whether shale gas and oil or tight gas and oil, faces the challenge of producing hydrocarbons from formations with very low porosities and permeabilities.

Geomechanics deals with the mechanical properties of rocks, including the strength, elastic, and plastic properties, and the deformation of the subsurface formations (source rocks, reservoirs, or overburden), resulting from initial and induced stresses and pressure changes accompanying field developments. Geomechanical engineering has become a significant aspect in the development of these resources, for several technical reasons. The importance of geomechanical engineering in unconventional resource development is based on the need to generate a man-made or artificial permeability network to drain the formations. This is achieved through tensile and shear failure of the formation during hydraulic fracturing and shear deformation of any natural fracture network. To make unconventional resources productive, operators have to crack or shear the rock via hydraulic fracturing.

In addition to generating a permeability network to enhance the existing low geological permeability, the stress state controls the drilling location; the direction in which laterals are drilled to generate optimally oriented transverse hydraulic fractures; the spacing of fracture stages; the fracture stimulation design; and any potential for refracturing later in the development life. Geomechanical engineering also plays a pivotal role in assessing the pore pressure and correct drilling fluid design, to successfully drill and complete the well.

Critically, geomechanical engineering considerations in the well design, hydraulic fracture design, containment of hydraulic fractures, shearing of natural fractures, and the generation of a stimulated reservoir volume have become central aspects of unconventional resource developments.

9.1.1 What Is Geomechanics?

Geomechanics comes from the Greek prefix geo "earth" and mechanics.

Geomechanical engineering is the science that studies the mechanical behavior of soil and rock under stress. The two main disciplines of geomechanics are soil mechanics and rock mechanics. These are the underlying principles that are used to assess the response of the subsurface to stress changes imposed during a field development.

9.1.2 Geomechanical Engineering in Unconventional Resource Development

Geomechanical engineering analysis of unconventional oil and gas field developments is more complex than in conventional reservoir developments. First, the hydrocarbons are in source rocks that can have high transverse anisotropy resulting from shale laminations and fine bedding. Second, the existence of natural fractures in low permeability rocks makes the characterization of the mechanical behavior under stress more complex. Third, there is often no industry-wide consensus for key parameters such as rock brittleness as it is prone to hydraulic fracturing. Plus no consistent standard measurement methodology for these parameters from core testing, borehole logging tools, or seismic attributes. Fourth is the difficulty in getting reliable pore pressure and fracture closure measurements through microfracture tests and the necessity of inducing fracture closure by controlled flowback in straddle packer microfracture tests due to the extremely low leak-off coefficient in these unconventional rocks. Finally, the complexity of the micropore structure mixed with the distributed organic matter makes the measurements of poroelastic properties and shale permeability at in-situ conditions challenging in laboratory facilities. However, these challenges can be negated when the geomechanical considerations are taken into account as further discussed in DFIT (Diagnostic Fracture Injection Test in Section 17.6.2) and laboratory core testing in Chapter 10.

9.1.2.1 Shale Gas and Shale Oil

Generally, the industry does not consider any intrinsic difference in the geomechanical rock and stress characterization, the geomechanical engineering response, or the specific geomechanical engineering analysis between shale gas and shale oil developments and conventional resource developments, other than the thermal maturation of the organic matter dictates what type of hydrocarbon

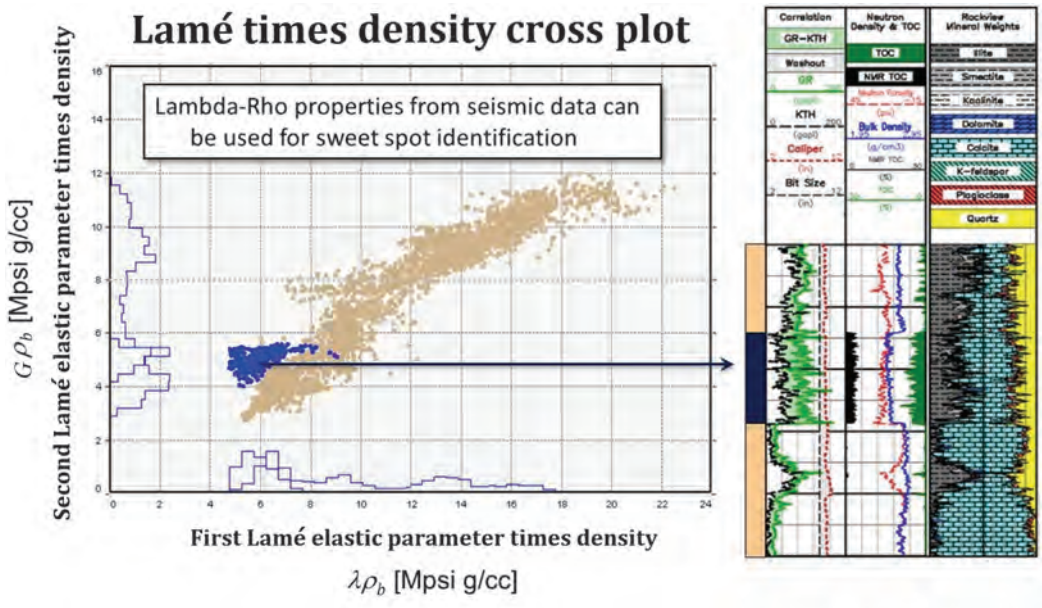

Fig. 9.1—Cross plot of the Lamé parameters times density in a vertical well drilled through the Eagle Ford shale. The black and green shading indicate high TOC values, and the blue dots in the cross plot indicate the sweet spot (pay zone).

will be produced (gas or liquids). The small pore volumes and pore throat diameters in these tight shale, gas-filled formations are expected to have significant capillary pressures (suction in civil engineering terminology) (Bishop 1959) that may lead to significant changes in the effective stresses driving the formation responses (Addis 1997). However, this is an area of recent focus and attention in the petroleum industry.

The main role of the geomechanic engineering discipline in unconventional resource developments can be grouped in three categories: characterizing and identifying geological sweet spots throughout the formation volume; orienting and drilling stable boreholes; and designing and modeling hydraulic fracturing stimulation jobs.

Geological sweet spot identification is the earliest application of reservoir geomechanic engineering to unconventional field developments. Stress and stress anisotropy estimation along with brittleness or being prone to hydraulic fracturing are estimated from a combination of 3D seismic (further detailed in Chapter 6) and well logs (further detailed in Chapter 8) in exploration and appraisal wells. Brittleness is a rock property proxy that is used to identify good intervals or zones to fracture in vertical or horizontal wellbores. High shale brittleness is associated to high fracturing complexity or effective rock failure during well stimulation jobs.

Brittleness indexes can be obtained from core triaxial tests, elastic properties estimates from from seismic attributes and acoustic logs, log-derived mineralogy from high-energy pulse-neutron instruments, and more recently from advanced mud logging using drill cuttings to estimate mineralogy.

The characterization of the Lamé elastic parameters from seismic attributes analysis and acoustic logs has shown good results in identifying zones with high total organic content (TOC), particularly with the cross plot of lambda-rho "lr_b" (first Lamé elastic parameter times bulk density) and "Gr_b" second Lamé elastic parameter (or Shear modulus) times bulk density. This cross plot is effective in identifying potential shale sweet spots because the presence of organic matter reduces the bulk density of the rock. This effect gets amplified as the lambda-rho and Gr_b parameters contain the bulk density square "r_b^2".

Fig. 9.1 illustrates the geological sweet spot due to high TOC in the Eagle Ford shale from the non-organic shales (above the pay zone) and the non-productive limestone (below the pay zone). Fig. 9.1 shows the log-derived mineralogy characterization of a vertical pilot well drilled in the Eagle Ford shale along the amount of TOC obtained by the excess carbon from mineralogy logging (in green) and the NMR porosity (in black). This technique can be used with seismic attributes allowing 3D subsurface sweet spot identification of high TOC zones.

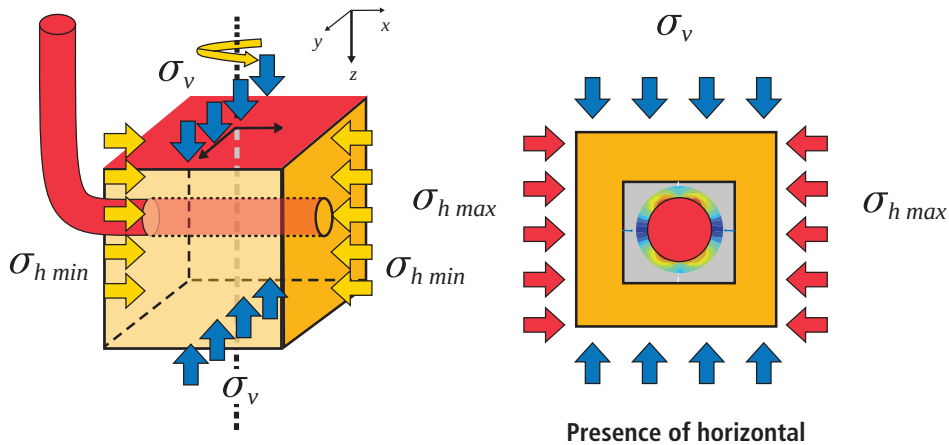

Fig. 9.2—Safety horizontal drilling in vertically transverse isotropic formations and wellbore stability analysis including weak planes and laminations.

High concentrations of natural fractures in shale and tight reservoirs in a conductive natural fracture network under favorable stress conditions can be stimulated through shear to provide higher reservoir contact during hydraulic fracture treatments. The frequency and distribution of natural fractures can be obtained from the 3D seismic attribute analysis, prior to drilling, and calibrated using image logs in early exploration and appraisal wells.

9.1.2.2 Wellbore Stability

Orienting and drilling stable wellbores for efficient drilling can reduce non-productive time (NPT) and drilling costs in the build, hold, and lateral sections of the wellbore. This is key to successful unconventional play development. A stable wellbore is required for proper wellbore completion, stage isolation, and effective stimulation. **Fig. 9.2** shows how horizontal wells are drilled in the direction of minimum horizontal stress to propagate transverse vertical fractures oriented perpendicular to wellbore direction. Fig. 9.2 also shows how the openhole stability may require the analysis of horizontal weak planes (beddings), laminations, or natural fractures. Addressing shale anisotropy in wellbore stability studies and the analysis of in-situ stress directions and magnitudes are important geomechanic engineering contributions in drilling unconventional reservoirs.

9.1.2.3 Completion Design

The impact of geomechanics on the completion design and the connectivity between the hydraulic fracture and the wellbore commonly is overlooked. The majority of completions in shale gas and oil plays in North America are plug and perforated completions.

The main issues include:

- The impact of the formation stress and stresses on the perforation depth. In a very competent formation, such as tight gas sandstones and carbonates, the perforation depth will be reduced greatly compared to standard perforation design tables, that leads to problems initiating hydraulic fractures.
- The characterization of stress distribution along the lateral, and the impact on the distribution of the stages design. Having too large a stress variation within an individual stage may lead to low cluster efficiency and productivity.
- Location of the hydraulic fractures stages depends upon the stress magnitude and brittleness estimation, as well as other petrophysical factors.

9.1.2.4 Hydraulic Fracture Modeling

The main contributions of geomechanics into hydraulic fracture design include the characterization of the minimum horizontal stress with depth in the reservoir and the quantification of the stress contrast above and below the target zone to be stimulated by hydraulic fracturing. The lateral variation of the stress is also important for optimizing rigorous designs (**Fig. 9.3**).

Inadequate horizontal stress profile characterization results in unreliable vertical fracture propagation prediction compromising the vertical fracture containment within

the prospective interval. The vertical fracture propagation is controlled by the net pressure imposed during fracture propagation and constrained by the stress contrast between the stratigraphic layers (Ahmed 1988).

Other geomechanic engineering contributions in designing reservoir stimulation job treatments include:

- The assessment of the horizontal stress anisotropy and the difference between the maximum and horizontal stresses. This is likely to be a controlling parameter on the generation of bi-wing versus complex fracturing, for example a stimulated reservoir volume (SRV) type stimulation.
- The stress state and whether the minimum stress direction is horizontal or vertical. The former results in vertical hydraulic fractures. The latter leads to horizontal fractures or a combination of vertical and horizontal hydraulic fractures such as T-shaped fracture geometries.
- The hardness and stiffness characterization of the shale rocks for placement of the lateral sections and the stage location as well as predicting proppant embedment and effective fracture width during flowback.

9.1.2.5 Water Disposal Wells and Fracture Design

The development of hydraulic fracture design has focused predominantly on production and stimulation optimization. However, much of the flowback water from the hydraulic fractures is disposed of in water disposal wells. This can be through matrix injection or through the use of hydraulically fractured wells. Conventional field development commonly addresses produced water re-injection into wellbores as an overall part of the field development. However, relatively little focus has been given to the injection and fracture design of downhole disposal of back flow fracturing fluids in unconventional field developments. This is likely to have a higher priority for international developments.

9.1.2.6 Coalbed Methane

Coalbed methane (CBM) (or coal seam gas) reservoirs exist in diverse geological settings and have different characteristics requiring different field development and wellbore completion strategies. CBM reservoirs have complex anisotropy due to the presence of orthogonal microfractures (cleats). These discontinuities make the hydromechanical behavior of coalbed methane reservoirs similar to a dual-porosity system.

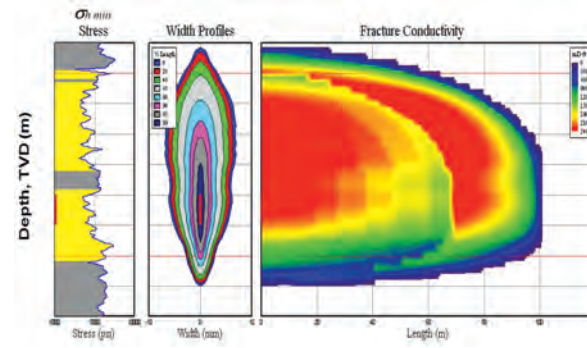

Fig. 9.3—Traditional hydraulic fracture propagation modeling from vertical profile of the minimum horizontal stress.

The main geomechanics concerns in developing CBM reservoirs are wellbore instability during drilling; effective hydraulic fracturing and shear stimulation; and solids production from inter-bedded clay-rich clastic rocks (particularly severe during the reservoir dewatering process). These field development operational challenges can be addressed and minimized with proper geomechanical engineering analysis during the drilling and production of CBM resources.

9.2 Rock Characterization

Rock mechanics properties define how source rocks deform and fail under stress. Petrophysical, mineralogical, and organic matter thermal maturity characterization in shale source rocks are covered in Chapter 8.

Four basic technologies are used to characterize the mechanical properties of rocks: (1) processing of seismic attributes, (2) petrophysical processing of well log responses, (3) laboratory analysis of rock samples from outcrops, full wellbore cores, or side-wall coring, and (4) advanced mud logging of drill cuttings. Rock mechanical properties have been derived from all of these technologies during unconventional reservoir developments. However, the technologies No. 1, No. 2, and No. 4 usually are calibrated to triaxial core experiment results at in-situ conditions to obtain comparable datasets. While triaxial tests are the benchmark for comparison, the seismic and petrophysical estimations of rock properties are dynamic and involve small amplitude (strain) high-frequency wave propagation. Triaxial tests are large-strain static measurements. Also, the volume of the rock volume tested varies tremendously with these techniques, from millimeters in the drill cuttings to tens of meters with the seismic methods, introducing a scale difference into any comparisons.

9.2.1 Rock Mechancial Properties

Rock mechanical properties are used in drilling, wellbore completion, and production decisions during the development of unconventional resources. The confined rock stiffness is used to predict:

- Tectonic induced stresses and quantifying the stress contrast between formations of different stiffness to model vertical fracture propagation and containment.
- Fracture aperture and proper proppant placement in hydraulic fracturing operations.
- Evaluate potential proppant embedment into the formations.

Rock compressive and tensile strengths are used in wellbore stability analysis to model shear and tensile failure around the hole during drilling and openhole well operations. Friction coefficients of natural fractures and matrix are used to simulate the potential for shear stimulation during hydraulic stimulation jobs.

Details on laboratory tests and core analysis on source rocks are in Chapter 10 including ultrasonic core velocity measurements, triaxial loading experiments, and indentation testing.

9.2.1.1 Dynamic Elastic Properties

Dynamic elastic properties of shale gas and shale oil can be measured either in the lab by ultrasonic core velocities with frequencies of around 1 MHz, by borehole acoustic tools with a frequency of 100kHz, or from seismic velocity analysis with frequencies between 2 and 100 Hz. Elastic rock properties derived from compressional and shear waves characterize the dynamic stiffness tensor of shale rocks.

Acoustic and ultrasonic measurements performed in the laboratory are non-destructive and should be performed at in-situ conditions. The number of acoustic or ultrasonic measurements required to fully characterize the stiffness tensor depends on the level of structural (intrinsic) anisotropy present in the rock fabric such as laminations, beddings, weak planes, or natural fractures.

Isotropic rocks can be characterized by only two acoustic measurements: compressional wave slowness (DTC) and shear wave slowness (DTS) in any direction and polarization. The dynamically derived elastic properties (Young's modulus Edyn and Poisson's ratio E_{dyn}) of an isotropic rock are defined below where r_b is the bulk density, and the number 13474.44 is the unit conversion factor to transform [g/cc] [ft²/ms²] into [Mpsi]. Typically acoustic slownesses and density are expressed in ms/ft and g/cc, respectively, while Young's modulus is expressed in Mpsi or x10⁶ psi.

$$\nu_{dyn} = \frac{1}{2}\left[\frac{\left(\frac{DTS}{DTC}\right)^2 - 2}{\left(\frac{DTS}{DTC}\right)^2 - 1}\right] \quad \textbf{(Eq. 9.1)}$$

$$E_{dyn} = 2\rho_b\left[\frac{1}{DTS}\right]^2(1 + V_{dyn}) \bullet 13474.44 \quad \textbf{(Eq. 9.2)}$$

Once two elastic dynamic properties are measured, the rest of the elastic properties such as shear G_{dyn} and volumetric (bulk) K_{dyn} moduli can be derived by linear elastic relationships for isotropic materials. The dynamically derived Lamé elastic parameter "λ_{dyn}" is related to shear and volumetric dynamic elastic moduli as shown in **Eq. 9.5** (Jaeger et al. 2007).

$$G_{dyn} = \frac{E_{dyn}}{2(1 + \nu_{dyn})} \quad \textbf{(Eq. 9.3)}$$

$$K_{dyn} = \frac{E_{dyn}}{3(1 - 2\nu_{dyn})} \quad \textbf{(Eq. 9.4)}$$

$$\lambda_{dyn} = K_{dyn} - \frac{2}{3}G_{dyn} \quad \textbf{(Eq. 9.5)}$$

Even though these dynamically derived elastic properties can be obtained either from core measurements or acoustic logs, it should be noted that to consistently compare the values measured from the different sources:

- The acoustic source amplitude and frequency of ultrasonic piezoelectric core transducers in the lab are different than the acoustic transmitters used in downhole acoustic tools.
- The core ultrasonic measurements should be conducted under confining stress at similar in-situ (downhole) effective stress conditions even though shale rocks exhibit very low stress sensitivity in comparison with porous sandstones (Tang et al. 1999).

- The wave propagation direction of borehole acoustic and ultrasonic core measurement need to be the same because shale rocks are anisotropic.
- The borehole compressional fullwave slowness could be affected by gas at in-situ conditions in comparison with core measurements (that probably have lost all its gas at surface condition).
- The core plug scale is not the same as the vertical resolution of the borehole acoustic properties.

The enhanced-vertical resolution borehole slowness profiles (obtained from 6 in. sub-array aperture fullwave stacking) match fairly well with the core ultrasonic velocities performed at the same confining in-situ conditions (Zhang et al. 2000). The conventional slowness profile obtained from 3.5 ft. receiver sub-array aperture tends to average (or smooth) the thin bed or lamination variations characteristic in shale formations.

9.2.1.2 Static Elastic Properties

Static mechanical properties are derived from the stress-strain rock deformation behavior measured in core samples under triaxial compression loading tests. The triaxial testing apparatus and loading procedures are covered in detail on Chapter 10.

The number of static elastic properties required to fully describe the deformation of rocks will depend on the type of anisotropy present in the formation. Isotropic rocks can be defined with only two elastic constants (typically by one Young's modulus and one Poisson ratio measured in any loading direction).

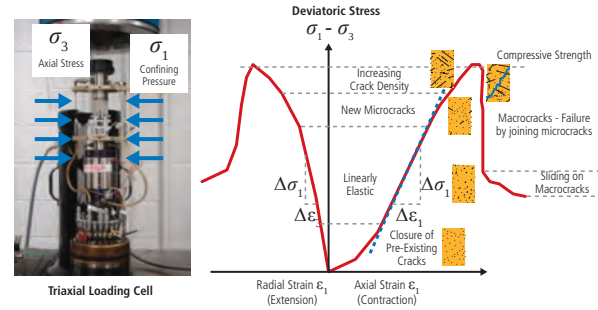

Fig. 9.4—Example of a core triaxial test where Young's modulus and Poisson's ratio are calculated as static elastic rock properties

The term ***shale***, when used in shale gas and shale oil plays, refers to tight, low-permeability formations, rather than geological shales: True geological shale formations contain a high percentage of argillaceous minerals with fine laminations and bedding. Shale rocks can exhibit highly transverse anisotropic behavior due to laminations, requiring the measurement of static elastic properties parallel and perpendicular to the intrinsic laminations.

Young's modulus is the slope of the stress-strain curve tested at atmospheric conditions, over the linear elastic portion the rock deformation, calculated as follows in the direction of deviatory loading (i direction) and illustrated in **Fig. 9.4**. The elastic moduli measured at different confining pressures, exceeding atmospheric pressure, are referred to as the confined elastic moduli:

$$E_i = \frac{\partial(\sigma_i - \sigma_j)}{\partial \varepsilon_i} \quad ; \quad E_{axial} = \frac{\partial \sigma_{axial}}{\partial \varepsilon_{axial}} \qquad \text{(Eq. 9.6)}$$

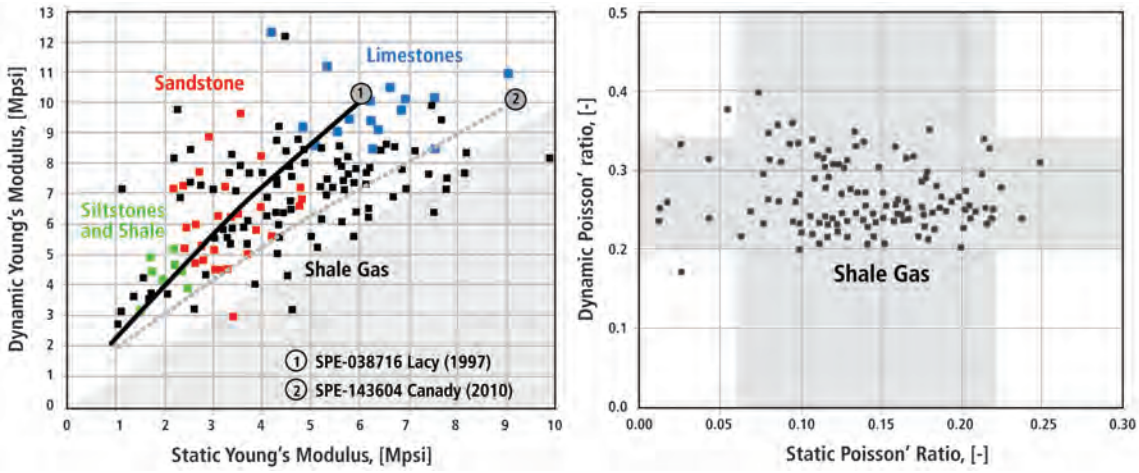

Fig. 9.5—Dynamic and static Young's modulus and Poisson's ratio from several shale gas core samples from North America.

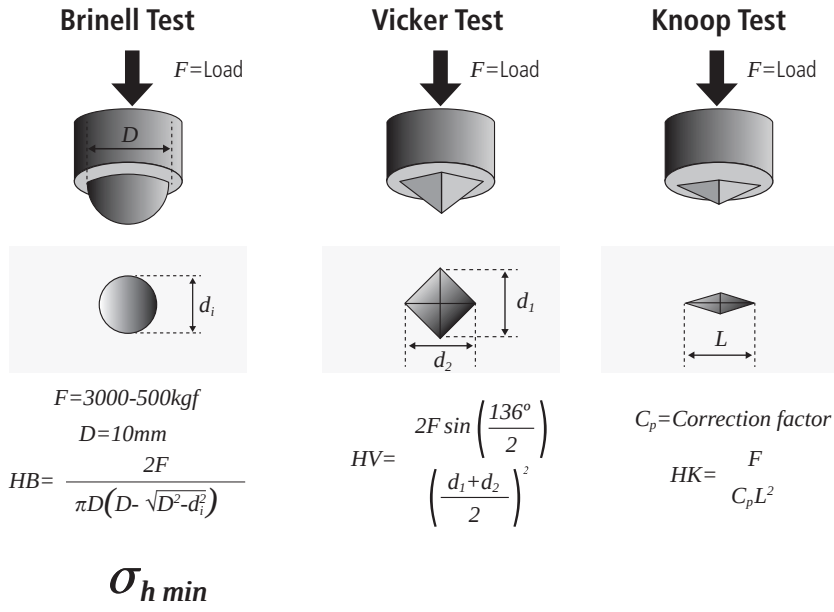

Fig. 9.6—Macroscopic and microscopic hardness indentation tests (Brinell, Vicker, and Knoop).

As the confining pressure (s_j) around the sample is held constant during the deviatoric loading, the Young's or confined modulus can be calculated from the change of axial strain and stress as the deviatoric loading is applied to the sample in the axial direction.

Poisson's ratio is the fraction of the axial strain that is transmitted in the radial direction. As axial compression produces lateral expansion, the definition of Poisson's ratio has a negative sign to produce positive Poisson's ratio numbers. The sign convention in geomechanics is positive strain for compression while negative strain for expansion.

$$\nu_{ij}=\frac{\partial\varepsilon_j}{\partial\varepsilon_i}\quad;\quad \nu=-\frac{\partial\varepsilon_{radial}}{\partial\varepsilon_{axial}} \qquad \textbf{(Eq. 9.7)}$$

The static elastic properties are different than the dynamic elastic properties mainly because acoustic waves do not activate large strains in the sample in comparison to core triaxial loading tests. Static Young's modulus is about half of the dynamic derived Young's modulus (**Fig. 9.5**).

Lacy (1997) and Canady (2011) proposed correlations for the upper and lower bounds to predict static Young's modulus from dynamic measurements that seem to bound the average values. However, no clear and consistent Poisson's ratio correlation has been obtained from triaxial loading and ultrasonic measurements in core laboratory experiments. It seems that the dynamic Poisson's ratio is higher and has less variability than the static one even when both tests are carried out under the same confining stress.

9.2.1.3 Rock Hardness

Rock hardness can be defined by three testing techniques: macro and micro indentation tests, rebound tests, and scratch tests (ISRM 1978).

The indentation tests are divided into several categories depending of the shape and size of the indenter tip (**Fig. 9.6**). Brinell hardness is based on a 10-mm-diameter ball indenter and is the most commonly used in rock characterization. Vicker and Knoop microhardness indexes are obtained by using four-faced pyramidal indenters typically used for testing materials and minerals (Winchell 1946 and Das 1974). Rockwell hardness uses a spherical diamond-tipped cone of 120° angle as indenter while Berkovich hardness uses a three-faced pyramidal indenter (Fischer-Cripps 2000).

The measurement of Brinell hardness in reservoir rocks has been documented by several authors such as Van der Vlis (1970) and Geerstma (1985). Its correlation to other rock mechanical properties, such as the elastic Young's modulus "*E*" and the unconfined compressive strength (UCS) have been validated in several rock types (Santarelli et al. 1991). All of these indentation index tests require field-specific calibration to laboratory measured UCS tests because no generic correlation has been found, or adopted, to date.

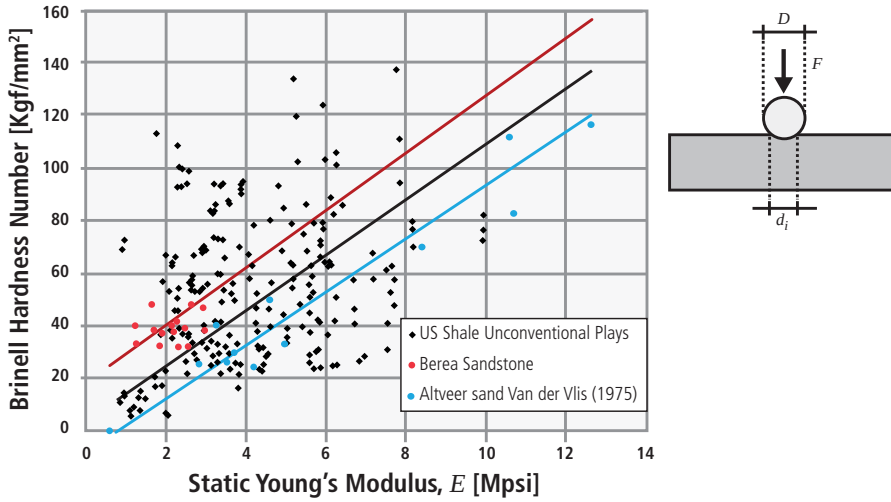

Fig. 9.7—Brinell hardness and Young's modulus from several US unconventional shale reservoirs.

The Brinell hardness of rocks is calculated from the maximum load supported by the indentation test divided by the area of contact at peak load, which is proportional to the indentation displacement. The elastic modulus of the rock can be obtained from the (unloading) slope of load versus displacement during the indentation tests. A small-diameter ball indentation test (1/16 in. with 100 kgf) is not recommended in testing rocks because the indentation contact area should cover at least 10 to 15 grains of the rock. This testing analysis was adopted from material science characterization (Oliver and Pharr 1992).

Shukla et al. (2013) published a relationship showing a good agreement between the Young's modulus obtained by nano indentation and the dynamic Young's modulus obtained by measuring bulk density, compressional, and shear wave velocities in several unconventional shales. This correlation provides a means to obtain microhardness and rock stiffness from small rock pieces obtained from drilling cutting, fragments, or sidewall coring.

Van der Vlis et al. (1975) used the rock hardness number from spherical indentation tests (Brinell) to estimate static Young's modulus and used it as a practical parameter for estimating rock stiffness and propped fracture conductivity. **Fig. 9.7** shows the linear relationship between static Young's modulus and Brinell hardness obtained by Van der Vlis along with multiple indentation and triaxial tests done in several US unconventional plays and Berea sandstones.

The rock hardness of unconventional shale samples could be sensitive to the type of fluid and the exposure time to a particular fluid. Typically, rock hardness tests are conducted on samples that have been exposured to fracturing fluids to quantify the rock hardness after the hydraulic fracturing stimulation treatment. The rock hardness and the estimated in-situ horizontal stress help to predict the proppant embedment into the formation after the flowback and the final propped effective fracture conductivity.

Rebound hardness tests use the principle of impact rebound forces to quantify the hardness of the material. The impact consists of a piston that is loaded with a spring that is projected against the surface and the height of the piston after the rebound is taken as empirical measurement of the hardness. The most commonly used rebound hardness device is the Schmidt hammer.

The scratch hardness test is more specific to minerals. Mohr (1822) proposed the hardness scratch scale that consists of the ten most commonly found minerals with values ranging from 1 to 10. Scratch sclerometers use diamond points to scratch the specimen, and it might provide inconsistent values in impure or poorly crystallized minerals. This type of hardness testing is not common in unconventional shale rocks.

9.2.1.4 Rock Brittleness

Rickman et al. (2008) highlighted the significance of shale brittleness for the success of hydraulic fracture treatments in shale gas and oil plays. Brittleness has been calculated in many ways in the oil and gas industry and no standardized or accepted concept has been generally accepted. This reflects the wide range of methodologies used to quantify the brittle/ductile behavior of rocks from core testing to borehole logging data (Altindag 2003, Holt, 2011). The

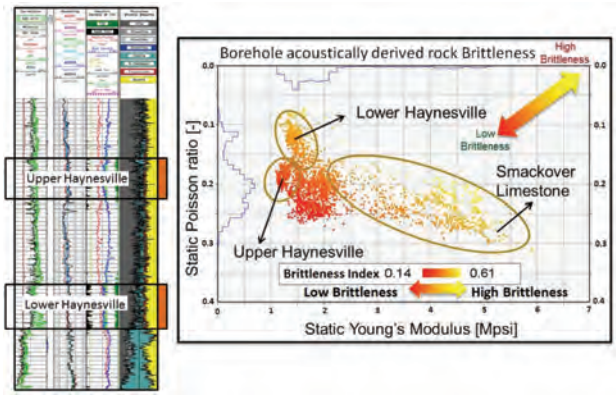

Fig. 9.8—Borehole acoustically derived brittleness in color coded on a cross plot between Young's modulus and Poisson's ratio (reverse scale) in a 1,500 ft. logged interval covering upper and lower Haynesville formations.

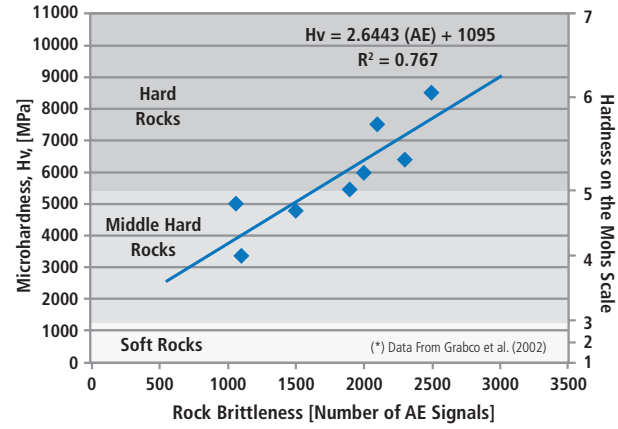

Fig. 9.9—Correlation between Vicker micro-hardness and rock brittleness index obtained from measurement of acoustic emitting (AE) signals.

most commonly adopted approach in the industry is the acoustically derived shale brittleness using log-derived Young's modulus and Poisson's ratio (indicating high brittleness zone in high Young's modulus and low Poisson's ratio) (Rickman et al. 2008). This borehole approach commonly is used because the data needed is available from standard density and acoustic borehole logs (DTC and DTS). Dynamic elastic properties from logs can be converted into static elastic properties either using empirical correlations or customized correlation obtained from core measurements (**Fig. 9.8**). The borehole acoustically derived brittleness $B_{elastic}$ is obtained as the average of two indexes obtained from Young's modulus and Poisson's ratio relative values along the logged interval.

This log-based acoustically derived brittleness cannot physically capture the full brittle or ductile behavior of

$$B_{elastic} = \frac{1}{2}\left(\frac{E - E_{min}}{E_{max} - E_{min}} + \frac{\nu_{min} - \nu}{\nu_{max} - \nu_{min}}\right) \quad \textbf{(Eq. 9.8)}$$

rocks just as elastic properties do not determine the failure behavior of rocks. There is still uncertainty whether this brittleness definition, proposed by Rickman et al. (2008), fully represents the relevant brittle characteristic needed for a particular field application (Holt et al. 2011). Many core analyses indicate a strong correlation between Young's modulus and brittleness at relative low temperatures and under relative low confining stress. However, Poisson's ratio has not shown a clear correlation with brittleness.

Another way to characterize brittleness in shale rocks consists of measuring the weight fraction or volume fraction of rock minerals/constituents from mineralogy logging, core measurements, or advance mud logging. In all of these techniques, the rock brittleness is obtained indirectly from the ratio between brittle minerals (calcite, dolomite, quartz, K-feldspar, and plagioclase feldspar) and the total rock constituents including all clay minerals and the organic matter. Jarvie et al. (2007) introduced the first mineralogy derived brittleness definition based solely on quartz weight fraction as the main proxy of brittleness from Barnett shale samples. However, other minerals such as calcite, dolomite, K-feldspar, and plagioclase feldspar also can contribute to the overall brittle behavior of the rock. The volume of clay and TOC show a strong correlation to ductility of shale gas and oil source rock formations. However, mineralogy-based analysis does not fully characterize the brittleness behavior of rock, as cementation between grains plays a fundamental role in how rock fails. For example, poorly consolidated sands containing 100% brittle quartz grains are very ductile and compliant due to high porosity and lack of grain cementation.

An alternative way to quantify rock brittleness is by capturing acoustic emitting (AE) signals during indentation tests on core samples. **Fig. 9.9** shows the correlation between the microhardness measured from Vicker pyramidal indentation tests and the rock brittleness obtained from the number of acoustic emission signals during the indentation test of various rocks (Grabco et al. 2002).

This correlation between the hardness of the rock and the number of acoustic emissions may be explained as high ductility rocks that can tolerate high plastic strain and that

would be expected to produce less micro-acoustic emissions during indentation. A similar concept could be applied in microseismic monitoring during hydraulic fracturing. Rocks with high brittleness should generate more microseismicity events while they are deformed due to the opening (induced strain) of the hydraulic fractures.

The most rigorous methods of measuring rock brittleness entail measuring the stress-strain behavior under triaxial loading beyond rock failure. However, there are multiple definitions to derive rock brittleness from stress-strain curves obtained in core triaxial tests. Yarali and Soyer (2011) proposed a brittleness definition using the uniaxial compressive strength UCS and the Brazilian tensile strength T_o of the rock in addition to the definitions proposed by Hunca and Das (1974) and Altindag (2002).

Even though Yarali and Soyer (2011) found a strong correlation between the rock's drillability index DRI defined by Dahl (2003) and the brittleness $B3_{UCS\text{-}To}$ and $B4_{UCS\text{-}To}$, none of these brittleness definitions captures the rock deformation and how the material fails under shear stress. Furthermore, none of these definitions is

$$B1_{UCS\text{-}To} = \frac{UCS}{T_0}$$

Hunca and Das (1974) **(Eq. 9.9)**

$$B2_{UCS\text{-}To} = \frac{UCS - T_0}{UCS + T_0}$$

Hunca and Das (1974) **(Eq. 9.10)**

$$B3_{UCS\text{-}To} = \frac{UCS*T_0}{2}$$

Altindag (2002) **(Eq. 9.11)**

$$B4_{UCS\text{-}To} = (UCS*T_0)^{0.72}$$

Yarali and Soyer (2011) **(Eq. 9.12)**

sensitive to confining stress that has a significant impact on rock failure and brittleness. Therefore, none of these definitions ($B_{UCS\text{-}To}$) is meaningful in a practical context to characterize shale brittleness in unconventional reservoirs.

Holt et al. (2011) and Yang et al. (2013) evaluated other rock brittleness definitions from shale samples including the one that measures the rock deformation and post failure behavior. The brittleness definition proposed by Coates and Parsons (1966) captures the rock deformation before failure. This definition uses the normalized elastic strain ε_{el} by the total strain at shear failure ($\varepsilon_{el} + \varepsilon_{pl}$), where ε_{pl} is the plastic strain at failure to quantify the rock brittleness.

Bishop (1967) introduced another brittleness definition that can be obtained from triaxial stress-strain rock behavior where the peak and the residual shear strengths are used to quantify the magnitude of the brittle failure.

$$B_{strain} = \frac{\varepsilon_{el}}{\varepsilon_{el} + \varepsilon_{pl}}$$

Coates and Parsons (1966) **(Eq. 9.13)**

The brittleness definition from strains (B_{strain}) describes how the plastic strain does or does not develop prior to rock failure, whereas the brittleness definition from peak and residual shear strengths ($B_{failure}$) is related with post

$$B_{failure} = \frac{\tau_{max} - \tau_{res}}{\tau_{max}}$$

Bishop (1967) **(Eq. 9.14)**

failure behavior. These two brittleness definitions include stress sensitivity because the rock brittleness decreases with increasing confining pressure. Rocks change their behavior from brittle to ductile failure as the confining stress increases (Holt et al. 2011, Yang et al. 2013). In contrast, the brittleness definition ($B_{elastic}$) derived from elastic parameters shows an opposite stress sensitivity with an increase of brittleness with confining stress as the rock velocities.The Young's modulus increases with effective confining stress (Kulhawy 1975; Holt et al. 2011).

Some of the log-based estimations of brittleness calculate the strain-derived brittleness definition (B_{strain}) from openhole logging data. These methods are based on the logging of mechanical properties (LMP) calculation and RockTest micromechanical stress-strain modeling that can be calibrated against the results against triaxial core measurement, if required. The $B_{failure}$ brittleness definition cannot be calculated from LMP as the RockTest micromechanical code cannot predict the post failure behavior of rocks based on openhole logging data.

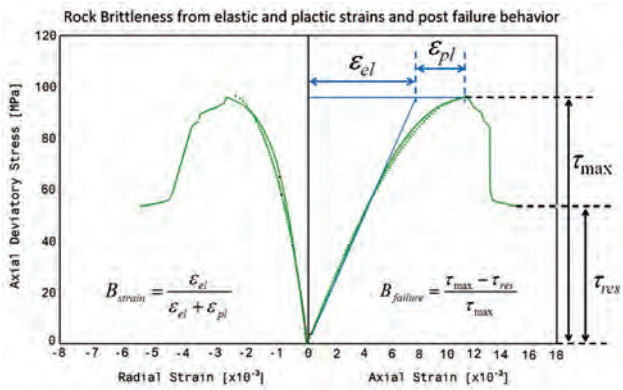

Fig. 9.10—Brittleness definitions based on the elastic and plastic deformation prior to failure (B_{strain}) (Coates and Parsons 1966) and the post failure behavior ($B_{failure}$) (Bishop 1967).

Fig. 9.10 illustrates one triaxial test with 3300 psi (22.75 MPa) of confining pressure conducted in a core sample taken from the Haynesville shale. The green solid curves are the axial and radial strains measured in a triaxial loading frame showing elastic deformation, pre-failure plastic behavior, and post-failure residual strength of the rock. The dotted curves correspond to the LMP-RockTest micromechanical simulation (Franquet et al. 2010). This shale sample from the Haynesville has a brittleness index (B_{strain}) equal to 0.7 using the pre-failure elastic and plastic deformations, while the brittleness index ($B_{failure}$) is just 0.44 using the maximum and residual shear strength of the rock. These two brittleness indexes measure different rock properties pre- and post-failure but both provide a relative quantification of how brittle the rock fails in comparison with others.

9.2.1.5 Rock Strength

Rock strength can be characterized using three parameters, depending on the loading path applied to the samples: the unconfined compressive strength (UCS), the tensile strength, (T_o), and the shear strength (S_o), better known as the cohesive strength (C_o). Rocks increase in strength with increasing confining pressures; the shear stress needed to fail the rocks increases with the confining pressure. This is often represented by a simplified linear shear failure envelope with confining stress described by the Mohr–Coulomb failure criteria.

In this equation, σ_n and t are the normal and shear stresses acting on the failure plane, whereas q is the internal angle of friction as illustrated in **Fig. 9.11**.

$$\tau = S_0 + \sigma_n \tan(\theta) \qquad \textbf{(Eq. 9.15)}$$

$$\sigma_1 = UCS + \sigma_3 \tan^2\left(\frac{\pi}{4} + \frac{\theta}{2}\right) \qquad \textbf{(Eq. 9.16)}$$

The Mohr–Coulomb failure criterion commonly is used in rock characterization and primarily predicts shear failure under compression. The Hoek and Brown (1980) nonlinear failure criterion can be used to predict more accurately the tensile rock failure. The Hoek and Brown failure criterion was developed to characterize rock strength in large excavations, tunneling, and mining applications. This model is based on two empirical parameters, *m* and *s*, which are defined as the characteristic rock type constant and the rock mass parameter, respectively.

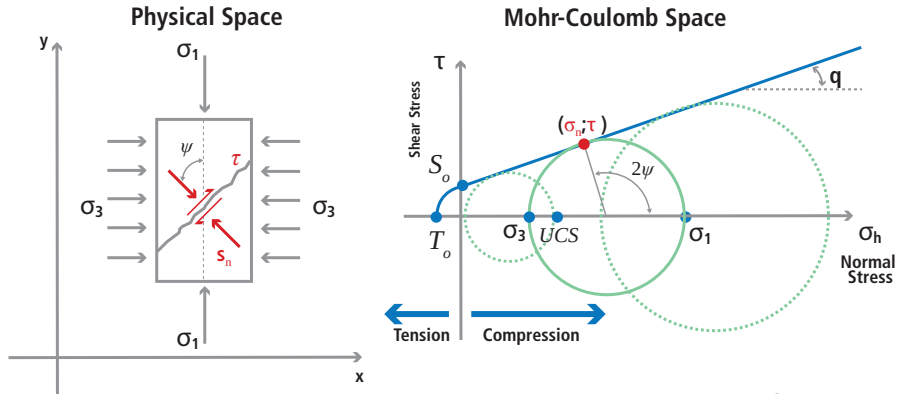

Fig. 9.11—Comparison between the physical space and the Mohr-Coulomb space, where the shear failure plane is created at a y angle between the normal direction of the plane of failure and the maximum loading compression direction s1.

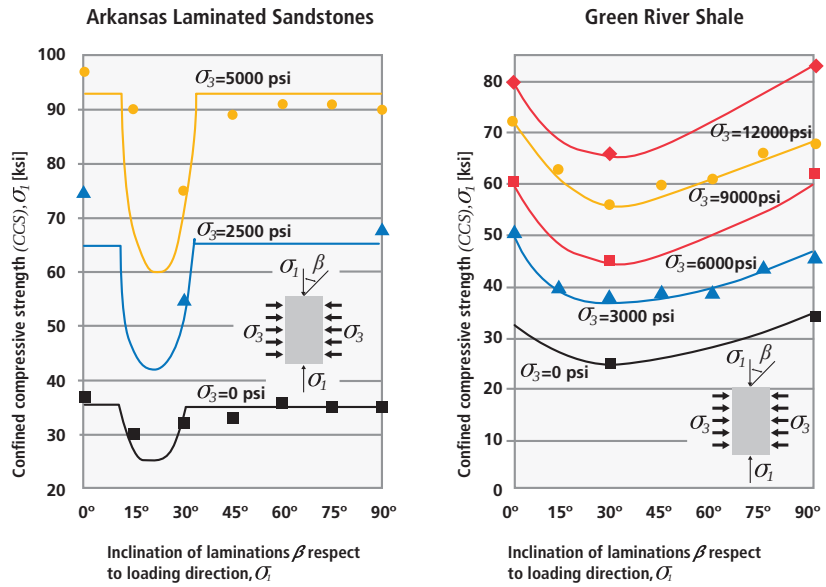

Fig. 9.12—Anisotropic shear failure behavior obtained in Arkansas laminated sandstone (left) compared against the single plane-of-weakness model from Jaeger (1960) and Green River shale (right). These also are compared against the variable cohesive and friction coefficient approach at various confining pressures (σ_3) respect to the inclination of the bedding planes (*b*), after. (Chenevert and Gatlin 1965.)

The Mohr–Coulomb and Hoek–Brown failure criteria are independent of the intermediate stress (σ_2) magnitude. Applying an intermediate stress, greater than the minimum stress (σ_3), to a rock sample can lead to increasingly larger shear strength, as the magnitude of the intermediate stress

$$\sigma_1 = \sigma_3 + \sqrt{m\sigma_3 UCS + s(UCS)^2} \quad \text{(Eq. 9.17)}$$

approaches the maximum principal stress (σ_1). The Drucker and Prager (1952) plasticity failure criterion includes s_2 and was extended from the von Mises yield criterion and developed for soil mechanics. This relationship considers the shear strength increase due to the intermediate stress to equal that of the minimum stress (Veeken et al. 1989). The Lade (1977) failure criterion includes s_2 but considers the shear strength increase due to changes in the intermediate stress to be less than those for changes in the minimum stress. This failure criterion originally was derived for soil material without cohesive strength. McLean and Addis (1990a and 1990b) demonstrated the significant impact of using different failure criteria, including the Mohr–Coulomb and Drucker–Prager, on wellbore stability calculations and mud weight predictions. As a consequence, Ewy (1999) modified the Lade criterion for rock with cohesive strength and applied it for wellbore stability applications in the petroleum industry.

Unconventional shale rocks may require anisotropic failure criteria to include the intrinsic shale anisotropy originated by depositional beddings, laminations, or natural fractures. Coalbed methane formations also may exhibit high intrinsic strength anisotropy created by the cleats.

Chenevert and Gatlin (1965) concluded from experimental triaxial testing that the classical isotropic model for describing the elasticity behavior of shales was inadequate. Their triaxial results also showed the failure behavior of anisotropic laminated shales should be described by the plane-of-weakness theory introduced by Jaeger (1960) or by the variable cohesive and friction coefficients approach. The latter consists of a continuous variation of the cohesive strength σ_0 and internal friction angle y of the rock depending to the inclination angle of the bedding or laminations β with respect to the maximum loading direction s_1. **Fig. 9.12** shows the anisotropic shear failure behavior obtained on a laminated sandstone and a shale rock based on the experimental results obtained by Chenevert and Gatlin (1965).

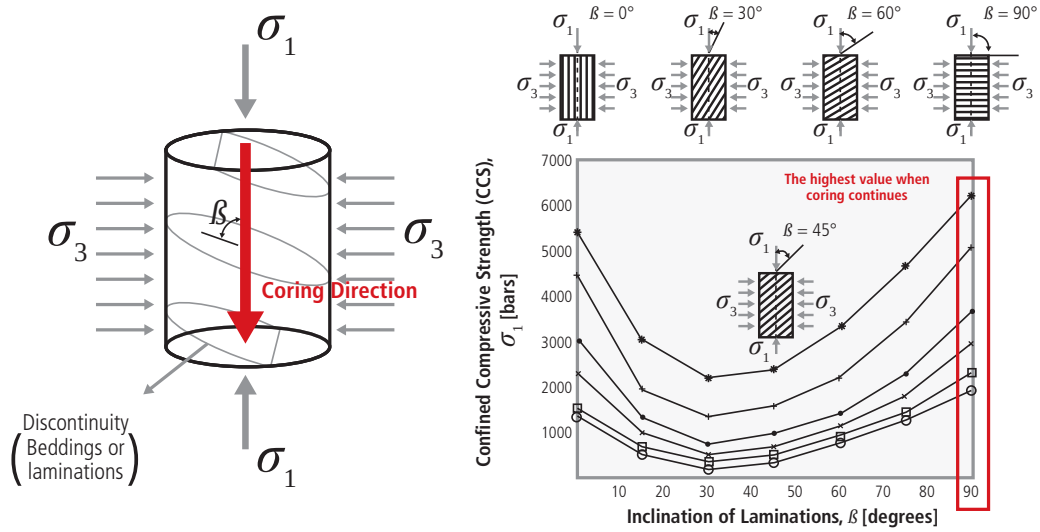

Fig. 9.13—Rock strength anisotropy modeling in a laminated metamorphic rock at several confining pressures and multiple lamination orientation β with respect to maximum loading direction s1 (Pei 2008; Donath 1964).

The anisotropic shear failure referred to as single plane-of-weakness theory (Jaeger and Cook 1979) can be modelled analytically from the intrinsic shear strength of the plane of weakness S_w and the coefficient of sliding friction on the plane of weakness m_w as follows:

In the equation, β is the inclination angle of the plane of weakness with respect to the maximum stress direction σ_1. This analytical model predicts the weakest loading direction

$$\sigma_1 = \sigma_3 + \frac{2(S_w + \mu_w \sigma_3)}{\left[1 - \mu_w \cot\left(\frac{\pi}{2} - \beta\right)\right] \sin(\pi - 2\beta)} \qquad \textbf{(Eq. 9.18)}$$

as 30° from the plane of weakness or laminations. This phenomenon also explains the severe borehole instability experienced when drilling at high inclination angles, within 20° to the bedding planes in highly transverse anisotropic shales with horizontal beddings. This strength anisotropy model first was applied to wellbore stability by Aadnoy and Chenevert (1975) and to borehole breakout modeling by Vernik and Zoback (1990). This concept is explained in detail at the wellbore stability section of this chapter.

Experimental studies (Donath 1964; Nasseri et al. 2003; Pei 2008) show that these shale rocks not only have anisotropic strength properties but also anisotropic elastic moduli (Young's modulus and Poisson's ratio) depending on the inclination of the laminations (e.g., bedding) with respect to the maximum loading direction during triaxial testing. This is illustrated in **Fig. 9.13** (Pei 2008).

The intrinsic shale anisotropy has a profound effect on the rock strength depending on the orientation of the maximum loading direction with respect to the bedding or laminations. The highest strength is achieved when the maximum loading is perpendicular to the bedding while the weakest strength is obtained at 30° angle between the loading direction and bedding direction.

Mokhtari et al. (2013) analyzed the failure behavior of anisotropic shales (particularly Mancos shales) at various bedding angles. Even though this study obtained similar results to Donath (1964) where the weakest strength is achieved at 30° angle to the bedding, the highest shale strength was obtained in samples drilled parallel to bedding.

Crawford et al. (2012) analyzed several core samples from 14 strongly transverse anisotropic fine-grained rocks including 6 argillaceous shales, 3 calcareous marls, 2 oil-shales; 1 limestone, 1 sandstone, and 1 coal. Both strength anisotropy models, single-plane-of-weakness and variable cohesive strength, and the friction coefficient approach were used in this extensive dataset. The experimental data seem to indicate that a continuous variation in cohesive strength with lamination orientation angle gives the best match while less systematic variability was found with the variable friction angle approach. This study also shows the highest cohesive strength reductions (45 to 80%) in calcareous and argillaceous shale samples. The lowest cohesive strength

reductions (20 to 25%) were in sandstones, limestones, and oil-shale samples due to lamination orientation with respect to loading direction.

The compressive strength of shale rocks can be affected not only by laminations but also by the chemical interaction between clay minerals and the water-based drilling fluids. Zhang et al. (2006) studied the rock strength of shales with the exposure of different ionic water solutions with various NaCl, $CaCl_2$, and KCl concentrations. This chemical interaction between clay minerals and water is time dependent and could severely affect the wellbore stability in horizontal wells as the shale strength deteriorates. For example, water-based muds are commonly used to drill vertical wellbores while oil-based muds are used to drill the deviated and horizontal laterals in the Marcellus shale. The oil-based mud maintains the stability of the wellbore while also providing additional lubricity for the drilling process.

9.2.1.6 Poroelastic Properties

The foundation of poroelasticity in the petroleum industry started with the general theory of 3D consolidation, with the work of Biot (1941). This was followed by Gassman's (1951) calculation of the change of stiffness of porous materials containing different fluids; the prediction of the effect of pore pressure depletion on reservoir compressibility (Geertsma 1957); and the re-interpretation of the elastic coefficients of the theory of consolidation (Biot and Willis 1957).

The most commonly used poroelastic coefficient in the oil and gas industry is the one that relates how efficiently the pore pressure opposes the total stress applied to porous media. This coefficient is known as Biot's pore pressure poroelastic parameter (a) and refines the concept of effective stress in rocks from the early effective stress concept introduced by Terzaghi (1936 and 1943) in soil mechanics where *a* was assumed to be equal to 1.

In the equation, σ' is the effective stress supported by the rock that drives deformation; σ is the total stress externally applied to the rock; P_r is the reservoir pore pressure.

The Biot poroelastic parameter can be obtained from several experimental techniques:

- The indirect method consists of measuring the bulk modulus K of the rock and the grain incompressibility modulus K_g (Biot 1956).

$$\sigma' = \sigma - \alpha P_r \qquad \textbf{(Eq. 9.19)}$$

- The direct method consists of measuring the change of pore volume ΔV_p and bulk volume ΔV simultaneously during a triaxial loading test (Biot 1956, Abousleiman and Ghassemi 1992).

$$\alpha = 1 - \frac{K}{K_g} \qquad 0 \leq a \leq 1 \qquad \textbf{(Eq. 9.20)}$$

- The pore pressure depletion test method consists of two triaxial tests. One test is the hydrostatic test with no pore pressure and the other is the hydrostatic test with pore pressure depletion (Franquet and Abass 1999).

$$\alpha = \frac{\Delta V_p}{\Delta V} \qquad \textbf{(Eq. 9.21)}$$

- The failure envelope technique consists of determining the Mohr–Coulomb failure envelope from triaxial test with no pore pressure and conducting one triaxial test with pore pressure (Franquet and Abass 1999). The pore pressure depletion test and the failure envelope techniques result in similar Biot coefficients but are about 10% lower than the results obtained by the indirect method.

All these rock laboratory measurement techniques have additional challenges in shale samples due to their extremely low permeability. These samples require a very long time for internal pore pressure equilibrium and extremely low strain rate deformation for drained tests. The third and fourth methods require multiple samples, which introduces potential errors due to sample variability.

Aoki et al. (1995) studied the anisotropic poroelastic parameters of anisotropic shales by conducting triaxial undrained tests. The true poroelastic behavior in shale samples is difficult to capture in laboratory conditions due to extremely low permeability in the microdarcy to nanodarcy range. Additionally, it is challenging to accurately measure the pore pressure inside shale samples during triaxial tests requiring extremely slow strain rate and a long consolidation time. Consequently, these triaxial shale tests are expensive and time consuming as one test can last many days or even weeks.

Most triaxial tests performed on shale samples are for undrained conditions because high strain rates are used for practical and cost-efficient reasons to obtain quick measurements of strength and quasi-static elastic properties. An alternative approach uses small disk samples at very low strain rates as a substitute for standard 1 or 1.5 in. diameter cylindrical samples (Gutierrez et al. 2013).

The transverse anisotropic nature of the Biot poroelastic coefficient and its stress dependency has been calculated from dynamic measurements in limestones samples (Azeemuddin et al. 2001). This study suggests a Biot transverse anisotropy around 8 to 12% (being higher in the horizontal direction) and a decreasing Biot anisotropy with confining stress. Similarly, acoustic and quasi-static triaxial measurements have been used to calculate the Biot coefficient in sandstones samples drilled parallel and perpendicular to beddings with different porosity values (Al-Tahini et al. 2005).

Different values of Biot's poroelastic coefficient (α) are obtained from different estimation methods on the same samples. The Biot coefficient calculated from the indirect method can be overestimated by 10% in comparison to the direct method. However, with low-porosity rock and high stiffness this difference is reduced significantly.

The anisotropy of the Biot's poroelastic coefficient has been measured in vertical and horizontal samples from the Woodford shale (Abousleiman et al. 2008). The results indicate a Biot coefficient 5% higher in the vertical direction, in contrast to the observations by Azeemuddin (2001), with slight stress sensitivity to confining stress and differential stress. This result differs substantially from the pronounced stress sensitivity of the Biot coefficient measured in samples of Mancos shale (Gutierrez et al. 2013) at around 50% after the first 2000 psi increment of effective mean stress. These experiments were conducted in constant rate of strain consolidation (CRS) on small disk samples allowing reliable measurements of shale permeability and compressibility in a short time and covering a wide range of effective stress change. The CRS test on Mancos shale shows an initial Biot poroelastic coefficient around 0.85 under low effective stress and a substantial decline to 0.4 after applying 2000 psi of effective mean stress (Gutierrez et al. 2013).

New techniques for measuring dual Biot poroelastic coefficient in laboratory conditions have been presented for tight gas and shale gas applications by Abass et al. (2009).

$$B = \frac{\Delta P_r}{\Delta \sigma_3} \qquad \textbf{(Eq. 9.22)}$$

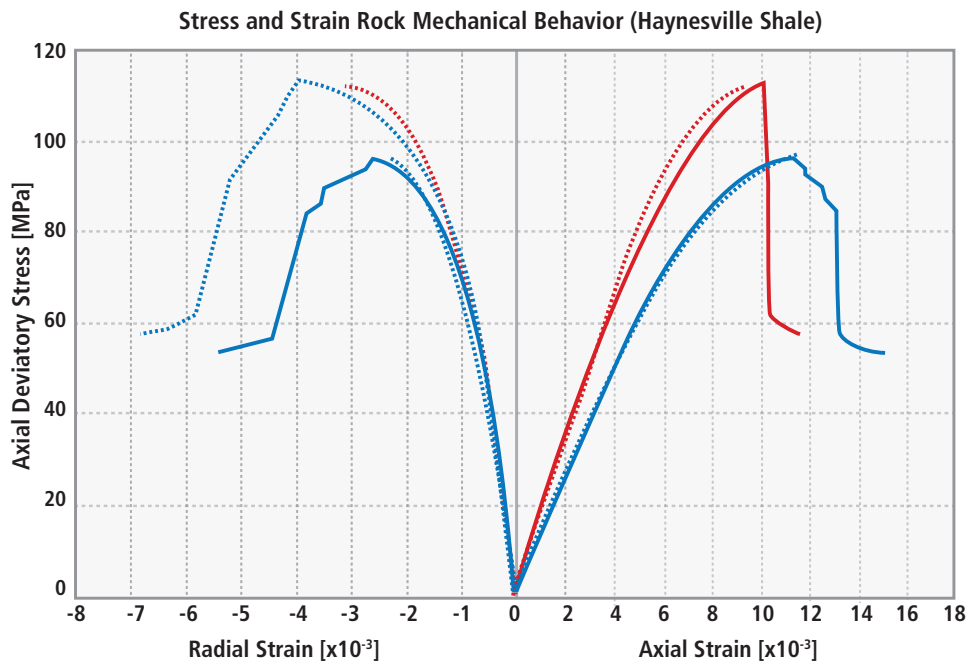

Fig. 9.14—Micromechanical stress and strain modeling of rock samples from the Haynesville shale at 3,300 psi (22.75 MPa) of confining pressure (Franquet et al. 2010).

Another parameter related to poroelasticity and important to characterize the behavior of rocks is the Skempton B parameter. This parameter relates the pore pressure response of a fully saturated soil or rock sample to an incremental increase of the total confining stress S_3 hydrostatically under undrained conditions.

$$\alpha = \frac{1}{B}\left(1 - \frac{K}{K_u}\right) \qquad \textbf{(Eq. 9.23)}$$

A relationship between Biot's (α) and Skempton (B) coefficients can be obtained if two hydrostatic compression tests are conducted on twin saturated samples. The bulk modulus K is obtained from the drained test at constant pore pressure while K_u is obtained from the undrained hydrostatic tests.

Biot's (α) coefficient versus petrophysical parameters: Zimmerman (1986) theoretically derived a relationship between Biot's (α) and porosity. While Fabre and Gustkiewicz (1997) measured both poroelastic coefficients (α and B) of several limestone and sandstone samples and described an experimental relationship between Biot's poroelastic parameter and porosity (Gustkiewicz, 1989). This relationship can be useful to estimate Biot coefficient from log-based porosity measurements.

Another log-derived alternative to estimate Biot coefficient is by using the LMP micromechanical modeling of the bulk modulus during the simulated hydrostatic loading and the average grain volumetric modulus obtained from the weight fraction of the minerals obtained from high-energy pulse-neutron mineralogy logging. The LMP micromechanical modeling is described in the next section.

9.2.2 Micromechanical Stress-Strain Modeling

Static mechanical properties of sedimentary rocks can be predicted from openhole logging data by using an analytical micromechanical stress-strain model. The first constitutive model to predict static mechanical properties from logs was introduced by Raaen et al. (1996) and named **FORMEL** (**FOR**mation **ME**chanical **L**ogging). This model was refined and generalized as part of a joint project between Baker Hughes and IKU (SINTEF) in 1998. The refinement consisted of enhancing the physical rock description and improving the numerical stability to become what is known as logging of mechanical properties (LMP).

The micromechanical approach for predicting static mechanical properties at in-situ conditions utilizes the fundamental behavior of grain-to-grain contacts and micro-crack deformation (sliding along the surfaces of micro-cracks) to construct a constitutive relationship between stress and strain for a given rock material. This model is able to predict static rock deformation in the axial (direction of deviatoric loading) and radial direction during hydrostatic and deviatoric loading of a virtual core sample that is modeled from basic petrophysical properties derived from openhole logging data. The model uses more than twenty micromechanical parameters for the grain-supported and clay-supported rock constituents that can be adjusted or calibrated from triaxial core tests at multiple effective confining conditions.

Franquet et al. (2010) reproduced the stress-strain behavior of conventional sandstones from the Gulf of Mexico and unconventional shale gas samples from the Haynesville using the LMP micromechanical constitutive modeling. **Fig. 9.14** shows the stress-strain mechanical behavior of two triaxial core tests measured in the lab (solid lines) performed with the same confining pressure (3,300 psi) while their corresponding micromechanical simulations from openhole data are plotted in dotted lines. The micromechanical modeling simulates the hydrostatic loading (not shown in Fig. 9.14) and the deviatoric loading of the sample until the macroscopic shear failure is achieved. Therefore, the dotted lines are not predicting the post-failure rock behavior. The red curve comes from a sample with 24% shale volume including the total organic carbon. The blue curve comes from a sample with 34% (V_{clay} + TOC). The sample with less clay and TOC volume behaves more brittle than either the ($B_{elastic}$) or ($B_{failure}$) rock brittleness definitions.

The prediction of log-derived static mechanical properties using micromechanical stress-strain modeling has been successfully implemented not only in conventional reservoirs but also in unconventional shale gas resources. Ong et al. (2000a, 2000b) and Franquet et al. (2005, 2007) used micromechanical log-derived mechanical properties in conventional reservoirs for sand production and wellbore stability applications. More recently LeCompte et al. (2009), Franquet et al. (2011), and Moos et al. (2011) applied the micromechanical approach to derive static mechanical in unconventional reservoirs to evaluate hydraulic fracturing wellbore completions.

9.2.3 Shale Anisotropy

Rock anisotropy is not a new subject in the oil and gas industry as it has been studied by geoscientists, geophysicists, and reservoir engineers for many decades. Chenevert and Gatlin (1965) measured not only 40% rock strength reduction in laminated rock samples tested at 30° from bedding but also observed substantial transverse anisotropy between core samples tested parallel and normal to bedding. Rock anisotropy also has been detected by 3D induction wellbore devices (Schoen et al. 2001) and borehole acoustic logging tools using cross dipole data (Tang and Chunduru 1999) and Stoneley waveforms (Tang 2003).

The macroscale anisotropy of subsurface volumes has been analyzed extensively with the use of multicomponent seismic technology (Hardage et al. 2011).

While well established in the mining and rock mechanics community, rock anisotropy has not received much attention in conventional reservoir development because these formations exhibit limited anisotropy except for the overburden shales, the natural fracture reservoirs, and the fine laminated sand-shale sequences. In today's unconventional shale developments, however, the hydrocarbons are trapped in tight, impermeable, naturally fractured, and highly laminated shale rocks that can be highly anisotropic in nature.

9.2.4 Seismic Anisotropy

The details of the mathematics defining seismic anisotropy are beyond the scope of this chapter, and this discussion is restricted to a description of the fundamental concepts.

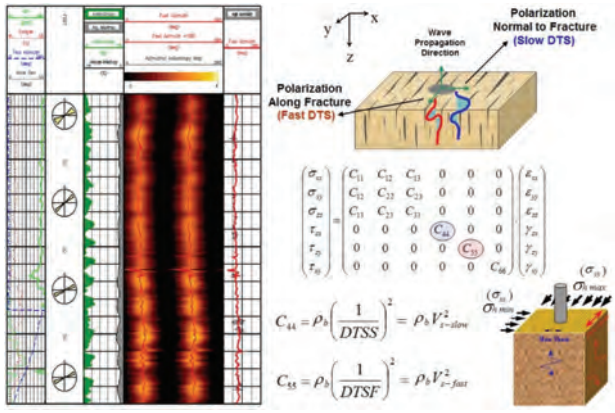

Fig. 9.15—Cross-dipole processing of a vertical well drilled into the Marcellus shale.

Seismic anisotropy is characterized by a dependence of the velocity or reflectivity of a seismic wave on its angle of incidence or direction of azimuth. Seismic anisotropy may be caused by the basic fabric of the rock itself, by the presence of natural fractures, or by the in-situ stress field. A medium is referred to as transversely isotropic when it has a single axis of rotational symmetry typically when the two horizontal directions have similar properties and differ from those in the vertical direction. The intrinsic anisotropy in shales is caused by the horizontal layering of the shale rock fabric resulting in a vertically transversely isotropic medium with a vertical axis of symmetry perpendicular to the layering. This is referred to as VTI anisotropy. Natural fractures occurring in an isotropic matrix that are vertically aligned in well-defined planes or corridors and are oriented in a preferred direction resulting in a horizontally transverse isotropic medium with a horizontal axis of symmetry perpendicular to the fracture planes. This is referred to as HTI anisotropy. A combination of horizontal layering and vertical fracture planes is referred to as orthorhombic or orthotropic anisotropy.

When a seismic P-wave (pressure wave) is incident on a planar boundary between two layers, some of the reflected and transmitted energy is converted into S-waves (shear waves). The angles and velocities of the reflected and transmitted P-waves and S-waves are defined by Snell's law. Karl Zoeprittz (1919) derived the equations for the reflected P, reflected S, transmitted P, and transmitted S-wave amplitude coefficients. The Zoeprittz equations are an exact solution but are complex and difficult to apply to seismic data. To avoid this computational complexity, linearized approximations to the Zoeprittz equations have been developed. Two common approaches are the Aki–Richards equation (Aki and Richards 1980) and the Fatti equation (Fatti 1994). These form the basis for many current seismic anisotropy prediction and inversion routines that are based on amplitude measurements of reflected seismic data.

VTI anisotropy of shales results in a change in the amplitude of a reflected wave versus its angle of incidence with no variation due to azimuth. Based on the Aki–Richards and Fatti equations, these techniques commonly are called AVO (amplitude versus offset) or AVA (amplitude versus angle) approaches and have been very powerful tools in predicting gas in sands (Fatti et al. 1994).

The study of HTI anisotropy resulting from the presence of natural fractures is of particular interest for unconventional shale reservoirs. In this case, the azimuth of the seismic path is a controlling factor. Some techniques are based on travel

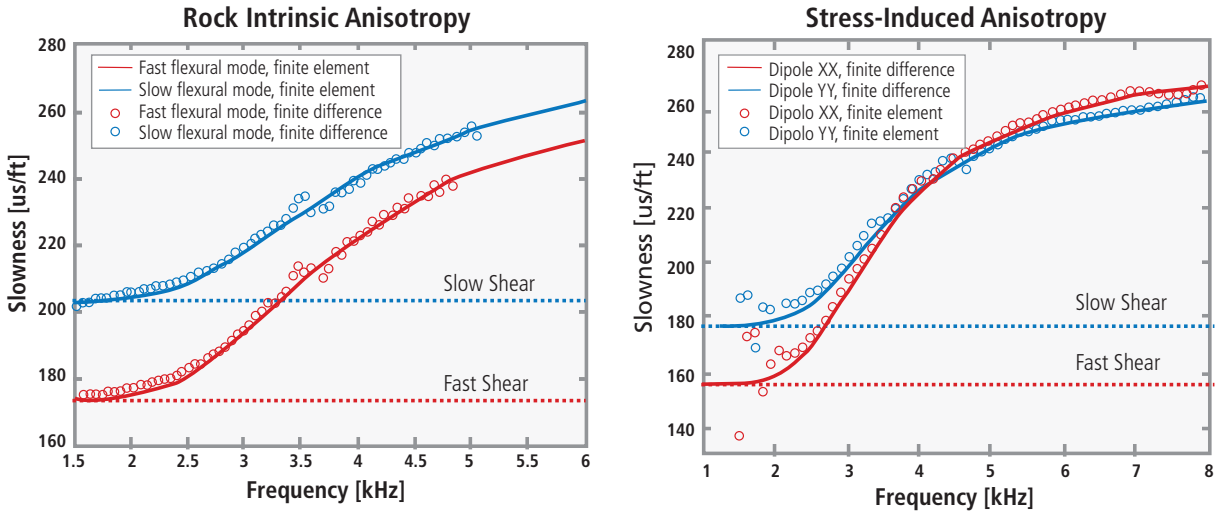

Fig. 9.16—Dispersion curves of fast and slow flexural acoustic modes in a vertical borehole drilled in a formation with intrinsic anisotropy (left) and dispersion curves of the two flexural modes polarized along (xx) and perpendicular (yy) to the maximum horizontal stress direction (right).

time variations caused by velocity anisotropy with azimuth. This is caused by vertically aligned fractures that cause the velocity to be slower perpendicular to the fractures. These methods include shear wave splitting and azimuthal AVO. Shear wave splitting requires a multicomponent 3D survey and measures the filtering effect of vertical fractures that split converted S-waves into fast and slow components. Azimuthal normal moveout (NMO) measures the variation in velocity with azimuth caused by the aligned fractures. HTI anisotropy was studied by Ruger (1998) analyzing the P-wave reflectivity variation with offset and azimuth. An example of the application of this in an unconventional reservoir is shown in another chapter.

9.2.5 Log Anisotropy

The two main logging technologies to characterize rock anisotropy from well logs are 3D induction logging devices and cross-dipole multi-array acoustic logs. The first approach uses three mutually orthogonal transmitter-receiver coil configurations to derive all necessary electrical data to solve the anisotropic resistivity tensor (Kriegshauser et al 2000). The second approach uses four-component cross-dipole and monopole transmitters to derive fast and slow polarized shear waves along the wellbore (Tang and Chunduru 1999) and the transverse shear polarized on the plane orthogonal to well direction from Stoneley-wave inversion (Tang 2003).

Fig. 9.15 illustrates the cross-dipole anisotropy in a vertical well drilled in the Marcellus shale in North America showing low (2 to 3%) azimuthal shear wave anisotropy. The cross-dipole anisotropy detected in wellbore could be originated by three main causes:

- High angle bedding respect to wellbore direction
- Intrinsic anisotropy due to near wellbore fractures
- Horizontal stress anisotropy on stress sensitive rocks

It is difficult to detect the acoustic anisotropy due to stress anisotropy around the wellbore in unconventional reservoirs because tight shale samples are insensitive to stress (small changes in acoustic velocities due to stress). Therefore, the main features detected in cross-dipole anisotropy processing in unconventional reservoirs are the rock intrinsic anisotropy and the near wellbore fractures.

The cross-dipole anisotropy processing of a vertical well would detect two vertical shear waves polarized in the fast and slow direction. The fast shear is polarized parallel to the strike of microfractures while the slow shear is polarized perpendicular to it when the anisotropy is created by intrinsic rock anisotropy. If the cross-dipole anisotropy is caused by borehole-induced stresses, the fast shear is polarized toward the direction of the maximum horizontal stress. The slow shear is toward the minimum horizontal stress direction.

It is possible to differentiate the source of cross-dipole azimuthal anisotropy in stress-sensitive formations by processing the radial variations of the shear-wave velocities near the wellbore. The azimuthal directions of fast shear waves

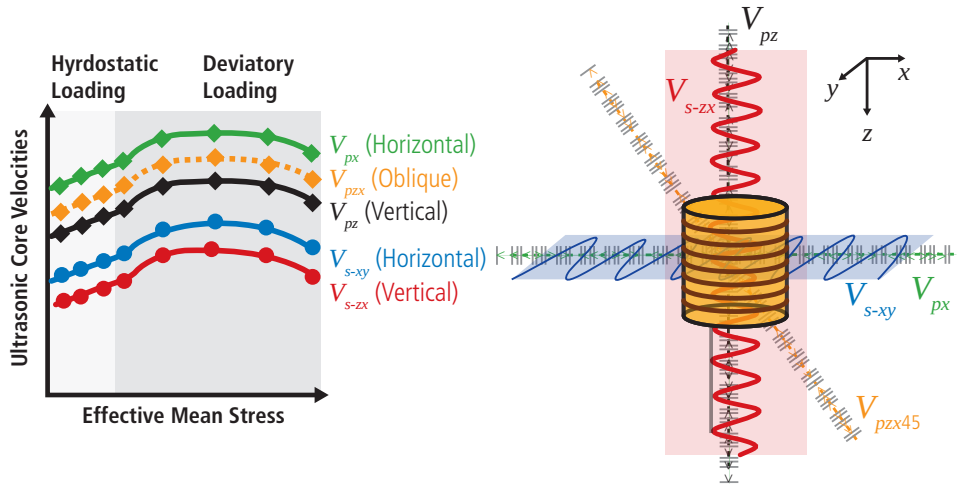

Fig. 9.17—Ultrasonic core velocities measured in shale rock sample for characterizing the VTI anisotropic stiffness tensor.

are calculated at low and high frequencies using a global optimization algorithm by exploiting redundancy of array waveforms from all available receiver combinations. The cross-dipole anisotropy is considered a result of intrinsic anisotropy if the difference of the fast shear angle at low and high frequencies is less than 45°; while it is mainly stress induced if the angle difference is close to 90° (Zheng et al. 2009). **Fig. 9.16** shows the modeling of the shear wave slowness dispersion curves versus frequency in a formation with intrinsic anisotropy (left) and in a stress-sensitive formation with borehole stress-induced anisotropy (right).

The cross-dipole azimuthal anisotropy processing performed in a horizontal wellbore provides direct measurement of the transverse intrinsic anisotropy of the shale formation due to beddings and laminations. The transverse anisotropy of shale formation can also be detected and quantified in vertical wellbores by processing the Stoneley wave (Tang 2003).

The methodology for deriving the horizontal shear-wave from the vertically propagating Stoneley tube wave data acquired by an acoustic logging tool consists of the inversion analysis between the Stoneley wave slowness and the weighted average of the wave's dispersion curve over the frequency range occupied by the wave spectrum. The wave dispersion equation can be derived from Tongtaow (1982) and Ellefsen (1990).

9.2.6 Core Anisotropy

The mechanical core anisotropy can be measured using either triaxial compression tests or ultrasonic velocity measurements on samples taken in multiple directions with respect to the intrinsic rock anisotropy: parallel and perpendicular to bedding or natural fractures.

Transversely anisotropic rocks like shale rocks require five independent acoustic measurements to fully characterize the stiffness tensor C_{ij} (**Fig. 9.17**). C_{ij} represents the simplified second-order stiffness tensor of the rock after the Voigh (1910) tensor index transformation. The dynamically derived stiffness tensor components can be obtained from two shear and three compressional wave velocities measurements for transversely isotropic rocks.

9.3 In-Situ Stress and Pore Pressure Characterization

The characterization of reservoir pressure (P_r) and in-situ stresses (sv, s_{hmax}, s_{hmin}) in reservoirs should be conducted simultaneously because they are considered to be dependent upon each other in a couple-balanced hydromechanical state.

Unconventional and conventional reservoirs alike undergo stress changes during production accompanying pressure depletion and the consequences of rapid pressure decline during the early stage of production. Similarly, total in-situ stresses are modified and increased in the vicinity of the hydraulic fracturing stimulation zones due to the deformation associated with the formation and opening of the hydraulic fractures. A large volume of the hydraulic fluid pumped into the target reservoir zone(s)

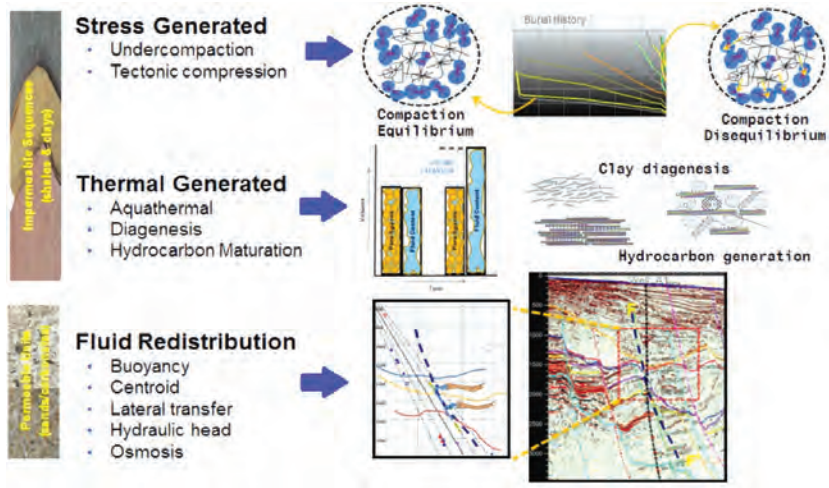

Fig. 9.18—Principal overpressure generating mechanisms prevalent in different sedimentary basins.

remains underground. Not all the fluid can return to the surface during the flowback period following the well stimulation treatments. This entrapped fluid in poorly connected induced fractures may affect the in-situ stresses in the subsurface.

The stresses acting in the subsurface can be defined by three mutually orthogonal principal stresses aligned to the principal stress directions: $s_1 > s_2 > s_3$. The vertical stress is commonly one of the principal stress directions in subsurface, in low-tectonic environments with horizontal beds without inclined or deformed layers. In contrast, structural features such as salt-diapirs. Thrust-related roll-over anticlines, drape structures perturb the in-situ stress state in the surrounding formations rotating the principal stress direction from the vertical direction. Regions with high tectonic stresses typically have principal stress directions rotated from the vertical and horizontal axes.

This chapter considers the in-situ stress state when one of the principal stresses is aligned with the vertical direction, comprising a simplified stress characterization acting in unconventional reservoirs. As a way forward, it is important to recognize the power of integrating microfrac, minifrac, core, and sonic logging for an optimized stress profile development (Ahmed 1991).

9.3.1 Pore Pressure Estimation

Pore pressure estimation in unconventional reservoirs presents a significant challenge, compared to conventional plays. Standard direct measurements (DSTs, wireline testing tools, RCI, MDT, etc.) are not suitable to measure the pore pressure in shale gas and oil reservoirs due to their low porosities and permeabilities. The porosity-based techniques are commonly used to derive pore pressure profiles in shales in conventional plays based on an under-compaction approach. They are not applicable and have limitations in unconventional plays as:

- Most of the shale gas and oil plays are not geological shales.
- The unique and variable sources of these formations are not constant and have a complex diagenetic history.
- The formations often are not in passive basins but in basins with a complex geological history.

The main cause of overpressure in unconventional reservoirs is not under-compaction (**Fig. 9.18**) but hydrocarbon generation (volume expansion) and at times even due to transference (fluid redistribution) through permeable faults and fractures (Haugland et al. 2013). Moreover, challenges in estimating pore pressures result from scarcity of sufficient datasets of logs and dependable stratigraphic correlation that offer additional challenges to integrate detailed geological understanding into the pore pressure models for these resources.

The difficulty in obtaining reliable direct pressure measurements in these tight source rocks is due to their extremely low permeabilities (microdarcy to nanodarcy) that also limit any model calibration from indirect pore pressure estimation methods. It is difficult to get any reliable pore pressure measurements from wireline formation tests in these shale rocks. However, microfracture and hydraulic fracture diagnostic test results can be misleading. The resultant effective stress ratios in many cases have been questionable and are considered invalid. There are also limitations in using various drilling parameters, including gas shows, as reliable indicators of the overpressure state of these formations. As these formations are tight, the reported connection gases and the overall background gas trend

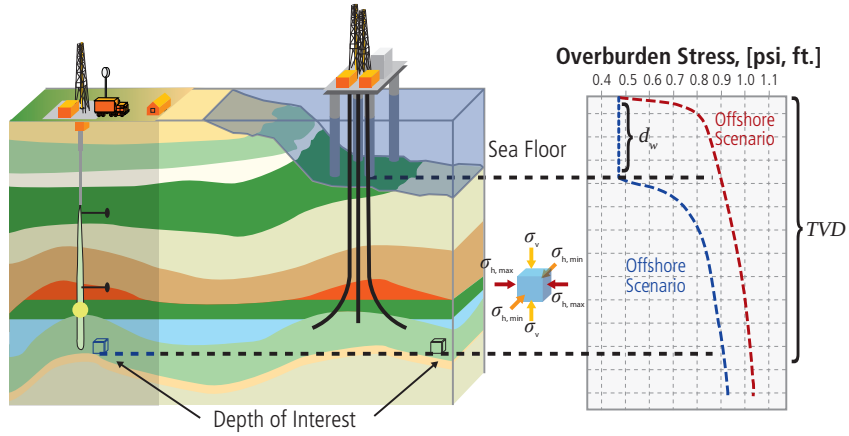

Fig. 9.19—Comparison between the density integration in onshore and offshore scenarios for the same TVD.

are not always reliable indicators of pore pressure. Moreover, the variations in the background gas are probably more related to mineralogical changes, effects of rate-of-penetration, the presence or absence of natural fractures, etc. The incidences of high gas counts while drilling are in direct response to the richness of the source. The variations in the total recorded gas are related to the changes in the organic content and expected gas-in-place in these unconventional reservoirs.

As overpressure generation in these rocks are mostly associated with source rock maturation. Both subsidence and temperature-related overpressure mechanisms play a role, with generation of hydrocarbons and overpressure being possibly concurrent events (Cander 2012). Therefore, their associated effect on rock elastic properties, porosity-permeability, and effective stress become difficult to ascertain. Moreover, as overpressure values in these unconventional plays are associated with hydrocarbon generation, the pore pressure magnitude is usually related to the total organic content (TOC), the thermal maturity, and the diagenetic history of these shale rocks (Theloy and Sonnenberg 2012). This underscores the need to develop new methodologies to estimate the pore pressures in these plays.

In addition to knowledge about possible overpressure causes, it is equally important to understand how overpressure is preserved vis-à-vis the basinal history both burial and any associated uplift. Therefore, basin-modeling techniques to model source rock maturity and petroleum generation, along with possible expulsion as well as hydrocarbons retained in these source rocks, provide important information about the overpressure state of these resources. Moreover, normalization of the reported gas trend with drilling events and parameters as well as gas-in-place information calculated from petrophysical data also can provide crucial information to help calibrate the interpreted pressure profiles in these challenging rock types.

$$\sigma_v = \int_0^{d_w} \rho_w \vec{g} dz + \int_{d_w}^{TVD} \rho_b(z) \vec{g} dz \qquad \text{(Eq. 9.24)}$$

9.3.2 Overburden Stress

The characterization of the in-situ stress state in both conventional and unconventional resources commonly assumes that the vertical, or overburden, stress is one of the principal stresses acting in the reservoir. This simplification is reasonable in field locations with nearly flat topography where the vertical compressive stress acting on the subsurface strata corresponds to the weight of the overburden rock layers. The weight of the water column needs to be considered as well in offshore reservoirs, as expressed in the density integration shown in **Fig. 9.19**.

Fig. 9.19 shows lower vertical stress acting on an offshore reservoir in comparison to a reservoir on shore at the same true vertical depth (TVD) because formation bulk density ρ_b is more than double that of seawater density ρ_w. The water depth d_w is measured from the mean sea level to the sea floor.

The acoustic logs are more commonly run in oil and gas fields from the total depth of the well to surface because they provide important depth control along with vertical seismic profile (VSP) for seismic data migration. Therefore, it is common to estimate formation density of the shallow formations (in absence of density logs) from empirical correlation between compressional velocity V_p and density for overburden stress integration. Similarly, the overburden stress field can be obtained in 3D using volumes of formation density derived from seismic attributes.

9.3.3 Minimum Horizontal Stress

The minimum horizontal stress magnitude is a key parameter for hydraulic fracture design, which can be estimated from theoretical considerations, from observations and trends, and from direct measurements. Anderson (1951) discussed the relative magnitudes of the stresses required to generate faulting in different geological environments and defined a stress polygon based on a Mohr–Coulomb failure criterion. The magnitudes of the maximum and minimum stresses required to generate a fault at frictional equilibrium bounds the magnitudes of the stresses which define the stress polygon at each vertical stress and reservoir pressure condition. Horizontal stresses cannot exist outside the polygon because shear failure and slip will occur. Hubbert and Rubey (1959) used the same assumptions of fault slip to assess the stress magnitudes required for thrust faulting in the presence of overpressures.

$$\sigma_{h\,\min} = K_{ESR}(\sigma_v - P_r) + P_r \qquad \textbf{(Eq. 9.25)}$$

Matthews and Kelly (1967) proposed that the increase of minimum horizontal stress $s_{h\,min}$ is proportional to the increase of the vertical stress s_v. They also proposed the effective stress ratio K_{ESR} is the ratio of these two stresses that varies with depth and compaction. This model as formulated, however, cannot accurately predict changes of horizontal tectonic stresses between formations with high stiffness contrast.

An alternative theoretical approach to estimate the magnitude of the minimum horizontal stress assumes not faulted rock, following Anderson, but intact rock and soil. This continuum approach estimates the minimum horizontal stress magnitude based on elastic theory. It has been used since the early days of geomechanical engineering, where

$$\sigma_{h\,\min} = \frac{v}{1 - v}(\sigma_v - P_r) + P_r \qquad \textbf{(Eq. 9.26)}$$

the ratio of the effective stresses ($s_{h\,min}$-P_r / s_v-P_r) can be estimated from the Poisson's ratio (n/1-n) for zero lateral strain or passive basin conditions (Terzaghi, 1943). Eaton (1969) adopted this elastic approach to predict fracture gradients in the Gulf of Mexico. Each rock layer is assumed elastic and isotropic. The resulting minimum horizontal stress profile reflects the variation of the Poisson's ratio, pore pressure gradient, and overburden stress.

Biot's pore pressure coefficient subsequently has been included in later formulations of this relationship.

These early approaches have been refined to different degrees but substantially retain the underlying assumptions of the original work. Following the earlier work of Anderson (1951), Zoback and Healy (1984) proposed an effective stress ratio approach based on frictional equilibrium. They refined the stress polygon and more clearly segmented it into the three triangles that define tectonic stress boundaries for each stress state regime in the subsurface: NSR normal faulted, SSR strike-slip, and RSR reverse stress regime (**Fig. 9.20**). The size of the polygon depends on the internal friction coefficient ***m*** and the pore pressure P_r of the formation. A high friction coefficient

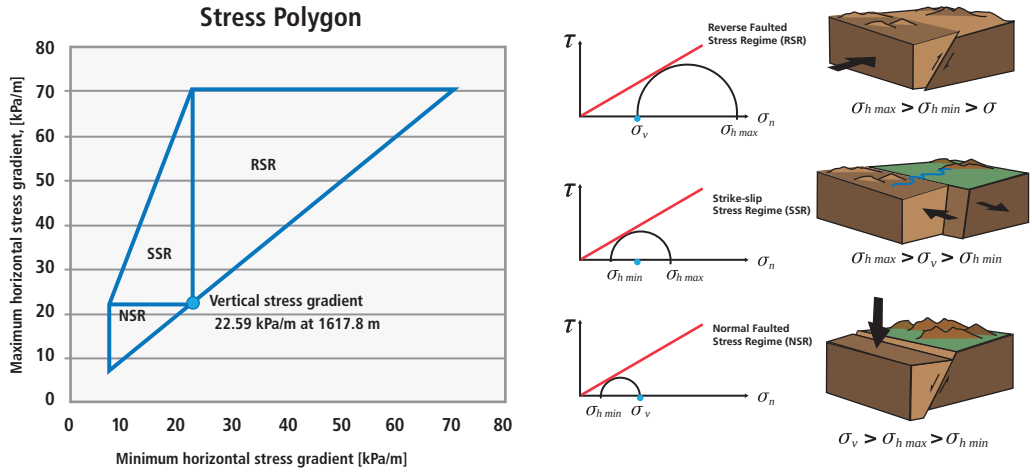

Fig. 9.20—Stress polygon and frictional equilibrium after Zoback and Healy (1984).

increases the size of the stress polygon while a high reservoir pressure reduces the polygon size. This frictional equilibrium approach constrains the magnitude of the minimum horizontal stress in a normal faulted stress regime environment as follows:

$$\sigma_{h\,\min} = \left[\sqrt{(\mu^2+1)} + \mu\right]^{-2}(\sigma_v - \alpha P_r) + \alpha P_r \quad \textbf{(Eq. 9.27)}$$

where ***m*** can be obtained from the Mohr–Coulomb internal friction angle of the rock, q: An effective stress ratio K_{ESR} = 3.1 is obtained from a friction coefficient of ***m*** = 0.6.

$$\mu = \tan(\theta) \quad \textbf{(Eq. 9.28)}$$

This Andersonian polygon approach contains inherent assumptions about the nature of faulting that have been updated to address these shortcomings, showing that the principal stresses during faulting are more complex than this simple model predicts. However, this approach still is widely used in the industry.

$$\sigma_{h\,\min} = \frac{\nu}{1-\nu}(\sigma_v - \alpha P_r) + \alpha P_r + \sigma_t \quad \textbf{(Eq. 9.29)}$$

$$\sigma_{h\,\max} = \left[\frac{\nu}{1-\nu}(\sigma_v - \alpha P_r) + \alpha P_r\right]\left(1 + \frac{\sigma_{ani}}{100}\right) \quad \textbf{(Eq. 9.30)}$$

The Eaton methodology to predict the minimum horizontal stress magnitudes also is widely used in the industry and in the development of unconventional reservoirs. In most of the cases, this approach underestimates the minimum horizontal stress because it does not include the lateral tectonic stresses acting in the crust. Zoback (2007) shows an example where several stress measurements from minifracture tests were not predicted by the Eaton method using a log-derived Poisson's ratio from compressional DTC and shear DTS wave slowness.

The log-derived minimum horizontal stress magnitude can be calibrated from leak-off tests (LOTs), extended leak-off tests (XLOTs), or microfracture tests conducted at multiple depths by adding a tectonic stress factor s_t (Daines 1982) and a horizontal stress anisotropy s_{ani} [%]. A good example of this log-derived stress calibration from microfracture tests is the work done by Gatens et al. (1990) in the Devonian shales for quantifying the stress contrast and static mechanical properties for hydraulic fracturing design and vertical fracture growth modeling.

Warpinski et al. (1998) compared the log-derived minimum horizontal stress from Eaton's method to stress measurements from microfracture tests. They found the log-derived stress method underestimates the in-situ stress obtained from the fracture closure and predicts smaller stress contrast between formations than measured from the microfracture tests. As such, even if a tectonic factor is used to calibrate the log-derived stress profile, the log predictions may fail to reproduce the stress contrast. This is the main drawback of trying to calibrate the uniaxial strain compaction or bilateral constrained method with a constant tectonic stress or stress gradient assuming isotropic rocks.

$$\sigma_h = \frac{\nu}{1-\nu}(\sigma_v - \alpha P_r) + \alpha P_r + \frac{E\alpha_t}{1-\nu}\Delta T + \frac{E}{1-\nu}\varepsilon_h \quad \textbf{(Eq. 9.31)}$$

Prats (1981) proposed an idealized horizontal stress model where only horizontal deformation results from changes in vertical loading, temperature, and lateral strains as presented below:

$$\sigma_{h\,\min} = \frac{\nu}{1-\nu}(\sigma_v - \alpha P_r) + \alpha P_r + \frac{E}{1-\nu^2}\varepsilon_{h\,\min} + \frac{\nu E}{1-\nu^2}\varepsilon_{h\,\max} \quad \textbf{(Eq. 9.32)}$$

$$\sigma_{h\,\max} = \frac{\nu}{1-\nu}(\sigma_v - \alpha P_r) + \alpha P_r + \frac{E}{1-\nu^2}\varepsilon_{h\,\max} + \frac{\nu E}{1-\nu^2}\varepsilon_{h\,\min} \quad \textbf{(Eq. 9.33)}$$

where αt is the thermal coefficient of linear expansion of the rock, ΔT is the change of temperature, and ε_h is the horizontal (lateral tectonic) strain assumed equal in both lateral directions. The two horizontal tectonic strains should not be equal as plate tectonics have a predominant direction for lateral deformation. Therefore, the two horizontal stresses can be modeled with two lateral strains to include the tectonic stresses in both horizontal directions ε_{hmin} and ε_{hmax}. The equations below include the tectonics stresses with two lateral strains acting on an isotropic formation with no thermal induced stresses.

The above horizontal stress relationships have a profound difference with respect to those of Eaton (1969) and Gatens et al. (1990) due to the inclusion of the Young's modulus (rock stiffness) in the equations. The variation of the Young's modulus

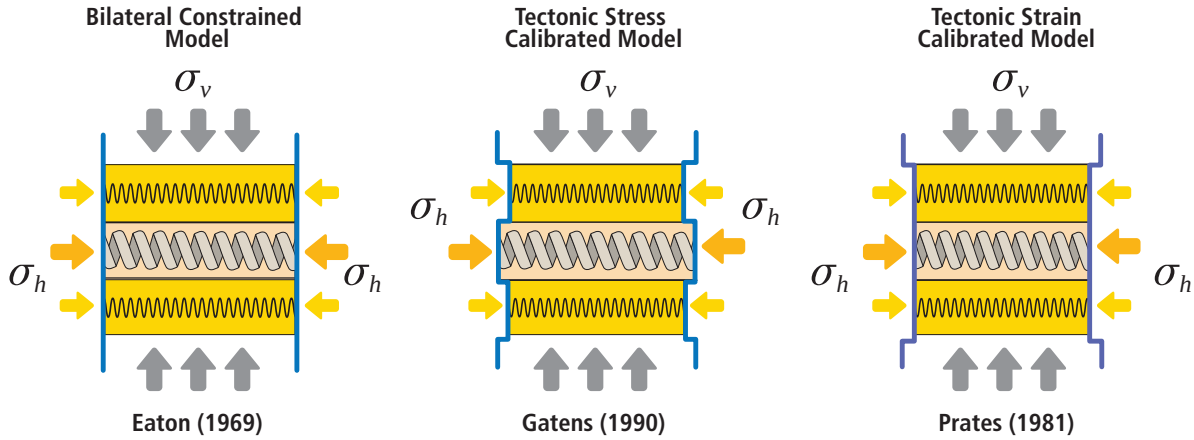

Fig. 9.21—Horizontal stress models for zero lateral strains (Eaton), tectonic stress calibrated (Gatens), and tectonic strain calibrated (Prats).

with depth of the layers could have a very different impact on the minimum horizontal stress magnitude in comparison to Poisson's ratio. In fact, these two curves could have opposite trends because high Young's modulus could be associated with formations with low Poisson's ratio. As a consequence, the vertical profile of the horizontal stress including lateral tectonic strains could have different stress contrast characteristics due to the presence of Young's modulus in the equation. **Fig. 9.21** shows the uniaxial strain compaction model (bilateral constrained), the tectonic stress calibrated model, and the tectonic strain calibrated mode. The calibrated tectonic strain model could end up with a different stress contrast in comparison to the other models because stiffer layers will support more stress than soft layers for the same amount of tectonic strains.

To obtain agreement with the field measurements, the inclusion of Young's modulus in these stress estimation equations requires an iterative approach to evaluate the appropriate horizontal strain magnitudes ($\varepsilon_{h\,min}$ and $\varepsilon_{h\,max}$), which are effectively calibration parameters. These elastic strain values cannot at present be obtained from geological history estimation or palynspathic reconstruction based on large strain plasticity approaches as these are inherently inconsistent approaches.

Many geomechanical engineers prefer to use the effective stress ratio K_{ESR} for characterizing horizontal stresses. They use the frictional equilibrium, borehole breakouts, or casing shoe leak-off tests to calibrate the effective stress ratio for petroleum applications such as wellbore stability and sand production prediction. For this approach, the effective stress ratio should be lithology dependent. This will account for local changes in the magnitude of the horizontal stresses among formations of different stiffness that is crucial for vertical fracture propagation modeling and prediction of fracture containment. This is the main reason why other log-derived estimations of horizontal stresses are used in the industry for hydraulic fracturing design and vertical fracture growth assessment.

Warpinski et al. (1982) conducted several in-situ stress measurements demonstrating that material property differences are incapable of containing hydraulic fractures. Warpinksi noted that the stress contrast between the pay zone and the bounding layers is the most predominant factor controlling fracture height while material interfaces show little effect. Warpinski confirmed the presence of large variations in the magnitude of the minimum horizontal stress over small vertical distance (a few feet), which also was observed from numerous microfracture tests performed by Evans et al. (1989) and Plumb et al. (1990).

$$\sigma_{h\,min} = \frac{E_h}{E_v}\,\frac{\nu_{zx}}{1-\nu_{xy}}(\sigma_v - \alpha(1-\xi)P_r) + \alpha P_r + \frac{E_h}{1-\nu_{xy}^2}\,\varepsilon_{h\,min} + \frac{\nu_{xy}E_h}{1-\nu_{xy}^2}\,\varepsilon_{h\,max}$$

(Eq. 9.34)

$$\sigma_{h\,min} = \frac{E_h}{E_v}\,\frac{\nu_{zx}}{1-\nu_{xy}}(\sigma_v - \alpha(1-\xi)P_r) + \alpha P_r + \frac{E_h}{1-\nu_{xy}^2}\,\varepsilon_{h\,max} + \frac{\nu_{xy}E_h}{1-\nu_{xy}^2}\,\varepsilon_{h\,min}$$

(Eq. 9.35)

The modeling of horizontal stresses using the lateral tectonic strains can be expanded to include anisotropic formations like shale gas. Higgins et al. (2008) used the borehole acoustic anisotropy and the ANNIE approximation to characterize VTI vertically transverse isotropic formations. They derived log-based horizontal stress profiles for hydraulic fracturing and completion design in the Baxter shale. This model uses two Young's modulus (vertical E_v and horizontal E_h) and two Poisson's ratio (vertical-to-horizontal n_{zx} and

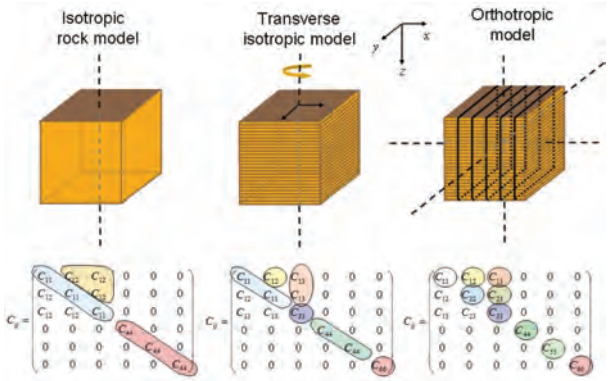

Fig. 9.22—Rock models and stiffness tensor characteristics for isotropic, vertically transverse isotropic, and orthotropic elastic rocks. These models require two, five, and nine independent elastic properties to define their stiffness tensors, respectively.

horizontal-to-horizontal n_{xy}) besides an anisotropic Biot poroelastic parameter ***x*** to derive horizontal stress profiles.

$$\sigma_{ij} = C_{ijkl}\,\varepsilon_{kl}$$

(general elasticity equation) **(Eq. 9.36)**

$$\sigma_{i} = C_{ij}\,\varepsilon_{j}$$

(after Voigt transformation) **(Eq. 9.37)**

Shale anisotropy has been studied extensively from seismic attributes (Sayers 2005) and borehole acoustic data (Walsh et al. 2006) to characterize the stiffness tensor of VTI formations. **Fig. 9.22** illustrates the 3 x 3 x 3 x 3 fourth-order stiffness tensor C_{ijkl} simplified into a 6 x 6 second-order tensor C_{ij} after Voigh (1910) tensor transformation for isotropic, VTI vertically transverse isotropic, and orthotropic formations.

The ANNIE approximation introduced by Schoenberg et al. (1996) consists of two assumptions:

- $C_{12} = C_{13}$: This assumes that all non-diagonal terms are equal as any TI material have $C_{13} = C_{23}$.
- d = 0: Thomsen's delta coefficient ***d*** defined in Thomsen (1986).

The benefit of using the ANNIE approximation in shale formations consists of estimating all five stiffness components for a VTI medium with only three independent borehole acoustic measurements acquired in a vertical pilot hole. The vertical DTC, vertical DTS, and horizontal shear DTSH from Stoneley wave inversion developed by Tang (2003) provide the data for characterizing the dynamic stiffness coefficients C_{33}, C_{44}, and C_{66}, respectively.

$$C_{33} = \rho_b \left(\frac{1}{DTS}\right)^2$$ **(Eq. 9.38)**

$$C_{44} = \rho_b \left(\frac{1}{DTS}\right)^2$$ **(Eq. 9.39)**

$$C_{66} = \rho_b \left(\frac{1}{DTSH}\right)^2$$ **(Eq. 9.40)**

$$C_{13} = C_{33} + 2C_{44}$$

ANNIE approximation (*d* = 0) (Eq. 9.41)

$$C_{13} = C_{13}$$

ANNIE approximation (Eq. 9.42)

$$C_{11} = C_{12} + 2C_{66}$$

Linear elastic relationship (Eq. 9.43)

The main problem with using the ANNIE approximation for characterizing unconventional shales from borehole acoustic logs is the contradictory core ultrasonic measurements obtained in several shale samples where the Thomsen delta coefficient is not zero and the non-diagonal terms C_{12} and C_{13} are not equal (Berge et al. 1991; Abousleiman et al. 2008).

$$C_{22} = C_{11}$$

VTI anisotropy condition **(Eq. 9.44)**

$$C_{23} = C_{13}$$

VTI anisotropy condition **(Eq. 9.45)**

$$C_{55} = C_{44}$$

VTI anisotropy condition **(Eq. 9.46)**

Franquet and Rodriguez (2012) expanded the analytical solution of the two horizontal principal stresses for orthotropic rocks using six of the stiffness tensor components. They did not use the pre-conceived ANNIE

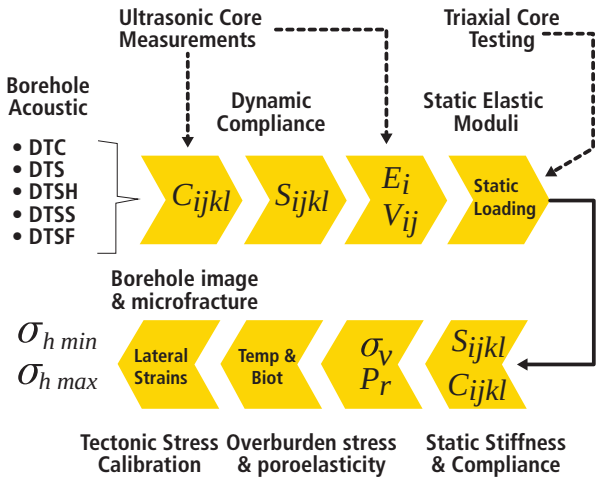

Fig. 9.23—Log-derived anisotropic stress profiling with core elastic anisotropy measurements and lateral tectonic strain calibration from microfracture and/or borehole breakout modeling (Franquet and Rodriguez 2012).

approximation on the stiffness tensor for TI rocks. The general orthotropic stress profiling is based on the following assumptions:

- The vertical direction is one of the principal stress directions of the far-field stress tensor.
- The borehole logging data comes from a vertical pilot well.
- The transverse and orthotropic anisotropies of the rock are created by horizontal beddings of shale laminations and vertical natural fractures, respectively.

Fig. 9.23 shows the workflow for getting the log-derived, core-calibrated, and tectonically calibrated horizontal stress profiling in anisotropic formations. The first step of the workflow is to define the rock model based on the acoustic anisotropy obtained from borehole cross-dipole logs and ultrasonic core measurements. Then, the dynamic stiffness and compliance tensors are converted into static elastic tensors following calibration against triaxial core tests on vertical (perpendicular to bedding), horizontal (parallel to bedding), and 45°-angle samples. Next, the overburden stress and pore pressure are included with the Biot's poroelastic coefficient estimated from core testing, micromechanical stress-strain modeling, or empirical correlations using shale porosity and weight fraction of the minerals. Finally, the horizontal stress profiles are obtained, after adjustment of the required lateral tectonic strains to reproduce microfracture test results and/or borehole failure evidence from breakouts and/or induced fractures.

A common misunderstanding is that lateral strains are constant with depth and always positive. Lateral tectonic strains vary with depth and the ($\varepsilon_{h\,min}$) can become negative in active extensional stress regimes.

$$\sigma_{h\,max} = \psi_2 (\sigma_v - \alpha_z P_r) + \alpha_x P_r + \psi_3 \varepsilon_{h\,min} + \psi_5 \varepsilon_{h\,max} \quad \textbf{(Eq. 9.47)}$$

$$\sigma_{h\,max} = \psi_2 (\sigma_v - \alpha_z P_r) + \alpha_y P_r + \psi_4 \varepsilon_{h\,max} + \psi_5 \varepsilon_{h\,min} \quad \textbf{(Eq. 9.48)}$$

The above equations consider the z direction as vertical and x in the direction of minimum horizontal stress and y in the direction of maximum horizontal stress. The y coefficients can be expressed in terms of the static stiffness tensor components C_{ij} as follows:

$$\psi_1 = \frac{C_{13}}{C_{33}} \quad \textbf{(Eq. 9.49)}$$

$$\psi_2 = \frac{C_{23}}{C_{33}} \quad \textbf{(Eq. 9.50)}$$

$$\psi_3 = C_{11} - \frac{C_{13}^2}{C_{33}} \quad \textbf{(Eq. 9.51)}$$

$$\psi_4 = C_{22} - \frac{C_{23}^2}{C_{33}} \quad \textbf{(Eq. 9.52)}$$

$$\psi_5 = C_{12} - \frac{C_{13} C_{23}}{C_{33}} \quad \textbf{(Eq. 9.53)}$$

Eq. 9.47 and **Eq. 9.48** are general for any type of anisotropy as they convey the same results for isotropic and transverse isotropic rocks. The y terms also can be expressed in terms of three Young's modulus (E_x, E_y, and E_z) and three Poisson's ratios (n_{zx}, n_{xy}, and n_{zy}) (Franquet and Rodriguez

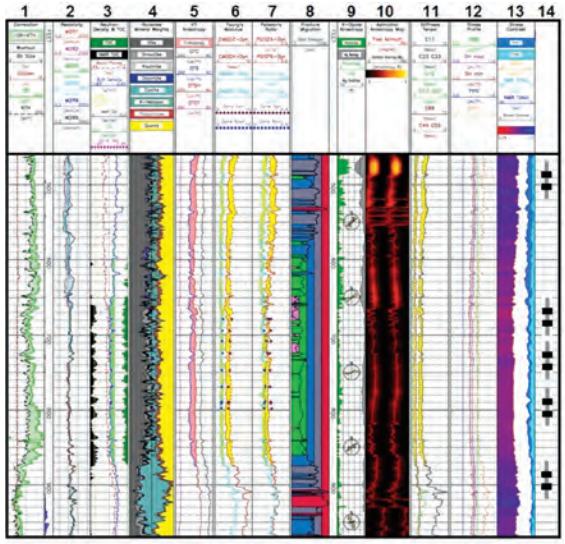

Fig. 9.24—Log-derived minimum horizontal stress profile in the Eagle Ford shale using an anisotropic model obtained from borehole acoustic anisotropies and calibrated with ultrasonic core measurements. (Franquet and Rodriguez 2012).

2012). An example of the stress profiles calculated using the azimuthal cross-dipole anisotropy and transverse anisotropy from Stoneley wave inversion in the Eagle Ford shale is presented (**Fig. 9.24**).

The figure shows the mineralogy track next to the transverse anisotropy, which is shaded in pink. The next two tracks illustrate the cross-dipole azimuthal shear anisotropy direction and magnitude around the wellbore. The last three tracks are the vertical fracture migration plot, anisotropy stiffness tensor components, and the minimum horizontal stress profile (fracture closure pressure gradient CLPG). The latter is the curve that is used for hydraulic fracturing modeling and fracture containment. The lowest minimum horizontal stress (indicated in red) in the middle of the log (depth range 250 to 400 ft.) corresponding to the high organic 150-ft.-thick interval of the Eagle Ford that can be effectively stimulated as sufficient stress contrast exists above and below the pay zone.

The tectonic strain calibration of the fracture closure pressure curve (minimum horizontal stress) is achieved with multiple measurements of fracture closure using a dual packer injection test from surface pumping or by downhole straddle packer tools capable of performing microfracture tests. Conventional microfracture tests identify the fracture closure pressure by natural leak-off after formation breakdown and fracture propagation. Conventional reservoirs have enough

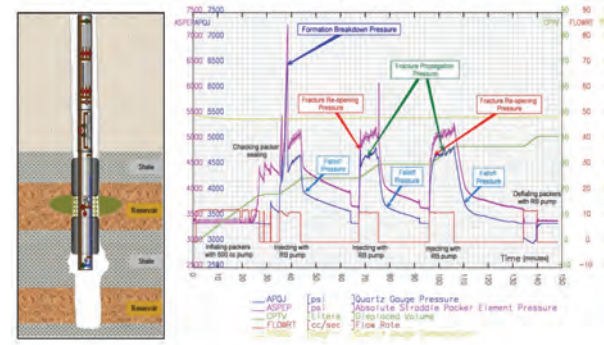

Fig. 9.25—Downhole straddle packer microfracture test performed in a conventional carbonate reservoir (Ihab et al. 2014).

permeability to identify in a short time the fracture closure by monitoring the pressure fall-off after shut-in. Multiple fracture closure identification methods are commonly used such as square-root of shut-in time, Log-Log plot, and GdP/dG plot. **Fig. 9.25** illustrates a downhole straddle packer microfracture tests done in a conventional carbonate reservoir (Ihab et al. 2014).

Wireline or pipe-conveyed straddle packer microfracture tests are performed by injecting the wellbore fluid into an isolated small interval (3 to 5 ft.) at a small flow rate (0.5 to 0.6 liter/min). The fracture is propagated for short periods of time (around 10 minutes) on each injection cycle. The straddle packer inflation pressure (plotted in magenta) is always above the isolated interval pressure (plotted in blue) by a few hundred psi (300 psi in the above example).

However, unless natural fractures are intersected by the hydraulic induced fracture, unconventional reservoirs don't have enough leak-off coefficient to observe fracture closure in a reasonable timeframe. The induced fracture can stay open for a long time due to the extremely low formation permeability and low leak-off. Therefore, straddle packer microfracture tests in unconventional reservoirs are performed to induce fracture closure after shut-in by a controlled flowback at a small rate. Controlled flowback to improve fracture closure in low permeability formations has been addressed in conventional reservoirs by De Bree and Walters (1989). Typically four to five injection cycles are conducted at the same straddle interval to validate the formation breakdown, fracture reopening, propagation, and closure. **Fig. 9.26** illustrates a wireline microfracture test in a shale gas with four injection cycles and four flowback tests. **Fig. 9.27** shows the fracture closure identification from a flowback test after fracture propagation in a shale gas interval.

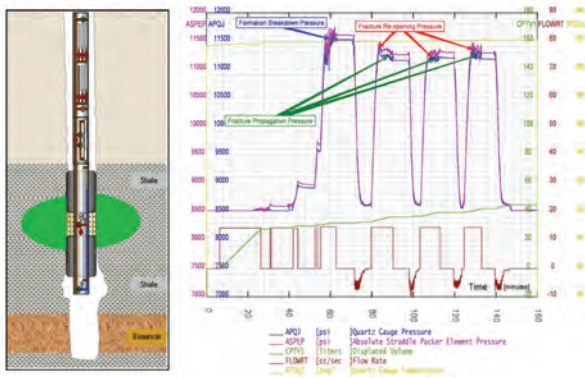

Fig. 9.26—Downhole straddle packer microfracture test performed in a shale gas reservoir.

Diagnostic plots of pressure decline analysis during a long period of time after a minifracture test are common pre-stimulation characterization stress tests for minimum horizontal stress and pore pressure estimation in unconventional reservoir development.

9.3.4 Maximum Horizontal Stress

The minimum horizontal stress is calibrated from fracture closure analysis either from surface low-rate injection tests (minifracture), downhole wireline straddle packer injection tests (microfracture). Then the magnitude of maximum horizontal stress can be estimated from the occurrence of borehole breakouts, induced fractures, or fracture initiation pressure (formation breakdown) recorded during

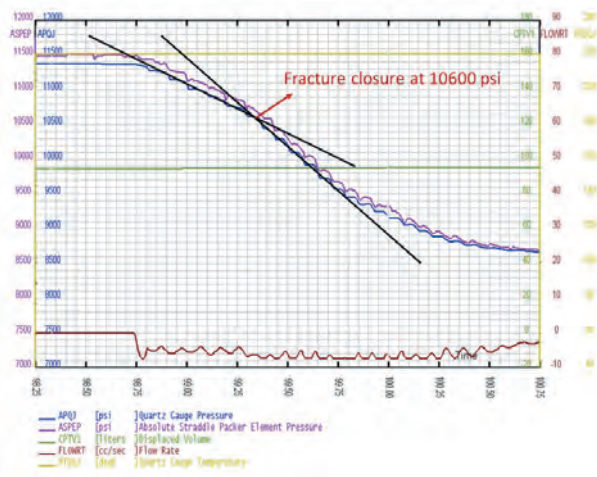

Fig. 9.27—Fracture closure identification during a flowback test during a straddle packer microfracture test performed in a shale gas interval.

openhole microfracture tests. The best-case scenario is when the magnitude of both horizontal stresses is obtained simultaneously from borehole breakouts and microfracture tests in multiple intervals along the wellbore.

Barton et al. (1988) proposed the methodology for the determination of $s_{h\,max}$ from observations of borehole breakout widths when the rock compressive strength and the minimum horizontal stress are known. Breakouts are formed in the two sectors of the hole where the induced tangential stress (hoop stress) gets amplified beyond the rock strength.

$$\sigma_{h\,\max} = \frac{(UCS + \alpha P_r + P_w + \sigma^{\Delta T}) - \sigma_{h\,\min}\,[1 + 2\cos(2\theta_b)]}{1 - 2\cos(2\theta_b)} \quad \textbf{(Eq. 9.54)}$$

$$2\theta b = \pi - w_{bo} \quad \textbf{(Eq. 9.55)}$$

Where P_w is the wellbore pressure that created the breakout, $\sigma^{\Delta T}$ is the thermal induced stress, and W_{bo} is the borehole breakout width.

Traditionally, the maximum horizontal stress magnitude has been estimated from the formation breakdown pressure and fracture reopening pressures measured during straddle packer microfracture tests. The fracture initiation at the wellbore is induced by increasing the wellbore pressure in a brittle formation interval (without natural fractures) when the hoop stress becomes negative beyond the tensile strength of the intact rock. Lower fracture initiation pressures are obtained where the isolated intervals have natural fractures. The maximum horizontal stress can be back calculated from the breakdown pressure P_b or reopening pressures of a microfracture test done in an interval with no leak-off (impermeable formation like shale gas rocks) of a vertical well:

$$\sigma_{h\,\max} = 3\sigma_{h\,\min} - \alpha P_r - P_b - T_0 - \sigma^{\Delta T} \quad \textbf{(Eq. 9.56)}$$

T_o is the tensile strength of the rock at the isolated interval.

Fig. 9.28 shows how the VTI anisotropic stress model of the horizontal stresses provides a better match to the

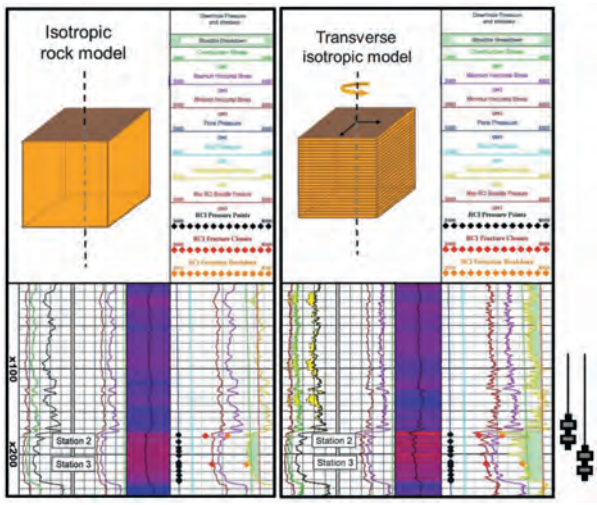

Fig. 9.28—Isotropic and vertically transverse isotropic model calibration from two straddle packer microfracture tests in a carbonate reservoir (Ihab et al. 2014).

results of two microfracture tests than the isotropic model. The microfracture tests were performed in a vertical well drilled on a carbonate reservoir separated by 30 ft. The fracture closure is plotted as two red dots, and the fracture initiation (formation breakdown) pressure is plotted as two orange dots. The VTI model reproduces the results of both microfracture tests.

9.3.5 Stress Direction

Bell and Gough (1979) first recognized that borehole breakouts were a result of borehole failure and that the orientation of the breakouts in vertical wellbores were aligned perpendicular to the maximum horizontal stress direction. **Fig. 9.29** shows the breakout locations in a vertical wellbore along the direction of $s_{h\,min}$. The tensile fractures were induced

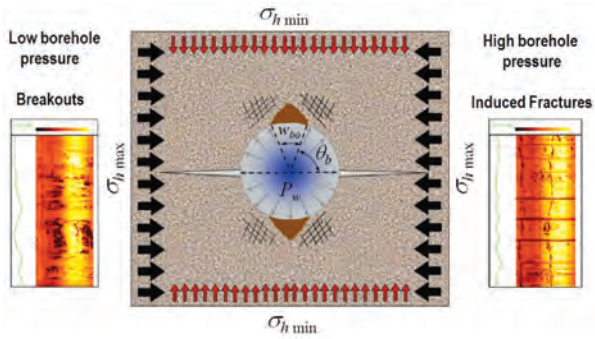

Fig. 9.29—Location of breakouts and induced tensile fractures in a vertical well.

in the direction of $s_{h\,max}$. Borehole image logs provide the best data to identify stress orientation in oil and gas fields from the occurrence of breakouts and drilling induced fractures. The development of unconventional plays requires drilling horizontal wells in the direction of the minimum horizontal stress so the multistage hydraulic fractures will propagate perpendicular to the well maximizing the reservoir contact area and production. Therefore, the stress directions need to be known before planning the horizontal drilling campaign.

9.4 Wellbore Stability

Wellbore stability problems such as tight hole, packoff, stuck pipe, inflow, and lost circulation are commonly associated with both conventional reservoirs and unconventional plays. Identification and prevention of wellbore instability saves time and money. They often can be achieved by deriving a field-specific geomechanical engineering model that provides input into the relevant drilling and completion recommendations. A basic geomechanical engineering model consists of an understanding of the pore pressure, vertical stress, orientation, and magnitude of the horizontal stresses and the rock properties. However, additional complexities sometimes need to be considered such as the presence of weak planes, the electrochemical gradient arising from the chemical makeup of shale and drilling fluids, and the thermal gradient due to differences in drilling fluid and formation temperatures.

Instability problems in unconventional plays often are observed while drilling the build section. Problems may occur particularly when the overburden shales are fissile in nature and the wellbore makes a low angle of attack to the bedding planes. However, some unconventional reservoirs also contain intervals of fissile shale (e.g., the Marcellus shale), which can seriously complicate horizontal drilling. Additionally, most shale formations are microfractured to some extent. The existence of a positive hydraulic gradient from mud overbalance allows the drilling fluid to penetrate the fractured networks. This fluid infiltration would equilibrate pore pressure within the fracture with mud pressure, potentially lubricate the fracture surfaces and further exacerbate the wellbore instability.

One or all of these complications may exist at a given time. The transport processes either acting solely or in concert can result in physical and chemical changes of the shale that ultimately govern its stability. While the study of wellbore stability in shale is incomplete without considering the chemical and thermal effects, it is beyond the scope of this section to include the intricate linkages between the different

transport processes. The focus is on mechanical instability resulting from loading of the wellbore by the far-field stresses and the additional complexities arising from the presence of weak planes, such as bedding and fractures. This will be illustrated using a generalized Marcellus shale example.

First, we investigate how much mud weight is required to prevent excessive wellbore collapse and associated drilling problems, such as tight hole, pack-off, and stuck pipe, when drilling through the fissile shale bedding intervals commonly seen in many areas of the Marcellus. In areas with horizontal or subhorizontal beds, such as the Marcellus region, sometimes the mud weight required to control the failure in highly deviated wells to a manageable level is significantly greater than the pore pressure, which can cause mud to invade the formation. We also discuss how the presence of natural fractures, such as the J1 and J2 joint sets in the Marcellus area, further complicates the situation because the potential for failure of isotropic rock and all planes of weakness must be considered, as must the risk of using too high or too low mud weight. We also investigate the feasibility of underbalanced drilling to minimize the risk of mud invasion while assuming mud invasion cannot be prevented through the use of lost circulation materials alone. Finally, the effect of model uncertainties on the predictions is investigated.

The details of this generalized Marcellus example are provided in **Table 9.1**. The stress state is strike-slip faulting ($S_{h,\,max} > S_v > S_{h,\,min}$), and the pore pressure is above hydrostatic. In this example, we use the Baker Hughes methodology to calculate the required mud weights to maintain stability. We would expect vertical wells to be drilled without incident at balance or possibly lower mud weights (air drilling is not uncommon in the Marcellus region), though problems may be encountered in the deviated and lateral sections of those same wellbores. When problems do occur, they are often in the form of tight holes, pack-off, stuck pipe, lost circulation events, and excessive cavings. Cavings are related to the failure of fractures and often appear blocky in shape or like rubble. Cavings related to the failure of weak bedding planes are tabular in shape and sometimes have large flat surfaces (Gallant et al. 2007). Inflows are not often experienced because of the tight nature of the rocks. However, there is always a risk of inflow if the mud weight is not high enough to hold back the formation fluid, especially if a fracture swarm is encountered.

Table 9.1—Generic Marcellus Example.

Parameter	Value	Unit
Depth	**8000**	**ft**
S_v	22	ppg
$S_{h,\,min}$	16	ppg
$S_{h,\,max}$	23	ppg
$S_{h,\,max}$ azimuth	60	degrees
P_r (pore pressure)	11	ppg
UCS	8000	psi
Well azimuth	150	degrees
Well deviation	89	degrees
a (Biot's coefficient)	0.6	unitless
n (Poisson's ratio)	0.3	unitless
m (Internal friction coefficient)	0.7	unitless

Callout 9.1—Allowable breakout and failure width.

A maximum breakout width of 90° is set for a vertical well. When breakouts are 90° wide or less, arch support is maintained at the wellbore wall and breakouts tend to get deeper, but not wider with time. If breakouts are allowed to grow wider than 90°, they tend to get both wider and deeper with time and can become washouts, Zoback (2007). The allowable breakout width is reduced to 60° for lateral wells not because they are inherently less stable, but because they are harder to clean.

In this text, breakout width refers to failure of istotropic rock, while failure width refers to the summed width of isotropic breakout and anisotropic failure.

9.4.1 Determining Required Mud Weights

There are many factors to consider when determining the appropriate mud weight and type when drilling a well. These factors include pore pressure, rock strength, in-situ stresses, and wellbore trajectory. However, additional factors must be considered in some shale plays, such as the presence of weak bedding planes or fractures. We use our generalized Marcellus shale example to illustrate the potential effect of failure due to bedding and fractures on wellbore stability and to investigate solutions.

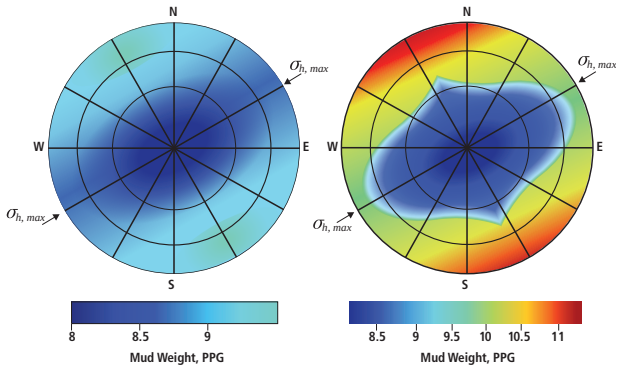

Fig. 9.30—Effect of weak bedding on mud weight required for stability. These stereonets show the borehole collapse pressure to limit breakout and failure width to the designed width (here 90° in a vertical well and 60° in a horizontal well) for any well trajectory. Vertical wells plot in the center. Deviation increases radially, such that wells deviated 30° plot on the innermost circle, wells deviated 60° plot on the next circle and horizontal wells plot on the edge. Cooler colors represent lower mud weight and hotter colors represent higher mud weight. The stereonet on the left shows the collapse pressure for our generalized Marcellus example in the absence of weak bedding planes. The stereonet on the right shows the same but includes the effects of weak bedding planes with bedding dip = 0°, dip azimuth = 0°, cohesion = 800 psi, and bedding friction coefficient = 0.6. The difference in recommended mud weight for a lateral well drilled in the direction of σh, min (150°) has increased by ~1.9 ppg (from ~9.5 to ~11.4 ppg) with the introduction of weak bedding planes. The same color scale (8.0 to 11.5 ppg) and Mohr–Coulomb failure criterion was used to create both plots.

The borehole collapse pressure represents the mud weight required to limit breakout and or failure to the designed width (here 90° in a vertical well and 60° in a horizontal well). **Callout 9.1** shows the details of how allowable breakout and/or failure widths are determined and the difference between breakout and failure width. The left plot of **Fig. 9.30** shows that with no weak bedding, well azimuth does not have a pronounced effect on the borehole collapse pressure for lateral wells in this example. When weak beds are not present, drilling a lateral well in the direction of $\sigma_{h',min}$ (150°) requires ~9.5 ppg mud weight versus ~9.1 ppg mud weight required when drilling a lateral well drilled in the direction of $\sigma_{h,max}$ (60°). The introduction of weak bedding planes can change the rock strength and borehole collapse pressure significantly, depending on the wellbore orientation with respect to the bedding planes (Aadnoy and Chenevert 1987; Willson et al. 1999; Zoback 2007).

Introducing weak bedding planes with bedding dip = 0°, dip azimuth = 0°, cohesion = 800 psi and bedding friction coefficient = 0.6, we can see in the right plot of Fig. 9.30 that the borehole collapse pressure increases significantly for wells deviated more than ~40° and well azimuth has a more pronounced effect on the required mud weight. When these weak bedding planes are present, drilling a lateral well in the direction of $\sigma_{h,min}$ requires ~11.4 ppg mud weight; whereas ~9.8 ppg is required for a lateral well drilled in the direction of $\sigma_{h,max}$. The difference in recommended mud weight for a lateral well drilled in the direction of σh min has increased by ~1.9 ppg (from ~9.5 to ~11.4 ppg) with the introduction of weak bedding planes. Note that so far, we have assumed there is cohesion on the bedding planes and that increasing the mud weight will help to stabilize the well. Also note that the mud weight required for stability in vertical wells in ~8.0 ppg whether or not weak bedding planes are present. This is because in a vertical well, the strength of horizontal beds do not have an impact on stability, as the well is perpendicular to the weak planes. Additional information on the impact of weak bedding planes on rock strength is in **Callout 9.2**.

9.4.2 Influence of Multiple Weak Planes

We have shown that for a lateral well drilled in the direction of $\sigma_{h,min}$, a mud weight of 11.4 ppg is required to limit failure to the designed width when weak bedding planes are present and that the allowable breakout angle varies with well deviation. But the beds are not necessarily the only weak planes present; natural fractures are present as well, in which case the failure of multiple planes of weakness needs to be addressed. For this purpose, vertical J1 and J2 joints sets, common to many areas of the Marcellus region, are assumed to be present parallel and perpendicular to the direction of $\sigma_{h,max}$ in our example.

In **Fig. 9.31A**, the red zone indicates the zone within which any of the modeled weak planes is expected to slip. Failure of the beds and J2 joint set is predicted when 11.4 ppg mud weight is used and 800 psi cohesion is assumed on the beds and the joints. However, when only one plane of weakness slips, it is unlikely to wash out and fall into the wellbore. The J1 joint set is not expected to slip at the modeled conditions. **Fig. 9.31B** shows that the slip region is reduced and confined to the wellbore wall when we require that both the beds and J2 joint set fail simultaneously. However, once slip occurs, the cohesion on the slipped surface is reduced to 0. Because slip of bedding and J2 joints did occur we must now consider the failure with zero cohesion. **Fig. 9.31C** shows the zone within which either the beds or J2 joints are expected to slip when the cohesion is 0. It is clear by

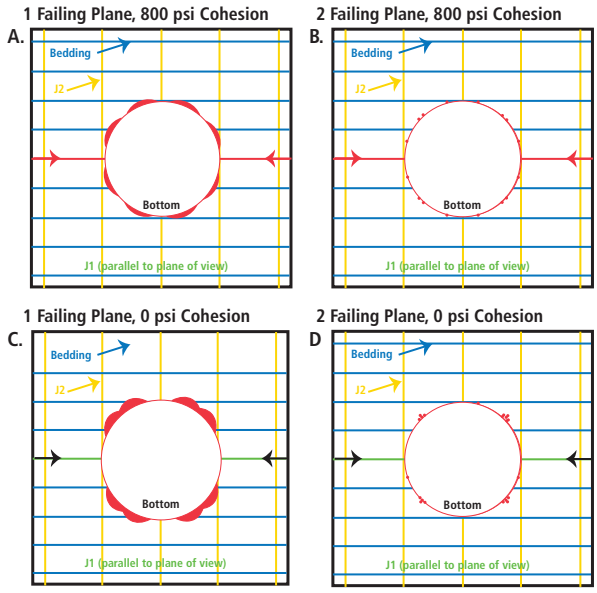

Fig. 9.31—Failure of multiple planes of weakness. These plots show the well in cross section together with a zone of failure (red color) and the individual weak planes as they would appear if they were cut by a plane perpendicular to the wellbore axis. Each fracture set is displayed in a different color. In this case, the bedding planes are in blue, and the J2 joint set is in green. The J1 joint set doesn't appear because it is parallel to the plane of view. The black arrows indicate that the direction of maximum compression is on the sides of the wellbore. Fig. 9.31A and Fig. 9.31C. Red zones indicate the zone within with any of the modeled weak planes is expected to slip. Slip of the bedding planes and J2 joint set is predicted. The J1 joint set is not predicted to slip. Other input parameters: J1 dip = 90°, J1 dip azimuth = 150°, J2 dip = 90°, J2 dip azimuth = 60°, bedding dip = 0°, dip azimuth = 0°, friction coefficient = 0.6, and cohesion = 800 psi (A.) and 0 (C.). Fig. 9.31B and Fig. 9.31D. The slip region (red zones) is reduced when we require that both the bedding and J2 joints slip simultaneously. Other input parameters: J1 dip = 90°, J1 dip azimuth = 150°, J2 dip = 90°, J2 dip azimuth = 60°, bedding dip = 0°, dip azimuth = 0°, friction coefficient = 0.6 and cohesion = 800 psi (A.) and 0 (C.).

comparing Fig. 9.31A to Fig. 9.31C that the loss of cohesion results in an increase in the potential zone of failure. **Fig. 9.31D** shows us the zone of overlapping failure of the beds and J2 joints. This is the amount of material we might expect to fall into the wellbore. The failed zone is quite small and would not be expected to result in drilling problems. However, we also must consider the potential for mud invasion to exacerabate the wellbore failure.

Callout 9.2—Weak bedding lab experiments versus weak bedding when drilling wells.

Theories have been developed and lab experiments performed to determine the impact weak bedding has on rock strength, Donath (1964), Jaeger and Cook (1979), and Vernik et al. (1992). Samples are tested with the orientation of weak planes at different angles, β, to the maximum principal stress, σ_1. The theories and lab experiments show that when β ~0° or ~90°, the bedding planes have little impact on rock strength, but that when β ~60°, the rock will fail at a much lower axial stress. One might conclude that wellbores drilled at 60° to weak bedding planes would require the highest mud weights to maintain stability. However, we have flat beds in our generalized Marcellus example, yet we can see in the right plot of Fig. 9.30 that wells drilled at 60° deviation require lower mud weight than wells drilled at 90° deviation. How can we explain this apparent discrepancy?

In the experimental set up σ_1 is always vertical, and the confining pressure around the sample, σ_h, is constant. When drilling a deviated well in an anisotropic stress state, like our generalized Marcellus example, σ_1 at the wellbore wall is not vertical and the stress varies around the wellbore. Even with flat beds, you can't directly compare the wellbore to the sample orientation in the lab.

If the stress field were isotropic ($\sigma_1 = \sigma_2 = \sigma_3$), and the bedding planes were flat, the highest mud weights would be required to maintain stability in wells with 60° deviation, as you see in the lab. In this simple case, the difference between the radial and tangential stresses at the wellbore wall determines whether the bedding will slip, and that difference does not change with well orientation. Therefore, the only thing dictating changes in mud weight (at constant allowable breakout width) is the well orientation with respect to the bedding. The calculations become far more complex with an anisotropic stress field. In this case, the orientation of the well causes the tangential stresses to change in both orientation and magnitude, and therefore the mud weight required to avoid slip changes due to these stress changes with respect to the bedding orientation.

Mud invasion can occur into any permeable zone, such as a rubble zone or a fracture that has some void space between the fracture surfaces. When mud invasion occurs, the pressure inside the fracture becomes equal to the mud weight, which can cause additional failure of the wellbore wall (Santarelli et al. 1992; Chen et al. 2002; Paul and Zoback 2006). The process of mud invasion is illustrated in **Fig. 9.32**. When weak planes are present, mud weights that are too high can lead to borehole collapse as well as lost circulation.

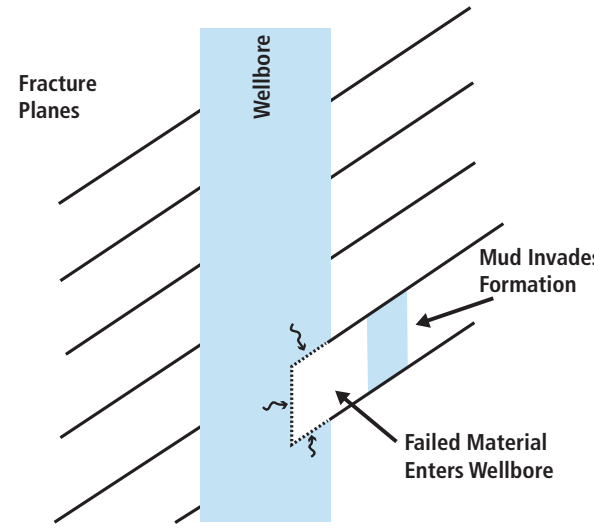

Fig. 9.32—Illustration of the effect of mud invasion into fractures. Mud invasion can occur into any permeable formation but is likely to occur when high mud weights are used in highly fractured formations. Before mud invasion, the pressure in the fracture is equal to the pore pressure. After mud invasion, the pressure in the fracture is equal to the mud weight, greatly increasing the chances of slip along the fractured surface.

9.4.3 Underbalanced Drilling

In some cases, underbalanced drilling may be an option to limit the potential of mud invasion and may have other benefits such as increased ROP as compared to drilling with a high overbalance. Up to this point, we have assumed that rocks deform elastically until the point of failure. To investigate the feasibility of underbalanced drilling, a poroelastic analysis is performed to compute the stresses and pore pressure surrounding a well at a fixed time after the bit has passed. The predicted zone of failure is a first-order function of the rock strength and degree of underbalance. It is also strongly dependent on the drilling rate, hole size, depth of investigation, and fluid mobility, which is the product of permeability and fluid viscosity (Moos et al. 2010).

In **Fig. 9.33** we examine the predicted breakout width ¼ in. and ½ in. into the wellbore wall for three rock strengths: 7,000, 8,000, and 9,000 psi UCS. Looking ¼ in. into the wellbore wall (left plot), 8,000 psi, UCS rocks are expected to be stable (less than 60° wide breakouts in a lateral well) up to about 0.8 ppg underbalance. At 9,000 psi UCS rocks are stable up to about 2.3 ppg underbalance. There may be some instability if weaker 7,000 psi UCS rocks are

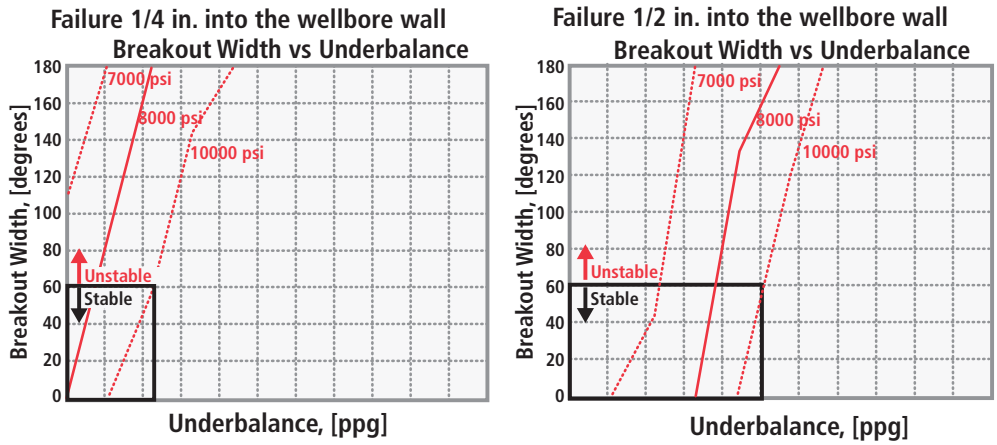

Fig. 9.33—Predicted failure during underbalanced drilling. Red contours show breakout width versus amount of underbalance for a specific UCS. The left plot is looking ¼ in. into the wellbore wall. The right plot is looking ½ in. into the wellbore wall. Other input parameters are: bit size = 8.5 in., ROP = 60 ft./hr; E = 3000000 psi; porosity = 5%; permeability: 0.0005 mD; Skempton's coefficient = 0.4; viscosity = 0.7 cP.

encountered because ~105° wide breakouts are predicted at on-balance conditions and washout is predicted at ~1 ppg underbalance. While this wide failure of weaker rocks might seem problematic, the failure will stabilize at some distance into the formation. Looking ½ in. into the wellbore wall (Fig. 9.33, right plot), 7,000 psi UCS rocks are stable up to ~2.3 ppg underbalance. At 8,000 psi UCS rocks are stable up to ~3.8 ppg underbalance and 9,000 psi UCS rocks are stable up to ~5 ppg underbalance. Several additional factors should be considered such as hydraulics and hole cleaning capability. However, in some cases, underbalanced drilling may keep wellbore failure within acceptable limits, with added benefits, such as limiting the potential for mud invasion and increased ROP. However, we only consider the failure of isotropic rock in Fig. 9.33. Additional failure of the bedding and fractures can be expected.

Unfortunately, we do not yet have the capability to model the failure of multiple planes of weakness at underbalanced conditions. However, we can assume the failure will be more severe than in Fig. 9.31 and that the failure will increase with increasing underbalance. However, the potential for mud invasion is reduced with underbalanced drilling. With only one failing plane, the material is unlikely to wash out and fall into the wellbore. Therefore, some amount of underbalance may be tolerable, even in the presence of multiple planes of weakness.

The presence and strength characteristics of natural fractures and fissile beds are difficult to establish. In the absence of wireline or LWD images, drilling experience and cavings are often the best real-time indicators of problematic fractures and or bedding. In some situations, it is possible to increase the angle of attack to bedding and raise the mud weight. However, this is only advisable if there is cohesion on bedding planes. These may not be viable solutions when the target is weakly bedded and slip of the bedding and fractures has already occurred, which reduces the cohesion of those surfaces to zero. The optimal approach while drilling into such formations will vary. One option may be to keep mud weights as low as possible and to formulate the mud properties to help prevent mud from penetrating into fractures and bedding. If mud penetration cannot be prevented, underbalanced drilling is worth investigating.

9.4.4 Geomechanical Engineering Modeling Uncertainties

Many of the parameters important to geomechanical engineering modeling are particularly difficult to constrain in shale plays. Pore pressure and Biot's coefficient are often unknown; allowable breakout widths are assumed as well as failure models (Mohr–Coulomb, Lade, Drucker–Prager) or allowable plastic strain criteria. Measurements are often unreliable due to the tight nature of the rocks. Standard log-based techniques do not apply because the tectonic history is complicated and undercompaction is not the overpressure generating mechanism. Log-based strength estimates are commonly not calibrated to laboratory core measurements and properties of bedding planes and fractures are guidelines at best. Fractures and high TOC can impact the log response and cause log-based UCS to be underestimated. Verification of the log-based UCS calculations requires detailed triaxial tests that are not often performed in unconventional reservoirs. Additionally, in weakly bedded reservoirs, the core is often too fissile to plug. Uncertainties also exist for the horizontal stress magnitudes due to a lack of data. Leak-off tests (LOT) or extended leak-off tests (XLOT) (Addis et al. 1998) are not typically conducted during drilling operations. Microfractures or minifractures are often neglected during completion operations, leading to uncertainty in the magnitude of $\sigma_{h,min}$. Considering the sometimes large error bars on the input parameters used to model $\sigma_{h,max}$ magnitude, the resulting $\sigma_{h,max}$ magnitude often has high uncertainties as well.

Given the uncertainties when modeling unconventional reservoirs, identify the sensitivity of a model to various input parameters in a wellbore stability analysis. This can be done with a Monte Carlo type simulation called a quantitative risk analysis (QRA) (Ottesen et al. 1999; Moos et al. 2003; Moos 2006) and is illustrated for our generalized Marcellus example in **Fig. 9.34**. We vary eight input parameters and examine the effect each has on the mud weight required for stability. This analysis provides an uncertainty range on the predicted mud weights and illustrates what parameters have the largest influence on the model results. This helps to set data collection priorities to reduce uncertainties in the predictions. In this example, the model is most sensitive to changes in $\sigma_{h,max}$ magnitude, pore pressure, allowable failure width, bedding cohesion, and bedding friction.

When planning a drilling program in an unconventional reservoir, many geomechanical engineering considerations need to be taken into account. We used a generalized example appropriate for the Marcellus shale to illustrate some of these considerations such as model uncertainties, the effect of any weak planes, and the benefits and the risks of overbalanced versus underbalanced drilling.

Because of the large uncertainties associated with these analyses, reliable mud weight recommendations or operations are dependent upon calibration of the predictions with field experience and the use of engineering judgment.

9.4.5 Horizontal Drilling

Horizontal drilling and wellbore completion are possibly the main technologies along with multistage hydraulic fracturing that revolutionized the shale gas developments in North America. Horizontal drilling requires understanding of in-situ stress orientation to induce multiple transverse fractures on each stimulation stage and maximize reservoir stimulation volume. Some unconventional plays require special attention in drilling the deviated section due to wellbore instabilities on laminated shales with plane of weakness.

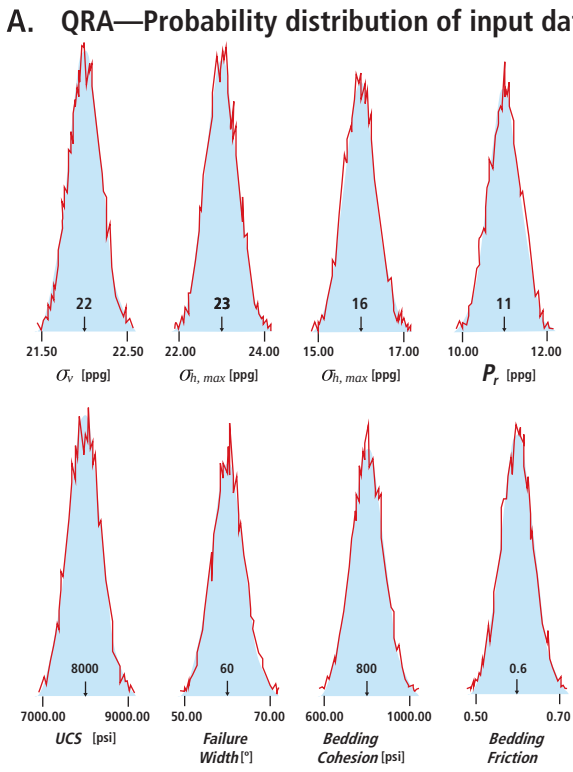

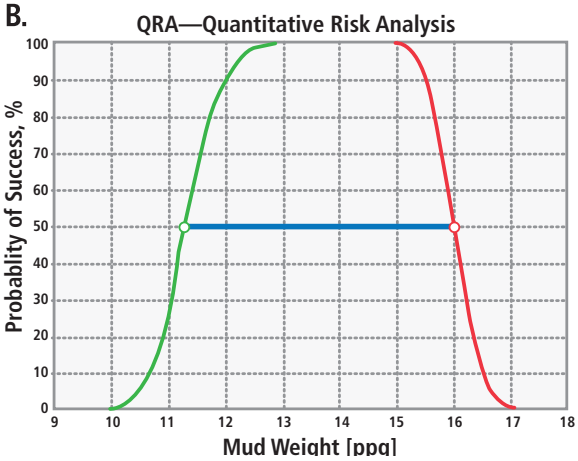

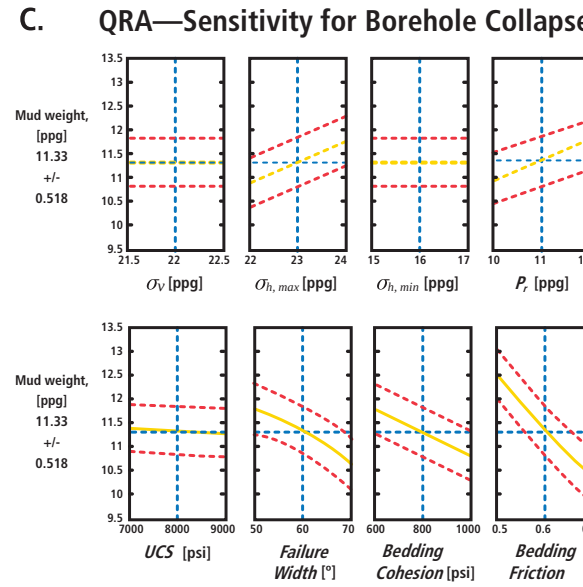

Fig. 9.34—Quantitative risk analysis (QRA) of our generalized Marcellus example, probability distribution of input parameters (1,000 simulations). Fig. 9.34A shows the most likely, minimum, and maximum values of the eight input parameters considered in this analysis. Fig. 9.34B shows the probability of limiting the failure width to the designed parameters (60° for a lateral well) at 8,000 ft. TVD for a lateral drilled in the direction of σh, min at particular mud weight. The green curve is the lower bound borehole collapse pressure and the red curve is the upper bound least stress. The P10 mud weight is ~10.7 ppg, the P50 is ~11.3 ppg, and the P90 mud weight is ~12.0 ppg. Fig. 9.34C shows the impact each input parameter has on the mud weight required to limit failure width to the same parameters described in B. Green lines show the most likely predicted mud weight. Red lines show the 99% confidence mud weight window. For example, decreasing pore pressure from 11 ppg to 10 ppg reduces the required mud weight from 11.5 ppg to 11.0 ppg. In this example, the model is most sensitive to changes in σh, max magnitude, pore pressure, allowable failure width, bedding cohesion, and bedding friction.

9.5 Geomechanical Engineering Considerations in Shale Stimulation

Effective shale stimulation relies upon creating an artificial permeability network to maximize the interconnected surface area in contact with the source rock that has most of the organic-rich sediments where hydrocarbons are entrapped in nano- or microscale porous space. The effectiveness

of the hydraulic shale stimulation depends on multiple geomechanic-related considerations, such as producing well-contained hydraulically induced fractures within the pay-zone, (avoiding fracturing out-of-zone); having low proppant embedment into the source rock; selecting appropriate intervals for fracture initiation in horizontal wellbores with the presence or not of natural fractures; and efficiently inducing shear stimulation inside the reservoir.

9.5.1 Stress Contrast and Fracture Containment

Petroleum geomechanical engineering provides the means to estimate and measure the magnitude of the minimum horizontal stresses used in hydraulic fracture design. More importantly, the relative change in magnitude with depth dictates how strong or weak the stress contrast will be between pay zones and non-pay zones. The larger the stress contrast, the more aggressive the hydraulic fracture stimulation job can be in terms of net pressure, fracture propagation time, volume injected, proppant placement, and fracture length. If the stress contrast is small, the hydraulic fracture may grow vertically while propagating into the pay zone, with a risk of connecting with shallower formations and aquifers. If the stress contrast is negative (meaning the non-pay zone above or below the target has lower minimum horizontal stress than the target) the fracture will follow the path of least resistance growing out-of-zone. Again, this can potentially result in leakage into the overburden. This is the paramount piece of information when designing a hydraulic fracture job safely, economically, and with minimum environmental impact, to conduct fluids and proppants injection into the targetted subsurface formations.

As mentioned in this chapter, the downhole straddle packer tool can measure the stress contrast between the nonproductive formations above and below the target stimulation zone. **Fig. 9.35** shows the anisotropic modeling of the magnitude of the horizontal stresses from borehole acoustic anisotropies and core measurements (ultrasonic velocities and triaxial testing) after the tectonic lateral strain calibration. This is based on several straddle packer microfracture tests conducted in the upper and the lower Haynesville productive formations, as well as the non-productive layers above and below the productive zones.

Track 13 of Fig. 9.35 illustrates a positive stress contrast above and below the lower Haynesville target. Blue shade indicates high minimum horizontal stress while red means low stress. Track 3 shows the amount of TOC from mineralogy and NMR logging in green and black shading, respectively. The ultrasonic elastic properties and static

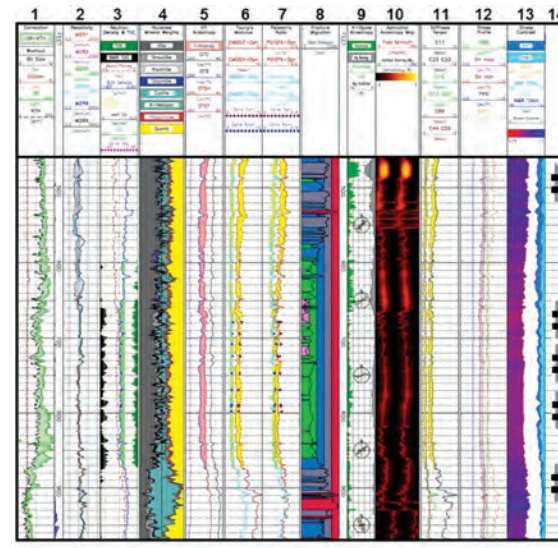

Fig. 9.35—Stress contrast measurement from multiple straddle packer microfracture tests at various depths in the lower Haynesville shale.

elastic moduli are validated with core measurements in Track 6 and Track 7. Depth-dependent lateral tectonic strains were back calculated from multiple straddle packer microfracture tests from upper Haynesville to lower Haynesville formations.

This type of stress contrast analysis in vertical pilot wells is important even for designing hydraulic stimulation treatments in horizontal wells because the stress contrast can only be acquired by fracture closure measurement in vertical wells that intersect the formation above and below the pay zone.

9.5.2 Shale Stiffness and Proppant Embedment

Losing fracture productivity is a major concern; one mechanism to account for this is attributed to the proppant embedment into the formation due to the action of the in-situ stresses after the flowback and the potential shale hardness degradation caused by the fracturing fluids. Rigorous Brinell hardness tests need to be carried out in shale samples with different times of fluid exposure to quantify the hardness lost due to the fluid-rock interaction. Chapter 10 about core analysis and testing discusses this important core measurement at laboratory conditions.

The combination of various rock mechanics measurements on core samples allows operators to obtain customized correlations between rock hardness and other elastic properties such as Young's modulus and a relationship with mineralogical composition. These correlations are

useful to generate log-derived formation hardness from borehole acoustic or mineralogy logging as the volume of clay minerals and organic matter tend to reduce the shale hardness and brittleness.

9.5.3 Fracture Initiation and Multistage Selection

The efficient optimization of the spacing between hydraulic fractures remains a significant challenge. Ideally, the process requires continuous pre and post job analysis coupling reservoir, geomechanical engineering, and economic models (Finkbeiner et al. 2011). Reservoir modeling, economics, and operational aspects provide individual hydraulic fracture spacing criteria that are not necessarily equal. Concurrently, geomechanics serves to quantify the risks of hydraulic fracture interference resulting in unstimulated or inadequately stimulated zones. Therefore, a complete solution takes into account all available spacing criteria and arrives at a minimum fracture spacing that is economic, efficiently drains the reservoir, and mitigates the risk of bypassing productive zones. This section highlights some geomechanical engineering considerations in the selection of stimulation stage length and cluster spacing in multistage horizontal wells. First, we start with evaluation of cluster spacing based on attaining development of multiple independent hydraulic fractures, within a particular stage. We then consider the interaction between multiple hydraulic fractures during simultaneous and sequential propagation. Finally, we highlight the range spacing criteria suggested in the literature.

Generating individual hydraulic fractures from each cluster within a fracture stage is the basis of limited entry designs. Nongeometric or targeted completions focus on characterizing the rock properties, stresses, and/or productive capability along the lateral utilizing logging (e.g., LWD, MWD, wireline) or seismic attributes to target specific zones for stimulation. The primary goal in nonuniform cluster spacing, associated with geomechanics, is to group zones with similar rock properties (primarily stress and elastic properties) and assume that process will mitigate variances in fracture initiation pressures. However, prediction of the pressure necessary for fracture initiation requires not only the description of the rock properties, stress distributions, and pore pressure but also pumping parameters and the geometry of discontinuities in the near wellbore region (which introduces a characteristic length scale; Detournay and Cheng 1992; Theircelin 1992). It remains difficult to describe the fracture initiation process through only rock mechanical properties and stress profiles (Abbas et al. 2013). However, these techniques may have the ability to resolve some issues related to variances in breakdown pressures (Walker et al. 2012).

Limiting the number of clusters reduces the risk of not breaking down every cluster within a stage. Ideally, a single cluster per stage removes the risk of unstimulated zones. Nonetheless, this configuration may include significant operational challenges and economic costs. Beyond the issue of fracture initiation across multiple clusters, the interaction of fractures during propagation and/or subsequent fracturing operations provides additional stage and cluster spacing considerations.

The interaction of hydraulic fractures by simultaneous and sequential propagation can be addressed in two ways. First, the competition between hydraulic fractures propagating within parallel arrays that do not deviate and remain parallel is discussed. In this case, fractures in parallel arrays compete primarily due to hydraulic and elastic mechanisms. Secondly, the propagation of hydraulic fractures perturbs the in-situ stress state and may lead to the deviation of an adjacent propagating fracture due to the rotation of stresses in the fracture tip region. These processes are not mutually exclusive and occur to various degrees. Furthermore, similar interaction mechanisms exist for complex or network fracture geometries though quantifying interaction between (and within) network type fractures remains difficult. For simplicity, we reserve this section to analysis of isolated opening mode bi-wing-type of hydraulic fractures.

Propagation of multiple, parallel, and equally spaced fractures is an idealization for the description of fracture interaction in an elastic medium. Some critical parameters for characterizing this interaction are fracture number and spacing, net fracturing pressures, fracture dimensions, and elastic properties. In well-confined hydraulic fractures (i.e., PKN, Perkins and Kern, Nordgren two-dimensional fracture geometry model); the ratio between the fracture height and fracture spacing is critical for quantification of fracture interference. Numerical and physical experiments have shown that in the intermediate case of two to ten parallel fractures, with constant net fracturing pressure, the exterior fractures of the array will dominate the flow capacity (Germanovich et al. 1998). **Fig. 9.36** contains a schematic of the fracture array geometry, along with data from Germanovich and Astakhov (2004), showing the reduction of fracture width due parallel fracture spacing ratio. The result of the reduction of fracture widths of interior fractures may lead to screening out these fractures during proppant stages (Cheng 2012). Reduced fracture width increases the risk of unequal fluid and proppant distribution between all clusters in a particular stage.

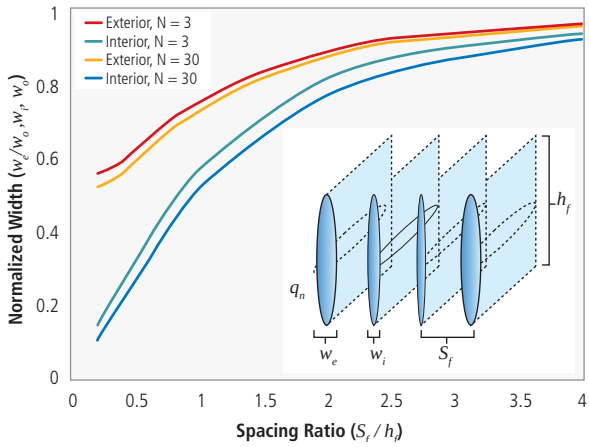

Fig. 9.36—Normalized fracture width versus fracture spacing ratio (S_f/h_f) plot. Fracture width data taken from Germanovich and Astakhov (2004). Schematic shown in the inset illustrates the parallel fracture array geometry. W_e and w_i are the average width of the external and internal fractures, respectively. Fracture width is normalized by the width (w_o) of a non-interacting fracture under the same net pressure. S_f is the fracture spacing and h_f is the fracture height. N is the number of parallel fractures within the array.

The perturbation of the in-situ stress regime may cause fractures to deviate from orthogonal to the original minimum stress direction (Roussel and Sharma 2011). The relationship between the intermediate fracture dimension, spacing, fracture net pressure, and in-situ stress anisotropy dominate the curving phenomenon between fractures (Bunger et al. 2012; Wu and Olson 2013). The boundary conditions of nearby fractures also play a critical role in determining the paths of propagating fractures. For fixed existing fractures (e.g., fractures closed on proppant packs), numerical models suggest that fractures will deviate away from existing propped fractures and may lead to a transition from transverse to longitudinal fracture geometry (Roussel and Sharma 2011). However, the existence of a pressurized existing fracture can lead to attraction and possible coalescence of a propagating hydraulic fracture (Bunger et al. 2012; Sesetty and Ghassemi 2013). Given that fracture closure times in unconventional wells are often greater than operational times between stages, the boundary conditions imposed from previous fracturing stages remain difficult to quantify. Still, magnitudes of stress anisotropy greater than the fracturing net pressure likely suppress fracture turning, due to interaction (Geilikman et al. 2013).

Determining spacing criteria in multistage horizontal wellbores largely remains an exercise in trial and error. In general, the literature suggests values of fracture spacing to fracture height ratios within a range of approximately 1.0 to 2.0 to mitigate fracture interference (Britt and Smith 2009; Roussel and Sharma 2011; Bunger et al. 2013). Interactions between fractures (either simultaneous or sequential) are negligible above a ratio of 2.0. Whereas, spacing to fracture height ratios of less than 1.0 suggest fracture interference may contribute to unequal or unstimulated zones in a horizontal well. Operational, economic, and production modeling aspects, however, drive many fracture spacing criteria. Geomechanics allows for estimation of the risks associated with unstimulated or under-stimulated zones for a given spacing criterion.

Against this theoretical background recent downhole measurement by Molenaar and co-workers (2011) using distributed acoustic sensing (DAS) demonstrates the impact of subsurface variability on the generation of hydraulic fractures from clusters, and the impact of operational procedures, such as diversion, in optimizing the distribution into the perforation clusters in any one fracture stage.

The downhole data demonstrate that stimulation fluids are not equally distributed and tend toward preferred clusters (Molenaar et al. 2011; Wheaton et al. 2014; Sookprasong et al. 2014). This is probably a result of the stimulation program, the subsurface variation between the clusters, including the minimum horizontal stress or anisotropy variations across the stage.

9.5.4 Shear Rock Stimulation

Since the beginning of the large-scale usage of hydraulic fracturing for well stimulation, conventional wisdom suggests that hydraulic fractures formed in a bi-wing, planar fashion (Howard and Fast 1970). However, with the use of slickwater fracturing fluids and the advent of more direct hydraulic fracture monitoring methods, like tilt-meters and, especially, microseismic monitoring, it became evident that hydraulic fractures were often not bi-wing and potentially nonplanar (Maxwell et al. 2010; Urbancic et al. 2012). Particularly in naturally fractured unconventional reservoirs, many microseismic results have shown a diffuse, nearly symmetrical pattern of events. This contrasts with the conventional wisdom that microseismic events should fall largely along a single plane delineating the location and, potentially, the length or zone of influence of the hydraulic fracture (**Fig. 9.37**).

As the early shale fractures suggested nonplanar behavior, the resultant production data often showed that production was higher than that achievable from simple, planar

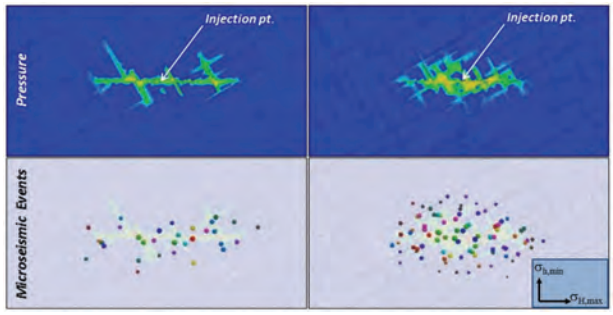

Fig. 9.37—Plan view of natural fracture pressure during injection (top) and simulated microseismic events (bottom). On the left is the behavior of a planar hydraulic fracture; on the right, the behavior of a hydraulic fracture with shear stimulation.

hydraulic fractures (King 2010; Chong et al. 2010). As the vast majority of field-measured microseismic events represent acoustic energy released during shear rock failure, this gave rise to the concept of shale shear stimulation (**Fig. 9.38**) (Lam and Cleary 1984).

Production from a hydraulic fracture is directly related to the reservoir contact surface area created and potential pressure losses within the propped hydraulic fracture and at the wellbore. In shale plays, shear stimulation, as interpreted from microseismicity, is believed to provide additional reservoir contact surface area through shear slippage along natural fractures and weakness planes (Barton and Bandis 1983; Barton et al. 1985). This results in an uneven match between the two fracture surfaces (self-propping) that, in-turn, increases the flow capacity (permeability) of the natural fractures and contributes to an increase in production (Blanton 1982; Aguilera 2006; Rahman et al. 2009).

Understanding and predicting the production contribution of shear stimulation is not trivial. In part this is due to the poor reservoir characterization of natural fractures and as a result the

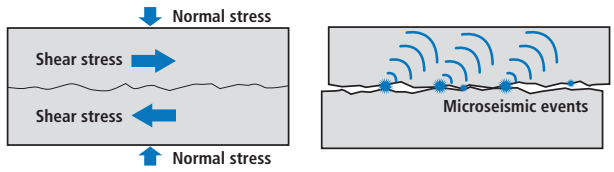

Fig. 9.38—When a natural fracture or weakness plane (left) is subjected to sufficient shear stress, slippage along the fracture surface occurs (right). This shear failure of the fracture can emit acoustic energy in the form of microseismic events and open up larger flow paths along the fracture surface itself.

paucity of subsurface discrete fracture network (DFN) models in shale gas and shale oil developments, which have been largely overlooked. The existence of shear events, both those recorded microseismic events and those below the recording threshold, and their associated shear rock failure, does not guarantee that the event location is in hydraulic communication with the main fracture or wellbore. Without hydraulic communication, the rock failure cannot contribute to production.

Early during the development of shale plays, it was commonly thought that microseismicity represented the extent of the pressure changes in the natural fracture network due to fluid injection and hydraulic fracturing. This was supported by the concurrent microseismicity, pressure, and production response in offset wells during stimulation (Cipolla 2014). However, evidence of a more complex relationship is observed in some plays. This is interpreted as an effective stress change and fracture slip resulting not from a pressure change but as a result of a total stress change. Consequently, interpretation of microseismicity accompanying stimulation considers both dry microseismic events and wet events (Nagel et al. 2013). Dry microseismic events are associated with a total stress change and unlikely to be in hydraulic communication with hydraulic fracture or wellbore. Wet events are associated with a pressure change and, therefore, likely to be in hydraulic communication with the hydraulic fracture or wellbore.

A number of field characteristics and operational practices can enhance or limit shear stimulation. The key field characteristics include in-situ pressure; in-situ stress magnitude, anisotropy and orientation; natural fracture or weakness plane strength; and natural fracture or weakness plane orientation relative to the stress field. In-situ pressure is not necessarily formation pressure, but the pressure in the natural fractures and weakness planes themselves. In-situ pressure along with the in-situ stress controls the effective stress acting on the natural fractures. As pressure increases, the effective stress on the natural fractures decreases, which promotes shear. All other things being equal, a shale rock with a greater in-situ pressure will be more prone to shear stimulation. Like pressure, the in-situ stress controls the effective stress acting on the natural fractures and weakness planes.

However, stress direction is also critical. Principal stresses are known in the industry as $s_{h\,min}$, $s_{h\,max}$, and s_v, the minimum and maximum horizontal stresses and the vertical stress, respectively. For natural fractures oriented orthogonal to the principal stresses, no shear stresses exist on these regardless of the magnitude and difference in the principal stresses. However, when the natural fractures are not aligned with the

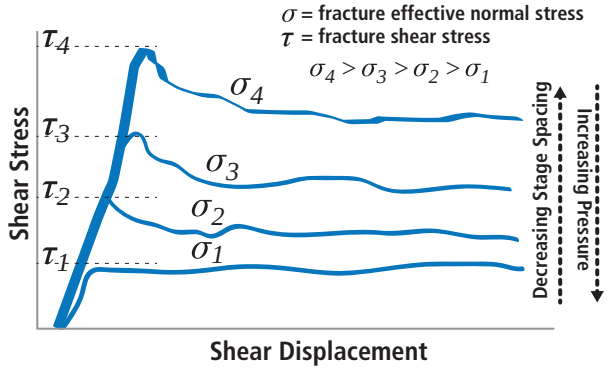

Fig. 9.39—Shear failure along natural fractures and weakness planes is controlled by a number of factors. One of these is the effective normal stress acting on the natural fractures and weakness planes. As shown, as the normal effective stress increases, hydraulic fracture stage spacing is reduced. It becomes more difficult to shear and shear stimulate natural fractures and weakness planes. However, as the pressure within the natural fractures increases, the effective normal stress decreases and shear stimulation is increased.

principal stresses, then a shear stress does exist. This shear stress is related to the orientation of the natural fractures in the stress field and the difference in magnitude between the principal stresses. This shear stress is energy available within the earth to shear the natural fractures and weakness planes that do not need to be provided by the hydraulic fracturing process. All other things being equal, as the magnitude of the principal stresses increases, the effective stress on the natural fractures and weakness planes increases inhibiting shear stimulation. However, as the difference in magnitude of the principal stresses increases, for those natural fractures not orthogonal to the stress field, the shear stress increases, which tends to enhance shear stimulation (**Fig. 9.39**) (Nagel and Sanchez-Nagel 2011; Nagel et al. 2012).

The strength characteristics of the natural fractures and weakness planes also controls shear stimulation. Often, rock strength is considered to be a function of cohesion and friction coefficient (friction angle). As either or both of these parameters increase in value, the natural fractures and weakness planes become stronger and more resistant to shear stimulation. Natural fractures may not have a cohesive strength (e.g., they lack cementation). The friction coefficient then controls the strength. As the friction coefficient (friction angle) increases, the natural fractures become more resistant to shear stimulation with all other things being equal (Barton and Choubey 1977).

Natural fractures at depth may not be conductive nor stress sensitive and may be re-cemented limiting the ability to shear and produce conductive pathways. This has been observed for conventional reservoirs by Dyke (1992) and Ameen et al. (2009).

Operational practices also affect the ability to shear stimulate shale formations. The stress field changes caused by a hydraulic fracture include the shear stress field at the tip of the propagating fracture as well as the increased stress behind the tip (often called the stress shadow) and the decreased stress ahead of the tip. A common misperception is that increasing injection rate increases shear stimulation; however, this is only true if there is an increase in net pressure (where net pressure is the injection pressure inside the hydraulic fracture minus the minimum in-situ stress). Net pressure controls the magnitude of shear stress at the tip of the hydraulic fracture (which determines the ability to shear/open closed and cemented natural fractures and weakness planes) as well as the magnitude of the stress shadow. As the stress shadow increases, the effective stress acting on the natural fractures increases and inhibits shear stimulation.

The pore pressure acting on the natural fractures or weakness planes is considered the most important factor that can be controlled during the stimulation treatment to generate a shear stimulation. As pressure increases, the effective stress on the natural fractures decreases, and that enhances shear stimulation. The ability to increase natural fracture pressure is itself controlled by both formation characteristics and operational practice. The change in natural fracture pressure during hydraulic fracturing is largely a diffusive process, meaning that it is proportional to the driving pressure (i.e., the net pressure), time (either pump time or shut-in time under pressure), natural fracture aperture (greater aperture leads to more diffusion) and is inversely proportional to viscosity i.e., as viscosity increases, pressure diffusion decreases. Consequently, a stimulation design that optimizes net pressure and pump time with reduced fluid viscosities offers the potential to maximize shear stimulation for a given natural fracture network or series of weakness planes in unconventional shale plays.

9.6 Geomechanics Considerations in CBM Developments

Development of coalbed methane (CBM), also called coal seam gas (CSG), reservoirs around the world has picked up rapidly in recent years. These reservoirs exist within a variety of geological settings, have different reservoir characteristics, and require different field development and well completion strategies.

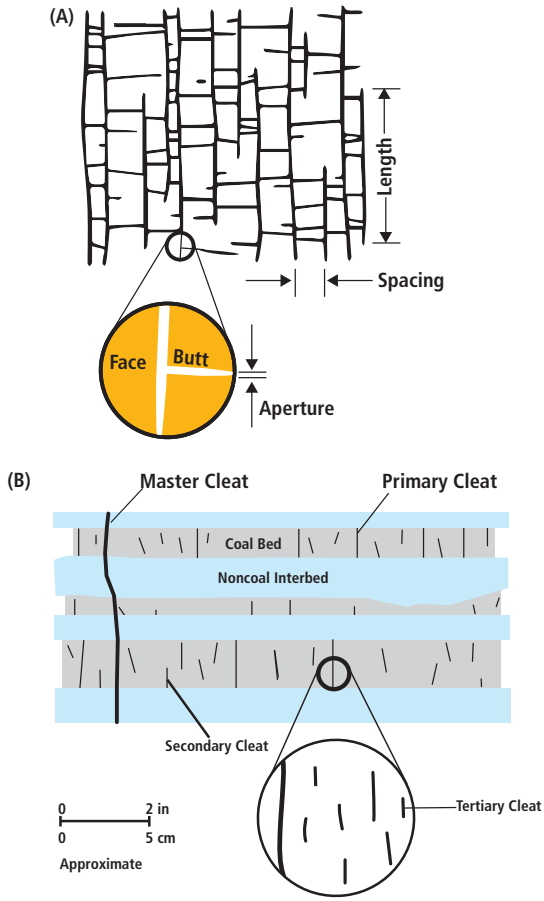

Fig. 9.40—Diagrammatic views from the top (A) and the side (B) of cleats in coal (from Laubach et al. 1998), illustrating the relationships between bedding, face, and butt cleats.

The common features among all CBM reservoirs is the presence of often abundant discontinuities in the form of orthogonal microfractures generally referred to as cleats that have developed during the coalification of organic-rich peat by matrix shrinkage through biological processes and the application of heat and pressure over geological time. Cleats in coal occur as two mutually perpendicular sets of opening-mode fractures. Face cleats tend to be continuous and are the primary cleats; butt cleats form subsequently and terminate on face cleats. **Fig. 9.40** is a schematic presentation of cleat systems in coal. The extent of the cleating system can be analyzed from core data and high-resolution borehole image logs (Laubach et al. 1998).

Matrix permeability of coal is generally very low, but the cleat system forms permeable pathways and presents opportunity for coalbed gas exploitation. The most productive regions of many coalbed methane plays are those that are the most heavily fractured. The presence of multiple cleat set, fracture network, and bed-boundary discontinuities, however, could pose a drilling risk as closely spaced cleats can cause severe problems while drilling due to disaggregation of the coal along their surfaces where increasing mud weight could exacerbate their effect. On the other hand, near-well transmissivity can be increased by appropriately exploiting these same weak planes through hydraulic fracturing and shear stimulation. As such the most productive wells could therefore likely be the most difficult wells to drill (Moos 2011). The drilling risks can be reduced through wellbore stability analysis and mud weights adjustment using geomechanical engineering principles and characterization of the coalbeds and their cleat system.

Various completion techniques have been utilized worldwide to develop CBM reservoirs. These techniques range from vertical well multiseam completion either open hole or cased and perforated with stimulations, to multiple lateral wellbores drilled into a single coal seam. Common stimulation techniques include open-hole under ream, cavity completions, and hydraulic fracturing (Caballero 2013). Fundamental reservoir parameters that should be considered in the selection of drilling and completion techniques for CBM wells include: reservoir thickness, coal matrix and cleat permeability and porosity, reservoir pressure, gas saturation, number of seams, geological complexity, coal rock strength, hole integrity and collapse risk. In general coal seams with lower permeability require a greater degree of stimulation such as hydraulic fracturing or cavity completion. Thick highly permeable (fractured) coal seams require relatively little stimulation while low permeability coal seams require stimulation techniques such as horizontal drilling; large number of coal seams or highly structured geologically complex seams may limit the completion option to vertical or low angle wells. Surface access or limitation in local services may drive the drilling and completion decision (Caballero 2013). The development of CBM reservoirs often involves a low-technology, low-cost approach due to shallow depth, relatively thin reservoirs, limited lateral extension, and very heterogeneous nature of CBM reservoirs. In contrast to conventional gas reservoir development where water production and reservoir pressure depletion result in lower gas flow, eventually leading to well abandonment, in CBM wells extracting gas from coalbeds often requires an initial dewatering stage, pumping out the water held in the seam to reduce the level of water saturation and formation pressure, to allow the gas to be released through desorption from the coal surface (**Fig. 9.41**). **Fig. 9.42** illustrates the difference in gas and water production profiles between conventional gas reservoirs and CBM (CSG) reservoirs.

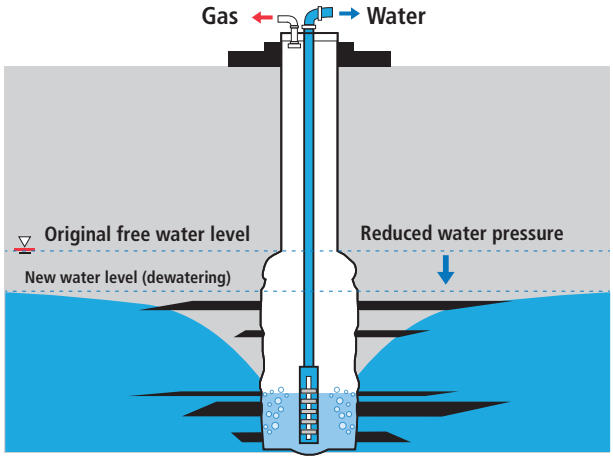

Fig. 9.41—Typical completion and dewatering process in a CBM well.

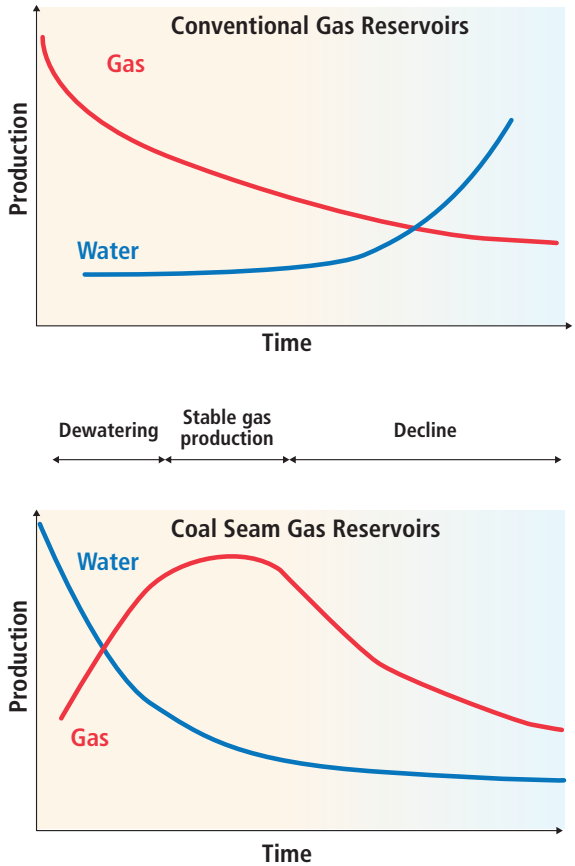

Fig. 9.42—Gas and water production stages in CBM and conventional gas reservoirs.

Production lowers the pore pressure, and, to a lesser extent, the reservoir stresses resulting in effective stress increases accompanying reservoir depletion. Generally a stress-path factor defined as the reduction of total stresses relative to a unit drop in pore pressure is used to determine the pore pressure-stress coupling of the reservoirs. The value of stress path factor in the conventional reservoirs typically is less than one and typically ranges between 0.4 and 0.9 (Addis 1997). In coal seam reservoirs the stress-path factor could be on the higher side and even greater than one due to the intrinsic elastic properties of coals and the shrinkage of coalbeds with gas desorption. Hence, compared with conventional reservoir rocks the unit increase in effective stress with depletion will be higher in CBM reservoirs. Pressure depletion and high drawdown pressures during the dewatering stage in CBM wells have been seen to increase the risk of wellbore and perforation instability in the form of solids and fine production caused by rock failure under a high effective stress environment even before onset of gas production.

In thinly bedded CSG reservoirs, solids production from coals may not be a concern but sanding or solids production from interbedded rocks can be the main source of solids production that will have an adverse effect on well productivity and integrity. Where the interbedded clastic rocks are clay rich with an abundant percentage of water sensitive clay minerals such as smectite, clay swelling and grain dispersion will be expected when the rocks are exposed to low-salinity water generated from coal dewatering. This in turn could reduce the overall rock strength, due to the loss of cementation in the rock matrix, hence increasing the risk of rock failure under low hole pressure and high drawdown conditions at early stages of the well life. This is in contrast to the conventional gas reservoirs where many gas wells will be sand free in early to middle stages of their lives and sanding may become an issue only when the reservoir becomes heavily depleted with or without water production.

Geomechanical engineering assessment of solids production and sanding evaluation is well established for conventional reservoirs and the same principles can be utilized for CBM wells too. Such sanding evaluation and coal failure analysis during production will be based on in-situ stresses, coal rock strength, wellbore trajectory, reservoir and wellbore pressure and can be used to identify the likelihood and mechanism(s) of solids production over the well life-cycle in CBM wells. Typical outputs include identification of solids prone zones, the critical well and reservoir pressures beyond which rock failure is expected, effect of dewatering, and chemophysical properties of formation water on rock failure and hence solids production.

9.7 Conclusion and Future Trends

The stress state of the rock at depth is influenced by drilling, completion, and production from oil and gas wells. Geomechanical engineering, the study of the rock response to such stress changes, has received a great deal of attention over the past few decades applied to drilling and production across North America's offshore and onshore basins to improve field development strategies. For unconventional resources, there is a large difference, between the expectations and the reality, due to the large subsurface uncertainties present in the field development. Geomechanical engineering addresses some of this uncertainty, within a variety of geological settings, and can provide solutions that underpin more robust field development plans. Geochemical assessment of source rocks and measurement of rock mechanical properties from core lab measurements provide a common means to distinguish zones of high deliverability along the lateral legs. Correlation between well logs and the measured rock properties gives an increased understanding of rock quality needed for reservoir modeling and hydraulic fracturing stimulations. Development of in-situ stress profile along with prediction and interpretation of mud weight window is critical to fully understand the operational issues and ensure the drilling operation is optimized. The presence of natural fractures and weakness planes in both shale and CBM could be potentially disadvantageous in terms of borehole stability during directional and horizontal drilling. However, some reservoir structural complexity (contained natural fractures within the pay zone) is beneficial to achieve effective reservoir stimulation during multistage hydraulic fracturing operations in horizontal wellbores.

It is in the interest of all stakeholders to ensure best practice is applied to any field development. Addressing the geomechanical engineering issues in the planning and operational phases helps reduce environmental impacts and optimizes the field development by minimizing well stability problems encountered during drilling and work-overs, and optimizing fracture containment during completion and stimulation increases the success of the field development. Geomechanical engineering also increases operational efficiency by providing improved understanding of the reservoir. Proper placement of horizontal wells and hydraulic fracture stages along the wellbore is critical to success of economic production from these tight and heterogeneous formations.

The extension of reservoir characterization to include geomechanical engineering parameters for unconventional resource development has been demonstrated over the past few years across the shale gas and shale oil plays in North America. Geomechanical engineering has become an integral part of the exploration and production workflow in every stage of field development plans. Geomechanical engineering analysis will continue to play an important role in addressing the significant number of challenges associated with unconventional resources development in North America and internationally as the industry seeks to unlock these energy resources in an efficient and responsible manner.

9.8 References

Aadnoy, B.S. and M.E. Chenevert, M.E. 1987. Stability of Highly Inclined Boreholes. ***SPE Drilling Eng***., **2** (4), pp. 364–374.

Abass, H.H., Al-Tahini, A.M., Abousleiman, Y., et al. 2009. New Technique to Determine Biot Coefficient for Stress-Sensitive Dual-Porosity Reservoirs. Paper SPE 124484 presented at the SPE Annual Technical Conferences and Exhibition, New Orleans, Louisiana, 4–7 October. http://dx.doi.org/10.2118/124484-MS.

Abbas, S., Lecampion, B., and Prioul, R. 2013. Competition between Transverse and Axial Hydraulic Fractures in Horizontal Wells. Paper SPE 163848 presented at the SPE Hydraulic Fracturing Technology Conference, The Woodlands, Texas, 4–6 February. http://dx.doi.org/10.2118/163848-MS.

Abousleiman Y.N. and Ghassemi, A. 1992. Laboratory Determination of Poroelastic Parameters, Part I–Biot's Effective Stress Parameter. The University of Oklahoma, School of Petroleum and Geological Engineering, RMI Consortium Report, RMC 92–12 (unpublished).

Abousleiman Y.N., Tran, M.H., and Hoang, S.K. 2008. Laboratory Characterization of Anisotropy and Fluid Effects on Shale Mechanical Properties Using Inclined Direct Shear Testing Device IDSTID. Paper ARMA 08-256 presented at the 42nd U.S. Rock Mechanics Symposium, San Francisco, California, 29 June–2 July.

Addis, M.A. 1997. The Stress–Depletion Response of Reservoirs. SPE 38720, Proc. 72nd SPE Annual Technical Conference & Exhibition, San Antonio, 5–8 October 1997.

Addis, M.A., Hanssen, T.H., Willoughby, D.R., Yassir, N., et al. 1998. A Comparison of Leak-off Test and Extended Leak-Off Test Data for Stress Estimation. SPE/ISRM 47235, Proc. Eurock '98 Conf., Trondheim, Norway, July.

Aguilera, R. 2006. Effect of Fracture Compressibility on Gas In-Place Calculations of Stress-Sensitive Naturally Fractured Reservoirs. Paper SPE 100451 presented at the SPE Gas Technology Symposium, Calgary, Alberta, Canada, 15–17 May. http://dx.doi.org/10.2118/100451-MS.

Ahmed, U. 1988. Fracture Height Prediction, *Journal of Petroleum Technology*, July 1988, pp 813–825.

Ahmed, U. and Markeley, M. 1991, Enhanced In-Situ Stress Profiling with Microfrac, Core, and Sponic Logging Data. *Journal of Petroleum Technology* (June 1991), pp 243–251.

Aki, K. and Richards, P.G. 1980. *Quantitative Seismology: Theory and Methods*. San Francisco: W.H. Freeman.

Al-Tahini, A.M., Abousleiman, Y.N., and Brumley, J.L. 2005. Acoustic and Quasistatic Laboratory Measurement and Calibration of the Pore Pressure Prediction Coefficient in the Poroelastic Theory. Paper SPE 95825 presented at the SPE Annual Technical Conferences and Exhibition, Dallas, Texas, 9–12 October. http://dx.doi.org/10.2118/95825-MS.

Altindag, R. 2002. The Evaluation of Rock Brittleness Concept on Rotary Blasthole Drills, *J. South Afr. Inst. Min. Metal*. **102**: 61–66.

Altindag, R. 2003. Correlation of Specific Energy with Rock Brittleness Concepts on Rock Cutting. *J. South Afr. Inst. Min. Metal*. **6**: 163–172.

Ameen, M.S., Buhidma, I.M., and Rahim, Z. 2010. The function of fractures and in-situ stresses in the Khuff reservoir performance, onshore fields, Saudi Arabia. *AAPG Bulletin*, **94**, no. 1: 27–60.

Aoki, T., Tan, C.T., Cox, R.H.T., et al. 1995. Determination of Anisotropic Poroelastic Parameters of a Transversely Isotropic Shale by Means of Consolidated Undrained Triaxial Tests. 8th ISRM Congress 95-037, Tokyo, Japan. 173–176.

Avseth, P., Mukerji, T., and Mavko, G. 2010. *Quantitative Seismic Interpretation: Applying Rock Physics Tools to Reduce Interpretation Risk*. Cambridge University Press.

Azeemuddin, M., Awal, M.R., Scott, T.E., et al. 2001. Transverse Anisotropy in Biot's Constant through Dynamic Measurements on Cordoba Cream Limestone. Paper SPE 68193 presented at the SPE Middle East Oil Show, Bahrain. 17–20 March. http://dx.doi.org/10.2118/68193-MS.

Barton, C.A., Zoback, M.D., and Burns, K.L. 1988. In-situ Stress Orientation and Magnitude at the Fenton Geothermal Site, New Mexico, Determined from Wellbore Breakouts. *Geophysical Research Letters*, **15** (5): 467–470.

Barton, N.R. and Choubey, V. 1977. The Shear Strength of Rock Joints in Theory and Practice. *Rock Mech*. **10** (1-2): 1–54. http://dx.doi.org/10.1007/BF01261801.

Barton, N.R. and Bandis, S. 1983. Rock Joint Deformation and Permeability Coupling. Proc. 5th Int. Congr. Rock Mech. Melbourne.

Barton, N., Bandis, S., and Bakhtar, K. 1985. Strength, Deformation and Conductivity Coupling of Rock Joints. *Int. J. Rock Mech. & Min. Sci. & Geomech*. Abstr. 22: 3: 121-140.

Bell, J.S. and Gough, D.I., 1979. Northeast–Southwest Compressive Stress in Alberta: Evidence from Oil Wells. *Earth Planet. Sci. Lett.*, 45, 475-482, 1979.

Berge, P.A., Mallick, S., Fryer, G.J., et al. 1991.In-Situ Measurement of Transverse Isotropy in Shallow-Water Marine Sediments. *Geophys. J. Int.* (1991), **104** (2): 241–254. http://dx.doi.org/10.1111/j.1365246X.1991.tb02509.x.

Biot, M.A. 1941. General Theory of Three Dimensional Consolidation. *J. Appl. Phys.*, **12** (2): 155–164. http://dx.doi.org/10.1063/1.1712886.

Biot, M.A. 1956. General Solutions of the Equations of Elasticity and Consolidation for a Porous Material. *J. Appl. Mech. Trans.* ASME, **78**: 91-96.

Biot, M.A. and Willis, D.G. 1957. The Elastic Coefficients of the Theory of Consolidation. *J. Appl. Mech*. **24**: 594–601.

Bishop, A.W. 1959. The Principle of Effective Stress. *Teknisk Ukeblad* **106** (39): 859–863.

Bishop, A.W. 1967. Progressive Failure with Special Reference to the Mechanism Causing it. Proc. Geotechnical Conference, Oslo, Norway 2: 142–150.

Blanton, T.L. 1982. An Experimental Study of Interaction between Hydraulically Induced and Pre-existing Fractures. Paper SPE 10847 presented at the SPE Unconventional Gas Recovery Symposium, Pittsburgh, Pennsylvania. 16–18 May. http://dx.doi.org/10.2118/10847-MS.

Britt, L.K. and Smith, M.B. 2009. Horizontal Well Completion, Stimulation Optimization, and Risk Mitigation. Paper SPE 125526 presented at the SPE Eastern Regional Meeting, Charleston, West Virginia. 23–25 September. http://dx.doi.org/102118/125526-MS.

Bunger, A.P., Jeffrey, R.G., and Zhang, X. 2013. Constraints on Simultaneous Growth of Hydraulic Fractures from Multiple Perforation Clusters in Horizontal Wells. SPE 163860. ***SPE J***. pre-print. http://dx.doi.org/10.2118/163860-PA.

Bunger, A.P., Zhang, X., and Jeffrey, R.G. 2012. Parameters Affecting the Interaction among Closely Spaced Hydraulic Fractures. SPE 140426. ***SPE J.*** **17** (1): 292–306. http://dx.doi.org/10.2118/124484-PA.

Caballero, J. 2013. Drilling and Completion Techniques Selection Methodology for Coalbed Methane Wells. Paper IPTC 17153 presented at the International Petroleum Technology Conference, Beijing, China, 26–28 March. http://dx.doi.org/10.2523/17153-MS.

Canady, W. 2011. A Method for Full-Range Young's Modulus Correlation. Paper SPE 143604 presented at the North American Unconventional Gas Conference and Exhibition, The Woodlands, Texas. 14–16 June. http://dx.doi.org/10.2523/143604-MS.

Cander, H. 2012. Sweet Spots in Shale Gas and Liquid Plays: Prediction of Fluid Composition and Reservoir Pressure. Search and Discovery Article paper 40936 presented at the AAPG Annual Convention and Exhibition, Long Beach, California. 22–25 April.

Chen, X, Tan, C.P., and Detournay, C. 2002. The Impact of Mud Infiltration on Wellbore Stability in Fractured Rock Masses. Paper SPE 78241 presented at the SPE/ISRM Rock Mechanics Conference, Irving, Texas, 20–23 October. http://dx.doi.org/102523/78241-MS.

Chenevert, M.E. and Gatlin, C. 1965. Mechanical Anisotropies of Laminated Sedimentary Rocks. SPE 890. ***SPE J.*** **5** (1): 67–77. Trans. http://dx.doi.org/10.2118/890-PA.

Cheng, Y. 2012. Mechanical Interaction of Multiple Fractures—Exploring Impacts of the Selection of the Spacing/ Number of Perforation Clusters on Horizontal Shale-Gas Wells. SPE 125769. ***SPE J.*** **17** (4): 992–1001. http://dx.doi.org/10.2118/125769-PA.

Chong, K.K., Grieser, W.V., Passman, A., et al. 2010. A Completions Guide Book to Shale-Play Development: A Review of Successful Approaches Towards Shale-Play Stimulation in the Last Two Decades. Paper SPE 133874 presented at the Canadian Unconventional Resources and International Petroleum Conference, Calgary, Alberta, Canada. 19–21 October. http://dx.doi.org/10.2118/133874-MS.

Cipolla, C. 2014, pers comm.

Coates, D. and Parsons, R. 1966. Experimental Criteria for Classification of Rock Substances. ***Int. J. Rock Mech. Min. Sci. & Geomech.***, **3** (3): 181–189. http://dx.doi.org/10.1016/0148-9062(66)90022-2.

Crawford, B.R., DeDontney, N.L., Alramahi, B., et al. 2012. Shear Strength Anisotropy in Fined-grained Rocks. Paper ARMA 2012-290 presented at the 46th U.S. Rock Mechanics Symposium, San Francisco, California. Chicago. Illinois. 24–27 June.

Dahl, F. 2003. DRI, BWI, CLI Standards. Norwegian University of Science and Technology, Angleggsdrift, Trondheim.

Das B. 1974. Vicker's Hardness Concept in the Light of Vicker's Impression. ***Int. J. Rock. Mech. Min. Sci. & Geomech.***, **11** (3): 85–89. http://dx.doi.org/10.1016/0148-9062(74)91536-8.

De Bree, P. and Walters, J. V. 1989. Micro/Minifrac Test Procedures and Interpretation for In-situ Stress Determination. ***Int. J. Rock Mech. Min. Sci. & Geomech. Abstr.***, **26** (60): 515–521.

Detournay, E.E. and Cheng, A.E. 1992. Influence of Pressurization Rate on the Magnitude of the Breakdown Pressure. Paper ARMA 92–0325 presented at the 33rd U.S. Rock Mechanics Symposium. Santa Fe, New Mexico. 3–5 June.

Donath, F.A. 1964. Strength Variations and Deformational Behaviour in Anisotropic Rocks. In ***State of Stress in the Earth's Crust***, W.R. Judd (ed). American Elsevier Publishing Co. 281–298.

Drucker, D. and Prager, W. 1952. Soil Mechanics and Plastic Analysis or Limit Design. ***Applied Mathematics***, **10**: 157–165.

Dyke, C.G. 1992. How Sensitive Is Natural Fracture Permeability at Depth to Variation in Effective Stress? Proc., IntI. ISRM Symposium on Fractured and Jointed Rock Masses, California.

Eaton, B.A. 1969. Fracture Gradient Prediction and Its Application in Oilfield Operations. Trans. *J. Pet Tech.* **21** (10): 1353–1360. SPE 2163. http://dx.doi.org/10.2118/2163-PA.

Ellefsen, K. J. 1990. Elastic Wave Propagation along a Borehole in an Anisotropic Medium. Sc.D. Thesis, Massachusetts Institute of Technology, Cambridge, Massachusetts. http://hdl.handle.net/1721.1/52915.

Evans, K.F., Engelder, T., and Plumb, R. 1989. Appalachian Stress Study 1–A Detailed Description of In-situ Stress Variations in Devonian Shales of the Appalachian Plateau. *J Geophys Res.* (1989) 94, B6, 7129.

Ewy, R. 1999. Wellbore-Stability Predictions by Use of a Modified Lade Criterion. *SPE Drill & Compl*, **14** (2): 85–91. SPE 56862-PA. http://dx.doi.org/10.2118/56862-PA.

Fabre, D. and Gustkiewicz, J. 1997. Poroelastic Properties of Limestones and Sandstones under Hydrostatic Conditions, *Int. J. Rock Mech. Min. Sci.* **34** (1): 127–134. http://dx.doi.org/10.1016/S1365-1609(97)80038-X.

Fatti, J.L., Smith, G.C., Vail, P.J., et al. 1994. Detection of Gas in Sandstone Reservoirs Using AVO Analysis: A 3D Case History Using the Geostack Technique. *Geophysics*, **59**: 1362–1376. http://dx.doi.org/10.1190/1.1443695.

Finkbeiner, T., Freitag, H.C., Siddiqui, M., et al. 2011. Reservoir Optimized Fracturing–Higher Productivity from Low-Permeability Reservoirs through Customized Multistage Fracturing. Paper SPE 141371 presented at the SPE Middle East Oil and Gas Show and Conference, Bahrain. 25–28 September. http://dx.doi.org/10.2118/141371-MS.

Fischer-Cripps, A.C. 2000. *Introduction to Contact Mechanics*. Springer-Verlag.

Franquet, J.A. and Abass, H.H. 1999. Experimental Evaluation of Biot's Poroelastic Parameter–Three Different Methods. Paper ARMA 99-0349 presented at the 37th U.S. Rock Mechanics Symposium, Vail, Colorado. 7–9 June.

Franquet, J.A., Mitra, A., Warrington, D.S., et al. 2011. Integrated Acoustic, Mineralogy, and Geomechanics Characterization of the Huron Shale, Southern West Virginia, USA. Paper CSUG/SPE 148411 presented at the Canadian Unconventional Resources Conference, Calgary, Alberta, Canada. 15–17 November. http://dx.doi.org/10.2118/148411-MS.

Franquet, J.A. and Rodriguez, E.F. 2012. Orthotropic Horizontal Stress Characterization from Logging and Core Derived Acoustic Anisotropies. Paper ARMA 2012-644 presented at the 46th U.S. Rock Mechanics Symposium, San Francisco, California, June. Chicago. Illinois. 24–27 June.

Franquet, J.A. Stewart, G., Bolle, L., et al. 2005. Log-based Geomechanical Characterization and Sanding Potential Analysis on Several Wells Drilled in Southern Part of Oma. Paper SPE/PAPG 111044 presented at the SPE/PAPG Annual Technical Conference, Islamabad, Pakistan. 28–29 November. http://dx.doi.org/10.2118/111044-MS.

Franquet, J.A., Verma, N.K., Azeemuddin, M., et al. 2007. Openhole Stability Analysis of Horizontal Wellbores under Production Scenarios in Jurassic Carbonate Reservoirs of West Kuwait. Paper SPE 105332 presented at the SPE Middle East Oil and Gas Show and Conference, Bahrain. 11–14 March. http://dx.doi.org/10.2118/105332-MS.

Franquet, J.A., Wolfe, C.A., and Rodriguez, E.F. 2010. Micromechanical Modeling of Rock Stress-Strain Curves from Log Data. Paper PEG-D1-02B-03 presented at the ICIPEG Int. Conference on Integrated Petroleum Engineering & Geosciences under the ESTCON World Engineering, Science & Technology Congress.

Gallant, C., Zhang, J., Wolfe, C.A., et al. 2007. Wellbore Stability Considerations for Drilling High-Angle Wells through Finely Laminated Shale: A Case Study from Terra Nova. Paper SPE 110742 presented at the SPE Annual Technical Conferences and Exhibition, Anaheim, California, 11–14 November. http://dx.doi.org/10.2118/110742-MS.

Gassmann, F. 1951, Uber die elastizität poröser medien: Vierteljahrsschrift der Naturforschenden Gesellschaft in Zürich, 96, 23.

Gatens, J.M., Harrison, C.W., Lancaster, D.E., et al. 1990. In-situ Stress Test and Acoustic Logs Determine Mechanical Properties and Stress Profiles in the Devonian Shales. *SPE Formation Evaluation* **5** (3): 248–254. SPE 18523-PA. http://dx.doi.org/10.2118/18523-PA.

Geertsma, J. 1957. The Effect of Fluid Pressure Decline on Volumetric Changes of Porous Rocks. Paper SPE 728-G., *Petroleum Trans. AIME* **210**: 331-340.

Geertsma, J. 1985. Some Rock Mechanical Aspects of Oil and Gas Well Completions. *SPE. J* **25** (6): 848–856. SPE 8073-PA. http://dx.doi.org/10.2118/8073-PA.

Geilikman, M., Xu, G., and Wong, S.W. 2013. Interaction of Multiple Hydraulic Fractures in Horizontal Wells. Paper SPE 163982-MS presented at the SPE Unconventional gas Conference and Exhibition. Muscat, Uman. 28–30 January. http://dx.doi.org/10.2118/163982-MS.

Germanovich, L.N. and Astakhov, D.K. 2004. Fracture Closure in Extension and Mechanical Interaction of Parallel Joints. ***J. Geophys. Res.*** 109 (B2). http://dx.doi.org/10.1029/2002JB002131.

Germanovich, L.N., Astakhov, D.K., Shlyapobersky, J., et al. 1998. Modeling Multisegmented Hydraulic Fracture in Two Extreme Cases: No Leakoff and Dominating Leakoff. ***Int. J. Rock. Mech. Min. Sci. & Geomech.*** **35** (4-5): 551–554.

Grabco, D., Palistrant, O., Shikimaka, R., et al. 2002. Hardness and Brittleness of Rocks Studied by Microindentation Method in Combination with the Registration of Acoustic Emission Signals. Paper presented at the 8th European Conference on Nondestructive Testing. Barcelona, Spain. 17–21 June.

Gustkiewicz J. 1989. Synoptic View of Mechanic Behavior of Rocks under Triaxial Compression. Proc. ISRM International Symposium. Pau, France 30 August–2 September. In ***Rock at Great Depth***, Maury, V., and Fourmaintraux, D. (eds) 3–9.

Gutierrez, M., Tutuncu, A., and Katsuki, D. 2013. Stress-Dependent Flow and Poro-Elastic Properties of Tight Shales. 3rd Unconventional Resources Geomechanics Workshop–ARMA San Francisco, California. 21 June.

Hardage, B.A., DeAngelo, M.V., Murray, P.E., et al. 2011. Multicompoment Seismic Technology, SEG Geophysical References Series no. 18, ***Society of Exploration Geophysicists***. http://dx.doi.org/10.1190/1.9781560802891.

Haugland, M., Zhang, J., Sarker, R., et al. 2013. Pore Pressure Prediction in Unconventional Resources. Paper IPTC 16849-MS presented at the International Petroleum Technology Conference. Beijing, China. 26–28 March. http://dx.doi.org/10.2523/16849-MS.

Higgins, S., Goodwin, S., Bratton, T., et al. 2008. Anisotropic Stress Models Improve Completion Design in the Baxter Shale. Paper SPE 115736 presented at the SPE Annual Technical Conference and Exhibition. Denver, Colorado. 21–24 September. http://dx.doi.org/10.2118/115736-MS.

Hoek, E. and Brown, E.T. 1980. Empirical Strength Criterion for Rock Masses. ***J. Geotech. Engng. Div. ASCE*** **106** (GT9): 1013–1035.

Holt, R.M., Fjaer, E., Nes, O.M., et al. 2011. A Shaly Look at Brittleness. Paper ARMA 11-366 presented at the 45th U.S. Rock Mechanics Symposium, San Francisco, California. 26–29 June.

Howard, G.C. and Fast, C.R. 1970. Hydraulic Fracturing, V2. 203 pp., ***SPE Monograph Series***, SPE.

Hunka V. and Das, B. 1974. Brittleness Determination of Rocks by Different Methods. ***Int. J. Rock Mech. Min. Sci. Geomech.*** Abst. **11** (10): 389–392. http://dx.doi.org/10.1016/0148-9062(74)91109-7.

Ihab, T., Naial, R., Moronkeji, D.A., et al. 2014. Wireline Straddle Packer Microfrac Testing Enables Tectonic Lateral Strain Calibration in Carbonate Reservoirs. Paper IPTC 17301-MS presented at the International Petroleum Technology Conference, Doha, Qatar. 19–22 January. http://dx.doi.org/10.2523/17301-MS.

ISRM. 1978 Suggested Methods for Determining Hardness and Abrasiveness of Rocks, ***Int. J. Rock Mech. Min. Sci. & Geomech***. **15**: 89–97.

Jaeger, J.C. 1960. Shear Failure of Anisotropic Rocks. ***Geol. Mag***. **97** (1): 65–72.

Jaeger, J.C. and Cook, N.G.W. 1979. ***Fundamentals of Rock Mechanics***, 593 pp., 3rd edition, Chapman and Hall.

Jaeger, J.C., Cook, N.G.W., and Zimmerman, R.W. 2007. ***Fundamentals of Rock Mechanics***, 488 pp., 4th edition, Blackwell Publishing.

Jarvie, D.M., Hill, R.J., Ruble, T.E., et al. 2007. Unconventional Shale Gas Systems: The Mississippian Barnett Shale of North-Central Texas as One Model for Thermogenic Shale-Gas Assessment. ***AAPG Bulletin***. **91** (4): 475–499.

King, G.E. 2010. Thirty Years of Gas Shale Fracturing: What Have We Learned? Paper SPE 133456 presented at the SPE Annual Technical Conference and Exhibition. Florence, Italy. 19–22 September. http://dx.doi.org/10.2118/133456-MS.

Kriegshauser, B., Fanini, O., Forgang, S. et al. 2000. A New Multicomponent Induction Logging Tool to Resolve Anisotropic Formation. Paper SPWLA-2000-D presented at the SPWLA 41st Annual Logging Symposium, Dallas, Texas. 4–7 June.

Kulhawy, F.W. 1975. Stress Deformation Properties of Rock and Rock Discontinuities. ***Engng. Geol.*** 9 (no. 4), 327–350

Lacy, L.L. 1997. Dynamic Rock Mechanics Testing for Optimized Fracture Designs. Paper SPE 38716 presented at the SPE Annual Technical Conference and Exhibition. San Antonio, Texas. 5–8 October. http://dx.doi.org/10.2118/38716-MS.

Lade, P. 1997. Elasto-plastic Stress-Strain Theory for Cohesionless Soil with Curved Yield Surfaces. ***Int. J. Soil and Structures***, **13** (11): 1019–1035.

Lam, K.Y. and Cleary, M.P. 1984. Slippage and Re-initiation of (Hydraulic) Fractures at Frictional Interfaces. ***Int. J. for Num. and Anal. Meth. in Geomech.***, **8** (6): 598–604. http://dx.doi.org/10.1002/nag.1610080607.

Laubach, S.E., Marrett, R.A., Olson, J.E., et al. 1998. Characteristics and Origins of Coal Cleat: A Review. *International Journal of Coal Geology* **35**: 175–207.

LeCompte, B., Franquet, J.A., and Jacobi, D. 2009. Evaluation of Haynesville Shale Vertical Well Completions with a Mineralogy Based Approach to Reservoir Geomechanics. Paper SPE 124227 presented at the SPE Annual Technical Conference and Exhibition. New Orleans, Louisiana. 4–7 October. http://dx.doi.org/10.2118/124227-MS.

Matthews, W.R. and Kelly, J. 1967. How to Predict Formation Pressure and Fracture Gradient. *Oil and Gas Journal* **65** (8): 92–106.

Maxwell, S.C., Rutledge, J., Jones, R., et al. 2010. Petroleum Reservoir Characterization Using Downhole Microseismic Monitoring. *Geophysics* **75** (5): 129–137. http://dx.doi.org/10.1190/1.3477966.

McLean, M.R. and Addis, M.A. 1990 (a). Wellbore stability: A Review of Current Methods of Analysis and Their Field Application. IADC/SPE paper 19941: IADC/SPE Drilling Conference, Houston, February. http://dx.doi.org/10.2118/19941-MS.

McLean, M.R. and Addis, M.A. 1990 (b). Wellbore Stability: The Effect of Strength Criteria on Mud Weight Recommendations. Paper SPE 20405 presented at the SPE Annual Technical Conference and Exhibition. New Orleans, Louisiana. 23–26 September. http://dx.doi.org/10.2118/20405-MS.

Mohrs, F. 1822. Essentials of Mineralogy (Grundriß der Mineralogie), translated, revised, and expanded by Wilhelm Haidinger as *Treatise on Mineralogy, or the Natural History of the Mineral Kingdom*, 3 vols. 1825. Edinburgh.

Mokhtari, M., Alqahtani, A.A., and Tutuncu, A.N. 2013. Failure Behaviour of Anisotropic Shales. Paper ARMA 13-312 presented at the 47th U.S Rock Mechanics/Geomechancis Symposium. San Francisco, California. 23–26 June.

Molenaar, M.M., Hill, D.J., Webster, P., Fidan, E., and Birch, B. 2011. First Downhole Application of Distributed Acoustic Sensing (DAS) for Hydraulic Fracturing Monitoring and Diagnostics. SPE 140561. SPE Hydraulic Fracturing Technology Conference and Exhibition, The Woodlands, Texas. 24-26 January 2011.

Moos, D., Peska, P., Finkbeiner, T., et al. 2003. Comprehensive Wellbore Stability Analysis Utilizing Qunatitative Risk Assessment. ***Jour. Petrol. Sci. and Eng***. **38** (3-4): 97–109. http://dx.doi.org/10.1016/S0920-4105(03)00024-X.

Moos, D. 2006. Geomechanics Applied to Drilling Engineering, ***Petroleum Engineering Handbook***, (ed.) Larry W. Lake, II, SPE, Richardson, Texas, 1–87.

Moos, D. 2011. The Influence of Coal Seam Discontinuities on Wellbore Stability and Productivity. ***SPE News***–Australia, April, **143**: 5–9.

Moos, D., Perumalla, S., Kowan, J., et al. 2010. A New Model for Wellbore Stability and Stress Prediction in Underbalanced Wells. Paper IADC/SPE 135894 presented at the IADC/SPE Asia Pacific Drilling Technology Conference and Exhibition. Ho Chi Minh City, Vietnam. 1–3 November. http://dx.doi.org/10.2118/135894-MS.

Moos, D., Vassilellis, G., Cade, R., et al. 2011. Predicting Shale Reservoir Response to Stimulation in the Upper Devonian of West Virginia. Paper SPE 145849 presented at the SPE Annual Technical Conference and Exhibition. Denver, Colorado. 30 October–2 November. http://dx.doi.org/10.2118/145849-MS.

Nagel, N.B. and Sanchez-Nagel, M. 2011. Stress Shadowing and Microseismic Events: A Numerical Evaluation. Paper SPE 147363 presented at the SPE Annual Technical Conference and Exhibition. Denver, Colorado. 30 October–2 November. http://dx.doi.org/10.2118/147363-MS.

Nagel, N.B., Sanchez-Nagel, M., and Lee, B.T. 2012. Gas Shale Hydraulic Fracturing: A Numerical Evaluation of the Effect of Geomechanical Parameters. Paper SPE 152192 presented at the SPE Hydraulic Fracturing Technology Conference. The Woodlands, Texas. 6–8 February. http://dx.doi.org/10.2118/152192-MS.

Nagel, N.B., Sanchez-Nagel, M., Zhang, F., et al. 2013. Coupled Numerical Evaluations of the Geomechanical Interactions between a Hydraulic Fracture Stimulation and a Natural Fracture System in Shale Formations. *Rock Mechanics and Rock Engineering*, **46** (3): 581–609.

Nasseri, M.H.B., Rao, K.S., and Ramamurthy, T. 2003. Anisotropic Strength and Deformational Behaviour of Himalayan Schists. *Int. J. Rock Mech. & Min. Sci.*, **40** (1): 3–23.

Nye, J.F. 1958. Physical properties of crystal: Their Representation by Tensor and Matrices. *J. Mech. & Phys. Solids*, **6** (4): 328–329. http://dx.doi.org/10.1016/0022-5096(58)90012-7.

Oliver, W.C. and Pharr, G.M. 1992. An Improved Technique for Determining Hardness and Elastic Modulus Using Load and Displacement Sensing Indentation Experiments. *J. Mater. Res.*, **7** (6): 1564–1583. http://dx.doi.org/10.1557/JMR.1991.1564.

Ong, S.H, Ramos, G.G., and Zheng, Z. 2000. Sand Production Prediction in High Rate, Perforated and Open-hole Gas Wells. Paper SPE 58721 presented at the SPE International Symposium on Formation Damage Control. Lafayette, Louisiana. 23–24 February. http://dx.doi.org/10.2118/58721-MS.

Ong, S.H., May, A., George, I., et al. 2000. An Accurate Characterization of Sand Strength in Weak and Unconsolidated Formations Aids Offshore Production Test Designs–A Bohai Bay Case Study. Paper SPE 64738 presented at the International Oil and Gas Conference and Exhibition. Beijing, China. 7–10 November. http://dx.doi.org/10.2118/64738-MS.

Ottesen, S., Zheng, R.H., and McCann, R.C. 1999. Borehole Stability Assessment Using Quantitative Risk Analysis. Paper IADC/SPE 52864 presented at the SPE/IADC Drilling Conference. Amsterdam, Netherlands. 9–11 March. http://dx.doi.org/10.2118/52864-MS.

Paul, P. and Zoback, M. 2006. Wellbore Stability Study for the SAFOD Borehole through the San Andreas Fault. Paper SPE 102781 presented at the SPE Annual Technical Conference and Exhibition. San Antonio, Texas. 24–27 September. http://dx.doi.org/10.2118/102781-MS.

Pei, J. 2008. Strength of Transversely Isotropic Rocks. PhD dissertation, Massachusetts University of Technology, Cambridge, Massachusetts. June.

Plumb, R.A., Evans, K., and Engelder, T. 1990. Lithology Dependent Stress Contrasts in Palaeozoic Sedimentary Rocks of New York State. *J. Geophysical Res*.

Prats, M. 1981. Effect of Burial History on the Sub-Surface Horizontal Stresses of Formations Having Different Material Properties. SPE 9017 *SPE J.* **21** (6): 658–662. http://dx.doi.org/10.2118/9017-PA.

Raaen, A.M., Hovem, K.A., Joranson, H., et al. 1996. FORMEL: A Step Forward in Strength Logging. Paper SPE 36533 presented at the SPE Annual Technical Conference and Exhibition. Denver, Colorado. 6–9 October. http://dx.doi.org/10.2118/36533-MS.

Rahman, M. M., Aghighi, A., and Rahman, S.S. 2009. Interaction between Induced Hydraulic Fracture and Pre-Existing Natural Fracture in a Poro-Elastic Environment: Effect of Pore Pressure Change and the Orientation of a Natural Fractures. Paper SPE 122574 Presented at Asia Pacific Oil and gas Conference and Exhibition. Jakarta, Indonesia. 4–6 August. http://dx.doi.org/10.2118/122574-MS.

Rickman, R., Mullen, M., Petre, J., et al. 2008. A Practical Use of Shale Petrophysics for Stimulation Design Optimization: All Shale Plays Are Not Clones of the Barnett Shale. Paper SPE 115258 presented at the SPE Annual Technical Conference and Exhibition. Denver, Colorado. 21–24 September. http://dx.doi.org/10.2118/115254-MS.

Roussel, N.P. and Sharma, M.M. 2011. Optimizing Fracture Spacing and Sequencing in Horizontal-Well Fracturing. SPE 127986-PA, *SPE Prod. & Oper.* **26** (2): 173–184. http://dx.doi.org/10.2118/127986-PA.

Ruger, A. 1998. Variation of P Wave Reflectivity with Offset and Azimuth in Anisotropic Media. *Geophysics* **63**: 935–947. http://dx.doi.org/10.1190/1.1444405.

Santarelli, F.J., Dardeau, C., and Zurdo, C. 1992. Drilling through Highly Fractured Formations: A Problem, a Model, and a Cure. Paper SPE 24592 presented at the SPE Annual Technical Conference and Exhibition. Washington, D.C. 4–7 October. http://dx.doi.org/10.2118/24592-MS.

Santarelli, F.J., Detienne, J.L., and Zundel, J.P. 1991. The Use of a Simple Index Test in Petroleum Rock Mechanics. Paper ARMA 91-647 presented at the 32nd U.S. Symposium on Rock Mechanics (USRMS). Norman, Oklahoma. 10–12 July.

Sayers, C.M. 2005. Seismic Anisotropy of Shales. *Geophysical Prospecting* **53** (5): 667–676.

Schoen, J.H., Yu, L., Georgi, D.T., and Fanini, O. 2001. Aspects of Multicomponent Resistivity Data and Macroscopic Resistivity Anisotropy. SPE 74334. *SPE Res. Eval. & Engin.* **4** (5): 415–429.

Schoenberg, M., Muir, F., and Sayers, C.M. 1996. Introducing ANNIE: A Simple Three Parameter Anisotropy Velocity Model for Shales. *Journal of Seismic Exploration* **5**: 35–49.

Sesetty, V. and Ghassemi, A. 2013. Numerical Simulation of Sequential and Simultaneous Hydraulic Fracturing. Paper ISRM 2013-040 presented at ISRM International Conference for Effective and Sustainable Hydraulic Fracturing. Brisbane, Australia. 20–22 May.

Shukla, P., Kumar, V., Curtis, M., et al. 2013. Nanoidentation Studies on Shales. Paper ARMA 13-578 presented at the 47th U.S Rock Mechanics/Geomechancis Symposium. San Francisco, California. 23–26 June.

Sookprasong, P.A., Hurt, R.S., Gill, C.C., et al. 2014. FibreOptic DAS and DTS in Multicluster, Multistage Horizontal Well Fracturing: Interpreting Hydraulic Fracture Initiation and Propagation through Diagnostics. SPE 170723. SPE Annual Tech. Conf. and Exhib., Amsterdam, The Netherlands, 27–29 October.

Tang, X.M., Cheng, N.Y., and Cheng, A.C.H. 1999. Identifying and Estimating Formation Stress from Borehole Monopole and Cross-Dipole Acoustic Measurements. Paper SPWLA 1990-QQ presented at the SPWLA 40th Annual Logging Symposium. Oslo, Norway. 30 May–3 June.

Tang, X.M. and Chunduru, R.K. 1999. Simultaneous Inversion of Formation Shear-wave Anisotropy Parameters from Cross-dipole Acoustic-array Waveform Data. *Geophysics*, **64** (5):1502–1511. http://dx.doi.org/10.1190/1.1444654.

Tang, X.M. 2003. Determining Formation Shear-wave Transverse Isotropy from Borehole Stoneley-wave Measurements. *Geophysics*, **68** (1): 118–126. http://dx.doi.org/10.1190/1.1543199.

Terzaghi, K. 1936. The Shearing Resistance of Saturated Soil and Angle Between Planes of Shear. Proc. 1st Intl. Conf. In *Soil Mech. and Found. Eng.*, v.1, 54–56.

Terzaghi, K. 1943. *Theoretical Soil Mechanics*. Wiley. http://dx.doi.org/10.1002/9780470172766.

Theloy, C. and Sonnenberg, S.A. 2012. Factors Influencing Productivity in the Bakken Play, Williston Basin. Paper presented at the AAPG Annual Convention. Long Beach, California. 22–25 April.

Thiercelin, M. 1992. The Influence of Microstructure on Hydraulic Fracturing Breakdown Pressure. In Structure et Comportement Mecanique des Gdomateriaux; Colloque Rene Houpert, 419–428.

Thomsen, L. 1986. Weak Elastic Anisotropy. *Geophysics*, **51** (10): 1954–1966.

Tongtaow, C. 1982. Wave Propagation along a Cylindrical Borehole in a Transversely Isotropic Formation. Ph.D. dissertation, Colorado School of Mines, Golden, Colorado.

Urbancic, T., Baig, A., and Goldstein, S. 2012. Assessing Stimulation of Complex Natural Fractures as Characterized Using Microseismicity: An Argument for the Inclusion of Sub-horizontal Fractures in Reservoir Models. Paper SPE 152616 presented at the SPE Hydraulic Fracturing Technology Conference, The Woodlands, Texas, 6–8 February. http://dx.doi.org/10.2118/152616-MS.

Van der Vlis, A.C. 1970. Rock Classification by a Simple Hardness Test. Proc. 2nd ISRM Congress, paper 3–4.

Van der Vlis, A.C., Haafkens, R., Schipper, B.A., et al. 1975. Criteria for Proppant Placement and Fracture Conductivity. Paper SPE 5637 presented at the Fall Meeting of the Society of Petroleum Engineers of AIME. Dallas, Texas. 28 September–1 October. http://dx.doi.org/10.2118/5637-MS.

Veeken, C.A.M., Walters, J.V., Kenter, C.J., et al.1989. Use of Plasticity Models for Predicting Borehole Stability. Paper ISRM IS-1989-106 presented at the ISRM International Symposium. Pau, France. 30 August–2 September.

Vernik, L. and Zoback, M.D. 1990. Strength Anisotropy in Crystalline Rock: Implications for Assessment of In-situ Stresses from Wellbore Breakouts. Paper ARMA 90-0841 presented at the 31st U.S. Symposium on Rock Mechanics (USRMS). Golden, Colorado. 18–20 June.

Voigh, W. 1910. Lehrbuch der kristallphysik, (textbook of crystal physics), 1st ed. Leipzip: B.G. Teubner.

Walker, K. J., Wutherich, K., and Terry, J. 2012. Engineered Perforation Design Improves Fracture Placement and Productivity in Horizontal Shale Gas Wells. Paper SPE 154582 presented at the SPE American Unconventional Resources Conference. Pittsburgh, Pennsylvania. 5–7 June. http://dx.doi.org/10.2118/154582-MS.

Warpinski, N.R., Peterson, R.E., Branagan, P.T., et al. 1998. In-situ Stress and Moduli: Comparison of Values Derived from Muliple Techniques. Paper SPE 49190 presented at at the SPE Annual Technical Conference and Exhibition. New Orleans, Louisiana. 27–30 September. http://dx.doi.org/10.2118/49190-MS.

Warpinski, N.R., Schmidt, R.A., and Northrop, D.A. 1982. In-Situ Stresses: The Predominant Influence on Hydraulic Fracture Containment. SPE 8932. ***J. of Pet. Tech.*** **34** (3):653–664. http://dx.doi.org/10.2118/8932-PA.

Walsh, J., Sinha, B., and Donald, A. 2006. Formation Anisotropy Parameters Using Borehole Sonic Data. Paper SPWLA 2006-TT presented at the 47th Annual Logging Symposium. Venezuela, Mexico. 4–7 June.

Wheaton, B., Miskimins, J., Wood, D., Lowe, T., and Barree, R. 2014. Integration of Distributed Temperature and Distributed Acoustic Survey Results with Hydraulic Fracturing Modeling: A Case Study in the Woodford Shale. URTeC 1922140, Unconventional Resources Technology Conference, Denver, Colorado, USA, 25-27 August 2014. http://dx.doi.org/10.15530/urtec-2014-1922140.

Willson, S.M., Last, N.C., Zoback, M.D., et al. 1999. Drilling in South America: A Wellbore Stability Approach for Complex Geologic Conditions. Paper SPE 53940 presented at Latin America and Caribbean Petroleum Engineering Conference. Caracas, Venezuela. 21–23 April. http://dx.doi.org/10.2118/53940-MS.

Winchell, H. 1946. Observations on Orientation and Hardness Variations. ***Am. Miner.*** **31**: 149–152.

Wu, K. and Olson, J.E. 2013. Investigation of the Impact of Fracture Spacing and Fluid Properties for Interfering Simultaneously or Sequentially Generated Hydraulic Fractures. SPE 163821, ***SPE Prod. & Oper.*** **28** (4): 427–436. http://dx.doi.org/10.2118/163821-PA.

Yang, Y., Sone, H., Hows, A., et al. 2013. Comparison of Brittleness Indices in Organic-rick Shale Formation. Paper ARMA 13-403 presented at the 47th U.S. Rock Mechanics/Geomechancis Symposium. San Francisco, California. 23–26 June.

Yarali, O. and Soyer, E. 2011. The Effect of Mechanical Rock Properties and Brittleness on Drillability. ***Scient. Res. and Ess.*** **6** (5): 1077–1088.

Zhang, T., Tang, X.M., and Patterson, D.J. 2000. Evaluation of Laminated Thin Beds in Formations Using High-resolution Acoustic Slowness Logs. Paper SPWLA 2000-XX presented at the SPWLA 41st Annual Logging Symposium Dallas, Texas. 4–7 June.

Zhang, J., Al-Bazali, T.M., Chenevert, M.E., et al. 2006. Compressive Strength and Acoustic Properties Changes in Shales with Exposure to Water-Based Fluids. Paper ARMA 06-900 presented at the 41st U.S. Symposium on Rock Mechanics (USRMS). Golden, Colorado, 17–21 June.

Zheng, Y., Tang, X.M., and Patterson, D.J. 2009. Identifying Stress-Induced Anisotropy and Stress Direction Using Cross-dipole Acoustic Logging. Paper SPWLA 2009-21660 presented at SPWLA 50th Annual Logging Symposium. The Woodlands, Texas. 21–24 June.

Zimmerman R.W., Somerton W.H., King M.S., 1986. Compressibility of Porous Rocks, ***Journal of Geophysical Research***, Vol: 91, Pages: 12765-12765, ISSN: 0148-022

Zoback, M. and Healy, J.H. 1984. Friction, Faulting, and In-Situ Stresses. ***Annales Geophysicae***, **2**: 689–698.

This page intentionally left blank

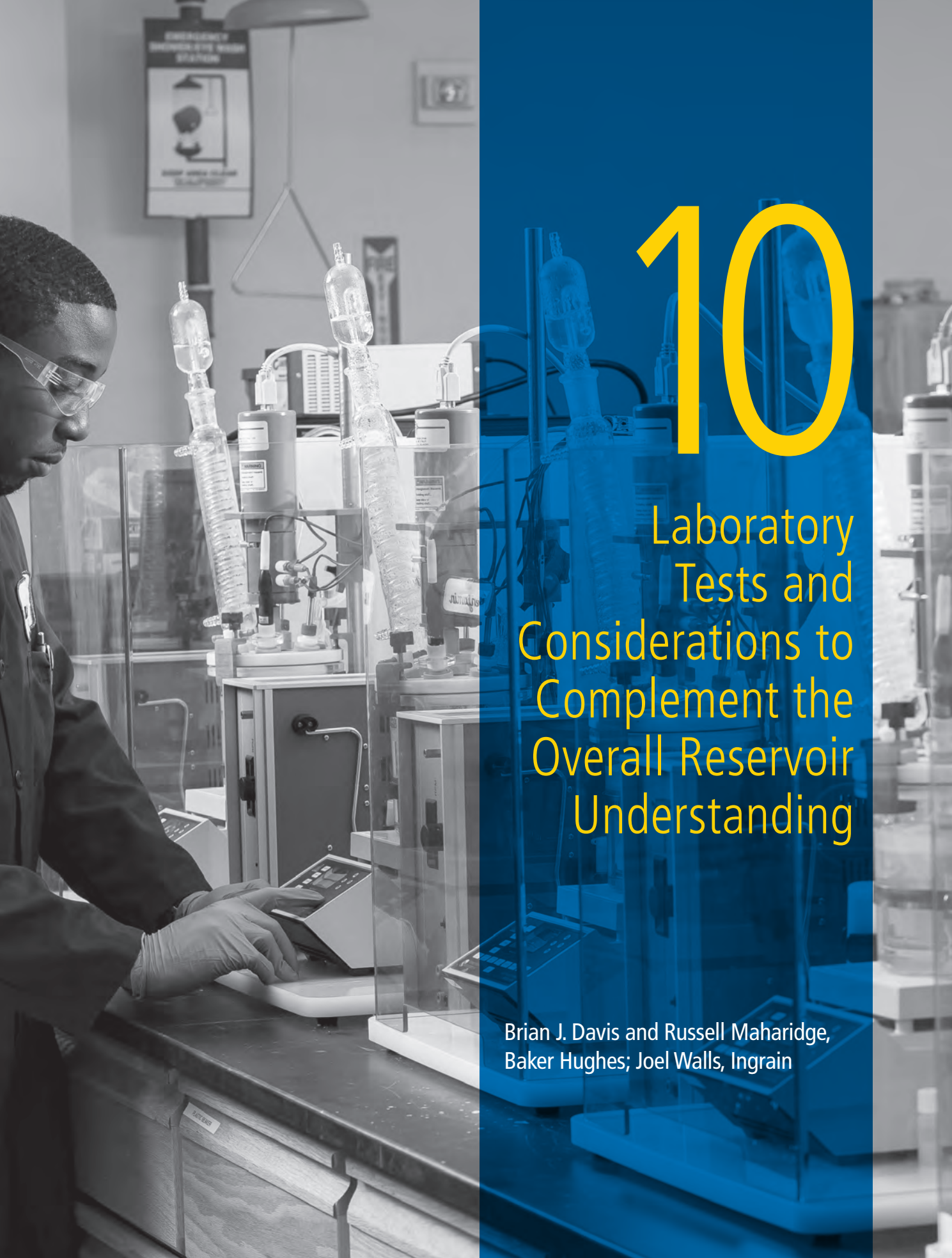

10

Laboratory Tests and Considerations to Complement the Overall Reservoir Understanding

Brian J. Davis and Russell Maharidge, Baker Hughes; Joel Walls, Ingrain

This page intentionally left blank

Chapter 10: Laboratory Tests and Considerations to Complement the Overall Reservoir Understanding

10.1 Introduction

Understanding the reservoir through laboratory analysis and digital rock imaging is one of the building blocks of petroleum reservoir development. This chapter focuses on the measurements and data acquired in the laboratory from unconventional reservoir rock samples and is aimed at characterizing the lithology and measuring the properties needed for reservoir modeling and hydraulic fracture stimulation. One goal of this chapter is to provide overviews of the analytical techniques and digital imaging methods used for specific data types and to discuss the strengths and limitations of each technique. All analytical procedures have limitations; the overviews discuss the impact of those limitations generally in relation to mudstone (also known as shale) reservoirs. As with much of the industry, this chapter includes the analysis of coal-bed methane reservoirs, and tight-gas and tight-oil reservoirs, but the focus is on the analysis of mudstone reservoirs.

10.2 Reservoir Samples for Lab Analysis

A variety of samples is commonly analyzed in laboratories to evaluate petroleum reservoirs and their bounding beds. Samples tested include cuttings, sidewall core plugs, whole core segments, core plugs drilled from whole core segments, formation outcrop samples, and rocks recovered during production from wellbores. **(Fig. 10.1.)**

Each sample type has accompanying pros and cons related to how the samples were obtained, questions about their original location in the reservoir, and the analytical limitations. Upscaling the laboratory data to reservoir scale continues to be a challenge within the industry. The following subsections describe the sample types and address the pros and cons mentioned above.

10.2.1 Drill Cuttings

Well drill cuttings are created during the drilling process by the chipping and/or shearing motion of the drill bit. The cuttings are recovered at the drilling rig from the shale shakers by a mudlogger, who does a variety of analyses on subsamples before archiving the samples for future analysis.

Depths for cuttings are calculated based on mud pump rates and the calculated lag time from drilling to separation on the shale shakers. Therefore, a greater amount of uncertainty is inherent in the recorded cuttings depths compared to samples obtained by coring methods. Cuttings sizes and degree of alteration results from a combination of forces, including hydrostatic pressures, mud weight, penetration rate, and–most importantly–drill bit type. Very large cuttings have been noted from igneous geothermal reservoirs (up to 2 cm by 1 cm by 1 cm) that were drilled with roller cone bits. **(Fig. 10.2.)**

Fig. 10.1—Whole core, core plugs, and cuttings.

Fig. 10.2—Roller cone bit.

At the other end of the spectrum, zones drilled with some polycrystalline diamond compact (PDC) cutter bits can yield particle sizes from silt- to powder-size. PDC bits can also yield rock aggregates that initially appear to be typical cuttings, but, when the cuttings are inspected microscopically, the results reveal that these are actually reconstituted cuttings. The shear forces ahead of the PDC cutter, combined with fluid hydrostatic pressures, cause collapse of the rock and pore network fabric and the immediate recementation of the material into stacked structures reminiscent of vermiculite.

Mineralogically, the resultant samples are a mixture of the sheared formation rock and entrained mud-weighting material. Destruction of the intergranular relationships makes these cuttings unusable for rock and pore network examination by scanning electron microscopy, thin section petrography, or other digital image analysis techniques. **Fig. 10.3** shows an example of these reconstituted cuttings.

Normal cuttings can be used to evaluate mineralogy and fluid compatibility with the capillary suction time (CST) test method. Typically, the mineralogical data must be normalized to remove barite sourced from the drilling mud. If the rock and pore network is undisturbed, scanning electron microscopy analysis on conventional reservoir sandstones provides reasonable insights in terms of intergranular cementation, porosity types, clay types, clay locations, associated potential completion problems, and potential formation damage mechanisms.

Scanning electron microscopy analysis of mudstone cuttings provides relatively limited insight due to the generally small size of the cuttings and the nanopore size range of mudstone porosity. It is possible to gain insight into lithology, microbedding, and degree of bioturbation, but these analyses are better conducted on core samples.

10.2.2 Conventional Whole Core

Conventional coring operations utilize hollow bits with integrated core-catchers and inner barrels to obtain continuous full-diameter cores. Typical core barrels are built in 30-ft. and 60-ft. lengths, and use steel, aluminum, or fiberglass inner barrels to containerize the core. In brittle or heavily fractured reservoirs that tend to jam the core barrel and limit recovery, telescoping sleeves can be used that allow multiple jams to occur during a coring run before the core barrel is retrieved to the surface, which increases core recovery. Core diameters range from 2 in. up to 6 in. The most popular diameters are 3½ in. and 4 in.

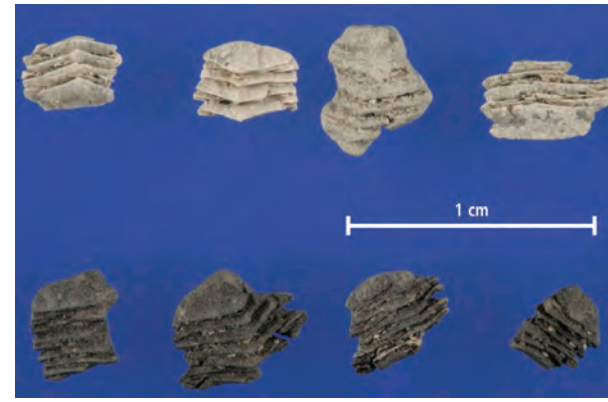

Fig. 10.3—Reconstituted cuttings.

Gamma ray profiles are collected for the cored interval in the laboratory. The profiles are used for correlation with the true vertical depth (TVD) measured downhole by wireline petrophysical tools. Depth shifts of one to six feet are common.

Commercial core analysis laboratories are capable of measuring basic reservoir properties (porosity and permeability) of full-diameter segments, following lengthy solvent extraction operations to remove residual hydrocarbons. The tested samples typically incorporate ½ to ¾ of each 1 ft. of core. This is typically conducted on carbonate lithologies, where vertical lithological variability and natural fracture occurrence makes data generated on core plugs non-representative in these heterogeneous reservoirs. Full diameter permeabilities are measured in two directions (0° and 90°), with the higher measured value designated K_{max}. Full diameter analysis is not normally conducted on unconventional reservoir cores, due to the lengthy preparation or analytical equilibration times associated with the microdarcy or nanodarcy permeability levels observed in these ultra-tight cores.

Horizontal (bedding-parallel) and vertical (bedding-perpendicular) core plugs sized at 1-in. and 1½-in. diameters are usually drilled from whole core segments for laboratory tests that require right-cylindrical core plugs, such as rock mechanical properties, porosity, and permeability measurements. After those tests are complete, the core plugs, endtrims, and whole core carcasses can be used for destructive tests such as mineralogy, scanning electron microscopy, thin section petrography, fluid compatibility tests, and geochemical measurements.

The general rule of thumb is "more rock, better data," which is why, whenever possible, whole core segment analysis is preferred over analyzing the smaller reservoir samples. Lithologically similar "sister samples" can be obtained from whole core segments; core plugs can be drilled in X-axis, Y-axis, and Z-axis directions; and abundant material is available for the variety of analyses that may be required to fully characterize the reservoir.

10.2.3 Sidewall Core Plugs

Percussion sidewall coring was originally developed as an oil-finding tool for immature, porous, and/or permeable conventional sandstones. Analytical techniques were created to calculate porosity and fluid saturations, and empirical correlations were developed to generate permeability values with inputs such as calculated porosity, grain size, sorting, shalyness, and saturated sample density. In well-cemented sandstones, carbonates, and shales, the high degree of rock induration results in the energy of the percussion sidewall bullet causing the rock to either shatter, or the bullet to bounce off the formation face, yielding no recovery. Percussion sidewalls are therefore rarely attempted in unconventional reservoirs.

Rotary sidewall core plugs are routinely obtained from unconventional reservoirs (**Fig. 10.4**). Based upon open-hole wireline petrophysical data, depths are selected for coring. Standard coring bit sizes are 1 in. or 1½ in. in diameter, and are obtained with a computer-controlled, electronically powered coring device via wireline. A maximum of 60 samples can be taken per coring run. Core plug quality is generally very good, although the 1½-in.-diameter core plugs are typically limited to a maximum length of 2½ in.

Compared to drill cuttings or percussion sidewall cores, rotary sidewall core plug locations are well established, and alteration of the rock fabric by the coring process is minimal. All of the analyses discussed in Section 10.5 can be performed on rotary sidewall core plugs, including rock mechanical property measurements.

Fig. 10.4—Rotary sidewall coring tool.

10.2.4 Outcrop and Quarried Samples

Quarried blocks and outcrop samples are used as analogs for testing where core material is unavailable, or if there is insufficient comparable core material available. Commonly, core plugs drilled from quarried formations, such as the Berea sandstone, are used in comparative tests like regained permeability evaluations. The analyses discussed in Section 10.5 can be conducted on these samples, but the degree of weathering and/or oxidation of the outcrop samples should be taken into consideration when relating the data to deeply buried sediments.

10.2.5 Produced Samples and Cavings

Although somewhat unusual, formation materials can be analyzed that have been obtained by bailing, fishing operations, or produced to the surface along with hydrocarbons.

Limiting factors in this analysis are the unknown depth that the samples originated from, and the generally small size of the rock chips. In the case of a horizontal fishing operation, a hollow overshot tool generated a short core, plus or minus 1 ft. long, with a diameter of 4¾ in. that was suitable for a wide variety of tests, since it was essentially a short, horizontal whole core segment.

10.3 Unconventional Rock Types

This book is primarily focused on mudstone reservoirs commonly referred to as shales, but other unconventional reservoirs include coalbed methane zones, tight oil reservoirs, tight gas and oil sandstones, and tight gas and oil carbonates.

10.3.1 Coalbed Methane

Coalbed methane (also known as coal seam gas) reservoirs are classified as unconventional reservoirs due to their dissimilarity from conventional sandstone and carbonate reservoirs. The majority of the methane in the reservoir is stored as gas adsorbed on the carbon matrix, rather than in interparticle pores. Coals are classified into four main types, or ranks, depending on the amount and type of carbon and producible heat energy. Coal ranks are a function of the amount of pressure and heat the coal was subjected to during deep burial. Lignite is the lowest coal rank, tending to be a relatively young coal deposit containing only from 25 to 35% carbon. Sub-bituminous coals typically contain from 35 to 45% carbon, while bituminous coals contain from 45 to

86% carbon, and the highest rank (anthracite) contains from 86 to 97% carbon (Energy Information Administration—EIA 2011). Generally, increasing carbon content translates to increased methane storage capacity, which is why most coalbed methane production is from bituminous or anthracitic coal zones.

A short list of nations with producing coalbed methane zones includes Australia, Canada, China, India, and the US (with multiple sedimentary basins). Frequently, coalbed methane zones are interbedded with shales, siltstones, and sandstones, which may provide additional hydrocarbon storage capacity and reserves. In comparison to the other types of unconventional reservoirs, coals are typically much more porous and permeable. The natural fracture overprint, referred to as the cleat system, is the dominant pathway for the movement of fluids within coal reservoirs.

Cleats develop initially during coalification in response to coal shrinkage associated with moisture loss, while cleats in higher rank coals develop in response to local and regional tectonic stresses. Details of this process were detailed in Chapter 9 on geomechanics. Moisture loss involves rearrangement of the coal structure rather than simple loss of interstitial water. Cleat spacing decreases with increasing coal rank because of continued loss of molecular water and volatile components. **Fig. 10.5** shows the end of a 2½-in.-diameter whole core segment, illustrating the well-defined cleat system in this anthracitic coal zone. "Face" and "butt" cleats are visible generally at right angles, creating a well-developed natural fracture overprint on the matrix. **Fig. 10.6** shows a thin section of a carbonate-rich coal sample that has been vacuum-impregnated with blue-dyed epoxy, filling the complex cleat system.

Fig. 10.5—Coal cleat system.

Coalbed methane reservoir permeabilities during depletion are affected by several factors: decreased permeability due to an increase in effective stress, and increased permeability due to coal matrix shrinkage as methane desorbs from the carbon. In shallow coalbed methane reservoirs where overburden stresses are moderate and reservoir pressures are low, coalbed methane permeabilities tend to increase during depletion.

10.3.1.1 Wet Coalbed Methane Zones

Coal is deposited in freshwater or brackish environments. With deep burial and coalification, compaction and generation of gases by biogenic and thermogenic processes expulses most of the water phase, and in most cases the coal becomes oil-wet. In cases where regional uplift and erosion occurs, the coal bed and adjacent sedimentary strata can be exposed to the surface, resulting in meteoric recharge of the zone, leading to high water saturations. Production from these water-saturated coals initially involves dewatering the coal to reduce zonal pore pressure, which results in desorption and diffusion of the methane from the coal matrix into the cleat system. Initial production, in some cases for extended periods, may be almost 100% water. Intermediate production may include both water and gas, before moving toward single-phase gas production.

10.3.1.2 Dry Coalbed Methane Zones

In cases where the coal zones remain deeply buried and not in direct contact with meteoric water sources, the residual water saturations are low and minimal water is produced. Dry coalbed methane reservoir's wettabilities tend to be

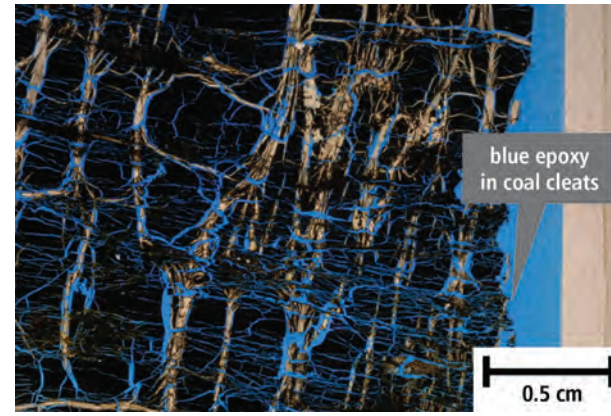

Fig. 10.6—Complex coal cleat system.

more strongly oil-wet than those noted in wet zones. Dewatering is seldom required since the water saturations are low, but dry coalbed methane zones are susceptible to treatment fluid water blocks due to relative permeability losses associated with capillary imbibition.

10.3.2 Tight Gas and Oil Zones

With advances in the 1980s in hydraulic fracturing modeling and treatment designs, the petroleum industry began targeting reservoirs with permeabilities significantly lower than was typical of conventional reservoirs. The predominant focus in the 1980s and 1990s was on tight gas reservoirs, typically sandstones with permeabilities in the microdarcy range. Increased oil prices (from $40 to $50—and more—per barrel) during the mid-2000s improved the economics of tight-oil production. This prompted operators to begin targeting formerly uneconomic reservoirs, both in siliciclastics and in carbonates. Extended-reach horizontal laterals and multistage hydraulic fracturing designs dramatically increased production rates in comparison to single-stage, vertical wellbores.

10.3.2.1 Sandstones and Siltstones

With hydraulic fracturing refinements and government incentives, low permeability, gas-rich sandstones, such as the Cotton Valley and Travis Peak of East Texas; the Morrow Sandstones of southeastern New Mexico and Oklahoma; Frontier, Muddy, Frontier and Dakota sandstones in Rocky Mountain basins; and the Cardium sands in Alberta were targeted early for development. The oil-bearing, clay-rich Wilcox sandstones of southwestern Louisiana have recently been developed, despite their low mobility ratios, with horizontal drilling and multistage hydraulic fracture treatments. Much of the North Dakota oil and gas production from the Bakken shale is actually from dolomitic siltstones within the middle member of the Bakken, as are the siltstones in the Montney shale in Alberta.

10.3.2.2 Carbonates

An example low-permeability carbonate that experienced development in the 1980s was the oil-bearing, naturally fractured Austin Chalk of East Texas. Oil-rich carbonates currently under development include the Lower Smackover Brown Dense Limestone of East Texas, and the Mississippian limes and cherts of north-central Oklahoma.

The play that started the current industry focus on shales was the Barnett shale of North Texas. The success in the Barnett led to a search by the industry for the "next Barnett." However, the petroleum industry has learned that "all shales are not created equal" when it comes to successful exploration and development.

10.3.2.3 Mudstone Classification

Given that mudstones are classified according to their size fraction (clay- and silt-sized particles < 62.5 microns) rather than their mineralogy, there is tremendous variability in mudstone mineralogies, primarily as a function of the original depositional environment.

Fig. 10.7 shows a ternary diagram of mineralogical compositions, which illustrates the dissimilar data trends in these six US mudstone reservoirs. For reference, the Barnett shale of North Texas composition is generally one-third clay, one-third carbonate, and one-third quartz plus feldspar. This plots slightly below the visual center of Fig. 10.7. Multiple classifications have been created by the petroleum industry and academia to address the various mudstone types, with category names such as silica-rich argillaceous mudstone, carbonate-rich siliceous mudstone, and clay-rich carbonate mudstone.

10.3.2.3.1 Silica-Rich Mudstones

Mudstone reservoirs recognized as being dominated by silica include the diatomite reservoirs of the Monterey shale in California, the siltstones within the Middle Member of the Bakken shale, and the Woodford of south-central Oklahoma. The Monterey shale includes highly argillaceous zones, clean diatomite zones, dolomitic zones, immature opal-rich zones, and porcelanite zones. The cleaner diatomite zones may have porosities in excess of 50%, due to the detrital fossil fragments (diatoms, radiolarians, foraminifera) being porous, yet the permeabilities are still very low due to the clay-sized nature of the fossil fragments. **Fig. 10.8** shows a scanning electron microscope view of a highly porous fossil hash from a San Joaquin Valley Monterey shale.

10.3.2.3.2 Carbonate-Rich Mudstones

Carbonate-rich mudstones targeted by the North American petroleum industry include the Eagle Ford shale of south Texas, the Utica/Point Pleasant shale of Ohio, and the Niobrara shale in the Denver-Julesburg basin of Colorado. The Eagle Ford has also been targeted in East Texas, but less successfully, at least in part due to the higher ductility related to the higher clay contents in East Texas.

An example of mudstone variability, even within the same formation in the same geographic area, is the Niobrara

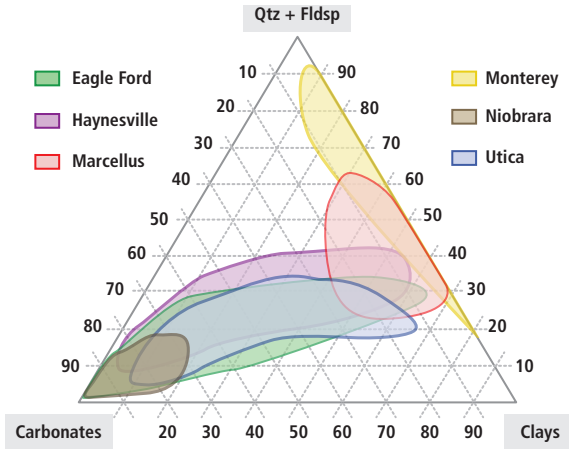

Fig. 10.7—Mineralogy ternary diagram.

formation in northeastern Colorado. The Niobrara is composed of three chalk benches sandwiched between argillaceous mudstone members. The clean chalk zones are composed primarily of extremely fine-grained carbonate fossil debris, including coccoliths, calcispheres, foraminifera, and broken fragments of each (similar to **Fig. 10.9**). The most productive zone, the B chalk bench, has the highest calcite content and the lowest clay content. The argillaceous C chalk bench exhibits a higher average clay content (12%), and is generally not targeted for production.

10.3.2.3.3 Clay-Rich Mudstones

Several clay-rich mudstones are also being targeted by the petroleum industry with variable success. The original depositional environments yielded clay mineral contents greater than 40%, and in many cases approaching 60%. Examples include the New Albany shale of the Illinois Basin, the Marcellus shale of the Appalachian Basin, the Tuscaloosa Marine shale of southwestern Mississippi, the Lower Bakken source-rock mudstones, and the Eagle Ford shale in the East Texas Basin. The dominant clay-type in these reservoirs is illite, or a mixed-layer illite/smectite with relatively low expandability. The high clay content of these formations is generally thought to increase the reservoir ductility, although all of these clay-rich mudstones contain natural fractures and are hydrocarbon-productive.

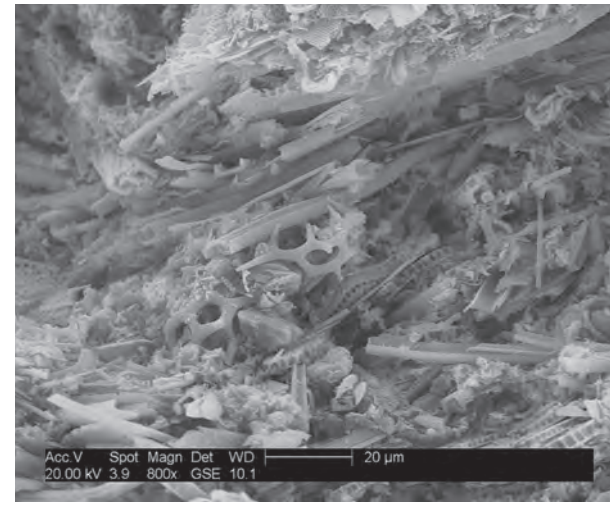

Fig. 10.8—Monterey diatomite.

10.3.3 Nano-Perm Mudstone Reservoirs

Increased horizontal drilling and hydraulic fracturing efficiencies, together with improved hydrocarbon prices, has led to the development of mudstone oil and gas zones that were previously considered too tight for economic production. These mudstone formations are the source of hydrocarbons, seal, and reservoir. The oil and gas currently in these mudstones are the remnants of the hydrocarbons that were thermogenically generated at depth, but were either adsorbed on, and in, kerogen macerals, or trapped in nano-sized pore spaces that prevented their expulsion into shallower reservoirs.

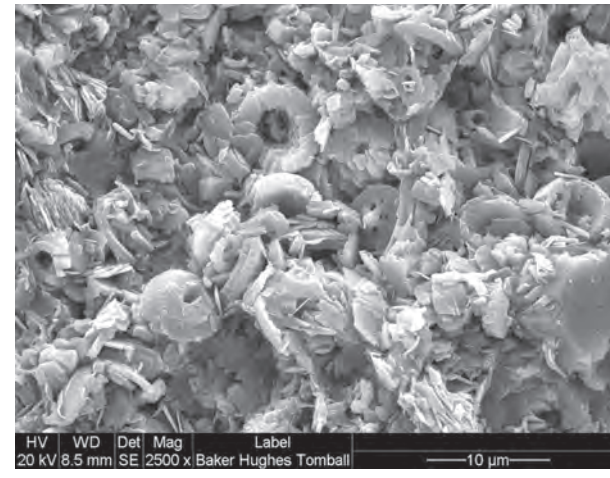

Fig. 10. 9—Coccolith fragments in clean chalk.

Mudstones are very fine-grained sedimentary rocks, of which the original constituents were clays or muds. Grain size can be up to 0.0625 mm (0.0025 in.) with individual grains too small to be distinguished without a microscope. Mudstones are formed from the compaction of silt and clay-sized mineral particles commonly called mud. Mudstone refers to the rock's average particle sizes, not the mineralogical composition, since many mudstones have clay compositions less than 25%.

10.3.3.1 Shale Versus Mudstone

The term ***shale*** is generally used to name formations of very finely grained rocks, similar to how rocks with sand-sized grains are called sandstones. The formation name is used as a geological nomenclature, rather than a description of the litho-type.

With increased overburden pressure at burial depth, platey clay minerals may become aligned, and display the appearance of fissility or parallel layering. This finely bedded material that splits readily into thin layers is called shale, as distinguished from mudstone. Unfortunately, fissility either can be a function of weathering in outcrop locations, or induced by extended core storage intervals. The designation mudstone is more consistent with standard naming conventions for siltstone and sandstones, since the categories are a function of grain size, rather than other physical attributes.

The lack of fissility or layering in most mudstones may be due either to original texture or to the disruption of layering by burrowing organisms in the sediment prior to lithification. The petroleum industry is currently targeting mudstone formations in the US such as in the Barnett, Niobrara, Monterey, Eagle Ford, Bakken, Marcellus, and Wolfcamp; in the Vaca Muerta in Argentina; and the Posidonia in Poland. All of these fine-grained formations are named as shales, but are classified as mudstones.

10.4 Core Preservation

This section discusses the need for core preservation, and describes different types of core preservation techniques commonly used at the well site and in the laboratory. Clay mineral desiccation is the most commonly encountered effect of inadequate preservation, which effects fluid saturations and basic rock property measurements. **(Fig. 10.10** shows an example from the other end of the spectrum.) In a study of a highly permeable conglomerate core stored in a

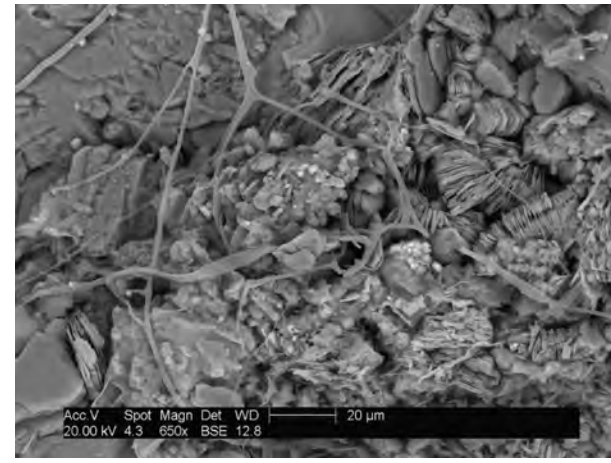

Fig. 10.10—Fungal growths inside a conglomerate core.

humid tropical environment, scanning electron microscopy examination revealed filaments of fungal hyphae, including asexual reproduction structures that had grown in the interior of the 4-in.-diameter core. **Fig. 10.11** shows a second example where iron- and chlorine-rich growths were observed inside a porous sandstone.

10.4.1 Preservation Purposes

Data generated from core samples can be negatively affected if the core is not preserved to some extent on arrival at the surface and afterwards during storage. However, not all analyses are affected by poor preservation; mineralogy is generally not influenced by inadequate preservation with a few exceptions. Measurements that can be drastically effected include post-coring residual saturations,

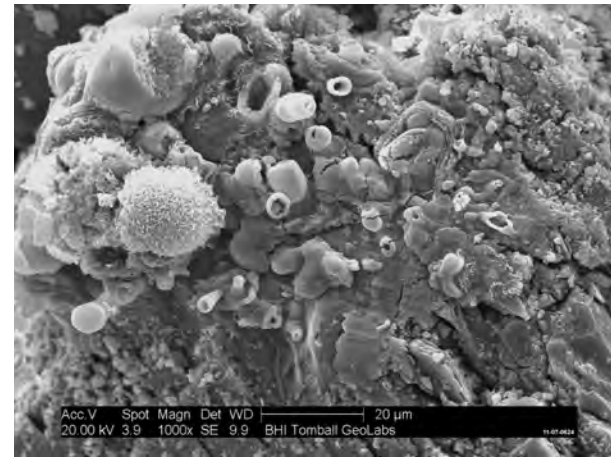

Fig. 10.11—Iron-chlorine rich growths inside sandstone core.

permeability measurements on clay-rich or shale-laminated sandstones, and both permeability and mechanical property measurements on softer sediments.

The goals of preservation vary with the planned analyses. Generally, the goals include limiting desiccation, preventing mechanical damage in soft sediments, preventing residual oil oxidation, and stabilizing the core for transport to laboratory facilities.

10.4.2 Wellsite Preservation Techniques

Well drill cuttings are typically retrieved from the wellsite shale shaker, rinsed to remove the majority of the drilling mud contaminants, dried, and archived in paper envelopes. Residual water is removed during the drying process, with only non-volatile oil fractions being retained in the cuttings. Laboratory testing of cuttings is generally limited to mineralogical analysis and fluid compatibility tests, although new digital imaging and computerized scanning electron microscopy elemental data acquisition techniques have been recently developed.

Rotary sidewall core plugs are retrieved from the tool by the coring engineer and wrapped in a clear plastic film (made out of polymers with very low permeability, created to preserve food). Sometimes an outer wrap of aluminum foil is added over the plastic, and then the core plug is sealed inside a glass jar with the appropriate sample identification information. The jars are then placed in segmented cardboard boxes for transport to the laboratory. Residual saturations are preserved by the sealed bottle; therefore, the Dean Stark solvent extraction, combined with helium porosity measurements, allows the calculation of oil and water saturations. If residual saturations are not to be determined, mechanical properties can be determined on the core plugs in their partially saturated state.

Whole core segments are also commonly wrapped at the wellsite with a layer of clear plastic film, followed by a layer of aluminum foil. Both layers provide a vapor barrier to some extent, but the plastic film becomes brittle with age, and exposing the aluminum foil to brine salts and oxygen leads to corrosion and/or oxidation of the aluminum, which in turn may lead to alteration of the core's wettability.

Another wellsite and laboratory preservation technique involves first wrapping the core sample in plastic wrap and aluminum foil, and then briefly suspending the wrapped core in a vat of melted paraffin-based or low-temperature (350°F) melted, strippable plastic. The segment is removed from the vat and allowed to cool suspended from a drying rack. The string or wire used to suspend the sample is trimmed, and the segment can be labeled. **Fig. 10.12** shows examples of the plastic-based and paraffin-based coatings.

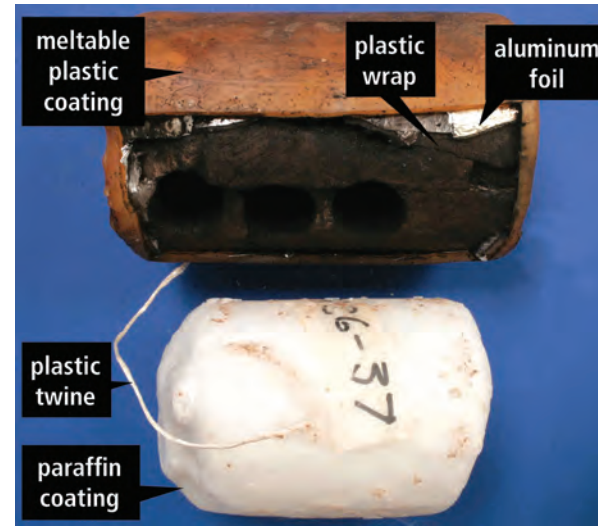

Fig. 10.12—Meltable coatings on core segments.

Problems that can be encountered with this technique included incomplete coatings, moisture wicking out of the core through the string and at the wire opening, and degradation of the plastic wrap and aluminum foil during lengthy storage.

Heat-sealable, laminated aluminum, polyethylene, and polyester tubes, sheets, and pouches were developed for the food industry and for the military. These products provide effective mechanical strength with a vapor barrier for food preservation. These aluminum and plastic materials have been adapted by the petroleum industry for core preservation to prevent desiccation of core and wettability alteration. This approach has also been used to preserve 3-ft.-long whole core segments, which are loaded into standard 3-ft.-long core boxes for transport from the wellsite to the laboratory. Problems encountered with this technique were due to the brittleness of the laminate, which was frequently punctured by sharp rock surfaces, and by breakage induced by folding the 3-ft.-long pouches into standard core boxes.

Resealable plastic bags with a tab slider or a matching-groove (zipper-type) closure are routinely used at the wellsite as a temporary preservation technique (see **Fig. 10.13**). The bags are opened and placed into 3-ft.-long cardboard core boxes, and then the whole core segments are loaded into the bags prior to sealing. Over short time periods, this is a moderately

Fig. 10.13—Three-ft.-long resealable bag in core box.

effective vapor enclosure, but should not be considered a long-term storage option. The ability to reseal the bags degrades quickly after several episodes of opening and closing, with accompanying core desiccation associated with evaporation of mobile water, irreducible water, and clay-bound water.

Core barrels may incorporate steel, aluminum, or fiberglass inner barrels to encapsulate the core during the coring process, and minimize core jamming. The core barrel can be attached to a cradle, which limits bending and other mechanical damage to the core when it is moved to a horizontal position at the wellsite. In soft sediment applications, either an epoxy resin, foam, or a gypsum slurry can be injected into the annular space between the core and inner barrel to stabilize the core. The inner barrel can be cut into 3-ft.-long segments using a chop saw, then sealed with rubber caps using hose clamps or duct tape, as seen in **Fig. 10.14**. This method is effective at preventing mechanical damage to competent cores, and preventing evaporation of core pore fluids. In soft sediment reservoirs, the inner barrel and core are typically frozen at the wellsite to further limit mechanical alteration of the core.

10.4.3 Lab Preservation Techniques

Storage requirements in the laboratory are generally aimed at minimizing desiccation before subsamples are obtained for the various planned analyses. The whole core segments typically remain in the 3-ft.-long resealable bags when used, even when their sealing capacity is diminished by use. Large PVC pipe segments sealed with rubber endcaps are also utilized in the laboratory to preserve whole core segments.

Core plugs drilled from the whole core segments are preserved in a variety of ways, including small resealable plastic bags, and in glass or plastic bottles. As needed, these bottles allow the core plugs to be immersed in brines or oils for long-term storage.

10.5 Laboratory Analyses

Examination and testing of reservoir samples in the laboratory entails a wide variety of measurements and tests, including, but not limited to, lithological descriptions, mineralogical composition, characterization of the rock and pore network and pore-size distribution, characterization of the organic geochemistry and thermal maturity, measurement of basic rock properties (porosity and permeability) and mechanical rock properties (Young's modulus, Poisson's ratio, unconfined compressive strength), and fluid compatibility testing.

10.5.1 Sedimentology

Examination of cores and cuttings generally begins with macroscopic reviews of hand specimens, both at the wellsite and in the laboratory. Broad description categories include color, lithology, texture, accessories, and fractures or partings.

10.5.1.1 Depositional Fabric

In mudstone descriptions, particular emphasis is placed on depositional fabric, since the original fabric in mudstones has a significant impact on ultimate porosity preservation. Documented textural features include attitude of bedding, depositional fabric (microbedding versus bioturbation), grain size, sedimentary structures (pellets, ripples, burrows, silt

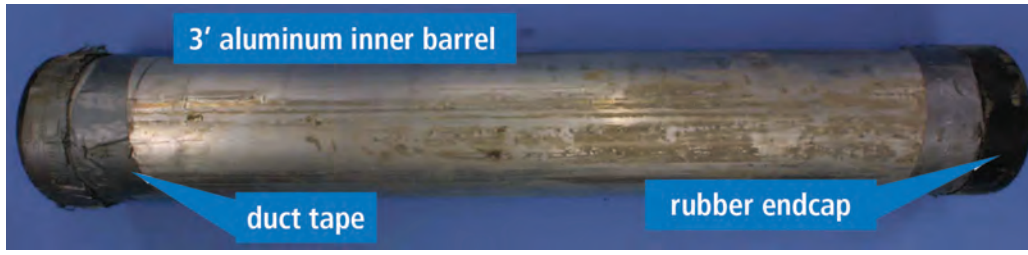

Fig. 10.14—Three-ft.-long aluminum inner barrel.

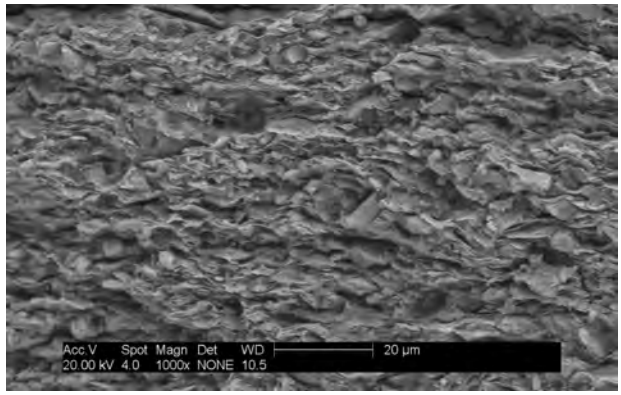

Fig. 10.15—Lenticular microbedding.

laminae, erosional surfaces, fossil concentrations, and lag deposits), accessories (fossils, pyrite), volcanic ash or tuff beds, fractures, and coring-induced partings along bedding surfaces.

Fig. 10.15 shows an example from the Haynesville shale of a mudstone fabric with clay-sized minerals aligned in lenticular, bedding-parallel structures. The bed-parallel fabric is primarily related to the conversion of smectitic clays to illitic clays, with the resulting alignment being perpendicular to the maximum compressive stress.

10.5.1.2 Optical Microscopy

Examination of hand specimens with low-power optical microscopes is essential in garnering an understanding of rock samples from a macro standpoint, and selecting representative samples for analysis. Stereomicroscopes are used from 10-to-50X magnifications to review cut surfaces, but more importantly, to view the freshly broken vertical surfaces of the reservoir. Insights into grain size, sorting, cementation degree and type, porosity, laminations and microbedding, fossil content, and the presence of bitumen are available even at these low magnifications.

Biostratigraphy studies can be conducted via optical microscopy to assign relative ages of sedimentary zones based on the fossil assemblage, and correlate strata between wells. Description of foraminifera, ostracods, radiolarians, inoceramid fragments, pelagic bivalves, and nanoplankton such as coccolithophores yields insights into correlatable units and paleo depositional environments.

10.5.1.3 Computed Tomography Scanning

X-ray computed tomography (CT) uses computer-processed X-rays to produce tomographic images (virtual slices) of specific areas of a scanned object, allowing visualization of the sample's interior. CT X-ray scanning creates a large series of

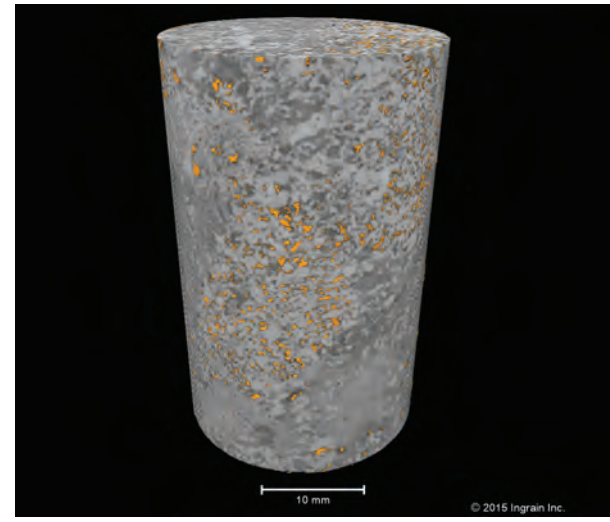

Fig. 10.16—Three-dimensional computed tomography (CT) scan of a carbonate core plug.

two-dimensional "slices" that can be processed to generate a three-dimensional image of the sample. CT scanning was originally used in the petroleum industry for unconsolidated sandstone reservoirs where the core is encased in an inner core barrel to identify coring-damaged areas and align the core barrel prior to core plugging so that drilled core plugs did not cross bedding planes or shale laminations. CT scanning of core samples allows the identification of lithological types, fractures (natural and coring-induced), bedding, burrows, and fossils in whole core segments, allowing avoidance of mechanical defects or other features when core-plugging locations are selected. When scans of whole core segments are unavailable, Micro-CT scans such as **Fig. 10.16** can be conducted on core plugs to perform screening prior to laboratory measurements to ensure data is generated on representative samples.

Animated images similar to the screen-captured image seen in **Fig. 10.17** can be created using CT imaging, allowing review of the pore network within a core plug from various angles as the image rotates.

Whole core samples can also be imaged by a dual-energy X-ray CT method that provides several key advantages for organic mudrocks, including quantitative bulk density and photoelectric factor (PEF). The principles of this method were published by Vinegar and others in a series of papers beginning in the 1980s (Vinegar, 1986; Coehen and Maas, 1994). However, commercial use of the technology for unconventional resource evaluation was first reported by Walls et al., 2011. This paper showed whole core dual-energy data from an Eagle Ford shale well in which the combination of bulk density and PEF was used

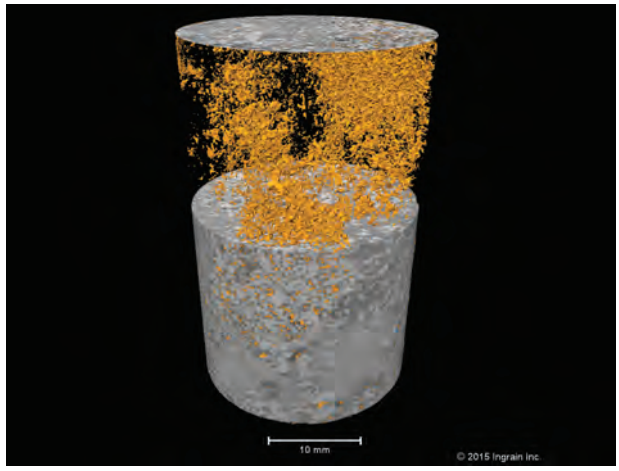

Fig. 10.17—3D computed tomography pore network image.

to find the best reservoir quality intervals. Since this time, at least 100,000 linear feet of whole core, mostly shale, has been imaged using the dual-energy X-ray CT method.

10.5.1.4 Natural Fractures and Fracture-Healing Minerals

The natural fracture overprint in nanodarcy reservoirs is one of the primary controls on reservoir productivity. Natural fractures in these reservoirs are rarely observed as open fractures, but are frequently noted in core samples as "healed" fractures. The natural fractures remain as planes of weakness throughout the reservoir that are believed to dilate during hydraulic fracturing if intersected by the treatment fluid/pressure.

10.5.1.4.1 Vertical Fractures

Vertical fractures in full diameter core segments observed in the laboratory range from commonly none, to the high-density fracture swarm visible in the mudstone sample seen in **Fig. 10.18**. Fourteen distinct calcite-healed vertical natural fractures were noted in this 4-in.-diameter core, all exhibiting the same trend through the mudstone matrix.

Occasionally, as seen in the microscopic photographs in **Fig. 10.19** and **Fig. 10.20**, natural fractures are noted in well drill cuttings. Both of these images are of Barnett shale cuttings from North Texas; the image with the dark background shows an iron-rich dolomite as the dominant fracture-fill, with individual pyrite crystals generally precipitated in the center of the fracture-healing material. The blue-background image shows calcite healing variably sized natural fractures, including a crosscutting fracture in one cutting.

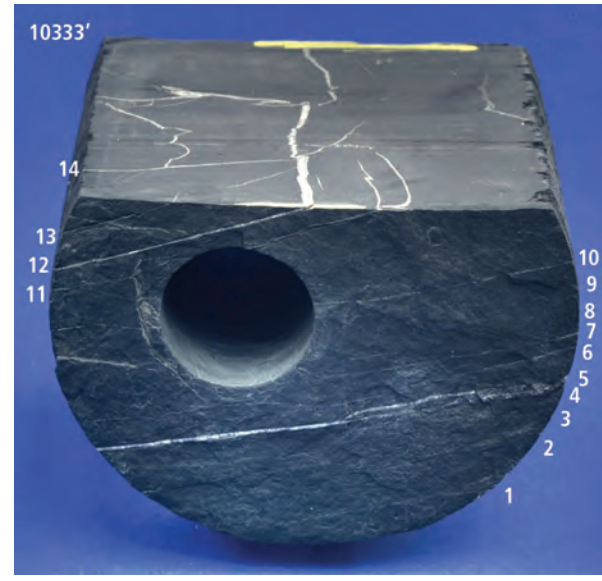

Fig. 10.18—Marcellus fracture swarm.

10.5.1.4.2 Bedding Parallel Veins of Fibrous Minerals—Horizontal "Beef"

Bedding-parallel natural fractures (beef) are observed throughout portions of the Haynesville shale formation of northwestern Louisiana and are documented in many other mudstone formations. "Beef" is very common in the Vaca Muerta formation in the Neuquén Basin of Argentina. The term "beef" originates from references to this horizontal fracture mineralization in the Dorset, England, area circa 1830s, when the calcite fibers were compared to fibers visible in animal musculature. The calcite crystals seen in the natural fracture visible in **Fig. 10.21** grew in cone-in-cone structures perpendicular to the original bedding planes, and

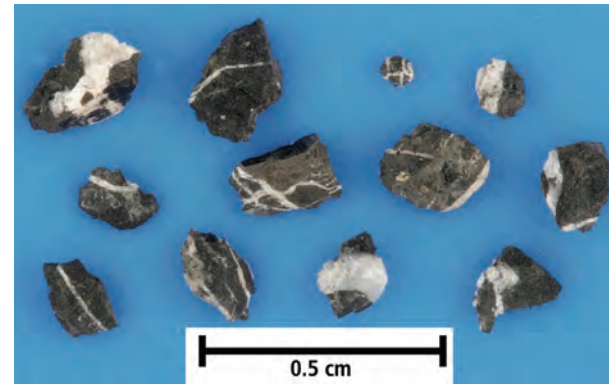

Fig. 10.19—Barnett shale cuttings, calcite-healed vertical fractures.

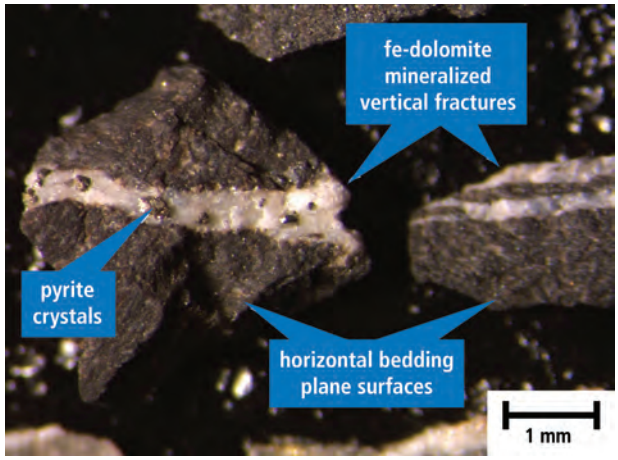

Fig. 10.20—Barnett shale, Fe-dolomite healed vertical natural fractures.

are believed to be evidence for fluid overpressure during compaction and hydrocarbon generation. The thickness of these fractures varies from microscopic to greater than six inches, with layering inside the mineralized fractures evidence of multiple cycles of precipitation.

10.5.1.4.3 Fracture Orientation Analysis

Oriented coring yields full diameter cores with known north-south and east-west orientations throughout the cored interval. As the core moves vertically past the drill bit and into the core barrel, three inward-facing tungsten blades in a shoe adjacent to the coring bit act as knives to cut three grooves (scribe marks) on the exterior of the core. The knives typically cut in an asymmetrical pattern with the groove that is offset from the other two grooves referred to as the primary groove. The direction of the primary groove can be determined by correlation with an electronic multi-shot survey instrument's time-stamped measurement of geographic or magnetic north. Multiple surveys are taken during coring to allow orientation of the entire interval, despite periodic breaks in the core's continuity caused by breakage or spinning along bedding surfaces.

A core orientation frame—or goniometer—is used in the laboratory to determine the dip and strike of the sedimentary strata, and any fractures visible in the core. Natural fractures can be vertical, subvertical, and horizontal (bedding-parallel).

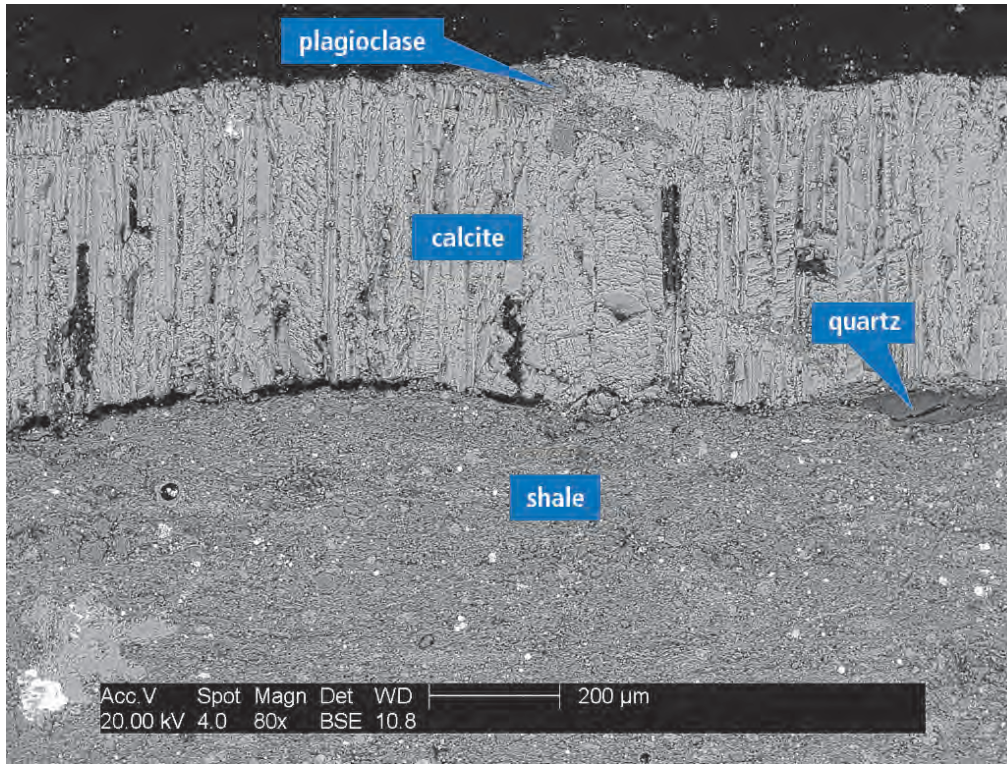

Fig. 10.21—Horizontal calcite-healed natural fracture.

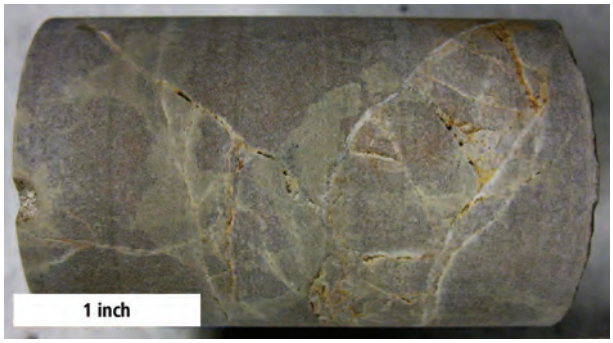

Fig. 10.22—Healed and open natural fractures.

Discriminating between coring-induced and natural fractures is essential. Natural fractures may or may not exhibit partial-to-total mineralization. **Fig. 10.22** shows a heavily fractured, quartz-cemented sandstone core plug containing both mineralized and partially open natural fractures.

10.5.2 Porosity

Over the last twenty years, the petroleum industry has become aware that storage capacity in mudstones is difficult to measure accurately, and is located in multiple pore types, including: interparticle pores, intercrystalline pores, intraparticle pores, phyllosilicate pores, organophyllic pores, and as adsorbed hydrocarbons in both porous and nonporous kerogen. The section below describes different porosity measurement techniques, their strengths, and their limitations. **Fig. 10.23** compares grain sizes, pore sizes, and porosity measurement techniques.

10.5.2.1 Helium Porosity on Core Plugs

Core plugs drilled from whole core segments are typically sized at 1 in. diameter by 2 in. long, or 1½ in. diameter by up to 3 in. long. These core plugs are typically drilled in a horizontal

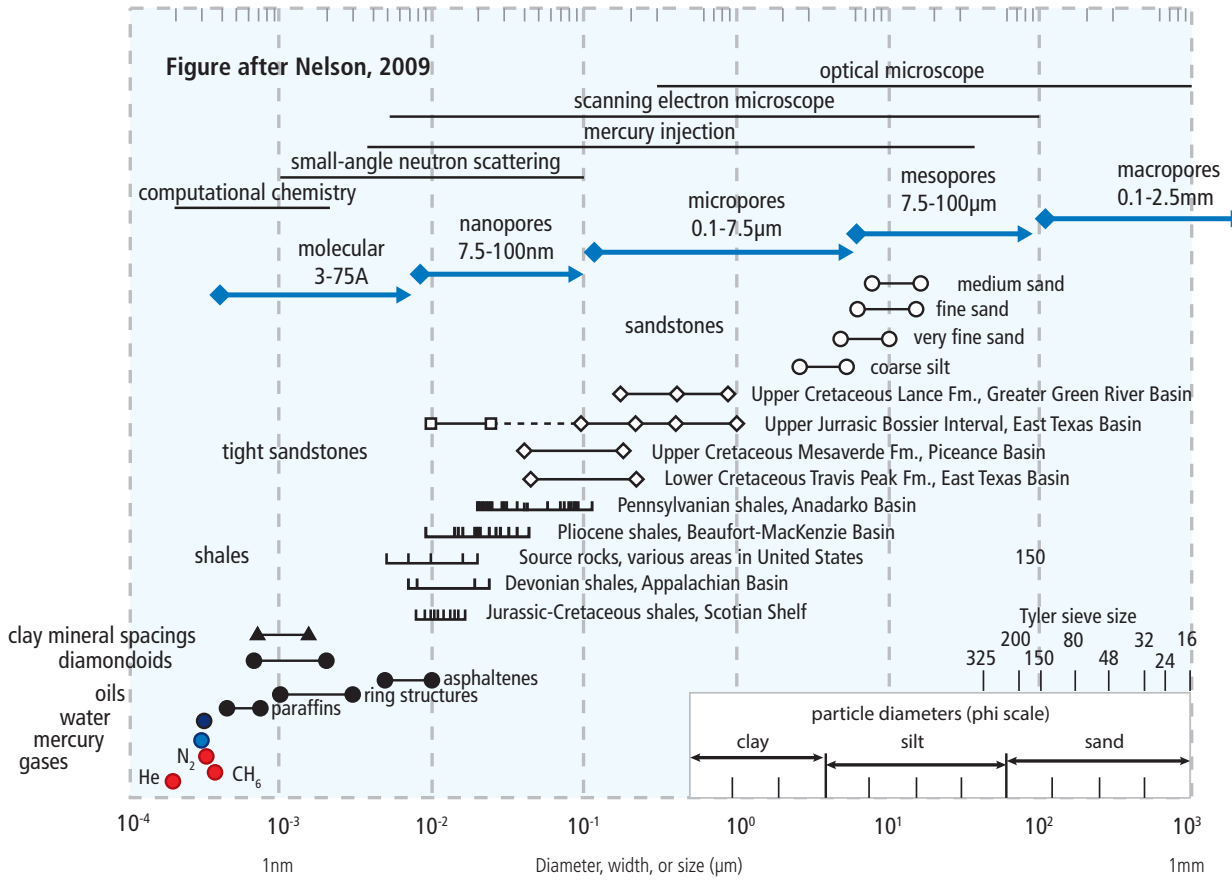

Modified from Nelson, AAPG Bulletin 93, 2009.

SPE 162612 J-H Chen, Georgi, J Chen, and Yang, Petrographic Features of Kerogen in Unconventional Shales and Their Effect on Hydrocarbon Petrophysics, 2012.

Fig. 10.23—Comparison of pores sizes and measurement techniques.

(bedding-parallel) orientation, but can also be drilled vertically (perpendicular to bedding). Following extraction to remove residual hydrocarbons and drying to remove the residual water saturation, dry weights are determined. Grain volumes are measured in a Boyle's law helium matrix cup, or pore volumes can be measured in a coreholder. Calculated grain density is used as a quality control measure on the grain volume measurement. Exterior bulk volumes are either calculated from calipered dimensions, or measured by Archimedes displacement techniques in selected liquids (typically mercury). Porosity data are calculated using the available bulk volume, grain volume, and/or pore volume data.

Difficulties in obtaining accurate porosity/permeability data on 1-in. and 1½-in.-diameter core plugs from ultra-tight reservoirs was recognized, due to the lengthy pressure stabilization periods and the low surface area to mass ratios when testing core plugs. This led to the development of the GRI technique discussed below.

10.5.2.2 Helium Porosity and Permeability on Crushed Samples

In the late 1980s and early 1990s, under the supervision of the Gas Research Institute—renamed the Gas Technology Institute, or GRI—a technique was initially developed for siltstones in Devonian shales of the Appalachians to determine porosities for nanopermeability-type rocks. The weight and Archimedes bulk volume (in mercury) of a fresh, irregularly shaped core sample are measured to allow calculation of bulk density. Approximately 300 grams of fresh core material are then crushed to yield 20/35 mesh rock pebbles, which are extracted for approximately one week by the Dean Stark technique. Following extended drying, the grain volumes are determined on the 20/35 mesh pebbles in a helium porosimeter, allowing calculation of porosity, grain density, and residual saturations. Utilizing helium in a computerized pressure-decay permeameter, the matrix permeability is also determined on the 20/35 mesh pebbles.

Several limitations are associated with this technique. If the samples are from a mudstone in the oil window, the Dean Stark solvent extraction process appears to remove oil from the kerogen macerals, yielding excessively high helium porosities. In addition, Dean Stark analysis measures sample water volume, which may include mineral-bound water in addition to pore water. Successfully measuring kerogen micropore porosity in thermally mature samples from the gas window by helium injection is questionable. Additionally, both the porosity and permeability data are generated on unconfined samples, probably yielding porosity and permeability values that are higher than those present in the reservoir. The poor permeability-to-porosity relationships generated with this approach on mudstones are believed to be—at least partially—a relic of the measurement techniques.

10.5.2.3 High-Pressure Mercury Porosimetry

Mercury porosimetry is a laboratory technique used to measure pore sizes and volumes on porous materials. The procedure involves the progressive intrusion of mercury into porous rock samples by gradually increasing the pressure on a mercury-filled sample chamber that contains the tested rock sample. Pore volumes, pore size distributions, and total porosity are calculated. Mercury is a non-wetting liquid that, due to its high interfacial tension, will not imbibe into a rock sample's pores unless sufficient pressure is used to inject mercury into the pores. The Washburn equation is used to relate injection pressures to pore diameters. High-pressure (60,000 psia) mercury porosimetry is commonly utilized in testing of mudstone reservoirs due to the extremely small pores and pore-throat sizes in mudstones.

Mercury porosimetry is performed on dry samples; the drying process may alter the pore structures in clay-rich mudstones, possibly yielding excessively high porosities. In contrast, since pore diameters smaller than 3 nanometers are not detectable by mercury porosimetry, the smallest pores in mudstones may not be included in calculated porosity values.

10.5.2.4 Small-Angle and Ultra-Small-Angle Neutron Scattering

Small-angle (SANS) and ultra-small-angle neutron scattering (USANS) units probe structures in materials on the nanometer (10-9 nm) to micrometer (10-6 nm) scale, which covers all the pore sizes common to mudstones. This capability is typically available at large government-supported laboratories, in countries such as France, Canada, and the US. SANS and USANS measurements are performed by the petroleum industry to characterize the range of pore sizes present in reservoir samples, calculate total porosities, and understand their connectivity. SANS and USANS porosity values tend to be systematically higher than helium porosity or subcritical gas adsorption values, possibly due to the gas measurements not accessing all micropores.

SANS and USANS experiments run at ambient pressure; therefore, the relief of overburden pressure may result in measured porosities higher than present in the reservoir. Due to the high facility and equipment capital expenses related to this equipment, only a handful of the SANS and USANS units are available, such as at the Oak Ridge National Laboratory

in Tennessee or the National Institute of Standards and Technology in Maryland. An extended wait (sometimes over one year) for access to the equipment is common.

10.5.2.5 Subcritical Gas Adsorption

Subcritical nitrogen (N_2) and carbon dioxide (CO_2) gas adsorption studies are used to provide specific surface area evaluation of materials by nitrogen multilayer adsorption, below the effective range of mercury intrusion porosimetry. A fully automated analyzer employs the BET method (Brunauer, Emmett and Teller) to determine pore area and specific pore volume using adsorption and desorption techniques. At low relative pressure, gas adsorbs to solid surfaces in a monolayer; multilayers form at higher pressures. By knowing the number of gas molecules in a monolayer and the dimensions of an individual molecule, the surface area covered by the monolayer can be calculated. Pore size distributions are typically calculated from the adsorption isotherms using the Barett–Joyner–Halenda (BJH) method.

This analysis is performed on dried samples; therefore, in mudstones that contain clay-bound water, a certain degree of uncertainty exists due to the potential for alteration of the pore network during drying. The measurements in the single-digit nanopore range using the BET transform exhibit nonlinearity, but the results can be used for comparison to similar sample types. Additionally, some questions arise as to the accuracy of the N_2 data where porous kerogen comprises a significant proportion of the porosity.

10.5.2.6 Nuclear Magnetic Resonance Porosity and Pore-Distribution

NMR data are generated when a liquid-saturated sample is placed in a magnetic field and then excited with a short pulse of radio frequency energy. The radio frequency pulse generates an NMR signal, which then decays with a characteristic relaxation time or decay rate known as the T2 relaxation time (**Fig. 10.24**). The amplitude of the signal is an indication of the volume of fluid present, while the relaxation time yields information about the physical environment of the liquids. The NMR signal is a composite of small, medium, and large pores present in the sample, with large pores exhibiting long relaxation times and the small pores having very short relaxation times. The data is processed yielding a T2 distribution that characterizes the pore size distribution. Integration of the area under the T2 curve yields total porosity data. Extensions of NMR data, in combination with other measurements, allow the generation of capillary pressure data, fluid saturations, pore wetting characteristics, and calculated permeability values.

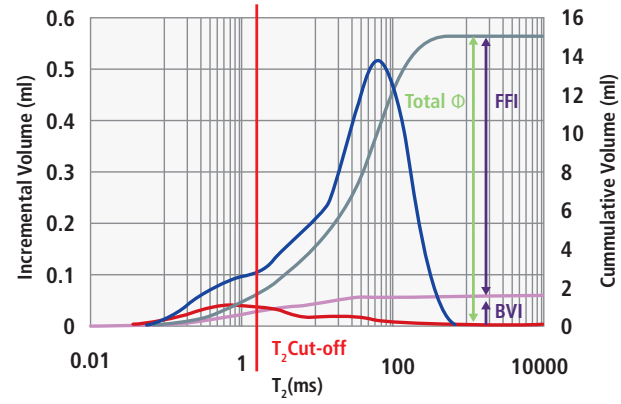

Fig. 10.24—NMR T2 results. (From Oxford Instruments online NMR brochure.)

The primary limitation of NMR measurements on mudstone reservoirs is in the difficulties producing accurate measurements of T2 distributions at the nanoscale, particularly from thermally mature, kerogen-rich samples with associated kerogen porosity. NMR data are also generated without confining pressure and the pore sizes may differ under confining stress.

10.5.2.7 Field Emission Scanning Electron Microscopes and Porosity

Porosity values can also be calculated given 3D FIB-SEM image volumes as described in Chapter 8 and later in this chapter. This digital rock methodology was, at one time, only available in research lab settings. However, the procedures have been streamlined so that it can be conducted in a timely manner and at commercial scale. For example, an integrated digital rock properties (DRP) project was conducted in Colombia to assess the unconventional resource potential of several key basins. This project involved analysis of about 30,000 feet of whole core from 140 wells, more than 4,000 plug samples, and about 450 FIB-SEM samples; the project was completed in a four-month period (Walls et al., 2014). Depending on the rock type and its pore size distribution, the DRP method can give porosity values that are roughly equivalent to standard physical lab methods like GRI (Driskill, et al 2013). Additional information about digital rock methods is provided in Section 10.5.15.

10.5.2.8 Water Immersion Porosity Measurement Technique

The water immersion porosity (WIP) measurement technique is conducted on small rock chips, which maximizes the surface area for water injection. The chips are degassed at an

elevated temperature, then they are pressure-saturated with deionized water before the weight increase and bulk volume are measured. This technique was validated by conducting the test on thermally mature and over-mature dry gas productive mudstones that contained minimal expandable clay; however, it has not been applied to mudstones in the oil or condensate window, or to reservoirs containing significant amounts of expandable clays. Questions remain about WIP's application in mudstones with mixed wettabilities and oil-wet kerogen macerals, and the capability of water molecules to enter all types of mudstone micropores.

10.5.3 Permeability

Permeability measurements on porous and/or permeable coal samples are conducted using routine core analysis techniques using air, nitrogen, or helium. Uncertainties in coal permeability data are related to high permeability losses noted with increases in effective stress, and permeability increases as methane desorbs from the carbon matrix. Argillaceous coals with clay-bound water may yield elevated values following laboratory drying, which may also generate coal fines and associated permeability reductions in cleaner coals. Extended measurement times associated with coal swelling have been noted during laboratory measurements using methane, making coal-methane permeability measurements problematic.

Measuring permeability in core samples from unconventional reservoirs is problematic due to the nano-permeability range. Overburden confinement is known to impact permeability measurement greater than porosity measurements, and stress-creep-stabilization times up to one month are well documented in the literature. Low pore-pressure measurements yield excessively high permeability values, and room temperature measurements are also typically higher than reservoir temperature measurements. Sample drying conditions, particularly on argillaceous samples, can yield excessive permeability values due to clay shrinkage or the development of microcracks in argillaceous laminations. Month-long stress creep stabilization times require both increased numbers of coreholders and a constant temperature environment, thus raising equipment costs and limiting application.

Beyond the limitations described previously, permeability measurements using helium rather than methane as the carrier gas yield excessively high permeability values. This is speculated to be due to the affinity for methane to adsorb on kerogen surfaces, resulting in the reduction of pore throat sizes due to kerogen swelling.

10.5.3.1 GRI Permeability

Utilizing helium in a computerized pressure-decay permeameter, permeability is determined on the 20/35 mesh pebbles previously used for the GRI grain volume measurement described in Section 10.5.2.2. Shortcomings associated with this technique include the lack of reservoir confining stress, a lack of Klinkenberg correction due to low pore pressure measurements, the particle size of the crushed sample, and the short time frame of the measurement.

10.5.3.2 Pressure Decay Permeability

Computerized permeameters are utilized to measure ultra-low permeability in exceptionally tight rock. These systems measure permeability ranging from 1 millidarcy down to 10 nanodarcies using helium gas. One inch- or 1½-in.-diameter core plugs are loaded into a hydrostatic coreholder, and confining pressure is applied. The sample is saturated with helium to pre-equilibrium. Saturation times can range from minutes to hours due to the nature of the reservoir rock. Differential pressure transducers are used to measure a pressure pulse initiated through the core plug. Absolute pressure, differential pressure, and time are computer-monitored as the pressure pulse approaches equilibrium. Permeability is calculated from the combination of the differential form of Darcy's equation and the continuity equation.

Pressure-decay permeameters typically use helium at room temperature at relatively low pore pressures and at low confining stress over short time intervals on core plugs that have been solvent-extracted and dried. Actual reservoir permeabilities are probably a factor of two-to-three times less than the laboratory measurements.

10.5.3.3 Permeability Correlations

Permeability values are routinely reported from several data sources that do not actually involve measurement of permeability. Correlations have been developed that calculate permeability values based on mercury injection capillary pressure (MICP) data (Swanson correlation), three-dimensional computed tomography (CT) data, TEM and field emission scanning-scanning electron microscopy data, and NMR data.

10.5.4 Fluid Saturations

Fluid saturation measurements on reservoir core samples can provide insights into downhole saturations, but are not an exact reflection of reservoir saturations. During the drilling and coring process, some degree of filtrate flushing occurs ahead of the bitface, which alters the core's saturations.

Low-invasion muds and specialized drill bits are available to reduce core flushing. As the core is tripped to the surface, pressure decreases result in gas bubbles evolving, which cause oil-shrinkage and expulsion of portions of the liquid phases. Factors that affect the degree of core saturation alteration include the core's porosity and permeability, wettability, the coring fluid and coring rate, reservoir fluid saturations and viscosities, reservoir relative permeabilities, and vertical lithological variability.

The next section describes laboratory techniques used to determine core fluid saturations, including their strengths and limitations.

10.5.4.1 Routine Core Analysis Retorting

High-temperature retorting of core material yields fluid volumes that can be used to calculate residual oil and water saturations. Typically, a known weight (100-125 grams) of pebble-sized material is loaded into a sealable retort cup. The retort cup is placed into the retort so that it fits into a condensing column that directs fluid vapor through a chilled water-condensing bath into a graduated receiving tube. The retort temperature is elevated to 350°F for 30 minutes, and an initial water reading is obtained for the water that is not chemically bound to the rock matrix. The retort temperature is then elevated to 1200°F to vaporize all water and liquid hydrocarbons, which are read in the graduated receiving tube. Oil and water saturation calculations are generated using the retort data and porosity data generated on adjacent samples. An alternate three-step procedure involves heating samples to 230°F for free pore fluids, to 660°F for capillary/interlayer clay water, and 1300°F for structural-hydroxyl water.

This retorting technique is primarily applied to conventional reservoirs, since the high final retort temperature may crack kerogen in the core, creating excessively high oil saturations. Additionally, oil correction factors required for ultra-low permeability samples would be high, making the saturation data further questionable.

10.5.4.2 Dean Stark Solvent Extraction

Dean Stark recirculating solvent extraction glassware allows the removal of soluble hydrocarbons and the collection of pore water in a graduated sidearm flask. Solvents such as toluene or xylene are used at a boiling temperature of approximately 230°F, and the extraction process can be conducted either on core plugs or on the crushed pebbles that were used in the GRI technique. Measured water volumes are corrected for salt content, and the oil volume is determined by a weight-loss calculation that is corrected by using an arbitrary oil density. A chloroform-methanol azeotrope solution can also be used before the helium porosity measurements to remove formation brine salts remaining after the initial solvent extraction.

Uncertainties in the analysis are related to the salt volume and oil density correction factors, and the potential for atmospheric moisture contamination during the extraction process. Solvent extraction periods can be lengthy, with the GRI technique calling for a one-week extraction period. Water saturation comparisons between Dean Stark and retorting methods indicate that the Dean Stark saturations appear to be excessively high, particularly in clay-rich lithologies. The extended extraction period may strip bound water from the sample's clays, causing artificially high porosity and permeability measurements. The extended solvent extraction also appears to remove oil adsorbed on kerogen in mudstones in the oil-window, altering the porosity and saturations. Again, oil and water saturations calculated by this technique are post-coring, post-tripping to the surface, with residual saturations that may be a poor reflection of reservoir saturations.

10.5.5 Mineralogy

Defining the mineralogy is one of the fundamental building blocks in understanding the reservoir. Knowledge of mineral types and abundance provides insights into lithology, diagenic alterations, potential damage mechanisms, and of particular concern, fluid compatibility issues. In lithologically mature unconventional reservoirs, mineralogy data is used in some "brittleness" calculations. Contrary to conventional thinking, hydrocarbon-productive mudstones are not composed primarily of clay minerals; instead, they are composed predominantly of quartz, calcite, or mixtures of these, with lesser amounts of clay minerals.

10.5.5.1 X-ray Diffraction (XRD)

X-ray powder diffraction (XRD) is an analytical technique that bombards a finely powdered rock sample with monochromatic Cu K- radiation and measures intensity of the scattered beam versus the 2-theta angle of the instrument. Minerals are identified by comparing the calculated d-spacings with a library of standard d-spacings. Bulk XRD samples are prepared by mechanically grinding the sample to a fine powder (< 5 μm) and packing the powder into a hollow-cavity sample mount. **Fig. 10.25** shows a bulk difractogram obtained from a slightly feldspathic, clay-rich sandstone that contains minor amounts of carbonate minerals.

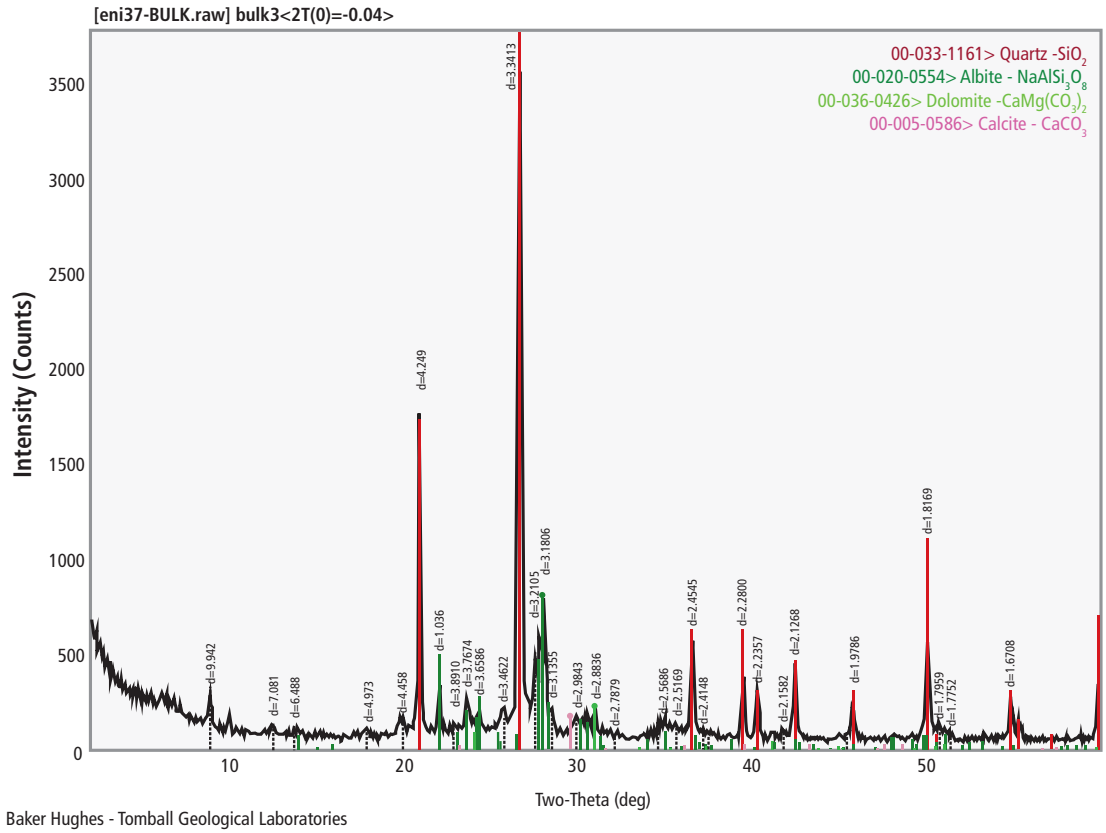

Fig. 10.25—Sandstone bulk XRD diffractogram.

Clay samples are prepared by separating the clay size-fraction from a bulk sample, and depositing a slurry containing the "clays" onto a glass slide. Additional treatments of clay samples by glycolating (to distinguish the expandable mixed-layer clays) and heat-treating (to discern kaolinite from chlorite) are performed as needed. **Fig. 10.26** shows a glycolated clay pattern overlain on the same sample's air-dried pattern. Note that on the left side of the diffractogram, there is a shift between the glycolated curve and the air-dried curve, indicative of expandable clays.

Quantitative XRD analysis is accomplished by using a whole-pattern fitting method utilizing measured and calculated XRD scans. The XRD measurements are commonly combined with a chemical analysis of the bulk sample (from X-ray fluorescence measurements) to improve the quantitative results. X-ray diffraction analysis is considered the ground-truth method for determining the weight percentages of mineralogical phases. Note that all other mineralogical identification techniques require correlations to XRD data for calibration.

Table 10.1 presents an example mineralogical dataset from a West Virginia Marcellus shale core. Given the limitations of data tables, mineralogical data is commonly presented in a graphical form to better understand the relationships and

Table 10.1—Mineralogical results (Marcellus).

Sample ID	1	2	3	4
Mineral Phases	6680	6691	6701	6702
Quartz (SiO_2)	32	31	39	45
Plagioclase Feldspar	3	4	3	3
Potasium Feldspar	Nd	nd	1	nd
Calcite ($CaCO_3$)	3	3	5	3
Dolomite ($CaMg[CO_3]_2$)	3	3	4	3
Pyrite (FeS_2)	5	6	5	5
Mica and/or Illite	48	41	28	27
Sulfur not in sulfides/ sulfates	trace	trace	trace	trace
Carbon-rich material	6	12	14	14
TOTALS	**100%**	**100%**	**100%**	**100%**

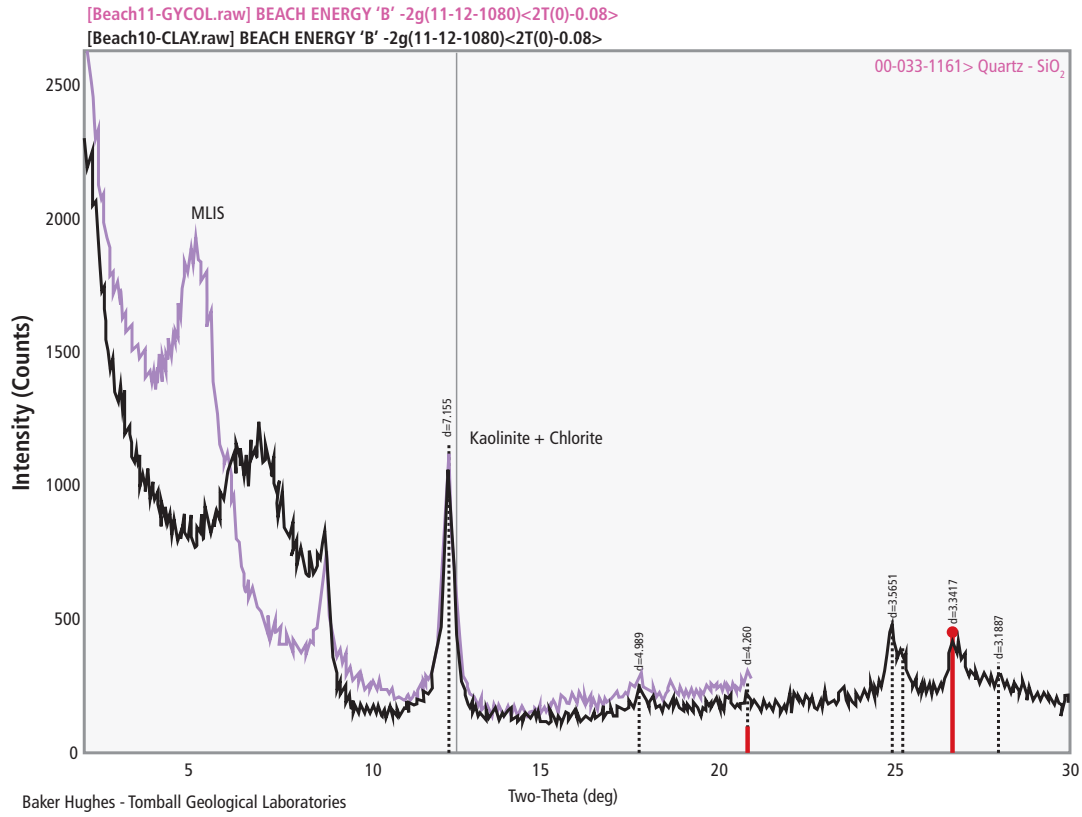

Fig. 10.26—XRD of air-dried and glycolated clay diffractogram.

differences in datasets, such as seen in the ternary diagram in **Fig. 10.7.**

Fig. 10.27 illustrates the significant differences noted in mudstone mineralogies, with silica-rich lithologies such as Woodford, Monterey, and Wolfcamp exhibiting similar thin oval trends, while the carbonate-dominated Eagle Ford exhibits a trend perpendicular to the silica-rich mudstones. In comparison, the trend for the North Texas Barnett is a much thicker oval, which reflects the general mineralogical composition of one-third clays, one-third carbonates, and one-third quartz plus feldspars.

Analytical turnaround time is the largest limitation of XRD analysis. Obtaining the most accurate data for clay-bearing rocks requires separating the clays to allow individual scans of the air-dried clays and glycol-solvated clays when expandable clays are present. This translates to three different XRD scans: the bulk run on the entire sample and a minimum of two clay runs. Preparation time plus equipment time on a batch-processing basis would be expected to be several days for 10-to-20 samples before data interpretation by the analyst.

10.5.5.2 SEM-EDS Mineralogical Analysis

Recent advances in electron beam technology, in combination with energy dispersive spectrometry (EDS) during scanning electron microscopy (SEM) analysis, have enabled generation of mineralogical data in an automated format. Equipment packages are available for both laboratory and wellsite analysis. This technique can be applied to all core samples, but it requires a flat, polished sample surface for analysis. Loose samples such as cuttings are typically mounted in resin for stabilization and then polished prior to analysis.

These computerized, automated services deliver high-resolution petrographic-style analyses and yield elemental data, calculated mineralogical data, matrix density values, and porosity data (percent, pore size distribution, and pore shapes) on a quantitative, point-count basis. Advanced elemental datasets are created using multiple energy dispersive spectrometry detectors with backscattered electron (BSE) and secondary electron (SE) detectors in the scanning electron microscope. Combining the elemental composition data with image "brightnesses" yields sample mineral maps. Data analysis of the mineral maps allows calculation of mineral phases and mineral volume abundances.

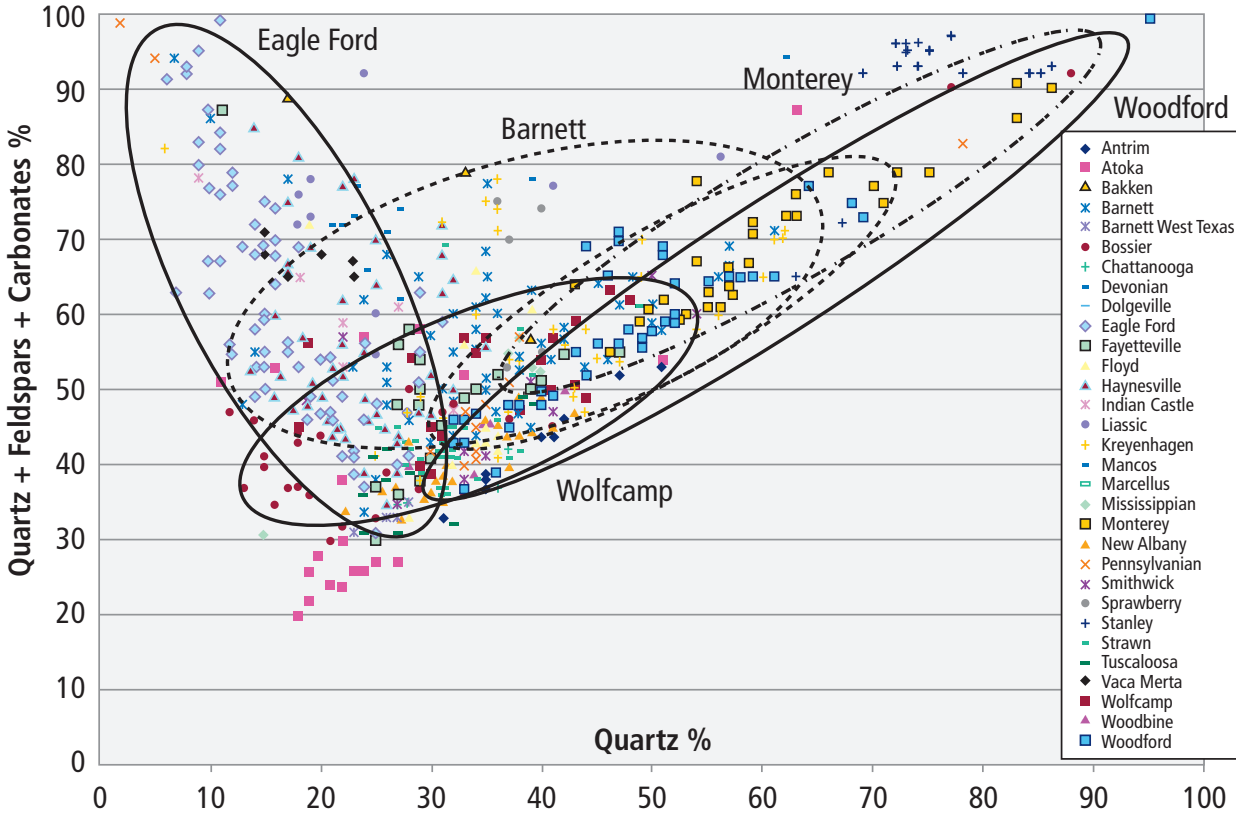

Fig. 10.27—Mineralogical trends by formation.

This analysis currently targets identification of the most "brittle" regions along a horizontal lateral using the generated mineralogical values, to optimize the location and spacing of hydraulic fracturing stages. Limitations of this technique are in the discrimination between aluminosilicates (clays and feldspars) at nanometer-level resolution, generation of porosity information in mudstones due to resolution limitations, and the lack of insights into the degree of expandability of mixed-layer clays such as mixed-layer illite/smectite (MLIS). Fine-grained and layered clays are difficult to resolve due to their similar chemistries and the maximum resolution of the EDS being two microns. In most (but not all) of the moderately mature mudstone reservoirs currently targeted by the petroleum industry, MLIS clays are the dominant clay type. Understanding the degree of expandability is essential to gain insights into rock and fluid compatibility.

10.5.6 Elemental Compositions by X-ray Fluorescence

X-ray fluorescence (XRF) spectrometry is an analytical technique that uses a high energy X-ray beam to bombard a sample. The bombardment causes the sample to produce X-rays that have energy levels that are characteristic of the element(s) from which they were generated. The X-ray count for a given energy level (element) is proportional to the abundance of that element in the sample. Compositionally similar standards are used to calibrate the system for quantitative analysis.

Standalone XRF analysis is typically used to support X-ray diffraction mineralogical interpretations, or to generate a chemostratigraphic column. The XRF elemental compositional data can be used as a constraint in the calculation of mineral percentages, particularly in atypical mineral assemblages. Hand-held energy dispersive XRF units are used on slabbed whole core sections to collect elemental data and to generate a detailed chemostratigraphic log throughout a cored interval. There is a relationship between elevated molybdenum and vanadium contents and total organic contents (TOCs). Therefore, XRF data may provide insights into TOC contents where geochemical data is unavailable. Hand-held XRF unit limitations are related to difficulties measuring sodium, barium, and phosphorus.

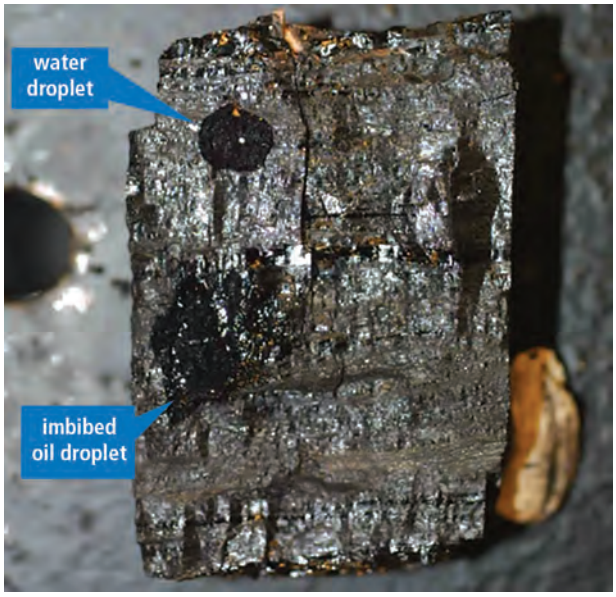

Fig. 10.28—Liquid droplets on coal surface.

10.5.7 Wettability Measurements

Sedimentary strata are typically deposited in water-borne environments, with the notable exception being eolian deposits (usually sandstones and siltstones) accumulated by wind action. Virtually all mudstones and coal deposits are initially water-saturated, and their initial state of wettability is believed to be strongly water-wet. Diagenic alterations associated with the thermal breakdown of organic material or the influx of liquid hydrocarbons into a reservoir may shift the wettability from strongly water-wet to strongly oil-wet, with a range of intermediate wettability states such as neutral-wet, mixed-wet, "Dalmatian-like" wetting, or speckled-wetting. The state of the reservoir's wettability affects production characteristics and the ultimate hydrocarbon recovery. Therefore, laboratory tests were developed for conventional reservoirs to provide insights into reservoir wettability conditions. Most of these tests are not applicable to mudstones.

10.5.7.1 Wettability by Surface Droplet

An example of a simple technique frequently used to obtain a qualitative insight about wettability is seen in **Fig. 10.28.** Droplets of water and a similar viscosity mineral oil are placed on the core surface, which in this example is coal. Visual observation of whether the droplets imbibe into the core or bead on the surface, plus the speed of the reaction, indicates post-coring wettability conditions.

10.5.7.2 Amott–Harvey Wettabilities

Liquid-saturated core plugs at irreducible water saturation (Swir) are sealed in a brine-filled glass container, resulting in spontaneous imbibition of the brine into the core plug, allowing the measurement of the displaced oil. Following a lengthy stabilization period, the core plug is flushed with a brine to displace any remaining mobile oil while encased in a coreholder. The sequence is then repeated with oil substituted for brine, and then water and oil imbibition indices are calculated, ranging from +1 (strongly water-wet) to -1 (strongly oil-wet).

The Amott–Harvey method relies on the sample having sufficient permeability to allow liquids to move relatively quickly through the rock matrix, which virtually eliminates this type of testing in nanodarcy mudstone reservoirs.

10.5.7.3 US Bureau of Mines: Wettabilities

The US Bureau of Mines (USBM) method employs a centrifuge to drive fluids out of a core plug or a porous plate capillary pressure cell. Liquid-saturated core plugs at irreducible water saturation (Swir) are spun in a brine-filled tube in a centrifuge to residual oil saturation (Sor), then spun similarly in an oil-filled tube. Calculations from the generated capillary pressure curves yield wettability estimates typically ranging from +1 to -1. Use of a high-speed centrifugal force in the USBM approach shortens data acquisition times, but the data must be corrected for saturation gradient effects induced by the centrifuge. Despite the fact that this technique employs high-speed centrifugal force to drive liquids through the rock matrix, the data generation on mudstones is questionable because of the mudstone's low permeability.

10.5.7.4 Contact Angle Measurements

Contact angle measurements typically use reservoir crude oil and crystals of calcite or quartz to evaluate wettability. A brine-aged crystal is placed in contact with a crude oil droplet, and movement of the crystal creates water-advancing and water-receding contact angles that can be measured to define wettability. Since the reservoir rock is not used in these contact angle measurements, a certain degree of uncertainty is inherent in this data.

A modified contact angle measurement technique was conducted on fresh or polished reservoir rock surfaces, as seen in the two images (**Fig. 10.29a** and **Fig 10.29b**). In the upper image, Fig. 10.29a, the water droplet is spreading

Fig. 10.29a—Contact angle images.

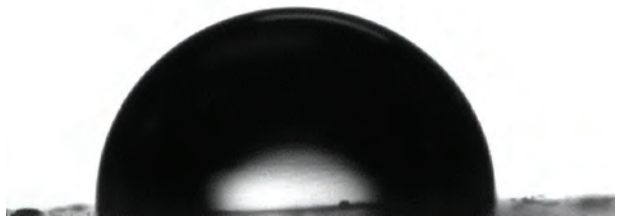

Fig. 10.29b—Contact angle images.

on the rock surface indicating a moderately water-wet condition. The lower image, Fig. 10.29b, shows a contact angle of about 88°, indicating an intermediate to very slightly water-wet condition.

10.5.7.5 Nuclear Magnetic Resonance for Wettability

Measurement of T2 relaxation times and distributions has recently been used to evaluate wettability in mudstones. After an initial polarization, ions on the rock surface can enhance relaxation times compared to fluids not in contact with the surface. The extremely small size of mudstone micropores, plus presence of oil-wet kerogen within mudstones, further complicates nuclear magnetic resonance (NMR) interpretation. The restricted-diffusion NMR method is now under development to address the normal NMR limitations in characterizing wettability.

10.5.8 Thin Section Petrography

Thin section petrography uses light transmitted through a thin (30 microns) section of rock to image the sample. Samples are prepared by injecting porosity with blue-dyed epoxy-resin under vacuum and pressure, attached to a glass slide, and ground to a final 30-micron thickness. Samples may be stained for rapid identification of calcite and/or potassium feldspar. Thin section petrology descriptions commonly include textural parameters such as grain size, sorting and roundness, and cementation, porosity types, and relationships.

Examples of thin section petrographic images are contained in **Fig. 10.30** and **Fig. 10.31**. Fig. 10.30 is an image from an unconventional tight-gas sandstone project in Oman, which shows porosity generally limited to dissolution

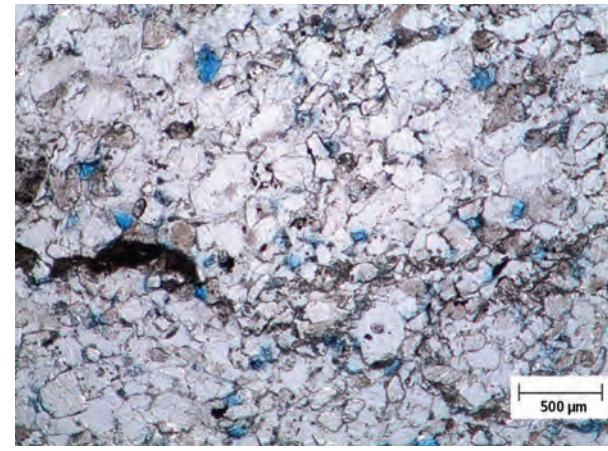

Fig. 10.30—Oman tight gas sandstone.

porosity in this heavily quartz-cemented, quartose sandstone. In comparison, a micro-bedded, argillaceous, calcareous mudstone from the Eagle Ford formation in south Texas is seen in Fig. 10.31.

Sample preparation for petrographic review is much more time-consuming than scanning electron microscopy analysis, which translates to extended analytical turnaround times. Thin sections may provide some limited data on clay morphologies, but scanning electron microscopy analysis is more effective for reviewing clay morphologies due to the higher magnifications available in scanning electron microscopy reviews. Petrographic analysis of mudstones provides information at the microscale, but neither thin section petrography nor normal scanning electron microscopy review of thin sections provides meaningful information about mudstone porosity. Nano-sized pores in

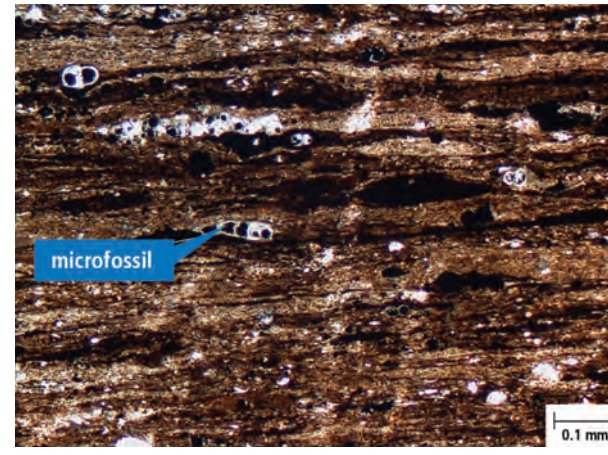

Fig. 10.31—Eagle Ford shale thin section.

mudstones are not discernable even from carefully polished thin sections due to the roughness of the surface. Argon milling—coupled with examination in focused ion beam (FIB) instrumentation—is required to discern the extremely small pores typical in mudstones.

10.5.9 Electron Microscopy

The limitations of optical microscopy prevent investigation of rock and pore networks generally above 500X magnifications. Therefore, imaging pores in the nano range must be performed with electron microscopes. Even in polished thin sections, surface irregularities also limit evaluation of mudstone meso- and micropores related to clays and kerogen. Electron microscopy (scanning electron microscopy, field emission and scanning electron microscopy, STEM) with BSE detectors allows a sample review from 20X to over 100,000X, which provides visual reviews and data collection that can yield critical information about mineral phase locations (particularly clays), pore locations, and pore size distribution in mudstones unavailable through stereomicroscopy or thin section petrography.

10.5.9.1 Mudstone Porosity Types

Prior to describing the various imaging techniques, a description of mudstone pore systems is needed since they deviate significantly from the pore systems normally imaged in conventional sandstone and carbonate reservoirs. Mudstone pores are classified into three types: macropores (> 50 nanometers), mesopores (2- to 50 nm), and micropores (< 2 nm). Fig. 10.31 shows a thin-section of Eagle Ford shale that illustrates the point that mudstone pores are so small that they are not well imaged by either transmitted or reflected light microscopy techniques. Reviews of field emission scanning with scanning electron microscopy indicate that in some mudstones, the macropores and mesopores are primarily located within aggregates of clay, kerogen, and/or carbonates. Micropores are also observed associated with both inorganic (quartz, clays, pyrite, apatite) and organic (kerogen) grains.

10.5.9.1.1 Interparticle Pores

Preserved interparticle pores along with phyllosilicate pores, and to a lesser extent, intercrystalline pores, can comprise a significant portion of the total pore space. At the time of deposition, mudstones are a chemical and biological soup with porosities approaching 80%, which are deposited as floccules of clays, quartz, organic material, and/or carbonate. The lithification process generally destroys most of this porosity through grain reorientation and compaction, recrystallization, and precipitation of authigenic cements such as quartz, calcite, dolomite, and feldspar. Interparticle pores are noted as triangular or slit-shaped pores within the stress shadows of compaction-resistant grains such as silt-sized quartz and pyrite framboids. Porosity has also been noted in very small vuggy pores and was interpreted to have been created by dissolution of carbonate grains and/or cements, possibly related to the formation of carboxylic acids during diagenesis.

Carbonate-rich mudstones undergo cycles of carbonate dissolution and precipitation, yielding interparticle pores created by calcite or dolomite dissolution.

10.5.9.1.2 Phyllosilicate (Clay) Pores

Clays and clay-sized grains commonly exhibit a bedding-parallel alignment related to the collapse of their original cardhouse fabric as a response to overburden compaction, or recrystallization of clay species. Microscopic examinations reveal several different phyllosilicate pore morphologies, including pores within partially open floccules, triangular pores at clay platelet junctions, or lenticular, slit-like pores between clay flakes.

Phyllosilicate pores may be more sensitive to porosity-reduction during hydrocarbon production, since the reduction in pore-pressure may result in compression of the slit-like pore structures as a response to increased net overburden stress. Phyllosilicate pores in mudstone plays may exhibit similar or different wettabilities than organophyllic pores, since wettability alteration is so closely related to hydrocarbon generation by the entrained kerogen.

10.5.9.1.3 Organophyllic Pores

Kerogen macerals tend to develop intraparticle pores as a function of increased thermal maturity during the evolution and expulsion of hydrocarbons from the kerogen. Different organic matter types may yield different organophyllic pore types. Microporous kerogen macerals have been observed in all mudstone plays, and are believed to represent a significant, if not predominant, fraction of the total porosity. The shapes of the larger organophyllic pores have been described as semispherical, bubble-like, and pendular. The larger bubble-shaped pores have been noted in reservoirs in the oil window, gas-condensate window, and the gas window. **Fig. 10.32** and **Fig. 10.33** show mudstone matrices containing organic particles that exhibit both large and small pores.

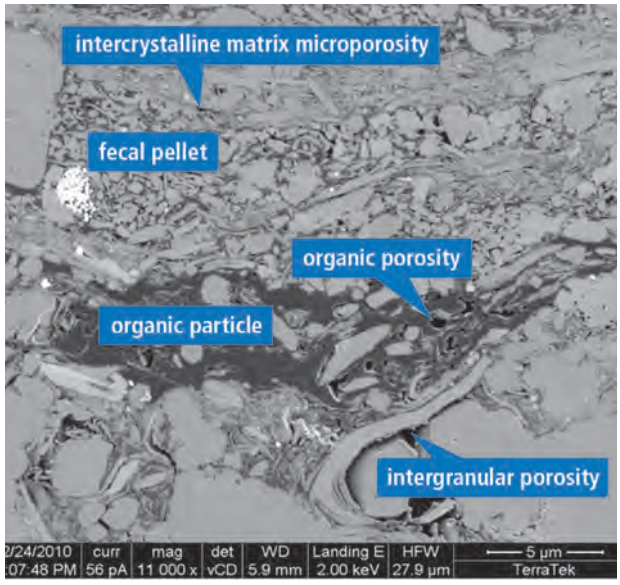

Fig. 10.32—Organophyllic pores. (Spain and Anderson 2010.)

Higher thermal maturity reservoirs tend to exhibit smaller organophyllic pores that pierce the larger bubble-shaped pores, creating a sponge-like internal structure with porosities approaching 50%. Since much of methane storage is in the sorbed state on pore surfaces and within kerogen pores, the spongy micropores in organic macerals have higher surface areas than larger pores, therefore the micropores contribute more to the total surface area within the rock.

Organophyllic porosity can be further enhanced by fractures within kerogen blebs from mudstones in the oil window, and shrinkage cracks within organic matter as seen in **Fig. 10.34**.

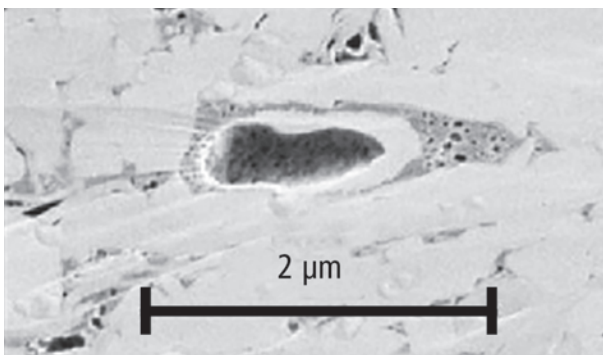

Fig. 10.33—Organophyllic pores. (Driskill et al. 2012.)

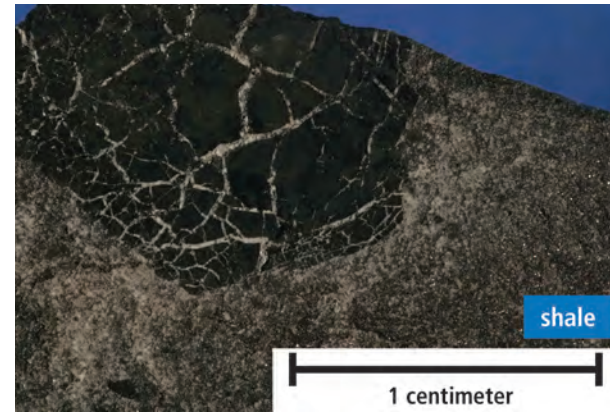

Fig. 10.34—Mineralized shrinkage cracks in plant matter.

10.5.9.1.4 Intraparticle Pores

Pores within particles are typically associated with porous interiors of small fossil fragments, pores within flattened fecal pellets, and gaps within pyrite framboids (**Fig. 10.35**). Porous apatite (calcium phosphate) grains have been noted, and pores have been noted in larger calcareous shell fragments from brachiopods and gastropods. Pyrite framboids are compaction-resistant and commonly have small pores between individual pyrite crystals, which contributes to reservoir storage capacity.

10.5.9.1.5 Fracture Pores

Mature mudstone reservoirs usually contain vertical, sub-vertical, and, in some cases, bedding-parallel (horizontal)

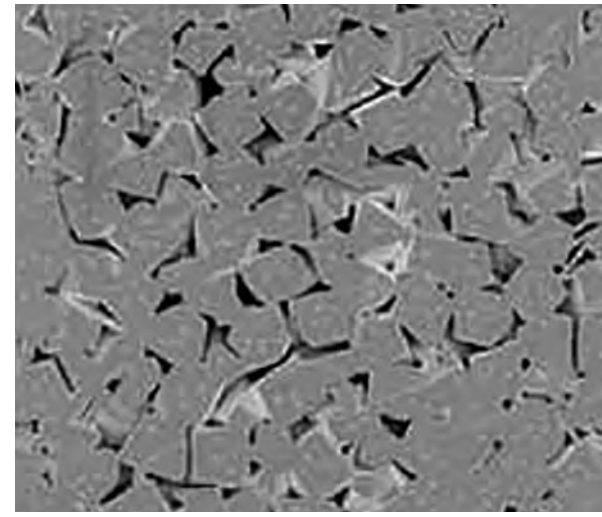

Fig. 10.35—Pyrite framboid intraparticle pores. (Klaver et al. 2011.)

natural fractures. The fractures are typically "healed" by mineral precipitates, such as calcite, dolomite, pyrite, barite, apatite, and clays. Due to irregularities in the fracture walls and crystal precipitates, pores are present that contribute to storage capacity. In cases like the brittle siltstones of the Middle Bakken in North Dakota, an extensive sub-horizontal reticulated, microfracture network developed associated with fluid release caused by superlithostatic pore pressures. These non-mineralized fractures are believed to be major contributors to Bakken storage capacity and exert a dominant control on reservoir permeability. In one dry gas play, the frequency of healed horizontal fractures (beef) has been linked to elevated production rates, associated with the overpressure that led to the beef.

10.5.9.2 Scanning Electron Microscopy and Energy Dispersive Spectrometry

Scanning electron microscopy combined with energy dispersive spectrometry uses an electron beam generated in a vacuum chamber to image the sample. Samples are prepared by extracting volatile hydrocarbons and drying them at a low temperature. The cleaned and dried samples are subsequently sputter-coated with a 30-Ångstrom-thick layer of gold under vacuum. As the electron beam strikes the sample surface, topography-sensitive, secondary electrons are generated, collected in a detector, and computer-imaged. X-rays are also generated while the sample is being scanned. The energy levels of these X-rays are characteristic of the elements from which they were generated. The X-ray energies are computer-imaged into an elemental (EDS) spectrum showing qualitative atomic composition of the sample. Scanning electron microscopy with EDS techniques are used to provide both high- and low-magnification views of the sample with great depth of field, which yields interpretations of the interrelationships between grains, pore types, cements, and clays. Scanning electron microscopy techniques are particularly useful to assess the occurrence of clays within the pore network in conventional reservoirs.

Samples are typically examined in a scanning electron microscope under high-vacuum conditions, but can also be reviewed in wet-mode in environmental scanning electron microscopes. Freshly broken surfaces allow the review of the rock and pore network to help define the mineral phase locations and to evaluate potential completion problems, such as mobile fines in porous and/or permeable reservoirs. **Fig. 10.36** shows a North Sea Rotliegende sandstone with grain-coating illite and "hairy illite" growths in pore-bridging forms. Given sufficiently large pore-throats, these fragile

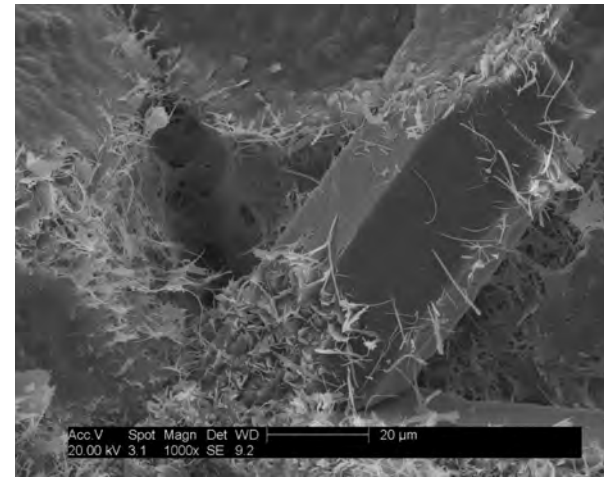

Fig. 10.36—Hairy illite in Rotliegende sandstone.

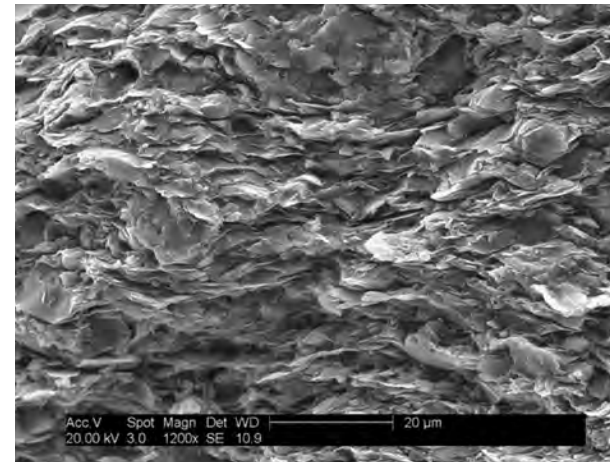

Fig. 10.37—Haynesville shale pseudo-porosity.

clays can migrate during well operations, plugging pore throats and reducing reservoir deliverability.

A limitation of scanning electron microscope analysis in mudstones is visible in **Fig. 10.37**, in a freshly broken surface of a Haynesville shale sample. The sample initially appears to be very porous, but the "pseudo-pores" are actually merely lab-created pores where the other side of the fresh surface pulled away during sample preparation (sometimes called the jigsaw puzzle effect). As discussed previously, the nano-sized pores in mudstones are not well imaged in normal scanning electron microscopy examinations. Argon milling to eliminate surface irregularities is required.

Thin sections can be easily imaged in the scanning electron microscope. An example from the Marcellus shale is visible

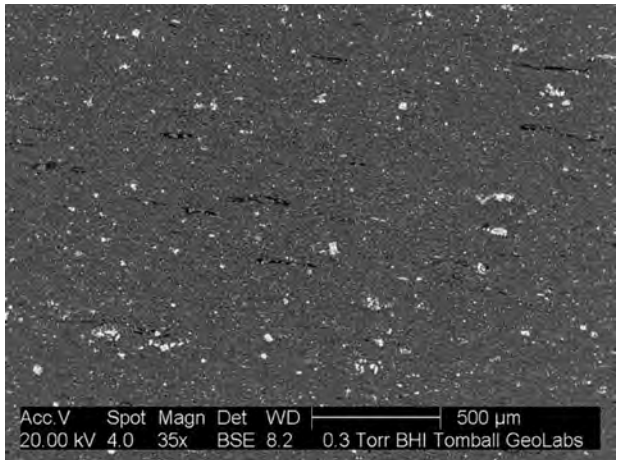

Fig. 10.38—Scanning electron microscope image of polished thin section.

in **Fig. 10.38** at 35X magnification. Whitish-colored dots throughout the image are authigenic barite and pyrite, while the linear, black-colored structures are kerogen, which is also seen in **Fig. 10.52** at higher magnification in the geochemistry section. Note that minimal information about the mudstone pore sizes or distribution is available from this type of scanning electron microscope imaging, even at much higher magnifications.

Fig. 10.39 shows an energy dispersive spectrometry elemental image map collected from a siliceous Marcellus shale core, with calcium being mapped in this image. The purple-colored areas indicate the calcium-rich areas, which are relatively isolated grains or replacements. A carbonate mudstone such as the Eagle Ford differs from the following image in that the Eagle Ford exhibits both coarse- and finely-granular calcium-rich areas in much higher abundance.

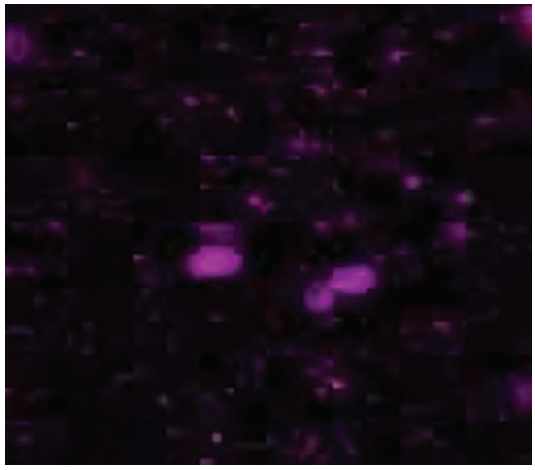

Fig. 10.39—EDS elemental mapping.

Interactions of the beam electrons with the outer-shell electrons in crystals can induce emission of visible light, a phenomenon called cathodoluminescence. The physics of cathodoluminescence is complex. The intensity and color of cathodoluminescence can be related to the intrinsic properties of the crystal lattice to trace elements that have substituted for the "normal" elements in the crystal and to crystal defects. Color cathodoluminescence imaging of clastic reservoirs provides insight into the relationships between detrital grains, authigenic precipitates, natural fractures, and fracture-healing minerals. A scanning electron microscope equipped with color cathodoluminescence detector allows the collection of color images in a single scan on flat or polished rock samples. Color variations indicate multiple cycles of quartz cementation around quartz detrital grains that is unavailable in normal secondary electron or backscattered electron imaging. Healed category I and II natural fractures are invisible to a normal scanning electron microscope or by transmitted light imaging, but are readily apparent in cathodoluminescence scanning electron microscope imaging. Cathodoluminescence images enable better understanding of grain fracturing and healing through quartz precipitation, and the development and healing of natural fractures.

10.5.9.2.1 EDS Analysis of Fracture Minerals

At moderate-to-high magnifications, the EDS detector in a scanning electron microscope can be used to determine the elemental composition of minerals healing natural fractures. In some cases, enough fracture mineralization material is available for XRD mineralogical analysis, but, more typically, the mineral content of the fracture is interpreted based upon the elemental data from the scanning electron microscope EDS. Multiple periods of fracture generation may lead to a variety of mineral types authigenically deposited in mudstone natural fractures and in coal cleats. The Haynesville shale image in Fig. 10.21 shows the mudstone matrix in the lower third of the image, and a horizontal natural fracture filled predominantly by coarsely crystalline calcite in the central-third of the image. Other authigenic fracture-filling minerals visible in Fig. 10.21 include quartz and plagioclase feldspar. Similar images from this same natural fracture included authigenic apatite (calcium phosphate) and pyrite (iron sulfide).

10.5.9.2.2 Imaging Tight Oil Sandstones and Siltstones

Scanning electron microscopes and thin section petrography are commonly used to understand the rock and pore network

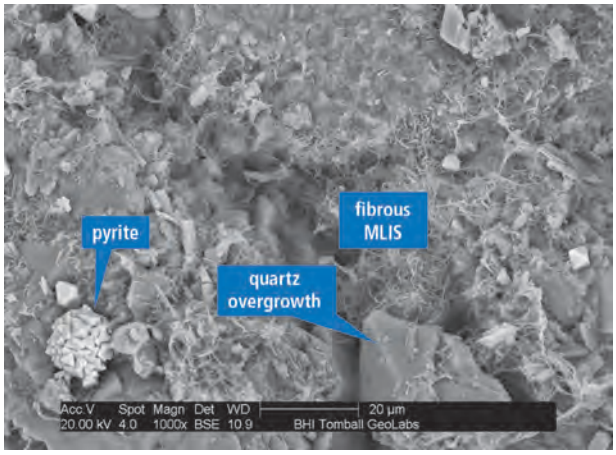

Fig. 10.40—Wilcox sandstone of southwestern Louisiana.

in tight-oil zones that are currently being developed. Freshly broken vertical reservoir surfaces provide two-dimensional views of surfaces that would be created by hydraulic fracturing, yielding insights into potential damage mechanisms. **Fig. 10.40** shows a tight-oil sandstone from the Wilcox formation in southwestern Louisiana. Partially expandable MLIS clays are visible coating grain surfaces, bridging pore throats, and reducing effective porosity. The reservoir's mobility ratio is low, primarily due to the low permeability typical of this argillaceous, very fine-grained sandstone.

10.5.9.3 Mudstones—Focused Ion Beam and Broad Ion Beam Milling

In most mudstones, meso- and micropores that cannot be imaged in normal scanning electron microscopes constitute a major, if not dominant, porosity type. Ion milling techniques have been developed to create delayered surfaces free of coarser polishing artifacts.

Focused ion beam (FIB) milling using argon gas is a sample preparation technique that creates a surface that can be imaged at higher magnifications in field emission scanning electron microscopes and transmission electron microscopes (TEM). FIB milling produces a flat surface that allows imaging of mesopores and micropores in mudstones that cannot be discriminated using a normal thin-section surface polishing approach. The major limitation of this technique is that the FIB-milled area is very small, creating concerns about effective representation of the pore network, and the capability to upscale to larger volumes. One approach to increase the area of investigation is polishing the sample by the broad ion beam (BIB) technique. BIB milling creates a polished surface approximately 1000 times larger than that generated by FIB preparation; FIB polished areas are approximately 2 square millimeters.

Repetitions (200 to 500 times per sample) of the milling and imaging sequence yield a series of images that can be utilized to generate a 3D rendering of a sample's rock and pore network. These data are used to calculate porosity, pore size distributions, and connectivity.

10.5.9.3.1 Field Emission Scanning Electron Microscope

Ion-milled samples imaged in a field emission scanning electron microscopes yield high-magnification views of mudstone macropores, mesopores, and micropores that are too small to be imaged by normal scanning electron microscopy methods. The major limitation of this technique is that only a small area of the sample is imaged due to the time and expense required for milling and data collection. However, using field emission scanning electron microscope and STEM imaging techniques yield pore and pore distribution insights previously unavailable by other imaging techniques.

10.5.9.3.2 STEM (Pseudo-3D Images)

Scanning transmission electron microscope imaging of ion-milled samples can yield both two-dimensional and pseudo-3D images of the macropores, mesopores, and micropores present in mudstones. In addition to the small size of the sample, other limitations inherent in field emission scanning electron microscopes and STEM imaging includes the limited size of the sample, inadequacy of sampling to accurately represent heterogeneous mudstone pore distributions, the analysis being performed at very low pressures rather than under confining pressure, and the extensive amount of equipment time required to generate the data.

10.5.10 Fluid Compatibility Testing

Hydraulic fracture stimulation treatments are essential to create sufficient drained-reservoir volume for economic production rates in mudstone reservoirs. Due to the presence of clays, in particular partially expandable clays, salts such as potassium chloride (KCl) are used in the base fluids to minimize reactivity with the rock matrix. As a function of salt commodity pricing, the expense related to the volume of salt used in the stimulation treatment may be significant. Alternatives to salt, such as KCl-substitutes and clay stabilizers, have been developed to decrease stimulation costs where applicable. Several fluid compatibility tests are conducted in the laboratory to evaluate rock and fluid

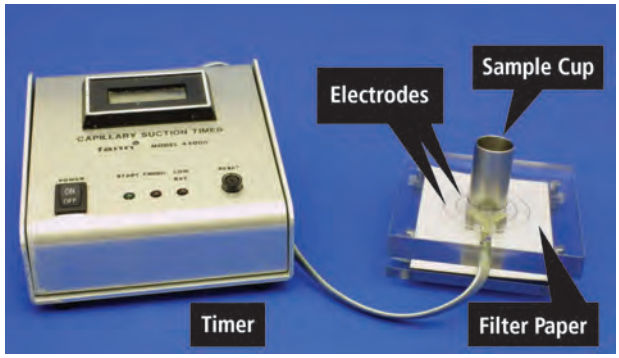

Fig. 10.41—CST apparatus.

sensitivity, salt loadings, and the feasibility of using clay protection additives instead of salts.

10.5.10.1 Capillary Suction Time Testing

Capillary suction time (CST) testing defines the time of movement of a water front between two electrodes **(Fig. 10.41**), which is related to the ability of the fluid to flocculate or disperse clays in a sample. CST results are presented as capillary suction time ratios. The selected liquids are tested without solids to create a baseline for comparison to sample-plus-liquid travel times. CST ratios are defined as the sample-plus-liquid travel time divided by the corresponding liquid-only travel time. When comparing multiple samples in the same fluid, the longer the time of water front movement, the greater the water sensitivity of the sample (the greater the dispersion and/or expansion). When comparing the same sample in different fluids, the higher CST ratios indicate poorer clay control by the fluid.

Fig. 10.42 shows a graphical presentation of CST data for four samples tested with five fluids. The data confirms a significant potential for formation damage with low salinity brines, the incomplete protection with the KCl-substitute/clay stabilizer additive package, and the decreased reactivity when KCl salt is added to the treatment water. This dataset also indicates that minimal additional protection is gained with a high KCl loading of 7%.

CST testing is performed on ground and dried rock material, rather than unaltered reservoir cores. CST analysis homogenizes rock samples, therefore exposing all clays or other reactive minerals to the testing solutions. This is not a valid simulation of the downhole reservoir, since, in conventional sandstone, any clays within shale laminations or shale clasts will be exposed to treatment fluids during this test. The CST procedure is believed to be more applicable to mudstone lithologies in comparison to coarser sandstones, since clays in mudstones are more evenly distributed

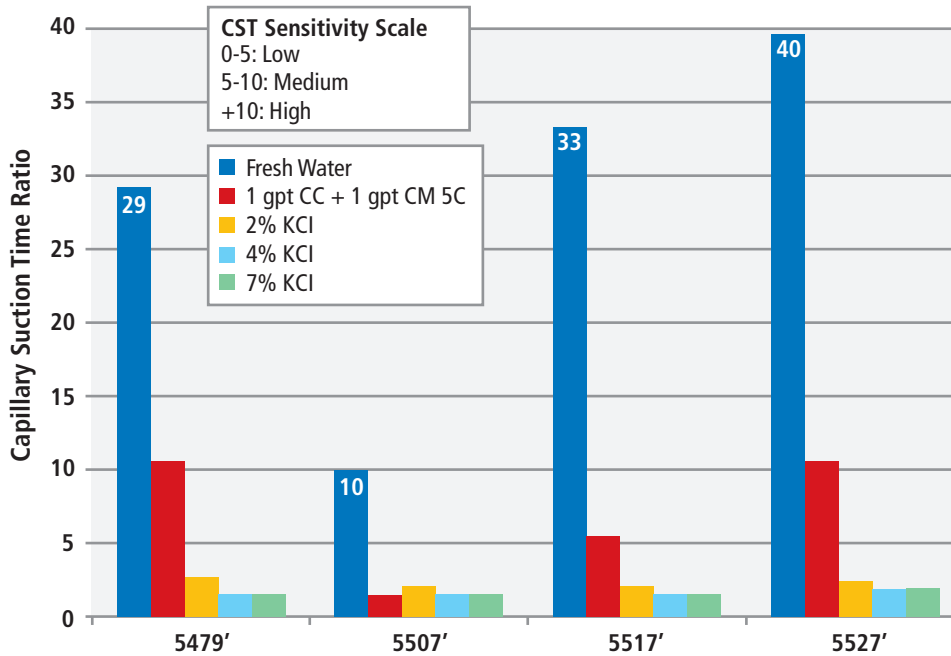

Fig. 10.42—Example CST results.

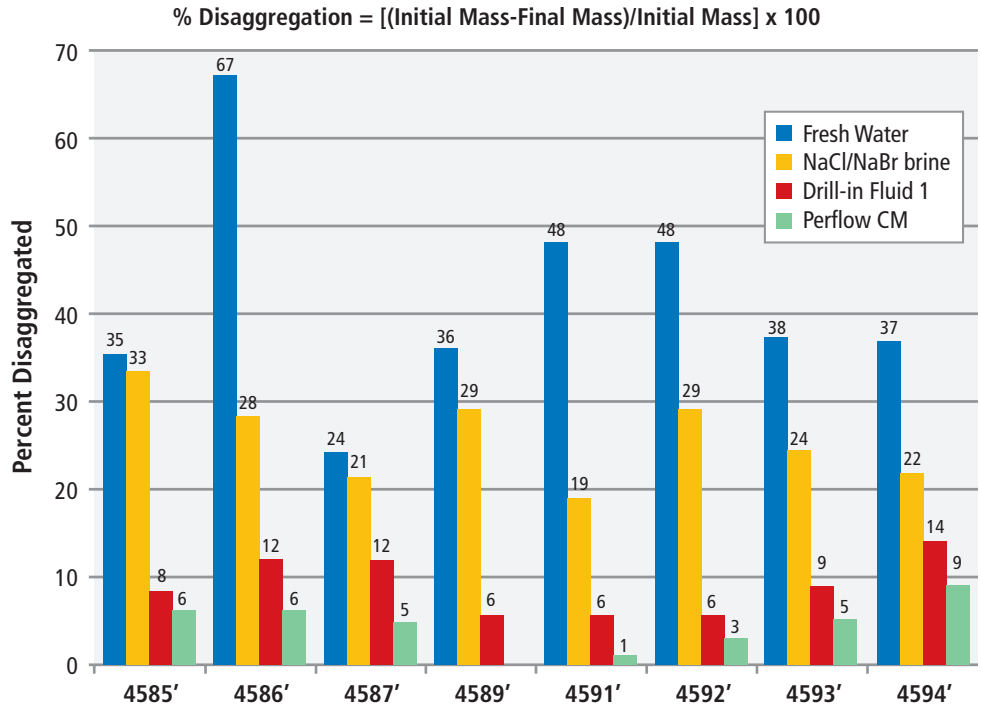

Fig. 10.43—Example roller oven testing results.

throughout the mudstone matrix. CST analysis tends to overestimate the sensitivity of formations to treatment fluids, but it can be used as a comparator to get a better feel for sensitivity-to-treatment solutions given the limitations of the analytical procedure.

10.5.10.2 Roller Oven Testing

Roller oven testing is a method used to evaluate the compatibility of formation samples with a suite of selected fluids. Formation samples are broken to a predetermined size fraction (between 12 and 70 mesh) for analysis. Sieved, dried, and weighed samples are placed into 250 milliliter HDPE plastic bottles filled with selected testing solutions. The bottles are then loaded into an oven equipped with motor-driven rollers that constantly roll the sample bottles. Following a specific rolling interval, the sample is rinsed across a 70-mesh screen with the testing solution, dried, and weighed. The results are reported as percent disaggregation. The disaggregation percentage is calculated by dividing the initial weight into the difference between the initial weight and the final weight, and then by multiplying the result by 100 to express the result as a percentage. The lower the percentage of material disaggregated, the higher the effectiveness of the clay control fluid, and vice versa.

The advantage this test has over CST testing is that the procedure utilizes unaltered rock fragments, rather than ground powder. The disadvantage of this procedure, which clouds the data interpretation, is that the rolling process has an erosional impact on the samples. The disaggregation percentage is therefore not strictly a function of rock and fluid compatibility, but does provide insights into fluid compatibility. **Fig. 10.43** shows an example graphic of roller oven testing data.

10.5.10.3 Brinell Hardness Scale

CST and roller oven testing provide data about rock and fluid compatibility, but there are limitations due to analytical procedures and sample types. The Brinell hardness scale/2 test measurements are now used to gain further insights into rock and fluid compatibility, with the Brinell hardness measurements typically being conducted on conventional core or rotary sidewall core plugs. It is recommended that core plugs are drilled in the direction in which the hydraulic fracture is expected to open (i.e., in the direction of minimum principal stress). The direction of minimum horizontal stress often lies in the horizontal plane (which generates in near-vertical hydraulic fractures). If near-horizontal fractures are anticipated, then vertically oriented cores should be tested. In either case, the surfaces of core plugs should be oriented in a way that is consistent with a propped fracture.

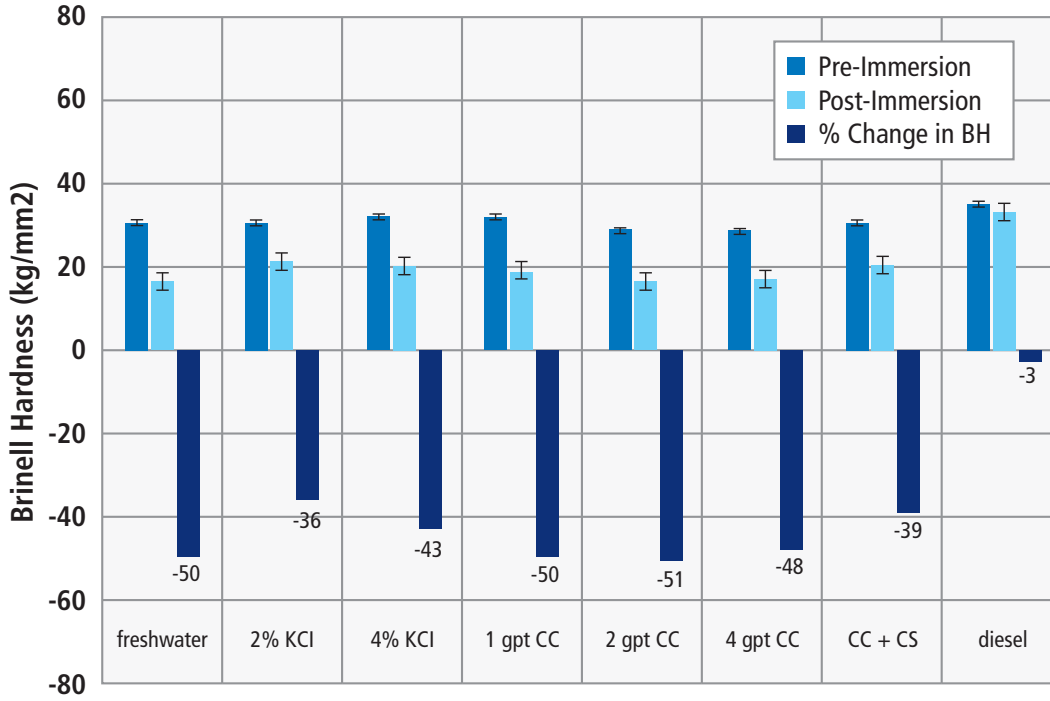

Fig. 10.44—Brinell hardness data graphic.

Brinell hardness values are determined on "as-received" samples, which, typically, are not preserved samples and can exhibit fairly extensive desiccation. Right-cylinder core plugs are typically ½ in. or greater in length. Shorter samples are avoided because they frequently break along the original horizontal bedding planes, which can yield erroneous data.

The pre-immersion values are used for comparison to post-immersion values; **Fig. 10.44** shows an example Brinell hardness dataset. Following the generation of the pre-immersion data, the core plugs are placed in bottles filled with selected fluids, and loaded into ovens or water baths that are near reservoir temperatures. Typical immersion times may range from a few hours to weeks, depending on the objective of the study. Following immersion, Brinell hardness is remeasured and compared to the initial values. Non-reactive diesel fuel is often used as a baseline for comparison to the aqueous phases because it has been observed to have very little effect on formation hardness in water-sensitive reservoir rock (see Fig. 10.44).

The Brinell method of testing for rock follows the ASTM E10-10 recommended practice for metals. Brinell hardness is measured using a device that supports the core and applies force to a tungsten-carbide ball in contact with the core. The mean diameter of the indentation is then measured, either directly, using image analysis tools, or indirectly, using a micrometer that measures the depth of penetration of the ball. The Brinell hardness number (HBW) is defined by the ratio:

$$HBW = 2F/(\pi D_b(D_b-(D_b^2-d^2)^{½}) \quad \textbf{(Eq. 10.1)}$$

F is the force applied to the ball, D_b, is the diameter of the ball, and d is the diameter of the indentation.

At least two measurements (if sample size permits) should be made at different locations on the core surface, and the average and range are calculated and reported.

Microscopic examination of the indentations often reveals the creation of fractures that might bias test results toward lower HBW values. When fractures are noticed, basic statistical analyses are made to determine bias by comparing HBW values associated with fractures versus those not associated with fractures. Microscopic observations of the core surface may also reveal a source of variance due to textural features such as laminations and bedding. Textural features that vary in grain size, mineral content, porosity, and cementation will likely vary in hardness. Consequently, evaluation of HBW test data that takes into account these textural features often helps to explain large variances in the overall dataset, and also helps determine whether bias from unrepresentative sampling on a single or multiple cores has occurred.

Fig. 10.45—Proppant embedment apparatus.

Another source of variance occurs when comparing HBW values made at different hardness scales. The hardness scale is defined by ASTM E10-10 as a particular combination of the applied force and indenter ball diameter. According to ASTM, comparisons of HBW values between different hardness scales are valid only when the ratios of the force on the indenter (F) divided by the square of the ball diameter (F/D_b^2) are the same. The simplest way to achieve this criterion is to create indentations at the same force for a given ball diameter.

Additional factors that require attention to reduce errors in measurement include:

1. Calibration of load cell and displacement devices.
2. Sufficient core thickness so that the effect of the indentation is not observed on the opposite face of the core.
3. Distance from center to center of adjacent indentations exceeds three times the mean indentation diameter.
4. Distance of an indentation from the edge of the core should be 2.5 times the mean indentation diameter.
5. Maintaining consistent load rates and dwell times between measurements.
6. Keeping the diameter of the indentation between 24% and 60% of the ball diameter.

Brinell hardness measurements have also been conducted on large drill cuttings, with the cuttings mounted in epoxy pucks to create a stable measurement platform. Epoxy flexing and the small surface area induce less confidence in the HBW data generated on cuttings. Data generated from as-received samples can be misleading, since the core plugs have typically undergone some degree of desiccation prior to testing, unless they were preserved at the wellsite. Even with nonreactive liquids, the initial HBW values are invariably higher than post-immersion values. Brinell hardness values, measured after drying previously immersed samples, usually yield values that rebound closely to the initial, pre-immersed measurements. This confirms that the initial values are artificially high, and that the true degree of softening with liquid immersion is concealed by the initial sample conditions.

10.5.10.4 Proppant Embedment Testing

Proppant embedment measurements are performed on core samples to evaluate the hydraulic fracture width's response to net closure stress and proppant pack embedment. This test is especially important in soft formations where hydraulic fracture designs are planned using very low concentrations of proppant two layers or less) and produced under high-net closure stress.

Currently, there is no ASTM or ISRM standard method of testing. A typical proppant embedment test uses a thick-walled cylinder in which a core plug is placed inside the cylinder (**Fig. 10.46**). The core (after immersion in hydraulic fracturing base fluid) fits snugly into the test cell so that

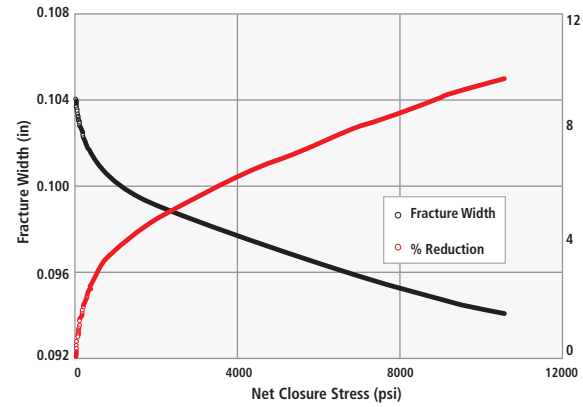

Fig. 10.46—Proppant embedment testing graphic.

the cylinder approximates a state of uniaxial compression on the core. A steel piston is placed on top of the core and the test cell placed in a hydraulic press. A cyclic axial load is applied to the core where the load-displacement response is recorded and analyzed for system compliance. Proppant is then added to the test cell, and the initial height of the proppant is measured by determining the difference in height of the steel piston before and after addition of the proppant. A computer-controlled pump is used to control the rate of increase in axial stress on the proppant. One or two linear variable differential transformers (LVDT) measure the displacement of the piston.

Following a set equilibration time, the load is reduced and the core is removed from the test cell to view the core plug surface. Surface photographs allow computerized measurements of the diameters of the indentations. The ratio of average diameter of the indentations to average diameter of proppant provides an estimate of proppant embedment. The proppant height (or reduction in fracture width) is calculated as a function of net closure stress using the displacement data from the test. Fig. 10.46 shows an example data graphic.

10.5.11 Mechanical Rock Properties

10.5.11.1 Introduction

Knowledge of elastic properties and strength of reservoir rock has application in all areas of drilling, completions, stimulation, and production. For example, in drilling, bit performance is affected by rock hardness and abrasion characteristics, which are often correlated to rock properties such as hardness and unconfined compressive strength. The range of acceptable mud weights needed to avoid fluid loss and wellbore collapse requires knowledge of the wellbore failure criterion in tension and compression. In cementing, formation and cement elastic properties and strength are required input into numerical models that predict cement integrity to changes in wellbore pressure, temperature, and depletion. In hydraulic fracturing, the elastic constants, formation hardness, and fracture-toughness are rock property input parameters to the numerical models that predict hydraulic fracture dimensions and the degree of proppant embedment. During production, unconfined compressive strength (UCS) and critical strain limits (CSL) are used to predict the onset of sand production from perforations and in open-hole completions.

The elastic constants are intrinsic rock properties that determine how a rock mass, a wellbore, a wellbore-cement-casing system, a hydraulic fracture, and a perforation cavity will deform under changes in stress and/or reservoir pressure. For homogeneous, linear, elastic solids, the constitutive relationship is expressed through Hooke's law (Love 1927).

$$\sigma_{ij} = C_{ijkl}\varepsilon_{kl} \qquad \textbf{(Eq. 10.2)}$$

σ_{ij} is the stress tensor, ε_{kl} is the strain tensor, and C_{ijkl} is the elastic stiffness tensor, in which repeated indices, k and l, imply summation over the three orthogonal axes. Equation (2) represents nine linear equations, with 81 elastic constants. The number of elastic stiffness constants can be reduced from 81 to 21 by considerations of energy balance and symmetry within the rock's texture and structure (Love 1927).

Linear elastic, homogeneous, isotropic solids only require two independent elastic constants to characterize the response to changing loads.

Following are the constitutive equations of elasticity for linearly elastic, isotropic solids expressed in terms of Young's modulus (E) and Poisson's ratio (ν).

$$\sigma_{xx} = E(1-\nu)\,\varepsilon_{xx}/(1+\nu)(1-2\nu) + \nu E(\varepsilon_{yy}+\varepsilon_{zz})/(1+\nu)(1-2\nu)$$

$$\sigma_{yy} = E(1-\nu)\,\varepsilon_{yy}/(1+\nu)(1-2\nu) + \nu E(\varepsilon_{xx}+\varepsilon_{zz})/(1+\nu)(1-2\nu)$$

$$\sigma_{zz} = E(1-\nu)\,\varepsilon_{zz}/(1+\nu)(1-2\nu) + \nu E(\varepsilon_{xx}+\varepsilon_{yy})/(1+\nu)(1-2\nu)$$

$$\tau_{xy} = E\varepsilon_{xy}/(1+\nu)$$

$$\tau_{xz} = E\varepsilon_{xz}/(1+\nu)$$

$$\tau_{yz} = E\varepsilon_{yz}/(1+\nu) \qquad \textbf{(Eq. 10.3)}$$

(Note: The σ's are normal stresses and the τ's shear stresses.)

The number of independent elastic constants increases if the solid is anisotropic. For rock possessing transverse isotropy (e.g., laminated sandstone and siltstone sequences), five independent elastic constants are required. For rock possessing orthorhombic symmetry (e.g., laminated shale with natural fractures oriented obliquely to the laminations), nine independent elastic constants are required.

In addition to elastic properties, the strength of formation and wellbore cement are required knowledge to determine failure criteria. Failure criteria provide the constraints for how much deformation or change in stress these materials can

undergo before losing the ability to perform their intended function.

For pure shear failure (mode II fracture), the most common criterion is the Mohr–Coulomb. The criterion is expressed as a linear relationship between shear and net effective normal stresses generated within the solid.

$$\tau \leq S_o + \mu\sigma' \qquad \textbf{(Eq. 10.4)}$$

τ is the shear stress, σ' is net effective normal stress, and S_o and μ are the coefficients of cohesion and internal friction, respectively. The net effective stress is defined as the difference between total stress and pore pressure.

The Mohr–Coulomb criterion considers only the minimum and maximum principal stresses. If the formation compressive strength depends strongly on the intermediate principal stress, then cores will have to be tested using a polyaxial hydraulic system where three independent, orthogonal stresses can be applied to the core sample. Strength data collected from these tests are then input into criteria, such as the von Mises or Drucker–Prager (Fjaer et al. 1996).

For mode I fractures (i.e., tension), a separate failure criterion is used. The failure criterion for pure tension of a rock with tensile strength, T_o, of the porous solid is expressed as:

$$\sigma \leq T_o \qquad \textbf{(Eq. 10.5)}$$

This criterion states that a porous rock will fail in tension when one of the principal stresses becomes less than the tensile strength of the rock (noting that, by convention, tensile stress and strength are considered negative values).

While the previous sections describe generalized failure criterions, fracture toughness K_{ic}, is a fracture propagation criterion. Fracture toughness quantifies a brittle materials resistance to crack propagation at a given loading condition, in the presence of a crack or flaw (Gidley et al. 1989; Griffith 1921). In a perfectly brittle material, linear elastic fracture mechanics (LEFM) holds and fracture toughness (or critical stress intensity factor) is a material constant. LEFM requires that any region of inelastic deformation ahead of the crack tip (e.g., process zone), must be small relative to the region dominated by the first term of the equation describing the complete stress field (this term contains the stress intensity).

In rocks and other quasi-brittle materials, deformation processes that precede crack propagation may increase the size of the process zone significantly. Consequently, fracture toughness is not a material constant but used as an effective parameter (e.g., scale and rate dependent). This is the root cause of issues with scaling of laboratory measurements of fracture toughness to relevant field scales.

ISRM describes a few methods for measuring fracture toughness on core. Unfortunately, obtaining K_{ic} from laboratory testing on core is not routine. However, fracture toughness remains an input parameter in some numerical hydraulic fracturing models. It appears to have limited use in hydraulic fracture numerical models for a number of reasons, a few of which are discussed next:

1. **K_{ic} depends on the state of stress.** K_{ic} has been reported (Schmidt, R.A. 1976) to be greater when measured on cores tested under confining stress compared to ambient stress conditions. Testing with confining stress lends an extra degree of complexity to the test procedure that has impeded its development into the suite of routine core analyses.

2. **K_{ic} depends on scale (size) of the fracture and rate of crack propagation.** The values of K_{ic} measured on cores, which have, at most, a 4-in. diameter, are not likely to be representative of field scale hydraulic fractures (except, perhaps, near the wellbore). Scaling laws for extrapolating core derived K_{ic}'s to field scale are rarely, if ever, published.

3. **Rock materials largely exhibit quasi-brittle behavior, therefore, LEFM is not strictly valid.** Inelastic behavior can lead to a process zone of significant size in which energy dissipation mechanisms (e.g., microcracking, shear banding, softening) can be substantial.

4. **Hydraulic fractures at field scales are largely within the viscosity-dominated regime.** That is to say, the amount of energy dissipated by the fracture process is small compared to energy dissipated through viscous fluid flow. As such, numerical models designed for engineering and analysis of field hydraulic fracturing treatments are typically insensitive to reasonable values of fracture toughness.

10.5.11.2 Laboratory Challenges in Mechanical Properties Tests of Unconventional Reservoirs

There are added considerations when planning a core test program in shale reservoirs that differentiates it from coring

programs in conventional sandstone reservoirs. A few of these considerations are discussed below:

1. **Anisotropy.** As discussed previously, shale and mudstone rock types can be highly anisotropic and very weak along bedding planes. Consequently, the elastic properties are no longer characterized by only two independent elastic constants. Typically, five or more elastic constants will be required. This will, in general, require core plugs to be taken parallel, perpendicular, and 45° to the bedding planes, which can be especially difficult when coring perpendicular and 45° to bedding. Special techniques may have to be invented to eliminate splitting along the bedding planes.

2. **Core Plug Orientation.** If the shale formation is anisotropic, then core plug orientation should be consistent with the objectives of the coring program. For example:

   - For hydraulic fracturing, the axis of the cylindrical plug should be parallel to the direction in which the hydraulic fracture is expected to open (i.e., in the direction of minimum principal stress). In this way, the stiffness of the formation is being measured in the same direction in which most elastic strain energy is being stored as potential energy. This same argument applies to measurements of formation hardness where an estimation of proppant embedment is the objective.
   - For calibration of wireline logs, core plugs should be oriented along the direction(s) in which the wireline tools measure properties in the wellbore.
   - For wellbore stability data, core plugs should be taken parallel, 45°, and perpendicular to bedding to characterize strength anisotropy.

3. **Poroelastic Effect.** The very low permeability of most shale cores makes it difficult to know whether the triaxial tests are being conducted under "drained" or "undrained" conditions. The presence of pore fluids introduces additional coupling terms to the constitutive equations, i.e., pore pressure and pore fluid volume displacement. Since rock strength and elastic constants respond to the net effective stress (Terzagi 1943 and Wang 2000) it is necessary to know (and measure) how pore pressure varies during the test. It should be recognized that the elastic constants (bulk modulus, Poisson's ratio, and Young's modulus) are greater measured under "undrained" versus "drained" conditions (Wang 2000). Testing at high-stress-strain rates should help promote an "undrained" response, but monitoring pore pressure is still recommended. A separate study may be needed to determine the proper strain or stress rate to run a triaxial test to obtain a "drained" response. Without knowledge of pore pressure, test results may show considerable variance depending on sample size, permeability, and loading rates.

4. **Mineralogy and Sensitivity to Fluids.** Some clay minerals are very sensitive to fresh water. When exposed, they have a tendency to absorb the water molecules into their lattice structure and swell. Associated with swelling is a reduction in formation hardness. When testing formation shale and mudstones for fluid sensitivity, core preservation is especially beneficial in providing a baseline formation hardness value to compare against the effect of water-based hydraulic fracturing fluids. Unpreserved, dry core usually results in too high an initial hardness value, and re-constitutive methods of restoring core to native state are very difficult to achieve. Consequently, efforts should be made to preserve shale cores at the wellsite.

5. **Detection and Quantification of Natural Fractures.** Natural fractures play an essential role in the production rate of shale reservoirs. Efforts should be made to measure and report the density (number per foot) from slabbed whole core sections, and the orientation with respect to bedding, whether filled or unfilled, filling minerals, and fracture width. Also, CT scanning of whole core and core plugs prior to testing can be beneficial in identifying where to take core plugs as well as interpreting test results that show large variances.

10.5.11.3 Considerations and Requirements for Core Selection and Preparation

The following section lists considerations required when selecting and preparing core samples.

ISRM recommends that the length-to-diameter ratio of core plugs be between 2:1 and 3:1 when testing for strength and static elastic properties.

Core plugs must be prepared as right cylinders and flat to within ±0.0.01 mm.

Every attempt to preserve core at the wellsite should be made. Additionally, it is important to maintain preservation in the transport to, and at, the laboratory. Testing for mechanical properties with in-situ fluids is recommended.

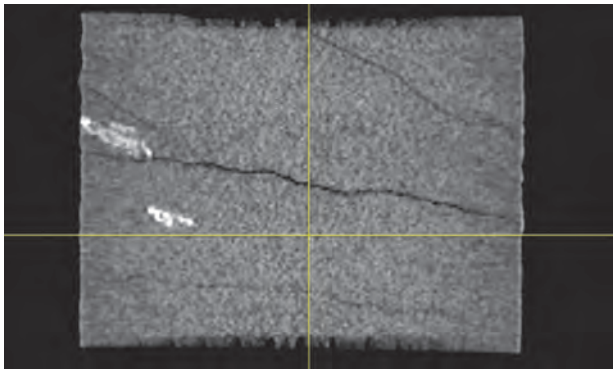

Fig. 10.47—CT scan of vertical core plug showing structural defects.

CT scanning the core before testing is recommended to highlight any density variations and internal voids and/or fractures that may help to explain unusually high variances in test results when comparing elastic-to-strength properties of cores from nearly the same depth interval and/or rock type. CT scans may also be used to preclude the use-damaged cores from the testing program. **Fig. 10.47** shows an example CT scan of a core plug with apparent structural defects.

If fluids saturate the cores, then the stress and strain rates applied during the triaxial testing should be slow enough to allow fluid drainage (i.e., constant pore pressure maintenance) during the test if the "drained" elastic properties are the objective. If "undrained" elastic properties are required, then the core sample and pore pressure lines need to be fully saturated, be free of air, and be connected to valves to eliminate flow of fluid from the cores during application of stresses. To help assess the strain and stress rates that should be applied, initial measurement of air-to-liquid permeability is recommended prior to mechanical property testing.

When taking a core to failure, continue the test beyond peak strength as far as the axial and radial displacement gauges allow. The post-failure stress-strain response provides information about the residual strength and an indication of brittle-versus-ductile behavior. When the residual strength is reached, a second axial deviatoric stress cycle is recommended to verify that the residual strength had been reached.

It is recommended that core plug size be as large (Moronkeji, Prasad, and Franquet 2014) as can be accommodated by the test apparatus. There have been numerous studies (Jaeger and Cook 1969) showing that smaller cores have a tendency to be stronger than larger cores, which biases formation strength toward higher values.

10.5.11.4 Laboratory Measurements

The elastic constants are routinely measured in the laboratory using conventional load-displacement type apparatus (for static values of the elastic constants), or a pulsed ultrasonic wave velocity (ultrasound) apparatus (for dynamic values of the elastic constants). The next two sections describe how these measurements are commonly performed to determine Young's modulus, Poisson's ratio, and bulk modulus.

10.5.11.4.1 Determination of Static Elastic Constants

A few reasons why elastic properties and compressive strength of rock are routinely measured under a triaxial rather than an unconfined state of stress are the following:

1. Studies have reported the increase in strength and increased tendency toward ductile response with increasing confining stress.

2. The dependency of strength (Handin 1963, Heard 1960, Robinson 1959) and elastic constants on pore pressure (Biot 1941).

3. Studies (Holt et al. 1998) showing that the release of overburden and horizontal stress associated with coring alters the mechanical properties of rock, biasing the compressibility of the cored rock to lower values.

4. Nonlinear stress-strain behavior common in many rocks results in nonunique values of the elastic constants.

Triaxial testing apparatus, in short, provides a means to measure rock properties at near reservoir conditions, which helps reduce bias introduced by the previously mentioned factors.

As previously mentioned, there are two general types of test systems: true polyaxial and triaxial axial symmetric (pseudo-triaxial).

True polyaxial test systems employ three independently controlled hydraulic rams that apply a set of orthogonal normal stresses on the sides of cube-shaped core samples. This test apparatus is especially suited to measure the effect of the intermediate principal stress on the failure criterion, as well as characterizing the elastic properties of reservoir materials under more exacting in-situ conditions.

Axial symmetric triaxial apparatus uses cylindrically shaped core samples. Testing procedures are described in ASTM and ISRM recommended practices. These systems typically consist of a confining pressure vessel and hydraulic press for applying

radial and axial stresses independently to the circumference and ends of the core.

Core plugs are typically sleeved in thin, impermeable, elastic membranes. The radial component of stress is applied using pressure generated in the confining fluid that surrounds the circumference of the core. Independently controlled axial pistons apply normal stress to the ends of the core. When synchronized, these two stress controls can generate hydrostatic, axial deviatoric, and radial deviatoric stress paths.

Axial, radial, and circumferential displacements are typically measured using strain gauges and linear variable differential transformers (LVDTs). Strain gauges have an advantage that they can be glued directly to the core sample, which avoids the need to correct for end platen and system compliance. The disadvantage of this arrangement is that the strain gauges can only be used once. Some test systems use strain gauges in the construction of cantilever type devices that can be used repeatedly.

Axial LVDTs, on the other hand, are often attached to rings that are attached to the steel end platens that contact the ends of the core. In this configuration, end platens contribute to the gross displacement measured by the axial LVDTs. If ignored, the axial strain will be biased toward higher values, which will result in a lower Young's modulus and larger Poisson's ratio. The displacement contributed by the end platens can be quantified by measuring the load-displacement response with the end platens placed in direct contact with each other. Alternately, a standard, such as aluminum or steel, of known modulus can be tested under the exact loading path as prescribed by the test procedures. The measured modulus is used to quantify the system compliance factor, which can be used to subtract out the effect of the end platens in subsequent measurements on the cores. Regardless of which type of strain gauge is used, all should be calibrated and traceable to a NIST standard. **Fig. 10.48** shows a triaxial load frame, data acquisition computer, and pressure intensifiers used to control confining stress and pore pressure. Readers interested in finding details of triaxial testing on one-meter cubic blocks under simulated confining and pore pressures should review Ahmed (1983).

Core plugs may be tested with or without pore fluids. If saturated with a fluid, the triaxial test requires an additional parameter to control the net effective stress: pore pressure. Tests conducted keeping pore pressure constant are referred to as a "drained" condition, which means that the pore fluids

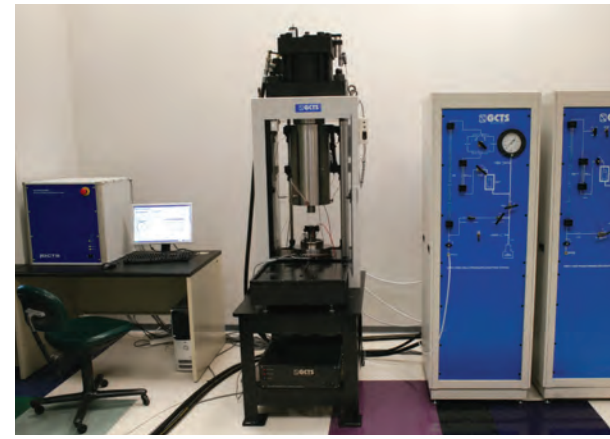

Fig. 10.48—Triaxial test system.

are allowed to freely flow in or out of the core. If pore fluid is not allowed to flow from the core during a particular stage of the test, an "undrained" condition exists. The degree to which the pore pressure increases (or decreases) depends on the mechanical coupling between rock and fluid. Using these two pore pressure control methods in conjunction with various stress paths, the pore-elastic constants can be determined and net effective stress laws examined.

Young's modulus (E) is calculated from the slope (linear least square fit) of the axial deviatoric stress to axial strain curve.

$$E = \Delta\sigma_a/\Delta\varepsilon_c \qquad \textbf{(Eq. 10.6)}$$

σ_a is the axial stress and ε_c is the axial strain corrected for system compliance.

Poisson's ratio (v) is measured from the slope (linear least square fit) of the radial versus axial strain curve.

$$v = -\Delta\varepsilon_r/\Delta\varepsilon_c \qquad \textbf{(Eq. 10.7)}$$

Bulk modulus (K) can be measured from the initial hydrostatic stage from the slope of change in hydrostatic stress (σ_{hydro}) to change in volume strain.

$$K = \Delta\sigma_{hydro}/\Delta\varepsilon_v \qquad \textbf{(Eq. 10.8)}$$

ε_v is volume strain, defined as (ε_c+2ε_r).

It is useful to monitor and record the volumetric strain throughout the test. During application of the axial deviatoric stress stage, the core usually goes through a compaction phase where the volume of the sample decreases with

increasing axial load. As the axial load continues to increase, a point is usually reached where the volume strain begins to increase with additional loading. This turning point (the point of maximum volume reduction) in the volume versus axial strain curve represents the start of dilation and an approximate measure of the point of yielding. This peak in volume strain is sometimes used as the upper bound to the axial strain interval over which the elastic constants are calculated. It is also used, at times, to determine the point of yield for single core, multistage tests, discussed below.

There are two stress paths that are commonly followed to determine the elastic constants and failure coefficients of rock specimens. The first method is the industry-preferred method to measure failure coefficients. The second is used when there is not enough core material to prepare identical core samples.

1. **Single Stages on Multiple Plugs.** This procedure generally follows the following steps:

    a. An initial, drained, hydrostatic ramp to a target confining stress is applied.

    b. A dwell time allowing the axial and radial strain gauges to equilibrate with the hydrostatic stress.

    c. While keeping confining stress constant, one or more axial deviatoric stress cycles are applied. Stress cycling of the core helps reduce stress hysteresis in the strain measurements in subsequent cycles. The last axial deviatoric cycle takes the core beyond peak stress to the point where a constant axial stress with increasing axial strain is observed. This constant value of stress is referred to as residual stress. Another axial deviatoric stress cycle is sometimes applied to detect the presence of strain hardening,

    d. The loads are reduced back to ambient conditions and the core photographed and possibly CT-scanned.

    Stages a. through c. are repeated on a set of identical core plugs, each tested under a different confining stress. The yield, peak stress, and residual stresses are then recorded. The collective peak stress values are plotted versus confining stress, where the slope and intercept of a linear regression of this plot are used to derive the Mohr–Coulomb failure coefficients (cohesion and internal friction). Young's modulus, bulk modulus, and Poisson's ratio are also determined from the stress-strain curves in stage c. as discussed previously.

2. **Multistage on a Single Core.** If there is not enough core material to prepare a set of identical samples, the following sequence of stages has been used to estimate the yield envelope from a single core plug.

    a. The first stage involves a hydrostatic ramp to the lowest confining stress.

    b. In the next stage, the confining stress is held constant, while the axial deviatoric stress is increased. Volume strain is monitored during this stage. Deviatoric stress is increased until a departure from linearity is observed in the volume strain versus axial stress curve. When detected, the axial stress is reduced back to the confining stress.

    c. The hydrostatic stress on the core plug is then increased to the next confining pressure, and stage b is repeated.

    d. Stage c. is repeated for as many different confining stresses desired.

    e. After the last confining stress is reached, the deviatoric stress is taken beyond peak stress to record the post failure response.

    f. The core is unloaded, photographed, and possibly CT-scanned.

10.5.11.4.2 Determination of Dynamic Elastic Constants

The dynamic elastic properties are commonly determined by measuring the ultrasonic compressional and shear wave velocities using a standard pulsed through-transmission method (ISRM, 2007). The wave velocities are often measured as a function of hydrostatic or deviatoric stress. Test apparatus often includes strain gauges or LVDTs so that the static and dynamic elastic properties can be concurrently acquired.

The ultrasonic signals are typically generated using a pair of transmitting and receiving piezoelectric transducers. Some commercial transducers stack shear and compressional piezoelectric crystals in a series so that each mode of wave propagation can be independently propagated. Other test systems, for example, may only use a pair of polarized shear wave transducers, using the mode-converted compressional signal to measure the compressional wave transit time. Both sound generating systems need calibration to correct for inherent transit times through the crystals and face plates that protect the transducers from the high pressures and stresses.

The transmitting transducers are typically energized using a high-voltage spike pulser-receiver unit. The ultrasonic signals are amplified, band-pass filtered, and displayed on an oscilloscope where the signal arrival times can be measured and recorded. Frequencies for ultrasonic transducers may range from 0.1 MHz to 2 MHz for rock specimens. The wave speeds of the compressional and shear modes are calculated by dividing the time of arrival of a particular propagation mode into the length of the sample. Corrections, due to inherent signal delay times through the end plates, are applied to the signal arrival times prior to the velocity calculations. Correction for change in sample length can also be taken into account by measuring the axial displacement during the test. The bulk density of each sample also has to be measured.

For linearly elastic, isotropic, and homogeneous solids, the dynamic values of Poisson's ratio, Young's modulus, bulk modulus, and shear modulus are calculated using **Eq. 10.9, Eq. 10.10, Eq. 10.11,** and **Eq. 10.12**. The dynamic Poisson's ratio (ν) is calculated from the expression:

$$\nu = (0.5(V_p/V_s)^2 - 1)/((V_p/V_s)^2 - 1) \qquad \textbf{(Eq. 10.9)}$$

V_p and V_s are the compressional and shear wave velocities, respectively. Shear modulus (G) is calculated from the expression:

$$G = \rho_b V_s^2 \qquad \textbf{(Eq. 10.10)}$$

ρ_b is the bulk density. Young's modulus (E) is calculated from the expression:

$$E = 2\rho_b (V_s)^2 (1 + \nu) \qquad \textbf{(Eq. 10.11)}$$

Bulk modulus (K) is calculated from the expression:

$$K = \rho_b (V_p^2 - 4V_s^2/3) \qquad \textbf{(Eq. 10.12)}$$

The strong possibility of elastic anisotropy in unconventional reservoirs is one challenge faced in deriving the dynamic elastic properties for wireline logs. The presence of anisotropy makes the above equations inaccurate, to some degree. Advances in dipole sonic logs now make use of five independent modes of wave propagation (and wave velocities), which allow determination of five elastic constants characteristic of transversely isotropic elastic solids. The problem becomes more complicated if more than five elastic constants are needed. In these instances, more sophisticated methods will have to be employed, possibly making use of wireline logs along with wave velocity measurements in core and integration of vertical seismic profile (VSP) data.

10.5.11.4.3 Brazilian Indirect Tensile Strength

While the Mohr–Coulomb failure criterion characterizes the failure envelope under compressive loads resulting in shear failure (Mode II), it does not account for failure of Mode I fractures, which occurs in tension. For tensile strength, a direct tensile strength test is the ideal, and consists of pulling a long, narrow rock specimen along its axis in direct tension. Unfortunately, for rock testing, the direct tension test is problematic to put into practice, so indirect methods have been devised. One such test is the Brazilian Indirect Tensile Strength test.

ASTM D3967-08 and ISRM recommended practices describe the Brazilian Indirect Tensile strength measurement. ASTM recommends that the cores be in the shape of cylindrical discs with a diameter-to-thickness ratio between 1.33 and 5. ASTM also recommends at least 10 samples be tested, unless the variation coefficient is less than 5%. (If it is less than 5%, then a lesser number is acceptable.) The diameter of the cores should be at least ten times greater than the largest grain diameter. The splitting tensile strength (σ_t) is calculated from peak strength using the expression:

$$\sigma_t = 2P/(\pi LD) \qquad \textbf{(Eq. 10.13)}$$

P is peak strength in units of Newtons (or lbf), L is the height of the core in mm (or in.), and D is the diameter of the core in mm (or in.). It should be noted that the test results from the indirect and direct methods of testing do not always agree.

10.5.11.4.4 Fracture Toughness

Fracture toughness is a criterion in the theory of Linear Elastic Fracture Mechanics (LEFM) that determines the stress conditions under which a fracture will propagate (Griffith, A.A. 1921). It is considered a material property for perfectly elastic brittle solids.

There are various ways to measure fracture toughness in the laboratory (ISRM, 2007). The Chevron-notch method appears the most common. Almost all of these describe methods where the core samples are tested unconfined. Due

to this limitation and to other factors discussed previously, very few laboratories have put much effort into making this measurement routine.

10.5.11.4.5 Scratch Testing

Scratch testing is used to assess formation strength heterogeneity, and for comparison to mechanical properties determined downhole by logging tools. This technique allows the generation of continuous unconfined compressive strength (UCS) values on cored intervals. Slabbed whole core segments are cut with a PDC cutter, allowing computer data acquisition of the scratch distance along the core and the horizontal and vertical cutting forces created during the scratching process. **Fig. 10.49** shows a 4-in.-diameter whole core segment that has been slabbed along the vertical core length. As seen in the inset photograph in **Fig. 10.50**, a preliminary scratch is cut to prepare a constant-depth surface for the subsequent final scratch measurements.

Correlations between UCS and the scratch measurements have been developed using UCS values measured on core plugs from scratched cored intervals. Scratch testing data can be used in selecting sample depths for UCS measurements, allowing enhanced calibration of log-derived mechanical properties.

Limitations of this technique are related to the condition of the core prior to scratching; i.e., state of preservation, alteration of the slabbed surface by incompatible fluids, and the presence of coring-induced fractures. Additionally, these measurements are conducted at room conditions rather than under reservoir stress conditions, which may significantly impact the scratch and UCS correlations. Lastly, the number of commercial vendors offering this service is limited.

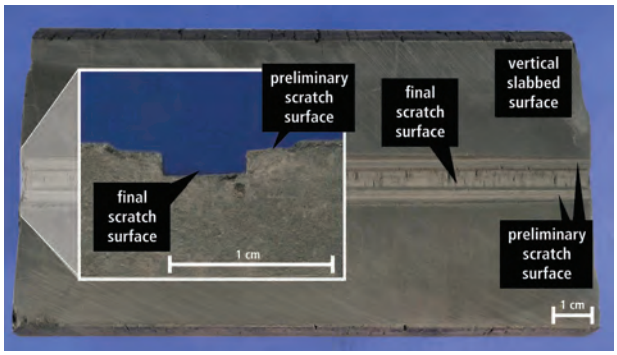

Fig. 10.49—Scratch testing groove.

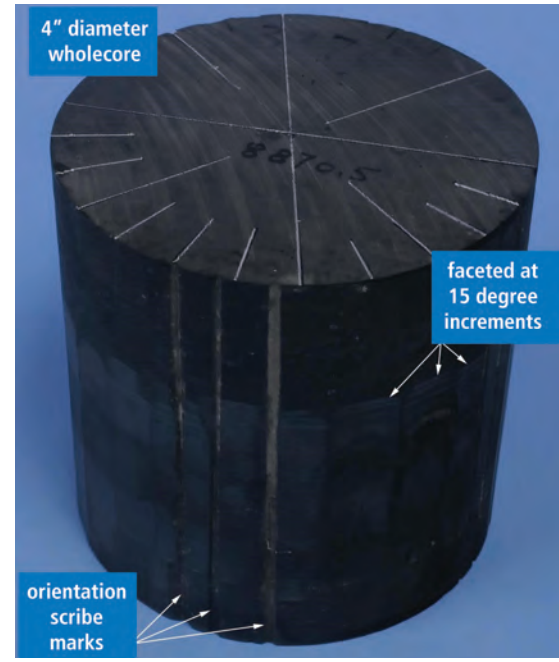

Fig. 10.50—Faceted whole core segment.

10.5.11.4.6 Using Oriented Whole Core Sections to Determine Stress Direction

In hydraulic fracturing, knowledge of the directions (and magnitudes) of the principal stresses, especially the directions of minimum and maximum horizontal stresses, is especially important in deciding not only lateral wellbore trajectory, but also the primary direction of induced hydraulic fractures.

SPE Monograph volume 12 (Gidley et al. 1989) devotes a chapter to fracture azimuth and geometry determination. One such method uses oriented whole cores to infer the directions of minimum and maximum horizontal stress. This method relies on the hypothesis that planes of compliance are created during the coring operation. Release of overburden and horizontal stresses will cause expansion of the core. The expansion should, if the core is elastically isotropic in the horizontal plane, be greatest in the direction of maximum horizontal stress.

Wave velocity anisotropy and differential strain analysis methods on oriented whole cores have been used to take advantage of this phenomenon. If measurements of the compressional and shear wave velocities are taken transverse to the whole core axis as a function of azimuth angle, then the sound velocities should be slowest when propagating perpendicular to the planes of compliance (i.e., in the direction of maximum horizontal stress) and fastest when propagating parallel to the planes of compliance.

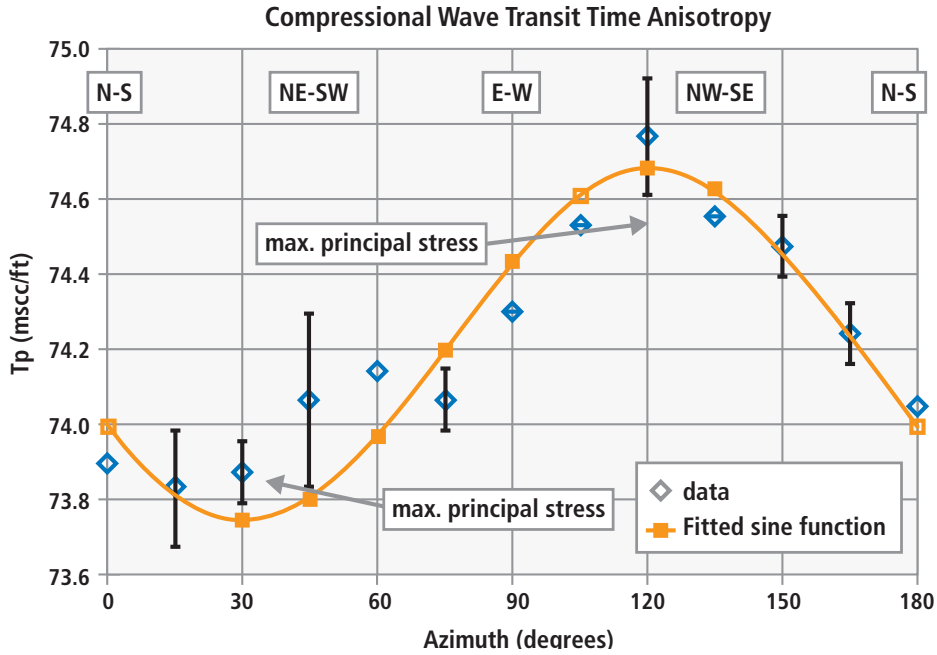

Fig. 10.51—Wave velocity versus azimuth.

Analogically, differential strain analysis of cores that are subjected to an applied hydrostatic stress will produce the largest strains in a direction perpendicular to the planes of compliance and in the direction of maximum horizontal stress.

When using the wave velocity anisotropy method, the measurement requires that the whole core be drilled in the vertical direction and inscribed along its side to signify the north-south azimuth.

Whole core sections are first prepared by surface grinding facets, about every 15°, around the perimeter of the whole core section, as seen in **Fig. 10.50**. These surfaces should be ground smooth on an end-face grinder (or equivalent machine). The distances between opposing facets are measured. Ultrasonic transducers are attached to the opposing facets where the transit time across each facet is recorded. The through-transmission method is used to record the time of flight of compressional and shear wave signals. The inherent transit time of transducers should also be measured and subtracted from the gross measurements.

The net transit times for each facet pair are divided into the distance between opposing facets to obtain the average wave velocity. A plot of wave velocity versus azimuth is plotted. The resulting sinusoidal curve with a period of 180°, as shown in **Fig. 10.51**, is interpreted as the existence of horizontal stress anisotropy, the direction of which is determined by the azimuth of the slowest wave speed (or largest reciprocal wave velocity).

One condition that needs to be met for the anelastic strain recovery methods to work is that there should not be a large density of tectonically induced fractures that were created in past epochs that no longer reflect the current local tectonic stress state of the reservoir. Existence of pre-existing fractures may lead to erroneous conclusions about the current directions of horizontal stress. Therefore, the inferred stress directions from oriented core should be corroborated with wellbore break-out and tensile fractures viewed using borehole imaging technologies.

10.5.11.5 Brittleness Index

Brittleness of mudstones has become a high profile (but controversial) parameter for identifying "sweet spots" when drilling and perforating unconventional reservoirs. Practitioners in the industry believe that creating fracture complexity (if desired) in mudstones requires a relatively high degree of "brittleness." The problem that currently faces the industry is that there is no consensus for how this parameter should be defined. One common method of defining brittleness is based on mineral content. For example, high quartz content containing little or no clay would generate a high brittleness index. Other methods rely on the elastic constants and formation hardness. For example, a high

Young's modulus value is sometimes used to imply a high degree of brittleness.

One of the difficulties in deciding upon a practical definition of brittleness is that this parameter is a function of the state of stress to which the formation is exposed. Porous solids tend to be most brittle when one of its principal stresses is near zero psi (an unconfined state of stress), and they become more ductile as the minimum principal stress becomes greater in compression. Characterizing the brittleness of rock using quantities that do not consider stress state are, therefore, often misleading and do not accurately predict in-situ behavior. Mineralogy-derived brittleness values should be restricted to diagenically mature sandstones, carbonates, and mudstones. Immature sediments with low clay contents may appear to be brittle based on mineralogy, but lack of cementation results in a ductile formation.

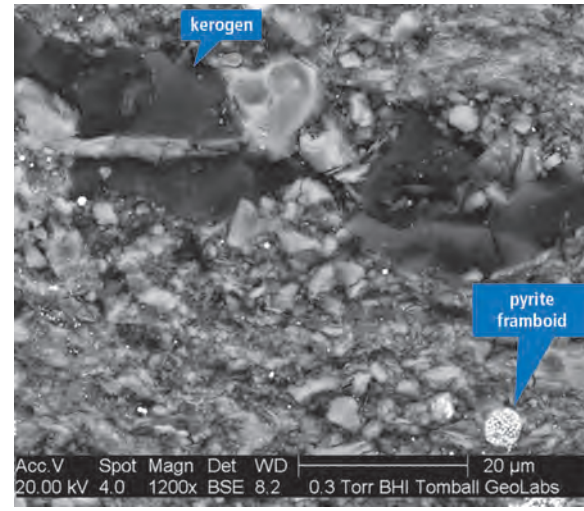

Fig. 10.52—Kerogen in mudstone.

10.5.12 Geochemical Analyses

Reservoir samples are tested by geochemical techniques to assess petroleum play characteristics. Generated data reflects the present-day, residual organic material remaining after thermal diagenesis. Geochemical testing measures the volume of residual liquid hydrocarbons present in the reservoir, determines the amount and type of kerogen present, and evaluates the reservoir's thermal maturity for insights into producible hydrocarbon types.

In unconventional mudstone plays, kerogen plays an important role in hydrocarbon storage capacity with hydrocarbons stored within kerogen pores and adsorbed on and in kerogen macerals. Kerogen represents residual organic matter detritus that was entrained in the reservoir at the time of deposition along with the inorganic fraction (quartz, carbonates, clays) that was deposited by sedimentary action (**Fig. 10.52**).

10.5.12.1 Organic Content Determinations

Total organic content (TOC) is typically determined by direct combustion. The LECO combustion technique involves acid-digesting a known weight of a sample, rinsing and drying it, then combusting it at about 1000°C. TOC contents in most mudstones under development range from < 1% up to 15%. Productive shales TOC contents typically average above 2%.

Rock-Eval™ pyrolysis determines kerogen type, maturity, and the amount of free hydrocarbons present in samples. Weighed samples are first heated to 300°C to determine the entrained free hydrocarbons (S1) that could be normally solvent-extractable. Pyrolyzable hydrocarbons (S2) are measured by heating the sample to 550°C in an inert environment. T_{max} is defined as the temperature at maximum S2 generation, and is considered a thermal maturity indicator; T_{max} increases with increasing thermal maturity. S2 and the TOC data are used to calculate the hydrogen index (HI). S3 is derived from the measurement of carbon dioxide generated during pyrolysis, and is used to calculate the oxygen index (OI). HI and OI are plotted on Tissot–Welte and van Krevelen type diagrams as kerogen type indicators.

TOC data limitations are related to different types of organic matter generating different types of hydrocarbons, if any at all. Hydrogen contents estimated from pyrolysis measurements refine the understanding of the types and amounts of hydrocarbons that can be generated from mudstones.

10.5.12.2 Thermal Maturity Characterization

Definition of thermal maturity variability within a sedimentary basin aids oil and gas companies when they select acreage and zones for exploration. Understanding whether reservoirs are immature, in the oil window, in the mixed oil and gas window, or in the dry gas window is particularly essential in the mudstone plays, since product pricing may preclude drilling in gas-rich areas. Two of the predominant techniques used to characterize reservoir thermal maturity are measurement of vitrinite reflectance (%R_o), and %R_o calculated from pyrolysis measurements. Thermal alteration index (TAI) is also discussed.

10.5.12.2.1 Vitrinite Reflectance

Vitrinite occurs as both cell wall material and cell-filling material in land-sourced plants. With increasing thermal

maturity, vitrine's chemical composition changes, increasing its ability to reflect light. A scale of vitrinite reflectance (%R_o) versus maturity developed by the coal industry is used to relate microscopically measured vitrinite reflectance values to the maximum thermal maturity of the subject reservoir.

Subsamples of rock samples are typically hand ground to a 0.5 to 0.18 mm size fraction, then mounted in an epoxy puck prior to grinding with coarse and fine sandpaper and polishing compounds. The sample is reviewed in a reflected-light microscope using filtered incident light in concert with data acquisition software for data storage and calculations.

Common limitations of vitronite reflectance measurements in black shales is the small amount of higher plant material deposited in these depositional environments, recycling of vitrinite from pre-existing sedimentary strata, and the presence of other organic materials that have vitrinite morphologies but do not have vitrinite chemistry. The reflectance of non-vitrinite particles has not been thoroughly calibrated. The subjectivity associated with discriminating vitrinite induces a level of uncertainty, which can be mitigated to some extent by combining fluorescence with vitrinite reflectance measurements.

10.5.12.2.2 Definition of T_{max}

T_{max} values are generated during Rock-Eval™ measurements; T_{max} is defined as the oven temperature at maximum S2 generation, and is considered a thermal maturity indicator. T_{max} values increase with increasing thermal maturity. Vitrinite Reflectance (%R_o) data can be calculated from pyrolysis data, using the equation $R_o\% = (0.0180 \times T_{max}) - 7.16$.

A limitation of T_{max} values calculated from pyrolysis measurements is associated with samples contaminated with oil-based mud, which yields anomalously high T_{max} values. Low organic contents also have a negative effect on pyrolysis T_{max} values.

10.5.12.2.3 Thermal Alteration Index

With increasing thermal maturity, kerogen color shifts from light yellow to black. A color scale was developed for microscopic examination with 5 indices (numbered 1 through 5) to track the kerogen color shift from light yellow, yellow, orange, brown, brownish-black, and black. The thermal alteration index (TAI) ranges from 1: unaltered in immature reservoirs to 5; metamorphosed in overmature or metamorphosed reservoirs.

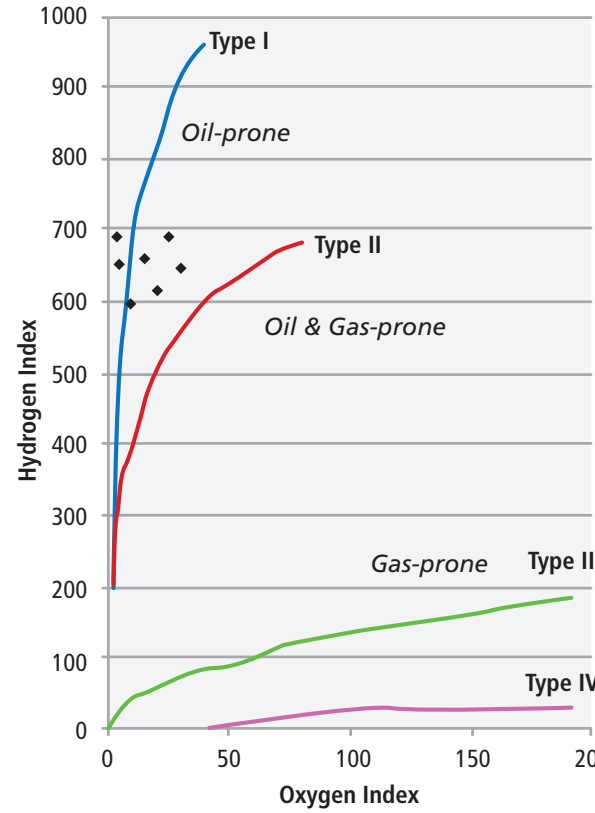

Fig. 10.53—Pseudo Van Krevelen diagram.

Interpretation of the average kerogen color in samples can be complicated by the different maturation rates noted in different spores and pollen. In carbonate reservoirs, recrystallization frequently causes kerogen color to shift to darker levels. Weathering and oxidation also cause color shifts that make the maturity levels appear to be higher.

10.5.12.3 Kerogen Type Determination

A diagram for classification of kerogen was developed by van Krevelen, and has been modified for classification of kerogen types and maturity level in the petroleum industry. HI is calculated from the TOC and pyrolysis measurements [HI= (S2 x 100)/TOC], and the OI is calculated similarly [OI= (S3 x100)/TOC]. HI and OI are plotted on Van Krevelen type diagrams as kerogen type indicators, while HI and T_{max} are plotted on modified Espitalie diagrams. **Fig. 10.53** shows an example pseudo-Van Krevelen diagram.

10.5.13 Canister Gas and Adsorption Isotherm

Natural gas storage, particularly in mudstone reservoirs, is not limited to storage within inorganic mineral-related

intergranular, interparticle, or intraparticle pores. Kerogen porosity, which is not well characterized by typical porosity measurement techniques, can comprise a large proportion of the total mudstone porosity. In the case of coalbed methane reservoirs, the gas storage mechanism is almost entirely as adsorbed gas throughout the coal.

10.5.13.1 Sorbed Gas and Desorbed Gas Content

Gas storage mechanisms can be evaluated through testing on samples "canned" at the wellsite. On arrival at the surface after coring, core samples or cuttings are rapidly sealed in airtight aluminum canisters. The initial natural gas evolved from the core is measured to estimate the amount of gas lost as the core was brought to the surface from the reservoir. In the laboratory, the sealed canisters' temperatures are raised to reservoir temperature, and evolved gas is measured to depletion. Residual gas is then measured while the core is crushed in a sealed container. Total gas is calculated from the sum of the wellsite and laboratory measurements.

10.5.13.2 Canister Gas Composition

Gas chromatography mass spectrometry (GCMS) techniques are used to define the composition of natural gases released by the rock matrix. In addition to methane content, carbon dioxide (CO_2), ethane, propane, butane, pentane, hexane, and nitrogen proportions are measured.

10.5.13.3 Adsorption Isotherm

Knowledge of the TOC content and adsorbed phase gas storage capacity in mudstones allows calculation of a reservoir's adsorbed gas storage capacity, which in mudstones comprises a major portion of the total storage capacity. Adsorption isotherm analysis yields the adsorbed phase gas storage capacity. Gas sorption analyzers are used to determine the specific surface area using the BET surface area technique, which is based on a mathematical model for the process of gas sorption including multilayer adsorption.

10.5.13.4 Natural Gas Classification

Evaluation of the biogenic or thermogenic origin of gases can often be defined by the composition of the C1-C4 hydrocarbons. GCMS methane/ethane ratios that are generally less than 100 suggest a thermogenic origin, while ratios greater than 100 would suggest a biogenic origin for the hydrocarbons. Natural gas can be altered during diagenesis, and may be a combination of biogenic and thermogenic gases. The best definition of natural gas sources is through isotope analysis, particularly evaluating the ratios of two stable carbon isotopes (C-12 and C-13) in the methane.

10.5.14 Hydraulic Fracture Conductivity

Hydraulic fracture conductivity testing is performed to evaluate conductivity changes in a proppant-loaded artificial fracture as a function of fluid contact, and/or confining pressure changes. Testing requires splitting a 1 in. or 1.5 in. diameter core plug in-two (in tension) to create a bedding-perpendicular surface, placing proppant between the two halves, then loading the core-plus-proppant inside an elastic sleeve (see the Bakken siltstone in **Fig. 10.54**). The core plug should be split perpendicular to the original horizontal bedding planes to emulate downhole conditions. The average amount of proppant placed in the artificial fracture is inferred from the weight of proppant and area of contact (i.e., lbs./ft^2). Flow distribution platens are placed at each end of the core, the assembly is placed inside a Hassler-type core holder for confinement, and the coreholder is placed inside a thermal bath.

Confining stress is applied in increments to at least 4500 psi, and the core is usually saturated with a simulated formation brine prior to flowing with fracturing fluids. Fluids are pumped through the proppant/fracture under constant flow rates while measuring the differential pressure across the proppant/fracture. Since fracture width is not well defined in this test, the Darcy equation for linear flow is solved for fracture conductivity, defined as the product of fracture permeability times fracture

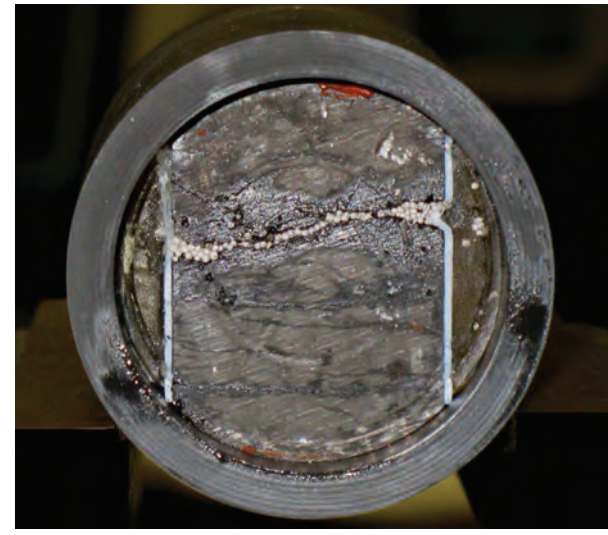

Fig. 10.54—Hydraulic fracture conductivity sample assembly.

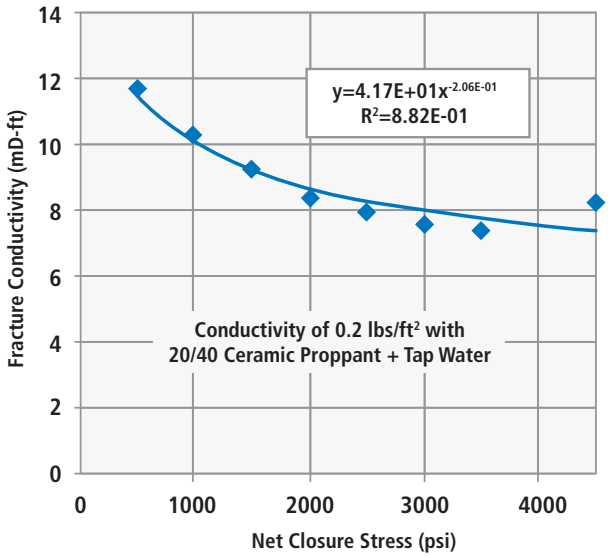

Fig. 10.55—Hydraulic fracture conductivity data graphic.

width. At each stress increment, fracture conductivity is measured. The core plug is recovered at the end of the test and the surface photographed. If proppant indentations can be observed, an estimate of proppant embedment is performed.

10.5.14.1 Net Confining Stress Changes

Fig. 10.55 shows an example data graphic for a Bakken siltstone using an intermediate strength ceramic proppant. Limited conductivity losses occur as a function of proppant embedment due to the heavily cemented nature of this quartzose siltstone.

10.5.14.2 Conductivity Response to Fluid Flow

Hydraulic fracture conductivity measurements comparable to those described in the previous section can be conducted while maintaining constant net closure stress, but altering the composition of the fluid flowing through the hydraulic fracture. This allows evaluation of the formation's compatibility with treatment fluids, and the impact on fracture conductivity.

10.6 Digital Rocks Methods for Mudstones: An Example from the Wolfcamp Formation

10.6.1 Introduction

The Wolfcamp formation is a major unconventional resource play in Texas. Oil versus water production has been observed to vary widely among the hundreds of horizontal wells that have targeted this formation. This variability is a serious challenge for many operators and there is a strong need to understand which rock properties have the greater effect on oil/water ratios and how to target the best intervals. Using slabbed core from the Texas Bureau of Economic Geology (BEG) in Austin, TX, and the tools of digital rock physics, some clues have emerged. The well will be referred to as Wolfcamp-1 and is located in the southern Midland basin.

10.6.1.2 Methodology

Digital rock properties (DRP) technology developed by Ingrain was applied in the Wolfcamp-1 well using a workflow especially designed for the characterization of shales. During stage 1, dual energy X-ray CT imaging was performed with a voxel resolution of about 0.25 millimeter. From this imaging, a high-resolution vertical profile of rock bulk density (RHOB) and PEF was computed. Bulk density is an indicator of porosity and organic matter content, while PEF is an indicator of mineralogy. The density and mineralogy information can be used to define shale facies. This process was used to separate the data into five facies classes, as well as to characterize and identify higher reservoir potential. In **Fig. 10.56**, the second track from the left shows the facies. Red and green colored facies represent higher porosity and/or organic content with the green areas being more silica rich than the red areas. Light blue zones are a more carbonate-dominated zone. This data can be generated in a matter of hours after the core has been recovered, thereby aiding in horizontal wellbore placement and stimulation design. Core-based rock typing from a combination of dual-energy X-ray CT imaging and spectral gamma ray scanning was used to select sample locations for the second stage of testing. In stage

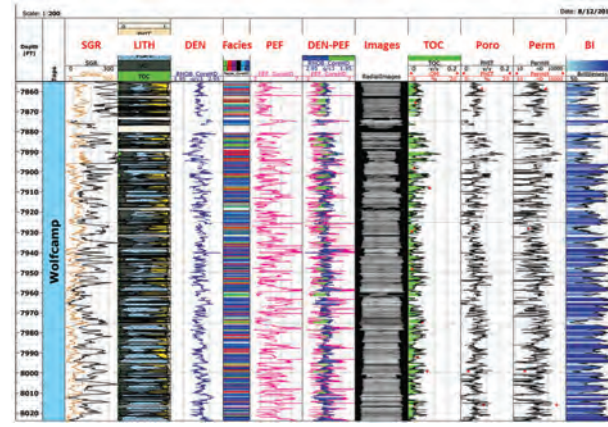

Fig. 10.56—Integrated digital rock properties log based on whole core, plug samples, and FIB-SEM data.

two of this shale core program, plugs were selected for greater analytical detail. Initially, the plugs were X-ray CT imaged at a resolution of 40 microns/voxel. These CT volumes not only were used to guide the selection of subsamples, but were also part of a very important visual catalog. During this second stage, scanning electron microscope (SEM) analyses were also conducted on argon ion milled samples. Scanning electronic microscopes were used to obtain high-resolution images of the shale mineral grains, solid organic material, and pore space. These images (**Fig. 10.57** and **Fig. 10.58**) were digitally analyzed to quantify the amount of organic matter, organic porosity, intergranular porosity, and high-density minerals (usually pyrite) present in the samples.

During stage 3 of the project, three-dimensional volumes of digital rock images were obtained from FIB-SEM (focused ion beam combined with scanning electron microscopy). These image volumes have a voxel resolution of about 5 to 15 nanometers and form a digital rock volume that is used for computing permeability and other types of special core analysis data. **Fig. 10.59** shows two examples. Segmentation and image processing allows the separation of the solid mineral, organic matter, and pore space for these 3D objects. Absolute permeability was calculated in each 3D FIB-SEM

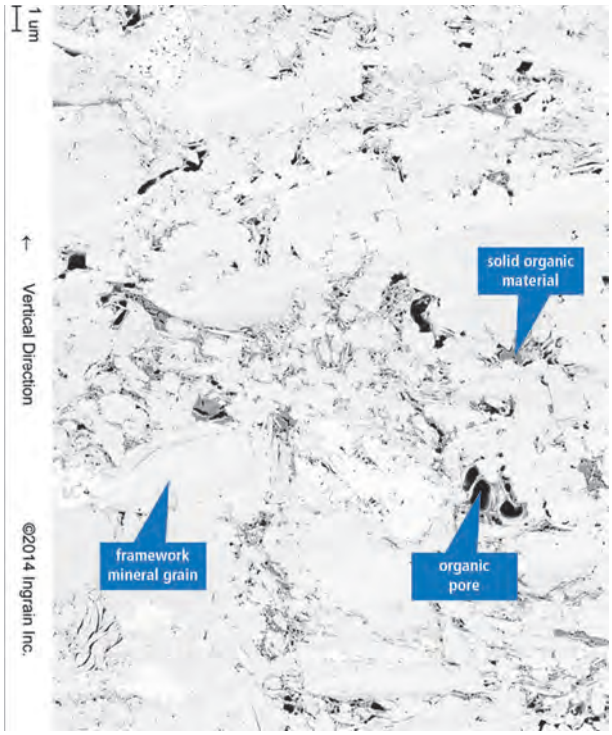

Fig. 10.57—SEM image from Wolfcamp-1 well, 7,928 ft., shows porosity inside organic material.

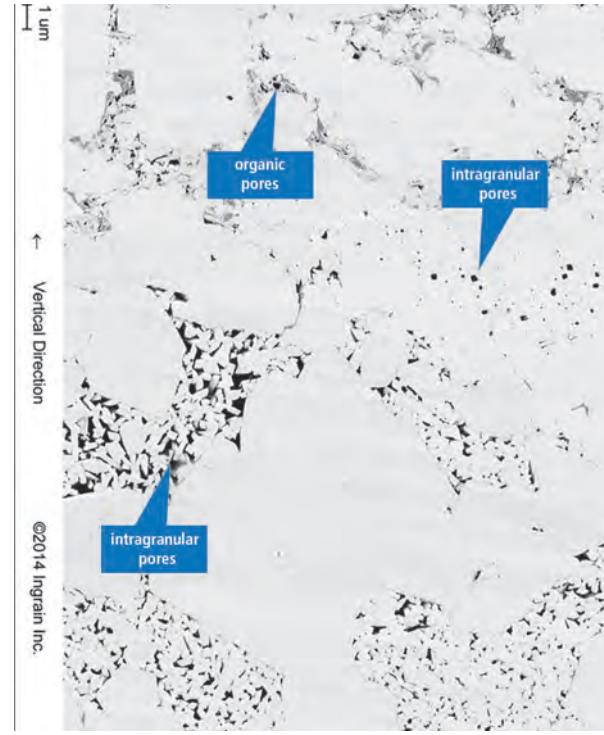

Fig. 10.58—SEM image from Wolfcamp-1 well, 8,016 ft., shows predominantly intra- and intergranular porosity.

volume using a numerical method known as Lattice–Boltzmann (Tolke, et al., 2010).

10.6.2 Results and Findings

In addition to total porosity, connected porosity, solid organic matter, and porosity associated with organic matter (PA_OM), we also computed vertical permeability, horizontal permeability, and pore size distribution. Results of these tests, and hundreds of others performed over several years, show that the Wolfcamp formation has not only large variability in porosity and permeability but also that organic porosity and intergranular porosity are both common. Both types of porosity are well interconnected and can contribute to fluid flow. **Fig. 10.60** shows the total porosity versus horizontal permeability for Wolfcamp-1 compared to the upper and lower bounds determined from other Wolfcamp samples in the Ingrain DRP database.

10.6.3 Data Integration and Interpretation

In the final part of this project, the results of dual-energy CT imaging, spectral gamma scanning, and local XRF (X-ray fluorescence) data was combined with FIB-SEM that was used to compute variations in TOC, lithology, brittleness index (BI),

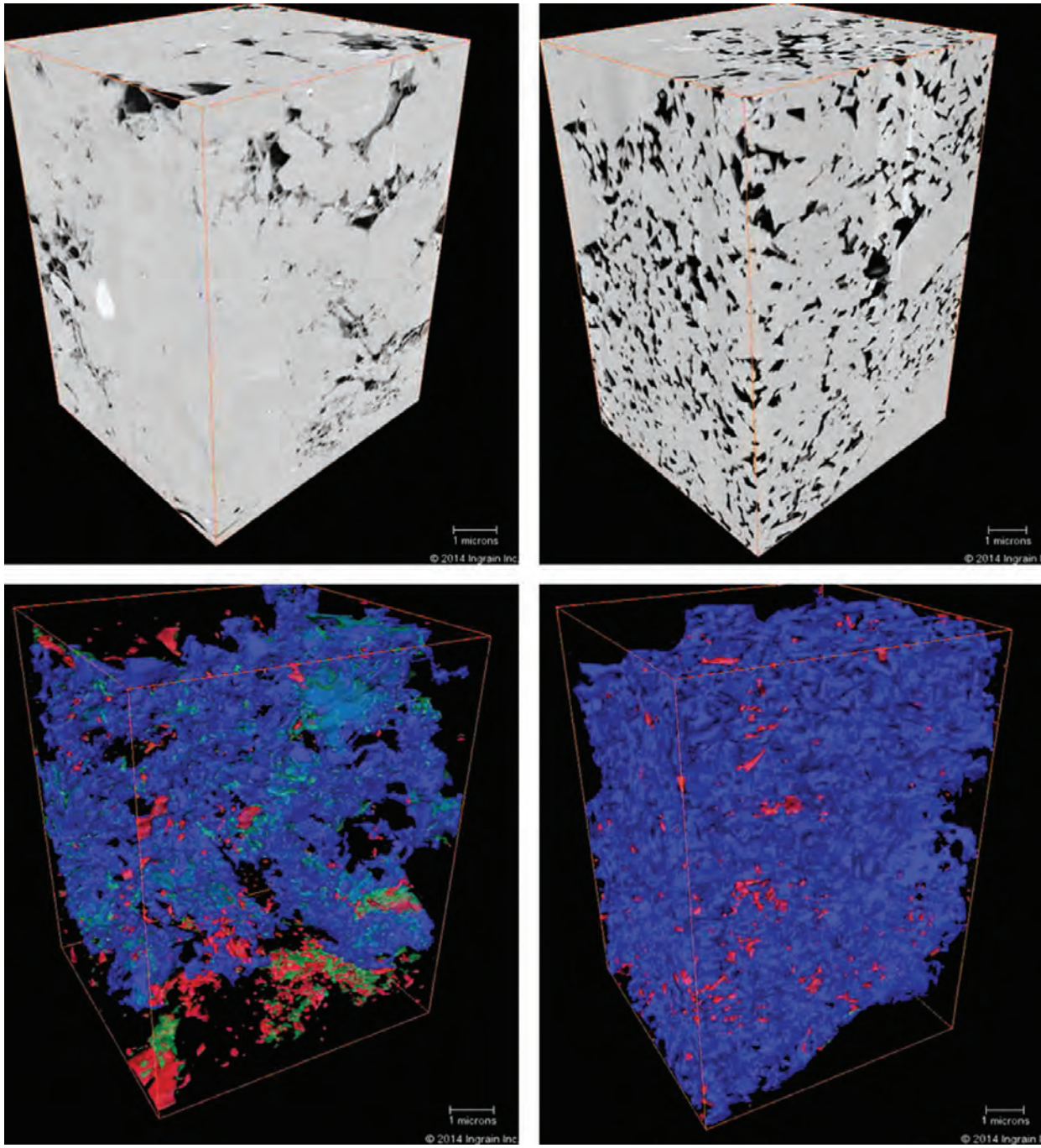

Fig. 10.59—High-resolution 3D FIB-SEM volumes are shown from the Wolfcamp-1 well. Images on the left are from 7,928 ft. and images on the right are from 8,016. In the bottom two images, the green color is solid organic matter, the blue color is connected porosity, the red color is isolated porosity, and the transparent areas are solid mineral grains. Note that the sample on the left (7,928 ft.) has much of its connected porosity closely associated with organic material. The sample on the right (8,016 ft.) has essentially no organic material or organic porosity.

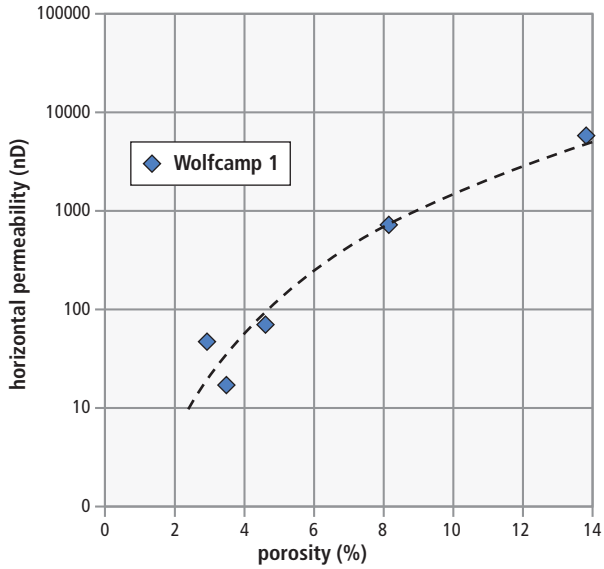

Fig. 10.60—The dashed line shows the best-fit porosity-permeability trend from the Wolfcamp-1 well. The trend compares favorably to many other Wolfcamp samples in the Ingrain database. Permeability in this figure was computed in the horizontal plane using FIB-SEM digital rock volumes.

porosity, and permeability over the entire cored interval. In this case, the FIB-SEM derived porosity-permeability trend was used as an empirical upscaling guide to compute permeability over the cored depth interval (Fig. 10.60). Based on the integrated DRP results, the upper one-third of this cored interval contains the highest organic porosity and permeability. The better reservoir quality streaks become thinner and less pronounced in the lower one-third. Note, however, that brittleness index is lower in the best reservoir quality zones.

10.6.4 Summary

The collection and integration of the data from this digital rock physics (DRP) study of whole core and plug samples from the Wolfcamp formation shows that rock types, porosity, and permeability are highly variable and that the Wolfcamp-1 well is fairly typical of the Midland basin. The DRP analysis further shows that some samples have mostly intergranular pores, while other samples have mostly porosity inside the organic material. Both sample types may have relatively high porosity and permeability. If we assume that water resides mostly in the intergranular pores, and that hydrocarbons are more common in the organic pores, then it suggests water cut may be reduced by targeting the completion in the intervals with greatest organic porosity.

10.7 Final Words

Given sufficient hydrocarbon product pricing, unconventional reservoir exploitation will continue for the foreseeable future. The inherent heterogeneity of mudstone reservoirs makes laboratory characterization one of the essential building blocks in understanding the reservoir. Basic concepts, such as hydrocarbon storage and hydrocarbon movement through a nano-permeable reservoir matrix, are not well understood. Reservoir models utilizing downhole data require correlations and calibrations based on laboratory measurements. Continued refinements of laboratory measurements and the development of new analytical techniques will be needed for better development insights and more efficient drainage of these challenging reservoirs.

10.8 Acknowledgments

Special thanks from the authors to the staff of the Baker Hughes Tomball Pressure Pumping Technology Center's Geological Services and Geomechanics laboratories for the data, images, and graphical presentations scattered throughout this chapter.

10.9 References

Abdallah, W., Buckley, J.S., Carnegie, A., et al. 2007. Fundamentals of Wettability. *Oilfield Review*, **19** (2): 44–61.

Agbalaka, C.C., Dandekar, A.Y., and Patil, S.L, et al. 2008. The Effect of Wettability on Oil Recovery: A Review. Paper SPE 114496 presented at the SPE Asia Pacific Oil and Gas Conference and Exhibition. Perth, Australia. 20–22 October. http://dx.doi.org/10.2118/114496-MS.

Ahmed, U. 1983. Effects of Stress Distribution on Hydraulic Fracture Geometry. A Laboratory Simulation Study in 1-Meter Cubic Blocks. SPE paper 11637.

ASTM E10-10, Standard Test Method for Brinell Hardness of Metallic Materials. West Conshohocken, Pennsylvania. ASTM Int'l.

ASTM D3967-08. 2008. Standard Test Method for Splitting Tensile Strength of Intact Rock Core Specimens. ASTM Int'l.

ASTM D7012-07, 2009. Standard Test Method for Compressive Strength and Elastic Moduli of Intact Rock Core Specimens under Varying States of Stress and Temperatures. ASTM Int'l.

Aumon, J.B. 1986. A Laboratory Evaluation of Core Preservation Materials. ***SPE Form Eval***, **4** (1): 53–55 Trans., SPE 15381-PA. http://dx.doi.org/10.2118/15381-PA.

Biot, M.A. 1941a. General Theory of Three-Dimensional Consolidation. ***J. Appl. Phys***. **12**: 155–164.

Bohacs, K.M., Passey, Q.R., Rudnicki, M., et al. 2013. The Spectrum of Fine-grained Reservoirs from 'Shale Gas' to 'Shale Oil'/Tight Liquids: Essential Attributes, Key Controls, Practical Characterization. Paper IPTC 16676 presented at the International Petroleum Technology Conference. Beijing, China. 26–28 March. http://dx.doi.org/10.2523/16676-MS.

Chalmers, G.R., Bustin, R.M., and Power, I.M. 2012. Characterization of Gas Shale Pore Systems by Porosimetry, Pycnometry, Surface Area, and Field Emission Scanning Electron Microscopy/Transmission Electron Microscopy Image Analyses: Examples from the Barnett, Woodford, Haynesville, Marcellus, and Doig Units. ***AAPG Bull***, **96** (6): 1099–1119. http://dx.doi.org/10.1306/10171111052.

Chen, J.H., Li, B., Georgi, D.T., et al. 2012. Petrographic Features of Kerogen in Unconsolidated Shales and Their Effect on Hydrocarbon Petrophysics. Paper SPE 162612 presented at the Abu Dhabi International Petroleum Conference and Exhibition. Abu Dhabi. UAE. 11–14 November. http://dx.doi.org/10.2118/162612-MS.

Civan, F. 2000. ***Reservoir Formation Damage: Fundamentals, Modeling, Assessment, and Mitigation***, Gulf Publishing Company.

Clarkson, C.R., Freeman, M., Agamalian, M., et al. 2012. Characterization of Tight Gas Reservoir Pore Structure using USANS/SANS and Gas Adsorption Analysis. ***Fuel***, **95**: 371–385. http://dx.doi.org/10.1016/j.fuel.2011.12.010.

Cobold, P.R. 2013. Sweetspots in Foreland Basins, Insights from the Neuquén Basin (Argentina), and from Physical Models. Presented to the Houston Geological Society, Applied Geoscience Conference. Houston, Texas. 18–19 February.

Coenen, J.G.C. and Maas, J.G. (1994) Material classification by dual-energy computerized X-ray tomography. Proc. Int. Symp. on Computerized Tomography for Industrial Applications, 8–10 June, Berlin, 120–127.

Curtis, M.E, Sondergeld, C.H., Ambrose, R.J., et al. 2012. Microstructural Investigation of Gas Shales in Two and Three Dimensions Using Nanometer-Scale Resolution Imaging. ***AAPG Bull***, **96** (4): 665–677. http://dx.doi.org/10.1306/08151110188.

Davis, B.J. 2011. Mythbusters: Formation Damage Myths Exposed! Paper presented at the 9th European Formation Damage Conference. Noordwijk, The Netherlands. 7–10 June.

Davis, B.J. 2014. Internal Baker Hughes presentation.

Dembicki, H. 2009. Three Common Source Rock Evaluation Errors made by Geologists During Prospect or Play Appraisals. ***AAPG Bull***, **93** (3): 341–356. http://dx.doi.org/10.1306/10230808076.

Driskill, B., Suurmeyer, N., Rilling-Hall, S., et al. 2012. Reservoir Description of the Subsurface Eagle Ford Formation, Maverick Basin Area, South Texas, US. Paper SPE 154528 presented at the SPE European/EAGE Annual Conference. Copenhagen, Denmark. 4–7 June. http://dx.doi.org/10.2118/154528-MS.

Edman, J.D. 2012. How Local Variations in Thermal Maturity Affect Shale Oil Economics and Producibility. ***World Oil, Special Section, Geology and Geophysics***, **233** (3).

EIA. 2011. US Energy Information Administration. 2014. Subbituminous and Bituminous Coal Dominate U.S. Coal Production. http://www.eia.gov/todayinenergy/detail.cfm?id=2670. (retrieved July 21, 2014).

Fjaer E., Holt R.M., Horsrud, P., et al. 1996. Petroleum Related Rock Mechanics. Elsevier Publ., ***Developments in Petroleum Science***, **33**.

Baker Hughes/BJ Services Company. 2014. Geological Laboratories Technical Reports 1990–2014, Tomball, Texas. (unpublished).

Economides, M.J. and Nolte, K.G. 2000. ***Reservoir Stimulation***, Chapter 3, 3rd edition. West Sussex, England: John Wiley and Sons, Ltd.

Gidley, J.L., Holditch, S.A., Nierode, D.E., et al. 1989. *Recent Advances in Hydraulic Fracturing*, No. 12. Chap. 3, Richardson, Texas. Monograph Series, SPE.

Griffith, A.A., 1921. The Phenomenon of Rupture in Flow of Solids. *Phil. Trans. Roy. Soc. London*, A221,163–98. http://dx.doi.org/10.1098/rsta.1921.0006.

Guo, R., Mannhardt, K., and Kantzas, A. 2007. Laboratory Investigation on the Permeability of Coal During Primary and Enhanced Coalbed Methane Production. Paper PETSOC-2007-042 presented at the Canadian International Petroleum Conference. Calgary, Alberta. 12–14 June. http://dx.doi.org/10.2118/2007-042.

Handin J., Hager, R.V., Friedman, M., et al. 1963. Experimental Deformation of Sedimentary Rocks Under Confining Pressure: Pore Pressure Tests, *Bull. Am. Assoc. Petrol. Geol*., **47**.

Handwerger, D.A., Willberg, D.M., Pagels, M., et al. 2012. Reconciling Retort versus Dean Stark Measurements on Tight Shales. Paper SPE 159976 presented at the SPE Annual Technical Conference and Exhibition. San Antonio, Texas. 8–10 October. http://dx.doi.org/10.2118/159976-MS.

Hart, B., Macquaker, J., and Taylor, K. 2013. Mudstone ("shale") Depositional and Diagenetic Processes: Implications for Seismic Analysis of Source-Rock Reservoirs. *Interpretation* (1): B7–B26. http://dx.doi.org/10.1190/INT-2013-0003.1.

Heard, H.C., 1960. Transition from Brittle to Ductile Flow in Solenhofen Limestone as a Function of Temperature, Confining Pressure and Interstitial Fluid Pressure, Rock Deformation, *Geol. Soc. Amer. Mem.* **79**.

Holt, R.M., Brignoli, M., Kenter, C.J., et al. 1998. From Core Compaction to Reservoir Compaction: Correction for Core Damage Effects. Presented at Eurock '98 in Trondheim, Norway, 8–10 July, SPE/ISRM 47263.

Hunt, J.M. 1979. *Petroleum Geochemistry and Geology.* W.H. Freeman and Company, San Francisco. California.

Hunt, P.K. and Cobb, S.L. 1986. Core Preservation with Laminated, Healed Sealed Package. *SPE Form. Eval.*, **3** (4): 691–695; Trans., SPE 15382-PA. http://dx.doi.org/10.2118/15382-PA.

ISRM. 2007, Suggested Methods for Determining the Strength of Rock Material in Triaxial Compression: Revised Edition. *The Complete Suggested Methods for Rock Characterization, Testing and Monitoring*: 1974–2006, Elsevier.

ISRM. 2007. Suggested Methods for Determining Sound Velocity from *The Complete Suggested Methods for Rock Characterization, Testing and Monitoring*: 1974–2006, Elsevier Publ.

ISRM. 2007. Suggested Methods for Determining Tensile Strength of Rock Materials from *The Complete Suggested Methods for Rock Characterization, Testing and Monitoring*: 1974–2006. Elsevier Publ.

ISRM. 2007. Suggested Methods for Determining the Fracture Toughness of Rock from *The Complete Suggested Methods for Rock Characterization, Testing and Monitoring*: 1974–2006. Elsevier Publ.

Jaeger, J.C. and Cook, N.G.W. 1969. *Fundamentals of Rock Mechanic*s. Methuen Publ., Chap. 5 and 6.

Keelan, Dare K. 1975. Rock Properties and Their Effect on Gas Flow and Recovery. Presented at the 22nd Annual Southwestern Petroleum Short Course, Texas Tech University, Lubbock, Texas, 17–18 April.

Klaver, J., Desbois, J., and Urai, J.L. 2011. Porosity Mapping of Shale Using Broad Ion Beam–Scanning Electron Microscopy (BIB-SEM): Preliminary Results of an Organic Rich Shale. Les Rencontres Scientifiques d'IFP Energies Nouvelles. Paris, France.

Kuila, U., Prasad, M., Derkowski, et al. 2012. Compositional Controls on Mudrock Pore-Size Distribution: An Example from Niobrara Formation. Paper SPE 160141 presented at presented at the SPE Annual Technical Conference and Exhibition. San Antonio, Texas. 8–10 October. http://dx.doi.org/10.2118/160141-MS.

Kuila, U., McCarty, D.K., and Derkowski, A. 2014. Total Porosity Measurement in Gas Shales by the Water Immersion Porosimetry (WIP) Method. *Fuel*, **117** (Part B): 1115–1129. http://dx.doi.org/10.1016/j.fuel.2013.09.073.

Love, A.E.H. 1927. *A Treatise on the Mathematical Theory of Elasticity.* Dover Publ., 4th Edition, Chap. 3.

Maharidge, Russell L. 2014. Internal Baker Hughes Inc. presentation.

Modica, C.J. and Lapierre S.G. 2012. Estimation of Kerogen Porosity in Source Rocks as a Function of Thermal Transformation: Example from the Mowry Shale in the Powder River Basin of Wyoming. ***AAPG Bull.***, **96** (1): 87–108. http://dx.doi.org/10.1306/04111110201.

Moronkeji, D.A., Prasad, U., and Franquet, J.A. 2014. Size Effects on Triaxial Testing from Sidewall Cores for Petroleum Geomechanics. Paper ARMA 14-7405 presented at the US Rock Mechanics/Geomechanics Symposium, Minneapolis, Minnesota, 1–4 June.

Nelson, P.H. 2009. Pore-throat Sizes in Sandstones, Tight Sandstones, and Shales. ***AAPG Bull***., **93** (3): 329–340. http://dx.doi.org/10.1306/10240808059.

Odusina, E.O., Sondergeld, C.H., and Rai, C.S. 2011. An NMR Study of Shale Wettability. Paper CSUG/SPE 147371 presented at the Canadian International Petroleum Conference. Calgary, Alberta. http://dx.doi.org/10.2118/147371-MS.

Pitman, J.K., Price, L.C., and Lefever, J.A. 2001. Diagenesis and Fracture Development in the Bakken Formation, Williston Basin: Implications for Reservoir Quality in the Middle Member. U.S.G.S. Professional Paper 1653.

Rickman, R., Mullen, M.J., Petre, J.E., et al. 2008. A Practical Use of Shale Petrophysics for Stimulation Design Optimization: All Shale Plays Are Not Clones of the Barnett Shale. Paper SPE 115258 presented at the SPE Annual Technical Conference and Exhibition. Denver, Colorado. 21–24 September. http://dx.doi.org/10.2118/115258-MS.

Roberto, S.R., Stenebraten, J., and Dagrain, F. 2002. Continuous Scratch Testing on Core Allows Effective Calibration of Log-Derived Mechanical Properties for Use in Sanding Prediction Evaluation. Paper SPE/ISRM 78157 presented at the SPE/ISRM Rock Mechanics Conference. Irving, Texas. 20–23 October. http://dx.doi.org/10.2118/78157-MS.

Robinson, L.H. 1959. Effect of Pore and Confining Pressure on the Failure Process in Sedimentary Rocks. ***Colo. Sch. Mines Q***., **54**, 1959.

Rodrigues, N., Cobbold, P.R., Loseth, H., et al. 2009. Widespread Bedding-Parallel Veins of Fibrous Calcite ("beef") in a Mature Source Rock (Vaca Muerta Fm, Neuquén Basin, Argentina): Evidence for Overpressure and Horizontal Compression. ***J. Geol. Soc.***, The Geological Society of London, **166**: 695–709. http://dx.doi.org/10.1144/0016-76492008-111.

Schieber, J., Southard, J.B., and Schimmelmann, A. 2010. Lenticular Shale Fabrics Resulting from Intermittent Erosion of Water-Rich Muds–Interpreting the Rock Record in the Light of Recent Flume Experiments. ***J. Sed. Res.***, **80**: 119–128. http://dx.doi.org/10.2110/sr.2010.005.

Schieber, J., Zimmerle, W., and Sethi, P.S. 1998. ***Shales and Mudstones Volumes I and II***. Verlagsbuchhandlung, Stuttgart.

Schmidt, R.A. 1976. Fracture Toughness Testing of Limestone. ***Experimental Mech.*** **16** (5): 161–67.

Shellenberger, M., Nordhaus, T., Trembath, A., et al. 2011. New Investigation Finds Decades of Government Funding Behind Shale Revolution. The Breakthrough Institute. http://thebreakthrough.org/archive/new_investigation_finds_decade (accessed July 2014).

Sinha, S., Braun, E.M., Determan, M.D. et al. 2013. Steady-State Permeability Measurements on Intact Shale Samples at Reservoir Conditions–Effect of Stress, Temperature, Pressure, and Type of Gas. Paper SPE 164263 presented at the SPE Middle East Oil and Gas Show and Conference. Manama, Bahrain. 10–13 March. http://dx.doi.org/10.2118/164263-MS.

Slatt, R.M., and Neal, R.O. 2011. Pore Types in the Barnett and Woodford Gas Shales. ***AAPG Bull.***, **95** (12): 2017–2030. http://dx.doi.org/10.1306/03301110145.

Sone, H. and Zoback, M.D. 2013. Mechanical Properties of Shale-Gas Reservoir Rocks–Part 1: Static and Dynamic Elastic Properties and Anisotropy. ***GEOPHYSICS***, **78** (5): D381–D392. 10.1190/geo2013-0050.1.

Spain, D. R. and Anderson, G. A. 2010. Controls on Reservoir Quality and Productivity in the Haynesville Shale, Northwestern Gulf of Mexico Basin: Gulf Coast Association of Geological Societies Transactions, **60**: 657–668.

Tolke, J., Baldwin, C. Mu, Y., Derzhi, N. Fian, Q. Grader, A., and Dvorkin, J. (2010). Computer Simulations of Fluid Flow in Sediment; From Images to Permeability. ***The Leading Edge***, 29(1), 68-74.

Walls, J., Ceron, M.R., and Anderson, J. (2014). Characterizing Unconventional Resource Potential in Colombia; a Digital Rock Physics Project, Unconventional Resources Technology Conference, URTEC-1913256, Denver, Colorado. 25–27 August.

Walls, J.D., Diaz, E., and Sinclair. S.W. (2011) Digital Rock Physics Reveals Link between Reservoir Quality and Pore Type in Eagle Ford Shale, Search and Discovery Article #40785 http://www.searchanddiscovery.com/pdfz/documents/2011/40785walls/ndx_walls.pdf.html.

Walls, J., Morcote, A., and DeVito, J. (2013). Shale Reservoir Evaluation Improved by Dual-Energy X-Ray Ct Imaging. International Symposium of the Society of Core Analysts, Napa, California, 16–19 September.

Vinegar, H. (1986). X-ray CT and MR Imaging of Rocks, *Journal of Petroleum Technology*, March.

This page intentionally left blank

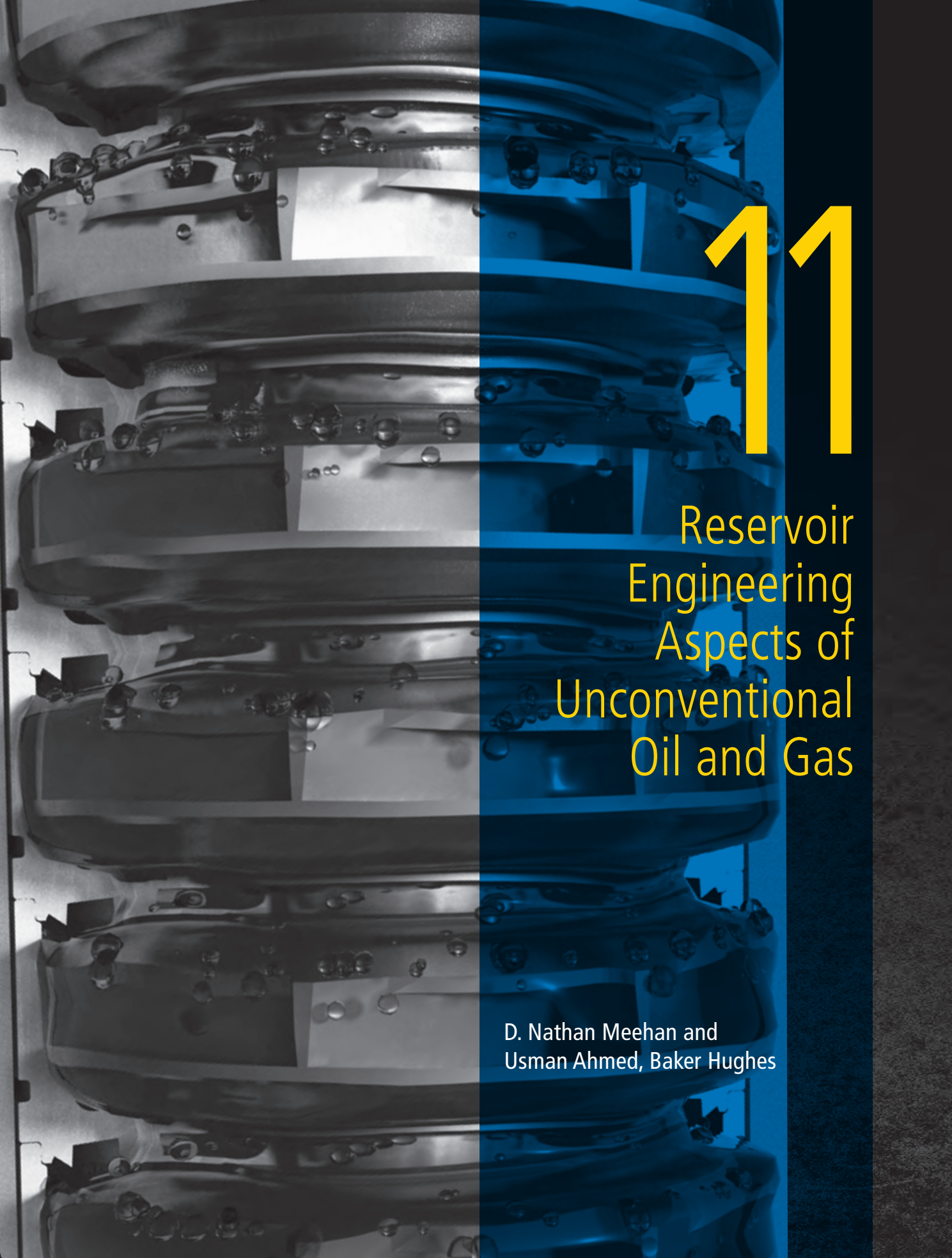

11

Reservoir Engineering Aspects of Unconventional Oil and Gas

D. Nathan Meehan and
Usman Ahmed, Baker Hughes

This page intentionally left blank

Chapter 11:
Reservoir Engineering Aspects of Unconventional Oil and Gas

11. 1 The Conventional Approach

As reservoir engineers, we can analyze most conventional oil and gas reservoirs and even tight gas plays by measuring or estimating the variables that constitute Darcy's law and the material balance equation. These include:

- PVT properties such as viscosity, formation volume factor, and isothermal compressibility
- Porosity and saturations
- Reservoir pressure and temperature
- Permeability including phase relative permeabilities
- Reservoir geometry including thickness and area
- In the case of hydraulic fractured wells, fracture geometry, and permeability

Complete descriptions of reservoir performance in conventional reservoirs and tight gas may further require knowledge of natural fractures and other detailed heterogeneities. The spatial variations of reservoir properties as dictated by geology represent the largest group of unknowns. The most critical aspect of this variability is often the spatial correlation of extreme values such as in natural fractures of faults. Conventional tools to address this problem include 3D or even 4D seismic to improve the spatial model, integration of geological knowledge about the reservoir along with petrophysical (and less frequently but likely no less important geomechanical) information into an integrated earth model.

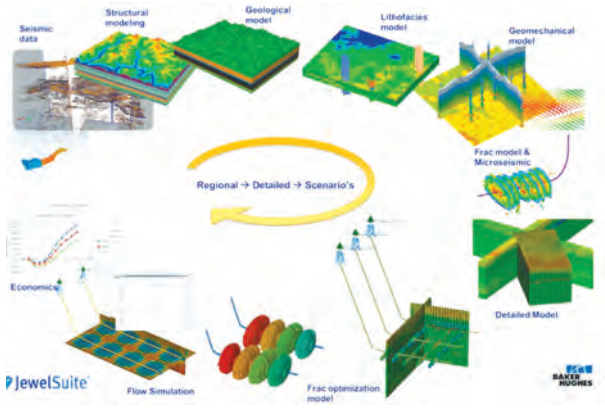

Fig. 11.1—Workflow used in reservoir modeling and simulation of field development studies.

Baker Hughes JewelSuite™ software (**Fig. 11.1**) is an example of such an earth model. The well and reservoir parameters from the earth model are discretized into a reservoir simulation model. The reservoir simulation model simultaneously solves flow and material balance equations and can be used to match historical data or forecast reservoir performance under a variety of alternative development scenarios. These alternative development scenarios allow economic optimization of decisions including well spacing, hydraulic fracture stage spacing and locations, hydraulic fracture design parameters, and operating conditions, to name a few.

11.2 The Unconventional Dilemma

Unconventional reservoirs are not as easily addressed as conventional or tight gas reservoirs for the following reasons:

- Fluid flow mechanisms in unconventional are different.
- Storage mechanisms for hydrocarbons are different and difficult to characterize.
- The distribution of natural fractures is different and not susceptible to conventional natural fracture modeling.
- The interaction and characterization of multiple hydraulic fractures generally is not captured in unconventional models. We discuss our present understanding.

11.2.1 Flow Mechanisms

Flow rates and pressure drops for a single-phase fluid can be calculated rigorously only for simple geometries and fluid-wall interfaces. For example, the Hagen–Poiseiulle equation calculates steady-state laminar flow through a cylinder. If Newtonian fluids are used, the model predicts flow velocities that are linear with pressure drop. Such approaches would be extremely complex for real porous media. Darcy's law is a phenomenologically derived constitutive equation to calculate flow velocity in porous media that presumes linearity and introduces permeability (k) as an empirical constant to approximate the aggregate complexities in cross-sectional area and connectedness of the reservoir pores. Although originally established empirically, it can be derived from the Navier–Stokes equation. The simplest form of Darcy's law is:

$$u = -\frac{k}{\mu}\frac{dP}{dL} \qquad \textbf{(Eq. 11.1)}$$

where:

u = the apparent velocity, cm/s
k = permeability, D
μ = viscosity, cp
p = pressure, atm
L = length of cylinder, cm

Darcy's law can be applied to most flow in porous media and forms the basis along with material balance of reservoir engineering. Even when reservoir conditions do not strictly show this linear relationship of flow rates with pressure drop, the standard approach is a modification of Darcy's law to adapt for unique reservoir conditions. For example, relative permeability is a construct that allows us to model phase permeabilities as a function of saturation.

Unconventional reservoir pores are thought to be so small that Darcy's law may not be applicable. In general, flow processes occur either as a result of advection or diffusion. Advection describes flow with a net mean fluid flow while diffusion represents more random flow behavior even if driven by concentration gradients. Both models are represented by conservation of mass and constitutive laws. Diffusion equations generally incorporate stochastic models based on random walks and central limit theorems with constitutive equations either at the microscopic level or mesoscopic level. For example, diffusion is critical to modeling the flow of gas in coalbed methane. It is the desorption of gas that allows for

$$C_m = 0.031\rho_B(V_L \times p) / (p_L + p), \qquad \textbf{(Eq. 11.2)}$$

where:

C_m = matrix gas concentration, scf/ft^3
ρ_B = bulk density, g/cm^3
V_L = dry, ash-free Langmuir volume constant, scf/ton
p_L = Langmuir pressure constant, psia
p = pressure in the fracture system, psia

Most coalbed methane (CBM) gas production is dominated by gas that is adsorbed in the microporosity of the coal with lesser amounts of free gas present in the natural fractures. Measures of the available gas in a coalbed methane reservoir generally are made with an isotherm as illustrated in **Fig. 11.2**. In this figure, a Langmuir isotherm is used to describe the gas storage content of the coal. The Langmuir volume of 375 scf/ton in this graph represents the total theoretical volume of gas that can be adsorbed in a given sample. The Langmuir pressure is that pressure that must be achieved for half the theoretical gas to be recovered. In this example, the initial reservoir pressure is 3210 psi at which the Langmuir isotherm match would have predicted a little over 318 scf/ton of adsorbed gas. The coalbed methane reservoir only has 281 scf/ton of adsorbed gas and will produce water until the reservoir pressure is reduced to 1700 psi, the critical desorption pressure. The isotherm then can be used to predict the volumes of adsorbed gas that are released until the abandonment pressure is reached.

While this approach is common for screening coalbed methane (CBM) projects, cores taken from shale gas projects often show relatively small volumes of adsorbed gas with exceptions such as the Antrim shale. There remains substantial debate as to the extent of adsorbed gas in shale gas recoveries and well performance. If adsorption plays a significant part in recoveries it is likely to be at late stages in the reservoir as pressures are highly depleted. It is also likely to result in lower late-time decline rates and necessitate artificial lift and compression for gas wells to minimize bottom hole flowing pressures. Significant gas adsorption may also necessitate closer well spacing for optimal drainage.

In small pores, fluid flow can occur in a wide range of flow mechanisms including:

- Knudsen diffusion, where the mean free path of a particle is relatively long compared to the pore size. Collisions with the walls are frequent and Knudsen diffusion is common for pore sizes in the 2-50 nm range.

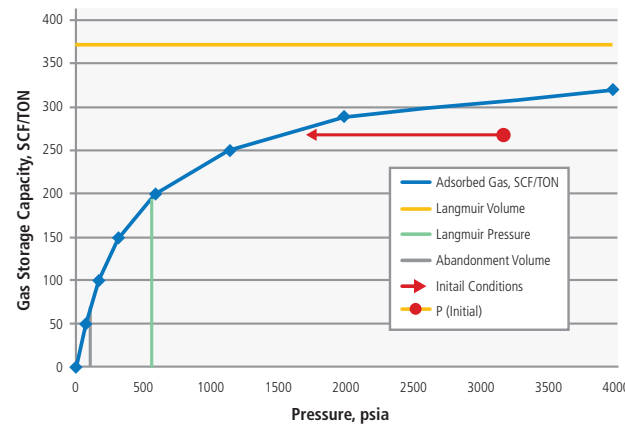

Fig. 11.2—An example coal gas isotherm (gas storage capacity, SCF/Ton versus pressure, psi).

- Fickian diffusion, this model describes molecular diffusion driven by differences in concentration gradients. By contrast to Knudsen diffusion, the mean free path of particles is relatively low compared to pore scales and this diffusion model is applicable to Brownian motion.
- Hydrodynamic flow is driven by pressure gradients along a flow channel.
- Viscous flow is flow in which the mean free path is small compared to the pore scale and pressure drops are determined mainly by the collisions of the molecules.
- Normal-mode diffusion describes flow of Brownian particles in the presence of friction.
- Single-file diffusion represents flow where flow paths are so small that they cannot pass each other in pore channels or throats.

Knudsen (diffusive flow) may be important in nanopores or in solid kerogen. Additionally, desorption from kerogen may contribute to production. Ozkan and Raghavan (2010) illustrated the impact of integrating diffusive flow in nanopores in addition to Darcy flow in the fractures and matrix. When permeabilities are very low, Darcy flow becomes insignificant and diffusive flow dominates. They conclude that at very low permeabilities it is essential to incorporate diffusive flow.

11.2.2 Storage and Flow Mechanisms

Conventional models of porous media incorporate the concept of a representative elementary volume (REV). This volume has aggregate properties (porosity, permeability, saturations) representative of a larger volume. Even in very heterogeneous porous media, the REV concept is useful. For example, the REV of a naturally fractured reservoir might be relatively large; however, the media can be described as a composite reservoir comprising unfractured matrix and fractures. The REV sizes of the component media may be quite small. Tight gas and conventional models assume that the bulk of all hydrocarbon storage is in matrix pores. Flow only occurs as interconnected pores communicate pressure changes initiated at wellbores. In the conventional/tight gas models hydraulic fractures provide large surface areas that more effectively communicate pressure changes to the reservoir but do not significantly affect the bulk properties of the matrix.

The created hydraulic fractures in unconventional wells can increase bulk matrix permeability. This can be the result of shear slippage of previously closed natural fractures, slowly slipping faults, and other factors. This is a somewhat controversial topic. Some experts do not believe that improving matrix permeability is necessary if created hydraulic fractures have sufficient surface area. Others strongly disagree and insist that unconventional reservoirs cannot be successful without this fracture-rock interaction. The truth is probably a complex amalgam of the two opinions. Additionally, storage of hydrocarbons in organic matter or adsorbed onto the matrix may be significant relative to those stored in pore spaces.

Javadpour described multiple scales for fluid flow. **Fig. 11.3** illustrates gas evolution and transport mechanism in shale formations at different scales. The differences in flow models for the smallest pores may incorporate different models for wall slip, the relative size of the molecules and the pore-throats, the mean free path of the molecule and chemical and physical interactions with pore surfaces. The Knudsen number is useful in describing flow regimes and is defined as

$$K_n = \frac{\lambda}{d} \qquad \textbf{(Eq. 11.3)}$$

where d is the pore-throat diameter and λ is defined as:

$$\lambda = \frac{k_b T}{\sqrt{2}\pi\delta^2 \mathrm{P}} \qquad \textbf{(Eq. 11.4)}$$

where:

k_b is the Boltzmann constant, 1.3806488 × 10-23 m^2 kg s^{-2} K^{-1},
T is the temperature (K).
P is pressure, atm,
σ is the particle hard shell diameter

The Knudsen number is a function of temperature and pressure (**Fig. 11.4**). Values below 0.001 correspond to no-slip (Darcy) flow. Values of Kn between 0.001 and 0.1 correspond to slip flow or Knudsen diffusion. Javadpour illustrates these flow regimes for different pore-throat sizes. They then describe an alternative approach applicable for constant diffusion coefficient flow with minimal viscous effects. Their measurements indicate that nanopores dominate flow behavior in many shale core samples.

Nelson provides an interesting comparison of porosity, permeability and pore-throat sizes in sandstones, tight sandstones, and shales (**Fig. 11.5**). The contrast in pore-throat sizes going from conventional to tight to shales is remarkable. The extraordinarily small pore-throat sizes suggest that some level of natural fractures may be necessary to improve the bulk permeability and that even low fracture conductivities can substantially enhance fluid flow.

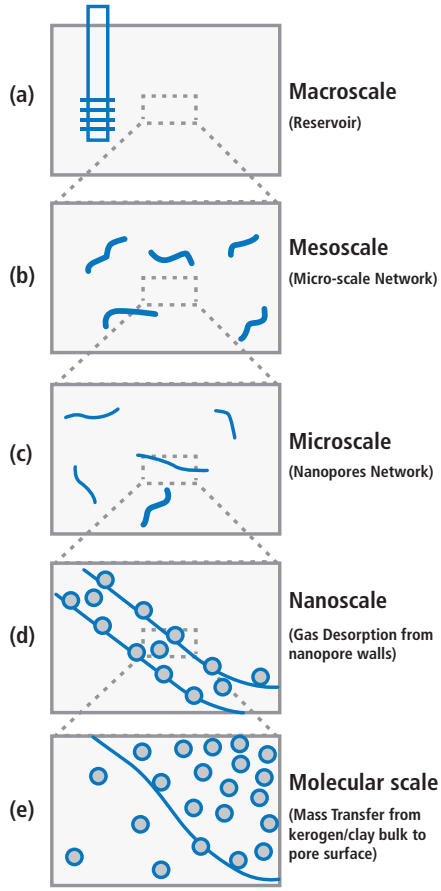

Fig.11.3—Gas evolution and transport at different scales in shales. (Javadpour et al. 2007.)

11.3 Well Variability Issues

Well-to-well variations in production from horizontal laterals that have nearly identical hydraulic fracture treatments may be significant. A common observation when production logs are run in horizontal laterals is that substantial fractions (20 to 50%) of hydraulic fractures are ineffective. There is wide variability in the relative contribution of each fracture stage and there is poor agreement with analytic solutions. Analysis of local fractures parameters derived from petrophysics may help explain the variations; however, there are few published results clearly explaining the variability. Reservoir characterizations that fail to predict the behavior are overly simplistic.

Fig. 11.6 shows the significant variability in mineralogy of the various shales. The Barnett shale is rich in sandstone and has very little calcite, whereas the Eagle Ford shale is rich in calcite and has very little sandstone. Flow mechanism will

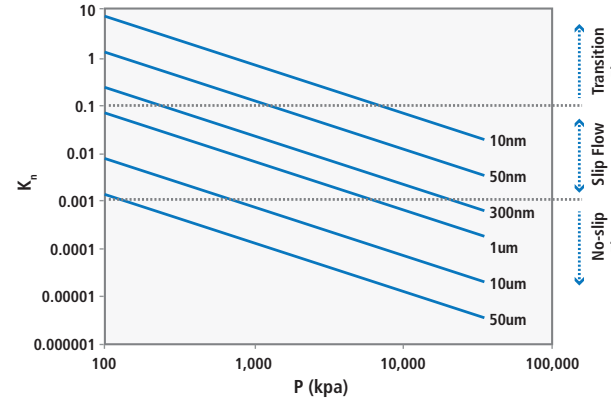

Fig.11.4—Knudsen number for a gas mixture for different pore sizes. (From Javadpour et al. 2007.)

be different within such variable mineralogy and lithology. Plus, such variation will impact the choice of drilling bits and the completion and stimulation fluids used. Within each of the shale resources we see similar levels of variation as one moves through the lateral length, suggesting a potential reason for hydraulic fractures not producing similar production results.

Vertical and horizontal well logs, particularly image logs, are critical to describing shales. Advanced logging tools now enable operators to image fractures and faults away from the wellbore using advanced logging techniques. Whole cores are relatively rare and operators increasingly rely on rotary sidewall cores for conventional measurements. The low permeabilities involved complicate conventional core analysis. Advances in digital rock physics are encouraging, particularly in making sense of the shales and in using cuttings.

The key drivers explaining the variability arise from multiple sources. However, geomechanical variations and variations in fractures, particularly in critically stressed fractures, may explain much of the lateral variability. Microseismic measurements (Chapter 20) often provide clues to lateral variability; current rock stresses along with the variations in natural fractures and the presence of faults contribute to the variability. Operators of low permeability horizontal wells requiring hydraulic fracturing including most unconventional wells generally settle on transverse fractures. This suggests that they drill parallel with the minimum horizontal compressive stress, σ_h. Operators in such reservoirs rarely try to parallel σ_H; this approach generates longitudinal fractures and is more common for higher permeability applications. Wells drilled in intermediate directions generally should be avoided. Fractures generated at the wellbore often result in multiple initiations

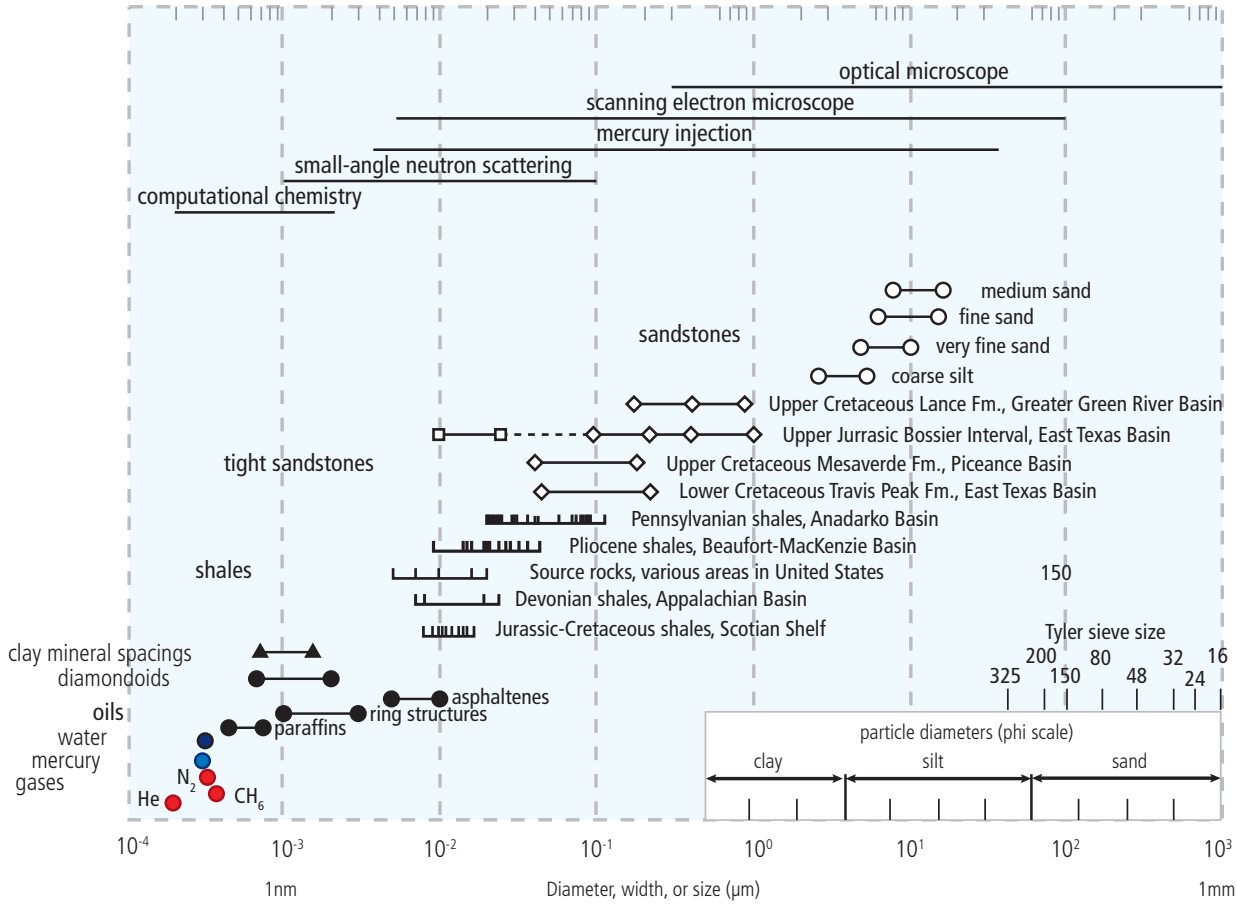

Fig.11.5—Pore-throat sizes in sandstones, tight sandstones, and shales. (From Nelson 2009.)

that compete for fluid and turn into a direction normal to the local minimum compressive stress, resulting in shear, narrow fracture widths, high net pressures, and potential screen-outs.

In active normal faulting stress environments where $\sigma_h<\sigma_H<\sigma_V$, the tendency is to create a number of parallel vertical hydraulic fractures orthogonal to the wellbore. Such behavior has been observed in multiple cases, particularly in tight gas sands. If the created fractures are sufficiently closely spaced, significant stress interference may arise between the created fractures and can manifest in increasing instantaneous shut-in pressures (ISIPs) and fracture initiation and net pressures with increasing job numbers, often reaching a maximum level. However, the presence of critically stressed fractures can complicate the simple model and improve the performance results.

Simple parallel fractures created in Mode I tensile failure in unaltered nanodarcy rock generally cannot explain the performance of successful wells. As fractures are created, the region of increased stress may activate substantial numbers of critically stressed fractures and slowly slipping faults. While the closure of the tensile failures may require proppant, the permeability created by activated critically stressed fractures may be responsible for a substantial fraction of all fluid flow (Barton 1997; Zoback 2012). The numerous linear features common in Barnett microseismic that are not parallel to the major faulting directions are unlikely to be fluid-filled or proppant-filled. When $\sigma_h \approx \sigma_H$, it is easier for the created hydraulic fracture to turn, particularly near pre-existing failures. However, vast numbers of microseismic events in such applications support the critically stressed fractures model. To the extent that they are created in shear because of slippage of critically stressed fractures, they have a tendency to be self-propped. Some authors refer to the behavior as fracture complexity and incorrectly assume that it is caused by the varying directions and paths of injected fluids. There is no doubt that created hydraulic fractures may follow complex paths; however, much of the created seismicity occurs well ahead of fluid-filled hydraulic fractures.

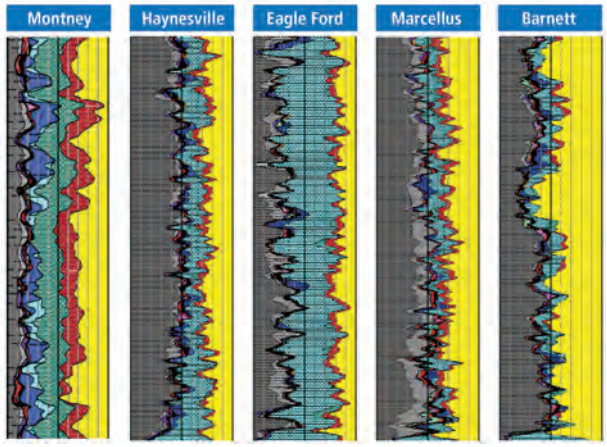

Fig.11.6—Variations of mineralogy and lithology of the various shale formations.

In strike-slip faulting environments, the maximum horizontal compressive stress exceeds the vertical stress. Estimation of the maximum horizontal compressive stress cannot be performed accurately by simple log measurements; an appropriate geomechanical model is required (Chapter 9). Important components of such a model include measurements from minifractures or microfractures and wellbore image logs. The presence or absence, size, direction, and other characteristics of drilling-induced tensile failures and wellbore breakouts are critical components of a geomechanical model. The geomechanical model is employed in many aspects of shale development including defining wellpaths, lateral placement, and hydraulic fracture design. However, the greatest value is derived from an understanding of the fundamental characteristics that dominate flow behavior.

As discussed in Chapter 8, shale porosity includes many pores that essentially are unconnected to poorly connected. Hydrocarbon generation in shales occurs over long periods of time and the increased pressures can fail the rock locally in tension. The fact that hydrocarbons migrate from shales implies some local permeability. Conventional reservoirs are sufficiently permeable that buoyant forces and traps dictate where the migrating hydrocarbons may accumulate. Unconventional reservoirs contain hydrocarbons that have not migrated and buoyant forces do not control their distribution in shales. Nes et al. 1993 used NMR to measure effective porosities. Like many other researchers, they found shale porosities to be complicated in that it is difficult to establish a ground truth. Very fine pores may not dry easily. The process of hydrocarbon extraction and helium porosity measurements may actually change the physical structure of the shale. Kerogen remaining in the rock may be porous as well. Dehghanpour and Shirdel (2011) hypothesized a triple porosity model of shale reservoirs and others have postulated greater complexity.

In practice, operators use porosity logs infrequently in horizontal wells and take cores in those wells less frequently. Digital rock models of porosity increasingly are useful in unconventional reservoirs to at least maintain consistent estimates of variability in rock properties. As a practical matter few unconventional horizontal laterals are instrumented with long-term production monitoring capabilities, and cased hole production logs are infrequent and complicated to correctly interpret. Many of the production logs run in such wells imply that a significant fraction of the hydraulic fractured intervals contribute negligible quantities of hydrocarbons. Are the fracturing jobs in those intervals wasted money? If so, is it due to fracture design or implementation, unavoidable statistical variation in rock properties, geosteering into a poor part of the interval, or other factor?

11.4 Impact of Fracture Characteristics

While shales and related unconventional rocks often are susceptible to hydraulic fracturing, substantial, well-connected natural fractures in such rocks are not common in modern resource plays. Highly fractured shales can produce without stimulation and storage of hydrocarbons in such reservoirs requires structural or stratigraphic traps. In other words, they wouldn't be unconventional reservoirs. The combination of interconnected, conductive fractures and matrix permeability allows unconventional reservoirs to produce commercial quantities of hydrocarbons.

Most natural fractures in unconventional reservoirs are sealed initially. If sufficient strain occurs because of proximity to a sufficiently large hydraulic fracture, most of them may become critically stressed. The generally increasing instantaneous shutdown pressures observed in subsequent stages illustrates how significant the stress shadow from created hydraulic fractures may be. Advanced modeling shows that the shape and direction of created hydraulic fractures are strongly impacted by this interaction. A substantial number of such previously closed natural fractures slip in shear as a result of the created hydraulic fractures. Measured microseismicity in typical unconventional wells likely measures as many or more such slipping natural fractures as it does those immediately caused by the

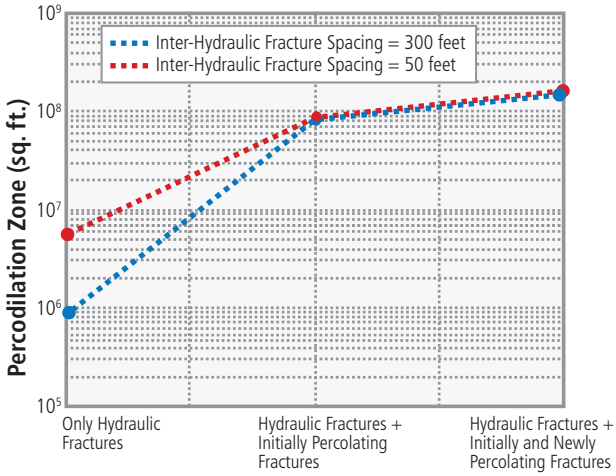

Fig. 11.7—Impact of hydraulic fractures on system permeability. (From Johri and Zoback 2013.)

hydraulic fracture. Many more such slip events are likely to be created whose magnitude is too small to be measured as microseismic events. Slowly slipping faults also are unlikely to create measured microseismic events.

Johri and Zoback (2013) modeled the interaction of natural fractures and created hydraulic fractures. The size of the percolation zone (an area of hydraulic activity that has bulk permeability in excess of the native rock) shows that as this percolation zone expands in a given system of natural and induced fractures, the magnitude of contribution from the stimulated rock (in excess of the hydraulic fractures alone) can be very substantial (**Fig. 11.7** and **Fig. 11.8**). The connectivity of the newly stimulated microcracks is impossible to predict directly. Similarly, it is not obvious how to predict the total number of such microcracks and faults or their permeability. As long as these values remain history-matching parameters for numerical simulation or production transient analysis, there will be a great deal of nonuniqueness in models of well performance.

11.5 Drainage Volume

One of the less understood aspects of the unconventional resource development is the drainage volume of the individual well and the individual hydraulic fracture stage. Most of the unconventional resource development was based on statistical drilling and as such not much attention was placed on the reasons for failures and success of an individual well let alone the individual hydraulic fracture stage or clusters. Industry surveys (Welling & Company 2012; Hart's E&P 2012) suggest the following statistics:

- Seven out of ten wells did not meet expected production.
- Six out of ten hydraulic fractures were deemed non-commercial.

When enquired as to the reasons for such not-so-good results, three out of four US-based operators mentioned that they did not know enough about the subsurface. This implies that they did not know enough about the reservoir flow mechanism of horizontal wells with several hydraulic fracture stages. Before we can address the drainage volume of individual wells we need to be able to comprehend the drainage volume of individual fracture stages.

Drainage volume of individual hydraulic fracture stage in conventional tight oil and gas reservoirs is well documented in the literature (Holdtich et al. 1978; Mukherjee and Economides 1991; Raghavan et al. 1997; Horne and Temeng 1995; Lolon et al. 2009) and is addressed in Chapter 14. Understanding and estimating drainage volume of induced hydraulic fracture stage in unconventional shale reservoirs is complicated by the presence of natural fractures. Outcrop analysis can and has allowed formulation of discrete fracture network (DFN) modeling. **Fig. 11.9** from the Appalachian Plateau shows the Marcellus shale reservoir to be fractured (Engelder et al. 2009; Meyer et al. 2011). In the illustration the J1 is more the common fracture and that hydraulic fractures should be targeted for this fracture network for enhanced production. The fracture porosity is indicated along the direction of the J1 strike while the matrix porosity is in between the J1 fracture paths. Similar saturated fracture spacing can be seen near the Oil Mountain area in Wyoming. This unfolded outcrop is a thrust-cored anticline with the fractures running up and down similar to the Marcellus outcrop. Several investigators used fracture patterns from outcrops to model the fracture network (Medeiris et al. 2010; Meyer et al. 2010) and integrate with the created hydraulic fracture and model the flow behavior by implementing a dual porosity dual fracture network system.

The following equations describe the governing relationships between hydraulic fracture system and its propagation in the reservoir:

Continuity equation:

$$\vec{\nabla} \cdot \vec{v} w + 2v_l + \frac{\partial w}{\partial t} = 0 \quad \textbf{(Eq. 11.5)}$$

Mass conservation equation:

$$\int_0^t q(\tau)d\tau - V_l(t) - V_{sp}(t) - V_f(t) = 0 \qquad \textbf{(Eq. 11.6)}$$

Momentum conservation equation:

$$\vec{\nabla}P = -\frac{1}{2} f\rho\vec{q}^2 / w^3 \qquad \textbf{(Eq. 11.7)}$$

Width opening pressure constraints:

$$w = \Gamma_w \frac{(P_f - \sigma) H_\varsigma}{E'} \qquad \textbf{(Eq. 11.8)}$$

Nomenclature:

E' = Effective Young's modulus
H_ς = Characteristic fracture half-height (or length)
Γ_w = Generalized influence function
f = Darcy friction factor
P = Pressure
P_f = Fracture pressure
σ = Confining stress
q = Injection or flow rate
t = Time, Closure time, $t_c > t_p$
τ = Time of fracture leak-off area creation
v_l = Fluid leak-off velocity
V_f = Fracture volume
V_l = Volume loss by leak off
V_{sp} = Spurt loss
w = Fracture width

With the assumption of homogeneous discrete fracture network (DFN) model and the associated uniform drainage volume, Meyer et al. (2009) designed the equidistant transverse fracture stages by leading to predicting production performance for oil wells in Bakken and gas wells in Marcellus. **Fig. 11.10** illustrates the oil production over time in Bakken for increasing number of transverse hydraulic fractures. Irrespective of the number of transverse fractures, the initial decline is steep. Initially the 12-stage well produces almost 20 times that of a single stage. By 100 days, the ratio drops to 14, and by three years the drop is at 10 indicating the change in flow pattern.

11.6 Other Reservoir Issues

Reservoir engineers frequently make relatively simplistic assumptions about abandonment pressures and the ability to produce wells to low bottom hole pressures. This is typically

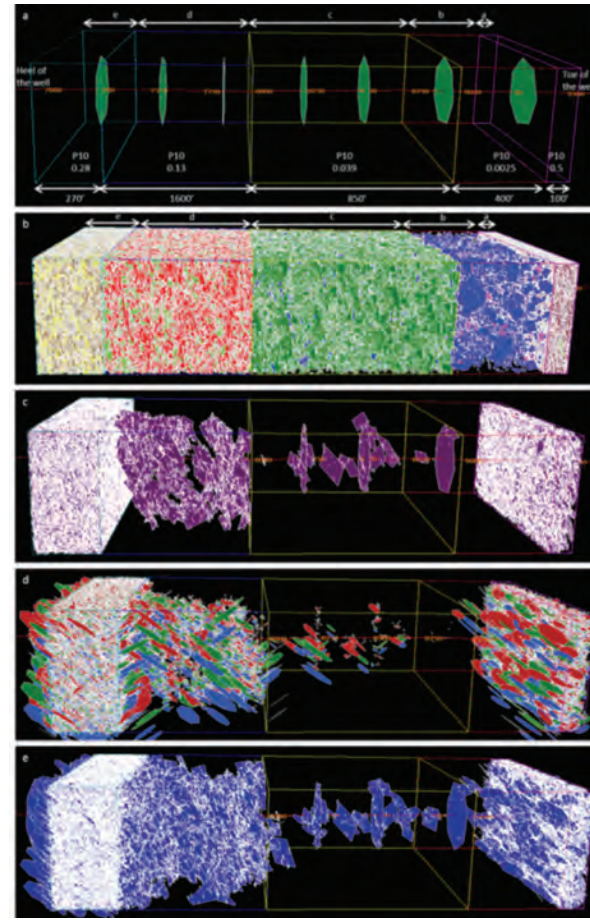

Fig. 11.8—Models showing (a) created hydraulic fractures, (b) DFN populated natural fractures, (c) critically stressed hydraulic fractures connected to the well, (d) newly created fractures generated by slip on poorly connected fractures, and (e) combined fractures. (From Johri and Zoback 2013.)

a reasonable simplification; however, this is not true for most unconventional wells. For vertical oil wells and liquid rich gas wells, sucker rod pumping can produce low bottom hole pressures with low liquid flow rates. In many cases the pump can be placed below the perforations if gas production is problematic or above it in cases with significant sanding. Electric submersible pumps (ESPs) are the preferred artificial lift method for high liquid flow rates. Recent advances such as the Baker Hughes FLEXPump™ series lowered the minimum liquid flow rates for ESPs to around 100 BFPD. More details are in Chapter 19. In horizontal wells, sucker rod pumps must be placed well above the horizontal section of the well and do not perform nearly as well as ESPs in lowering pressures. Modern field development approaches emphasize pad drilling in which many, perhaps dozens, of unconventional wells are drilled from adjacent surface

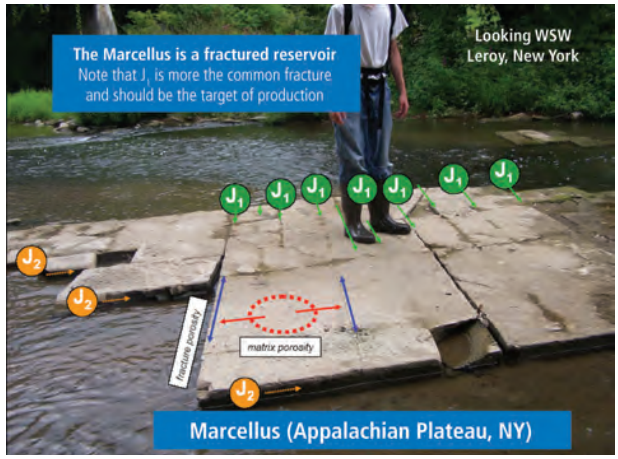

Fig. 11.9—Marcellus outcrop in the Appalachian Plateau, NY. (From Engelder et al. 2009, modified by Meyer et al. 2011.)

locations. The advantages of this approach are plentiful and include:

- Minimize the total surface footprint of development, particularly with respect to production facilities that remain long term
- Decrease rig moves
- Decrease transportation and road costs with the corresponding impact on the environment
- Enable commercial use of produced natural gas and minimizing venting or flaring
- Enable produced or flowback water to be reused
- Eliminate duplicate fluid and chemical storage sites
- Improve operational continuity and HSE performance

With twelve or more nearby wellheads it is more likely to be unacceptable to have a large number of highly visible surface sucker rod pumping units. Environmental and community relations suggest that alternative pumping such as ESPs may be preferable throughout the life of the well.

The ideal pump for artificial lift has a surface impact similar to that of an ESP but operates through a large range of liquid flow rates (1 to 1,000 BFPD), handles sand and gas well, and is reliable and energy efficient. In such cases the reservoir pressures can be effectively lowered to the point of optimizing production and ultimate recovery.

Similarly, well designs, particularly lateral junctions, must be stable for the long term. If a high volume unconventional well is damaged or fails mechanically early in its lifetime, the remaining reserves may be sufficient to either redrill the well or add a lateral from a nearby well. Reservoir pressures would not have been reduced so much as to cause substantial lost circulation. The likelihood of restimulating the formation is reasonable. At later dates there might not

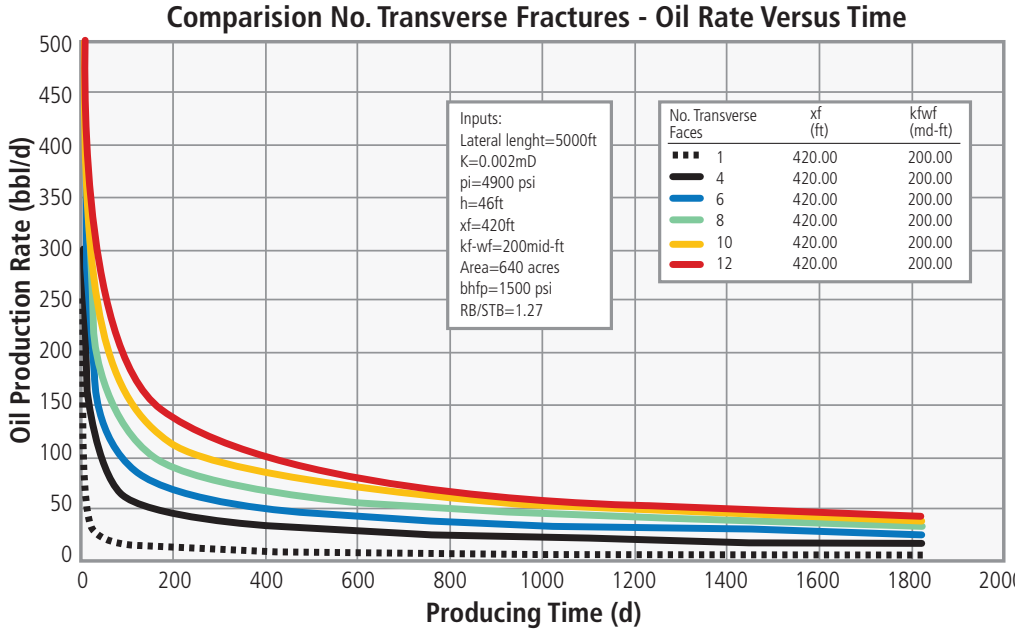

Fig. 11.10—Impact of increasing number of transverse fracture stages on production performance. (From Meyer et al. 2010.)

be adequate reserves to justify a redrilling of wells lost to mechanical means or the reservoir pressure may be so low as to pose costly drilling challenges. This concern has limited the number of multilateral wells used in unconventional developments. Because so much of the cost of the wells is due to the cost of the created hydraulic fractures, the loss of a multilateral well would be extremely expensive. However, in situations where the surface and vertical well drilling portion of well costs is high, multilateral wells will become increasingly attractive because the technology needed for such completions has been developed and proven in other applications.

11.7 References

Andrade, J.S., Costa, U.M.S., Almeida, M. P., et al. 1999. Inertial Effects on Fluid Flow through Disordered Porous Media. ***Physical Review Letters***, **82** (26): 5249–5252.

Barton, C.A., Moos, D., and Zoback, M. 1999. In Situ Stress Measurements Can Help Define Local Variations in Fracture Hydraulic Conductivity at Shallow Depths. ***The Leading Edge***, **16**: 1653–1656.

Dehghanpour, H. and Shirdel, M. 2011. A Triple Porosity Model for Shale Gas Reservoirs. Paper SPE 149501 presented at the Canadian Unconventional Resources Conference. Alberta, Canada. 15–17 November. http://dx.doi.org/10.2118/149501-MS.

Engelder, T., Lash, G.G., and Uzcategui, R.S. 2009. Joints Sets That Enhance Production from Middle and Upper Devonian Gas Shales of the Appalachian Basin. ***AAPG Bulletin***, **93** (7): 857-889.

Holditch, S.A., Jennings, J.W., Neuse, S.H., et al. 1978. The Optimization of Well Spacing and Fracture Length in Low Permeability Gas Reservoirs. Paper SPE 7496 presented at the SPE Annual Fall Technical Conference and Exhibition, 1–3 October, Houston, Texas. http://dx.doi.org/10.2118/7496-MS.

Horne, R.N. and Temeng, K.O. 1995. Relative Productivities and Pressure Transient Modeling of Horizontal Wells with Multiple Fractures. Paper SPE 29891 presented at the Middle East Oil Show. Bahrain. 11–14 March. http://dx.doi.org/10.2118/29891-MS.

Hosticka, B., Norris, P.M., Brenizer, J.S., et al. 1998. Gas Flow through Aerogels. ***Journal of Non-Crystalline Solids***, **225** (1): 293–297.

Javadpour, F., Fisher, D., and Unsworth, M. 2007. Nanoscale Gas Flow in Shale Gas Sediments. ***J. Cdn. Pet. Tech***, **46** (10). PETSOC-07-10-06.

Johri, M. and Zoback, M.D. 2013. The Evolution of Stimulated Reservoir Volume during Hydraulic Stimulation of Shale Gas Formations. Paper SPE 168701/URTeC 1575434 presented at the Unconventional Resources Technology Conference. Denver, Colorado. 12–14 August. http://dx.doi.org/10.1190/URTEC2013-170.

Levitt, D.G. 1973. Dynamics of a Single-File Pore–Non-Fickian Behavior. ***Physical Review A***, **8** (6): 3050–3054.

Lolon, E., Cipolla, C., Weijers, L., et al. 2009. Evaluating Horizontal Well Placement and Hydraulic Fracture Spacing/Conductivity in the Bakken Formation, North Dakota. Paper SPE 124905 presented at the SPE Annual Technical Conference and Exhibition. New Orleans, Louisiana. 4–7 October. http://dx.doi.org/10.2118/124905-MS.

Malek, K. and Coppens, M.O. 2003. Knudsen Self- and Fickian Diffusion in Rough Nanoporous Media. ***Journal of Chemical Physics***, **119** (5): 2801-2811.

Medeiros, F. Kurtoglu, B., Ozkan, E., et al. 2010. Analysis of Production Data from Hydraulically Fractured Horizontal Wells in Shale Reservoirs. ***SPE Res Eval & Eng*** **13** (3): 559–568. SPE 110848-PA. http://dx.doi.org/10.2118/110848-PA.

Meyer, B.R. and Bazan, L.W. 2011. A Discrete Fracture Network Model for Hydraulically Induced Fractures–Theory, Parametric and Case Studies. Paper SPE 140514 presented at the SPE Hydraulic Fracturing Technology Conference. The Woodlands, Texas. 24–26 January. http://dx.doi.org/10.2118/140514-MS.

Meyer, B.R., Bazan, L.W., Jacot, R.H., et al. 2010. Optimization of Multiple Transverse Hydraulic Fractures in Horizontal Wellbores. Paper SPE 131732 presented at the SPE Unconventional Gas Conference. Pittsburgh, Pennsylvania. 23–25 February. http://dx.doi.org/10.2118/131732-MS.

Mukherjee, H. and Economides, M.J. 1991. A Parametric Comparison of Horizontal and Vertical Well Performance. ***SPE Form Eval***, **6** (2): 209–216. SPE 18303-PA. http://dx.doi.org/10.2118/18303-PA.

Nelson, P.H. 2009. Pore-throat sizes in sandstones, tight sandstones and shales. *AAPG Bulletin*, **93** (3): 329–340. http://dx.doi.org/10.1306/10240808059.

Olav-Magnar Nes, Horstud, P., and Sketjne, T. 1993. Shale Porosities as Determined by NMR. Paper SEG-1993-0088 presented at the SEG Annual Meeting, Washington, DC. 26–30 September.

Ozkan, E. and Raghavan, R. 2010. Modeling of Fluid Transfer from Shale Matrix to Fracture Network. Paper SPE 134830 presented at SPE Annual Technical Conference and Exhibition. Florence, Italy. 19–22 September. http://dx.doi.org/10.2118/134830-MS.

Raghavan, S.R., Chen, C.C., and Agarwal, B. 1997. An Analysis of Horizontal Wells Intercepted by Multiple Fractures. *SPE J*, **2** (3): 235–245. SPE 27652-PA. http://dx.doi.org/10.2118/27652-PA.

Sholl, D.S. and Fichthorn, K.A. 1997. Normal, single-file, and dual-mode diffusion of binary adsorbate mixtures in AlPO4- *Journal of Chemical Physics*,**107** (11): p. 4384–4389.

Singh, H. and Javadpour, F. 2013. Nonempirical Apparent Permeability of Shale. 168724-MS SPE Conference Paper.

Weber, M. and R. Kimmich. 2002. Maps of Electric Current Density and Hydrodynamic Flow in Porous Media: NMR Experiments and Numerical Simulations. *Physical Review E*, **66** (2): p. 026306.

Zoback, M.D. 2012. Identification and Hydraulic Properties of Critically-Stressed Fault and Anticipating Triggered Seismic and Aseismic Fault Slip. https://pangea.stanford.edu/researchgroups/scits/sites/default/files/Zoback%20Presentation.pdf (accessed August 2014).

This page intentionally left blank

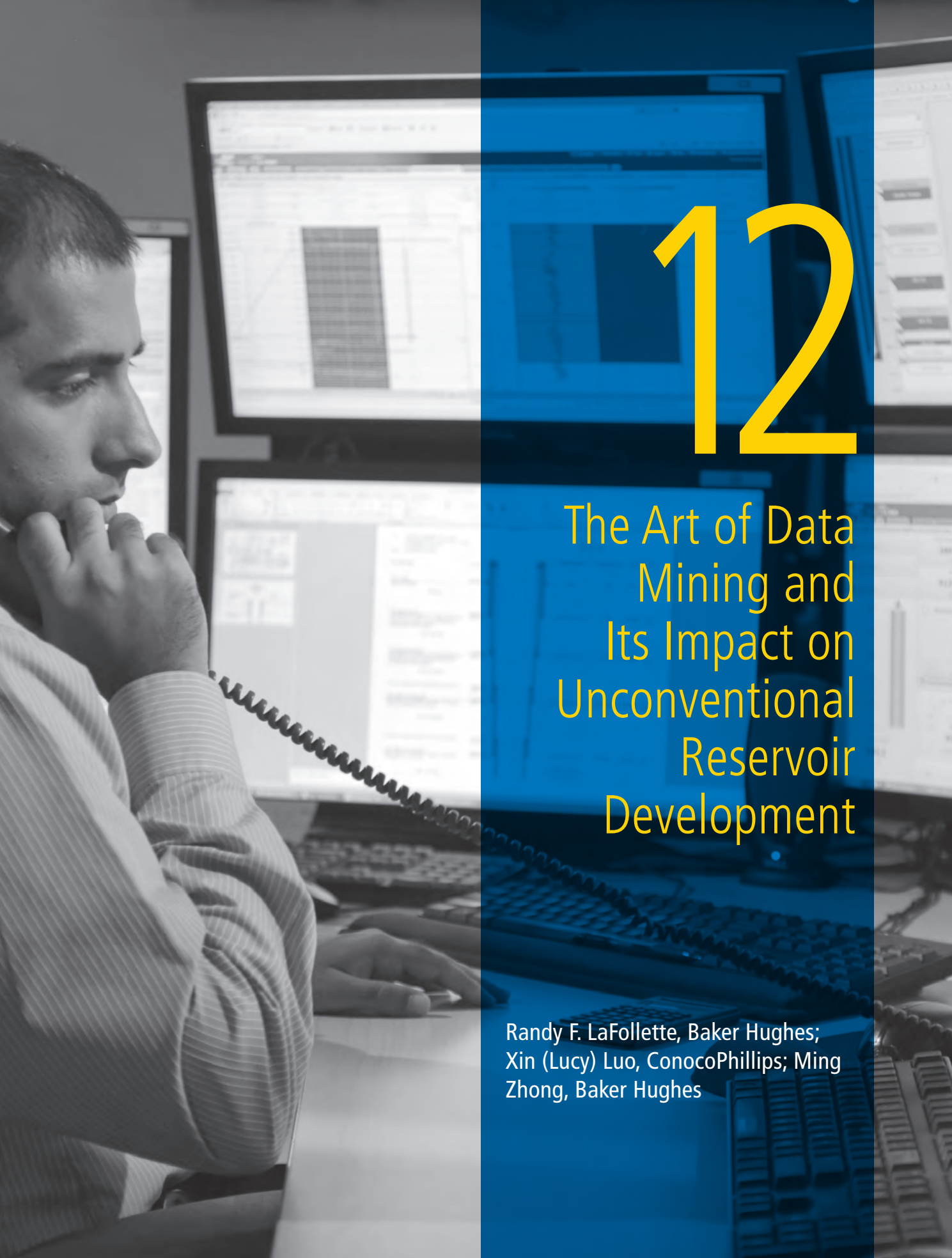

12

The Art of Data Mining and Its Impact on Unconventional Reservoir Development

Randy F. LaFollette, Baker Hughes; Xin (Lucy) Luo, ConocoPhillips; Ming Zhong, Baker Hughes

This page intentionally left blank

Chapter 12:
The Art of Data Mining and Its Impact on Unconventional Reservoir Development

12.1 The Importance of Data Mining in Unconventional Reservoirs

12.1.1 Introduction

Unconventional reservoir development is a process in which multi-million-dollar decisions must be made in a commodity environment that is both technically and fiscally sensitive. An operator's decision to acquire a certain unconventional leasehold or concession is a huge financial risk, perhaps one hundred million US dollars or more, that may or may not ever pay out. Reservoir quality is the first requirement, but even if the resource is adequate, changes in operational practices may either substantially improve—or ruin—an operator's success.

North America has been, and remains, the testing laboratory for unconventional reservoirs around the planet. Many thousands of vertical wells were completed in tight gas sandstones and mixed conventional and tight reservoirs since the 1970s (Hufft, 1977; Meehan and Pennington, 1982). The modern era of "shale" reservoir drilling and completion began in the 1980s in the Barnett shale (Steward 2007), although much of the groundwork was laid by the United States Department of Energy's Eastern Gas Shales Project studies of the 1970s. (Shellenberger et al. 2011, Ahmed, et al. 1991, Yost et al.1980).

The previous paragraphs should be sufficient for the reader to understand the importance of careful analysis of the available data, so that expensive and risky decisions can indeed be data-driven. However, there is more. The unconventional resource owner has access to quantities of data unheard of even 10 years ago. The effect is simple–too much data, too little knowledge. This chapter is intended to discuss the important topic of practical data mining and what it can mean to the reader. The authors have presented a discussion of variables, available data, database quality control, and analytical methods. Case studies of different reservoirs are also documented.

12.1.2 Fundamental Reservoir Quality Issues in Unconventional Reservoirs

Early in the modern era of mudstone reservoirs, also known as "shales," these reservoirs were often thought to have relatively uniform natural properties, perhaps with the exception of large faults that bounded different producing areas. This view led to an industry belief system that production results depended mainly on completion and stimulation parameters. There was some truth in that belief, but it was incomplete. Inadequate stimulation, that is, pumping treatments that are too small for the zone in question, produced less than desired production. At the other end of the treatment size range, too-large treatments in the Barnett could also result in poor well results. The reasons varied, but in general, the results were due to larger treatments contacting unknown geohazards, either karsts or faults, that were in communication with the underlying Ellenberger saline aquifer. Subsequent data mining work over the years has shown that the natural variability in unconventional well production is heavily dependent on variations of naturally occurring rock properties. Data mining results have also shown that well architecture, completion, and stimulation parameters can be key productivity drivers. These results hold true whether tight gas sandstones, mudstones, or light-tight oil reservoirs are under consideration.

The fundamental natural rock properties in unconventional reservoirs are found at the intersection of geochemical, geological, and geomechanical properties in the reservoir and bounding beds. For data mining purposes, geochemical parameters are less important in tight gas sandstones where migration out of the source rock has occurred. In the mudstone reservoirs, geochemical maps indicating thermal maturity yield one of the keys to understanding production variability in the source rock reservoirs.

Key geological engineering properties are represented in some of the factors of the fundamental rate equation (that is, permeability, thickness, reservoir pressure, and reservoir fluid viscosity). For the importance of the fundamental rate equation in understanding oil and gas well production, see Economides and Nolte 2000. These values do vary geologically across producing areas. Certain values, particularly matrix permeability and its variability, are difficult or impossible to obtain across tens to ten thousand or more wells, and this complicates the data mining process. The importance of natural fractures to system permeability in these reservoirs further complicates the reservoir quality picture.

Reservoir fluid viscosity impacts productivity in unconventional reservoirs. And, particular mudstone reservoirs typically show substantial variability in gas gravity as the thermal maturity varies across different areas of a play.

Reservoir thickness is a much more tractable value than permeability and is also a key to production results.

However, it should not be assumed that greater thickness would ***automatically*** result in greater production. Non-sympathetically varying parameters such as thermal maturity or presence or absence of fracture height growth barriers have shown in some instances to compete with pay height to reduce production.

Reservoir pressure is also a key productivity factor. Unconventional reservoirs that work tend to be over-pressured to strongly over-pressured.

From the previous discussion, it would be easy to conclude that any data mining exercise would be doomed to failure. System permeability is a substantial uncertainty. Reservoir fluid viscosity measurements are rarely available for data mining work. Pay thickness can be a bit more reliable. The good news for data mining efforts using less granular data sets, such as public data, is that natural reservoir quality typically varies systematically across geographic areas and may be proxied by the well location variables.

12.1.3 Variability of Key Geomechanical Properties

In addition to the above fundamental factors, there are many other parameters that may strongly influence well production in unconventional reservoirs. Geomechanical properties comprise one set of influencing parameters because they are critical to hydraulic fracture initiation, propagation, complexity, containment, conductivity, and durability.

Elastic mechanical properties of shale gas reservoir rocks were shown by Sone and Zoback (2013) to vary widely within and among reservoirs. From their experimental laboratory work, the main drivers of variability were mineralogy and rock fabric anisotropy. Practitioners also need to concern themselves with the mechanical properties of all bounding beds that may be fractured, or those that may act as fracturing barriers across any given area of study.

An early GIS-based analysis of the Barnett shale indicated that the presence or absence of the Viola–Simpson formation will determine if, and where, there is a hydraulic fracturing barrier. Where the Viola–Simpson formation underlies the Barnett shale across part of the Fort Worth basin, it acts as a hydraulic fracturing barrier. Where the barrier is missing, the GIS analysis shows clear evidence of a negative impact on vertical well performance.

12.1.4 Time-Dependence of Well Architecture, Completion, and Stimulation Trends

Workers with some history in unconventional reservoirs understand intuitively that well architecture, completion, and stimulation approaches have varied substantially over time.

One way to understand the macro trends is through the use of a graphic timeline, such as that shown for Barnett shale from its tentative beginning in 1981 through 2009 (LaFollette and Holcombe et al. 2012). In **Fig. 12.1**—Barnett update 2009, vertical wells are shown in yellow, deviated wells are in red, and horizontal wells are shown in blue. The dates for introduction of key technologies are shown by the annotations.

Another example is shown in tabular format (LaFollette et al. 2011) in **Table 12.1**. The abbreviation MHF is ***massive hydraulic fracturing***. SWF is ***slick water fracturing***.

Examination of the table reveals that, over the relatively short time frame of 6 years, completed lateral well lengths increased from an average of 1,800 feet to over 2,600 feet, while fracture treatment volume per foot decreased from 2,200 ft to 1,400 ft. Additionally, proppant quantity increased from approximately 670 lbm/ft to 960 lbm/ft. Thus, the completion date can be a key variable describing well productivity.

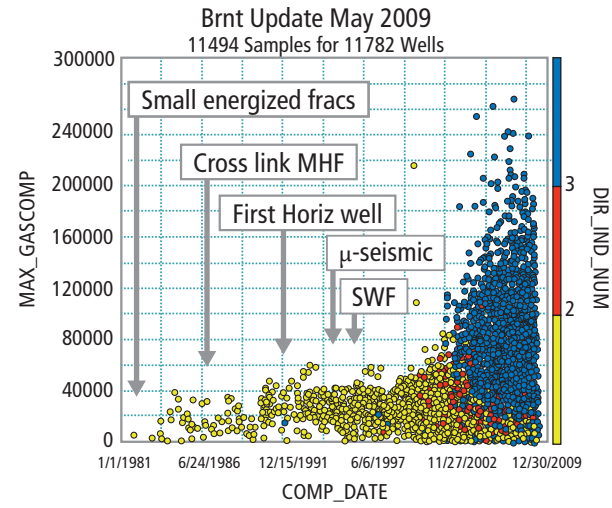

Fig. 12.1—Barnett update 2009.

Table 12.1—Statistical data for whole field Barnett horizontal completions, 2004 to 2009.

Average Statistics for Barnett Horizontal Completetions						
	Completion Year					
Parameter	2004	2005	2006	2007	2008	2009
Number of Completions	255	697	1239	2303	2662	1380
Perforated Length, ft	1793	1874	2054	2187	2363	2675
Peak Monthly Gas Mscf/mo	52098	53150	49851	52640	54098	58689
1 year Cumulative Gas, MMscf/yr	378.3	355.2	325.2	340.2	358.4	365.2*
1 year Cumulative Liquids, BBl	2267	2048	1552	1469	1911	2438*
1 year Cumulative Water, BBl	44050	63915	64825	73026	89721	77329*
Treatment Volume, Mgal	3849	3793	3686	3353	3587	3796
Treatment Volume /pcrf ft, gal/ft	2206	1951	1779	1497	1418	1410
Proppant Quantity, Mlbs	1141	1400	1867	2287	2562	2624
Proppant Quantity/pcrf ft, lbs/ft	672	711	886	995	993	953
Number of Stages	2.1	2.8	4.0	3.2	3.2	3.6
Peak Monthly Gas P10, MMscf/mo	17.0	17.3	17.3	17.4	19.0	21.2
Peak Monthly Gas P25, MMscf/mo	29.1	27.4	26.5	27.9	30.3	34.2
Peak Monthly Gas P50, MMscf/mo	45.6	46.6	42.0	45.4	47.4	53.7
Peak Monthly Gas P75, MMscf/mo	69.6	68.2	64.1	68.8	69.2	74.9
Peak Monthly Gas P90, MMscf/mo	93.1	98.6	93.1	96.8	95.9	103.3

*Limited Sample Size

12.2 Evolution of Data Mining

12.2.1 Non-Oilfield Data Mining

Data mining is an analytic process of knowledge discovery. In a data-mining project, we collect raw data, examine the quality of the data, and explore the data to find intrinsic relationships and consistent patterns. Ultimately, we want to apply these findings to help us make predictions on new datasets. Data mining may sound like an abstract concept, but it's actually underlying many things, influences many aspects of our daily life, and shapes our future.

Market survey questionnaires are distributed to random customers to gain feedback on specific products or services to enable the provider to make improvements. Think of those short online surveys printed on your restaurant receipts that contain several feedback questions! Responses are data-mined to provide guidance to the management.

In clinical trials, all subjects' vital statistics are collected periodically together with the drug usage, including placebo usage and drug dose, to make an inference on the drug toxicity and efficacy. All drugs have to go through multiple-phase clinical trials before being approved by the US Food and Drug Administration (FDA).

In financial services, every bank has its own set of criteria for loan applications. In this type of data-mining exercise, a statistical model is built upon large historical datasets that automatically pulls all the applicants' credit information, including but not limited to, credit scores, loans and mortgages, and delinquency history. The data-mining algorithm then uses that data to evaluate the risk of charge-off. If the predicted risk is lower than a preselected threshold, the application will be approved.

Social media companies apply algorithms to look into users' emails, forum posts, videos viewed—and even who their friends are—to allocate hobbies and interests before they send out targeted advertisements.

Data mining has a close similarity to statistical methods, and the terms have been used in the literature interchangeably. Exploratory data analysis methods, such as scatter plots and histograms, can be used to describe different perspectives of the data and summarize them. Linear models provide straightforward preliminary descriptions of variable relationships. Principal component analysis, factor analysis, and cluster analysis bear important merits in high-dimension datasets. Due to the rapid development in computer technology, machine learning has emerged as a new trend in data mining recently, including random forest, boosting, and support vector machines. Unlike traditional statistical models, these methods don't require an explicit expression of the model in the beginning.

12.2.2 Early Oilfield Formation Studies: Number 2 Lead Pencils and Graph Paper

Practicing engineers have attempted to put pencil to paper and correlate field practice with production and economics for a very long time. When the earliest formation, completion, and stimulation studies known to the authors were done in the 1960s, modern data mining methods were in their infancy. Early work from engineers in the oilfield consisted of compilations of existing practices, perhaps with calculations designed to offer an understanding of the theory and practice. These studies involved very limited data and effectively represented "current events."

12.2.3 Computers and Univariate Statistics: Spreadsheets and Cross Plots

Early formation studies in which relatively large datasets (for the time) were used include a study of the Second Frontier formation of the Moxa Arch, southwest Wyoming, US (LaFollette and Davis, 1993.)

In that project, public datasets were gathered from a subscription to Petroleum Information (now IHS Energy). Monthly production streams from approximately 500 wells were decline-analyzed by hand to generate production metrics. A computer spreadsheet application was then used to graph and correlate data, such as sedimentary depositional environment, porosity and permeability, fracturing fluid type, and so on. The data was used for correlation to target variables such as estimated ultimate recovery (EUR) and initial potential (IP) metrics using linear regression. Studies such as this are univariate statistical studies, where independent variables are each correlated in isolation to a target variable. In these types of studies, interactions among the so-called "independent variables" are not typically considered.

Univariate statistical studies at the time did not generally take advantage of the more modern understanding of the importance of reservoir quality proxies, and thus suffered from the fact that much of the driving force (that is, the interaction of permeability, pressure, thickness, and hydrocarbon viscosity) behind well productivity was excluded from the analysis.

12.2.4 Map-Based Analysis: Geographical Information Systems (GIS)

While spreadsheets and cross plots have certain uses, map-based GIS analysis brings a geoscience-based perspective to the analysis, interpretation, and display of complex integrated datasets. Certainly, the early work of this nature in the earth sciences field came from geologists and geochemists putting their data on hand-drawn maps. With the advent of GIS mapping applications such as ESRI's ArcView™ (supplanted by ArcGIS™), IHS Energy's Petra™, and Schlumberger's Petrel™, workers have been much more productive in terms of the sheer numbers of maps they could generate. However, this was only the beginning, as the speed with which maps can be modified to show, for example, the best and worst 10% of wells in a given play, can allow direct question and answer using the map. Present-day GIS applications have evolved far beyond their original geological and geochemical uses.

GIS applications are useful for analysis and display of all data categories from well architecture through production. Even simplistic well azimuths drawn as straight lines from surface to bottom-hole locations were used in groundbreaking work that proved the importance of well azimuth to productivity in the Barnett shale. Attribute functions can be easily used to show stage counts. Specialized functions such as the drainage radius function in the IHS Energy Petra™ application can be used to directly show treatment size as high aspect ratio ellipses that can be aligned in the maximum horizontal stress direction where it is known. Work with GIS methods begins by enabling workers to store all available data in a well-centric manner, using a unique well identifier (UWI) number assigned to each well's data. Critical to good interpretation, GIS applications can store geological, geochemical, and geomechanical data along with well logs, plus engineering and production data. Much of the data from tables within a GIS application may be analyzed internally and then displayed directly on the map. This offers the advantage of immediately taking data—such as treatment size, fracturing fluid type, well azimuth, completion stage count—and immediately putting it into a geographic and geologic perspective.

GIS is so useful to us because it makes use of the human brain's inherent pattern recognition ability. An example to think about is our innate ability to instantly recognize the faces of the people we know. Use of GIS methods not only allows engineering inputs to be analyzed in geological, geomechanical, and geochemical perspective, but it also enables the practitioner to study and recognize patterns on the map. This makes GIS a very powerful analytical tool, not only to aid the data miner in interpretation, but to also show data and knowledge on the map in patterns that can be easily comprehended and explained.

12.2.5 Present Day: Multivariate Statistics Combined with GIS

There are many different methods used in multivariate statistical work. For a more complete study of the different methods available, refer to Zangl and Hannerer 2003; Nisbet et al. 2009; and Hastie et al. 2009.

Early GIS work for well optimization was presented in Economides and Martin, 2007. Evolving workflows have taken GIS work with multivariate statistical work and combined them to create a powerful workflow method that can be used by other workers. This allows the practitioner to take advantage of the power of each set of methods. In these workflows, "sanity checked" datasets are developed and analyzed using boosted tree methods to develop the influence plots highlighting key well productivity drivers. A commercial GIS application is then used to further develop the interpretation and to display key insights on maps.

12.3 Data Availability

There are many different sources of data, public and proprietary, that are available for study. The data is classified into different types, and then categorized into subgroups. This section discusses the issues associated with the variety of data streams available (or not) for data mining.

12.3.1 Data Categorization

There are numerous random variables in our daily work. We can classify them into a few categories based on their intrinsic characteristics. Generally, there are two types of variables: numeric variables and categorical variables. A numeric variable can be either an integer or a decimal. A variable with integer values is termed a ***discrete numeric variable***. Two examples would be the number of fracture stages and well completion year. On the other hand, a variable with possible decimal values is termed a ***continuous numeric variable***. Two examples of continuous variables are total proppant quantity and cumulative lateral length. In other words, continuous variables can have any value within a ***theoretically possible*** range of values. A categorical variable can only take values from a few categories. If these values can be ranked and sorted, the variable is ordinal, otherwise it is nominal. Proppant mesh size is an example of an ordinal categorical variable, while well completion type is an example of a nominal categorical variable.

Variable classification is very important, since we need to apply different methods to visualize the different categories in exploratory data analysis. This will be discussed in more detail in Section 12.5.2. Correct variable classification can also be helpful in data quality control. If a fracture stage count value was 8.5, or a proppant mesh size was shown as 204.0 in the raw data, it would be clear to a domain expert that something was wrong, as those values would not be possible. Those data points would then need to be flagged for further investigation and correction, removal, or marked as suspicious.

It is worthwhile to mention that the API (UWI) number is a crucial variable in all oil and gas data manipulation, since it is the "unique, permanent, numeric identifier." A 14-digit API number is composed of 2-digit state code, a 3-digit county code, a 5-digit well identifier for the permit, a 2-digit directional sidetrack code, and a 2-digit event sequence code.

Well data can be subdivided into reservoir quality, well architecture, well completion, stimulation, and production classes.

Knowledge of the reservoir is crucial to optimize shale play production. Reservoir quality can be characterized based on total organic carbon (TOC) kerogen, thermal maturity, porosity, permeability, mineralogy, lithology, brittleness, thickness, stress regime, depositional environment, reservoir pressure, viscosity, flow regimes, and distribution of natural fractures, to name but a few. Different hydrocarbon types may be characterized by their cumulative gas-to oil ratio (GOR). Fluid types evolve basinward from black oil to volatile oil, condensate, and finally to dry gas, and vary with increasing formation depth, pore pressure, API gravity, and thermal maturity. When resources for petrophysical analysis are not available on the scale required for work with thousands of wells, and when public data are used, X-Y surface location can be used as a proxy for the data sources.

Well architecture data includes completed lateral length, well azimuth, and well dip angle. Completed lateral length is calculated as the measured depth of the bottom perforation or sleeve, minus measured depth of the top perforation or sleeve. Average azimuth calculations were taken from the actual directional survey in the completed lateral section of the well. Special care was taken when calculating well azimuth when survey points crossed the due north dividing line between the northwest and northeast quadrants. These wells were flagged, azimuths were projected onto

the southeast/southwest quadrants, average azimuth was calculated, and then projected back to their original directions. Well dip angle was averaged from the actual directional survey over the completed section of the lateral. Wells with dip angles less than 90° are toe down, wells having dip angles greater than 90°are toe up, and wells at 90° are flat.

The well completion can be either open-hole or cased-hole (plugged and perforated). Well completion data contains casing size, casing length, cementing depth and method, bore hole diameter, number of stage counts, clusters counts or clusters per stage, and the length of stage.

Well stimulation treatment data will be focused on generic fracturing fluid type and volume, proppant type, proppant quantity, mesh size, average pressure concentration, injection rate, and additives.

Well production and production proxies, such as maximum oil rate in the first 12 producing months and normalized 12-month cumulative production, were often selected and merged with the other data for analysis. The best-producing month in the first 12 producing months (BO) gives an indicator of the factors studied that can drive overall well early time production rate. The BO/ft. is a measure of efficiency of completed well length. Cumulative 3-month and 12-month oil/gas production was based on 3 and 12 months of active production beginning with the peak month.

For unconventional reservoir development, how to optimize drilling and completion and how to effectively predict production remains a major challenge in the oil and gas industry. Thus, data integration and analytic innovation are becoming more and more important.

12.3.2 Public Data Sources

In the North American oil and gas industry, state governments generally give the public the right to access government oil and gas records. Certain exceptions may apply to the disclosure of the information. The Railroad Commission of Texas maintains historical information that is used by employees, other state agencies, local government, the oil and gas industry, and the general public in its Central Records and Imaging units. An estimated 132 million pages of analog and digital documents encompassing the history of each Texas oil and natural gas well—from the drilling permit application to the final plugging report—are preserved. The oil and gas potential profile includes applications to drill, oil and gas completion reports, plugging reports, producer's transportation authority, and miscellaneous records from 1964 to the present. The well log (WL) profile includes images of all well logs received since July 2004.

The following is the data link from Railroad Commission of Texas:

http://www.rrc.state.tx.us/data/index.php#

Similar to Texas, the following states' websites contain information related to oil and gas well permits, leases, rigs, and production or drilling reports. Some states have online mapping applications and the well locations are updated daily. The following states' websites are active as of the date of this writing:

Arkansas	http://www.aogc.state.ar.us/JDesignerPro/JDPArkansas/default.htm
Colorado	http://cogcc.state.co.us/Home/gismain.cfm
Kentucky	http://oilandgas.ky.gov/Pages/ProductionReports.aspx
Montana	http://www.bogc.dnrc.mt.gov/webapps/dataminer/
New York	http://www.dec.ny.gov/energy/1603.html
North Dakota	https://www.dmr.nd.gov/oilgas/
Utah	http://gis.utah.gov/data/energy/oil-gas/
Virginia	http://www.dmme.virginia.gov/dgoinquiry/frmMain.aspx?ctl=1
West Virginia	http://www.dep.wv.gov/oil-and-gas/databaseinfo/Pages/default.aspx

Fracfocus

http://www.fracfocus.org/

In 2011, the FracFocus.org national chemical registry website was created. The website was formed to give the public access to detailed information on every fracturing treatment pumped in the United States. It is currently managed by the Ground Water Protection Council and the Interstate Oil and Gas Compact Commission. The well data sheet contains the

technical information about the fluid type, proppant type, all fluid additives with purpose and concentration, trade name, supplier, ingredients, chemical abstract service number, ingredient percentage in additive by percent of mass, and the ingredient concentration in hydraulic fracturing fluid percentage by mass. The well data sheet also includes key well data such as fracture date, location, API number, depth, operator, well name, total water volume, and production type. All data is based on the total material injected into the well, but the data is not broken down by stage or the number of stages.

Vendors' Data

Commercial datasets about well history, completion practices, and monthly production are available to be purchased from vendors, such as IHS, or Drilling Info, but are not available from the states' websites.

IHS

http://www.ihs.com/products/oil-gas-information/production-data/index.aspx

The **IHS Energy** well database contains well header data, location, key well dates, producing formations, actual directional survey, well test, treatment information, and production stream data.

http://www.ihs.com/products/oil-gas-information/production-data/index.aspx)

The IHS web site states: "IHS has a team of experts who work daily to transform original raw data received in multiple formats and in several languages, following different company or country standards and from various sources into the critical information fit for customer's requirement. IHS Production Data covers the world from Canada, the United States and 85 countries."

Canadian production data is available on over 800 approved and pending down-spacing applications to Alberta's Energy Resources Conservation Board. Canadian fluid analyses and pressure information is updated regularly, as well as providing written and visual depictions of well production and performance.

US well and oil, gas, and water cumulative and monthly production volumes are available on over 1.7 million producing entities. IHS has the following to say:

> IHS Drilling and Rig Activity products cover every facet of US drilling activity, from permits through completion, along with instant access to detailed analysis of daily updated well activity across the country.

IHS Oil and Gas Log Data products provide critical data for well properties, hydrocarbon zones, and optimal production methods. Digital and raster log databases contain the historical well log coverage in the industry for both continental and off-shore exploration.

Drilling info

http://info.drillinginfo.com/products/

"Drilling Info provides an online permit, completion mapping, historical well and scout information, nationwide production data, and international regional information. DI Desktop is one of their powerful production analysis tools. It will not only deliver well production, decline curve analysis, and estimated ultimate recoveries, but contains transporter, gas plant/refinery and pricing data."

RigData

http://www.rigdata.com/Index3.aspx

RigData says they provide the information pertaining to drilling activity in the United States, the Gulf of Mexico, and Canada. It has comprehensive reporting on drilling permits, drilling activity, and tracking for drilling rig locations. RigData collects and publishes extensive information on permits-to-drill, completions data, drilling rig locations, and overall oil and gas drilling activity.

12.3.3 Proprietary Data Sources

Besides public and vendor databases, operators and service companies will have their own proprietary data sources. In-house databases have been used extensively for data mining purposes. Most of the time, these are more reliable than public data sources, although none yet has been found to be without some level of error.

At Baker Hughes, we have the PowerVision™ stimulation and cementing database, hydraulic fracturing JobMaster™ database, drilling and evaluation MaPS system database, product line financial SAP database, and rig data.

The Baker Hughes PowerVision™ applications allow engineers to enter job information simultaneously into one

centralized database. The system allows all authorized users to view and create job proposals from any location. It provides quality services and products to our customers. The database contains general information, regarding the customer, business and technique contact name etc., and well information, such as name, rig name, API, location, etc., service line information, such as cementing, acidizing, fracturing, casing, etc. Based on the wellbore hole OD, measured depth, and true vertical depth, the system will provide calculated annular volumes of slurry, shoe track volume, along with pump via data, displacement volume, etc. PowerVision has detailed pressure-pumping jobs, such as stages, injection rate, fluid type, volumes, proppant type, quantities, mess size, and mass, etc.

JOB master contains detail fluid, proppant, tubing, and casing databases. Job events are logged automatically, entered manually, selected from a pre-defined list, or recorded from a compatible device. Job data may be played back for purposes of demonstration or parameter recalculation. The customer version is available for post-job analysis and remote monitoring.

Rig data. Baker Hughes has issued the rotary rig counts as a service to the petroleum industry since 1944, when Hughes Tool Company began weekly counts of US and Canadian drilling activity. Hughes initiated the monthly international rig count in 1975. The North American rig count is released weekly at noon central standard time on the last day of the workweek. The international rig count is released on the fifth working day of each month. The Baker Hughes Rig Counts are an important business barometer for the drilling industry and its suppliers. When drilling rigs are active, they consume products and services produced by the oil service industry. The active rig count acts as a leading indicator of demand for products used in drilling, completing, producing, and processing hydrocarbons.

> Baker Hughes Rig Counts are published by major newspapers and trade publications, are referred to frequently by journalists, economists, security analysts and government officials, and are included in many industry statistical reports. Because they have been compiled consistently for 60 years, Baker Hughes Rig Counts also are useful in historical analysis of the industry. The working rig location information is provided in part by RigData. http://www.rigdata.com/index.aspx

MaPS. The Maintenance and Performance System (MaPS) provides Baker Hughes with operational data, equipment repair and maintenance data, and tool failure and quality incident data. MaPS makes the entire equipment life-cycle transparent, because it covers all aspects of the tracked equipment, and helps to achieve important business goals like improving the overall reliability and quality, reducing maintenance costs, and providing up-to-date equipment and service information at any time. The maintenance, operational, and tool failure data that is entered by MaPS users worldwide, or is pulled from other systems like SAP®, Advantage, and Power, enables Baker Hughes to predict tool maintenance intervals, track tool repair and maintenance efforts, and to query information for generating standardized and custom reports on product configuration, product reliability, and performance.

12.4 Data Quality Control

Ideally, we would like to see a fully automatic system, within which raw data collection, data processing, and data storage functions are seamlessly integrated. However, many data are still hand-written recorded by field engineers, then extracted from paper and typed into the database. Human error like fat fingers is inevitable in this procedure. Before starting any data interpretation work, we need to scrutinize our raw datasets with various criteria for quality control. Sanity check can never be exaggerated. Remember that "garbage in, garbage out."

12.4.1 Verifying and Validating Units

The commonly used units for proppant quantity in the US are pounds, sacks, or tons and the units for fracturing fluid volume are gallons or barrels. However, we cannot take units as guaranteed in real datasets. Actually, it is common to see erroneous units in large datasets, especially from public data sources. The following table (**Table 12.2**) is a frequency table showing the distribution of fracture fluid units from a public dataset. We can see that the majority records have correct units with either gallons (GAL) or barrels (BBL). But, a fair number of units are missing and some erroneous units exist in the dataset.

After verifying and validating units of records, an essential step in data processing is to reconcile and unify the units in subsequent work. In other words, all proppant amounts need to be converted into values in pounds and fracturing fluid volumes need to be converted to values in gallons. The transformation includes:

- 1 SACK = 100 LBS,
- 1 TON = 2000 LBS, and
- 1 BBL = 42 GALS.

12.4.2 Known Limits and Ratios

When there is a negative value in a proppant or fluid column, we immediately know it is an error. The largest fracture job size we've seen in the studies has approximately

Table 12.2—Frequency table with distribution of fracture fluid units from a public dataset.

	BBL	CF	GAL	HOLE	LB	MCF	QT	SACK	TON
65217	190548	2695	135076	1	36	9441	2	6	128

10 MM lbs of proppant and 10 MM gals of fracturing fluid. If a record contains a tenfold bigger job size, it is suspicious and needs to be revisited and validated. Another very useful criterion is to check if proppant concentration is in a reasonable range. Proppant concentration is the value of total proppant over total fracture fluid and is expressed in pounds/gallon. The theoretical upper limit is 25 lbs/gal, but the realistic values are most likely less than 10 lbs/gal. A record containing 2 MM lbs of sand and 75,000 gallons of cross-linked gel is clearly problematic.

12.4.3 Other Outlier Checks

It's always helpful to visualize the data and plot the distribution of each variable. If a few data points are far from the others, we need to verify and validate those distant points. Both histogram and scatter plot methods, which will be introduced in 12.5.2, are very efficient ways to identify outliers.

12.5 Analysis Methods

12.5.1 Map-Based Methods

GIS maps can be used for many different analyses of unconventional reservoirs. First, GIS maps can be used to gain the interpretive perspective of geologically driven, geographic location-based changes in fundamental reservoir properties. For example, reservoir depth and thickness frequently change in a predictable, but nonlinear, fashion. Thermal maturity can be mapped directly and can show geographical change. Simple mappings of hydrocarbon types or well classifications can lead to an increased perspective, which contributes to the prediction of production variation related to gross well location within the study area. In another example, geological features, such as faults, may be associated with poor wells.

In an early example of GIS-based analysis (that is regretfully proprietary), of the Barnett, consistently derived petrophysical parameters were mapped, contoured, and then overlain by an estimated ultimate recovery (EUR) bubble map. Examination of the map clearly demonstrated that the EUR was not consistent with the petrophysical variables. In that instance, the best indicator of vertical well EUR was the water-to-gas ratio (WGR), with the poorest wells having the highest WGR values. At issue was fracture stimulation treatments hitting faults, or otherwise communicating with, the wet Ellenberger dolomite and bringing salt water into the completion.

At the point when a proper understanding is reached about the impact of geoscience on production, then the author's GIS workflow enters into the "considerations of well architecture" phase. Cumulative frequency histograms of production metrics are used to identify the distribution's tails, and the (for example) best and worst 10% wells can then be displayed on the map, excluding the middle 80%. The goal of this analysis is to identify natural geographic sweet- and not-so-sweet spots by observing whether the best and worst wells are intermixed or if they are geographically separated into specific parts of the study area. Overlays can be used to outline sweet spots. Less-than-optimum producers within sweet spot areas can be further investigated for problems associated with original well architecture, completion, and stimulation that may or may not be possible to remediate.

Direct display of actual well paths from directional surveys is a key to pattern recognition methods of GIS analysis, although surface and bottom-hole locations may be used if they are all that is available. It should be noted that an assumption of a straight-line well path may be incorrect in the plays in which "turnizontal" wells were drilled in order to gain the geomechanically most favorable well path in an unfavorably oriented lease. Examining the well path data via the map is a means of identifying optimum and non-optimum well paths and too-short laterals in different parts of the play.

The attribute function of GIS programs provides a means of visually identifying stage count groups. Proceed with caution when better producers within a geographic area show higher stage counts, because a more detailed investigation may be needed to separate the stage-count effect from the treatment-size effect.

As indicated previously, treatment volumes and proppant quantities can be shown on the map through the use of drainage radius or perhaps other functions. In one example, the method plots a high aspect-ratio ellipse with size and color showing the proppant quantity pumped in each well. When plotted in conjunction with the stage count and production

metric, oversized and undersized treatments can be readily identified and compared to production results.

The level of analytical detail and understanding that can be achieved using GIS analysis is first and foremost based on the level of granularity of the dataset being studied. Equally important is using the full interpretive power of the different disciplines working together on projects. A geologist trained in understanding reservoir geometries, thermal maturity patterns, and so on, brings much more insight to the interpretation of the engineering parameters, while the engineer(s) bring insights and experience from their own discipline to aid the final integrated study result.

12.5.2 Exploratory Data Analysis

The first two questions that arise when we tackle any analytic problem are, "what is my goal?" and "what data do I have?" A quick tour of the available dataset will plot the profile of our task. Despite the advances in modern sophisticated statistical methodologies, several traditional methods play important roles in exploratory data analysis.

The frequency table (**Table 12.3**) displays the distribution of a categorical variable in the dataset by associating the possible values of the variable with the corresponding frequency or relative frequency (i.e., percentage). An example of a frequency table for the well distribution over districts in the Wichita-Albany formation from a proprietary dataset is shown next. A table that displays a single variable is also known as a one-way table.

A two-way table (**Table 12.4**) shows the joint distribution of two categorical variables. The two-way table often helps with identifying the association between these variables. There are different criteria for the well completion type. The two-way table, next, indicates that all engineered wells used sleeves in the completion example shown.

The bar plot in **Fig. 12.2** visualizes the related frequency table for better readability. We converted the previous one-way table example to a bar plot. In this example Gaines County has most of the wells.

Both frequency tables and bar plots are apparatuses for categorical variables. A widely used visualization method for numeric variables is the histogram, which looks very similar to a bar plot. A histogram shows the frequency distribution of a numeric variable upon a set of consecutives bins. The number of bins can be adjusted to serve the presentation purpose. However, either too many bins or too few bins can dilute the information from the data. There are typically 5-to-10 bins in a histogram. The following histogram for the variable maximum monthly oil production in BOE shows a highly right-skewed distribution, with only a small percentage of the wells showing production over 6,000 BOE (**Fig. 12.3**). Note that the vertical scale is relative frequency in this example, which ensures that the area under the overlaid fitted curve is normalized to one. Also, the wells with ultra-high production (over 12,000 BOE) are outliers, based on the distribution and need to be validated.

Table 12.3—Frequency of well distribution over districts in the Wichita-Albany formation from a proprietary dataset.

ANDREWS	CRANE	ECTOR	GAINES	WARD	WINKLER
79	58	20	194	49	29

Table 12.4—Two-way table showing that all engineered wells used sleeves in the completion.

	Ctype2	
Ctype1	Engineered	Geometric
Plug & Perf	0	2
Sleeves	65	2

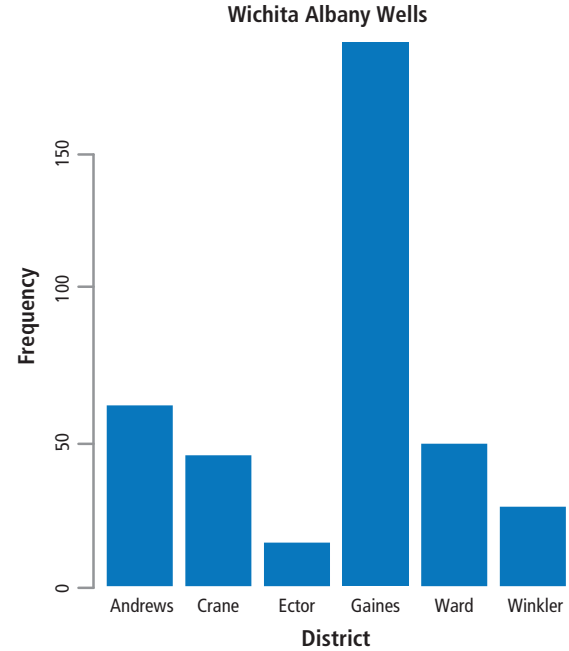

Fig.12.2—Bar plot showing the data for the related table in Table 12.4.

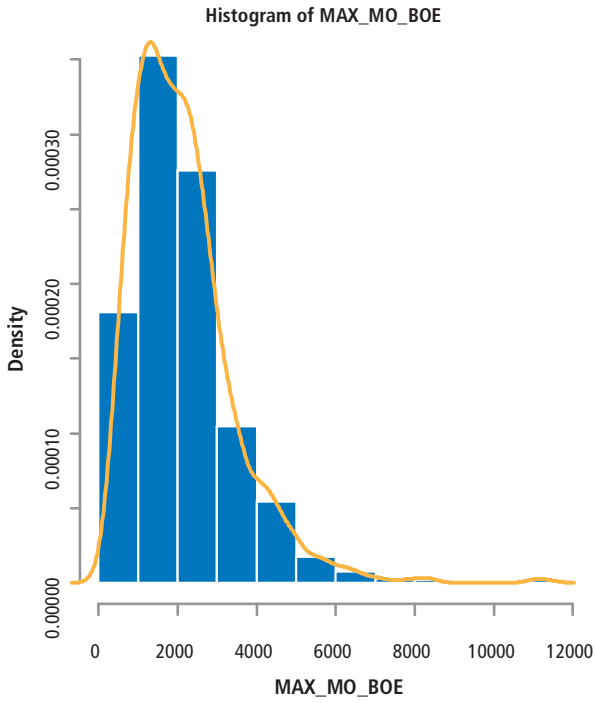

Fig. 12.3—Histogram of MAX_MO_BOE bar plot.

A scatter plot (shown in **Fig. 12.4**) uses Cartesian coordinates to display values of two or more variables from a dataset. It shows various kinds of correlations between these variables, as well as the existence of outliers. The scatter plot, next, indicates that there is a positive correlation between fracture fluid and proppant. There is an outlier that is far away from the others that needs further verification.

When a dataset contains many variables, it will take a lot of scatter plots to inspect the pairwise relationship between them. It's neither convenient nor efficient to flip through dozens of plots. Instead, we can integrate selected scatter plots into a scatter plot matrix and review all the pairwise relationships simultaneously. The scatter plot matrix, next in **Fig. 12.5**, contains 91 independent scatter plots taken from 14 variables. The target variable is the cumulative 30-day production, beginning with peak production within the first 12 producing months. The predictor includes fracture stage count, average stage length, gross fracture fluid amount, proppant quantity, and other well parameters. Each off-diagonal cell c_{ij} is a scatter plot between two variables; one is listed in the diagonal cell c_{ii} along the horizontal direction and the other can be found in the diagonal cell c_{jj} along the vertical direction. Note that the scatter plots in cell c_{ij} and c_{ji} are essentially the same. One is the mirror image of the other after 90° counterclockwise rotation. According to the scatter

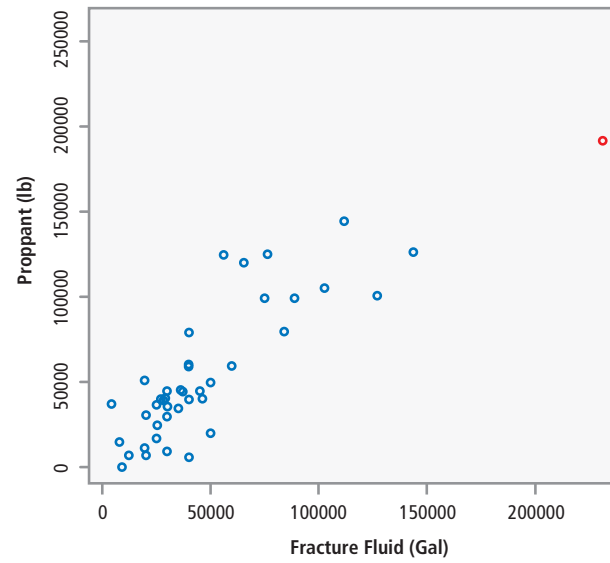

Fig. 12.4—Scatter plot with Cartesian coordinates showing dataset variables.

plot matrix, we can find (aside from the positive correlation between the fracture fluid and proppant, as we mentioned before), the number of fracture stages is also strongly correlated with these two variables.

There are other frequently used methods in exploratory data analysis we didn't discuss here, such as the pie chart and box plot. Interested readers can easily find an introduction to these two chart types in reference books or online.

12.5.3 Linear Methods

In statistics, regression analysis is the analysis of the relationship between a response or outcome variable and another one or more explanatory variables. For one explanatory variable, it is called simple linear regression. For more than one explanatory variable, it is called multiple linear regressions. It is different from multivariate linear regression, where multiple correlated dependent variables are predicted, rather than a single scalar variable.

The relationship is expressed through a statistical model equation that predicts a response variable (or dependent variable) from a function of regressor variables (or called independent variables or explanatory variables) and parameters. In a linear regression model, the predictor function is linear in the parameters. The parameters are estimated so that a measure of fit is optimized.

Fig. 12.5—Example of 91 separate scatter plots created from 14 variables.

The multiple linear regression equation is as follows:

$$\hat{Y} = b_0 + b_1X_1 + b_2X_2 + \ldots + b_pX_p \quad \textbf{Eq. 12.1}$$

where $\hat{Y}$ is the predicted value of the dependent variables, X_1 to X_p are $_p$ distinct independent variables, b_0 is the value of Y when all of the independent variables (X_1 to X_p) are equal to zero, and b_1 to b_p are the estimated regression coefficients. Each regression coefficient represents the change in Y relative to a unit change in the respective independent variable.

While mining production or production efficiency in major shale plays, the production (initial production, three-cumulative-month production, etc.) is usually the dependent variable and parameters from reservoir properties, well architectures, completions, and stimulations are independent variables to be regression studied through statistical modeling. (See the case study as example.)

12.5.4 Tree Boosting Methods

Machine learning methods have gained momentum across various fields recently. Benefiting from rapid advances in computer science and technology, machine-learning methods can be applied to modeling problems in a different way than traditional statistical modeling. Traditional statistical models start from an explicit expression with a set of unknown parameters, and then those parameters are tweaked to achieve the best match with real data according to certain criteria (typically, minimizing a metric).

Machine learning methods, instead, have no specific predefined models, but instead rely on the "brute force" power from the computer to learn the relationship between the variables and find dominant patterns between the target and predictors. Two widely used machine-learning methods—*random forest* and *boosting*—are both decision-tree based. A decision tree is a tree-like hierarchical model used to map observations of a subject to conclusions about the subject's target value. Fisher's iris dataset consists of 50 samples from each of three species of iris: setosa, versicolor, and virginica. Four characteristics were measured for each sample, including the length and the width of the sepal and petal (in centimeters). A decision tree was built to use these four characteristics to predict the species of iris (**Fig. 12.6)**. From the results:

- Node 2 contains 50 samples from branch, with petal length ≤ 1.9, and the species are all setosa
- Node 5 contains 46 samples from branches with 1.9 < petal length ≤ 4.8 and petal width ≤ 1.7, and the species are mostly versicolor
- Node 6 contains 8 samples from branches, petal length > 4.8 and petal width ≤ 1.7, and they are half versicolor and half virginica
- Node 7 contains 46 samples from branches with petal length > 1.9, and petal width > 1.7, and the species are mostly virginica

To verify the accuracy of this decision tree, we can check the cross table between the predicted species and the true species. In the table below (**Table 12.5)**, the columns label the prediction and the rows the true species. We can see that only 6 cases out of 150 are misclassified under a single decision tree.

Boosting the method builds a series of trees subsequently during modeling. Each tree is built upon a random subsample of the train dataset and the residual from the previous tree, which is treated as target variable. Note that tree boosting

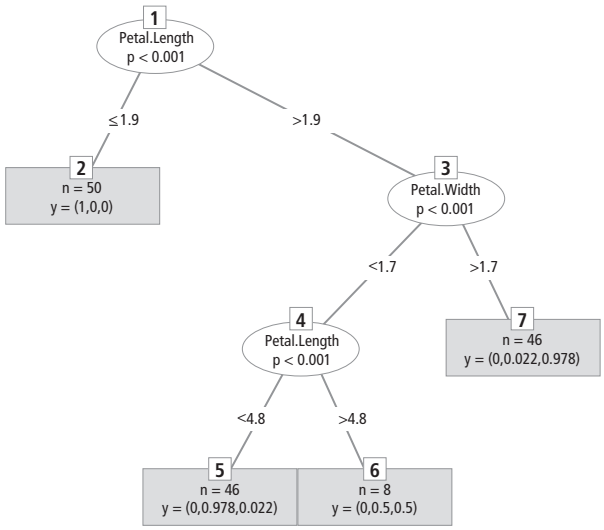

Fig. 12.6—Iris species prediction decision tree.

Table 12.5—Iris data table showing data for predicted and true species.

	setosa	versicolor	virginica
setosa	50	0	0
versicolor	0	49	5
virginica	0	1	45

requires a minimum of assumptions about data structure, and is more resistant to common data quality issues like outliers and missing data than traditional statistical modeling is. We can evaluate the impact of individual predictors upon the target, based on the output of the relative importance chart. From that output, we can observe the marginal effect of individual predictors upon the target, while the influence of other predictors is "integrated" out. We will illustrate the application of this method using a few case studies in the next section.

12.6 Case Studies

The remainder of the chapter is devoted to case studies about three well-known unconventional reservoir plays in North America. Each case study is presented as a means of reinforcing the data sources, quality control, data exploration, data mining concepts, and key lessons learned using the methods described above.

12.6.1 Barnett Shale

The Barnett shale of the Fort Worth basin is a complex mudstone reservoir. X-ray diffraction (XRD) analysis of 66 samples of Barnett shale from 13 counties indicates that quartz, feldspars, carbonate minerals (mainly calcite, dolomite, and siderite), and clays (mainly illite/smectite) are the main minerals present. **Fig. 12.7** highlights the variable nature of Barnett mineralogy.

The Barnett offers much data to study and has been data mined extensively by the authors (LaFollette, 2011 and LaFollette, 2012.) The major goals of these Barnett studies were to analyze well and production data from Barnett vertical and horizontal wells in order to better understand critical and not-so-critical productivity drivers. (See **Fig. 12.9** and **Fig. 12.10** later in this section for a graphical representation of the data.)

Study well data were taken from the IHS Energy US Well Database subscription, and from the Baker Hughes internal PowerVision™ database. Over 211,000 wells were selected for analysis (LaFollette, 2012) including the over 15,000 Barnett wells producing in 2011. Standard procedure is to load all well header and production data into a commercial GIS application.

The process of quality control began immediately by checking well locations against map overlay boundaries. Wells shown were color-coded by well type, with gas wells in red, oil wells in green, and injectors in blue (**Fig. 12.8**). Background geological studies indicated that all conventional reservoirs in the study area were sourced by the Barnett shale. Thus, the map became a proxy for gross thermal maturity variation across the basin.

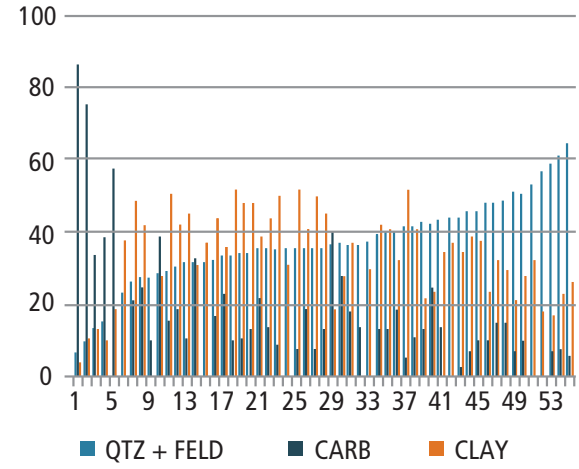

Fig. 12.7—Main minerals present in the Barnett shale highlight the variability mineralogy.

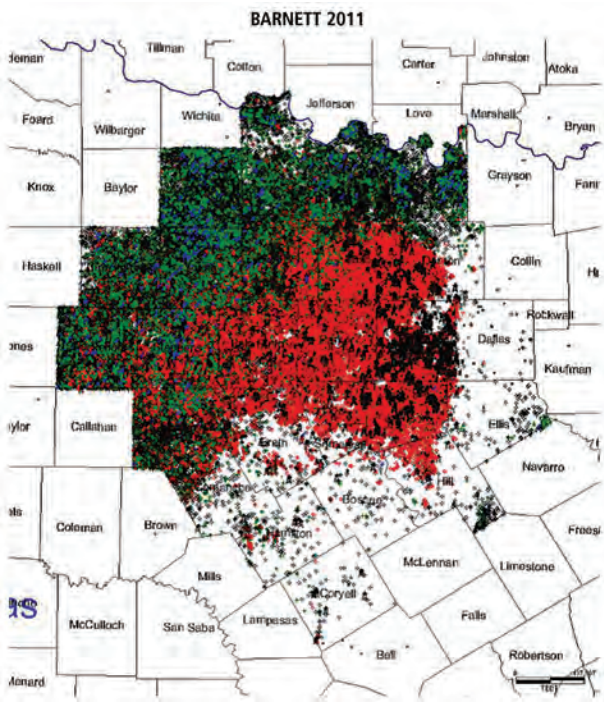

Fig. 12.8—Data plot for production wells. (LaFollette and Holcomb 2012.)

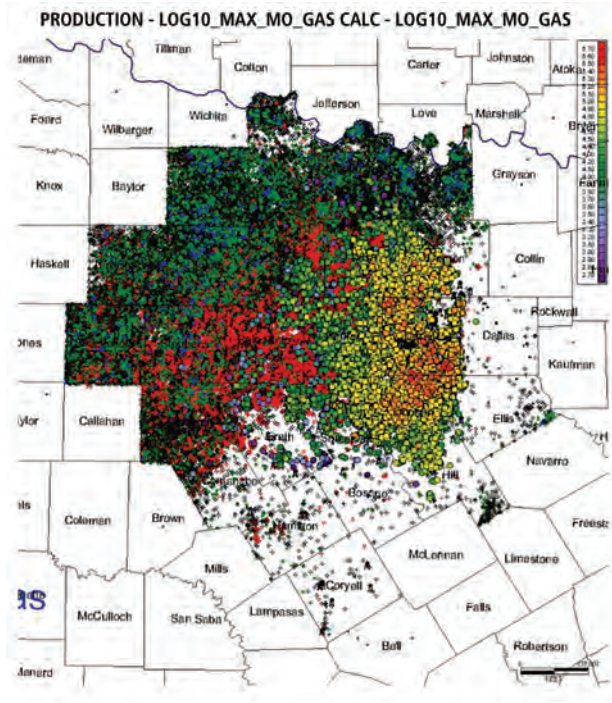

Fig. 12.9—Map of well data. (LaFollette and Holcomb 2012.)

Public and proprietary data from well architecture, completion staging, well tests and treatments and production were also merged into a common database and quality control checked. Examples of quality control checks included checking calculated well azimuth values to be within the known limit of 0-360° and checking to ensure that well length was in the "reasonable" range. Another example is to cross-reference public and proprietary values of the same variable, e.g., fracturing fluid, proppant quantity, etc. Many other sanity checks were performed in the course of the study.

Selecting the right production metric(s) is important in data mining. The tradeoff is that the longer time a well must be produced to be selected as a study well, the fewer wells are available for study. Further, results are pushed further into the future. One of the goals of data mining is to use the data to drive significant operational change, leading to selection of production metrics as short term as possible. However, selecting a production metric that is too short may not adequately predict longer-term production.

The authors typically select such short-term metrics as peak monthly rate, and 3-, 6-, and 9-month normalized cumulative production for regression against the 12-month normalized cumulative production. Then the shortest-term metric that correlates acceptably with 12-month normalized cumulative production is selected.

For the purpose of mapping production data for comparison to geographical, geological, and other trends, bubble-mapping the log10 value of the peak gas rate was used, as shown in Fig. 12.8 and Fig. 12.9.

GIS mapping using a log10 production metric and a rainbow color scheme with each shade difference having a 0.1 value indicates a 25% production improvement per increment. This allows rapid pattern-recognition of production trends across the study area. The map can also be used to identify both better and poorer producing areas by displaying, for example, best and worst 10% wells. **Fig. 12.10**, next, shows such a plot of Barnett vertical wells.

Study of the map shows that locations most favorable for vertical wells were restricted to areas to the northeast of the Viola Pinchout, were generally at some distance from major faults, were geographically separated from the poorest 10% wells, and did not extend to the northwest into the oil leg area of northern Wise and Montague Counties.

Examination of **Fig. 12.11**, next, shows that favorable locations for best 10% horizontal wells could be on either

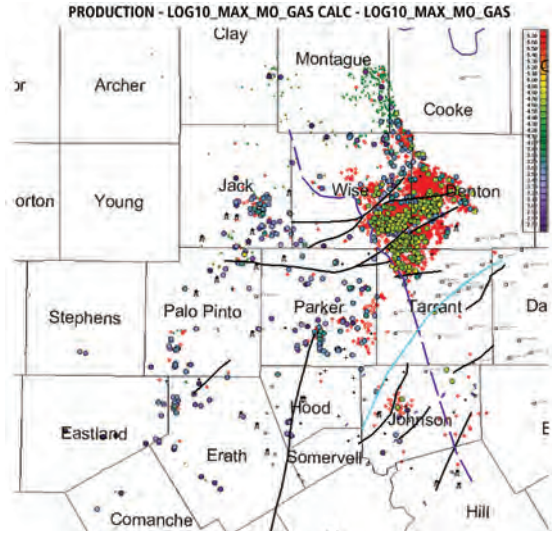

Fig. 12.10—Map highlighting the best and worst 10% of Barnett vertical wells with large-scale structure. Fault lines are in black; Viola Pinchout is in purple (dashed). (LaFollette and Holcomb 2012.)

side of the Viola Pinchout. An important lesson was that vertical wells could condemn acreage in a shale play that could be productive when drilled and completed as horizontal laterals.

The importance of well azimuth to productivity was first learned using GIS analysis in an unpublished study circa 2004, and was validated again in 2011 (LaFollette, 2011).

Public and proprietary stimulation treatment data were input stage-wise in their original databases. The data were aggregated and summarized to well level for analysis. It is important to note that stage-by-stage stimulation data would be useful in data mining projects only in the unlikely event that production data were also collected stage-wise.

Examination of the distributions of all variables studied indicated that certain variables were skewed or bimodally distributed. This led to choosing a boosted regression tree method of analysis.

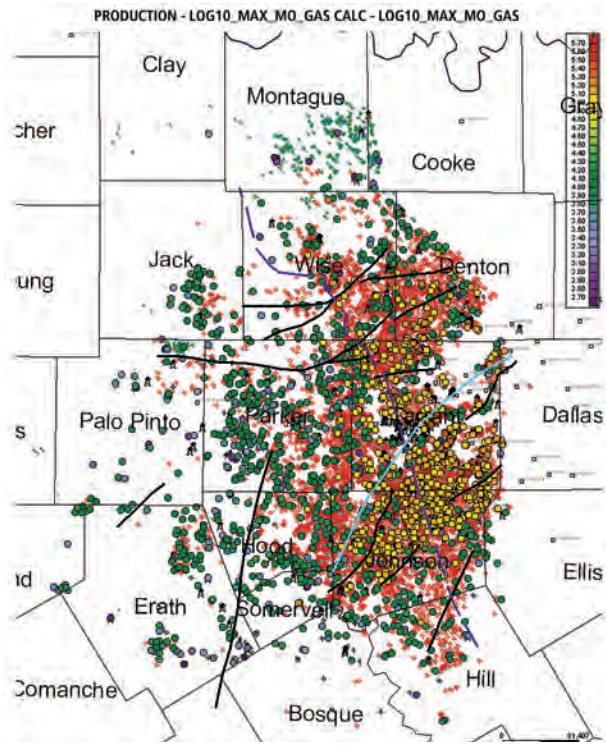

Fig. 12.11—Map highlighting favorable locations for the best 10% of Barnett shale horizontal wells on either side of the Viola Pinchout. Fault lines are in black. (LaFollette and Holcomb 2012.)

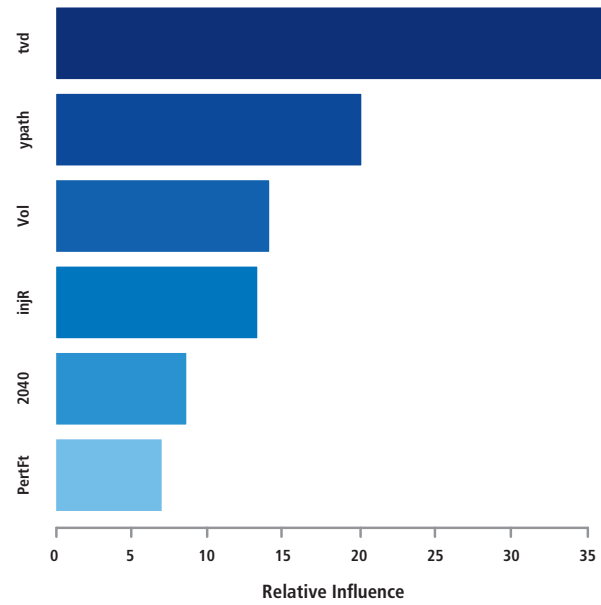

Fig. 12.12—Response surface diagram highlighting the importance of both injection rate and treatment fluid volume on maximum gas rate in Barnett study wells. (LaFollette 2013.)

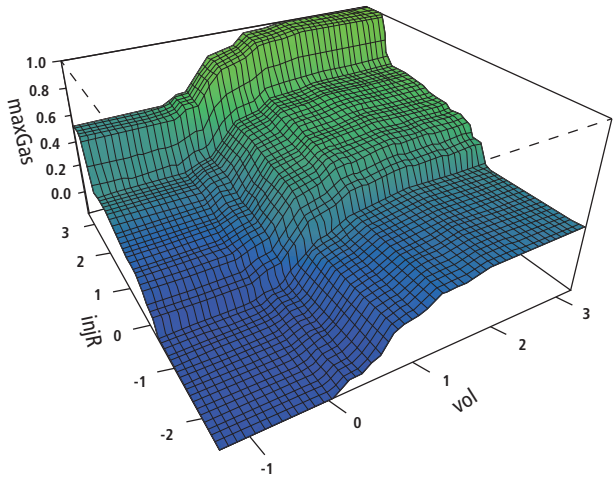

Fig. 12.13—Importance plot showing main stimulation influences on maximum gas rate (MMG) target. (LaFollette and Holcomb 2012.)

The influence plot from the boosted tree analysis using the target production variable maximum monthly gas rate (MMG) is shown in **Fig. 12.13.**

The bar chart in **Fig. 12.12** shows the top six variables influencing MMG in the study area. True vertical depth (TVD) is most influential, followed by N-S location (ypath), fracture treatment fluid volume (Vol), injection rate (InjR), percentage of 20/40 mesh sand, and completed lateral length (PerfFt). Of these, completed lateral length drops below the commonly used double-digit threshold of significance in the dataset used in the study.

The importance of both injection rate and treatment volume to well performance in unconventional reservoirs was discussed early on by King.

Lessons learned may be categorized by variable class.

12.6.2 Bakken Play

The Bakken formation of the Williston Basin occurs mainly in eastern Montana, western North Dakota, and southern Saskatchewan. This study is focused on wells producing from the Middle Bakken interval of the Bakken-Lodgepole Total Petroleum System south of the 49th parallel (Figure 1, Pollastro, et.al., 2008). It does not include Bakken-Three Forks completions.

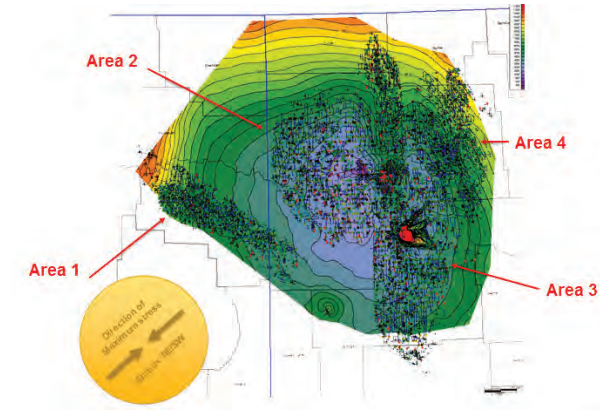

Fig. 12.14—Middle Bakken producing areas across the US side of the basin.

The Bakken shale play discussed here is a shale-sourced, light, tight oil play in which laterals are drilled, completed, and stimulated in the Middle Bakken interval. The Middle Bakken is an interval of mixed carbonate and siliclastic mineral suites, according to producing area (**Fig. 12.14**).

The goals of this study are to update and expand prior well optimization data mining efforts in the Bakken. There are over 3500-plus horizontal wells included in our Bakken analysis. Our efforts were focused on the impacts of well location, well architecture, completion, and stimulation on production results. One of the production metrics considered is "best month oil production" in the first 12 producing months (BO) in barrels.

The dataset histograms in **Fig. 12.15** reveal the distribution of individual variables. The target variable BO is highly skewed to the right, while both the surface X location and the cumulative lateral length (CLAT) have bimodal distributions.

A multiple linear model was built upon the Bakken data after variable selection. This model highlights the importance of well location, total fracturing fluid amount pumped in the well, area code, the presence of coarse-mesh proppant in the treatment, and increased proppant concentration in the fracturing fluid as predictors of improved maximum monthly oil production performance.

Linear models (**Table 12.6**) are straightforward, but need to be built upon many assumptions. The model shows that the fracture fluid volume has a positive impact upon the production. Actually, you can't expect the production to keep climbing with the increased fracture fluid volume in the field. The real-world relationship is much more complex and generally nonlinear.

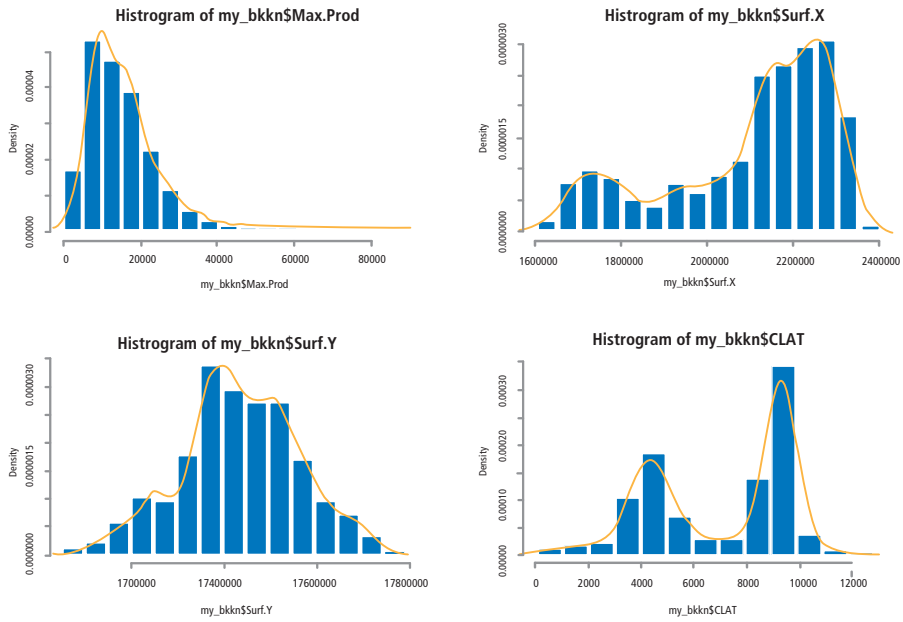

Fig. 12.15—Histogram of selected variables showing frequency distributions. Note the bimodal distribution of CLAT and Surface X direction.

Next, we applied the boosted tree method in the analysis (**Fig. 12.16**). When multiple variables influence the target variable simultaneously, the goal is to learn which ones are the key influence factors. The relative influence is essentially a weighted average of the frequencies a variable is used for splitting trees. The higher value on the influence plot suggests a stronger effect on the target variable. The influence value is proportional to the length of the blue horizontal bar, which is scaled to have a sum of 100.

Table 12.6—A multiple linear model for max monthly oil production. Nature logarithm has been applied to some variables to comply with the normality assumption of linear modeling.

```
Call:
lm(formula = log(Max.Prod) ~ log(Surf.X) + log(Surf.Y) + log(ffa_tot) +
    Area.Code + CPROP + ratio, data = na.omit(my_bkkn[, -c(15:17)]))

Residuals:
    Min      1Q  Median      3Q     Max
-4.5438 -0.3447  0.0430  0.3826  1.8923

Coefficients:
                Estimate Std. Error t value             Pr(>|t|)
(Intercept)   254.14056   30.86012   8.235 0.000000000000000260 ***
log(Surf.X)    -1.28235    0.45820  -2.799              0.00516 **
log(Surf.Y)   -13.81892    1.69754  -8.141 0.000000000000000561 ***
log(ffa_tot)    0.30765    0.01708  18.011 < 0.0000000000000002 ***
Area.CodeRegion 2 -0.39703    0.08612  -4.610 0.000004182166989809 ***
Area.CodeRegion 3 -0.41930    0.10765  -3.895              0.00010 ***
Area.CodeRegion 4 -0.09823    0.13102  -0.750              0.45349
CPROP1          0.10218    0.02440   4.188 0.000028892970413116 ***
ratio           0.17680    0.01622  10.898 < 0.0000000000000002 ***
---
Signif. codes:  0 '***' 0.001 '**' 0.01 '*' 0.05 '.' 0.1 ' ' 1

Residual standard error: 0.5987 on 3139 degrees of freedom
Multiple R-squared: 0.1743,     Adjusted R-squared: 0.1721
F-statistic:  82.8 on 8 and 3139 DF,  p-value: < 0.00000000000000022
```

Note: To avoid the distraction of technical details, we only quoted the results here.

The relative importance plot indicates that well location is the single most important consideration to predict well productivity from our dataset, followed by the total proppant agent amount. Location and proppant quantity variables show double-digit values on the influence plot, which is a good indicator of their significance. Fracturing fluid amount is only slightly less influential than proppant quantity (high single-digit influence). Proppant quantity is relatively consistent related to the fluid volume. Proppant concentration (in lb/gal, expressed as a "ratio") has less influence, as does CLAT. Well azimuth through the completed interval (AZM and AZM2) seems to have relatively little influence in the basin-wide model. Note that AZM is well azimuth on a 360° scale and AZM2 is well azimuth on a 180° scale. Neither of these predictors stands out as substantially more significant than the other. The influence of area code indicates that the particular gross field area effects well productivity—which is no surprise to workers in the Middle Bakken play.

More analysis details can be found in the Society of Petroleum Engineers conference paper, SPE 163852 Application of Multivariate Analysis and Geographic Information Systems Pattern-Recognition Analysis to Production Results in the Bakken Light Tight Oil Play, February 2013, available from https://www.onepetro.org/conference-paper/SPE-163852-MS).

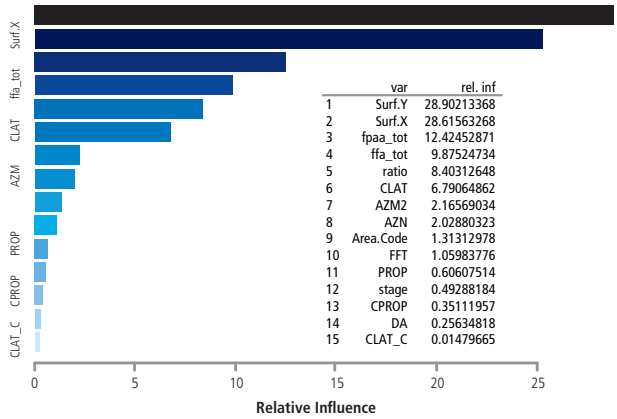

	var	rel. inf
1	Surf.Y	28.90213368
2	Surf.X	28.61563268
3	fpaa_tot	12.42452871
4	ffa_tot	9.87524734
5	ratio	8.40312648
6	CLAT	6.79064862
7	AZM2	2.16569034
8	AZN	2.02880323
9	Area.Code	1.31312978
10	FFT	1.05983776
11	PROP	0.60607514
12	stage	0.49288184
13	CPROP	0.35111957
14	DA	0.25634818
15	CLAT_C	0.01479665

Fig. 12.16—Boosted tree model influence plot of Bakken wells with directional surveys across the Williston Basin. The model is based on approximately 3500 wells.

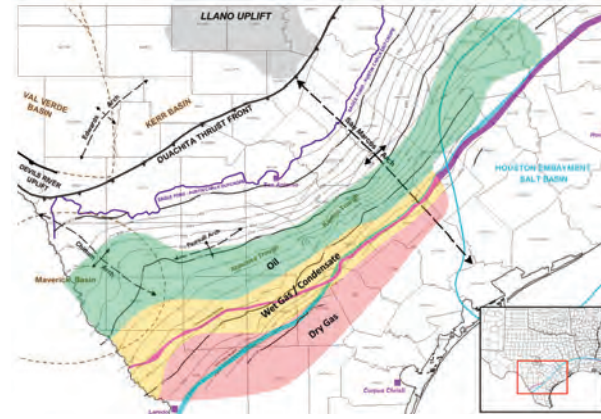

Fig. 12.17—LaFollette 2014. Location map showing the general study area of Eagle For production, South Texas, US. Map courtesy of Momentum Oil and Gas. Used with permission.

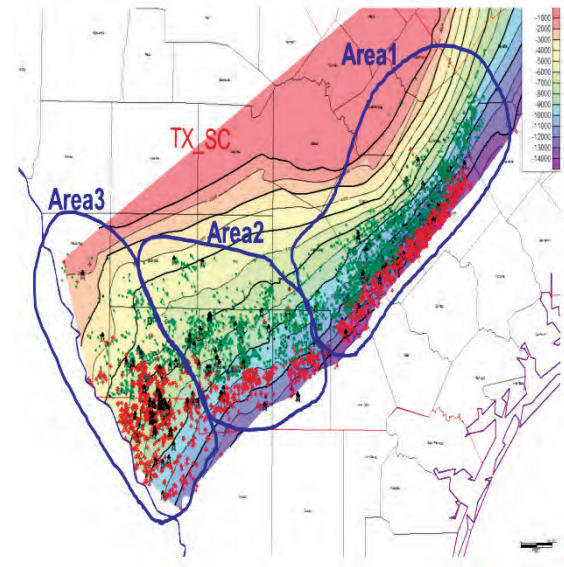

Fig. 12.18—LaFollette 2014. Map highlighting the study sub-areas within the Eagle Ford play of South Texas, US.

12.6.3 Eagle Ford Shale

The Eagle Ford formation is a Late Cretaceous Age sedimentary rock formation that underlies much of South Texas. The rocks are mainly organic matter-rich fossiliferous marine shales of the Lower Eagle Ford interval. The play extends over an area of approximately 11 million acres overall, and the main body of the play stretches from the Texas-Mexico border to the eastern borders of Gonzales and Lavaca counties (**Fig. 12.17**). The northern part of the play (highlighted in green) is in the oil maturation window, and, in addition to producing crude oil, the oil window also contains lesser amounts of natural gas and natural gas liquids (NGLs). Situated to the south and southeast of the oil window, the wet-gas region (highlighted in yellow) produces gas along with high volumes of NGLs. The southernmost region (highlighted in red) contains mostly dry natural gas. Because oil and natural gas liquids command a higher price than natural gas, producers have mostly focused on extracting the formation's oil and NGL resources.

Our Eagle Ford database contains data for around 4,000 horizontal wells from public and proprietary data sources. The wells were divided into three major producing areas. We evaluated the effect of various well parameters upon the production metrics in each area. One of the target variables is maximum monthly oil production within the first 12 producing months (MMO). The available predictors include: X/Y surface locations (which serve as the proxies of the reservoir quality in the absence of large-scale petrophysical analysis data), CLAT, number of fracture stages, well azimuth, drift angle, gas oil ratio (GOR), total fracture fluid volume, total proppant quantity, and proppant concentration.

Exploratory data analysis and a "sanity check" was conducted iteratively for data quality control. Both the histograms and the scatter plot matrix (created from the selected variables shown in the chart, next) suggest the complexity nature of the dataset. A multiple-linear model is not competent to address the non-normality and nonlinearity within the data.

We applied a tree boosting method, gradient boosting, to build our predictive model in each of the three areas from the Eagle Ford play (**Fig. 12.18**). For producing Eagle Ford wells in Area 1, GOR stands out as the most influential

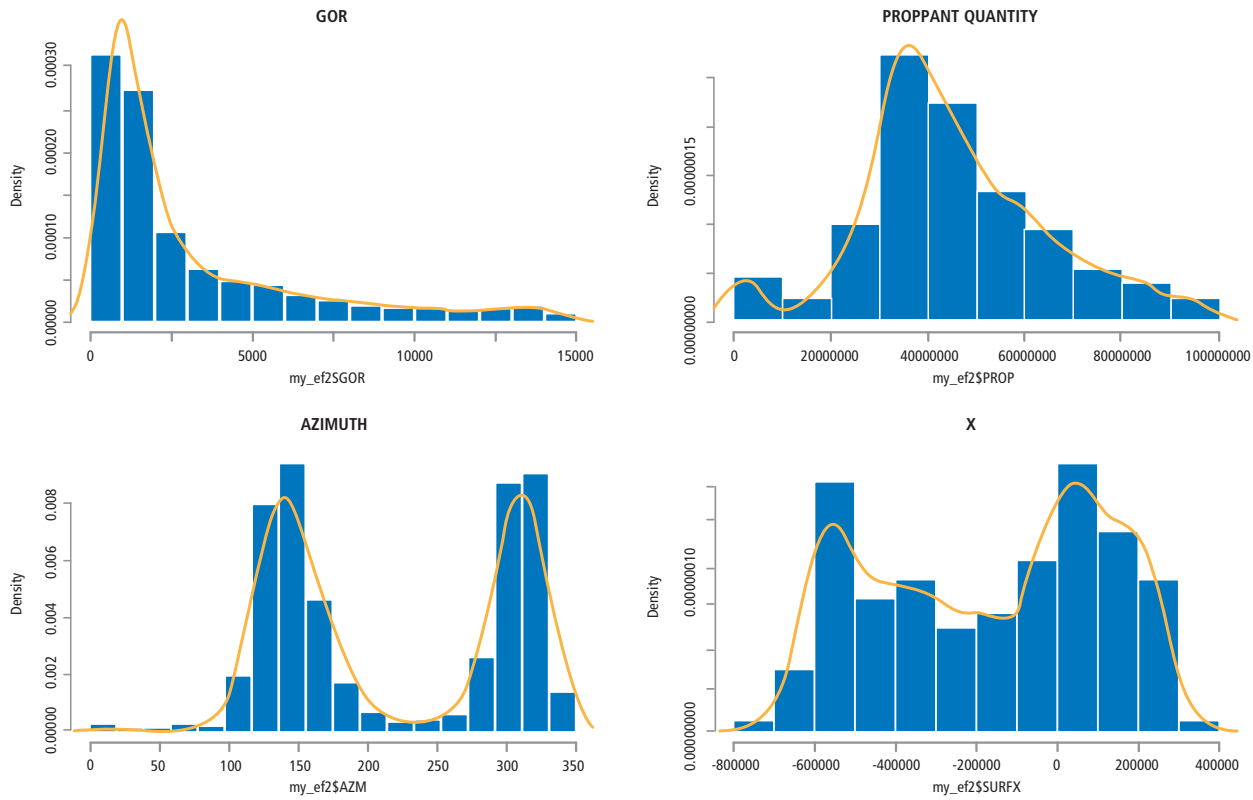

Fig. 12.19—Histogram suggesting the complexity of the dataset.

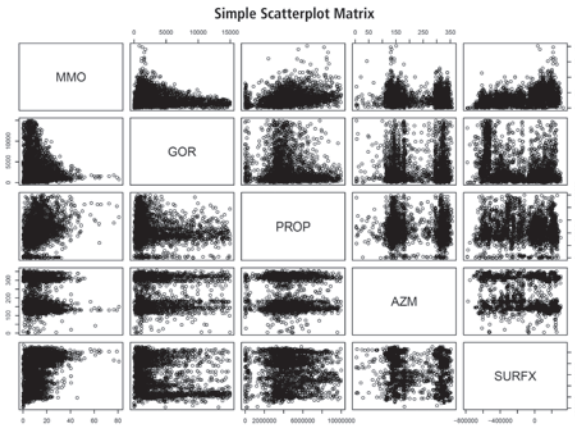

Fig. 12.20—Scatter plot matrix suggesting the complexity of the dataset.

predictor, followed by proppant amount, X-Y-location, and CLAT. The remaining variables are somewhat less influential (**Fig. 12.19**). **Fig. 12.20** is a matrix scatter plot diagram that suggests the complexity of the dataset.

The relative influence quantifies the overall effect of a variable upon the production, but it can't reveal how this effect could vary when the variable changes its value. As another output from the boosting model, partial dependence plots show the marginal effect of the chosen variable(s) on the target variable. These plots provide useful clues for interpretation.

Fig. 12.21 shows the partial dependence plots of the top six predictors in the relative influence-ranking list. The upper left, partial dependence plot highlights GOR as a major cause of peak month oil productivity in Area 1. This is reasonable, since the higher GOR means more gas—or less oil—and lower peak production is a natural inference. The partial dependence plot of proppant quantity shows that more proppant is generally associated with increased productivity at least up to the maximum eight-million-plus pound treatments shown in the dataset. Well location is also a key factor that suggests the importance of sweet spots. Last, but not least, according to the partial dependence plot of CLAT (bottom center), the optimal choice of CLAT for peak oil rate is over the range of approximately 3,000 to 6,000 feet. More analysis details can be found from SPE 168628.

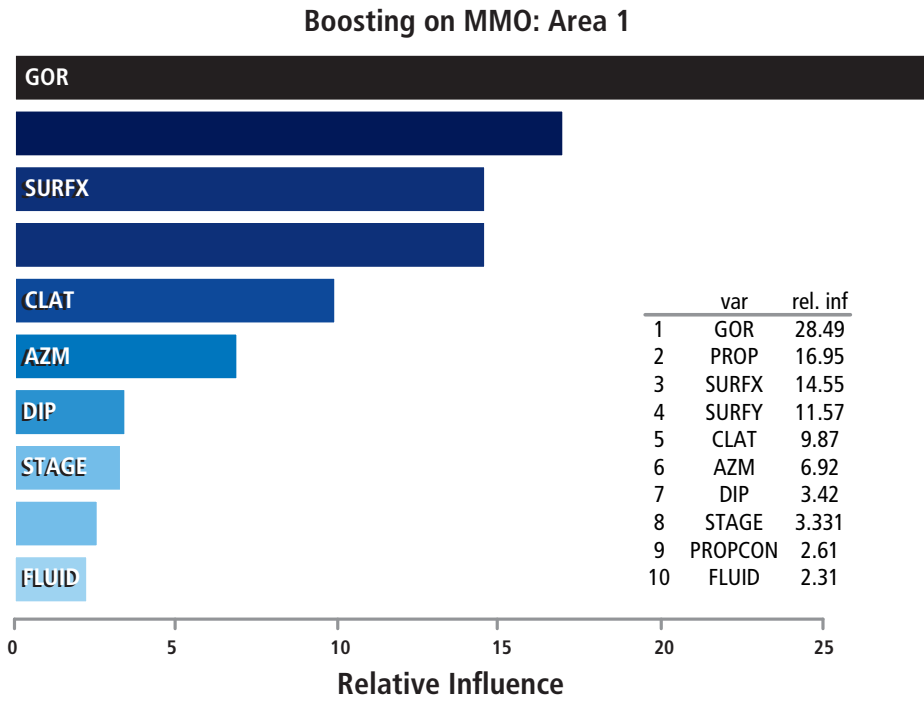

Fig. 12.21—Boosting on MMO for Area 1.

12.7 Concluding Remarks

As stated at the beginning of the chapter, data mining is important in unconventional reservoirs because multi-million dollar decisions are being made daily in the industry, often with limited data to inform the decision-makers. This is largely a result of inadequate reservoir and bounding bed characterization, caused mainly by cost and risk considerations.

While data mining adds important tools to the practitioner's toolbox, we would be remiss if we did not include the following cautions:

- Do follow good statistical and data mining practices. Seek help from a qualified statistician, if statistics is not your field of expertise.
- Understand that "correlation does not imply causation." For any given correlation, there may be an underlying fundamental variable not studied that is the real cause.
- Seek to understand what variables are unknowns, e.g., karst locations relative to Barnett wells, and what impact they would have on interpreting study results.
- Use extreme caution when applying the results of a study outside its original study area. Geological conditions may not have changed, but it is more likely that conditions have indeed changed.
- Do not extrapolate study results. Seeing a trend of increasing treatment volume having a strong influence on increasing well production does not imply that the trend will continue indefinitely.
- Never apply the results of any data mining study blindly.

Data mining allows examination of large numbers of historical well datasets using statistical and machine-learning methods. This approach can be combined with map-based pattern-recognition methods that give the analyst geological and geographical perspective. Together, these tools allow operators, service companies, investors, and others to effectively and efficiently find hidden relationships among variables that may significantly impact their business strategy and decisions.

12.8 References

Ahmed, U., Crary, S., and Coates, G., Permeability Estimation: The Various Sources and Their Interrelationship, ***JPT***, May 1991, pp. 578-587.

Economides, M., Martin, T., (Eds.) 2007. ***Modern Fracturing: Enhancing Natural Gas Production***. Energy Tribune Publishing Inc., Texas, USA.

Economides, M.J. and Nolte, K.G. 2000. Reservoir Stimulation, Third edition, Wiley & Sons Ltd. NY, Baffins Lane, Chichester, West Sussex, England.

Hastie, T., Tibshirani, R., and Friedman, J.H. 2009. ***The Elements of Statistical Learning***. 2nd edition, Springer, New York, USA.

Hufft, H.F. 1977. The Evolution of a Fracturing Technique for the Cotton Valley. Paper, SPE 6868.

LaFollette, R.F. and Holcomb, W.D. 2011. Practical Data Mining: Lessons Learned from the Barnett Shale of North Texas. Paper, SPE 140524.

LaFollette, R.F., Holcomb, W.D., and Aragon, J. 2012. Practical Data Mining: Analysis of Barnett Shale Production Results With Emphasis on Well Completion and Fracture Stimulation, Paper, SPE 152531.

LaFollette, R.F., Izadi, G., and Zhong, M. 2013. Application of Multivariate Analysis and Geographic Information Systems Pattern-Recognition Analysis to Production Results in the Bakken Light Tight Oil Play, Paper, SPE 163852.

LaFollette, R.F., Izadi, G., and Zhong, M. 2014. Application of Multivariate Statistical Modeling and Geographic Information Systems Pattern-Recognition Analysis to Production Results in the Eagle Ford Formation of South Texas, Paper, SPE 168628.

Meehan, D.N. and Pennington, B.F. 1982. Numerical Simulation Results in the Carthage Cotton Valley Field. ***SPE Journal of Petroleum Technology***, 0149-2136/82/0001–9838, January.

Nisbet, R., Elder, J., and Miner, G. 2009. ***Handbook of Statistical Analysis and Data Mining Applications***. Elsevier, UK.

Shellenberger, M., Nordhaus, T., Trembath, A., et al. New Investigation Finds Decades of Government Funding Behind Shale Revolution, The Breakthrough Institute. http://thebreakthrough.org/archive/ new_investigation_finds_decade.

Sone, H. and Zoback, M.D. 2013. Mechanical Properties of Shalegas Reservoir Rocks–Part 1: Static and Dynamic Elastic Properties and Anisotropy. ***Geophysics***, **78**: No. 5. D381–D392. September–October.

Steward, D.B. 2007. The Barnett Shale Play–Phoenix of the Fort Worth Basin. The Fort Worth Geological Society, Texas, The North Texas Geological Society, Texas.

Thearling, K. (2007): An Introduction to Data Mining, White Paper, p.4, http://www.thearling.com/text/dmwhite/dmwhite.htm.

Yost, A.B., Frohne, K-H, Komar, C.A., et al. 1980. Techniques to Determine Natural and Induced Fracture Relationships in Devonian Shale, Paper, SPE 9271.

Zangl, G. and Hannerer, J. 2003. ***Data Mining: Applications in the Petroleum Industry***, Round Oak Publishing, Katy, Texas.

This page intentionally left blank

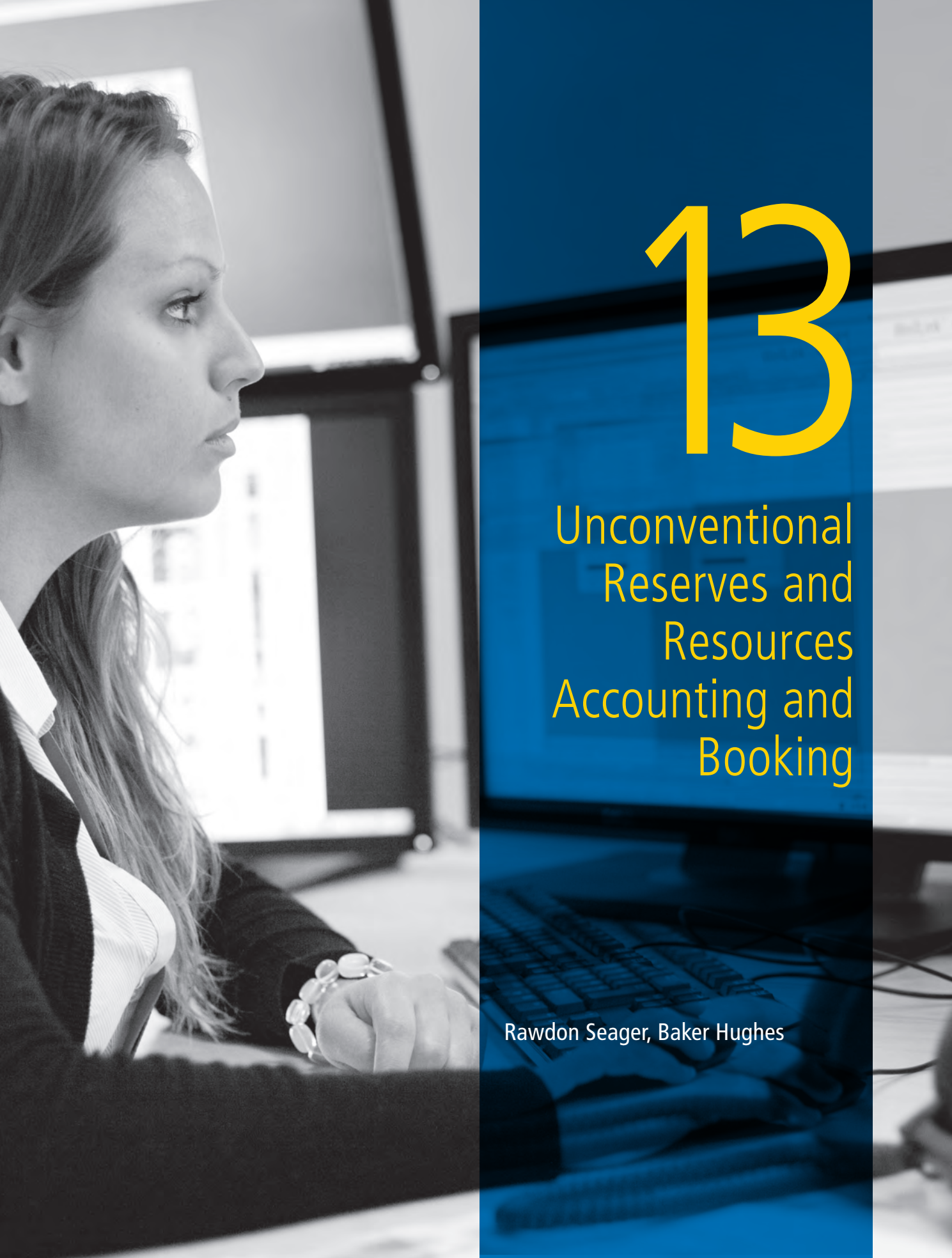

13

Unconventional Reserves and Resources Accounting and Booking

Rawdon Seager, Baker Hughes

This page intentionally left blank

Chapter 13: Unconventional Reserves and Resources Accounting and Booking

13.1 Introduction

Oil and gas reserves and resources are the fundamental assets of oil companies. That is why it is critical that those assets are correctly evaluated, classified, and categorized. This chapter deals with the basic definitions that are used in the industry, both in the United States and worldwide, and will discuss, in particular, the differences between assessment of conventional and unconventional accumulations.

13.1.1 Chapter Content Overview

After a discussion about what we mean by "reserves and resources," we will review the importance of these numbers to the various stakeholders (i.e., the users of this information). There are many different entities that rely on reserves statements for a variety of reasons, including the management of oil and gas companies, investors, stock exchange regulators, national oil companies or ministries, and multinational study groups. Each of these entities may have different interests. Therefore, the reported volumes **must** clearly relate to the stated and established set of definitions.

The title of the chapter includes the term "booking" in relation to reserves and resources. What does this mean? We will discuss the concepts of "rights, risks, and rewards" that convey the capability of a company to report reserves. There are many different types of fiscal regimes around the world, of which many do not allow companies to report reserves. Others use fiscal regimes that bring about nonintuitive quantitative results, so we will review the main types in some detail.

When we decide that it is appropriate to book reserves, we need to consider the definitions required by the reporting authority (if any). For instance, most major stock exchanges have regulations that govern what a company must (and can) report and the basis upon which volumes should be calculated.

The next section will address the most important definitions for oil and gas reserves and resources. Definition sources include the United States (US) Securities and Exchange Commission (SEC) and the Petroleum Resources Management System [prepared by the Society of Petroleum Engineers (SPE) and a number of other industry-related societies]. Mention will be made of some other important sets of definitions and guidelines (such as that required for use in Canada and an umbrella framework developed by the United Nations), but the emphasis will be on the two that are the most common in the international oil and gas industry. This discussion includes the definitions and methodologies employed to derive the estimates, but this chapter does not attempt to deal with a detailed set of instructions about how to carry out fundamental geological and engineering analysis.

Having covered the basic framework, the chapter will deal with the assessment of reserves and resources for unconventional reservoirs. We will outline the major differences that distinguish such accumulations from conventional reservoirs and review the methodologies that can be applied in their quantitative evaluation. Since the unconventional industry is still in its relative infancy and understanding is still evolving, we will make note of the key areas of uncertainty and highlight potential red flags for regulators.

13.1.2 What Are Reserves and Resources?

The PRMS (SPE 2007) provides the following definitions:

Reserves:

Reserves are those quantities of petroleum anticipated to be commercially recoverable by application of development projects to known accumulations from a given date forward under defined conditions. Reserves must further satisfy four criteria: They must be discovered, recoverable, commercial, and remaining (as of a given date) based on the development project(s) applied.

Resources:

The term "resources" as used here is intended to encompass all quantities of petroleum (recoverable and unrecoverable) naturally occurring on or within the Earth's crust, discovered and undiscovered, plus those quantities already produced. Further, it includes all types of petroleum, whether or not currently considered "conventional" or "unconventional" (see Total Petroleum Initially-in-Place). In basin potential studies, total petroleum may be referred to as "total resource base" or "hydrocarbon endowment."

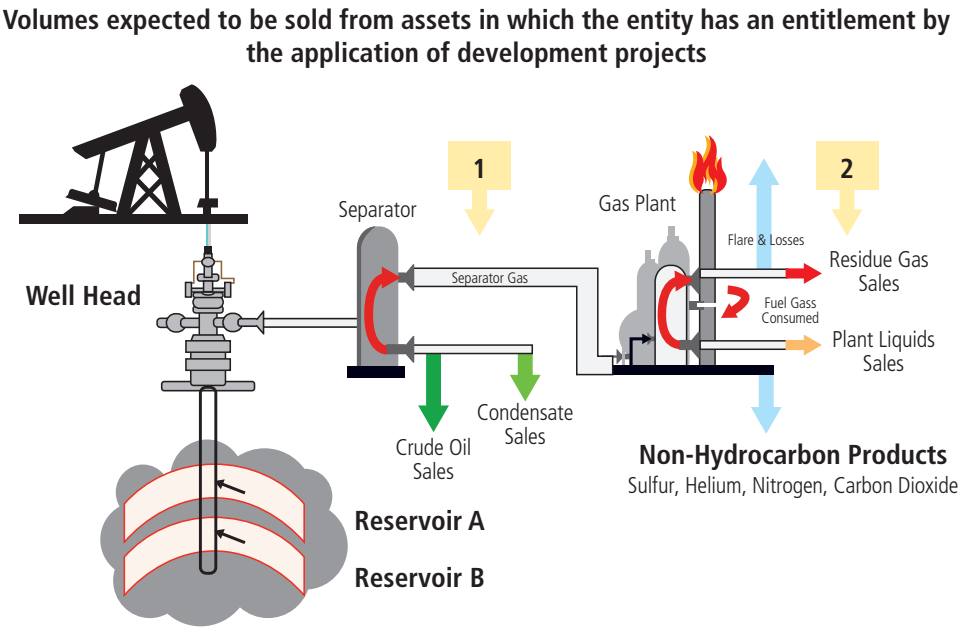

Fig. 13.1—Illustration of sales points (SPE 2007).

These definitions are important, and we will return later to discuss in detail the elements of each. It may be helpful to think of reserves (and resources) in the following ways:

1. Volumes expected to be sold from assets in which the entity has an entitlement by the application of development projects.

   The basic principle is that volumes are reported in the condition in which they are sold. In the previous illustration (**Fig. 13.1**), if production were sold at point 1, the volumes reported would be the wet gas from the lease separator together with the crude oil or condensate liquids. Even if the wet gas were subsequently treated in a gas plant, the custody (ownership) transfer takes place at point 1, and this is where the volumes are measured. However, if the gas were sold at point 2, the reported volumes would be the dry (residue) gas, plant liquids (natural gas liquids or NGLs), plus the crude or oil condensate from the lease separator. Note that if there are small amounts on non-hydrocarbons in the gas (such as carbon dioxide), and it is not required by the purchaser of the gas that they be removed, then the volume reported includes those volumes, as well. On the other hand, if it is necessary to remove impurities before sale, then the reduced volume is recorded.

2. The summation of estimated future production from a given date forward to the economic, contract, or lease limit.

   The volume of oil or gas reported should be derived based on an estimate of future production from whatever project is required for its extraction. (The project consists of wells, plus treatment and transportation facilities.) However, there are some limits on what can be reported by the company as entitlement.

Reserves must prove to be economical, so it is always necessary to use an economic limit test (ELT) to assess when revenue derived from the sale of production is no longer sufficient to cover operating costs for the asset. In **Fig. 13.2**, next, the economic limit (which depends on the price of the sales products and the operating costs for the field) is shown by the horizontal red line at about 10,000 b/d. Production for the last three years (marked as years 15 to 17 in Fig. 13.2) is not economic; therefore, these volumes (that could be technically feasible to produce) are not included in reported reserves. In principle, the company could capture these technically recoverable—but uneconomical—volumes as contingent resources, but most companies do not do so.

Second, there may also be a time limit on the company's rights to operate the field; for example, perhaps the concession expires. In Fig. 13.2, this happens after year 11, so the volumes that might be produced in years 12 to 14, although potentially economic, are not counted as reserves because,

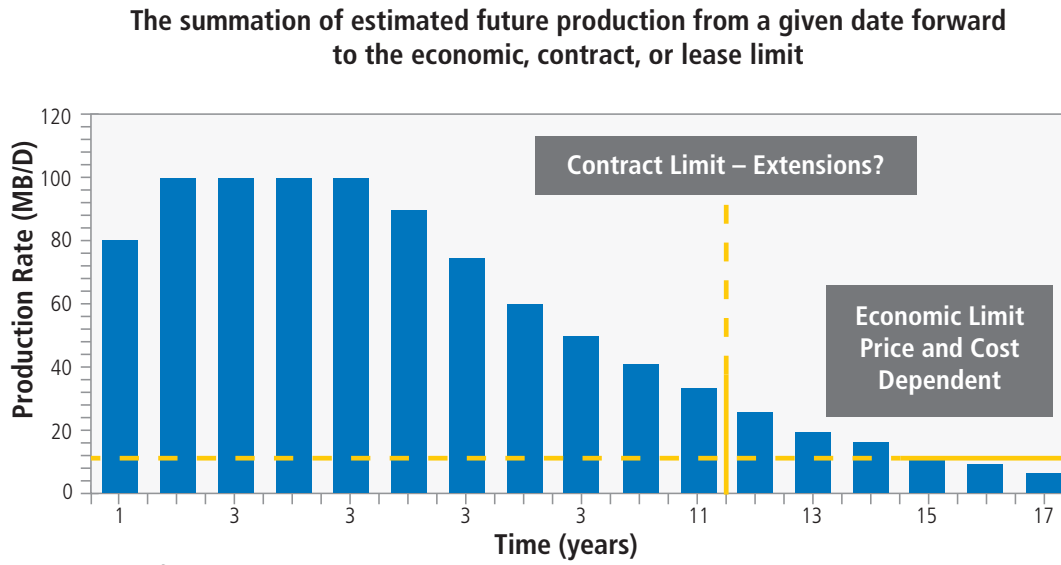

Fig. 13.2—Production profile and economic limit (GCA).

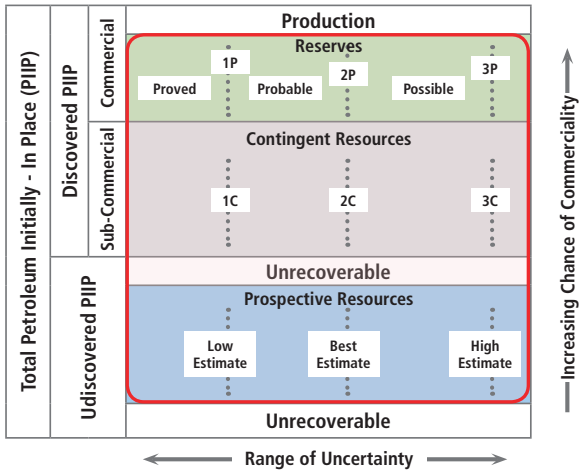

Fig. 13.3—Resources classification framework (PRMS 2007).

by that time, the company has no rights to produce them. Therefore, in this illustration, the company would report reserves (at whatever level of confidence corresponded to the production profile) for years 1 through 11 only. Similar time limits can apply to sales contracts, such as for gas, especially in areas that lack a well-developed spot market.

13.1.3 Why Are Reserve and Resource Estimates Important?

Many stakeholders rely upon reserve and resource estimates. The definitions, guidelines, and regulations are structured to accommodate as many of these users as possible. This section briefly addresses some of the key users of reserves and resources information.

13.1.3.1 Companies

Oil and gas companies need a framework to capture and record all hydrocarbon assets in their portfolio to make appropriate management decisions in connection with potential acquisitions, divestments, developments, etc. SPE PRMS provides a total framework encompassing all types of assets from exploration opportunities, to recent discoveries, to developing and developed oil and gas fields. **Fig. 13.3** shows the PRMS framework for classification and categorization of resources. A later section will discuss this in more detail.

13.1.3.2 Regulators

Regulators including the Securities and Exchange Commission (SEC) in the United States, have a duty to protect the interests of investors by providing rules and guidelines for the public reporting of oil and gas reserves. In this way, the public can be assured that all companies are using a common set of definitions and are (or at least should be) deriving their estimates based on the same principles. As discussed in the next section, the SEC definitions are very similar to the PRMS definitions, but they are not identical. Other regulators have adopted the PRMS definitions and control what each company is required to report.

13.1.3.3 Governments and NOCs

Government entities and national oil companies (NOCs) in countries with oil- and gas-producing operations are also keenly interested in the "bounty of the state" to assist with national resource planning, fiscal policy, and general management of the resource. Such entities' interest may be more about total resource potential, rather than volumes that might more narrowly meet the definitions of reserves. For example, operating companies may get requests for reports dealing with "life-of-field" projections rather than just the volumes to which they may be entitled through to the end of their current concession.

13.1.3.4 Banks and Other Lending Institutions

Organizations that lend money for oil and gas development or infrastructure projects are also very interested in the underlying resources, which are often the collateral (either directly or indirectly) for the loans. Commercial banks will frequently only lend on the highest-confidence volumes ("proved reserves," and sometimes only lend based on "proved developed producing reserves"). Other lenders, such as private equity firms, will lend based on more risky volumes in return for a non-operating stake in the business. Multinational lenders, such as the World Bank, also provide financing for certain energy projects, usually via the host country that will benefit from the activity.

13.1.4 How Is the Work Carried Out and by Whom?

There are three fundamental levels of involvement when deriving and verifying reserves information: evaluation, audit, and process audit.

- **An evaluation is the most fundamental factor.** The evaluation represents a "grass-roots" estimation of the in-place and recoverable volumes. This estimate is typically done by the technical and economic staff within an oil company, which starts with the staff gathering basic data such as seismic data, well logs, test and production data, etc. Consultants or contractors may be brought in to assist, but the onus is on the company staff (or at least their management) to ensure that the evaluation is carried out appropriately. The company must have suitable guidelines and procedures in place to be able to demonstrate that all rules, guidelines, definitions, and regulations are being met.
- **An audit of the declared volumes.** External third-party consultants most often perform the audit. These consultants are totally independent of the company under audit, so that they can provide an unbiased view of the reasonableness of the company's declared volumes. Such an audit will involve a significant degree of checking, but a limited amount of "ab initio" (from the beginning) evaluation. An unqualified audit letter will state agreement, within specified limits, with the volumes declared.
- **The process audit.** This audit contains a review and confirmation that the required procedures exist and have been implemented correctly. The process audit result is not an opinion about the volumes, but only a judgment of the processes.

13.2 What Do We Mean by Reserves Booking?

Before continuing to the discussion about how the reserve numbers are derived, it is important to understand the term "booking." In the oil and gas industry, booking is understood to mean the formal recognition of reserve and resource volumes by a company or other organization, in that those volumes are reported either internally for management purposes, or externally to the public, regulator, or other authority. There is always an implicit requirement that the volumes reported are complete, accurate, and in compliance with the relevant reporting standards.

13.2.1 Qualifications

Many companies and regulators specify education and experience qualifications required of the person in responsible charge of preparing and approving such "booked" volumes. An example is provided in the Society or Petroleum Engineers' *Standards Pertaining to the Estimating and Auditing of Oil and Gas Reserves Information Approved by SPE Board in June 2001, Revision as of February 19, 2007* (SPE Standards 2007):

> **Section 3.2, Professional Qualifications of Reserves Estimators**
>
> A Reserves Estimator shall be considered professionally qualified in such capacity if he or she has sufficient educational background, professional training, and professional experience to enable him or her to exercise prudent professional judgment and to be in responsible charge in connection with the estimating of reserves and other Reserves Information. The determination of whether a Reserves Estimator is professionally qualified should be made on an individual-by-individual basis. A Reserves Estimator would normally be considered to be qualified if he or she (i) has a minimum of 3 years' practical experience in petroleum engineering

or petroleum production geology, with at least 1 full year of such experience being in the estimation and evaluation of Reserves Information; and (ii) either (A) has obtained, from a college or university of recognized stature, a bachelor's or advanced degree in petroleum engineering, geology, or other discipline of engineering or physical science or (B) has received, and is maintaining in good standing, a registered or certified professional engineer's license or a registered or certified professional geologist's license, or the equivalent thereof, from an appropriate governmental authority or a recognized self-regulating professional organization. [See remainder in original article.]

Section 3.3, Professional Qualifications of Reserves Auditors

A Reserves Auditor shall be considered professionally qualified in such capacity if he or she has sufficient educational background, professional training (similar to that described above), and professional experience to enable him or her to exercise prudent professional judgment while acting in responsible charge for the conduct of an audit of Reserves Information estimated by others. The determination of whether a Reserves Auditor is professionally qualified should be made on an individual-by-individual basis and with the recognition and respect of his or her peers. A Reserves Auditor would normally be considered to be qualified if he or she (i) has a minimum of 10 years' practical experience in petroleum engineering or petroleum production geology, with at least 5 years of such experience being in responsible charge of the estimation and evaluation of Reserves Information; and (ii) either (A) has obtained, from a college or university of recognized stature, a bachelor's or advanced degree in petroleum engineering, geology, or other discipline of engineering or physical science or (B) has received, and is maintaining in good standing, a registered or certified professional engineer's license or a registered or certified professional geologist's license, or the equivalent thereof, from an appropriate governmental authority or professional organization. A Reserves Auditor should decline an assignment for which he or she is not qualified.

While the qualifications stated in the two preceding paragraphs provide a reasonable basis for qualifications, each company is free to develop its own guidelines. Note, however, that some regulators specify minimum experience and qualifications for "Qualified Reserve Evaluators" or "Qualified Reserve Auditors."

13.2.2 Concepts of Rights, Risk, and Reward

There are certain key criteria that must be met before a company has the right to book reserves, which are summarized by the concepts of "rights, risk, and reward."

Fundamentally, the contractor must have a direct economic interest in the volumes of oil or gas produced as a result of the activities contemplated under the contract. The following factors are typically considered when deciding on the appropriateness of booking reserves:

- The right to extract oil or gas.
- The right either to take produced volumes in kind or share in the proceeds from their sale.

This right may not of itself provide any meaningful guidance. There are cases (for instance, some risk service contracts) where there is no such right, but reserves are still booked on the basis of the other criteria being satisfied.

Equally, some contracts provide for payment in crude oil, but this of itself is not sufficient for the booking of reserves.

- The exposure to market risk and technical risk.
- Compensation tied in some meaningful fashion to the production achieved.

It is unlikely that reserves would be allocable to purchase contracts, loans, or pure service agreements (such as fee for service).

Because there are many different types of contracts in existence (and even within one legislative framework, individual concession agreements can differ), it is critical that the specific details of the agreement being considered are assessed on their own merits regarding the possibility of booking reserves.

The next figure (**Fig. 13.4**) shows some of the main types of petroleum contracts from around the world. The contracts are listed in a continuous spectrum based on the likelihood of being able to recognize (book) reserves.

13.2.3 Entitlement under Tax Royalty and PSC Contracts

Company oil and gas volumes entitlement depends significantly on the type of concession under which the company is operating. The tax and royalty regime in the US is the most straightforward. Calculations under production sharing contracts (PSCs) are well understood but are more

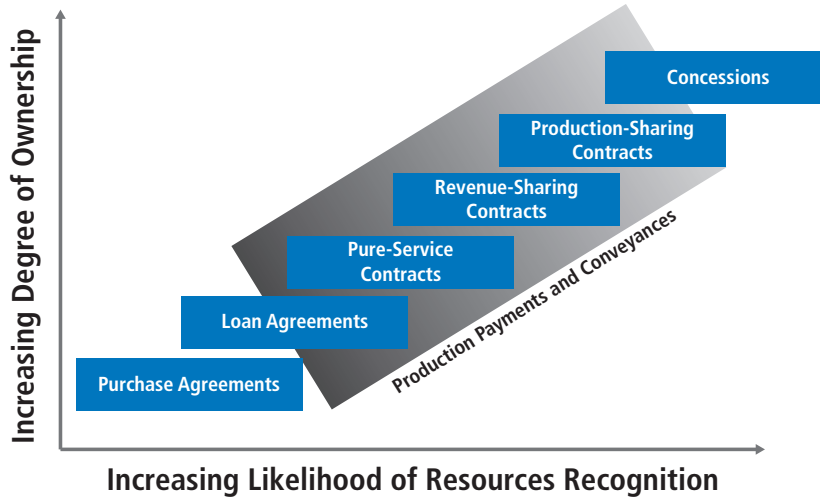

Fig. 13.4—Spectrum of petroleum fiscal systems (Young 2012).

complex and potentially confusing. Daniel Johnston's book, *International Exploration Economics, Risk and Contract Analysis*, provides an excellent discussion of various types of international petroleum contracts. The correct way to calculate volumes entitlement under selected fiscal regimes is addressed in the following section.

13.2.3.1 Working Interest and Net Revenue Interest

In the US, the oil company makes an agreement directly with the mineral owner (for instance a landowner or, for offshore development, the state or federal authorities), and is thereby allowed to drill for and produce oil and gas. The contractor, in the sense previously defined, has a working interest of 100%. If there are several companies jointly and equally (pari passu) participating in the operation, each will have its own working interest percentage. The sum of all such interests will be 100%. However, the companies must pay a "royalty" to the mineral owner in order to compensate him or her for the right to explore for, and produce, hydrocarbons. Under customary US treatment, such a royalty represents a "volume due to the mineral owner" and that part of the production cannot be claimed as reserves by the oil companies. This is the case (as usually happens) even if the value of the royalty is paid in cash rather than the delivery of hydrocarbons.

Historically, US royalties have been in the range from 12.5% to 16.33%, but with the recent high demand for acreage in the shale plays, landowners are currently commanding royalty rates of up to 25% or so. Therefore, the company's reserves entitlement is determined from its "net revenue interest." Using the example of a single company operating in an onshore US shale play for which the royalty is 20%, the company's working interest would be 100%, and its net revenue interest would be 80%. The reserve entitlement volume would be the sales volume that meets the relevant definition for each reserve or resource category multiplied by 0.8 (see Section 13.3).

The situation in other countries can be quite complex. Even if the fiscal regime is nominally one of tax and royalty, there are cases in which the royalty can be paid in cash only. In such situations, some companies elect to treat it as a tax, and not as a deduction from volumes. It is advisable to seek a specialist's advice in such circumstances.

13.2.3.2 Production Sharing Contracts Entitlement and "Tax Barrels"

Calculating bookable reserve volumes under production sharing contracts (PSCs) is completely different from that described for tax and royalty regimes. The best way to illustrate this is with an example.

1. An operating company (group) is appointed as the contractor in a specific area.

2. The contractor operates at sole risk and expense, but under the control of the host country.

3. The production, if any, belongs to the host country until it is exported.

4. The contractor is entitled to recover the expended costs out of a proportion of production revenue from the contract area ("cost oil").

5. After the cost recovery, the balance of production is shared by a predetermined percentage split between the host country and the contractor ("profit oil").

6. The contractor's income is taxable with the tax often being paid from the host country share.

7. Equipment and installations are the properties of the host country.

The following example (**Fig. 13.5**) is from Indonesia, one of the first countries to develop and apply the PSC concept.

This example contains the following features:

- Out of total field production, a certain proportion of that production—the First Tranche Petroleum (FTP)—is allocated to profit oil (see the bullet about "Profit oil" later in this section). This allocation guarantees that the state entity receives some share of production, even in the early stages of the field's life, during which there are many accumulated costs to recover (often mainly development capital). In some jurisdictions, this same function is accomplished by the imposition of a royalty, which is paid directly to the state, or by a cap on the cost recovery percentage.
- The remaining petroleum is allocated first to cost recovery to allow the contractor to recover investments and other allowed costs. Some costs are recoverable in full immediately (typically operating costs), while, for others, the deduction is based on capital depreciation. Any remaining production after FTP and cost oil becomes profit oil.
- Profit oil is divided between the contractor and state according to the terms of the agreement. A typical Indonesian after-tax split would be 85% to the state and 15% to the contractor.
- The state pays corporation tax on behalf of the contractor.
- There may also be a domestic market obligation (DMO) that requires the contractor to dedicate a certain amount of production to meet local requirements. This DMO is sold to the state at a discounted price.

When these calculations have been made for every year of the forecast recovery, the contractor's entitlement is defined as the sum of "cost oil" and share of "profit oil." If the state pays corporation tax on behalf of the contractor, some companies elect to add back in these "tax barrels" because reserves evaluation is usually considered on a before-tax basis. However, it is critical to ensure that the resulting calculation makes sense, and, more importantly, that volumes greater than 100% of field sales are never calculated! Then, the reserve entitlement is calculated by dividing the contractor's revenue by the oil price. It is easy to see how the entitlement volume can be affected (sometimes quite significantly) by the oil price when this calculation is used. Note that high oil prices result in lower volumes, and, conversely, low oil prices result in higher volumes, which is somewhat counterintuitive.

It is beyond the scope of this chapter to describe all of the intricacies of the various types of PSCs around the world (and there are many). Daniel Johnston's book (*International Exploration Economics, Risk, and Contract Analysis*) provides more detail on this topic.

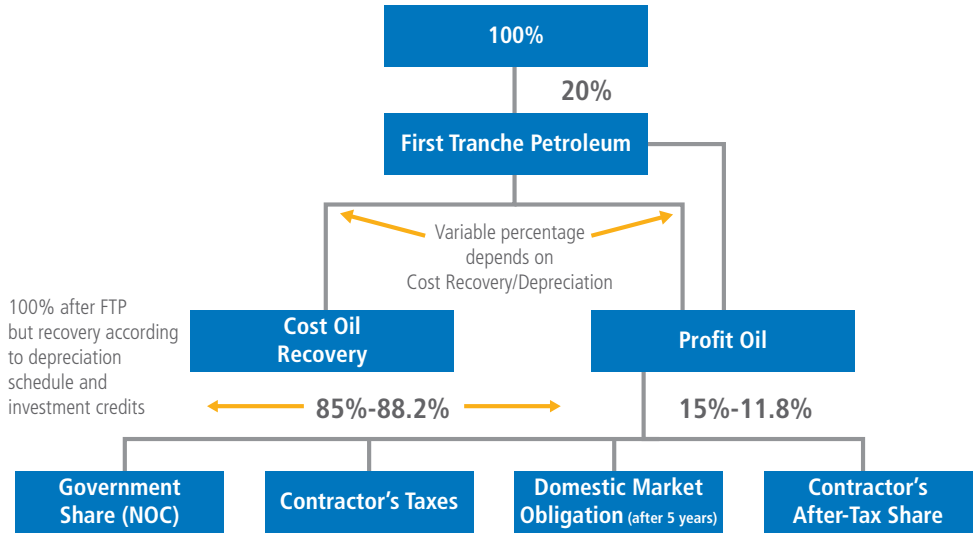

Fig. 13.5—Example allocation in pre-2002 Indonesian production-sharing contract (GCA internal presentation; not available to the public).

13.2.3.3 Risk Service Agreements

In many ways, risk service agreements (RSAs) are similar to PSCs in that the volume entitlement is derived from the economic calculation. RSAs usually pay the contractor a fee that is based on production achieved rather than explicitly allowing the contractor to recover costs and share in profits. In this case, the total revenue received by the contractor under the terms of the RSA is divided by the relevant oil price, resulting in an equivalent volume of oil. As with PSCs, there are many types of RSAs. It is important to study the RSA terms carefully in order to make the correct calculation.

13.2.4 Formal Reporting to Regulatory Authorities

Most financial jurisdictions and national governments have rules that govern what companies must and may formally report. Both regulators, who are protecting the interests of investors, and governments that are concerned with setting policy, require standardized reporting on oil and gas reserves (and resources, where permitted).

13.2.4.1 The US Securities and Exchange Commission and the Financial Accounting Standards Board

Within the United States, the Securities and Exchange Commission (SEC) is charged with regulating all institutions that have a listing on the securities and stock exchanges in the US. As will be discussed next, companies must comply with the SEC's established definitions for reserves. Separate from the SEC regulations, the US Financial Accounting Standards Board (FASB) specifies the financial information that should be reported, and how that reporting must be achieved. The most well-known FASB report is the "standardized measure of discounted future net cash flows relating to proved oil and gas reserve quantities" (SMOG), which provides an after-tax 10% discounted net cash flow value. In principle, this measure is more representative of the company's expected benefits from its operations than just volumes of oil and gas, because it takes account of the price received for selling the oil and gas, the costs of the operations, and the timing of cash flows.

13.3 Definitions for Reserves and Resources

This section provides an overview of the key sets of definitions for oil and gas reserves in use around the world. It starts with a discussion of the PRMS because this provides a framework for capturing all types of resources, and because many other systems are either based on or very similar to the PRMS.

13.3.1 Overview and History of Reserves and Resources Definitions

A definition for oil and gas reserves has existed in some form since the early years of the last century. The SPE introduced a formal definition for proved reserves in 1965. These definitions have been updated several times, as shown in **Table 13.1**, next. Most recently, the definitions have been revised in conjunction with other industry organizations with the addition of definitions for probable and possible reserves and resources. The SEC's definition for proved reserves was formalized in 1978, and that was the basis for corporate reporting until the modernized regulations were released effective January 1, 2010 (Modernization of Oil and Gas Reporting 2009).

13.3.2 PRMS Framework: The Basis for Most Corporate Planning

The PRMS was published in March 2007 and has, since then, been very widely adopted in the industry throughout the world. It provides a framework in which a company can capture all of its oil and gas assets from exploration, to discoveries, to fields under development, and on to production (**Fig. 13.6**).

The following paragraphs will provide a brief description of each of the resource classes and categories; however, the reader is encouraged to review the PRMS to obtain full details.

13.3.2.1 Reserves (Proved, Probable, Possible, 1P, 2P, and 3P)

As defined in the PRMS, "Reserves are those quantities of petroleum anticipated to be commercially recoverable by application of development projects to known accumulations from a given date forward under defined conditions. Reserves must further satisfy four criteria: They must be discovered, recoverable, commercial, and remaining (as of a given date) based on the development project(s) applied." Let us look at each of these criteria in turn.

13.3.2.2 Criteria

13.3.2.2.1 Discovered

The first requirement for a discovery is a well. It is not possible to have a "known accumulation" without a wellbore penetration. Potential accumulations that have not yet been discovered are accounted for using the "prospective resources" class.

Table 13.1—History of major reserves and resources definitions.

Year	Definition Event
1930s-1940s	American Petroleum Institute (API) and American Gas Association (AGA); Former Soviet Union Systems
1965	SPE definition of proved reserves
1972	McKelvey Box
1978	SEC Proved Reserves definitions
	SEC Staff Accounting Bulletin, Topic 12 "interpetive responses"
1987	SPE definitions for probable and possible reserves
1987	WPC resource system and definitions
1997	SPE/WPC reserve definitions
2000	SPE/WPC/AAPG resource definitions and classification system
2000-2001	SEC Website "classifications"
2001	SPE/WPC/AAPG guidelines for the evaluation of petroleum reserves and resources
2002	Canadian Oil and Gas Evaluation Handbook (COGEH) Volumes 1 and 2
2007	SPE/WPC/AAPG/SPEE Petroleum Resources Management System
2007	COGEH Second Edition Volume 1 and Volume 3
2009	SEC revised regulations (1/1/2010 effective date)
2011	SPE, WPC, AAPG, SPEE, and SEG Guidelines for the Application of the Petroleum Resources Management System

13.3.2.2.2 Recoverable

When an entity is estimating and reporting any class of resource (reserves, contingent resources, and prospective resources) the more interesting data is about the quantities that can be recovered and sold or otherwise monetized. There will always be some part of the in-place volume that cannot be recovered due to the limitations of the physical processes involved. This unrecoverable amount is shown as "Unrecoverable" in the PRMS framework. The amount of oil or gas that is recoverable will depend on both the details of the extraction project (for instance, natural depletion, aquifer drive, carbon dioxide flooding, etc.) and the physical properties of the rock and fluid (high- or low-permeability, high- or low-fluid viscosity, "wetness" of the rock, etc.). The amount of hydrocarbons that can be recovered from a reservoir may change over time based on prevailing economic conditions and available technology.

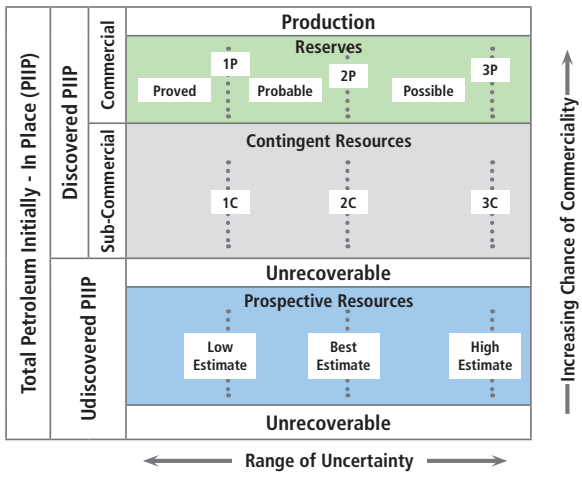

Fig. 13.6—Petroleum Resources Management System Framework (PRMS 2007).

13.3.2.2.3 Remaining

Reserves or other resources statements always reflect the amount that is estimated to be recoverable from a given date forward. Therefore, the reports will always have an effective "as-of" date. Adding the historical production (if any) to an estimate of future recovery provides the "estimated ultimate recovery" (EUR) amount.

13.3.2.2.4 Economic or Commercial

For a recoverable volume to qualify as a reserve, a number of other criteria must be met. In addition to the basic requirement for economics (see below), there are a number of other conditions specified in the PRMS that must be met

that fall under the general concept of "commercial." The statements are as follows:

> Discovered recoverable volumes (Contingent Resources) may be considered commercially producible, and thus Reserves, if the entity claiming commerciality has demonstrated firm intention to proceed with development and such intention is based upon all of the following criteria:
>
> - Evidence to support a reasonable timetable for development.
> - A reasonable assessment of the future economics of such development projects meeting defined investment and operating criteria.
> - A reasonable expectation that there will be a market for all or at least the expected sales quantities of production required to justify development.
> - Evidence that the necessary production and transportation facilities are available or can be made available.
> - Evidence that legal, contractual, environmental, and other social and economic concerns will allow for the actual implementation of the recovery project being evaluated.
>
> To be included in the Reserves class, a project must be sufficiently defined to establish its commercial viability. There must be a reasonable expectation that all required internal and external approvals will be forthcoming, and there is evidence of firm intention to proceed with development within a reasonable time frame. A reasonable time frame for the initiation of development depends on the specific circumstances and varies according to the scope of the project. While years is recommended as a benchmark, a longer time frame could be applied where, for example, development of economic projects are deferred at the option of the producer for, among other things, market-related reasons, or to meet contractual or strategic objectives. In all cases, the justification for classification as Reserves should be clearly documented.

13.3.2.2.5 Economic Limit Test

The economic limit test (sometimes abbreviated as ELT) is an assessment of the volumes of oil or gas that can be produced economically. The "economic limit" is the point in time beyond which the revenue from the declining production is no longer sufficient to cover the operating cost of the project. That is the limit for the projection of recovery for reserves purposes. Volumes that might be technically recoverable beyond the economic limit might be captured as contingent resources (contingent on a higher price or lower operating cost than can be accounted for at the time of the estimate). However, many companies do not do this, and simply truncate the profile at the economic limit.

13.3.2.2.6 Developed and Undeveloped Volumes

The PRMS (and the SEC) definitions distinguish between volumes that have already been developed and those that require future investments. Developed volumes are estimated to be recovered by existing projects, while undeveloped volumes require relatively major additional capital expenditures.

13.3.2.3 Contingent Resources

Following is the definition of contingent resources from the PRMS, which says in part:

> Contingent Resources are those quantities of petroleum estimated, as of a given date, to be potentially recoverable from known accumulations by application of development projects but which are not currently considered to be commercially recoverable due to one or more contingencies. Contingent Resources may include, for example, projects for which there are currently no viable markets, or where commercial recovery is dependent on technology under development, or where evaluation of the accumulation is insufficient to clearly assess commerciality.

So, contingent resources have been discovered, but have not yet been confirmed to be commercially recoverable. We saw, above, the criteria that need to be met for contingent resources to move into the Reserves class.

13.3.2.4 Prospective Resources

As defined by the PRMS, prospective resources are: "… those quantities of petroleum estimated, as of a given date, to be potentially recoverable from undiscovered accumulations by future development projects." It goes on to say:

> Potential accumulations are evaluated according to their chance of discovery and, assuming a discovery, the estimated quantities that would be recoverable under appropriate development projects. It is

recognized that the development programs will be of significantly less detail and depend more heavily on analog developments in the earlier phases of exploration.

Prospective Resources have not yet been discovered (which, as we saw, requires, at a minimum, a well), but we are still interested in estimating the volumes that could be recoverable based on potential development projects.

13.3.2.5 Concept of a Project

The "project" concept is fundamental to the evaluation of recoverable volumes of any class. For reserves in particular, the project (or projects) is described in the approved field development plan. The identified and committed plan allows the company to demonstrate the "firm intention to proceed" that is a requirement for the allocation of reserves.

13.3.2.6 Methodologies

This chapter is not intended to delve deeply into the "how to" of reserves and resources estimation. We are more concerned about what to do with the numbers when they have been derived (i.e., their "booking"), but it may still be helpful to mention briefly the main methods that are applied to derive estimated recoverable volumes.

13.3.2.6.1 Analogy

When there are little data available about a particular field or accumulation, it is useful (and perhaps necessary) to look at similar accumulations in order to understand the potential of the new situation. There are definitions for what constitutes "analog field project data" or "analog" in both the PRMS and SEC definitions, but in general, it should have properties no better than the subject reservoir. The challenge with unconventional reservoirs is that most seem to be sufficiently different from each other that they cannot be used as analogs for newer reservoirs. In a shale gas play, for instance, the play becomes its own analog as data from around the (usually extensive) area are gathered.

13.3.2.6.2 Volumetric

The standard volumetric approach is of limited value for unconventional reservoirs due to the large uncertainty in recovery efficiency. An attempt should still be made to assess the quantities of oil and gas in place, both free and adsorbed, in order to be able to check that the inferred recovery efficiency from performance methods is sensible.

13.3.2.6.3 Performance

The method that is applied most often to the evaluation of shale gas and other unconventional reservoirs is based on projections of well performance using historical data from existing wells and type curves for use for future wells. This topic will be discussed further later in this chapter and in detail in Chapter 14.

13.3.3 SEC—Revised Regulations and FASB

Companies listed on a stock exchange in the US must comply with the SEC reporting requirements. For oil and gas companies, the relevant definitions are in Regulation S-X Rule 4.10(a) and reporting requirements are contained in Regulation S-K (Modernization of Oil and Gas Reporting 2009). These rules were modernized in 2009 and have been in effect since January 1, 2010. The previous rules had been in effect since 1978, and the industry had seen many changes since then.

The four main areas that the SEC identified for change that took effect in 2010 are as follows:

1. The requirement for the use of a single-day pricing when calculating reserves has been replaced by a 12-month, first-day-of-the-month arithmetic average.

2. The limitation against reporting of "non-traditional" hydrocarbons (such as bitumen) has been removed.

3. The use of "reliable technologies" is permitted.

4. Companies may elect to (but are not required to) report probable and possible reserves, in addition to proved reserves.

13.3.3.1 Similarities and Differences with PRMS

The new SEC definitions are very similar to those set out in the PRMS, but they are not identical. Practitioners should be aware of the differences when preparing reports for submission to the SEC. One of the main differences is in relation to the price that can be used. As noted above, the SEC prescribes how the price is to be calculated. The PRMS is based on pricing forecasts (as typically being the basis upon which companies make their investment decisions). This difference may have limited impact in practice because most US assets are evaluated under a tax and royalty regime, but the effect could be much greater under the entitlement calculation required for a production sharing contract. A discussion of this in detail

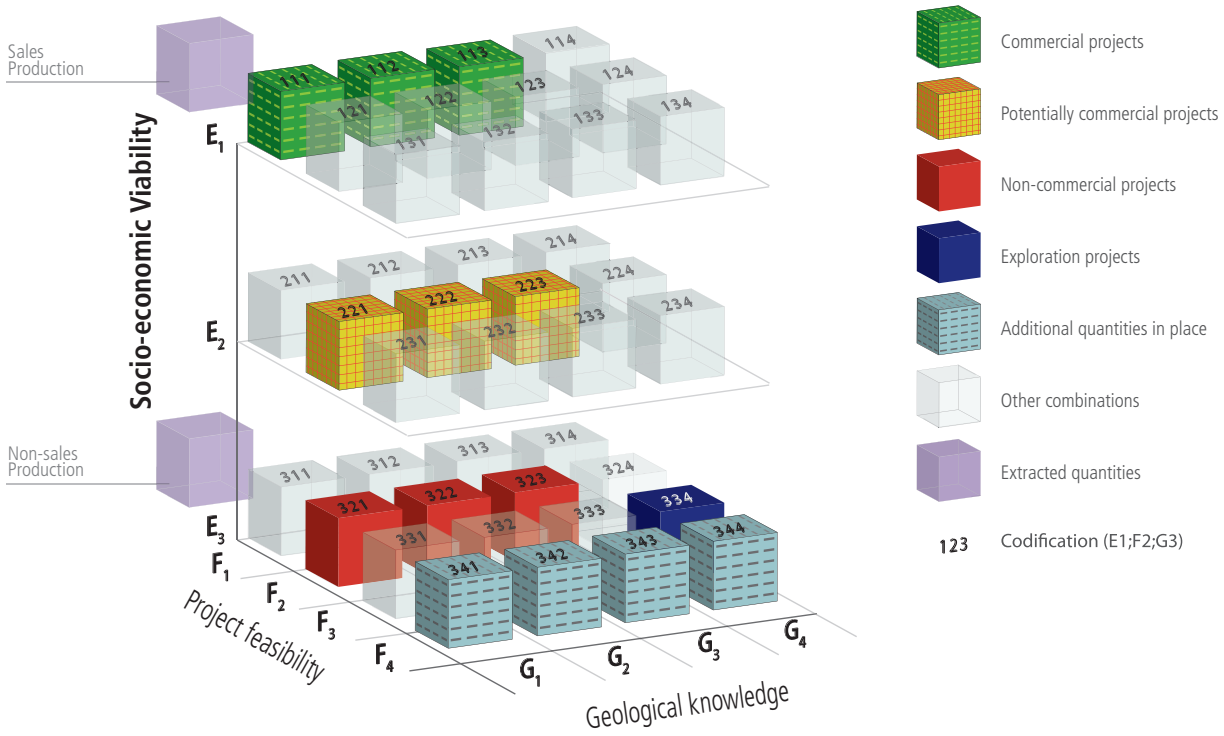

Fig. 13.7—United Nations Framework Classification (UNFC-2009). (Reproduced courtesy of the United Nations Economic Commission for Europe.)

is beyond the scope of this chapter, but interested readers are encouraged to review Daniel Johnston's excellent book, *International Exploration Economics, Risk and Contract Analysis*.

13.3.3.2 Additional Reporting Requirements (FASB)

Without going into detail, it will be useful for you to know that reserves reporting is also governed by the Financial Accounting Standards Board (FASB). FASB released a reference document, Topic 932, in early 2010 to update the prior regulations contained in FAS 69, and to incorporate the changes introduced by the SEC. You can search for, and access, the information related to Topic 932 online at FASB.org.

13.3.4 *The Canadian Oil and Gas Evaluation Handbook* and the PRMS

Companies reporting oil and gas reserves or resources to any Canadian stock exchange must comply with National Instrument (NI) 51-101. The definitions, and a great deal of discussion about estimating volumes, are contained within the *Canadian Oil and Gas Evaluation Handbook* (COGEH), which is a three-volume set. The core definitions are contained within Chapter 5 of Volume 1 and are fundamentally similar to those of the PRMS. There are a few differences that practitioners should be aware of if reporting to a Canadian exchange. Volume 3 deals with unconventional reservoirs, especially coalbed methane.

13.3.5 UNFC—PRMS Provides the Hydrocarbon Specifications

The United Nations has developed a framework for classifying extractive minerals within one three-dimensional system. It is called the "United Nations Framework Classification for Fossil Energy and Mineral Reserves and Resources 2009 (UNFC-2009)." "UNFC-2009 is a generic principle-based system in which quantities are classified on the basis of the three fundamental criteria of economic and social viability (E), field project status and feasibility (F), and geological knowledge (G)," and uses a numerical and language-independent coding scheme. Combinations of these criteria create a three-dimensional system" (**Fig. 13.7**).

The system is numeric to avoid the differences in meaning of certain words when they are translated into other languages. While this system is not in common use in the oil and gas industry, it is important to mention that the PRMS provides the underlying specifications for oil and gas within the UNFC-2009.

13.3.6 Additional Guidelines

13.3.6.1 As-Of Date

As mentioned in the section about definitions, every reserves or resources report must have an effective date. For US companies, this is the final day of the fiscal reporting period, usually December 31. No data that relates to events after the as-of date can be included in the evaluation. (In the author's view, it would be appropriate to mention the impact of any subsequent event before the date of issuance that would have a material effect on reported volumes with the goal of full and fair disclosure.)

13.3.6.2 Reference Point

All volumes to be reported are as measured at a specified reference point. That would normally be a custody transfer point when the production is sold to another party. The volume recorded would be in the condition when sold, so if, for instance, it were a stream of gas that included 3% nitrogen, the volume would be as sold, and not reduced by 3% to account for the inert gas.

13.3.6.3 Fuel and Flare

Under SEC guidance, it is permitted to include fuel used in field operations as a reserve, presumably on the basis that it has value. It is not permitted to include fuel in Canada. The PRMS recommends exclusion, but recognizes that some jurisdictions (such as the SEC) do permit it. It is good practice to identify any volume of fuel included in the reserve estimate separately.

Flared, vented, or otherwise lost volumes should not be included in any reserve or resource estimates. Such volumes are captured for the purposes of engineering material balance studies, but they do not generally form a part of reserve or resource booking.

13.3.6.4 Contract and Lease Term

Companies should report only those volumes to which they are entitled. That entitlement may expire at the end of a defined lease term so volumes that might be projected to be economically producible beyond such expiry date are not reserves to the company. They may indeed be to the host country, but that is another matter. If there is a clause in the license terms that permits an extension, volumes after the expiry date may be considered as Contingent Resources until such time as the renewal and its terms are sufficiently well-defined to provide the high level of confidence needed for qualification as reserves.

13.3.6.5 Royalty

A royalty represents a volume of hydrocarbons that is owned by someone other than the producing company, usually the state or, in the onshore US in particular, the landowner. If this is truly a "volume due to others," then it is a deduction to the company's reserve base. If, as may be the case in certain foreign jurisdictions, this is merely another form of taxation, then it may be treated as such and not deducted from volumes. Each contract can be different, so advice should be sought if there is any doubt as to the appropriate treatment of a royalty.

13.3.6.6 Non-Hydrocarbons

No adjustment is usually required for non-hydrocarbons that remain in the product as it is sold. If it is necessary for them to be removed before sale (for instance, to meet pipeline specifications), then the reduced volume is reported.

13.3.6.7 Aggregation

Aggregation refers to the summation of individual estimates to derive totals for reporting purposes.

13.3.6.7.1 Arithmetic

If estimates of volumes are prepared deterministically, then arithmetic aggregation is the only option. Individual category estimates of proved, probable, and possible for different projects are summed to arrive at total category values for the business entity or corporation. It is recognized that summation of all proved quantities gives a total that is more conservative than any of the individual estimates, but there is no deterministic mechanism to accommodate this. Equally on the high side, summation of all possible (or 3P) values could be too optimistic.

13.3.6.7.2 Probabilistic

If probabilistic methods are used, the definitions allow for stochastic aggregation up to the field, property, or (for PRMS) project level. Thereafter, aggregation should be by simple arithmetic summation.

13.4 What Do We Mean by "Unconventional Resources"?

According to the PRMS, "Unconventional resources exist in petroleum accumulations that are pervasive throughout a large area and that are not significantly affected by hydrodynamic influences (also called "continuous-type deposits"). Examples include coalbed methane (CBM), basin-centered gas, shale gas, gas hydrate, natural bitumen (tar sands), and oil shale deposits. Typically, such accumulations require specialized extraction technology (e.g., dewatering of CBM; massive fracturing programs for shale gas, steam and/or solvents to mobilize bitumen for in-situ recovery; and, in some cases, mining activities). Moreover, the extracted petroleum may require significant processing before the sale (e.g., bitumen upgraders). (Also termed "non-conventional" resources and "continuous deposits.")

The Society of Petroleum Evaluation Engineers (SPEE), Monograph 3 (2010), Guidelines for the Practical Evaluations of Undeveloped Reserves in Resource Plays uses a slightly different definition: "Resource play reservoirs cover a large areal extent and have a continuous hydrocarbon accumulation throughout the reservoir. However, the reservoir is not homogeneous; that is, the wells in the same producing interval exhibit dramatic differences in producing rates and EURs." The Monograph goes on to identify four "Tier 1" criteria that are nearly always observed in resource plays:

1. Wells exhibit a repeatable statistical distribution of estimated ultimate recoveries (EURs).
2. Offset well performance is not a reliable predictor of undeveloped location performance.
3. A continuous hydrocarbon system exists that is regional in extent.
4. Free hydrocarbons (non-sorbed) are not held in place by hydrodynamics.

Further, an additional four "Tier 2" criteria are identified that are commonly observed in resource plays:

1. Requires extensive stimulation to produce at economic rates.
2. Produces little in-situ water (except for coalbed methane and tight oil reservoirs).
3. Does not exhibit an obvious seal or trap.
4. Low permeability (< 0.1 md).

While all criteria are important, it is the first, "Wells exhibit a repeatable statistical distribution of EURs," that forms the basis for the method proposed. If this criterion is not met then the method should not be applied.

While this approach is similar in some ways to the PRMS definition, the Monograph 3 wording specifically relates to the statistical nature of the accumulation, which has an effect on the proposed method of evaluation (refer to Section 13.5.3).

Fig. 13.8, next, illustrates the differences between conventional and unconventional reservoirs. Some characteristics are also presented in **Table 13.2**.

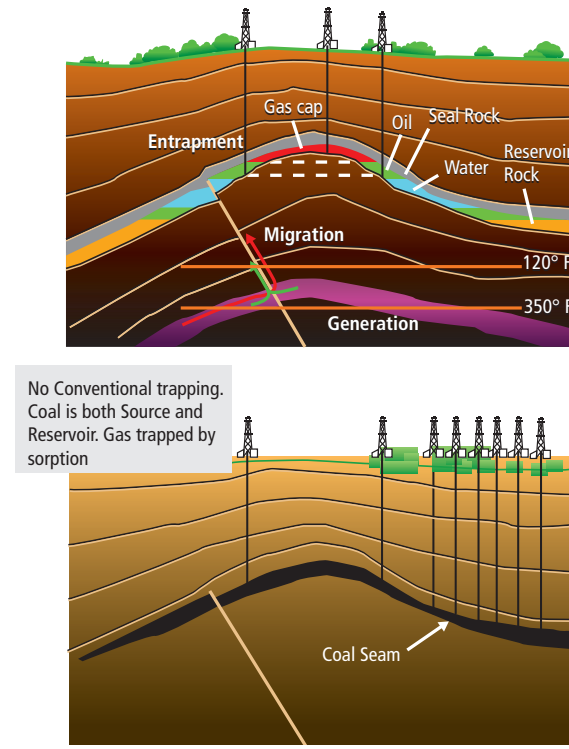

Fig. 13.8—Illustration of conventional and unconventional accumulations (Top: Rhein Petroleum and Bottom: GCA).

13.5 Approach to Assessing Reserves and Resources in Unconventional Reservoirs

Having discussed the basic definitions for reserves and resources in some detail, this final section will deal with some of the issues being faced by the industry in the assessment and reporting of reserves and resources in unconventional reservoirs. Consistent with the theme of this book, the focus will be on shale gas, although many of the principles will apply to other unconventional accumulations such as shale oil, coalbed methane (CBM), tight gas and oil, etc.

As will be shown in Chapter 14, each shale play is unique and has its own performance characteristics. This uniqueness means that one of the tools that is often applied for conventional reservoirs, that of the analog, is much harder to justify with unconventionals. Each play becomes its own analog, so a large number of wells is needed in order to be able to assess the likely future performance of any particular asset.

The key questions that we need to answer are:

- What constitutes a discovery?
- When a discovery has been made, how should we estimate volumes to be included into the Contingent Resources and Reserves classes? As a part of this question, we need to consider what we mean by a "project" and how we assess confidence in the realization of the project as well as its outcome.
- What is the projected recovery from current and future wells?

We will address each of these points in turn.

Table 13.2—The difference between conventional and unconventional accumulations. Adapted from PRMS and Elliot 2008.

Conventional	Unconventional
■ Trapping dominated by hydrodynamics	■ Trapping not significantly affected by hydrodynamics
■ Controlled by local structure and statigraphy. ■ Well-defined limits (caprock and fluid contacts). ■ Discrete fields.	■ Controlled by regional stratigraphy (pervasive throughout large area). ■ Poorly defined limits. ■ Continuous-type deposits.
■ Many produce without stimulation.	■ Requires specialized extraction and/or processing technologies.

13.5.1 What Constitutes a Discovery?

The first and one of the most critical aspects of the evaluation of an unconventional reservoir is to ascertain "what has been discovered?" In many cases, the existence of the formation has been known for many years and may have been penetrated by hundreds of wells drilled to deeper reservoirs. However, it has only recently been shown that it is possible to extract hydrocarbons from these formations. Therefore, the reservoir has been "discovered" in the sense of being known to exist, but initially there is no demonstration of (potentially) commercial producibility. According to the PRMS framework, it should, therefore, be identified as Discovered Petroleum Initially In Place. If there were no evidence of the potential for recovery (for instance, from valid analogs), it would be appropriate to assign volumes as "Unrecoverable." The PRMS defines Unrecoverable Resources as:

> That portion of Discovered or Undiscovered Petroleum Initially-in-Place quantities which are estimated, as of a given date, not to be recoverable. A portion of these quantities may become recoverable in the future as commercial circumstances change, technological developments occur, or additional data are acquired.

The PRMS includes the following requirements for a discovery:

> A discovery is one petroleum accumulation, or several petroleum accumulations collectively, for which one or several exploratory wells have established through testing, sampling, and/or logging the existence of a significant quantity of potentially moveable hydrocarbons. In this context, "significant" implies that there is evidence of a sufficient quantity of petroleum to justify estimating the in-place volume demonstrated by the well(s) and for evaluating the potential for economic recovery.

As can be seen from the criterion "testing, sampling, and/or logging," a well test is not necessarily required to establish a discovery. The authors of the PRMS included this comment intentionally in order that the definition would apply to unconventional reservoirs from which it may not be feasible to test productivity at the time of exploration due either to fluid properties (e.g., bitumen) or reservoir properties (e.g., shales).

Although the Application Guidelines (Guidelines for Application of the Petroleum Resources Management

Systems 2011) were not intended to change the principles of the PRMS, a small but significant amplification was made to the requirement for a "discovery" for shales in those guidelines (in Chapter 8):

> For shales, there are several criteria that should be considered before an accumulation is declared to be 'discovered.' **The first is a well test**, which may require fracture stimulation that produces enough gas to the surface to be of commercial interest. **The second is core and log data** that provide convincing evidence of a significant volume of moveable hydrocarbons. **The third is identification of a commercially productive analog** with sufficient similarity to the subject reservoir to conclude that it should be able to produce gas at comparable rates and recoveries. It is the combined weight of these three criteria that is important, which means, for example, if the gas flow rate is thousands of cubic feet per day, then the evidence from core, logs, and analogs needs to be more compelling than if the gas flow rate is millions of cubic feet per day. [Emphasis added.]

So in this case a well test is required to demonstrate the "proof of concept" that potentially commercial quantities of gas can be flowed to surface. (Note that for a discovery, i.e., for the recognition of Contingent Resources, actual proof of commerciality is not required. That is only needed when we aim to establish the existence of Reserves.) In practice, it may be necessary to obtain (at least) several months of production data to confirm that the reservoir will be able to maintain commercial production over a reasonable time period. Further, it will be necessary to demonstrate that potentially commercial levels of producibility can be obtained throughout the area (that can be very large) that is being considered for eventual development.

13.5.2 Estimation of Contingent Resources and Reserves

13.5.2.1 How Far from a Discovery Can Be Considered Contingent Resources?

As discussed previously, when we have decided that a discovery has been established, in the early stages of evaluation, we must assess how much of the shale reservoir might then fall into the contingent resources class. Those volumes that cannot be included in contingent resources will remain as prospective resources. (We will deal with reserves later.) Unfortunately, there is no "industry standard" answer to this question, since it will depend largely on the results of the testing to date, the number of locations evaluated throughout the entire area under consideration, the distance between them, and the properties of the reservoir.

The following suggestions are taken from the application guidelines:

> Since shale gas plays extend beyond the limits of conventional traps, the decision regarding how far away from existing well control Contingent Resources should be assigned can be difficult. Two guidelines that should be applied in this work are (1) information from seismic data showing that the shale is a continuous accumulation of similar character extending away from well control and is not cut by a sealing fault, and (2) indications that reservoir properties from wells that bound the Contingent Resources area are sufficiently similar to those of the discovery well that their well performance is expected to be similar.

This latter point suggests that the evaluation should be focused mainly on interpolation within the area outlined by well control. There should be little if any extrapolation of contingent resources beyond well control; instead, such areas should remain prospective until drilled.

One admittedly arbitrary method is to consider that contingent resources can be assigned within a three-mile radius from established production. There is no real basis for this assignment, since most evaluators agree on one fact: unconventional reservoirs are generally heterogeneous, so proximity to a productive area is no guarantee that similar productivity will be attained within that area. Remember that contingent resources are not yet necessarily commercial—there is the **potential** for commerciality. In order for contingent resources to become reserves, many other criteria need to be met [see *PRMS Framework,* Section 13.3.2.2.4]. How far this approach can be applied will depend significantly on the quantity and quality of data available for evaluation. Just a handful of wells spread over a large lease (for instance, one million acres; see **Fig. 13.9**) is not adequate to infer much about the overall potential. Nevertheless, this method does provide a way to begin to capture volumes for company consideration.

It is important to remember that, according to the PRMS, any resource assessment should be based on projects that could be implemented in order to recover the estimated volumes. This is discussed further below in connection with the assignment of reserves, but the same philosophy applies to the quantification of contingent resources. Any

volumes that are to be booked as contingent resources should be considered based on the idea that the area under investigation will be drilled using a defined spacing and that the company concerned is planning to do so, subject to confirmation of commerciality.

13.5.3 Estimation of Reserves

Oil and gas companies have a particular interest in the volumes that they can report as reserves. For most unconventional plays in North America, estimates of future recovery are based on the number of wells that can be assigned to each reserve category (proved, probable and possible), based on the assessed confidence in recovery and the projected recovery from each one. This sounds simple, but as always, the difficulty is in the details.

A key factor in assigning reserves to an unconventional reservoir is "what constitutes a project?" The PRMS is a project-based system (refer to the PRMS Framework section earlier in this chapter). The PRMS instructs us to seek to estimate the recovery from defined projects that are draining underground resources. However, the definition of a project can be more complex for unconventional reservoirs. Ultimately, it may take thousands of wells to develop a particular shale play.

There are two main ways to consider how many wells should be included when deriving estimates of future recovery:

1. The number of wells that will offset established production.

2. The number of wells that have actually been approved for drilling.

Many evaluators use a version of what may be termed the "concentric rings" method of evaluation to assign wells to the different Reserves categories. This is illustrated in the **Fig. 13.10** (locations are shown as squares for simplicity; in reality they would be rectangles for horizontal wells):

The concentric rings approach is to assign higher confidence to wells that are to be drilled closer to existing production. In the example, there is one productive, proved developed producing (PDP) well (the red dot) and eight adjacent locations (in pink) are assigned as proved undeveloped (PUD). Beyond that are a number of locations (in blue) to which probable reserves have been assigned, based on their greater distance from the existing data point. Further still, it may be reasonable to assign possible reserves and/

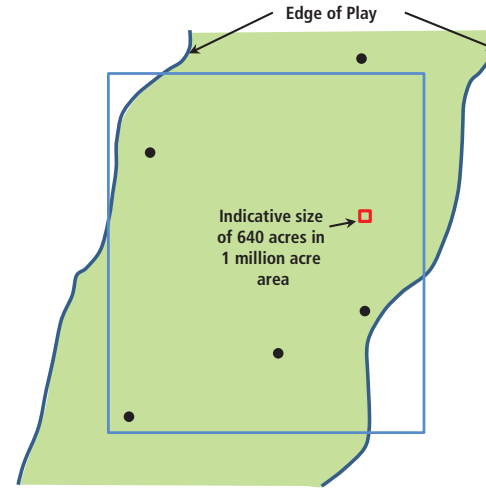

Fig. 13.9—Large lease with a few wells widely spaced (GCA).

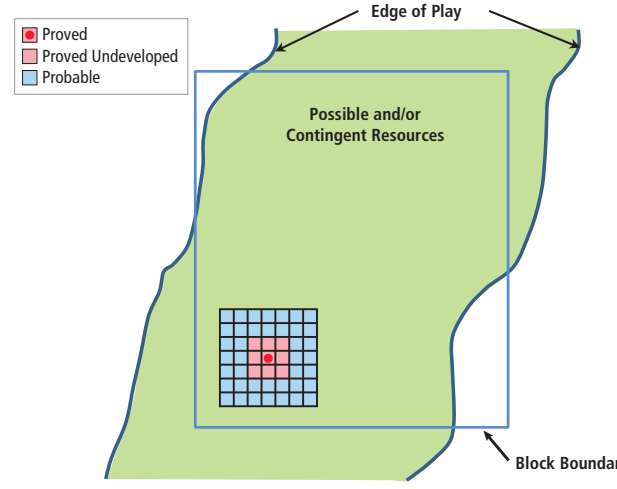

Fig. 13.10—Illustration of the concentric rings method (GCA).

or contingent resources and/or prospective resources, depending on what is known about the reservoir in other parts of the play. To do this, we are assuming that other appraisal wells exist with confirmation of the existence and potential commerciality of the play throughout the area within the block boundary.

This incremental approach to reserve assignment is typical of conventional onshore developments and has been adopted by many for unconventional assets as well. One fact that must not be overlooked is that for any location to which reserves are assigned, there should be a demonstrated commitment to drill a well. This is not an exercise in geometry, but one that takes account of what a company is actually planning to do.

The *Guidelines for Application of the Petroleum Resources Management System* provides the following advice:

> [Excerpted}…the large variability in individual well IPs [initial production rates] and EURs [Estimated Ultimate Recoveries] can make the assignment of PUDs problematic at distances beyond one development spacing unit from a producing well. In general, if there is consistency in the initial rates and estimated ultimate recoveries of producing wells, then it seems reasonable to assign PUDs at a distance of two or perhaps three development spacings from these wells as long as these PUD locations are bounded by other PDP wells." (Note that here also the emphasis is on interpolation.)
>
> In practice, it seems reasonable to assign Probable Reserves to 2 to 3 drilling locations beyond PUDs, and Possible Reserves to 2 to 3 drilling locations beyond the Probable Reserves area.

Using the higher recommended ranges for the offset spacings noted above, there would be a total of up to 225 locations that could be assigned reserves (proved, probable, or possible) based on just one existing well. In other words, we would be assigning reserves to 99.5% of an area based on data in 0.5% of the area. Depending on the overall amount of information available throughout the play, this might be rather optimistic.

13.5.3.1 Statistical Method

The challenge with the approach described previously is the simultaneous recognition that distance from the existing well control is typically not a determinant of the confidence that can be placed on the estimated production from future wells. Even though unconventional reservoirs may be considered regionally homogeneous, they are locally heterogeneous. For this reason, it may be appropriate to use statistical methods when a sufficient number of wells has been drilled. This approach is described in SPEE Monograph 3. It is not appropriate to attempt to duplicate a description of this sophisticated and analysis-heavy method here, but it may be summarized as follows:

1. Establish that it is a resource play. This means that it meets all of the Tier 1 criteria, and most, if not all, of the Tier 2 conditions.

2. Check the minimum number of wells needed to apply the method.

3. Identify analogous wells. Wells should all be within a common geological setting and be drilled and completed in a similar way.

4. Create a statistical distribution of analogous wells based on a suitable parameter such as EUR. It is a fundamental premise of the method that all wells form part of a common statistical distribution. This is essential because it is assumed that all future wells (that can be called proved) will also be part of the same distribution with the same mean, standard deviation, and distribution shape.

5. Determine the number of drilling opportunities or well count.

6. Prepare a Monte Carlo simulation. (A Monte Carlo simulation is a method to solve a problem by estimating the outcome probabilities with trial runs, termed "simulations," that use a random sampling of input variable probability distributions).

7. Calculate proved, probable, and possible reserves using appropriate definitions.

It should be pointed out that the SPEE Monograph 3 approach requires a large number of wells from a consistent geological environment with reliable forecasts of EUR before it can be applied. Because of that, there may be only a few situations in which this method might yield reliable results. The statistical basis for the methodology of the monograph is not rigorous but is considered to be "practical" by its authors.

13.5.3.2 Five-Year Rule

Another consideration for assigning reserves, especially for companies in the US that report to the SEC, is the five-year limit for future development activity. Although the SEC regulations provide the possibility for exceptions, generally, for proved reserves (at least), volumes should be limited to those wells (or other development projects) that are planned for implementation within the next five years from the date of the estimate. This constraint can be combined with the areal assessment described above to assign volumes to the various reserves categories. Wells that a company plans to drill beyond the five-year limit can be included in the probable or possible categories.

Note that the PRMS suggests five years as a guideline for considering projects to be included for reserves assessment, but that guidance is considered to be less stringent than the SEC's regulation.

13.5.3.3 How Do We Estimate and Incorporate Forecasts of Future Recovery?

One of the most challenging aspects of estimating reserves and resources for unconventional reservoirs is projecting future production. At present, production history for most shale plays is limited to just a few years. It is unlikely that boundary dominated (or influenced) flow has been reached. Extrapolating historical production behavior into the future, therefore, is subject to significant uncertainty. Nevertheless, we need to make such projections, and the main methods for accomplishing this are dealt with in detail in Chapter 14.

There are two types of forecasts needed. First, we need to project the recovery of already-producing wells. Second, we need to provide estimates for wells that are to be drilled in the future. The most common approach used for producing wells is decline curve analysis (DCA) based on fitting the Arps hyperbolic equation (Arps 1945) to historical data. Usually, because flow through the stimulated reservoir volume (mainly in the induced fractures) is largely linear, the hyperbolic exponent "b" is greater than one and often approaches two at early time. This is unsustainable in the long term (extrapolation would lead to infinite recovery); so many practitioners apply a terminal exponential decline rate.

There are numerous other curve-fitting approaches that have been proposed in the literature, each claiming to fit the data better than the simple Arps formula. Some are relatively straightforward, while others are complex and time-consuming. Additionally, software is available to provide analytical solutions to aid in production forecasting, and full 3D reservoir simulation is also a possible approach to evaluation of an unconventional reservoir. Regardless of the method used, the underlying assumptions about the unknown future performance of wells will have a significant impact on projected recovery and, therefore, estimates of reserves. All of this is discussed in detail in Chapter 14, but it is mentioned here because the reserve evaluator or auditor must be aware of the range of uncertainties.

For wells to be drilled in the future, it is common practice to construct type curves from existing wells that are considered analogous. There is a very large variation in production performance for wells in unconventional plays, even from ostensibly the same (or very similar) geological environments. Meaningful type curves can only be constructed with confidence when there are a significant number of wells with enough history to assess that a reasonable range of recoveries can be made.

Fig. 13.11 shows many wells' production, normalized in time, for one of the shale plays.

A note about analogs: most shale plays are geologically different. Therefore, it is not usually feasible to attempt to

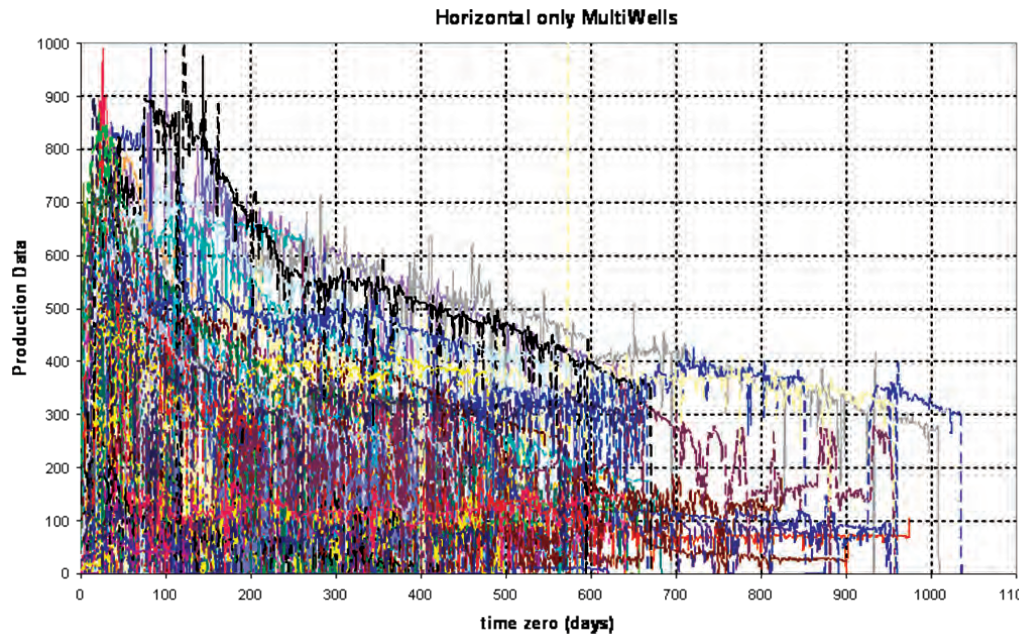

Fig. 13.11—Normalized well production—pick your type well!

use the performance of one shale play as a predictor for another. Each shale becomes its own analog, hence the need for a large number of wells.

When analysis has been carried out and projections have been prepared for current and future wells, the rendered values can be applied to the ongoing drilling program to derive forecasts for each reserves category.

13.5.3.4 Compliance with Requirements for Proved Reserves

When it is established that it is appropriate to book reserves (See Concepts of Rights, Risk, and Reward, earlier in this chapter), estimates of proved Reserves may be made that meet all of the confidence criteria set out in previous sections of this chapter. Some of the factors to keep in mind are as follows:

- Is there a defined development plan (the project or projects) on which the estimation of volumes is to be based?
- Are the projected recoveries appropriately conservative and reasonably certain of being recovered?
- Are the wells considered for proved undeveloped within a reasonable distance of established production? (See also the discussion above).
- Is there a firm commitment by the company (or companies) to carry out the program (drilling, facilities, etc.)?
- Are all approvals, including, if necessary, by the government or state, in place or reasonably certain of being obtained?
- If relevant, are sales contracts in place?
- Is the program limited according to the definitions for proved (i.e., five years for SEC and same as guidance for PRMS)? Note that appropriate (lower) levels of confidence regarding technical recovery may be applied to probable and possible reserves.

13.5.4 Potential Pitfalls or "Red Flag" Issues for Regulators

The following list is a selection of some of the issues that have been raised by the SEC in comment letters to companies in recent years. This information is all publicly available on EDGAR (the Electronic Data Gathering, Analysis and Retrieval system on the SEC website).

- Use the SEC definitions, not the PRMS definitions.
- Explain reporting proved reserves for activities to take place after five years.
- Remove PUD reserves for activities that have been reported for more than five years, but not implemented.

13.6 Closing Remarks

The proper estimation and reporting of all classes of resources (reserves, contingent resources, and prospective resources) is critical to the efficient management of an oil and gas company, to banks and other lending institutions, to securities regulators and to national oil companies, and to ministries and governments. A thorough understanding of the relevant definitions and guidelines is essential for all those who prepare, audit, or use these estimates.

While many companies and organizations are relatively comfortable with assessments of conventional reservoirs, there are unique challenges in the correct application to unconventional reservoirs. The industry is still learning how to understand the reservoirs in order to optimize recovery and reduce costs.

This chapter has provided a high-level discussion of the key factors that need to be considered in such evaluations, but it is important to keep an open mind as we all learn more about these hydrocarbon accumulations that are expected to provide the world with oil and gas for decades to come.

13.7 References

Arps, J.J. 1945. Analysis of Decline Curves. Paper SPE 945228-G. In *Petroleum Development and Technology*: **160** (1): 228–247. New York: In Transaction of the American Institute of Mining and Metallurgical Engineers, AIME. http://dx.doi.org/10.2118/945228-G.

Elliott, D.C. 2008. The Evaluation, Classification, and Reporting of Unconventional Resources. Paper SPE 114160 presented at the SPE Unconventional Resources Conference. Keystone, Colorado. 10–12 February. http://dx.doi.org/10.2118/114160-MS.

Guidelines for Application of the Petroleum Resources Management System, sponsored by the Society of Petroleum Engineers, American Association of Petroleum Geologists, World Petroleum Council, Society of Petroleum Evaluation Engineers, and Society of Exploration Geophysicists, November 2011. http://www.spe.org/industry/docs/PRMS_Guidelines_Nov2011.pdf (accessed June 2014).

Guidelines for the Practical Evaluation of Undeveloped Reserves in Resource Plays, Society of Petroleum Evaluation Engineers, SPEE Monograph 3, December 2010.

Johnston, D. 2003. ***International Exploration Economics, Risk, and Contract Analysis***. Pennwell Books.

Petroleum Resources Management System, 2007, Society of Petroleum Engineers, American Association of Petroleum Geologists (AAPG), World Petroleum Council (WPC), Society of Petroleum Evaluation Engineers (SPEE), http://www.spe.org/industry/docs/Petroleum_Resources_Management_System_2007.pdf (accessed June 2014).

Rhein Petroleum. 2012. Planned 3D Seismic Surveys (Geplante 3D seismische Vermessungen), Weinheim, Germany. July 2012. http://publish.cmcitymedia.de/news/getFile

Securities and Exchange Commission, Modernization of Oil and Gas Reporting Part 2, 2009, effective January 2010, *Federal Register* (**74, No. 9**), 2158–2197 http://www.sec.gov/rules/final/2009/33-8995fr.pdf (accessed June 2014).

Standards Pertaining to the Estimating and Auditing of Oil and Gas Reserves Information Approved by SPE Board in June 2001, revision as of February 19, 2007, Society of Petroleum Engineers. http://www.spe.org/industry/docs/Reserves_Audit_Standards_2007.pdf (accessed June 2014).

United Nations Framework Classification for Fossil Energy and Mineral Resources, 2009, http://www.unece.org/energy/se/reserves.html (accessed June 2014).

Young, E.D. 2012. Reporting Reserves under Modern Fiscal Agreements. Paper SPE 162708 presented at the SPE Hydrocarbon, Economics and Evaluation Symposium. Calgary, Alberta, Canada. 24–25 September. http://dx.doi.org/10.2118/162708-MS.

This page intentionally left blank

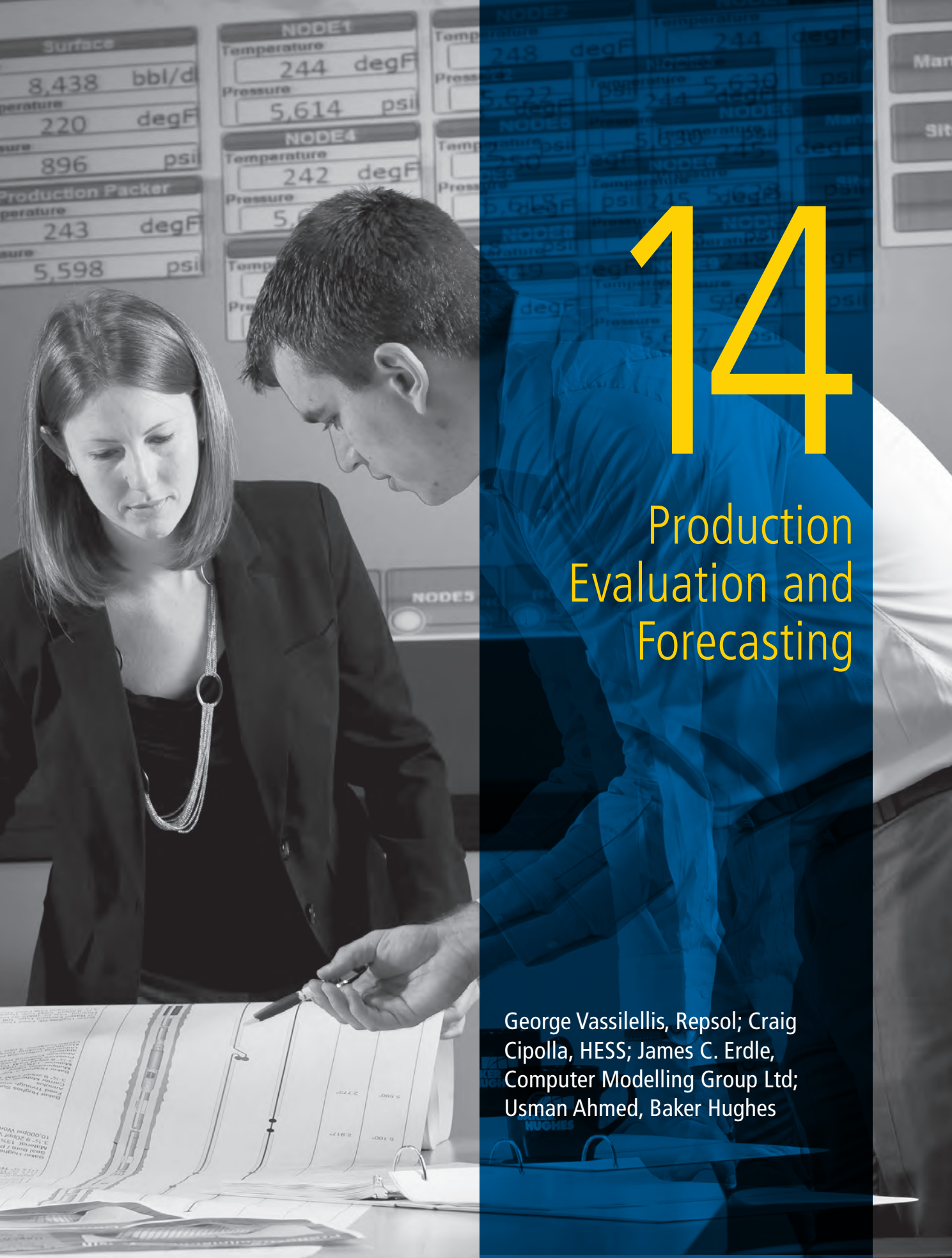

14

Production Evaluation and Forecasting

George Vassilellis, Repsol; Craig Cipolla, HESS; James C. Erdle, Computer Modelling Group Ltd; Usman Ahmed, Baker Hughes

This page intentionally left blank

Chapter 14:
Production Evaluation and Forecasting

14.1 Introduction

This chapter focuses on production evaluation and forecasting well performance in unconventional reservoirs. Evaluating well performance in unconventional reservoirs provides key data to optimize the number of fracture treatment stages, fracture treatment design, and well spacing. In most cases, early time production behavior (e.g., 6- to 12-months) is analyzed to estimate hydraulic fracture length, fracture conductivity, and reservoir permeability. In contrast to reserves accounting (Chapter 13), production forecasting focuses on improving completions and well spacing. Thus, it is necessary to model how changes in completion strategy, well spacing, and placement affect reservoir performance. In this chapter we make use of both analytical and numerical models to facilitate the discussion and explanations.

Economic viability of unconventional resources hinges on effective stimulation of extremely low permeability rock, typically in the 10- to 1000-nanodarcy (10-6 md) range. Many conventional hydraulic fracture treatments use high-viscosity fluids and relatively high proppant concentrations to maximize propped fracture width and permeability. The use of low-viscosity fluids (slick water) and relatively low sand concentrations for low-permeability reservoirs was popularized after work by Union Pacific Resources in the 1990s such as the work by Mayerhofer and others in 1997 (Mayerhofer et al. 1997). This groundbreaking paper led to the widespread use of such slick water fractures and the commercialization of unconventional reservoirs in the Barnett. Following observations of microseismicity that showed numerous microseismic events in approximately linear trends other than what would have been assumed based on conventional models, the concept of fracture complexity was coined (**Fig. 14.1**). Among the many potential reasons that slick water hydraulic fracturing may work, it is possible that this complexity is promoted by the use of thin fluids. As the development of unconventional resources has expanded, fracture treatment designs and completion strategies have been tailored to specific reservoir and rock properties, which yield a much more diverse mixture of conventional and unconventional approaches to completion optimization. Hybrid jobs starting with slick water and converting to conventional polymer loads and proppant concentrations are common in many plays and reverse hybrid jobs are also used. Improvements in production evaluation and forecasting techniques have contributed significantly to our understanding of the relationship between fracture treatment design, completion strategy, and well performance.

Examination of the rocks that constitute typical unconventional reservoirs by scanning electron microscopes reveals porosity networks that are two orders of magnitude smaller than typical tight reservoirs with pores measuring in nanometers rather than microns. Early reservoir engineering researchers like Klinkenberg (1941) and others showed that Darcy's law must be modified when molecular forces, Brownian motion, and diffusion skew the proportional relation between pressure differential and flow rate. Gas desorbed into organic matter may be released at lower pressures. Although hydrocarbons will be produced in shale wells mostly by pressure depletion, as in conventional reservoirs, physical mechanisms involved are more complex than those of conventional reservoirs.

The process of hydraulic fracturing is complex and approximate. Knowledge about fracture geometry is difficult to obtain, and the physics of fracturing is more complex than early models. Hydraulic fracture geometry estimates from fracture models have been difficult to verify. Numerous diagnostic techniques have been developed to improve our understanding of hydraulic fracturing in this area , including fracture modeling, rate transient analysis (RTA), pressure transient analysis (PTA), and numerical simulation techniques. These techniques are widely used because the required data are readily available. These approaches can provide estimates of fracture dimensions, effective fracture length, and fracture conductivity, based on indirect measurements such as the pressure response during the propped fracture treatment or the pressure and flow rate during production. By making assumptions about the physical processes that are involved, the observed net pressure or production and pressure responses can be matched using reservoir and/or fracture models, which provides an estimate of fracture dimensions, fracture conductivity and effective fracture length. Available models range from analytical solutions to complex numerical simulators (Cipolla et al. 2009).

Microseismic (MS) mapping has significantly improved our understanding of hydraulic fracture growth in unconventional reservoirs, leading to better stimulation designs. Hydraulic fracture growth in many unconventional reservoirs is complex and difficult to predict. Fig. 14.1 shows an MS event pattern for a Barnett shale water-fracture stimulation treatment, illustrating the complex fracture networks typical in many unconventional gas reservoirs

(Fisher et al. 2002). The dots represent microseismic events and show spatial locations where fractured shear slippage in the reservoir has taken place. They DO NOT necessarily represent where hydraulic fracture fluid has gone. The MS events in Fig. 14.1 are certain to include previously closed natural fractures that slipped in shear as a result of the strain created from hydraulic fractures. Shear slippage creates more MS energy than does Mode I tensile failure. The authors point out "possible aligned fractures;" however, this is completely speculative and many lines that were drawn in their figures are unlikely to be fluid-filled fractures. It is necessary to assume complex fracture growth to explain these linear features. There is an excellent likelihood that they are slippage events that do not contain injected fracture fluid. The fracture network in Fig. 14.1 depicts a large area that covers about 75 acres and connects millions of square feet of reservoir surface area to the wellbore. Without this "picture" of the fracture, we may never have appreciated the extreme complexity of fracture connections in the Barnett shale. Hydraulic fracture growth may not always be complex in unconventional reservoirs. Planar hydraulic fractures may be dominant in some plays and there will be a mixture of planar and complex fracturing in a given horizontal well completion as shown in **Fig 14.2**.

New hydraulic fracture models are being developed to simulate these complex networks of created fractures and shear slippage to help improve stimulation designs. Occasionally, larger and more complex MS event patterns have been shown to correlate positively to production (Mayerhofer et al. 2008). Flow capacity or conductivity of the fracture network also affects gas recovery. Integrating fracture diagnostic technologies and hydraulic fracture modeling is an important component of production evaluation and forecasting workflows, providing constraints on hydraulic fracture geometry and fracture complexity.

14.2 Production Forecasting

It is not possible to uniquely determine hydraulic fracture length, fracture conductivity, and reservoir permeability using production data alone. Unlike conventional reservoirs where matrix permeability can be easily measured in the laboratory (core) and in the field (pressure buildup test or PBU), it is very difficult to obtain reliable, representative measure matrix permeability in unconventional reservoirs.

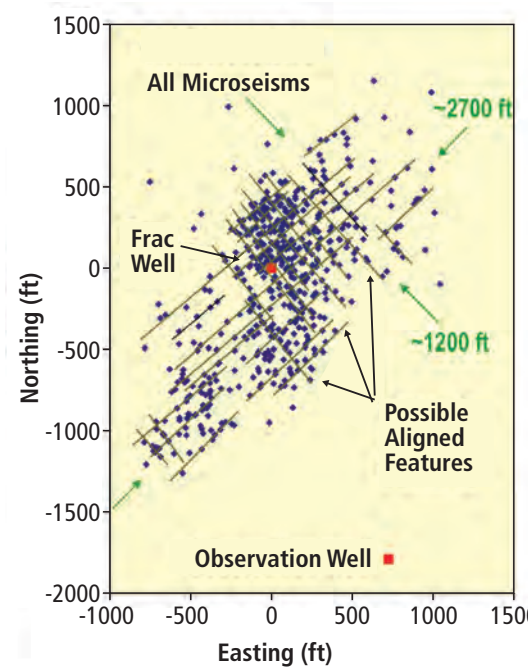

Fig. 14.1—MS event pattern for a typical Barnett shale water-fracture, vertical well. (After Fisher et al. 2002.)

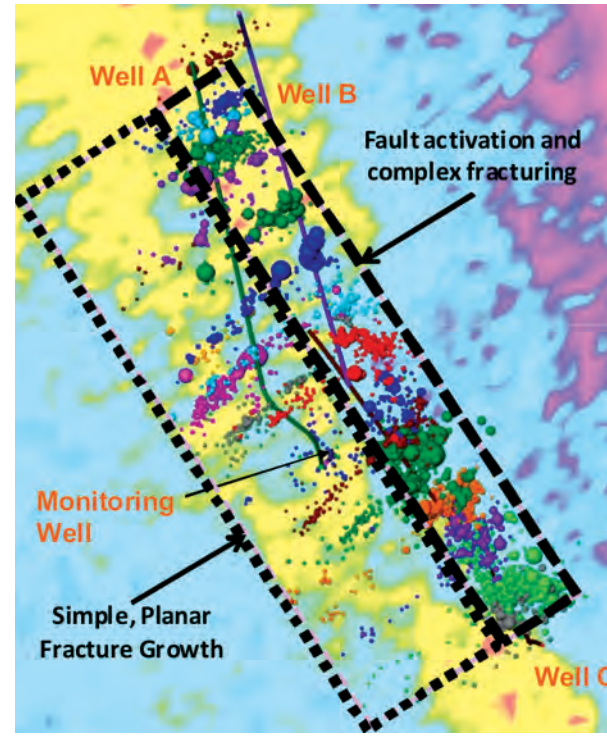

Fig. 14.2—Microseismicity recorded during multiple stages of three wells, and Poisson's ratio contours (hot colors are low values). (From Maxwell and Cipolla 2011.)

14.2.1 Hydraulic Fracture Design and Well Spacing

Completion optimization in tight gas reservoirs developed using vertical wells is relatively straightforward, focusing on selecting the optimum hydraulic fracture length (and proppant type) and evaluating if hydraulic fracturing actually provides sufficient economic benefit. The most complex part of this optimization process is reservoir characterization, i.e., understanding vertical and spatial variation in permeability. The most critical parameter to optimize is well spacing because the largest component of capital expenditure for onshore fields is well cost. Many simplistic optimization approaches focus on optimizing stage spacing and fracture design. In unconventional reservoirs where horizontal wells with multiple hydraulic fractures are required for economic development, the completion optimization process is more complex. The number of reservoir variables is so large that field trials to optimize independent values are not practical. Machine learning approaches may be required. Additionally, optimized well spacing, well length, and fracture design is likely to vary by area.

Due to complexities associated with multiple-fractured horizontal well completions, significant reservoir heterogeneity, and large variability of well performance in most unconventional reservoirs, completion optimization requires a combination of empirical field-trials and model-based production forecasting to select the appropriate fracture treatment design and completion strategy.

14.3 Conventional Techniques for Characterizing Fracture Geometry

This section summarizes the strengths, weaknesses, and limitations of fracture modeling, RTA, PTA, and numerical reservoir modeling.

14.3.1 Fracture Modeling

Fracture modeling with net pressure analysis can provide information about fracture dimensions and conductivity. These values can be estimated by using fracture modeling software to match observed net pressures (fracturing pressure across from the perforation, minus minimum rock stress). This technique typically provides non-unique solutions, but can be unreliable if not calibrated, and requires baseline rock and stress data. Fracture geometry also changes with net pressure. **Fig. 14.3** shows two modeling solutions for the same treatment if 500 psi stress contrast exists around the pay zone. This observation from net

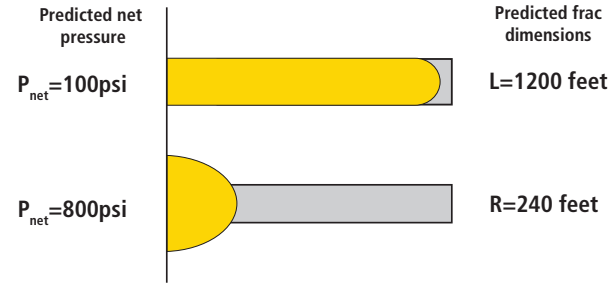

Fig. 14.3—Two modeling solutions for the same treatment if 500 psi stress contrast exists around pay zone. (From Cipolla 2008.a.)

pressure analysis predicts that stress barriers can effectively contain fracture height growth. Such models typically predict thick shales to be such barriers.

Net pressure history matching can be implemented by adding more sophisticated rock physics to fracture models. However, inferred geometry from net pressure matching does not always agree with directly measured geometry. Fracture geometry is inferred from net pressure and leakoff behavior is non-unique, requiring careful and consistent interpretation for useful results. Fracture modeling is most useful when results are integrated or calibrated with results of other diagnostics, production data and well test analysis and direct fracture diagnostics. Details can be found in the discussion of shale models by Meyer et al. (2010).

The benefits of real data fracture treatment analysis can be enormous. This approach has been shown to reduce screen-out risks, improve production economics, and improve fracture conductivity. In addition, measurement of real data is relatively simple and cheap. The right analysis assumptions and a consistent approach can lead to useful and reasonable answers, but the geometry requires calibration with direct measurements.

14.3.2 Pressure Transient Analysis

Pressure transient analysis (PTA) is an effective technique for evaluating stimulation effectiveness in low-permeability hydraulically fractured wells by providing an estimate of fracture half-length and fracture conductivity. Knowledge of reservoir permeability, either from a pre-fracture well test or from an independent source (Rushing and Blasingame 2003) is usually required to compute fracture properties. If a well is shut-in for a sufficient time to reach the pseudo-radial-flow period, reservoir permeability can be determined from a post-fracture pressure buildup test (PBU). Unfortunately, wells completed in tight formations usually require very

long shut-in times (months to years) to reach pseudo-radial flow and build-up responses can be distorted in early time by wellbore storage and in late time by interference (Economides et al. 2006). Most operators are reluctant to shut-in a well for the time required to reach pseudo-radial flow. (Rushing and Blasingame 2003).

As an application of well test data, dimensionless fracture conductivity (the ratio of fracture conductivity to reservoir permeability) can be measured using a post-fracture PBU and is defined using **Eq. 14.1**.

$$F_{cD} = \frac{k_f w_f}{X_f k} \qquad (\textbf{Eq. 14.1})$$

In general, an F_{cD} greater than 300 results in theoretical behavior indistinguishable from that of an infinite conductivity fracture (Cinco-Ley and Samaniego-V 1981). An F_{cD} of 30^{+} is often considered sufficient for most fracturing applications. The shape of the post-fracture PBU will normally allow an easy identification of the approximate magnitude of F_{cD}. The most significant limitation of post-fracture well test estimates of fracture length is uncertainty in reservoir permeability and pressure. If these parameters are not known prior to the post-fracture test, the analysis can be non-unique and unreliable. **Fig. 14.4, Fig. 14.5,** and **Fig. 14.6** show log-log diagnostic plots of the pressure buildup behavior for a generic non-fractured well and the same well with a low and high conductivity fracture (of the same length). The presence of linear flow is typical of a highly conductive fracture (relative to the reservoir), while bilinear flow indicates a less conductive fracture. Actual field data may exhibit more complex behavior than the idealized data shown, but much of this complex behavior can be adequately matched using conventional PTA.

14.3.3 Rate Transient Analysis

RTA can be used to estimate reservoir quality (kh), completion effectiveness (fracture conductivity and length), hydrocarbons-in-place and ultimate recovery. Conventional type curve analysis of production data is a viable alternative for evaluating well performance without shutting in the well (Rushing and Blasingame 2003). Like PTA, RTA cannot obtain unique estimates of fracture half-length. Rushing and Blasingame (2003) compared post-fracture performance of 22 wells producing from the Bossier tight gas sand and observed good agreement with effective fracture half-lengths computed from RTA and pressure transient analysis (PTA) methods. According to these authors, most differences in

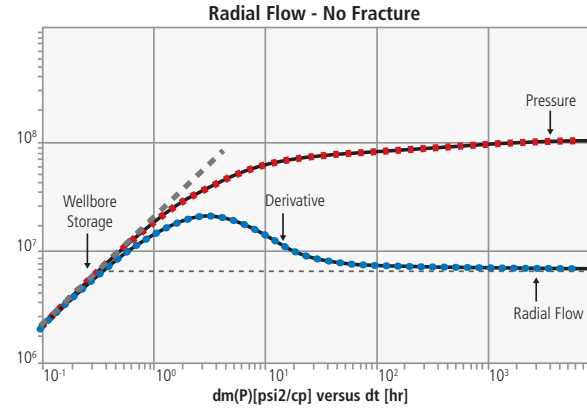

Fig. 14.4—Example of pre-fracture PBU.

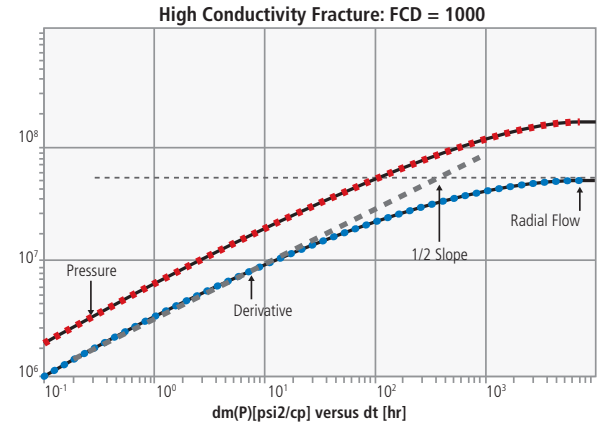

Fig. 14.5—Example of post-fracture PBU high conductivity fracture.

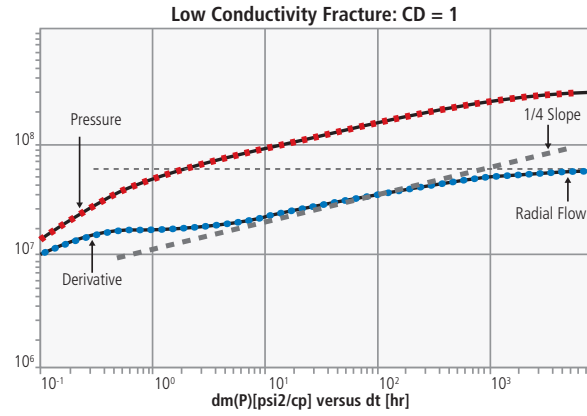

Fig. 14.6—Example of post-fracture PBU, low conductivity fracture.

estimated fracture half-lengths can be attributed to wells with low or conductivity fractures. Some type curves were developed for an infinite-conductivity vertical fracture, so they may not be appropriate for wells with very low

fracture conductivities (Rushing and Blasingame 2003). A critical element in the successful application of the decline type curve methodology is the frequency and quality of the well production data. (Rushing and Blasingame 2003). The authors had the most success with well performance evaluations when accurate daily production data, including well flowing pressures, are used.

Mattar and Anderson (2003) presented a paper highlighting the strengths and limitations of the methods used for analyzing production data. Blasingame method (Blasingame et al. 1991) and Agarwal–Gardner (Agarwal et al. 1998) are similar to Fetkovich's traditional method (1980) in that they use type-curves. The primary difference is that the modern methods incorporate the flowing pressure data along with production rates and they use analytical solutions to calculate hydrocarbon-in-place (Al-Reshedan et al. 2009). The main weaknesses of these approaches are the assumption of a simple geologic model (i.e., single layer or dry gas) and the quality of the production data (which is usually noisy, especially rate and the pressure derivative). Rushing et al. (2005) concluded that the major problems with production data generally are poor data quality, incomplete or infrequent data sampling, and/or erroneous data.

In practice, RTA data rarely approach the quality, quantity, or accuracy of data obtained during a pressure transient test. The challenge of analyzing production data remains that of understanding what information the data may convey. For example, we should not expect to be able to estimate permeability and skin factor with confidence using monthly production rates and pressures from a well in a moderate- to high-permeability reservoir. These data simply lack the detail to provide a competent analysis. In contrast, monthly production and flowing bottomhole pressure data may be sufficient for wells in low-permeability reservoirs where the transient state may be maintained for months or even years.

14.3.3.1 Rate Transient Analysis (RTA) in Unconventional Reservoirs

Building on the stimulated reservoir volume (SRV) concept proposed by Mayerhofer and others (2008), RTA and linear flow analysis techniques have been developed that approximate complex fracture networks using a region of enhanced permeability around a planar hydraulic fracture. Such techniques are useful for production forecasting, decline curve development, and reserve estimates. However, the estimates of fracture half-length and reservoir permeability from RTA is not unique and may not be appropriate for completion optimization and well spacing for several reasons.

The "apparent" system permeability (k_{srv}) may not provide sufficient detail to predict the effect of changes in treatment design or stage spacing, as different completion strategies may change the system behavior, resulting in a different k_{srv}. Additionally, the "effective" fracture half-length from RTA may not properly describe the actual drainage architecture. In a simplistic case where hydraulic fractures are evenly spaced in a horizontal well and the properties of the SRV are constant, the k_{srv} can be determined by identifying the time to end of linear flow (t_{EL}). **Fig. 14.7** illustrates the RTA graphical analysis and equations used to calculate k_{srv} and fracture half-length (x_f) (Ye et al. 2013). The slope, m_{CRL}, is inversely proportional to well productivity and provides a means to calculate $x_f\sqrt{k}$.

The critical element of this analysis is the assumption that the deviation from the initial straight-line behavior in Fig. 14.7 represents the uniform interaction of all the hydraulic fractures. For a given distance between hydraulic fractures, as k_{srv} increases, the t_{EL} decreases. The non-uniqueness in fracture half-length and permeability is problematic in unconventional reservoirs where completions consist of horizontal wells with multiple, closely spaced, different length hydraulic fractures. Lateral lengths of 5,000 to 10,000 ft. are typical, with 15 to 40 hydraulic fracture treatments with multiple perforation clusters in each stage. Reservoir heterogeneity is common in unconventional reservoirs and productivity can vary significantly along laterals (Baihly et al. 2010, Miller et al. 2011). The more actual conditions deviate from assumptions inherent in the RTA theory, the greater the uncertainty in the results. For example, Fig. 14.9 shows the RTA results for a 10-stage completion in a very low-permeability reservoir (75 nd) with a natural fracture corridor modeled using a thin high-permeability strip (90 ft. wide, 0.02 md). The apparent end of linear flow (t_{EL}) is dictated by the size and properties of the fracture corridor and dominates the early-time RTA behavior. The "apparent" k_{srv} is 0.0066 md and the "effective" fracture half-length is 105 ft. The model fracture half-length was 500 ft., with the majority of the reservoir at 75 nd. RTA fracture half-length is about 20% of the modeled length and k_{srv} is almost two orders of magnitude higher than the input matrix permeability. In this case, using the results from RTA to optimize completions and make well spacing decisions could lead to inaccurate decisions. Without production logs, the likelihood for error when interpreting these models increases.

14.4 Numerical Reservoir Modeling

Reservoir simulation history matching has proved to be useful for determining effective fracture length. Uniqueness problems common to simulator history matching are minimized when

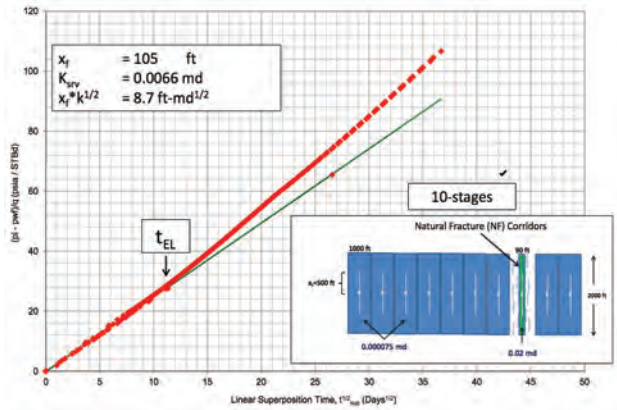

Fig. 14.7—Effect of reservoir heterogeneity on RTA results.

trying to match test data obtained on the well and the long-term production history of the well. Numerical reservoir modeling is an excellent technique for handling simultaneous effects of fracture conductivity, reservoir boundaries, multiphase and non-Darcy flow effects, and complex reservoir systems. **Fig. 14.8** illustrates a numerical model for hydraulic fracture. The model can account for multiphase flow from fractured intervals, multiple zones with different permeabilities, pressures, fracture lengths and conductivities, vertical and horizontal well, multiple fractures, non-Darcy flow, and fracture fluid cleanup.

RTA and PTA methods do not account for varying inflow along the wellbore. Most production logs in unconventional wells show high variations in flow along the wellbore. Some data suggests that 40% of the perforations show negligible inflow (Hart's E & P report 2012, Vincent 2010). RTA and PTA do not predict this; however, simulation models can. Uniform models of reservoir permeability will not predict the actual inflow in heterogeneous systems. Production logs are powerful tools for improving reservoir models.

14.5 Stimulated Reservoir Volume, Microseismic Data, and Production Evaluation and Forecasting

The interpretation of microseismic data was initially focused on hydraulic fracture length and height, which provides an important measurement to calibrate planar fracture propagation models (Mayerhofer et al. 2005, Warpinski et al. 1998 and 2009, King 2010). However, microseismic data in the Barnett shale exhibited significantly more complex patterns compared to typical tight-gas sands (Fisher et al. 2002). The concept of stimulated reservoir volume (SRV) is widely used when discussing well performance and

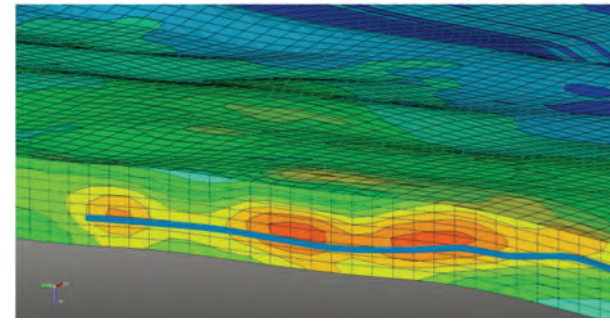

Fig. 14.8—A numerical model for hydraulic fracture.

stimulation effectiveness in unconventional reservoirs. This conceptually was developed to provide a semiquantitative measure of stimulation effectiveness in the Barnett shale based on the size of the microseismic "cloud." However, SRV and similar techniques provide little insight into two critical parameters: hydraulic fracture area and conductivity. Each of these can vary significantly based on geologic conditions and fracture treatment design. The simplifying assumptions in many SRV-based rate transient models may lead to estimates of hydraulic fracture length and reservoir permeability that are not well suited for completion optimization. Completion optimization will require a more holistic approach to the application of microseismic measurements and RTA, and one that includes mass balance and fracture mechanics.

14.5.1 Microseismic, Rate Transient Analysis, and Stimulated Reservoir Volume: A Historical Perspective

The concept of SRV was first introduced by Fisher et al. in 2004 and presented as a means to correlate microseismic images to well performance in the Barnett shale. Hydraulic fracture models applicable to these complex environments did not exist, so previous applications of microseismic images for fracture model calibration were impossible. Thus, SRV was used as a proxy for fracture geometry and the area of enhanced permeability near created fractures.

SRV concepts, as applied to RTA, can provide estimates of drainage volume and EUR (Kabir et al. 2010). However, the relationship between SRV and hydraulic fracture geometry is not understood, as microseismic measurements capture only a small portion of the overall deformation (Maxwell and Cipolla 2011, Warpinski et al. 2012). Additionally, well performance is dictated by many well and reservoir variables (Cipolla et al. 2008, Mayerhofer et al. 2008). While microseismic images can provide an estimate of fracture height, length, and location, microseismic images cannot provide details of the hydraulic fracture

structure, total fracture area, and location of proppant (Cipolla et al. 2011b and 2012). This critical issue is often overlooked when interpreting microseismic images and the subsequent application of microseismic data in production modeling workflows. These issues are further complicated by the proliferation of horizontal wells with multistage completions.

There have been attempts to use microseismic data alone to guide reservoir simulation (Williams-Stroud 2008, Du et al. 2009 and 2010, Detring and Williams-Stroud 2012) using a dual porosity/dual permeability approach within the SRV to approximate the hydraulic fracture network or simply by assuming a region of enhanced permeability in the SRV (k_{srv}). Other approaches include modeling planar hydraulic fractures with half-lengths calibrated to the microseismic data and then adding regions of enhanced permeability or dual porosity/dual permeability around the planar fractures to approximate the fracture network (with dimensions guided by the SRV) (Cipolla et al. 2009). Some approaches attempt to extract the hydraulic fracture geometry directly from the microseismic data or to determine permeability enhancement using the density and strength (i.e., magnitude) of the microseismic events. While these approaches may be useful for production forecasting, type curve development, and reserve estimations, they are less well-suited for completion optimization and well spacing evaluations. SRV-based evaluations of well performance cannot be used to evaluate changes in completion strategies or fracture treatment designs.

Potential misapplications of SRV and rate transient analysis (RTA), as they relate to completion optimization and well spacing, include three primary misconceptions:

1. Hydraulic fracturing does not create permeability, but it results in greater connectivity between the wellbore and the reservoir. Terms such as "shatter" and "rubbelize" are inapplicable when describing hydraulic fracturing in unconventional reservoirs. Characterizing fracture area and fracture conductivity should be the focus of fracture modeling and microseismic interpretation.

2. Evaluating effect of changes in fracture treatment design and stage spacing on well performance requires integrating hydraulic fracture geometry and the distribution of fracture conductivity with production modeling. Without a direct link between fracture modeling and reservoir simulation, production optimization remains a trial-and-error process. Given the limitations of current microseismic interpretation techniques, characterizing the hydraulic fracture geometry and conductivity using microseismic data (SRV) is impossible.

3. RTA techniques that utilize SRV concepts may result in estimates of permeability and/or fracture length that are inappropriate for use in completion optimization and well spacing evaluation. As fracture treatment designs and stage spacing change, it is likely that the overall system behavior including k_{srv} will change. RTA results may not adequately describe the complexity of the fracture geometry and fluid flow.

14.5.2 Microseismic, Network Fracture Modeling, and Reservoir Simulation

Hydraulic fracture modeling has been problematic in unconventional reservoirs because of the absence of fracture propagation models suited for these complex environments. With recent advances in fracture modeling (Rogers et al. 2010, Weng et al. 2011, Meyer and Bazan 2011, Kresse et al. 2012), it is possible to model network fracture propagation and predict the interactions of the hydraulic fractures with natural fractures in a given stress regime. More advanced network models can estimate stress-shadowing effects between network fractures (i.e., within a given network fracture and between stages in a horizontal well). Such models require estimates of intermediate horizontal stress (σH), not just the minimum stress (σh), as stress bias ($\Delta\sigma$) affects network fracture growth. A description of background natural fractures is also required, typically modeled by a discrete fracture network (DFN). Advanced network models require an approximation of the mechanical properties of the DFN. Network fracture models can be calibrated using microseismic images (Cipolla et al. 2011a). The integration of these complex network fracture geometries with numerical reservoir simulation requires efficient automated gridding routines that can replicate the fracture geometry and distribution of conductivity (Cipolla et al. 2011).

14.6 Completion Optimization and RTA in Unconventional Reservoirs

In this section, two examples are provided to illustrate issues and challenges encountered when applying RTA data and microseismic images to optimize completion in unconventional reservoirs. **Fig. 14.9** illustrates the basic workflow for integrating complex hydraulic fracture models with microseismic images in a numerical reservoir simulation to estimate fracture geometry and complexity.

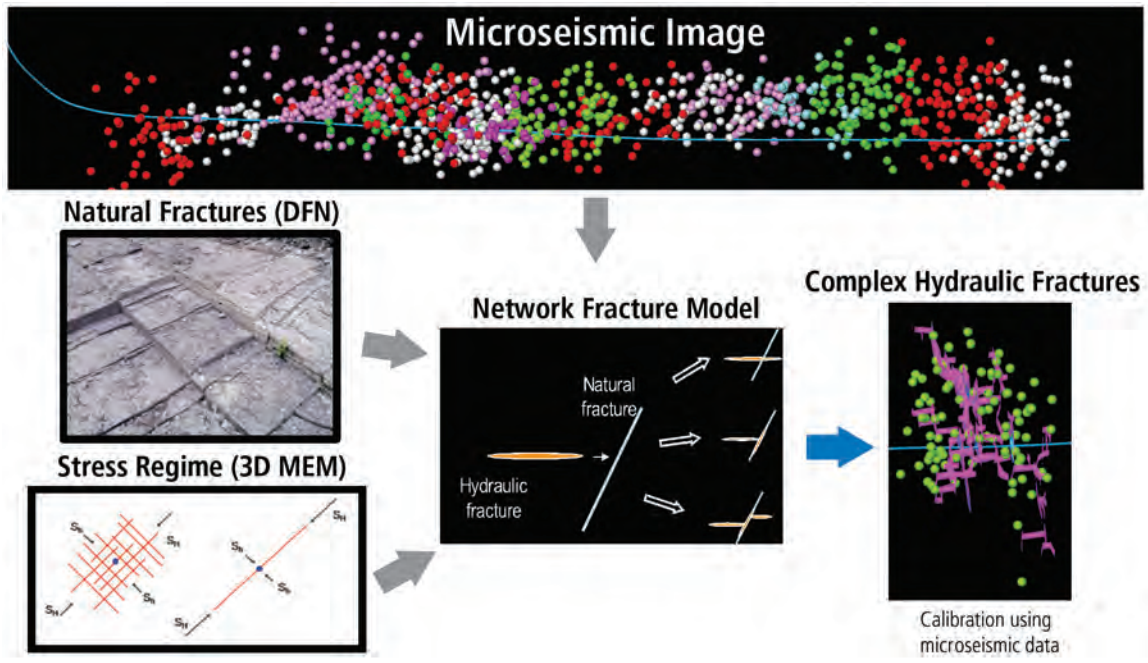

Fig. 14.9—Integration of complex hydraulic fracture modeling and microseismic images.

14.6.1 Shale Gas Example

The first example to evaluate completion performance is a shale gas well with 500 days of production data. This well was completed using a cased and cemented lateral (~4,500 ft.), 15 fracture treatment stages, and four perforation clusters per stage (limited entry design). A total of 109,000 bbl of fluid and 4.4 million lbs of proppant were pumped at 70 bpm using a hybrid treatment design. Proppant stages consisted of 100-mesh sand (12%), 30/50 ceramic proppant (75%), and 20/40 (13%) ceramic proppant with a maximum proppant concentration of 3 ppg. The pad volume was 20% of the treatment volume. **Table 14.1** provides reservoir properties used in this example.

Both planar and network fracture geometries were modeled and the history was matched. Several natural fracture scenarios or DFNs for a 15-stage completion as presented in **Table 14.2** were evaluated and compared to the microseismic image assuming un-propped fractures contributed to production. A case of planar fracture geometry and two cases of DFNs with orthogonal natural fractures spaced 50 ft. and 75 ft. apart were evaluated. A case is also presented assuming that un-propped fractures did not contribute to production (UPC~0) for the 50 ft. DFN case (**Fig. 14.10**). The network fracture geometries were consistent with the microseismic image with a fluid efficiency of about 75%. To achieve a planar fracture geometry consistent with the microseismic image required an unrealistic fluid efficiency (~40%), but is included for comparison.

Table 14.1—Shale gas example, reservoir properties.

P_i	7650	psi
ø	4.7	%
Gas GR =	0.65	
h =	132	ft
T_r	180	°F

As shown in Table 14.2, the complex fracture modeling indicated about 30 million square feet of fracture area, but only 8.4 (28%) million square feet are propped. The complex fracture geometry and distribution of fracture conductivity, both propped and un-propped regions of the hydraulic fracture were represented in a numerical reservoir simulation model. Fig. 14.10 shows the reservoir simulation grid for 50-ft. DFN case (Fig. 14.10) geometry, representing the details of the complex hydraulic fracture and maintaining the fidelity between the fracture model and reservoir simulation model.

Geomechanical effects of increasing closure stress on both propped and un-propped fracture conductivity were modeled in the reservoir simulator using compaction tables. **Fig. 14.11** shows the reservoir simulation history matches

and production forecasts for the four cases evaluated. Acceptable matches of the actual production history were achieved for all four cases by varying matrix permeability. If the un-propped fractures contribute to production, matrix permeability ranged from 20 nd to 32 nd, but if the un-propped fracture did not contribute to production (UPC~0 case), then a much higher matrix permeability of 270 nd was required to match production history. This emphasizes the importance of constraining matrix permeability. Forecasted production was the highest for the planar fractures due to somewhat longer fracture lengths and a larger drainage area. This emphasizes that fracture length has a significant effect on drainage area in unconventional reservoirs.

The impact of stage spacing and fracture complexity on well performance was evaluated by comparing the production forecasts for an 8-stage completion to that of a 15-stage completion. The fracture geometries for an 8-stage completion were modeled, both planar and complex fracture, using the same treatment design and completion strategy as the 15-stage completion. However the perforation clusters were twice as far apart in the 8-stage completion. **Fig. 14.12** compares the 1-year and 10-year gas recovery for an 8-stage and 15-stage completion, illustrating the important of properly characterizing fracture complexity when optimizing stage spacing. Although the 15-stage completion utilizes almost twice the fluid and proppant (1.875 times to be exact), the 1-year production is increased by only 18% when fracture complexity is high (50 ft. DFN) and the 10-year production is essentially the same offset. However, the production forecast for the case of planar fractures shows a 69% increase in 1-year gas recovery, much more consistent with conventional expectations for nanodarcy reservoirs. The significant difference between the complex and planar fracture cases is due to the significant overlap of fracture geometry when complexity is high. Although stage spacing is an economic optimization, it is clear that fracture complexity will play a significant role in completion optimization.

14.6.1.1 Rate Transient and Linear Flow Analyses in Unconventional Reservoirs

Rate transient analysis (RTA) and linear flow analysis (LFA) are often used to estimate the average effective hydraulic fracture length and system permeability (k_{srv}) for wells completed using multistage fracture treatments. As discussed previously, results from these SRV-based reservoir engineering models may not be well suited for completion optimization. To illustrate this issue, and using the same shale gas example, production forecasts for the complex

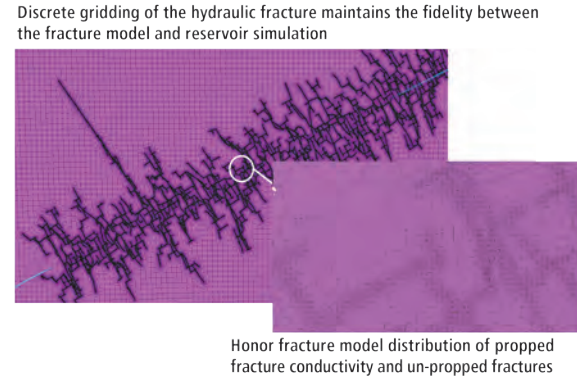

Fig. 14.10—Reservoir simulation grid for complex hydraulic fracture, 50 ft. DFN.

fracture cases were analyzed using commercial RTA software packages to estimate fracture half-length and system permeability (k_{srv}). The results are summarized in **Table 14.2**, illustrating that RTA and LFA results often indicate fracture half-lengths that are much radically shorter than the actual lengths (actual fracture lengths from the complex fracture model were quite variable from stage to stage, but the average was about 400-500 ft). The permeability from the RTA and LFA is a composite of the matrix permeability and complex hydraulic fracture network, which is much higher than the matrix permeability. Reviewing the RTA and LFA (sqrt-of-time analysis) results shows that permeability changes as stage spacing changes. RTA can also be very non-unique, as illustrated in **Fig. 14.13**, which is an alternate match of the 50-ft. DFN case (15-stages) using a different commercial RTA software package and different RTA model. The alternate match indicates a fracture half-length of 400 ft. and a permeability of 42 nd.

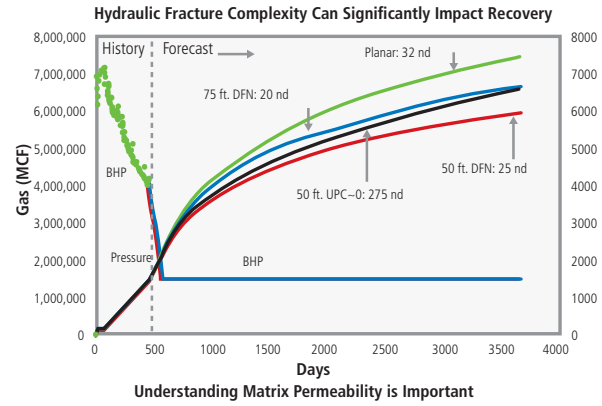

Fig. 14.11—Reservoir simulation history match and production forecast for different fracture.

Table 14.2—Comparison of 15-stage and 8-stage completions.

15 Stages	Fracture Area ($MMft^2$)	Propped Area ($MMft^2$)	Pay Area ($MMft^2$)	Pay Propped ($MMft^2$)	History Match Permeability (nd)
Planar	18	7.3	12	5.4	32
50-ft DFN	30	8.4	16	3.7	25
50-ft DFN, UPC~0				3.7	275
75-ft DFN	31	8.9	17	3.9	20
8 Stages	**Fracture Area ($MMft^2$)**	**Propped Area ($MMft^2$)**	**Pay Area ($MMft^2$)**	**Pay Propped ($MMft^2$)**	**History Match Permeability (nd)**
50-ft DFN	19	5	11	2.2	25
75-ft DFN	19	5.7	11	2.6	20

This example highlighted a number of important issues associated with the interpretation of microseismic images and the application of RTA and linear flow analysis. The production behavior for this well could be adequately matched using planar and network fractures, illustrating that production modeling will likely yield non-unique solutions unless matrix permeability, stress regime, and the DFN can be constrained. Non-unique solutions are compounded by uncertainty in fracture conductivity, especially in the un-propped regions. The comparison of RTA results for the various simulation cases showed k_{srv} is a function of the completion (e.g., number of stages) and the DFN and x_f from RTA may not be representative of actual fracture half-length for network fractures. It should be emphasized that the DFNs in this example were very homogeneous. Increasing heterogeneity would result in an even more problematic application of x_f and k_{srv} from RTA.

14.6.2 Tight Oil Example

This example utilizes the Bakken microseismic data presented by Dohmen et al. (2013) and builds on the work of Chu et al. (2012) to illustrate the impact of fracture geometry and complexity on well performance and RTA. The

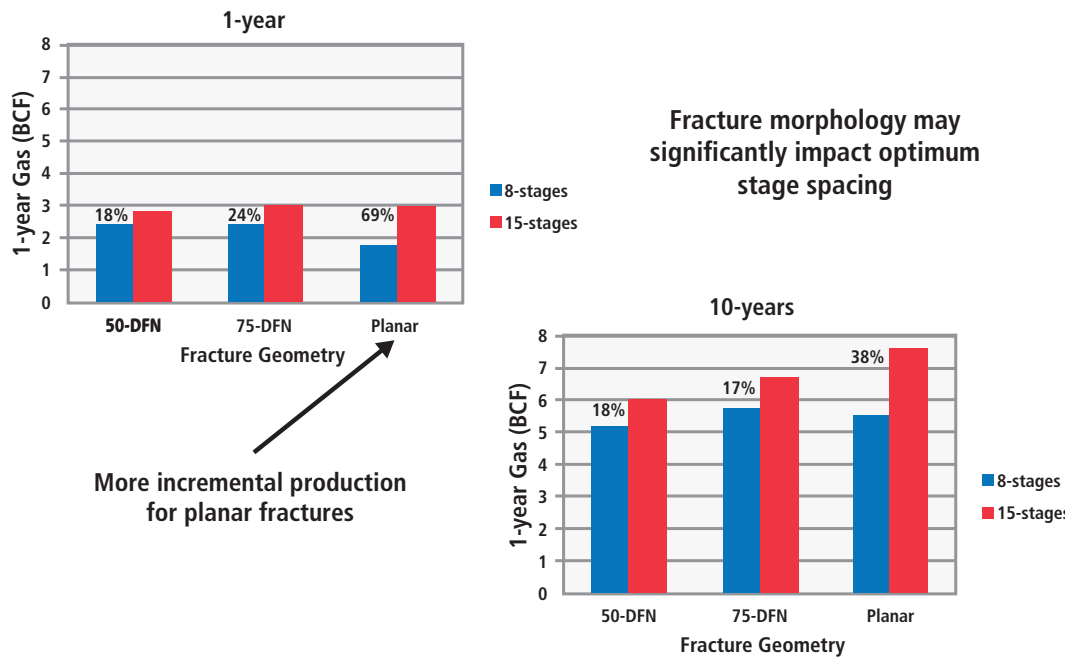

Fig. 14.12—Effect of fracture complexity and stage spacing on well performance. (From Cipolla and Wallace 2014.)

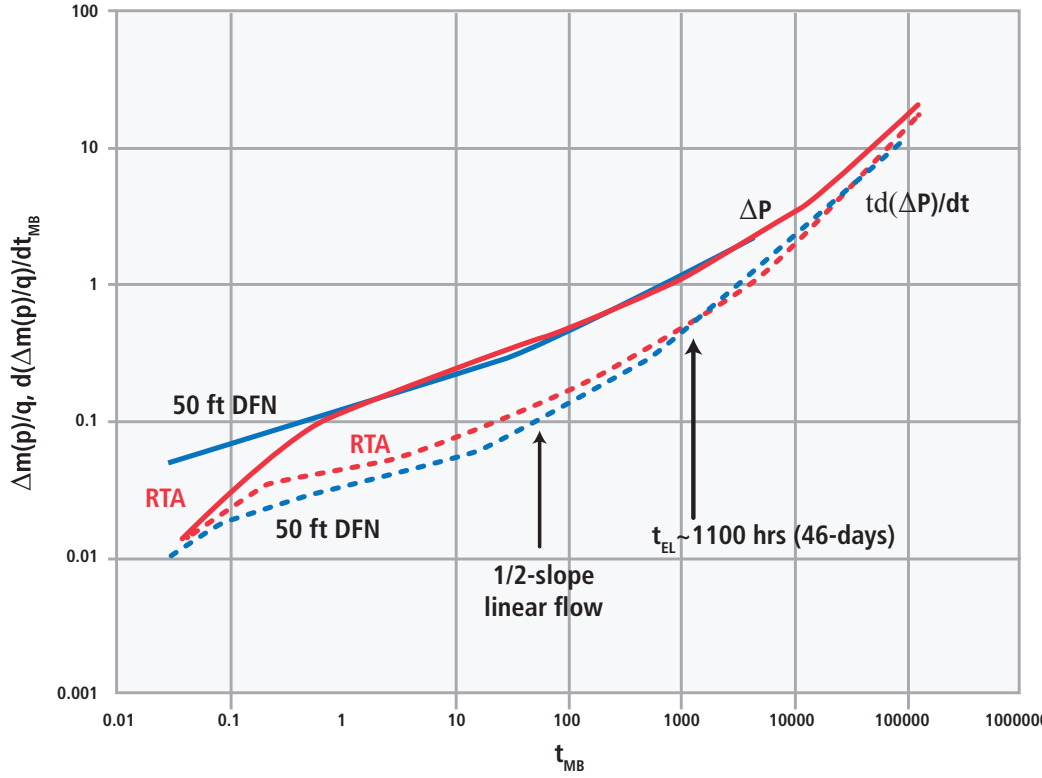

Fig. 14.13—Alternate RTA results, multifractured horizontal well model: 50-ft. DFN, 15 stages, and simulation input k = 25 nd. RTA match indicates x_f = 400 ft., k = 42 nd.

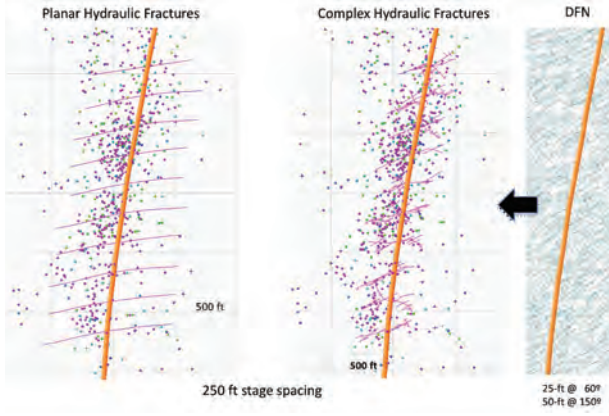

Fig. 14.14—Tight oil example: complex and planar fracture geometries.

reservoir and fluid properties are shown in **Table 14.4**. Rock compaction was also considered in the simulation study.

The fracture model was guided by the microseismic events for a 3,000-ft. section of the lateral, DFIT results, and "fracture hits" in nearby observation wells. The fracture modeling for all cases used a treatment design consisting of 1,600 bbl of cross-linked fluid and 110,000 lbs of 20/40 ceramic proppant per stage (5 ppg maximum concentration) pumped at 45 bpm (un-cemented liner, one fracture port per stage, ball-drop completion system), which is consistent with the actual treatments pumped in this well. The fracture height was calibrated to match microseismic data for all cases.

Two fracture geometry cases were evaluated to illustrate the impact of fracture geometry on RTA, completion optimization, and well spacing decisions: simple planar hydraulic fractures and complex network fractures. The discrete natural fracture network (DFN) used for the complex fracture modeling assumed orthogonal natural fractures: 25-ft. spacing oriented at 60° and 50-ft. spacing oriented at 150° (Sarg 2011). The planar and complex fracture geometries are shown in **Fig. 14.14** for a fracture spacing of 250 ft. and compared to the microseismic data.

The average fracture half-length for the planar fracture is 500 ft. and average height is 220 ft., with an average net pressure of 550 psi. The net pressures in the planar cases were adjusted to match field observations by increasing fluid friction. The total fracture area for the planar case is 2.2 MMft^2, with 80% of the fracture area propped (0.63 lbs/ft^2 average proppant

Table 14.3—Summary of RTA and LFA for tight gas example.

Case	RTA-Analytical Model						SQRT of TIme Analysis			
	x_f(ft)	k(nd)	F_c (md-ft)	F_{cD}	SRV ($MMft^3$)	$x_f k^{1/2}$ ($ft*md^{1/2}$)	$x_f k^{1/2}$ ($ft*md^{1/2}$)	SRV ($MMft^3$)	x_f(ft)	k(nd)
50-ft DFN (15 stages) - 25nd	239	220	53	1008	290	3.5	3.0	320	263	125
50-ft DFN (8 stages) - 25nd	220	200	180	4091	267	3.1	4.8	261	215	490
50-ft DFN (UPC~0) - 275nd	180	750	260	1926	219	4.9	3.3	214	176	346
50-ft DFN (15 stages) - 20nd	225	350	79	1003	274	4.2	3.2	359	296	119
50-ft DFN (8 stages) - 20nd	300	63	15	794	364	2.4	4.4	297	245	321

concentration). With a few exceptions, the fracture length extends beyond the highest density microseismic events. Fracture lengths are relatively consistent with the microseismic image, indicating that planar fractures could be interpreted in this example. Predicted hydraulic geometries for the network fractures are complex, as the hydraulic fractures interact with the natural fractures and are influenced by stress shadowing much more than the planar case. The average fracture half-length for the complex case is 250 ft. and the average height is 160 ft., with an average net pressure of 600 psi. No adjustment to fluid friction was used when modeling complex network fractures. The total fracture area for the complex fractures is 3 $MMft^2$, with 53% of the fracture area propped (0.68 lbs/ft2 average proppant concentration). The complex network fractures have about 30% more fracture area compared to the planar fractures, but the propped area is about 10% greater in the planar case because of the inability of proppant to enter portions of the complex fracture network. Complex fractures are mostly shorter than indicated by the microseismic data, but are more consistent with the complex microseismic event patterns.

14.6.2.1 Production Modeling–250-ft. Stage Spacing

Fracture geometries were added into the reservoir simulation model, which used unstructured grids to match the hydraulic fracture structure and distribution of conductivity. Both propped and un-propped fracture areas were included in production modeling. In situ propped fracture conductivity was about 150-to-300 md-ft. at production conditions. Un-propped fracture conductivity was modeled using the base and low-case curves shown in **Fig. 14.15** (Zhang et al. 2013, Suarez 2013). FBHP was reduced from 5,000 to 1,250 psi during the first 40 days and held constant at 1,250 psi thereafter.

Production for the planar and network cases is compared in **Fig. 14.16**. Although the two cases exhibit similar production during the first year, the planar case produces about 40% more oil. The pressure distribution after 10 years of production for the planar fractures is shown in **Fig. 14.17**, while the

Table 14.4—Reservoir properties, tight oil example.

k_0 =	600	nd
Pi =	7030	psi
ø =	5.1	%
B_0 =	1.82	STB/RB
P_{BP} =	3150	psi
μ_0	0.37	cp
c_0 =	1.13E-05	psi^{-1}
h =	77	ft
R_{si} =	1552	scf/bbl

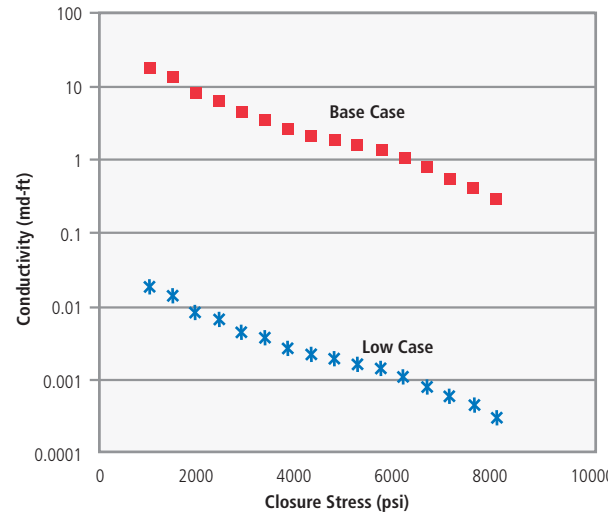

Fig. 14.15—Un-propped fracture conductivity, tight oil example.

network fracture case is shown in **Fig. 14.18**. The apparent drainage distance normal to the lateral for the planar fracture case is about 1,200 ft., compared to 700 ft. for the network fractures. The longer fracture lengths result in an increased drainage area. This illustrates a limitation of the SRV approach. Drainage area and production are dictated by fracture geometry, not microseismic volume.

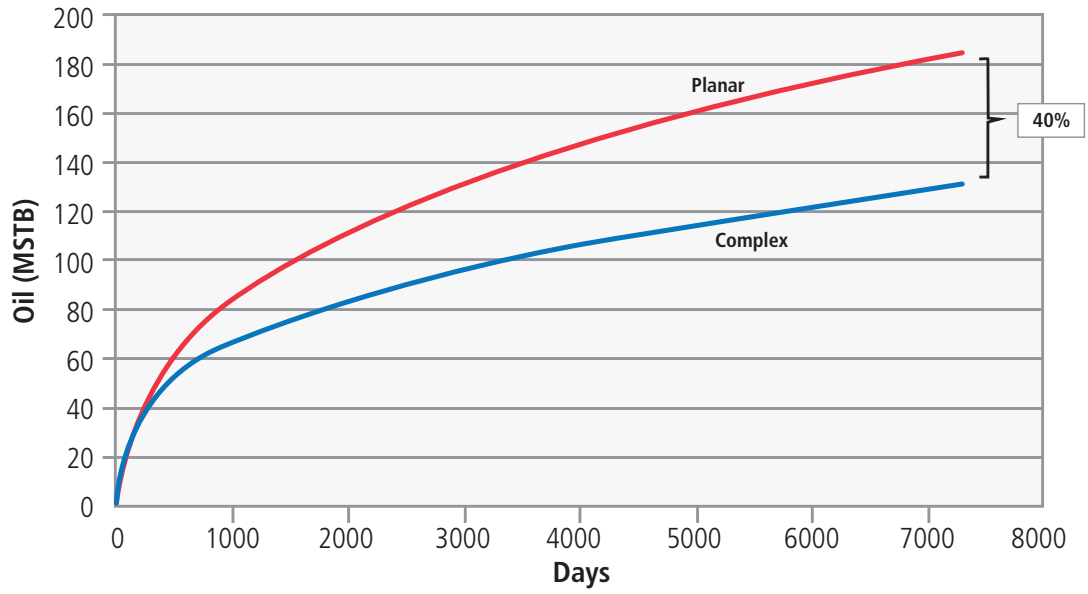

Fig. 14.16—Cumulative production, planar and network fractures, 250-ft. stage spacing. (From Cipolla and Wallace 2014.)

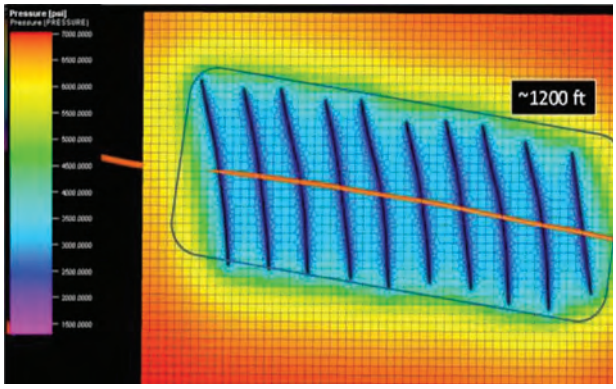

Fig. 14.17—Pressure distribution after 10 years with planar fractures and 250-ft. stage spacing.

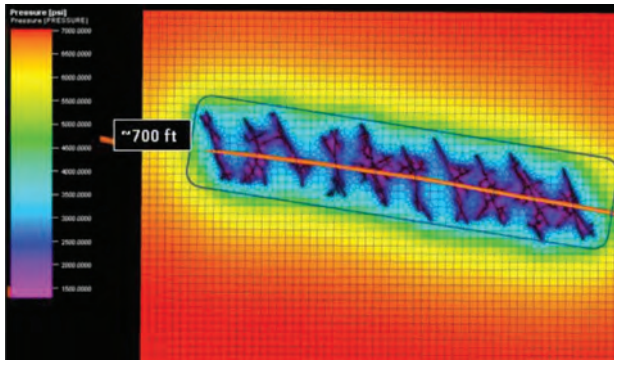

Fig. 14.18—Pressure distribution after 10-year, network fractures, 250-ft. stage spacing.

The previous modeling assumed the base-case, un-propped conductivity profile shown in Fig. 14.16. If un-propped conductivity is very low, as represented by the low case curve in Fig. 14.16, well performance would be significantly reduced. The impact of un-propped fracture conductivity is shown in **Fig. 14.19**. Un-propped fracture conductivity has a more pronounced effect on the production from network fractures compared to the planar case. This result is intuitive: half of the network fractures are un-propped, compared to only 20% for the planar fractures. In general, modeling shows that as fracture complexity increases, so does the amount of un-propped area due to proppant bridging in secondary fractures.

14.6.2.2 Linear Flow Analysis

To compare linear flow analysis results for planar and network fractures, 1,000 days of production at 1,500 psi FBHP was simulated for each case. The RTA analysis is based on the work of Ye et al. (2013). **Fig. 14.20** compares the linear flow analysis for planar and network fracture for the 250-ft. stage spacing. The departure for linear flow (t_{EL}) is much earlier for the network fractures compared to planar fractures, resulting in a much higher estimate of permeability (k_{srv}). Matrix permeability is 600 nd in the simulations in both cases. The k_{srv} estimate for the planar case is 0.002 md, with a fracture half-length of 305 ft. ($x_f\sqrt{k} = 13.6$). Although the average fracture half-length in the planar case was ~500 ft. and permeability was 600 nd ($x_f\sqrt{k} = 12.2$), the results are

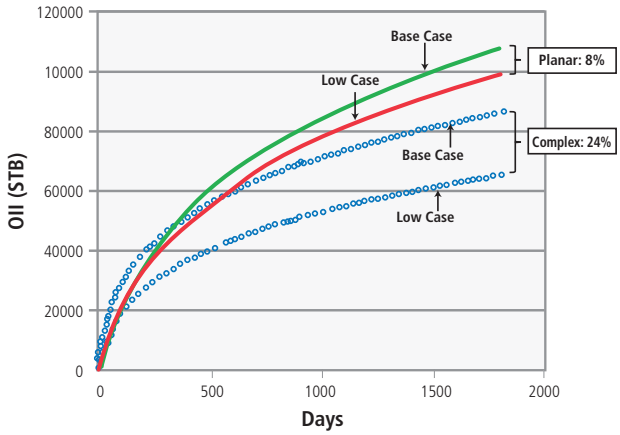

Fig. 14.19—Effect of un-propped conductivity on well performance, tight oil example, 250-ft. stage spacing. (From Cipolla and Wallace 2014.)

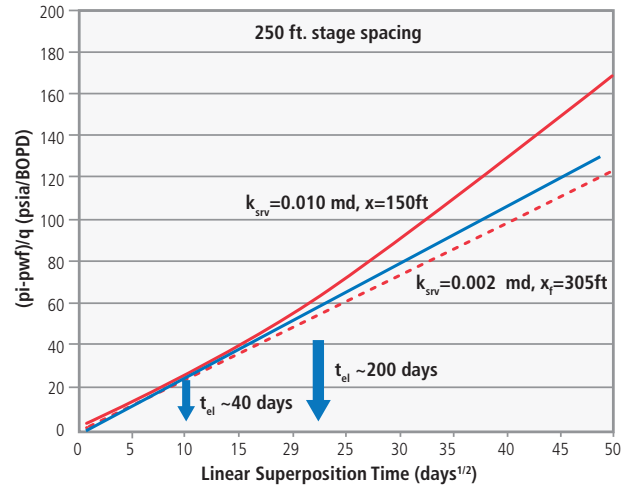

Fig. 14.20—Comparison of linear flow analysis results for planar and network fractures, 250-ft. stage spacing.

within reasonable agreement given the difficulties comparing single-phase linear flow analysis and two-phase numerical modeling where both fracture conductivity and matrix permeability are changing based on local pore pressure.

The linear flow results for the network fractures indicate an apparent system permeability (k_{srv}) of 0.01 md and a fracture half-length of 150 ft. ($x_f\sqrt{k} = 15$). The k_{srv} and x_f from this work are consistent with the results presented by Chu et al. (2013) and Ye et al. (2013). The $x_f\sqrt{k}$ product for the planar and network fractures is similar, consistent with the early time production behavior for the two cases. However, the k_{srv} for the network case is five times higher than the planar case and 16.7 times higher than the numerical simulations. This may appear consistent with the SRV representation of network fractures with an enhanced permeability region around the hydraulic fracture. However, the SRV implication can lead to erroneous conclusions concerning stage spacing and well placement, as each network fracture changes the overall system behavior when stage spacing is increased or decreased. This issue is illustrated in the following section.

14.6.2.3 Stage Spacing and Well Placement

Optimizing stage spacing is a critical economic decision that is significantly affected by interpretations of reservoir permeability and fracture geometry. Simply put, larger stage spacing is indicated as permeability increases, and closer well placement is typical as fracture lengths decrease. The linear flow results for the network fractures Fig. 14.20 were used to predict the 10-year oil recovery for stage spacing of 192 ft., 250 ft., 333 ft., and 500 ft. and were compared to the numerical reservoir simulation results. The fracture geometries for each stage's spacing were modeled and input into the numerical reservoir simulator. The base case un-propped fracture conductivity was used for all the numerical simulations (Fig. 14.19).

The results from linear flow analysis (k = 0.01 md, x_f = 150 ft.) were used as input for a single-phase numerical reservoir simulation model to evaluate stage spacing. The drainage boundary was set at 160 ft. from the lateral. Thus, only the SRV was assumed to contribute to production. Given the linear flow analysis of k_{srv} = 0.01 md and x_f = 150, results from a 10-year oil production per 1,000 ft. of completed lateral as a function of stage spacing, showed that there is little benefit in decreasing stage spacing below 333 ft. and only a 12% increase in recovery when stage spacing is decreased from 500 to 333 ft. However, the network fracture model and subsequent numerical reservoir simulations predict significant improvements in oil recovery as stage spacing is decreased. In comparison to the RTA-based results, the network fracture model predicts that oil recovery will increase by 66% when stage spacing is decreased from 500 to 333 ft. The two cases continue to differ as fracture spacing is decreased below 333 ft. The network model predicts a 20% increase in oil recovery when stage spacing is decreased from 333 to 192 ft., while the model using the linear flow analysis results predicts a 4% increase in recovery. Although stage spacing is ultimately an economic decision, the results presented here indicate that using k_{srv} and x_f from linear flow analysis could lead to incorrect conclusions concerning optimum stage spacing.

The simplifying assumptions inherent in linear flow analysis may not adequately capture the complex depletion behavior

of network fractures. To illustrate this behavior further, the linear flow analysis results for network fractures with stage spacing of 192 ft., 250 ft., and 333 ft. are compared in **Fig. 14.21**. The FBHP for all cases is 1,500 psi and 1,000 days of production were simulated (daily data). Although picking tEL is somewhat subjective, there is a general trend showing a decrease in the k_{srv} and an increase in x_f as stage spacing is reduced. These trends may be useful when applied in a comparative manner, but cannot be used for completion optimization. This example is not intended to capture all the complexities associated with any specific play, including the Bakken, but to illustrate the limitations of using SRV from microseismic data and results from linear flow analysis for completion optimization.

14.6.2.4 Tight Oil Example

The tight oil example illustrated that properly characterizing fracture geometry and conductivity is required for completion optimization. As with the previous shale gas example, the tight-oil example showed that understanding un-propped fracture conductivity is important for network fractures, but less important for planar fractures. The example highlighted potential shortcomings of using reservoir permeability (k_{srv}) and x_f from linear flow analysis to evaluate stage spacing, as k_{srv} changes with stage spacing as illustrated in **Fig. 14.22** and may not adequately describe production mechanisms for network fractures, while x_f from linear flow analysis will likely underestimate the actual fracture half-length.

14.6.3 Summary

SRV derived from microseismic data can be a good starting point to guide fracture modeling, providing a measure of overall hydraulic fracture extent. However, SRV may not be a good indication of the stimulated volume or of the effectiveness of the fracture treatments.

Microseismic interpretations can guide hydraulic fracture models, leading to a better understanding of fracture area and the distribution of fracture conductivity. The application of "calibrated" network hydraulic fracture models provides a tool for predicting fracture geometry when treatment designs and completion strategies are changed. Preserving the details of the network fracture geometry and distribution of fracture conductivity in reservoir simulation models is critical for completion optimization and well-spacing studies.

The two examples discussed herein illustrate that properly characterizing matrix permeability, DFN, and hydraulic fractures is necessary to evaluate completion strategies reliably. Modeling the distribution of fracture conductivity also provides important insights into well performance and the drainage area. The examples also highlight drawbacks of directly using permeability and fracture half-length from RTA or linear flow analysis in completion optimization and well spacing workflows. The apparent system permeability or k_{srv} can change dramatically depending on completion strategy (e.g., stage count) and, thus, may be inappropriate when evaluating stage spacing and well placement. However, RTA can provide important insights when comparing well performance, forecasting production, and estimating reserves, and should be part of a holistic approach when evaluating well performance in unconventional reservoirs.

The issue of non-uniqueness is pervasive in production modeling workflows. It is difficult to separate the effects of fracture area, fracture conductivity, and reservoir permeability. Additional measurements and data are required to constrain hydraulic fracture and production models.

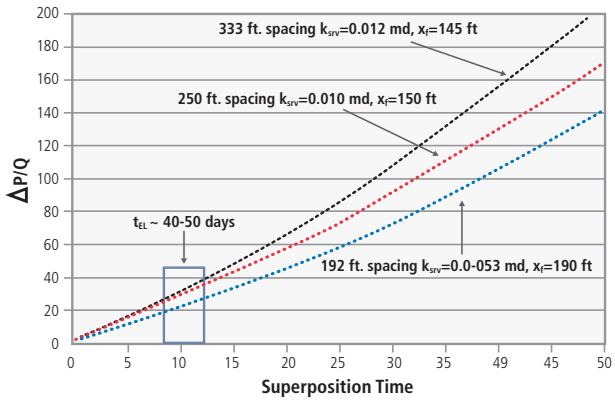

Fig. 14.21—Linear flow analysis results for network fractures, and stage spacing at 192 ft., 250 ft., and 333 ft.

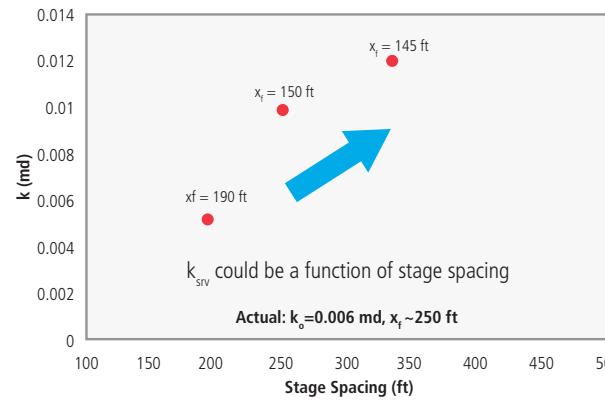

Fig. 14.22—Effect of stage spacing on k_{srv}, tight oil example.

Although the details of the hydraulic fracture structure cannot be determined from microseismic images, advanced interpretations of microseismic may provide important insights into natural fracturing and stress regime. With the increasing use of pad drilling and well-spacing pilots, important data on well-to-well interference is being gathered to better describe fracture geometry and the distribution of fracture conductivity. An integrated approach that includes hydraulic fracture propagation models linked to reservoir simulations will be important.

14.7 Production Forecast Approximation

Fetkovitch (1980) and others (Ehligh-Economides and Ramey 1981) showed the relation of decline parameters to reservoir properties and the possibility of having more complicated hyperbolic trends in multilayer reservoirs, or when other drive mechanisms (other than pressure depletion) are involved. Generally hyperbolic exponents (b less than 1.0) are expected in such circumstances. In the same context, it was shown that hyperbolic exponents larger than 1 could be possible in transient behavior. More precisely, transient flow could produce decline patterns in which a "best fit" of the data using a model derived for a different flow regime could be greater than unity. Fitting b-values greater than unity to early transient data is rarely valuable for characterizing reservoir data or for forecasting production and reserve. Theoretically, when the hyperbolic exponent is greater or equal to unity, the decline rate in infinite time becomes zero, indicating infinite production at infinite time. This argument prompts the introduction of a terminal condition (for example using a minimum decline rate), which is equivalent to accepting that decline trends with a hyperbolic coefficient equal, or greater than unity represent transient flow conditions.

Introduction of natural fractures complicates the analysis of production trends. In one simplified model of naturally fractured systems, the fracture storage parameter (ω) and the inter porosity flow parameter (λ) are used. These dual-porosity approaches are not useful for unconventional reservoirs. Notwithstanding those limitations for a practical interpretation of corresponding production trends for natural fractured reservoirs, the architecture of induced fractures in shales may and tight formations may present more complicated networks of interconnected fractures. According to some early researchers (Camatcho-Velasquez et al. 2008, Beier 1990, Chang 1990) production and pressure response resembles those of fractal networks suggesting that the fractures that result from slick water stimulation vary in scale and hierarchy and may not be described by simplistic planar models. Several researchers (Kurtoglu et al. 2011, Ambrose et al. 2011) have suggested formulations and methods that take into account the placement of transverse fractures in horizontal wells.

Various production plots are provided for a typical Barnett well (**Fig. 14.23**). Characteristic decline shapes, or "type curves" are usually employed in shale play evaluations provided that there is a sufficient group of wells with relevant production data that can be grouped and summarized.

If we examine one of the horizontal wells in the Barnett example shown in **Fig. 14.24**, it can be seen that a characteristic decline shape has the form of rapid-early decline, followed by an extended period of lower declines in flow rates (Fig. 14.24).

In the course of the first year, this particular well has lost 55% of its initial rate. After eight years of continuous decline, the well has begun a period of very shallow decline. The temptation here (as shown on the figure from time 2192 to the end of the graph) may be to interpret the slow decline rates as a "plateau." This is wrong. Theoretical and actual behavior will show declining rates (at a constant flowing bottomhole pressure) even if the decline rates are low. Although this well has a long production history with a relatively smooth decline, it is still uncertain for how long this well will be producing, and at what rate, or what the conditions would be at abandonment. A different plot of the well history in a semi-log plot reveals that, with exception of the first two years, the well exhibits almost a constant decline at 15% per annum (see **Fig. 14.25**).

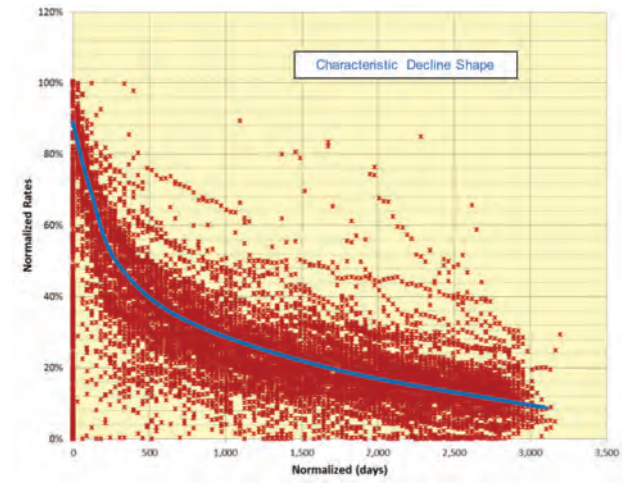

Fig. 14.23—Normalized gas rates versus normalized time for selected Barnett wells.

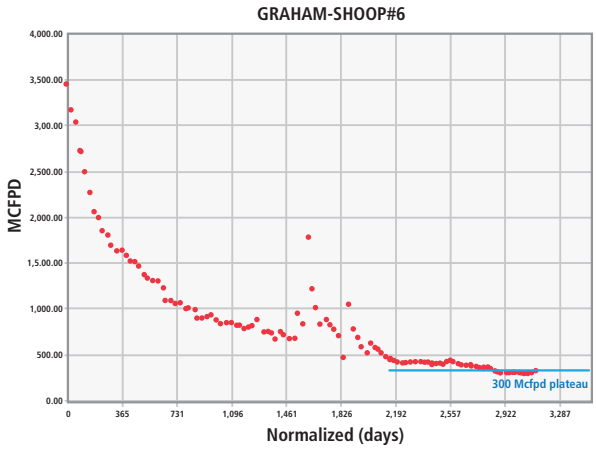

Fig. 14.24—Horizontal Barnett well example.

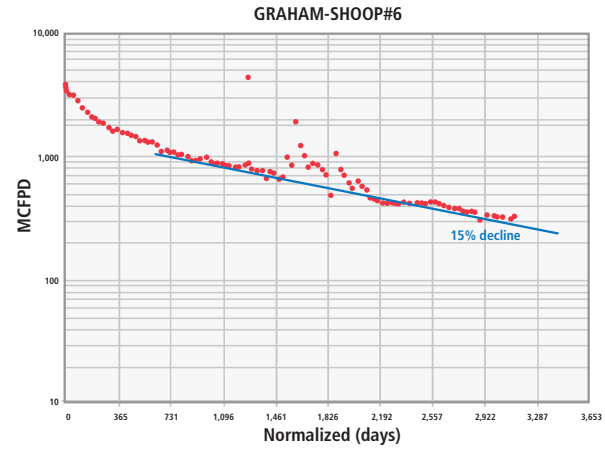

Fig. 14.25—Example Barnett well decline.

This behavior is typical low-permeability well performance, the exception being not exactly knowing when to expect a well to follow an exponential decline trend if such a trend is not already established. By plotting the same data in a different form, we might get linear flow trends at the first four years of production. Linear flow in a formation is associated with flow of matrix into fractures that have high conductivity relative to the matrix permeability and are connected directly to the wellbore. Linear flow patterns have been documented in tight gas and shale gas wells as early as 1976 (Bangall and Ryan 1976). Many researchers (Wattenbarger et al. 1998, Nobakht et al. 2010) have shown the practicality of such rate plots when cumulative production, or the inverse of rate is plotted versus the square root of time. When a well exhibits a linear flow regime, a straight line fits production data as a function of square root of time closely. As the flow regime is impacted by boundaries that could be the extent of the stimulated rock volume, or a mirror well infringing into the drainage area, the flow regime changes to boundary dominated flow as shown in **Fig. 14.26** after four years' lapse, next.

While it may be possible for engineers to plot production data in a form that produces straight-line fits, such lines cannot be extrapolated without previous knowledge of which regime prevails (linear or boundary).

In this particular example, someone may provide a linear fit of the last 3 years of production, and extrapolating that, it is estimated that the 30 year EUR would be close to 4 Bcf, as shown in **Fig. 14.27**.

Relating this regime to hyperbolic decline curves, it can be shown that, when a linear regime prevails, production-rate versus time data conforms to a hyperbolic decline with a hyperbolic coefficient that is often close to, or greater than, 1.0.

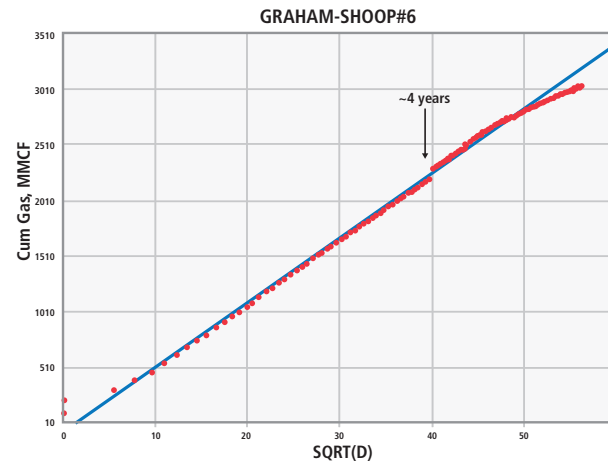

Fig. 14.26—Example Barnett well performance in linear terms.

There is no theoretical basis to fit shale well data with high b-values for hyperbolic declines in the early time and then allow for production data to extrapolate to an exponential decline. Doing so leads to the adoption of hyperbolic trends with hyperbolic coefficients greater than 1.0 that revert to exponential declines by introducing an arbitrary minimum decline. Approaches that vary b-values with time also miss the point that the Arp's approach is not well suited for multiple hydraulic fractured horizontal wells with varying permeability regions in long-term transient flow. The following example in **Fig. 14.28** shows how the example Barnett well could be fitted with such a hybrid decline scheme in which early production data are conforming to a hyperbolic decline scheme and by adopting a tangential minimum exponential decline of 15% per year.

Although hybrid decline schemes [after their introduction by Rushing et. al. (2007)] are widely used as a simple approach in

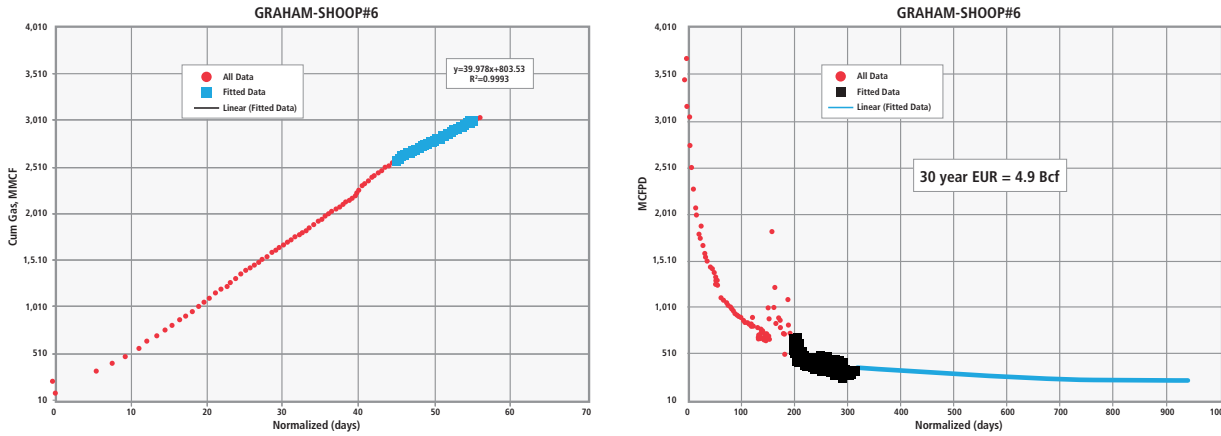

Fig. 14.27—Extrapolation of linear trends in the example well.

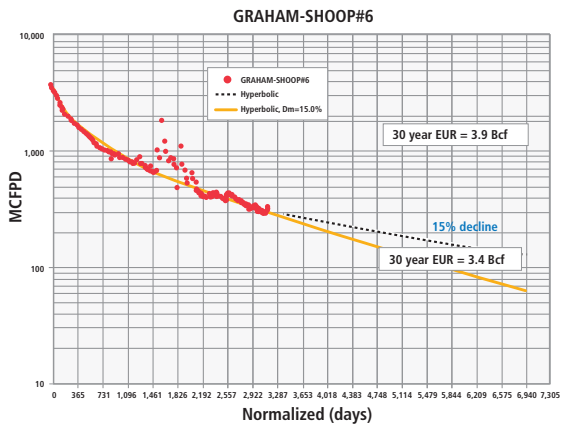

Fig. 14.28—Example Barnett well, hybrid decline scheme.

shale plays, their implementation requires empirical guidance to adopt appropriate hyperbolic parameters and calculate the appropriate minimum decline rate. This is not an unbiased approach and an expert in one area may feel impaired when adopting his or her experience in an analogous area with limited production.

The Barnett experience in the early 2000s offered a plethora of production data analyzed by many researchers in the pursuit of a universal fit that may apply to early and late production performance and will be independent of making assumptions on flow regime transitions or other well attributes. There are several methods (Lee and Sidle 2010, Lee 2011) proposed to accomplish this task, none of which presents a definite advantage or a solid theoretical foundation that relates to the physics of the subject wells.

14.7.1 Power Law

The method of extrapolating decline schemes is basically a mathematical consolidation of the minimum decline concept in a single formulation that was introduced by Ilk et al. (2008).

Applying this method to the example Barnett well, we can arrive at the following analysis (see **Fig. 14.29**).

14.7.2 Stretched Exponential

This empirical method was introduced by Valkó in 2009 (Valkó 2009). This method claims to provide a continuous fit of production data in the early and late time with the least controlling fit parameters. The stretched exponential formulation can be derived from the power law, when the decline rate at infinity is set to zero. The decline method can be explained as a sum of exponential declines that their respective time constants have a characteristic probability distribution that is skewed toward the low values. The formulation [as it is explained in more detail by Valkó and Lee

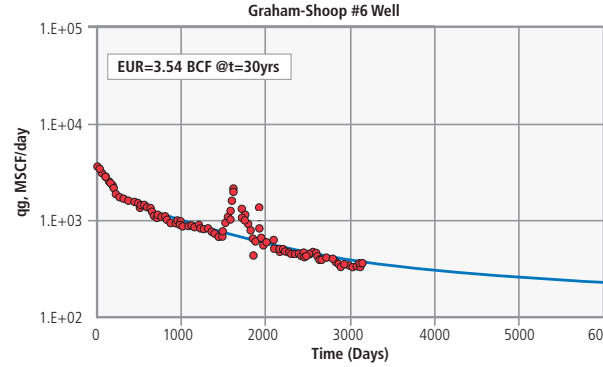

Fig. 14.29—Power law fit, for example Barnett well.

(2010)], involves the Gamma function in its derivation and has the advantage of being constrained to a finite cumulative production at infinite time.

Applying this method to the example Barnett well, we arrive at the following analysis, shown in **Fig. 14.30**.

14.7.3 Duong's Method

This method uses the concept of constant depletion schemes that is assumed in the exponential and linear flow equations. For exponential decline, depletion is constant.

$$\frac{q_i - q}{G_p} = D \qquad \textbf{(Eq. 14.2)}$$

For linear flow (Hara 1986; Knott and Hara 1991) the ratio between instantaneous rate and cumulative production is related to time:

$$\frac{q}{G_p} = \frac{(1 - n)}{t} \qquad \textbf{(Eq. 14.3)}$$

Duong proposed a scheme that fits shale wells very closely by using the following relation:

$$\frac{q}{G_p} = at^{-m} \qquad \textbf{(Eq. 14.4)}$$

In summary, the formulations and nomenclature for these equations are provided in **Table 14.5** and **Table 14.6**, respectively.

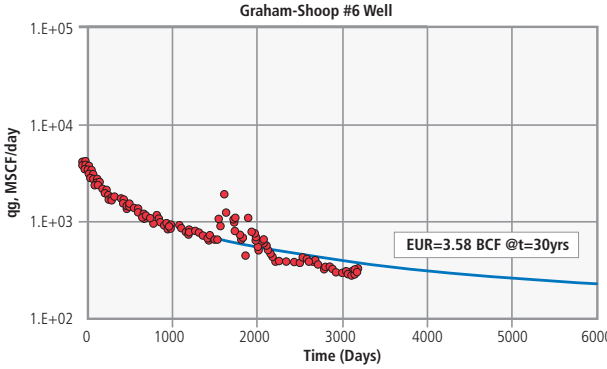

Fig. 14.30—Stretched exponential fit in example Barnett well.

Applying this method to the example Barnett well, we arrive at the following analysis (see **Fig. 14.31**).

Table 14.5—Decline trend formulations.

Decline Method	Formulation	Introduced by
Exponential	$q = q_i e^{(-Dt)}$	Arps, 1944
Hyperbolic	$q = q_i \frac{1}{(1 + bD_i t)^{(1/b)}}$	Arps, 1944
Linear flow	$q = q_i t^{-n}$	Bangall and Ryan, 1976
Power law	$q = q_i e^{(-D_\infty t - D_i t^n)}$	Ilk et al., 2008
Stretched exponential	$q = q_i e^{\left[-\left(\frac{t}{\tau}\right)^n\right]}$	Valkó et al., 2009
Duong	$\frac{q}{G_p} = at^{-m}$ or $q = q_i e^{\left[\frac{a}{1-m}\left(t^{(1-m)}-1\right)\right]}$	Duong, 2010

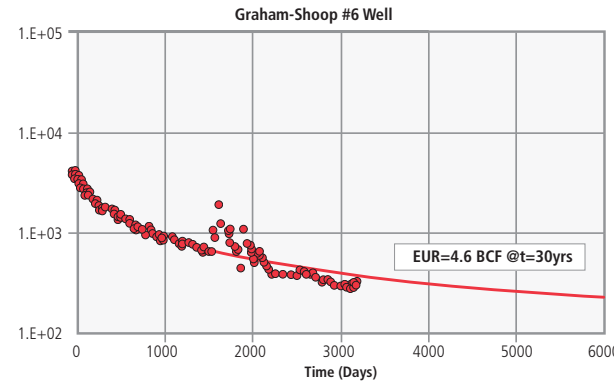

Fig. 14.31—Applying Duong's fit in the example Barnett well.

where:

Table 14.6—Decline trend nomenclature.

Symbol	Explanation	Typical Units
q	Rate at time (t)	Mcf/day
q_i	Initial rate	Mcf/day
t	Time	(years, months or days)
D	Decline rate	Fraction (per year, month, or day)
D_i	Initial decline rate	Fraction (per year, month, or day)
b	Hyperbolic exponent	Dimensionless
τ	Characteristic periods	(years, months, or days)
n	Exponent (linear, Ilk, Valkó)	For linear flow n=0.5 For-bi-linear flow, n=0.25
D_∞	Terminal decline rate (Ilk)	Fraction (per year, month, or day)
G_p	Cumulative production at time t	Mcf
a	Constant (Duong)	Dimensionless
m	Exponent (Duong)	Dimensionless

In summary, by applying all different methods mentioned in the example Barnett well, which has a relatively long history, the following comparison can be made for the corresponding recoverable volumes estimated at 30 years, shown in **Table 14.7**.

In retrospect, having a relatively large production performance example stretching over 8 years with smooth production trend (absence of interventions or other obvious interference), there is a broad range of estimates ranging from 3.4 to 4.6 Bcf. The average is 3.9 Bcf with a standard deviation 0.6 (+/- 14% error). The most likely values are the ones provided by the modified hyperbolic, the stretched exponential, and the power law. Given the fact that in all these methods some late time response needs to be experienced in order to adjust initial decline trends, it appears that the stretched exponential fits as proposed by Valkó et. al. may provide a better alternative in absence of any other way to project performance in shale gas wells. According to Valkó and Lee (as referenced earlier) this method has been tried in a large number of horizontal wells in the Barnett shale with satisfactory results.

Table 14.7—Comparison of different EUR estimates for the example Barnett well.

Decline Method	EUR at 30 years, Bcf
Exponential (after 4 years)	3.4
Hyperbolic	3.9
Hyperbolic with D_{min}=15%	3.4
Linear flow	4.9
Power law	3.54
Stretched exponential	3.58
Duong	4.60

14.7.4 Pitfalls of Decline Trends

Several researchers have recently pointed out the pitfalls and practical obstacles in adopting decline schemes in the analysis of shale well production taking a "statistical" approach and by following a type curve principal. These include:

- Does not involve natural constraints.
- Difficult to explain well design effects.
- Optimization is based on "trial and error," i.e., many attempts may fail and then attempts are readjusted to avoid errors in the next round of tries.
- Large investment for "know how" needed, i.e., direct experience with decline schemes
- Geomechanical effects are ignored.
- Analogies may not be extrapolated due to changing formation characteristics and conditions.
- Long-term predictions are questionable.

14.8 Numerical Models

In this section, the term *numerical model* is used to refer to the discretized representations of subsurface hydrocarbon-bearing reservoirs and the wells connecting those wells to the surface and facilities. (**Fig. 14.32**)

Numerical models are typically used as enter data for reservoir fluid flow simulators to determine a reservoir's response to operating decisions. These calculations simulate actual changes in operations through history-matching or proposed decisions through forecasting.

Physical aspects that can be modeled for each well include, but are not limited to:

- Casing and tubing sizes
- Type of artificial lift system
- Fracture treatment style, fluid and proppant types and volumes, and number of stages
- Well density and spacing

Well and field operating strategies may include:

- Post-fracturing flowback rates
- Decision to either shut-in or maintain continuous production in the well
- Multiwell fracturing options
- Whether to use enhanced oil recovery (EOR) methods or which EOR method to use

Reservoir simulation and numerical modeling (RSNM) has been used in the petroleum industry since the 1960s. Many improvements have been made in the types of physical phenomena that can be modeled and in the performance (speed) at which modern commercial reservoir simulators can run. In addition to these improvements in simulator physics and numerical solver technology, the past five or so years have witnessed the arrival of reservoir simulation engineer

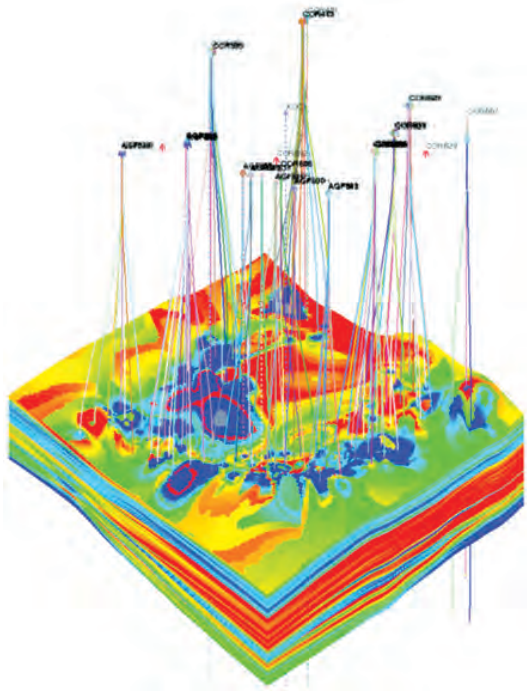

Fig. 14.32—Numerical models describe both the reservoir and wells connecting the reservoir to the surface.

Table 14.8—Known properties.

Property	Value
Depth at top of reservoir, ft.	10,800
Reservoir thickness, ft.	150
Initial reservoir pressure, psi	8,100
Initial reservoir temperature, °F	270
Oil bubble point pressure, psi	3,010
Oil gravity, °API	43
Initial solution gas/oil ratio, scf/STB	950
Lateral length, ft.	4,000
Number of fracturing stages pumped	10

productivity enhancement (PE) tools. These tools have dramatically shortened the time required to achieve usable results from RSNM and have increased the ability to quantify the magnitude and sources of uncertainty in those results.

RSNM can be combined with PE tools to accomplish three important tasks faced by engineers working with unconventional reservoirs:

1. Calculating estimated ultimate recoveries (EUR) for unconventional wells before boundary-dominated behavior is observed

2. Optimizing the number and size of propped fractures for a single well, with or without prior history

3. Optimizing well spacing, with or without prior history

These particular applications are significant because of the limitations of conventional and advanced decline-curve analysis (DCA) methods (i.e., they require observation of boundary-dominated flow) and rate-time-analysis-based methods (i.e., they are unable to model multiple wells, multiphase flow, or heterogeneous reservoir properties).

A workflow for applying RSNMs to answering these three questions using productivity enhancement tools is presented with a general discussion of the simulator features and gridding design required to accurately calculate the transient flow behavior of unconventional reservoirs.

Because no tools or methods are foolproof, a review of some of the current research about the physics fluid flow and phase behavior through nanoscale-diameter pore throats is also presented.

Table 14.9—Ranges estimated for uncertain properties.

Property (unit)	Min Value	Max Value
Reservoir matrix porosity (fraction)	0.04	0.10
Reservoir matrix permeability (nanodarcies)	10	1,000
Reservoir matrix permeability (nanodarcies)	0.0006	0.0006
Reservoir natural fracture effective porosity (fraction)	40	40
Reservoir natural fracture x-direction spacing (ft.)*	50	50
Reservoir natural fracture y-direction spacing (ft.)*	50	50
Reservoir natural fracture z-direction spacing (ft.)*	0	0
Propped fracture spacing (ft.)	100	400
Propped fracture half-length (ft.)	50	400
Propped fracture permeability (darcies)	1	30
Initial water saturation (fracture water) in natural fractures (fraction)	0.15	0.45
Initial water saturation (fracture water) in propped fractures (fraction)	0.15	0.45
Reservoir matrix relative permeability	Corey functions are sufficient but uncertain	
Reservoir natural fracture relative perm	Straight line behavior is expected in open slots	
Propped fracture relative permeability	Straight Line behavior is expected in hi-perm proppants	
Reservoir matrix capillary pressure	Reasonable to assume to be correlated with matrix relative permeability Corey functions	
Reservoir natural fracture capillary pressure	Reasonable to assume to be zero in open slots	
Propped fracture capillary pressure	Reasonable to assume to be zero in hi-perm proppants	
Reservoir matrix pore volume compaction	Reasonable to assume to be a constant	
Reservoir natural fracture pore volume compaction	Reasonable to assume to be a constant	
Propped fracture pore volume compaction	Unknown variable which can be determined via proppant stress-test data	

14.8.1 Application No. 1—Calculating EUR for Unconventional Wells with or without Observed Drainage-Boundary Dominated Behavior

This method is applied regardless of whether drainage-boundary-dominated behavior is observed.

Consider an Eagle Ford oil window well completed with a 10-stage fracturing job over a 4,000-foot lateral length that has been producing for more than 7 months (222 days). Oil, gas, and water production rates and flowing bottomhole pressures were measured on a daily basis. To calculate the well EUR, the available data and RSNM with PE tools were used.

Step 1. Gather Known Information

List the known information about the well, the producing interval (for the reservoir), and the fluid properties of the oil and gas being produced (**Table 14.8**).

Step 2. Assign Values to Unknowns

List the unknown reservoir and fracturing treatment parameters (**Table 14.9**), many of which can be assigned reasonable ranges.

The natural fracture properties* (X, Y, and Z-direction spacing, effective porosity, and effective permeability) are assumed to be constant and known for this example, but that is not a requirement or limitation of the technology or workflow being described (i.e., those values could also have been allowed to vary). In some situations, all reservoir and propped fracture properties will be allowed to vary with position in the reservoir, which would account for lateral and vertical variations in rock lithology and facies and for variations in propped distribution at closure.

For now, the problem is kept on a simpler level to correspond with the typical available information. The assumption is that neither reservoir property distributions in the form of 2D maps or 3D geologic models, nor hydraulic fracture treatment simulation

design results, are available for this workflow. For this example, the assumed values correspond to open vertical slots spaced every 50 ft. in both horizontal directions; slot widths are set to approximately 0.5 microns (or 500 nm).

Relative permeability and capillary pressure data are rarely available because gathering this data normally requires expensive and time-consuming special core analysis lab (SCAL) tests. Very low permeabilities associated with the unconventional reservoirs in this chapter make it even more difficult, if not impossible, to perform the lab tests required to obtain such data. Some 3D-imaging methods now available may offer an alternative source, although the validity of their derived relative permeability and capillary pressure data is unproven.

However, there is good news when it comes to relative permeability and capillary pressure behavior for many unconventional reservoir numerical models, including the Eagle Ford example as described, next:

- Fluid flow in the matrix during the first few years of primary depletion is likely to be single phase in nature for the following reasons:
  - In-situ water is mostly bound to the clay surfaces and, therefore, immobile; this means the flow of oil from and through the reservoir matrix in the Eagle Ford example is effectively single-phase oil.
  - Imbibed fracturing water could create a situation in which mobile water exists in the reservoir matrix. However, given the very low matrix permeabilities associated with tight or shale reservoirs, mobile water flow in the matrix is likely to be negligible in most situations.
  - Matrix pore pressures take a long time to drop below the bubble point pressure or the dewpoint pressure in reservoirs containing condensates, volatile or black oil, or tight or shale liquids; single-phase oil flow can be expected to dominate the early-time production behavior in the Eagle Ford oil well example.

- Natural and propped fractures are where most of the injected fracturing fluids reside, and where pressures can, and do, drop quickly below the bubble (or dewpoint) pressures of condensate, volatile oil, and black oil fluid systems. In these areas, multiphase oil, gas, and fracturing fluid and water flow are effectively described by straight-line relative permeability curves with no capillary pressure effects as a result of the very high intrinsic permeabilities associated with open slots (natural fractures) and proppant-filled hydraulically created fractures. This state leads to a situation in which fluid flow is mostly segregated, resulting in little reduction in relative permeability to the oil, gas, or water phases as a result of the existence of those three phases in the propped and open natural fractures.

Given the previous assumptions, a typical set of relative permeability curves that were used for the matrix and for the natural and propped fractures is shown in **Fig. 14.33**, **Fig. 14.34**, and **Fig. 14.35**.

Capillary pressure effects were assumed to correlate with the matrix relative permeability curves (used in Fig. 14.33, Fig. 14.34, and Fig. 14.35). Zero was used for the reservoir natural fractures and propped fractures.

The last type of data in Table 14.9 is the pore volume compaction for the reservoir matrix, the reservoir natural fractures, and the propped fractures. Both the porosity and the permeability of porous media decrease as the net effective stress acting upon the pores and pore throats increases. Note that declining pore pressures over the producing life of a well are a major source of increased net effective stress. This decrease in porosity and permeability is

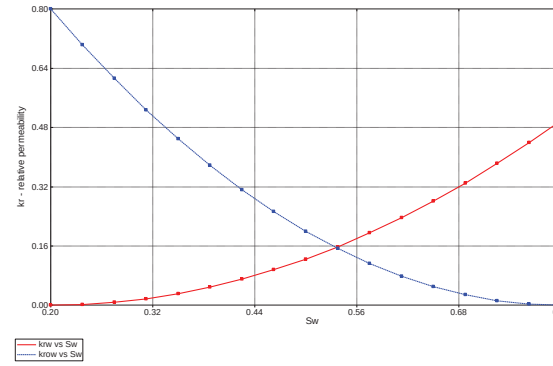

Fig. 14.33—Oil and water relative permeability versus water saturation in matrix.

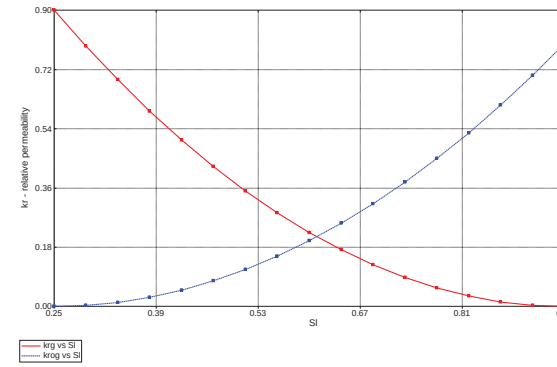

Fig. 14.34—Gas and oil relative permeability versus total liquid saturation in matrix.

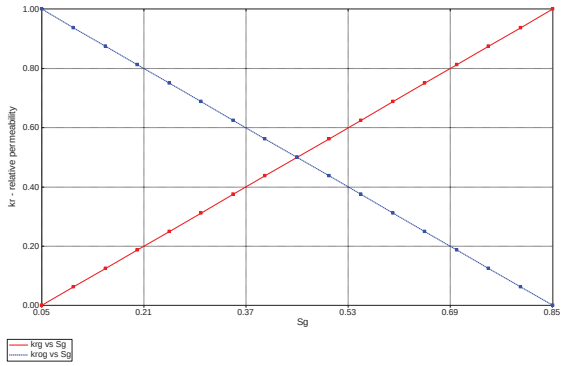

Fig. 14.35—Gas and oil relative permeability in fractures (propped and natural).

typically represented by tables of decreasing pore pressure using pressure-dependent porosity and permeability multipliers such as in **Fig. 14.36**, which shows four different curves representing four different models of permeability decline for the propped fractures.

Proppant permeability can decrease during the production life of hydraulically fractured tight, shale gas, or liquid wells as the effective stress increases over time. This stress leads to compaction, possibly crushing the proppant, and also possibly embedding the proppant into the walls of the propped fracture (the reservoir rock matrix). Lab tests of proppant porosity and permeability provide good initial indicators of the potential effects of compaction. However, unless the lab tests are done with fracture walls consisting of reservoir rock, the test results will not include the effects of embedment. For this reason, and because many previous sensitivity analyses have shown that tight or shale well productivity can be severely decreased by proppant compaction, the figures show four different sets of proppant compaction data in the EUR workflow example.

Step 3. Design a Grid

Design a flow simulation grid representing the discretization of the reservoir (matrix and natural fractures), the propped fractures, and the well. Populate that grid with the data assembled in Step 1 and Step 2.

Because the well being modeled is a single well that was drilled on 640-acre spacing, the simulation grid covers an area of 640 acres at a total reservoir thickness of 150 ft. The recommended practice is to set the length of the sides of each gridblock to be equal to, or less than, the natural fracture spacing. The gridblocks in this model are 50 ft. by 50 ft. Because log data suggests there are 5 distinct hydraulic flow units in the Eagle Ford where this well is located, we

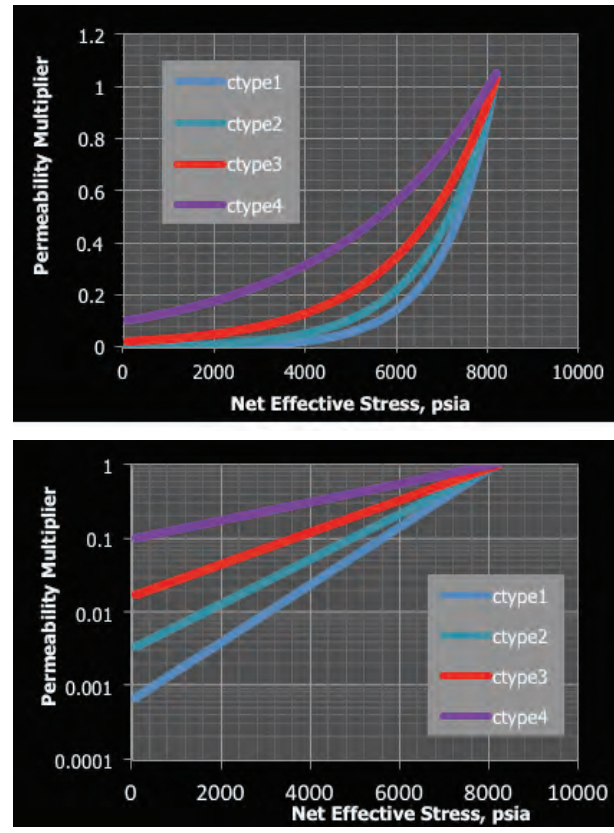

Fig. 14.36—Compaction data representing four different models of permeability decline for propped fractures on Cartesian (top) and log (bottom) scales.

subdivided the total thickness into 5 layers of equal 30-ft. thickness. The decision to make these five layers equal thickness was at the discretion of the model builder and not a limitation of the technology or workflow being used.

Two additional levels of grid discretization are required to model the presence of natural fractures and propped fractures in reservoir simulators.

Natural fractures could be represented explicitly by adding grids that follow the direction and width of those fractures. However, that would be very expensive in terms of run time because it requires a large number of additional gridblocks, and numerical instabilities can be introduced if very small gridblocks are included in the model. Fortunately, modern reservoir simulators have a more efficient method for including the effects of natural fractures, known as dual-continuum modeling (**Fig. 14.37**).

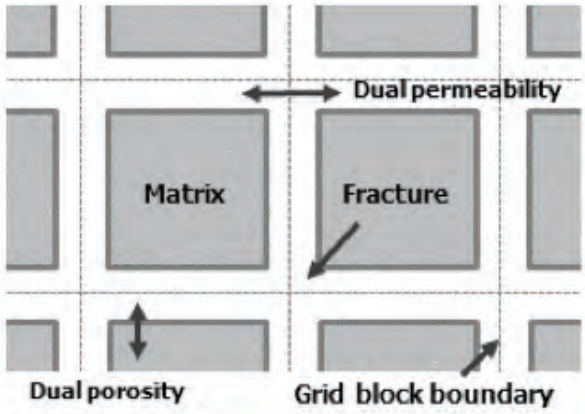

Fig. 14.37—The dual-continuum concept for representing natural fractures in reservoir simulators.

- In the dual continuum approach, each gridblock consists of a matrix block centered within a fracture block so that the simulator can model the matrix at one porosity and permeability and the fracture at another. If the designer chooses to model the formation as dual porosity, the simulator allows flow to go from matrix to fracture but not between matrix gridblocks. If it is dual permeability, fluid can flow between directly connected matrix gridblocks in addition to flowing between matrix and fracture gridblocks. The dual-permeability approach has important advantages over the dual-porosity approach.
- Propped fractures, unlike natural fractures, are best represented in reservoir simulation models using explicit gridblocks that follow the geometry of the fractures. Propped fractures are surrounded by a series of gridblocks of ever-increasing width that can properly capture the transient nature of fluid flow from very low-permeability rock matrix to the high-permeability proppant in the propped fracture matrix corridors.
- A grid design feature that automatically creates logarithmically spaced, locally refined gridblocks can model the propped fractures and surrounding matrix. It can also accommodate dual permeability to the mix to model any natural fractures that become opened during the hydraulic fracturing treatment operation. Because the resulting grid looks somewhat like a Scottish plaid, the term *tartan* is used for simplicity. A more technically precise definition for the tartan grids is LS-LR-DK grids, which stands for logarithmically spaced, locally refined, dual-permeability grids. **Fig. 14.38** shows two tartan grids, one for planar and the other for complex (intersecting) propped fracture geometries.

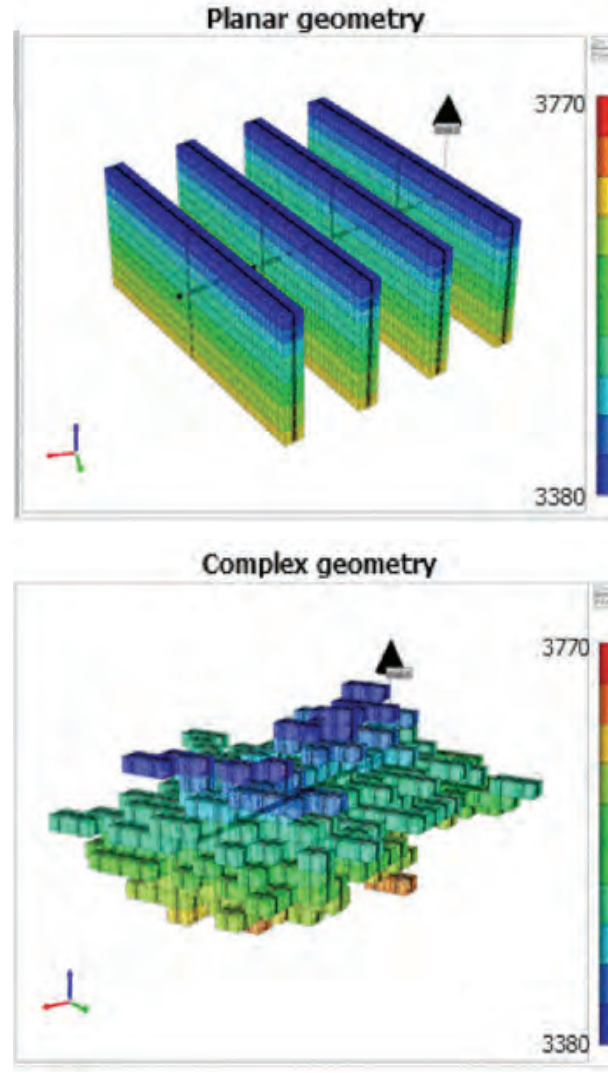

Fig. 14.38—Tartan gridding represents propped fractures in reservoir simulation models of unconventional wells.

- The discretized grid of the single Eagle Ford well includes both visible matrix and invisible natural fracture gridblocks, as well as the visible LS-LR gridblocks used to represent the 10 fracturing stages that were pumped into this well. The assumption was that each of the four perforations in each stage created a single planar geometry propped fracture whose dimensions vary according to the data ranges in **Table 14.10**. In the following 2D areal views of the simulation grid (**Fig. 14.39**), the planar propped fracture gridding is visible and prominent.

Fig. 14.40 is a 3D perspective view in transparency mode and shows the well location with respect to the propped fractures from the inside of the grid.

Step 4. Perform a Sensitivity Analysis

Perform the sensitivity analysis to determine which uncertain reservoir, well, and fracturing treatment parameters have the greatest influence on the observed production. This analysis can provide useful information that can help with direct data-gathering decisions and reduce the number of variables used in the next step for history matching.

The sensitivity analysis step involves using the PE tool to automatically make multiple passes of the reservoir simulation model, with each pass being referred to as an experiment, to assess the sensitivity of cumulative oil, gas, and water production volumes, as well as flowing bottomhole pressure (BHP), to changes in the values of the 8 parameters in Table 14.9 as having a range of possible values.

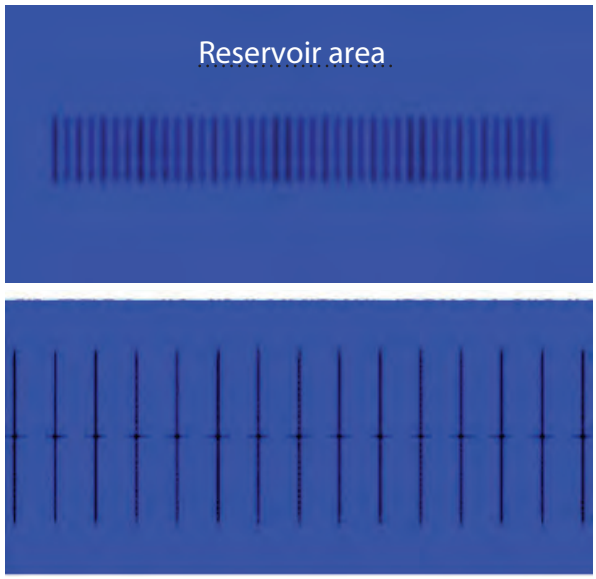

Fig. 14.39—The 2D areal tartan grids show the 41 propped planar geometry fractures. The zoomed-in bottom view shows propped fracture corridor.

Table 14.10—Simulation grid statistics.

Grid Property	Value
X and Y direction lengths, ft.	50
Z direction length, ft.	30
No. of X and Y direction grids	105
No. of Z direction grids (layers)	5
No. of parent gridblocks	55,125
No. of tartan grids when Xf = 275 ft.	33,825
Total gridblocks when Xf=275 ft.	88,950

Fig. 14.40—A 3D perspective view of simulation grid includes the planar propped fractures.

The PE tool used accommodates the use of discrete or continuous values, with the latter being supplemented with a probability density function. The values used for this sensitivity analysis in this example are in **Table 14.11**.

The PE tool used allows the user to select the sampling technique and the total number of patterns, or combinations of data. In this case the Latin hypercube sampling method was used to generate 100 patterns. The PE tool then presents the results of the sensitivity analysis in a variety of formats. Among these, tornado plots (**Fig. 14.41**) may be the most useful for understanding the results.

These tornado plots show two important sets of information. The magnitude and direction of the bars next to each of the uncertain parameters indicate the size and direction of their effect. The other important information is clustered at the top of the charts, where the maximum, target, and minimum bars are found. If the maximum and minimum bars bracket the target bar for a given variable, then at the very least the ranges supplied for the uncertain variables will allow a history-match to be achieved for that objective function (e.g., Cum_Oil, Cum_Gas, Cum_Water or FBHP).

For this specific set of input data and range of uncertain parameters, the most sensitive parameter affecting cumulative oil is matrix permeability. A wide range of values was used in this situation to mimic the real-world situation in which matrix permeability may well be unmeasured or unmapped at the time the EUR calculation is done. The second most sensitive parameter for cumulative oil is propped fracture half-length.

Table 14.11—Discrete values used in sensitivity analysis.

Matrix Perm, md	Matrix Porosity, fraction	Nat Fracturing Swi, fraction	Rock Comp Table No.	Fracturing Half-Length, Ft.	Propped Fracturing		
					Perm, md	Spacing, Ft.	Swi, fraction
0.00001	0.04	0.15	"ctype1.inc"	50	1,000	100	0.15
0.0001	0.06	0.25	"ctype2.inc"	150	10,000	200	0.25
0.0005	0.08	0.35	"ctype3.inc"	250	20,000	300	0.35
0.001	0.10	0.45	"ctype4.inc"	400	30,000	400	0.55

Cumulative water production is most sensitive to propped fracture half-length and the initial water saturation in the propped fractures, which is not surprising.

FBHP is most sensitive to propped fracture half-length and propped fracture spacing, parameters that help control flow capacity, and therefore, pressure drops that contribute to the flowing BHP calculation.

Step 5. Perform an Aided History Match

Calculated EUR is important and potentially time-consuming. It involves making a series of simulation model runs while changing the many possible reservoir, well, and completion parameter values to arrive at multiple combinations of parameters that produce equally or near-equally good history matches.

As with the sensitivity analysis the PE tool selects a set of continuous or discrete values for each uncertain parameter

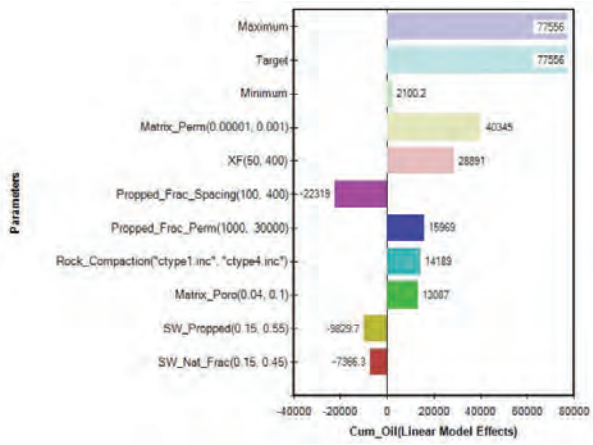

Fig. 14.41—Tornado plots show the effects of the eight factors on cumulative oil and water and BHP.

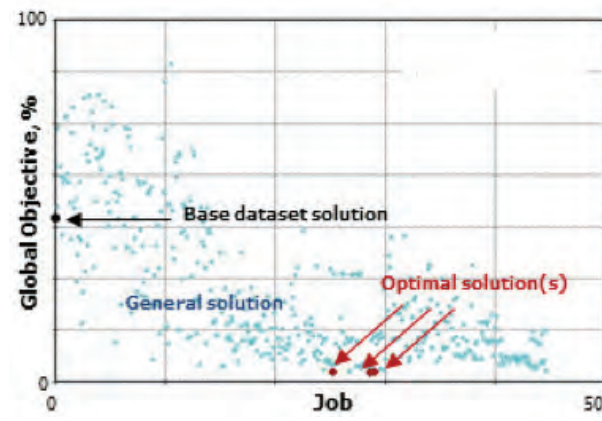

Fig. 14.42—Output from the PE tool indicates that 15 of the possible combinations produce a global objective error less than 3. Run 286 was identified as the optimal combination, with an error rate at only 1.87%.

as the PE tool makes its way through the many, many combinations of parameters the optimization engine indicates it should explore. Those values are listed in **Table 14.12**.

This list of continuous and discrete values for the eight uncertain parameters selected for this history match results in a set of possible combinations of data (i.e., models) totaling 6.22 million. The PE tool allows users to simply monitor the plots of their defined global objective function versus run number while working on other projects. In this case, the global objective function to be minimized was designed to include the weighted average error between the simulated versus the observed and/or measured cumulative oil, cumulative gas, cumulative water, and flowing BHP values. A plot of that global objective function versus simulator run number is shown in **Fig. 14.42**.

The PE tool reduced the global objective function error from a little over 30% for the base case model to a minimum value

Table 14.12—Discrete values used in sensitivity analysis.

Matrix Perm, md	Matrix Por, fraction	Nat Fracturing Swi, fraction	Rock Comp Table #	Fracturing Half- Length, ft.	Propped Fracturing		
					Perm, md	Spacing, Ft.	Swi, fraction
0.00001	0.04	0.15	"ctype1.inc"	50	1,000	100	0.15
0.00005	0.05	0.16	"ctype2.inc"	150	5,000	150	0.20
0.0001	0.06	0.17	"ctype3.inc"	150	10,000	200	0.25
0.0002	0.07	0.18	"ctype4.inc"	200	15,000	250	0.30
0.0003	0.08	0.20		250	20,000	300	
0.0004		0.25		300			
0.0005		0.30					
0.0007		0.35					
0.001							

of 1.87% for run number 286 (from the tabular form of the data). Fifteen of the run passes (i.e., combinations of data) produced a global objective function error less than 3%.

The PE tool continued searching the solution space for a total of 446 run passes before concluding that it had already found the best solutions to this problem. It is advantageous to see the plots of simulated versus production data to verify that the PE tool is converging on a good match (**Fig. 14.43**).

Matches of oil rate and cumulative oil are easier to obtain because observed oil rates were specified for the model with the observed oil production history. In order to produce what was observed, the model had to have sufficient flow capacity. Transient inflow performance is a significant source of that flow capacity in very-low-permeability reservoirs. Therefore, the reservoir must be gridded properly similar to modeling a short-term pressure buildup or drawdown test. In this example, a radial grid was used with a logarithmically spaced grid circling the well in ever-increasing radii away from the well to capture the transient pressure response.

In the case of unconventional reservoirs, transient response is in both the production rate and flowing BHP (i.e., both are changing with time throughout the very long transient flow duration), and it persists for a long time (until drainage-boundary effects are felt, either from a physical boundary or a man-made one such as interference from another well).

Matches for the other production variables are good, since the process of generating these matches is systematic and automatic. The work hours and computer time required to perform this history match are discussed at the end of this exercise on EUR calculation.

Step 6. Forecast Future Production from the Best History-Matched Models

Extend the best history match models into the future to calculate a range of EURs. This was done for the top 15 history match datasets.

This process concludes with a range of possible EURs for oil and gas, with an associated ranking in terms of history match quality (error). Results can be summarized as shown in **Table 14.13**.

Using numerical models to determine EURs in unconventional reservoirs using the six-step process described above produced a range of physically possible EUR values that are based purely on first principles that do not

Table 14.13—Statistical analysis of EURs.

	Oil EUR (stb)	Gas EUR (MMscf)
Maximum	724,059	981
Minimum	571,847	851
Average	654,125	926
Median	649,323	922
Std Dev	45162	44

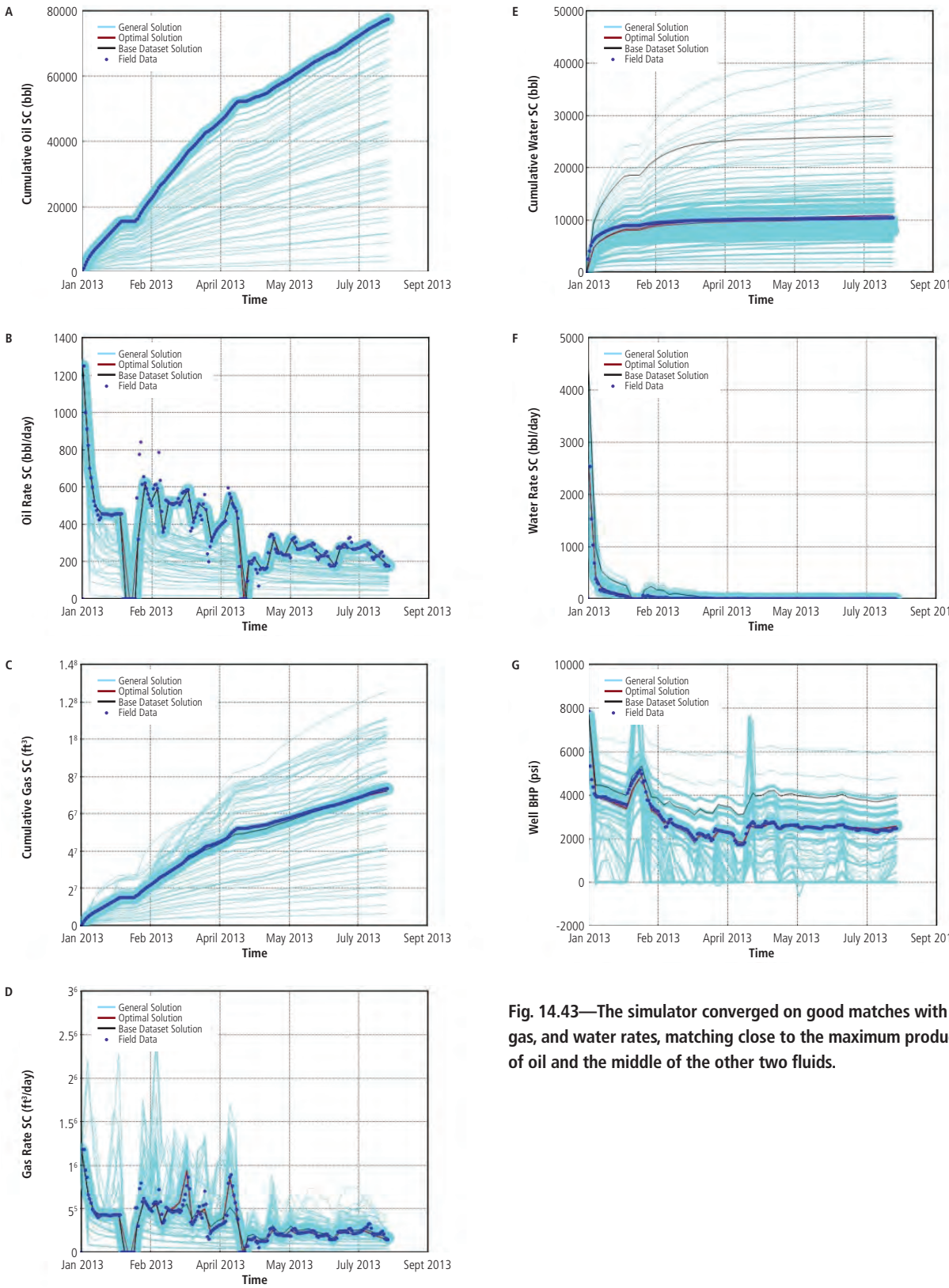

Fig. 14.43—The simulator converged on good matches with oil, gas, and water rates, matching close to the maximum production of oil and the middle of the other two fluids.

depend on curve-fitting, pattern recognition, or the large list of limiting assumptions associated with DCA-based and RTA-based production data analysis methods.

Table 14.14 summarizes the man-time and calendar time required to make the 561 reservoir simulation runs made for this analysis.

Table 14.14—Time to make runs.

Task	Time (hours)	Time/run (min)
Engineer's time to set up base model and PE tool input	8	NA
Time to make 100 SA model runs*	5.5	3.3
Time to make 446 HM model runs*	21	2.8
Time to make 15 30-year forecast model runs**	1	4.0
Total time for all model runs	27.5	2.9

* 2 simultaneous 2-way parallel black oil simulator runs on a Dell M4700 laptop

** Sequential 4-way parallel black oil simulator runs on a Dell M4700 laptop

14.8.2 Application No. 2. Optimizing the Number and Size of Propped Fractures for a Single Well

Forecasting EUR for a single well using the physics-based approach described previously naturally leads to the extension to multiwell EUR calculation and optimization, in terms of optimum fracturing design and optimum well spacing. The previously used Eagle Ford oil window data will be used to optimize the fracturing design for a single well in this section. This exercise will take advantage of the previous example, but that is not a prerequisite for successfully performing this task.

The objective is to maximize net present value (NPV) of new wells over a (arbitrary) 30-year producing lifetime by using the result of the previous EUR calculation and to condition the results for risk. As was the case for Application No. 1, this optimization was performed using the available data and RSNM+PE technology. The process was as follows.

Step 1. List the Well Information

List the known or assumed information about nearby wells, including the producing interval (the reservoir) and the fluid properties of the oil and gas that will likely be produced. These values are shown in **Table 14.15**.

Table 14.15—Known properties.

Property	Value
Depth at top of reservoir, ft.	10,800
Reservoir thickness, ft.	150
Initial reservoir pressure, psi	8,100
Initial reservoir temperature, F°	270
Oil bubble point pressure, psi	3,010
Oil gravity, °API	43
Initial solution gas/oil ratio, scf/STB	950
Lateral length, ft	4,000
Number of fracture stages pumped	10

Step 2. List the Properties and Uncertain Parameters

List the unknown or assumed reservoir properties and the proposed well properties (such as permeability, capillary pressure, and well spacing), and fracturing treatment parameters, as shown in **Table 14.16**.

Also required is an assumed set of economic parameters as shown in **Table 14.17**.

Finally, the PE tool allows for handling both continuous and discrete values for unknown parameters when used for optimization tasks. Those values are listed in **Table 14.18**.

Step 3. Design a Base RSNM model

As was the case for Application No. 1, this step is to design a base RSNM representing the discretization of the reservoir (matrix and natural fractures), the propped fractures, and the well, and to populate that grid with the data assembled in Step 1 and Step 2. This base RSNM is similar in appearance to that for Application No. 1; that section provides a description of the model construction details, including the grid design.

Step 4. Perform the NPV Optimization

The optimization process is next, which is performed by the PE tool. The PE tool is used to help define which parameter value combinations to run as the optimization process moves forward from the one or more equally optimum values of the user's objection function. For Application No. 2, the optimum value is the NPV of 30 years' worth of oil and gas production revenue. This production value is, in turn, offset by the initial cost to drill and complete the well under a variety of fracturing treatment design scenarios. The design scenarios are selected by the PE tool as a basis that leads to one or more optimal solutions, as shown in **Fig. 14.44**.

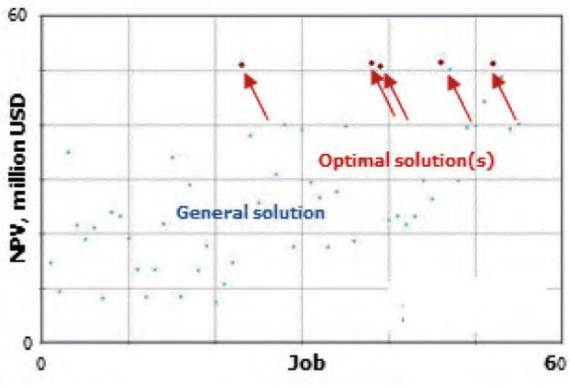

Fig. 14.44—Fifty-five identified propped fracture design combinations from the PE Tool, including five that led to an equally optimal NPV of USD 48.5 million.

Of the 240 total possible value combinations, the PE tool identified 55 combinations to use in full-simulation model runs. From these 55, there were 5 different sets of propped fracture design combinations that led to equally optimal values of NPV (48.5 million USD after subtracting the 3 million USD drilling cost).

What is interesting about this example, and perhaps not intuitive given the assumed matrix permeability of 500 nd, are the final values the PE tool selected for the 5 equally optimal combinations. Those values are given in the three-parameter histograms shown in **Fig. 14.45**.

What the histograms reveal is that all optimum NPV combinations of parameters used the minimum propped fracture spacing and the maximum propped fracture half-length (the maximum cross-sectional area exposed to the matrix), and that any propped fracture permeability above 9 darcies was sufficient.

These results were further tested by running the optimization at matrix permeabilities of 100 nd and 1,000 nd (**Fig. 14.46**).

Although the optimum NPV changed (23.5 million USD for 100 nd and 63.2 million USD for 1,000 nd), the propped fracture treatment parameters that produced those optimum NPVs were the same for all 3 matrix permeabilities. This will not necessarily hold true for other values of matrix permeability.

Table 14.16—Ranges for unknown or assumed reservoir parameters and proposed well and fracturing treatment properties, reservoir parameters, and proposed well and fracturing treatment properties. 14—Time to make runs.

Property	Min. Value	Max. Value
Reservoir matrix porosity, fraction	0.05	0.05
Reservoir matrix permeability, nd	400	400
Reservoir natural fracture effective porosity, fraction	0.0006	0.0006
Reservoir natural fracture effective permeability, nd	40	40
Reservoir natural fracture x-direction spacing, ft.	50	50
Reservoir natural fracture y-direction spacing, ft.	50	50
Reservoir natural fracture z-direction spacing, ft.	0	0
Proposed well spacing, acres	640	640
Proposed well lateral length, ft.	4,000	4,000
Proposed propped fracture spacing, ft.	200	800
Proposed propped fracture permeability, darcy	50	400
Reservoir matrix relative permeability	1	20
Reservoir natural fracture relative permeability	Corey functions from Application No. 1 used	
Propped fracture relative permeability	Straight lines from Application No. 1 used	
Reservoir matrix capillary pressure	Straight line from Application No. 1 used	
Reservoir natural fracture capillary pressure	Corey function based Pc from Application No. 1	
Propped fracture capillary pressure	Assumed to be zero as in Application No. 1	
Reservoir matrix pore volume compaction	Assumed to be zero as in Application No. 1	
Reservoir natural fracture pore volume compaction	Constant natural fracture PV compressibility	
Propped fracture pore volume compaction	ctype4.inc from Application No. 1 used	

Table 14.17—Assumed Economic Parameters

Economic Parameter	Value
Oil price (USD/bbl)	100
Gas price (USD/Mscf)	3
Well drilling cost (millions USD)	3
Fracturing cost (USD/Stage)	250,000
Forecast period (years)	30

In **Fig. 14.46**, the slope reduction at a matrix permeability of approximately 480 nd suggests that the benefit of maximum cross-sectional exposure begins to be reduced there.

In **Fig. 14.47**, the 5 optimal propped fracture designs are compared with all 50 of the other examined combinations. With few exceptions, the optimal designs outperform all of the others for most of the simulated production period.

Table 14.19 summarizes the work hours expended (8 hours) and the time required to make the 55 runs (3.4 hours) that were required to optimize the propped fracture design for a single well in a 640-acre section.

14.8.3 Application No. 3.—Optimizing Well Spacing

Determining the number of wells to be drilled per section to optimize NPV is easier with the PE tool. For this example, four additional RSNMs were constructed using the optimum propped fracture design parameters determined in Application No. 2 and applying them to models that included 2, 3, 4, and 5 wells in the original 640-acre section. The four-well grid is shown in **Fig. 14.48**.

Table 14.18—Proposed Fracturing Treatment Parameter Values.

Propped fracturing spacing, ft.	Propped fracturing permeability, darcy	Propped fracturing half-length, ft.
200	1	50
300	3	100
400	6	200
500	9	300
600	12	400
800	15	
	18	
	20	

Cumulative oil production and NPV over the 30-year forecast period is presented in **Fig. 14.49** for all 5 well spacings and densities.

After 30 years of production in the 4-well and 5-well cases, regions in the corners of the 640-acre section still have not experienced a significant drop in matrix pore pressure for the case of 500 nd matrix permeability, which is a typical permeability value for shale reservoirs..

The influence of boundary effects, both between the wells within a section and between sections, can perhaps best be appreciated by re-running this same exercise with a much higher matrix permeability. **Fig. 14.50** compares NPV for the number of wells in a 640-acre section for both the original case (matrix permeability of 500 nd) and a much higher matrix permeability case of 100,000 nd (0.1 md), which is closer in matrix permeability to the Middle Bakken formation.

NPV continues to increase from one to five wells even in the higher matrix permeability case, although the slope of the line reduces significantly after the second well comes online. This suggests that interference effects become important when reservoir permeability is closer to conventional reservoir magnitudes. This is the case with special shales like the Middle Bakken, which is actually more like sandstone and carbonate, and has a matrix permeability ranging from tenths of a millidarcy to several millidarcies.

Table 14.20 summarizes the hours expended (8 hours) and the calendar time required to make the five runs (3.4 hours) that were required to optimize the well spacing for this 640-acre section.

14.8.3.1 RSNM Features and Grid Design

RSNM features and grid design are required to accurately calculate the transient fluid flow behavior observed in most unconventional reservoirs.

A listing of the physics required to model fluid flow in unconventional reservoirs and the features available in two commercially available reservoir simulators (one using a black oil PVT model and the other an equation-of-state PVT model) are shown in **Table 14.21**.

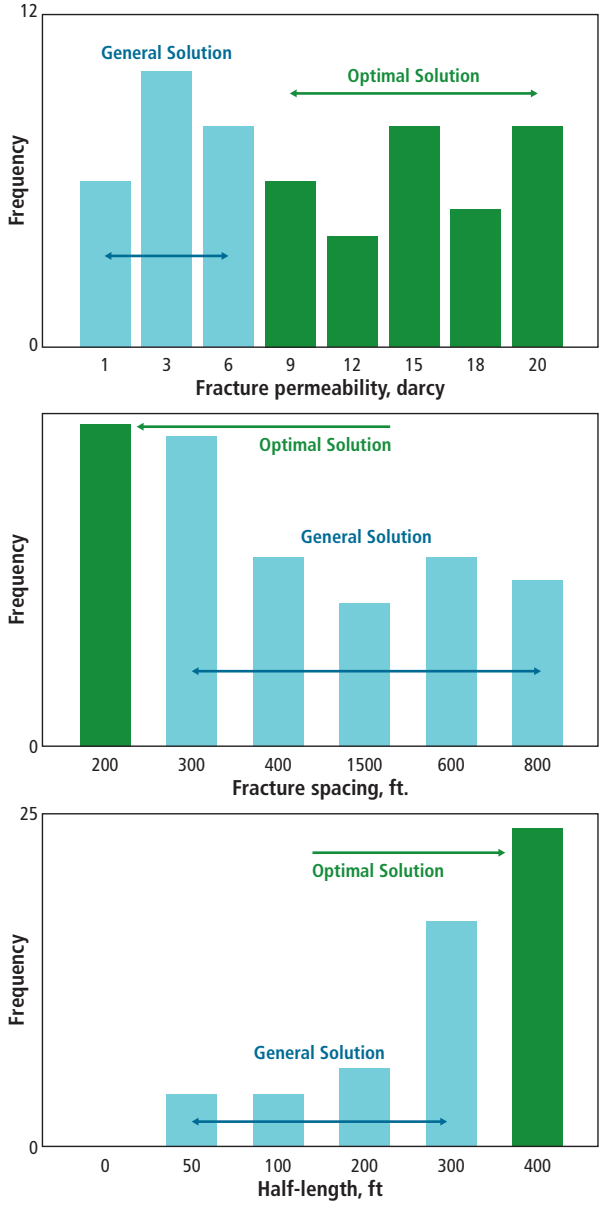

Fig. 14.45—All optimal parameter combinations had long half-lengths, closely spaced fractures, and propped fracture permeability of at least 9 darcies.

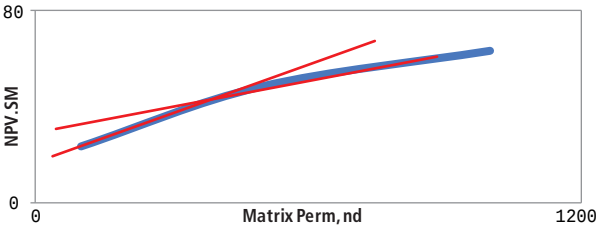

Fig. 14.46—Optimum NPV decreases rapidly at matrix permeabilities less than about 480 nd.

14.8.4 Review of Current Research on the Physics of Fluid Flow and Phase Behavior through Nanoscale Diameter Pore Throats

14.8.4.1 Nanoscale Pore Throat Diameter Effects

Many researchers are investigating the effects of nanometer-scale pore throat diameters on rock-fluid interactions (i.e., relative permeability and capillary pressures) and fluid properties (i.e., PVT data) and how they are represented in RSNMs. Phenomena like bubble point depression, Knudsen diffusion, and transient (i.e., non-equilibrium) capillary pressure behavior are all being discussed, and in some cases, quantified, with associated correction factors offered for current commercial RSNMs.

In most conclusions to date at the level of pore throat diameters where different behavior has been demonstrated, the resulting matrix permeabilities are too low to be of commercial significance. For example, several papers refer to 50 nm as the pore throat diameter at which the bubble point depression phenomenon begins to be observed. Using a correlation developed by Katz and Thompson (1986) and presented in Nelson's paper on unconventional reservoirs (2009):

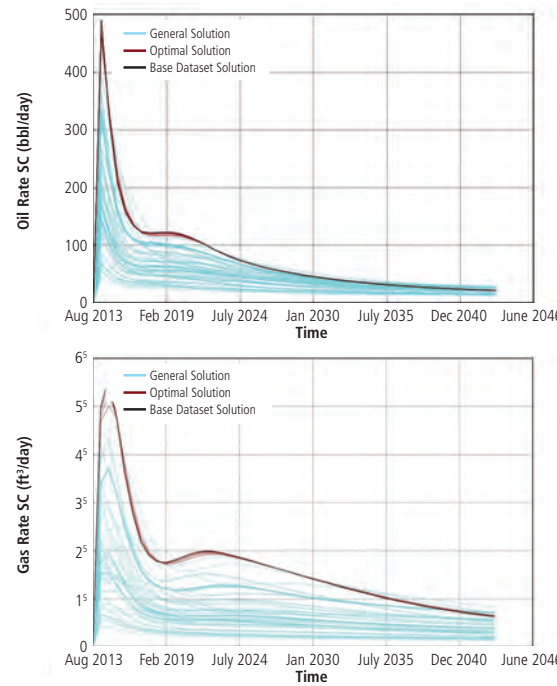

Fig. 14.47—The five optimal designs outperform all of the other designs for both oil and gas rate for most of the life of the wells.

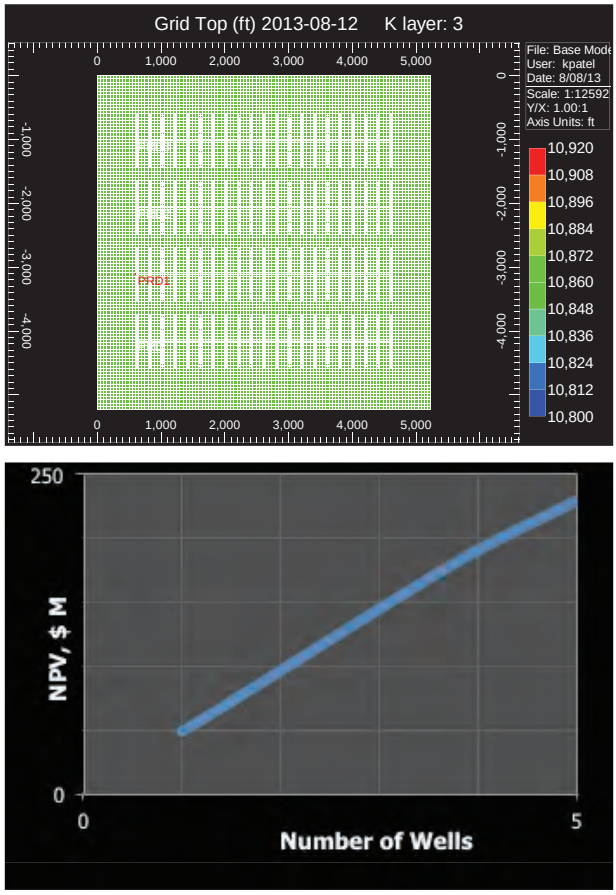

Fig. 14.48—Wells in 640-acre spacing.

where:

k = matrix perm (md)

d = pore throat diameter (micrometers)

ϕ = matrix porosity (fraction)

$$k \approx 4.48\, d^2\, \varphi^{2|} \qquad \textbf{(Eq. 14.5)}$$

A 50-nm pore throat diameter translates to a 28-nd matrix permeability at a 5% matrix porosity, which is substantially below the matrix permeabilities being exploited by currently commercial shale or tight liquids production plays.

The equivalent straight capillary tube permeability for a 50 nm capillary tube diameter is 15,832 nD (or 0.016 md). This is a potential source of confusion regarding how applicable the nanoscale pore throat diameter research is. In terms of straight capillary tube permeability, the magnitudes of permeability appear to be in the upper range of currently exploited shale/tight liquids plays, and thus the nanoscale phenomena should be taken into consideration in reservoir simulators.

Table 14.19—Work hours and computer time expended to produce a physics-based optimum propped fracturing design.

Task	Time, hours	Time for Model-Run, in Minutes
Engineer's time to set up base model and PE tool input	8.0	NA
Time to make 55 OPT model runs*	1.6	19.2

* Sequential four-way parallel black oil simulator runs on a Dell™ Precision M4700 Mobile Workstation M4700

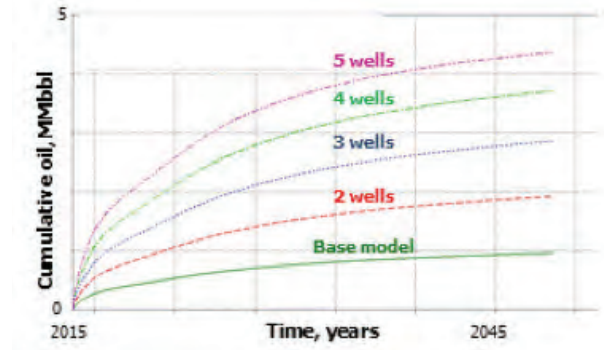

Fig. 14.49—Cumulative oil production over 30 years for the five cases (top) will result in NPVs just under 50 million USD per well (bottom).

14.8.4.2 Geomechanics and Geochemistry

A more significant effect on our ability to model the behavior of unconventional reservoirs is likely to be derived from the effects of geomechanics to the modeling of the hydraulic fracturing process and to compaction of propped fractures during production, and geochemistry on the mechanical properties of proppant that is exposed to fracturing fluids and in situ hydrocarbons and formation brines. Some commercial reservoir simulators already have these capabilities, although adding the extra layers of complexity may limit their routine use.

14.8.4.3 Low-Permeability Reservoir Rock-Fluid Interaction

A significant concern exists regarding the current capabilities of RSNMs to model the physics of unconventional reservoirs is the limited ability to define and/or predict matrix relative

Table 14.21—Unconventional reservoir fluid flow physics required and available in commercial reservoir simulators.

Physics	Black Oil Simulator	EOS Simulator
PVT	BO, VO, GC, and WG	Any fluid type
Adsorbed components	Gas phase only	All components
Molecular diffusion	No	All components within oil, gas, and water phases
Diffusion-like process for matrix to fracture fluid flow	No	Yes
Non-darcy (turbulent) fluid flow	Yes	Yes
Klinkenberg (slip) fluid flow	No	Yes
Multiple rock-fluid regions	Matrix, natural fractures and propped fractures	Matrix, natural fractures and propped fractures
Natural fractures	Dual porosity or permeability	Dual porosity or permeability
Propped fractures	Explicit tartan grids	Explicit tartan grids
Pressure-dependent compaction	Yes	Yes
Stress-dependent compaction	No	Yes (using coupled geomechanics)
Tartan (LS-LR-DK) gridding	Yes	Yes

Table 14.20—Work hours and computer time expended to produce a physics-based optimum propped fracturing design.

Task	Time, hours	Time for Model-Run, in Minutes
Engineer's time to set up base model & PE tool input	8.0	NA
Time to make 5 well density model runs*	3.4	7

* 2 simultaneous 2-way parallel black oil simulator runs on a Dell M4700 laptop

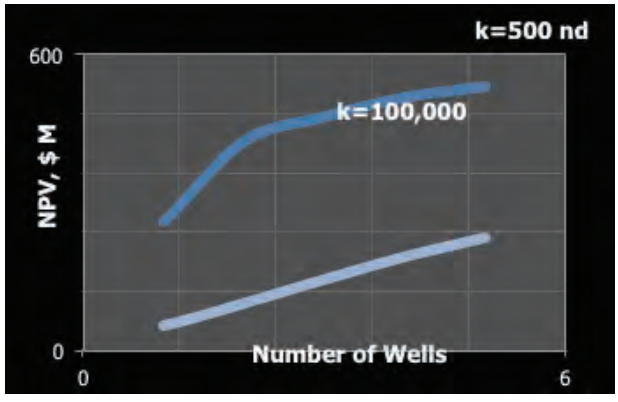

Fig. 14.50—In higher-permeability formations, interference effects become apparent beginning with the addition of the second well.

permeability and capillary pressure behavior under what amounts to an unmeasurable dataset. We know the general shape that very low permeability conditions impose on relative permeability and capillary pressure data, but we will not know for certain how real-world unconventional reservoirs behave with respect to matrix relative permeability and capillary pressure until we have a substantial population of wells exhibiting boundary-dominated flow behavior with matrix pressures below bubble point or dew point values.

We can certainly show the impact of a reasonable range of Corey exponents and endpoint relative permeabilities and saturation endpoints for very tight rocks, but until we have real-world data that is under the influence of multiphase flow conditions in the matrix we cannot be certain.

14.9 References

Agarwal, R.G, Gardner, D.C., Kleinsteiber, S.W., et al. 1998. Analyzing Well Production Data Using Combined-Type-Curve and Decline-Curve Analysis Concepts. Paper SPE 49222 presented at the SPE Annual Technical Conference and Exhibition. New Orleans, Louisiana. 27–30 September. http://dx.doi.org/10.2118/49222-MS.

Agarwal, R.G, Gardner, D.C., Kleinsteiber, S.W., et al. 1999. Analyzing Well Production Data Using Combined-Type-Curve and Decline-Curve Analysis Concepts. *SPE Res Eval & Eng.*, **2** (5): 478–486. SPE 57916-PA. http://dx.doi.org/10.2118/57916-PA.

Alvarez, C.H., Holditch, S.A., and McVay, D.A. 2002. Effects of Non-Darcy Flow on Pressure Transient Analysis of Hydraulically Fractured Gas Wells. Paper SPE 77468 presented at the SPE Annual Technical Conference and Exhibition. San Antonio, Texas. 29 September–2 October. http://dx.doi.org/10.2118/77468-MS.

Ambrose, R.J., Clarkson, C.R., Youngblood, J., et al. 2011. Life-Cycle Decline Curve Estimation for Tight/Shale Gas Reservoirs. Paper SPE 140519 presented at the SPE Hydraulic Fracturing Technology Conference. The Woodlands, Texas. 24–26 January. http://dx.doi.org/10.2118/140519-MS.

Anderson, D.M., Rushing, J.A., and Mattar, L. 2006. Production Data Analysis—Challenges, Pitfalls, Diagnostics. Paper SPE 102048 presented at the SPE Annual Technical Conference and Exhibition. San Antonio, Texas. 24–27 September. http://dx.doi.org/10.2118/102048-MS.

Baihly, J., Malpani, R., Edwards, C., et al. 2010. Unlocking the Shale Mystery: How Lateral Measurements and Well Placement Impact Completions and Resultant Production. Paper SPE 138427 presented at the SPE Tight Gas Completions Conference. San Antonio, Texas. 2–3 November. http://dx.doi.org/10.2118/138427-MS.

Bangall, W.D. and Ryan, W.M. 1976. The Geology, Reserves and Production Characteristics of the Devonian Shale in Southwestern Virginia. National Technical Information Service MERC/SP-76/, 41-53: ***Proceedings of the Seventh Appalachian Petroleum Geology Symposium,*** Morganstown, West Virginia, March 1976.

Barree, R.D., Cox, S.A., and Barree, V.L., et al. 2003. Realistic Assessment of Proppant Pack Conductivity for Material Selection. Paper SPE 84306 presented at the SPE Annual Technical Conference and Exhibition. Denver, Colorado. 5–8 October. http://dx.doi.org/10.2118/84306-MS.

Barree, R.D., Cox, S.A., Gilbert, J.V., et al. 2003. Closing the Gap: Fracture Half Length from Design, Buildup, and Production Analysis. Paper SPE 84491 presented at the SPE Annual Technical Conference and Exhibition. Denver, Colorado. 5–8 October. http://dx.doi.org/10.2118/84491-MS.

Beier, B.A. 1990. Pressure Transient Field Data Showing Fractal Reservoir Structure. Paper SPE 21553 presented at the CIM/SPE International Technical Meeting, Calgary, Alberta, Canada. 10–13 June. http://doi.org/10.2118/21553-MS.

Blasingame T.A., McCray, T.L., and Lee, W.J. 1991. Decline Curve Analysis for Variable Pressure Drop/Variable Flow rate Systems. Paper SPE 21513 presented at the SPE Gas Technology Symposium. Houston, Texas. 22–24 January. http://dx.doi.org/10.2118/21513-MS.

Camatcho-Velasquez, R., Fuentez-Cruz, G., and Vasquez-Cruz, M. 1988. Decline Curve Analysis of Fractured Reservoirs with Fractal Geometry. ***SPE Res Eval & Eng***, **11** (3): 606–619. SPE 104009-PA. http://dx.doi.org/10.2118/104009-PA.

Chang, J. and Yortsos, Y.C.1990. Pressure Transient Analysis of Fractal Reservoirs. ***SPE Form Eval***, **5** (1): 31–38. SPE 18170-PA. http://dx.doi.org/10.2118/18170-PA.

Cheng, Y., Lee, W.J., and McVay, D.A. 2007. A New Approach for Reliable Estimation of Hydraulic Fracture Properties in Tight Gas Wells. Paper SPE 105767 presented at the SPE Hydraulic Fracturing Technology Conference. College Station, Texas. 29–31 January. http://dx.doi.org/10.2118/105767-MS.

Chu, L., Ye, P., Harmawan, I., et al. 2012. Characterizing and Simulation the Non-Stationariness and Non-Linearity in Unconventional Oil Reservoirs: Bakken Application. Paper SPE 161137 presented at the SPE Canadian Unconventional Resources Conference. Calgary, Alberta, Canada. 30 October–1 November. http://dx.doi.org/10.2118/161137-MS.

Cinco-Ley, H. and Meng, H.-Z. 1981. Transient Pressure Analysis: Finite Conductivity Fracture Case Versus Damaged Fracture Case. Paper SPE 10179 presented at the SPE Annual Technical Conference and Exhibition. San Antonio, Texas. 4–7 October. http://dx.doi.org/10.2118/10179-MS.

Cinco-Ley, H. and Samaniego-V, F. 1981. Transient Pressure Analysis for Fractured Wells. ***J. Pet Tech.*** **33** (9): 1749–1766. SPE-7490-PA. http://dx.doi.org/10.2118/7490-PA.

Cipolla, C.L. 2014. Microseismic Interpretations and Applications: Beyond SRV. Presented to MicroSeismic, Inc. User Group Meeting. February 19, 2014, http://www.microseismic.com/brochures/Cipolla-Presentation-Public.pdf (accessed July 2014).

Cipolla, C.L., Fitzpatrick, T., Williams, M., et al. 2011c. Seismic to Simulation for Unconventional Reservoirs. Paper SPE 146876 presented at the SPE Reservoir Characterization and Simulation Conference and Exhibition. Abu Dhabi, UAE. 9–11 October. http://dx.doi.org/10.2118/146876-MS.

Cipolla, C.L., Lolon, E., Erdle, J.C., et al. 2009. Reservoir Modeling in Shale-Gas Reservoirs. Paper SPE 125530 presented at the SPE Eastern Regional Meeting. Charleston, West Virginia. 23–25 September. http://dx.doi.org/10.2523/125530-MS.

Cipolla, C.L., Maxwell, S., and Mack, M. 2012. Engineering Guide to the Application of Microseismic Interpretations. Paper SPE 152165 presented at the SPE Hydraulic Fracturing Technology Conference. The Woodlands, Texas. 6–8 February. http://dx.doi.org/10.2118/152165-MS.

Cipolla, C.L., Lolon, E., and Mayerhofer, M.J. 2008a. Resolving Created, Propped and Effective Hydraulic Fracture Length. Paper IPTC-12147 presented at the International Petroleum Technology Conference. Kuala Lumpur, Malaysia. 3–5 December. http://dx.doi.org/10.2523/12147-MS.

Cipolla, C.L., Lolon, E., and Mayerhofer, M.J. 2009. Resolving Created, Propped and Effective Hydraulic Fracture Length. *SPE Prod & Oper.* **24** (4): 619–628. SPE 129618-PA. http://dx.doi.org/10.2523/129618-PA.

Cipolla, C.L. and Mayerhofer, M.J. 1998. Understanding Fracture Performance by Integrating Well Testing and Fracture Modeling. Paper SPE 49044 presented at the SPE Annual Technical Conference and Exhibition. New Orleans, Louisiana. 27–30 September. http://dx.doi.org/10.2118/490445-MS.

Cipolla, C.L., Maxwell, S., Mack, M, et al. 2011b. A Practical Guide to Interpretation Microseismic Measurements. Paper SPE 144067 presented at the SPE North American Unconventional Gas Conference and Exhibition. The Woodlands, Texas. 14–16 June 2011. http://dx.doi.org/10.2118/144067-MS.

Cipolla, C.L. and Wallace, J. 2014. Stimulated Reservoir Volume: A Misapplied Concept. Paper SPE 168596 presented at the SPE Hydraulic Fracturing Technology Conference. The Woodlands, Texas. 4–6 February. http://dx.doi.org/10.2118/168596-MS.

Cipolla, C.L., Warpinski, N.R., Mayerhofer, M.J., et al. 2008b. The Relationship between Fracture Complexity, Reservoir Properties, and Fracture Treatment Design. Paper SPE 115769 presented at the SPE Annual Technical Conference and Exhibition. Denver, Colorado. 21–24 September. http://dx.doi.org/10.2118/115769-MS.

Cipolla, C.L., Weng, X., Mack, et al. 2011a. Integrating Microseismic Mapping and Complex Fracture Modeling to Characterize Fracture Complexity. Paper SPE 140185 presented at the SPE Hydraulic Fracturing Technology Conference and Exhibition. The Woodlands, Texas. 24–26 January. http://dx.doi.org/10.2118/140185-MS.

Cipolla, C.L., Williams, M.J., Weng, X., et al. 2010. Hydraulic Fracture Monitoring to Reservoir Simulation: Maximizing Value. Paper SPE 133877 presented at the SPE Technical Conference and Exhibition. Florence, Italy. 19–22 September. http://dx.doi.org/10.2118/133877-MS.

Cipolla, C.L. and Wright, C.A. 2000. Diagnostic Techniques to Understand Hydraulic Fracturing: What? Why? And How? Paper SPE 59735 presented at the SPE/CERI Gas Technology Symposium. Calgary, Alberta. Canada. 3–5 April. http://dx.doi.org/10.2118/59735-MS.

Crafton, J.W. and Anderson, D. 2006. Use of Extremely High Time-Resolution Production Data to Characterize Hydraulic Fracture Properties. Paper SPE 103591 presented at the SPE Annual Technical Conference and Exhibition. San Antonio, Texas. 24–27 September. http://dx.doi.org/10.2118/103591-MS.

Daniels, J., Waters, G., LeCalvez, J., et al. 2007. Contacting More of the Barnett Shale through an Integration of Real-Time Microseismic Monitoring, Petrophysics, and Hydraulic Fracture Design. Paper SPE 110562 presented at the SPE Annual Technical Conference and Exhibition. Anaheim, California. October 12–14. http://dx.doi.org/10.2118/110562-MS.

Detring, J. and Williams-Stroud, S. 2012. Using Microseismicity to Understand Subsurface Fracture Systems and Increase the Effectiveness of Completions: Eagle Ford Shale, TX. Paper SPE 162845 presented at the SPE Canadian Unconventional Resources Conference. Calgary, Alberta, Canada. 30 October–1 November. http://dx.doi.org/10.2118/162845-MS.

Dohmen, T., Zhang, J., Li, C., et al. 2013. A New Surveillance Method for Delineation of Depletion Using Microseismic and Its Application to Development of Unconventional. Paper SPE 166274 presented at the SPE Annual Technical Conference and Exhibition. New Orleans, Louisiana. 30 September–2 October. http://dx.doi.org/10.2118/166274-MS.

Downie, R., Xu, J., Grant, D., et al. 2013. Utilization of Microseismic Event Source Parameters for the Calibration of Complex Hydraulic Fracture Models. Paper SPE Paper 163873 presented at the SPE Hydraulic Fracturing Technology Conference. The Woodlands, Texas. 4–6, February. http://dx.doi.org/10.2118/163873-MS.

Du, C., Zhang, X., Melton, D., et al. 2009. A Workflow for Integrated Barnett Shale Reservoir Modeling and Simulation. Paper SPE 122934 presented at the SPE Latin American and Caribbean Petroleum Engineering Conference. Cartagena, Columbia. 31 May–3 June. http://dx.doi.org/10.2118/122934-MS.

Du. C., Zhang, X., Zhan, L., et al. 2010. Modeling Hydraulic Fracturing Induced Fracture Networks in Shale Gas Reservoirs as a Dual Porosity System. Paper SPE 132180 presented at the International Oil & Gas Conference and Exhibition. Beijing, China. 8–10 June. http://dx.doi.org/10.2118/132180-MS.

Duong, A.N. 2010. An Unconventional Rate Decline Approach for Tight and Fracture-Dominated Gas Wells. Paper SPE 137748 presented at the Canadian Unconventional Resources and International Petroleum Conference. Calgary, Alberta, Canada. 19–21 October. http://dx.doi.org/10.2118/137748-MS.

Ehlig-Economides, C.A. and Ramey, H.J, 1981. Transient Decline Analysis for Wells Produced at Constant Rate. Paper SPE 8387, July 1979, *Society of Petroleum Engineering Journal*, **21** (1): 98–104, SPE 8387-PA. http://dx.doi.org/10.2118/83878-PA.

Ehlig-Economides, C.A., Valko, P., Dyashev, I.S., et al. 2006. Pressure Transient and Production Data Analysis for Hydraulic Fracture Treatment Evaluation. Paper SPE 101832 presented at the 2006 SPE Russian Oil and Gas Technical Conference and Exhibition. Moscow, Russia. 3–6 October. http://dx.doi.org/10.2118/101832-MS.

Elbel, J. and Ayoub, J. 1992. Evaluation of Apparent Fracture Lengths Indicated from Transient Tests. *J. Cdn, Pet Tech*, **31** (10). PETSOC92-10-05. http://dx.doi.org/10.2118/92-10-05.

England, K.W., Poe, B.D., and Conger, J.G. 2000. Comprehensive Evaluation of Fractured Gas Wells Utilizing Production Data. Paper SPE 60285 presented at the SPE Rocky Mountain Regional/Low Permeability Reservoirs Symposium. Denver, Colorado. 12–15 March. http://dx.doi.org/10.2118/60285-MS.

Fetkovich, M.J. 1980. Decline-Curve Analysis Using Type Curves. *J. Pet Tech*, **32** (6): 1065–1077. SPE 4629-PA. http://dx.doi.org/10.2118/4629-PA.

Fisher, M.K., Davidson, B.M., Goodwin, A.K., et al. 2002. Integrating Fracture Mapping Technologies to Optimize Stimulations in the Barnett Shale. Paper SPE 77441 presented at the SPE Annual Technical Conference and Exhibition. San Antonio, Texas. September 29–October 2. http://dx.doi.org/10.2118/77441-MS.

Fisher, M.K., Heinze, J.R., Harris, C.D., et al. 2004. Optimizing Horizontal Completion Techniques in the Barnett Shale Using Microseismic Fracture Mapping. Paper SPE 90051 presented at the SPE Annual Technical Conference and Exhibition. Houston, Texas. 26–29 September. http://dx.doi.org/10.2118/90051-MS.

Hara, S. K. and Stanecki J. A. 1986. A simplified Model for Fluid Flow in South Belridge Diatomite. Shell Development Company, Bellaire Research Center, Sept 15.

Hart's E & P. 2012. News and resource provider for exploration and production. http://www.epmag.com.

Holditch, S.A., Lee, W.J., and Gist, R. 1983. An Improved Technique for Estimating Permeability, Fracture Length and Fracture Conductivity from Pressure Buildup Tests in Low Permeability Gas Wells. *J. Pet Tech*., **35** (5): 81–90. SPE-9885-PA. http://dx.doi.org/10.2118/9885-PA.

Ilk, D., Anderson, D., Stotts, G., et al. 2006. Production-Data Analysis–Challenges, Pitfalls, Diagnostics. Paper SPE 102084 presented at the SPE Annual Technical Conference and Exhibition. San Antonio, Texas. 24–27 September. http://dx.doi.org/10.2118/102084-MS.

Ilk, D., Perego, A.D., Rushing, J.A., et al. 2008. Integrating Multiple Production Analysis Techniques to Access Tight Gas Sand Reserves: Defining a New Paradigm for Industry Best Practices. Paper SPE 114947 presented at the CIPC/SPE Gas Technology Symposium 2008 Joint Conference, 16–19 June, Calgary, Alberta, Canada. http://dx.doi.org/10.2118/114947-MS.

Inamdar, A., Malpani, R., Atwood, K., et al. 2010. Evaluation of Stimulation Techniques Using Microseismic Mapping in the Eagle Ford Shale. Paper SPE 136873 presented at the SPE Tight Gas Completions Conference. San Antonio, Texas. 2–3 November. http://dx.doi.org/10.2118/136873-MS.

Kabir, C.S., Rasdi, F., and Igboalisi, B. 2010. Analyzing Production Data from Tight Oil Wells. Paper SPE 137414 presented at the Canadian Unconventional Resources and International Petroleum Conference. Calgary, Alberta, Canada. 19–21 October. http://dx.doi.org/10.2118/137414-MS.

Katz, A.J. and Thompson, A.H. 1986. ***Phys. Rev. B.*** 34: 8179(R).

Kennaganti, K.T., Grant, D., Oussoltsev, D., et al. 2013. Application of Stress Shadow Effect in Completion Optimization Using a Reservoir-Centric Stimulation Design Tool. Paper SPE 164526 presented at the SPE Unconventional Resources Conference. The Woodlands, Texas. 10–12 April. http://dx.doi.org/10.2118/164526-MS.

King, G.E. 2010. Thirty Years of Gas Shale Fracturing: What Have We Learned? Paper SPE 133456 presented at the SPE Annual Technical Conference and Exhibition. Florence, Italy. 19–22 September. http://dx.doi.org/10.2118/133456-MS.

Klinkenberg, L.J. 1941. The Permeability of Porous Media to Liquids and Gases. Paper API-41-200 presented at the 11th API Drilling and Production Practice Conference. New York, New York. 1 January.

Kresse, O., Cohen, C., Weng, X., et al. 2011. Numerical Modeling of Hydraulic Fracturing in Naturally Fractured Formations. Paper ARMA-11-363 presented at the 45th U.S. Rock Mechanics / Geomechanics Symposium. San Francisco, California. June 26–29.

Kresse, O., Weng, X., Wu, R., et al. 2012. Numerical Modeling of Hydraulic Fractures Interaction in Complex Naturally Fractured Formations. Paper ARMA-2012-292 presented at the 46th U.S. Rock Mechanics/Geomechanics Symposium. Chicago, Illinois. June 24–27.

Kresse, O., Weng, X., Chuprakov, D., et al. 2013. Effect of Flow Rate and Viscosity on Complex Fracture Development in UFM Model. Paper ISRM-ICHF-2013-027 presented at the International Conference for Effective and Sustainable Hydraulic Fracturing. Brisbane, Australia. May 20–22.

Kurtoglu, B., Cox, S.A., and Kazemi, H. 2011. Evaluation of Long-Term Performance of Oil Wells in Elm Coulee Field. Paper SPE 149273 presented at the Canadian Unconventional Resources Conference, Alberta, Canada. 15–17 November. http://dx.doi.org/10.2118/149273-MS.

Lee, W.J. and Holditch, S.A. 1981. Fracture Evaluation with Pressure Transient Tests in Low-Permeability Gas Reservoirs. ***J. Pet Tech***, **33** (9): 1776–1791. SPE 9975-PA. http://dx.doi.org/10.2118/9975-PA.

Lee, J. 2011. Estimating Reserves in Unconventional Gas Reservoirs. Seminar organized by Hanson Wade, Charter House, London, England.

Lee, J. and Sidle, R. 2010. Gas-Reserves Estimation in Resource Plays. Paper SPE 130102 presented at the SPE Unconventional Gas Conference. Pittsburgh, Pennsylvania. 23–25 February. http:dx.doi.org/10.2118/130102-MS.

Lolon, E., Quirk, D.J., and Enzendorfer, C.K. 2008. Hydraulic Fracture Feasibility, Design, On-Site Supervision and Post Job Evaluation in Southeast Pakistan Gas Fields. Paper SPE 113932 presented at the SPE Annual Technical Conference and Exhibition. Denver, Colorado. 21–24 September. http://dx.doi.org/10.2118/113932-MS.

Lolon, E.P., McVay, D.A., and Schubarth, S.K. 2003. Effect of Fracture Conductivity of Effective Fracture Length. Paper SPE 84311 presented at the SPE Annual Technical Conference and Exhibition. Denver, Colorado. 5–8 October. http://dx.doi.org/10.2118/84311-MS.

Mattar, L. and Anderson, D.M. 2003. A Systematic and Comprehensive Methodology for Advanced Analysis of Production Data. Paper SPE 84472 presented at the SPE Annual Technical Conference and Exhibition. Denver, Colorado. 5–8 October. http://dx.doi.org/10.2118/84472-MS.

Mattar, L., Gault, B., Morad, K., et al. 2008. Production Analysis and Forecasting of Shale Gas Reservoirs: Case History-Based Approach. Paper SPE 119897 presented at the SPE Shale Gas Production Conference. Fort Worth, Texas. 16–18 November. http://dx.doi.org/10.2118/119897-MS.

Maxwell, S.C. and Cipolla, C.L. 2011. What Does Microseismicity Tell Us About Hydraulic Fracturing? Paper SPE 146932 presented at the SPE Annual Technical Conference and Exhibition. Denver, Colorado.30 October–2 November. http://dx.doi.org/10.2118/146932-MS.

Maxwell, S.C., Pope, T.L., Cipolla, C.L., et al. 2013. Understanding Hydraulic Fracture Variability through Integrating Microseismicity and Seismic Reservoir Characterization. Paper SPE 144207 presented at the North American Unconventional Gas Conference and Exhibition. The Woodlands, Texas. 14–16 June. http://dx.doi.org/10.2118/144207-MS.

Maxwell, S.C., Kresse, O., and Rutledge, J. 2013. Modeling Microseismic Hydraulic Fracturing Deformation. Paper SPE 166312 presented at SPE Annual Technical Conference and Exhibition. New Orleans, Louisiana. 30 September–2 October. http://dx.doi.org/10.2118/166312-MS.

Mayerhofer, M.J., Richardson, M.F., Walker, R.N. et al. 1997. Proppants? We Don't Need No Proppants. Paper SPE 38611 presented at the 1997 Annual Technical and Conference, San Antonio, Texas. 5–8 October. http://dx.doi.org/10.2118/38611-MS.

Mayerhofer, M.J., Bolander, J.L., Williams, L.I., et al. 2005. Integration of Microseismic-Fracture-Mapping Fracture and Production Analysis with Well-Interference Data to Optimize Fracture Treatments in the Overton Field, East Texas. Paper SPE 95508 presented at the SPE Annual Technical Conference and Exhibition. Dallas, Texas. 9–12 October. http://dx.doi.org/10.2118/95508-MS.

Mayerhofer, M.J., Lolon, E.P., Warpinski, N.R., et al. 2008. What Is Stimulated Reservoir Volume (SRV)? Paper SPE 119890 presented at the SPE Shale Gas Production Conference. Fort Worth, Texas. 16–18 November. http://dx.doi.org/10.2118/119890-MS.

Meyer, B.R. and Bazan, L.W. 2011. A Discrete Fracture Network Model for Hydraulically-Induced Fractures: Theory, Parametric and Case Studies, Paper SPE 140514 presented at the SPE Hydraulic Fracturing Conference and Exhibition. The Woodlands, Texas. January 24–26. http://dx.doi.org/10.2118/140514-MS.

Meyer, B.R., Jacot, R.H., Bazan, L.W., et al. 2010. Technology Integration: A Methodology to Enhance Production and Maximize Economics in Horizontal Marcellus Shale Wells. Paper SPE 135262 presented at the SPE Annual Technical Conference and Exhibition. Florence, Italy. 19–22 September. http://dx.doi.org/10.2118/135262-MS.

Miller, C., Waters, G., and Rylander, E. 2011. Evaluation of Production Log Data from Horizontal Wells Drilled in Organic Shales. Paper SPE 144326 presented at the SPE Americas Unconventional Gas Conference. The Woodlands, Texas. 14–16 June. http://dx.doi.org/10.2118/144326-MS.

Nelson, R. 2009. Unconventional Reservoirs. ***AAPG Bulletin***, 93 (3): 329–340.

Neuhaus, C. and Miskimins, J. 2012. Analysis of Surface and Downhole Microseismic Monitoring Couple with Hydraulic Fracture Modeling in the Woodford Shale. Paper SPE 154804 presented at the EAGE Annual Conference and Exhibition. Copenhagen, Denmark. 4–7 June. http://dx.doi.org/10.2118/154804-MS.

Nobakht, M., Mattar, L., Moghadem, et al., 2010. Simplified yet Rigorous Forecasting of Tight/Shale Gas Production in Linear Flow. Paper SPE 133615 presented at the SPE Western Regional Meeting, 27–29 May, Anaheim, California. http://dx.doi.org/10.2118/133615-MS.

Nott, D.C. and Hara, S.K. 1991. Fracture Half-Length and Linear Flow in the South Belridge Diatomite. SPE 21778. http://dx.doi.org/10.2118/21778-MS

Pratikno, H., Rushing, J.A., and Blasingame, T.A. 2003. Decline Curve Analysis Using Type Curves–Fractured Wells. Paper SPE 84287 presented at the SPE Annual Technical Conference and Exhibition. Denver, Colorado. 5–8 October. http://dx.doi.org/10.2118/84287-MS.

Rogers, S., Elmo, D., Dunphy, R., et al. 2010. Understanding Hydraulic Fracture Geometry and Interactions in the Horn River Basin through DFN and Numerical Modeling. Paper SPE 137488 presented at the Canadian Unconventional Resources and International Petroleum Conference. Calgary, Alberta, Canada. 19–21 October. http://dx.doi.org/10.2118/137488-MS.

Rushing, J.A. and Blasingame, T.A. 2003. Integrating Short-Term Pressure Buildup Testing and Long-Term Production Data Analysis to Evaluate Hydraulically-Fractured Gas Well Performance. Paper SPE 84475 presented at the SPE Annual Technical Conference and Exhibition. Denver, Colorado. 5–8 October. http://dx.doi.org/10.2118/84475-MS.

Rushing, J.A., Sullivan, R.B., and Blasingame, T.A. 2005. Post-Fracture Performance Diagnostics for Gas Wells with Finite-Conductivity Vertical Fractures. Paper SPE 97972 presented at the SPE Eastern Regional Meeting. Morgantown, West Virginia. 14–16 September. http://dx.doi.org/10.2118/97972-MS.

Rushing, J.A., Perego, A.D., Sullivan, R.B., et al. 2007. Estimating Reserves in Tight Gas Sand at Hp/HT Reservoir Conditions: Use and Misuse of an Arps Decline Curve Methodology. Paper SPE 109625 presented at the SPE Annual Technical Conference and Exhibition, 11–14 November, Anaheim, California. http://dx.doi.org/10.2118/109625-MS.

Sarg, J.F. 2012. The Bakken: An Unconventional Petroleum and Reservoir System. Final Scientific/Technical Report: September 18, 2008–December 31, 2011. DOE/NETL report issued March 2012. Submitted by the Colorado School of Mines, http://www.netl.doe.gov/file%20library/research/oil-gas/enhanced%20oil%20recovery/nt0005672-final-report.pdf (accessed July 2014).

Seager, R. and Vassililles, G. 2011. Shale Engineering. Paper presented at the SPEE Annual Meeting. Amelia Island Resort, Florida. June 6.

Smith, M.B., Bale, A., Britt, L.K., et al. 2004. An Investigation of Non-Darcy Flow Effects on Hydraulic Fractured Oil and Gas Well Performance. Paper SPE 90864 presented at the SPE Annual Technical Conference and Exhibition. Houston, Texas. 26–29 September. http://dx.doi.org/10.2118/90864-MS.

Stimlab Predict K Pro. http://www.corelab.com/stimlab/Predict-K (accessed July 2014).

Suarez, R. 2013. Fracture Conductivity Measurements on Small and Large Scale Samples–Rock Proppant and Rock Fluid Sensitivity. Slides presented at the SPE Workshop on Hydraulic Fracture Mechanics Considerations for Unconventional Reservoirs. Rancho Palos Verdes, California. 11–13 September.

Valkó, P.P. 2009. Assigning Value to Stimulation in the Barnett Shale: A Simultaneous Analysis of 7,000 Plus Production Histories and Well Completion Records. Paper SPE 119369 presented at the SPE Hydraulic Fracturing Technology Conference, The Woodlands, Texas. 19–21 January. http://dx.doi.org/10.2118/119619-MS.

Valkó, P.P. and Lee, J.W. 2010. A Better Way to Forecast Production from Unconventional Gas Wells. Paper SPE 134231 presented at the SPE Annual Technical Conference and Exhibition, 19–22 September, Florence, Italy. http://dx.doi.org/10.2118/134231-MS.

Vassilellis, G.D., Bust, V.K., Li, C., et al. 2011. Shale Engineering Application: The MAL-145 Project in West Virginia. Paper SPE 146912 presented at the Canadian Unconventional Resources Conference. Alberta, Canada. 15–17 November. http://dx.doi.org/10.2118/146912-MS.

Vincent, M.C. 2010. Restimulation of Unconventional Reservoirs: When Are Refracs Beneficial? Paper SPE 136757 presented at the Canadian Unconventional Resources and International Petroleum conference. Calgary, Alberta, Canada. 19–21 September. http://dx.doi.org/10.2118/136757-MS.

Warpinski, N.R., Branagan, P.T., Peterson, R.E., et al. 1998. Mapping Hydraulic Fracture Growth and Geometry Using Microseismic Events Detected by a Wireline Retrievable Accelerometer Array. Paper SPE 40014 presented at the Gas Technology Symposium. Calgary, Alberta, Canada. 15–18 March. http://dx.doi.org/10.2118/40014-MS.

Warpinski, N.R. 2009. Integrating Microseismic Monitoring with Well Completions, Reservoir Behavior, and Rock Mechanics. Paper SPE 125239 presented at the Tight Gas Completions Conference. San Antonio, Texas. 15–17 June. http://dx.doi.org/10.2118/125239-MS.

Warpinski, N.R., Mayerhofer, M.J., Agarwal, K., et al. 2012. Hydraulic-Fracture Geomechanics and Microseismic-Source Mechanisms. Paper SPE 158935 presented at the SPE Annual Technical Conference and Exhibition. San Antonio, Texas. 8–10 October. http://dx.doi.org/10.2118/158935-MS.

Wattenbarger, R.A., El-Banbi, A.H., Villegas, M.E., et al. 1998. Production Analysis of Linear Flow into Fractured Tight Gas Wells. Paper SPE 39931 SPE Rocky Mountain Regional/Low-Permeability Reservoirs Symposium, 5-8 April, Denver, Colorado. http://dx.doi.org/10.2118/39931-MS.

Weijers, L., Wright, C., Mayerhofer, M., et al. 2005. Developing Calibrated Fracture Growth Models for Various Formations and Regions Across the United States. Paper SPE 96080, presented at the SPE Annual Technical Conference. Dallas, Texas. 9–12 October. http://dx.doi.org/10.2118/96080-MS.

Weng, X., Kresse, O., Cohen, C., et al. 2011. Modeling of Hydraulic-Fracture-Network Propagation in a Naturally Fractured Formation. ***SPE Prod & Oper***, **26**: (4): 368–380. SPE-140253-PA. http://dx.doi.org/10.2118/140253-PA.

Williams-Stroud, S. 2008. Using Microseismic Events to Constrain Fracture Network Models and Implications for Generating Fracture Flow Properties for Reservoir Simulation. Paper SPE 119895 presented at the SPE Shale Gas Production Conference. Fort Worth, Texas. 16–18 November. http://dx.doi.org/10.2118/119895-MS.

Ye, P., Chu, L., Harmawan, I., et al. 2013. Beyond Linear Flow Analysis in an Unconventional Reservoir. Paper SPE 164543 presented at the SPE Unconventional Resources Conference. The Woodlands, Texas. 10–12 April. http://dx.doi.org/10.2118/164543-MS.

Zhang, J., Kamenov, A., Zhu, D., et al. 2013. Laboratory Measurements of Hydraulic Fracture Conductivity in the Barnett Shale. Paper IPTC 16444 presented at the International Petroleum Technology Conference. Beijing, China. 26–28 May. http://dx.doi.org/10.2523/16444-MS.

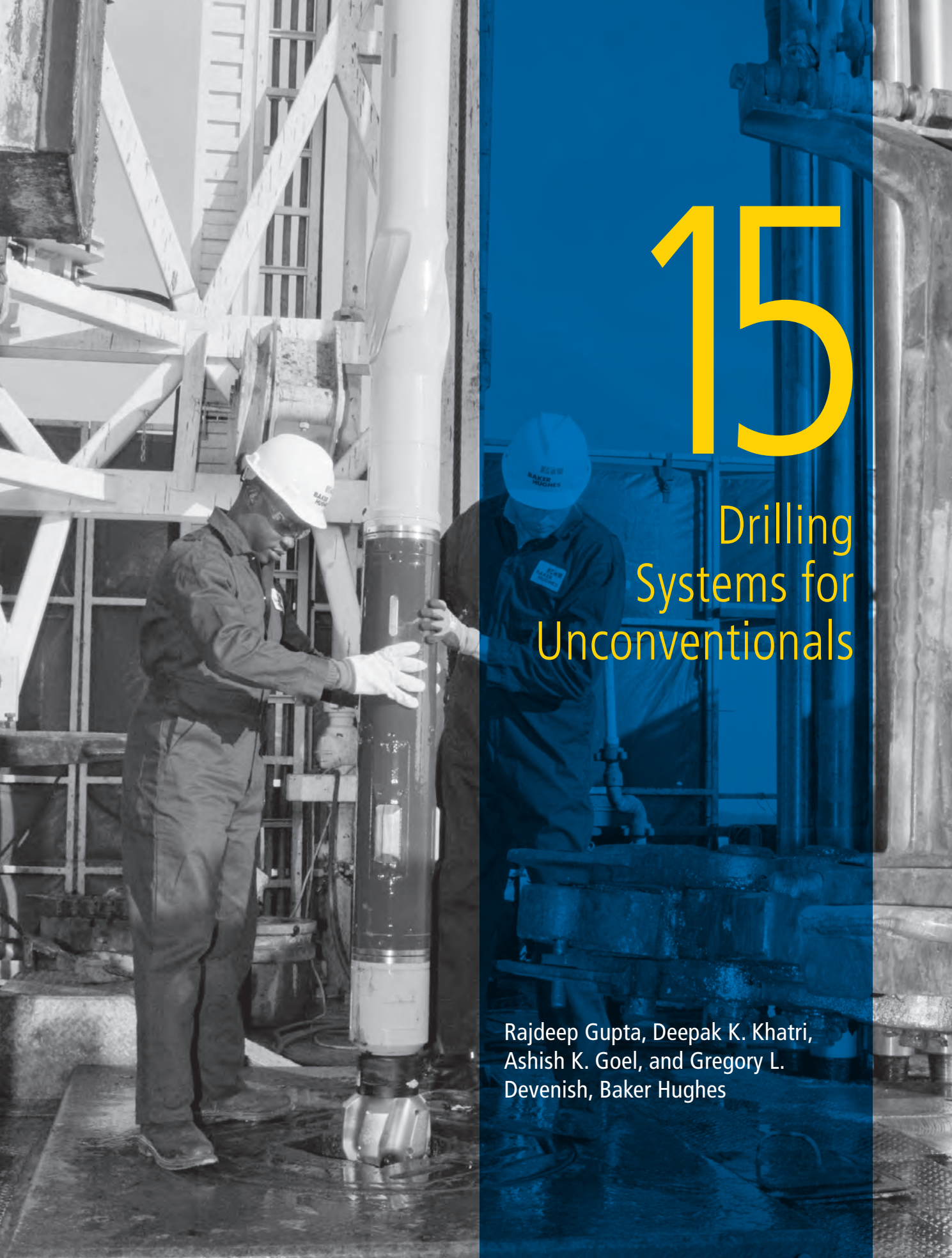

15

Drilling Systems for Unconventionals

Rajdeep Gupta, Deepak K. Khatri, Ashish K. Goel, and Gregory L. Devenish, Baker Hughes

This page intentionally left blank

Chapter 15: Drilling Systems for Unconventionals

15.1 The Early Days

Drilling in the Barnett shale started in the early 1980s, but it took over 20 years and technology advancements, as well as a conducive fiscal, regulatory, and infrastructure environment, to bring about the shale gas revolution. Early shale gas wells in the Barnett were mostly vertical. Verticals were drilled to collect data along with some horizontal appraisal wells to test hydraulic fracturing and mechanical well completion designs. These wells were also used to obtain estimates of initial production potential of the designs. It was not until 2003 that there was a total shift to horizontal wells for developing shale in the Barnett as well as all the other US shale basins that followed.

On the technology side, the introduction of horizontal drilling allowed operators to access larger reservoir volumes with reduced costs. The introduction of cost-efficient hydraulic fracturing using "slick-water" provided access to the resources. During the same time frame, openhole and cased hole completion systems were developed that allowed stimulating fifty and more zones in a continuous pumping operation with the added advantages of increasing cost effectiveness and well productivity.

As an example, wells in the Barnett were completed in 2007 with four-to-eight fracture stages per well. Just 5 years later, wells were completed with upwards of 20 stages per well in the Haynesville and Marcellus shales.

This change came about due to increases in exploration and development work on drill bit technology as more wells were drilled to maintain production rates. Some questions remained unanswered, such as the reasons for inconsistencies in production rate, in spite of drilling horizontal wells and combining them with increased fracturing stages and multistage completions.

Due to shale's unique nature, every basin, play, well, and pay zone requires a unique treatment. This distinctiveness poses technological challenges when operators need to address the geological uncertainties present with production variation and economics. Major opportunities for improvement are available for applications to characterize the reservoir (both from petro-physical and geomechanical viewpoint) and for targeted drilling technologies that could reduce the cost and improve efficiency.

15.2 Drilling Unconventional Wells

Drilling unconventional wells requires thorough understanding of the reservoir make up, well architecture, and associated costs and rig requirements. Cementing and planning to optimize drilling efficiency when encountering challenges (such as faults and open fractures) without compromising the reservoir contact are also discussed.

15.2.1 Reservoir Understanding

Data acquisition requirements will vary during the shale reservoir exploration and appraisal stages. Requirements may even vary within a single stage, depending on the heterogeneity and geologic complexity of each specific shale reservoir.

It is important that maximum information is obtained in the exploratory stage so that the best technical decisions can be made concerning well placement, stimulation, and completion design as one moves into appraisal drilling. The priority objective is to acquire a consistent set of high-quality datasets about these shale wells that will allow one to verify any variations in any important reservoir characteristics in the area or in vertical wells.

- Variations in mineralogy will affect geomechanical properties of the reservoir.
- Variations in TOC wt %, vertical distribution, kerogen type, and maturity will affect the type of hydrocarbons that will be produced (dry gas? condensate? oil?) as well as affect the net thickness of the organic-rich shale interval.
- Variations in the fracture network across the exploratory area must be identified as well as any variations in the stress regime.
- Understanding areal variation in reservoir properties is central to identification of sweet spots.

Understanding the reservoir will help with optimized well construction and logging requirements for the drilling program.

15.2.2 Well Architecture

Based on North American shale gas and oil experience, a large number of wells develop unconventional plays. Both vertical and horizontal wells are required to be drilled. During the appraisal phase, more horizontal wells are drilled than in the exploration phase. Almost all development wells will be horizontal.

Listed are current practices and observations for drilling horizontal wells.

- Wells are often drilled in a direction normal to the maximum principal stress. In some areas this is modified to maximize well placement based on state well-spacing rules.
- Vertical sections and build curve sections are typically 8°/100 ft. to 12°/100 ft.
- Optimum (and shorter) lateral lengths may be preferred over longer lateral lengths. The length of the horizontal sections varies from play to play, with a range of 3,000 to 6,000 ft. for gas wells and 7,000 to 10,000 ft. for oil wells.
- Using longer laterals can mean facing increased risk of encountering a geohazard problem (fault, karst, or water), when initiating the fracturing at the well toe. This may cause losing the wellbore. Longer laterals are also more difficult to geosteer into a narrow window.
- Most operators convert drilling fluid to some form of oil-based mud (OBM) prior to drilling the curve and lateral.
- Some wells in the US are being drilled with environmentally friendly, water-based mud (WBM). It is likely that most horizontal shale wells will be drilled with WBM in the future.
- Mud weights depend on formation pore pressure, which ranges from subnormal to over-pressured.
- Operators use drilling motors—usually positive displacement motors—to drill the well's vertical section.
- In a cost-sensitive environment, motors are also used to drill the curve and the lateral sections. Sliding with a positive displacement motor can be challenging due to tool face control and drag issues, which result in less penetration while drilling long horizontals and attempting to steer through the reservoir. Although it is possible to drill and still remain in a horizontal target with positive displacement motor, there is a better way. A rotary steerable system (RSS) is typically more efficient because of the continuous near-bit information that is available and the automatic steering capability discussed later in this chapter.
- Polycrystalline diamond compact (PDC) bits are used in most shales.
- Higher bottom-hole temperatures occur in the deeper Haynesville shale and parts of the Eagle Ford shale.
- An early preference for drilling wells in the toe-up mode is gradually changing to drilling the lateral as flat as possible and perfectly horizontal (Kennedy et. al 2012a). The toe-up attitude selection is based on the fact that gravity facilitates draining any fluids that may collect along the lateral into the mother hole, allowing production and lifting from the well.
- Drilling time for a typical horizontal well is now significantly reduced; e.g., the time spent drilling in the Barnett and Marcellus shales is 12 days and drilling time in the Eagle Ford is 17 days (Kennedy et al. 2012a).
- Pad drilling is being used for both logistics and environmental reasons at 4-to-10 wells per pad in the US, with larger 16-well pads in Canada. Pad drilling is primarily being used during the development phase of the shale play. As of early 2014, 70% of US shale wells are being drilled from pads.
- Drilling constitutes 40% to 50% of the total well costs. Well completion (wellbore completion plus hydraulic fracturing treatment) is the major part of completed well costs.

Horizontal wells are the norm for developing US shale plays. **Fig. 15.1** shows a typical well profile for the Woodford shale play. **Table 15.1** and **Table 15.2** show a general comparison between various shale oil and plays and the associated development costs. **Fig. 15.2** from Baker Hughes rig count shows the dominating trend of horizontal and directional wells in North America.

15.2.3 Rig Requirements, Costs, and Flexibility

As the development of unconventional reservoirs has evolved, so have the drilling units required to deliver the wells (**Fig. 15.3**). In the early day of single well locations, rig requirements were driven by the need for high reliability, increased drilling efficiency, reduced operating costs, and the ability to change locations quickly. Drilling contractors responded to these requirements by embracing automation, instrumentation, and digital information. Flexible rigs were built which included top drives, AC motors, automated pipe handling, iron roughnecks, fewer personnel, as well as the ability to rig down, move, and rig up in half the time of standard rigs. Emphasis was placed on reducing down time between wells and reducing the number of loads to move the rig.

The use of multiwell pads as a drilling strategy reduces environmental impact, minimizes surface costs, provides greater efficiency, and can deliver better reservoir drainage. This strategy allowed batch drilling, reduced transport costs, reduced flat time, and reduced drilling time between wells from one-to-two days to four-to-six hours. Unconventional

operators quickly adopted this strategy. As a result of the move from single wells to pad drilling, the rigs added skidding or walking capability to the rig and substructure, a blow out prevention (BOP) handling system capable of suspending the BOP, and the capability to move with pipe in the derrick. The central facility for power and fluids remains stationary while 50 ft. suitcases of umbilical conduit are added, as needed, to reach the rig's new location.

15.2.4 Cementing

In 1903, the first oil well operator performed a cementing job using a shovel and cement mixer to pour cement around the steel casing in the well to isolate the wellbore. Since then, the process continues with improved technology and mixing capability, placement, and materials. Creating zonal isolation within a wellbore continues to rely on cement.

Many people believe that using cementing with good zonal isolation is the best foundation for a well. It is only recently that the industry has started to recognize and appreciate the real importance of cementing in the well-drilling-to-production process.

15.2.4.1 What Is Cementing?

Cementing is the process of adding water (termed as a "mixed fluid," which consists of water plus additives) with dry cement to prepare the cement slurry. The slurry is pumped down the pipe and up the annulus with high-pressure equipment. Often, a triplex pump is utilized so that the cement slurry can be placed between the openhole and casing. The objectives are to:

- Isolate different zones (**Fig. 15.4**)
- Protect the casing.
- Protect the formation.
- Continue drilling for the next section, or complete the well.

15.2.4.2 Cementing: The Process

The process of cementing different casing strings during drilling operation is referred to as primary cementing. When the primary cement job fails and the cement needs repair, the repair is referred to as secondary or remedial cement job. A remedial cement job can be performed by placing cement

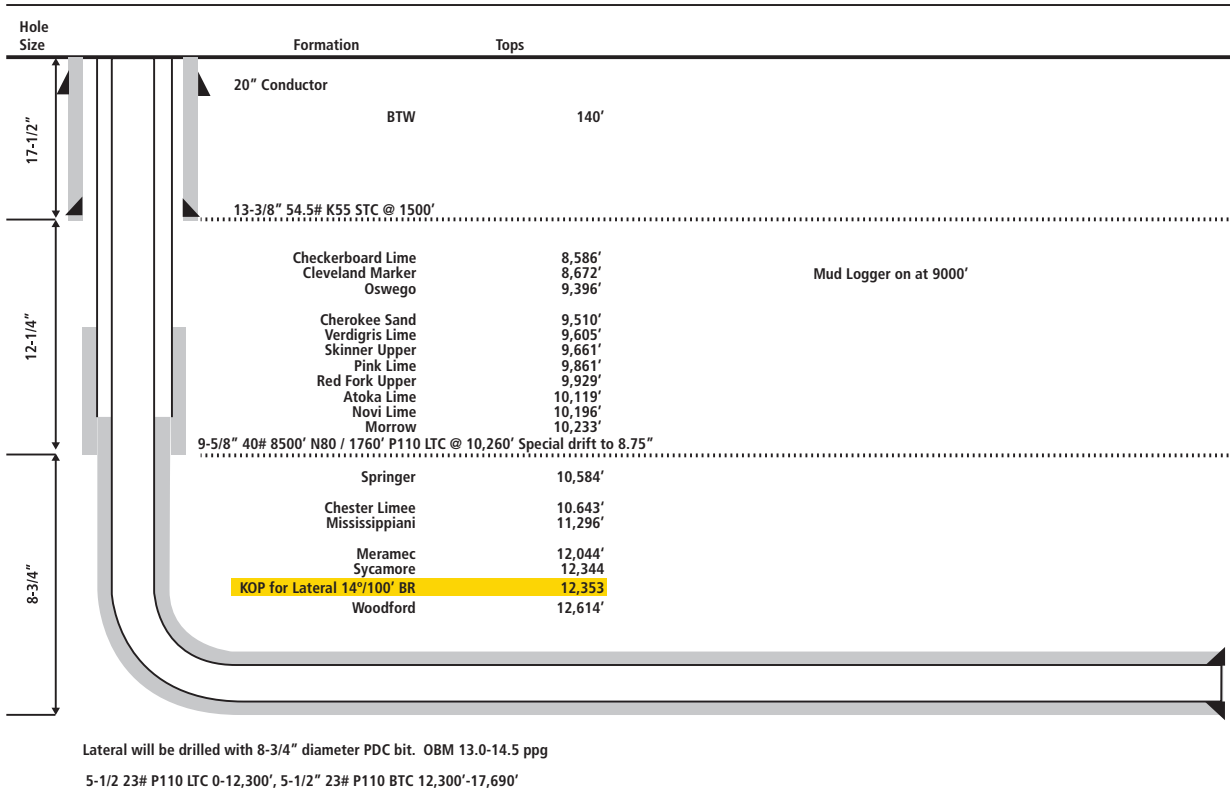

Fig. 15.1—Typical well profile for a well in the Woodford shale play. Cased hole wells typically use a 4½-in or 5½-in. completion string (with the 5½-in. string preferred for more efficient fracturing). (From Kennedy et al. 2012b.)

Table 15.1—US shale gas plays comparison. (From EIA 2011.)

PLAY	BARNETT	FAYETTEVILLE	WOODFORD	EAGLE FORD	HAYNESVILLE	MARCELLUS
Area, Mi^2	4,075	9,000	3,700	1,100	9,000	95,000
Depth, Ft	6,500 – 8,500	1,000 – 7,000	5,000 – 9,500	10,500 – 11,300	10,500 – 13,500	4,000 – 8,500
Thickness, Ft	100 – 600	20 – 200	150 – 250	180 – 375	200 – 300	50 – 200
IP Rate, MMcfd	2.5	2.8	3.6	7.0 + Cond	14+	3.5
EUR/Well, Bcf	1.6	2.1	3.0	5.0	6.5	3.5
Avg Lateral, Ft	3,950 – 4,350	4,700 – 5,500	3,000 – 5,000	5,000 – 5,300	4,400 – 4,700	4,200 – 4,900
Well Spacing, Acres	116	80	160	160	80	80
TRR, Tcf	43	32	22	21	75	410
Well Spacing, Acres	116	80	160	160	80	80
TRR, Tcf	43	32	22	21	75	410

Table 15.2—US shale oil plays comparison. (From EIA 2011.)

PLAY	BAKKEN	EAGLE FORD	NIOBRARA	UTICA	WOLFCAMP
Depth, Ft	8,500 – 10,000	4,000 – 12,000	6,000 – 8,000	2,000 – 14,000	5,500 – 11,000
Thickness, Ft	8 – 14	300 – 475	150 – 300	70 – 750	1,500 – 2,600
IP Rate, BOPD	200 – 1,800	250 – 1,500	400 – 500	4.5 – 17 MMcfd 200 – 1,500 Bopd	1,050
EUR/Well, MBO	700	600	250 – 450	3.6 – 5.4 Bcf 500 – 900	650 – 750
Avg Lateral, Ft	8,700 – 10,000	6,000 – 7,000	4,050 – 5,100	4,700 – 6,200	4,550 – 6,700
TRR, BBO	4.5 (20)	7 – 10	1.5	3.0 (5.5)	4,550 – 6,700

plugs at the required depth and either allowing the plugs to set or by placing the cement plugs, closing the annulus, and then applying pressure to squeeze the cement slurry into the leaking points or zones to isolate. This is also referred to as a squeeze cementing operation.

15.2.4.3 Data Gathering

The process of cementing starts with data gathering. Critical data include depths (total vertical as well as total depth), hole size, and bottom hole static temperature. When available, understanding permeability, porosity, type of formation, and type of drilling fluids is helpful to determine the best slurry system. Based on this data, simulators can be used to determine circulating temperatures and placement rates to ensure that pressures are maintained considering well control.

Fluids to be placed during a typical cementing operation are either used as spacers or as a wash to effectively displace the drilling fluid. This process is also referred to as cleaning the wellbore and is done to prepare the well for cementing, followed by cement slurry, to provide zonal isolation. The more effective the mud removals, the better the chances of good bonding between cement and pipe and cement and formation.

15.2.4.4 Laboratory Qualification

Fluid systems are tested and qualified in the laboratory using the API tests before placing the fluids in the wells.

Spacers are tested for mixability, density, rheology, and stability to make sure the fluid is qualified for downhole conditions. The cement slurry is tested for mixability, density, rheology, and stability and also pumpability, by using a high pressure, high temperature consistometer at bottomhole temperature and pressure to make sure the cement can be placed in the well safely.

15.2.5 Current Drilling Challenges

Shale reservoirs are unique; each well needs a unique treatment in terms of well placement, wellbore stability,

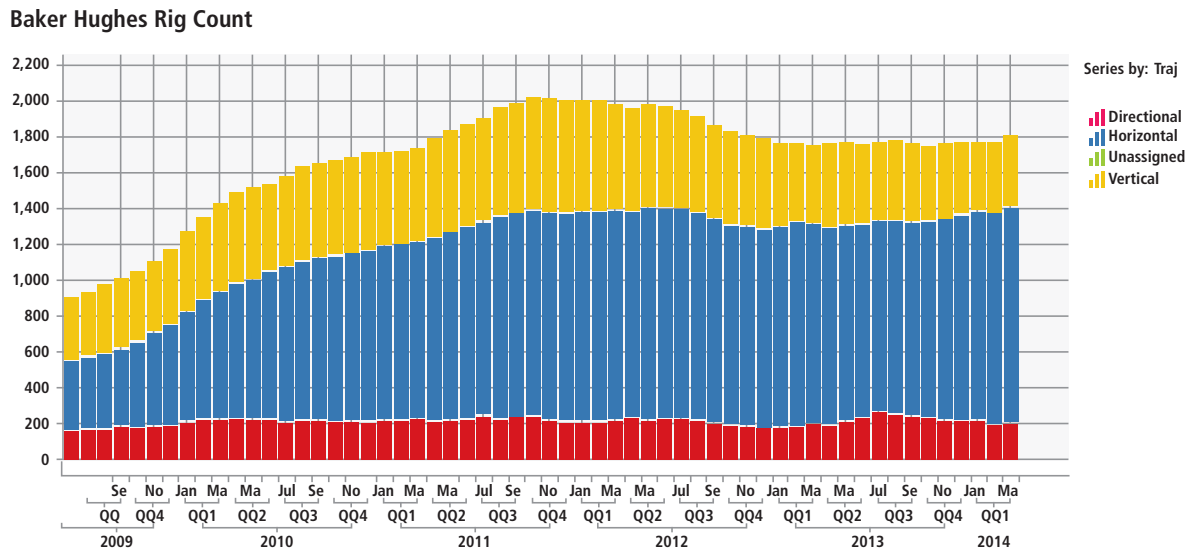

Fig. 15.2—Development in rig count across North America showing the changing trends in type of drilled wells.

torque and drag, inconsistent build rates, geological uncertainties, lost circulation zones, and other technical challenges. The so-called factory drilling approach is aimed at reducing costs but does not fully take into account the significant variability that exists in these plays.

Here are some of the major challenges:

- Minimizing the trip time
- Optimizing drilling to increase rate of penetration
- Steering to the right spot in the formation

15.2.5.1 Identifying Opportunities for Performance Improvement

Drilling shale wells presents many technical challenges that affect the overarching goal to optimize drilling costs and reduce the number of days drilling per well. Performance improvement is an important consideration. The quality of pre-well planning influences both the cost of drilling and the ultimate hydrocarbon recovery. Therefore, an integrated approach is needed to identify opportunities for performance improvement, by ensuring the availability of reservoir data, geoscience, geomechanical knowledge, and downhole conditions before planning the drilling details of shale wells.

If well delivery costs are reduced, the following benefits can be achieved:

- Improved progress rate and overall reduced cost-per-foot.
- Increased drilling efficiency by having complete drilling string application, including bit selection, which also can extend bit life.
- Improved wellbore quality and placement—enhancing formation evaluation (FE) log quality and casing installation.
- Enhanced wellbore stability.
- Fluids optimization, drilling dynamics, spiraling, ledging, directional control, steerability, pressure management, and equivalent circulating density (ECD).
- Hole cleaning.
- Reduction in trips.

The process of designing an effective well begins with a thorough knowledge of the subsurface and offset well information. There are questions to ask that can assist in gathering that knowledge.

What if we could identify:

- Open fractures and faults in the wellbore? Would we complete it any differently?
- Conductive fractures from an offset completion? Would we move stages?

Fig. 15.3—Typical single well site in North America.

- Differences between ductile and brittle rock? Would we change our target or complete the well any differently?
- Different stresses on the wellbore? Would we complete any differently?
- Fracture system? Could we optimize completion and increase recoverable reserves?

When the data have been gathered, create the initial well plan design and layout drill string. Parameters to be considered for this design should include the following:

- Health, safety, and environmental requirements
- Customer objectives
- Drilling environment
- Objective formation
- Rig and surface equipment
- Trajectory and targets
- Measurement-while-drilling (MWD) and logging-while-drilling (LWD) integration
- Fluids needed and fluid disposal mechanism
- Liner, completion, pass through
- Drilling and production optimization
- Reliability
- Logistics

During this process, every effort must be made to influence performance and reduce cost by avoiding a low rate of penetration, high torque and drag, excessive slide drilling (oriented) in lateral intervals, damaging drill string vibrations, premature damage to PDC bits, and inconsistent build-up rates.

15.3 Drilling Systems

Drilling systems for conventional wells are similar to those for horizontal land wells with a few variations. This section discusses the key components of drilling systems.

15.3.1 Developments in Deflection Tools

As a requirement for directional drilling, deflection tools are used to deviate the well trajectory from the vertical direction to the desired course of direction. In this section, the focus is on the two most common types of directional techniques.

15.3.1.1 Conventional Motors

Positive displacement motors (PDM) have been the cornerstone of directional drilling service delivery for decades. In unconventional wells, positive displacement motors are used extensively to drill horizontal trajectories because of their ready availability and inherent cost effectiveness.

A PDM is powered by a hydraulics system with circulating fluid (drilling fluid). This fluid provides rotation and torque to the bit without the need to rotate the drill string. Positive displacement motors operate by efficently converting hydraulic energy generated by rig pumps into mechanical energy to turn the bit.

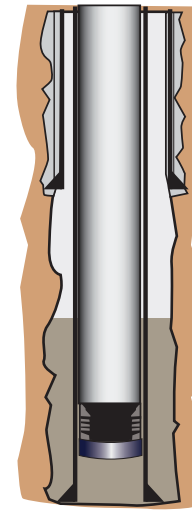

Fig. 15.4—Zonal isolation.

The positive displacement motor consists of basic components: an optional float valve, a power section, a flexible shaft, and the bearing assembly. The optional float valve acts as a check valve preventing backflow into the motor cavity when it is running in the hole.

The motor's power section is made up of a rotor and a stator. Hydraulic energy originating from drilling fluids is converted into mechanical energy in the power section. This energy, in turn, provides torque, bit speed, and also generates residual heat. Motor power sections are available in a variety of torque, RPM, and efficiency ranges. The stator in the power section has one more lobe than the rotor. Positive displacement motors are characterized by the ratio of rotor lobes to that of the stator. For example, a 5:6 motor features 5 lobes on the rotor and 6 lobes on the stator. Fluid pumped through the drill string displace the rotor inside the progressive cavities of the stator, forcing the rotor to turn. The mechanical characteristics of a positive displacement motor means that the number of rotor or stator lobes increases, the RPM and mechanical efficiency decreases, but torque output increases. Based on the application, motor power sections should be selected to match the bit speed and torque requirement for optimal operational efficiency.

Ultra motors are Baker Hughes standard motor technology that uses a conventional steel stator tube, filled with the required elastomer contour.

The elastomer has always been considered to be a weak part of the overall design of a downhole motor. The elastomer can swell or shrink, leading to less efficiency. The elastomer can also gain or lose hardness and can create internal heat due to the working of the rotor on the contour of the stator. This can be problematic, because the heat build-up cannot escape due to the elastomer's efficient insulation properties. In extreme cases, the bonding system (glue) between the elastomer and the steel tube can be destroyed, resulting in rubber chunking and tool failure.

Baker Hughes X-treme® Motors use a precontoured stator tube, which is coated with a thin layer of elastomer (**Fig. 15.5**). The advantages are obvious:

- Less shrinking or swelling occurs inside the stator tube, because less elastomer is used.
- Less heat build-up occurs in the stator because the thinner elastomer layer provides less insulation. In addition, heat is dissipated much more easily into the borehole through the steel of the stator.
- In case of high torque (which is caused by a high differential pressure between the neighboring chambers), the rubber cannot be pushed aside, which prevents rubber chunking. Also, less leakage between the chambers is possible, thus the volumetric efficiency of the power section is improved, and motor stalling can be avoided.

A flexible shaft connects the lower end of the rotor and the upper end of the drive sub. This shaft transmits power generated by the power module through the drive sub to the bit. In addition, the universal joint assembly and flexible shaft translates the eccentric motion of the rotor into concentric rotation for the bearing assembly.

The bearing assembly consists of a series of balls and races designed to accommodate the high-downhole weights required to penetrate the formation, along with upper and lower radial bearings that support the side force on the drive sub. These mud-lubricated components support the drive sub that delivers the power to the bit in the form of rotational speed and torque.

Positive displacement motors (**Fig. 15.6**) operate effectively with all types of drilling mediums at any mud weight, including water, salt water, oil-base, oil emulsion, fluids with high viscosity, or fluids that contain lost circulation material and compressible fluids.

The motor design is modular in construction. Positive displacement motor systems differ mainly in the power module used. Depending on the required application, the various modular assemblies can be modified or replaced enabling motor geometry to be constructed for specific applications.

Today's motors (2015 timeframe) are capable of a wide range of build rates because they can be configured with different bend angle and stabilization options. The housing bend angle and the stabilization geometry determine whether or not the motor can be rotated, and if so, the maximum revolutions per minute (RPM) that can be used in rotary mode.

The following is a list of the types of wells that are commonly drilled with positive displacement motors:

- Profiles-S shape, J shape, and horizontal wells
- Vertical section
- Build-up and drop
- Tangent sections
- Lateral and horizontal sections

With these advanced capabilities, complex wells can be drilled in complex geological structures. Drilling a directional well is economically desirable because it enables one well to intersect multiple targets. Horizontal wells provide an additional benefit by increasing reservoir productivity, providing well spacing, and reducing the total number of wells required for full field development.

Two modes of directional control methods associated with drilling motors to drill and maintaining the directional objectives are:

Oriented (Slide) Mode:

- Controlled curvature
- Controlled direction
- No drillstring rotation

Rotary Mode:

- Behaves in the same way as a rotary drilling assembly
- Hole is slightly overgauged

Other additional bottomhole assembly (BHA) design considerations will have significant effect on steerable motor dogleg development. By reducing the diameter of the motor top-end string stabilizer, the motor's build rate capability can be enhanced and an angle-build tendency in the rotary mode can be developed. Similarly, movement of the motor top-end stabilizer to a higher position will generally reduce dogleg capabilities, although the drilling assembly deflection between the bearing housing and the motor top-end stabilization will eventually offset this tendency. The normal mode of operation through intervals of significant angle change is to alternate the oriented and rotary footage. After establishing actual dogleg development performance, the course length of oriented "sets" is controlled to minimize oriented drilling. Typically, course lengths for oriented sets are from 15-to-90 ft. (4.6-to-27.7m), depending on required DLS and the formation characteristics.

15.3.1.2 Rotary Steerable Systems

Rotary steerable directional drilling systems (RSS) was introduced to the offshore drilling market in the mid 1990s and was commonly deployed in directional wells there. These systems have high-level formation evaluation capability, which often eliminated the need for wire line logging programs.

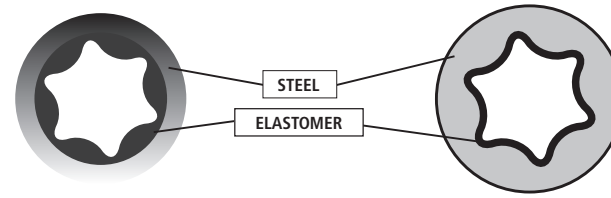

Fig. 15.5—Schematic of different elastomer technology used in PDM.

A rotary steerable system employs the use of specialized downhole equipment to replace conventional directional tools such as mud motors. They are generally programmed by the measurement while drilling (MWD) engineer or directional driller who sends commands using surface equipment (typically using either pressure fluctuations in the mud column or variations in the drill string rotation), to which the tool responds and gradually steers in the desired direction. In other words, a tool designed to drill directionally with continuous rotation from the surface eliminates the need to slide drilling as opposed to a mud motor.

The methods used to direct the well path fall into two broad categories: "push the bit" or "point the bit." Push-the-bit tools use pads on the outside of the tool that press against the well bore. This causes the bit to press on the opposite side, which causes a direction change. Point-the-bit technologies cause the direction of the bit to change relative to the rest of the tool by bending the main shaft running through it. The latter require a non-rotating housing or reference housing to create this deflection within the shaft.

Fig. 15.7 shows examples of different bit deflections for rotary steerable systems.

RSS brings many advantages for geoscientists and drillers. This technology reduces wellbore tortuosity in complex geometries allowing drillers to have better control over the wellbore trajectory compared to when working with motors. Continuous rotation of the drill string results in a better hydraulic performance and a smoother wellbore. A smoother wellbore helps crews to worry less about stuck pipe issues, and focus more on other aspects of the operation. Increased

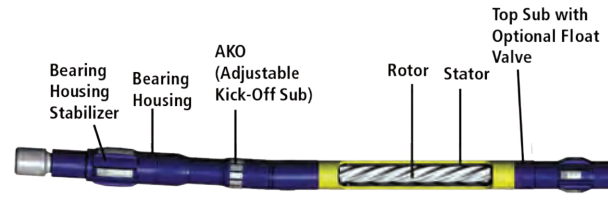

Fig. 15.6—Schematic of a positive displacement motor.

wellbore quality can also help geoscientists with imaging capabilities and accurate measurement of formation properties. The low rig rates and relatively short duration of the wells in the land market did not justify the deployment of expensive rotary steerable systems with extensive formation evaluation capabilities. But, with the increasing number of horizontal wells being drilled in these plays, the growing complexity of well profiles, and the need to overcome the current motor drilling challenges, operators are looking for other, more efficient means of drilling these wells. Rotary steerable systems (RSS) are playing a significant role in the development of shale plays. For optimized drilling, there are two main features of these systems:

1. Continuous drill string rotation while steering.

2. Highly automated steering control and easy directional target changes via surface commands. This option delivers reduced drilling risk in terms of drilling a smoother wellbore, better wellbore stability, and maximum reservoir contact. Using automated steering control can result in increased production and ultimate recovery, as well as increased rig efficiency.

Increased rig efficiency from optimized drilling systems (as discussed previously) can provide greater net rate of penetration without the need for orienting or sliding issues, thus allowing optimized bit selection for performance. The greater reach capability ensures better weight transfer, continuous pipe rotation, less friction, and tight TVD control over long intervals, which, when used together, would create a smooth 3D well trajectory and superior gauge hole quality. The easy directional control and the effective reservoir navigation service using integrated sensors can result in increased production with precise wellbore placement in the reservoir and reduced drilling risk.

15.3.1.3 Measurement while Drilling Services

Measurement while drilling (MWD) services supports reliable transmission of downhole data to the surface, which can assist field and engineering personnel to make real-time wellbore decisions that will reduce nonproductive time. These measurements include taking directional surveys, measuring amounts of natural gamma rays, gauging drilling dynamics, temperatures, and annular pressure. MWD applications include geometric wellbore placement, reservoir navigation, and drilling optimization.

MWD tools transmit real-time measurements to the surface by using different data transmission methods commonly known as a telemetry system.

The most commonly used data transmission methods are listed below and in **Table 15.3** based on the typical depth and well-length limitations:

- Short reach
  - Electromagnetic pulse
  - Acoustic drill string
- Medium reach
  - Coiled tubing (E-line)
- Long reach
  - Mud pulse
  - Wired pipe

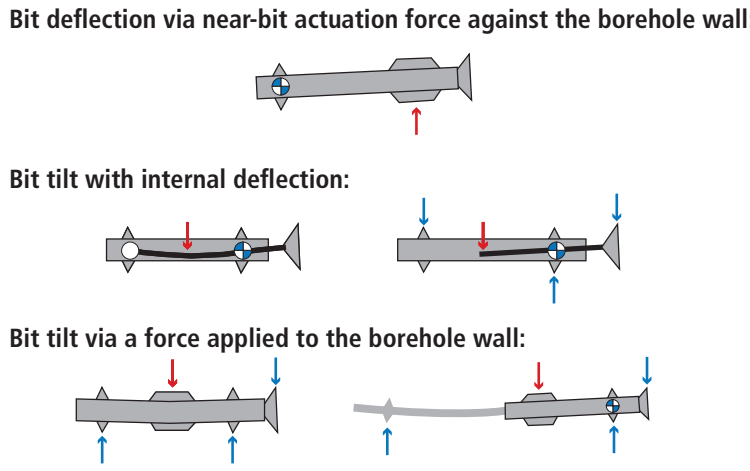

Fig. 15.7—Different rotary steerable technologies.

Table 15.3—Different data transmission methods and their associated data rate and range of reach. (Data from Wassermann et al. 2008*.) (Refer to the table, next, for source notations with asterisks: Wang et al. 2014, Jellison et al. 2003***, Baker Hughes 2014****, and other various sources).**

Attribute	Acoustic Drill-string	Electromagnetic	Mud Pulse	Coiled Tubing (E-line)	Wired Drillpipe
Data Rate, bps	20-100	10–100***	1–40*	10,000	1,000,000
Reach, m	5,000	Up to 3,000****	Up to 12,000**	7,000	Up to 15,000**

15.3.1.4 Mud-Pulse Telemetry

The economic success of many drilling operations depends on availability of real-time information about the drilling process (Wasserman et al. 2008). Drilling fluid telemetry systems, often called mud-pulse telemetry, are the most common type of transmitting MWD and LWD data and extremely useful in unconventional oil and gas drilling because of the opportunity to measure and provide important data during drilling operations. Mud-pulse MWD tools use three types of signal generation to generate mud pulse signals: negative pulse, positive pulse, and continuous wave. This is the most common method of data transmission used by MWD tools. Downhole, a valve is operated to restrict the flow of the drilling mud (slurry) according to the digital information to be transmitted. This creates pressure fluctuations representing the information. The pressure fluctuations propagate within the drilling fluid toward the surface where they are received from pressure sensors. On the surface, computers process the received pressure signals to reconstruct the information. When underbalanced drilling is used, mud pulse telemetry can become unusable. This is usually because, in order to reduce the equivalent density of the drilling mud, a compressible gas is injected into the mud. This causes high signal attenuation, which drastically reduces the ability of the mud to transmit pulsed data. In this case, it is necessary to use methods different from mud pulse telemetry, such as electromagnetic waves propagating through the formation or wired drill pipe telemetry. Current mud-pulse telemetry technology offers bandwidths of up to 40 bit/s (Wasseman et al. 2008). The data rate drops with increasing length of the wellbore. Surface-to-downhole communication is typically done via changes to drilling parameters; i.e., either a change to the drill string rotation speed or change to the mud-flow rate, commonly known as downlinking.

The mud-pulse telemetry for MWD most often is comprised of an uplink transmitter with encoder, continuous-value mud pulse transmitter, and a receiver with decoder, depending on the system used. Various software systems have been developed to decode data from the mud-pulse tools, such as the Pason Directional System, used together with the Baker Hughes mud pulse tools with Pason electronic drilling recorder to decode the mud pulse data. The system can provide information about the tool face, survey, gamma, and other diagnostic information.

15.3.2 Other Enabling Technologies

There are other enabling technologies that could significantly improve the performance of the drilling process. Bits and fluids are such examples.

15.3.2.1 Bits

Drill bits are either roller-cone or fixed-cutter. From a directional drilling perspective, the choice of bit is as critical as the selection of any other component in the well design. Different bits are selected based on the formation type and hardness.

15.3.2.1.1 Roller Cone Bits

A roller-cone bit removes rock through impact. A roller-cone bit comprises three conical rollers with teeth made of a hard material, such as tungsten carbide. The two-cone drill bits were designed and patented more than 100 years ago in 1909 by Howard Hughes, Sr. Twenty years later, Tricone roller drill bits (**Fig. 15.8**) were introduced to maximize drilling effectiveness and improve reliability and steerability. The basic cutting mechanics of these bits are through crouching and gouging. The features and concerns associated with the tricone roller drill bits are the following:

Features:

- Moving cones with pressed-in tungsten-carbide inserts (TCI) or steel teeth.
- Generates low torque and easy to steer. Torque fluctuation (TF) is almost nonexistent.

Concerns:

- Low durability and limited drilling rotations/hours because of moving parts
- Typical formations:
  - Top hole, soft rocks
  - Hard volcanic formations (basalt)

The cutting structure of the bits varies according to the rock formation. Soft bits will have longer protruding teeth or chisel-shaped buttons, and fewer, more widely arranged teeth. Medium formation bits will have much closer teeth than soft formation bits, and the protrusion of the teeth is reduced. The teeth are very short and closely arranged on hard formation bits.

15.3.2.1.2 Fixed Cutter Bits

A fixed-cutter bit (**Fig. 15.9**) removes rock through shearing or grinding away the rock, depending on the cutter type and size.

Two types of fixed cutter bits are commonly used:

- PDC bits
- Impregnable bits

15.3.2.1.3 PDC Bits

Polycrystalline diamond compact bits were introduced in the late 1980s. PDC bits have no moving parts.

Basic cutting mechanics of a PDC bit is through shearing and dragging. The following describes the features, concerns, and the typical formations that PDC bits are used with:

Features:

- Separate blades with built-in diamond cutters
- High durability due to absence of the moving parts
- Good for high-torque, low-speed operations

Concerns:

- Stick slip is an issue with aggressive bits, also resulting in cutter damage

Typical Formations:

- Currently there are PDC bit designs available to drill almost all types of formations, apart from very hard and abrasive sandstones.

The achievable dogleg severity (DLS) is a function of the bit-gauge length, gauge profile, side-cutting ability, cutter layout, and many other factors. The achievable weight on bit (WOB), or ability to flex the BHA, will be determined by the amount of torque required to effectively turn the bit. The torque is affected by the cutter size, type, and layout.

Modern bit design addresses the common drilling challenges associated with PDC bits, which has resulted in more directional-friendly bits by changing the bit profile, cutter size, orientation, rake angle, and count. Improved cutter technology has enabled operators to use PDC bits to drill in the wide spectrum of formation types that can be encountered throughout the bit run.

15.3.2.1.4 Talon 3D PDC bit

Further enhancements in technology specific to shale play development have resulted in specific solutions to optimize performance and reduce costs. Talon PDC bit (**Fig. 15.10**) enables increased mechanical, hydraulic, and operational efficiency without compromising bit and BHA stability for faster drilling and longer section lengths.

The Talon 3D high-efficiency, vector-accurate PDC bit is an optimized PDC frame designed to improve hydraulic efficiency and provide longer life in tough formations when operations call for reducing trips, especially in shale-play environments with the following features:

- Optimized junk slot volume and geometry provide hydraulic efficiency in low-horsepower-per-square inch (HSI) situations.
- Application-specific cutters tailored to the formation and operation to improve cutting efficiency and evacuation.
- Hard facing material and polished cutters increase durability to improve run life.
- Improves overall drilling efficiency by reducing buildup on the cutting face through the drill bit system's polished cutters.
- Increases build-up rate aggressiveness and enhances steerability through short bit-to-bend dimension.

15.3.2.1.5 Synthetic Diamond-Impregnated Drill Bits ("Impreg")

Impregnated bits are PDC type bits in which the diamond cutting structures are completely impregnated in the matrix material (**Fig. 15.11**). The features and concerns associated with the impregnated drill bits and the typical formation they are designed for are presented here:

Fig. 15.8—Schematic of a tricone bit.

Fig. 15.9—Schematic of a fixed-cutter bit.

Features:

- Small diamonds are impregnated into the matrix material
- Requires very high rotation speeds (>500 rpm) due to the low depth-of-cut control (DOC)
- Used in two-speed (TS) motors, turbines, and high-speed (HS) motor applications

Concerns:

- Matrix material hardness should be adjusted to the formation hardness to prevent grinding the formation with the matrix or premature diamond exposure and fast bit wear.

Typical Formations:

- Sandstone
- Very hard limestone and shale (> 25k psi)

15.3.2.1.6 Kymera Hybrid Drill bit

Operators are often challenged when it comes to making a choice between a roller cone bit and a PDC bit when drilling through the interbedded soft and hard formation. Leveraging the cutting superiority of PDCs in soft formations and the rock-crushing strength and stability of roller cones in hard or interbedded formations, the hybrid bit has the potential to maintain a higher overall rate of penetration for more footage than a roller cone or PDC could individually. Hybrid drill bit technology combines PDC and roller cone bit technology for smoother drilling, remarkable torque management, and precise steerability. **Fig. 15.12** shows the Baker Hughes Kymera hybrid drill bit.

15.3.2.2 Fluids

Drilling fluid systems design and selection should take into account the following:

Proper hole cleaning

- Stabilization of clays in the formation
- Overall wellbore stability
- Reduction of drag and stuck pipe
- Improved rate of penetration
- Sufficient lubricity
  - Long horizontal sections
  - Tortuous well paths
  - Rig limitations
  - Casing runs
  - Balling
- Wellbore stability
  - Shale stability (reactivity)
  - Sloughing
  - Breakout
  - Lost circulation
- Environmental and worker safety

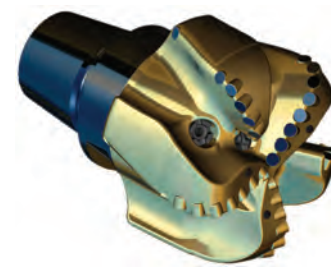

Fig. 15.10—Schematic of a Talon 3D PDC bit.

Fig. 15.11—Synthetic diamond-impregnated drill bit.

Fig. 15.12—Schematic of a Kymera hybrid drill bit.

Many operators of shale plays often look at fluids as a commodity item because they are not aware of the positive effects of working with a high-performance drilling fluid. It's important to consider the advantages of using an advanced drilling fluid due to the high impact on well construction success. Because of the high environmental sensitivity of many shale operators, water-based mud was developed to give customers superior performance while at the same time lowering environmental impact and reducing disposal costs. Today's newest WBM—LATIDRILL™ gives higher performance, is environmentally friendly, and cost-effective. The choice of drilling fluids should also consider local environmental regulations and facilities for treating and reusing spent drilling fluids.

The importance of a high-quality hole cannot be emphasized too much. A poor-quality hole will, in many cases, either lead to a poorly completed well, or one where significant amounts of well repair must take place before the well can be completed.

15.4 The Changing Needs of Unconventional Drilling

Drilling unconventional resources constantly requires finding ways to increase efficiency and reduce costs by employing the right processes and technology.

15.4.1 Common Pitfalls

Based on US experience, it requires a large number of development wells to develop shale gas and oil reservoirs. The so-called factory drilling approach is aimed at reducing costs and does not fully take into account the significant variability that exists in these plays. In the factory drilling approach, drilling practices are focused on reducing costs and not on reducing the geologic uncertainty. In this scenario, use of expensive, yet needed, technologies to characterize the reservoir is often discouraged. Horizontal wells are typically planned to maximize wells per leasehold. Gamma ray technology is often the only tool used to geosteer through the reservoir. These common practices have led to many wells being placed and completed in reservoir intervals with poor rock, which has a direct effect on production performance (Ahmed 2014).

15.4.2 Operating for Efficiency

Starting around 2008, the major operators and IOCs started acquiring leases to participate in the shale gas and oil revolution. These participants brought a more "data-rich" approach with them in terms of subsurface characterization than what most of the independents had done in the past. Based on experience from the early days of shale well drilling, and by use of modern fit-for-purpose technologies, industry is successfully aiming toward reducing costs and making these plays economic and efficient.

Operators have started to understand the importance of using wellbore-imaging data to position the fracturing stages better. They have also turned away from wireline data acquisition to the newer generation of logging while drilling tools, which frees the drilling rig earlier to move to the next well.

Additionally, advancements in drilling technologies enabled faster penetration rates and extended lateral lengths, while delivering a quality wellbore with precise steering in the prospective zone.

Table 15.4—Features and benefits of Navi-Drill ultra curve motor.

Features	Benefits
Reduced bit-to-bend length	Achieves higher and more consistent build-up rates at a smaller deflection angle setting.
High performance elastomer	Delivers more torque and power downhole for demanding, high-endurance PDC bits with premium, high-performance elastomer
Extended-length power sections	Provides higher torque output, greater rate of penetration, and improved reliability
Optimized connections and high make-up torque	Reduces the possibility of downhole back-off during tough and dynamic drilling applications for increased motor reliability and drilling performance

15.4.2.1 Improvements in Downhole Drilling Motors

Restrictions in the size of leases and the need to maximize reservoir exposure drove the trajectory design to higher dogleg severity (DLS) and also longer lateral lengths than was commonly used in conventional wells. The operating companies challenged the service companies to drill the well as cheaply and quickly as possible and to deliver the well curvature with a minimum of oriented (low rate of penetration) drilling. With the ever-increasing need for more horizontal reservoir exposure and the growing occurrence of pad drilling in major shale plays, the need for a more precise build-up rate (BUR), combined with consistent directional drilling control, has become even more critical. Advances in drill bit technology and optimization of drilling operations have pushed forth the design of a new steerable motor solution.

Service companies responded by developing motors with shorter bit-to-bend distance (to allow greater DLS) and more powerful power sections. The Baker Hughes Navi-Drill Ultra Curve motor features reduced bit-to-bend length to address the new requirement for steerable motors that can complete the vertical, curve, and lateral sections in one run, that also provide higher BURs in the curve section and improve overall drilling performance (**Table 15.4**). With a smaller adjustable kickoff angle requirement to achieve high BUR, Baker Hughes' Navi-Drill Ultra Curve motor enables precise wellbore placement and while delivering vertical, lateral, and curve sections in one run, maximizing overall performance and reducing well costs. Baker Hughes' Navi-Drill Ultra Curve motors (**Fig. 15.13**) provide improved BURs from kick-off throughout the curve and are capable of rotation at BURs that standard motors can only achieve in slide mode. While the standard Ultra series motors are suited for traditional wellbore profile applications, the Navi-Drill Ultra Curve motor has reduced bit-to-bend length that maximizes steering response and delivers reliable, high-BUR for ultimate performance in directional wells.

The industry has also developed friction-breaking tools that are installed along the drill string, which enabled oriented drilling at protracted depths. Automated top drive controls and related software was also introduced to maintain stable steering (tool face) orientation and extend the capability to drill in an oriented mode. Bit designs were refined to enable better side cutting ability and more durability. Traditional matrix bit body materials were replaced with steel bodies to reduce costs.

15.4.2.2 High Dogleg Rotary Steerable System

Using high dogleg RSS can achieve improving operational efficiency including:

- Reduces days on well
- Lands in the reservoir sooner
- Drills a smoother wellbore
- Places the well in the sweet spot
- Completes and produces faster
- Drills more wells per year
- Improves ultimate recovery

Traditional RSS often could not achieve the higher build rates needed for the unconventional wells, which meant that some of the lateral length in the pay zone had to be used to achieve the 90° angle. Using the lateral length in this way negatively affected production and deterred the traditional RSS use in unconventional wells.

Operators using traditional RSS struggled to meet the expectations of delivering high build-up rate to land the well and drill the lateral in one run. Which means that to drill wells with build-up 8-to-12°/100-ft., the operator had to first use a motor BHA to land the well, and then the lateral section was drilled using standard RSS. Two or more BHA runs were required, which have proven uneconomic in many applications.

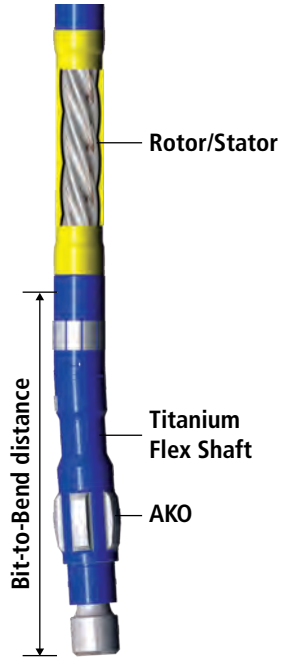

Fig. 15.13—Navi-Drill Ultra Curve™ motor.

While motor drilling was less expensive than RSS, there were some negative effects associated with their use:

- Multiple trips had to be made to adjust motor adjustable kick-off (AKO) angle and heavy-weight pipe placement. Different BHAs were required to drill each of the vertical curves and lateral sections.
- Hole quality was often poor, which meant that additional rig time was required to make cleanout trips and to condition the hole to run casing or completion string.
- Cement coverage and sealing around the casing was often inconsistent due to hole geometry.
- Setting packers and fracture and proppant distribution was problematic due to the rugosity of motor-drilled boreholes.
- Lateral lengths and wellbore placement were compromised due to the inability to slide from the cumulative friction of the drill string lying on the low side of the wellbore.

To address the operators' changing needs, drilling services companies developed high-build-rate rotary steerable systems combined with formation evaluation capability (gamma ray). These tools are capable of drilling the three sections in one run with a curvature of 8-to-15°/100'. To deliver the high doglegs, bits were developed that specifically matched the RSS systems.

While drilling the longer lateral section, keeping the well as flat as possible is the key. Wells with porpoising can cause difficulty with running casing, and low spots can collect liquids, which can cause hydrocarbon flow obstruction or liquid loading of gas wells.

The AutoTrak™ Curve high-build rate rotary steerable system with Talon™ bits can achieve "one-run curve and lateral" wells (one BHA, one bit, one trip). Cases are available in the Barnett, Woodford, Marcellus, and Eagle Ford, resulting in savings of several drilling days.

High-build rate rotary steerable systems (HBRSS) (such as the AutoTrak™ Curve) provides the following advantages:

- One bottomhole assembly (BHA) configuration for all intervals
- Oriented kick-off from vertical
- Controlled vertical drilling with a rotary bha
- Drill the curve up to 15° per 100 ft. build rate
- Drill the lateral precisely and fast
- Eliminate BHA trips
- Higher borehole quality
- Reduce days on wells

These new HBRSS were often combined with motors to enhance rate of penetration. The continuously rotating systems provided better hole cleaning, a better quality hole, more precise placement, and longer lateral reach. Cementing casing and completion operations become more effective. The improved efficiency also reduces drilling days and eliminates the need for wiper trips.

15.4.2.3 Pad Drilling Technology

The pad-drilling concept originated with offshore drilling, and was adapted to use on land during the last decade where it was used for tight gas wells in the US Rocky Mountains in the late 2000s (which consisted of 24 S-type wells on mountain and plateau tops). The results of multi- pad drilling (**Fig. 15.14**) are clearly evident in the Barnett shale area of North Texas where Devon started with 2 wells-per-pad in 2010 and has reached as high as 36 wells-per-pad (according to a Devon Energy Corporation report, 2014). The large number of wells per pad could only be achieved in the Barnett, where direction of S_{Hmin} is approximately equal to S_{Hmax}. Wells are not restricted to being drilled in the direction of S_{Hmin} to have the hydraulic fractures run perpendicular (transverse) to the horizontal lateral well, which creates the largest stimulated volume.

According to the US Energy Information Administration (EIA), by mid-2012, Statoil, Range Resources, and other drilling contractors started touting the advantages of pad drilling using 4-to-6 wells per pad (EIA 2012). Acceleration of the trend took place with the following results:

- The Eagle Ford grew from less than 40% of wells using pad drilling to more than 60% by mid-2013 (with 4-to-6 wells per pad).
- The Bakken had two-thirds of the wells being drilled on 4-to-6 well pads by mid-2013.
- The Marcellus had nearly the same percentage of wells being drilled from pads similar to Bakken.

Near the end of 2013, over 70% of all horizontal shale wells in the US were being drilled on pads with 4-to-6 wells. Today, less than a year later, 85% of the horizontal shale wells in the Eagle Ford, Marcellus, and Bakken are being drilled on 4-to-6 well pads.

Pad drilling offers a good solution to many issues, because it reduces the environmental impact, as well as improving operational efficiency and reducing cost. Modern rotary steerable systems are a key technology component in this approach. Increased drilling efficiency delivers more wells per rig per month, which helps to maintain—or increase—production rates.

The advantages of pad drilling are numerous and the potential benefits can be classified into three areas: environment, hydraulic fracturing, and production. The benefits are as follows:

Environmental

- Dramatically minimizes surface disturbance by consolidating surface drilling and production equipment.
- Reduces an operator's impact on developable land.
- Minimizes wildlife disturbance.
- Requires fewer access roads to multiple pads versus traffic to single pads for multiple wells.
- Reduces truck traffic (and emissions).
- Creates a smaller surface footprint, which is a benefit for populated areas, and supports better community relations.
- Rig moves, operations, and drilling efficiency.
- Moving rigs between locations typically takes only two to three days.
- On pad, rig moves are only about 20 ft. to the next well location taking a few hours.

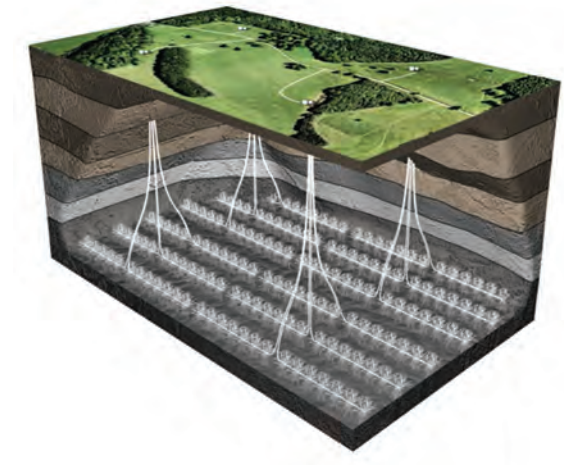

Fig. 15.14—Pad drilling has many advantages, such as targeted sweet spots, data-rich planning and design, improved production performance, and optimized logistics and costs. Reduced number of suppliers means single point of accountability. (Image from Statoil.com.)

- Decreased time and traffic for rig setup, breakdown, and move.
- Supports "batch drilling" of (upper part of well) to gain efficiency.
- Reduces capital expenditures for the location and roads, and drilling water and mud; storage tanks and pits.
- Eliminates the need for additional lease roads.
- Reduces ancillary drilling costs; i.e., trucking material and supplies, operating fuel and electricity because pad drilling only requires a central location.
- Overall, operators can drill multiple wells in less time than drilling one well per site.

Hydraulic Fracturing

- Proppant and water transport to single location savings.
- Fracturing manifolds with access to all wells on pad, which provides a single point connection for fracturing fluid, proppant, and slurry.
- Possible skid-mounted fracturing pumps designated to remain on pad for longer periods of time.
- Fracturing fluid and drill water treatment and storage.
- Central location for water source and disposal wells.
- Allows for simultaneous hydraulic fracturing operations, such as two and three well zipper fractures. Zipper fracturing can reduce days and costs up to 50%.
- Flowbacks are optimized by consolidating equipment and resources.

Production Benefits

- Produce wells efficiently
- Consolidate operations, personnel, driving time
- Reduce capital expenditures for a number of liquid separators, storage tanks, vapor recovery units, piping, lease transfers and sales, and equipment and pipelines

All the above advantages can be easily eliminated if the efficiency process overlooks the reservoir characterization and understanding.

15.4.3 Data-Driven Approach and FE

When the target zone has been identified, it is important to place the wellbore in the optimal part of the reservoir, taking into account bed dip as well as formation discontinuity due to faulting. With today's modern MWD and LWD tools, it is possible to use reservoir navigation services where pre-drill models are built based on available seismic data and offset well reservoir characterization data. During drilling, the LWD data is used to maintain the wellbore in the optimum zone, or the sweet spot. A variety of sensing techniques is used, depending on the play. In some cases, oriented gamma ray measurement has proven useful, while in other cases deep reading azimuthal resistivity images or high-resolution borehole images have enabled real-time decisions to maintain the well trajectory within the productive zone.

15.4.3.1 Advanced Mud Logging Techniques

Mud loggers are the first (and sometimes the only) people at the rig site to actually look at mud log analysis, and describe the cuttings that are being drilled. These brief descriptions on the mud log based on a quick examination under a low powered microscope are for many the only information available describing the actual geology of the formations being drilled.

Today's operators need much more information about the formations than traditional mud logging analysis can deliver. Questions such as:

- What type of clay minerals is in this shale?
- What is the total organic carbon (TOC) content of the formation?
- Where is the best place to hydraulically fracture?
- How much dolomite is present?

Historically, the answers to these questions have required laboratory analysis, which was usually done after the well was completed. Now, we can answer these questions while drilling at the well site, because advances in technology enable us to access information to help make informed decisions while drilling, which also helps the operators to refine their completion strategy.

The Geologic Evaluation Service with advanced cuttings evaluation from Baker Hughes uses the latest analytical technologies to give real-time elemental, mineralogical, organic content, and petrophysical analysis of cuttings for enhanced formation evaluation while drilling. Real-time geochemical data can also be used for near real-time geosteering and to support smart completion solutions in unconventional shale plays.

The advanced cuttings evaluation uses a comprehensive range of analytical methods that can be used either singly or together to give you a full understanding of the reservoir while still drilling. The service includes:

XRF

X-ray Fluorescence (XRF) is used to measure the emission of characteristic "secondary," or fluorescent X-rays, from a sample that has been bombarded with high-energy X-rays. The frequency of this fluorescence identifies the elemental composition of the sample. Elements from magnesium to uranium can be identified in minutes.

XRD

X-ray Diffraction (XRD) analysis measures the scattering of a beam of X-rays when passed through a crystalline material. The crystal structure produces a unique X-ray fingerprint of X-ray intensity versus scattering angle, which is used to identify the minerals present in the sample, including clay minerals.

Pyrolysis

Pyrolysis analysis uses established oil industry analytical techniques, usually run post well in the laboratory to identify the amount, type, and maturity of the kerogen in the formation at the rig site. This enables real-time identification of productive and nonproductive zones.

RoqSCAN™

Baker Hughes and CGG have combined their portfolios to bring CGG Robertson RoqSCAN™ wellsite mineralogical analysis to the rig site. This technology uses a portable scanning electron microscope (SEM) fitted with X-ray detectors to give an automatic quantitative and diagnostic analysis of mineralogy and texture (including porosity) within 30 minutes of the sample arriving at the surface.

RoqSCAN™ can distinguish more than 100 minerals, over 70 elements, accurately differentiate clay minerals and clay mineral phases, and also provide quantitative textural information.

Digital Microscope

The high-resolution digital microscope provides the geoscientists the capability to examine the cuttings in detail at the rig site or in town.

By using all this information along with other log information, the operator has the opportunity to optimize and redefine the completions program before the well drilling is finished. In this case, the operator could improve chances of a successful completion job by ignoring poor zones and concentrating on stimulating prospective zones in the horizontal lateral.

15.4.3.2 Logging while Drilling

Introducing logging while drilling (LWD) systems can have profound effect on the ultimate value delivered by a wellbore. LWD tools not only help to provide critical assurance in optimal wellbore placement and precise reservoir description, but LWD also allows the operator to optimize drilling dysfunctions and mitigate hazards. Further, added advantages of LWD services include real-time structural model updates and better designed, enhanced completions.

Historically, instrumentation that was used to obtain high-quality formation evaluation in shale reservoirs has been restricted to the wireline method of logging. As technology advanced, more and more shale plays have horizontal sections in the well plans. Longer horizontal sections help increase reservoir contact and improve single well production. Driven by cost, time, and difficulty associated with acquiring wireline measurements in horizontal intervals, only the vertical sections were logged and interpreted and then used to define the reservoir profile for the horizontal target. This has been proven to be a less effective method of drilling shale plays due to its non-unique structural modeling solutions.

With current advanced technologies, most wireline conveyed measurements are available in logging while drilling (LWD). Logging wells with LWD is an efficient and more economical alternative of acquiring measurements along the lateral. Integration of logging sensors in the drilling BHA provides critical formation evaluation information while requiring little additional time, effort, and cost. As well drilling costs constitute a huge percentage of a typical unconventional well's total construction cost, LWD technologies play a critical role in enhancing recovery and making unconventional plays profitable. Relevant LWD acquisitions are listed in the following paragraphs. Details of these measurements can be found in Chapter 8.

15.4.3.3.1 Gamma Ray

Natural gamma ray measurement is a measurement of total natural radioactivity that is measured in API units. Mostly shales and clays are responsible for natural radioactivity and hence gamma ray is a good indicator of presence of these formations.

15.4.3.3.2 Resistivity

It is a measure of ability of a formation to conduct electrical current. Rock has pore spaces filled with fluids that can be conductive (saline water) or nonconductive like oil, gas, etc. High resistive formations indicate the presence of hydrocarbons as it indicates a low water content and higher hydrocarbon content.

15.4.3.3.3 Neutron Porosity and Density

Using low-level radioactive sources, it is possible to estimate the formation density and porosity. Porosity is derived from interaction of high-speed neutrons emitted by radioactive nuclei with the hydrogen atoms present in the formation and fluids. Hydrogen causes these fast moving neutrons to slow down. Measuring and detecting the amount of slow neutrons can be directly correlated to the porosity of the formation. This is because hydrogen—as water or hydrocarbons—is mostly found in the pore spaces of rocks.

For density measurement, a gamma rays emitting source is used. The amount of gamma rays absorbed in any medium is directly related to the electron density of the material. Therefore, the density is derived from the amount of dissipated gamma rays in the formation.

Combining the density and porosity measurements can provide invaluable information about the rock matrix and the fluid in the pore spaces.

15.4.3.3.4 Acoustic

Acoustic is a method to measure the formation's acoustic property. A sound source is placed in the downhole tools and is spaced with an array of receivers that measure the speed of sound propagating through the formation rocks. The information obtained is used for various applications such as:

- Calibrate already existing seismic data
- Determine acoustic porosity
- Correlate stratigraphic data
- Identify lithologies, fractures, and compaction
- Identify over-pressure conditions

15.4.3.3.5 Seismic while Drilling

This technology allows a true look ahead into the well formations and structure by helping to generate a real-time high-resolution seismic map tied to the existing surface seismic data. This "look ahead" is achieved by utilizing a surface seismic source with tools that act as a downhole receiver. Seismic while drilling (SWD) captures seismic data without interrupting drilling operations, which can save money and reduce risk. SWD also provides the ability to predict pore pressure ahead of the bit.

15.4.3.3.6 Electrical Imaging

The LWD electrical imager uses a single electrode to measure the resistivity as the drill string rotates. The electrode emits a current at a known voltage into the formation, using the conductive mud as a medium, and the return voltage is recorded. A high sampling rate combined with the shallow, focused measurement enables generation of very high-resolution images, while the rotating sensor offers a true 360° image of the borehole for advanced structural analysis.

There are other LWD technologies like nuclear magnetic resonance (NMR) logging, formation pressure testing, fluid sampling that are rarely used in the unconventional wells, and hence this discussion excludes these technologies.

15.4.4 Reservoir Navigation with Image Logs

Depth correlation using LWD measurements is relatively easy when drilling through formation strata in vertical wells; however if one is drilling parallel to the bedding planes, it becomes more complex. Various imaging tools can be used to effectively steer well drilling in real time and keep the lateral being drilled in the target zone. Using reservoir navigation systems (RNS) techniques, the operator can be aware, in real-time, of the near-wellbore apparent dip, stratigraphic position, and subseismic faulting (**Fig. 15.15**). This knowledge can improve the decision-making process and the probability of a higher net-to-gross well. Additionally, many of the geologic interpretations can be confirmed using an LWD electrical imaging tool with high-resolution image. In shale reservoirs, the laminated nature of shale formations makes using borehole LWD images an ideal steering tool (**Fig. 15.16** and **Fig. 15.17**).

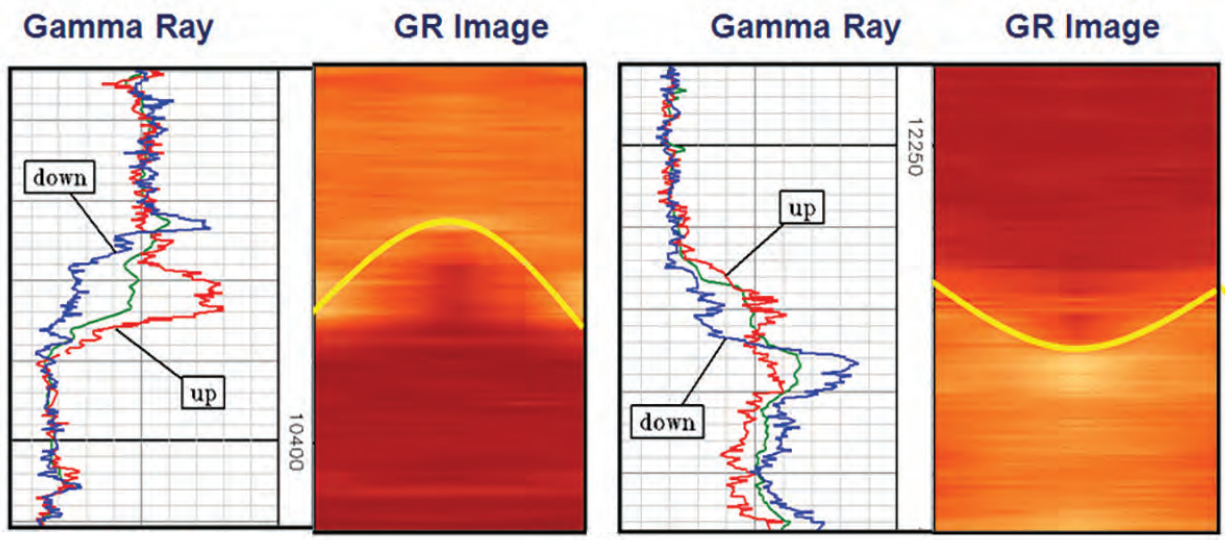

Fig. 15.15—Example of how imaging tools are used to calculate apparent DIP. (From Thomas et al. 2014.)

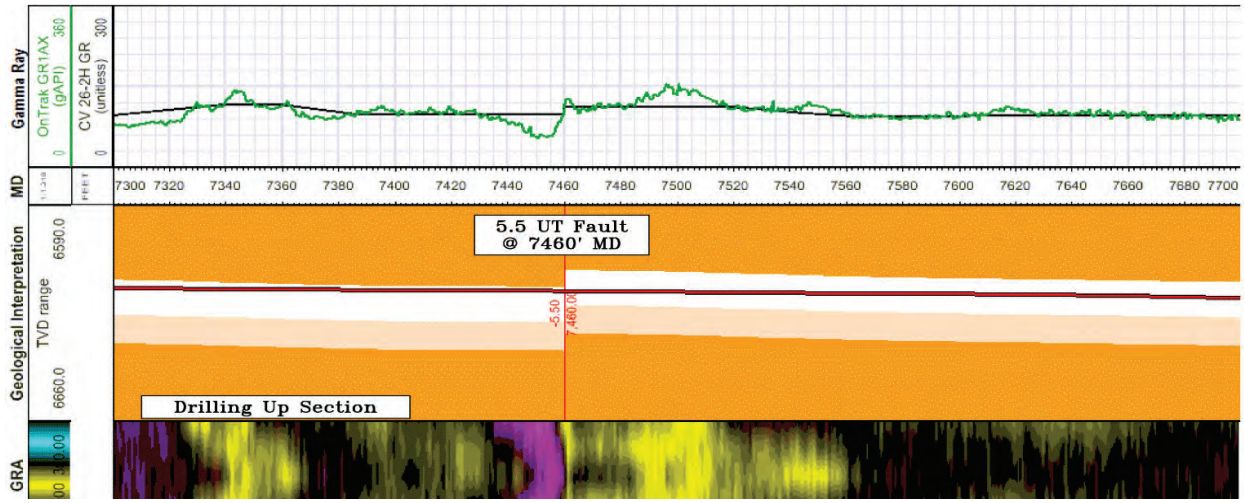

Fig. 15.16—A typical horizontal well navigation using gamma ray imaging. (From Thomas et al. 2014.)

Real-time dip picking and validating structural models allow reservoir navigational specialists to effectively steer the wellbore within thin targets or sweet spots within the reservoir thus having a great impact on the overall life and output of a wellbore.

Electrical images can be used to interpret bedding and structural information, fracture type and orientation, and faults with orientation. Using the improved accuracy of high-resolution electrical images, they are often used to confirm and provide accurate depth for faults and features identified by gamma imaging, or if gamma or resistivity imaging results are too subtle, faults are confirmed with the high-resolution electrical imager (**Figs. 15.18** and **15.19**).

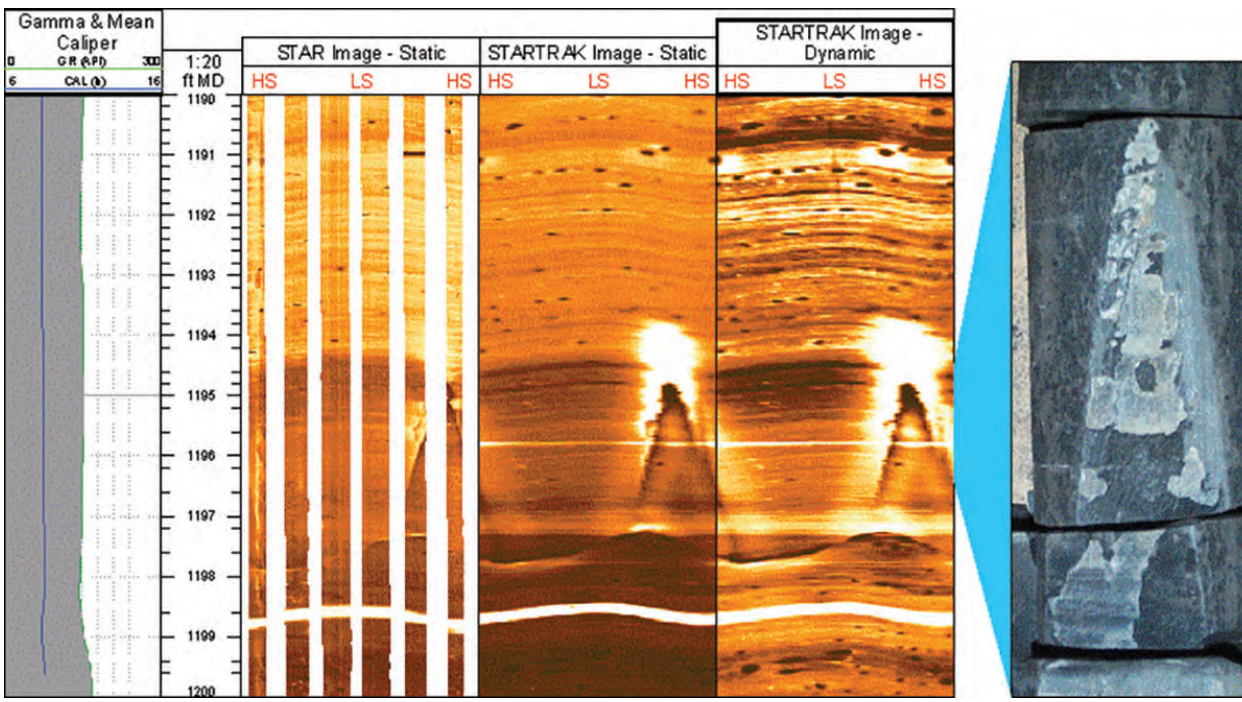

Fig. 15.17—Image quality of LWD tools versus wireline tools compares vary favorably. (From Janwadkar et al. 2012.)

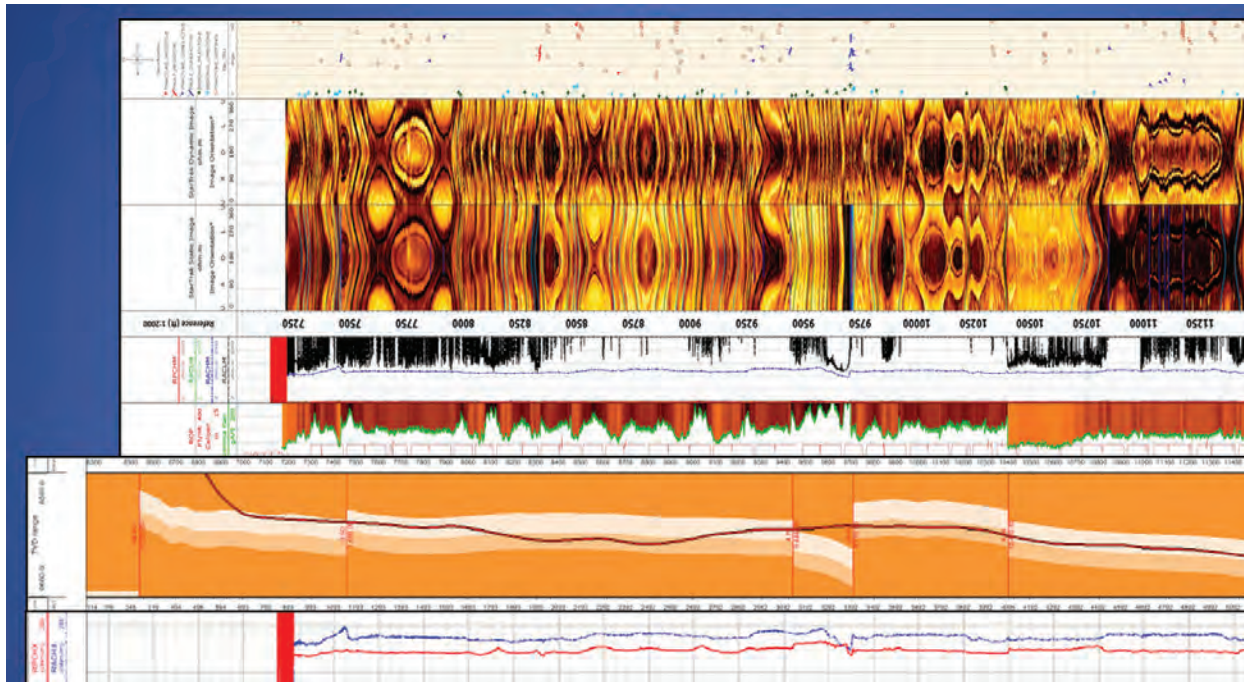

Fig. 15.18—Shows a typical reservoir navigation deliverable combined with the interpreted high-resolution electrical imager. (From Thomas et al. 2014.)

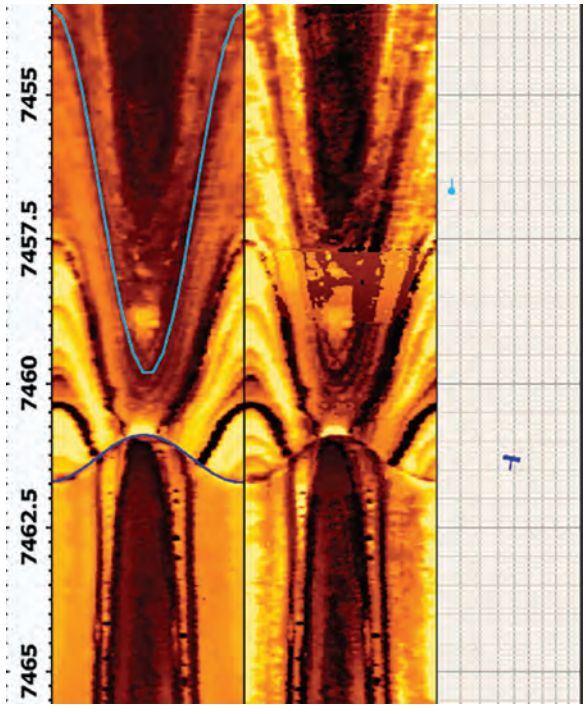

Fig. 15.19—A bedding plane (turquoise) and a fault (blue). (From Thomas et al. 2014.)

15.4.5 Completion Optimization Using Logging while Drilling Logs

It is recommended that the lateral section of the well be characterized in order to gain critical information about natural and conductive fractures. The results of the characterization will help plan completion process to maximize production. It is recommended to run LWD imaging tools along the lateral, because the service is relatively inexpensive, and the process is valuable to the drillers and others.

Imaging tools can identify natural fractures, faults, bedding planes, and even induced fractures from nearby offset wells. Along with the imaging tools used for analyzing the drill cuttings for top-of-cement and mineralogy, and employing advanced mud logging (to include gas chromatography). Together, these methods can help to understand the entire picture.

Tools for characterizing certain reservoir information along the lateral, such as high-definition electrical resistivity imaging LWD tools (Baker's StarTrak™), can provide valuable information for placement of fracture stages and perforation clusters (in plug-and-perf) for well completion. **Fig. 15.20** shows that 3D seismic has limited resolution and cores have

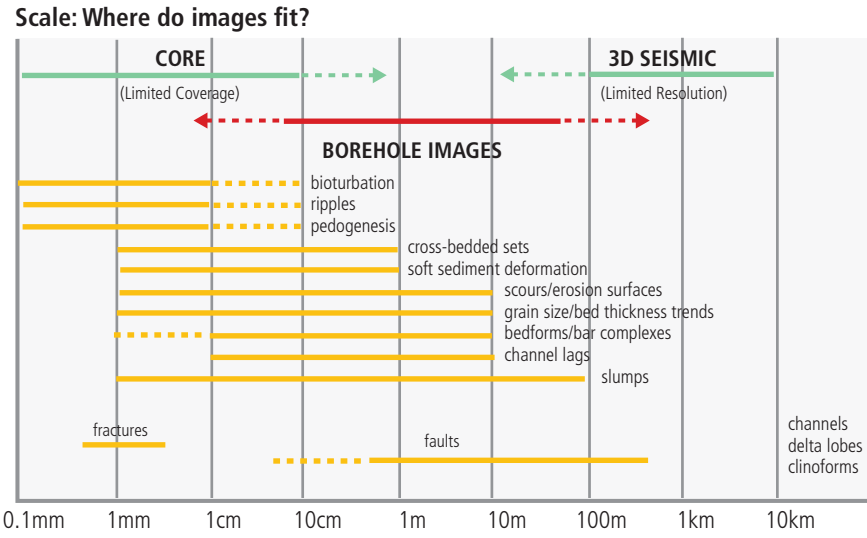

Fig. 15.20—Where do the images fit? (From Kennedy et al. 2012b.)

limited coverage; therefore, high-definition resistivity images truly fill this gap of addressing typical stage and cluster intervals between 1 and 100 meters.

High-definition resistivity images can help to identify natural fractures, induced fractures (from nearby offset wells), faults, and bedding planes. This information can be used to help optimize the fracturing (placement) program, while helping to avoid areas where fracturing will be inefficient and, more importantly, help to identify areas where fracturing will be most beneficial; i.e., locations of natural fractures (see **Fig.15.21**, **Fig. 15.22**, and **Fig. 15.23**).

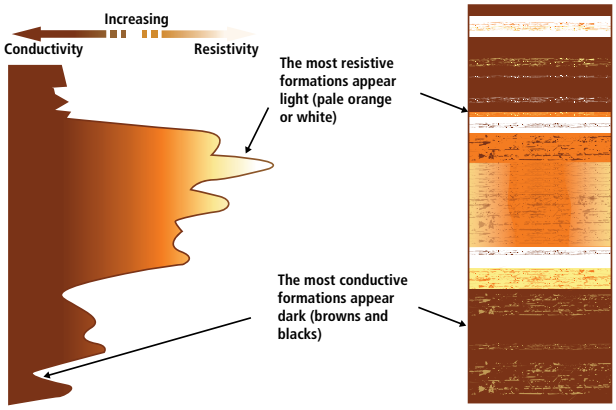

Fig. 15.21—How image colors are assigned. (From Janwadkar et al. 2012.)

Next, we provide an example with an overview of the wellbore trajectory along with the high-definition image log. The fracture characterization for the eight-fracture stages are included in this particular well example. Color codes are listed below.

In **Fig. 15.25**, the bottom shows the gamma ray curve shaded in earth tones. Next, above the gamma ray curve are the dip type and angle data. Third from the bottom is the depth column. Fourth from the bottom is the LWD resistivity image. The next four columns above the image log give the strike direction based on a Schmidt plot. The strike direction given in each column is color-coded the same as the dip and angle data with blue as the open strike direction, red as the partial strike direction, brown as the shear fracture strike direction, and pink as the strike direction for the faults. The next four columns above that show fracture density. Fracture stages (numbered) are in next column. The column above this illustrates the wellbore path built on the path developed from the stratigraphic vertical wells. Next is the depth column that applies to the very top column depicting the modeled gamma ray plotted against the real-time gamma rays.

This detailed analysis that identifies natural fractures, along with their orientation and distribution, helps to distinguish natural fractures from drilling-induced fractures or borehole breakouts. As described previously, petrophysical analysis, combined with electrical imaging, provides a comprehensive quantitative fracture analysis. This analysis can be used to compute fracture density, fracture aperture, and fracture

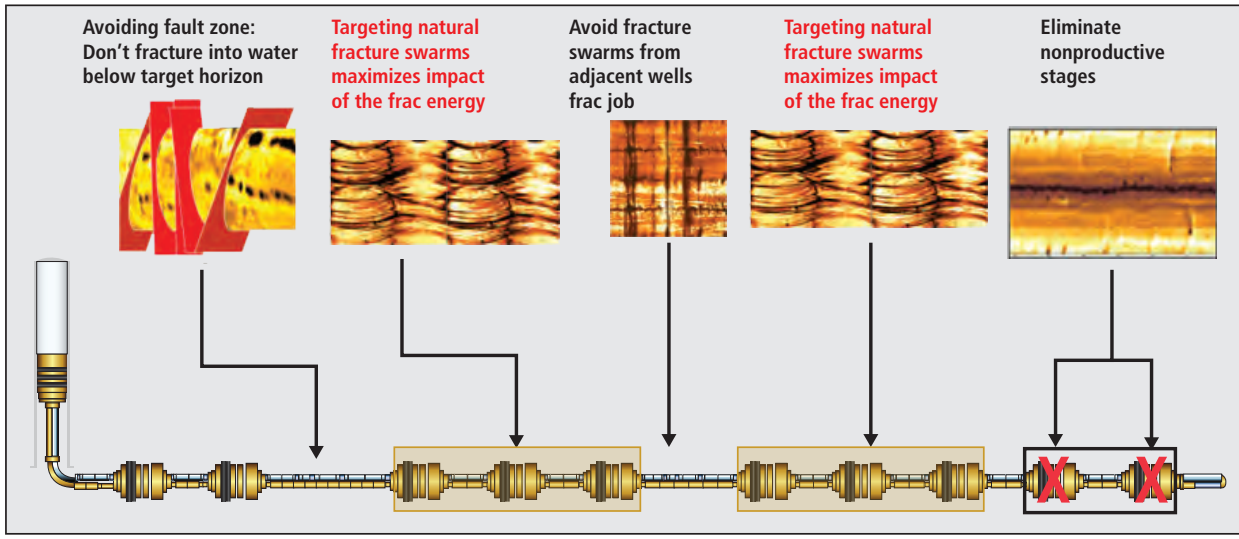

Fig. 15.22—LWD resistivity imaging tool provides valuable information on stage placement. (From Kennedy et al. 2012b.)

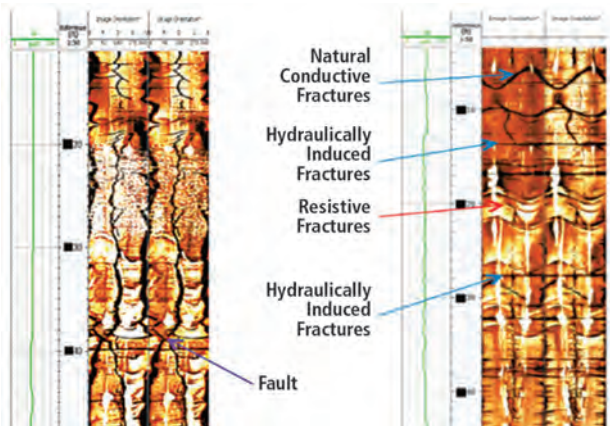

Fig. 15.23—Fracture and faults on log display. The red array shows partially open fractures, blue shows open fractures, and violet shows faults. (From Kennedy et al. 2012b.)

lengths. Then, fracture stage placement can be enhanced by targeting natural fractures, avoiding fracture swarms from adjacent wells, and by eliminating nonproductive stages.

15.4.6 Modern Cementing Technologies

Modern cementing technologies emphasize best practices in cementing and protecting the well integrity and the environment and require the delivery of zonal isolation via an integrated suite of solutions. These practices and technologies are under one comprehensive well integrity roof. The focus here is on maximizing long-term zonal isolation, ensuring a solid bond for the well, and a post-job evaluation to ensure that the execution data matches with the pre-job simulation.

15.4.6.1 Maximizing Zonal Isolation Success with Careful Planning and Simulations

A good cement job starts with proper understanding of well design objectives and application of cementing best practices. These practices, including mud conditioning, optimal pump rates, right densities, centralization, and other factors that maximize mud displacement efficiencies ensuring effective mud removal, are critical elements for long-term zonal isolation. By staying engaged, we can ensure that we fully understand all of the challenges and have all the critical data needed to perform the job.

An early step to reducing well construction risks is performing an in-depth, pre-job evaluation by determining the objectives and challenges for building the well before designing the cementing job.

Experienced cementing specialists complete such a vital step by creating computer models using a number of cementing simulation software applications.

The CemFACTS™ advanced cement placement software incorporates the planned cement setting depth, hole size, desired pump rates, and bottomhole temperatures and pressures to simulate cement slurry placement. It also performs interactive calculations of the necessary slurry and spacer volumes, mixing and displacement rates, and anticipated pressures. The simulation also factors in fluid compressibility and multiple temperature regimes. Taken together, this allows for accurately predicting downhole density changes enabling us to better predict a more realistic

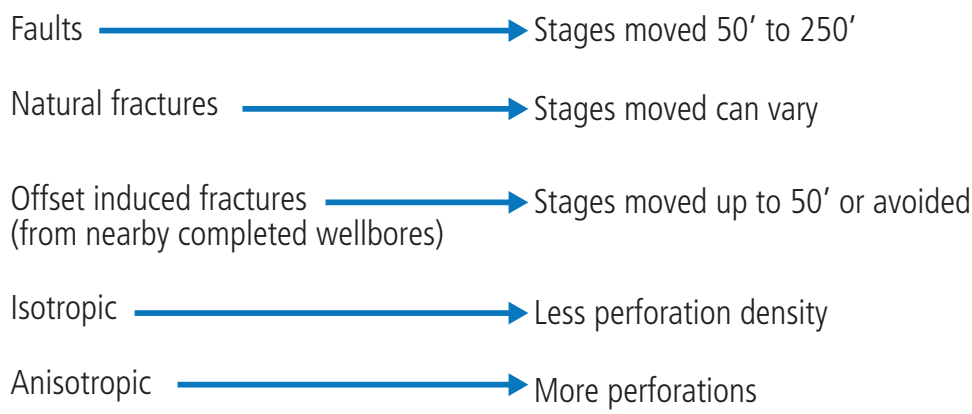

Fig. 15.24—Typical stage adjustments.

equivalent circulating density and, when necessary, modify pump rates to avoid lost circulation or fluids migration.

To better understand the expected wellbore stresses that can impact long-term integrity, Baker Hughes engineers use IsoVision™ software to model the radial and tangential stresses on the set cement and determine whether the planned cement sheath will perform effectively over the full life of the well. If needed, changes can be made to the cementing program to adjust the cement's compressive and tensile strength, Young's modulus, and Poisson's ratio, and make it more resilient to downhole stresses.

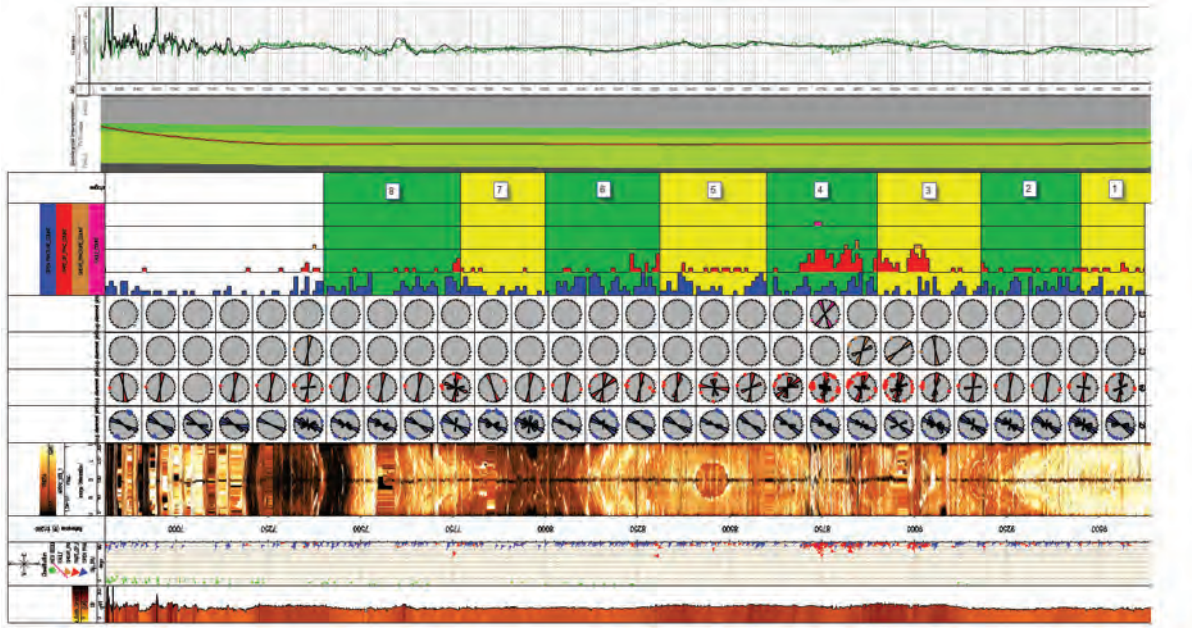

Fig. 15.25—StarTrak™ completion optimization lot. (From Janwadkar et al. 2012.)

Fig. 15.26—Baker Hughes Optimized Drilling (OASIS) process.

The benefit of these simulation offerings goes beyond the ability to make changes to the cement job design. They help engineers make informed decisions about the stage placement, slurry design, and cement system selection—minimizing risk throughout the well's life.

CemVision™ 3D cement simulation software offers Baker Hughes engineers a better understanding of fluid contamination risks.

The combined benefits of these simulation tools go beyond the ability to make changes to the cement job design. They help engineers make informed decisions regarding the stage placement, slurry design, and cement system selection—minimizing risk throughout the well's life.

15.4.6.2 Preparing the Well for a Solid Bond

Once the simulation is completed, the engineer works with the operator to select the optimal spacer system, which helps ensure that the wellbore is free of drilling mud and other debris, and water-wets the casing string and formation rock for vastly improved cement bonding. To further optimize a cement job, operators need assurances that the cement is delivered to the desired location in the wellbore, without causing lost circulation issues or other damage to the producing formation. Baker Hughes offers a selection of spacers so that regardless of the situation, one can apply the appropriate one or a combination of two of the following:

- The MultiBond™ spacer system is a stable fluid designed to recover expensive oil- and synthetic-based drilling fluids while preparing the well for a cement job
- The SealBond™ cement spacer system mitigates lost-circulation issues by reducing slurry fallback after placement, which prevents induced losses and eliminates costly remedial cement jobs
- The UltraBond™ spacer system effectively displaces the drilling fluid in the annulus, improves fluids compatibilities, optimizes displacement efficiencies, provides superior cement bonding, and promotes effective mud removal.

15.4.6.3 Delivering Zonal Isolation That Is Permanent, Long-Lasting

Once the wellbore has been properly conditioned, cement slurry is chosen that will ensure the best long-term resilience against stresses in the cement sheath.

It is prudent to work with a family of cement system, customized solutions that can address downhole conditions and well requirements. Baker Hughes DeepSet for Life™ is an example of such a solution that includes:

- The DeepSet™ system controls shallow water and gas-flow in deepwater wells.
- The DuraSet™ system withstands stresses induced by hydraulic fracturing, high-injection pressures, and temperature fluctuations.
- The FoamSet™ system provides wellbore integrity and ensures proper zonal isolation for diverse environments by lowering lost-circulation risks, protecting against shallow gas flows, and improving hole cleaning and cementing performance.
- The LiteSet™ system delivers superior-quality lightweight cements with higher compressive strengths.
- The PermaSet™ system provides maximized cement longevity in CO_2 and other corrosive environments.
- The XtremeSet™ system ensures long-term zonal isolation in wells with bottomhole temperatures as high as 600°F (316°C) and pressures up to 40,000 psi (275.8 MPa).

15.4.6.4 Closing the Loop with Job Evaluation

When the cement job is complete at the well site, evaluation of the results using Baker Hughes CemFACTS software can be performed to analyze how well the execution data matches with the pre-job simulation. The software highlights any deviations between the simulation and actual job

execution data, enabling one to make changes to the cement job design for future wells to optimize the process.

15.4.6.5 Putting It All Together

By collaborating closely with operators and drawing from a comprehensive portfolio of design processes, cementing technologies and equipment, and leveraging experienced field personnel, Baker Hughes helps minimize risks and ensure long-term integrity for wells around the world.

Combining job simulation, cementing, evaluation, and mechanical barrier technologies under one comprehensive well integrity solution lets Baker Hughes better address various well integrity challenges by deploying the optimal combination of advanced technologies and principles of flawless execution.

The cement sheath that seals the well is, ultimately, an investment in safety and environmental stewardship. In addition to supporting the casing, the sheath offers a sealed barrier that protects the casing from corrosion and underground source drinking water from contamination.

A well-designed Zonal Isolation Suite combines optimized cement systems and automated mixing equipment to enable precise slurries matched to well conditions that deliver the well integrity needs for the life of the well while minimizing rig time. Baker Hughes Zonal Isolation Suite is designed to address such a challenge.

15.4.7 Drilling Optimization and Remote Drilling Technology

Drilling shale wells presents technical challenges that impact the overarching goal of optimizing drilling costs and reducing days on wells. The quality of pre-well planning impacts both drilling spend and ultimate recovery. Therefore, an integrated approach is required to ensure that all the available reservoir data, geoscience, and geomechanical knowledge and down-hole conditions are well understood prior to planning the details of shale wells.

Following a strict regimen of careful planning and execution is vital to a long-term well integrity solution as illustrated in the Drilling Optimization process referred to as OASIS in (**Fig. 15.26.**) The service is based on the Continuous Improvement Cycle. Each project has slightly different challenges, but in each case the positive impact of the service on drilling efficiency is achieved through the process. The results of the planning phase are critical as is a careful post-drilling evaluation. By carefully utilizing this process Baker Hughes drilling planners and engineers can demonstrate to our customers the effectiveness of our technologies and processes in helping them to maximize the return on their investment.

15.5 Concluding Remarks

Applying classic drilling and well construction engineering techniques is considered to be inadequate for meeting the unique challenges posed by unconventional shale oil and gas formations. With the current small profit margins available for operators and service companies, improper horizontal well placement can result in failure with any subsequent completion and production operations, which is not acceptable.

Experience with US shale has shown that, in order to capture full reservoir potential and deliver the economic value of the assets, drilling technology must accommodate sweet spot identification. Moreover, drilling technology should be further optimized to reduce costs and mitigate operational risks including appropriate zonal isolation. Operators are now realizing the importance of well-bore imaging and real-time data, which is documented in numerous case studies and obviously successful field implementations. Various drilling system components (drilling rigs, drilling fluids, downhole drilling motors, cementing, and drill bits) are constantly being improved and introduced to the market to maintain environmental compliance, while offering greater return on investments. These tools and services are not only designed specifically to meet each operator's objectives at the initial phase of the exploration and appraisal but also during the development phase. These tools also offer flexibility to seamlessly integrate with one another by adding multi-dimensional functionality to the drilling system during the development and rejuvenation phases of the field development plan.

Baker Hughes OASIS strategic approach is the industry's most comprehensive drilling solution in planning and execution that improves well productivity and mitigates operational risks regardless of the drilling challenge.

15.6 References

Ahmed, U. 2014. Optimized Shale Resource Development: Balance between Technology and Economic Considerations. Paper SPE 169984 presented at the Trinidad & Tobago Energy Resources Conference, Port of Spain, Trinidad & Tobago, 9–11 June 2014.

Baker Hughes 2013. Driving Innovations in Well Integrity. *CONNEXUS*, **4** (1): 22. http://assets.cmp.bh.mxmcloud.com/system/96599d804d94403e9215de5516d322ef/pdfs/f0/00cc80aed811e382d54d156dd14b16/CONNEXUS_6.pdf (accessed July 3, 2014).

Baker Hughes 2013. WellLink Fit Remote Directional Drilling Service. http://assets.cmp.bh.mxmcloud.com/system/v1/1a28e95712c1795dd4a928315c36958d/37462.WellLink_Fit_Overview_HiRes.pdf (accessed July 18, 2014).

Baker Hughes 2014. E-MTrak Electromagnetic Telemetry, http://www.bakerhughes.com/products-and-services/drilling/drilling-services/measurement-while-drilling/e-mtrak-electromagnetic-telemetry (accessed September 2014).

Baker Hughes. 2014. Zonal Isolation Suite Delivering Reliable Wellbore Integrity with an Integrated Suite of Solutions. http://assets.cmp.bh.mxmcloud.com/system/46/3099a01e7311e490b84fe12de84bdc/41050.Zonal-Isolation-Suite_Brochure_Web.pdf (accessed September 2014).

Caruzo, A., Hutin, R., Reyes, S., et al. 2012. Advanced Design and Execution Techniques for Delivering High Data Rate MWD Telemetry for Ultradeep Wells. Paper OTC-23749 presented at the OTC Arctic Technology Conference. Houston, Texas. 3–5 December. http://dx.doi.org/10.4043/23749-MS.

Devon Energy Corporation report. http://www.dvn.com/CorpResp/initiatives/Pages/MultiwellPads.aspx#terms?disclaimer=yes (accessed July 2014).

Energy Information Administration (EIA). 2011. Review of Emerging Resources: U.S. Shale Gas and Shale Oil Plays, July 2011. Prepared by INTEK Inc., for the U.S. Energy Information Administration (EIA) Department of Energy, Washington, DC. http://www.eia.gov/analysis/studies/usshalegas/pdf/usshaleplays.pdf (accessed June 2014).

Energy Information Administration. 2012. Today in Energy, Pad Drilling and Rig Mobility Lead to More Efficient Drilling. http://www.eia.gov/todayinenergy/detail.cfm?id=7910 (accessed June 2014).

Hahn, D., Peters, V., and Rouatbi, C. 2005. Hydraulically balanced reciprocating pulser valve for mud pulse telemetry. US Patent No. 6898150 B2.

Kennedy, R.L., Gupta, R., Kotov, S., et al. 2012b. Optimized Shale Resource Development: Proper Placement of Wells and Hydraulic Fracture Stages. Paper SPE 162534 presented at the Abu Dhabi International Petroleum Conference and Exhibition. Abu Dhabi, UAE. 11–14 November. http://dx.doi.org/10.2118/162534-MS.

Kennedy, R.L., Knecht, W.N., and Georgi. D.T. 2012a. Comparison and Contrasts of Shale Gas and Tight Gas Development, North American Experience and Trends. Paper SPE 160855 presented at the SPE Saudi Arabia Section Technical Symposium and Exhibition. Al-Khobar, Saudi Arabia. 8–11 April. http://dx.doi.org/10.2118/160855-MS.

Janwadkar, S., Thomas, M., Denney, S., et al. 2012. High-Resolution LWD Images Used to Optimize Completions in Unconventional Play–North America. Paper SPE 152303 presented at the SPE/EAGE European Unconventional Resources Conference and Exhibition. Vienna, Austria. 20–22 March. http://dx.doi.org/10.2118/152303-MS.

Jellison, M.J., Hall, D. R., Howard, D.C. et al. 2003. Telemetry Drill Pipe: Enabling Technology for the Downhole Internet. Paper SPE 79885 presented at the SPE/IADC Drilling Conference. Amsterdam, Netherlands. 19–21 February. http://dx.doi.org/10.2118/79885-MS.

Thomas, M.G., Gupta, R., and Martin, S.J. 2014. Application of Real-Time Reservoir Navigation and High-Definition Electrical Imaging Services for Enhanced Well Placement and Optimal Completion Design. Paper URTeC 1933458 presented at the Unconventional Resources Technology Conference. Denver, Colorado. August 25–27.

Wang, Z., Li, T., McDougall, M., et al. 2014. Wireless Data Transmission Options in Rotary in-Drilling Alignment (R-IDA) Setups for Multilateral Oil Drilling Applications. International *Journal of Information Theories and Applications.* **21** (2): 154–161.

Wasserman, I., Hahn, D., Nguyen, D.H., et al. 2008. Mud-pulse Telemetry Sees Step-Change Improvement with Oscillating Shear Valves. *Oil & Gas J.* **106** (24): 39–47.

This page intentionally left blank

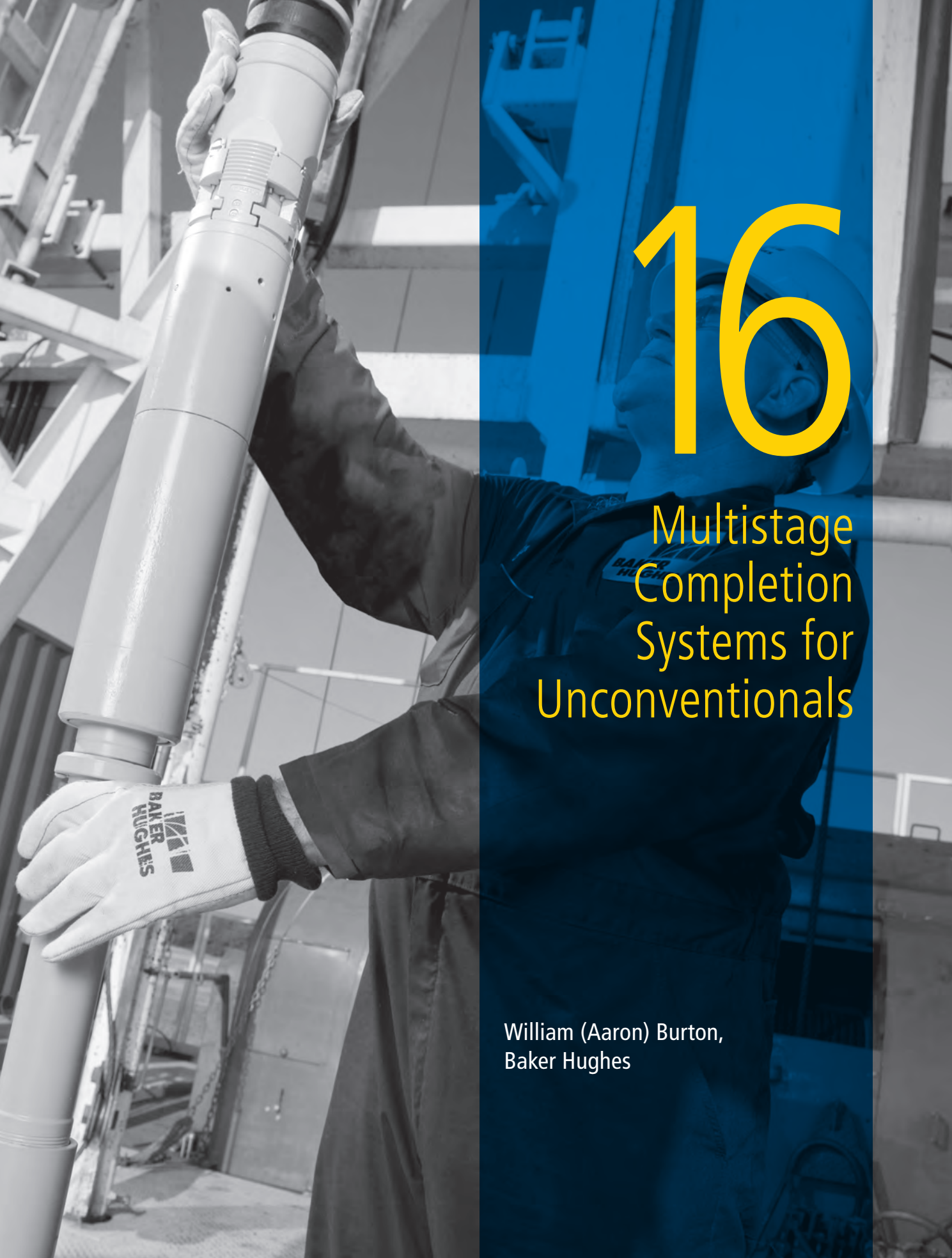

16

Multistage Completion Systems for Unconventionals

William (Aaron) Burton,
Baker Hughes

This page intentionally left blank

Chapter 16: Multistage Completion Systems in Unconventionals

16.1 Basics of Unconventional Wellbore Completions

Wellbore completions turn a well from a hole in the ground into a producing well. Wellbore completion tools are installed after a well is drilled and enable any completion techniques required to make the well product, such as acidizing or perforating. Completion tools may remain in the well to be used for production. Wellbore completions in unconventional plays isolate different sections in the well for hydraulic fracturing. There are a variety of different techniques used in these applications; each one enables multistage hydraulic fracturing.

16.1.1 Completing a Well

Wells are completed using steel pipe, called casing, to install the completion in the well. This casing lines the wellbore so it is commonly referred to as a liner. The assembled casing and completion tools are referred to as the completion string or the liner string. The completion string will contain any completion tools that will be installed in the well that will allow completion and production of the well. When the completion string is placed in the well, the weight of the completion string needs to be supported, and there are several ways to do so. One option is to hang the weight of the completion string in the intermediate casing. This support can be provided with a liner hanger or a permanent casing packer. Both of these tools use slips to hang and support the weight of the completion in the casing, hence the term *liner hanger*. Slips are devices used to grip casing and hold the tools at that position in the well. Slips are used in a variety of tools and applications in the industry and are illustrated in **Fig. 16.1**.

Fig. 16.1— When set, slips grip the casing and hold the completion in place.

Typically, a liner hanger is used in cemented applications because the slips that hang (hold) the weight of the completion can be set and still maintain circulation for the cement job. As illustrated in **Fig. 16.2**, a casing packer may be run with the liner hanger to provide isolation from above and below the hanger to add additional isolation and keep the cement contained at the intended depth. Circulation is possible during cementing because the packer is set after the cement job has been completed. A completion string without cement can use either a liner hanger or a permanent casing packer. When a permanent casing packer is used, the packer is set at the same time as the slips, so when the weight of the completion is supported, it is no longer possible to circulate fluid or cement through the annulus. This is illustrated in **Fig. 16.3**.

When using a liner hanger or permanent casing packer, the system is installed and run to the intended depth with drill pipe. The completion string is attached to the drill pipe with a running tool for the liner hanger or permanent casing packer, and it releases from the drill pipe by applying the appropriate amount of pressure (or rotation) in the drill pipe. When the intended depth is reached, and all of the appropriate completion tools are set and functioned, the running tool is released, and the drill pipe is pulled out of the hole.

When the drill pipe is removed from the well, another string of casing can be run and connected to the completion string. When it is not possible or advised to perform the fracturing job through the intermediate casing, connecting another casing string into the top of the liner to perform the fracturing job is common. This casing string is known as a *fracturing string*, and it is used to provide additional protection during the fracturing

Fig. 16.2—Liner hanger and casing packer.

job. After the fracturing is completed, the fracturing string can be removed, and then the well is produced through the intermediate casing. A string of casing called the production string can also be installed to "produce through" if needed.

Another commonly used practice is to run the liner string back to the surface and support the completion's weight with slips in the wellhead. This is called a ***long string***. Long strings are usually used in shallower formations with short laterals where the completion is not too heavy, and the weight of drill pipe is not required to get the completion to the intended depth.

16.1.1.1 Float Equipment

While the completion string is being run in the wellbore, protection through the inside of the liner is required to ensure the well cannot start producing during installation. This protection is accomplished with float equipment containing check valves that allow circulation from the surface to the annulus, but prevents the well fluids from entering the liner and going to the surface. There are a variety of different style valves that can be used to provide this type of isolation. The isolating valve at the very bottom of the completion string is called the float shoe. It provides protection at the bottom of the completion string and it is rounded to help guide the string into the wellbore.

Because the float shoe is at the toe of the completion string, it will hit the formation, which puts the valve at risk of sticking in the open position due to impact and/or formation debris. That is why it is a best practice to run a float collar spaced several feet above the float shoe. The float collar is a completion tool that has the same type of valve that allows circulation, but prevents wellbore fluids from entering the string from the annulus. The float equipment usually has two of these valves for redundancy. This float equipment prevents the wellbore fluids from coming into the completion string.

16.1.2 Installing Completion Strings

This section contains information about the process of installing cemented and openhole completion strings into the wellbore. Although similar, there are differences in installing the completion using cement and systems using openhole packers.

16.1.2.1 Cemented Completions

Cemented completions use cement to isolate the annulus between the liner and the formation. When the well is drilled and the drilling equipment is retrieved, the completion will be run in the wellbore to complete it. The casing joints are

Fig. 16.3—Permanent casing packer slips and element set simultaneously.

connected together and installed into the wellbore. Any completion tools, such as float equipment and fracturing sleeves, will be installed and spaced out according to the completion plan between the joints of casing. The completion string is then run into the well until it reaches the intended depth. When this depth is reached, the completion is placed in the well by setting it in the wellhead slips, or by setting the liner hanger and engaging the hanger slips. It is then time to perform the cement job. A clean fluid flush is pumped into the completion string to clean the inside of the completion string, followed by pumping the cement according to the mixture and volumes set out in the completion plan. The cement is followed by a cement wiper plug. The wiper plug has rubber fins that drag along the inside of the casing to clean up the cement as it is being pumped down. The wiper plug and fins cleaning the casing are illustrated in **Fig. 16.4**.

When the wiper plug arrives at the bottom of the completion string, all of the cement is in the annulus of the well. A cemented system has a landing collar that has been installed at the toe of the completion during the installation. The landing collar has a special profile that will catch the wiper plug and not allow it to go any further in the well. A pressure spike will occur when the wiper plug catches in the landing collar, because circulation between the liner and annulus is blocked off. This pressure spike is commonly called a ***plug bump***. At this point, the float equipment and the wiper plug keep the cement from flowing back into the completion and the cement hardens to isolate the annulus.

16.1.2.2 Openhole Completions

An openhole completion is installed the same way that a cemented completion is, using the casing to space out and run the completion equipment into the well. In addition to completion tools like fracturing sleeves, the openhole completions require openhole packers to isolate the annulus. The system will still use the float equipment to protect from the well coming through the liner. When this completion is at the intended depth, the weight is supported like the cemented system, with either the slips in the wellhead, the liner hanger, or a permanent casing packer. Instead of cementing at this point, the openhole packers are set to provide the annular isolation. The openhole packers provide annular isolation, which is the only difference between the two completion strings.

16.1.3 Difficulty Installing the Completion

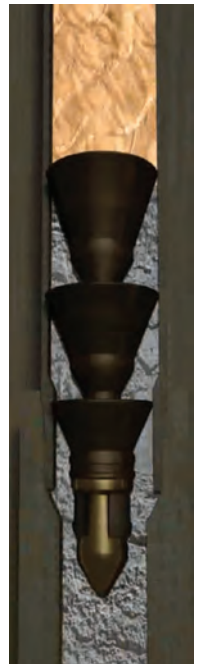

Fig. 16.4—Cement wiper plug cleaning cement in the casing.

Fig. 16.5—Watermelon string mill.

Sometimes it is difficult to get the completion system to the intended depth. Completion tools add stiffness to the casing string and can make it more difficult to install into a horizontal well. Some tools will also have an increased diameter, making installation even more difficult.

16.1.3.1 Preventative Measures

There are some preventative measures that can be taken before installation to avoid these problems. During installation, there are contingencies to help if the completions string does not reach the intended depth.

If completion tools are run in a horizontal well in a significant number, they add additional diameter and stiffness into the completion string making it more difficult to get to the intended depth. In this application, it is recommended to run a simulator to verify that the completion string will physically fit into the well with the additional stiffness and diameters. It is also recommended to run a reamer in horizontal wells with direction inconsistencies or rough laterals. **Fig. 16.5** shows a drawing of a common type of reamer in these applications: the watermelon string mill.

Multiple reamers are run in the well on drill pipe and rotated to clean and smooth the wellbore. The reamer setup run will vary in different formations, but it is a best practice to design the reaming assembly to mimic the diameter and the stiffness of the completion string to be installed. The assembly is rotated as needed to the bottom of the well while fluid is pumped through the drill pipe and back to surface through the annulus to remove debris from the wellbore. When the reaming assembly has reached bottom and it is believed that there is a good wellbore to run the completion, it is possible to test if the wellbore is in good shape. If the reaming assembly can be removed without having to circulate or rotate, it is a good indication the completion system can slide to the bottom.

16.1.3.2 Contingencies during Installation

There are three contingency options if the completion string has trouble getting to the intended depth: reciprocating, circulating, and rotating. These three options are mentioned in the order they should be attempted, based on risk level and success.

- **The first option is reciprocating the pipe.** The reciprocating action picks up the string and takes it back down while using the weight and momentum of the string to

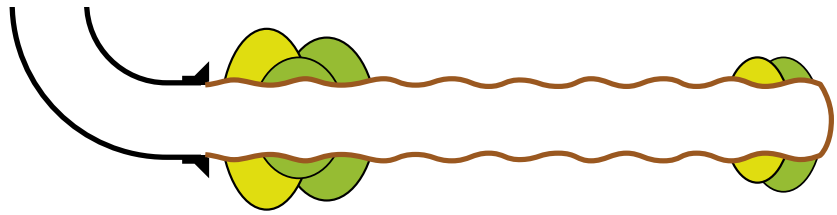

Fig. 16.6—Fractures growing to the path of least resistance in a barefoot completion.

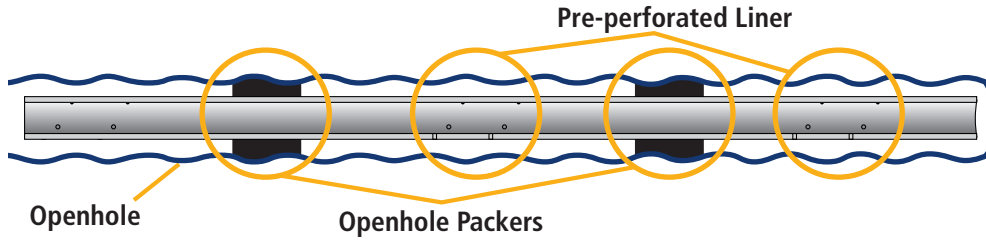

Fig. 16.7—Pre-perforated liner completion.

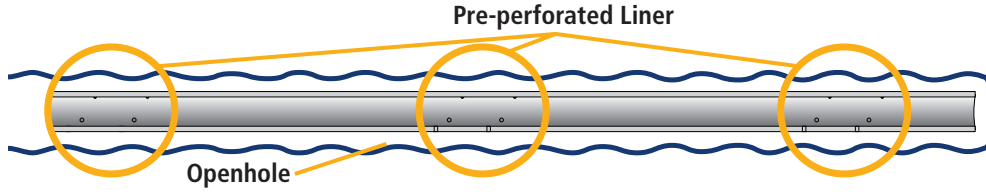

Fig. 16.8—Pre-perforated liner completion with openhole packers.

try to push it through obstacles. This is a low-risk option that provides a high success rate, depending on the obstacle.

- **The second option is circulation.** Sometimes debris is left in the well during the drilling and the reaming process, and there is too much to try and push through. The circulation option should be considered if this happens. A high-viscosity fluid can be circulated through the casing into the annulus to try to clear the debris and bring it back to surface. The fluid returning from the well should be monitored to see if the debris is coming back to surface and when it stops, indicating the debris is mostly removed. This is a relatively low-risk contingency if clean fluids are circulated and the annulus has enough flow area with the debris to be able to circulate. It is very critical to use clean fluid to circulate, particularly if hydraulic-activated tools are in the completion string. If debris is in the fluid, it could plug up in a tool, like the float collar, and cause an abrupt pressure spike. This pressure spike could prematurely set or release the tools.
- **The third option, if neither of the other options works, is to attempt to rotate the pipe.** *Important: this option* ***should not*** *be considered if a mechanical running tool is being used to* deploy *the completion!* The release mechanism on a mechanical running tool is rotating the pipe, so it is possible to disconnect from the completion. Another high-risk situation is using non-premium casing connections with low torque values. In horizontal applications with low torque connections, applying torque is a risk. Applying too much torque to the connections risks twisting off and losing part of the completion, and putting low amounts of torque may not provide any benefit. If the system has a hydraulic setting tool designed for rotating and the system has premium connections, this may be a viable and useful contingency. The completion string can be designed for high torque if it is known ahead of installation that rotation will be required.

16.1.4 Early Methods of Completing Unconventionals

The Barnett shale play was the original unconventional reservoir that kicked off the unconventional race. Experimentation and small production began in this play in the

early 1980s. There were several well completion types tested, starting with vertical wells with small, energized fracturing jobs.

Horizontal wells and different fracturing fluids were introduced, but the results were no better than those with the vertical wells. It was not until the early 2000s that horizontal wells were divided into multiple, individually fractured stages, and truly unlocked these types of plays. This section will discuss the variety of techniques that were used to experiment with in North America to try to economically produce these plays.

16.1.4.1 Single-Stage Massive Hydraulic Fracturing

Before liners started being used in this application, there were horizontal wells that were drilled and left as openhole wells without any lining in the wellbore. This is commonly referred to as a barefoot completion. Attempts were made to increase the reservoir contact area by placing a single massive hydraulic fracturing job in the lateral. Without multiple stage isolation, this is not a viable option in this application because these wells fracture at the paths of least resistance, leaving sections of the well unstimulated or under stimulated. A "barefoot" completion with fractures growing to the path of least resistance is illustrated in **Fig. 16.6**.

16.1.4.2 Slotted and Pre-Perforated Liner

Another attempt to increase the reservoir contact area was using slotted and pre-perforated liners to place the hydraulic fracture treatment Illustrated in **Fig. 16.7**. These liners already have the holes in the casing when they are installed into the well. The theory was that the openings in the casing would create multiple diversion points and help distribute the fluids and increase the surface area. However, this technique had the same flaw as the barefoot completions: there was no isolation of individual stages, so the fractures followed the path of least resistance.

Advances in this technique included adding openhole packers between the slots in the liner. This did improve results because it gave annular isolation between stages, but it still did not have the through-tubing stage isolation needed to divert the fluid to each stage individually and remained uneconomical. A diagram of these completions can be seen in **Fig. 16.8**.

16.2 Plug-and-Perforate Completion Systems

The plug-and-perforate (or plug-and-perf, also abbreviated PNP) completion system is the multistage completion technique that was originally used to unlock these unconventional plays, and is still the most common type of multistage completion system used today. This system traditionally uses cement to isolate the annulus, perforations to breach the cemented liner to provide a fluid-flow path during fracturing and production, and fracturing plugs to isolate from the previously fractured stages and divert the fluids out of the perforations. When the fracturing job is finished, the plugs are milled out to put the well on production.

16.2.1 Composite Fracturing Plugs

Composite fracturing plugs are designed as temporary isolation devices. The plugs are set in the liner to isolate and divert the fluids, and then the plugs are removed from the well. The plugs are available in two types: ball-isolating plugs and self-isolating plugs, each of which has advantages depending on the type of completion in use. Both types of plugs are illustrated in **Fig. 16.9**.

16.2.1.1 Ball-Isolating Plugs

The ball-isolating plugs rely on a fracturing ball to provide the isolation. This plug is open through the mandrel, and it allows flow from both above and below the plug until a ball is placed on the ball seat. There is still flow to the previously fractured stage through this plug until a ball is dropped from the surface and it lands on the seat for isolation.

Fig. 16.9—Ball-isolating and self-isolating fracturing plugs.

16.2.1.2 Self-Isolating Plugs

The self-isolating plugs have an isolation device installed inside the mandrel. There are a couple of different types of isolation devices, such as a poppet or a caged ball. These plugs allow flow from below, but not from above. As soon as these plugs are set in the liner, there is isolation from the previously fractured stage.

16.2.2 Perforating the Well

With the PNP method, it is preferred to perforate multiple clusters of perforations per stage to "fracture through" to increase efficiency. This "clustering" is made possible by using select firing perforation systems. These systems have multiple sets of perforation guns that can be fired selectively using electronic signals sent through the wireline. When the first set of perforations is shot, the assembly is moved uphole. Then, when the wireline is in position, another electronic signal is sent to fire the second set of guns. This process is repeated until all the clusters are perforated. For more information about perforating strategy, see Chapter 17.

These multiple perforation clusters per stage mean there are multiple entry points for the fracture to go through. It is also technically possible to only use one set of perforations for a single entry point, but due to added inefficiencies, it is not practical in most applications. Single entry and multiple entry will be discussed later in this chapter.

16.2.3 Plug-and-Perforation Installation

The PNP completion is traditionally a cement liner string. The completion string consists of a float shoe, float collar, and a landing collar at the toe of the string, plus casing to cover the lateral, and either a liner hanger or a long string of casing back to the surface. (The installation of this completion string is described in the previous section.) When the completion string is tested and it is confirmed that the well is isolated, the drilling rig is moved off of the location.

Fig. 16.10—Wireline pump-down assembly.

16.2.4 Plug-and-Perforation Fracturing Operations

When it is time to fracture the PNP completions, pressure pumping is required as well as wireline and/or coiled tubing (CT). Because the well has been cemented into place and there is no circulation, a through-tubing trip, usually performed on CT, is required to perforate and regain communication with the formation. The CT assembly is pulled out of the hole, and the pressure pumping units are connected to the well. The first stage fracture is performed through these perforations. Now that there is flow into the formation again, it is common to go to pump down wireline assemblies. (**Fig. 16.10** shows these assemblies consisting of perforation guns, a setting tool, and a composite fracturing plug.)

This assembly is pumped down to the intended depth and the plug is set by sending an electronic signal to the setting tool. The setting tool will set the plug and then release from it. If it is a self-isolating plug, the plug can be pressure-tested before the perforations are fired. The perforation guns are pulled uphole to the intended depth, and the first cluster of perforations is fired using another electronic signal through the wireline. The assembly is pulled uphole to the next cluster depth and the second cluster is fired by sending another electronic signal. This process is then repeated until all of the perforation clusters are shot and then the wireline is retrieved. The wireline unit is disconnected and the pressure pumping units are set up. A stage using a self-isolating plug can begin fracturing right away. If a ball-isolating plug is used, the ball is dropped into the well and pumped onto the plug. When the ball seats on the plug, there will be an abrupt pressure increase and that indicates isolation from the stage below. When isolation is achieved, the fracture begins. After the fracturing is performed on this stage, the pressure pumping units are disconnected from the well and the wireline unit is set up again with a new wireline assembly, and this process is repeated until all stages are fractured. **Fig. 16.11** illustrates a well using PNP.

Using the ball-isolating plug requires pumping down a ball to the plug, but it has advantages if the job does not go as planned. After the plug is set, fluid can be pumped into the previously fractured stage because the ball-isolating plug can still be pumped through, whereas the self-isolating plug isolates immediately and fluid flow is lost. If the perforation guns do not fire when using the ball-isolated plugs, the perforation guns can be redressed on surface and pumped downhole again. In this scenario with a self-isolating plug, the guns would have to be redeployed using a through-

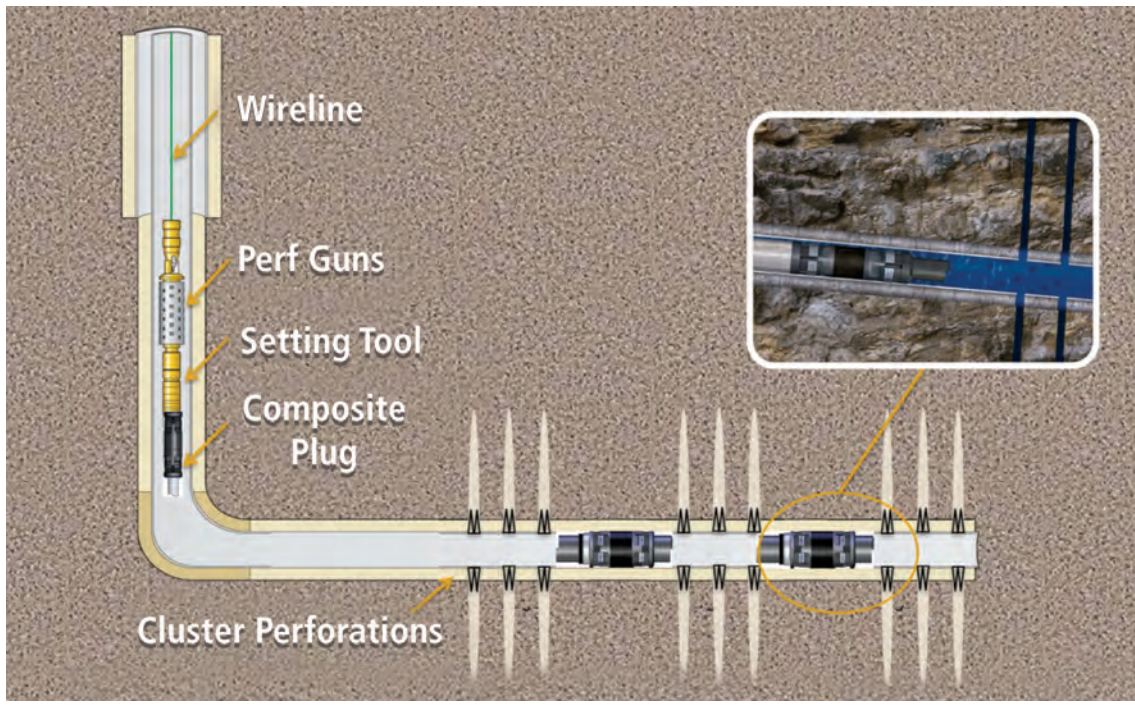

Fig. 16.11—Wellbore diagram of a plug-and-perforation job.

tubing trip on CT. The availability and mobilization time of the CT unit will determine how long the nonproductive time will be on the well.

It is also possible to run the same bottomhole assembly (BHA) that is used on the wireline on CT. The most common application (where CT is used to deploy the plugs and the perforating guns) is using high pressure and high temperature (HPHT) plugs. Some of these plugs are not optimized for pump-down application because they require additional metal components to support the HPHT. These plugs can have a higher risk of presetting while pumping down. Another application to consider using CT deployment is when controlling the amount of fluid displaced is critical. The CT does not require the plugs to be pumped down, because the plug is run to depth on the CT string. Not having to pump down equipment through previously fractured stages will prevent over-displacement of fluids and save the overall amount of water required.

16.2.5 Milling Out the Composite Bridge Plugs

After the fracturing job is completed with PNP, the plugs will have to be milled out and removed before the well is put on production. Most mill-out applications rely on weight-on-bit (WOB) while milling, but it can be difficult to get enough WOB when milling out in horizontal wells with CT. In this application, the mill-out is designed to try to reduce the dependency on WOB drilling as much as possible. This section discusses the components and the process of milling out the plugs.

16.2.5.1 Bottomhole Assembly Design and Mill Selection

The milling BHA consists of a motor and mill. The motor is a smaller version of the motors that are used in the drilling process described in Chapter 15. The motor is selected based on the fluids that will be circulated and the amount of torque output that is needed.

A variety of mill designs are effective in this application. The mills will vary, but some parameters stay mostly the same: mill size, shape of the mill face, and the cutting structure. The mill size is typically designed to be 95% to 99% of the drift diameter of the casing to ensure the mill can pass through the casing. The profile of the mill is designed so that there is enough flow area to circulate the milled out debris around the mill and back toward surface. The face of the mill needs to be concave. A convex face that points outward will vibrate and kick away from the plug, hindering the mill-out process.

In addition, the cutting structure is very important. The cutting structure needs to be aggressive on the plug, and very durable. The durability of the cutting structure will determine how quickly the mill will wear down and how often it will need to be retrieved from the well to be replaced. Numerous trips in and out of the well can add a significant amount of time and cost.

16.2.5.2 Fluid Selection

The fluids should be designed to help with the milling process as well as to remove the debris. The fluid should be viscous enough to circulate the debris and bring it back to surface. The fluids should also reduce the amount of friction of the coiled tubing and at the mill face to ensure all of the applied weight and power is being transferred to the mill, rather than lost to friction. Reducing friction will also help optimize the pump pressure, and a properly designed fluid will prevent differential sticking.

16.2.6 Alternative Systems and New Technologies

There are two recent technological advances developed for PNP completion that are focused on improving the efficiencies during the fracturing job and allowing access to new applications. These technologies are the cemented pressure-activated fracturing sleeve and the large-bore fracturing plugs. The cemented pressure-activated fracturing sleeve can be used to replace the CT trip required to perforate the first stage. It is deployed on the completion string and installed at the toe of the string just above the float equipment. When it is time to begin the fracturing job, the pressure pumping units set up and apply pressure to open this sleeve. When the sleeve is opened, the first-stage fracturing begins. This sleeve saves the time and cost of deploying a CT unit and performing a through-tubing trip to perforate the first stage.

The large-bore fracturing plug is a ball-isolating plug that is designed to remain in the wellbore after the fracturing job and to be produced through. It is used in conjunction with a disintegrating fracturing ball that provides isolation on the plug during the fracturing job, but it will disintegrate in the production fluid afterwards. Once the fracturing is complete, the balls disintegrate and the well can be put on production without milling out the plugs.

The combination of these technologies improves operational efficiencies of PNP completions because through-tubing runs are not needed beforehand to perforate, or afterward to mill-out plugs. With these tools a CT unit is not required for a PNP completion. This capability makes PNP a more feasible option in plays that have longer laterals that exceed the length or operational limitations of CT.

16.3 Ball-Activated Completion Systems

16.3.1 Fracture Sleeves and Isolation Valves

The ball-activated completion system (BACS) uses ball-activated fracturing sleeves to perform multistage hydraulic fracturing. Balls and ball seats are used to open the sleeves and divert the fracturing fluid into the individual stages. This section will discuss details of the components used with these types of systems.

16.3.1.1 Pressure-Activated Sleeves

The pressure-activated fracturing sleeve is run at the toe of the well and can be opened by applying pressure into the completion string. This sleeve has the same functionality as the cemented pressure-activated sleeve mentioned previously. When it is time to begin the fracturing job, the appropriate amount of pressure is applied, opening the sleeve and the first-stage fracture stimulation is performed through this sleeve. This sleeve allows access to the formation without through-tubing intervention, which is important because there are ball seats with diameter restrictions above it that may not allow intervention tools to pass.

16.3.1.2 Wellbore Isolation Valve

The wellbore isolation valve (WIV) is run at the toe of the completion when a pressure-activated sleeve is used as the first stage at the toe. The WIV will allow circulation from the completion string to the annulus during run-in so that fluids can be displaced and circulated should the system have trouble getting to the intended depth. When the system reaches the intended depth the ball that corresponds to the WIV is dropped in the well and pumped to the WIV. Applying pressure closes the WIV and it acts as a plug at the toe of the completion. All circulation is shut off between the liner and the annulus, providing well protection, a point to apply pressure against, and to set any hydraulic equipment in the completion.

16.3.1.3 Ball-Activated Sleeves

The ball-activated fracturing sleeves are the key component to this completion type. These sleeves contain a ball seat that corresponds to a fracturing ball. Each of these sleeves has a different size ball seat so that each sleeve can be selectively opened. Because each sleeve has an individual ball and ball

seat combination for selective opening, the sleeves must be run in order of the smallest ball seat at the toe of the well and the largest at the heel of the well. This is the only way that all of the balls can pass through the ball seats of the sleeves above it.

When the ball is pumped down and it lands on the corresponding ball seat, pressuring up will open the fracturing sleeve and expose the fracturing ports on the sleeve. The ball remains on seat during the fracturing job to divert the fluid out of the fracturing ports and to isolate from the previously fractured stage. The fracturing sleeve in the opened and operating position is shown in **Fig. 16.12**.

The fracturing sleeve remains in the open position after the fracturing job so that the well can produce through the sleeve. To prevent the sleeve from closing and blocking off production, the sleeve locks in the open position as soon as it is opened. The balls will flow back to the surface if there is enough velocity in the production. The ball seats can be produced through, but they are also designed to be milled out if the application calls for it. If the fracturing balls remain in the well, they can be milled out as well.

16.3.1.4 Reclosable Sleeves

There is also a reclosable version of the ball-activated fracturing sleeve. This sleeve has the same functionality to divert the fracturing job and isolate it from the stage below with a ball and ball seat in the fracturing sleeve. However, the reclosable sleeve version can be shifted with CT after the fracturing job. These sleeves have a shifting profile that a shifting tool locks into to shift the sleeve open and closed. It may be preferred or required to mill out the ball seats before the shifting tool can be used. After the ball seats are milled out, a CT or work-over string is run in the well with a hydraulic-activated shifting tool that can selectively latch into each sleeve. The sleeves can be selectively closed and opened with this shifting tool. If it is known the seats will need to be milled out, it is best to mill them out before the well is put on production. Producing the well helps to remove the ball seat debris.

Fig. 16.12—Ball-activated fracturing sleeve in the open position.

These sleeves can be used in applications where water breakthrough is possible or in a refracturing application. If water starts producing through a stage, the sleeve can be shifted closed to isolate that stage and save the rest of the well. The fact that all of the sleeves can be reclosed and the liner isolated again allows for some refracturing options. If it is desired to have new injection points in the well, all sleeves can be closed and an openhole plug-and-perforation job can be performed between the packers. If the refracturing is done through the same injection points, all of the sleeves can be reclosed to isolate the liner again and the following procedure can be used:

1. Selectively open a sleeve.
2. Refracture through the open sleeve.
3. Reclose the sleeve.
4. Repeat until all desired stages are refractured.
5. Open all refractured stages for production.

Only having one sleeve open at a time will force the fracture into the desired stage.

16.3.2 Openhole Packers

The role of the openhole packers is to isolate the annulus between the completion string and the openhole formation. There are a variety of different packers that have different setting and isolation methods, but their role is the same. All of the packers are designed to conform to the shape of the openhole and irregularities within it. There is no way to test each packer individually, but production results have shown us that the openhole packers do effectively isolate multiple stages in the wellbore. There are a couple of reasons that these packers may be able to isolate multiple stages even in inconsistent wellbores and with difficult applications. Imagine the packer as an O-ring in the wellbore, which is a fairly accurate analogy. Just like an O-ring, when pressure is applied, the rubber-packing element is energized and will cover an even larger surface area. Also, most of these applications use proppants, so even if the packer does not completely seal due to an irregularity in the formation, the proppant

could still plug this path and complete the isolation. It is also important to remember that an airtight seal is not required in this application. As long as the packer creates enough of a blockage to contain the path of least resistance in that stage, the packer will provide effective isolation.

16.3.2.1 Hydraulic-Activated Packers

One type of openhole packer is the hydraulic-activated packer. This packer relies on applied pressure to set the packer. When the packer sets, the components shift parallel to the packer, forcing the rubber-packing element outward toward the formation. The rubber also has a metal backup ring around it that extrudes with the rubber and conforms to the openhole, enabling a more reliable and higher-rated packer. When the components of the packer shift, the internal mandrel does not shift. This means that the length of the completion string will not change when setting the packers, so an unlimited number of these packers can be set at the same time.

16.3.2.2 Fluid-Activated Packers

Another packer commonly used for openhole isolation is the fluid-activated or reactive-element packer. This packer relies on fluid to activate and swell the rubber out to contact the formation. When these packers reach the intended depth, an activation fluid is pumped across the packers if it is needed. The packers will swell and contact the formation to provide isolation. These packers are highly customizable to each application. The rubber element is wrapped around a piece of casing, so it is easy to match the properties of the liner, such as the threads, metallurgy, weight, and other parameters. Also, the sealing length and OD of the packer can be customized for the application, and the activation fluid can be a water-based or oil-based fluid. A predictor software is used to determine how long it will take for the packers to provide a complete seal and to design the packer length and OD based on the well conditions and operating parameters. Typically, these packers are designed to have the maximum OD that will go into the well and the shortest length. However, if there is an application where the OD needs to be smaller and the length longer, it can be designed to meet that need as well. These packers are designed to leave enough space between the openhole diameter and the OD of the completion tools, so it is easier to get the system to the intended depths.

16.3.3 Ball-Activated Completion Systems Installation

When the well is drilled and the drill string is out of hole, the drilling rig will run the completion string. The completion string is made up of the fracturing sleeves, packers, and all other completion components, and casing is used to space out the components and place them at the intended depths. To ensure the components go into the well in the correct place it is recommended to mark the casing with paint where the components will be installed while the casing is on the pipe rack. The marks should be at the box of the casing joint below and the pin of the joint above to identify a piece of equipment belongs between the joints of casing. This is shown in **Fig. 16.13**.

The completion string is run to the intended depth using the methods mentioned in the first section. When the completion has reached the target depth and all fluids have been displaced, the first ball, which is the smallest, is dropped and pumped onto the WIV. Applying pressure will close the WIV, isolating the completion string from the formation, and create a point to pressure up against to set any hydraulic equipment.

If a hydraulic-activated system is run, the activation pressures will be staggered so that the components can be activated at different times. For example, the hydraulic-activated openhole packers and the casing packer would set at 1500 psi. The hydraulic running tool would be set at 3000 psi, so that the casing packer can be tested before the running tool is released. The pressure-activated sleeve would be set to 5,000 psi. This would allow all of the completion isolation equipment to be set, the casing packer tested, and the running tool released without opening this sleeve. The running string can then be removed and the rig can be moved off the location with the well isolated. The WIV will isolate the well through the liner, and the casing packer isolates from the annulus. **Fig. 16.14** shows a wellbore diagram of a hydraulic-activated BACS.

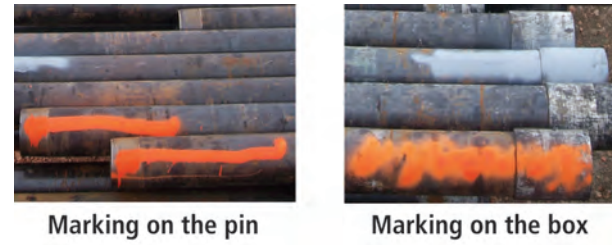

Fig. 16.13—Marking the joints of casing before installing the completion equipment.

The fluid-activated packers are often run without the WIV and pressure-activated sleeve, although they can be used. If these components are not in the completion, the running tool will have the components needed to set the casing packer whether it's mechanically or hydraulically set. Installing the completion would follow the same steps as above, but the openhole packers would be changed out. When the system gets to depth, the activation fluid is circulated around the packers (if needed), the casing packer is set and provides annular isolation, and the float equipment will provide the liner isolation from the well. The running tool will be retrieved, and over the appropriate amount of time, the packers will set.

16.3.4 Ball-Activated Completion Systems Fracturing Operations

When the fracturing crew arrives on location, they rig up and apply pressure to open the pressure-activated sleeve. If there is not a WIV and pressure-activated sleeve, fluid will be pumped out of the float equipment and into the formation. The ball corresponding to the first ball-activated sleeve is dropped in the well and pumped onto the ball seat. Applying pressure against the seated ball opens the sleeve. Either way, when the first sleeve is opened, the first-stage fracturing begins. After the first stage is fractured, a small amount of additional fluid, called a flush, is pumped through the completion string to clean out any proppant that remains in the liner. While this flush is being pumped, the ball corresponding to the second stage is dropped into the fluid flow and pumped to its ball seat. The ball is dropped into the fluid flow using a manifold or a ball-dropping head, so the fracturing job does not have to shut down between stages. When the fracturing ball lands on the ball seat, applying pressure opens the sleeve, and the ball isolates from the stage below the fluid through the ports on the sleeve. The second stage is then fractured. The process is then repeated until all stages are fractured:

1. Drop the ball for the next stage into the clean fluid flush for the previous stage.
2. The ball lands on the seat isolating it from below.
3. Applying pressure against the ball opens the sleeve.
4. The fracturing begins without ever shutting down the pressure pumping units.

Ideally, the pressure signatures can be seen when the fracturing sleeves open. The ball landing on the seat causes a pressure increase, and opening the sleeve causes a pressure decrease. Unfortunately, this looks very similar to a formation breakdown, and there is no guarantee that this pressure signature can be seen during the fracturing. To

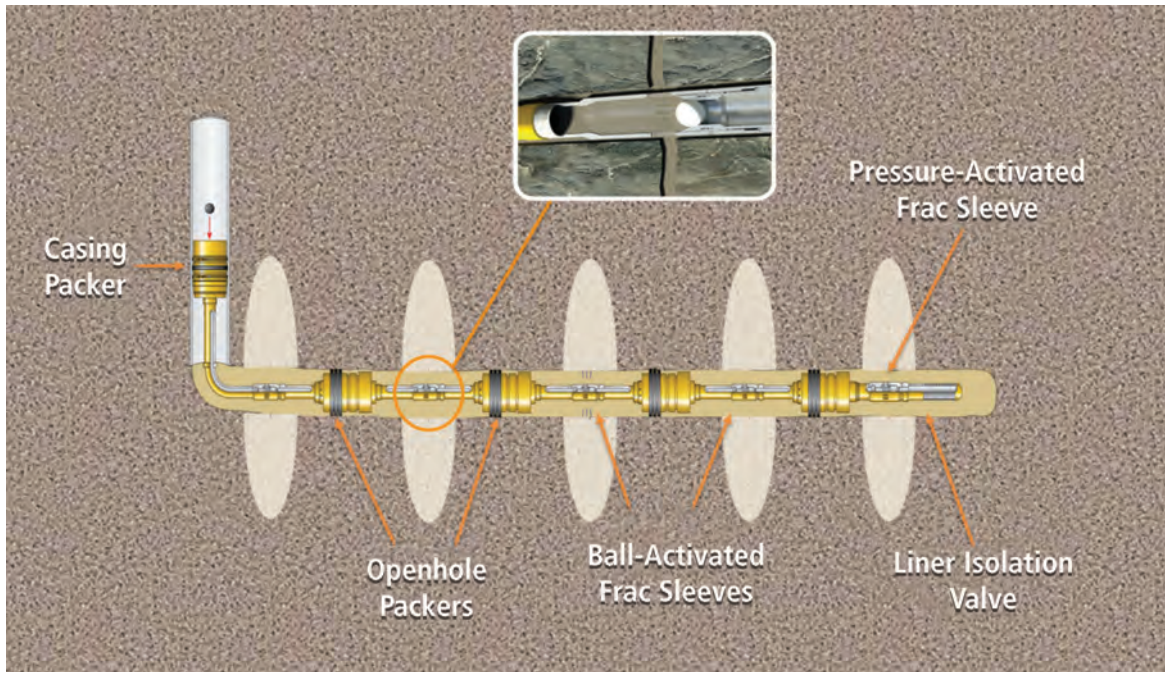

Fig. 16.14—Wellbore diagram of the BACS.

assist with being able to see this sleeve shift open, it is recommended to slow the pump rate down as the ball is approaching the ball seat, so that there is a better chance of observing the pressure signatures.

16.3.5 Ball-Activated Completion Systems Post-Fracturing Operations

After the fracturing job, pumping units are moved off location and the well can be put in production. The fracturing balls will flow off the ball seats, and the ball seats can be produced through. Most ball seats have been designed to be milled out easily if it is decided to do so. If reclosable fracturing sleeves are used, they can be functioned with CT at this point.

There are instances where the fracturing balls cannot be produced to surface. If there is a differential in pressure between stages, it is possible that the balls could be held on the seat until the pressures balance out. Also, there may not be enough velocity in the production to bring the balls back to surface. The balls would remain in the well and settle into the low spots of the well, potentially creating a debris barrier. If there are concerns about the balls remaining in the well after the fracturing, disintegrating fracturing balls can be used. These fracturing balls will provide the isolation needed during the fracturing job, but will disintegrate in the production fluid afterwards, ensuring that the balls will not hinder production without performing a through-tubing intervention.

16.3.6 Alternative Systems and New Technologies

Recent advances in the BACS technology allow this completion to use cement to isolate the annulus. The fracturing sleeves have the same functionality as the openhole sleeves, but with minor changes to adapt them to cementing operations. The modifications to these sleeves are primarily to prevent cement from entering the internal components of the sleeve and to prevent it from opening. This system also uses the cemented pressure-activated sleeve that is mentioned under the PNP new technologies at the toe of the well.

The fracturing process is exactly the same with this system: pumping a fracturing ball to the corresponding seat, opening the sleeve, fracturing that stage, and repeating the process until all stages are fractured. The only difference is in the installation procedures. The openhole packers will not be used in this system, but the sleeves are still installed and spaced out using the casing string. When the system reaches the intended depth, it is cemented in the wellbore using the procedures mentioned previously in this chapter.

16.4 Coiled Tubing-Activated Completion Systems

Coiled tubing-activated completions systems (CTACS) use coiled tubing (CT) to achieve multistage isolation. There are two primary methods with CT, using either an abrasive perforator or CT-activated sleeves to access the stages in the well. A coiled-tubing packer or a sand plug can be used to isolate from the previous stage.

16.4.1 Components of Coiled Tubing-Activated Systems

This section describes the components commonly used with coiled tubing systems, including components such as fracturing sleeves and abrasive perforators, and how they are used in different applications under different conditions.

16.4.1.1 Coiled Tubing-Activated Fracturing Sleeves

The CT-activated fracturing sleeves provide the flow path for the fracturing fluids to enter each stage. There is a variety of these types of sleeves in the industry. One type is the mechanically shifted sleeves that rely on mechanical force from the CT to shift the sleeve open. The CT tools lock into the sleeve and applying downward force opens the sleeve. Another option is the pressure-balanced sleeves. These sleeves have internal pressure ports at the top and the bottom of the sleeve. As long as these ports have the same amount of pressure applied to each one, they remain pressure balanced and in the closed position. These sleeves are opened by using a CT packer to create a pressure imbalance across these ports. The CT packer is run through the liner into the fracturing sleeve, and it is set in between the two pressure ports. The ports are now isolated from each other and pressure is applied to the annulus. Because of the CT packer isolation, the top port will have applied pressure, but the bottom one will not. This creates the imbalance and the sleeve shifts into the open position, exposing the fracturing ports.

16.4.1.2 Abrasive Perforator

An abrasive perforator is an alternative to conventional perforating guns. The abrasive perforator is a CT tool that creates holes in the casing by pumping fluid and sand through the CT and into the casing in an abrasive manner. As shown in **Fig. 16.15**, this tool uses a water and sand mixture to cut the casing with an abrasive jet coming through the nozzle. When the casing is cut, these perforations are used to divert the fracturing fluid into the formation at that point. The abrasive perforator can be seen in **Fig. 16.16**.

16.4.1.3 Coiled Tubing Packers

The CT packer is used to create a mechanical barrier to isolate below the CT assembly. This will isolate the previously fractured stage and divert the fracturing fluid through the fracturing sleeve ports or abrasive perforations. The packers are also used to isolate the top and bottom ports on the pressure-balanced sleeves so that the sleeve can be opened. The CT packers for this application are specially designed to rely on weight as little as possible, just like the plug mill-out application. When the CT is extended to certain lengths in the horizontal lateral, it can be very difficult to get weight down to the bottom of the CT string.

16.4.1.4 Sand Plug

Another way to isolate the abrasive perforation or the fracturing sleeve is to pump a sand plug at the end of each stage. A sand plug is created by increasing the sand concentration in the fluid to a high enough level that it plugs off and fluid can no longer enter the formation through that injection point. Because fluid cannot pass into the formation at that injection point, it is isolated from the next stage fracturing without the use of the CT packer. The sand plugs do require a clean out trip with the CT when the fracturing is complete.

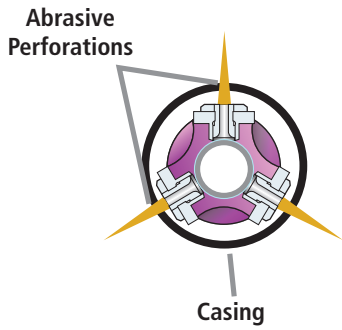

Fig. 16.15—Abrasive perforator cutting through the casing.

Fig. 16.16—Abrasive perforator.

16.4.1.5 Casing Collar Locator

The casing collar locator (CCL) is used to determine the location of the CT BHA in the wellbore, so the CT tools are placed for opening the sleeve or the abrasive perforator placed for cutting. Between each connection of casing, there is a casing collar that connects to the next joint. When the connection is made between joints, there is a small gap between the two joints of casing. The CCL is part of the CT BHA and has spring-loaded latches that touch the inside of the casing as it moves up and down the wellbore. When these latches pass over a casing collar, the springs push the latches into the gap and the CCL locks into place. There is enough force applied through the springs that it will require pulling tension with the CT unit to release the CCL from the collar. This feature allows each casing connection to be located to know where the CT assembly is in the wellbore. The CCL and the spring-loaded latch are shown in **Fig. 16.17**.

If a premium casing thread is used, there will not be a gap between each joint of casing. In this application a locating sub will be used to identify the depths in the hole. A locating sub is a small piece of casing that has a groove machined into it that mimics the gap between the joints of casing openhole, and will catch the CCL as it passes over it. This sub would be run in and then spaced out with the completion string, strategically placing it to help identify where the sleeves and other tools are in the wellbore.

16.4.2 Coiled-Tubing-Activated Completions Systems Installation

If the CT-activated completion system will rely primarily on an abrasive perforator, there will be no completion equipment to install on the completion string. Blank casing will be installed and cemented into the well using the techniques previously discussed in 16.1.2.

When using CT-activated sleeves, the sleeves are installed with the drilling rig, using the casing to space the sleeves to the correct depths. If this is an openhole completion, then the openhole packers will be spaced between the sleeves to provide the annular isolation and installed as discussed in 16.1.2. Typically, these completions are cemented completions.

The casing string with the sleeves is installed at the intended depth and the completion string is cemented in place. The installation procedures described in 16.1.2 are used to install and set this type of completion. When the completion is installed and pressure-tested, the rig is moved off-location.

16.4.3 Coiled Tubing-Activated Completions Fracturing Operations

CT-activated systems use annular fracturing behind coiled tubing to achieve multistage hydraulic fracturing. There are a variety of tools available to achieve isolation and diversion and this section will go through the operations for each type of setup.

16.4.3.1 Fracturing Using Abrasive Perforations as the Injection Point

To fracture this type of completion, pressure pumping and CT are required. When it is time to perform the first fracture, the CT assembly is deployed in the well using the CCL to identify where the BHA is in the wellbore and locate where to abrasive perforate. Then, a sand-and-water mix is pumped through the CT and out of the nozzles on the abrasive perforator. This creates a force that cuts the casing by abrasion. The CT packer is then set and the first stage fracture begins through the annulus of the CT and the casing. When the stage is finished, the fracturing is shut down and tension is applied to the CT to unset the CT packer. The assembly is then pulled uphole to the depth of the next stage and the process is repeated until all stages are fractured. This type of completion is shown in **Fig. 16.18**.

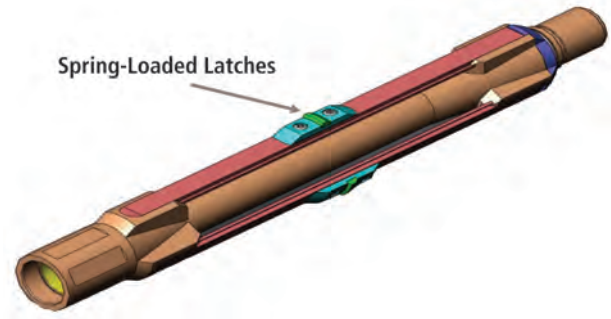

Fig. 16.17—Casing collar locator with spring-loaded latches.

After the abrasive perforation is performed, the annular fracturing will need to have a step-rate increase, rather than pumping aggressively right away. During the perforating, all the sand that was used to cut the casing remains in the casing, and this sand will be picked up by the fluid flow and moved into the formation. This additional sand in the fracturing fluid can plug up the injection point and create an accidental sand plug that causes a loss of fluid flow to the

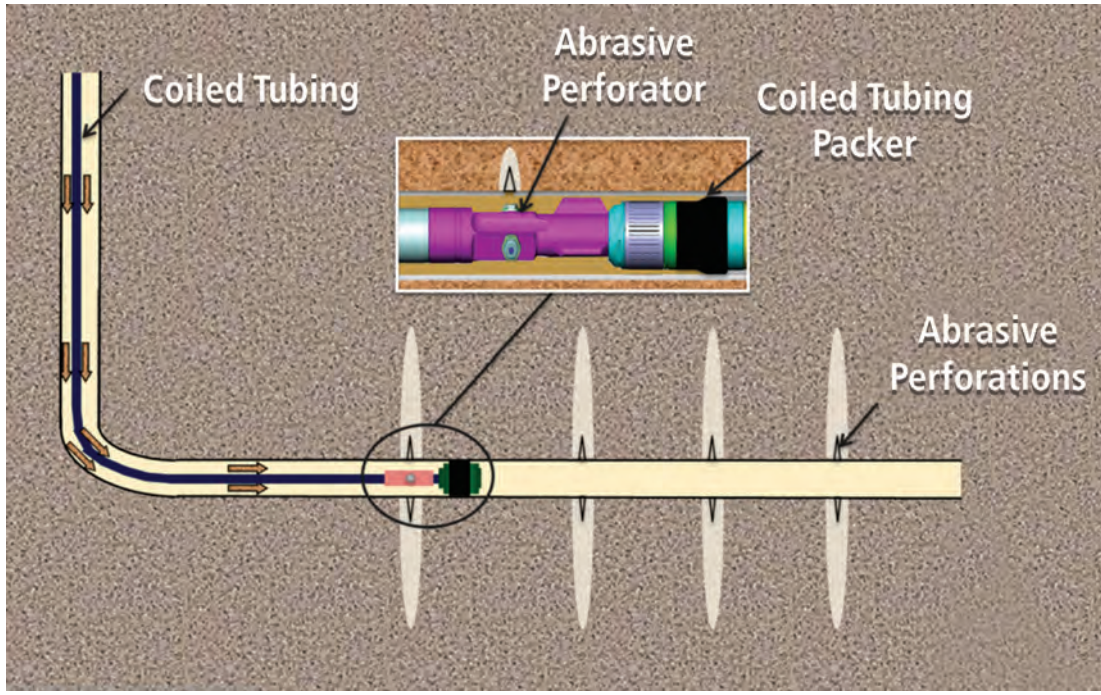

Fig. 16.18—Example CTACS using an abrasive perforator to create entry points into the casing.

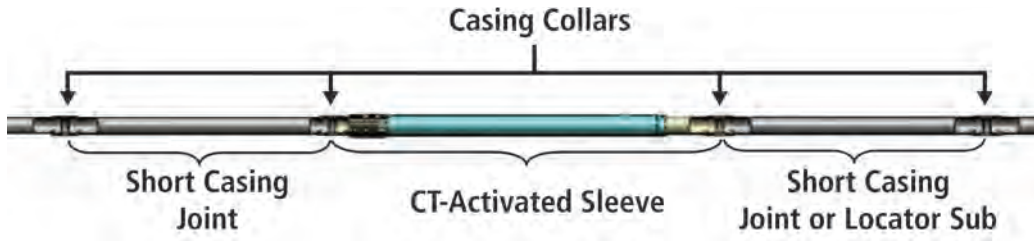

Fig. 16.19—The CT-activated sleeve is installed on short casing joints.

formation, also known as a screen-out. The screen-out can be cleaned out by circulating fluid through the CT annulus, but this creates nonproductive time. It is better to ramp up the fracturing flow rates in increments to disperse the sand in smaller volumes and avoid screen-outs.

Another alternative to this method is using sand plugs to isolate each stage rather than the CT packer. The CCL would locate the depth in the wellbore, and the abrasive perforation would be used to cut the injection point through the casing. When the casing is cut the annular fracturing would be performed, and a sand plug would be pumped at the end of the fracturing job to intentionally create a screen-out so that fluid could not enter that injection point any more. The CT assembly is moved uphole and the casing is cut again. Because the previous injection point has a sand plug, the new perforation is the only open injection point in the well, so the fluid diverts into the new perforation.

16.4.3.2 Fracturing Using Coiled Tubing-Activated Sleeves

When the CT-activated sleeves are used, the CT BHA is used to locate and open the fracturing sleeve. The CCL locates the sleeve by using the casing collars or locator subs. The sleeves will have short joints of casing on the top and bottom of the sleeve to give positive identification of the sleeves. This is achieved because each joint of casing is approximately 40-ft long, but the short joints on the sleeves are only 6-ft. long. As shown in **Fig. 16.19** when the CCL hits another casing collar after pulling up only 6 ft., it is obvious that the assembly is in the sleeve.

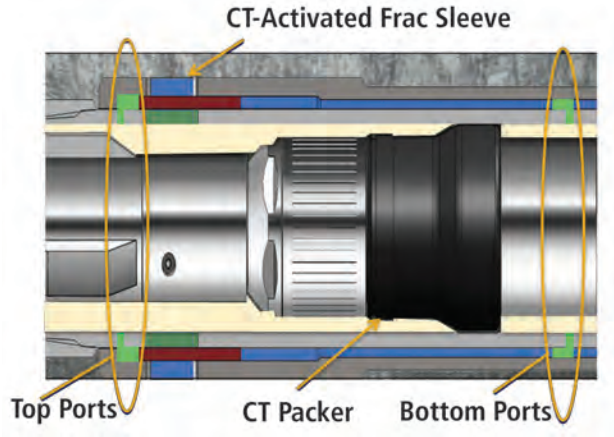

Fig. 16.20—Setting the CT packer between the top and bottom ports on the fracturing sleeve. (Modified from Castro et al 2013.)

When the assembly reaches the correct depth, the sleeve will be opened. If it is a mechanical sleeve, the coiled tubing latches into the sleeve and mechanical force will be applied to shift the sleeve open. If it is a pressure-balanced sleeve, the CT packer is set and it isolates the top and bottom ports of the pressure-balanced sleeve. As shown in **Fig. 16.20**, pressuring up the annulus causes the top set of ports to have applied pressure that the bottom set does not have. This causes a pressure imbalance in the sleeve, and opens the sleeve. The other sleeves in the completion string are not isolated, so the ports stay in a pressure-balanced and closed position.

When the sleeve is opened, the annular fracturing begins, using the CT packer to isolate from below and divert the fluid out of the ports. When that stage is finished, the fracturing is shut down, tension is applied to the packer to release it, and the assembly is moved to the next sleeve. The process is repeated until all stages are fractured. The completion is seen in **Fig. 16.21**.

The fracturing does shut down between stages, but it is still an efficient process. The CT packer will need time to equalize and go into a relaxed position. Once the CT-packer is equalized, the BHA is moved uphole to the next stage. Shutting down the fracturing job and being able to move instantaneously has benefits. Like the CT deployed PNP, there is direct control of how much fluid is displaced into each stage so over displacement can be avoided. By only fracturing out of one injection point and having the capability to instantaneously shut down, there is direct control of the volume of fluid placed in each injection point. If it is known how the fracturing will grow in that formation, controlling the volume of fluid will give indirect control of the

height and length of the fracture. This can be used to avoid fracturing into water-bearing zones or offset wells. Another scenario in which this would be useful is while using real-time microseismic monitoring. If the microseismic monitoring shows the fracturing growing into a nonproductive or water-bearing zone, the fracturing can be shut down and moved to the next stage to save time and money and avoid that zone.

While annular fracturing with CT, there will be a small amount of fluid being pumped in the CT and out of the abrasive perforator. The primary purpose of doing this is to apply internal pressure so that the annular pressure will not collapse the CT during the fracturing. This column of fluid is at a low enough pump rate to deliver accurate real-time downhole pressure monitoring capabilities, because the static nature of this fluid does not have the friction losses that are seen in the high rates in the annulus. This downhole pressure data can help you detect, and prevent screen-outs.

Should a screen-out occur, fluid can be circulated through the CT to the annulus to clean out the excess sand in the wellbore. The abrasive perforator is still on the CT assembly even though the sleeves are the primary means into the formation. It is used as a contingency option if there is a screenout that cannot be recovered from or if another stage needs to be added. If either of these scenarios occurs, the abrasive perforation will be used to cut a new injection point into the casing.

16.4.4 Alternative Systems and New Technologies

Another alternative with the CTACS is using a straddling device on CT to isolate individual perforations. In this scenario, a casing string would be installed into the well and cemented into place. Perforation guns would then be deployed to perforate each of the entry points into the well. A CT assembly would then be run in the well with a BHA

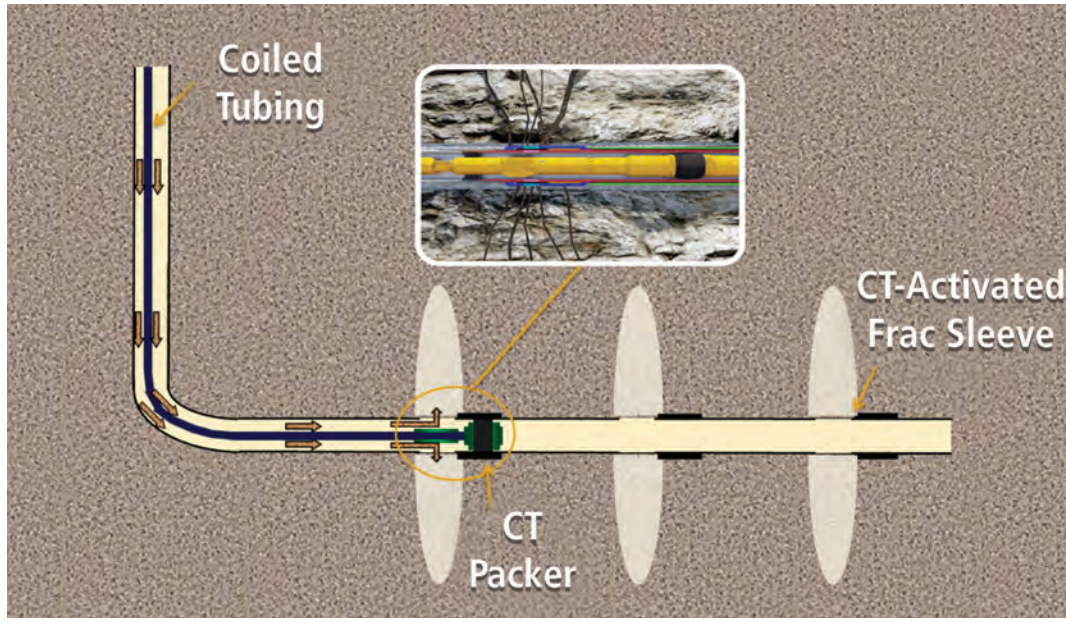

Fig. 16.21—CTACS using CT-activated fracturing sleeves.

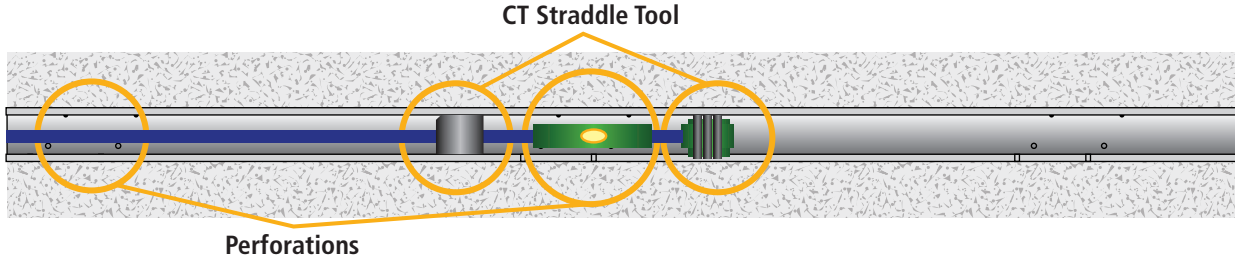

Fig. 16.22—Coiled tubing straddle tool isolating perforations.

Table 16.1—Summary of benefits and considerations compared for PNP, BACS, and CTACS. (From Burton 2013a.)

	PNP	BACS	CTACS
Number of Stages	Virtually unlimited	Limited	Virtually unlimited
Stage Placement	Flexible	Fixed	Fixed with fracturing sleeves; flexible with abrasive perforator
Contingency Options	Full diameter	Diameter restrictions	Full diameter and CT in completion string
Fracturing Logistics	Pressure Pumping, Wireline, CT	Pressure pumping	Pressure pumping, CT
Fracturing Operational Efficiency	Set up/down between stages	Nonstop	Brief fracturing job shut down between stages
Post Fracture	Mill out plugs	Restricted diameter	Full production diameter

containing a straddle tool. The straddle tool is capable of isolating above and below each of the perforated entry points. The straddle tool is placed over a set of perforations and the fracture is pumped through the CT and between the straddling tools. This is illustrated in **Fig. 16.22**.

This technique is also being used in refracturing applications for a previously fractured well that is no longer producing at an economic rate. The straddle tool is positioned over the existing perforations or the previously opened fracturing sleeve, and the refracturing is performed through the CT. For more on refracturing see Chapter 17.

16.5 Benefits and Considerations of Each Completion System

This section will discuss the benefits and considerations of each completion system. **Table 16.1** provides a quick reference summary of the completion systems as discussed in these sections. This section has been modified from Burton (2013a).

16.5.1 Plug-and-Perforation Completion Systems

Plug and perforation completion systems have the following benefits and considerations:

- **Number of stages.** The number of stages is virtually unlimited because each plug and set of perforation guns is run on separate trips. The only limitation is the length of the wireline to deploy the tools, and the length of the coiled tubing to deploy tools and/or mill out the plugs.
- **Stage placement.** The placement of the stage is not final until the perforations are fired, so the placement can be changed during the fracturing job. The perforation guns can be moved up or down the well to the optimal target before they are fired. This allows time to gather and analyze more data before determining stage placement.
- **Contingency options.** Should a screen-out or other downhole problems arise, there are not any diameter restrictions above the stage being fractured, so it is possible to use through-tubing tools to recover.
- **Fracturing logistics.** Pressure pumping services are not the only requirement during the fracturing job. Either wireline and/or coiled tubing services are required to perforate the first stage, deploy tools, and mill out plugs. All these services have to be coordinated to avoid any nonproductive time for the other services.
- **Fracturing operation efficiency.** This completion technique is not the most efficient during the fracturing job because pressure pumping and wireline have to be set up and disconnected between each stage. When pad drilling is used and several wells are placed close together, the efficiency can be improved using simultaneous operations. While wireline services are being performed on one well, the pressure pumping will be performed on a nearby well. Once these services are complete, the services are switched between the two wells, minimizing the nonproductive time for wireline and pressure pumping
- **Post fracture.** When the fracturing job is completed, the composite fracturing plugs require mill out to put the well on production. Removing the plugs leaves a full production diameter through the liner. Using the new large-bore plugs with disintegrating fracturing balls

will avoid the mill-out run. Then, the well can be put on production after the fracturing job is complete.

16.5.2 Ball-Activated Completion Systems

Ball-activated completion systems have the following benefits and considerations:

- **Number of stages.** Because the fracturing sleeves are dependent on incremental ball and ball seat sizes, the number of stages is limited to the number of ball and ball seat combinations. Currently the number of ball and ball seat combinations exceeds the average number of stages in each well.
- **Stage placement.** When the system is set, the stages are fixed at the depth of the sleeves and packers. If a geological hazard or nonproductive zone is located, a stage can be skipped by not dropping the ball that corresponds to the fracturing sleeve in that stage.
- **Contingency options.** There can be very limited contingency options if a screen-out or other downhole problems occur. The ball seats create diameter restrictions in the completion string that can hinder the use of through-tubing tools. Contingency options depend on the diameters above the stage where the incident occurs and if through-tubing tools can reach the problem area. It may be possible to open the next stage using mechanical force from CT, or to skip a couple of stages and mechanically open a sleeve. The worst-case scenario would be a screen-out at the toe of the well with diameter restrictions causing a loss of a significant portion of the stages. If this occurs and it is decided that too many stages will be lost, the ball seats can be milled out and an openhole PNP can be performed between the packers.
- **Fracturing logistics.** Pressure pumping is the only service required on location during the fracturing job.
- **Fracturing operation efficiency.** The nonstop fracturing operations translate to very efficient fracturing operations.
- **Post fracture.** The fracturing balls are designed to come off the ball seats, so the well can be produced through the ball seats. However, the production diameter is restricted if the ball seats are not removed. The ball seats are designed to be milled out, so they can be removed if needed. Using the disintegrating fracturing balls will ensure that the balls will not hinder production because they disintegrate in the wellbore after the fracturing job is completed.

16.5.3 Coiled Tubing-Activated Completion Systems

Coiled tubing-activated completion systems have the following benefits and considerations:

- **Number of stages.** These systems have a virtually unlimited number of stages. The length of the CT and the ability to effectively operate the tools in longer laterals are the primary limitations.
- **Stage placement.** Using the abrasive perforator to create the diversion of the fluid enables the flexibility to adjust the stages during fracturing by moving the CT up or down the well to the optimal stage depth. If using the fracturing sleeves, the stages are fixed at the depths that the fracturing sleeves are set. It is possible to skip a stage by not opening the sleeve, and an abrasive perforator is still run on the CT BHA so stages can be added during fracturing.
- **Contingency options.** If a screen-out or other downhole problem occurs during the fracturing job, CT is already in hole and at the depth of the incident. The BHA is set up to circulate from the CT through the annulus, or vice versa. This makes the recovery of a screen-out relatively easy and minimizes nonproductive time.
- **Fracturing logistics.** During the fracturing job, pressure pumping and coiled tubing services are required on location.
- **Fracturing operation efficiency.** Fracturing briefly shuts down between each stage to move the CT tool assembly to the next stage. Because the fracturing job is performed with the CT in the well, there is no setting up and setting down CT between each stage, so it is still very efficient, even though the fracturing shuts down between stages.
- **Post fracture.** After the fracturing is complete, the well can be put on production without an additional through-tubing trip and with a full diameter in the liner.

16.6 Operational Comparison of Each Completion System

16.6.1 Comparing Multiple-Entry and Single-Entry Points

Multistage completion systems provide a variety of options to consider when selecting a system. One of the primary considerations is the number of entry points per stage: should it be a single entry point or multiple entry points? This will determine how much pump rate will be needed in each stage, and how much hydraulic horsepower will be required on location. It also controls fluid volumes in each stage and indirect control of fracture growth.

Traditionally PNP uses cluster perforations creating multiple points of entry for the fracturing fluids. Traditional ball-activated and coiled tubing-activated fracturing sleeves only use a single point of entry out of a single sleeve, but there are sleeves that are designed to open multiple sleeves at once creating multiple points of entry. This section will discuss the benefits and the considerations of single-entry and multiple-entry completion designs.

16.6.1.1 Fracturing Out of Single- and Multiple-Entry Points

When fracturing out of a single entry point, the theory is very simple: the fluid volumes and rates pumped at the surface are going out of that entry point. There is only one flow path, so all of the fluid has to go out of that point. There are other factors to consider when fracturing out of multiple perforation clusters at one time. The very basic theory behind fracturing stages with multiple entry points is that the fracturing fluid will distribute evenly. There are fluid friction losses between each cluster though. There will be a path of least resistance toward the heel of the well, because it will have the least amount of distance to travel and therefore the least amount of friction losses. The cluster toward the toe of the well is the deepest in the well, so it has the most friction losses and would be the path of most resistance. The fluids will naturally flow to the path of least resistance.

To help compensate for the friction losses, there is a technique called limited entry perforating. This technique uses the flow area of the perforation clusters to help negate the effect of the friction losses. The perforations toward the heel would have the least amount of flow area and the perforations toward the toe would have the most flow area. This makes it easier for the fluid to flow out of the perforation toward the toe. The idea is to make the energy required for the fluid to enter the top set of perforations the same as the energy required to enter the bottom set of perforations. This will balance all of the perforation clusters and there will not be a path of least resistance, creating a more even distribution of the fluids. For more details on the technique of limited entry perforating, see Chapter 17.

16.6.1.2 Horsepower Requirements

When fracturing out of multiple entry points at one time, it will require more horsepower because all of the entry points are being fractured at the same time. **Table 16.2** shows the results from comparing a well using multiple entry points, and a well using single entry points in the same area of a field. In this example, Well A used PNP with 10 individual stages and 3 clusters per stage for a total of 30 entry points, and Well B used a CTACS with 30 individual entry points with CT-activated sleeves. The entry points were spaced the same distance from each other, and the parameters of the fracturing job were the same. Well A had to use 99 bbls/min to treat the 3 clusters per stage, which translates to 33 bbls/min out of each entry point. Because of the single entry point, Well B was able to drop the overall treatment rate to 40 bbls/min. The treatment per entry point was more

Table 16.2—Multiple entry versus single entry fracturing job. (Modified from Castro et al. 2013.)

Parameter for Well	A (Plug and Perf)	B (Targeted)	Variance
Number of Fracture Stages	10 (with 3 clusters per stage)	30	None
Fracture Spacing (ft):	165	164	None
Fluid Type:	HCl Spearhead, slickwater fluid	HCl Spearhead, slickwater fluid	None
Proppant Type:	100 mesh sand, 40/70 Ottawa white and resin coated with 2% resin coating	100 mesh sand, 40/70 Ottawa white and resin coated with 2% resin coating	None
Total Clean Fluid Pumped (gal):	9.344,170	9.568,993	+2.4%
Total Proppant Placed (lbs):	3,675,280	3,772,380	+2.6%
Average Fracturing Rate (bpm):	99	40	-60%
Average Treating Pressure Range (psig):	5,852 to 6,801	4,125 to 6,935	-30% to +2%
Average HHP Range:	13,889 to 16,387	3,004 to 5,517	-78% to -66%
Maximum HHP Required:	20,630	6,693	-68%

aggressive in Well B, but the overall rate was significantly lower. This lower rate also rendered a much lower maximum horsepower requirement. Fracturing through three entry points per stage required nearly 21,000 HHP, where the single entry of Well B was able to stay under 7,000 HHP. If this type of savings can be planned, it can reduce the amount of horsepower needed on location, in turn reducing the amount of space needed.

It is worth noting that all three of the completion types can use a single entry. The BACS and the CTACS were designed to fracture out of a single entry point. PNP can also be single entry by simply placing one set of perforations per stage, but it further amplifies the inefficiencies during the fracturing job. In the example above it would require setting up and setting down the wireline and pressure pumping units a total of 30 times, if Well A were to use single entry points. This would cause a significant increase in the total amount of time required to perform the fracturing job.

16.6.1.3 Direct Control of Fluid Volumes and Indirect Control of Fracture Growth

Another benefit of using single entry points during the fracturing job is the direct control of how much fluid volume is placed into each injection point. Even when using the limited entry perforating strategy to balance the amount of energy required at each entry point, the formation will still dictate how the fluids will distribute based on the weak points in the formation. These types of formations are heterogeneous, and as mentioned above, the fluids will follow the paths of least resistance. This increases the chance that most of the fluid will go through only a few of the entry points, potentially resulting in some clusters being over stimulated and some clusters being under stimulated as shown in **Fig. 16.23**.

This could lead to missing out on production from the under stimulated clusters and having poor conductivity leading to low production in the over stimulated clusters. It also means that the over stimulated clusters have a fracture geometry that is larger than intended. That can be a very important factor in applications with unwanted zones or producing wells nearby. For example, certain sections of the Barnett shale do not have a natural fracturing barrier between the Barnett shale and the saltwater-bearing Ellenberger zone below it. If the Ellenberger zone is fractured into and the fracture stays conductive to the wellbore, the well will be a saltwater-producing well rather than a hydrocarbon-producing well.

In applications like this where it is critical to control the growth of the fracture, a single point of entry should be used. This will not give direct control over the growth of the fracture because it will still be formation dependent, but it will give direct control of the volume of fluid placed in that injection point. If the formation is understood and it is somewhat known how the fracture will grow, controlling the volume of fluid and the rates out of the single entry point will give indirect control of the fracture growth. This can be used to avoid fracturing into surrounding zones or nearby offset wells. This is demonstrated in **Fig. 16.24**.

16.6.2 Wells with Long Laterals

Wells with long laterals present unique challenges to completions. A common well profile in the Bakken formation is a 10,000-ft.-deep well with a 10,000-ft. lateral. With these depths, it can be difficult to locate a CT unit or wireline unit that has 20,000 ft. or more of length. Even if units with the lengths required are located, it is still difficult to perform through-tubing operations in these long laterals, particularly with CT. It would be challenging to effectively operate tools or perform mill outs at these depths. Additional CT tools and specialty fluids can be used to increase effectiveness in longer laterals, but there are

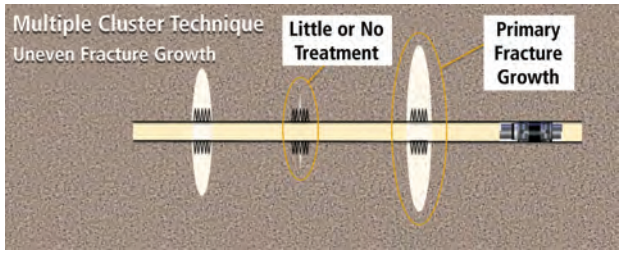

Fig.16.23—Uneven fluid distribution and fracture growth through multiple clusters. (Modified from Burton 2013b.)

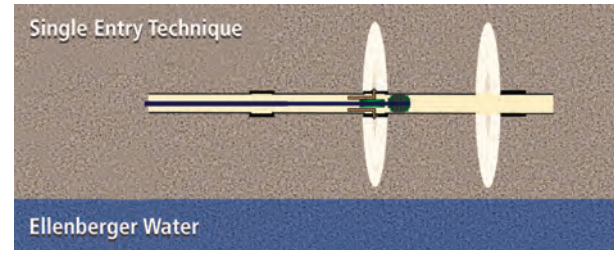

Fig. 16.24—Fracturing through single entry points can help avoid fracturing into unintended zones. (Modified from Burton 2013b.)

still risks and limitations. Operations that require WOB to perform, such as mill outs, may have to consider using a workover rig with tubing to perform these operations.

These challenges make the BACS the most appealing completion system in this application. The BACS does not require through-tubing operations during or after the fracturing job, simplifying the process in these long laterals. If more stages are desired than can be accomplished with the BACS, this system could also be combined with other completion types to form a hybrid system that is more optimal for this application. The BACS would be run at the toe of the well at the depths that would be difficult for through-tubing operations, and a PNP or CTACS would be run toward the heel of the well at the shallower depths where these operations are more feasible.

Another option would be to use a hybrid system using the large-bore fracturing plugs with disintegrating fracturing balls at the deeper depths toward the toe of the well. These plugs are left in the well and produced through, and composite fracturing plugs or CTACS can be used toward the heel of the well where the CT operations are more practical.

16.6.3 Increased Number of Stages

An increased number of stages is often associated with the longer laterals. When the number of stages increases in the wellbore, the nonproductive time associated with the inefficiencies during the fracturing job increases exponentially. Consider the following example in **Fig. 16.25** comparing PNP to BACS with 40 individual stages. It is assumed that there is 1 hour per stage in the fracturing plan and there are no operational issues. With the BACS that means it will require 40 hours to stimulate the well, translating to 2 days with a 24-hour pressure pumping crew and 4 days with a 12-hour crew. PNP requires an additional assumption of the time to set up and set down wireline and pressure pumping between stages. This example assumes 3-hours between stages. This will require 160 hours to stimulate the well, which translates to 7 days with a 24-hour crew and 14 days with a 12-hour crew. In this example, the BACS reduces the fracturing cycle time from weeks to days, and will most likely be the most economical solution.

16.6.4 Low Number of Stages

Not all wells will have long laterals and an extended number of stages though. Consider the example shown in **Fig. 16.26** that compares a five-stage fracturing job between BACS and PNP. The same assumptions of one hour per stage, no operational issues, and three hours of set up and set down time per stage for PNP are used in this example. The BACS will require five hours total time to stimulate, which will only take one day with either a 24-hour or 12-hour crew. The PNP completion will require 20 hours total time to stimulate, translating to one day with a 24-hour crew and two days with a 12-hour crew. In this example, there is not a drastic difference in the fracturing cycle time between the two systems, so an economic analysis will need to be performed to determine the most cost-effective solution.

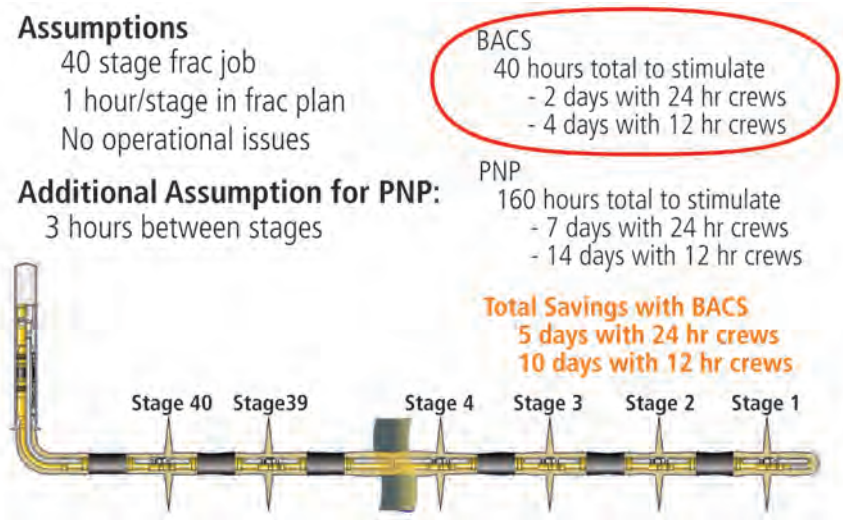

Fig. 16.25—Comparison of a 40-stage PNP and BACS. (Modified from Burton 2013b.)

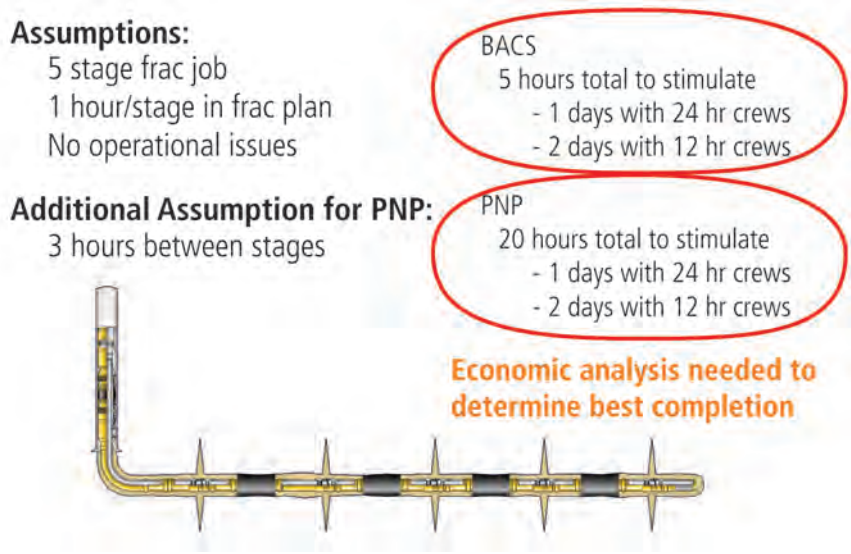

Fig. 16.26—Comparison of a five-stage PNP and BACS. (Modified from Burton 2013b.)

16.6.5 Shortage of Supplies for Fracturing

There are also applications where the availability of fracturing components, such as water and proppants, will play a major role in the cost effectiveness of the completion. For example, in some areas there is only enough water or other supplies to fracture one or two stages per day. It does not matter how efficient or how many stages can be done with the completion system if the availability of the fracturing supplies limits the number of stages per day. In this application, an economic analysis will need to be performed to compare the cost of services to cost of completion tools.

16.6.6 Appraisal Phase of the Asset Life-Cycle

The appraisal phase of the asset life-cycle has different objectives than any other phase in the life-cycle. Because this is a new formation, the primary objective is to gather data and understand this formation. During this phase there is a higher risk of drilling a poor-quality wellbore and having a screen-out during the fracturing job, simply because formation is not known yet. Also, it may be desired to run additional logs or additional time may be needed to analyze logs captured while drilling and it is not known exactly where to place the stages as soon as the well is drilled.

The ideal completion system for this application is a system with the following benefits:

- Allows the stage placement to be adjusted during the fracturing job. (The stage depth is not determined until perforations are placed in the casing.)
- Contains no completion tools that would increase the diameter and stiffness of the completion string. (Increasing diameter and stiffness of the completion string makes it more difficult to install in the well, particularly if it is poorly drilled.)
- Has a full diameter in the liner above the stage being fractured so that through-tubing operations can be performed if a screen-out occurs. (A full diameter above the stage being fractured allows through-tubing tools to be deployed to assist in recovery.)

The PNP completion fits the description of this completion system. The CTACS using an abrasive perforator as the primary means of creating the injection points could also be considered.

16.6.7 Development Phase in the Asset Life-Cycle

When the asset transitions to the development phase, it is assumed the formation is mostly understood. This understanding changes the objectives and there is more focus on cost and time efficiencies while maintaining—or increasing—production. All three completion types (BACS, CTACS, and PNP) are viable options in this phase.

The BACS only requires pressure-pumping services during the fracturing job, simplifying the onsite service logistics.

This system can drastically reduce the fracturing cycle time in wells with a large number of stages, in some cases reducing the cycle time from weeks to days. There are no through-tubing operations required during, or after, the fracturing job, so it is also effective in long laterals outside of the normal operating limits of CT.

The CTACS has the most efficient contingency options for a screen-out. This feature is particularly useful in formations where it is difficult to design the stimulation and screen-outs are more likely. CTACS also allows direct control of the fluid volume placed in each stage, which provides indirect control of the growth of the fracture. This gives a significant advantage in formations that do not have good fracturing barriers and risk breaching into unwanted zones, or in a field with wells spaced closely together to prevent fracturing into nearby producing wells. In addition, the flexibility to shut down the fracturing and move to the next stage is ideal in areas where real-time fracturing monitoring, like microseismic, is being performed. Running this system with an abrasive perforator also builds-in the flexibility to adjust the depth of the stage during the fracturing job.

PNP is the completion option that was used to unlock these types of plays, and is still the most commonly used today. It remains one of the most flexible systems because the stage depth is not determined until the casing is perforated, and there is an unlimited number of stages within the operating depths of wireline and CT. During the development phase, the overall efficiencies are increased, and some of those increase the efficiency of PNP as well. Using simultaneous operations during pad drilling will decrease the services' nonproductive time and increase the overall efficiency of PNP. The efficiency is gained by the capability to run wireline operations in one well while simultaneously performing the fracturing job at a nearby well. When these services are completed, they switch out wells so that neither service is completely idle between stages. Also, this may be the most economical solution in areas where the fracturing supplies are not readily available to perform a large number of stages per day.

16.7 Services Correlation

It is very important that the services collaborate in these plays. The way the well is drilled will directly affect the completion type that can be installed, and the way the well is completed will directly affect the success of the fracturing job.

16.7.1 Effects of Drilling on the Wellbore Completion System

The size of the casing and the openhole can reduce the completion options available to be installed in that well. The quality of the wellbore will determine if annular isolation can be achieved better with cement or openhole, or if it can be achieved with either choice. The capability to get the completion to the intended depth also depends on the quality and shape of the well.

16.7.2 Effect of the Wellbore Completion System on Fracturing Operations

The type of completion used determines the efficiency during the fracturing job as well as the number of services required. The flow areas and the pressure ratings in the well are dependent on the completion type that is selected. The completion determines the number of entry points per stage, which controls the volumes of fluid pumped into each injection point and indirectly controls the fracture geometry. Also, the amount of fluid required to pump down equipment is determined by the type of completion, and is critical in formations that are sensitive to over displacement of fluids. Designing the fracturing job and the wellbore completion independently from each other could result in incompatibility and limitations to the original fracturing plan during the fracturing job.

16.8 Concluding Remarks

All three of the completion techniques are viable options in formations that require multistage hydraulic fracturing. Each one has the capability to use cement or openhole packers to isolate the annulus, and each one has the capability to use single- or multiple-entry points per stage. Therefore, if either an openhole or a cemented completion, or single- or multiple-entry is superior for that particular formation, any of the systems can still be used. Over the years, the production results have proven that each of these systems provides effective multistage isolation. The choice can be made based on the application, as well as cost and availability of services, after determining which technique is truly the best completion for that area.

16.9 Acknowledgments

The author would like to thank James King of Baker Hughes and Monte Madsen of Whiting Petroleum for reviewing the chapter and providing feedback. Although

there are too many to list by name, he would also like to thank the mentors and coworkers at Baker Hughes that have provided the experience and knowledge to write this chapter.

16.10 References

Burton, A. 2013a. Unconventional Completions: Which One Is Right for Your Application? Paper SPE 166431 presented at the SPE Annual Technical Conference and Exhibition. Louisiana, New Orleans. 30 September–2 October. http://dx.doi.org/10.2118/166431-MS.

Burton, A. 2013b. Unconventional Completions–An Operational Comparison. Paper SPE 167030 presented at the SPE Unconventional Resources Conference and Exhibition–Asia Pacific, Brisbane, Australia. 11–13 November. http://dx.doi.org/10.2118/167030-MS.

Castro, L., Bass, C. Pirogov, A., et al. 2013. A Comparison of Proppant Placement, Well Performance, and Estimated Ultimate Recovery Between Horizontal Wells Completed with Multi-Cluster Plug & Perf and Hydraulically Activated Frac Ports in a Tight Gas Reservoir. Paper SPE 163820 presented at the SPE Hydraulic Fracturing Technology Conference. The Woodlands, Texas. 4–6 February. http://dx.doi.org/10.2118/163820-MS.

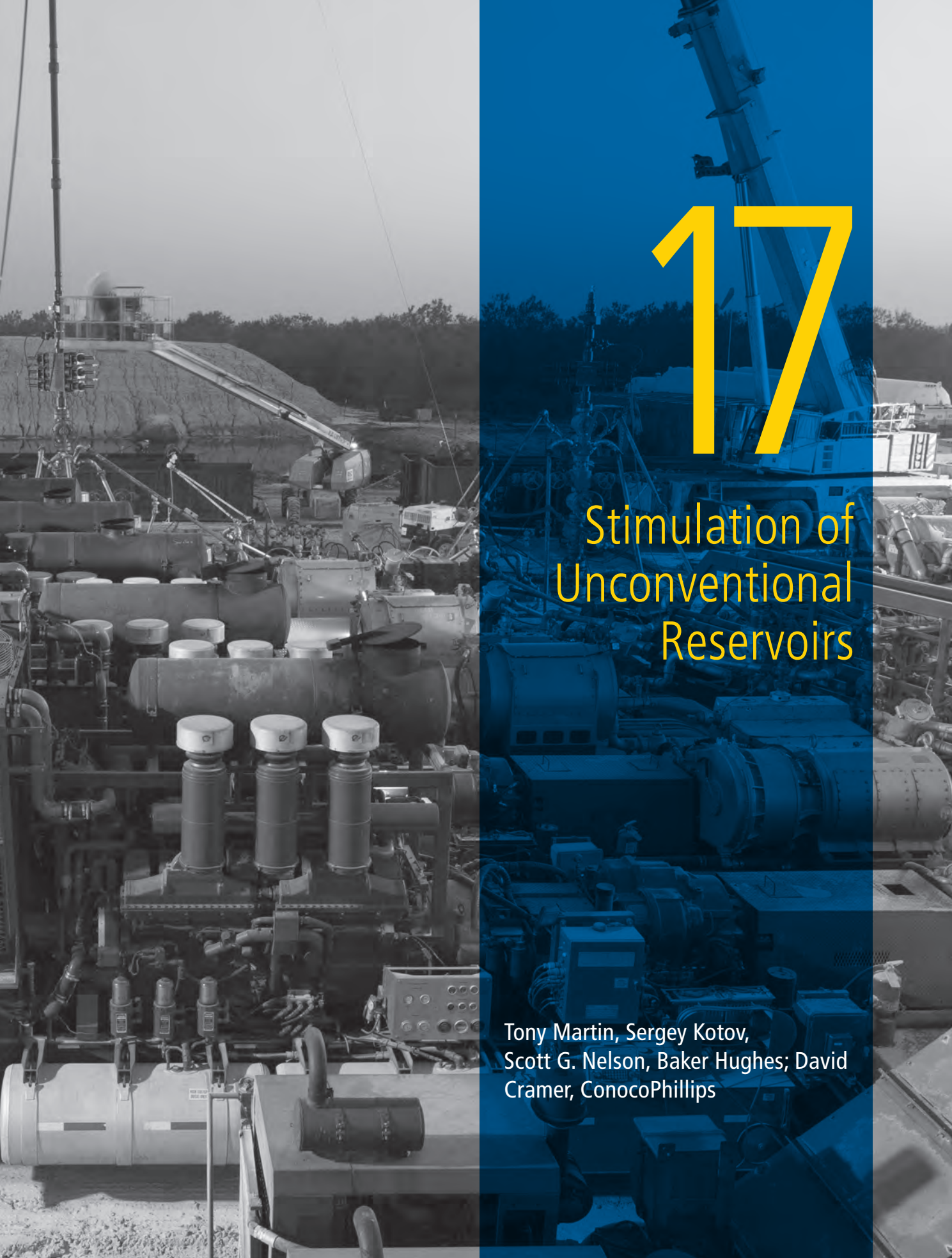

17

Stimulation of Unconventional Reservoirs

Tony Martin, Sergey Kotov, Scott G. Nelson, Baker Hughes; David Cramer, ConocoPhillips

This page intentionally left blank

Chapter 17: Stimulation of Unconventional Reservoirs

Authors' Note

This chapter attempts to cover a lot of information in a quite short space: a single chapter for a subject that can fill whole books. Necessarily, the authors have focused on the aspects of hydraulic fracturing that are specific to unconventional reservoirs. Consequently, we assumed that the reader already has a certain level of background knowledge about the subject. For those readers who lack this background knowledge, or those who perhaps wish to refresh their knowledge of certain aspects of fracturing, the authors recommend the following excellent publications: Howard and Fast (1970), Ely (1994), Gidley et al. (1989), Economides and Nolte (2000), Economodes, Nolte, and Ahmed (1998), Economides and Martin (2007), and Martin (2009).

It should also be noted that oil and gas reservoirs—especially unconventional oil and gas reservoirs—are stochastic mediums within which to work. Unconventional oil and gas reservoirs are highly variable in character and properties; even the amount by which they vary is highly unpredictable. What this means is that case histories and oil field experiences based on single-well or single-location understanding are ultimately meaningless in the context of global unconventional reservoir fracturing. What we seek to capture in this chapter are distilled general trends and accumulated best practices, rather than specific instructions intended to work under every circumstance for every reservoir. There is still considerable room for sound engineering judgment to be used when applying the principles and practices discussed here.

17.1 Introduction to Unconventional Fracturing

Hydraulic fracturing has been around for over 60 years. The successful implementation of this technology in the Barnett shale during the 1990s started a new era in economic development of unconventional resources.

17.1.1 Evolution of Hydraulic Fracturing

The first attempts at fracturing formations were not hydraulic in nature. Early fracturing involved the use of high explosives to break the formation apart and provide "flow channels" from the reservoir to the wellbore. There are records indicating that this took place as early as 1890. Some companies even used nitroglycerine to explosively stimulate formations. This type of reservoir stimulation reached its ultimate conclusion with the experimental use of nuclear devices to fracture relatively shallow, low-permeability formations in the late 1950s and early 1960s (Howard and Fast 1970).

In the late 1930s, acidizing had become an accepted well development technique. Several practitioners observed that above a certain "breakdown" pressure, injectivity would increase dramatically. It is probable that many of these early acid treatments were in fact acid fractures.

In 1940, Torrey recognized the pressure-induced fracturing of formations for what it was (Torrey 1940). His observations were based on squeeze cementing operations. Torrey presented data to show that the pressures generated during these operations could part the rocks along bedding planes or other lines of "sedimentary weakness." Similar observations were made for water injection wells (Yuster and Calhoun 1945a and 1945b).

The first intentional hydraulic fracturing process for stimulation was performed in the Hugoton gas field in western Kansas in 1947. The Klepper No. 1 well was completed with four gas producing limestone intervals, one of which had been previously treated with acid. Four separate treatments were pumped, one for each zone, with a primitive packer being used for isolation. The fluid used for the treatment was Vietnam-era war-surplus napalm, which was surely an extremely hazardous operation. In spite of the danger, 3000 gallons of fluid were pumped into each formation. The process was later patented by Riley F. Farris at Stanolind Oil and Gas Company, which was one of the predecessors of Amoco (Farris 1953).

By the mid-1960s, propped hydraulic fracturing had replaced acidizing as the preferred stimulation method in the Hugoton field. Early treatments were pumped at 1 to 2 bbl/min with sand concentrations of 1- to 2-ppa.

Today, thousands of these treatments are pumped every year, ranging from small skin bypass fractures at $20,000, to massive fracturing treatments that end up costing well over $1 million. Many fields only produce because of the hydraulic fracturing process. In spite of this, numerous industry practitioners remain unfamiliar with the processes involved and with what can be achieved.

17.1.2 Unconventional Versus Conventional Hydraulic Fracturing

"There are no optimum, one-size-fits-all completion or stimulation designs for shale wells." (King 2010.)

The fundamental differences between conventional and unconventional reservoirs are explained in detail elsewhere in this work (see Chapter 3). Until the end of the 1970s, fracturing was mainly performed on wells that would flow naturally without fracturing, with the process used primarily to turn sub-economic wells into economic wells, and economic wells into even better wells. Significant work was performed on both oil and gas formations.

In 1980, the US federal government introduced the Alternative Fuels Production Credit [Energy Information Administration (EIA) 1999]. Originally, set up to run until 1989, but subsequently extended until 1992, this tax credit was designed to boost production of several different US-based sources of alternative fuels, but by far the biggest beneficiary was tight gas (defined as gas coming from formations of less than 0.1 md permeability). This meant that many producing companies could essentially drill and complete tight gas wells for free. Hydraulic fracturing very quickly became an essential part of the completion process, often proving to be essential for economic production. In a very short space of time, fracturing became a fundamental part of the tight gas extraction industry.

The success of hydraulic fracturing marked the advent of a whole new class of reserves—unconventional reservoirs—for whom no significant exploitation of the often-huge resources could be achieved without hydraulic fracturing. Three types of unconventional reservoirs exist:

1. Sandstone and carbonate oil and gas reservoirs. The only main difference to conventional reservoirs is very low permeability (this category includes tight gas).

2. Coalbed methane (CBM), also referred to as coal seam methane or CSM. These reservoirs consist of gas released during the formation of coal that has not migrated into other formations.

3. Shale oil and gas reservoirs. These are reservoirs of almost no native permeability, which are generally the source rock for the oil and/or gas and from which the oil and/or gas has not significantly migrated.

This chapter will concentrate on the aspects of fracturing associated with the stimulation of shale oil and shale gas reservoirs. It will concentrate on the materials used in fracturing unconventional reservoirs, treatment design, geomechanics and fracture modeling, perforation strategy, calibration and diagnostic tests, and finally unconventional fracturing operations.

It is difficult to over-state the size, complexity, and extent of unconventional fracturing operations in North America. For instance in 2014, the US land fracturing industry is expected to use 94 billion lbs. of proppant and fracturing sand (PacWest 2014a). This is a number so large as to be abstract—so let's put it another way—it is a volume sufficient to cover an NFL football field to a depth of just over three miles. Furthermore, the North American fracturing industry is expected to average 19.7 million hydraulic horsepower (HHP) pumping capacity in 2014 (PacWest Consulting 2014b). With each pump truck averaging around 2,000 HHP, that's nearly 10,000 trucks just for pumping—and these trucks will be busy. It is estimated that they will pump over 510,000 individual fracturing jobs in North America in 2014 (PacWest 2014c). In terms of capital expenditure, logistics, and manpower, the commitment made by the industry to the fracturing of unconventional reservoirs in North America is quite simply staggering—especially so given that most practitioners do not fully understand the processes involved.

Fig. 17.1 shows a typical North American fracturing location for an unconventional reservoir.

Fig. 17.1—Haynesville shale location with two complete fracturing spreads performing a "simo-fracturing" on two separate wells. It is difficult to overstate the massive logistics and capital expenditure associated with the hydraulic fracturing of unconventional resources in North America.

17.2 Fracturing Fluids and Proppants

The selection of proper proppant and fracturing fluids is an important component of any successful hydraulic fracture treatment. Any flaws in the selection of these materials will be detrimental to the efficiency of the created hydraulic fractures and ultimately, production from the wells.

17.2.1 Fracturing Fluid Systems

Fracturing fluid systems can be categorized by the base fluid as water-based (slickwater, gelled fluid systems including linear and crosslinked gels;) viscoelastic fluids; and non-aqueous, hydrocarbon-based fluid (oil, gas condensate, diesel, liquid LPG, and so on). Other systems such as acid-based and multiphase fluids (emulsions, foams, energized fluids), liquid CO_2-based, and methanol-based fluids are also used.

Water-soluble polymers based on either polysaccharides (e.g., starch, cellulose, guar, and their derivatives) or synthetic polymers (e.g., polyacrylamide) are used to viscosify water-based fracturing fluids. Guar is the dominant viscosifying agent in use today.

Oil-based fracturing systems were the first fracturing fluids to be used. The technology has evolved from sodium-carboxylated associative polymers, to aluminum-carboxylated associative polymers, to aluminum-phosphate associative polymers. In the last decade, use of oil-based fluids has transitioned to iron-phosphate ester technology (Economides and Martin 2007). Although they are compatible with most reservoirs, currently oil-based fluids are rarely used due to the higher cost compared to water-based fluids, as well as because of environmental restrictions.

Each fluid type has unique characteristics. To provide the required performance, the fracturing fluid has to possess several properties including, but not limited to:

- Adequate viscosity and rheology provides the efficient transport and placement of proppant into the fractures.
- Low friction properties to reduce tubular friction, thus reducing the horsepower requirements and providing higher safety factors for surface equipment pressure limitations.
- Controlled degradation of viscosified fluids ensures easy cleanup and minimizes polymer damage to the proppant pack and the formation.
- Minimized leakoff promotes optimum fracture geometry and maintains the fracture width to allow placement of proppant.
- Compatibility with the formation, reservoir fluids, and proppant.
- Environmental acceptance to minimize or ideally eliminate any potentially harmful biological and/or environmental effects.
- Operational safety acceptance.

To be practical, the fracturing fluid should also be operationally simple and cost-effective. The reservoir conditions and the objective of the fracture treatment will dictate the fluid type and the properties.

17.2.1.1 Fracturing Fluid Additives

Depending on the type of the fluid and specific fluid characteristics, there could be a variety of additives used in the preparation of these various types of fracturing fluids. The description and the application criteria for all the fracturing fluid additives is beyond the scope of this chapter; however, the following is a description of the most common types of additives.

The additives depicted in **Fig. 17.2** represent less than 0.5% of the total fluid volume. There is no one-size-fits-all formula for the volumes for each additive; therefore, the application and the concentration of additives may vary depending on the objective of the fracture treatment and specific reservoir conditions.

The following provides descriptions of typical fracturing fluid additives:

- **Gelling Agents.** Used to viscosify the fluid.
- **Buffers.** Used to control the pH of the fracture fluid for polymer hydration as well as crosslinking and gel stability.
- **Crosslinkers.** Used to exponentially increase the fluid viscosity.
- **Biocides.** Used to kill bacteria in the mix water, biocides are designed to prevent a colony of bacteria from developing in the first place, rather than for killing an existing colony.
- **Surfactants.** Used to reduce the surface tension, interfacial tension between water and formation fluids, and also to change the contact angle of the leakoff fluid for easier recovery.
- **Friction Reducers.** Used to reduce the friction pressure and hence associated horsepower requirement for the pumping operation, friction reducers also protect equipment from wear and tear due to the high pumping rates of slickwater jobs.
- **Gel Stabilizers.** Used to increase the fluid stability of crosslinked gels at elevated temperatures.

Fig. 17.2—Common fracturing fluid additives. Water and sand constitute the vast majority of the materials used in fracturing of unconventional reservoirs.

- **Breakers.** Used to "break" the viscosity of the fracturing fluid, reduce the molecular weight of the polymer, and help with cleaning the proppant pack and the filter cake on the fracture face.
- **Clay Stabilizers.** Used to control swelling, migration, and disintegration of clay minerals such as illite, smectite, chlorite, and montmorillonite.

A more detailed description of fracturing fluids may be found in Chapter 7 of Economides and Martin (2007).

17.2.1.2 Slickwater and Linear Gel Systems

Many fracturing treatments in unconventional reservoirs are performed using low-viscosity fluids such as friction-reduced water ("slickwater"). Combined with a friction reducer and linear gels, this approach provides lower friction pressure loss during the treatment and minimizes horsepower requirements, as well as promoting fracture complexity with minimal or no proppants at all (Meehan, 1997).

Linear gel fracturing fluids are formulated with a wide variety of different polymers in an aqueous base. Common polymers used for linear gels include: starch, guar, hydroxypropyl guar (HPG), carboxymethyl hydroxypropyl guar (CMHPG), carboxymethyl guar (CMG), cellulose, hydroxyethyl cellulose (HEC), carboxymethyl hydroxyethyl cellulose (CMHEC), xanthan, xanthan derivatives, and various synthetic polymers. Guar gum and its derivatives, such as HPG and CMHPG, account for most of the gelled fracturing fluids.

Before the dry polymer is added to water, the individual molecules are tightly curled upon themselves. As the polymer molecule hydrates in water, it straightens out—

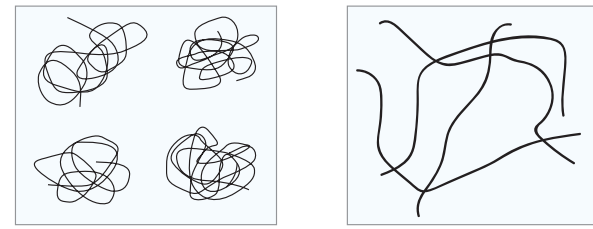

Fig. 17.3—Hydration of polymer gels in water, which shows a polymer molecule before hydration in water (A) and a polymer molecule after hydration in water (B). (Martin 2009.)

which is why these fluids are referred to as linear gels—as illustrated in **Fig. 17.3**.

Due to low viscosity, slickwater and linear gels rely entirely upon turbulence in the fluid to keep the proppant suspended. Friction reducers are typically added to the water at a concentration of 0.25- to 2-gal/1000 gal to allow this fracturing fluid to be pumped at higher rates with reduced friction pressure, compared to water without the friction reducer. Although the objective is to reduce the friction pressure of the fluid system, rather than to provide any viscosity-based proppant transport characteristics, the linear gel has higher viscosity than slickwater, and, therefore, is a better proppant transport media. Some advanced high-molecular-weight friction reducers can increase viscosity similar to the level of linear gels thus improving proppant transport while reducing friction (proppant transport is covered in more detail later in this chapter).

17.2.1.3 Crosslinked Gel Systems

Depending on the reservoir conditions, treatment design requirements, and/or technical constraints, more-viscous fluids may be required to stimulate unconventional reservoirs. Viscosity of the fluids is typically generated by polymers. Hydrated guar and derivatives create linear gels that do not achieve the required viscosity for proppant transport at elevated temperatures. Therefore, crosslinking agents are added to linear gels resulting in high-viscosity fracturing fluids with a complex 3D structure that provides higher proppant transport performance, relative to linear gels. When used for crosslinked systems, linear gels are often referred to as base gels. The most commonly used linear gels are guar and its derivatives: HPG, CMG, and CMHPG. A crosslinked gel, as illustrated in **Fig. 17.4**, consists of a number of hydrated polymer molecules, which have been joined together by the crosslinking chemical. The series of chemical bonds between the polymer

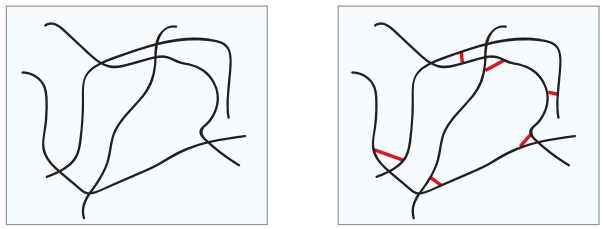

Fig. 17.4—(A) Crosslinked polymer shows the hydrated polymer before the crosslinker is added and (B) the crosslink chemical bonds between the polymer molecules. (Martin 2009.)

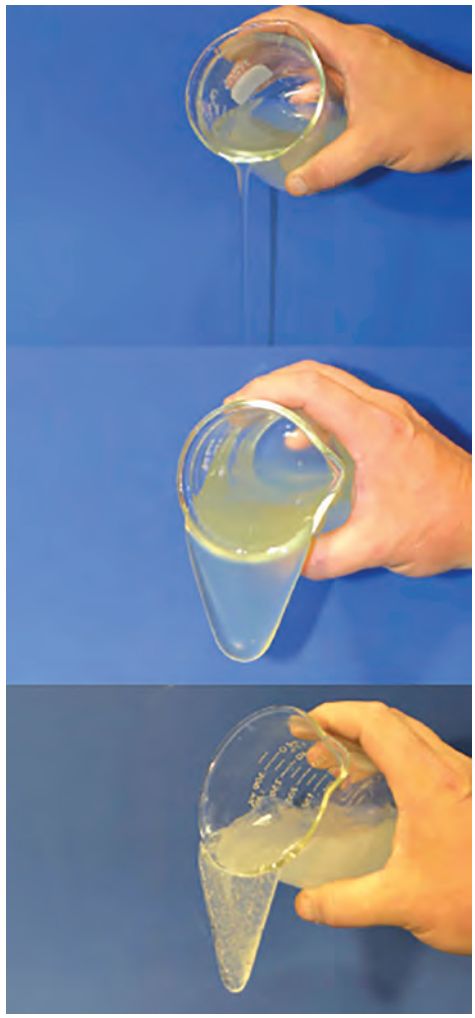

Fig. 17.5—Appearance (from top to bottom) of the base gel, borate crosslinked gel, and zirconium crosslinked gel. (Economides and Martin 2007.)

molecules greatly increases the viscosity of the system, sometimes by as much as 100 times.

Crosslinking is the most cost-effective way of increasing the viscosity of the fluid by chemically linking the polymer chains. Water-based fluids can be crosslinked at high- or low-pH conditions.

In order for an efficient crosslink to occur, two requirements must be met. First, the base gel must be buffered to a pH that will allow the crosslinking chemical to work. Usually, this is a different pH than is optimum for polymer hydration, so a pH buffer must be used. Secondly, the crosslinking radical needs to be present at a sufficient concentration. If both these conditions occur, the gel will experience a dramatic increase in viscosity.

The crosslinked systems used today can be divided into two categories: borates and metallics.

Borate-crosslinked fracturing fluids utilize borate ions, while metallic ion crosslinked fluids utilize zirconium, aluminum, titanium, chromium, and other metallic ions to crosslink the hydrated polymers and increase viscosity. Zirconium-based fluids are the most widely used of metallic crosslinked systems today. Aluminum, titanium, and chromium have not been used since the late 1990s due to their lack of high-temperature stability, shear stability, and environmental restrictions.

Hydrated guar gum is usually crosslinked with borates, whereas derivative guar gums such as CMG, HPG, and CMHPG are mostly crosslinked with transition metal crosslinkers (e.g., zirconium). Borate crosslinked fluids are preferred due to their reversibility to mechanical shearing, their favorable environmental properties, and their enhanced tolerance to water quality related issues. Also borate crosslinked fluids are best suited for treatment of lower temperature wells (less than 300°F) unlike metal-based crosslinked fluids, which are more commonly used for treatment of higher temperature wells (Legemah et al. 2014).

Fig. 17.5 shows the appearance of the base gel, borate crosslinked gel, and zirconium crosslinked gel.

Fracturing fluid technology is constantly advancing to meet the requirements of the more challenging environment of unconventional reservoirs. Contemporary borate fluids can tolerate temperatures exceeding 300°F. Zirconium-based fluids can provide better temperature stability than borate fluids, and may be used up to 450°F.

To reduce both the formation and proppant pack damage from polymer residues and to reduce overall fluid cost, the industry has been developing and improving low- and no-polymer systems. The low-polymer systems were introduced in fluids developed by Gupta and Franklin (1994). Dawson et al. (2000) further developed a theoretical basis for these systems. Lei and Clark (2004) discussed the concept of a minimum effective polymer concentration for crosslinking to occur. More recent developments in crosslinker chemistry have allowed crosslinking to occur with guar or guar derivatives at concentrations much lower than the critical overlap concentration, thus reducing the loading of polymer required for crosslinking (Legemah et al. 2014).

Each crosslinker has unique reaction requirements and behavior. All crosslinked gels tend to be shear thinning; i.e., the apparent viscosity of the fluid decreases with shear rate due to the shear breaking the crosslink bonds between the hydrated polymer molecules. Borate crosslinked fluids are both shear-degradable and thermally thinning, but they will recover their viscosity when shear is removed.

Zirconate bonds are much more shear-sensitive and may not reconnect. Therefore, it is essential to consider the level of shear that a fluid will experience when selecting a crosslinker. To minimize shear degradation and loss of fluid viscosity, crosslink time may be delayed by using crosslinking delay additives. The primary purpose of delaying the crosslink time is to minimize the friction—and to avoid having to pump a highly viscous fluid because of the resultant high horsepower requirements (see Chapter 7 of Economides and Martin 2007). The ideal crosslink delay system would delay the onset of crosslink as long as possible, but ensures that the fluid is fully crosslinked by the time it reaches the perforations or formation.

When the fracturing fluid has performed its function to deliver proppant into the fracture, it has to be effectively broken to provide a maximum fluid recovery and ensure that the created proppant pack is clean and conductive. The most common types of breakers used with fracturing fluids are oxidizers, enzymes, and acids—oxidizers and enzymes can also be used in combination.

17.2.1.4 Hybrid Formulations

In some reservoirs, so-called "hybrid" systems have proved to be the most effective type of fracturing fluids. Hybrid fracturing is a process of pumping fracturing fluids with different viscosities in sequences, i.e., slickwater followed by linear gel and/or by crosslinked fluid, and different combinations of the above fluids (a more detailed discussion on hybrid fracturing is provided later in this chapter).

Reverse-hybrid (Liu et al. 2007) and alternate-slug fracturing (Malhotra et al. 2013) use high-viscosity fluid (linear or crosslinked gel) to create the fracture: the proppant is pumped subsequently in a low-viscosity fluid (such as slickwater). Laboratory testing has indicated that the low-viscosity fluid carrying proppant, "fingers" through the high-viscosity fluid, potentially placing proppant deeper in the fracture.

17.2.1.5 Alternative Fluid Systems

Multistage fracturing requires a significant amount of water. Water availability has become a worldwide concern. To address the water shortage issue, the industry has identified the alternatives to fresh water. These include: recycled water (treated flowback water), produced water (treated), formation water (water source wells), and/or sea water. Many companies are re-evaluating these resources as a cheaper and better base for fracturing fluids. In areas with developed oil and gas infrastructure, the cost of processing and using this fluid for fractures is both economically and technically attractive to using often-scarce fresh water (King 2012).

Foams and emulsions are also used in treating shallow unconventional reservoirs. Foaming a fracturing fluid improves rheological properties of the fluid and provides increased energy to enhance cleanup and flowback of the fracturing fluid after the treatment. This has been particularly useful in under-pressured gas reservoirs. The most common foams contain either carbon dioxide or nitrogen and a chemical foaming agent (surfactant)—with binary foams containing both N_2 and CO_2. Fluids containing N_2 or CO_2 could be considered energized if the volume percentage of the energizing medium to the total volume (defined as "quality") is less than 53% at bottomhole conditions, and they are considered to be foams if the volume percentage is greater than this (Mitchell 1969). Energized fracturing fluids of 25 to 30% quality are quite common. When the quality exceeds 53% (i.e., 53% by volume is gas at bottomhole conditions), there is bubble-to-bubble interference and system viscosity increases exponentially until about 90% quality, when misting starts to occur, dramatically reducing viscosity. When the internal phase is a non-liquid, it is considered foam; when it is a liquid, it is considered an emulsion. (See Section 7-4.1 of Economides and Martin 2007.) The typical foams used for fracturing applications contain water gelled with guar and foamed with nitrogen or carbon dioxide to between 65 and 75% quality.

The liquid phase may be reduced even further. Viscoelastic surfactant-enhanced elasticity of the liquid phase can facilitate the fracturing application of foams with gas qualities less than 90% (Brannon et al. 2009). Viscoelastic surfactant (VES) foams are particularly well suited for treating ultra-low permeability reservoirs because they minimize both the interfacial tension and the amount of water used in the fracturing fluid. This significantly reduces the permanent retention of water and the amount of water trapped in the near-wellbore region that would impair the ability of gas to flow (Gupta 2009).

VES fluid systems are polymer-free fracturing fluids that use surfactants in combination with inorganic salts or other surfactants to form interacting micelles in water, resulting not only in increased viscosity but also elasticity. These fluids provide exceptionally high viscosity under the low-shear conditions required for proppant transport. They are not wall-building and provide excellent regained fracture conductivity and cleanup characteristics. VES fluids do not require any biocides, because they do not contain any biopolymers. Clay control additives are not required due to the use of salts or cationic surfactants that have clay control properties similar to KCl substitutes. Having inherently low surface and interfacial tension, VES fluids do not require additional flowback surfactants.

Fluids based on liquid CO_2 could be a viable alternative to conventional water-based fluids in water-sensitive formations. Several authors have described the unique nature of liquid CO_2 and liquid CO_2/N_2 mixtures as fracturing fluids (Lillies 1982, Tudor et al. 1994, Mazza 1997, Gupta and Bobier 1998). In these systems, the proppant is placed in the formation without causing damage of any kind and without adding any other carrier fluid, viscosifier, or any other chemicals. The use of a reservoir friendly substance like CO_2 (or inert N_2) offers unique advantages through the elimination of capillary fluid retention and clay swelling (Mazza 1997).

Phase trapping due to retention of water pumped into low-permeability formations may result in productivity impairment, particularly in reservoirs where sub-irreducible water saturation exists. In these formations, replacing 40% of water phase used in conventional CO_2 foams (emulsions) with methanol can minimize the amount of water, which results in rapid cleanup and improved production results (Gupta et al. 2007). In formations with severe liquid (aqueous and hydrocarbon) phase-trapping problems, non-aqueous methanol may be a solution. The advantages of alcohol-based fluids include, but are not limited to, low freezing point, low surface tension, high water solubility, high vapor pressure, and formation compatibility, although there are several safety concerns when using methanol (low flash point, high vapor density, and flame invisibility). With special precautions, methanol can be safely used in the field (Thompson et al. 1992, and Hernandez et al. 1994).

Water-sensitive formations may require hydrocarbon-based fracturing fluids to reduce the potential damage from the contact with water. Most of the modern oil-based fluids use aluminum phosphate-ester chemistry. Oil-based fracture treatments typically utilize refined oils as base fluid, but crude oil and condensate, as well as other liquid hydrocarbons, may also be used. These oil-based, polymer-free fracturing fluid systems do not work like a conventional water-based crosslink system. There is no base gel viscosity when the gelling agent is added, because it does not react with the base hydrocarbon. Instead, the gelling agent disperses in the hydrocarbon. The second additive, the crosslinker (XL), joins the gelling agent (GA) molecules, trapping the hydrocarbon molecules within the GA-XL matrix and producing viscosity. Because the gelling agent does not react with the base hydrocarbon, it is possible to use the gel with any fluid system in which this product can be dispersed. As a result, the system can be used in a wide variety of hydrocarbon-based fluids (Gupta et al. 2005 and 2009). Modern hydrocarbon-based fluids can be used in applications up to 300°F and they can be foamed with N_2 or CO_2.

One of the most recent additions to the family of unconventional fracturing technologies is liquefied petroleum gas- or propane-based gel systems, as discussed by Loree and Mesher (2007). This patent proposes that LPG can be viscosified and proppant added to the fluid much like conventional fracturing fluid. The application further describes a unique and novel process that safely handles LPG and meters proppant into a gelled LPG stream for fracturing treatments. LPG gases are a mixture of petroleum and natural gases existing in a liquid state at ambient temperatures and moderate pressure (less than 200 psi). Unlike conventional hydrocarbon-based fracturing fluids, the common LPG gases, such as propane and butane, are tightly fractionated products with over 90% purity. There are many advantages in using liquefied petroleum gases for hydraulic fracturing, if it can be done safely. The properties of density, viscosity, and surface tension with complete solubility in formation hydrocarbons are very beneficial. Recovery of the LPG very nearly approaches 100%, cleanup is very rapid (often within 24 hours), phase trapping is virtually eliminated, and LPG properties allow for extended shut-in times without detriment. Additionally, direct flowback to an available pipeline can be readily achieved. The result is

potential cost-effective stimulation with effective fracture length, excellent post-treatment production and the potential zero flare cleanup (Gupta 2009).

17.2.1.6 Guide to Fracturing Fluid Selection

When selecting a fracturing fluid, a number of factors have to be considered: compatibility with the reservoir mineralogy and reservoir fluids (as discussed previously), stress regime, rock mechanical properties, reservoir pressure, completion type (i.e., openhole or cased hole, and casing and tubing and liner diameters, number of clusters), etc. All of the above need to be taken into account when designing a hydraulic fracture treatment to achieve the desired fracture geometry and conductivity. Cost, logistics, environmental compliance, and safety requirements are also key considerations when planning a successful fracture treatment. Logistics and efficiency of hydraulic fracturing operations are covered in detail later in this chapter.

Reservoir mineralogy plays a significant role in fracturing fluid selection. Clay swelling and dispersion could be a concern in clay-rich formations when water-based fluids are used. Quartz-rich and calcite-rich shales with 30% clay content or less will show negligible fluid interaction. Data indicates that there is a certain clay content threshold somewhere between 30% and 62% at which fluid interaction begins to negatively affect fracture conductivity (Pedlow and Sharma 2014). To mitigate the potential formation damage due to the contact with water-based fluids, potassium chloride, calcium chloride, or ammonium chloride salts could be used.

When stimulating unconventional reservoirs with extremely low permeability, it is critical that a non-damaging fracturing fluid is used. Many reservoirs can be described as "water sensitive," even when expandable clays are not present in the reservoir due to relative permeability reductions caused by capillary imbibition of aqueous treatment fluids. This imbibition effect, also known as aqueous phase trapping, has been noted in both oil and gas reservoirs, and has been observed as a particularly severe problem in reservoirs where sub-irreducible water saturation exists (Bennion et al. 1994).

To address the phase-trapping issues associated with fracture treatment water retention in low-permeability reservoirs, water-based fluids could be replaced with non-aqueous fluids such as methanol-, oil-, or gas-based fracturing fluid systems. Energizing stimulation fluids with gases to "pressure charge" the near-wellbore area can enhance formation cleanup following the treatment. To both reduce the amount of water in the treatment and pressure charge the reservoir, foamed fluids may be used. When using water-based fluids, surfactants may enhance well cleanup by lowering the interfacial tension between water and gas. Adding methanol to water-based treatment fluids may also be beneficial to reduce water content, lower interfacial tension, and to enhance the evaporation of the water-based filtrate during reservoir cleanup.

The methodology for fracturing fluid selection has been described by many authors (Holditch et al. 1993, Xiong and Holditch 1995, Xiong et al. 1996, and Economides and Martin, 2007); however, the selection of fracturing fluid for a particular application is still as much an art as it is science. Fracturing fluid selection based on laboratory-generated data has been detailed by Devine (2005). This procedure utilizes mineralogical evaluation using x-ray diffraction analysis and scanning electronic microscopy of the formation core to understand potential sensitivities of the formation material to fracturing fluids. Other testing methods include immersion, capillary suction time, and core flow analysis. However, unconventional reservoirs' core testing procedures may differ from the "conventional" core testing, which is covered in detail in Chapters 8 and Chapter 10 of this publication. Detailed fluid selection criteria for identifying the right fracturing fluid for gas wells are presented in Chapter 7 of Economides and Martin (2007). General guidelines for fluid selection, with distinctions made between oil and gas wells, are also presented in Chapter 10 of Economides and Nolte (2000).

A general belief that oil wells require more conductivity than gas wells is due to the fact that oil is less mobile than gas. Hydrocarbon mobility plays a key role in the productivity of a particular reservoir rock and pore fluid system. It can also affect stimulation design—multiphase oil production requires significantly greater fracture conductivity than what is accepted for single-phase gas production (El Shaari et al. 2011).

Although slickwater provides very poor proppant transport, with high pumping rates, substantial fluid volumes, adequate proppant selection, and suitable pumping schedules, slickwater treatments may enhance gas production better than crosslinked fluids for a particular reservoir. Slickwater treatments appear to be more successful in hard brittle rock with low horizontal stress anisotropy. Hybrid or crosslinked types of treatments may be considered for oil wells to provide better fracture conductivity.

The main purpose of unconventional fracture stimulation is to increase the reservoir contact area; therefore, the fracture

Table 17.1—Suggested treatment types for dry gas, wet gas, and oil-bearing unconventional formations.

	PNP	BACS	CTACS	
Fracture Fluid Type	Formation	Pump Rate	Conductivity	US Play Application
Slickwater/Linear Gel	Dry Gas or Low Liquid	High Rates 100+ bpm	Infinite to Gas	Barnett, Marcellus, Fayetteville
Hybrid	Gas Condensate	60-to-80 bpm	Moderate Conductivity Fracture	Eagle Ford, Utica

complexity of the hydraulic stimulation is highly desirable. The created SRV (see Mayerhofer et al. 2010) is affected by fracture spacing, fluid volume, proppant volume, pumping rate, and fluid viscosity. The breakdown of the shale and the created fracture complexity are greatly dependent on the flow behavior of fracture fluids just before the fracture initiation. Gomaa et al. (2014a) investigated the effect of fracture fluid viscosity on the breakdown pressure of shale. A lower fluid viscosity will result in lower pressure needed to breakdown the shale formation, while a higher fracture fluid viscosity will require a higher pressure to break down the same shale formation. Several authors used a concept of brittleness as a guideline to the fracturing fluid type selection (for example Rickman et al. 2008; and Chong et al. 2010). It is important to note that the fracturing fluid cannot be selected based on rock mechanical properties alone. **Fig. 17.6** shows how the selection of a fracturing fluid changes when moving from a high-permeability, ductile rock to a low-permeability, brittle rock.

The Barnett shale is one of the best examples of a successful application of slickwater fracturing. No two shales are alike (King 2010), and there is no other shale exactly like the Barnet; i.e., with the identical rock properties. Other ultra-low permeability reservoirs require a unique completion and stimulation strategy.

Although slickwater fracturing has proved itself in a number of US shales, there are many cases where slickwater fracturing has not provided sufficient propped flow capacity to develop a gas or oil productive shale. For these cases, a hybrid fluid using a slickwater fracturing to open the fissures and a more viscous fluid to place the main body of the proppant may be warranted (King 2010).

Proper selection of the fracturing fluids is very important for the successful hydraulic fracture stimulation treatment. There is a wide variety of fracturing fluids, and the optimum one must be chosen depending on the shale reservoir type, i.e., dry gas, wet gas, or oil. **Table 17.1** compares suggested fracture treatment types for dry gas, wet gas, and oil. The industry continues to optimize fracturing fluids, improving the performance of the fluids and addressing environmental concerns.

17.2.2 Fracture Conductivity and Proppant Selection

As described previously, the objective of the hydraulic fracture treatment is to increase the production rates and improve the ultimate recovery by creating a conductive flow path from the reservoir into the wellbore. To maximize production in unconventional reservoirs, a large surface area of the stimulated reservoir is required. Reservoir contact is achieved by creating multiple fractures with an interconnected fracture network of adequate conductivity that improves the flow of hydrocarbons into the well. Conductivity or the fracture flow capacity is defined as the product of proppant permeability in the fracture and the average propped fracture width ($k_f w$). It determines how easily the fluid moves through a fracture. The fracture conductivity is usually reported in millidarcy feet (md-ft.) and is a key design parameter.

Many fracture optimization "rules of thumb" suggest that the required conductivity of a fracture can be optimized by simply knowing the reservoir permeability and the fracture half-length—for instance trying to reach certain dimensionless fracture conductivity (C_{fD}), which represents the contrast between the flow capacity of the fracture and the formation deliverability, and is defined as:

$$C_{fD} = \frac{k_f \overline{w}}{x_f k} \qquad \text{(Eq. 17.1)}$$

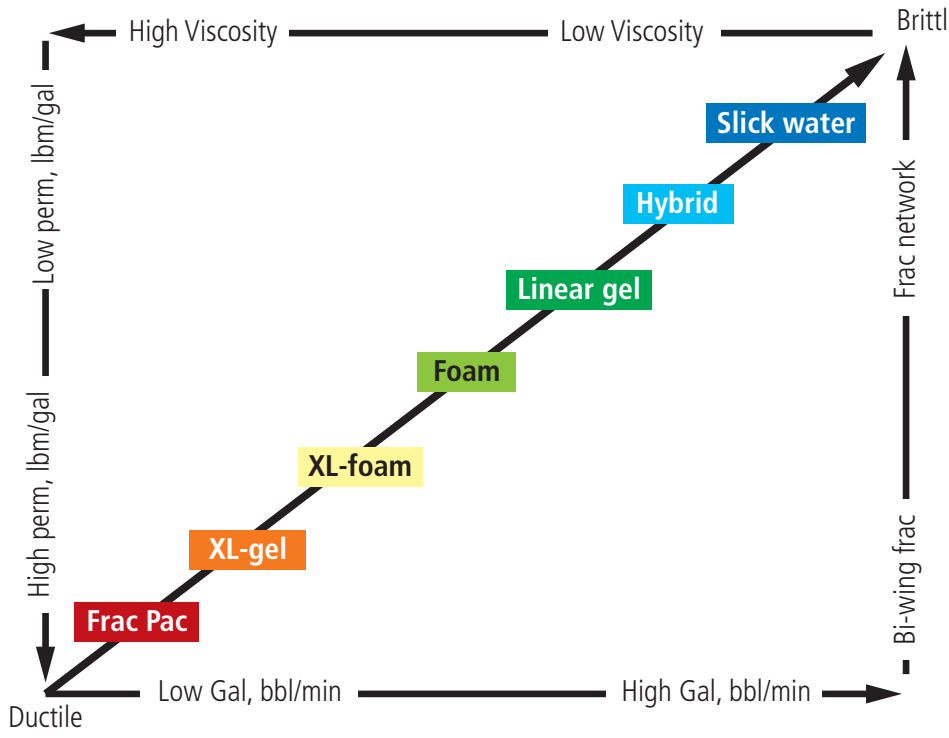

Fig. 17.6—Relationship between fluid type and rock mechanical properties. (Chong et al. 2010.)

where k is the formation permeability, kf is the fracture or proppant permeability, w is the average propped fracture width, and x_f is the fracture half-length.

This approach may not always apply in horizontal wells, as it does not consider the intersection between the wellbore and the fracture and the associated flow convergence (Warpinski et al. 2008). Dedurin et al. (2006) and Besler et al. (2007) have demonstrated that transverse fractures have entirely different conductivity requirements compared to longitudinal fractures. Several authors, (especially Mukherjee and Economides, 1991, Vincent, 2009, and Shah et al., 2010) discuss the need for higher conductivity due to inadequate contact between the transverse fracture and the horizontal wellbore.

The concept of dimensionless fracture conductivity has been used since the 1950s. Prats (1961) and McGuire and Sikora (1960) have developed correlations using the C_{fD} concept to optimize the fracture stimulation design. These methodologies balance the fracture half-length and drainage area with the fracture conductivity. These methods are valid for steady or pseudo-steady state flow in oil wells. In the 1970s, work focused on the nature of the transient-flow period, which is much more significant in lower-permeability gas reservoirs. Cinco-Ley and Samaniego (1981) showed that to maximize the transient production rate (which is higher than the steady-state flow as analyzed by Prats), it is typically necessary to have even higher dimensionless fracture conductivity (Pearson 2001). The dimensionless fracture conductivity concept is also used in the Unified Fracture Design approach, introduced in 2002 (Economides et al. 2002). Due to the assumptions of simple planar fractures, consistent flow regimes within the reservoir and the fracture, hydraulic continuity throughout the fracture, these analytical tools have their limitations when designing a fracture treatment in unconventional reservoirs. C_{fD} calculation is quite challenging especially in unconventional reservoirs due to the extremely low reservoir permeability (which is difficult to estimate) and the complex fracture geometry. While C_{fD} is a widely used tool for fracture design optimization, a realistic conductivity must be used for C_{fD} calculations.

Proppants are evaluated according to the standard testing procedures ISO 13503-2/API Recommended Practice 19C for crush test and ISO 13503-5/API RP 19 (International Standards Organization 2006a and 2006b) for long-term conductivity. These proppant tests are not designed to account for multiphase flow, non-darcy effects, gel damage, proppant embedment, long-term proppant degradation, fines migration and plugging, flowback of proppant out of the fracture, etc.

Thus all the advertised proppant conductivity data should be modified for the above-mentioned effects. In addition, most production models and published conductivity data presume that fractures are linear, planar, of uniform width, have smooth fracture faces, and are not damaged by gel (Warpinski et al. 2008). However, more realistic testing conducted on narrower fractures subjected to realistic flow rates of liquid and gas subjected to cyclic stress and gel damage may show 50 to 100 times higher pressure losses. Fracture conductivity may be reduced by over 90% when accounting for realistic conditions, as reported by Palisch et al. (2007).

The need for fracture conductivity in micro- and nanodarcy rock is often regarded as unimportant, and instead fracture designs focus on increasing reservoir contact volume. However contacted reservoir volume (CRV) or stimulated reservoir volume (SRV) may not necessarily equate to better stimulation if the fracture conductivity that transmits the fluids to the wellbore is inadequate (Meyer et al. 2013). Even in extremely low-permeability reservoirs, increasing the conductivity of the fracture network can have a significant effect on well productivity and estimated ultimate recovery or EUR (Cipolla et al. 2012).

The fracture conductivity depends on several factors, including, but not limited to, the proppant type, size, shape, and concentration, as well as the properties of the fracturing fluid.

The following section of this chapter discusses the proppant types used in unconventional stimulation today as well as the proppant selection criteria. The main categories of proppants used today are natural sand of various origins, resin-coated sand, and ceramic proppants.

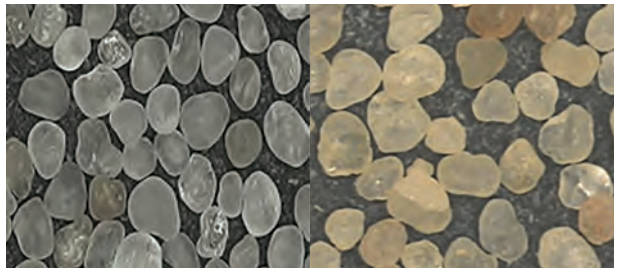

Fig. 17.7—Left picture shows Ottawa "white" sand grains. Right picture shows Brady "brown" sand grains. (From Economides and Martin 2007.)

17.2.2.1 Natural Sand

Naturally occurring sand was first introduced as proppant in the late 1940s and is still the most widely used type of proppant today, primarily due to low cost and availability. After mining, natural sand is processed to remove fines and traces of minerals, clays, and other organic matter. It is washed, dried, and screened to obtain the required mesh size. Sand has the specific gravity of 2.65, which enables good suspension in fracturing fluids. Ottawa ("white") and Brady ("brown") sands are the predominant types of sands used in hydraulic fracturing today (see **Fig. 17.7**). Ottawa sand is found mostly in the sandstone formations spanning north-to-south from Minnesota to Missouri and east-to-west from Illinois into Nebraska and South Dakota. White sands are mined primarily from St. Peter (near Ottawa, Illinois), the Jordan (South Central Minnesota), and the Wonewoc (Wisconsin) sand deposits. Ottawa sand also known as "Northern," "White," or "Jordan" sand is the highest-quality natural fracturing sand used in the oil and gas industry. It has superior conductivity and crush resistance compared to other fracturing sands due to its monocrystalline structure, roundness, sphericity, and purity. White silica sand is recommended for formations with net closure stresses up to 6,000 psi. "Northern White" sand is 99.8% high-purity quartz, it is chemically inert and has a high melting point.

Brown sands have been used since the late 1950s, when "brown" sand quarries were opened in the Hickory sandstone formation near Brady, Texas. Brady sand contains impurities, contributing to its color. These sands have a higher percentage of coarser grain sizes than other fracturing sands. Brown sands have polycrystalline structure, and each grain is composed of multiple crystals bonded together. The existence of cleavage planes within each grain results in greater proppant crush and reduced strength properties (See Chapter 7 of Economides and Martin 2007). Brown sands have more irregular shapes and are not as round and spherical as white sand. Brady sands are suitable for the shallower wells with closure stresses below 5,000 psi.

17.2.2.2 Artificial Proppants

Although natural sand is widely used in unconventional hydraulic fracturing, resin-coated sands or more spherical and stronger proppants such as ceramic materials could improve overall fracture conductivity resulting in higher production rates and increased ultimate recovery. More challenging environments in deeper and hotter wells require more advanced proppant technologies. As an alternative to naturally occurring sands for these challenging reservoir conditions, the industry offers man-made proppants such as resin-coated and ceramic proppants. The various intermediate- and high-strength synthetic proppants are briefly discussed as follows.

Ceramic proppants are generally classified as lightweight, intermediate density, and sintered bauxite. Ceramic proppants are derived from sintered aluminosilicates such as bauxite.

17.2.2.3 High-Strength Sintered Bauxite

High-strength sintered bauxite proppants are usually made from bauxite and kaolin ore by crushing the ore, compacting it into spherical particles and subsequently firing in a furnace at very high temperatures. Due to these manufacturing processes, sintered bauxite proppants maintain their integrity under the harshest downhole conditions. They offer excellent roundness and sphericity. These proppants contain corundum, one of the hardest materials known, and offer the greatest strength available for deep wells with high stress (greater than 12,000 psi) and temperature environments, providing high fracture conductivity. Sintered bauxite proppants are available in sizes ranging from 12- to 70-mesh with a specific gravity of 3.4 and greater (see **Fig. 17.8**).

Due to its relatively high cost, sintered bauxite proppants are generally limited to wells with high closure stresses in excess of 12,000 psi. New technologies are being developed to reduce the cost and address the proppant transport issues due to high density of sintered bauxite proppants. Alternative raw materials derived from industrial waste streams such as basalt-based mine tailings and drill cuttings from shale gas wells, recycled glass cullet, fly ash, and metallurgical slag could potentially be used to manufacture proppants with properties and performance rivaling those of state-of-the-art sintered bauxite proppants (Hellman et al. 2014).

Strength is crucial to the performance of any proppant. The current standard for extreme conditions (high temperature and high stress) is sintered bauxite, which is suitable for stresses up to 15,000 psi.

Contemporary advanced technologies offer high performance ceramic proppants with superior characteristics significantly exceeding the compressive strength and durability of the typical bauxite-based proppants at the highest closure stresses and providing the conductivity levels nearly twice as high as conductivity exhibited by conventional high-strength bauxite proppants at 20,000 psi (Palish et al. 2014).

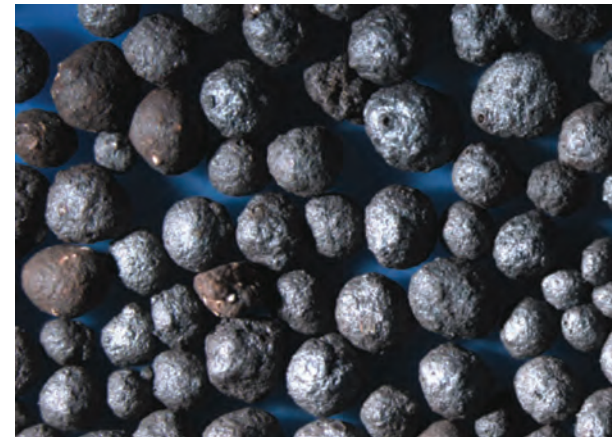

Fig. 17.8—Sintered bauxite grains. (Photo courtesy of Sintex Proppants.)

17.2.2.4 Intermediate Strength Proppants

Intermediate strength proppants (ISP) are also manufactured from high alumina ores. These alumina oxide and silicate fused ceramic proppants have a specific gravity ranging from 2.9 to 3.3. The variance in specific gravity is related to the composition of raw materials used by different manufactures of the proppant. Due to their lower cost, lower density, and comparable strength and conductivity in moderate depth, high-stress wells, intermediate strength proppants provide a cost-effective alternative to bauxite proppants. ISPs are also less abrasive to the fracturing equipment and surface lines. The density of ISPs is lower than bauxites, which improves the proppant transport and reduces the risk of screen-outs, while providing excellent resistance to high closure pressures up to 14,000 psi. Intermediate strength proppants are commercially available in sizes ranging from 16- to 70-mesh. Similar to bauxites, ISPs exhibit very good roundness and sphericity (**Fig. 17.9**, left).

17.2.2.5 Lightweight Ceramic (LWC) Proppants

Proppant transport challenges in low-viscosity fluids are well known. Low-density proppants reduce the settling rate resulting in proppant transport further into the fracture. Alumina silicate lightweight ceramic proppants have a specific gravity of approximately 2.6 to 2.8. While LWC proppants are not as strong as intermediate strength proppants and high-strength bauxites, they provide much higher conductivity than high-quality natural sand due to improved strength, greater sphericity, and more uniform size distribution. LWC proppants are suitable for applications with the closure stress range above sand stress limitations

(from 6,000 to 10,000 psi). Due to superior conductivity over natural sand, LWC proppants could also be used at lower stresses but in applications where the highest possible conductivity is required, such as high-performance wells exhibiting non-darcy effects and/or multiphase flow characteristics within the proppant pack. LWC proppants are commercially available in sizes ranging from 12- to 70-mesh. (See Fig. 17.9, right hand side.)

17.2.2.6 Ultra-Lightweight Ceramic

Ultra-lightweight ceramic (ULWC) proppants have a specific gravity ranging from 2.2 to 2.7, which makes them ideal for slickwater fracturing applications. Having similar or lower density than sand, but providing significantly higher flow capacity than similar sizes of sand, ULWC proppants offer a great combination of proppant transport and conductivity. ULWC proppants have also significantly better thermal stability compared to sand and/or resin-coated sand. ULWC proppants are available in sizes ranging from 16- to 80-mesh.

17.2.2.7 Resin-Coated Sand and Proppant

As covered previously, silica sand has limited application due to its low strength properties. In deeper wells with closure stresses exceeding 6,000 psi, stronger materials than silica, such as resin-coated sands and ceramic proppants are required. Resin-coated proppants (RCP) have been used for several decades. The primary purpose of resin coating is twofold: to improve the performance of the core proppant at higher stress levels by encapsulating each grain, which increases the stress tolerance and maintains particle integrity, and also to mitigate proppant flowback by adhering the proppant grains to each other. The resin improves the crush resistance by distributing the stress load over a larger area of the proppant grain, reducing the point loading. Furthermore, when proppant grains are crushed, the resin coating serves to encapsulate the fines and fragmented portions, preventing small particles from migrating and plugging the proppant pack pore throats and flow channels.

Fig. 17.9—Left side shows ISP proppant grains. (Photo courtesy of Saint Gobain.) Right side shows LWC proppant grains. (Photo courtesy of Carbo Ceramics Inc.)

Resin also reduces the angularity of the sand grains, improving the conductivity. Resin coating technologies continue to evolve and improve the strength of proppants, and now resin-coated sands can be used at closure stresses greater than 8,000 psi. In general, there are three types of resin coatings: pre-cured, partially cured, and curable. The resin coating is usually at least partially cured during the manufacturing process to produce a non-melting, chemically inert surface film. Both curable and fully pre-cured resin coatings are available for and are widely used in fracturing treatments. Resin coatings are available for most proppant types (sand to bauxite) of varying size and strength to fit a variety of downhole conditions.

Pre-cured or tempered resin-coated proppant is designed to increase the strength of individual proppant grains. The likelihood of the proppant failure is reduced due to a more even point stress distribution over the thin deformable coating. The increased surface area of the grain-to grain contact reduces fines generation, and the resin coating encapsulates the generated fines, preventing fines migration and conductivity reduction. The pre-cured coating strengthens the uncoated proppant and encapsulates fines, but it does not have the ability to prevent proppant flowback. The pre-cured resin coated proppant grains do not consolidate in the proppant pack, therefore a partially cured or curable resin coating is required to prevent flowback. (See **Fig. 17.10**.)

Partially cured and curable resin-coated proppants are typically used in producing zones that otherwise tend to flow back proppant during production operations. Due to the curable coating, the proppant grains bond together after they are placed in the formation. The consolidated pack prevents the proppant from flowing back out of the fracture. These proppants provide greater reduction in fines generation than pre-cured proppants due to a greater surface area of grain-to-grain contact. Multiple grains bonding together create a network of deformable surfaces, reducing the stress on individual proppant grains. This network of bonded particles also prevents the fines from migrating through the proppant pack and reducing the flow. Curable resin coating on proppant reduces embedment by redistributing stresses on the pack within the fracture (Penny 1987). Proppant embedment can reduce the fracture width, which leads to a lower fracture capacity especially in soft shale formations. Terracina et al. (2010) showed that the embedment profile of curable resin-coated sand (CRCS) is

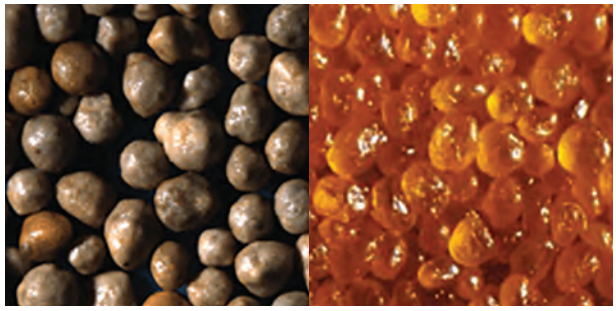

Fig. 17.10—Left side is pre-cured resin-coated proppant. Right side is curable resin-coated proppant. (Both photos courtesy of Santrol.)

noticeably different compared to uncoated sand and ceramic proppant due to bonded grains distributing the load along the core face, resulting in much less embedment. Curable resin-coated proppants are typically pumped at the end of the treatment, often referred to as a resin-coated "tail-in" stage. After the treatment, the well is typically shut in for a time to allow the resin to bond proppant particles and to cure into a consolidated, permeable pack. Certain resin coatings are designed for the specific downhole conditions such as confining stress and temperature. Curable proppants only require temperature to start the bonding process, while partially cured proppants require the specific temperature and closure stress. The temperature applications range from as low as 100°F (special chemical activators may be used for low temperature applications) to temperatures above 350°F. (See Fig. 17.10.)

17.2.2.8 Neutral Density Proppants

High-rate, large-volume, low-proppant concentration slickwater fracturing treatments have become quite common in many unconventional reservoirs. The inability of slickwater to efficiently transport conventional proppants inside the fracture is well known and documented (e.g., King 2012). A potential solution to this problem can be the use of neutral density proppants, which can be easily transported by low-viscosity fluid such as slickwater.

The settling rate of proppant in the fracturing fluid is strongly influenced by the specific gravity of the proppant. As the specific gravity of the proppant approaches that of the fluid, a nearly neutral buoyancy condition is approached and proppant-settling velocity nears zero. Ultra-lightweight (ULW) proppants were commercially introduced in 2004, exhibiting both lower specific gravities and the requisite mechanical properties to successfully function as a fracturing proppant at reservoir temperature and stress conditions (Brannon et al. 2002, Warpinski et al. 2008, Rickards et al. 2003, Wood et al. 2003). The ULW proppants have been shown to provide sufficient strength for application in reservoirs with closure pressures up to 8,000 psi and BHSTs exceeding 275°F.

Walnut shells, hollow glass spheres, low-density plastics, porous ceramics and other materials were initially evaluated. The first generation of ULW proppants were comprised of resin-modified walnut hulls with an apparent specific gravity of 1.25, which is less than half that of sand (2.65). Subsequent development has yielded additional ULW proppants with specific gravities of 2.02 and 1.50. The most recently introduced ULW proppant is a heat-treated, thermoset nano-composite having an apparent specific gravity of 1.05 (see **Fig. 17.11**). Transport of this proppant in fracture fluid is extremely efficient, and inherently slow settling rates provide greater effective fracture length and optimal fracture height coverage compared to heavier proppants. This type of proppant has near-perfectly spherical particles with smooth surface. Due to the low specific gravity, ULW proppants provide a greater pack volume per unit of mass compared to heavier proppants.

When low-viscosity fluid is used, smaller sizes of conventional proppants are pumped to improve the proppant transport. Employment of a smaller sized conventional proppant is not nearly as effective in reducing proppant-settling rate as reducing the particle specific gravity (Brannon and Starks 2009). The low specific gravity of ULW proppants allows effective transport of larger particle sizes, providing greater fracture conductivity. The minimized proppant settling afforded by the ULW proppants enables effective placement of proppant partial monolayers (PML).

The partial monolayer theory has been discussed by many authors, such as Howard and Fast 1970, Brannon et al. 2004, and others. The concept of partial monolayers suggests that

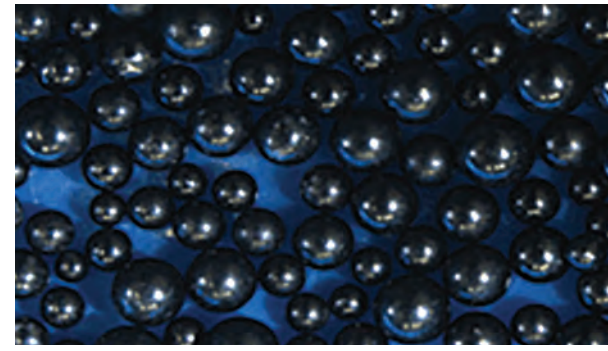

Fig. 17.11—Neutral density ULW proppant, made from a thermoplastic nanocomposite.

an areal proppant concentration below that of a full proppant monolayer may yield conductivity much higher than that of not only a full monolayer, but of even proppant packs comprised of several layers (Darin and Huitt 1959). A properly placed partial monolayer exhibits conductivity equivalent to packed fractures having greater than ten proppant layers (Brannon and Starks, 2009). ULW proppants are available in sizes ranging from 14- to 80-mesh.

The industry continues to develop new proppant technologies. A new addition to the family of "lightweight" proppants is self-suspending proppant. The concept is based on encapsulating conventional proppant particles with a thin layer of high-molecular-weight hydrogel polymer, which in contact with water expands and forms a space-filling cushion around each granule (Mahoney et al. 2013).

17.2.2.9 Multiphase and Non-Darcy Flow Effects

Non-darcy flow (sometimes inaccurately referred to as turbulence), which is not accounted for by Darcy's law, may affect the production rates of oil and gas wells quite significantly. The reservoir fluid travels along the tortuous flow path, such as the fracture network, at variable velocities, accelerating and decelerating at the turns. As the velocity of the reservoir fluids increases along the fracture, a large amount of energy is lost due to inertial flow effects—changes in direction. The inertial effects in a propped hydraulic fracture (for a single phase) are influenced by the proppant size distribution, surface roughness, proppant roundness and angularity, permeability and porosity of the proppant pack, etc. Non-darcy flow becomes more pronounced in the near-wellbore area particularly at the intersection of the transverse fracture and the wellbore. The relation between pressure gradient and velocity is described by Forchheimer's equation (Forchheimer 1901) (**Eq. 17.2**) for a single-phase fluid. The equation combines the Darcy pressure drop (viscosity- and permeability-dominated) and non-darcy pressure drop (which is dominated by the velocity squared term). In addition, the limited communication area between the transverse fracture and the wellbore generates an additional pressure drop and a choking effect for all transversely fractured horizontal wells. This extra pressure drop contributes to the effective fracture conductivity reduction and can be estimated to reach the level of 50 to 85% (Palisch et al. 2007). Non-darcy flow behavior in tight gas and tight oil formations exists even at low production rates (Penny and Jin 1995; Zhang and Yang 2014).

$$\Delta p/L = \mu v/k_f + \beta \rho v^2 \qquad \textbf{(Eq. 17.2)}$$

Multiphase flow is another phenomenon that negatively affects the production rates. Alteration of fluid saturation and changes in relative permeability contribute to multiphase pressure drop, but most of the multiphase pressure losses are caused by the phase interaction between the fluids (i.e., gas-water, gas-condensate, etc.). Due to mobility differences, reservoir fluids move at drastically different velocities, interfering with the flow of each other. This is particularly evident in gas-liquid flow (Palisch et al. 2007). Multiphase non-darcy flow and its effect on well productivity and impairment has been widely discussed in the literature (Wang and Mohanty 1999; Barree et al. 2003; Olson et al. 2004; Miskimins et al. 2005; Mohan et al. 2006; Barree and Conway 2009). The combination of high-velocity and multiphase flow has dramatic effect on the productivity in hydraulically fractured wells (Cooke 1973; Geertsma 1974; Holditch and Morse 1976; Martins et al.1990; Vincent et al. 1999, and many others). When designing a hydraulic fracture treatment, non-darcy and multiphase flow are too important to be disregarded. Proppant size, type, porosity, and permeability are critical for non-darcy flow conditions and have to be taken into account to address these effects and provide an optimum stimulation.

17.2.2.10 Fracturing Fluid Damage

In addition to several mechanisms of fracture conductivity reduction identified by the industry, such as proppant crushing, fines migration, stress cycling, non-darcy flow, multiphase flow and viscous fingering (caused by a potential contrast in post-treatment mobility between the viscous and nonviscous "phases" during cleanup), there are several conductivity reducing factors associated with the use of fracturing fluids. These factors include: unbroken gel residue, filter cake residue on the fracture face, proppant embedment due to fluid-induced formation softening, phase trapping and proppant diagenesis. As described previously, these cumulative effects can reduce the effective flow capacity by over 90% as compared to the advertised measured conductivity data. In previous sections, the possible damage mechanisms related to the use of fracturing fluids are addressed and guidance is provided on the optimum fracturing fluid selection.

Polymer damage could be detrimental to the proppant pack and the reservoir, especially if it is an unconventional reservoir with extremely low permeability. In recent years the industry has developed advanced low polymer and polymer-free fracturing fluid systems as well as the effective breaker chemistry to minimize the polymer residue and maximize productivity. Breaker performance and non-damaging fluid

properties are extremely important for effective fracture cleanup and improved well productivity.

Increased fluid viscosity improves proppant transport, however the use of polymer-based fluids may damage the formation permeability and reduce the proppant pack conductivity to some extent (due to the fluid/filtrate invasion into the formation, filter cake forming, unbroken gel, etc.). Palisch et al. (2007) defined several gel damage mechanisms including distributed residual fracture damage, loss of width due to filter cake, and loss of effective length due to static gel at the tip. Gel plugging at the tip of the fracture is caused by insufficient flow velocity required to remove both broken and unbroken gel. Effective gel cleanup in the fracture depends not only on the fracturing fluid breaker mechanism, but also on the proppant type, size, and concentration. Laboratory data consistently demonstrates more efficient cleanup with higher proppant pack conductivity (larger proppant particle sizes and higher proppant concentrations), e.g., Stim-Lab 1986–2007; Palisch et al. 2007.

Gel damage can be quite detrimental to fracture conductivity in moderate- to high-permeability formations. In naturally fractured formations, gel damage to the natural fractures may be even more serious (Warpinski et al. 1990, Gall et al. 1988). In ultra-low permeability reservoirs it is believed that the absolute permeability damage by invasion of polymeric fracturing fluids into the matrix of the reservoir does not happen due to the large size of the polymer molecules compared to the size of the pore-throats in this type of reservoir. Due to extremely low leak-off rate (which is primarily controlled by the reservoir permeability) of the fracturing fluid filtrate, a filter cake does not form. However, polymer residue within the induced and natural fractures may result in severe damage (Ahmed, et al. 1979). As per Wang et al. (2009), the gel strength of the remaining fracturing fluid in the fracture is the most important factor that reduces the fracture fluid cleanup and gas recovery.

Another mechanism that might cause slow cleanup is phase trapping. Water blocking, resulting in productivity impairment in "tight" oil and gas reservoirs, has been recognized by many authors (Holditch 1979; Kamath and Laroche 2003; Mahadevan and Sharma 2005; and others). As covered earlier in this section, phase trapping due to the retention of water-based fracturing fluids in low-permeability reservoirs, particularly in oil-wet formations with sub-irreducible water saturation, may cause a reduction in productivity. Capillary imbibition is the primary hydrocarbon recovery mechanism in ultra-low permeability naturally fractured reservoirs and an effective matrix-fracture interaction is required for hydrocarbon extraction (Babadagli et al. 1999). Wettability affects flow behavior and, when altered, imbibition mobilizes oil because of capillary pressure changes from negative to positive (Wang et al. 2012). The alteration of rock wettability to water-wet and/or the reduction in interfacial tension by means of surfactants added to fracturing fluids is widely discussed in the literature (Chen et al. 2001; Shuler et al. 2011; Sharma and Mohanty 2013; and others). Aladasani et al. (2014) suggested that there might be a trade-off between the dominance of viscous forces and the significance of decreasing capillary pressures. A balance between wettability alteration and interfacial tension reduction should be reached when designing a fracturing fluid for unconventional liquid-rich reservoirs. When the surfactants change wettability, it is suggested not to decrease the capillary pressure excessively in order to prevent imbibed fluids from draining from the matrix (Alvarez et al. 2014).

Bertoncello et al. (2014) identifies two different processes of water displacement. The pressure differential during the hydraulic fracture treatment forces water into the oil-wet pore network. Subsequently, the water naturally imbibes into the water-wet pore network by capillary action. As a water block remediation, either immediate flowback or an extended shut-in may be recommended. Even though early cleanup and immediate fluid recovery are beneficial for water imbibition prevention, they may be impractical in horizontal multistage completions due to the period of time required to perform multiple fracture treatments. Also the fracture closure time should be considered when flowing back the fracturing fluid. Flowback procedures and recommendations are discussed later in the chapter.

The exposure of some clay-rich shales to fracturing fluids can cause significant softening. Clay swelling in these "soft" rocks leads to the loss of fracture width due to proppant embedment and formation spalling. The subsequent reduced width results in lower fracture conductivity and also leads to non-darcy pressure losses due to the increased fluid flow velocity. The difference between the reported lab conductivity data measured under laminar flow conditions and realistic field data is well documented (Barree et al. 2003; Schubarth et al. 2006; and many others).

Bazin et al. (2010) demonstrated that a clay-damaging water-based fluid could cause irreversible absolute permeability reduction by a factor of four in low-permeability illitic sandstone core samples, by the illite and montmorillonite clays swelling and by kaolinite clay migration. The formation

softening effect can be evaluated by a Brinell hardness test and a proppant embedment test. The combination of the formations' mineralogy, along with the temperature, proppant, fracturing fluid, and formation water, can potentially decrease the Brinell hardness and proppant "tensile strength" (LaFollette and Carman 2010).

The fracturing fluid should be "compatible" with the reservoir and proppant (especially resin-coated proppant) and carefully tailored to take into account the potential gel damage, phase trapping, rock softening effects, as well as proppant diagenesis, to ensure long-term effective fracture conductivity.

17.2.2.11 Guide to Proppant Selection

Unconventional fracturing technologies are developing rapidly, however there is still a significant amount of uncertainty as to the effect of different stimulation processes (pumping techniques, fluids, additives, proppants) on the well productivity. Due to a large number of variables, such as reservoir quality, lateral placement, completion techniques, etc., simple "rules-of-thumb" for shale fracturing probably do not exist, except for some generally accepted basic engineering principles.

Hydraulic fracturing is a large component of the overall well construction and completion cost. Many practitioners believe that the key factor in making the development of unconventional reservoirs economic is minimizing upfront cost, including increased drilling and completion efficiency, as well as "factory" fracturing designs with low-end materials and technology. However, a long-term strategy for increasing ultimate recovery may require a more thorough economic analysis, which is a complicated process and should be considered in the context of the block/area/field development. Laboratory data may suggest that one technology is superior over the other, however due to the complexity of the fracturing design process, only fit-for-purpose technologies in combination with the optimum completion and fracturing design will provide the maximum economic benefit.

The success of hydraulic fracture treatments in unconventional reservoirs depends on many factors, and selection of fit-for-purpose proppant is one of the most important ones. In the real world—aside from sound engineering judgment—one of the primary drivers in proppant selection for unconventional reservoirs is availability and cost. Proppant is currently in high demand and quite often the proppant is selected from what is available, rather than what is best suited for a particular application. See **Fig. 17.12** for a closure stress-based guide to proppant selection.

Since the beginning of the "unconventional revolution," which started in the Barnett shale in the late 1990s to early 2000s, multiple experiments with different combinations of fluids and proppants have been performed. Some wells were even treated with slickwater without proppant (see Mayerhofer et al. 1997). The initial production was high, but the decline rate was very rapid. Several authors have discussed hydraulic fracture treatments in unconventional stimulation without proppant (Ehlig-Economides and Economides, 2011). Zhang et al. (2013) demonstrated that the unpropped conductivity of displaced (fracture surfaces are irregular, representing shear displacement of the fracture walls) and aligned fractures (the fracture faces completely match) can be up to one order of magnitude different; however, when proppant is introduced in the fracture, the conductivity of both fracture types becomes similar. This indicates that the proppant pack is the dominant factor that affects conductivity of propped fractures. The shear displacement plays a major role only if the fracture is unpropped. When the pre-existing fissures or fractures are activated during pumping, some of the cementing material may be removed at the moment of fracture initiation and further eroded by the high-velocity slurry. Therefore, even if those natural fractures remain unpropped, they may still have sufficient conductivity to contribute to the overall productivity of the stimulated volume, especially when they are developed in clusters within the fracture network.

As is briefly discussed earlier, fracture conductivity is one of the most critical parameters affecting successful fracture treatment and well performance. Meyer et al. (2013) summarized well-known fracturing "design guidelines" for the optimum fracture performance as a function of fracture length and relative fracture conductivity (McGuire and Sikora 1960; Pratz 1961; Cinco-Ley and Samaniego 1981; Economides et al. 2002, and others) and demonstrates that dimensionless fracture conductivity is one of the key parameters for both traditional and unconventional wells. Many still believe that any hydraulic propped fracture placed in an ultra-low-permeability reservoir will have "infinite" conductivity. It is well documented in the literature that the above assumption is misleading. As has been concluded by the industry, there is a significant difference between the reference conductivity measurements and the actual realistic conductivity. It is now apparent that most fractures either have "finite" conductivity or are "conductivity-limited" (Palisch et al. 2007). Even in the unconventional reservoirs, particularly those that produce liquids or condensate, increasing the fracture conductivity will increase production—the only question is whether it is economic to do so (Palisch et al. 2012).

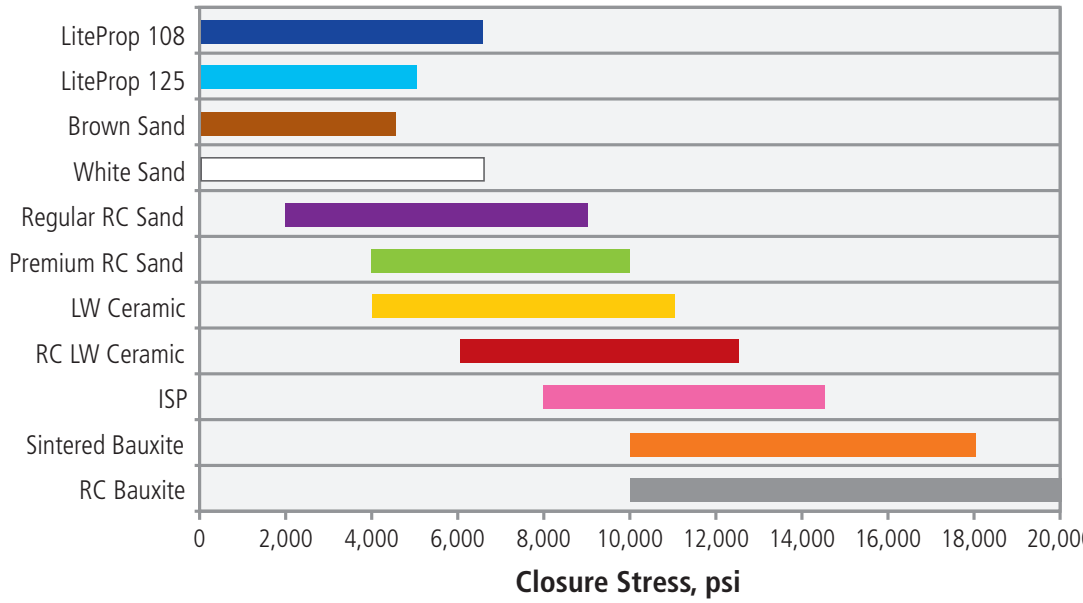

Fig. 17.12—Recommended closure stress ranges for various types of proppants. (Data provided by Stim-Lab 2007.)

Many considerations affect the stimulation design. Proppant can bear a great portion of the total fracture stimulation treatment cost, but it cannot be selected solely based on the price. In general, proppants selection is based on the type, grain size distribution, compressive strength, density, and cost. Unfortunately, in the US proppant (especially sand) is also increasingly selected on the basis of availability.

Although there is a lot of laboratory data and published case histories on different types of proppants, the selection of proppant might not be as simple as it may appear.

Today there are many choices on the market from brown sand, white sand, curable and pre-cured resins, light weight and intermediate weight ceramics, bauxite proppants, etc. More confusion is added with multiple manufacturers. Proppant selection should be based on careful specification, examination, and quality control. As per Vincent and Besler (2013), the industry has seen up to 500% quality and durability variation in the currently offered commercial "top quality white sand," and over 400% variation between "premium ceramics" misleadingly described as interchangeable commodities. There is a lot of debate in the industry, as to whether it is economically feasible to use ceramic proppants instead of sand. It is quite challenging to make a fair comparison due to a great number of variables. In general (with all the parameters being equal, such as proppant volumes, concentrations, fluids, and completion design) field data suggests that ceramic proppants outperform natural sands, although each individual case should be evaluated with regard to the economic benefit.

Conductivity is the main criteria representing proppant performance. As discussed in the sections above, the baseline conductivity does not take into account several "real-life" factors, such as non-darcy flow, multiphase flow, gel damage, fines migration, resistance to cyclic stress, proppant flowback, proppant embedment, etc.

When selecting proppant, there are other important properties that require consideration: crush resistance, temperature and chemical resistance, roundness and sphericity (see **Fig. 17.13**), fluid compatibility, etc. Although all of these factors have to be taken into account, quite often proppant is selected based on the crush test. As discussed by Cutler et al. (1985), conductivity comparisons cannot be made on the basis of crush tests due to variance in crush results associated with method of loading and other variables. Different types of proppants crush differently: sand (quartz crystals) tends to crush in a greater number of fine shards, ceramics cleave or part into fewer larger pieces, resin-coated proppants deform and fail inside the resin capsule and do not generate many fines (Palisch et al. 2010).

The fracturing fluid also impacts proppant selection. As per Stokes' law, proppant settling rate is directly proportional to the density difference between the proppant and fluid, and inversely proportional to the fluid viscosity. It is also proportional to the square of the diameter, which means

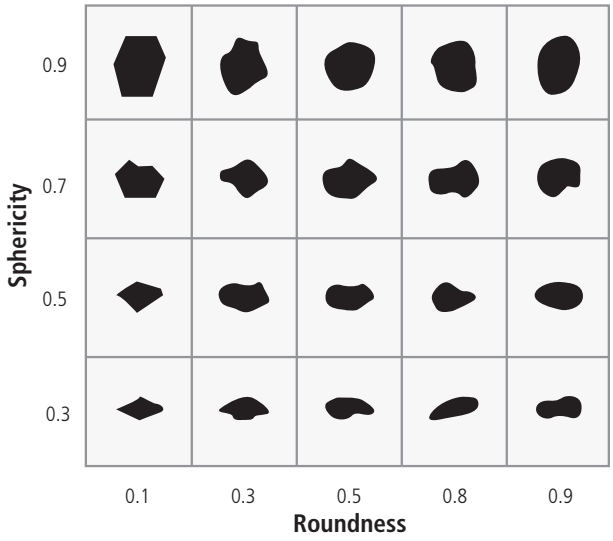

Fig. 17.13—The well-known Krumbein and Sloss roundness and sphericity chart. (From Krumbein and Sloss 1963.) Although the test is somewhat subjective, API Recommended Practice 56 and International Organization for Standardization (ISO) 13503-2, Proppant Crush Test for Hydraulic Fracturing and Gravel-Packing Options recommends roundness and sphericity both to be greater than 0.7 for sand and to be greater than 0.9 for artificial proppants.

that a relatively minor change in grain size can significantly affect the settling rate. Stokes' law describes single-particle settling mechanism in a stagnant liquid medium and has to be corrected for dynamic conditions, nevertheless the basic principles of proppant settling are still valid. Whereas proppant density and diameter determine the proppant-settling rate, the fluid and proppant selection are also interrelated. For example, in ultra-low-permeability dry gas reservoirs, low-viscosity Newtonian fluids such as slickwater are typically used as fracturing fluids. Due to poor proppant transport characteristics of slickwater, lower concentrations and smaller mesh size proppants (100 mesh, 40/70 sand and RCS and 40/80 LWC) are selected to ensure proppant placement further into the fracture. 100-mesh sand is used primarily for maximizing propped length and for blocking natural fissures to increase the density of the fracture network. When designing fracture treatments with low-viscosity fluids and low proppant concentrations, proppant crush and near wellbore flow convergence in transverse fractures should also be considered, suggesting the need for higher near-wellbore conductivity. Low proppant concentrations pumped in low-viscosity fluids result in narrow fracture width. In addition to flow restriction along the narrow fracture, higher proppant crush can further reduce the fracture conductivity; therefore, a balance between proppant size, density, strength, and cost should be considered for long-term fracture performance. The proppant will experience significantly greater stress concentrations and increased crush in narrow fractures, a phenomenon that is not reported in simplified tests (Palish et al. 2010).

Ultra-low-density proppants can be used in partial monolayer fracturing designs to improve conductivity. Ultra-light-weight proppant (ULWP) is much more effectively transported in low-viscosity applications than conventional proppants. Many of these proppants are designed to deform under stress and do not crush as conventional rigid proppant particles. Typically ULWP is used in lower stress environments, at closure stresses up to 7,000 psi, although the technologies are constantly improving. When designing a partial monolayer fracture treatment, several considerations should be given to ULWP selection: crush resistance, concentrated stress on individual proppant particles and embedment. In the reservoirs with high clay content (especially kaolinite), proppant embedment might be an issue. In the event embedment occurs, partial monolayer treatment may not be effective. To address this potential fracture conductivity reduction, higher proppant concentrations and larger proppants may be required.

If treatment design dictates that higher fracture conductivity for the specific reservoir conditions is required and that this conductivity could be achieved by the higher proppant concentration, as well as by larger and stronger/higher-density proppant, then an appropriate fracturing fluid would be required to effectively place the selected proppant in the fracture. Higher-viscosity linear gels provide better proppant suspension properties than slickwater and therefore allow the use of higher proppant concentrations and coarser proppants such as 30/50 and 20/40. Crosslinked and VES fluids provide much more effective proppant transport characteristics and are mostly used to carry higher density, larger mesh size proppants, and higher proppant concentrations in the final treatment stages to improve near-wellbore conductivity. It has been demonstrated that high-conductivity fractures are less affected by multiphase flow and may provide benefits in fracturing past condensate blocks (Vincent 2002). There is a general consensus in the industry that completions benefit from higher near-wellbore conductivity in transverse fractures (Besler et al. 2007; Shah et al. 2010; Vincent 2011; Ehlig-Economides et al. 2012). In general liquid-rich reservoirs require higher fracture conductivity than dry gas reservoirs due to lower oil mobility compared to gas. In these formations higher proppant concentrations and larger proppants, such as 30/50, 20/40, 16/30, and even 12/18, may be used to maximize conductivity.

While there are many ways to increase the fracture conductivity, and all should be considered when designing fracture stimulations, one of the easiest and most common ways is to upgrade the proppant size and/ or type. CARBO Ceramics Inc. developed a "Proppant Conductivity Pyramid" (see **Fig. 17.14**) demonstrating the improvement in conductivity and production with moving up the pyramid. However, these proppant "upgrades" typically increase completion (proppant) cost. Therefore, the decision to increase conductivity must ultimately be an economic decision (Saldungaray and Palisch 2012).

When selecting a proppant based on strength, one should consider the proppant density both from the proppant transport and from the occupied volume perspective. Intermediate density proppant (ISP) with the apparent specific gravity (ASG) 3.1 to 3.4 occupies approximately 20% less volume in the fracture compared to the same mass of sand or LWC proppant with ASG of 2.65 to 2.7; thus, a greater amount of ISP will be required to achieve the same volumetric proppant concentration per unit area in the fracture. Should the high-density bauxite be used versus LWC, the contrast in the propped fracture volume will be even greater up to 33% (Vincent 2009). If the same proppant masses of ISP and LWC are used, and assuming equal fracture height and length, the width of the fracture propped with ISP will be smaller, compromising the fracture conductivity. Pressure losses related to non-darcy effects, potential embedment, and filter cake damage will make the effect of fracture width reduction even more pronounced. Proppant density can also affect the fracturing operations. For example, high-strength high-density sintered bauxite proppants are usually recommended when it is necessary to withstand the highest closure stresses. The high density of these proppants does not only lead to the proppant transport issues inside the fracture when lighter carrier fluids are used, but also increases the risk of premature screen-outs in the near-wellbore zone. Multistage hydraulic fracturing in unconventional reservoirs requires high volumes of proppant. Reliability of the treatment equipment is a major concern for the successful execution of the stimulation process. The considerable abrasiveness of sintered bauxite needs to be taken into account when planning a stimulation treatment in order to minimize treatment equipment failure.

When designing a fracture treatment, downhole temperature should be considered not only from the treatment fluid design standpoint, but also from the proppant selection perspective. Proppants degrade over time, but some proppants are much more durable than others. Sand and resin-coated sand suffer from thermal degradation. Downhole temperature affects the long-term fracture conductivity, and at temperatures greater than 200°F natural sand-based products can experience a significant loss in strength and subsequent decrease in conductivity. When exposed to 250°F, uncoated sand at 6,000 psi stress loses 40% of its conductivity compared to 150°F published data. Resin coating improves the conductivity and the reduction in conductivity is 30% at 300°F and 8,000 psi, compared to 80% loss for uncoated sand for the same conditions (Palish et al. 2012; Stim-Lab 1986–2007). Ceramic proppants are much more temperature stable and the ISO/API conductivity tests are performed at 250°F are in comparison with sand at 150°F.

In certain formations proppant flowback could be a serious problem. As described in the following section, proppant flowback can lead to a loss of fracture conductivity, resulting in significant production decrease, deposition in the lateral resulting in restricted production. It can also

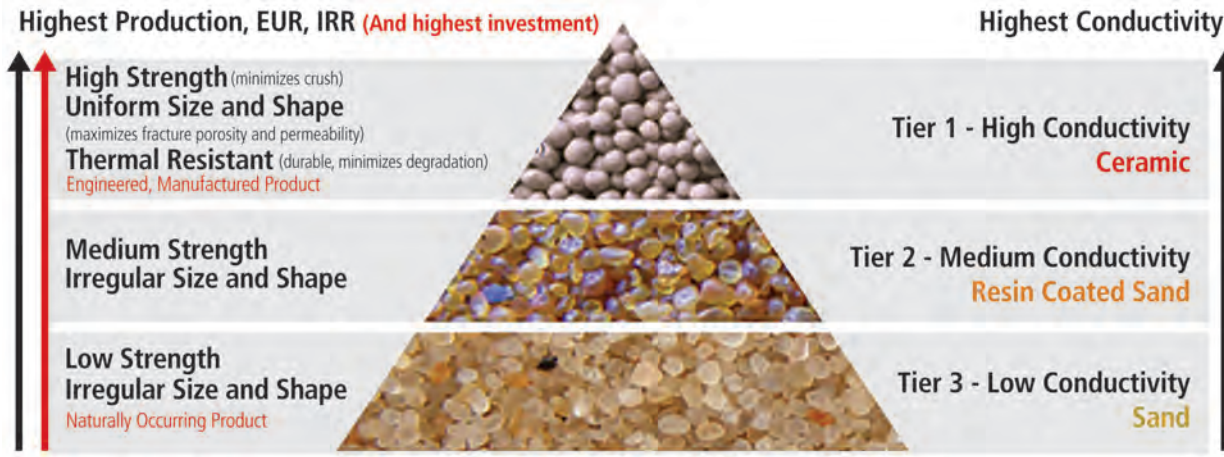

Fig. 17.14—"Proppant Conductivity Pyramid" aid to proppant selection for unconventional reservoirs. (Saldungaray and Palisch 2012.)

cause damage to downhole and surface equipment, leading to the increased intervention cost. Curable resin-coated proppants (CRCP) could be a solution for proppant flow back prevention. CRCP can be pumped throughout the treatment, but usually these proppants are pumped as tail-in at the end of the treatment at the ratio of 15 to 30% of the total proppant amount. Due to grain-to-grain bonding these proppants form a consolidated proppant pack preventing proppant flowback. CRCP can also improve fracture conductivity in soft formations, where embedment can be a cause of fracture width reduction. More detail in CRCP can be found in the previous section.

In summary, when selecting proppant for multistage horizontal fracturing in an unconventional reservoir, in addition to several conductivity reducing factors, one should account for flow convergence in transverse fractures, proppant transport in low-viscosity fluid, and more pronounced proppant crush when low proppant concentrations are used.

The effective conductivity of the proppant under bottomhole producing conditions should be taken into account. Proppant selection should not be made solely on the basis of well depth, stress, or what proppant historically was used in the field. Instead, the proppant should be selected based on the economic analysis of the fracture conductivity versus expected production rates. The proppant type selection should be based on the sensitivity analysis of the optimal conductivity for the particular reservoir and the economic benefit of increasing fracture conductivity should be validated by the field production data. Theoretically, most wells should benefit from greater conductivity, however a thorough return on investment analysis should be conducted to make sure that only fit-for-purpose technologies are used (see **Table 17.2**).

17.2.3 Proppant Flowback Prevention

Proppant flowback (also called proppant back production) is long-term production of the proppant from the fracture, or fractures, into the wellbore. Proppant flowback should not be confused with the initial and short-lived production of proppant that occurs as the fracturing fluid is recovered after the treatment has finished. A small and limited quantity of proppant will always return to surface with the recovered fluid, and this should be allowed for in the design of the flowback equipment. Generally, this volume of proppant is limited to between 500 to 5000 lbm, depending upon how many intervals have been treated. This consists of proppant that was left in the wellbore (e.g., due to under-displacement) and proppant that has come out of the very-near-wellbore region as the material packs itself into place. This initial proppant production should cease after two-to three-wellbore volumes of fluid have been recovered.

The rest of this section is concerned with longer-term production of proppant and its prevention.

17.2.3.1 Treatment Design—Prevention Is Better Than Cure

In shale gas wells, the entire purpose of drilling, completing, and fracturing the well is to place proppant deep into the reservoir. Generally, production will come from regions of the reservoir where we have placed proppant and kept it connected to the wellbore. Some production may come from fractures that have opened and then closed in a slightly changed orientation, which can produce some residual conductivity (for an example of this, see Mayerhofer et al. 1997), but in general, we need proppant to get production.

So in a very real sense, the entire purpose of the wellbore, completion, wellhead, and off-take system is to connect the proppant to the gas distribution pipeline grid.

Operating companies will spend a lot of time, effort, and money carefully placing the proppant into the formation, so the last thing anyone wants is to see it coming back again. Unfortunately, proppant flowback is very difficult to cure when it has started, so engineers should concentrate their efforts on preventing it from happening in the first place.

- Always end a treatment with high proppant concentration in the near-wellbore area. The higher the conductivity, the lower the drag forces on the proppant grains from the reservoir fluids. Although a screen-out at the end of the treatment may be problematic from an operational perspective, it is ideal for controlling proppant flowback, because the screen-out leaves the near wellbore with high concentrations of proppant packed as closely as possible.
- Avoid slickwater fracturing if at all possible. Because slickwater has very poor proppant transport properties, at the end of the treatment, all the proppant will tend to settle to the bottom of the fracture. This produces a "pipeline" across the top of the fracture, as illustrated in **Fig. 17.15**. This small area at the top of the proppant pack will have close to infinite conductivity. Consequently, gas will move across the top of the proppant at very high speeds, enabling the gas to entrain individual grains of proppant as it passes. This may not sound that significant, but over long periods this can lead to the production of a significant fraction of the original proppant placed—even up to 100%.

Table 17.2—Suggested proppant mesh sizes and concentrations for dry gas-, wet gas-, and oil-bearing unconventional formations.

Type of Reservoir Fluid	Type of Fluid System	Mesh Size	Concentration Range, ppa
Dry Gas	Slickwater	100, 40/70. 30/50	0.1–2.0*
Condensate	Linear Gel, Hybrid	30/50, 20/40	0.5–3.0
Oil	Hybrid, Crosslinked/VES	30/50, 20/40, 16/30	1.0–5.0

** Note that while operating companies continue to use relatively high concentrations of proppant in slickwater systems, concentrations above 1 to1.5 ppa (depending upon mesh size) can cause severe equipment damage.*

- If at all possible, avoid over-displacing the treatment. Put simply, this has the opposite effect to the first item above (namely ending with a high proppant concentration at the wellbore).
- Consider using a technique called "forced closure" (Ely 1996), where the fracture is closed rapidly. In this technique, as soon as the treatment is finished, the well is flowed back through a choke at a very low, controlled rate—perhaps 0.5- to 0.75-bpm. As this happens, the fracture rapidly closes, and tightly packed proppant collects in the near-wellbore area. While this technique is not practical for many multizone completions (and can be problematic) there is sufficient case history data to suggest that—under the right circumstances—it can be highly effective.

17.2.3.2 The Significance of Internal Friction

In order for proppant to be produced out of a fracture, there has to be movement of grains relative to one another. Proppant does not come back as large coagulated lumps—instead it comes back as individual grains. This means that

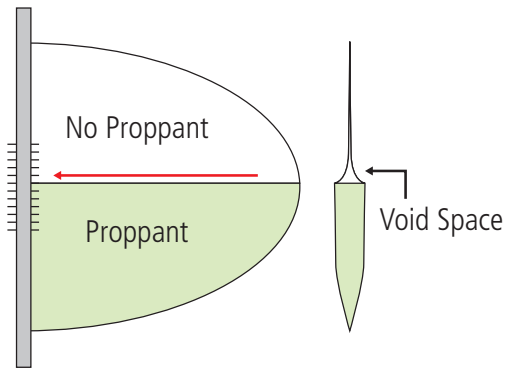

Fig. 17.15—Illustration of the "pipelining" effect in which high-velocity gas moves across the top of the proppant pack, entraining grains and producing them into the wellbore. (Martin 2009.)

controlling and even eliminating movement of grains relative to each other is key to its prevention. In other words, making and keeping the internal friction of the grains in the proppant pack as high as possible is the main method (aside from good treatment design, that is) for preventing proppant flowback.

Proppant flowback is one of the few areas in fracturing where natural sand has a technical advantage over using artificial proppants. This is because the highly angular nature of the natural sand automatically produces a higher internal friction pressure, as illustrated in **Fig. 17.16**.

17.2.3.3 Methods for Artificially Increasing the Internal Friction of the Proppant Pack

- **Resin Coating.** The most widely used method for increasing the internal friction of the proppant pack is to coat the grains with a resin that will adhere them to one another. Curable and partially cured (but not pre-cured) resins will change chemically under the temperature and pressure conditions inside the fracture, physically sticking the grains together. Resin-coated "tail-ins" are used as a common precaution against proppant flowback, where the last 10 to 30% or so of the proppant volume is resin-coated. However, caution is advised when doing this—there is no guarantee that just because a volume of proppant is pumped last, it will end up propping the part of the fracture closest to the wellbore. To be certain, it is recommended to use resin-coated proppant for at least the last 50% of the proppant volume.
- **Micro Fibers.** Small polymer fibers added to the sand or proppant form a mesh inside the proppant pack, significantly increasing the internal friction. Operationally, these fibers can be difficult to handle at surface and need to be evenly distributed among the proppant grains. However, when employed correctly, this technique can be highly effective.
- **Deformable Particles.** These particles are designed to be slightly larger than the proppant grains and also to be slightly

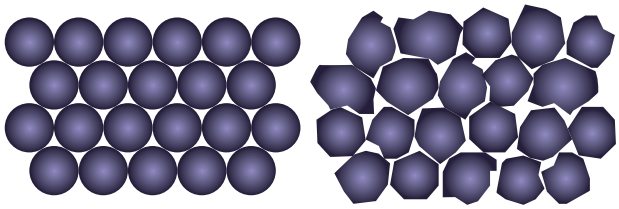

Fig. 17.16—The high degree of sphericity and roundness (see Fig. 17.8) found in artificial proppants (A) tends to reduce the internal friction of the proppant pack, whereas the natural angularity of sand (B) tends to increase the internal friction. (Martin 2009.)

softer. When added to the proppant at between 10 and 15% by weight, the particles will deform slightly in the pack as the fracture closes, allowing the proppant grains to "key in" to the deformable particle. This can dramatically increase the internal friction pressure of the proppant pack (Rickards et al. 1998).

- **Hard Needles.** These are particles designed to be relatively long and thin (as compared to the proppant grains), as well as being harder than the proppant. This acts to affect the internal friction of the proppant pack in much the same way as the microfibers, above.
- **Surface Active Agents (a.k.a. surfactants).** These chemicals are typically sprayed onto the proppant or natural sand as a fine mist, on-the-fly as the proppant is being delivered to the blender hopper. They act by altering the surface properties of the sand or proppant grains, making them increasingly mutually attractive—the overall effect being similar in manner to the way a magnet attracts iron filings.

17.3 Fracture Design Considerations

Before designing any hydraulic fracturing process, it is critical to evaluate the formation flow potential and to understand the relationships between the reservoir characteristics, well drainage area, and their influence on the optimum fracture geometry and fracture flow properties.

17.3.1 Fracture Geometry and Conductivity

The primary objective of hydraulic fracturing is to create fractures with optimum geometry and conductivity to maximize well production and ultimate recovery.

17.3.1.1 Impact of Reservoir Permeability on Treatment Design

One of the fundamentals of petroleum engineering is that pressure is energy, or more precisely, energy per unit volume. When we drill a gas well, we are creating a localized region of low pressure (the wellbore) in a region of high pressure (the reservoir), and basic fluid mechanics tells us that if there is a flow path between the two, fluids—i.e., liquids and gases—will flow from the high-energy area to the low-energy area. Some energy will be lost as the fluid moves from the reservoir to the wellbore—the lower the permeability, the more energy it takes. If we are really lucky, there is sufficient energy left in the fluid to overcome the hydrostatic pressure at the bottom of the well and actually make it all the way to the surface.

One of the main ways that hydraulic fracturing works is to reduce the amount of energy it takes to get from the reservoir to the wellbore. This happens in two ways:

1. The hydraulic fracture provides a flow path of massive conductivity, specifically designed to provide a huge contrast in conductivity between the fracture and the formation, so that fluids preferentially flow down the fracture to the wellbore, rather than through the formation. In low-permeability reservoirs this contrast in conductivity is so extreme that the reservoir fluids experience no significant pressure drop (= loss of energy) as they pass through the fracture. In such situations, the fracture is said to have infinite conductivity. Additionally, a hydraulic fracture will bypass any skin damage that has been induced around the wellbore (Rae et al. 1999).

2. Because the fracture can extend for a significant distance into the reservoir, the actual flow regime in the reservoir can be changed from very inefficient radial flow toward the wellbore, to much more efficient linear flow toward the fracture. The more the fracture penetrates into the reservoir, the greater this effect.

One of the areas that supports these efficiencies, especially item 2, is the inflow area, which is the area of contact between the "wellbore" and the reservoir. **Table 17.3** illustrates the effect on inflow area of hydraulic fractures. The basic fact is that no other completion technique even comes close to providing similar areas of contact with the formation and this is why hydraulic fracturing remains the only technique for completing ultra-low-permeability formations.

As discussed, the two factors controlling the production rate from a reservoir-propped fracture system are the ability of the

formation to deliver fluids to the fracture and the ability of the fracture to deliver the fluids to the wellbore. This is often expressed as dimensionless fracture conductivity or C_{fD}, as illustrated in Eq. 17.1. Note that you may also see C_{fD} written as FcD, which is now obsolete. What C_{fD} expresses is the ability of the fracture to deliver fluids to the wellbore, divided by the ability of the formation to deliver fluids to the fracture. When fracturing conventional reservoirs, maximum possible productivity is achieved by getting the optimum value for C_{fD}, as discussed by Economides et al. (2002).

From Eq. 17.1 we can see that in high permeability formations, in order to stop C_{fD} from having very low values, we need to maximize fracture conductivity (i.e., wk_f) and minimize fracture half-length. This means that very short, wide, and highly conductive fractures are required. In high permeability formations, fluids flow easily through the formation. The limiting factor for the reservoir-fracture system is not moving fluids to the fracture, but instead ensuring that the fracture has sufficient conductivity contrast with the formation in order to provide the required production increase.

Conversely, in low-permeability formations, it is easy to provide a huge contrast between the conductivity of the fracture and the conductivity of the formation. What limits the productivity of the system is the ability of the reservoir to deliver fluids to the fracture in the first place. Consequently, fractures are designed to be as large as possible to maximize inflow area while maintaining minimal (but still sufficient) conductivity.

There is an approximate inverse-square-root relationship between well productivity and area of contact with the reservoir, if all other factors remain unchanged. For example, if the reservoir permeability is 100 times less than anticipated, then the area of contact with the reservoir needs to increase by 10 times in order to provide the same productivity. Given that it takes roughly the same amount of money to drill a well of given geometry regardless of whether it is placed in a tight gas reservoir or a shale gas reservoir, then a drop in permeability from 0.1 md (the top end of tight gas permeability) to 1 nanodarcy (i.e., 10^{-9} darcy, which is the low end of shale permeability to gas), or a drop by a factor of 1 million, means that the reservoir contact area has to increase by 1000 times in order to provide the same productivity.

The effect of reservoir permeability on fracture design is illustrated in **Fig. 17.17**.

From Fig. 17.17 we can see that, as we progress from high permeability to the lower permeability ranges for tight gas, the only way to get a sufficient inflow area is to position the wellbore horizontally and to stack the fractures along the wellbore. However, as we progress into even lower permeability formations, such as the nanodarcy permeabilities found in shale gas reservoirs, even stacking the fractures along horizontal wellbores cannot produce sufficient inflow area to produce economic productivity. So a slightly different approach, as illustrated in **Fig. 17.18**, has to be used.

For shale reservoirs, the permeability of the formation is so low that the only way to develop sufficient inflow area is to move away from the conventional planar fracture geometry and instead fracture into the existing natural fracture network. This will be discussed in more detail later. For now it is sufficient to know that the existence of suitable natural fractures and the ability to place a propped fracture treatment in them can make the difference between a good well and a poor well in shale formations.

Table 17.3—Inflow areas for various types of completion.

Completion Type	Inflow Area	
	PNP	BACS
100 ft vertical, 8.5" OH	222.5	67.8
3000 ft horizontal, 6" OH	4,712	1,436
Radial fracture, 50 ft diameter	15,707	4,788
Elliptical fracture 400 ft x 100 ft.	251,327	76,605

Note: OH = Open Hole

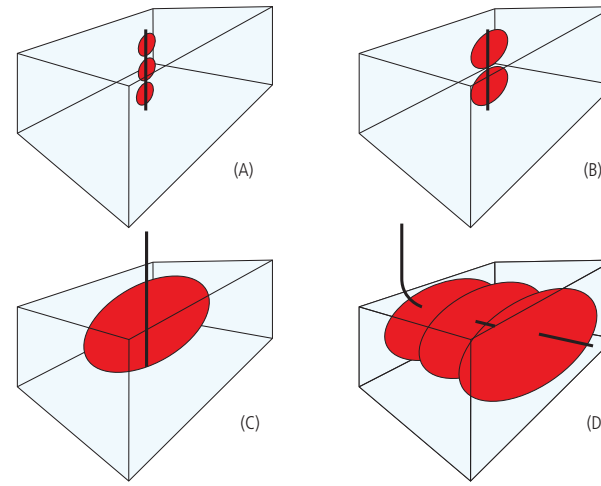

Fig. 17.17—The effect of permeability on required fracture geometry: (A) high permeability, (B) medium permeability, (C) low permeability (upper range for tight gas), and (D) very low permeability (lower range for tight gas). (Rylance and Martin 2014.)

17.3.1.2 Propped Fracture Length

When we refer to propped fracture length, x_f, we are actually talking about the fracture half length, or the distance from the center of the wellbore to the tip of the fracture, as illustrated in **Fig. 17.19**, which is an idealized representation of a reality that is without doubt considerably more complex. In practice, it is usual to talk about the average half-length of a single, regular, planar fracture that has the equivalent effect as the more complex reality. The *propped* fracture half-length is often significantly less than the *created* fracture length, as proppant may not reach the fracture tip during pumping or may become embedded as the fracture closes. Plus, if fracture height growth is more than designed, then the fracture length will be further compromised (Ahmed 1988).

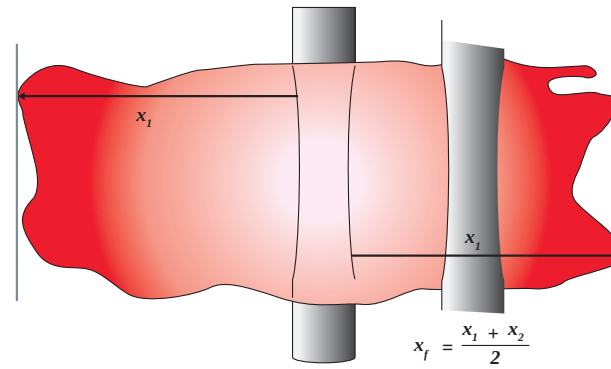

17.19—Fracture half-length, x_f.

17.3.1.3 Propped Fracture Width

The average propped fracture width, w, is the effective average width of the part of the fracture that is propped open after the fracture closes. It is quite different from the created fracture width, as illustrated by **Fig. 17.20**, which is the width while pumping the treatment. This is a dynamic quantity that can vary considerably during the treatment. When pumping stops, the fracture closes on the proppant and the width reduces until faces of the fracture close on the proppant. Consequently, *created* fracture width is always equal to or greater than *propped* fracture width.

17.3.1.4 Proppant Pack Permeability

The permeability of the proppant pack, k_f, is a complicated and highly variable quantity. It will vary with closure stress (which itself is dependent upon pore pressure and so may vary over the producing life of the fracture), flow velocity (non-darcy flow effects), and fluid type (multiphase flow). A more detailed description of this was published by Vincent et al. (1999), who demonstrated that the combination of multiphase and non-darcy flow effects could reduce the effective proppant pack permeability by well over 90%.

Non-darcy flow is especially prevalent in high rate gas wells, especially those with limited contact with the wellbore (such as transverse fractures) and is described by the Forchheimer equation (Forchheimer 1901):

where Δp is the pressure drop, L is the fracture length, μ is the fluid viscosity, v is the superficial velocity of the

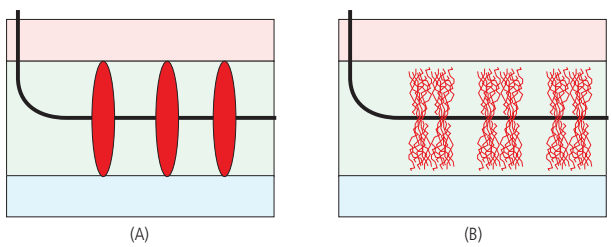

Fig. 17.18—As permeability decreases into the nanodarcy range common in shale reservoirs, the approach taken from fracture design shifts from stacking multiple planar fractures along a horizontal wellbore (A—low-permeability tight gas fracturing), to fracturing into the natural fracture network (B—shale fracturing). (Rylance and Martin 2014.)

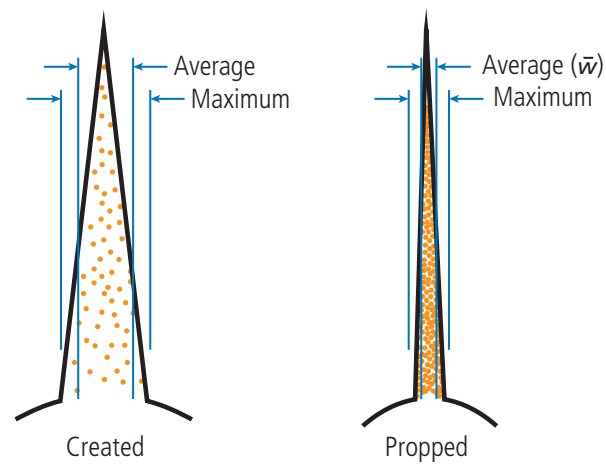

Fig. 17.20—Diagram illustrating the differences between created and propped fracture width as well as between maximum and average fracture width.

fluid (i.e., as if the porosity were 100%), k_f is the proppant permeability, β is the coefficient of inertial resistance [which can either be calculated (Cooke 1973) or obtained for specific conditions from tables supplied by proppant vendors], and ρ is the fluid density. In **Eq. 17.2**, the term $\Delta p/L$ represents the energy (or pressure) loss per unit length of the fracture, $\mu v/k_f$ represents the energy lost due to viscous, or darcy flow effects and $\beta\rho v^2$ represents the energy lost due to inertial flow effects. Clearly, the relative effects of non-darcy flow will dominate the pressure or energy loss in high-velocity flow situations (i.e., gas wells). $\beta\rho v^2$ can also be thought of as a kinetic energy effect as it is directly proportional to both the mass and the velocity squared.

In the context of shale gas fracturing, it is often believed that because the permeability of the formation is so tiny, just about any proppant conductivity will produce the massive contrast in conductivity required to create an infinite conductivity fracture (i.e., no significant pressure loss in the fracture). This has led to the use of poor-quality non-API fracturing sands, very small grain sizes, very low proppant concentrations, and the use of low-strength proppants and sands in high closure strength environments. This is a mistake, as any amount of liquid flow through the fracture can eliminate this conductivity contrast. This is particularly true during fracture fluid cleanup. A more detailed discussion of this topic is included previously.

17.3.1.5 Reservoir Factors Determining Proppant Distribution in the Fracture

In order for proppant to be placed within any given part of the fracture, two things need to happen. First, proppant-laden fluid needs to penetrate into this section, and second, the proppant needs to stay there after the fluid has stopped moving.

In order for proppant-laden fluid to penetrate into a particular section of the fracture, the fracture has to have sufficient width to accept the proppant—without this, fluid may continue to flow down the fracture, but proppant will "pile up" at the entrance to the narrow section. This will result in that section of the fracture "screening out" and being effectively isolated from the rest of the fracture network. If this piling up of proppant occurs near the wellbore, the whole treatment can end prematurely.

There are several factors that may cause a variation in fracture width:

- Fracture width is directly related to net pressure (p_{net}), which is the excess pressure of the fluid in the fracture above closure pressure—or put another way, the energy left in the fracturing fluid to make the fracture(s) grow, as defined in **Eq. 17.3**. As this energy dissipates as the fluid moves away from the wellbore—due to the effects of leakoff and friction—fracture width also decreases with distance from the wellbore.

$$p_{net} = p_c - p_f \qquad \textbf{(Eq. 17.3)}$$

where p_c is the closure stress and p_f is the fluid pressure within the fracture. The closure stress is the minimum effective stress in the formation and is the minimum pressure the fluid in the fracture must be at in order to keep the fracture open. Because fracture width decreases with distance from the wellbore, eventually a point is reached were proppant can no longer pass and whatever fracture has been created past this point will remain unpropped. This effect is common—as anyone who has done post-fracturing pressure and/or rate transient analysis will confirm. The effective fracture length is often much shorter than that predicted by modeling (although this can also be caused by proppant embedment; see next).

Obviously, the closure pressure (a.k.a. minimum effective stress) also has a great effect on the width of the fracture and hence the ability of proppant to be placed in any particular section. This means that a localized variation in stress—often caused by localized variations in material properties such as Poisson's ratio (ν) or Biot's poroelasticity factor (α) (see Chapter 9)—can have a significant effect. This is particularly prevalent when we consider the vertical movement of fluids and proppant between different layers in a particular formation.

- Fracture width is also proportional to Young's modulus, E, or more precisely the plane strain Young's modulus E' (equal to $E/[1—\nu^2]$) (see Chapter 9). Again, variations in material properties—especially vertical variations—can significantly affect the ability of the treatment to place proppant.
- As discussed, in general the fracture(s) naturally tends to grow perpendicular to the minimum horizontal stress, σ_h. Many of the natural fractures will also be in this direction—but many will not. By definition, any natural fracture that is not on this plane will experience a greater normal stress (i.e., the stress in the direction perpendicular to the plane of the fracture) referred to as σ_n—the magnitude of which will be a trigonometrical function of the three principal stresses (σ_v, σ_H, and σ_h), and the angle of the normal stress to these principal stresses. If we define angles α, β, and γ as being the angles between σ_n and principal stresses σ_v, σ_H, and σ_h, respectively, (such that the angles between the plane of the natural fracture and the principal stress are $(90° - \alpha)$, $(90° - \beta)$, and

(90° – γ)), as illustrated in **Fig. 17.21**, we can define l, m, and n in **Eqs. 17.4** and **17.5** as follows (Hurt 2014):

$$l = \cos\alpha \qquad m = \cos\beta \qquad n = \cos\gamma \tag{Eq. 17.4}$$

Such that:

$$l^2 + m^2 + n^2 = 1 \tag{Eq. 17.5}$$

Therefore, that the stress normal to the plane of the natural fracture is given by **Eq. 17.6:**

$$\sigma_n = l^2\sigma_v + m^2\sigma_H + n^2\sigma_h \tag{Eq. 17.6}$$

Finally, the minimum net pressure required to open this natural fracture is:

$$p_{net,\min} = \sigma_n - \sigma_h \tag{Eq. 17.7}$$

Eq. 17.7 is significant in that it defines the minimum net pressure required to produce a propped fracture network. As discussed, in order to achieve an effective fracture network, we need to produce or exploit fractures that are away from the preferred fracture plane. So it is only by opening these natural fractures, at pressures above that required to open fractures on the preferred fracture plane, that we can achieve this. Failure to achieve adequate net pressure during a treatment is a well-documented cause for poor post-treatment productivity (King et al. 2008).

However, Eq. 17.7 should be used with caution. First, if the natural fracture is at an angle to the principal stresses, it is likely that it will also be experiencing shear stresses. Applying fluid pressure to this fracture may cause it to shift due to the shear stresses, at pressures lower than the pressure required to actually open it. This may or may not produce significant fracture conductivity (see Mayerhofer et al. 1997), but it will not produce any of the fracture width required to transmit proppant. Second, the derivation of Eq. 17.7 assumes that the in-situ shear stresses dissipate as the fracture opens and are not significant when the fracture is open. This in turn means that it may take more pressure to open the natural fracture than it takes to keep it open. If these stresses do not dissipate, the pnet,min will be greater than that predicted by Eq. 17.7. Third, Eq. 17.7 assumes that there is no interference from the existing hydraulic fracture, acting to reduce the natural fracture width in the region close to the hydraulic fracture (the greater the angle between the hydraulic and natural fractures, the less significant this effect will be). Fourth (and last), Eq. 17.7 defines the minimum fluid pressure required to open the natural fracture—pressure in excess of this will be required to make this fracture propagate and to produce sufficient width to comfortably transmit proppant.

Eq. 17.7 also means that the same net pressure that produces a certain width in a fracture (natural or hydraulic) perpendicular to σ_h, will produce less width in a natural fracture at an angle to σ_h. This means that while it is ***relatively*** easy to transport proppant along the preferred fracture plane, it is much more difficult to distribute the proppant between parallel fractures or fracture networks. This is one reason why the industry has moved toward clusters of perforations in recent years, so that proppant is entering the fracture network along several parallel flow paths and thus has more chance of moving into fractures that are away from the principal fracture plane.

Propped fracture width can also be affected by a phenomenon known as ***embedment***, which is illustrated in **Fig. 17.22**. Embedment occurs when a relatively soft formation closes on a proppant pack with sufficient force to cause the rock to plastically deform around the proppant grains, effectively reducing propped fracture width. This has to be allowed for in the treatment design, otherwise insufficient effective propped width may be generated. Embedment can be assessed from rock mechanical testing of core (see Chapter 4 of Economides and Martin 2007), where a Brinell hardness (BH) test measurement of less than 5 or 6 kg/mm^2 indicates that embedment could be a problem. Note that seemingly resilient formations can have their BH significantly reduced by exposure to an incompatible

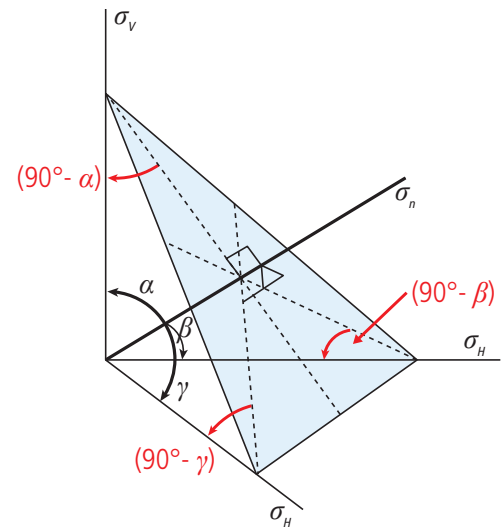

Fig. 17.21—Diagram illustrating the position of the angles α, β, and γ relative to the natural fracture and the normal stress σ_n.

fracturing fluid—a relatively common effect when water-based fluids contact shale formations.

17.3.1.6 Complex Fracture Networks and Stimulated Reservoir Volume

Up until now we have discussed fractures as if they are planar, ***elliptical***, and singular in nature. Almost certainly this is not the case even in conventional reservoirs and the reality is that we use elliptical analogies to mimic fractures of unknown complexity. Nevertheless, in conventional reservoirs we usually do our best to minimize this complexity, such as when selecting a perforating strategy (see Chapter 6 of Economides and Martin 2007).

However, this is not the case when dealing with shale reservoirs. As discussed above, in order to generate sufficient inflow area in such low-permeability reservoirs, we are deliberately targeting natural fracture networks, in order to exploit the contact area that this gives us. The resulting complex fracture network (as illustrated in **Fig. 17.23**) is very difficult to predict and model, although significant advances are being made in this area–see Section 17.4.5 (Meyer and Bazan 2011, Meyer et al. 2013).

Because fracture networks are being developed, rather than simple planar fractures, it is more useful and practical to assess the SRV, rather than the area or length of the fractures (Mayerhofer et al. 2010). This has been assisted by the advent of microseismic fracture mapping (see Chapter 20) which allows us to assess—within the accuracies of the measurement technique—what the actual volume of reservoir affected by the treatment is (see **Fig. 17.24**). Of course, this is a somewhat qualitative assessment. There is no guarantee that any given microseismic event represents a fracture (natural or otherwise) that is connected to the wellbore and even if it is connected to the wellbore, there is no guarantee that it will stay that way, or that it contains any proppant. However, SRV is a useful concept as it allows us to compare the effectiveness of offset treatments and to target unstimulated reservoir volume.

17.3.2 The Influence of Wellbore Orientation

17.3.2.1 Vertical, Deviated, and Horizontal Wellbores

Like most things in nature, hydraulic fractures follow the path of least resistance. This means that fractures tend to produce maximum width in the same direction as the minimum effective stress, which in turn means that the overall gross direction of fracture propagation is perpendicular to this

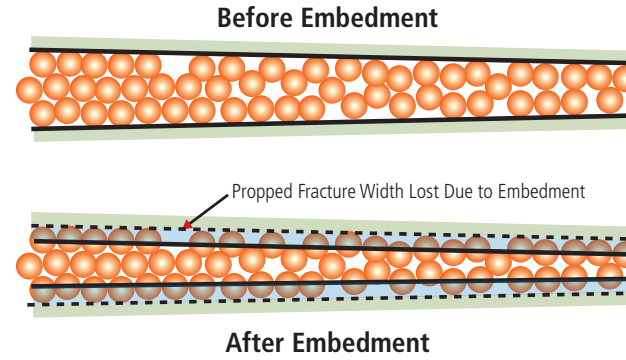

Fig. 17.22—Illustration showing the effect of proppant embedment on propped fracture width.

(see Chapter 9). In practice, in the vast majority of reservoirs, the maximum effective stress is vertical (σ_v), which means that the minimum effective stress will be on the horizontal plane (σ_h). This in turn means that the fracture will produce maximum width on the horizontal plane, and will propagate on a plane perpendicular to this plane (i.e., in the same direction as the maximum effective horizontal stress, σ_H) and will be oriented on a vertical plane.

Of course, when fracturing shale reservoirs, the natural fracture network will be targeted, with the express intent of creating a complex fracture network (see the previous section). However, the influences of the effective stresses in the rock will mean that the fracture will grow preferentially in the direction of σ_H and will orient preferentially on a vertical plane. The greater the stress anisotropy in the

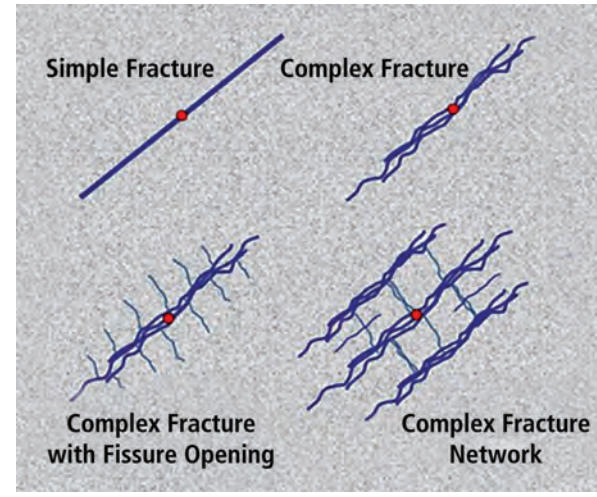

Fig. 17.23—Diagram illustrating the difference between a simple planar fracture and a complex fracture network. (Mayerhofer et al. 2010.)

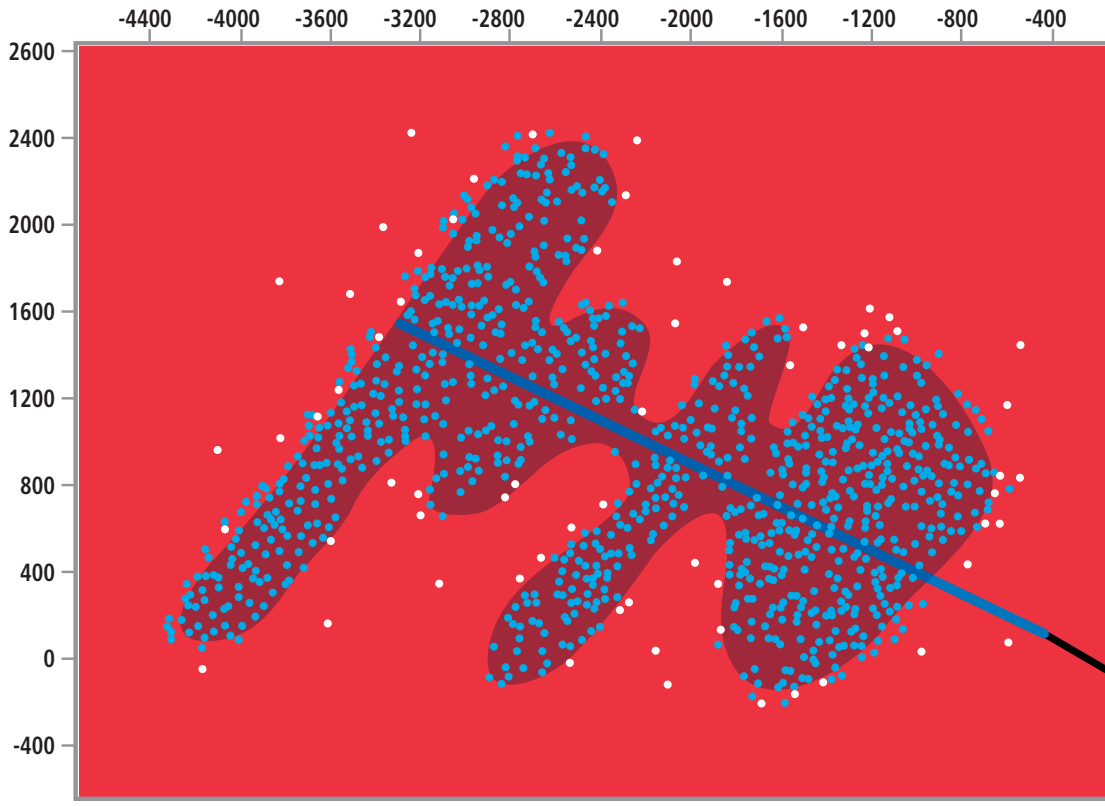

Fig. 17.24—Diagram illustrating the concept of SRV estimated from microseismic. (Cipolla et al. 2012.) Each of the dots represents a microseismic event, while the shaded area is a qualitative interpretation of the volume of rock that has been stimulated. This estimation allows future stimulation treatments and even wells to be planned to target unstimulated reservoir volume.

reservoir, the more the fracture network will tend to grow preferentially along a single plane. Conversely, this means that low stress anisotropy will help promote a more complex fracture network (see Chapter 9).

What this means is that fractures will propagate in a direction determined by the stresses in the formation regardless of wellbore orientation. This is illustrated in **Fig. 17.25**, which shows vertical wellbores transitioning into deviated and then horizontal sections. In the case of wellbore A, which is drilled parallel to σ_H, the fracture tends to propagate along the wellbore regardless of its deviation from the vertical. This kind of fracture is referred to as longitudinal. By contrast, wellbore B is drilled perpendicular to σ_H. While the wellbore is vertical, the fracture will propagate along the wellbore. However, as soon as the wellbore deviates away from vertical, the area of contact between the wellbore and the fracture is reduced to a minimum. This kind of fracture is referred to as transverse.

It should also be noted that when the plane of the fracture deviates more than roughly 15° from the orientation of the wellbore, the fracture will behave as a transverse fracture. This means that for wellbores drilled without any consideration for the stress azimuth, it is very likely that the fractures will be transverse.

17.3.2.2 Transverse or Longitudinal Fractures

The choice between vertical and horizontal wellbores and between horizontal wellbores with longitudinal or transverse fractures is complex (Economides and Martin. 2010). **Fig. 17.26** illustrates the differences between longitudinal and transverse fractures placed along a horizontal wellbore. From this figure we can see that there is a limit to how many longitudinal fractures can be placed along the wellbore, before they begin to overlap and waste effectiveness. In practice, when at least 80% of the wellbore is covered by fractures there is no further need to place any more longitudinal fractures. By contrast, the number of transverse fractures that can be effectively placed along the wellbore is really only limited by completion technology and treatment economics. Initial productivity is

directly proportional to the number of producing transverse fractures, although the closer the fractures are to each other, the quicker this productivity will decline.

17.3.2.3 Wellbore Type Selection

For conventional reservoirs, the guidelines in **Table 17.4** can be followed.

For shale reservoirs, effective permeability is so low that the best technical solution is always to drill horizontal wells so that transverse fractures are produced—that is to say, the preferential direction of fracture network growth is perpendicular to the wellbore. This allows maximum potential stimulated reservoir volume. As discussed, in order to achieve this, the wellbore needs to be drilled in the same direction as σ_h. This in turn means that a reliable knowledge of the in-situ stress azimuth in a shale reservoir is essential for a successful development (see Chapter 9).

17.3.3 Proppant Transport

One of the main functions of the fracturing fluid is to carry the proppant and place it deep within the fracture or fracture network. In unconventional formations, as discussed previously, maximizing the area of contact with the reservoir and the complexity of the fracture network is essential—but so is making sure that this network is connected to the wellbore with sufficient conductivity when the treatment is over. It is not sufficient to simply break the rock apart and then allow it to close—while this may produce some conductivity under the right conditions (e.g., Mayerhofer et al. 1997) for fractures which have propagated along the dominant fracture plane, proppant is essential to maintain sufficient conductivity for the life of the well. Understanding the mechanisms that allow proppant to be placed thousands of feet away from the wellbore, via what is often a very thin, twisting and complex flow path, is an essential part of treatment design.

17.3.3.1 Settling and Convection

Proppant settling is the basic, gravity-driven downward motion of a heavy particle in a less dense fluid. Obviously, the bigger the contrast in density between the particle and the fluid, the faster the particle tends to fall. Other factors are also relevant—larger diameter particles are prone to fall more quickly than smaller, as mass increases with the cube of particle radius, whereas viscous drag forces—which are proportional to the cross sectional area of the particle—are only proportional to the square of the radius. The velocity at which a particle will fall is governed by Stokes' law (**Eq. 17.8**):

$$F_d = 6\pi\mu r v \qquad \textbf{(Eq. 17.8)}$$

where F_d is the drag force on a particle suspended in a fluid, μ is the dynamic viscosity of the fluid (which is the same as the standard "viscosity" used in the oil industry), r is the radius of the particle and v is the velocity of the fluid moving past it.

Stokes' law is usually used to find the terminal viscosity (v_∞) of the falling particle—that is to say the maximum velocity it will reach. At this point acceleration is zero, so that force due to gravity is equal to the viscous drag force predicted by Stokes' law, as given in field units in **Eq. 17.9**:

$$v_\infty = 1.15 \times 10^3 \left(\frac{d_{prop}^2}{\mu_f}\right)(\gamma_{prop} - \gamma_f) \qquad \textbf{(Eq. 17.9)}$$

Table 17.4— Wellbore type selection for various permeability ranges. (Economides and Martin 2007.)

Permeability Range, md	Best Technical Solution	Comments
> 5	Horizontal Wellbore, Longitudinal Fractures	In all cases
0.5 to 5	Horizontal Wellbore, Longitudinal Fractures OR Vertical Well with Fracture	Dependent upon project economics and the relative costs of vertical and horizontal wellbores and zonal isolation techniques
0.1 to 0.5	Horizontal Wellbore, Transverse Fractures	Above 0.5 md, the "choked" connection between the fracture and the wellbore makes transverse fractures relatively inefficient
< 0.1 md	Horizontal Wellbore, Transverse Fractures OR Vertical Well with Fracture	Dependent upon project economics and the relative costs of vertical and horizontal wellbores and zonal isolation techniques

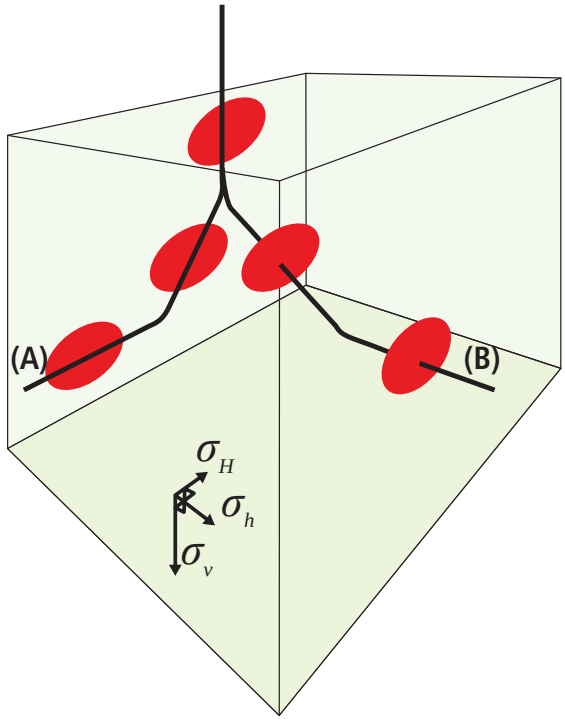

Fig. 17.25—Fractures will propagate on a plane that is perpendicular to the minimum effective stress, regardless of wellbore orientation.

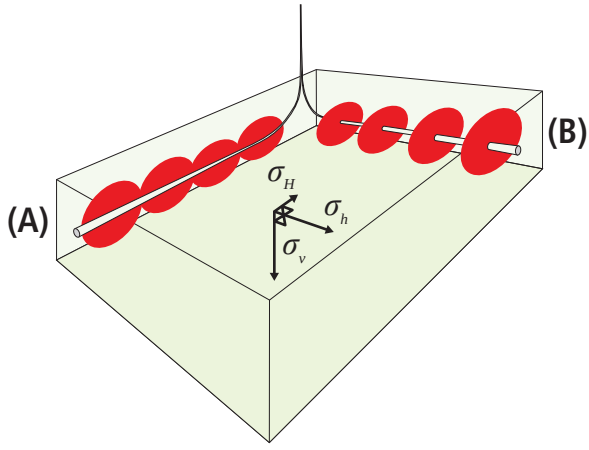

Fig. 17.26—Diagram illustrating that while there is a limit to how many effective longitudinal fractures may be placed on a horizontal wellbore (A), a similar limitation does not apply to transverse fractures (B).

where v_∞ is in ft/min, d_{prop} is the proppant diameter in inches, μ_f is the fluid viscosity in cp, γ_{prop} is the proppant specific gravity (dimensionless), and γ_f is the fluid specific gravity.

The main problem with Eq. 17.9 is understanding the viscosity of the fluid. For a Newtonian fluid such as slickwater, the viscosity is not dependent upon shear rate and can be regarded as constant. However, for most fracturing fluids with any significant viscosity, there is a significantly more complex relationship between shear rate (the amount of agitation a fluid is receiving) and the viscosity at that shear rate (referred to as the apparent viscosity—see Chapter 7 of Economides and Martin 2007). This means that actually finding the viscosity to use in Eq. 17.9 can be very problematic.

Mack and Warpinski (2000) produced a more user-friendly power law version of Eq. 17.9, in Chapter 6 of Economides and Nolte, 2010 (see **Eq. 17.10**, which is in SI units).

$$v_\infty = \left[\frac{(p_{prop} - \rho_{fl})\, g\, d_{prop}^{\,n'+1}}{3^{n'-1} 18 K'} \right]^{1/n'} \qquad \textbf{(Eq. 17.10)}$$

where ρ_{prop} is the density of the proppant, ρ_{fl} is the density of the fluid, g is the acceleration due to gravity (= 9.81 m/s2), n' is the power law fluid exponent and K' is the power law fluid consistency index.

It is important to realize that viscous drag forces act in two directions during proppant transport (**Fig. 17.27)**.

From Fig.17.27 we can see that unless the apparent viscosity of the fracturing fluid is effectively infinite, or the density of the proppant is the same as the density of the fluid, the proppant will always tend to head downward. This is known as proppant settling and the primary mechanisms for preventing this are to maximize apparent viscosity or to place the fluid in turbulent flow (in which case Eq. 17.9 and Eq. 17.10 become invalid).

While proppant settling is a phenomenon best described and calculated on an individual proppant grain basis, proppant convection is a phenomenon that works on large volumes of slurry as they move within the fracture or fractures. This is illustrated in **Fig. 17.28**.

The simple fact is that slurry with a high concentration of proppant is denser than slurry with a low concentration of

proppant. Consequently, given sufficient time and flow rate, the high concentration slurry tends to flow under the low concentration slurry, displacing it upward. This phenomenon, called ***proppant convection***, means that the last stage pumped in a fracture treatment may not necessarily end up being the stage next to the wellbore, when the fracture has closed on the proppant. This is a factor that needs to be allowed for during the treatment design.

17.3.3.2 Proppant Transport in High-Viscosity Fracturing Fluids

It is common practice to assume that when a fracturing fluid has achieved a certain apparent viscosity, it has "perfect" proppant transport characteristics. This means that at the low shear rates experienced within the fracture, the apparent viscosity of the fluid is essentially infinite, which in turn means that the vertical gravity-driven drag force is zero and the drag force caused by the fluid flow is such that the proppant grain moves at the same velocity as the fracturing fluid, in the same direction as the fracturing fluid.

When designing treatments, it is common practice to assume perfect proppant transport in the fracturing fluid and then retroactively design the fluid itself to meet certain minimum criteria for the life of the treatment, at bottomhole conditions. Typically there will be a minimum apparent viscosity, at a specified shear rate, for a minimum time, in order to qualify the fluid as perfect with regard to proppant transport. For example, when testing on a HPHT fluid rheometer, a common criterion used is to maintain at least 200 cp apparent viscosity at a shear rate of 40 s^{-1}. This must be maintained for the estimated life of the job (from the start of pumping to post-treatment fracture closure) at the estimated bottom hole static temperature. While use of such criteria is common in the industry, there is no industry standard so variations (often subjective) are common.

Most fracture simulations using high-viscosity fluids assume perfect proppant suspension and concentrate more on the effects of convection than settling.

Moreover, there is no doubt that a criterion based on a minimum apparent viscosity is a fairly crude way to assess whether or not a fluid has sufficient proppant transport characteristics. Work by Goel and Shah (2001), and Harris et al. (2009) suggests that a better measure of whether or not a fluid can transport proppant is to assess the linear elastic character of the fluid via the storage modulus (G') and the loss or viscous modulus (G''). These are assessed using special viscometers (such as a Thermo-Haake Rheostress 300), which

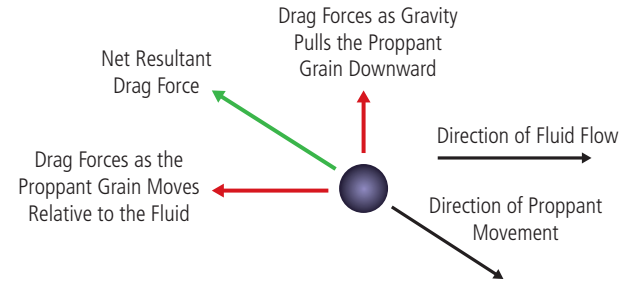

Fig. 17.27—Diagram illustrating the net effect of the two drag forces—one that is resisting gravity and the other that is resisting the fluid flow.

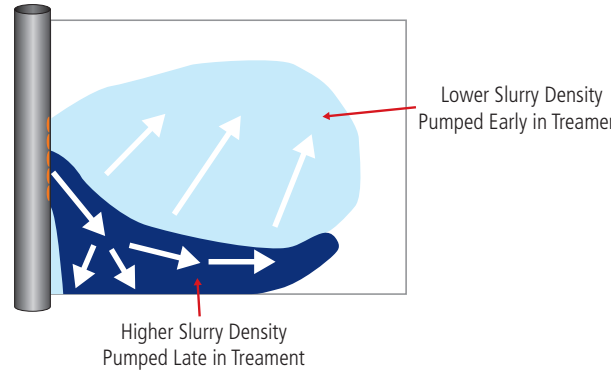

Fig. 17.28—Diagram illustrating proppant convection, as a high-density slurry vertically displaces a low-density slurry within the fracture. (After Martin 2009.)

measures the viscoelastic properties by placing the sample fluid between two circular parallel plates (perhaps 1 mm apart) and then radially oscillating one plate relative to the other. In purely elastic materials the stress and strain occur in phase, so that the response of one occurs simultaneously with the other. In purely viscous materials, there is a phase difference between stress and strain, where the strain lags the stress by a $\pi/2$ radians (90°) phase lag. Viscoelastic materials exist somewhere between the two extremes of elastic and viscous, exhibiting some phase lag between 0 and $\pi/2$ radians (0° – 90°) (Meyers and Chawla 2008). The storage modulus (G') represents the energy stored during elastic shear, while the loss or viscous modulus (G'') represents the energy lost as heat during viscous shear deformation. Under these test conditions high-viscosity fracturing fluids (crosslinked and VES) display viscous behavior at very low oscillating frequencies (equivalent to shear rate) and elastic behavior at higher shear rates (good examples of this behavior can be found in Gomaa et al. 2011).

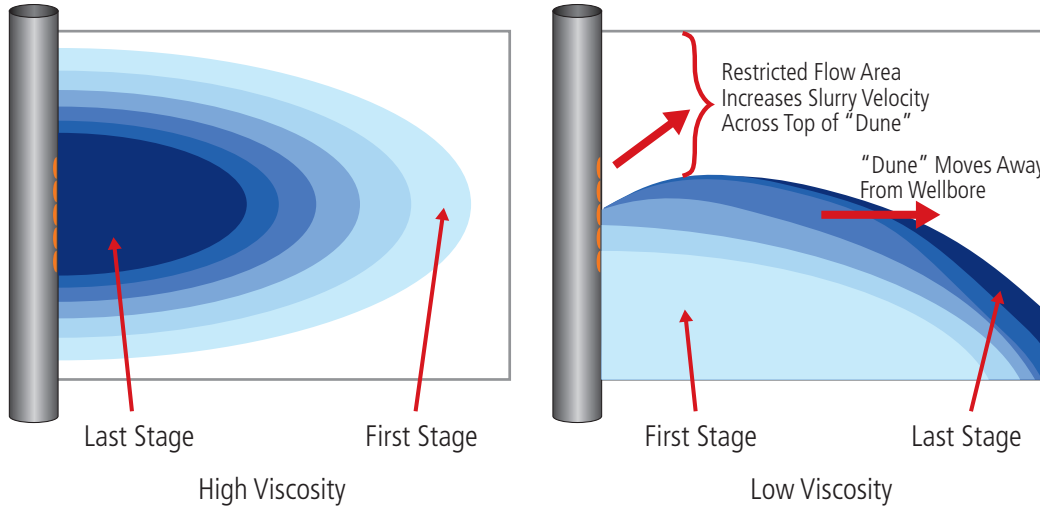

Fig. 17.29—Diagram illustrating how proppant is deposited by low-viscosity fluids, as compared to how it is suspended by high-viscosity fluids.

Goel and Shah (2001) provided experimental data to support a hypothesis that perfect proppant transport can be obtained under the condition given in **Eq. 17.11**.

$$G' > 0.5 + 20\omega - 8\omega^2 \qquad \textbf{(Eq. 17.11)}$$

where G' is measured in Pa and ω is the angular velocity (in rad/s) of a Bohlin rheometer (which uses an upper rotating cone and a fixed lower plate—the plate is 60 mm in diameter and the cone has a 4° angle and is 40 mm in diameter).

Gomaa et al. (2014b) suggested that when $G'' > G'$ (i.e., viscous energy loss is dominant), the proppant will settle downward (however slowly, depending upon the apparent viscosity) as the fluid is dominated by viscous behavior. However, when $G' > G''$ (i.e., elastic energy storage is dominant) the proppant will stay suspended as the fluid is effectively in a semi-solid state, where the fluid will provide a significantly higher internal resistance to proppant settling.

17.3.3.3 Proppant Transport in Low-Viscosity Fracturing Fluids

Proppant transport in low-viscosity fluids continues to be modeled and visualized on a much more empirical basis. This is because the only available mechanism to move the proppant is the energy provided by turbulent flow. In order to establish whether or not a fluid is in turbulent flow, the Reynolds number must be calculated, which in turn is highly dependent upon the flow area and geometry. So without any reliable estimate of both the dimensions of the flow channel (i.e., the fracture) and the number of flow channels, it is very difficult to calculate whether or not a fluid is in turbulent flow.

When carrying proppant in a low-viscosity fluid, the dense proppant will very quickly settle out of the fluid at any point where turbulent flow ceases, as illustrated in **Fig. 17.29**, which compares the proppant placement characteristics of high-viscosity fluids to those of low-viscosity fluids.

With regard to Fig. 17.29, as soon as the slurry enters the fracture (a relatively low shear environment) proppant rapidly settles to the bottom of the fracture, building a proppant "dune." As the dune gains height, fluid velocity across the top of the dune increases as the flow area becomes increasingly restricted. Eventually the velocity increases to a point where the fluid enters turbulent flow again and proppant at the top of the dune becomes re-entrained in the slurry. For any given flow rate, fracture geometry and fluid characteristics, there will be an equilibrium dune height, above which the dune will not rise. Instead, proppant is deposited beyond the top of the dune, as the flow area increases and the fluid again drops out of turbulent flow. So the far edge of the "dune" moves away from the wellbore as more proppant is pumped into the fracture.

This effect has three significant consequences for the treatment:

1. No matter how much proppant is pumped, it can never cover the entire vertical height of the created fracture. After fracture closure, this leaves the top of the fracture with negligible fracture conductivity and the bottom of

the fracture with excessive fracture conductivity. It can also lead to problems with proppant flowback due to the pipelining effect described previously (see Section 17.2.3.1).

2. In general, the first proppant to be pumped will remain close to the wellbore, while the last proppant to be pumped will be furthest away. This is the opposite of how the proppant is placed when using high-viscosity fluids.

3. Significant changes in pumping rate should be avoided when performing slickwater treatments. Any changes in slurry rate will affect the equilibrium dune height and could lead to either a sudden rise in dune height (drop in rate) or a high concentration "slug" of proppant being entrained into the slurry (rise in rate). Either phenomenon will dramatically increase the chances of a premature screen-out.

Nevertheless, fracturing with slickwater can be very successful in unconventional reservoirs and there is little doubt that proppant is penetrating further into the fracture network than the current models predict. One reason for this may be the phenomenon described as sheet flow (see **Fig. 17.30**). Sheet flow has been replicated under laboratory conditions and occurs when the slurry flows in the narrow gap between two fracture faces. Surface effects from the fracture faces act to slow the flow velocity adjacent to the faces, beyond what is normally predicted. Because mass is being conserved, the flow velocity in the center of the gap has to increase. This has the effect of concentrating the proppant into a higher-velocity "sheet" in the center of the fracture, which allows the proppant to penetrate further into the fracture network.

17.3.3.4 Proppant Transport in Hybrid Treatments

While considerable volumes of slickwater are pumped into the fracture network during a hybrid treatment, most of the proppant mass is slurried into high-viscosity fluids. Under the relatively low shear conditions inside the fracture network, high-viscosity and low-viscosity fluids will not mix together. Instead, as the high-viscosity fluid is pumped into the fracture or fractures, it will flow along the path of least resistance, displacing the low-viscosity fluid into other parts of the fracture.

This "path of least resistance" is defined by two phenomena: convection and the tendency of the viscous fluid to follow the widest flow channel available (larger width = lower resistance to flow). This second phenomenon means that the slurry will follow channels created by contrasts in rock mechanical characteristics, especially effective closure stress and Young's modulus (see **Fig. 17.31**). This effect, which is often referred to as viscous fingering, is quite beneficial, as it means that the proppant-laden slurry can often penetrate a lot further into the fracture than simulations predict—and is probably one of the main reasons why hybrid fracturing has proven to be so successful in unconventional reservoir fracturing (that is, provided the widest flow channels are not located in unproductive strata). However, it should be remembered that this phenomenon can only occur in fractures with significant vertical contracts in fracture width. In a uniformly wide fracture, the "least energy" solution is a piston-like displacement of the low-viscosity fluid by the high-viscosity fluid, across a relatively uniform front. Consequently, knowledge of the rock mechanical properties and whether or not there will be sufficient vertical contrasts to provide regions of increased width can be a significant factor in deciding whether or not to perform a hybrid treatment.

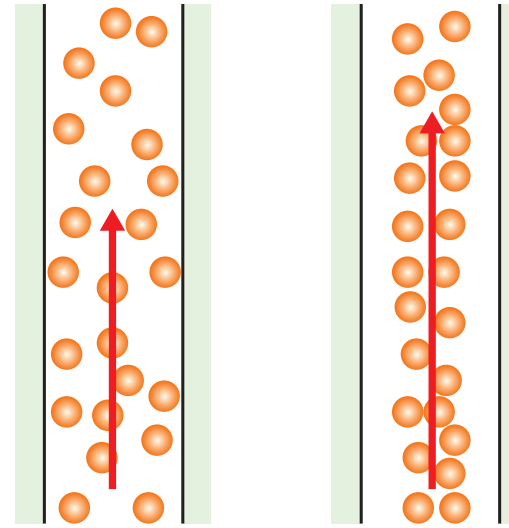

Fig. 17.30—Diagram illustrating how proppant is concentrated into a "sheet" in the middle of the flow channel when entrained in a low-viscosity fluid.

17.3.4 Reservoir-Specific Considerations

Reservoir response to the hydraulic fracture stimulation and fluid recovery from reservoir rocks is governed by several parameters, including reservoir pressure, water saturation, and the rock mineralogy.

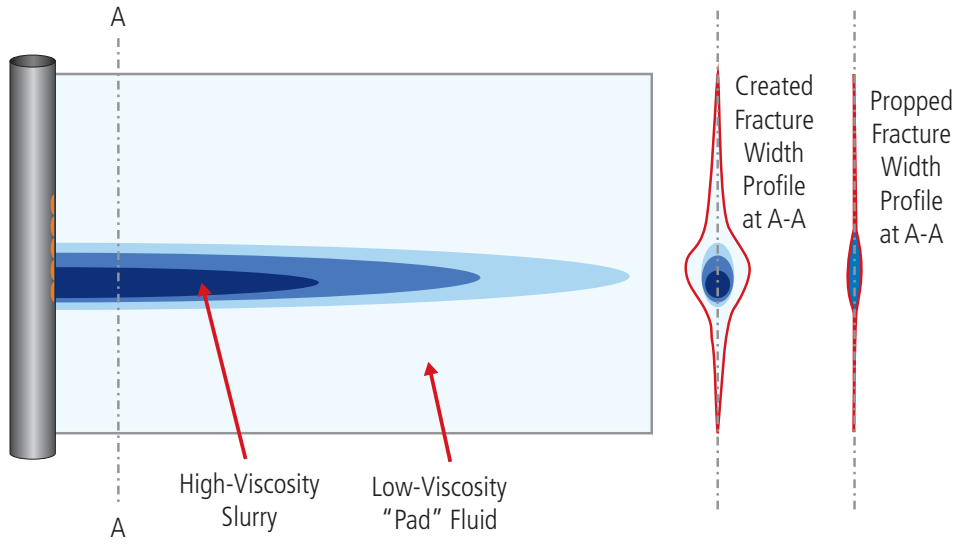

Fig. 17.31—Diagram illustrating the "viscous fingering" effect that can lead to proppant being successfully placed deep into the fracture network during hybrid treatments.

17.3.4.1 Reservoir Pressure

Reservoir pressure has four main effects on hydraulic fracture treatments in unconventional reservoirs:

1. In gas reservoirs, pressure is reserves, quite literally. The higher the pressure, the more reserves are present in the formation. Consequently the economic viability of both the individual fracturing operation and the reservoir development as a whole is heavily influenced by reservoir pressure.

2. In conventional reservoirs, with significant fluid leakoff into the rock matrix, reservoir pressure is one of the factors that control this leakoff—the lower the reservoir pressure, the greater the leakoff. Thus, when designing treatments, greater allowance for fluid leakoff has to be made for low-pressure reservoirs. In the case of unconventional reservoirs, fluid leakoff (or more correctly, fluid loss) is primarily via natural fractures rather than through the rock matrix. In this case, reservoir pressure heavily influences the ability of the fracturing fluid to penetrate and then open the natural fractures.

3. As discussed in more detail later in this chapter, reservoir pressure can significantly influence the effective stresses in a formation. A depleted interval can have radically different stress characteristics compared to a similar interval at virgin pressure, even to the extent of altering fracture azimuth. This effect can also influence the closure stress experienced by the proppant and hence proppant type selection.

4. Reservoir pressure has a massive influence on fluid recovery after fracturing operations. Although significant fluid can usually be recovered from a formation by flowing it back as soon as possible after the cessation of pumping operations (and thus using the energy stored as elastic strain in the rock around the fracture(s)), ultimately we are relying on reservoir pressure to maximize fluid recovery. In spite of many well-publicized isolated instances of wells thriving after little or no post-fracturing fluid recovery, in general the more fracturing fluid we recover, the better the well will be. Indeed, one of the main reasons why such a high percentage of fractured intervals fail to produce after fracturing (Hodenfield 2012, Bazan et al. 2010) is because of the inability to recover treatment fluids, due to localized variations in reservoir pressure (and other formation properties) along the wellbore. If the reservoir pressure is below the hydrostatic gradient of the fracturing fluid, then extra energy will be needed to recover the fluid—usually in the form of a pump, gas lifting or from incorporating gasses (usually CO_2 and/or N_2) into the treatment fluid (which both adds energy to the system and reduces the hydrostatic head). So in this instance reservoir pressure is hugely significant, as the recovery of the fracturing fluid from the formation is just as important as the treatment itself.

17.3.4.2 Water Saturation

Aside from the obvious effect that water saturation has on the reserves held in a formation, there are also a few considerations that need to be taken into account when designing and performing fracture stimulation treatments.

Reservoirs with high water saturation are likely to produce significant quantities of water. This will have a major effect on productivity due to the effects of multiphase flow in the propped fractures and capillary pressures (see Chapter 7 of Economides and Martin 2007). These effects are especially significant in unconventional wells, where fracture propped width and conductivity is relatively much smaller than for conventional wells. Formations that are expected to produce significant quantities of water must be designed with greater fracture conductivity to compensate for these effects.

Reservoirs with low water saturation—especially "dry" gas reservoirs—are likely to be undersaturated. This means that the formation will absorb water from the fracturing fluid and that this water will react with minerals in the formation. The effect of this can be to radically alter the characteristics of the formation, turning hard formations into locally soft rocks and releasing huge quantities of fines. It is vital that this is taken into account when designing the fracturing fluid, in order to minimize changes to the formation adjacent to the fracture(s).

17.3.4.3 Mineralogy

This section deals with the very specific aspects of shale mineralogy that affect fracture propagation and treatment design. A more detailed discussion on this subject can be found in Chapter 8 of this book.

17.3.4.3.1 Rock Mechanical Properties

The mineralogical composition of shales can have a significant effect on the outcome of a stimulation treatment. Work by Sonnenberg (2012) and Alqahtani (2013) suggests that shales with a clay composition greater than around 60% will behave in a ductile fashion (see **Fig. 17.32**). This has serious implications for generating a fracture network and maximizing stimulated reservoir volume. Put simply, brittle rocks fracture easily while ductile rocks do not. This is the difference between hitting a pane of glass (brittle) with a hammer and a piece of mild steel (ductile). Both materials are mechanically strong, but only one of them exhibits low fracture toughness (a.k.a. brittleness). Moreover, ductile rocks are unlikely to possess the natural fracture network required in order to develop the required stimulated reservoir volume (ductile rocks are just as resistant to the propagation of natural fractures as they are to the propagation of hydraulic fractures).

This means that (in general) shales with high clay content are probably much more difficult to develop economically, as they cannot be easily fractured effectively. Consequently, knowledge of the mineralogy can have a very significant effect on reservoir development decisions. On a smaller scale, localized variations in clay composition along an individual wellbore could easily turn the local rock from brittle to ductile and vice versa. This means that knowledge of the mineralogy is essential when selecting which specific intervals to fracture.

17.3.4.3.2 Fracturing Fluid Composition

With regard to the effect of mineralogy on fracturing fluid composition, formations tend to fall into one of three categories:

1. Formations that can be fractured with water-based fracturing fluids with little or no detrimental effects on post-treatment productivity. This includes formations that require basic clay control via systems such as 2% KCl, low-cost KCl substitutes, or sea water.

2. Formations that require significant treatment fluid alteration in order to use water-based fluids. This "alteration" can involve the use of sophisticated clay control, surfactant, and fluid recovery additives, as well as the replacement of some of the water by methanol, N_2, and/or CO_2.

3. Formations that should not be fractured using water-based systems.

Clay composition is the main area to pay attention to, and not just the overall clay composition. The individual composition of minerals such as smectite, montmorillonite, chlorite, illite, kaolinite, and mixed-layer clays can also be significant. Feldspars and (especially) xeolites can also be problematic. To make matters more complex, the percentage present is only an indication of potential problems. Formations with undersaturated clays (especially smectite and montmorillonite) can soak up water like a sponge, even when the clay composition is relatively low (see Bennion 1996, Davis and Wood 2004). Formations with disintegrating clays (such as kaolinite) can see dramatic reductions in hardness, which can lead to proppant embedment. The problems are manifest and while an accurate knowledge of the mineralogy can be of real benefit, the only way to be sure of fluid compatibility is to test with well-preserved core

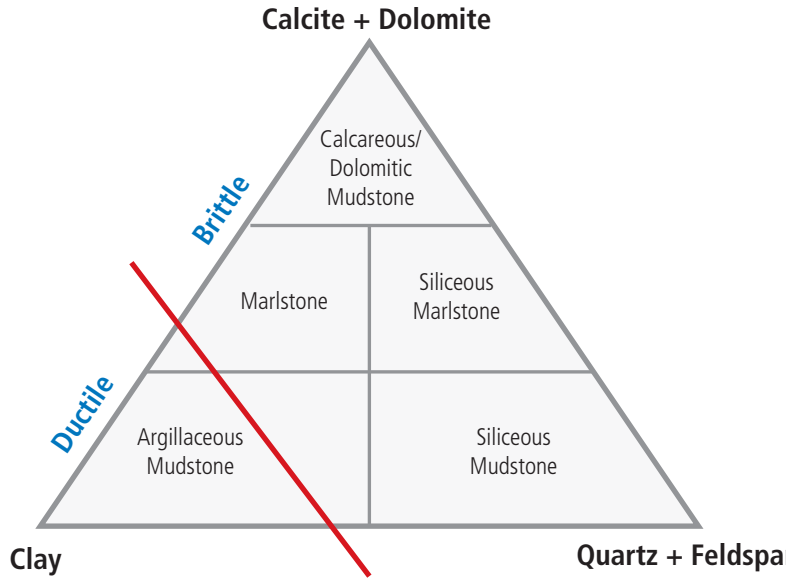

Fig. 17.32—Diagram illustrating the mineralogical characterization of shale reservoirs and the particular effect of clay composition on ductility and brittleness. (Adapted from Sonnenberg 2012.)

samples. See Chapter 7 of Economides and Martin (2007) for a more detailed discussion on this subject.

17.3.4.4 Oil and Liquids-Rich Reservoirs

Two major factors must be accounted for when designing treatments for oil- and liquids-rich unconventional reservoirs:

1. Treatments must be designed to produce increased fracture conductivity to account for multiphase flow effects in the fracture and for the fact that the oil or condensate has a much lower mobility than gas. Consequently, greater proppant concentrations are required per unit area in the fracture, which can be offset to a certain extent by using larger grain sizes and/or better quality proppant. This means higher proppant concentrations in the treatment fluid and even the use of highly viscous fluids with which to transport the proppant.

2. Fluids must contain a non-emulsifier in order to prevent emulsions from forming with the native crude. This is also true of "liquids-rich" reservoirs and the retrograde condensate they produce—in spite of the "light" nature of the condensate, there have been enough documented instances of emulsions forming with fracturing fluids that precautions still need to be taken. Ideally, fracturing fluids should be tested with the crude or condensate from the actual formation to be treated in order to ensure the functionality of the emulsion prevention/breaking additives (Ely 1994, Baker Hughes Inc., 2014b). Failing this, they must be tested with the closest and freshest offset fluids available.

17.3.4.5 Gas Reservoirs

Unconventional gas reservoirs—and especially dry gas reservoirs—are the easiest to design for in terms of treatment fluid requirements. Slickwater fracturing is common and there is no need to design for the presence of crude oil or condensate. Instead, the emphasis is on fluid recovery and compatibility with the often water-sensitive formation. Fluids should be designed for minimum surface tension, minimum interaction with the minerals in the formation, and for maximum fluid recovery (Bennion 1994, Davis and Wood 2004, also Chapter 7 of Economides and Martin 2007).

17.3.5 Treatment Style Selection

17.3.5.1 Fracturing Fluid Methodology

With reference to the fluid systems described in the previous section, unconventional fracturing operations can be roughly split into three main types of treatment, of which types 1 and 3 are the most prevalent.

1. **Slickwater Treatment.** This type of treatment uses water with no increased viscosity. Proppant transport is via turbulent flow. Very few chemical additives are used in the

fluid, other than friction reducers, surfactants, clay control additives, and/or biocides. This type of treatment is often the default position for fracturing shale reservoirs, due to the fluid's low cost, the relative ease to flow back and either recycle or dispose of the flowback fluids. This treatment has been demonstrated to promote more complex fracture growth than viscous fluid systems (Mayerhofer et al. 1999, Schein et al. 2004, and Schein 2005). However, slickwater fracturing has several disadvantages:

- Because turbulent flow is the only mechanism for transporting proppant, pumping rates have to be very high in order to keep the proppant moving down the fracture. Empirical operational experience has shown that the faster these treatments are pumped, the better the post-treatment production. This is quite simply because the faster the treatment is pumped, the easier it is to maintain turbulent flow in the furthest parts of the fracture network and hence the more likely it is to place proppant further away from the wellbore.
- Again, because turbulent flow is the only proppant transport mechanism, proppant will quickly settle out in areas of the fracture that do not experience turbulent flow. This results in large areas of the fractures—especially the upper parts—being left unpropped, especially in the often-lengthy period of time between the end of pumping operations and fracture closure.
- Because the ability to keep the proppant moving is inversely proportional to proppant density, slickwater fracturing is not recommended when using higher strength (i.e., higher density) proppant systems.
- Slickwater fracturing is very hard on fracturing equipment, especially the fluid ends of the high-pressure pumps. The inability of the fluid to suspend the proppant except under very high shear conditions results in proppant dropping out in the fluid end and ultimately causing sometimes quite catastrophic failure. This means that most fracturing service companies will not pump proppant in excess of 1.0 to 1.5 ppa concentrations in slickwater.

2. **Viscous Fluid Treatment.** More often used in conventional fracturing, a viscous fluid treatment uses either a crosslinked polymer gel or a viscoelastic surfactant (VES) to provide sufficient viscosity to transport the proppant, regardless of the level of shear being seen by the fluid. These fluid systems are much more benevolent to the fracturing equipment and are capable of carrying even high-density proppant systems to the extremes of the fracture network. Unfortunately, microseismic monitoring and empirical production data have demonstrated that viscous fluid treatments tend not to generate the same level of fracture complexity as non-viscous fluid systems, presumably because of the difficulty of forcing an extremely viscous fluid into a very narrow natural fracture. In addition, these fluids are more expensive, harder to flow back and more difficult to recycle or dispose of than slickwater systems.

3. **Hybrid Treatments.** As the name suggests, hybrid treatments are a combination of slickwater and viscous fluid treatments, attempting to harness the advantages of both while minimizing the disadvantages. Hybrid treatments use slickwater fluid systems for the pad stages of the treatment (the pad is a stage containing no proppant, designed simply to create and extend the fracture or fractures, prior to the proppant being placed in subsequent stages), linear gels for low proppant concentrations (up to perhaps 1.5 ppa), and a crosslinked polymer gel or VES system for higher proppant concentrations. The idea is to spend as much time as possible pumping slickwater to maximize the complexity of the fracture network and use the minimum sufficient viscous fluid to carry the proppant.

Hybrid fluid treatments are becoming increasingly popular as more challenging shale reservoirs and plays are becoming developed. The need for higher proppant concentrations and higher density proppant systems, while at the same time continuing to maximize fracture complexity, has led to a rapid expansion in their use. Hybrid fluid treatments are recommended as the default position for any treatment design, unless there is significant offset data to recommend an alternative treatment method.

17.3.5.2 Influence of Temperature

Temperature is the mortal enemy of viscosity and fluid stability. As the formation temperature rises, it becomes increasingly difficult to maintain the proppant transport characteristics of crosslinked and VES fluid systems. So while temperature doesn't have that massive an effect on the design of slickwater treatments, it can have a significant effect on the design of viscous fluid and hybrid treatments. However, considerable high temperature fluid system technology exists, developed for conventional and tight gas fracturing. Generally speaking though, the more temperature stability that is required, the more expensive a viscous fluid system will end up being in order to be compliant with all the systems' requirements.

Temperature does also have an effect on the additives used in slickwater systems, especially surfactants and clay control additives, but this is relatively minor compared to the effects it has on fluid viscosity.

The other major effect of temperature is on the completion system. Fracturing fluids will cool down the wellbore dramatically during a treatment, even if they do rapidly heat up as they penetrate into the formation. Cool down of the completion can cause significant thermal shrinkage of tubular components, a phenomenon that is made worse by the internal pressure effects of the treatment. If this shrinkage is not designed for, considerable damage can be caused to critical completion components. See Chapter 16 for a more detailed discussion about completion systems.

17.3.5.3 Influence of Closure Stress

The closure stress of the formation is stress that has to be overcome in order to keep the fracture open. Remembering that pressure and stress are essentially the same thing, the closure stress is, therefore, the minimum pressure the fluid needs to be in order to keep the fracture open. The fluid has to be above this pressure to make the fracture or fractures propagate. Closure stress is equal to the effective stress in the formation in a direction perpendicular to the plane of the fracture. In most cases, this means that the closure stress is equal to σ_h. Closure stress has two main direct effects on treatment design:

- Closure stress directly affects the surface treating pressure (STP) or injection pressure, p_{inj}, as demonstrated in **Eq. 17.12**:

$$p_{inj} = p_c + \Delta p_{tort} + \Delta p_{pf} - \Delta p_{head} + p_{pipefriction} \quad \textbf{(Eq. 17.12)}$$

where p_c is the closure pressure (or stress), Δp_{tort} is the pressure loss due to tortuosity, Δp_{pf} is the pressure loss due to perforation friction, p_{head} is the hydrostatic head or pressure of the fluid in the wellbore and $p_{pipefriction}$ is the friction pressure of the fluid in the wellbore. Put simply, the higher the closure pressure, the higher the injection pressure will be, which has implications for equipment MWP (maximum working pressure) ratings and for the pumping capacity (i.e., hydraulic horsepower) required in order to pump the treatment.

- Closure stress also affects the proppant selection. As closure stress is the stress trying to force the fracture closed, it is also the stress that the proppant needs to resist in order to keep the fracture propped open. Consequently, the higher the stress, the stronger the proppant needs to be. As closure stress generally increases roughly proportional to depth, deeper formations require stronger proppant. When selecting proppant, remember that closure stress is not a constant. The effective minimum stress in the formation is a function of pore pressure and so reservoir depletion should be allowed for when selecting a proppant.

17.3.5.4 Influence of Proppant Type and Concentration on Treatment Fluid Selection

The majority of fracturing operations in unconventional reservoirs are performed using slickwater systems. This is the fluid system of choice due to low cost, easy fluid recovery, ease of fluid disposal or recycling, and the capability to comfortably over-displace the treatment at the end of an interval. There is also considerable evidence that slickwater systems will produce increased fracture complexity and a more efficient stimulated reservoir volume, than more highly viscous fluid systems (Mayerhofer et al. 1999, Schein 2004 and 2005).

However, the Achilles' heel of slickwater fracturing is its inability to transport proppant by any other means than turbulent flow. This means that any time sand is pumped at more than around 1.25 ppa, or any time high-density proppants are used, additional viscosity must be added to the fracturing fluid. This can take the form of a very weakly crosslinked fluid system (Brannon and Bell 2011), designed purely to transport the proppant past the point where it makes a right-angled turn from the wellbore and into the fracture(s), conventional crosslinked fluid systems, and viscoelastic surfactant fluid systems. Large areas of the Barnett shale—the first shale play to see widespread economic exploitation—can be successfully fractured using 100% slickwater systems. However, operators soon found that when this technology was transferred to more difficult to exploit shale plays (e.g., the Haynesville or the Eagle Ford) the proppant types and concentrations that worked for the Barnett were insufficient for effective stimulation. This led to the advent of hybrid treatments, which combine the efficiencies and effectiveness of slickwater treatments, with the proppant transport capabilities of highly viscous fracturing fluids.

Finally, do not let the tail wag the dog. Treatment design and proppant selection should never be driven by an overwhelming desire to simply use slickwater because that's what works elsewhere. Instead, proppant type and concentration should be driven by formation characteristics and this in turn should drive fluid selection (Rylance and Martin 2014).

17.4 Geomechanics and Fracture Modeling

17.4.1 Open Versus Cased Hole Stimulation

A more detailed discussion on this topic can be found in Chapters 8 and 15 of this book.

From a stimulation perspective, openhole completions allow for a much cleaner connection between the wellbore and the fracture, especially for transverse fractures. Generally speaking, far less tortuosity is experienced when using openhole completions. They are also much cheaper than cased, cemented, and perforated completions. However, they also have their disadvantages:

- Because the packer elements are generally 300 to 500 ft. apart, precise control of fracture initiation is not possible.
- Zonal isolation is dependent upon the quality of the seal between the packer elements and the wellbore. If wellbore quality is poor, isolation will be problematic.
- The packer elements tend to affect the hoop or circumferential stresses around the wellbore, increasing the chances of the fracture(s) initiating close to the packer. Not only does this affect the sealing qualities of the packer, it can also reduce stimulation efficiency, as the fracture(s) in the interval on the other side of the packer may also initiate at the same place, providing double stimulation of one area and zero stimulation of others.
- When the packers have been set, there is very little scope for changing stimulation strategy, other than the design of the treatment stages themselves. By contrast, when using a cemented and perforated completion, the stimulation strategy for intervals further up the wellbore can be changed as a result of the performance of stimulation treatments further down the wellbore.

It is recommended that openhole completions only be used in well-known formations, where stimulation characteristics of the formation are well understood and there is little need to change the stimulation strategy from one interval to another. Cemented and perforated completions should be used in cases where there is significant uncertainty or in cases where the bottomhole conditions (e.g., temperature, wellbore quality) prevent the use of openhole completions.

17.4.2 Near-Wellbore Effects

17.4.2.1 Formation Breakdown

Normally, it takes pressure significantly in excess of the pressure required to propagate a fracture or fractures, in order to initiate the fracture from the wellbore. This additional pressure is often referred to as the breakdown pressure, p_b, and is caused by the geometry of the wellbore and the influence of pore pressure on the effective stresses. It has been demonstrated that the breakdown pressure for a vertical wellbore can be calculated from **Eq. 17.13**, provided that the rock around the wellbore has no significant tensile strength or any significant plastic deformation before failure occurs (Martin 2009).

$$p_b = \left(\frac{2\nu}{(1-\nu)}\right)(g_{ob}H - \alpha p_r) + \alpha p_r \quad \textbf{(Eq. 17.13)}$$

where ν is the Poisson's ratio, g_{ob} is the overburden stress gradient, H is the true vertical depth, α is Biot's poroelasticity constant (Biot 1941 and 1956), and p_r is the local reservoir or pore pressure. Rearranging this equation gives a slightly different emphasis:

$$p_b = \left(\frac{2\nu}{(1-\nu)}\right)g_{ob}H + \left[1 - \left(\frac{2\nu}{(1-\nu)}\right)\right]\alpha p_r \quad \textbf{(Eq. 17.14)}$$

From **Eq. 17.14** we can see that the local pore pressure has varying effects upon the breakdown pressure. This is illustrated in **Fig. 17.4a**, which shows us that if $\nu > 1/3$, then the function $\left[1 - \left(\frac{2\nu}{(1-\nu)}\right)\right]$ is negative, while if $\nu < 1/3$ then this function is positive. This in turn means that if $\nu > 1/3$ then an increase in localized pore pressure will act to decrease the breakdown pressure, while if $\nu < 1/3$ then an increase in localized pore pressure will act to increase the breakdown pressure.

This result is important if we remember that a localized increase in pore pressure is usually caused by pumping into the formation. It explains why some formations are easy to break down, while others are difficult. It also explains why some formations are easy to initially break down, but are very difficult to break down during subsequent injections.

It should be remembered that the above effect is for a vertical well. The relationship between Poisson's ratio, pore pressure, and breakdown pressure is significantly more complex for a horizontal wellbore, as it also involves the azimuth of the wellbore to the principle horizontal stresses. This will be the subject of further work. However, it is clear that pore pressure and Poisson's ratio still have a significant effect on breakdown pressure (see **Fig. 17.33**).

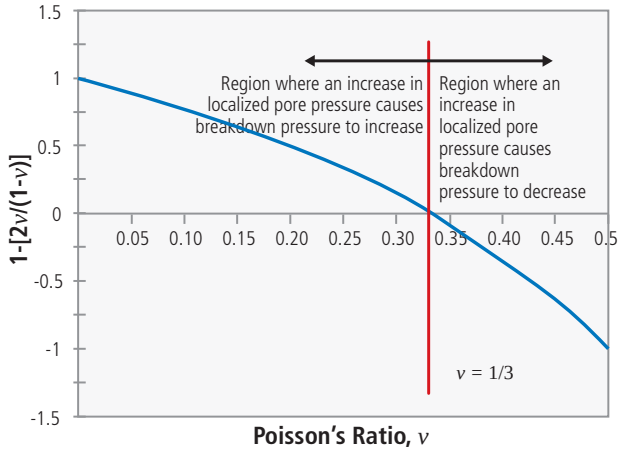

Fig. 17.33—Chart illustrating how Poisson's ratio controls the effect that pore pressure has on formation breakdown, for a vertical wellbore.

17.4.2.2 Tortuosity

Tortuosity is a huge topic and a full discussion is beyond the scope of this work. The reader is invited to read Chapter 6 of Economides and Martin (2007) plus the associated references, for a detailed description of this phenomenon.

Tortuosity can be thought of as a restricted flow path between the wellbore and the main body of the fracture or fractures. It manifests itself as loss of pressure (= loss of energy) in the fracturing fluid as it passes through the near wellbore region, over and above that caused by perforation friction. This means that fracture simulations that do not account for tortuosity assume that the fracturing fluid contains more energy to propagate the fracture than it actually does. This in turn produces a simulation with larger fractures and hence the potential for an early screen-out (as proppant volumes and concentrations are designed for longer, wider fractures), as well as less effective stimulation in low-permeability reservoirs (as the area of contact with the reservoir is smaller than planned for).

The restricted flow path caused by tortuosity can also severely limit the proppant concentration that can be transmitted to the main body of the fracture(s). Often, a low proppant concentration can be transmitted without any significant problems, while a higher concentration cannot, resulting in a very rapid screenout as the higher proppant concentration reaches the near wellbore region. Near wellbore screen-outs caused by tortuosity are responsible for the vast majority of premature screen-outs.

Factors that tend to increase the effects of tortuosity include:

Too many perforations. Every perforation is a potential source of fracture initiation and so the more perforations that exist, the greater the potential for a complex connection between the wellbore and the fracture(s). Do everything possible to minimize the number of perforations—when fracturing, always go with a small number of large holes, rather than a large number of small holes. By implication, this also means that openhole completions tend to suffer from much less tortuosity than cased and perforated completions.

Wellbore azimuth and deviation. As discussed previously (see Section 17.3.2), hydraulic fractures propagate along the path of least resistance, which usually means that they run on a vertical plane, parallel to the azimuth of the maximum horizontal stress. They will propagate in this direction, regardless of the azimuth and deviation of the wellbore. This means that unless the wellbore is drilled either vertically or perpendicular to the azimuth of the minimum effective in-situ stress, the fracture will be on a different plane to the wellbore. As the fracture propagates through the region close to the wellbore, it will move from a region where the stresses are dominated by wellbore-based effects, to a region where the stresses are unaffected by the wellbore. This can often mean a radical and sudden change in orientation of the fracture plane. This sudden turn can result in a very restricted flow path.

Transverse fractures. As discussed previously, transverse fractures have a very limited area of contact with the wellbore. This can lead to a very restricted area of flow for the fracturing fluids.

Formation characteristics. Hard (i.e., high Young's modulus) and brittle (i.e., low fracture toughness) formations tend to be more susceptible to tortuosity than soft and ductile formations.

Perforation type. For reasons not yet clearly understood by the industry, perforations cut by abrasive jetting tend to generate less tortuosity than perforations generated by explosive charges. While much of this effect may simply be due to the fact that there tends to be fewer perforations cut when using abrasive methods than when using explosive methods, there is also very significant empirical evidence indicating that something more fundamental is also occurring (Demarchos and Porcu 2006, Schultz et al. 2007, Castaneda et al. 2010).

17.4.2.2.1 Strategies for Mitigating Tortuosity and Its Effects

- Whenever possible reduce the number of perforations to a minimum.
- Whenever possible, try to perforate in vertical lines of perforations, rather than in spirals.
- Whenever possible, align the wellbore with the fracture azimuth.
- Whenever possible, align the perforations with the fracture azimuth.
- Try to avoid deep penetrating perforations, unless these are perfectly aligned with the fracture azimuth. Short, wide holes are better for fracturing.
- Avoid fracturing deviated wellbores unless it is perfectly aligned with the fracture azimuth—instead, try to drill S-shaped wells that penetrate the formation vertically.
- When drilling horizontal wells, longitudinal fractures exhibit less tortuosity than transverse fractures.
- In most cases, especially in horizontal wells, openhole completions exhibit less tortuosity than cased, cemented, and perforated wellbores.
- Never add more perforations to a wellbore that already exhibits significant tortuosity. All you will do is bring additional complexity to an already over-complicated near wellbore region. In general, you cannot perforate through or past tortuosity.
- Try to minimize the number of intervals being fractured simultaneously and to minimize the vertical height of the perforated interval.
- There is no substitute for fluid viscosity when trying to transmit proppant through near wellbore tortuosity. Crosslinked or VES fluid systems are far less likely to screenout than slickwater systems.

Tortuosity is one area were prevention is much better than cure. Everything possible and practical should be undertaken to mitigate the potential for tortuosity. However, often options are limited for a variety of reasons. Furthermore, some formation can exhibit significant tortuosity effects no matter what mitigation steps are taken. In these situations, remedial action can be taken, but this is costly and not guaranteed to be reliable. Descriptions of these techniques can be found in Kogsbøll et al. (1993), Cleary et al. (1993) and De Melo et al. (2012).

17.4.2.3 Geometric Skin Effects

As already discussed earlier in the chapter, transverse fractures have a very limited area of contact with the wellbore. This leads to a choking effect, which occurs as the flow in the fracture changes from linear in the very large main area of the fracture, to radial by the wellbore (see **Fig. 17.34**). This choking effect is common to both oil and gas reservoirs, because it is purely a function of flow geometry. However, gas wells—especially high rate gas wells—will also experience additional turbulent non-darcy flow effects, as the gas velocity increases massively as it approaches the wellbore (refer to the discussion on the Forchheimer Equation earlier in this chapter). In very high permeability gas formations, the phenomenon is so pronounced that even vertical fractured wells are more productive than transversely fractured horizontal wells. See also Table 17.2.

Mukherjee and Economides (1991) demonstrated that in transverse fractures, the very small area of contact between the fracture and the wellbore resulted in an additional skin effect (a "choke skin," *sc*) as demonstrated in **Eq. 17.15**:

$$sc = khwkf\ln h2rw - \pi 2 \qquad \textbf{(Eq. 17.15)}$$

where h is the net height of the formation and rw is the wellbore radius. Wei and Economides (2005) demonstrated the effect of this choke skin on wellbore productivity in **Eq. 17.16**:

$$J_{DTH} = \frac{1}{\frac{1}{J_{DV}} + s_c} \qquad \textbf{(Eq. 17.16)}$$

Where J_{DTH} is the dimensionless productivity index for a single transverse fracture on a horizontal wellbore and J_{DV} is the dimensionless productivity index for a single fracture on a vertical wellbore (for a full discussion on dimensionless productivity index and its applicability to hydraulic fracturing, see Martin and Economides 2010).

This limited area of contact between the fracture and the wellbore has two further effects. First, in gas wells the energy loss caused by non-darcy flow effects is further exacerbated as the gas flows into an ever-decreasing area. Second, the restricted flow applies in both directions, such that pumping the fracture treatment can be difficult, often resulting in premature screen-outs as the proppant fails to pass through the restricted area and on into the main body of the fracture (a phenomenon which is referred to as tortuosity—see the previous section).

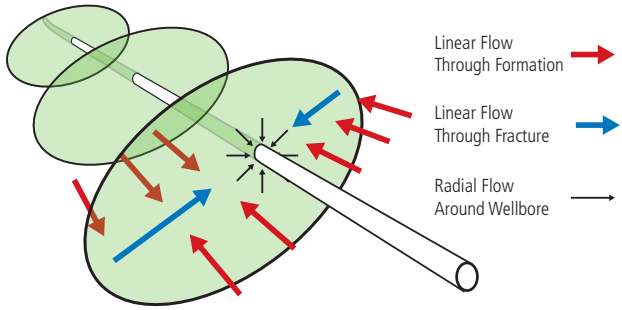

Fig. 17.34—Diagrammatic illustration showing how flow changes from formation linear to fracture linear and then to radial as the reservoir fluids approach the very limited area of contact with the wellbore

17.4.3 Stress Effects

For further detailed discussions about stress effects, please refer to Chapter 9.

17.4.3.1 Interaction of Multiple Parallel Hydraulic Fractures

Propagating parallel fractures interact with each other in two main ways. The first way they interact is through fluid leakoff—as fluid leaks off from one fracture it increases the pore pressure in the rock adjacent to the fracture and if the parallel fracture is close enough, reduces the leakoff from the parallel fracture and vice versa. Thus competing parallel fractures—provided they are sufficiently close—can decrease fluid leakoff and thus increase fluid efficiency and fracture volume. However, primary fluid leakoff (i.e., through the rock matrix) is considered to be almost negligible in shale formations and so this effect is not considered to be significant in unconventional fracturing.

The second way that parallel fractures interact mechanically is considered to be significant in unconventional reservoirs as the significance and extent of this interaction is a function of the mechanical properties of the formation and not the permeability. A qualitative illustration of how multiple parallel fractures interact is shown in **Fig. 17.35**, where d is the horizontal separation between fractures, and h is the fracture height.

To what extent each fracture influences each other is largely determined by the ratio h/d and the formation's rock mechanical properties, and is described by a dimensionless function known as the stiffness or Ψ, which itself is a function of E. The mathematics behind Ψ is complex but the function is defined such that as d/h $\rightarrow \infty$, $\Psi \rightarrow 1$ (indicating no reduction in width) and as d/h $\rightarrow 0$, $\Psi \rightarrow 0$ (indicating zero fracture width). Most published literature on this subject agrees that for values of d/h > 3, no significant mechanical interaction occurs between the parallel fractures. In the region 3 > d/h > 1 fracture width is reduced and below d/h < 1 mechanical interaction could significantly affect the interior fractures' ability to accept and transmit proppant. More details of this process can be found in Warpinski and Teufeul (1987), Dahi-Taleghani and Olsen (2009), Britt and Smith (2009), and Meyer and Bazan (2012).

17.4.3.2 Influence of Pore Pressure and Depletion

Assuming no tectonic influence over the horizontal stresses, the closure stress, σc (which is equal to the effective minimum in-situ stress, usually σh), can be expressed as follows:

$$\sigma_c = \frac{v}{(1 - v)}(\sigma_v - \alpha p_r) + \alpha p_r \qquad \textbf{(Eq. 17.17)}$$

Differentiating **Eq. 17.17** (which is essentially the same as **Eq. 9.28** in Chapter 9 without the tectonic component) with respect to pore pressure yields the following result (from Chapter 13 of Economides and Martin 2007):

$$\frac{\delta \sigma_c}{\delta p_r} = \alpha \left[1 - \frac{v}{(1 - v)}\right] \qquad \textbf{(Eq. 17.18)}$$

Eq. 17.18 allows us to estimate the effect of depletion on closure stress for given values of Poisson's ratio, as illustrated in **Fig. 17.4d**.

Ultimately, pressure depletion-driven effective stress change is one of mechanisms that drive the effectiveness of refracturing in conventional reservoirs (Ebel and Mack 1993; Wolhart 2004). Because the fracture tends to deplete the reservoir preferentially along one plane, the effective stresses are also altered preferentially along this plane (see **Fig. 17.36**). This can lead to a radical change in direction of the minimum effective stress in the formation, which in turn can lead to a new hydraulic fracture propagating in an entirely different azimuth. This phenomenon is well documented in conventional reservoirs. There have also been some well-documented instances of successful refracturing in shale reservoirs, although it is not clear whether these successes were due to fracture reorientation, or simply the application of more appropriate and effective treatment design (Lantz et al. 2007; Potapenko et al. 2009)—or indeed, both.

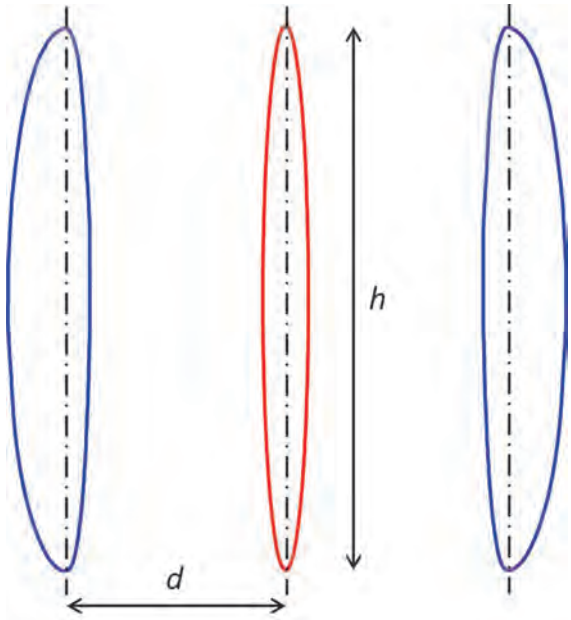

Fig. 17.35—Diagram illustrating how multiple parallel fractures can experience a reduction in width due to increased effective stresses between the fractures, caused by compaction of the rock either side of the fractures as they expand. Adapted (Meyer and Bazan 2011).

17.4.3.3 Far-Field Diversion

In unconventional fracturing, far-field diversion occurs when hydraulic fractures from different wellbores interact, affecting the stimulated reservoir volume of one or both of the fracture networks. Most commonly this occurs when fractures from parallel wellbores interact with each other. Evidence from both laboratory experiments and microseismic fracture mapping indicates that when fracture networks interact, one of two different patterns will be followed:

If one network is still propagating and has fluid with positive net pressure inside it, while the second network is pre-existing and does not have high-pressure fluid inside it, then when the high-pressure network contacts the low-pressure network, growth in the high-pressure network stops abruptly, as the high-pressure fluid starts to flow into the low-pressure network. As fluid pressure bleeds off rapidly in the high-pressure network, the net pressure quickly falls below zero and new (originally high pressure) fracture network rapidly closes, prematurely ending the treatment and resulting in a smaller than planned stimulated reservoir volume.

If both fracture networks are "pressured-up" and contain fluid with positive net pressure, then the "stress shadowing"

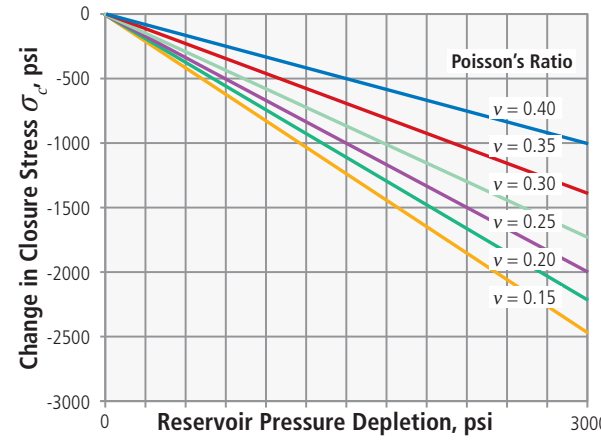

Fig. 17.36—Chart illustrating the reduction in closure stress caused by reservoir depletion (assumes α = 1.0).

effect around the fracture network acts to drive propagating fractures apart. This means that the fracture networks tend to avoid each other rather than fracture into each other.

The effect described in Item 2 above can be deliberately harnessed to help improve fracture network development and maximize stimulated reservoir volume. Two ways in which this effect can be used are illustrated in **Fig. 17.37a** and **Fig. 17.37b**.

With reference to Fig. 17.37, in the "Simo-Frac" process (left-hand side) treatments are pumped down wellbores A and B simultaneously, so that the networks are deliberately pumped into each other, in order to promote both axial fracture network growth and more complex growth within the SRV. On the right-hand side of Fig. 17.37 and also in **Fig. 17.38**, the zipper-fracture process pumps alternate treatments down the parallel wellbores, with the perforation clusters staggered relative to each other. The gray fracture networks in the right-hand side of Fig. 17.37 are fracture networks from further parallel wellbores off to the sides of the diagram and not illustrated. **Fig. 17.39** shows treatments being performed from three different locations simultaneously.

17.4.4 Geological Hazards ("Geohazards")

As discussed previously in several sections of this chapter, the development of a complex and extensive fracture network is essential to the successful development of an unconventional reservoir. In addition, it is essential to keep this fracture network from extending into water-bearing formations. There are many potential causes for failure to develop an extensive, water-free fracture network, many of which are only identifiable after they have been contacted by a propagating fracture network.

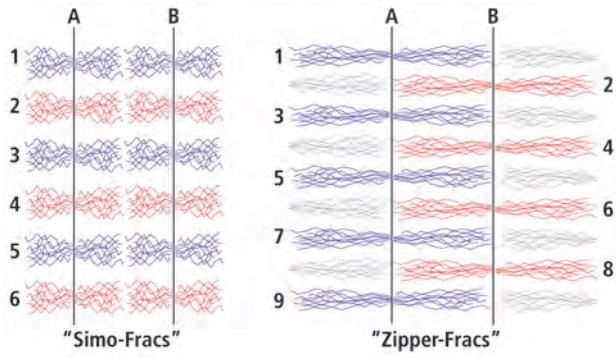

Fig. 17.37—Diagram showing a top-down plan view of two parallel horizontal wellbores, A and B, illustrating how "stress shadowing" effects can be harnessed beneficially to promote stimulated reservoir volume (SRV), with the numbers and colors indicating the order in which the treatments are pumped.

- **Karsts.** In the context of unconventional reservoir fracturing, a karst is an ancient sinkhole in a limestone or dolomitic formation that has been filled up over time with sediments. This produces a region in the limestone or dolomite formation that can have completely different rock mechanical properties—usually resembling the overlying formation, which has filled up the karst as it was deposited. This also means that any fracture that is propagating through the overlying formation will also tend to propagate down into the karst. This has two effects. First, it tends to limit the horizontal growth of the fracture network and second, it has the potential to send the propagating fracture network down into underlying water-bearing formations. This effect has been well documented in the Barnett shale, where microseismic fracture mapping has been used to halt treatments that have been observed to be developing predominantly downward rather than laterally.
- **Faults.** Faults can have the same effect as karsts in that they will stop lateral fracture network growth and send the propagation going upward or downward (or even both) into non-reservoir formations. Clearly, lateral separation from known fault systems, especially lateral separation in the dominant fracture propagation azimuth, is a significant factor in wellbore and treatment design. LaFollette et al. (2012) presented data from more than 211,000 wells in the Barnett shale of east Texas, much of it mapped geographically. These maps showed a significant trend with the best 10% of the wells largely being located away from major fault systems.
- **Barriers to fracture height growth.** Ideally, we want the fracture network to develop laterally from the wellbore and not penetrate out of zone into non-reservoir formations above and below the productive interval. Over- and underlying formations that resist the penetration of conductive fractures tend to force the network to grow laterally, increasing stimulated reservoir volume. Barriers also protect the fracture network from penetrating into water producing intervals. The classic example of this is the Viola-Simpson formation that sits underneath the east Texas Barnett gas shale and above the Ellenberger limestone. The Viola acts as a barrier, which generally prevents fracturing into the highly water-productive Ellenberger. However, the Viola-Simpson pinches out on a line running roughly from the north west corner of Wise county down to central Hill county—wells drilled north east of this pinch-out have no Viola-Simpson to prevent fracture growth down into the Ellenberger. As a result, fracture treatments have to be smaller and wells are subsequently less productive. In order to act as a barrier to upward or downward fracture height growth, there needs to be a contrast in rock mechanical properties between the shale and the barrier. Typically this means increased in-situ effective stress and/or Young's modulus in the barrier, but can also come from higher fracture toughness or even plasticity.

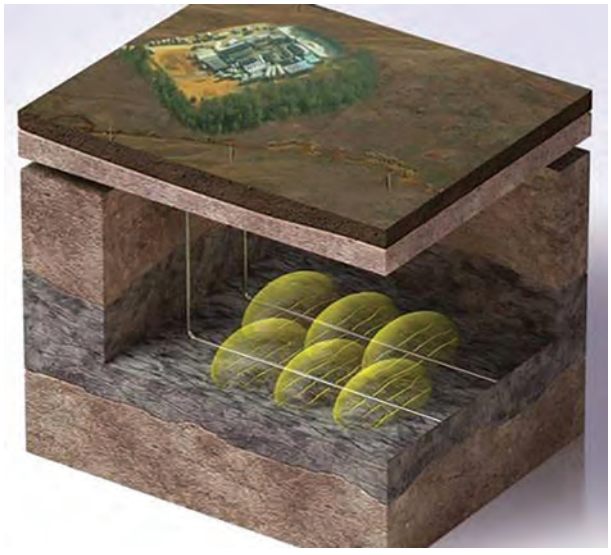

Fig. 17.38—Depiction of how parallel lateral stimulations (zipper fractures) can overlap one another.

17.4.5 Fracture Modeling in Unconventional Reservoirs

Fracture modeling in conventional reservoirs remains problematic. While a discussion on the efficacy of the various fracture propagation models employed by the industry would be inappropriate for this publication, it is fair to say that for the same input data, these models will produce different results. Which is closest to the "truth" is hard to say. However, in reality the more significant problem

is the difficulty in obtaining accurate and reliable data to input into these models. Not only is basic input data such as Young's modulus and permeability often unavailable, even if that data is available, it is probably only valid for a very small region of the formation. We are dealing with a highly stochastic medium, after all. Ultimately, no matter how sophisticated and accurately we can simulate the propagation of the fracture, the leakoff of the fracturing fluid, and the transport of the proppant, the simulation will never be completely accurate due to this lack of input data, as it is impossible to know every relevant formation characteristic for every minute and discrete volume of rock affected by the fracture. Ultimately, successful treatment simulation in conventional reservoirs is as much a product of experience and sound engineering judgment, as it is of physics and engineering science.

So if fracture modeling in conventional reservoirs is problematic, what then of fracture modeling in unconventional reservoirs?

The bad news is that because the fractures in unconventional reservoirs are an order of magnitude more complex than for conventional reservoirs (networks rather than planar fractures), fracture simulations are also an order of magnitude more complex. Even the most advanced attempts to model fracture networks require considerable "tuning" to the formation and so can only be called "predictive" in a specific formation after a considerable amount of fracturing has already been performed. This means that for the foreseeable future, treatment design for unconventional reservoirs will continue to rely more on experimentation and offset case histories, than it will on simulation. While this seems to work adequately in US and Canadian shale plays, the lack of publicly available information and the low numbers of wells makes this a significant issue for operators wishing to exploit unconventional reservoirs elsewhere in the world (Martin 2011 and 2012).

At the time of publication, the most advanced discrete fracture network (DFN) simulator models the fracture network as a series of orthogonal fractures. The model starts with a dominant fracture that propagates on the preferred fracture plane (i.e., perpendicular to the minimum stress) (see **Fig. 17.40**), which then spreads orthogonally on the planes normal to the preferred plane, as illustrated in **Fig. 17.41**.

The user defines a reservoir aspect ratio or λ, which is effectively the ratio of the dimension of the fracture network normal to the preferred fracture plane, divided by the dimension of the fracture network on the preferred fracture

Fig. 17.39—Simultaneous fracturing operations from three separate locations.

plane. The DFN is based on an original concept by Warren and Root (1963) (see **Fig. 17.42)** in which the dominant fracture is allowed to grow on the y-z plane and orthogonal fractures are allowed to grow on the y-x and x-z planes if the fluid pressure exceeds the effective stresses normal to these planes.

Allowances for mechanical interaction and leakoff interaction between parallel fractures are an integral part of this model. This means that a fracture positioned between parallel fractures and which is too close to them, can be "squeezed out" to the point where proppant cannot be placed into that fracture.

In order for the simulator to model the growth of the DFN, several additional input parameters are required, over and beyond that required to simulate a conventional planar fracture (Meyer & Associates, 2013). These include:

- Proppant distribution (uniform between all fractures, dominant fracture only or user specified ratio)
- Fracture interaction (stiffness and fluid loss)
- Aspect ratio
- Azimuth of minimum horizontal stress relative to wellbore

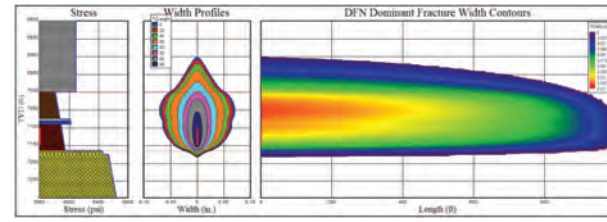

Fig. 17.40—The figure shows a 2-D view of DFN dominant fracture geometry. (Meyer and Bazan 2011.)

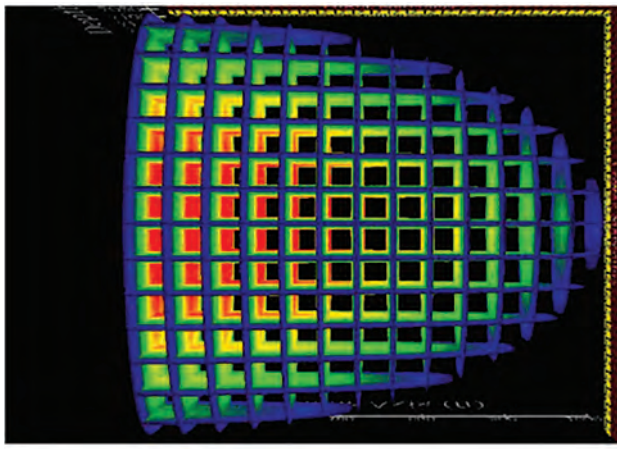

Fig. 17.41—The figure shows a 3-D view of DFN on the horizontal plane, and illustrates the orthogonal fracture network. (From Meyer and Bazan 2011.) Shading indicates fracture width, with blue being small and red being large.

- Dimensionless well location (an assessment of where the fracture initiation point (or points) are relative to the natural fracture network)
- Spacing along axes (the distances between fractures on the three planes)
- Aperture ratio [the relative widths of the fractures on the y-z (dominant), y-x, and x-z planes]
- Mid-field fracture complexity (Jacot et al. 2010)

The need for all this additional input data—the majority of which is not available until significant treatment-related data is available from a particular formation—means that DFN simulators are still a long way from the "predictive" 3-D and pseudo 3-D simulators used for conventional fracturing. As a result, the fracturing industry continues to rely on empiricism and case history data for treatment design in unconventional formations, rather than on model-based simulations.

17.5 Perforation Strategy

17.5.1 Perforating for Hydraulic Fracturing

17.5.1.1 Introduction

The primary objective of perforating cased and cemented wells completed in unconventional reservoirs is to control the allocation of fracturing fluid and proppant into multiple intervals in one simultaneous operation. This is done to reduce the number of fracturing stages and treatment cost. Perforating for hydraulic fracturing normally features the use of a shaped-charge jet perforator conveyed by a hollow-steel carrier. In horizontal wells, perforating is commonly accomplished by pumping a wireline conveyed, select-fire jet perforating gun string into the lateral section of the well along with a bridge plug. This process is known as plug-and-perforate (Castro et al. 2013a) and has been generally successful in establishing adequate connections from the perforations to the hydraulic fractures. There are several basic practices that enhance the effectiveness of perforating in hydraulic fracturing applications. These practices include limiting the length of the perforation interval or cluster along the wellbore, pumping HCl as a spearhead at the start of the fracturing treatment to remove soluble annular flow restrictions (such as the cement sheath along the path from each perforation to the plane of least principal stress), and continuing to condition the hole and/or casing annulus by pumping in a scouring stage of fine particle-size proppant to remove annular flow restrictions that were not dissolved by the acid.

17.5.1.2 Jet Perforation Characteristics:Configuration and Placement Options

The following topics address various design and mechanical aspects of perforating for hydraulic fracturing in unconventional reservoirs.

- **Perforation tunnel.** Fractures initiate from the wellbore in a plane normal to the minimum rock stress. Lab testing has shown that a perforation needs to be within 10° to 30° of this plane to have a fracture initiating from it. In the cases in which a fracture initiated from a perforation, these tests indicated that the fracture grew from the base of the perforation—the perforation tunnel within the reservoir rock did not participate in the process (Behrmann and Elbel 1991, Behrman and Nolte 1999). Field evidence for perforation tunnels not participating in fracture initiation includes mine-back experiments at the US Department of Energy Nevada Test site. As shown in **Fig. 17.43**, dyed fluid injected during a hydraulic fracturing test avoided the perforation tunnel entirely (Warpinski 1983). This result has been attributed to a stress cage enveloping each perforation tunnel, which was caused by the outcome of rock compression and crushing from the jet-perforating event. Additional insight was provided by hydraulic fracturing applications utilizing ported sleeves that open to a cemented pipe and hole annulus without the presence of perforation tunnels. These applications typically exhibit normal-to-reduced breakdown and treating pressures (Rytlewski and Cook 2006, Castro 2013a). In general, perforation tunnels within the reservoir rock are at best a non-factor in hydraulic fracturing applications and in some cases cause additional resistance to fracture initiation due to the associated stress cage.

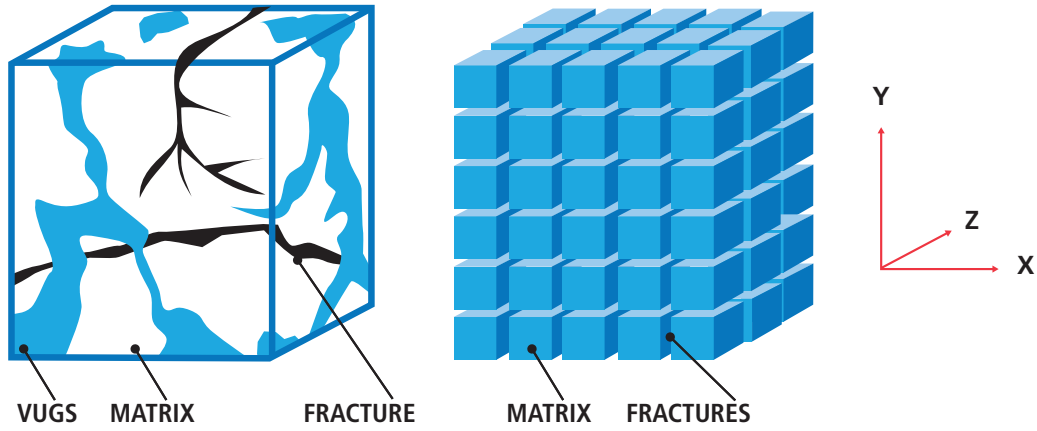

Fig. 17.42—Idealization of the discrete fracture network (DFN). (After Warren and Root 1963.)

- **Perforation phasing and orientation.** As noted above, perforations that are close to the part of the wellbore intersecting the plane of minimum stress will have a more direct path to the hydraulic fractures. Initially, flow will be less restrictive through these perforations; this has sometimes led to using oriented perforating to avoid excessive treating pressure and proppant bridging, especially with high-angle or deviated wells with a limited wellbore connection to that plane (Pearson et al. 1992). If oriented in the plane normal to the least stress at the wellbore, perforations phased 0° or 180° will have the cleanest path to the primary fracture and promote a relatively low fracture breakdown pressure. In horizontal wells, this plane is typically on the high and low sides of the well where radial stress is lowest. As well, zero degree phasing minimizes the variation in perforation diameter due to uniform gun standoff distance, which is advantageous in predicting and controlling perforation friction pressure. However, orienting perforating in practice introduces operational complexities and often the plane normal to the least stress is not known with certainty. It is usually more practical to use 60° perforation phasing at a high shot density. The concentrated energy of detonating closely spaced perforation charges promotes debonding of the cement sheath in the region of the perforations, which enables flow from each perforation via a microannulus to the preferred fracture plane (Behrmann et al. 1992); see **Fig. 17.44**. When combined with limited entry best practices, establishing a high-pressure drop across each perforation, combined with injection of HCl acid and particulate scouring material, removes the cement sheath in the hole and/or casing annulus adjacent to the perforations (Daneshy 2013). This conditioning process eventually leads to excellent communication from all perforations to the preferred fracture plane.
- **Perforation diameter.** To prevent the proppant from bridging in the perforations, it is only necessary that the perforation diameter is at least six times greater than the average particle size diameter of the propping agent (Gruesbeck and Collins 1982). Even small-diameter perforations meet those criteria, since a small-particle-size proppant is commonly used in unconventional reservoir treatments. For instance, the minimum required perforation diameter for 20/40 mesh proppant is 6 x 0.248 in = 0.15 in. This provides significant leeway to adjust the perforation entry-hole diameter to get the targeted perforation friction pressure drop for the limited entry method. However, the entry-hole diameter can vary significantly with variation in perforator gun clearance; i.e., the distance between the external surface of the gun assembly and the internal surface of the casing or liner. If the limited entry method discussed below is to be effective, it's important to minimize the variation in entry-hole diameter among the perforations within the cluster or from cluster to cluster. This can be accomplished by either centralizing the perforating gun string (which is not commonly implemented in horizontal well plug-and-perforate operations), or by selecting a perforator in which the entry-hole diameter is relatively insensitive to gun clearance. Also, it's helpful to minimize gun clearance by using the largest-diameter hollow steel carrier that is practical.
- **Perforation cluster length.** It is desirable to drive a single transverse fracture from each perforation cluster when using multiple perforation clusters in a horizontal well fracturing stage. When multiple fractures are created from a single perforation cluster, the length and width of each fracture is compromised due to splitting of the fluid and slurry streams partitioned to that interval and the fracture widths are further reduced by the mechanical compression caused by

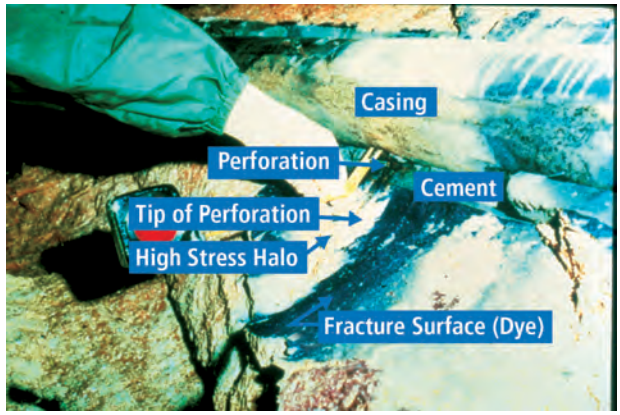

Fig. 17.43—In-situ hydraulic fracturing experiments via cemented, perforated casing. Mineback observations indicated that hydraulic fractures tended to avoid the high stress regions associated with shaped charge produced perforation tunnels. (Warpinski 1983.)

interactions among the multiple competing fractures (Daneshy 2013). To enhance the probability of propagating a single, long transverse fracture from each cluster, it is important to minimize the length of the perforation cluster. Lab studies indicate that the maximum perforated interval length should be limited to four times the wellbore diameter (El Rabaa 1990). For example, the perforation interval should be 32 inches or less for an 8-inch-diameter wellbore when using this guideline. Note that it is desirable to create an enhanced permeability region away from the wellbore by intersecting and reopening natural fracture networks that connect with and extend laterally away from the primary transverse hydraulic fracture.

Similarly, in vertical wells, the height of perforations should also be limited to increase the probability of creating a single, long primary fracture (Lestz et al. 2002). In limiting fracture access in a vertical well, it's important to place proppant across most of the extent of the fracture height. If there are high stress/ high modulus intervals that act to exclude proppant or seal off during fracture closure, multiple perforation sets should be placed between these potential pinch points (Cramer 1987).

- **Perforation cluster location.** As suggested above, near-wellbore fracture complexity is not a desirable feature, as it compromises hydraulic fracture width and can potentially lead to the near-wellbore bridging of proppant. It is important to perforate in mechanically stable rock intervals. Perforating in rock characterized by abundant planes of weakness will lead to chaotic fracture initiation and high near-wellbore pressure drop. Additionally, perforation clusters should be located to avoid external casing upsets such as centralizers and collars. The cement sheath exhibits increased resistance to shear failure at these wellbore locations, which inhibits the beneficial debonding process (see above) and can restrict fracture width at the wellbore (Daneshy 2013).
- **Perforation cluster density.** The number of perforation clusters per fracture treatment has varied from one to as many as ten. In general, increasing the number of individual perforation clusters increases the risk that a cluster interval will not be treated, even when applying the limited entry methodology. At some point, the loss of injection into a single interval will not make an appreciable difference in perforation friction or backpressure at the upstream side of perforations. As well, increasing the gross interval per treatment stage (i.e., the distance between the nearest and farthest perforation cluster) leads to increasing difference in tubular friction pressure among intervals, exacerbating the difference in entry pressure among intervals. In cases in which the total injection rate is limited due to treating pressure restrictions or horsepower availability, increasing the number of perforation clusters results in a reduction of injection rate per interval, which leads to reduced fracture width, length, and often height. As a result of these factors, many operators limit the number of perforation clusters and gross interval per multi-interval fracturing stage to a range of 3 to 5 ft. and 200 to 300 ft., respectively.
- **Perforation cluster spacing.** Due to the mechanical displacement induced by opened hydraulic fractures, in-situ stress in the reservoir rock increases above virgin conditions during and immediately after fracture treatments, especially in the direction normal to the fracture planes. The magnitude of the stress increase is a function of net pressure in the fractures, elastic rock properties, fracture height, and distance from the fracture surface (Warpinski and Branagan 1989). Closely spaced, parallel transverse fractures propagating from individual perforation clusters can be affected by this stress increase if sufficiently close to the adjacent fractures, i.e., within the stress shadow of those fractures (Cheng 2012). The stress shadow effect tends to reduce hydraulic fracture width, especially when the fracture is bounded on both sides by competing fractures. This can favor fracture propagation from the uphole perforation cluster during a plug-and-perforate operation, since it is bounded on only one side by competing fractures. Fractures propagating from both of the outside perforation clusters are advantaged when performing the first of multiple fracturing stages or if net pressure has significantly decreased due to a suitably long shut in time between fracturing stages. In limited entry applications, perforation

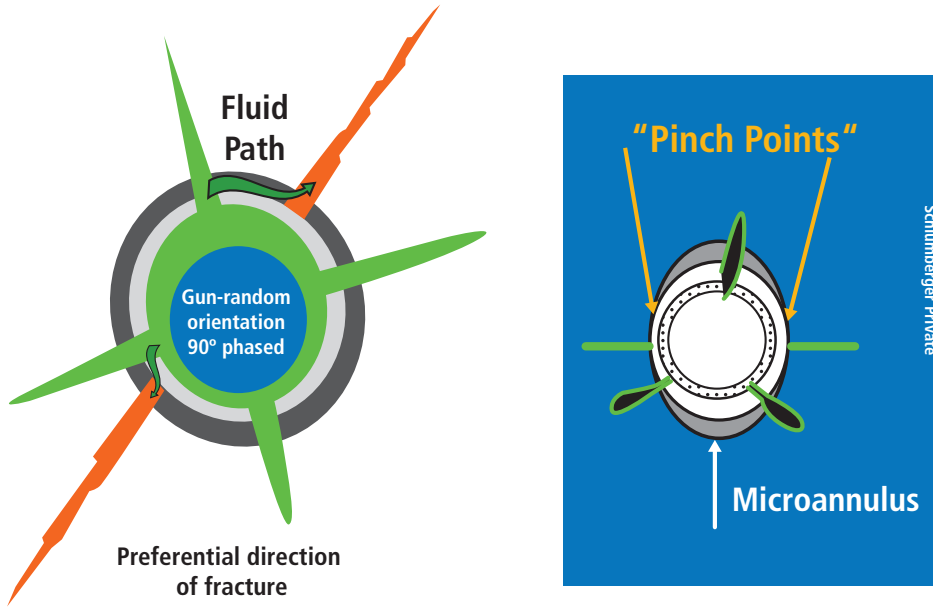

Fig. 17.44—This figure shows the flow in the microannulus from perforations to fracture wings. Big block testing verified results obtained from the mineback field trials. (After Behrmann and Nolte 1999.)

density can be underweighted in the less-bounded clusters to partially counteract this advantage. But in general, the impact on the width and possibly the trajectory of the interior fractures becomes more significant as the distance between clusters shortens, increasing the risk of pumping an inefficient treatment. Even more significant in determining perforation cluster spacing is the drainage area impacted by the individual fractures, which is a strong function of inter-fracture mobility (k/μ). Computer simulation is advantageous in evaluating the impact of cluster spacing on fracture propagation and reservoir drainage.

- **Single-interval treatments.** Treating each perforation cluster or interval individually may be optimal for cases that are not conducive to limited entry treatments, e.g., when large variation exists in fracture propagation pressure (600 psi or greater) among the intervals contacted by the perforation clusters for a given fracturing treatment stage (Cramer 1987). One recently developed application is coiled tubing enabled ported fracturing sleeves, which are hydraulically activated by setting a coiled tubing conveyed isolation packer in the sleeves (Castro et al. 2013a). Other methods include just-in-time perforating (Angeles et al. 2012), annular coiled tubing fracturing (McDaniel et al. 2008), and casing conveyed perforating combined with remote on-demand actuation and isolation (Eller et al. 2002).
- **Abrasive perforating.** Abrasive perforating features the use of specialized jetting nozzles which inject slurries of water and fine sand to erode holes through casing, cement sheath, and formation rock (McDaniel et al. 2008). It is often combined with annular coiled-tubing multistage fracturing applications in vertical, inclined, and horizontal wells. Since the eroded materials are removed from the freshly created perforations rather than compressed, as is the case with the jet perforating process, a stress cage is not created around the perforation tunnels and contiguous portions of the wellbore. As a result, fracture initiation pressure is often reduced as compared to using jet perforators. This is a good application for situations plagued by difficult-to-breakdown intervals that are strongly impacted by stress cage phenomena and also for select-interval treatments targeted in coiled tubing fracturing applications. However, the abrasive perforating process is not conducive for simultaneous treatment of multiple intervals as 1) it is difficult to control perforation entry-hole dimensions and this is necessary for applying the limited entry process and 2) proppant-induced perforation erosion occurs relatively quickly since an erosion-resistant work-hardened layer is not produced along the perforation hole in pipe as is the case with jet and bullet perforators (Cramer 1987). Additionally, abrasive material and debris byproducts must be circulated up the well to avoid solids-bridging at the beginning of the fracturing treatment and the jetting tool is subject to internal and external abrasive wear. Consequently, abrasive perforating is generally used on an as-needed basis.

17.5.1.3 Other Perforating Methods and Perforation Enhancing Techniques

Bullet perforating uses a bullet-shaped projectile to punch a hole through the casing, cement sheath, and formation. The bullets are propelled by gas generated by detonated explosive powder in a similar manner to jet perforators. Bullets provide a precise entry-hole diameter, which is advantageous for limited entry applications (Small 1986; Cramer 1987). However, the flexibility and reliability of bullet perforating is limited and often inadequate for massive fracturing applications. There is a limited selection of bullet sizes and it's difficult to maintain gun integrity over multiple firings. Consequently, bullet perforating has become an obsolete technique in most parts of the world.

Propellant sleeves have been used to increase the energy and gas volume associated with the jet perforating operation, inducing fractures which propagate several feet into the reservoir rock (Gilliat et al. 1999). Although this method has proven helpful in reducing fracture breakdown pressure, it requires a large number of perforations to prevent damage to the well and consequently is incompatible with limited entry methods.

Reactive perforating charges generate a secondary reaction in the perforation tunnel immediately after formation of the tunnel (Bell et al. 2009). Similar to propellant sleeves, the reaction is claimed to be highly energetic and drives the breakup and expulsion of crushed zone material and compacted debris. It is also compatible with the limited entry process. Yet the application of this technique has been very limited, partly due to the incremental cost and also to the effectiveness of conventional perforation conditioning materials and techniques, i.e., HCl acid spearhead, particulate scouring material.

17.5.2 Limited Entry for Control of Treatment Allocation

Limited entry is the process of limiting the number or reducing the entry-hole diameter of perforations in such a way that significant perforation friction pressure is achieved during a hydraulic fracturing treatment. Perforation friction establishes a backpressure in the wellbore that tends to allocate flow among the multiple perforation intervals or clusters, thus improving control of the hydraulic fracturing process when treating multiple intervals simultaneously. Limited entry is one of the most economical processes available to stimulate both vertical and horizontal wells completed in unconventional reservoirs.

To implement effective limited entry treatments, it is important to understand the mechanisms impacting pressure drop across perforations and use that knowledge to take appropriate measures when designing and implementing the treatment.

17.5.2.1 Limited Entry Mechanics

Due to stress concentrations around perforation tunnels created by shaped charge jet perforators, hydraulic fractures tend to initiate in rock unaffected by the perforating event, in the plain normal to the least stress. Therefore, the usual connection path of the wellbore to the primary hydraulic fractures is via the entry hole in the casing, along the perimeter of the cement/wellbore annulus, to the preferred fracture plain. Fractures can initiate at the base of perforations that are in line with the preferred fracture plane, but generally to the exclusion of the perforation tunnel in rock (Warpinski 1980). Therefore, the characteristics of the entry hole through the casing are of primary importance for determining flow from the wellbore to fractures during hydraulic fracturing treatments.

As shown in **Fig. 17.45**, perforation entry holes in pipe resemble orifice plate holes (Gross 1985) and the predictive equation for pressure drop through an orifice in **Eq. 17.19** can be used to estimate perforation friction pressure during hydraulic fracturing treatments (McClain 1963). It is important to remove annular flow restrictions in the path between the perforated pipe and hydraulic fractures to be able to use the predictive equation effectively. This is achieved early in the treatment by using hydrochloric acid (HCl) and scouring material such as 100-mesh sand or proppant.

$$\Delta p_{pf} = \frac{0.2369 q^2 \rho_f}{C_d^2 n^2 d^4} \qquad \textbf{(Eq. 17.19)}$$

where Δp_{pf} is the pressure drop across the orifice or perforation (psi), q is the injection rate (bpm), ρ_f is the density of the fracturing slurry (lbm/gal), C_d is the discharge coefficient, n is the number of perforations and d is the orifice or perforation diameter (inches). Eq. 17.19 is based on the Bernoulli theorem.

17.5.2.2 Input Parameter Variability

Shaped charge perforators produce holes through pipe that exhibit somewhat irregular surfaces and are impacted by environmental factors such as casing grade and thickness, gun clearance, bottom hole temperature, etc. The above factors will result in variability in the perforation diameter. As well, the

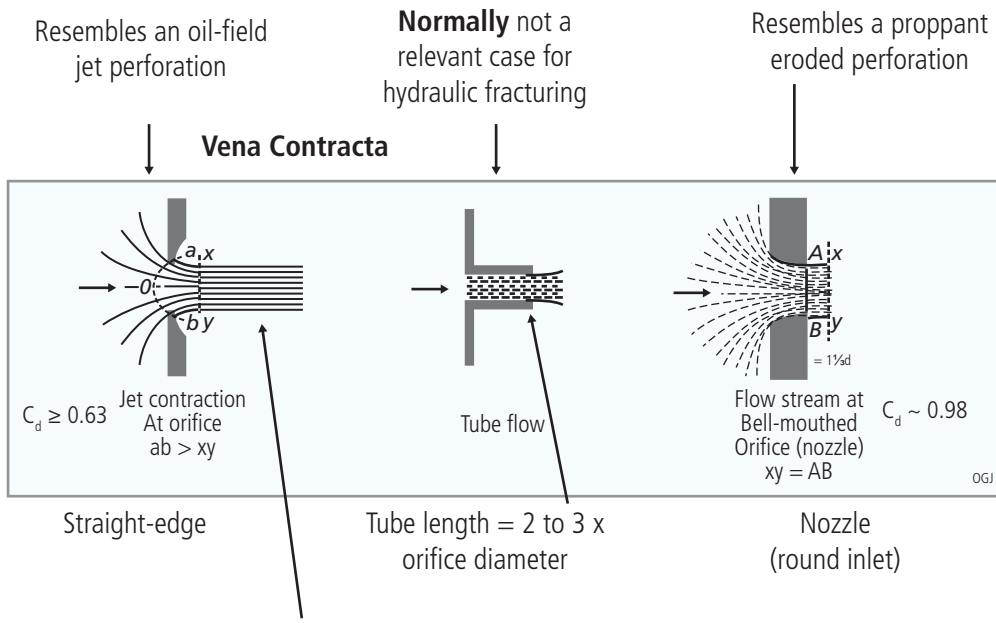

Fig. 17.45—Flow through an orifice. (Gross 1985.)

irregular, dimpled entrance hole through casing tends to increase the perforation discharge coefficient by reducing the vena contracta effect. Variability in perforation diameter and discharge coefficient leads to a degree of uncertainty in perforation friction pressure behavior during fracturing treatments.

Differences in fracture propagation pressure behavior in simultaneously treated intervals have a strong influence on the treatment volume distribution among those intervals. This is because the fracture pressure variation results in a different pressure drop across each perforation interval. Unfortunately, knowledge of the fracture propagation pressure within individual zones is often imprecise, both initially due to lack of knowledge of the in-situ stress distribution, and during the course of the treatment due to changes in net pressure. Inaccurate prediction of fracture propagation pressure behavior can promote undesired treatment allocation among intervals, and prevention or cessation of fracture propagation in intervals exhibiting relatively high fracture initiation or propagation pressure (see Fig. 17.33).

Achieving high excess perforation friction pressure increases the bottomhole "backpressure" within casing, which lessens the impact of unforeseen variations in interzonal fracture propagation pressure and perforation characteristics (see **Fig. 17.46**, an example taken from the Eagle Ford shale of south Texas). Planning for and achieving high perforation friction pressure (i.e., average $\Delta p \geq 1000$ psi) will lessen the negative impact of the above factors on treatment distribution among perforation clusters, improving control of the limited entry process and leading to improved post-treatment well productivity. Note how the excess perforation friction varies with the fraction of the treatment volume—this is an important concept, illustrating how increasing the excess perforation friction pressure leads to more uniform allocation of the treatment over the intervals.

17.5.2.3 Perforation Erosion

Surface flow tests have shown that proppant erodes the inlet of the casing entry hole and the perforation takes on a nozzle-like configuration (**Fig. 17.47**). Fluid-jet contraction (vena contracta effect) ceases, which increases the discharge coefficient. Eventually, proppant interactions can remove the thin, work-hardened, erosion-resistant layer or skin at the cylindrical perforation walls, leading to perforation diameter enlargement. Erosional effects reduce perforation friction pressure. Reducing perforation friction during the treatment is undesirable since it leads to reduced control of the treatment volume distribution among intervals. Using high-grade casing (e.g., P-110), and relatively small spherical proppant grains help maintain the Δp across perforations by reducing perforation erosion. As well, minimizing the variance in the initial entry-hole diameter among perforations will reduce the tendency for perforations to erode asymmetrically.

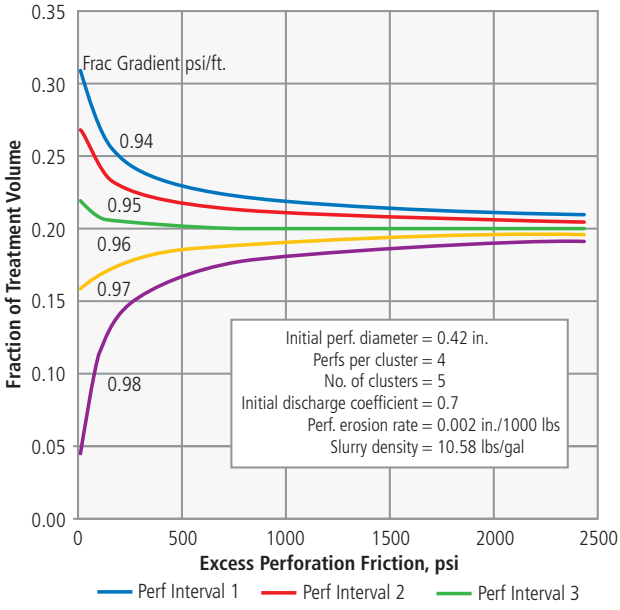

17.46—Excess perforation friction improves control of treatment distribution. The excess perforation friction is defined as the difference between the actual perforation friction and the bottomhole fracturing pressure differential or Δp^{BHFP} (which in turn is equal to the difference between the maximum and the minimum fracturing pressures at the perforation clusters). Note that this chart is a plot of pre-erosion conditions.

Field studies have verified that proppant-induced erosion occurs during limited entry massive hydraulic fracturing treatments. As indicated in **Fig. 17.48** and **Table 17.5**, the erosion seems to be a two-step process (where the hydraulic diameter - H is defined in **Eq. 17.20**).

$$\hat{H} = d\sqrt{C_d} \qquad \textbf{(Eq. 17.20)}$$

Initially, proppant interactions round the perforation inlet as expected, increasing the hydraulic (apparent) perforation diameter due to the increase in the perforation discharge coefficient (Cramer 1987). After a quiescent period during which the skin of work-hardened metal at the perforation walls resists erosion (Early 1977), the hydraulic perforation diameter exhibits a second growth period due to a progressive, steady-state increase in the actual perforation diameter. This increase is believed to be triggered by the removal of the work-hardened skin, which exposes the base metal to the erosive slurry jet. A significant increase in perforation flow capacity occurs during this second stage erosion, producing a significant decrease in perforation friction unless compensated for by increasing the injection rate. Another consideration is that the pressure drop across perforations is greater for the intervals exhibiting a relatively low fracture propagation pressure. This means that fluid and proppant flow rates will be greater through perforations in the lower fracture pressure intervals, which could lead to accelerated erosion and progressively increasing allocation of treatment volume into those intervals.

17.5.2.4 Treatment Design and Evaluation

Commercial and proprietary hydraulic fracturing software packages are available that enable calibration of perforation configuration and erosion-process parameters, as well as evaluation of interzonal fracture propagation pressure during fracturing treatments, providing an essential tool for evaluating limited entry effectiveness. As shown in **Fig. 17.49**, key parameters include the initial discharge coefficient, final discharge coefficient, volume of proppant necessary to remove the work-hardened skin layer (i.e., critical proppant mass) and growth (erosion) rate of the perforation diameter following removal of the work-hardened layer.

A study of limited entry treatments in a south Texas shallow oilfield has provided additional insight into the limited entry process. Limited entry parameters and coefficients were determined by use of a pressure-history matching routine within the MFrac hydraulic fracturing simulator (see **Fig. 17.50** and **Table 17.6**). It was discovered that the rate of perforation diameter growth due to second-stage erosion was about seven times greater than observed in the DJ Basin study (above). As well, second-stage erosion occurred relatively early in the treatment. The main differences in completion design as compared to the previous field study were the use of lower-grade casing (J-55 versus N-80) and coarser proppant (12- to 20-mesh sand versus 20/40 mesh sand), indicating the dominant impact of metal hardness and proppant particle size on the perforation erosion process. Tubular hardness usually has the most dominant impact on the rate of perforation erosion.

In the south Texas limited entry treatments, the aggressive erosion rate resulted in a significant loss in perforation friction during proppant displacement, as shown in the MFrac plot (**Fig. 17.51**). Low perforation friction can lead to a loss of control in distributing the treatment volume among the perforated intervals, thus diminishing or eliminating the effectiveness of the limited entry process. Taking steps to mitigate perforation erosion will lead to improved limited entry results.

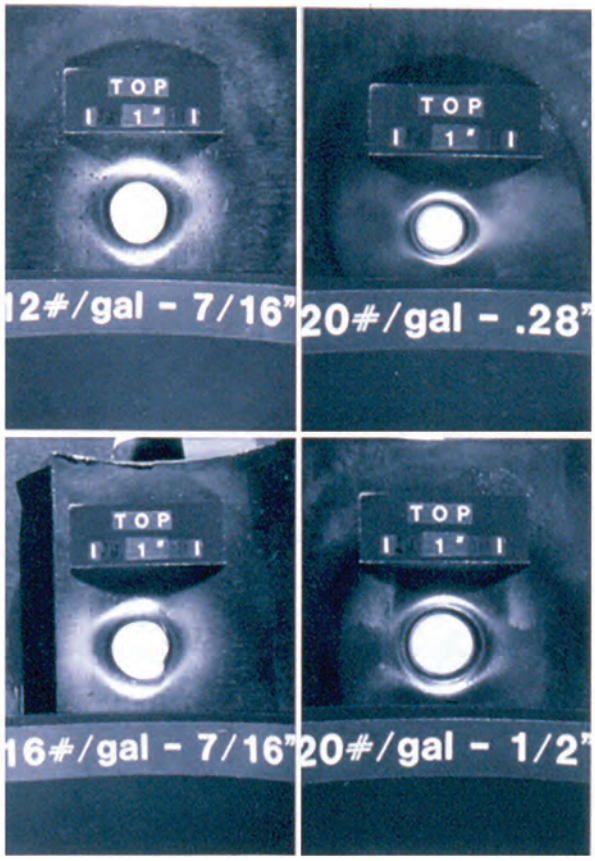

Fig. 17.47—Perforation erosion indicated in surface tests. Proppant rounds the entry-hole inlet and has the potential to enlarge the perforation diameter in the casing. Both effects reduce perforation friction pressure. (Crump and Conway 1988.)

17.6 Calibration and Diagnostic Tests

17.6.1 Applicability of Traditional Calibration Tests to Unconventional Reservoirs

Generally speaking, traditional calibration tests are not very applicable to unconventional fracturing operations, for a number of reasons:

- The analysis techniques used to interpret data derived from calibration tests are generally based around the assumption of a single planar fracture. This is usually not the case for unconventional fracturing, where the completion and perforation strategies are usually designed to promote complex non-planar fracture growth.
- The presence of natural fractures adds a degree of difficulty and significant complexity to the analysis of fracture closure and fluid leakoff.

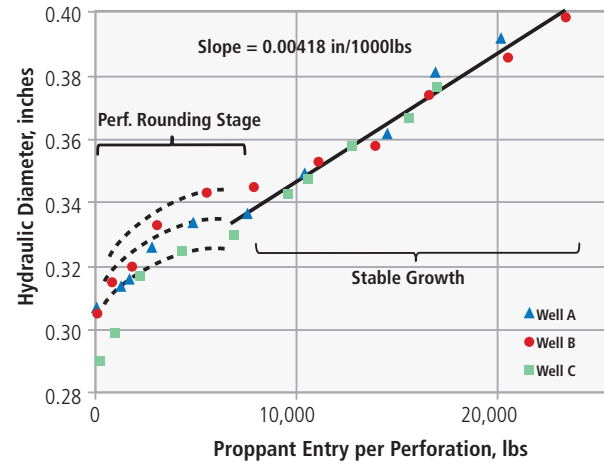

Fig. 17.48—Proppant-induced erosion appears to be a two-step process. This data is from a limited entry study performed in Colorado's Denver-Julesberg ("DJ") basin. (Adapted from Cramer 1987.) See also Table 17.5.

Table 17.5—Additional data and results from the perforation erosion example are illustrated in Fig. 17.48.

Casing	4 ½" 11.5 lbs/ft N-80
Proppant	20/40 sand
Number of perfs.	variable
Initial perforation diameter	0.375 in.
Initial discharge coefficient	0.75
Final discharge coefficient	0.93
Erosion rate	0.0042 in./1000 lbs
Critical proppant mass	6000 lbs

- The almost complete absence of fluid leakoff through the pore spaces—due to the ultra-low primary permeability of the reservoir rock—means that tests designed to calculate leakoff coefficients or fluid efficiency are almost irrelevant. For the same reason, tests designed to detect closure pressure can also result in extremely long test times and results that are often ambiguous and/or vague.
- Many shale reservoirs exhibit sensitivity to fluid injection such that the localized buildup of pore pressure adjacent to the wellbore combined with mineralogical sensitivity to the fracturing fluid, results in the inability to rebreak the formation after calibration tests have been performed.

However, there are some instances when traditional calibration tests may be useful. These are discussed in the following sections.

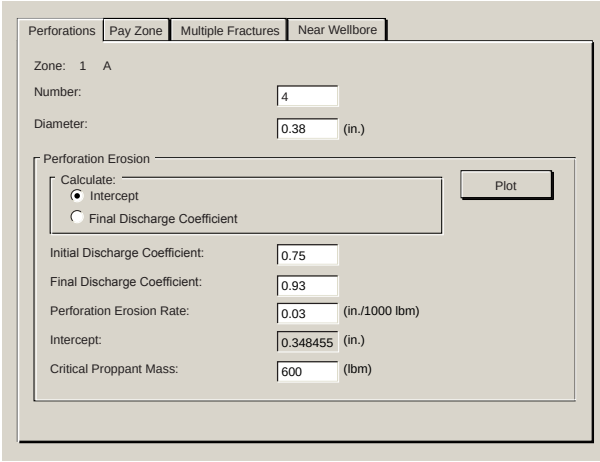

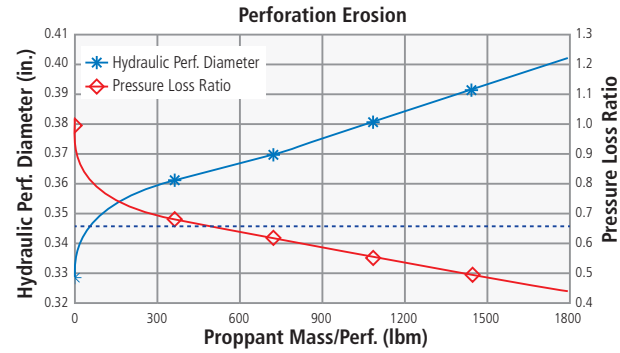

Fig. 17.49—Illustration of the limited entry design and zone data. Several hydraulic fracturing software packages (in this case MFrac) enable rigorous evaluation of the parameters effecting limited entry treatments.

17.6.1.1 Step-Up and Step-Down Tests

The step-up test is used to determine the fracture extension pressure and to establish an injection rate for a specific fluid, above which a fracture is being formed and below which matrix injections operations can be performed. The step-down test is used as part of the diagnostic process for near-wellbore friction—namely tortuosity and perforation friction. Good descriptions of how these tests are applied to conventional reservoirs can be found in Martin (2009) and Chapter 4 of Economides and Martin (2007).

The applicability of these tests to unconventional reservoir fracturing is mainly limited to the assessment of tortuosity and perforation friction problems in wells where a specific interval can be isolated for testing.

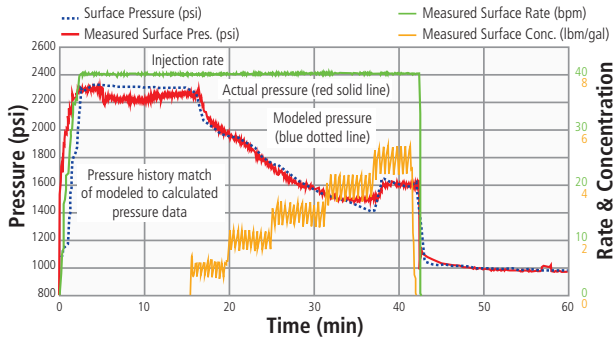

Fig. 17.50—South Texas limited entry field study, MFrac job plot. Erosion rate coefficients with J-55 casing and 12/20 mesh sand were 7 times greater than for N-80 and 20/40 mesh. See also Table 17.6.

17.6.1.2 Minifractures

Minifracturing is used for four main purposes: to determine the closure pressure of the formation; to determine fluid leakoff to a specific fluid system; to allow some assessment of potential main treatment fracture geometry; and to further test any suspected tortuosity problems for the ability to transmit proppant by the use of proppant slugs. Again, good descriptions of how these tests are applied to conventional reservoirs can be found in Martin (2009) and Chapter 4 of Economides and Martin (2007).

For reasons already discussed, the main use of the minifracturing process in unconventional reservoir fracturing—other than as a good starting point for a diagnostic fracture injection test (or DFIT—is to test near-wellbore transmissibility via the use of proppant slugs.

Table 17.6—Additional data and results from the limited entry field study illustrated in Fig. 17.50.

Total perforations, n	4 x 4 per cluster = 16
Initial perforation diameter, d	0.38 in.
Initial discharge coefficient, C_d	0.75
Final discharge coefficient	0.93
Erosion rate	0.03 in./1000 lbs
Critical proppant mass	600 lbs
Estimated EOJ perforation diameter	0.57 in.

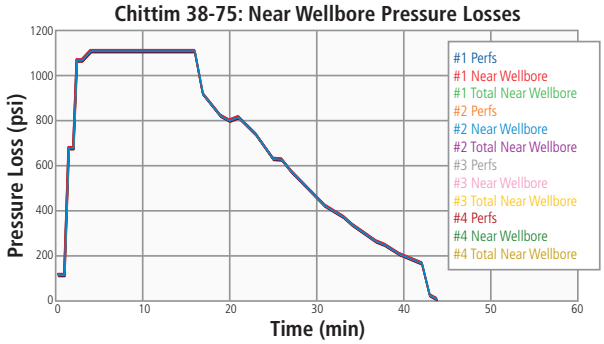

Fig. 17.51—Change in perforation friction due to erosion, derived from pressure match. In this case, erosion resulted in a significant loss of perforation friction. The use of low-hardness J-55 casing and coarse proppant (12/20 fracturing sand) exacerbated this effect. Taken from the same south Texas study as Fig. 17.50.

17.6.2 Diagnostic Fracture Injection Tests

Well testing is the technique of establishing fluid flow in the reservoir by either producing from or injecting into a well, and then changing or discontinuing the flow rate to create a transient event, usually by shutting in the well at the surface. Then, the resulting wellbore-to-sand-face pressure response is evaluated to derive reservoir flow properties and pressure capacity, such as kh and initial reservoir pressure (p_i). In tight or damaged rock, it is time-consuming and expensive to do a production flow test (i.e., drawdown/buildup test), especially when more than one sub-interval needs to be tested. In regard to doing injection fall-off testing in this type of rock, we typically cannot pump at a sufficiently low surface injection rate to stay below fracturing pressure, especially from a short perforation interval. As suggested in **Fig. 17.52**, creating a hydraulic fracture bypasses wellbore damage and near-wellbore stress concentrations and connects wellbore to a significant portion of the reservoir layer thickness, enabling a representative investigation of reservoir fluid flow properties by methods shown below. This method is known as the diagnostic fracture injection test (DFIT).

An additional benefit of DFIT is that geomechanical properties, chiefly minimum in-situ stress, can be deduced by identifying fracture closure signatures from the pressure fall-off data.

17.6.2.1 Diagnostic Fracture Injection Test Sequence

A typical diagnostic fracture injection test (DFIT) sequence is shown in **Fig. 17.53**.

Initially, the well is filled with water or brine and care is taken to purge the fluid column of entrained air and gas. Then, a surface pump establishes an injection rate with water/brine, and the wellbore fluid is compressed; the time of compression is a function of wellbore volume, injection rate, and breakdown pressure. In low permeability reservoirs, little if any of the injected fluid flows into the reservoir during this time. Eventually, formation breakdown or breakover pressure is reached, signifying that a hydraulic fracture is being propagated into the reservoir rock. Injection at the surface is continued until the wellhead pressure stabilizes (i.e., it is changing very slowly.) Then, surface injection is stopped, resulting in an instantaneous shut-in pressure (ISIP), which is inclusive of wellbore and near-wellbore friction pressure and from which net pressure at shut-in (i.e., the sand-face pressure and/or fracture closure pressure) can eventually be determined. The shut-in well pressure is then monitored for signs of fracture closure (which is considered to be equivalent to the minimum principal effective stress) and the after-closure period is evaluated for pseudo-linear and pseudo-radial flow signatures. Radial flow solution methods are used to derive kh/μ and p_i and linear flow can be evaluated for p_i.

17.6.2.2 Diagnostic Plots and Analysis

The shut-in pressure data is evaluated graphically to look for trends (Barree et al. 2007). The examples shown (**Fig. 17.54, Fig. 17.55, Fig. 17.57, Fig. 17.59, and Fig. 17.60**) are from a single DFIT conducted in a low permeability shale interval. Log-log plots of the semi-log derivative (red line) and pressure change (ISIP—measured wellbore-to-sand-face pressure; blue line) versus time are shown in Fig. 17.54.

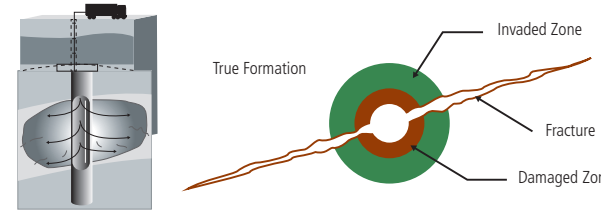

Fig. 17.52—Hydraulic fracturing bypasses the near-wellbore damage zone and connects the wellbore to more interval thickness (Santo 2011.)

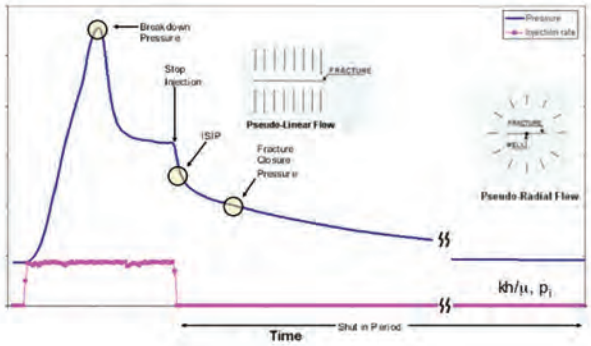

Fig. 17.53—Typical DFIT pressure response. (Cramer and Nguyen 2011.)

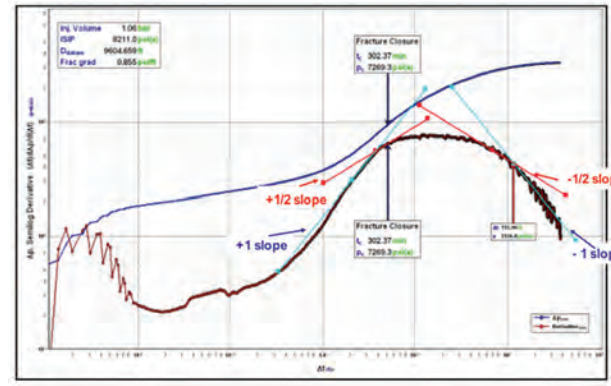

Fig.17.54—Diagnostic log-log plot of pressure fall-off. (Martin et al. 2012.)

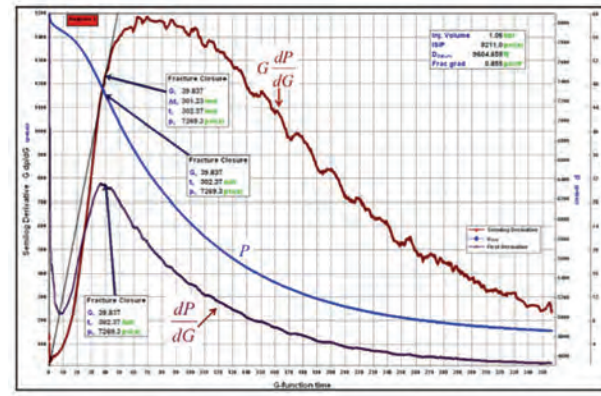

Fig. 17.55—G-Function plots for fracture closure identification. (Martin et al. 2012.)

The derivative plot shows characteristic slopes that indicate the pressure response is being strongly influenced by various flow regimes. Positive trending slopes occur during the fracture closure period. The positive unit slope is characteristic of wellbore or fracture storage, possibly indicating that a closing secondary fracture set is supplying fluid to the primary fracture. Fracture height recession and closing transverse fractures are two potential fracture storage mechanisms. The positive ½ slope trend is indicative of linear flow and suggests the presence of an open fracture. A departure from the positive ½ slope suggests the fracture has closed. Negative trending slopes occur during the after-closure period and verify that hydraulic fracture closure has occurred. The negative ½ slope and unit slope trends are characteristic of pseudo-linear and pseudo-radial flow, respectively.

Fracture Closure Analysis. Specialty plots are used to evaluate flow regimes and events suggested by the diagnostic log-log plot. Fig. 17.55 shows G-Function plots that are used for the identification of fracture closure and fracture complexity. (See Nolte 1979 and Martin 2009, for an explanation of G-Function analysis.)

Using guidelines introduced by Barree et al. (2007), fracture closure is indicated by the break-off from the origin-rooted tangent line in the semi-log derivative ($G\mathrm{d}p/\mathrm{d}G$) plot and the stable declining trend from the plateau region in the primary derivative ($\mathrm{d}p/\mathrm{d}G$) plot. Furthermore, Mattar and Zaoral (1992) noted that a steadily decreasing primary derivative trend is reflective of reservoir-dominated flow behavior, with the wellbore pressure response not being significantly influenced by noise or geomechanical processes such as fracture closure. The pressure versus time curve (p) shows a lack of signature at the time of indicated fracture closure and is not very useful in its selection. Although not shown, the square root of time plots of the semi-log and primary derivatives show analogous character to the G-Function plots.

Fracture Closure Dynamics. Fracture closure is a process, not an instantaneous event. As shown in **Fig. 17.56**, it starts when asperities on opposing fracture faces touch and continues with increased pressure decline and shut in time (Warpinski et al. 1997).

During the after-closure period, some residual fracture width and conductivity is retained. Yet since propping agent is not placed in the fracture, near complete closure can eventually occur, usually starting at the tips of the fracture.

Pseudo-Radial Flow Analysis. An after-closure flow regime type curve plot is shown in Fig. 17.57.

Using fracture closure as the initialization time, the semi-log derivative and pressure change data are plotted versus the linear time function squared (Nolte et al. 1997). In this case, the pressure change value is equal to the measured

wellbore/sand-face pressure less the assumed initial reservoir pressure (p_i). A negative unit slope trend in the semi-log derivative exists during a significant portion of the test, from 90 to 174 hours of elapsed test time (see Fig. 17.57). This confirms the unit slope observed in the log-log diagnostic plot in Fig. 17.54 and is one necessary identifier for pseudo-radial flow. The other identifying signal is the formation of a negative unit slope trend in the pressure change curve, with the pressure change and derivative values identical/overlying within the region of the negative unit slope trend. Within a reasonable range, the assumed initial reservoir pressure can be adjusted to force the above condition. The pressure adjustment process is a method also used to refine the selection of p_i.

The pseudo-radial flow period is analyzed further with the radial flow specialty plot shown in **Fig. 17.58**, which compares pressure to the reciprocal of total test time (Soliman et al. 2007, Santo 2011).

kh is derived from trend-line slope, the volume injected or leaked off during the fracture propagation and closure periods, and mobile reservoir fluid viscosity. pi is derived from the trend-line intercept with the y-axis. The *kh* and p_i values are compared to the flow regime plot in Fig. 17.57 for consistency.

Pseudo-Linear Flow Analysis. Sometimes, the pseudo-radial flow period is absent during the after-closure period, yet a long-duration pseudo-linear flow period, evinced by a negative half-slope trend in the semi-log derivative, is observed in the flow regime plot. This scenario can happen in low-permeability reservoirs when permeability is dominated by an anisotropic, unidirectional natural fracture set. In these cases, the pseudo-linear flow period can be evaluated for p_i (Nolte et al. 1997). An example is shown in Fig. 17.59, which is taken from another shale gas reservoir.

Using fracture closure as the initialization time, the semi-log derivative and pressure change data are plotted versus the linear time function squared (Nolte et al. 1997). A negative half slope trend in the semi-log derivative exists during a significant portion of the test, from 46 to 155 hours of elapsed test time. Within a reasonable range, p_i can be adjusted until the Δp curve develops a negative ½ slope trend in the same time region as the semi-log derivative curve, with the values of the Δp trend line twice the time-equivalent values of the derivative trend line. In this way, the initial reservoir pressure can be derived. The y-axis intercept of the linear flow plot, shown on Fig. 17.60, is an estimate of initial reservoir pressure and equals 11,424 psi, confirming the 11,425 psi that was derived in flow regime plot. Note that there is no capability to derive kh from linear flow analysis.

Injection Rate. In hydraulic fracture injection falloff tests, the true injection rate into the reservoir is governed by the leakoff rate of the fracturing fluid at the fracture faces (see Chapter 8 of Gidley et al. 1989), and not the surface injection rate used to propagate the fracture. In the case shown below in **Fig. 17.61** for an injection test in a low permeability interval, a significant volume of water is compressed in the wellbore prior to fracture breakdown, with little, if any, fluid leaking off before the breakdown event.

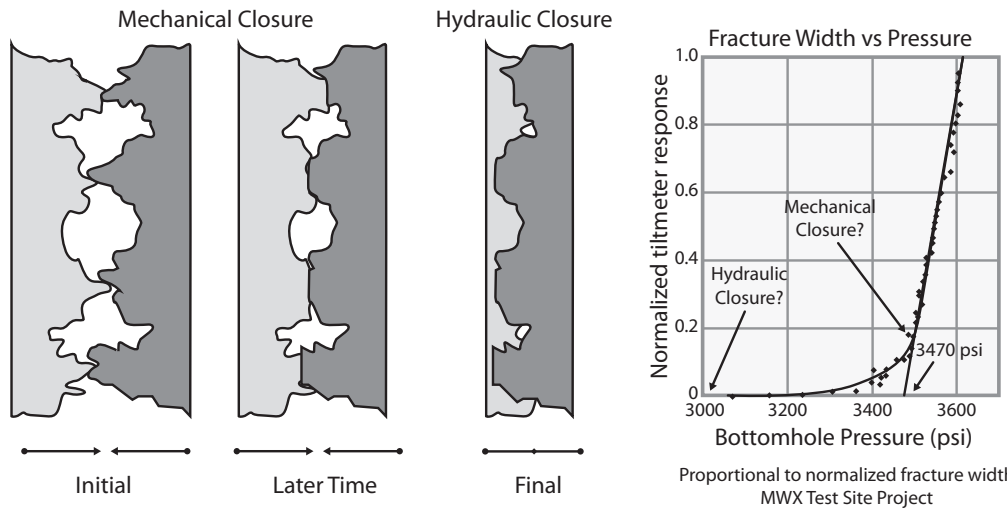

Fig. 17.56—Fracture closure is a gradual and often incomplete process. (Cramer and Nguyen 2013.)

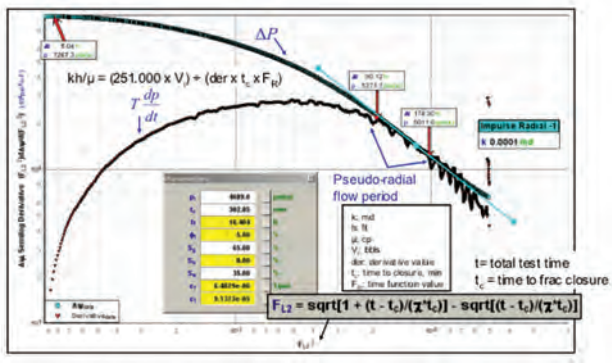

Fig. 17.57—After-closure flow regime type curve analysis. (Martin et al. 2012.)

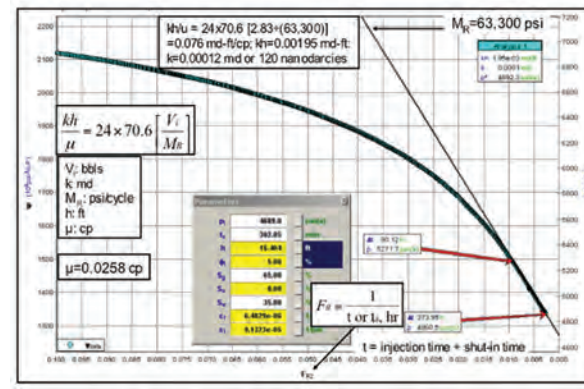

17.58—After-closure radial flow plot analysis. (Martin et al. 2012.)

The decompression of wellbore fluid following formation breakdown causes a high peak downhole injection rate, but that energy goes into creating hydraulic fracture area and width (note: the downhole rate was computed by evaluating surface treating pressure difference, wellbore volume, and water compressibility). Normally, fracture propagation terminates shortly after the end of the relatively high rate surface injection period. Fluid leakoff from the fracture provides the pulse into the reservoir flow network and dictates the pressure response of the reservoir to the DFIT injection. Due to its low compressibility, low viscosity, lack of filter cake-building characteristics and low cost, plain fresh water, or sometimes KCl or brine water, is the favored DFIT injection fluid.

The instantaneous source response function as outlined by Cinco-Ley et al. (1986) underpins DFIT after-closure analysis (Gu et al. 1993). This concept implies a sudden release of fluid at the source (i.e., the fracture-extended wellbore) in the reservoir, creating a pressure change throughout the system. Cinco-Ley et al. showed that at test durations greater than twice the injection/fracture opening time (pre-closure time), the instantaneous source solution for reservoir transmissibility (kh/μ) is within 10% of the exact solution using detailed rate history and superposition. As noted above, in the case of a hydraulic fracturing event, it is the fluid leaking off from the fracture that serves as the injection pulse into the formation/ reservoir. The duration of the leak-off/injection period is the time difference from formation breakdown until fracture closure. Instantaneous source solutions require knowledge only of the total injected or leaked-off fluid volume during that time period. Instantaneous source solutions are particularly useful in DFIT analysis given the constantly changing leakoff rate typical of the fracture propagation and closure periods.

Wellbore Storage. The relationship of sand-face pressure response to the leakoff and injection rate is strongly influenced by wellbore storage. Designing for a smaller test chamber or wellbore storage volume (e.g., the use of a downhole shut-in device), and using low compressibility wellbore/injection fluid, leads to a more rapid pressure response.

Treatment Size and Fracture Length. In low-permeability rock, it's important to minimize fracture length to shorten the time to pseudo-radial flow (Gringarten et al. 1974, Cinco-Ley et al. 1981). Achieving a pseudo-radial flow period is necessary for derivation of kh and p_i. For the case of a conductive fracture intersecting the wellbore, the earliest onset of pseudo-radial flow (tD = 1) can be estimated by using **Eq. 17.21**.

$$t = \frac{\varphi c_t \mu x_f^2}{0.000264k} \qquad \textbf{(Eq. 17.21)}$$

where t is time (hours), k is formation permeability (md), μ is the viscosity of the mobile fluid phase (cp), φ is the porosity (decimal), c_t is the total system compressibility (psi-1), and x_f is the fracture half-length (ft.).

As noted previously, the DFIT is a special case of an unpropped fracture and fracture conductivity may diminish as fluid pressure decreases in the fracture during the shut-in period. In the limiting case, the fracture may start to close off tightly at the tips and this process could progress toward the wellbore until the entire fracture is closed completely. Recessing fracture length and diminishing fracture aperture will hasten the time to pseudo-radial flow. As well, minimizing the injection volume and rate will hasten fracture closure, reduce fracture length, and minimize residual fracture width at the onset of closure, also speeding

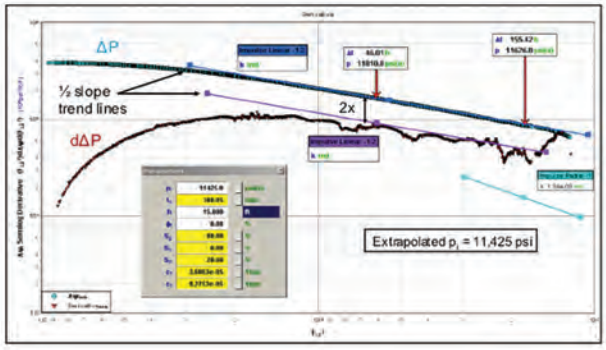

17.59—After-closure flow regime type curve analysis—evaluating a pseudo-linear flow period. (Martin et al. 2012.)

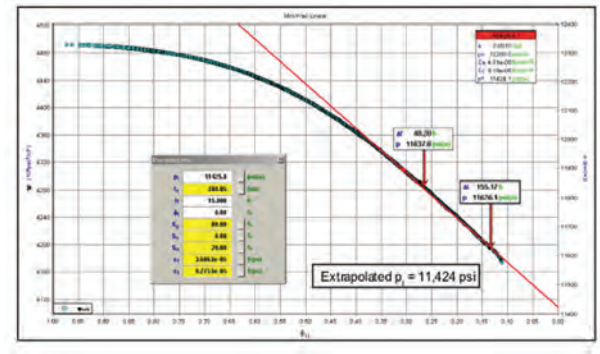

Fig. 17.60—After-closure, pseudo-linear flow analysis for estimating reservoir pressure. (Martin et al. 2012.)

the arrival of pseudo-radial flow. As such, most of the layered diagnostic fracture injection tests utilize a very small injection volume, in the range of 1 to 12 barrels of fluid. Even when using small injection volumes, for cases of low hydraulic diffusivity ($k/\mu\varphi c_t$) and high-strength reservoir rock, an interpretable pseudo-radial flow period can take many hours or even days to achieve.

Mobility. In order to compute kh, it is important to know the viscosity of the mobile reservoir fluid. The leaked-off injection fluid occupies very little of the total rock volume investigated during the test. Its main function is to create a disturbance or impulse into the reservoir pore network. The in-situ fluids that are mobile will move in response to the push. The relative ease of the reservoir fluid movement will dictate the nature of the pressure decline response.

Factors impacting the ease or resistance of far-field fluid flow are mostly related to reservoir properties: k, h, μ, φ, c_t, Δp (i.e., sand-face pressure (p_w) – p_i) and lateral changes in pore network and saturation characteristics. The measured permeability is system permeability within the tested rock volume or investigated area and includes the impact of open natural fractures.

Test Height. The height of the test interval is often uncertain given the extremely low vertical permeability that is characteristic of tight reservoirs. Hydraulic fractures connect the wellbore to greater interval thickness. Fracture modeling can be used to estimate fracture height growth and aid in selecting test height for improved characterization of reservoir permeability.

17.6.2.3 Diagnostic Fracture Injection Tests: Tactical Points and Guidelines

- Hydraulic fracture modeling can provide guidance on perforation location and perforation cluster spacing in the case of multilayer DFIT projects.
- Pseudo-radial flow development is necessary for deriving reservoir transmissibility (kh/μ) and can be hastened by limiting the injection rate and volume to minimize fracture length.
- Perform repeat injection/falloff cycles as necessary to confirm fracture closure selection when observing a fuzzy or ambiguous closure signal from the first cycle.
- When doing multiple DFIT cycles, plan to have a long shut-in period following the first injection to facilitate development of pseudo-radial flow.
- Downhole shut-in is recommended when working with under-pressured reservoirs and presents several general advantages including increased DFIT pressure

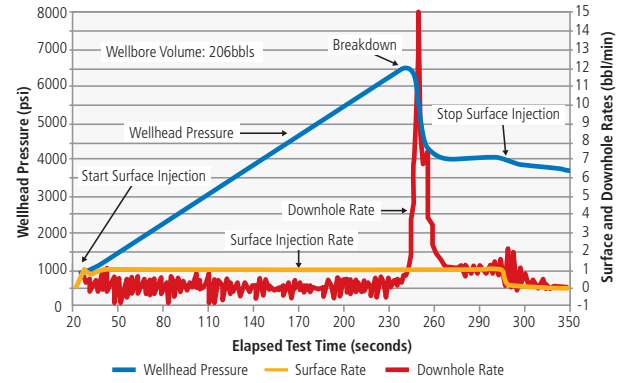

Fig. 17.61—A comparison of surface and downhole injection rates during the breakdown and fracture propagation events. (Cramer and Nguyen 2011.)

responsiveness by reducing wellbore storage, and facilitates the testing of multiple intervals.

- Well preparation measures include circulating the well at least 24 hours prior to conducting the DFIT (not necessary with downhole shut-in), and over-balanced perforating to reduce the risk of gas inflow prior to injection.
- Fracture height growth can be extensive even for very small DFIT injections. When doing multiple-interval DFITs, space test perforations at least 50 ft. apart, unless fracture modeling efforts and field experience dictate otherwise.
- Inject long enough to develop a stable pressure trend; this indicates that sufficient far-field fracture volume is available to enable dissipation of excess pressure resulting from fracture complexity within the near-wellbore hoop stress region. Near-wellbore fracture complexity has been indicated in multiple-interval vertical DFIT communication tests and is more severe in horizontal well DFITs.
- Natural fracture networks will be sensitive to increase in the net effective stress associated with reservoir pressure drainage during production. In these cases, DFIT-derived permeability represents a maximum initial value and may need to be adjusted downward when doing production analysis.
- A long period of pseudo-linear flow in the after-closure period is often indicative of reservoir flow being dominated by unidirectional natural fractures.
- In regard to DFIT, vertical wells present significant advantages as compared to horizontal wells including reduced near-wellbore fracture complexity, the ability to modify perforation intervals to test a desired horizon, and the ability to test multiple intervals.
- In multiple-interval DFIT projects, install pressure gauges beneath isolating bridge plugs to assess the presence or absence of pressure communication in passive, previously tested intervals during testing of the uphole interval.

17.7 Unconventional Fracturing Operations

17.7.1 General Introduction to Fracturing Operations

The hydraulic fracturing industry has progressed in developing the tools, techniques, and equipment required to economically develop the tightest permeability reservoirs to date, which fall under the overall description of unconventional resource plays. A general understanding of the concepts surrounding all aspects of unconventional stimulation comes from the realization that a single fracture, placed into a reservoir from a single vertical wellbore, has a limited ability to produce enough oil or gas to be economically viable. However, a horizontal wellbore drilled into the same reservoir allows for dozens, to over 100, of individual fractures to be propagated out of a single horizontal lateral, thereby multiplying the total amount capable of being produced from the reservoir by the number of fractures propagated successfully into the formation. The scope and size of these multistage horizontal fracturing treatments, almost by definition, makes them massive hydraulic fracturing operations (see **Fig. 17.62**).

The stimulation methods by which these horizontal wellbores are completed further define the equipment used in the execution of hydraulic fracturing operations. Today three basic methods of completion are used to execute new well multistage horizontal lateral stimulations. They include a plug-and-perforate method where multiple perforation sets are placed in the casing and those perforation clusters are then treated simultaneously at a high rate within an individual stage. The concept and techniques of "limited entry" (see Section **17.5.2**), through the application of diversion-utilizing perforation friction pressure, are performed with high fracturing fluid rates, with the intent of diverting the fluid equally into each of the intended perforation sets. This type of treatment requires high rate pumping and blending equipment, with many of these treatments varying in rate from 70- to 120-barrels per minute (bpm). Next would be the use of mechanical isolation techniques in which a multistage fracturing completion system is placed in the open-hole horizontal lateral. These systems can be cemented in the wellbore or packers can provide isolation between multiple-stage, ball-activated fracturing sleeves. Several variations to this technology exist whereby each stage treatment is pumped and then a sized ball is dropped into the well and is pumped to the correspondingly sized target ball seat. Upon the ball being engaged in the ball seat, the previous open fracture sleeves are isolated from further treatment and the next set of sleeves to be fracture stimulated uphole are opened when pressure is applied against the ball. The entire horizontal wellbore stimulation treatment, therefore, does not stop between stages. The pumping rate only slows allow for each ball to drop at the surface and then the ball is pumped into the well, where the ball is seated on the ball seat. This repeatable operation successively opens one or more sleeves to allow for the execution of each fracturing stage. Another stimulation method, which is typically executed with coiled tubing, isolates each individual fracturing sleeve. This method allows for the targeted stimulation of one fracture at a time through coiled tubing activated fracturing sleeves. The hydraulic fracturing treatment is pumped down the coiled tubing and casing annulus. A packer bottomhole assembly is used to provide

zonal isolation from the previously treated sleeves and opens the next sleeve adjacent to the intended point along the lateral to propagate a fracture (Castro et al. 2013b). The total time required to stimulate the entire horizontal lateral is extended in this type of completion due to the lower pumping rates that are utilized when fracturing down the casing and coiled tubing annulus. This treatment, out of the three described, is considered to be the most effective method for placing a hydraulic fracture at each intended location along the length of a horizontal lateral wellbore.

17.7.1.1 Brief Introduction to Fracturing Equipment

The methods and technologies surrounding the process of hydraulic fracturing are accomplished through the use of specialized equipment. The performance of the pumping, blending, and associated auxiliary pumping units have been advanced to meet specific needs within the industry for more than six decades. Basic concepts regarding equipment performance still remain, in that the fracturing fluid must be pumped at sufficient pressure to initiate and propagate the fracture into the formation, and that the blending equipment must control the mixing of precise formulations of fluid, proppant, and other materials to optimize the stimulation of the reservoir in the form of improved conductivity.

Today, the treatment of unconventional reservoirs uses pumping and blending equipment in addition to chemical additive units, polymer hydration units, proppant storage, fracturing manifold trailers, high pressure treating iron, and computer monitoring and control units. Frac pumps are rated to deliver between 2,000 and 3,000 hydraulic horsepower per unit. These high rate fracturing pumps and the high pressure treating iron are capable of withstanding working pressures in excess of 15,000 psi. The blending equipment is computer-controlled so that the ratio of proppant and products correlates to the amount of fluid being mixed and pumped through the blender. The basics of conventional fracturing equipment have not changed greatly to handle unconventional horizontal well hydraulic fracturing operations, but numerous improvements have been made that are directly associated to this work. These multistage fracturing operations now take days to complete the stimulation of each horizontal wellbore. This additional time and accelerated use of the equipment has reduced the life of equipment component parts and systems. Since the maintenance periods between component replacement has been shortened due to the accelerated hours of utilization, equipment has been redesigned to allow for faster replacement of worn out elements. Also attributed to the extended time on the well site are personnel safety and

Fig. 17.62—Photograph illustrating the massive hydraulic fracturing of an unconventional reservoir. Note that the huge quantities of water required for treatment are stored in a specially dug pit outside the photograph to the left.

environmental aspects that have been incorporated into new equipment. These include computer control and automation of equipment, which reduces the number of people required to execute a treatment. Upgraded capabilities have reduced engine emissions through the development of dual fuel fracturing pumps that utilize both diesel and natural gas, while current developments are ongoing to develop electrically powered fracturing pump technology. Other advances that have emerged include those in dust control, noise reduction, the pumping of dry-on-the-fly polymers, and the deployment of technologies that can prevent equipment leaks or product spills on the well site from reaching the ground. Examples of the different types of fracturing equipment are included in **Fig. 17.63**. A diagram illustrating how all this equipment fits together is given in **Fig. 17.64**.

17.7.1.2 Fracturing Operations: Before, During, and After the Treatment

Unconventional hydraulic fracturing operations are a collaboration of human and machine that is brought together in order to safely, effectively, and efficiently stimulate horizontal multistage wellbores. To accomplish this feat takes continuous logistical support to deliver to the well site the required water, proppants, complementary products and materials and fuel, to be used in the treatment, as well as provisions for the personnel performing the fracturing operation. Processes and standards that apply to the well stimulation are the basic functions that drive the actions before, during, and after the fracturing operation.

Weeks before a stimulation treatment is scheduled to be pumped, the date for the well treatment is added

to the fracturing calendar. From then until the time the equipment is mobilized to location, logistical processes take place in order to fulfill and deliver the intended wellbore stimulation treatment. Reviews of the fracturing design provide the parameters that will be needed in order to execute the job. The equipment capabilities will revolve around the desired pumping rate along with the corresponding hydraulic horsepower requirements and the design of the fracturing fluids will determine the types of auxiliary units that will be needed to meet the stimulation criteria. This review of the fracturing operations then quantifies the specific equipment and the total number of units that will be required for the execution of the fracturing treatment. Associated personnel will be utilized to implement the plan and to operate the equipment at the well site with the number of people, experience, and training coinciding with the equipment selected.

Beginning at the time of the mobilization of equipment to location, multiple safety meetings will occur with service company personnel. They will cover the travel to location and the rig-up of treating iron and equipment at the well site. Discussions will later outline the planned execution of the treatment, the methods to be used in the pumping of the fracturing operation, and the specific duties of each person on location. All potential HS&E conditions are also identified so that they can be corrected and eliminated prior to the beginning of the multistage fracture treatment.

Pre-job checklists are used to verify the operational capability of the equipment to perform its role. This process confirms that the equipment has been inspected and tested prior to the job and that it is in operating condition. The equipment on location is connected to the computerized control cabin or treatment monitoring center where all job-related data from the fracturing operation will be collected (see Fig. 17.64). This data will be used to analyze and make decisions regarding the stimulation treatment, control blending and pumping equipment on location, and monitor the fracturing fluid and the proppant being injected into the wellbore.

During the job, equipment sensors monitor the performance of the equipment in order to provide alerts in the event a unit is not functioning within standard operational ranges. Computer control of equipment such as blenders, fracturing pumps, sand delivery units and chemical additive units, helps to simplify the fracturing operation. Computer warnings also display issues with the performance of equipment so that proper maintenance can be directed to the particular problem in order to provide a remedy to the situation. Many critical operational problems occur with

Fig. 17.63—Examples of modern fracturing equipment: A–control van, B–2700 HHP "Gorilla" fracturing pump, C–125 bpm blender, D–2500 cu ft., 4-compartment proppant storage trailer, E–manifold trailer, rigged-up on location, and F–body-load hydration unit. (All photos courtesy of Baker Hughes.)

the high-pressure pumping equipment so it is a common practice to have surplus capability on location to handle the horsepower requirements in the event any of the fracturing pumps cannot be utilized.

The coordination and delivery of water and proppant to the blender are essential elements in the proper execution of the designed fracture treatment. Typically, dedicated personnel provide oversight of these areas in order to ensure that the correct amounts are available, as well as to oversee the proper placement of the proppants on location into the correct compartments or proppant storage units.

After the conclusion of each stage of the horizontal wellbore completion, the equipment is evaluated to identify any possible maintenance requirements that need to be addressed prior to the start of the next stage. At the conclusion of the entire multistage fracturing treatment operation, the equipment is likewise evaluated for maintenance issues before being scheduled to perform another job. To reinforce the strict environmental standards enforced during all fracturing operations, following the rigging down of the equipment from the wellhead and the removal of all the trucks from location, a thorough inspection of the location is performed. This allows the removal of

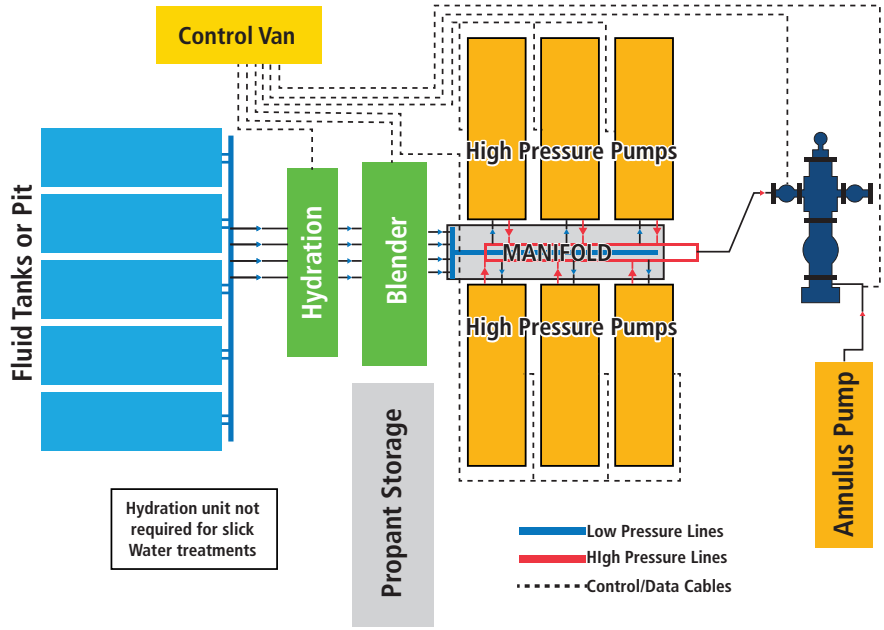

Fig. 17.64—Schematic diagram illustrating how the fracture equipment fits together and how the fluid, proppant, and slurry flows through the various different equipment types. (After Martin 2009.)

all unwanted materials and to immediately address any concerns relating to equipment leaks or spills that may have gone undetected during the completion of the well.

17.7.2 Issues Specific to Unconventional Fracturing

The size and scope of multistage horizontal well fracturing operations that are used to complete unconventional shale reservoirs are relatively new to the industry. Although wells have been hydraulically fractured since the late 1940s, it is the combination of horizontal drilling techniques along with the industry's ever-growing understanding of the complexities associated with stimulating shale formations that are now progressing. Through dedicated engineering and the understanding of these reservoirs, best practices are being developed leading to improved economic delivery through ever-increasing well production and advancements in the long-term performance of these wells. The engineered placement of numerous hydraulic fractures, propagating from a single horizontal wellbore, has taken the place of many vertical wells drilled from individual surface locations. This reduces the surface footprint of ongoing field development operations, but the tremendous volumes of water and materials required can be challenging from the standpoint of logistics.

The mobilization of high-rate hydraulic fracturing equipment capable of performing the stimulation of horizontal wells has segmented completion strategies into a few distinct methods. One treatment method that grew out of the stimulation of horizontal wellbores is the use of mechanical isolation and sliding sleeve technologies. This process of placing a completion string into the horizontal lateral from which to treat the formation with dozens of propagated fractures, allows the entire wellbore to be treated without interruption. While methods such as "plug and perforate" shut down operations for a period of hours between stages to prepare the well, a continuous multistage treatment can be executed along the lateral with the dropping of balls that successively open new sleeves with which to treat through and seal off the already treated intervals.

When the industry had adapted to manage massive hydraulic fracturing treatments in horizontal wellbores it was then only a small step to see the advantages of drilling multiple wellbores from a single surface location. The same techniques that allowed for multiple wells to be drilled from an offshore drilling platform were now the preferred method to utilize directional drilling expertise on land to place parallel horizontal wellbores throughout the reservoir.

17.7.2.1 Logistics of Unconventional Fracturing

The planning and the logistical support needed to accomplish a stimulation operation are critical to the efficient delivery of the multistage fracturing treatment. Operators

and pressure pumping service companies begin their collaborations well in advance of the fracturing process. They work to ensure the location size will be adequately prepared to accommodate the necessary hydraulic horsepower in the form of pumping equipment that will perform the treatment. Consideration is also given to the handling and continuous delivery of consumable products during the fracturing operation. Materials such as water, gel, chemicals, proppants, and fuel will be brought on site throughout the operation and they will need to be handled without disrupting the flow of ongoing operations.

The key deliverables in performing a horizontal well stimulation are the fluid and the proppant. It is important to plan for them in advance of the job since the water and proppant volumes will be significant. It is critical for the operator to develop a water management plan that will deliver the quantities of fluid that are designed to be pumped throughout the multistage stimulation operation. Water will need to be partially stored on location with the remainder accessible from storage in close proximity to the well site (see **Fig. 17.65**). As water is pumped in the treatment process, additional water can then be transferred to storage on location. Proppant quantities are also significant and will likely require delivery by rail and by truck. These sand and ceramic proppants are sourced from mines and manufacturing plants that are, in most instances, located considerable distances from the wells.

17.7.2.2 Continuous Multistage Operations

Continuous operations are uniquely suited for horizontal well operations where water, proppant, and materials are available for pumping without disruption. Unlike the "plug and perforate" completion method that interrupts the stimulation process between stages, in order to execute the setting of a plug and perforating the next stage's perforation clusters, a mechanical isolation treatment is preconfigured and placed in the well after the horizontal lateral is drilled. The paths of the initiated fractures from the wellbore are then directed to be adjacent to the sliding sleeves. The sleeves are ball-activated in that they are opened as a ball passes their location in the horizontal wellbore, or opened when the ball is seated and pressure is applied. The final landing position of the ball is in a ball seat where it acts as a plug. This prevents further fluid from being placed into the previously treated sleeves positioned along the wellbore.

Mechanical isolation tools are run into the openhole horizontal lateral and can be cemented in the wellbore, or packers can be used to provide isolation between the stages of ball-activated fracturing sleeves. There are several variations of this technology available in the industry where the stages are isolated from one another through the pumping and seating of a sized ball. The ball can be seated in a correspondingly sized target ball seat where it activates the opening of a fracturing sleeve, or it can be pumped along the horizontal lateral opening several sleeves until finally being captured in the last ball seat. The last ball seat then acts as a plug to isolate the previously treated sleeves from the subsequent stimulation treatment. This process allows for the continuous treatment of the multistage stimulation along the entire horizontal wellbore. The treating rate of the fracturing operation is only slowed sufficiently to allow for the dropping of each ball between the stages. When the sliding sleeves have been opened and the ball has seated, the pump rates are increased in order to execute the next hydraulic fracturing treatment along the horizontal lateral. The entire operation is then repeated for each stage so that one or more new sleeves are opened during each stage until the entire horizontal wellbore stimulation is completed.

17.7.2.3 Multiwell Operations: About Well Factories, Simo-Fractures, and Zipper Fracs

The efficiency gains realized through supply chain process improvements have helped to control costs and reduce periods of non-productive time on multistage fracturing treatments. The ability of multiple horizontal wells to be drilled parallel to each other adds the ability of those wells to be initiated from a single surface location. The efficiency gains tied to the supply chain logistics of bringing water, proppants, products, and fuel to a single location to treat a single well can then be further leveraged when multiple wells are drilled and then fracture stimulated from one location or pad.

It has been demonstrated that horizontal laterals that are landed in close proximity to one another can propagate complex fracture networks that can intersect and overlap each other. When a first well is treated and flowed back, a fracture network is created that corresponds to the total contacted fracture surface area. It is that total fracture geometry that is used to produce the reservoir. When another well in close proximity to the initial well is stimulated there is a probability that some of the second well multistage fracture treatments will intersect the fracture network created from the first well's treatment. Hydraulic fractures always propagate in the direction requiring the least energy so any fractures that intersect already existing fractures will re-propagate in the same direction. The fluid will then follow the same complex fracture network

building fracture width and carrying proppant into the already treated area of the reservoir. This causes an overall reduction in new contacted fracture area that could have been otherwise generated from the second well stimulation had it not intersected the first well. These concepts of well stimulation interference are confirmed each time a nearby producing well's production is detrimentally affected following the stimulation of an offset well. Fracturing fluid is likely placed into connecting natural fractures, or along the bedding planes of the formation, until it intersects with previous fractures that were propagated during the multistage stimulation of the initial well. When connected to the source of new fracturing fluid, many producing wells will experience a detrimental reduction in production, as additional fracturing fluid has to now be recovered before production can be restored.

Methods have been developed to overcome the detrimental effects of stimulating nearby horizontal laterals (see also Section 17.4.3.3). One such operation includes simultaneously fracture stimulating two or more offset wellbores at the same time. This treatment method, known as a "simo-fracturing" for short, treats two, three, or four wellbores simultaneously from wells drilled from separate surface locations or on the same pad (Schein and Weiss 2008). Each well is rigged up with its own fracturing equipment and the multistage fracturing stimulations are performed at the same time (see **Fig. 17.66**). Any intersection of fracture networks that occurs during the treatment then causes the propagation energy from both treatments to be directed toward the initiation of additional fracture area. It is this concept that works to add additional production capability to the wells rather than duplicating some of the contacted fracture face area as described previously.

Often operators that utilize the "plug and perforate" completion method will drill and complete several wells at the same time in succession while working on a single pad location. This method of stimulation is known as a zipper fracture. The fracturing equipment is placed on location so that the high pressure treating iron can be shifted between the wellheads of multiple individual wells. Following the fracture stimulation of the first stage of the first well, the treatment shifts to the stimulation of the first stage on the second well and so on, until all the wells are finished. In between each stage, as the fracturing equipment is stimulating the next well, the plug-and-perforate operation is being performed to prepare another well for its next stage treatment. The fracture stimulation of each stage, followed by the subsequent plug-and-perforate operation, is repeated over and over again until the final stage of the last well has been completed. Similar to a simo-fracture treatment

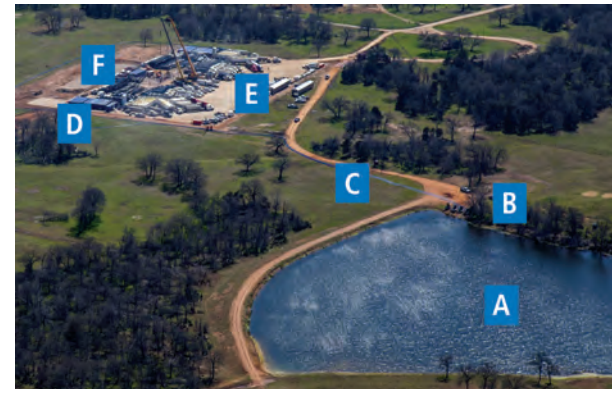

Fig. 17.65—Aerial view of an East Texas two-well "simo-fracture" location. The labels indicate the following: A–the huge pond required to store all the water needed for the whole operation; B–the pumps to move the water from the pond to the equipment, usually incorporating 100% redundancy; C–the pipelines between the water pumps and the equipment; D–several of the 500 bbls tanks, used as "surge" tanks between the water pumps and the blending equipment; E–two complete fracturing equipment spreads; and F–the flowback pit used to catch water for treatment and disposal.

Fig. 17.66—This massive hydraulic fracture treatment in the Barnett shale demonstrates the engineering and technical commitment required to work in these complex plays. The illustration shows a three-well, simultaneous fracturing operation.

where wells resist fracture retreatment of the same fracture network, a zipper fracture accumulates the fracture net pressure increase gained from the recently stimulated fracture networks. That residual, post-fracture net-pressure build-up, and the accompanying stress-shadowing effects, act to direct fractures in new paths, rather than along already established fractures. In the event an already established fracture is intersected, the existing fluid located within the fracture can be pressured and directed to deliver additional

fracture length that may then intersect additional natural fractures. The combined effects of treating a zipper-fracture series of wells allows for the creation of new fractures to be developed or extended. This completion method is intended to develop more created fracture area through the generation of additional fracture complexity associated with this multiwell, multistage, horizontal fracturing technique.

17.7.3 Fracturing Fluid Recovery

The hydraulic fracture stimulation of a horizontal wellbore is designed to place a particular amount of fluid and proppant within a given individually created hydraulic fracture, or within multiple fractures when treated together in a single stage. The production of an unconventional shale reservoir from a horizontal wellbore is ultimately proportional to the amount of created and propped fracture area resulting from the multistage fracture stimulation treatment. The total created fracture area in many shale formations is a combination of the newly generated hydraulic fractures along with the opening of pre-existing natural fractures within the reservoir. The total of these two fracturing mechanisms together relates to the concept of fracture complexity. The more fluid that is pumped, the more created fracture area has the potential to be developed. This is the basis for the tremendous volumes of water-based fluids that are pumped and later returned to the surface. That produced fluid is commonly referred to as the flowback water, or load water.

The multistage hydraulic fracturing operation that is performed does not end with the completion of the final fracturing stage. There remains a critical step between the fracturing treatment and the ultimate production of oil or gas, which includes the cleanout of the wellbore and the recovery of the fracturing fluid flowback water. The pumping of a horizontal stimulation is a water-intensive operation requiring several millions of gallons of water to complete a single well. Following the completion of the stimulation treatment, a portion of the fracturing fluid mixed with water from the formation will be produced back to the surface. Depending on the shale formation and the particular area within each basin, the amount of flowback water produced will typically range between 10% and 40%. This total amount of flowback fluid can be predominantly returned in the first weeks of production or may continue steadily for several months before falling off to lower rates.

The components within the flowback water will have changed from the constituents that were placed in the original fracturing fluid. The mixing of formation brine water along with the dissolving of minerals and salts in the formation and within natural fractures will increase the total dissolved solids (TDS) content of the flowback water. The salinity of the water will be increased and the hardness level, indicating the amount of dissolved minerals in the water, will also be higher in the produced fluid. The handling of this produced flowback water encompasses the practices of water management today. Flowback waters that are produced will, in some instances, be processed for use as fracturing fluids, following filtration. Other recovered water may be treated with processes such as reverse osmosis, ion exchange, and other technologies so that the water can be reused in fracturing fluids. In many instances, the total amount of water required on a subsequent fracturing treatment will exceed the flowback water produced. Additional sources including produced water from offset wells in the field, brackish well water produced from locally sourced formations, fresh water, or varying combinations of waters can be used to make up the volume difference, hence the term "make-up water." Flowback water may also be sent to disposal facilities that process salt water for injection into disposal wells.

17.7.3.1 Flowback

Soon after the conclusion of the fracturing operation on a multistage horizontal well, the equipment and treating iron are rigged down and removed from the well site. The next step in the post-fracturing process often utilizes a coiled tubing unit to begin the cleanout of the wellbore prior to the initiation of fluid recovery. The coiled tubing unit drills out any plugs that were placed in the horizontal lateral to provide stage isolation, or removes any of the non-dissolvable type balls that were dropped to open sleeves, and is used to circulate out any proppant and debris that remain in the horizontal lateral. During this beginning step in the preparation to initiate the flowback of fracturing fluids, standard operating procedures involving the acid pickling of the coiled tubing string should be followed. Coiled tubing strings contain a large amount of internal surface area that is prone to rust while the string is on the reel at the surface. During the cleanout of a well, slickwater fluid containing polyacrylamide friction reducer is widely used to increase flow rates and to reduce circulating pressures. The combination of the polyacrylamide polymer with high iron content water will cause the friction reducer to flocculate and to precipitate out of solution. The polymer solids may then be left in the wellbore where they could become a cause for concern.

Unconventional shale reservoir stimulation presents additional challenges when using the techniques involved in multistage fracturing of the horizontal wellbores. These shale reservoirs are very low permeability formations and, therefore, it takes a tremendously long time for the initiated fractures to close.

This allows ample time for the proppants to settle within the created fracture as well as allowing for proppant convection that can pull proppant away from the wellbore before a confining stress on the proppant occurs (see Chapter 13 of Economides and Martin 2007). Those items, coupled with other engineering considerations such as the inability to perform forced closure operations in order to draw proppant back into the near wellbore region, present a possible lack of proppant conductivity near wellbore. Another factor that detrimentally contributes to near wellbore conductivity concern is the over-flushing of the tubular volume following the placement of the final proppant stage. This practice is performed during some treatments to better clean the casing of residual proppant so that mechanical bridge plugs will be more effectively set in the wellbore to provide isolation from the previous treatment. The over-flushing of fracture stages, however, is proven to have a negative impact on the amount of proppant that is left in the near wellbore region. This reduces the fracture conductivity and affects the wellbore's connection to the far field complex fracture network.

As unconventional horizontal shale development technology moved across the basins of the United States, high initial production (IP) numbers were prized over other production parameters. This led operators to aggressively draw down new wells on large choke sizes in order to obtain high IPs. Today, numerous operators have determined that the large initial drawdowns that were associated with higher IPs from reservoirs were not sustainable over long periods of time. Many wells within fields demonstrated production declines from IP levels of 90% within the first year. Today, a more moderate approach is widely favored whereby the initial flowback of fracturing fluids is being executed with very small choke sizes and reduced flow rates. This method of flowback is taking place over longer periods of time as the wells are cleaned up. It is noted that a growing consensus among operators is now that these reduced rate flowback methods are contributing to higher long-term production levels over high rate cleanup methods. It can then be postulated that excessive flowback rates may contribute to the flow of proppant into the wellbore from the fracture thereby reducing conductivity. The associated drawdown, if great enough, could also cause damage to the proppant. Lower rate flowback methods may be contributing to improved conductivity of the fractures when all other reservoir and treatment parameters between comparison wells are essentially equal. Based on the previously outlined concepts that proppant during the fracturing of the stages is likely being displaced or drawn away from the near wellbore area, it is highly probable that the slower and steady flowback of the fracturing fluid during the initial producing period could be helping to draw proppant back to the near wellbore area where it is then filling in and bridging correlating to an improvement in conductivity.

It is becoming more apparent that the cleanup of the horizontal wellbore and the return of fracturing fluids following a multiple day fracturing operation are of vital importance to the overall long-term production life of many wells. The operational management on location of the flowback process and the techniques used are proving to be a critical aspect relating to production and the maximizing of a well's estimated ultimate recovery (EUR), and are, therefore, of importance to the proper completion practices of the fracturing operation.

17.7.3.2 Recycling and Disposal

The usage and management of water is a primary factor in the successful development of unconventional resource plays. The ability to source the water required for fracturing operations, as well as the handling of the flowback and produced water that follow, are factors that can positively affect the ultimate profitability of projects and operations. Factors relating to the intensive water requirements supporting the hydraulic fracturing of multistage horizontal wells have created a need for recycling water resources. Service companies and operators are increasingly reducing the demand for fresh water resources by developing practices that use flowback, produced, recycled, and non-potable water sources.

Before the proliferation of horizontal unconventional shale drilling, fracturing operations used vastly smaller amounts of fresh water to hydraulically fracture stimulate conventional reservoirs. These water-based treatments were either sourced from rivers, ponds, and lakes, or from fresh water aquifers, as well as municipally treated potable water. Historically, any flowback water recovered was transported to a disposal well for injection. The transition to horizontal unconventional stimulations has brought an era where water-intensive fracturing treatments are required to adequately stimulate these low-permeability reservoirs. The overall increased water volume requirements therefore correlate to cost increases associated in the sourcing, transportation, and disposal of these water-based fluids. It has now become feasible and cost-effective to treat and recycle flowback water, rather than paying for its disposal and replacement with equivalent additional fresh water volumes. **Fig. 17.67** shows the typical equipment used for water recycling.

The need for the industry to utilize treated, recycled flowback and produced water in fracturing operations has coincided with advancements in fracturing fluid chemistry by leading

Fig. 17.67—Typical equipment spread used to recycle flowback water on a US land wellsite. Note the mats beneath each skid for catching spills of the flowback water, the concentrated effluent, and the treating chemicals. (Photo courtesy of Baker Hughes.)

service companies. Their knowledge of reservoirs and of fluid chemistry has advanced fracturing fluid system innovations in two critical areas. First, the ability to hydrate synthetic polymer friction reducers in high-TDS and high-hardness environments was overcome, along with the ability to crosslink premium performance guar-based polymer systems in these same flowback and recycled waters. The ability to perform fracturing operations consistently with recycled and brackish water has transformed a former wastewater byproduct from the fracturing process into a cost-saving alternative to fresh water fracturing fluid systems.

The methods used in water management processes for the treatment of flowback water can vary within several categories. The removal of the larger particles from the fluid is accomplished through filtration where some of the suspended solids are captured. These solids can include formation and proppant fines, iron particles, and polymers (both broken and unbroken). Next, smaller colloidal-size particles such as clays and hydrocarbons can be treated with electrocoagulation. This process makes use of anodes and cathodes to remove the smallest particles from the flowback fluid following filtration. The anodes produce positively charged ions, which bond to fine particles in the flowback fluid that are negatively charged. The particles coagulate or agglomerate together, and, as they become heavier, they settle to the bottom of the treatment tank. In conjunction, the treatment also uses cathodes that produce gas bubbles that can attach and lift small, coagulated particles and hydrocarbon to the surface, where these constituents can be skimmed off and removed (Walsh 2013). Further processes of chemical flocculation and precipitation can be used to eliminate elements within the water, such as barium, that may be a concern because of scaling tendencies. When a sulfate solution is added to flowback water the barium content in the water will be converted to barium sulfate and efficiently precipitate out of the water. Lastly, the process of desalination can be employed to reduce the levels of salts and minerals through the use of reverse osmosis technology. All of these methods can be utilized to recycle flowback water, with varying degrees of initial contamination, and return the majority to recycled fracturing quality fluid (see **Fig. 17.68**). Following the treatment of the flowback water, only a small portion of the original volume will be sent for disposal. This represents a reduction in cost to the operator from the elimination of much of the transportation

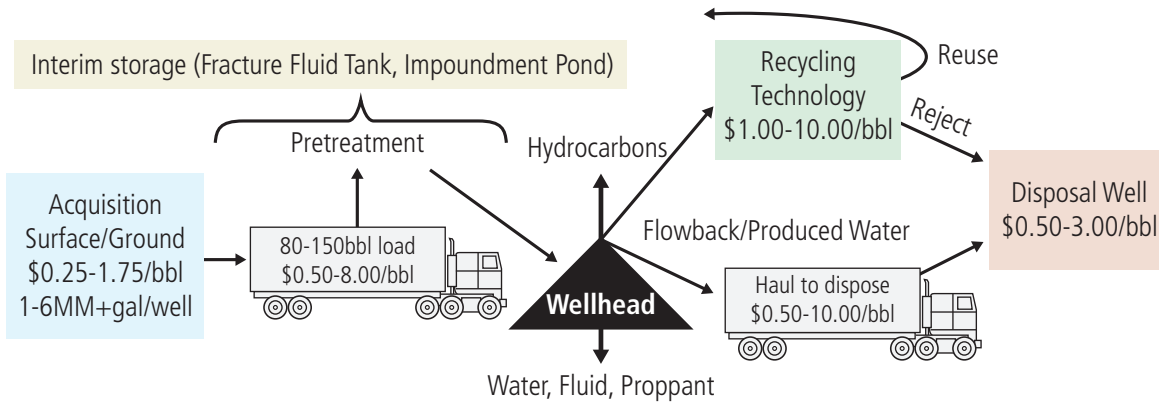

Fig. 17.68—All-in-cost of water for hydraulic fracturing. (Jeffries, GE, NETL 2013.) Note the huge variations in cost for transport, recycling, and disposal of the flowback water.

and disposal costs previously associated with the flowback of fracturing fluids. An ongoing savings to the operator can also be captured as the produced water stream from wells is diverted for recycling instead of disposal in order to support the fluid requirements of the next horizontal well's multistage hydraulic fracturing operation.

17.8 Acknowledgments

The authors would like to thank the following for their assistance in the preparation of this chapter: Randy LaFollette, Robert Hurt, Paul Carman, and Ahmed Gomaa of Baker Hughes.

17.9 Nomenclature

c_t	Total formation compressibility
Cd	Discharge coefficient
C_{fD}	Dimensionless fracture conductivity
d	Diameter (general); perforation diameter; distance between fractures
d_{prop}	Proppant grain diameter (usually average)
E	Young's modulus
E'	Plane strain Young's modulus (= E/[1 – ν2])
F_{cD}	Dimensionless fracture conductivity (obsolete)
F_d	Drag force
g	Acceleration due to gravity (= 9.81 m/s2)
g_{ob}	Overburden stress gradient
G	G-Function (see Nolte, 1979)
G'	Storage modulus for viscoelastic fluid
G''	Loss or viscous modulus for viscoelastic fluid
h	Height (general), net height, fracture height
H	Depth (usually vertical)
H	Perforation hydraulic diameter (= $d\sqrt{C_d}$)
J_{DTH}	Dimensionless productivity index for a single transverse fracture on a horizontal wellbore
J_{DV}	Dimensionless productivity index for a single fracture on a vertical wellbore
k	Permeability (general); formation permeability
k_f	Fracture or proppant permeability
K'	Power law fluid consistency index
t	Cosine of angle α
L	Length (general)
$\hat{m}$	Cosine of β
n	Cosine of angle γ; number of perforations
n'	Power law fluid exponent
p	Pressure (general)
p_b	Breakdown pressure
p_c	Closure pressure
p_f	Fluid pressure in fracture
p_{head}	Hydrostatic pressure or "head"
p_i	Initial reservoir pressure
p_{inj}	Injection or wellhead pressure
$pnet$	Net pressure
$p_{net,min}$	Minimum net pressure
$p_{pipe\ friction}$	Fluid friction pressure in pipe
p_r	Reservoir or pore pressure
q	Flow rate
r	Radius

r_w	Wellbore radius
s_c	Choke skin
t	Time (general)
t_D	Dimensionless time
v	Velocity
$v\infty$	Terminal velocity
w	Average propped width

17.10 Symbols

α	Biot's poroelasticity factor; angle of plane to σ_v
β	Coefficient of inertial resistance; angle of plane to σ_H
γ	Specific gravity; Angle of plane to σ_h
γ_f	Fracturing fluid specific gravity
γ_{prop}	Proppant specific gravity
$\overline{\Delta p}$	Pressure change, pressure loss
Δp_{BHFP}	Limited entry pressure differential
Δp_{pf}	Pressure loss due to perforation friction
Δp_{tort}	Pressure loss due to tortuosity
λ	Fracture network aspect ratio
μ	Viscosity
μ_f	Fracturing fluid viscosity (not slurry viscosity)
ν	Poisson's ratio
ρ	Density
ρ_f	Fracturing fluid density
ρ_{prop}	Proppant density
σ_c	Closure stress
σh	Minimum horizontal stress
σ_H	Maximum horizontal stress
σ_n	Stress normal to a plane
σ_v	Vertical stress
φ	Porosity
Ψ	Stiffness factor
ω	Radial velocity

17.11 References

Ahmed, U., 1988. Fracture Height Prediction, ***JPT***, July 1988, pp. 813-825.

Ahmed, U., Abou-Sayed, A., and Jones, A. 1979. Experimental Evaluation of Fracturing Fluid Interaction with Reservoir Rocks and Propped Fractures. SPE Paper 7922 presented at the annual TIS Gas Conference in Denver, CO, 19 May 1979.

Aladasani, A., Salehi S., Bai, B., et al. 2014. Optimizing the Development of Tight Formations. Paper SPE 167742 presented at the SPE/EAGE European Unconventional Resources Conference and Exhibition. 25–27 February. Vienna, Austria. http://dx.doi.org/10.2118/167742-MS.

Alqahtani, A.A., Mokhtari, M., Tutuncu, A.N., et al. 2013. Effect of Mineralogy and Petrophysical Characteristics on Acoustic and Mechanical Properties of Organic Rich Shale. Paper SPE 168899 presented at the Unconventional Resources Technology Conference. 12–14 August. Denver, Colorado. http://dx.doi.org/10.2118/168899-MS.

Alvarez, J.O., Neog, A., Jais, A., et al. 2014. Impact of Surfactants for Wettability Alteration in Stimulated Fluids and the Potential for Surfactant EOR in Unconventional Liquid Reservoirs. Paper SPE 169001 presented at the SPE Unconventional Resources Conference. 1–3 April. The Woodlands, Texas. http://dx.doi.org/10.2118/168001MS.

Angeles, R., Tolman, R., Gupta, J., et al. 2012. One Year of Just-In-Time Perforating as Multistage Fracturing Technique for Horizontal Wells. Paper SPE 160034 presented at the SPE Annual Technical Conference and Exhibition. 8–10 October, San Antonio, Texas. http://dx.doi.org/10.2118/160034MS.

Babadagli, T., Al-Benami. A., and Boukadi, F. 1999. Analysis of Capillary Imbibition Recovery Considering the Simultaneous Effects of Gravity, Low IFT, and Boundary Conditions. Paper SPE 57321 presented at the SPE Asia Pacific Improved Oil Recovery Conference. 25–26 October. Kuala Lumpur, Malaysia. http://dx.doi.org/10.2118/57321-MS.

Barree, R.D., Barree, V.L., and Craig, D.P. 2007. Holistic Fracture Diagnostics. Paper SPE 107877 presented at the Rocky Mountain Oil & Gas Technology Symposium. 16–18 April. Denver, Colorado. http://dx.doi.org/10.2118/107877-MS.

Baree, R.D. and Conway, M.W. 2009. Multiphase Non-Darcy Flow in Proppant Packs. ***SPE Prod & Oper***, **24** (2): 257–268. SPE 109561-PA. http://dx.doi.org/10.2118/109561-PA.

Barree, R.D., Cox, S.A., Barree, V.L., et al. 2003. Realistic Assessment of Proppant Pack Conductivity for Material Selection. Paper SPE 84306 presented at the SPE Annual Technical Conference and Exhibition. 5–8 October. Denver, Colorado. http://dx.doi.org/10.2118/84306-MS.

Bazin, B., Bekri, S., Vizika, O., et al. 2010. Fracturing in Tight Gas Reservoirs: Application of SCAL Methods to Investigate Formation Damage Mechanisms. Paper SPE 112460 presented at the SPE International Symposium and Exhibition on Formation Damage Control. 13–15 February. Lafayette, Louisiana. http://dx.doi.org/10.2118/112460-MS.

Bazan, L.W., Larkin, S.D., Lattibeaudiere, M.G., et al. 2010. Improving Production in the Eagle Ford Shale with Fracture Modeling, Increased Conductivity and Optimized Stage and Cluster Spacing along the Horizontal Wellbore. Paper SPE 138425 presented at the SPE Tight Gas Completions Conference. 2–3 November. San Antonio, Texas. http://dx.doi.org/10.2118/138425-MS.

Behrmann, L.A. and Elbel, J.L. 1991. Effect of Perforations on Fracture Initiation. ***J Pet Tech***, **43** (05) 608-615. SPE 20661-PA. http://dx.doi.org/10.2118/20661PA.

Behrmann, L. A. and Nolte, K. G. 1999. Perforating Requirements for Fracture Stimulations. ***SPE Drill & Compl***, **14** (04): 228-234. SPE 59480-PA. http://dx.doi. org/10.2118/59480-PA.

Behrmann, L.A., Pucknell, J.K., and Bishop, S.R. 1992. Effects of Underbalance and Effective Stress on Perforation Damage in Weak Sandstone: Initial Results. Paper SPE 24770 presented at the SPE Annual Technical Conference and Exhibition. 4–7 October. Washington, D.C. http://dx.doi.org/10.2118/24770-MS.

Bell, M., Hardesty, J., and Clark, N. 2009. Reactive Perforating: Conventional and Unconventional Applications, Learnings and Opportunities. Paper SPE 122174 presented at the 8th European Formation Damage Conference. 27–29 May. Scheveningen, The Netherlands. http://dx.doi.org/10.2118/122174-MS.

Bennion, D.B., Cimolai, M.P., Bietz, F.R., et al. 1994. Reductions in the Productivity of Oil and Gas Reservoirs due to Aqueous Phase Trapping. ***J. Cdn. Pet. Tech.*** **33** (9): 45–54. PETSOC-94-09-05. http://dx.doi.org/10.2118/94-09-05.

Bertoncello, A., Wallace, J., Blyton, C., et al. 2014. Imbibition and Water Blockage in Unconventional Reservoirs: Well Management Implications during Flowback and Early Production. Paper SPE 167698 presented at the SPE/ EAGE European Unconventional Resources Conference and Exhibition. 25–27 February. Vienna, Austria. http://dx.doi.org/10.2118/167698-MS.

Besler, M.R., Steele, J.W., Egan, T. et al. 2007. Improving Well Productivity and Profitability in the Bakken–A Summary of Our Experiences Drilling, Stimulating, and Operating Horizontal Wells. Paper SPE 110679 presented at the SPE Annual Technical Conference and Exhibition. 11–14 November. Anaheim, California. http://dx.doi.org/10.2118/110679-MS.

Biot, M.A. 1941. General Theory of Three-Dimensional Consolidation. ***Journal of Applied Physics***, **12** (2): 155–164, 1941. http://dx.doi.org/10.1063/1.1712886.

Biot, M.A. 1956. General Solutions of the Equations of Elasticity and Consolidation for a Porous Material. ***Journal of Applied Mechanics***, **23**: 91–96.

Brannon, H.D. and Bell, C.E. 2011. Eliminating Slickwater Compromises for Improved Shale Stimulation. Paper SPE 147485 presented at the SPE Annual Technical Conference and Exhibition. 30 October–2 November. Denver, Colorado. http://dx.doi.org/10.2118/147485-MS.

Brannon H.D., Malone, M.R., Rickards, A.R., et al. 2004. Maximizing Fracture Conductivity with Proppant Partial Monolayers: Theoretical Curiosity or Highly Productive Reality? Paper SPE 90698 presented at the SPE Annual Technical Conference and Exhibition, 26–29 September. Houston, Texas. http://dx.doi.org/10.2118/90698-MS.

Brannon H. D., Kendrick D.E., Luckey, E., et al. 2009. Multi-Stage Fracturing of Horizontal Wells Using Ninety-Five Quality Foam Provides Improved Shale Gas Production. Paper SPE 124767 presented at the SPE Eastern Regional Meeting, 23–25 September. Charleston, West Virginia. http://dx.doi.org/10.2118/124767-MS.

Brannon, H.D., Rickards, A.R., and Stephenson, C.J. 2002. Lightweight Methods for Well Treating. US Patent No. 6,364,018.

Brannon, H.D. and Starks, T.R. 2009. Maximizing Return on Fracturing Investment by Using Ultra-Lightweight Proppants to Optimize Effective Fracture Area: Can Less Really Deliver More? Paper SPE 119385 presented at the SPE Hydraulic Fracturing Technology Conference. 19–21 January. The Woodlands, Texas. http://dx.doi.org/10.2118/119385MS.

Britt, L.K. and Smith, M.B. 2009. Horizontal Well Completion, Stimulation Optimization, and Risk Mitigation. Paper SPE 125526 presented at the SPE Eastern Regional Meeting, 23.25 September, Charleston, West Virginia. http://dx.doi.org/10.2118/125526-MS.

Castaneda, J.C., Castro, L., Craig, S., et al. 2010. Coiled Tubing Fracturing: An Operational Review of a 43-Stage Barnett Shale Stimulation. Paper SPE 130678 presented at the SPE/ICoTA Coiled Tubing and Well Intervention Conference and Exhibition. 23–24 March. The Woodlands, Texas. http://dx.doi.org/10.2118/130678-MS.

Castro, L., Bass, C., Pirogov, A., et al. 2013a. A Comparison of Proppant Placement, Well Performance, and Estimated Ultimate Recovery Between Horizontal Wells Completed with Multi-Cluster Plug & Perf and Hydraulically Activated Frac Ports in a Tight Gas Reservoir. Paper SPE 163820 presented at the SPE Hydraulic Fracturing Technology Conference. The Woodlands, Texas. 4-6 February. http://dx.doi.org/10.2118/163820-MS.

Castro, L.A., Johnson, C.C., and Thacker, C.W. 2013b. Targeted Annular Hydraulic Fracturing Using CT-Enabled Frac Sleeves: A Case History from Montana's Bakken Formation. Paper SPE 166511 presented at the SPE Annual Technical Conference and Exhibition. New Orleans, Louisiana. 30 September–2 October. http://dx.doi.org/10.2118/166511-MS.

Chen, H.L., Lucas, L.R., Nogaret, L.A.D., et al. 2001. Laboratory Monitoring of Surfactant Imbibition with Computerized Tomography. ***SPE Res Eval & Eng***, **4** (1): 16–25. SPE 69197 http://dx.doi.org/10.2118/69197PA.

Cheng, Y. 2012. Mechanical Interaction of Multiple Fractures–Exploring Impacts of the Selection of the Spacing/ Number of Perforation Clusters on Horizontal Shale-Gas Wells. ***SPE J.***, 17 (04): 992.1001. SPE 125769-PA. http://dx.doi.org/10.2118/125769-PA.

Chong, K.K., Grieser, W.V., Passaman, A., et al. 2010. A Completions Guide Book to Shale-Play Development: A Review of Successful Approaches Towards Shale-Play Stimulation in the Last Two Decades. Paper SPE 133874 presented at the Canadian Unconventional Resources and International Petroleum Conference. Calgary, Alberta, Canada. 19–21 October. http://dx.doi.org/10.2118/133874-MS.

Cinco-Ley, H. and Samaniego-V. F., 1981. Transient Pressure Analysis for Fractured Wells. ***SPE J.***, **33** (9): 1,749–1,766. SPE 7490. http://dx.doi.org/10.2118/7490-PA.

Cinco-Ley, H., Kuchuk, F., Ayoub, J., et al. 1986. Analysis of Pressure Tests through the Use of Instantaneous Source Response Concepts. Paper SPE 15476 presented at the SPE Annual Technical Conference and Exhibition New Orleans, Louisiana. 5–8 October. http://dx.doi.org/10.2118/15476-MS.

Cipolla, C., Maxwell, S., and Mack, M. 2012. Engineering Guide to the Application of Microseismic Interpretations. Paper SPE 152165 presented at the SPE Hydraulic Fracturing Technology Conference. The Woodlands, Texas. 6–8 February. http://dx.doi.org/10.2118/152165-MS.

Cleary, M.P., Johnson, D.E., Kogsbøll, H-H., et al. 1993. Field Implementation of Proppant Slugs to Avoid Premature Screen-Out of Hydraulic Fractures with Adequate Proppant Concentration. Paper SPE 25892 presented at the Low Permeability Reservoirs Symposium. Denver, Colorado. 26–28 April. http://dx.doi.org/10.2118/25892-MS.

Cooke, C.E. 1973. Conductivity of Fracture Proppants in Multiple Layers. ***J Pet Tech***, **25** (9): 1101–1107, Trans. AIME, SPE 4117-PA. http://dx.doi.org/10.2118/4117-PA.

Cramer, D.D. 1987. The Application of Limited-Entry Techniques in Massive Hydraulic Fracturing Treatments. Paper SPE 16189 presented at the SPE Production Operations Symposium. 8–10 March. Oklahoma City, Oklahoma. http://dx.doi.org/10.2118/16189-MS.

Cramer, D.D. and Nguyen, D.H. 2011. Determining Reservoir Properties Using Fracture Injection Falloff Tests. SPE Technical Luncheon, Calgary, 25 May.

Crump, J.B. and Conway, M.W. 1988. Effects of Perforation Entry Friction on Bottomhole Treating Analysis. ***J Pet Tech***, **40** (8): 1041–1048. SPE 15474-PA. http://dx.doi.org/10.2118/15474-PA.

Cutler, R.A., Enniss, D.O., Jones, A.H., et al. 1985. Fracture Conductivity Comparison of Ceramic Proppants. ***SPE J.*** **25** (2): 157–170. SPE 11634. http://dx.doi.org/10.2118/11634-PA.

Dahi-Taleghani, A. and Olsen, J.E. 2011. Numerical Modeling of Multistranded-Hydraulic-Fracture Propagation: Accounting for the Interaction Between Induced and Natural Fractures. ***SPEJ***. **16** (3): 575-581. SPE 124884-PA. http://dx.doi.org/10.2118/124884-PA.

Daneshy, A. 2013. Horizontal Well Fracture Initiation and Extension from Cemented Cased Wells. Paper SPE 166086 presented at the SPE Annual Technical Conference and Exhibition. 30 September–2 October. New Orleans, Louisiana. http://dx.doi.org/10.2118/166086-MS.

Darin, S.R. and Huitt, J.L. 1960. Effect of a Partial Monolayer of Propping Agent on Fracture Flow Capacity. Paper SPE 1291-G.

Davis,B.J. and Wood, W.D. 2004. Maximizing Economic Return by Minimizing or Preventing Aqueous Phase Trapping During Completion and Stimulation Operations. Paper SPE 90170 presented at the SPE Annual Technical Conference and Exhibition. 26–29 September. Houston, Texas. http://dx.doi.org/10.2118/166086-MS.

Dawson, J.C., Le, H.V., and Kesavan, S. 2000. Polymer Expansion for Oil and Gas Recovery. U.S. Patent No. 6,017,855, 2000.

Dedurin, A.V., Majar, V.A., Voronkov, A.A., et al. 2006. Designing Hydraulic Fractures in Russian Oil and Gas Fields to Accommodate Non-Darcy and Multiphase Flow–Theory and Field Examples. SPE 101821 presented at the SPE Russian Oil and Gas Technical Conference and Exhibition, 3–6 October, Moscow, Russia. http://dx.doi.org/10.2118/101821-MS.

Demarchos, A.S., and Porcu, M.M. 2006. Transversely Multi-Fractured Horizontal Wells: A Recipe for Success. SPE 102263 presented at the SPE Russian Oil and Gas Technical Conference and Exhibition. 3–6 October. Moscow, Russia. http://dx.doi.org/10.2118/102263-MS.

De Melo, R.C.B., Curtis, J.A., Gomez, J. R., et al. 2012. Phosphonic/Hydrofluoric Acid: A Promising New Weapon in the Tortuosity Remediation Arsenal for Fracturing Treatments. Paper SPE 152624 presented at the SPE Hydraulic Fracturing Technology Conference. 6–8 February. The Woodlands, Texas. http://dx.doi.org/10.2118/152624-MS.

Devine, C.S. 2005. Approaches to Fracturing Fluid Selection Based on Laboratory Generated Data. Paper CIM 2005228 presented at the Canadian International Petroleum Conference. 7–9 June. Calgary, Alberta, Canada. http:// dx.doi.org/10.2118/2005-228.

Early, W.L. 1977. Metals and Their Resistance to Penetration by Shaped Charges. MS Thesis, University of Texas at Arlington. December.

Ebel, J.L. and Mack, M.G. 1993. Refracturing: Observations and Theories. Paper SPE 25464 presented at the SPE Production Operations Symposium. 21–23 March. Oklahoma City, Oklahoma. http://dx.doi.org/10.2118/25464-MS.

Economides, M.J. and Martin, T. 2007. ***Morden Fracturing: Enhancing Natural Gas Production***, ET Publishing Co., Houston, Texas.

Economides, M., Nolte, M., and Ahmed, U. 1998. Reservior Stimulation Pennwell Publications.

Economides, M.J. and Nolte, K.G. 2000. ***Reservoir Stimulation***, Chap. 3, 3rd edition. West Sussex, England: John Wiley and Sons, Ltd.

Ehlig-Economides, C.A., and Economides, M.J. 2011. Water as Proppant. Paper SPE 147603 presented at the SPE Annual Technical Conference and Exhibition. 30 October–2 November. Denver, Colorado. http://dx.doi.org/10.2118/147603-MS.

Ehlig-Economides, C.A., Liu, T., Economides, M.J, et al. 2012. A Study of Transversely vs Longitudinally Fractured Horizontal Wells in a Moderate-Permeability Gas Reservoir. Paper SPE 163317 presented at the SPE Kuwait International Petroleum Conference and Exhibition. 10–12 December. Kuwait City, Kuwait. http://dx.doi.org/10.2118/163317MS.

El Rabaa, W. 1989. Experimental Study of Hydraulic Fracture Geometry Initiated from Horizontal Wells. Paper SPE 19720 presented at the SPE Annual Technical Conference and Exhibition. 8–11 October. San Antonio, Texas. http://dx.doi.org/10.2118/19720-MS.

El Shaari, N., Minner, W.A., and LaFollette, R.F. 2011. Is There a "Silver Bullet Technique" for Stimulating California's Monterey Shale? Paper SPE 144526 presented at the SPE Western North American Region Meeting. 7–11 May. Anchorage, Alaska. http://dx.doi.org/10.2118/144526MS.

Eller, G.J., Garner, J.J., Snider, P., and George, K. 2002. A Case History: Use of a Casing-Conveyed Perforating System to Improve Life of Well Economics in Tight Gas Sands. Paper SPE 76742 presented at the SPE Western Regional/AAPG Pacific Section Joint Meeting. 20–22 May. Anchorage, Alaska. http://dx.doi.org/10.2118/176742-MS.

Ely, J.W., 1994. ***Stimulation Engineering Handbook***, PennWell Books: Tulsa, Oklahoma.

Ely, J.W. 1995. Experience Proves Forced Closure Works. ***World Oil***, **217** (1): 37–41.

Energy Information Administration (EIA). 1999. Federal Financial Interventions and Subsidies in Energy Markets 1999: Primary Energy, US Department of Energy. http://www. eia.gov/oiaf/servicerpt/subsidy (accessed July 2014).

Farris, R.F. 1953. Fracturing Formations in Wells. US Patent No. Re. 23,733, re-issued 10 November 1953.

Forchheimer, P. 1901. Water Movement through Soil (in German), ***ZVDI*** **45**, 1782–1788.

Gall, B.L., Sattler, A.R., Maloney, D.R. et al. 1988. Permeability Damage to Natural Fractures Caused by Fracturing Fluid Polymers. Paper SPE 17542 presented at the SPE Rocky Mountain Regional Meeting. 11–13 May. Casper, Wyoming. http://dx.doi.org/10.2118/17542-MS.

Geertsma, J. 1974. Estimating the Coefficient of Inertial Resistance in Fluid Flow through Porous Media. ***SPE J.*** **14** (5): 445–450. SPE 4706-PA. http://dx.doi.org/10.2118/176742-MS.

Gidley, J.L., Holditch, S.A., Nierode, D.E. et al. 1989. Recent Advances in Hydraulic Fracturing, ***SPE Monograph Volume*** **12**, SPE: Richardson, Texas.

Gilliat, J., Snider, P.M., and Haney, R. 1999. A Review of Field Performance of New Propellant/Perforating Technologies. Paper SPE 56469 presented at the SPE Annual Technical Conference and Exhibition. 3–6 October. Houston, Texas. http://dx.doi.org/10.2118/56469-MS.

Goel, N. and Shah, S. 2001. A Rheological Criterion for Fracturing Fluids to Transport Proppant during a Stimulation Treatment. Paper SPE 71663 presented at the SPE Annual Technical Conference and Exhibition. 30 September–3 October. New Orleans, Louisiana. http://dx.doi.org/10.2118/71663-MS.

Gomaa, A. M., Cawiezel, K.E., Gupta, D.V.S., et al. 2011. Viscoelastic Evaluation of a Surfactant Gel for Hydraulic Fracturing. Paper SPE 143450 presented at the SPE European Formation Damage Conference. 7–10 June. Noordwijk, The Netherlands. http://dx.doi.org/10.2118/143450-MS.

Gomaa, A.M., Gupta, D.V.S., and Carman, P. 2104b. Viscoelastic Behavior and Proppant Transport Properties of a New Associative Polymer-Based Fracturing Fluid. Paper SPE 168113 presented at the SPE International Symposium and Exhibition on Formation Damage Control. 26–28 February. Lafayette, Louisiana. http://dx.doi.org/10.2118/168113MS.

Gomaa, A.M., Zhang, B., Chen, J., et al. 2014a. Innovative Use of NMR to Study the Fracture Fluid Propagation in Shale Formation. Paper SPE 168619 presented at the SPE Hydraulic Fracturing Technology Conference, 4–6 February. The Woodlands, Texas. http://dx.doi.org/10.2118/168619MS.

Gringarten, A., Ramey, H., and Raghavan, R. 1974. Unsteady-State Pressure Distributions Created by a Well with a Single Infinite-Conductivity Vertical Fracture. ***SPE J.*** **14** (4): 347–360. SPE 4051. http://dx.doi.org/10.2118/4051PA.

Gross, R. 1985. Orifice Contraction Coefficient for Inviscid Incompressible Flow. ***Journal of Fluids Engineering***, **107** (1): 36.43.

Gruesbeck, C. and Collins, R.E. 1982. Particle transport through Perforations. ***SPE J.*** **22** (6): 857.865. SPE 7006-PA. http://dx.doi.org/10.2118/7006-PA.

Gu, H., Elbel, J., Nolte, K., et al. 1993. Formation Permeability Determination Using Impulse-Fracture Injection. Paper SPE 25425 presented at the SPE Production Operations Symposium. 21–23 March. Oklahoma City, Oklahoma. http://dx.doi.org/10.2118/25425-MS.

Gupta, D.V.S., Leshchyshyn, T.T., and B.T. Hlidek, 2005. Surfactant Gel Foam/Emulsion: History and Field Application Western Canadian Sedimentary Basin. SPE 97211 presented at the SPE Annual Technical Conference and Exhibition. 9–12 October. Dallas, Texas. http://dx.doi.org/10.2118/97211MS.

Gupta, D.V.S., Hlidek, B.T., Hill, E.S.W., et al. 2007. Fracturing Fluid for Low Permeability Gas Reservoirs: Emulsion of Carbon Dioxide with Aqueous Methanol Base Fluid: Chemistry and Applications. Paper SPE 106304 presented at SPE Hydraulic Fracturing Technology Conference. 29–31 January. College Station, Texas. http://dx.doi.org/10.2118/106304-MS.

Gupta, D.V.S. and Bobier, D.M. 1998. The History and Success of Liquid CO2 and CO2/N2 Fracturing System. Paper SPE 40016 presented at SPE Gas Technology Conference. Calgary, Alberta, Canada. 15–18 March. http://dx.doi.org/10.2118/40016-MS.

Gupta, D.V.S. and Franklin, V.L. 1994. Method for Fracturing High Temperature Subterranean Formations. U.S. Patent No. 5,305,832.

Gupta, D.V.S., Jackson, T.L., Hlavinka, G.J.,et al. 2009. Development and Field Application of a Low pH, Efficient Fracturing Fluid for Tight Gas Fields in the Greater Green River Basin, Wyoming. ***SPE Prod Oper***, **24** (4): 602–610.SPE 116191-PA. http://dx.doi.org/10.2118/40016-PA.

Gupta, S. 2009. Unconventional Fracturing Fluids for Tight Gas Reservoirs. Paper SPE 119424 presented at the SPE Hydraulic Fracturing Technology Conference. 19–21 January. The Woodlands, Texas. http://dx.doi.org/10.2118/119424-MS.

Harris, P.C., Walters, H.G., and Bryant, J. 2009. Prediction of Proppant Transport from Rheological Data. ***SPE Prod Oper***, **24** (4): 550–555. SPE 115298-PA. http://dx.doi.org/10.2118/115298-PA.

Hellmann, J.R., Scheetz, B.E., Luscher, W.G., et al. 2014. Proppants for Shale Gas and Oil Recovery. ***American Ceramic Society Bulletin***, **93** (1): 28.35.

Hernandez, J.M., Fernandez, C.T., and Scianca, N.M. 1994. Methanol as Fracture Fluid in Gas Wells. Paper SPE 27007 presented at the. SPE Latin America/Caribbean Petroleum Engineering Conference, 27–29 April, Buenos Aires, Argentina. http://dx.doi.org/10.2118/27007-MS.

Hodenfield, K. 2012. Operators Seek Fracture Consistency. The American Oil & Gas Reporter, National Publishers Group Inc., January 2012.

Holditch, S.A. and Morse, R.A. 1976. The Effects of Non-Darcy Flow on Behavior of Hydraulically Fractured Gas Wells. ***J. Pet Tech***, **28** (10): 1169–1179. SPE 5586-PA. http:// dx.doi.org/10.2118/5586-PA.

Holditch, S.A. 1979. Factors Affecting Water Blocking and Gas Flow from Hydraulically Fracture Gas Wells. ***J. Pet Tech***, **31** (12): 1515–1524. SPE 7561-PA. http://dx.doi.org/10.2118/7561-PA.

Holditch, S.A., Xiong, H., Rueda, J., et al. 1993. Using an Expert System to Select the Optimal Fracturing Fluid and Treatment Volume. Paper SPE 26188 presented at the SPE Gas Technology Symposium. 28–30 June. Calgary, Alberta, Canada. http://dx.doi.org/10.2118/26188-MS.

Howard, G.C. and Fast, C.R.1970. ***Hydraulic Fracturing, Monograph Series***, Vol 2, SPE, Dallas, Texas.

International Standards Organisation, 2006a. ISO 13503-2 Petroleum and Natural Gas Industries–Completion Fluids and Materials–Part 2: Measurement of Properties of Proppants Used in Hydraulic Fracturing and Gravel-Packing Operations.

International Standards Organisation. 2006b. 13503-5 Petroleum and Natural Gas Industries–Completion Fluids and Materials–Part 5: Procedures for Measuring the Long-Term Conductivity of Proppants.

Jacot, R.H., Bazan, L.W., and Meyer, B.R. 2010. Technology Integration–A Methodology to Enhance Production and Maximize Economics in Horizontal Marcellus Shale Wells. Paper SPE 135262 presented at the SPE Annual Technical Conference and Exhibition. 19–22 September. Florence, Italy. http://dx.doi.org/10.2118/135218-MS.

Kamath, J. and Laroche, C. 2003. Laboratory-Based Evaluation of Gas Well Deliverability Loss Caused by Water Blocking. ***SPE J***. **8** (1): 71–80. SPE 83659-PA. http://dx.doi.org/10.2118/83659-PA.

King, G.E. 2010. Thirty Years of Gas Shale Fracturing: What Have We Learned? Paper SPE 133456 presented at the SPE Annual Technical Conference and Exhibition. 19–22 September. Florence, Italy. http://dx.doi.org/10.2118/133456-MS.

King, G.E. 2012. Hydraulic Fracturing 101: What Every Representative, Environmentalist, Regulator, Reporter, Investor, University Researcher, Neighbor and Engineer Should Know about Estimating Frac Risk and Improving Frac Performance in Unconventional Gas and Oil Wells. Paper SPE 152596 presented at the SPE Hydraulic Fracturing Technology Conference. 6–8 February. The Woodlands, Texas. http://dx.doi.org/10.2118/152596-MS.

King, G.E., Haile, L., Shuss, J., et al. 2008. Increasing Fracture Path Complexity and Controlling Downward Fracture Growth in the Barnett Shale. Paper SPE 119896 presented at the SPE Shale Gas Production Conference. 16–18 November. Fort Worth, Texas. http://dx.doi.org/10.2118/119896-MS.

Kogsbøll, H-H., Pitts, M.J., and Owens, K.A. 1993. Effects of Tortuosity in Fracture Stimulation of Horizontal Wells–A Case Study of the Dan Field. Paper SPE 26796 presented at the Offshore Europe. 7–10 September. Aberdeen, United Kingdom. http://dx.doi.org/10.2118/26796-MS.

Krumbein, W.C. and Sloss, L.L. 1963. ***Stratigraphy and Sedimentation***, 2nd Edition, W.H. Freeman & Co: New York.

LaFollette, R.F. and Carman, P.S. 2010. Proppant Diagenesis: Results So Far. Paper SPE 131782 presented at the SPE Hydraulic Fracturing Technology Conference. 24–26 January. The Woodlands, Texas. http://dx.doi.org/10.2118/131782-MS.

LaFollette, R.F., Holcomb, W.D., and Aragon, J. 2012. Practical Data Mining: Analysis of Barnett Shale Production Results with Emphasis on Well Completion and Fracture Stimulation. Paper SPE 152531 presented at the SPE Hydraulic Fracturing Technology Conference. 6–8 February. The Woodlands, Texas. http://dx.doi.org/10.2118/152531-MS.

Lantz, T., Greene, D., Eberhard, M., Norrid, S., et al. 2007. Refracture Treatments Proving Successful in Horizontal Bakken Wells: Richland Count, Montana. Paper SPE 108117 presented at the Rocky Mountain Oil & Gas Technology Symposium. 16–18 April. Denver, Colorado. http://dx.doi.org/10.2118/108117-MS.

Legemah, M., Debenedictis, F., Workneh, N., et al. 2014. Successful Treatment of Green River Sandstone Formation Using a Novel Low-Polymer Crosslinked Fluid. Paper SPE 168186 presented at the SPE International Symposium and Exhibition on Formation Damage Control, 26–28 February, Lafayette, Louisiana. http://dx.doi.org/10.2118/168186MS.

Lei, C. and Clark, P.E. 2004. Crosslinking of Guar and Guar Derivatives. Paper SPE 90840 presented at the SPE Annual Technical Conference and Exhibition. 26–29 September. Houston, Texas. http://dx.doi.org/10.2118/90840-MS.

Lestz, R.S., Clarke, J.N., Plattner, D., et al. 2002. Perforating for Stimulation: An Engineered Solution ***SPE Drill & Compl***, **17** (01): 37–44 SPE 76812-PA. http://dx.doi.org/10.2118/76812-PA.

Lillies, A.T. 1982. Sand Fracturing with Liquid Carbon Dioxide. Paper PETSOC-82-33-23 presented at the Annual Technical Meeting of the Petroleum Society of CIM. 6–9 June. Calgary, Alberta, Canada. http://dx.doi.org/10.2118/82-33-23.

Liu, Y., Gadde, P.B., and Sharma, M.M. 2007. Proppant Placement Using Reverse-Hybrid Fracs. ***SPE Prod Oper***, **22** (3): 348–356. SPE 99580. http://dx.doi.org/10.2118/99580-PA.

Loree, D.N. and Mesher, S.T. 2007. Liquefied Petroleum Gas Fracturing Systems. US Patent Application No. 2007204991.

Mack, M. G. and Warpinski, N. R. 2000. ***Mechanics of Hydraulic Fracturing. In Reservoir Stimulation***, 3th edition, ed.

Mahadevan, J. and Sharma, M.M. 2005. Factors Affecting Cleanup of Water Blocks: A Laboratory Investigation. ***SPE J***. **10** (3): 238.246. SPE 84216-PA. http://dx.doi.org/10.2118/84216-PA.

Mahoney, R.P., Soane, D., and Kincaid, K.P., 2013. Self-Suspending Proppant. Paper SPE 163818 presented at the SPE Hydraulic Fracturing Technology Conference. 4–6 February, The Woodlands, Texas. http://dx.doi.org/10.2118/163818-MS.

Malhotra, S., Lehman, E.R., and Sharma, M.M. 2013. Proppant Placement Using Alternate-Slug Fracturing. Paper SPE 163851 presented at the SPE Hydraulic Fracturing Technology Conference. 4–6 February. The Woodlands, Texas. http://dx.doi.org/10.2118/163851-MS.

Martin, A. N. 2009. ***Baker Hughes' Hydraulic Fracturing Manual***, version 2. Baker Hughes.

Martin, A. N. and Economides, M.J. 2010. Best Practices for Candidate Selection, Design and Evaluation of Hydraulic Fracture Treatments. Paper SPE 135669 presented at the SPE Production and Operations Conference and Exhibition. 8–10 June. Tunis, Tunisia. http://dx.doi.org/10.2118/1356694MS.

Martin, A.N. 2011. The Potential Pitfalls of Using North American Tight and Shale Gas Development Techniques in the European Environment. Paper OMC-2011-155 presented at the Offshore Mediterranean Conference and Exhibition, 23–25 March, Ravenna, Italy.

Martin, A.N. 2012. The Potential Pitfalls of Using North American Tight and Shale Gas Development Techniques in the North African and Middle Eastern Environments. SPE Economics & Management, **4** (3): 147–157. SPE 141104, PA. http://dx.doi.org/10.2118/141104-PA.

Martin, A.R., Cramer, D.D., Nunez, O., et al. 2012. A Method to Perform Multiple Diagnostic Fracture Injection Tests Simultaneously in a Single Wellbore. Paper SPE 152019 presented at the SPE Hydraulic Fracturing Technology Conference. 6–8 February. The Woodlands, Texas. http://dx.doi.org/10.2118/152019-MS.

Martins, J.P., Milton-Tayler, D., and Leung, H.K. 1990. The Effects of Non-Darcy Flow in Propped Fractures. Paper SPE 20709 presented at the SPE Annual Technical Conference and Exhibition. 23–26 September. New Orleans, Louisiana. http://dx.doi.org/10.2118/20709-MS.

Mattar, L. and Zaoral, K. 1992. The Primary Pressure Derivative (PPD) – A New Diagnostic Tool in Well Test Interpretation. ***J. Cdn. Pet Tech***. **31** (4): 63–70. PETSOC-92-04-06. http://dx.doi.org/10.2118/92-04-06.

Mayerhofer, M.J., Richardson, M.F., Walker Jr., et al. 1997. Proppants? We Don't Need No Proppants. SPE 38611 presented at the SPE Annual Technical Conference and Exhibition. 5–8 October. San Antonio, Texas. http://dx.doi.org/10.2118/38611-MS.

Mayerhofer, M.J., Lolon, E., Warpinski, N.R., et al. 2010. What Is Stimulated Reservoir Volume? ***SPE Prod & Oper.***, **25** (1): 89–98. Paper SPE 119890. http://dx.doi.org/10.2118/17594-MS.

Mayerhofer, M.J., Lolon, E.P., and Warpinski, N.R., et al. 2010. What Is Stimulated Reservoir Volume? ***SPE Prod Oper***, **25** (1): 89–98. SPE 119890-PA. http://dx.doi.org/10.2118/119890-PA.

Mazza, R.L. 1997. Liquid CO2 improves Fracturing. ***Hart's Oil and Gas World***, 22 February 1997.

McClain, C. 1963. Fluid Flow in Pipes. ***The Industrial Press***, 117–128.

McDaniel, B.W., Surjaatmadja, J.B., and East, L.E. 2008. Use of Hydrajet Perforating to Improve Fracturing Success Sees Global Expansion. Paper SPE 114695 presented at the CIPC/SPE Gas Technology Symposium 2008 Joint Conference. 16–19 June. Calgary, Alberta, Canada. http://dx.doi.org/10.2118/114695-MS.

McGuire, W.J. and Sikora, V.J. 1960. The Effect of Vertical Fractures on Well Productivity. ***J Pet Tech***, **12** (10): 72–74, October 1960, also ***Trans. AIME***, 219, 1960. SPE 1618-PA. http://dx.doi.org/10.2118/1618-PA.

Meyer & Associates, 2013. ***MShale help file***.

Meyer, B.R. and Bazan, L.W. 2011. A Discrete Fracture Network Model for Hydraulically Induced Fractures: Theory, Parametric and Case Studies. SPE 140514 presented at the SPE Hydraulic Fracturing Technology Conference. 24–26 January. The Woodlands, Texas. http://dx.doi.org/10.2118/1618-MS.

Meyer, B.R., Bazan, L.W., Brown, E.K. et al. 2013. Key Parameters Affecting Successful Hydraulic Fracture Design and Optimized Production in Unconventional Wells. Paper SPE 165702 presented at the SPE Eastern Regional Meeting, 20–22 August, Pittsburgh, Pennsylvania. http://dx.doi.org/10.2118/165702-MS.

Meyers, M.A. and Chawla, K.K. 2008. ***Mechanical Behaviour of Materials.*** Cambridge University Press, 2nd Edition.

Miskimins, J.L., Lopez-Hernandes, H.D., and Barree, R.D. 2005. Non-Darcy Flow in Hydraulic Fractures: Does It Really Matter? Paper SPE 96389 presented at the SPE Annual Technical Conference and Exhibition. 9–12 October. Dallas, Texas. http://dx.doi.org/10.2118/96389-MS.

Mitchell, B.J. 1969. Viscosity of Foam. Ph.D dissertation, University of Oklahoma, 1969.

Mohan, J.P., Pope, G.A., and Sharma, M.M. 2006. Effect of Non-Darcy Flow in Well Productivity in a Hydraulically Fractured Gas/Condensate Well. Paper SPE 103025 presented at the SPE Annual Technical Conference and Exhibition, 24–27 September, San Antonio, Texas. http://dx.doi.org/10.2118/103025-MS.

Mukherjee, H. and Economides, M.J. 1991. A Parametric Comparison of Horizontal and Vertical Well Performance. ***SPE Form Eval***, **6** (2): 209–216. SPE 18303-PA. http://dx.doi.org/10.2118/8341-PA.

Nolte, K.G. 1979. Determination of Fracture Parameters from Fracturing Pressure Decline. Paper SPE 8341 presented at the SPE Annual Technical Conference and Exhibition, 23–26 September, Las Vegas, Nevada. http://dx.doi.org/10.2118/8341-MS.

Nolte, K., Maniere, J., and Owens, K. 1997. After-Closure Analysis of Fracture Calibration Tests. SPE 38676 presented at the SPE Annual Technical Conference and Exhibition. 5–8 October. San Antonio, Texas. http://dx.doi.org/10.2118/38676-MS.

Olson, K.E., Haidar, S., Milton-Tyler, D., et al. 2004. Multiphase Non-Darcy Pressure Drop in Hydraulic Fracturing. Paper SPE 90406 presented at the SPE Annual Technical Conference and Exhibition, 26–29 September, Houston, Texas. http://dx.doi.org/10.2118/90406-MS.

PacWest. 2014a. ProppantIQ: Market Analysis. (13 June 2014), http://pacwestcp.com/market-outlook/proppantiq. (accessed July 2014).

PacWest. 2014b. PumpingIQ: Market Analysis. (16 May 2014), http://pacwestcp.com/market-outlook/pumpingiq. (accessed July 2014).

PacWest. 2014c. WellIQ: Market Analysis, (25 April 2014), http://pacwestcp.com/market-outlook/welliq/ (accessed July 2014).

Palisch, T., Duenckel, R., Bazan, L., et al. 2007. Determining Realistic Fracture Conductivity and Understanding Its Impact on Well Performance–Theory and Field Examples. Paper SPE 106301 presented at the SPE Hydraulic Fracturing Technology Conference. 29–31 January. College Station, Texas. http://dx.doi.org/10.2118/106301-MS.

Palisch, T., Duenckel, R., Chapman, M., et al. 2010. How to Use and Misuse Proppant Crush Tests: Exposing the Top 10 Myths. Paper SPE 119242 presented at the SPE Hydraulic Fracturing Technology Conference. 19–21 January. The Woodlands, Texas. http://dx.doi.org/10.2118/119242MS.

Palisch, T., Wilson, B., and Duenckel, B. 2014. New Technology Yields Ultra High-Strength Proppant. Paper SPE 168631 presented at the SPE Hydraulic Fracturing Technology Conference, 4–6 February, The Woodlands, Texas. http://dx.doi.org/10.2118/168631-MS.

Palisch, T.T., Chapman, M. A., and Godwin, J. 2012. Hydraulic Fracture Optimization in Unconventional Reservoirs–A Case History. Paper SPE 160206 presented at the SPE Annual Technical Conference and Exhibition, 8–10 October, San Antonio, Texas. http://dx.doi.org/10.2118/160206-MS.

Pearson, C.M. 2001. Dimensionless Fracture Conductivity: Better Input Values Make Better Wells, SPE 60184, ***SPE J.*** **53**. http://dx.doi.org/10.2118/60184-JPT.

Pearson, C.M., Bond, A.J., Eck, M.E., et al. 1992. Results of Stress-Oriented and Aligned Perforating in Fracturing Deviated Wells. ***J Pet Tech***, **44** (1): 10.18. SPE 22836-PA. http://dx.doi.org/10.2118/22836-PA.

Pedlow, J. and Sharma, M.M. 2014. Changes in Shale Fracture Conductivity due to Interactions with Water-Based Fluids. Paper SPE 168586 presented at the SPE Hydraulic Fracturing Technology Conference. 4–6 February. The Woodlands, Texas. http://dx.doi.org/10.2118/168586MS.

Penny, G.S. 1987. An Evaluation of the Effects of Environmental Conditions and Fracturing Fluids Upon the Long-Term Conductivity of Proppants. Paper SPE 16900 presented at the SPE Annual Technical Conference and Exhibition. 27–30 September. Dallas, Texas. http://dx.doi.org/10.2118/16900-MS.

Prats, M. 1961. Effect of Vertical Fractures on Reservoir Behavior – Incompressible Fluid Case. ***SPE J.*** **1** (2): 105.118. SPE 1575-G, also Trans. AIME, 222, 1961. http://dx.doi.org/10.2118/1575-G.

Potapenko, D.I., Tinkham, S.K., Lecerf, B., et al. 2009. Barnett Shale Refracture Stimulations Using a Novel Diversion Technique. Paper SPE 119636 presented at the SPE Hydraulic Fracturing Technology Conference. 19–21 January. The Woodlands, Texas. http://dx.doi.org/10.2118/119686MS.

Rae, P., Martin, A.N., and Sinanan, B. 1999. Skin Bypass Fracs: Proof That Size Is Not Important. Paper SPE 56473 presented at the SPE Annual Technical Conference and Exhibition. 3–6 October. Houston, Texas. http://dx.doi.org/10.2118/56473-MS.

Rickards, A.R., Brannon, H.D., Wood, W.D., et al. 2003. High Strength, Ultra-Lightweight Proppant Lends New Dimensions to Hydraulic Fracturing Applications. Paper SPE 84308 presented at the SPE Annual Technical Conference and Exhibition. 5–8 October. Denver, Colorado. http://dx.doi.org/10.2118/84308-MS.

Rickards, A., Lacy, L., Brannon, H., et al. 1998. Stress Relief? A New Approach to Reducing Stress Cycling Induced Proppant Pack Failure. Paper SPE 49247 presented at the SPE Annual Technical Conference and Exhibition, 27–30 September, New Orleans, Louisiana. http://dx.doi.org/10.2118/49247-MS.

Rickman, R., Mullen, M., Petre, E., et al. 2008. A Practical Use of Shale Petrophysics for Stimulation Design Optimization: All Shale Plays Are Not Clones of the Barnett Shale. Paper SPE 115258 presented at the SPE Annual Technical Conference and Exhibition, 21–24 September. Denver, Colorado. http://dx.doi.org/10.2118/115258-MS.

Rylance, M. and Martin, A.N. 2014. Flushing away the Profit: The Potential Misapplication of Unconventional Fracturing Technology on a Global Scale. Paper SPE 170773 presented at the SPE Annual Technical Conference and Exhibition. 27–29 October. Amsterdam, The Netherlands. http://dx.doi.org/10.2118/170773-MS.

Rytlewski, G.L. and Cook, J.M. 2006. A Study of Fracture Initiation Pressures in Cemented Cased-Hole Wells without Perforations Paper SPE 100572 presented at the SPE Gas Technology Symposium. 15–17 May. Calgary, Alberta, Canada. http://dx.doi.org/10.2118/100572-MS.

Saldungaray, P. and Palisch, T.T. 2012. Hydraulic Fracture Optimization in Unconventional Reservoirs," SPE 151128 presented at the SPE Middle East Unconventional Gas Conference and Exhibition. 23–25 January. Abu Dhabi, UAE. http://dx.doi.org/10.2118/151128-MS.

Santo, M. 2011. Use of Minifrac Tests in Shale/Tight Formations. Fekete and Associates. http://www.fekete.com/ technical-resources/Technical%20 Newsletters/n-spring2011.pdf (accessed July 2014).

Schein, G.W. 2005. The Application and Technology of Slickwater Fracturing. Paper SPE 108807 presented as a SPE Distinguished Lecture during 2004–2005 season.

Schein, G.W., Carr, P.D., Canan, P.A., et al. 2004. Ultra Lightweight Proppants: Their Use and Application in the Barnett Shale. Paper SPE 90838 presented at the SPE Annual Technical Conference and Exhibition, 26–29 September, Houston, Texas. http://dx.doi.org/10.2118/90838-MS.

Schein G.W. and Weiss S.A. 2008. Simultaneous Fracturing Takes Off. ***Hart's E&P***, **81** (9): 55–56.

Schubarth, S.K., Spivey, J.P., and Huckabee, P.T. 2006. Using Reservoir Modeling to Evaluate Stimulation Effectiveness in Multilayered "Tight" Gas Reservoirs: A Case History in the Pinedale Anticline Area. Paper SPE 100574 presented at the PE Gas Technology Symposium.15–17 May. Calgary, Alberta, Canada. http://dx.doi.org/10.2118/100572-MS.

Schultz, D., Thompson, D., and Whitney, D. 2007. Abrasive Perforating via Coiled Tubing Revisted. Paper SPE 107050 presented at the SPE/ICoTA Coiled Tubing and Well Intervention Conference and Exhibition. 20–21 March. The Woodlands, Texas. http://dx.doi.org/10.2118/107050MS.

Shah, S.N., Vincent, M.C., Rodrigez, R., et al. 2010. Fracture Orientation and Proppant Selection for Optimizing Production in Horizontal Wells. Paper SPE 128612 presented at the SPE Oil and Gas India Conference and Exhibition. 20–22 January. Mumbai, India. http://dx.doi.org/10.2118/128612-MS.

Sharma, G. and Mohanty, K. 2013. Wettability Alteration in High-Temperature and High-Salinity Carbonate Reservoirs. ***SPE J.*** **18** (4): 646–655. http://dx.doi.org/10.2118/147306-PA.

Shuler, P.J., Hongxin, T., Zayne, L., et al. 2011. Chemical Process for Improved Oil Recovery From Bakken Shale. Paper SPE 147531. Presented at the Canadian Unconventional Resources Conference, 15–17 November, Alberta, Canada. http://dx.doi.org/10.2118/147531-MS.

Small, G.P. 1986. Steam-Injection Profile Control Using Limited-Entry Perforations. ***SPE Prod Eng***, 1 (05): 388–394. SPE 13607. http://dx.doi.org/10.2118/13607-PA.

Smarovozov, A., Nelson, S., and Hudson, H. 2014. Sustainable Fracturing Fluids Transform Water from Burden to Benefit. ***Hart's E&P***, **87** (7): 100–105.

Soliman, M., Craig, D., Bartko, K., et al. 2005. Post-Closure Analysis to Determine Formation Permeability, Reservoir Pressure, and Residual Fracture Properties. Paper SPE 93419 presented at the SPE Middle East Oil and Gas Show and Conference, 12–15 March, Kingdom of Bahrain. http://dx.doi.org/10.2118/93419-MS.

Sonnenburg, S. 2012. The Niobrara Petroleum System, Rocky Mountain Region. AAPG article 80206, adapted from a presentation at The Tulsa Geological Society. Tulsa, Oklahoma.

Stim-Lab, 1986–2007. Proppant Conductivity and Fluid Damage Consortia Reports. Stim-Lab, PredictK, v 7.0, 2007.

Terracina, J.M., Turner, J.M., Collins, D.H. et al. 2010. Proppant Selection and Its Effects on the Results of Fracturing Treatments Performed in Shale Formations. Paper SPE 135502 presented at the SPE Annual Technical Conference and Exhibition, 19–22 September. Florence, Italy. http://dx.doi.org/10.2118/135502-MS.

Thompson Sr., J.E., McBain, C., Gregory, G., et al. 1992. New Continuous-Mix Process for Gelling Anhydrous Methanol Minimizes Hazards. ***J. Pet Tech***, **44** (7): 832–839. SPE 22800. http://dx.doi.org/10.2118/22800-PA.

Torrey, P.D. 1940. Progress in Squeeze Cementing Application and Technique. ***Oil Weekly***, **98** (8): 68.84.

Tudor, R., Vozniak, C., Banks, M.L., et al. 1994. Technical Advances of Liquid CO2 Fracturing. Paper PETSOC-94-36 presented at the Annual Technical Meeting of the Petroleum Society of CIM. 12–15 June. Calgary, Alberta, Canada. http://dx.doi.org/10.2118/94-36.

Vincent, M.C. 2002. Proving It–A Review of 80 Published Field Studies Demonstrating the Importance of Increased Fracture Conductivity. Paper SPE 77675 presented at the SPE Annual Technical Conference and Exhibition. 29 September–2 October. San Antonio, Texas. http://dx.doi.org/10.2118/77675-MS.

Vincent, M.C. 2009. Examining Our Assumptions – Have Oversimplifications Jeopardised Our Ability to Design Optimal Fracture Treatments? Paper SPE 119143. presented at the SPE Hydraulic Fracturing Technology Conference. 19–21 January. The Woodlands, Texas. http://dx.doi.org/10.2118/119143-MS.

Vincent, M.C. 2011. Optimizing Transverse Fractures in Liquid-Rich Formations. Paper SPE 146376 presented at the SPE Annual Technical Conference and Exhibition. 30 October–2 November. Denver, Colorado. http://dx.doi.org/10.2118/146376-MS.

Vincent M.C. and Besler, M.R. 2013. Declining Frac Effectiveness–Evidence That Propped Fractures Lose Conductivity, Surface Area, and Hydraulic Continuity. Paper SPE 168744 presented at the Unconventional Resources Technology Conference, 12–14 August, Denver, Colorado. http://dx.doi.org/10.2118/168744-MS.

Vincent, M.C., Pearson, C. M., and Kullman, J. 1999. Non-Darcy and Multiphase Flow in Propped Fractures: Case Studies Illustrate the Dramatic Effect on Well Productivity, SPE 54630 presented at the SPE Western Regional Meeting. 26–27 May. Anchorage, Alaska. http://dx.doi.org/10.2118/54360-MS.

Walsh, J.M. 2013. Water Management for Hydraulic Fracturing in Unconventional Resources–Part 3 Water Treatment Technologies: Coagulation/Flocculation and Electrocoagulation. ***SPE Oil and Gas Facilities***, 2 (5): 10–15.

Wang, D., Butler, R., Zhang, J., et al. 2012. Wettability Survey in Bakken Shale Using Surfactant Formulation. Paper SPE 153853 presented at the SPE Improved Oil Recovery Symposium, 14–18 April, Tulsa, Oklahoma. http://dx.doi.org/10.2118/153853-MS.

Wang, J.Y., Holditch, S.A., and McVay, D. 2009. Modeling Fracture Fluid Cleanup in Tight Gas Wells. Paper SPE 119624 presented at the SPE Hydraulic Fracturing Technology Conference. 19–21 January. The Woodlands, Texas. http://dx.doi.org/10.2118/119624-MS.

Wang, X. and Mohanty, K.K. 1999. Multiphase Non-Darcy Flow in Gas-Condensate Reservoirs, SPE 56486 presented at the SPE Annual Technical Conference and Exhibition, 3–6 October, Houston, Texas. http://dx.doi.org/10.2118/56486-MS.

Warren, J.E. and Root, P.J. 1963. The Behavior of Naturally Fractured Reservoirs. ***SPE J***, **3** (3): 245-255. SPE 426-PA. http://dx.doi.org/10.2118/426-PA.

Warpinski, N. 1983. Investigation of the Accuracy and Reliability of In Situ Stress Measurements Using Hydraulic Fracturing in Perforated Cased Holes. Paper ARMA-83-0773 presented at the 24th U.S. Symposium of Rock Mechanics. 20–23 June. College Station, Texas.

Warpinski, N.R. and Branagan, P.T. 1989. Altered Stress Fracturing. ***J. Pet Tech***, 41 (09): 990–997. SPE 17533-PA. http://dx.doi.org/10.2118/17533-PA.

Warpinski, N.R., Branagan, P.T., and Sattler, A.R. 1990. A Case Study of a Stimulation Experiment in a Fluvial, Tight, Sandstone Gas Reservoir. ***SPE Prod Eng***, 5 (4): 403–410. SPE 18258-PA. http://dx.doi.org/10.2118/18258-PA.

Warpinski, N.R. and Teufel, L.W. 1987. Influence of Geologic Discontinuities on Hydraulic Fracture Propagation (includes associated papers 17011 and 17074). ***J. Pet Tech***, 39 (2): 209–220. SPE 13224-PA. http://dx.doi.org/10.2118/13224-PA.

Warpinski, N.R., Mayerhofer, M.J., Vincent, M.C., et al. 2008. Stimulating Unconventional Reservoirs: Maximizing Network Growth while Optimizing Fracture Conductivity. Paper SPE 114173 presented at the SPE Unconventional Reservoirs Conference. 10–12 February. Keystone, Colorado. http://dx.doi.org/10.2118/114173-MS.

Wei, Y. and Economides, M.J. 2005. Transverse Hydraulic Fractures from a Horizontal Well. Paper SPE 94671 presented at the SPE Annual Technical Conference and Exhibition. 9–12 October. Dallas, Texas. http://dx.doi.org/10.2118/94671-MS.

Ahmed, U., 1988. Fracture Height Prediction, ***JPT***, July 1988., pp. 813-825.

Wolhart, T. 2002. Hydraulic Fracturing Re-Stimulation. Paper SPE 101458 presented as an SPE Distinguished Lecture during the 2001–2002 season.

Wood, W.D., Brannon, H.D., Rickards, A.R., et al. 2003. Ultra-Lightweight Proppant Development Yields Exciting New Opportunities in Hydraulic Fracturing Design. Paper SPE 84309 presented at the SPE Annual Technical Conference and Exhibition. 5–8 October. Denver, Colorado. http://dx.doi.org/10.2118/84309-MS.

Xiong, H. and Holditch, S.A. 1995. A Comprehensive Approach to Formation Damage Diagnosis and Corresponding Stimulation Type and Fluid Selection. Paper SPE 29531 presented at the SPE Production Operations Symposium. April 2–4. Oklahoma City, Oklahoma. http://dx.doi.org/10.2118/29531-MS.

Xiong, H., Davidson, B. M., Saunders, B. F., et al. 1996. A Comprehensive Approach to Select Fracturing Fluids and Additives for Fracture Treatments. Paper SPE 36603 presented at the SPE Annual Technical Conference and Exhibition. October 6–9. Denver, Colorado. http://dx.doi.org/10.2118/36603-MS.

Yuster, S.T. and Calhoun, Jr., J.C. 1945a. Pressure Parting of Formations in Water Flood Operations. Part I. ***Oil Weekly***. March 12.

Yuster, S.T. and Calhoun, Jr., J.C. 1945b. Pressure Parting of Formations in Water Flood Operations. Part II. ***Oil Weekly***. March 19.

Zhang, J., Kamenov, A., Zhu, D., et al. 2013. Laboratory Measurement of Hydraulic Fracture Conductivities in the Barnett Shale. Paper IPTC 16444 presented at the International Petroleum Technology Conference. 26–28 March. Beijing, China. http://dx.doi.org/10.2523/162548-PA.

Zhang, F. and Yang, D. 2014. Determination of Fracture Conductivity in Tight Formations with Non-Darcy Flow Behavior. ***SPE J.*** **19** (1): 34–44, SPE 162548-PA. http://dx.doi.org/10.2118/162548-PA.

18

Flow Assurance

Stephen Szymczak, Baker Hughes

This page intentionally left blank

Chapter 18: Flow Assurance

18.1 Introduction

18.1.1 Overview—Production Assurance in the Unconventional Arena

As an introduction to this chapter, some terms are defined. The first is ***production assurance*** and the second is ***unconventional resource***. The stimulation process frames this discussion, and some refer to this as reservoir flow assurance in that it is the application and placement of production chemicals behind the pipe in the stimulated area that is defined by the extent of a propped fracture. These definitions will be used in this chapter in the discussions related to production assurance in unconventional resources. As is the case in all technical and academic pursuits, there is material that some readers think should be included but for a variety of reasons is not present. The material presented in this chapter is certainly germane to the topic but is not exhaustive in scope as an entire textbook by itself.

The term ***flow assurance*** has historically been used in reference to problems associated with the formation and deposition of scale, paraffin, and asphaltene as well as the downhole blocking problems associated with the formation of gas hydrates. This chapter will also include a discussion on bacteria because biocides are routinely used to sterilize fluids going downhole during stimulation. The discussion will not cover corrosion, hydrogen sulfide scavengers, oxygen scavengers, emulsion breakers, or other traditional production chemicals not routinely used during the stimulations. This chapter focuses on the use of specialty chemicals as inhibitors or control agents that are applied with the stimulation fluid and placed behind the pipe. The term ***reservoir flow assurance*** will be used to designate a flow assurance chemical treatment that is added to the stimulation fluid and placed into the formation via the stimulation operation. The traditional approach and practice for flow assurance is surface administered liquid chemicals added through chemical inject mandrels, down the back side or into flow lines as a means to address deposition after the production has entered the wellbore. An exception to this traditional application is a chemical squeeze. This is a case where the traditional approach and the reservoir-flow-assurance approach intersect.

As for unconventional resources, this chapter will use shale production as the default unconventional resource. Characteristic of shale wells for the purpose of flow assurance is little or no connate water, a lack of contiuity of the rock, and steep production declines. Shale presents less of a technical problem to the flow assurance technologies than those involved in reservoir analysis, drilling, and completions. The prime concern of flow assurance is unwanted deposition due to a change in thermodynamics. When the pressure and/or temperature changes, fluid constituents once soluble in either water or oil are now insoluble. Insoluble particles will soon aggregate and precipitate. When that occurs in undesirable locations such as the near wellbore, perforations, or tubulars, it becomes an operational problem because of the direct impact on flow rates and cumulative flow. These problems occur in all types of production and for that reason shale or other unconventional wells are just as, if no more, problematic than conventional production.

18.1.2 Costs

If a flow assurance solution can be added to the well during the completion process such that the post-stimulation costs of operation are significantly reduced, it should be an easy decision to spend money up front to reduce operational expense.

In the case of reservoir flow assurance the cost is carried in the completion budget, and the benefit is seen in the production budget. For example, adding a scale inhibitor and biocide to the stimulation fluid is a conventional and accepted treatment cost. However, the historical reason for this was to protect equipment from scaling and to assure the integrity of the guar in the stimulation fluid. More recent experience illustrates that by adding high quantities of those chemicals during the stimulation, there is a direct benefit seen in post-stimulation production. Corrosion due to bacteria is reduced and damage-inflicting scale deposition at the near wellbore is reduced. This is a case where the expenditure of a dollar on chemical added to the stimulation pays off in the elimination of a two dollar spend for well intervention and remediation after the fact. As in all practices that will influence the bottom line, a cost-benefit analysis will determine the proper amount to spend to achieve the required benefits.

18.1.3 Operations

There are three critical components to a successful reservoir flow assurance program. These are pre-stimulation analysis, job-site operations, and post-stimulation monitoring and

reporting. In the pre-stimulation period, the fluids are evaluated. The stimulation source-water, any connate water and oil or water from offset production need to be evaluated to make a determination as to the need for a flow assurance treatment. Typically, the analysis of source water is for bacteria to determine which biocide is necessary to sterilize and control subsequent bacterial growth. A complete water analysis should be run to determine potential for scale precipitation and deposition. A representative sample of the crude oil needs to be analyzed for paraffin and asphaltene deposition potential. Bacteria and scale tests are quantitative; the testing for paraffin and asphaltene is qualitative. In all sampling, there is a concern that the sample recovered at the surface is not completely representative of what may be found in the well bottom or in the formation. This is more of a concern for organics than for water. Thus, the tendency is to err on the side of precipitation potential for paraffin or asphaltene.

18.1.4 Prevention, Mitigation, and Remediation

Reservoir flow assurance is like health insurance, in that you pay for a service and hope that you do not need it. Chemical costs should be scrutinized to assure, as well as possible, that benefits exceed costs. There are differences, sometimes orders of magnitude differences, in the cost of not providing flow assurance. On one end of the spectrum, an operator may produce a well that has a high potential for calcium carbonate scale deposition. Calcium carbonate is acid soluble. If the well has easy access for an acid job and if the cost of a job is acceptable, then an operator may decide to forego any flow assurance protection and accept the cost of remediation as a cost of business. On the other end is a multistage horizontal well with high oil production and the potential for barium sulfate scale deposition. The cost to remediate barium sulfate may be prohibitive. In the first case, the cost benefit of a reservoir flow assurance program may not justify the expense. In the second case, the cost-benefit argument may be the entire basis for going forward with the project. Every well and field will have different characteristics and financial factors. The flow assurance technologist's job is to ascertain the potential for damaging deposition and to report that to the operator. The operator will then make a decision based on the cost benefit for the project.

18.2 Inorganic Scale

The constituents of inorganic scale are in solution for any given water. Such water under one set of conditions will not scale and under another set of conditions will scale. The primary conditions that drive scaling are thermodynamic (temperature and pressure) and mixing. Think of the ubiquitous water heater found in all modern homes. Now think of the rumbling noise one hears whenever the hot water is used in the house. Depending on the water chemistry and the temperature setting, scaling constituents in the water were driven out of solution, formed a scale particle, aggregated, and formed sufficient mass to drop out of solution and reside as a solid in the bottom of the tank. When the hot water is used and cold water enters the tank, the solid mass is agitated, and moves, which causes the sound. Fundamentally, the same phenomenon occurs in the well. The pressure and temperature changes that take place as the produced water enters the stimulated zone travel to the wellbore and enter the tubulars are sufficient to force ions out of solution. This thermodynamic event coupled with connate water mixing with stimulation water can exacerbate scale formation and deposition. Because the greatest thermodynamic shift will occur at perforations, that is the point that is most likely to see deposition. The deposit constricts flow paths in the near wellbore and results in reduced fluid production.

18.2.1 Characterization of Scale

To understand the scaling potential of particular water or mixture of waters, it is necessary to run a complete water analysis, including pH and gas content at the point of sampling. The water analysis will show the anion and cation constituents of the water. The water is mixed electronically under various conditions including the mix ratio, pH, and temperature. There are two outputs from this operation. First will be the scale prediction and second will be the momentary excess. The scale prediction will show if scale will form under the well conditions and what type(s) of scale will form. The momentary excess shows the amount of scale that will form per unit of water volume. For example, one analysis may show a potential for calcium carbonate with a high momentary excess. Another analysis may show a potential for barium sulfate with a low momentary excess. Both cases need to be evaluated on a cost-benefit basis. Although calcium carbonate is acid soluble and may be relatively easy to remediate, the high momentary excess prediction may lead an operator to use a preventive approach. For the barium sulfate example, although the momentary excess is low, it is also cumulative. Barium sulfate is quite problematic from a remediation standpoint. The operator may decide that it is best to pursue a preventative approach because the cost of a failure would be too high. Thus, it is critical to get a full

and complete picture of the scaling potential to make the best decision for prevention or remediation.

18.2.2 Conditions for Forming and Depositing Scale

As mentioned above, the formation and precipitation of scale is related to both thermodynamics and mixing of water. Consider a common scale inhibition test, the tube blocking apparatus. Two waters are prepared separately. One contains scaling anions (carbonate and sulfate, primarily) and the other contains scaling cations (calcium, barium, and iron primarily). The system is in an isothermal environment that reflects the temperature at which scaling is suspected to occur. This water is mixed and fed through a constrictive capillary tube. A differential pressure measuring system measures the pressure across the constriction. This test is designed to see scaling as a function of the high differential pressure after untreated waters are mixed. This will establish the baseline for an untreated scenario. In this case, the constrictive capillary tubing accelerates the time at which the effect of scale formation and precipitation is seen. This is analogous to water with a positive scaling index entering the near wellbore and perforations. If the water has a positive scaling potential, then deposition is most likely to be realized at the near wellbore.

18.2.3 Impact on Operations

When scale has formed and aggregated, it will deposit in the same proximity as the aggregation. This is often in the near wellbore or in the tubulars. The scaling process may take place uphole of the near wellbore. Scale may form at the wellhead choke or in the surface treating facilities. When scaling occurs downhole, is it much more problematic than when it occurs at the surface. When it occurs in the formation it is much more problematic than when it occurs in the tubulars. The impact of scale deposition on the operations and the operations cost will be directly attributable to the type of scale (whether acid-soluble or not) and the location of the scale (at the formation, tubulars, or surface). As mentioned earlier the formation of an acid soluble scale in an easy-to-reach wellbore easily can be addressed with an acid job. Formation of an acid insoluble scale in the formation in a multistage horizontal well might be sufficient to cease all operations and plug and abandon (P&A) the well.

18.2.4 Remediation and Mitigation Strategies

A common theme is the cost benefit of any operation. This becomes most obvious when the onset of scale deposition results in the need for well remediation. Two primary considerations on the cost side directly relate to the benefit side of the equation. The two primary cost items are the operating cost for remediation and deferred production. Any time a well is shut in for remediation means that the revenue is zero from the asset. When a cost is added on top of the shut in, then the situation becomes a significant cost issue for the operator. That is why it is important to understand what type of scale will potentially form in a particular well. An acid job may require a shut-in period of three days for mobilization and remediation. When the well is put back on production, the oil production may exceed the pre-remediation rate. In this case, the cost benefit of dealing with scale as a remediation cost may be justified. However, if barium scale is the issue and if the remediation requires excess time and dollars, then the cost benefit of dealing with the scale as a remediation may be ill advised.

For reservoir flow assurance, there are two basic approaches to prevention. Both of these occur during the stimulation. In one case, a liquid scale inhibitor is added and placed with the stimulation fluid. Variations of this would be to squeeze the liquid ahead of the stimulation. In the other case, a proppant-like substrate onto which a scale inhibitor has been adsorbed is placed in the formation with the proppant. There are pros and cons to both approaches. The primary consideration for selecting a liquid or a solid prevention method has to do with the life of the treatment. Typically, a liquid scale inhibitor flows back at a rate that is significantly higher than the minimum effective concentration (MEC) necessary to inhibit scale formation. This is expected because the liquid inhibitor has no natural affinity to stick to the formation rock and, thus, is apt to flow back with well production. However, one can still expect a treatment life, depending on the cumulative water flow of the well, to last between three to twelve months. The presence of the inhibitor is measured through regular water sampling and analysis. When the chemical residual falls below the MEC, the operator can decide to squeeze the well or apply a treatment from the surface.

The other approach to preventing and mitigating scale formation and deposition is adding a solid, chemical laden particle the same size as the proppant or sand used in the stimulation. This approach is growing in popularity and has been applied in thousands of land wells in the US and Canada. Basically, the chemical affixed onto the substrate releases at a rate above the MEC but within the same order of magnitude as the MEC in this controlled release approach. For example, a typical MEC for controlling calcium carbonate is 1 to 3 ppm as measured in the tube-blocking test. It is common to see initial

flowback rates for a liquid inhibitor in the tens or thousands of ppm, which are one or two orders of magnitude greater than what is needed. For the controlled release solid inhibitor, initial inhibitor residual will be in the range of 5 to 20 ppm and will maintain a flat chemical release profile for prolonged periods of time, often exceeding one year.

Following the tube block test, the scale inhibitor selection process is the same for liquids or solids. The next step is to select the right inhibitor. To do that the liquid inhibitor (for the solid product one would use the liquid version of the chemical that is placed onto the solid substrate) is added into the cation water source. When the cation and anion water(s) mix, the inhibitor is well dispersed and starts to kinetically inhibit scale. The fluid then reaches the capillary tube. The time for the differential pressure to register scaling is compared to the blank and to the other chemicals that are tested. The product that provides the longest period of inhibition at the lowest injection rate will be selected as the product of choice for the application.

If the cost of remediation is sufficiently high that a preventative measure needs to be considered, the operator has two basic choices for scale inhibition. First, we add a liquid, and second add a solid. The liquid is very effective and has been used for years. It has a shorter treatment life than a comparable solid. The solid has been in use for more than ten years. The one drawback has to do with crush strength and the potential for conductivity effect. Its benefit is a longer treatment life. Regardless of the approach chosen an operator is always advised to consider a preventative approach to achieve the best cost benefit for the asset. A dynamic blocking test was performed to evaluate the performance of different four scale inhibitors (RSI-10333, SCW4828, SCW8234, SCW5277) in the presence of iron. **Table 18.1** shows the synthetic brine that was prepared for this inhibition testing. **Fig. 18.1** illustrates the inhibition performance of these four inhibitors at 70°C and 750 psi. Under the testing condition, a blank scaling time of approximately 30 minutes was observed. After about 30 minutes, 60 ppm of SCW8234 and SCW5277 failed this test, but RSI-10333 and SCW4828 both achieved effective scale control at 30 ppm. RSI-10333 performance data shows that it can offer complete inhibition at 30 ppm concentration with a gradual pressure build-up as its concentration approaches 20 ppm. The SCW4828 follows a similar trend but at a slightly higher pressure rate. Therefore, the MEC for these two inhibitors would be between 20 and 30 ppm.

Table 18.1—Synthetic flowback water for inhibition testing.

	Concentration (ppm)
Sodium	30046.7
Calcium	8458
Magnesium	637
Potassium	237
Barium	5300
Strontium	1798
Iron	80
Chloride	67166.7
Sulfate	4
Bicarbonate	750
pH	7.25

Table 18.2—Calcite scale calculations.

T	P	Calcite		
°F	psia	pH	SI	Momentary Excess (mg/L)
77	15	7.26	2.18	466
88	96	7.22	2.21	471
99	178	7.18	2.23	477
110	260	7.15	2.26	483
121	342	7.12	2.29	489
132	423	7.10	2.31	495
143	505	7.08	2.34	501
154	587	7.07	2.37	506
165	668	7.05	2.40	512
176	750	7.05	2.43	518

18.2.5 Scale Potential Calculation

Table 18.2, **Table 18.3**, and **Table 18.4** present the results of the scale potential calculation performed by ScaleSoft-Pitzer software (Rice University), a program that is based on the Pitzer theory of electrolytes (Pitzer 1977). Scale prediction yields the scaling potential expressed as saturation index (SI). The greater the SI, the stronger the driving force promoting the precipitation of scaling ions (Szymczak et al. 2013). The severity of scaling can be compared between calcite, barite, and iron. The output on the calculations tells the user that scale will form, that is the SI, and how much will form, that is the momentary excess.

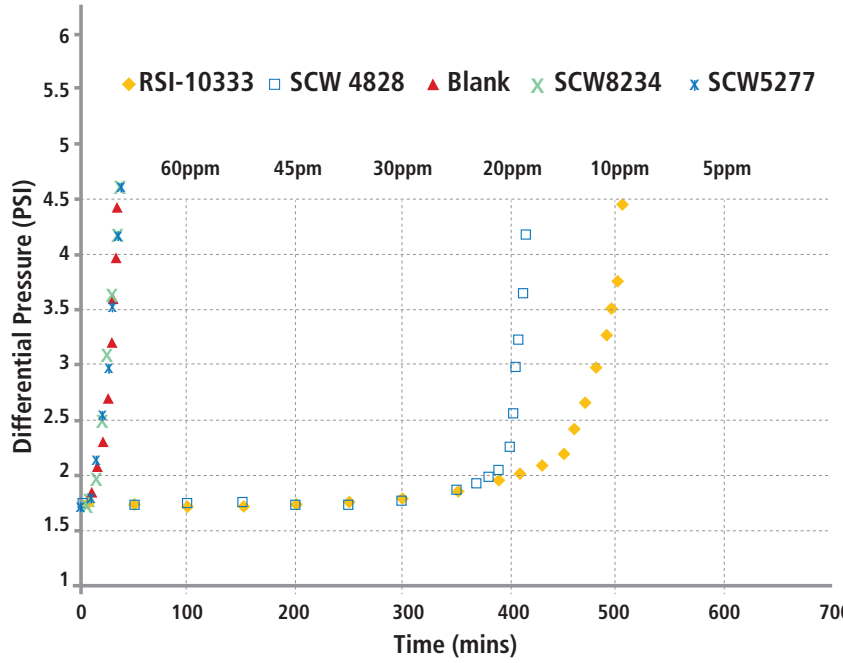

Fig. 18.1—Minimum effective concentration test (MEC). The best product runs the longest before showing a differential pressure response.

Table 18.3—Barite scale calculation.

T	P	Barite	
°F	psia	SI	Momentary Excess (mg/L)
77	15	1.90	10
88	96	1.82	10
99	178	1.74	10
110	260	1.67	10
121	342	1.61	9
132	423	1.55	9
143	505	1.50	9
154	587	1.45	9
165	668	1.40	9
176	750	1.36	9

Table 18.4—Iron carbonate scale calculation.

T	P	Iron carbonate	
°F	psia	SI	Momentary Excess (mg/L)
77	15	1.82	154
88	96	1.89	156
99	178	1.94	157
110	260	2.00	158
121	342	2.05	159
132	423	2.09	160
143	505	2.14	161
154	587	2.18	162
165	668	2.21	162
176	750	2.24	162

18.3 Paraffin

Paraffin in the oil field includes hydrocarbons of a chain length greater than 18 and normally in the range of 18 to 40+ carbon atoms. Under typical oilfield temperature and pressure domains the hydrocarbon fraction that precipitates is usually in that carbon-chain-length range. Carbon chain length is directly associated with the API gravity of a crude. The reason paraffin is a topic of discussion in a conversation on flow assurance has to do with the effects and impact that deposited paraffin has on oilfield operations. Scale is referred to as inorganic scale. One may see paraffin

referred to as organic scale, although it is more correct to refer to it as an organic deposition. Paraffin does not precipitate, aggregate, and deposit because of cation and anion salting. Rather it is a matter of the aggregate mass becoming dense to the point where the solvent cannot keep it in solution. Much like inorganic scale, the deposition of paraffin is related to the changes, often sudden, in temperature and pressure. Paraffin has another dimension not found with scale. Whereas scale, once removed has no economic value, paraffin once remediated and dissolved makes an economic contribution. The high carbon-chain-length fractions of crude oil are highly valued highly in the cosmetic and pharmaceutical industries.

18.3.1 Paraffin Characterization

A crude oil characterization for paraffin analyzes the crude for the percent asphaltene, percent solids, and percent oil and waxes. The percent oil and waxes are defined as C-10 to C-17 hydrocarbons and C-18+waxes. C represents the number of carbon atoms in the chain. Often this test is coupled with a pour point test in which a crude sample is cooled in 5°F increments to find the temperature at which the crude does not pour when the container is turned onto its side. From those analyses, a technician can determine the presence of paraffin and the severity of its impact as represented by the pour point test (ASTM D-97 method). For example, two crude samples could contain the same percent of C-18+wax. However, one may have a pour point of 40°F and the other have a pour point of -20°F. In the well environment the first sample will be significantly more problematic in that the paraffin starts to affect the flow characteristics at a much higher temperature than the second sample. Other test methods such as the cold finger are used to both evaluate the paraffin impact and test for paraffin inhibitor performance against a blank sample.

18.3.2 Conditions for Depositing Paraffin

As in the case for scale, paraffin deposition is a function of thermodynamics. In the pre-drill subterranean environment, paraffin fractions of the crude oil are in solution. When that environment is disturbed via a production well, the pressure and temperature will drop. As the pressure drops—from the reservoir, to the near wellbore, to the surface—and as the temperature drops over the same pathway, the crude will respond by shedding itself of constituents not light enough to stay in solution. Heavier hydrocarbon-chain-length molecules will crystallize, aggregate, and precipitate to form a paraffin deposit (**Fig. 18.2**). Just as we saw for scale, this deposition will be most pronounced in the near wellbore, perforations, tubing, surface chokes, and surface treating facilities. One

Fig. 18.2—The rod coupling with wax buildup after a hot water treatment.

effect of a drop of pressure is the in situ separation of the lighter hydrocarbons from the heavier hydrocarbons. Because paraffins are heavier than the shorter chain oil molecules, their degree of solubility will be more affected by the presence of the lighter ends. Under high formation pressure the methane fraction of the oil and the C-40 fraction are in solution. When the pressure drops at the perforations, the lighter methane, ethane, and propane gas will separate from the higher weight oil. This will exacerbate deposition problems.

18.3.3 Impact on Operations

Again, as with scale, the impact on operations has to do with depositions that interfere with the free flow of oil from the well. When paraffin deposits at the near wellbore, pathways available for oil flow are reduced and the volume of production is reduced. Just as for scale an intervention and remediation are required to bring the well back to the pre-damage conditions. Whereas some scale can be re-solubilized using acid, paraffin can be re-solubilized using a thermal method and/or a solvent approach. In both cases, the re-solubilization is assisted with the addition of paraffin dispersants. In some cases, the operator tries to remove deposited paraffin using wireline and a cutter. In this operation the wireline operator physically removes paraffin from the tubing until the well can flow on its own. When a well is shut-in for a paraffin work, production drops to zero and operating cost rises. Thus, it is in the operator's best interest to identify and remediate the well as quickly as possible.

18.3.4 Remediation and Mitigation Strategies

When a paraffin-related failure occurs, the operator must have an approach to intervene, correct the problem, and put the

well back on production. In all areas where paraffin is a known problem, there is a service industry segment that specializes in thermal methods to re-solubilize crude oil. This is referred to as hot oiling or hot watering. Initially in the industry it was most common for the hot oil company to secure a quantity of light crude oil from a source. This oil would then be heated using the heater on the hot oil truck. When the oil reached the desired temperature, e.g., 180°F, the oil would be circulated down the back side of the well. When the hot oil contacted the paraffin deposit in the tubing the wax would dissolve into the hot oil and the deposit would be removed. Research studies show that the use of hot oil over a prolonged period, i.e., several treatments, had a tendency to push heavier, nonsoluble fractions of paraffin into the formation and cause permanent damage. In more recent times, the industry uses hot water as the preferred thermal method. Hot water has a higher heat capacity and with the addition of paraffin dispersants does a good job of keeping the oil dispersed in the water until it reaches the surface. Today hot water is the preferred thermal method.

In the event that hot water is not available or if the completion does not allow for circulation, a solvent soak may be an alternative. In this case, a solvent is bull-headed into the tubing in an effort to slowly dissolve the deposit into the light oil. A dispersant is also recommended in this case to assure that the dissolved paraffin stays in solution until the oil is produced from the well.

Another approach to control paraffin is the addition of a solid substrate onto which a paraffin inhibitor has been adsorbed. Similar to the solid chemically charged product used for scale control, this paraffin inhibitor based product serves to provide prolonged paraffin deposition control by slowly releasing an active inhibitor into the oil phase (**Fig. 18.3**).

Fig. 18.3—The rod coupling after four months of production using a paraffin inhibition program.

18.4 Asphaltene

Unlike paraffins, which are long chain molecules made from hydrogen and carbon, asphaltenes are heterogeneous molecules dominated by hydrogen and carbon molecules but with other atoms such as oxygen, nitrogen, and sulfur. They also may contain small amounts of metals such as vanadium and nickel. Asphaltenes are colloidal, i.e., they are not truly dissolved in the crude oil. They exist in an associated form in the crude oil. However, it is common to read or hear about asphaltenes "coming out of solution." This is a misnomer. Asphaltenes will aggregate and precipitate like paraffin but there is a difference. Whereas paraffin forms a seed crystal as the first step in precipitation, an asphaltene is already formed. When the conditions change, asphaltene will precipitate. In addition to temperature and pressure leading to precipitation, asphaltene can also deposit when associated resins, maltenes, and other light ends separate. These components help keep the asphaltene dispersed within the crude. In the absence of these natural dispersants, asphaltene is more prone to deposit. In summary, asphaltenes are problematic because they deposit and create flow constrictions. Like paraffin, they are best inhibited by adding chemical inhibitor when the fluid is at its warmest and pressure at its highest.

18.4.1 Asphaltene Characterization

The first step in characterizing a crude oil for asphaltene is to run a saturate, aromatic, resin, and asphaltene (SARA) analysis. Saturates are normal oil and paraffin. Aromatics have an aromatic ring (e.g., benzene), and resins are similar to asphaltene. The difference is that resins are soluble in an alkane solvent such as heptane or hexane whereas an asphaltene is insoluble. Once the SARA is complete, various bench tests can be run to ascertain severity of asphaltene deposition under field conditions. Asphaltene as a production problem is not as prevalent as paraffin. When asphaltene is a problem, it can be significantly more severe than paraffin. Unlike paraffin, asphaltene is not truly soluble. If the deposit is not too heavy and if a high temperature is maintained, then a hot water treatment with a dispersant may have some effect. However, in many cases, to re-solubilize asphaltene in situ requires the application of an aromatic solvent such as xylene.

18.4.2 Conditions for Depositing Asphaltene

Like paraffin, asphaltene will deposit as a function of a change in temperature or pressure. The same fluid under high pressure and temperature versus low pressure and temperature will have a different deposition profile.

Like paraffin, when the pressure drops and the lighter molecules evolve away from the heavier molecules, the rate of deposition for asphaltene will increase. Like paraffin, asphaltene will begin to deposit at the near wellbore area, the perforations, and the tubulars. Once the oil has made it to the surface there is also potential for deposition. However, it is more common to see paraffin deposit in surface equipment than it is to see asphaltene deposit.

18.4.3 Impact on Operations

Like paraffin, asphaltene deposits when conditions force them out of solution. The typical locations for deposition are at points of pressure and/or temperature drop. This could be the perforations, tubing, safety valve, or surface equipment. If the deposited mass is of sufficient mass to constrict flow then the well production drops and the operator must expend resources to intervene and remediate the well. A well-executed flow assurance program is designed to prevent this deposition and to avoid or reduce the frequency of well interventions. **Fig. 18.4** illustrates the impact of cumulative treatment costs in comparison to costs associated with not implementing any remedial method.

18.4.4 Remediation and Mitigation Strategies

Like paraffin, asphaltene re-associates in an aromatic solvent (**Fig. 18.5**). Asphaltene will not dissolve in an alkane solvent such as diesel. If the deposit is not too severe, it may be possible to remove an asphaltene deposit

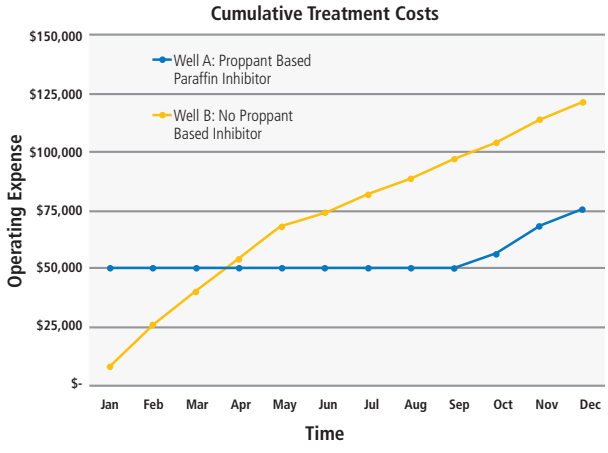

Fig. 18.4—Cumulative treatment costs. This chart shows the comparison of post-fracturing operational cost for paraffin treatment. At four months the cost of wax remediation for the untreated well exceeds the cost of the solid paraffin particle added during the fracture.

Fig. 18.5—Asphaltene deposition–a deep-water tool coated with asphaltene. This forced the operator to side track the well and install a chemical injection mandrel for chemical treatment.

using hot water and dispersant. However, the water needs to be hot, i.e., 180°F, and sufficient dispersant needs to be added to keep it in solution until it flows to the surface.

Just as with paraffin and scale, there is a relatively new technology that uses a solid substrate onto which an asphaltene dispersant has been adsorbed. A chemically charged substrate is added to proppant during the fracture. Upon contact with the produced oil, the asphaltene dispersant on the particle slowly releases and provides sufficient dispersancy to avoid asphaltene deposition (**Fig. 18.6**). Once the chemical on the substrate is depleted, the operator needs to either re-squeeze the substrate with an asphaltene dispersant or use a surface delivery system to feed a chemical into the production upstream of the point of asphaltene deposition.

18.5 Bacteria and Bacterially Related Corrosion

Bacteria are the cockroaches of the oil and gas industry. A minute trace of bacteria in produced water indicates a bacteria problem. Bacteria are present in all life forms. They can even exist as spores in extremely high temperature regimes only to return to a fully active state in a more moderate temperature. One cannot eliminate bacteria from a formation. However, one can control the growth and impact of bacteria in an oil and gas system. In practice, bacteria in and of themselves are not a problem. The

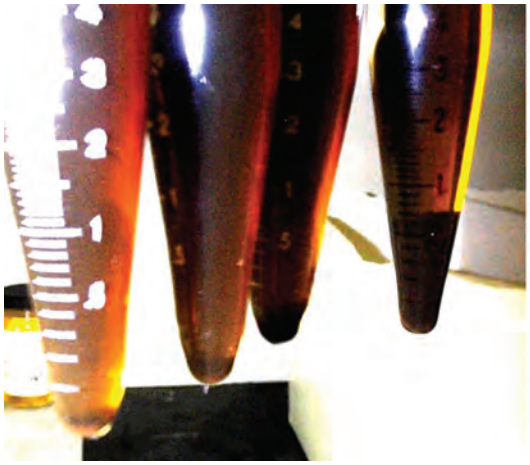

Fig. 18.6—In an asphaltene deposition test, asphaltene is forced out of solution with aliphatic solvent. The presence of asphaltene indicates it may not be depositing downhole. This photo shows asphaltene deposition in a deep-water tool coated with asphaltene. This forced the operator to side track the well and install a chemical injection mandrel for chemical treatment.

problem occurs when bacteria change from a free-floating form (planktonic) to a biomass (sessile).

18.5.1 Characterization of Bacteria

In the oil field, bacteria exist in two forms, planktonic and sessile. Planktonic bacteria are free floating in the water and are not a problem. Sessile bacteria are static and can form a biomass on the metal surfaces in the well, typically on the tubing. Once that colony has formed it creates an impenetrable outer coating that protects the colony from erosion and most chemical interference. At the interface between the colony and the metal, the bacteria act on the metal and thereby extract the iron from the pipe. Over time, the metal weakens and leaks. This is called microbial induced corrosion (MIC).

Two primary types of bacteria are a concern in the oil and gas industry: sulfate reducing bacteria (SRB) and acid producing bacteria (APB). Both anaerobic bacteria live in an oxygen-free environment, i.e., the environment typical of downhole in a well. Whereas aerobic life depends on oxygen, these anaerobic life forms depend on sulfur. The SRB metabolism is fueled by the sulfur found in sulfate-containing water. At the interface of the sessile bacteria colony and the metal pipe, the chemical process reduces the sulfate and creates both iron sulfide (FeS) and hydrogen sulfide (H_2S). In an environment that contains sulfate, hydrogen, and iron combined with SRB that are present the corrosion will weaken and make the affected pipe useless.

APB are corrosive through a mechanism by which the bacteria create an acid that, in turn, lowers the pH to a range that makes the metal corrode.

18.5.2 Conditions for Propagating Bacteria

Bacteria thrive within particular temperature ranges. Unfortunately, the temperature of many oil and gas wells is the preferred temperature for most oil field bacteria. One only has to think of the time for food to go bad. Food that is left out in the ambient summer temperature will go bad in a short time. The same food that is refrigerated will last for days before it goes bad. Instead of refrigerating bacteria, the industry used biocides to control bacterial growth. Most wells have a temperature range between 120°F and 300°F. The sweet spot for bacterial growth is roughly between 160°F and 200°F. However, on either side of that range bacterial growth still can be prolific. As the temperature drops below 100°F or above 300°F, bacterial growth will be arrested. However, when those fluids reach temperatures within the preferred range the bacteria that are present will start to grow at accelerated rates.

The other condition necessary for bacteria to form sessile colonies is quiescence. Any section of the well where the flow is non-turbulent is a good place for sessile growth to occur.

18.5.3 Impact on Operations

The operations cost for corrosion control and remediation is among the highest for any flow assurance related cost in the industry. More money is spent on corrosion control and repairs than for any other area. Although scale and paraffin arguably have a larger impact on the oil and gas production, corrosion has a larger overall impact on the total spend for well remediation.

18.5.4 Remediation and Mitigation Strategies

The focus in this chapter is remediation and mitigation that takes place during the completion. It is at this point that the operator has the best chance to establish control over subsequent bacteria growth and proliferation. Historically, the stimulation industry applied biocides to control bacterial growth in the fracturing water storage facilities. Guar is the most common chemical used in the stimulation market. Guar is a natural agricultural product that viscosifies fluids. It is also an excellent food source for bacteria. It is common for fracturing tanks filled with guar to be left in ambient conditions for several days in preparation for the fracture. To assure fluid integrity it

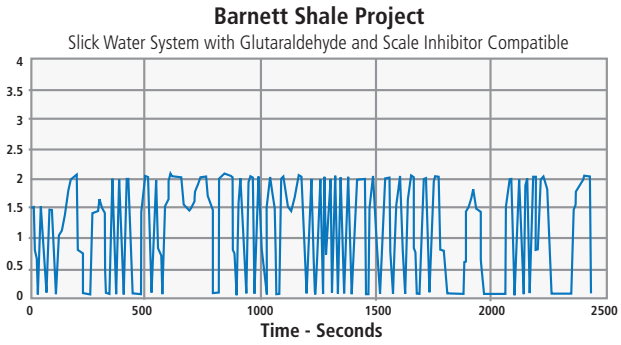

Fig. 18.7—Lab test to measure compatibility of a biocide with a slickwater stimulation fluid. The addition of a biocide in the test showed no response in the differential pressure thus assuring the biocide is compatible and approved for use in the fracturing system.

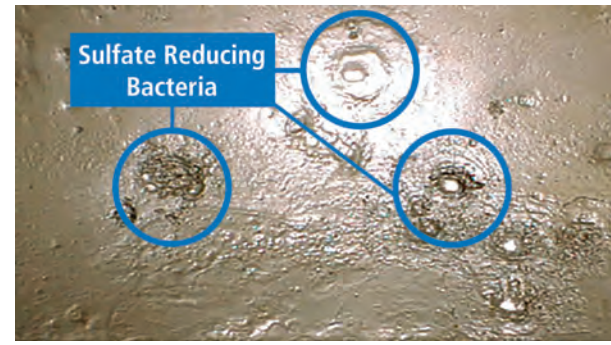

Fig. 18.8—Sulfate reducing bacteria is most prevalent source of microbial-induced corrosion in the oil field.

is necessary to add a biocide to the tanks to keep the bacteria under control. In the absence of a biocide, bacteria will digest the guar and significantly degrade fluid integrity. From those days when biocide was seen as only necessary to preserve the guar fluid, the industry has moved to a posture of using the stimulation as the prime manner by which a formation-sterilizing quantity of biocide can be applied to kill the bacteria and create a sterile environment in the propped formation (**Fig. 18.7**).

The present thinking for bacterial control calls for adequate amounts of an organic biocide to be added during the stimulation. Every water has different requirements but it is typical to see the biocide treatment range from 250 to 1,000 ppm based on water quality. This would be between 0.025 to 0.1% of the total water used for the stimulation. Among the standard products used are glutaraldehyde, tetrakishydroxy methyl phosphonium sulfate (THPS), and quaternary amines. The industry continues to develop new biocides that kill bacteria, but that has less of an effect on other life forms.

The industry also uses an oxidative approach to bacterial control. It is not uncommon to use chlorine dioxide (ClO_2) gas. In this case a ClO_2 generator is brought to the site. The gas constituents are present in the liquid form. The generator creates the ClO_2 gas, which is then fed directly into the fracturing water ahead of the blender. ClO_2 is also used to sterilize fracturing tanks that contain source water, similar to the use of organic biocides for the same purpose.

Organic biocide and ClO_2 have pros and cons. The organic products present a risk in transportation and potential for harm if spilled into a waterway. However, they have an excellent residual life. Once applied, they will continue to kill bacteria for a period of time. ClO_2 is generated onsite so it has less of a transportation or spill issue. Environmental risks are minimized when multiple wells are drilled from a single pad, decreasing transportation risk. However, it offers no residual life. It kills bacteria immediately after contact but has no sustainable killing power. Both products have handling and human contact concerns. All operators must be fully trained in the use and handling of biocides.

An emerging technology for bacterial control is the use of a biostat or preservation to treat bacteria in the wellbore over a prolonged period of time (**Fig. 18.8**). Biostats can be applied as a liquid as part of the stimulation. By design these have a prolonged effect on bacteria. Whereas a product such a glutaraldehyde kills quickly and can sterilize a particular water, biostats are slow killers but last longer.

Another approach to the biostat application has been the incorporation of biocide onto a solid substrate much like those described for scale and paraffin control. In this case the biocide-laden substrate is added to the proppant and fed as a proppant. Once in the formation biocide that resides on the substrate will release in the presence of produced water.

Because the bacteria reside in the water phase of the well fluids, the controlled release biocide is continually present and kills and controls bacteria for prolonged periods.

The presence and effect of a biocide and biostat are measured by collecting water samples and running tests designed to show the current population of bacteria and to measure the residual of available biocide available to control the bacteria population.

18.6 Program Design and Operations

By designing a flow assurance program in concert with the overall well design there will be less need for remediation over the life of the well. However, as discussed earlier, all completion costs must be weighed from a cost-benefit standpoint. If an operator used corrosion resistant alloys (CRA) tubing and installed a host of chemical injection mandrels (CIM) throughout the lower completion, then he or she might expect to avoid all future remediation for flow assurance. However, the cost should be such as to make the well unprofitable. Balance and smart design are keys to establishing a workable flow assurance methodology and program.

18.6.1 Ascertaining Production Assurance Requirements

Reservoir flow assurance is based on the premise that a chemical treatment placed behind the pipe is the best way to inhibit scale, paraffin, and asphaltene. If one were to examine a nodal analysis as the pressure and temperature change from the reservoir, through the proppant pack to the near wellbore the trend would show lower pressure and temperature from reservoir to wellbore. In the reservoir the fluid is in a state of equilibrium, i.e., any scale, paraffin, and asphaltene that would have precipitated would have done so. Once that equilibrium is disturbed by exposure to the wellbore and as fluids migrate toward the wellbore, fluids will seek to establish a new equilibrium dictated by the new pressures and temperatures. It is the job of the flow assurance expert to predict the degree and magnitude of deposition problems brought about by that shift in equilibrium. The tools to make that determination are fluid analyses, reservoir parameters, and experience.

18.6.2 Analysis and Treatment Recommendations

Fluids analysis is essential for determining a chemical recommendation to mitigate flow assurance related problems.

The information gained from a water analysis is simple and direct. Scaling index and momentary excess can be determined using several available software packages. Following an assessment of the scaling tendencies the lab can run a tube-blocking test or other suitable evaluation test to determine which inhibitor is best suited to inhibit the scale.

With a water sample, a technician can run a 28-day bacteria incubation and kill study. This will determine the best biocide based on the best kill rate.

Paraffin and asphaltene content of the crude can be determined using the tests described in earlier sections. For paraffin inhibition testing the various inhibitors can be evaluated using a cold finger apparatus or a pour point test. The cold finger test is based on forcing the deposition of paraffin onto a chilled tube (the finger) inserted into a warm crude sample. As the finger is chilled paraffin will crystallize, aggregate, and deposit onto the finger. The paraffin mass that accumulates on the finger is compared with a series of tests in which a single variable, usually the inhibitor and the inhibitor dosage, has been changed. The product that creates the least amount of deposited paraffin at the lowest dosage rate is deemed to be the best to use.

As described above, the pour point compares the temperature at which the crude fails to pour when the vessel is tipped onto its side. The untreated blank and the least effective inhibitors will fail to pour at higher temperatures. The products of choice are those that continue to pour at low temperatures and at the lowest dosage.

For asphaltene a forced precipitation test is used. In this test a blank is compared with samples that have been treated with various asphaltene inhibitors and dispersants. The blank and treated fluids are then mixed with an alkane solvent such as hexane or heptane. Asphaltene is not soluble in this type of solvent. Thus, uninhibited asphaltene will deposit. The sample with the least amount of precipitation is deemed to be the best technical product.

Once characterizations and product testing is complete, it is necessary to determine the best application for the prescribed products. As mentioned earlier, when one considers reservoir flow assurance, i.e., behind the pipe, several traditional methods of application are left out. For example, the bulk of flow assurance chemicals used in the production chemical business are fed through the annulus, through capillary tubing placed near the perforations, or bull headed down the tubing. Additionally a vast amount of chemicals are applied at the wellhead to prevent problems in surface flowlines and treating facilities. The squeeze is the one traditional method that places chemicals behind the pipe.

In addition to the squeeze for placing chemical into the formation there are two other methods. The first method is to identify a liquid flow assurance chemical that is compatible with the stimulation fluid and then add the chemical on the fly during the stimulation. Whereas a squeeze operation is conducted at pressures below the fracture pressure, chemicals added to the stimulation fluid are placed at the fracturing pressure. Thus, the flow assurance chemicals added during

the stimulation travel further away from the wellbore and as far as the fluid travels. This could be several hundred feet into the formation and could even leak off into the unfractured rock. A squeeze usually is limited to 3 to 10 ft. from the wellbore. Thus the stimulation addition method allows for more chemical to be placed and for the chemical to be placed further out into the formation. The argument for this treatment is that the treatment should last longer because of the bulk of chemical added and the increase in contact area that translates to increased inhibition further from the wellbore. If deposition due to the lack of flow assurance occurs close to the perforations where the temperature and pressure are relatively low, it is an advantage to have inhibitor acting against deposition before the fluid reaches the thermodynamic state that brings on the onset of deposition.

The final method of applying a chemical into the formation is through the use of a chemical placed onto a proppant-like substrate providing a controlled release of chemical into the formation to provide prolonged flow assurance. This technology exists for all of the traditional flow assurance inhibitors including scale, paraffin, asphaltene, corrosion, and bacteria. The treatment life for this approach, as well as for the stimulation added method and the squeeze, is directly proportional to the cumulative flow of the fluid. This is true for scale, corrosion, and bacteria control as well as for paraffin and asphaltene control. The advantage of the solid controlled release technology is that the chemical releases at a known rate under known conditions. The liquid comes back at a rate determined by the bulk fluid production. A liquid chemical, regardless of being water soluble or oil soluble, will flow back with the bulk produced fluids. The advantage of the controlled release solid has to do with solubility.

Most wells produce oil before they produce water, or at least the oil to water ratio is typically highest at the onset of production. Over time the water cut will typically increase. If the operator is placing a controlled release solid into the formation to control scale deposition then the ideal case is for all of the scale inhibitor to be available when water first starts to flow. The controlled release solid product is chemically inert in the presence of oil. However, once water production starts the scale inhibitor that is adsorbed onto the substrate will start to release. Thus the full amount of scale inhibitor is available until the water production starts. With the liquid scale inhibitor added to the stimulation fluid the chemical starts to flow back with the bulk production even if that production is all oil. That means less scale inhibitor is available when the water does start to produce. Thus some of the value in adding the liquid scale inhibitor is lost before it can return the value.

The question comes up as to the dynamics of scale inhibition for shale wells. Often these wells have no connate water. Thus the scaling that does occur will occur during flowback. Why would it matter if the scale inhibitor were present in the liquid or solid form? Although the initial flowback period will see the highest cumulative amount of water, residual water is produced for some time afterward. It is quite possible that the liquid inhibitor will be exhausted completely before the water and scaling potential ceases to be an issue. Liquid chemicals typically flow back at dosage rates well above what is required. Thus even in the dry shale production there is merit in examining the use of a controlled release solid scale inhibitor.

18.6.3 Cost-Benefit Analysis

The cost-benefit analysis of any operation requires quality information. It also calls for some appreciation for probabilities. In the case of mitigating the problems associated with flow assurance it is important to compare the cost of prevention with the cost of remediation. The challenge has to do with the assessment of the known versus the unknown. If the operator employs a deposition mitigation program during the completion then the cost of that program is known. If the well produces beyond the period of untreated offset wells before requiring remediation and if the value of the problem-free period exceeds the cost of the initial program, then the operator can be satisfied that the choice was sound and had a positive cost-benefit. However, the question always lingers as to whether or not a flow assurance problem would have occurred in a well for which a preventative program had not been employed. Just like the decision to buy or not buy life insurance, the operator must make a decision based on local offset experience and the cost of being wrong. For example, as reported in SPE 168169 an operator in the Eagle Ford employed a solid controlled release paraffin inhibitor into 20 wells. When they compared the cost of the solid versus the remediation costs of the untreated offset wells they determined that they needed four months of zero operations cost for the treated wells to equal the cost of remediation for the untreated wells. In fact, the treated wells produced over a year before any remediation was required indicating positive treatment economies.

18.6.4 Monitoring and Reporting

To understand the true value of the flow assurance program, operators and suppliers must agree on the manner by which the performance is measured and monitored. Time and experience show that a post-stimulation monitoring

program can provide long-term information with a sampling program that averages one sample per month. Immediately after the well is put on production some operators want to see relatively frequent data. Once a performance trend line is established, the monitoring period can often drop back to bimonthly or quarterly. On average 10 to 12 samples a year are sufficient to provide the performance trend for a flow assurance chemical program.

Sampling and analysis for water-based chemistries is simpler and more direct than that for the oil-based chemistries. Sampling and analyzing for scale, corrosion, and biocide residuals is straightforward. The initial performance testing in the lab that led to the selection of a particular chemical would have established the MEC for that product. The analysis of a subsequent produced water sample will tell the technician if the chemical residual is above that MEC. If so, then the program is said to be active and providing protection. As residual results drop over time and approach the MEC, the supplier needs to inform the operator that the initial chemical treatment is approaching its terminal life. That allows the operator to consider an alternative program to continue treating for the problem. Those alternatives include a squeeze or some form of a surface treatment.

Sampling frequency for paraffin and asphaltene inhibitor performance also can be set up for monthly sampling. The molecules used to treat paraffin and asphaltene do not lend themselves to easy analytical identification. For example, a wax crystal modifier or inhibitor is chemically related to a paraffin molecule. With the normally available lab analytical equipment and the time allowed for testing, it is virtually impossible to identify the paraffin inhibitor molecule in crude oil. Because of this, the industry uses a variety of comparative testing methods. Whereas the water-soluble inhibitor testing provides a quantitative answer as to the remaining chemical in place and available to inhibit, oil-soluble inhibitor testing provides a qualitative answer as to the remaining chemical in place and available to inhibit.

Two of the most common methods for evaluating a paraffin inhibitor are the cold finger and the pour point test. These were discussed in the paraffin section. Industry experts may argue which tool better serves the purpose. What is more important than the method is the manner by which it is used to align the testing with what is seen in the field? If Product X is used throughout an area and if the well failures due to paraffin are extremely low then there is a good chance that Product X is working. When someone develops a test that shows that Product Y is superior to X in a bench test but where there are no examples of Product Y ever having worked in the field, one must question the viability of the test method. In those cases where the application is new and for which there is no treatment precedent, the expert must develop a test that shows consistent performance under various test parameters. He or she must then monitor the field results to assure that the field performance matches the expectation from the bench testing.

An example of using a comparative method for observing paraffin inhibitor performance is a case from the Permian Basin involved in an active fracturing program. The wells for this operator averaged producing 100 bbls per day. After three to four months the wells began to fail due to paraffin build up on the rods leading to rod separation, etc. The operator agreed to place a solid controlled release paraffin inhibitor in the formation during the hydraulic fracture. His measure of success was four months of production without a paraffin-related failure. After 29 months the first well required an intervention for paraffin. During that 29-month period a sample was taken on a regular basis. The pour point of the sample was measured and compared with a standard sample taken from an offset well. For several months the difference in the pour points of the two samples was over 20°F. This pour point difference together with the extended life performance lined up such that the confidence in the pour point test as a measure was accepted by the operator. By tracking the performance over time, the operator was assured that the well was on track. When the pour-point results from the treated sample started to merge with the blank results, the operator knew it was time to start an alternative treatment program.

18.7 Summary and Conclusion

Production assurance is the objective of the post-stimulation period for a well and a field. Simply put it refers to the practices designed to prevent a production loss due to scale, paraffin, or asphaltene deposition as well as to the production impact of significant bacterial growth and the resulting corrosion of metal goods. Although there are practices related to materials such as corrosion resistant metal alloys, most of the production assurance practices and applications call for specialty chemicals designed to inhibit, mitigate, or eliminate associated problems of flow stopping deposition.

During the stimulation process it is advantageous to apply these flow assurance chemicals with the stimulation so as to place the chemicals as far away from the near wellbore as possible. In doing so, the inhibition process initiates before the deposit-prone particles can form and agglomerate. By

inhibiting solid deposition away from the near wellbore, there is less likelihood for harmful deposition to occur there. This maximizes flow through the near wellbore zone into the tubulars. This flow assurance process that started in the fracture zone will continue to mitigate harmful particle formation in tubulars and even into surface facilities.

Although unconventional resource hydrocarbon and rock formation have a significant impact on stimulation design they have minimal impact on the design of a production assurance program. Inorganic scale, paraffin, asphaltene, and bacteria are not different, nor do they display different behaviors, when going from a conventional resource to an unconventional resource. In all cases the inhibitory chemistry must contact the fluid prior to the onset of seed crystallization. This crystallization is a direct function of temperature and pressure. The largest pressure and temperature drop is seen across the perforations in the near wellbore. By placing these inhibitors far away from the near wellbore the chemistry can take advantage of the time for mixing as the fluid moves toward the near wellbore as well as enter the fluid before any significant crystal formation has occurred.

Every good production assurance program calls for well monitoring. By regularly collecting samples and analyzing the fluid for either a chemical residual or for a benchmark performance comparison, the supplier and the operator gain greater confidence in the program efficacy. Over time in a particular field a performance trend will emerge that gives the operator a greater sense of confidence in the longevity of a production assurance program. Any chemical that is placed in the formation eventually will be consumed. When the monitoring program shows that the useful life of the program is about to expire then it is prudent for the operator to introduce either a chemical squeeze program or a continuous application program.

Operators spend millions of dollars to drill and complete a well. Once the well comes on line that operator also must assure that the production is maximized. A well thought-out and cost-efficient chemical program is the best way to proceed with production assurance. By starting with the placement of chemical in the stimulation and then following up with a conventional continuous treatment program the operator has the best assurance that the well will remain economically viable for the designed life of the asset.

18.8 Acknowledgment

The author would like to thank William Steiner and Tony Smith of Baker Hughes for their contributions to this chapter.

18.9 References

ASTM D-97. Standard Test Method for Pour Point of Petroleum Products. West Conshohocken, Pennsylvania: ASTM International. http://dx.doi.org/10.1520/D0097-12.

Pitzer, K.S. 1977. Electrolyte Theory–Improvement since Debye and Huckel. *Accounts of Chemical. Research*, **10** (10), 371–377. http://dx.doi.org/ 10.1021/ar50118a004.

Szymczak, S., Gupta, D.V.S., Steiner, W., et al. 2014. Well Stimulation Using a Solid, Proppant-Sized, Paraffin Inhibitor to Reduce Costs and Increase Production for a South Texas, Eagle Ford Shale Oil Operator. SPE Formation Damage Control Symposium. Paper SPE 168169.

Szymczak, S., Shen, D., Higgins, R., et al. 2013. Minimizing Environmental and Economic Risks with a Proppant-Sized Solid Scale Inhibitor Additive in the Bakken Formation. ***SPE Prod Oper.***, **29** (1): 14–20. Paper SPE 159701. http://dx.doi.org/10.2118/159701-PA.

19

Artificial Lift Technologies

Alex Vilcinskas, Baker Hughes

This page intentionally left blank

Chapter 19: Artificial Lift Technologies

19.1 Introduction

This chapter covers some of the applications, technical challenges, tactics, and needs related to designing electrical submersible pumps (ESPs) for unconventional oil plays. The focus is on the applications and technical challenges that an application engineer may come across when working with unconventional oil plays.

This chapter is divided into specific challenges and tools and general practices that may be helpful to any professional involved with application of ESPs in unconventional oil plays. The text refers to unconventional oil plays in the US, but there is no reason to believe that most techniques and tools mentioned will not apply to any other similar plays overseas.

The term unconventional oil plays includes the now ubiquitous shale plays, certain plays that are not real shales but come close in regard to drilling requirements, and production strategies such as tight sands, chalks, cherts, and the combination of these in any oil or gas well. The term unconventional oil plays includes the shallow oil sands that are produced either by open-hole mining or by the steam-assisted gravity drainage (SAGD) method. Although ESPs are a large part of SAGD operations, this subject will not be covered.

19.2 Unconventional Oil Plays and General Issues

This chapter focuses on shales and other unconventional oil plays that produce enough oil to be the target of artificial lift with ESPs in particular. The term unconventional oil plays covers these shales and other similar geological structures that are usually trapped between shales and are affected by their behavior. Multiple sands and conventional rocks comprising strata are very thin, are locked in by shale-like structures above and below, and behave from the production aspect much like the pure shale rock reservoirs. A strongly developing unconventional oil reservoir north of Oklahoma and south of Kansas, known as the Mississippi chat (chat from chert, a siliceous rock), overlies the Mississippi lime, a limestone rich in hydrocarbon. These formations are significantly different from the true shales such as the Bakken in North Dakota or the Eagle Ford in South Texas but present similar challenges for ESP applications.

Operators targeting unconventional oil plays are mindful of their economics and approach drilling and completing and fracturing their new wells with the intent of keeping costs in line. This initial approach is not the best for ESP suppliers, who like to see large casings and straight casings wherever possible. Without taking artificial lift into consideration, the perfect shale play well is a small casing going straight down to the shale rock, making a 90° turn into the play, and proceeding horizontally as far as it can go with an even smaller liner. Smaller drill bits and smaller casing diameters reduce the final cost of the well. ESPs need elbow room and gradual curves if they are to make any turns.

Apart from the difficulties posed by well construction, production in these wells varies significantly due to the evolution of the reservoirs in the unconventional plays. The most typical scenario has the operation starting out with high rates while handling abundant fracturing sand in the fluid and some gas. Over a relatively short time, production rates fall, fracturing sand will start falling off, but gas production will tend to rise (**Table 19.1**). Additionally, sand production is common at early times.

19.2.1 Operator Production Strategy

Baker Hughes artificial lift systems (ALS) specific strategy manages artificial lift in a changing production environment. Declining production over a short time and gas evolution typically prevents one single installation from covering production needs over a very long period of time. The strategy for handling changes over time varies from one play and/or operator to another, involving diverse technical and marketing approaches. Some of this will become apparent as challenges to ESP application are discussed. Technical tactics involve making the most of the solutions and approaches at hand and identifying key opportunities to develop new technologies.

However, one defining factor for the ALS strategy is the operators' approach to the play's production regime. Two approaches are common: maximum recovery over a short period of time and a conservative production regime designed to obtain the maximum total hydrocarbons recovery from the well, field, or play. The main difference between the two is the resulting rate of decline in pressure and productivity in the wells. The first approach draws down the pressure in the well more aggressively. This affects the pressure profile

Table 19.1—Main characteristics of US land principle shale plays.
(HPDI and Simmons & Company International 2011 and various sources.)

Shale Play	30 Day IP Rate	1st YR. Decline	2nd YR. Decline	3rd YR. Decline	EUR	API	Prod. GOR	DEPTH (Ft.)	Typical Casing/ Line R Sizes	Pay Thick (Ft.)	Porosity (%)	Permea-biL (mD)	TOC (%)	SBHP	BHT (F)
Bakken	732	–71%	–34%	–23%	784	38–46	>450	7,000–11,000	7"/4–1/2"–5	<150	4–6	<0.01	6–20	<7000	200–260
Three Forks	>1,000							>10,000		<270					
DJ Niobrara	352	–78%	–41%	–29%	400	35–36	500–100K	4,000–8,000	5–1/2"(17#) 7"(26–29#)	270–375	4–14	<0.01	4–4.5	<2500	210–250
Eagle Ford (Oil)	870	–78%	–42%	–30%	575	30–45	800	7,500–11,00 (Oil Window)	5–1/2" (17, 20 & 23#)	75–500	4–11	<0.01	3–7	6,200	260
Miss. Chat	239	–56%	–28%	–20%	400	43	500–100	4,000–6,000	7"					500–900	120–140
Cana Wordford								6,000–11,000		900			5.7 Ave.		
TX Bone Spring*	500–700	–56%	–37%	–27%	600	20	40,000	6,500–13,000			7–18	0.5–7.2	4–10	2122	
Tuscaloosa Marine	~400					38–42		10,000–14,000		2,500–3,000	2.3–8				
Granite Wash	1,552	–79%	–35%	–23%	1,000	36–40	7500	11,000–13,000		100–1,500	8				200
Barnett					320	38–40	wet gas?	6,500–9,000		100–700	0.5–6		2–7	2,900	130
Utica					455	35		2,300–6,000		100–1,000	3–12	<0.01	1–3.1		
Wolfcamp**	~800				598	40–46		5,500–11,000		200–400	7–15		2–15		
Cline**	575				570	38–42		>9,000		200–350	8–12		2–8		

Notes: All information in spreadsheet is typical. Big swings possible as some plays may include interspersed sands or limestone layers.
It is important to mention that some of the production information (30 day IP and EUR) is changing over time as drilling and completion techniques improve. For example, in some areas there is almost a linear relationship between lateral length and 30 day IP.
(*) Bonespring is made up of 3 Bone Springs sands, Bone Springs carbonate, and Avalon shale.
(**) Wolfberry (Wolfcamp + Spraberry). Wolfbone (Bone Springs + Wolfcamp), Strawberry (Wolfberry + Strawn), etc.

in the reservoir volume closest to the well. As pressure is drawn down, a possibility is that fractures will collapse and crush proppant particles. This problem is more likely to occur in deeper and over-pressured formations. Mississippi Lime operators, for example, have not reported seeing this happen as they are at a depth of less than 5,000 ft. The proppant is usually made up of sand or ceramic, the latter being harder and more resistant to crushing. Ceramic proppants are a more expensive choice. Operators are beginning to see the benefits they offer and are gradually switching over to them for high stress completion.

The two approaches have an immediate effect on the strategy required for artificial lift. The aggressive approach gives way to a very rapid production decline that in turn makes it hard to design an artificial lift plan that covers the production range from start to finish. The finish is defined as a somewhat stabilized production rate and flowing bottom hole pressure (FBHP) maintained for an extended period of time.

Fig. 19.1 and **Table 19.2** show how quickly a well in the Bakken shale play (Parshall/Sanish area) will decline over time. When compared with the originally targeted wells for ESPs, found in fields with waterfloods or water drive reservoirs that sometimes had zero decline over a few years, it is easy to understand how difficult it is to find the right ESP for the application.

If a design is required for the well in this example, the ESP has to start out with a rate of approximately 700 BPD. This is at the extreme right-hand side of its performance range. They have to be able to produce at

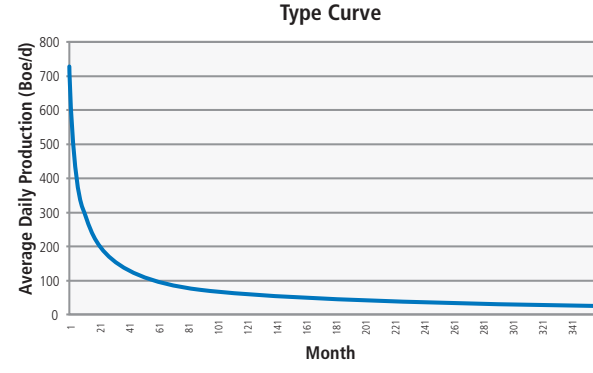

Fig. 19.1—Production decline curve and table for Bakken shale play, Parshall/Sanish area. (HPDI and Simmons & Company International 2011.)

Table 19.2—Key assumptions and threshold price on half cycle basis.

Key Assumptions/Threshold Price on Half Cycle Basis	
Assumptions	**Bakken Parshall Sanish**
Well Cost ($MM)	$7.3
EUR Per Well (Mboe)	784
Implied F&D Cost ($/boe)	$11.69
30-Day IP Rate (boe/d)	731.5
Production Costs	$8.00
Production Taxes	11%
1st Year Decline (%)	-71%
2nd Year Decline (%)	-34%
3rd Year Decline (%)	-23%
Well % Oil	86%
Oil DIff to WTI (%)	-10%
Well % NGLs	8%
Well % Gas	6%
Threshold Oil Price Necessary for 10% ATROR	$44.13
15% ATROR	$51.59
20% ATROR	$59.06
25% ATROR	$63.79

the minimum point of its range less than 100 BPD. No pump can do this efficiently. However, any pump with a rising head curve to the left, if built to handle the resulting downthrust and provided the motor can be kept cool with the low production rate, could meet the expectations of this production range. Better results can most likely be obtained by using two different pumps that better fit the ranges over time as the well declines; for example, a pump that starts out at 700 BPD and which is replaced one year later at the point where the production rate has fallen to just under 300 BPD. At this point it is replaced with a smaller pump that has a maximum operating rate of 300 BPD. This situation is even more severe in plays where the initial rate for most wells is much higher. ESP application with declining rates is the subject of a chapter found later in this book.

Both the perception that ESPs cannot work at very low rates and the possible need for equipment change, as well as equipment reliability in some of the harsher conditions found in unconventional plays have led many operators to disregard ESPs as an ALS solution for their wells or, as we have observed in many situations, the ESP is used for the initial high-production phase of the well. When the ESP fails or produces at the lower end of its range, it is replaced by another ALS, usually a rod pump.

Baker Hughes artificial lift systems' initiative, ProductionWave™ flexible production solution, is a concentrated effort to lead the industry's artificial lift systems with ESPs, particularly employing the new FLEXPump™ 3.2, which has a good low-end range and is able to manage solids and gas somewhat better than typical small rate radial stages. The demonstrated performance of the FLEXPump3.2 may discourage operators from automatically switching to rod pumps when production rates drop below a certain point (the point the operator deems to be the transition point and is not the same for all operators) and also replacing those rod pumps (or other artificial lift system) that develop problems in the shale play well conditions and/or are not cost effective when compared to a good ESP run. ProductionWave solution, however, is much more than just a better pump. A range of equipment, services, and commercial models cover the operator's full production needs over a long period of time and one hopes the whole production life of the unconventional play oil well.

19.3 Summary of Application Issues

The general issues give an idea of the trials awaiting the ESP application engineer charged with making this artificial lift system work in shale plays.

Apart from some exceptions, the shale plays are deep, which requires long pumps with many stages. If the casing size is small, the pump diameter has to be small, and because small diameter pumps generate low lift per stage, more stages (pump length) are required. A long motor may be required to drive the long pump.

The long motor, coupled with the buildup curve required to get the well to go horizontal, means the pump intake is set a substantial distance from the lowest spot in the well. This becomes an issue when the well needs to be drawn down as much as possible to get production.

The previous paragraph brings up the issue of the buildup curve. Electrical submersible pumps do not like to be bent and must be set in a straight section of casing. They cannot

be operated in a bind causing fatigue failures to occur in the shafts after a few days or weeks.

As mentioned earlier, most shale plays are deep and produce gas along with oil in the best of cases. A deep formation usually means high bottomhole temperature (BHT), which affects ESP equipment. If the wells produce gas, we have the issue of managing the gas to where the pump does not gas lock and a secondary effect regarding temperature, as gas has very little specific heat and does not contribute much to cooling the motor. Horizontal wells also have an inherent complication regarding gas, as they are usually not perfectly horizontal and have small or gradual hills and valleys. The hills are notorious collectors of gas. As production accumulates, gas slugs move horizontally until they get to the heel or the vertical portion of the well, where the ESP system sees the slug and tends to gas lock.

Further complicating ESP applications, shale completed wells are hydraulically fractured using proppants like sand. Initial well production may have a large content of fracture sand which diminishes over time. However, the pump will see some sand in the early stages of production and must be able to handle this sand without serious damage. Fracturing opens artificial paths within the rock to gather the oil from the pores. These fractured cracks spread out a given distance from the wellbore. When getting further and further away from the wellbore, the density of the cracks in the rocks falls away and the inflow from the surrounding rock slows down. As production from the well empties out the reservoir volume located closest to the wellbore, the well will see a gradual production decline. The initial decline is quite severe, and the decline curve turns asymptotically toward a very low number. This decline typically happens over a few months. Typically, after only one year, a well completed in a shale rock has its production decline by 60 to 75%. The ESP installed in this well must be able to handle this decline acceptably.

As all ESP operators and suppliers know, the issues with application can be very complicated given the multiplicity of components in the ESP system. Thus, apart from the problems mentioned above, others can be pressure-related or chemically related issues that affect solids precipitation, incrustations, and corrosion on the materials used to build the ESP components.

In the following sections of this chapter, all the issues affecting ESP application are independently analyzed and solutions are provided for each problem or challenge. However, there are always multiple challenges at any given time, and some solutions may not solve a given issue when others are present. Complex and multiple issues also are addressed.

All unconventional plays are not consistent and are dissimilar one to another. Just as with conventional ESP installations, every well is like a fingerprint and needs to be analyzed on its own. Feedback from reliability over time (as inevitable failures occur) is an important tool for equipment sizing.

19.3.1 Well Design

The secret of success in unconventional oil shale plays is the long reach horizontal well.

Fig. 19.2 is an example of a specific pad configuration in which the wells are fit into units made up of two sections each (2 x 640 acres), on both sides of the single drilling pad, which is also the area where the wellheads will be located. Some of these wells can be drilled in very large numbers to cover a very large surface and volume down in the formation.

These are expensive wells where to address drilling costs (getting more well in the shale play, i.e., the horizontal section, per linear foot drilled) make it beneficial for the operator to drill a well that has as short as possible curved section and as long as possible a horizontal section or branch, lying within

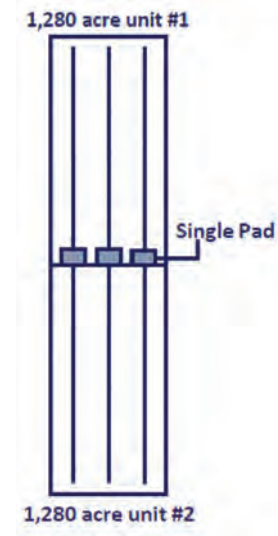

Fig. 19.2—Layout of horizontal wells in shale plays.

the oil or gas bearing shale. A curved section is a buildup section, starting at the kick-off point or KOP. A gradual buildup after the kick-off point means a longer unproductive section of the well and a shorter horizontal section. The horizontal section will usually be drilled with a smaller bit and will remain uncased or cased with a smaller tube size than the vertical section of the well. The smaller section, the liner, starts at a liner hanger that may be set in the vertical section of the well or may lie after the horizontal section has started. However, we have not seen many operators do this.

Limitations imposed by mineral rights and legal aspects usually related to mineral rights issues, as well as drilling costs (getting more well in the shale play, i.e., the horizontal section, per linear foot drilled), make it beneficial for the operator to drill a well that has as short as possible curved section and as long as possible horizontal section or branch, lying within the oil or gas bearing shale. A curved section is a buildup section, starting at the kick-off point or KOP. A gradual buildup after the kick-off point means a longer unproductive section of the well and a shorter horizontal section. The horizontal section will usually be drilled with a smaller bit and will remain uncased or cased with a smaller tube size than the vertical section of the well. The smaller section, the liner, starts at a liner hanger that may be set in the vertical section of the well or may lie after the horizontal section has started. However, we have not seen many operators do this.

Modern drilling technology such as drilling motors and steering systems allow for a fairly quick buildup rate, thus making the curve very short and very sharp. This is discussed in detail in Chapter 15. This type of curve allows for fluids to flow without problems but makes it difficult to run any kind of production or repair tool past this section and into the horizontal well. The limit to the radius of the curve (BUR or buildup rate) is dependent on the drilling system and tools. The resulting buildup rate also is affected by unplanned motion of the drill bit, an unexpected detour that can be caused by hard or soft spots in the rock and/or by tool malfunction. For this reason, wells with good profiles but with occasional doglegs can exceed what ESP installers would be comfortable with (in excess of 12°/100 ft. and frequently exceed 15°/100 ft.).

The objective of installing an ESP in the horizontal section is to get the maximum submergence possible when the well is drawn down as far as possible. An example is a horizontal well drilled with a buildup rate of only 3°/100 ft. and the ESP unit is set in the bottom of the vertical section, i.e., just above the kick-off point. The distance drilled to get to the horizontal position from kick-off point is a quarter circle with a length of 90/3*100 ft. = 3,000 ft. The radius of this quarter circle, the vertical depth between kick-off point. and the horizontal section is 1,909 ft. If the fluid in the well is fresh water, the pressure differential between these two points is 827 psi. If the length of the motor and seal is increased, it will be a few psi more. Many wells drilled in shale plays decline quickly and have a flowing bottomhole pressure (FBHP) of less than this. Consequently, setting in the horizontal would be very desirable. However, an operator does not want to drill 3,000 – 1,909 = 1,091 ft. of extra unproductive well before reaching the target formation. If the buildup rate is a more acceptable 12°/100 ft., the radius becomes 477.5 ft. and the pressure differential is now only 207 psi. In a gassy fluid, the gradient would be much lower and one could easily expect the pressure differential to be somewhere between 10 and 50% of this value. With this tighter curve, the operator can gain almost 1,500 ft. in the horizontal section of the well, i.e., in the target formation for the same drilling work.

As providers of ESP equipment and given this scenario, there are several courses of action:

- An up-front approach (working with drilling services colleagues and/or customers) that will try to ensure the operator drills an ESP-friendly well. This approach depends on the original intentions of the operator and the casing/liner sizes, top of liner, length of vertical and horizontal sections, kick-off point, etc. The intention is to convince the operator to consider looking at the benefits of laying the ESP unit in the horizontal section of the well, with the increased production this would provide versus a quicker buildup rate and having to hang the ESP unit in the vertical section of the well. The economics of increased production will follow a curve as shown further below in **Fig. 19.3**, and even provide a better long-term recovery (**Fig. 19.4**). The second issue related to the well design is the small diameter liner or open hole completion that is chosen for the horizontal section, particularly where the liner will start. Operators are running the liner hanger in the vertical section of the well above the kick-off point, thus severely limiting the option for running an ESP in the horizontal section as the ESP will have to be of a smaller series and may be subjected to additional stresses when going around the curve in cases where this is possible. The ideal solution for an ESP is a moderate buildup rate below the kick-off point and a liner installed after drilling the well horizontally a few hundred feet, to fit the ESP unit in the larger, horizontal section at the heel of the well.

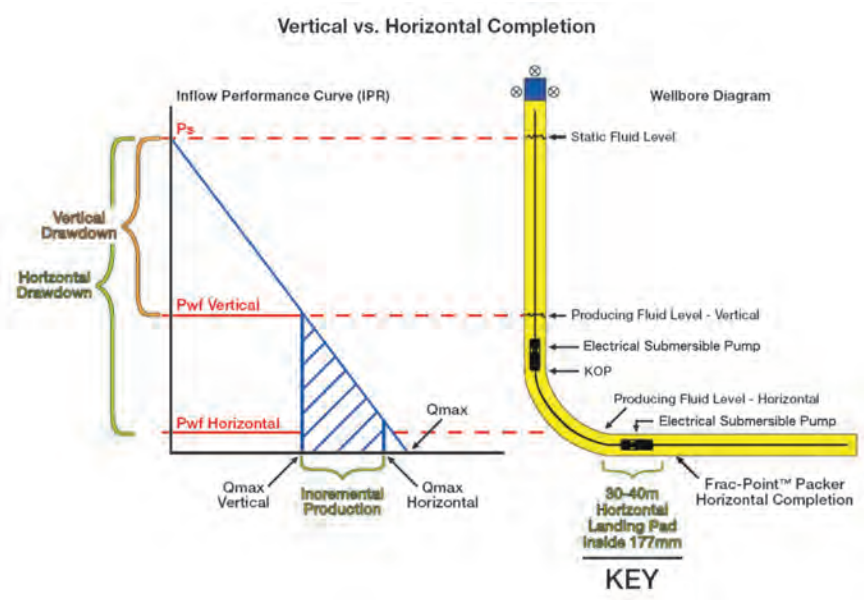

Fig. 19.3—Incremental production with ESP in the horizontal section of the well.

- Once the well has been drilled, the operator should look at the well profile and the existing casing and liner dimensions and buildup ratios, as well as other dogleg severities (DLS) if present, to see if setting the ESP in the horizontal section is a possibility. If so, the potential ease or difficulty in doing so determines the risk of success or failure and a cost/benefit analysis with the customer (now incorporating the risk of damage to the ESP unit) so that a decision can be reached regarding the course of action. This section covers the determination of stresses within the ESP materials using AutographPC™ software ASAP option to decide whether equipment can be safely run in a given case, along with discussion on changes and improvements to be made to the ESP unit to make it able to negotiate substantial buildup rates in the casing curvature. The AutographPC software ASAP option can be downloaded from the Baker Hughes website and the license can be obtained by filling out a form.
- There is an argument in favor of doing just the opposite. That is to drill the well with the sharpest turn to horizontal possible thus making the vertical section closer to the horizontal section. In this case the ESP unit is close to the deepest possible position, for example lying in the horizontal section, without the risks involved in running the unit through a tight casing curvature. Add to this the possibility of running a bottom intake pump. The pump intake pressure (PIP) is close to the value attainable with horizontal setting. A supporting argument for this is if the gas content in the fluid is high, the fluid gradient is low and the pressure that can be gained from increasing submergence by a few feet is small (**Table 19.3**). The graphic production analysis in **Fig. 19.4** changes substantially as the PIP increment is greater or smaller.
- There is one additional option for setting the ESP in between the vertical and the horizontal sections of the well. The operator drills a tangent section, typically at an angle varying between 45° and 85°. There are some advantages to this, especially considering that some ESP units may not have to be very long and, therefore, the tangent section need not be either. There is a benefit in handling gas, as the incline assists in separating the gaseous and liquid phases by gravity, especially in low flow regimes that may approach a laminar regimen. It also may provide a benefit in preventing in rushing of fracturing sand into the pump and/or obstructing the annular space between ESP motor and casing/liner. This approach, however, does not resolve the issue of the need to drill more well before the horizontal section is reached, unless a sharp angle (~85°) allows for penetration in the production zone or a more relaxed mineral issue exists. Numerous operators in the Mississippi Chat and Lime are testing this well design.

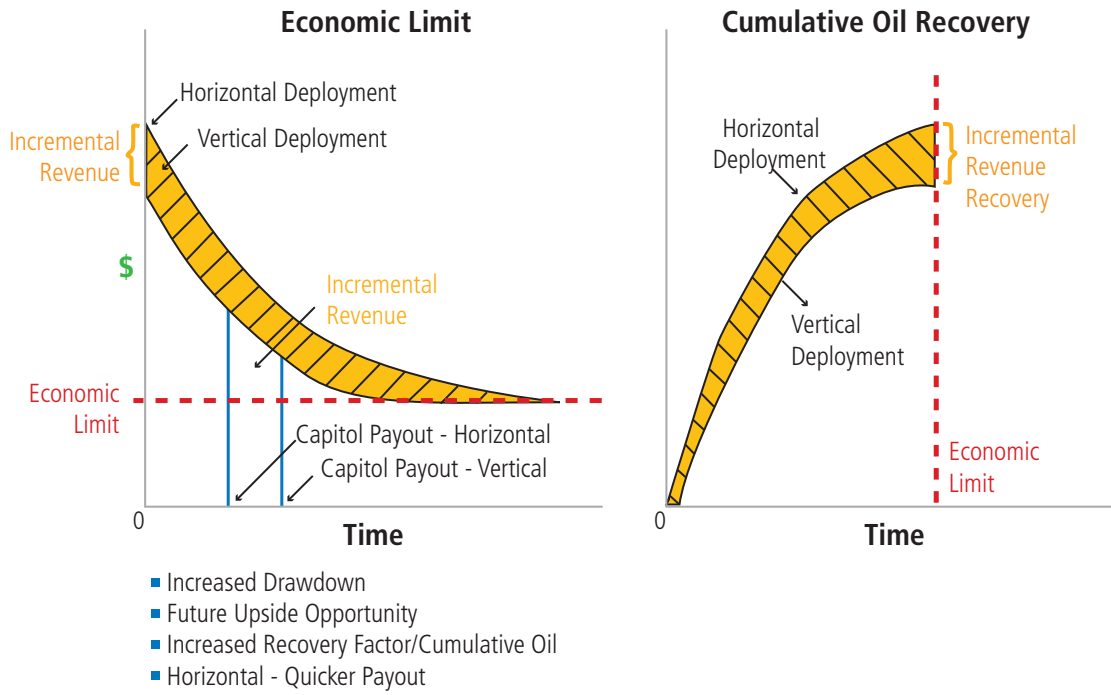

Fig. 19.4—Incremental reservoir recovery with ESP in the horizontal section of the well.

19.3.1.1 Standard Practice for Unconventional and Shale Well Buildup Rate

The standard buildup rates used in the Bakken, for example, vary between 8 to 12°/100 ft. The average target is in the middle (10°/100 ft.), and maximum buildups have usually been limited to 15°/100 ft. Caution: planning more gradual buildup rates may end up with sharper doglegs.

Drilling Services' AutoTrak™ system with measure while drilling and logging while drilling tools, will typically drill 30 ft. and obtain a survey point, adjust if necessary, and drill another 30 ft., repeating the survey. After a 90 ft. section is drilled they typically come back out, do a back-reaming operation, and clean out the last 90 ft. drilled. This process ensures a clean wellbore and a smooth buildup rate. When casing is later installed the micro-kinks (for lack of a better word) are ironed out and ESP installers can almost guarantee that the buildup rate is good for running in the ESP unit.

When installing ESPs in shale plays, proper selection of materials for heads, bases, and flange bolts, and good

Table 19.3—Small pressure (PIP) gain when installing in horizontal when fluid s.g. (gassy) is low.

ΔPIP Between Above KOP and in Horizontal Well Section as Function of Build-Up Rate and SP. GR.										
B.U.R.	SP. GR. OF MIX (BELOW MOTOR)									
	0.8	0.7	0.6	0.5	0.4	0.3	0.2	0.15	0.12	0.1
3	661.6	578.9	496.2	413.5	330.8	248.1	165.4	124.0	99.2	82.7
6	330.8	289.4	248.1	206.7	165.4	124.0	82.7	62.0	49.6	41.3
8	248.1	217.1	186.1	155.1	124.0	93.0	62.0	46.5	37.2	31.0
10	198.5	173.7	148.9	124.0	99.2	74.4	49.6	37.2	29.8	24.8
12	165.4	144.7	124.0	103.4	82.7	62.0	41.3	31.0	24.8	20.7
14	141.8	124.0	106.3	88.6	70.9	53.2	35.4	26.6	21.3	17.7
16	124.0	108.5	93.0	77.5	62.0	46.5	31.0	23.6	18.6	15.5
20	99.2	86.8	74.4	62.0	49.6	37.2	24.8	18.6	14.9	12.4
25	79.4	69.5	59.5	49.6	39.7	29.8	19.8	14.9	11.9	9.9

installation practices, should almost guarantee success in running through the vertical to horizontal buildup rate when drilled with Baker Hughes and other top-rate drilling services and staying within the 8 to 12°/100 ft. buildup rate.

A problem harder to overcome is the operators' choice of running smaller liners in shale play wells and hanging these liners in the bottom of the vertical section of the well. Although a slimline unit can be installed in a typical 4-1/2 in. liner provided it is not too heavy, it is a tighter fit. Running through the deviation or the buildup rate is harder to do.

If smaller liners are used (rare) it will not be possible to run an ESP into this section of the well. If the ESP is installed in the horizontal section, though, it creates other problems in regard to handling gas and solids production.

19.3.1.2 Running ESPs through Deviated Well Sections

Oil wells come in many shapes and forms, and the resulting well track may have many types of deviations, either caused by poor drilling techniques and/or tools, or simply because geological impediments require a complicated well profile. So, whether they are intentional or not, sharp curves or doglegs are common in oil wells. ESP equipment components are best suited for straight well sections, both for traveling through them on the way to the designated pump setting depth (PSD) and the section of the well in which the ESP unit will be permanently set. Depending on the size of the casing, the ESP components, and the materials used for manufacturing the ESP unit, the unit is capable of getting through more or less severe doglegs in transit to pump setting depth. However, once at the permanent setting depth, the well section must be relatively straight.

19.3.1.3 Running through Doglegs or Buildups

Parts of the ESP assembly are particularly sensitive to deviation such as the motor lead cable, the pothead insertion point, and the smaller diameter necks of the motor, pump, and seal sections.

When turning into a dogleg or buildup to an intentionally deviated/horizontal section of the well, if the cable and/or the pothead sit on the top of the assembly, they will typically suffer compression combined with scraping. This also depends on the inside diameter of the casing and the casing joint connections. One fortunate occurrence is that if the equipment is run in slowly at the point of deviation, the forces acting on the unit try to turn it slightly so the cable or pothead rest to one side and damage is avoided. Therefore a probability usually somewhat greater than 50% governs success with the cable installation in the deviated well.

The equipment section necks (reduced diameter so that flanges can be bolted together) are affected by a different situation. They cannot turn in any beneficial direction, so if they are flexed beyond the elastic limit, they suffer permanent deformation. Permanent deformation of this type leads to the shaft in the section (pump, seal, or motor) operating in a bind and generally failing after a short period of time due to fatigue, with the typical conical breakage to show for it. A typical shaft fatigue failure occurs in a 90- to 120-day period.

A smaller diameter unit passes through a larger casing size with less deviation than a similar unit with a larger OD, so the possible combinations of casing and equipment size are many. Tables have been prepared as guidelines for successful installation through a deviation, but the use of the AutographPC™ software deviated well tool (ASAP) is a good way to determine if material stresses will exceed elastic limits. The ASAP tool can be tedious to operate and requires some experience to correctly set up the specific case and interpret the results.

The problem of running through tighter doglegs and buildup rates will be resolved with the new FLEXlift Curve system, which is in the process of being launched commercially by the time this book is published (2015).

19.3.1.4 Using ASAP

This software tool takes into consideration the length of all the ESP components, well angle, dogleg severities (same for buildup rates), and casing and tubing dimensions. An option is available for the design to take into consideration tubing effect and equipment weight. **Fig. 19.5** shows the main ASAP screen with the equipment fit in the casing. Although the screen displays the equipment in a horizontal position, calculations involving weight are made for whatever the

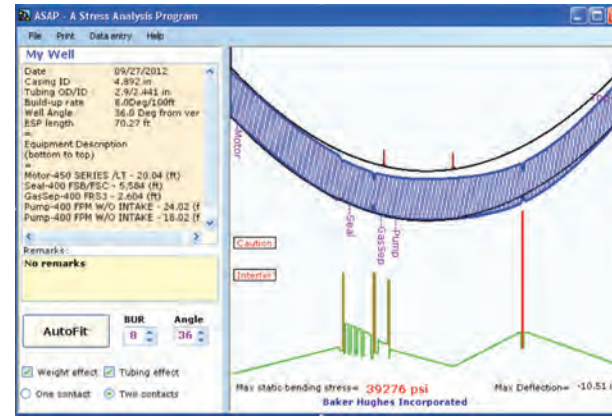

Fig. 19.5—AutographPC software ASAP screen.

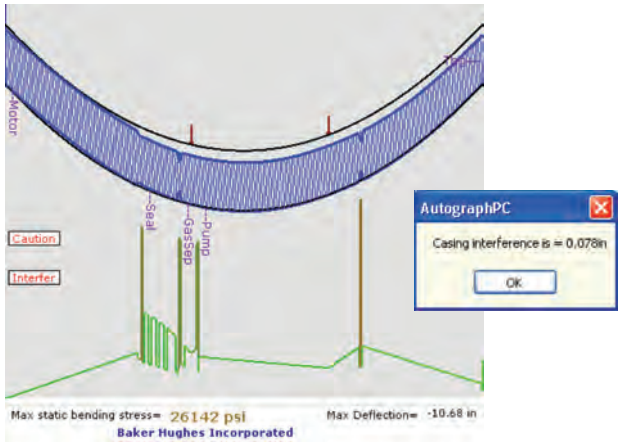

Fig. 19.6—ASAP maximum stress and casing interference.

true angle in the well is and input in the data entry screen. However, the display is always horizontal. As the angle is changed, the stress calculations change, but not the layout diagram. An AutoFit button makes a first attempt to fit the unit in the casing with a single point contact approach. If this is not possible, a dialog box gives the option of a two-point fit.

Published guidelines indicate that the acceptable stress limits are in the order of 24 to 25 kpsi for immediate acceptance of the design, whereas, 44 to 46 kpsi results require extra care such as review of design, installing with special precautions. Anything exceeding this stress limit requires product engineering support while stress limits between 26 to 43 psi require further data review.

Fig. 19.6 shows a section of the ASAP screen. Two notes in the lower section indicate the maximum stress for this example (26,142 psi) and maximum equipment deflection (-10.68 in.). However, there is also a caution box and an interference box. When clicking these boxes with the cursor, a warning comes up indicating that the stress exceeds 25,000 psi. In this example the casing interference is 0.078 in.

The latest version of the ASAP subroutine makes an accurate attempt at two point contact fit. If there is no fit, a dialog box tells the application engineer that the fit solution may require a three-point contact analysis, which ASAP is not automated. The dialog box tells the application engineer to try to fit the equipment manually by clicking on the graph and moving the contact points. Every time a contact point is moved, a new bending stress comes up and the figure changes. However, it is difficult to get a good fit, and multiple attempts may have to be made. The dialog box recommends reducing the well angle until the equipment fits in the casing. This makes sense because although the stresses indicated in ASAP are calculated, they are based on the deviations shown in the diagram. The diagram allows the equipment to lie outside the physical limits of the casing. So, by changing the angle of the well, the calculation does not create an unrealistic solution.

The interference box appears until the unit can be fit entirely into the casing. Experience indicates that if the interference shown is less than 0.5 in., it can be ignored. The problem can be considered as solved provided the stresses are at levels that can be handled either with conventional equipment or with the precautions indicated above and further in the text. This is an advantage as the interference box is hard to eliminate.

The American Petroleum Institute (API) published guidelines regarding deviated wells (API Recommended Practice–RP11S3. API 1999). This recommended practice is conservative, setting a BUR/DLS of 6°/100 ft. as a safe limit and indicating that deviations above this and up to 10°/100 ft. require special attention and precautions such as well cleanout, running a dummy unit of similar dimensions. The stress values indicated above are included in API's RP11S3.

The bottom line is that when deviation exceeds certain limits, ASAP may or may not be accurate in determining if the unit will suffer permanent deformation and an element of risk will have to be accepted. When confronted with these extreme cases, discuss with the operator and reach some agreement on how to handle the risk, including sharing the risk from an economic standpoint.

It is important to note that some application engineers, customer account managers, and operators provide extreme examples of lucky installs. An operator may say, "I was able to run an ESP through a 17°/100 ft. dogleg and the unit worked fine." These are not the norm and cannot be expected to be repeated routinely.

The ESP unit must be set in a straight section of the casing, regardless of the angle of inclination. The ESP unit can operate at any inclination from 0° to 90° and has operated at a slightly negative angle. ESPs can operate in an inverted position, typically for injection applications. But for this case or for high-negative angles, major modifications must be made to the equipment. A straight section is a section with no doglegs and with a maximum deviation of 1-1/2° to 2°/100 ft.

Beyond a certain length of the ESP unit, there is no change to the bending imposed on the unit. This issue is not yet fully understood. The doubts come from the fact that is it not the housing that is the weak point but, as mentioned earlier, it

is the smaller diameter necks at the base of the equipment sections, where the flanges are bolted onto the section below. A well-by-well analysis using ASAP should be carried out whenever possible to ensure a better chance of success. Also, if the buildup rates exceed 8°/100 ft., a dummy unit can be installed to determine if there will be tight spots. Protectors need to be installed to prevent damage to the pothead and the motor lead cable.

Fortunately for ESP manufacturers, the usual buildup rates pursued by operators are in the 8° to 12°/100 ft. range.

These buildup rates are easily managed by taking the right precautions such as equipment modifications and field service procedures. The latter are not the subject of this chapter but are included due to the importance of the subject and the need for the application engineer to be aware and to make all others involved aware of these changes and operational requirements.

Precautions when installing an ESP in a deviated well and a well with doglegs:

1. Make sure the information regarding the location of deviations or doglegs is accurate. Obtain a survey.

2. Run ASAP with the best information regarding dogleg severity and accurate description of ESP equipment, casing, and tubing.

3. If stresses do not exceed 25 kpsi, equipment can be standard, but installation precautions still apply.

4. If stress exceeds 25 kpsi but is below 44 kpsi, the ESP equipment should be built with materials stronger than low carbon steel (LCS). A standard corrosion resistant unit with AISI 460 stainless steel heads and bases, ferritic housings, and Monel® bolts is rated to withstand these levels of mechanical stress. The heads and bases when bent going through a dogleg put a lot of stress on the flanges and thus the bolts holding them together, therefore the need for Monel® bolts.

5. The motor lead cable (MLE) and pothead need to be protected when going through doglegs. The use of a pothead protector (V-type or walrus tooth protectors) is recommended and/or use of centralizing protectors located at the necks of the section connections (protectolizers) contribute significantly to prevent squashing the motor lead cable.

6. The motor lead cable to the power cable splice, and the lower end of the power cable (the section of power cable that goes through the doglegs and/or lies below the casing kick-off point) should be equipped with cable protectors. There are many types of these protectors, usually placed at the tubing couplings (cross-coupling cable protectors) and there are many manufacturers in different parts of the world.

7. The next issue to take care of is the installation process itself. The ESP unit can be run in the hole at the usual speed of installation until the first dogleg or the kick-off point is approached. Slow the speed significantly as the whole length of the ESP up to the power cable to motor lead cable splice goes though the deviation. The speed of running in equipment should still be kept slower after this as the power cable is still at some risk. If other doglegs are encountered below the first, or the kick-off point, reduce the speed again. During this part of the installation, the cable integrity should be checked frequently from the surface.

19.3.2 Fluid-Related Challenges

Excessive gas and production and scale depositions can severely impact the reliability of ESP systems and degrade the efficiency of the lift mechanism. Technologies have been developed to make ESPs more resistant to abrasion caused by sand production and fluid-related challenges such as gas production.

19.3.2.1 Sand and Abrasives—Fracturing Sand (Proppants)

ESPs have, over time, become a viable choice for artificial lift systems (ALS). As any of the original design problems have been improved upon, with both operators and suppliers devoting considerable time and funds for research, they now are a good choice for wells drilled in emerging new oil plays.

The following are guidelines for operating ESPs in wells that will be subject to fracturing sand production (whether drilled in shale plays or other types of reservoirs) covering techniques and diverse types of equipment available today to reduce the impact of fracturing sand as it moves through the pump, and remedial action that may extend the life of installations in the wellbore.

Fracturing sand and other types of sand hurt ESP equipment over time. There are no two ways about this. But in the right conditions and with the right equipment, fracturing sand can be:

- Avoided
- Separated
- Handled

19.3.2.1.1 Avoiding Fracturing Sand

The intent of using fracturing sand is to keep this sand in the formation and maintain its proppant function. Excess sand injected in the formation returns with production. How much of it returns depends on the success of the fracturing operation including selection of the right type of sand, injection pressures, injection rates, and the volume of fluids and correct additives.

To maintain the fracturing sand in the formation: The addition of resins (resin-coated sand) improves retention of the sand in the formation. Resin-coated sand is more costly than uncoated sand. Although it may not apply to all fracturing jobs, it is in most cases a cost-effective solution.

Return of fracturing sand can be avoided in the same manner as unconsolidated or sedimentary sands are kept in check by means of gravel packing or screening. These techniques add cost to the completion and may contribute to plugging, so operators would rather see the sand go away. An intermediate solution is to let most of the sand out with initial high production. Then, when sand production has decreased substantially, a permanent screen can be installed. This is not a good practice if the well is to be fractured again. Baker Hughes offers different solutions for sand control, be it for cased holes (screens) or open holes (expandable screens, GeoFORM™ technology, etc.).

The use of a sacrificial ESP or other type of artificial lift system can clean out most of the initial flow of fracturing sand, leaving a smaller amount of sand that steadily decreases in amount and may be handled by means of abrasion resistant ESPs.

Using a jet pump is a common method for cleaning out wells. These are low-cost downhole pumps; however, this type of AL requires a source of power fluid at the surface and a bottom hole assembly that must be installed and retrieved.

Fracturing sand may not be the only sand encountered in shale play wells. Some shale formations are found between sedimentary stratifications that may be traversed by the well profile during the drilling operation. In these cases, returns from the wells may include both fracturing sand and conventional sedimentary sand and either may continue to appear in the produced fluid long after well production is initiated.

19.3.2.1.2 Separating Fracturing Sand

Multiple desander products are available for installation below the pumping system to prevent sand from entering the pump.

Fig. 19.7a shows a typical desander attached to the bottom of an ESP motor. A pack off on the desander forces the well fluid into the sub where an auger gives the fluid a spinning motion, separating the heavier sand particles, which are allowed to drop into the rathole of the well or are collected at the bottom of the desander body.

Fig. 19.7b and **Fig. 19.7c** show screens such as the Baker Oil Tools EXCLUDER 2000™ sand screen, which can be screwed onto a standard motor shroud or hung from a joint of tubing, off the bottom of the motor, and packed off against the casing.

Desanders and screens are selected based on fracturing sand particle size, production rates, and amounts of sand expected to be produced.

These systems are of relatively low cost but require the well to be cleaned out over time as sand collects in the well unless collecting sand in the desander body,

For well cleanouts, Baker Hughes offers products and services through Coiled Tubing Services, such as the Sand-Vac™ cleanout system, with a low profile tool that can in special circumstances run simultaneously with other downhole equipment and tools.

19.3.2.1.3 Handling Fracturing Sand

Handling the sand translates to producing fracturing sand through the pump. This requires making the pump resistant to wear caused by fracturing sand and making it somewhat immune to plugging.

To do this, the pump must be designed to meet the following criteria as described in the following paragraphs.

Abrasion Resistant Bearings

Notwithstanding any benefits that may be obtained by speed control, the surfaces of the bearing areas inevitably are subjected to wear. Bearing surfaces must be manufactured with hard materials such as tungsten carbide (WC), a material, which is harder than the hardest component found in sands (SiO_2 quartz).

Hardened Wetted Surfaces

The bearings are the first areas to go when dealing with wear, but time also causes all surfaces that come into contact with well fluids to erode. The harder the surface, the longer the pumps will last. Pump stage materials have defaulted to NiResist Type I alloys for a long time. This material is a relatively good abrasion and corrosion resistant material and has the advantage that it can be coated. Many types of coatings have been applied to pump stages to handle wear and different types of incrustations and deposition. The best coatings for stage surface hardening have been nickel-based coatings. Different types of nickel coatings can be applied either by electroplating or chemical deposition and thus achieve a uniform coating over the whole surface. Coatings are covered in a separate section.

Large Vane Openings to Let the Sand through without Plugging

The smaller the rate required of an ESP, the smaller the vane openings usually are. This is a natural law affecting the geometry of centrifugal pump impeller design in general. One way to get around this is to select a larger pump than what is necessary for the required flow rate and use the Affinity Laws by running the pump at a slow speed (frequency). This entails an additional cost because the pump is more expensive than a smaller pump operating at the normal frequency of 60 Hz. However, two advantages are obtained: the larger vane openings and a reduced rate of wear, as abrasion/erosion induced wear is a function of the relative speed of surfaces in the erosion process to the fourth power.

This last statement is of significance. A simple example gives a better idea of the importance of speed.

If wear is considered to be 100% at 60Hz,

At 55 Hz, wear will be 70.7%

At 50 Hz, wear will be 48.2%

At 45 Hz, wear will be 31.6%

So a 25% reduction in speed yields a 68.4% reduction in wear.

Criterion for Selecting Abrasion Resistant Protection Level

In 1994, Baker Hughes developed a criterion for determining what level of protection should be incorporated in a pump as a result of analyzing sand samples from a field or well. The objective was to prevent early equipment failures due to pump wear, particularly when ESPs were to be used in an operator's field for first time.

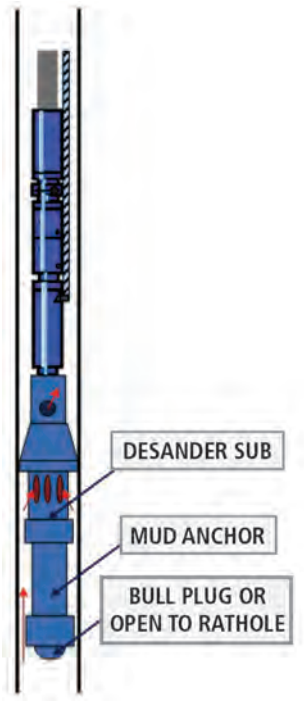

Fig. 19.7a—Cyclonic desander.

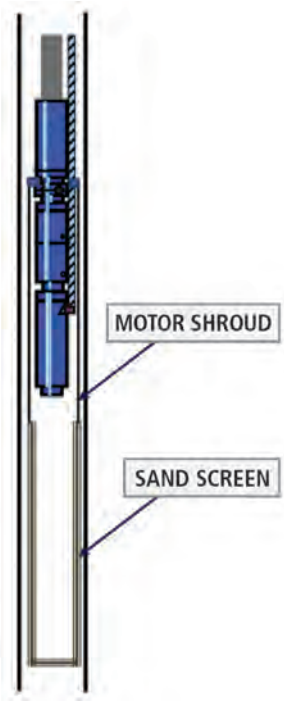

Fig. 19.7b—Sand screen with shroud.

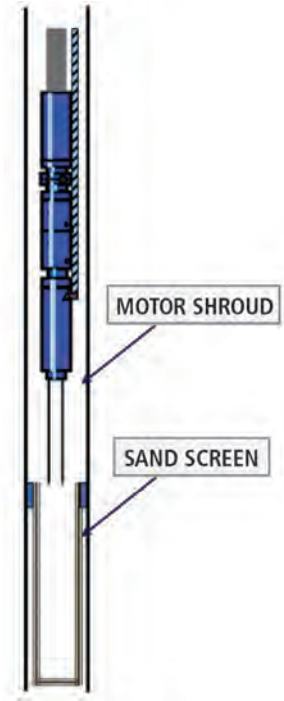

Fig. 19.7c—Sand screen with casing packoff.

The criterion resulted in the material recommendation index (MRI). The index was calculated using an empirical formula using sample characteristics easily tested in a basic laboratory set up for this purpose.

The MRI system is a starting point. Adding or removing levels of protection over time would give the optimal and cost effective protection level for the specific environment. The MRI is explained in detail at the end of this section.

When these solutions are put into place, separately or in some combination, a viable ESP for sandy and fractured shale play applications is in play. However, one item remains to be taken care of: sand fallback.

19.3.2.1.4 Sand Fallback

Sand fallback occurs when an ESP that has been producing for a while is stopped, for whatever reason, and the fluid in the production tubing falls back into the wellbore, going through the pump. If the amount of sand is large enough, it can completely plug the top end of the pump and may prevent the unit from being able to start again or to produce flow up the tubing again. In any case, it contributes to additional wear in the pump's top stages.

Fallback can be avoided by using one or more check valves in the production tubing. The check valve holds the fluid in the column and the fracturing sand collects on top of the valve. If the amount of sand is excessive or if the well produces gas, the valve may be prevented from reopening when the pump is restarted. Multiple check valves, spaced out along the string, may help to prevent the sand accumulation issue. When gas is the problem, check valves should not be used because the gas has nowhere to go (cannot bubble up) and the gas loaded/gas locked pump is usually not able to produce enough pressure to overcome the long column of liquid sitting above the check valve.

A recent tool development is the diverter valve (**Fig 19.8**). This valve is designed so that ports are opened to the well annulus when production is interrupted as the ESP is turned off or stalls due to a gas locking condition. The change in differential pressure triggers a piston or ball type device that opens ports allowing the fluid in the tubing to fall back into the well, around the ESP assembly. When production is restored, the incremental pressure below the diverter valve closes the ports and allows the fluid to go up the tubing string again.

The diverter valve shown in Fig. 19.8 is manufactured by a third party (RMS-PumpTools). Baker Hughes manufactures its own diverter valve, with models for ESP use and for ESP cavity pumps.

Baker Hughes' ESP diverter valve, called the pressure actuated valve (PAR) (**Fig. 19.9**), is more sensitive to opening and closing (with less flow and differential pressures) and is more compact and a more cost-effective design. Other manufacturers provide diverter valves, such as Zenith Oilfield Technology, Ltd., whose valve is the Auto-Flow Valve.

Diverter valves have been known to get stuck in the open position, which negates production from the ESP. This is a serious condition. Although the cost of the valve is low and repairing may be easier and even more cost effective, it requires pulling the unit out of the well, which is costly and time consuming.

Fig. 19.8—Diverter valve.

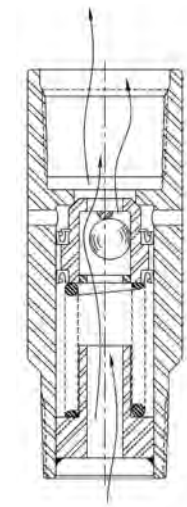

Fig. 19.9—Baker Hughes PAR valve.

19.3.2.1.5 Material Recommendation Index

Many factors go into selecting the proper abrasion resistant (AR) options for an ESP in a particular abrasive environment. Just to say the well makes sand is not adequate information to be able to estimate which options are required. Because all wells are different, specialized designs are needed to fit the application and well economics. This is why Baker Hughes offers a wide range of abrasion resistant pumps.

Electrical submersible pumps are exposed to three types of wear patterns in an abrasive environment (**Fig. 19.10**, **Fig. 19.11**, and **Fig. 19.12**): radial wear in the head and base bushings as well as the stages; up or downthrust wear on the stage's thrust surfaces; and erosive wear in the flow path area of the stages due to the high velocity and abrasiveness of the fluid. This last wear type is generally not a problem because the pump usually wears out from the first or second wear pattern described above.

Several factors must be weighed to make a proper pump configuration determination. The quantity of sand, usually represented by weight/volume (mg/L) or percent, is of obvious concern. However, several other characteristics of the sand are also of major concern. The characteristics that have to be examined when determining the abrasive nature of a particular sample are:

1. Quantity of sand. This is the quantity of produced sand.

2. Acid solubility. This is the percentage of sample not soluble in concentrated acid.

3. Particle size distribution. This is the percentage of sample that will fit within the pump tolerances. The total percent of the sample retained on and passed through a US Standard Sieve No. 100 (ASTM-E11) spec (Tyler equivalent 100 mesh).

4. Quantity of quartz. This is the percentage of the sample that is quartz.

5. Sand geometry. This is the sand grain shape (angularity), determined by microscopic examination. The shapes can be jagged, barbed, or smooth; the sharper the sand, the more aggressive it will be with respect to abrasion.

Use of all of the aforementioned criteria helps in estimating the proper abrasion resistant technology. Baker Hughes can analyze a sand sample to determine the above sand characteristics. Having all of the above information allows Baker Hughes to make the best possible recommendation for a customer's pumping needs.

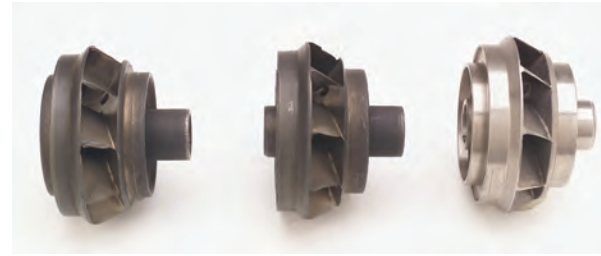

Fig. 19.10—Radial wear.

Fig. 19.11—Downthrust wear.

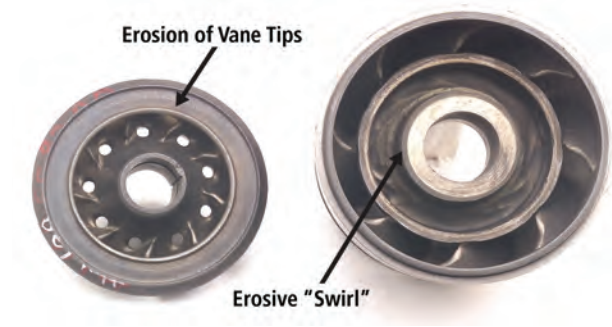

Fig. 19.12—Erosive wear.

The method of predicting abrasive wear is not an exact science and, therefore, nothing substitutes for information on the condition of previously run equipment (ESPs, tubulars, well head, flowline equipment, and previous downhole artificial lift equipment).

To best determine the equipment material needed to reduce a customer's abrasion problems, Baker Hughes has developed the Material Recommendation Index (MRI). This determination is complex but the following formula aids in lessening the complexity.

where:

SAN—Quantity of produced sand. This is represented as mg/L. See the conversion chart below for factors to convert between other units.

(SAN<*>SOL) × (PSD + QTZ + ANG) = MRI

SOL—Percentage of sample not soluble in concentrated acid.

PSD—The percentage of sample that will fit within the pump tolerances. The total percentage of the sample that is retained on and passed through a US Standard Sieve No. 100 (ASTM-E11) spec (Tyler equivalent 100 mesh).

QTZ—The percentage of the sample that is quartz.

ANG—The angularity of the sand grains.

Parameter Values:

SAN:	[mg/L]	Value
	100	See SAN/SOL Graph
	200	
	300	
	400	
	500	
	600	

SOL:	% Non-acid Soluble Material (Determined analytically)	Value
	0-100	See SAN/SOL Graph (Fig. 19.13)

PSD:	% of Particles that fit within Pump Tolerances[1]	Value
	0-25	1
	26-50	2
	51-75	3
	76-100	4

[1] Total percentage retained on and passing through a US Standard Sieve No. 100; Tyler equivalent 100 mesh.

QTZ:	% Quartz in Sample	Value
	0-25	1
	26-50	2
	51-75	3
	76-100	4

ANG:	Angularity	Value
	Smooth	1
	Moderate	2
	Sharp	3

The aggressive nature of sand can be defined as mild, moderate, or aggressive. These quantities are determined by adding the PSD, QTZ, and ANG.

Mild	3-5
Moderate	6-8
Aggressive	9-11

Conversion Chart

To Convert From	To	Action
mg/L*1	ppm	Multiply by 1.000
ppm	%*2	Multiply by .0001
%*2	ppm	Multiply by 10,000
gal/barrel	%	Divide gallons by 42 then multiply by 100
lbs./barrel	%	Determine mass of fluid in pounds then divide numerator by this number and multiply by 100

For water mg/L = µg/g = mg/Kg = ppm

*1—When fluid density is 1, this is a direct conversion. Otherwise, the density of the fluid has to be taken into consideration or use this number as an approximation.

*2—The % can be weight/weight, volume/volume, or weight/volume. When the percentage is expressed in weight/volume, the density of the fluid needs to be taken into consideration.

MRI Example:

Data	Parameter Value
SAN = mg/L	SAN/SOL Graph
SOL = 100%	SAN/SOL Graph
PSD = 55%	3
QTZ = 60%	3
ANG = MODERATE	2

MRI -> (3.4) * (3 + 3 + 2) = 27.2

Using **Fig. 19.13** and the AR Configuration Recommendation Charts (**Fig. 19.14**), the MRI minimum recommendation falls within the 1:X radial support bearing area ARS.

Table 19.4 shows pump configurations that are available from Baker Hughes that can help slow down the wear process of one or more of the wear types described above.

The advent of the new FlexPump product line has added a new construction option to the existing list above, the hybrid construction. Hybrid is a combination of stabilized severe duty (SSD) with stabilized heavy duty (SHD). Some stages only have a radial support based on the L/D ratio, while being contained in a unit or module that is provided with downthrust support. The only stage type that offers this construction is the FLEXPump10. The reason for this is the low downthrust this stage generates (based on hydraulic design, including a new thrust compensating device which is patent pending). The FLEXPump10 Hybrid is 1:3 radially supported SHD and 1:9 downthrust protected stabilized extreme duty (SXD). An MRI rating has not been determined yet for this configuration.

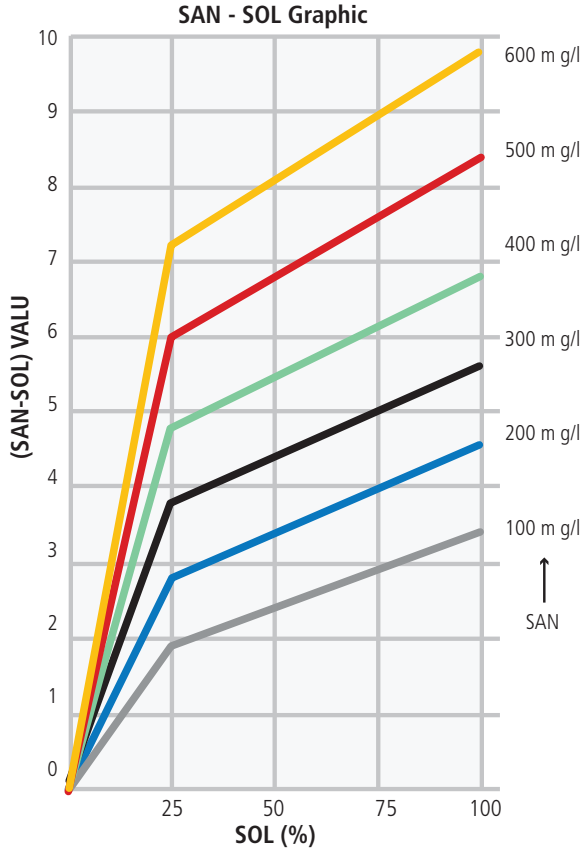

Fig. 19.13—SAN/SOL graph.

An important variable not included in the MRI is the running and pulling economics. If this cost is high, you may want to select a pump model that has increased support over what the MRI number may indicate for a more conservative, higher reliability approach. In the example above, the guideline indicates that the 1:X radial support bearing design is only marginally acceptable for this MRI value. Also, because the sand angularity is high on the moderate ranking, it may be beneficial to upgrade to an ARC or AR configuration for improved run life.

19.3.3 Gas

When the use of ESPs as a viable method of artificial lift became common in the 1960s and 1970s, gas was a big issue and it was believed that ESPs could not handle much more than 10% to 15% free gas at the intake.

The industry has evolved significantly since and the use of gas handling stages, active and passive gas separators, and downhole avoidance completions, space permitting, has made it possible to operate with ESPs in extremely gassy wells.

Obtain good production data and analyze the conditions of the fluid to be pumped. Bubble point pressure must be known and pump intake pressure (PIP), as well as the expected evolution of PIP and possibly fluid properties over time, as an application may be very viable in initial operating conditions. However, as time goes by liquid rates may decrease along with the PIP, and gas rates may increase, rendering the equipment useless for the new downhole conditions.

ESP applications in shale plays are often gassy. Evolution of production in most shale plays indicates that, as productivity decreases, gas production increases, compounding the problem. Adding even further to the gas problem is the presence of gas slugs, which cannot normally be handled by centrifugal pumps. Gas slugs will typically form in horizontal wells, which will inevitably have slight hills and valleys. The gas gradually accumulates in the upper sections (hills) and the liquid in the lower sections. Eventually flow is blocked and the whole slug moves along the horizontal section until it gets to the vertical well and moves up and away. This is a problem seen frequently in shale play applications, as most of the wells are horizontal.

Section 19.8 contains a comprehensive analysis and explanation of gas and its effect on centrifugal pumps, particularly ESPs. Please refer to this section to better understand the various factors that affect pump performance

Table 19.4—AR Pump Configuration and MRI Rating.

Summary of Abrasive Resistance Terminology and MRI					
400P	**New Terminology**	**Old Terminology**	**Radial Support**	**Axial Support**	**MRI Rating**
	Floater	Floater	Ni-Resist Bearing	None	0-12
	SND	"S" plus 1 ARS	3 WC Bearings	None	0-20
	SHD	ARS 1:R	WC Bearings ("R" based on L/D)	None	0-30
	SSD (radial flow)	Sand Pump	WC Bearings (ratio based on L/D)	WC Bearing modules (ratio based on L/D)	0-86
	SSD (mixed flow)	ARM 1:X	WC Bearings ("X" based on L/D or PV)	WC Bearings ("X" based on L/D or PV)	0-86
	SXD (radial flow)	AR 1:1	WC Bearings (ratio based on L/D)	SiC Bearing modules (ratio based on L/D)	0-100
	SXD (mixed flow)	AR 1:1	WC Bearings Throughout	WC Bearings Throughout	0-100
538P	**New Terminology**	**Old Terminology**	**Radial Support**	**Axial Support**	**MRI Rating**
	Floater	Floater	Ni-Resist Bearing	None	0-12
	SND	"S" plus 1 ARS	3 WC Bearings	None	0-20
	SHD	ARS 1:R	WC Bearings ("R" based on L/D)	None	0-30
	SSD (radial flow)	Sand Pump	WC Bearings (ratio based on L/D)	WC Bearing modules (ratio based on L/D)	0-86
	SSD (mixed flow)	ARM 1:X	WC Bearings ("X" based on L/D or PV)	WC Bearings ("X" based on L/D or PV)	0-86
	SXD (radial flow)	AR 1:1	WC Bearings (ratio based on L/D)	SiC Bearing modules (ratio based on L/D)	0-100
	SXD (mixed flow)	AR 1:1	WC Bearings Throughout	WC Bearings Throughout	0-100
562P	**New Terminology**	**Old Terminology**	**Radial Support**	**Axial Support**	**MRI Rating**
	Floater	Floater	Ni-Resist Bearing	None	0-12
	C	Compression	Ni-Resist Bearing	Compression (thrust bearing in seal)	0-20
	SND	"S" plus 1 ARS	3 WC Bearings	None	0-20
	CSND	"CS" plus 1 ARC	3 WC Bearings	Compression (seal's thrust bearing)	0-40
	SHD	ARS 1:R	WC Bearings ("R" based on L/D)	None	0-30
	CSHD	ARC 1:R	WC Bearings ("R" based on L/D)	Compression (thrust bearing in seal)	0-86
	SSD (mixed floor)	ARM 1:X	WC Bearings ("X" based on L/D or PV)	WC Bearings ("X" based on L/D or PV)	0-86
	SXD (mixed floor)	AR 1:1	WC Bearings Throughout	WC Bearings Throughout	0-100
675	**New Terminology**	**Old Terminology**	**Radial Support**	**Axial Support**	**MRI Rating**
	C	C	Ni-Resist Bearing	Compression (thrust bearing in seal)	0-20
	CS	CS	2 WC Bearings	Compression (thrust bearing in seal)	0-30
	CSND	"CS" plus 1 ARC	3 WC Bearings	Compression (thrust bearing in seal)	0-40
	CSHD	ARC 1:R	WC Bearings ("R" based on L/D)	Compression (thrust bearing in seal)	0-86
	SSD	ARM 1:X	WC Bearings ("X" based on L/D or PV)	WC Bearings ("X" based on L/D or PV)	0-86
	SXD	AR 1:1	WC Bearings Throughout	WC Bearings Throughout	0-100

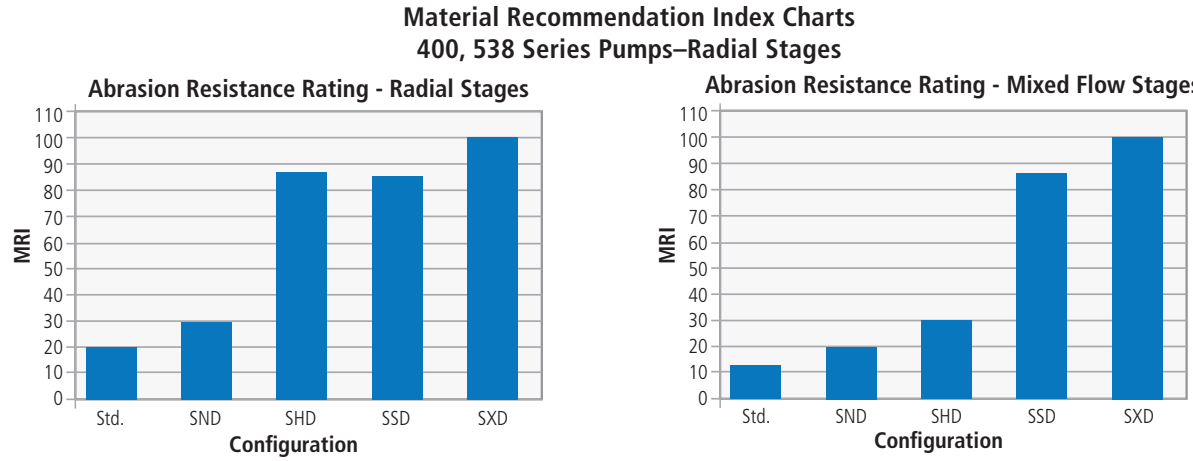

Fig. 19.14—Abrasion resistance MRI charts.

in the presence of large amounts of gas, such as pressure, bubble size, velocity, etc. The section that follows assumes knowledge of these issues.

19.3.3.1 Solutions for Dealing with Gas in Unconventional Plays

The following section covers existing and experimental solutions for dealing with the gas problem. Some of these solutions may be ideal for certain situations but may not be acceptable to the field operators due to cost. Some may require action before the well is drilled; some are after-the-fact solutions.

Dealing with gas in unconventional wells promises to be a complex issue due to other issues. Many solutions for gas handling will have to be combined with others such as handling fracturing sand, setting the ESP unit in the horizontal section of the well, handling decreasing flow rates, etc.

Apart from the difficulties posed by well construction, production in these wells varies significantly due to the evolution of the reservoirs in shale plays. The most typical scenario is an operation starting out with high rates while handling abundant fracturing sand in the fluid and some gas. Over time (relatively short time by normal reservoir evolution) production rates fall quickly, fracturing sand starts fading but gas production tends to rise and be a problem throughout the production cycle.

Due to the logical approach to gas handling (avoiding, then separating, and finally, handling), solutions presented here start with the most expensive.

19.3.3.2 Gas Avoidance

Three types of techniques are used to avoid the gas associated with producing wells. These techniques include drilling a side pocket or sump, creating an artificial sump by use of riser tubes, and a gas avoiding tool.

Drilling a Side Pocket or Sump

When a horizontal well is to be drilled and gas is an obvious problem, one of the ideal solutions is a pocket for collecting the liquid phase (basically creating a sump), while letting the gas bypass the pocket (**Fig. 19.15**). When production rates are relatively low, this solution can almost guarantee that gas will be 100% separated.

The ESP that is run in the side pocket will need to be shrouded to cool the motor. Alternatively, a recirculation tube can be used to achieve the same effect. This solution is similar to running the ESP or other artificial lift system in a rat hole below the perforations, when present. Drilling a lateral sump is, of course, substantially more complicated and expensive than drilling a little deeper in a vertical well to obtain the rat hole. For this reason, few operators accept this solution. Nevertheless, this solution has been attempted numerous times with positive results.

Another caveat in regards to the lateral sump is sand production. If the well is to produce formation sand or fracturing sand, it is likely that sand will accumulate in the sump and negate the advantages of this solution. However, if sand production is temporary, a bridge plug can be placed at the top of the sump during the initial sand-producing phase and removed later.

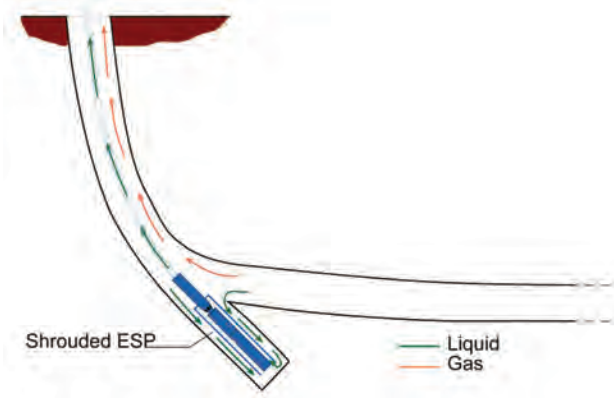

Fig. 19.15—Well with sump.

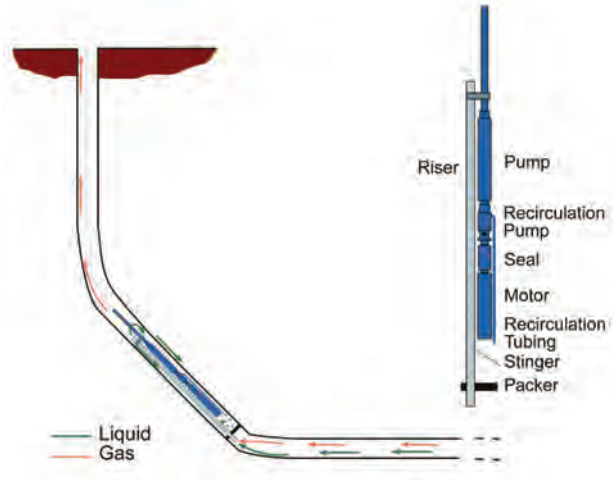

Fig. 19.16—Riser with recirculation pump.

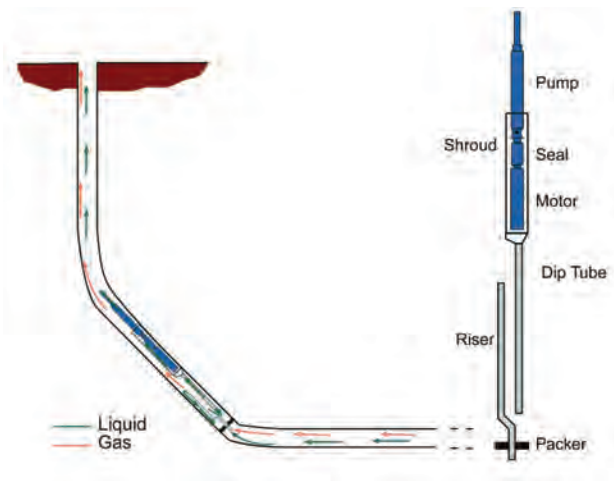

Fig. 19.17—Dip tube.

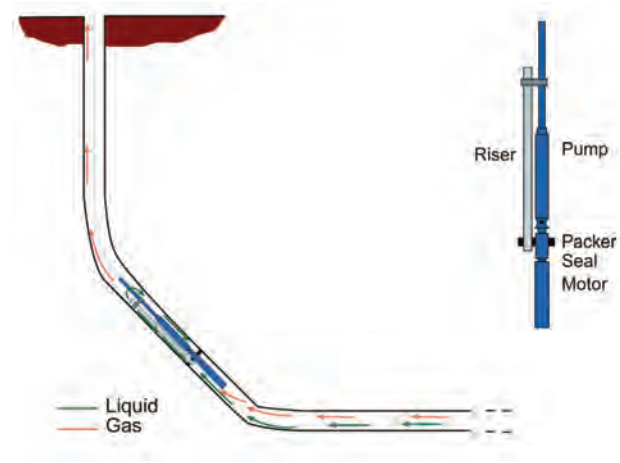

Fig. 19.18—Riser with integrated packer.

The sump can also be cleaned out by any number of means, but well economics determine if this is a practical option. Finally, the pump may be able to produce the sand along with the fluids. This is possible and depends on the sand characteristics and the pump stage vane sizes, material hardness, etc

Artificial Sump Arrangements—Use of Riser Tubes

When drilling a sump becomes impractical, a sump can be created artificially by means of some gas bypassing artifice. The following are some common examples. Note the example ESPs are set in tangent sections. **Fig. 19.16**, **Fig. 19.17**, **Fig. 19.18**, **Fig. 19.19**, and **Fig. 19.20** are all examples of artificial sump arrangements.

A simpler version of the riser with encapsulated pump and dip tube arrangement omits the riser and packer below. The dip tube can be used to draw the fluid from the well from a depth below perforations in conventional oil wells that have no room to install the whole ESP unit below perforations or when liners are present that are too tight for ESP equipment. It has an application in horizontal wells, such as found in unconventional plays. The dip tube can be run down into the tight liner also and provides a gas handling benefit as the tip of the dip tube lies low in the casing, allowing most of the gas to flow on by above the opening.

This gas handling solution has been used many times in conventional wells and with good results. The system has been tried in the Rocky Mountains in unconventional plays.

It is possible to find situations in which the dip tube and the length of the capsule equate to a substantial drop in pressure

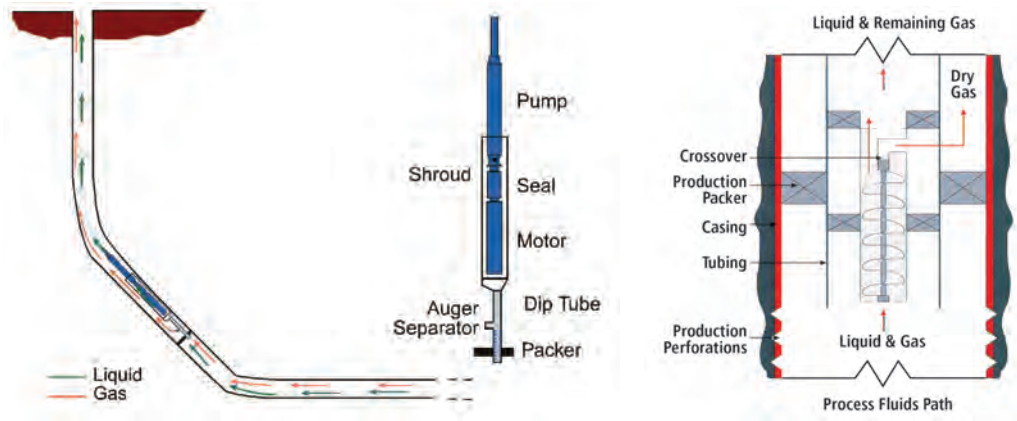

Fig. 19.19—Dip tube and auger combination.

at the pump intake, not only from the intake being higher up in the casing but also from friction loss in the dip tube and in the capsule, especially with long motors. This makes for more gas liberation (the dip tube will most likely only separate part of the gas) so these projects need to be evaluated carefully. A small opening is desirable at the bottom of the dip tube to lie lower in the casing and reduce ingress of gas. However, above the first small tubing joint, the dip tube can have a large OD rising to the capsule. Target flow rates, of course, also influence the choice of tubing sizes.

A gas separator can also be used with this arrangement, if necessary.

Bottom Intake Pump

When a pump is to be set above the liner hanger, keep the pump intake pressure as high as possible to pump the well down in the latter phases of horizontal well production and/or to keep gas in solution. Whether using a dip tube to partially get below the gas or not, use an inverted ESP arrangement, known as a bottom intake pump. The original design was targeted at cavern type oil reservoirs used for storing oil in large volumes, such as might be done by the government with the strategic oil reserves. This approach also can be used in horizontal wells if there is enough room in the casing to install an encapsulated ESP unit.

In **Fig. 19.21**, the motor is installed above the system, wired to run in reverse, and special seal sections are installed below and above to seal off the motor. The intake of the pump hangs below the whole assembly and, with the rest of the pump, hangs below the capsule. The top of the pump is at the bottom of the capsule, discharging well fluid inside the capsule. The fluid rises up the capsule, wetting and cooling the seals and the motor, and then is routed into the tubing string at the top end of the capsule.

A gas separator can be added to the bottom of the pump and a dip tube can be designed to be flanged onto the bottom of the pump instead of using a pump intake.

Arrangements also can be conceived using packers, but this concept prevents natural gas separation.

Inverted Shroud

This gas avoidance system (**Fig. 19.22**) has been successful in natural gas well dewatering applications and is a great tool for handling slugs. The length of the inverted shroud can be calculated easily to provide the necessary liquid accumulator volume. As long as the area between the inverted shroud and the tubing string is large enough to ensure that the velocity of the descending fluid is low enough, the top of the shroud acts as a good separator.

Testing demonstrated that if the downward liquid flow velocity is kept below 0.5 ft./sec., gas separation approaches 100%. This can be assisted by installing a small tubing diameter above the pump and up to the top of the inverted shroud.

When a gas slug comes through (100% gas) there is no downward flow, and the pump produces only the liquid accumulated in the inverted shroud. Inverted shrouds as long as 500 ft. have been installed successfully.

To be able to use long inverted shrouds, there must be enough room in the casing to have annular space outside the shroud as well as inside. Also, if the shroud is to be long, there must be available pump intake pressure to ensure that the fluid level above the pump is also above the top of the inverted shroud.

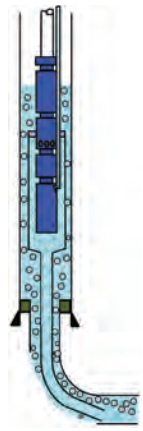

Fig. 19.20—Capsule and dip tube only.

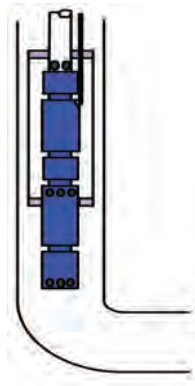

Fig. 19.21—Bottom intake pump.

Fig. 19.22—Inverted shroud.

If a lower than expected flowing bottomhole pressure FBHP (PIP) were encountered, a long inverted shroud would end up with its opening above the fluid level and thus would be rendered useless. However, this solution can still be used in a horizontal well (providing the casing size is large enough and there is a good horizontal section to lay the shroud and the ESP unit) as the requirement for the shroud to work is only that the top section be set a few feet into the vertical section of the well (**Fig. 19.23**).

Gas Avoiding Tool

This tool takes advantage of the fact that fluid flow in the horizontal section of the well will tend to separate naturally due to gravity. The longer the straight horizontal section and the lower the flow rate, the less turbulence there is and the better natural separation is. The gas avoider only allows entry to the flow on the underside of the tool, which is effectively an intake, in the expectation that this fluid is mostly in liquid phase, allowing all or most of the gas to proceed down the well in the annular space between the pump and the casing or liner.

Fig. 19.24 shows a cutoff diagram of the most commonly used gas avoiding design. All around the tool are successive ports in which weighted cups with a conical shape are aligned with the intake ports and are able to pivot with gravity to cover the upper ports, leaving the lower ports as the only intakes. This tool is available in the 400 and 500 series, for 5-1/2-in. and 7-in. casing, respectively.

Another newer gas avoiding design is the bowspring type (**Fig. 19.25**). Similar placed ports have a weighted swing gate and a pusher attached to the gate and to a flexible steel bow-shaped spring. The spring is attached to the tool on the upper (left in diagram) side and is allowed to slide on the other. As this tool is installed in the horizontal section of a well, the lower side weighs down on the casing I.D. The springs push open the intake ports, while the upper side bow-shaped springs remain uncompressed and the ports remain closed.

Except for the dip tube with auger and gas intake, all of the avoidance methods create a sump or fluid reservoir that allows for liquid accumulation. This arrangement is essential when dealing with slugs, especially when slugs are large, thus starving the ESP/completion from liquids for a short period of time.

The sump creating methods mentioned above, except for the case in which a sump is drilled in the well, require a large casing so that the pump can be shrouded or encapsulated or so that a bypass tube can be installed parallel to the pump.

In vertical wells, an ESP unit can be run below perforations when a rat hole is present. This constitutes the required sump.

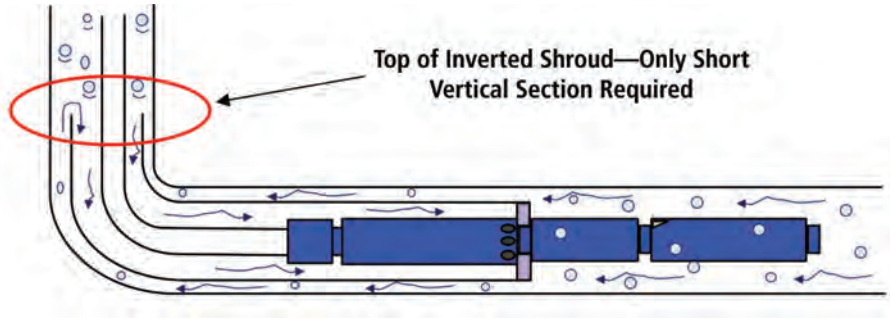

Fig. 19.23—Inverted shroud for horizontal application.

This luxury does not exist in horizontal wells. In some rare cases, laterals are added to vertical wells and a rathole may be present. Most unconventional wells are horizontal, with a single lateral, drilled in one operation, to have the space limitation unless the casing is fairly large. Fortunately, many shale wells are drilled with 7-in. casing, so there is room for running 400 series or even 338 series equipment in the well with a capsule or parallel tube.

A drawback for this type of complex completion is the risk of losing equipment or getting it stuck downhole. Operators avoid complex completions because they may pose the risk of losing an expensive well.

No pump gas separating or gas-handling device can operate with gas slugs. Unless the sump or liquid phase reservoir can be artificially created, a slug puts a stop to steady production. This is made up of the time taken to realize a slug is going through the pump, plus the time for the fluid to flow back down the tubing string after the pump is shut down, and the time it takes for the fluid to be pumped up to surface again. This could add up to many hours in a deep, low flow well.

Other solutions do exist for this problem, such as surface control options, use of a diverter or a dispersion flow system. These are addressed in more detail in the gas handling section.

19.3.3.3 Gas Separation

When gas cannot be avoided, a second level of action is separation. Although the devices indicated above can arguably also be called separators, some devices are considered to be true separators. These are mechanical devices attached to the pump, usually in lieu of a standard pump intake. However, natural separation must be discussed before going into detail on gas separation equipment.

However, before we go into detail on the subject of gas separation equipment, we must discuss natural separation.

Natural Separation

Any artificial lift equipment installed in a well must have a diameter that allows it to be installed and pulled with some ease, and must be capable of being fished using adequate fishing tools. Even when equipment is tight in the casing, there must be room for fluid passage.

This required room, although it may be quite small, allows for free gas to separate naturally by gravity. Although it is not intuitively easy to accept, a larger amount of gas than seems possible will separate by this means. Thus natural separation may at times be considered as helping in dealing with gas downhole.

AutographPC Software and Natural Separation

AutographPC software allows for a separation factor to be introduced into equipment design. In the well screen (data entry screen) a box allows for one separation value. Natural separation can be obtained for conditions entered in the well screen by going to the tools icon and selecting "estimate

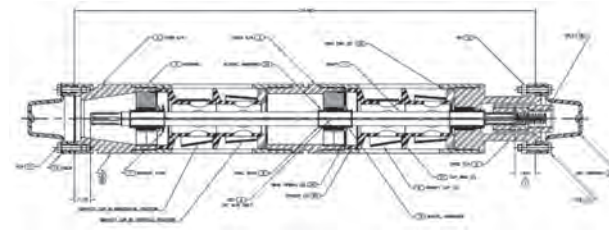

Fig. 19.24—Baker Hughes gravity cup.

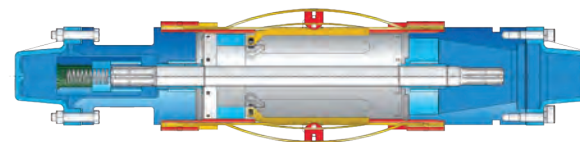

Fig.19.25—Baker Hughes bow spring-type intake.

natural separation" from the drop-down menu. For the tool to work, the gas separator selector under the "Gas Sep" button must be set to "None."

This is intentional, as natural gas separation is not happening normally when a gas separator is being used. This is due to the separator recirculating gas constantly between the gas discharge ports and the intake. Natural gas separation may help, however, if the equipment series is small for the casing size it is being installed in (for example, 400 series equipment in 7-in. casing). In these cases it may make sense to add a couple of percentage points to the separator efficiency chosen for a given gas separator. The natural separation tool in Autograph PC software does not apply to ESPs run below perforations.

A different situation entirely occurs when deciding separation efficiency in cases where the ESP unit is installed below producing perforations. Separation efficiency will now be a function of the velocity of the liquids descending to the pump intake. If the fluid velocity is small (≤ 0.5 ft./sec.) it is safe to assume that separation will approach 100%. The problem lies with estimating how much separation can be attained when fluid moves at a larger velocity than this. A somewhat conservative and general rule of thumb for this is in **Table 19.5**.

Table 19.5—Natural separation as a function of downward flowing fluid velocity—rule of thumb.

Liquid Velocity (ft/sec)	Separation Description	Gas Separation %
$V_L < 0.5$	Good	GS% >85%
$0.5 < V_L < 1$	Fair	40% < GS% <85%
$V_L > 1$	Poor	GS% < 40%
Gas Separation Indicator		

Gas Separators

Gas separator technology has evolved substantially over the last decade or so. The secret of gas separation is that there must be enough pressure in the separating tool so that after separation has been accomplished, separated gas is still at a pressure higher than the surrounding annular pressure so it can be expelled. All rotary separators need to generate some lift/pressure after the intake ports, then provide a path through the separation chamber and flow splitter/diverter with the lowest possible pressure drop, leaving enough to expel the gas. As flow increases through the separator, pressure drop increases, as it would when flowing through a pipe. Thus there is always a limit to the amount of throughput a gas separator can handle and still separate gas from the liquid phase. Larger and/or better designed separators have a wider range of flow.

The Baker Hughes artificial lift system's latest gas separator design, the GM™ Performance Series gas separator, focused on providing the best boost at the base and the least pressure drop at intake and exit ports, bearing supports, and in the separation chamber. **Table 19.6** shows the performance capability of some older gas separator models compared to the GM™ Performance Series gas separator. The table also compares the differences in capacity for handling rate with size (outer diameter or series).

The GM Performance Series gas separator product line is better equipped than older models to handle abrasives, which have been known to cut through the housing of gas separators due to abrasives being flung against the housing surface by the rotor chamber or vortex inducer. This separator has options for handling extreme abrasive conditions, including lining the interior of the housing with a tungsten carbide sleeve.

Does It Make Sense to Install a Gas Separator Below Perforations?

It may not seem intuitive to install a gas separator in a unit placed below the perforations because fluid coming down the casing will drag any gas exiting the separator ports back down to the intake. Although this is true and some small amount of separated gas may rise above the perforations, the gas separator nevertheless acts as a beater. This effect contributes to the turbulence that in turn contributes to chopping up the fluid and making smaller bubbles. Smaller gas bubbles are better handled by the pump, and this effect alone may avoid a gas lock condition.

Testing has been done with gas separators including a set of tubes or discharge ring with tubes attached to the gas separator's gas exit ports (**Fig. 19.26**). Tubes are run up to the point where they sit above the perforations and descending fluid. Baker Hughes engineers designed a ring mounted around the separator gas discharge ports to collect gas and then feed it into a single larger diameter tube. This arrangement has a positive effect when dealing with gas slugs.

19.3.3.4 Gas Handling

When avoidance and separation are impossible or insufficient, the pump must be able to handle the gas

Table 19.6—Features of standard Baker Hughes XP™ gas separator products.

Gas Separator Product Line								
Feature	**338 series**	**400 series**			**500 series**			**675 series**
Type	**Rotary**	**Old FRS**	**GM Rotary**	**GM Vortex**	**Old GRS**	**GM Rotary**	**GM Vortex**	**Vortex**
O.D. (in.)	3.38″	4.00″	4.00″	4.00″	5.13″	5.38″	5.38″	6.75″
Max. Rate (RBPD)	2,700		5,000	8,000		10,000	15,000	25,000
Shaft Size	11/16″	11/16″	11/16″	11/16″ LS - 7/8″	7/8″	7/8″	7/8″ LS – 1-3/16″	
60 Hz BHP (water)	3	>3	4.5	3	5	5	4	~25
AR protection	OPT	OPT	STD+	STD+	OPT	STD+	STD+	OPT

without suffering gas lock. The ESP system must be able to clear the lock and, if not able to do so, will shut down power to the downhole unit to protect it from:

- Motor burn, due to the produced fluid no longer cooling the motor
- Pump premature wear, as the pump runs dry it also gets hot, sometimes enough to destroy the thrust washers and subject the stages to metal-to-metal contact and premature wear
- Motor lead cable and/or pothead burn. These components may fail due both to the motor and the pump getting too hot for the insulation and jacket materials to survive.

When the surface protection equipment works properly, the downhole unit shuts down. However, this creates a problem for the operator as production is lost or deferred and sand fallback issues may cause other serious wear issues.

Traditional operating practices recommend leaving the unit shut in for a period of time long enough to guarantee that the fluid in the tubing has all run back down through the pump and that the fluid levels in the tubing and in the casing have leveled out. If the pump should start while running backwards during this period of back flow, the pump shaft could easily be twisted or broken.

Back flow can be prevented by using a check valve above the pump and a drain valve to empty the tubing string at the time the ESP needs to be pulled, to avoid pulling a wet string. This creates another set of problems.

- How can the operator be sure the check valve works after some time has gone by? The valve seat and flapper/poppet could have become worn, or some foreign object could be stuck in such a way as to keep the valve fully or partially open. For this reason, the surface equipment is usually allowed to time out.
- A check valve set too close to a pump can be a stopper for gas in the pump trying to exit and clear the pump for a full load start. This can usually be resolved by setting the check valve one to three stands above the pump.
- Falling sand or scale can also stick the check valve in the closed position, putting an end to production with the ESP. Multiple check valves can spread the load of sand and scale, but more valves downhole also add more risk.
- The use of a check valve negates the possibility of pumping fluids back down through the pump, actions that may be necessary to clean out sand or scale or other foreign objects from a partially blocked pump.

A tool that has helped in this regard is the backspin relay, a device that detects the current generated by the motor turning backward. It prevents a restart until the motor has stopped turning. This is an efficient way to prevent a backspin start situation, as it does not depend on calculations and does not require extra "insurance time," a waste of production to the operator.

The other problem with a gas lock shutdown or any shutdown is the additional time wasted in pumping up to the surface to restore normal production. In deep wells, the total downtime can amount to hours.

Gas Handling Stages

Over the years, hydraulic engineers or stage designers have worked on modifications to the typical, standard centrifugal stage design to make them able to handle more than the free gas normally associated with an electrical submersible centrifugal multistage pump. Although knowing that higher intake pressures allow for handling substantially more free gas (Fig. 19.31), most applications require producing wells with ESPs and low pump intake pressures, typically in the 100 to 300 psi range.

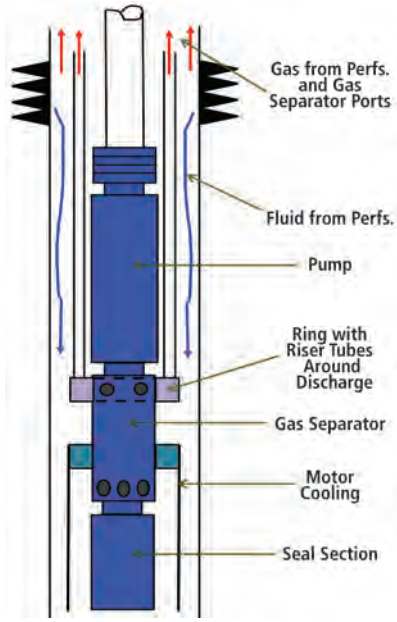

Fig. 19.26—Gas separator with gas collector and tubes.

Gas handling stage designs are centered on preventing gas from accumulating in low-pressure areas and/or preventing phase separation, due to centrifugal force, inside the impeller itself. The Baker Hughes artificial lift system offers two different types of gas handling stages.

Gas Insurance Stage

The current availability covers the GINPSHL (400 series) and GINPSHH (538 series). GINP represents gas insurance net positive and SHL and SHH are model indentifiers representing suction head low and suction head high. They are basically similar stages (**Fig. 19.27**) and are recommended for use when the intake pressure is very low (~ 100 psi). This pump stage design has a large hub, both impeller and diffuser, and leaves little allowable radial displacement for the pumped fluid, thus allowing little possibility of centrifugal separation. It has a high specific speed for an ESP stage and looks like a turbine element. The gas insurance pump/stage is used as a charge pump

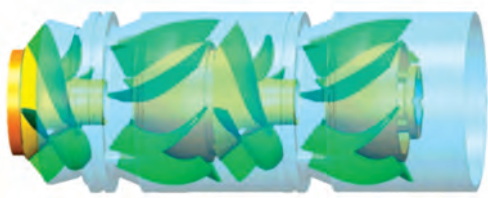

Fig. 19.27—GINP low NPSH gas handling stage.

only and is capable of providing some head even though the produced fluid mixture is highly gassy. Another benefit of a gas insurance stage pump is that gassy fluids can be handled by a centrifugal pump if the fluid is homogeneous. The gas insurance stage, acting as an agitator, breaks up large gas bubbles into small ones, and thus makes the two phases harder to separate as they go through the lower stages of the pump. The fluid becomes increasingly homogeneous and pumpable.

This stage may at times be used to produce at rates that make it somewhat inefficient unless running close to best efficiency point (BEP) and, as such, might be used to its best advantage if combined with another gas handling stage. The gas insurance stage has large vane openings, making it a very good stage for applications where there is a strong scaling tendency. (See **Fig. 19.28.**)

Multivane Pump Stages

Designed and patented in the early 2000s, the Baker Hughes MVTP™ multiphase gas handling pump stage is a radical change from the standard ESP centrifugal pump stages and from traditional gas handling stages. This is not a turbine style design. The approach taken for this design was based on an idea for preventing the gas bubbles from accumulating and coalescing in the low pressure area behind the vanes of the impeller. Vane length was interrupted with a small port, allowing some fluid to move into the low-pressure area and displace accumulating gas, as well as inducing turbulent mixing. Large balance holes were placed in the impeller to allow for some fluid flow from the top (high pressure) area to the low-pressure area behind the vanes, and to keep pressure differentials and thrust loading at a minimum.

An additional detail was taken into consideration when the tip of the multivane pump stage vane was turned backward from the normal angle, giving it a more aggressive angle of attack. This design allows a lighter fluid such as a gassy liquid, to receive an additional push and provide the stage with more lift capacity. (See **Fig. 19.29** and **Fig. 19.30**). The end result was a stage that provided better operating conditions and efficiency when the fluid is gassy. When pressure is higher and/or the fluid is more homogeneous, the stage becomes less effective and efficient when compared to a standard type ESP stage, a good reason why the multivane pump stage typically should be employed as a charge pump.

Tests carried out in the Claremore Gas Loop (a Baker Hughes gas loop facility built in Clarence, Oklahoma) showed that the gas insurance (GIN) type stage may outperform multivane

Fig. 19.28—A low NPSH (gas insurance stage) impeller.

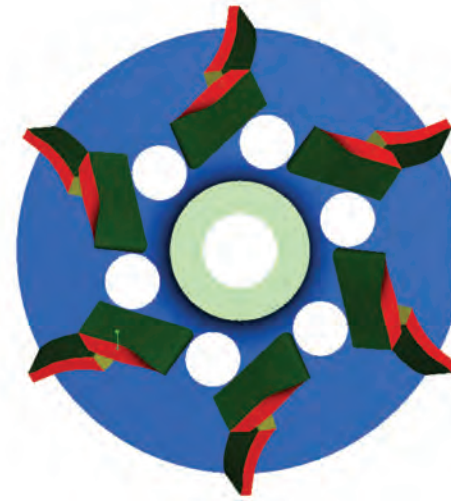

Fig. 19.29—Schematic of MVP impeller.

pumps in low pump intake pressure applications. Gas insurance stages and MVP stages frequently are combined to get better gas handling and efficiency is some very gassy applications.

Experience has demonstrated that the multivane pump stage should be applied in such a way that the operating points remain as much as possible to the right side of the best efficiency point, as gas handling performance deteriorates somewhat at the left side of the performance range as it does in most centrifugal pump stages. For this reason, if a given application is going to see production drop significantly over time (most unconventionals), the better choice may be the gas insurance stage or a combination of gas insurance and multivane pump stages.

The gas insurance stage is manufactured in one size only for each of the 400 and 500 series, but the multivane pump stage provides four sizes for the 400 series and three sizes for the 500 series. There are additional multivane pump stages, either in existence or in development, per the following multivane pump stage table (**Table 19.7**).

An important application consideration is that after having traversed a series of GINP and/or MVP stages, fluid going into the main pump may still show to have a large amount of free gas. The Turpin graph in AutographPC software (**Fig. 19.31**) should always be used as a reference, but even if it seems to indicate that the fluid still has too much gas for a standard stage, the agitation provided by the charge pump stages has most likely changed the characteristics of the two-phase configuration to the point that the fluid is now much more homogenized and more pumpable, i.e., more likely to be handled adequately by the standard type ESP stage. The fluid has been conditioned to make the pump better able to handle it.

Gas lock effect typically occurs in a small number of stages at the bottom of the pump, where the free gas is present in the highest volumetric fraction. If gas lock does not take place there, it is not likely to do so further up the pump. The charge pump assures that the upper (standard) stages do not gas lock.

Applications engineers may at times be tempted to add a larger amount of GINP or MVP stages than is required after looking at the free gas curves in the software. Test different amounts of gas handling and standard stages to obtain the most efficient way to operate. Effective gas handling may be guaranteed by a lower number of stages than that which is considered to be optimum (**Fig. 19.32**).

When using AutographPC software to design an application, the fluid volume in the calculations is affected by the free gas and the formation volume factor resulting from the portion of the gas that is in solution in the oil. A smaller amount of gas also dissolves in water. When all the effects of the gas

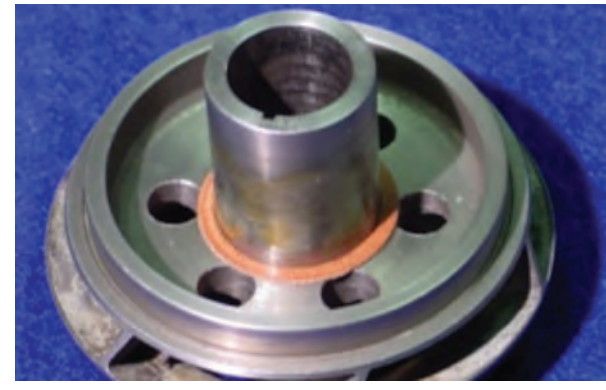

Fig. 19.30—Photograph of MVP impeller (400G22).

Table 19.7–MVP options available for casing sizes 7 in. and smaller.

SERIES	STG. TYPE	O.D.	RANGE (BPD)	AR. PROT.	CONFIGS.
338	G5	3.38"	400-700	UT	SSD, SXD
400	G4	4.00"	300-500	DT	SXD
	G12	4.00"	800-1700	UT	SSD
	G22	4.00"	1000-3000	UT	SSD
	G42	4.00"	2200-5800	DT	SSD
538	G31	5.38"	1800-4400	UT	SXD
	G68	5.38"	400-9500	UT	SSD, SXD
	G110	5.38"	6000-14000	UT	SXD
562	G200	5.62"	12000-24000	UT	ALL

with compressed volume adjusted to intake pressure is taken into consideration by the program the operating point lies further to the right on the pump performance curve when compared to the stock tank barrel volume. More stages are required to generate the required total dynamic head (TDH), so AutographPC software takes into consideration the larger volume of fluid going through the pump. This is normally referred to as RBPD or Reservoir BPD.

One issue that the software cannot address automatically is the actual performance deterioration of the stage because of free gas in the fluid. Not all stages behave the same way. A general practice to applications of ESPs in gassy wells is overstaging the pump. Some application engineers simply add a percentage, as much as 10 to 20%, of stages to the calculations resulting from TDH and head per stage and this would work well in the field. The more scientific way is to use a modifier in the pump screen (**Table 19.8**). The advantage of the modifier is that it can be applied with some intelligent criteria, especially if the pump will be a tapered type, as different modifiers can be used for each pump. The use of modifiers is a good solution but experience is required in using them, although there is a generic guideline for this. The theory behind this is something called head lock versus gas lock and it is explained in the next paragraph.

An example is a 200 stage pump generating 6,000 ft. of head (30 ft./stage) is operating in an application with little gas but with occasional surges. When a small amount of gas is coming through the pump, the head generated by the stages is only slightly affected and the operation goes smoothly. If there is a sudden increase in gas, and the first 50 stages are affected enough to lose 30% of their head capacity but not enough to gas lock, the pump can now only generate 5,550 ft. of head (6,000 – .3 X 50 X 30). If the pump head curve is somewhat

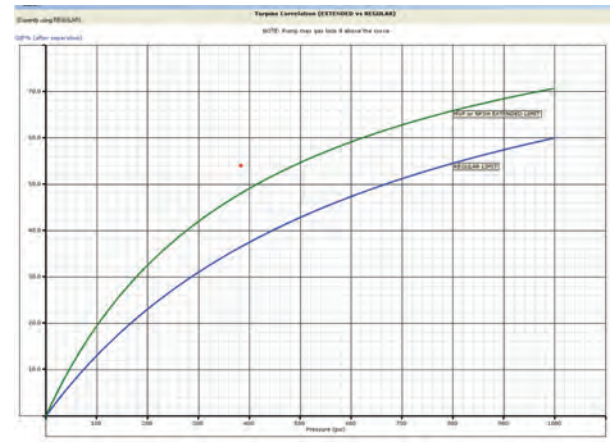

Fig. 19.31—Modified Turpin curve (AutographPC software) for standard stages and MVP. Note location of the operating point.

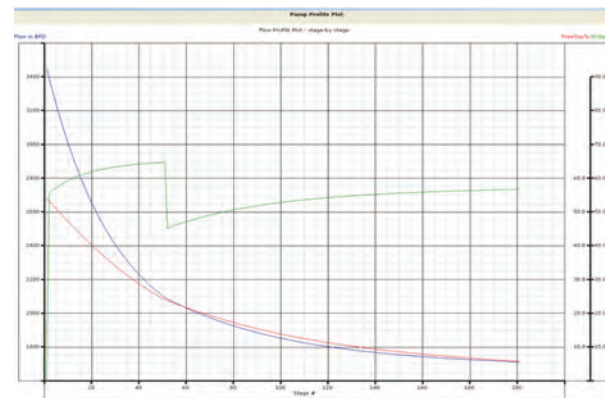

Fig. 19.32—The pump profile graph shows the head transition from an MVP stage to a standard electrical submersible pump stage. At the transition point, the free gas is in excess of 20%, but the top pump receives an agitated, somewhat homogeneous and pumpable fluid.

Table 19.8—Suggested modifiers for head capacity when pumping gas (AutographPC Software).

GIP (Free Gas into Pump)	Head Modifier
0 – 10%	1.0
10 – 20%	1.0 – 0.9
20 – 30%	0.9 – 0.8
30 – 40%	0.8 – 0.7
40 – 50%	0.7 – 0.6

flat to the left of the previous operating point, the pump performance may slide all the way to shut in, as the total head generated is now not enough to move the fluid column in the tubing, and the pump is described as head locked.

This process is likely part of the whole gas locking process as, even though a lower group of stages (a small number) is gas locked, the upper stages would still tend to move fluid up the pump, but the combination of the two effects can cause gas locking at the bottom of the pump when the fluid slows down due to head locking.

When using a VSD, the application engineer is somewhat protected from small errors in well data as the effect of frequency on pump performance is significant, thus allowing for easy corrections in the field by adding or removing maybe only fractions of a Hertz in the drive setup. Notwithstanding good calculations and the use of drives (one does not want to end up operating at very high frequencies, as this will lead to premature wear) knowledge and experience are additional input that can be expressed in the use of the modifiers in the AutographPC software pump screen. When producing substantial amounts of gas, stage performance is significantly affected. The application engineer can get off to a good start by judiciously using modifiers or just adding even more stages. The extra stages will cover the fact that AutographPC software cannot include the performance deterioration caused by the specific operation of a given type of ESP stage with elevated amounts of free gas. When using MVP or gas insurance stages in a charge pump, a presence of, say, 35% of free gas causes a 20 to 30% loss of head. The modifiers for the charge pump can be set at 70%, which affects frequency of operation and/or the number of stages used or the charge pump or the main producing pump. These modifiers must be used carefully and their use should be affected by feedback from the field as further applications are carried out.

When applications are made using switchboards at the surface, the problem is exacerbated. It is convenient to add extra stages not only because of performance deterioration but also because gas production is not constant and sizings are done for a given amount of gas production. This usually is based on the well test, which is an average production for a day or even a few hours. Be prepared for the potential higher gas production peaks likely to occur frequently during any given day. This can be seen when looking at amp charts (paper or electronic) or looking at amperage and pressure data on AMBIT™ ESP monitoring services (Baker Hughes trademark for remote monitoring services) or other data collection analysis software. Case-LOWIS, and X-Spoc are other remote monitoring services available in the industry. The occasional peaks in gas production frequently cause gas-locking conditions and pump shutdowns. Sometimes they will be large slugs and then as explained below most gas handling solutions do not apply as they are ineffective. One of the techniques that has been tried by many operators with mixed levels of success is increasing the tubing pressure at the wellhead.

The immediate effect of increasing the tubing pressure is an increase in total displacement head (TDH), which in turn will push the operating point on the pump's head curve to the left. The lower production from the pump caused by this action is reflected in the pump intake pressure as the well reacts per its productivity index. Now the higher pump intake pressure means less free gas is at the intake and the pump operates with fewer gas locking incidents. However, this procedure is usually carried out in conjunction with raising the speed (frequency) of the unit when a drive is available.

So does this higher tubing pressure (TP) make a difference if production rate is reinstated using the variable speed drive?

A complex process cycle goes on in the tubing string: The pump is operating steadily with a given amount of gas coming into the intake (gas separator or otherwise) and some gas is entering the pump. The pump discharge fluid is compressed enough that there is no free gas (or it's compressed to a volume small enough to disregard). As the fluid climbs the tubing string and pressure falls, some gas starts to break out/expand, but production is somewhat stable and pump discharge pressure remains fairly constant and equals to net lift to surface + friction loss + tubing pressure. Note that net lift to surface implies the column in the tubing being fairly steady, although specific gravity (gradient) changes as it rises, due to changes in formation volume factor and gas gradually breaking out. At some point, a small surge of gas enters the separator or pump, not enough to cause any serious disruption, but it changes the gas-to-oil ratio in the pump slightly. As the fluid exits the pump and goes up the

tubing, more gas breaks out as pressure reduces and lightens the column slightly. The lighter column means that the pump is pushing against a lower pump discharge pressure, so the operating point on the head performance curve moves slightly to the right. The slight increase in flow pulls the pump intake pressure down just a little and more gas enters the pump, still no disruption, though, but the increased gas breaks out and further lightens the column. The vicious circle continues until the change in pump discharge pressure and flow is enough to allow so much gas to enter that it does cause a gas lock.

This vicious circle can be mitigated with additional tubing pressure, as it desensitizes the process by limiting the gas breakout in the tubing caused by the small changes. It is intuitive that the pressure required at the tubing head to effectively desensitize this process must be rather high, making this process expensive, as the pump must be designed with even more stages or the drive must operate at a higher frequency, using up electric power just to maintain a higher TDH output from the pump.

Amazingly enough, the amount of ESP shut-ins is often reduced by only a couple of hundred psi, so it almost benefits the field service technician to try this partial solution. It doesn't work in every case but it always makes sense to try. It may be convenient to have some extra stages in the design, especially in applications without a variable speed drive (VSD).

19.3.3.5 Dealing with Gas Slugs—Prevention and Breaking a Gas Lock Condition

The worst gas-related condition is the gas slug. It is a very large bubble, usually formed in the horizontal section of a well where there may be small hills and valleys which allow for accumulation of a gas cap. A gas slug can also be formed in the reservoir close to the wellbore.

The passage of a gas slug equates to a period of time in which only gas enters the ESP unit. As there is no liquid phase, there is no possibility of separation or even of handling. Pumps do not generate enough head when there is a low-density medium in the stages to overcome the pressure of the liquid column above the pump. The pump would have to run approximately 10 times as fast and basically act as a compressor to generate the required head. As the gas enters the pump, the phenomena explained above will quickly halt production completely.

Other than the techniques mentioned to avoid the gas slug and how to help handle it, the best way to treat this situation is to let the pump shut down and allow for the liquid in the tubing string to fall back and wash out the gas while letting any remaining gas dissipate up the tubing string. The problem with this approach is not so much technical as it is commercial. The operator does not want to see production stop to clear the gas out of the pump and wait to restart the unit (making sure there is no backspin) and then wait for the fluid to be pumped to the surface again. Technically, the only potential problem is mild wear damage from downthrust when the pump backspins excessively fast during the liquid fallback period. In addition, if abrasives are being produced, these will also fall back into the pump, some of it going through, but some of it potentially accumulating in the top stages of the pump, creating additional wear on startup or even plugging the pump in extreme cases.

This book was prepared to support and aid application design, so it will not cover detailed ESP operation in the field. However, certain aspects of operating ESP equipment must take into consideration the operating mode when designing the ESP application, both for equipment features and for ancillaries. The completions explained earlier in this section are the first approach for dealing with slugs, but there are tools and processes that can further help.

Dispersion Flow System

Dispersion flow system (DFS) is a system designed for use with heavy oil. Performance of centrifugal pumps deteriorates very quickly with the rise in viscosity. Low API gravity oils have a higher viscosity and are usually found in shallow reservoirs, which are relatively cool. Oil viscosity is very sensitive to temperature and is much higher at low temperatures, so these reservoirs are hard to produce with ESPs. ESPs have been used for this type of reservoir, with viscosities between 500 and 2,000 cp. Gas deteriorates ESP performance, mainly lift per stage, and reduces the load on the pump. Viscous fluids deteriorate both flow and lift and quickly increase the load on the pump and motor. As a result of this, efficiency plummets.

Faced with this situation, many ideas were devised and tested to overcome this loss of performance. Before most of these applications went to PCPs that are much more efficient with viscous crudes, one solution offered a significant improvement: diluents injection.

Operators in Venezuela injected diesel oil and/or light crudes from other fields and it was discovered that a 20% diluents rate would increase pump performance by as much as 100%. The tool for delivering this diluent became the DFS. In the DFS, a capillary tube of larger than usual dimensions was used to inject the lighter fluid down to the pump intake. The fluid

wasn't just allowed to flow to the intake but was injected in a special intake assembly that included an auger for pre-mixing the heavy oil with the diluent.

A similar idea has been proposed for assisting with gas handling, allowing for production of some liquid while a gas slug is being cleared by the well.

Although the fluid (water is the cheapest and most convenient, although recirculated oil would benefit bearing surfaces in the pump) can be spotted at the pump intake (with or without a special intake), this solution would better serve high gas applications but not the slugging kind. The ideal injection solution for a gas slug is to inject the liquid phase into an inverted shroud. The shroud would not have to be very long and could fit more snugly around the pump as there would be less of a requirement for a large reservoir of liquid.

This solution may be considered costly but, whenever an inverted shroud can be made to fit in the casing, it is almost infallible. The shroud can solve the problem on its own or be combined with other solutions, designed to protect the motor from overheating, as there will be no cooling fluid passing the motor while the pump produces only from the fluid reservoir in the shroud.

Optimized Drive Software

The ideal solution for handling slugs in gassy applications (such as encountered in unconventional and shale plays) will likely be software based.

The new Advantage drive (part of the AutographPC software) has an optional MaxRate™ software. The basis of this subroutine is a sequence in which a gas lock tendency is detected (through a reduction in motor torque) and the pump is slowed down just enough that it cannot hold the column of fluid in the tubing string. This allows for some back flow through the pump, which clears out the gas (purge). After a short period of time, the pump speeds up again to restore production but, if the gas effect is detected again, such as would happen if a slug were passing through the casing at the ESP setting depth, the process will be repeated, and so on. The program can be modified with various setting points such as torque setting, time delays, number of attempts, etc.

A second control loop is included in the software to control drawdown in the well, as the process above should not allow the pump to draw down the well to the point that it pumps off. It is also necessary to find a point where the pump intake pressure stabilizes so that the gas purge sequence is not initiated too often, be it caused by excessive gas liberation due to low pump intake pressure or because of slugs. Ideally, the purge should only occur when slugs are the cause.

MaxRate is the result of various earlier attempts to do this with different speed changes, either carried out with the drive software and/or with external PLC solutions. Some of the previous attempts did meet with different levels of success and some are still operating in the field. PLC solutions are still employed with older variable speed drive models that cannot be updated with MaxRate software.

Diverter Valve

The same diverter valve mentioned in the section covering abrasives can be used to assist with slugs. It may be possible to combine the use of a drive setting with the capability of the diverter valve to dump the tubing fluid in the annular space providing a rapid increase of pump intake pressure. However, the software solution alone will probably be a better choice if it can be made to work as desired.

19.3.4 Scale and Other Depositions

There are other fluid-related factors that can seriously affect ESP performance. These are deposits that form on the ESP unit, sometimes on the outside of the equipment housings, sometimes on the internals of the pump. These are chemical issues that can cause a pump to be completed plugged or can even cause an ESP unit to be stuck at the bottom of a well.

The chemical issues are a function of not only the chemicals that make up the produced fluid but also of pressure and temperature. The phenonomen has been discussed in detail in Chapter 18. Both of these can tip the balance of chemical reactions, which are constantly taking place, even without noticing any adverse or positive effects. Deposition can even be aided by electrical and mechanical phenomena. The mere presence of downhole equipment with specific metallurgy or chemistry can alter the balance of the chemistry in the well.

There are two main types of chemical depositions that affect ESP performance and/or life in a given oil well: inorganic salts, commonly known as scale and organic compounds, which take the form of paraffin or asphaltene and sometimes are simply referred to as wax.

19.3.4.1 Scale

These are typically salts and they are found in the water that accompanies oil and gas in the reservoir. This water usually is

referred to as brine, because the salt content is normally high, enough to significantly raise the specific gravity of the solution. Although normal brines found in oil wells have SGs ranging from 1.01 to 1.05, values in excess of 1.2 are not unheard of.

The most common scales are made up of calcium carbonate, calcium sulfate, barium sulfate, strontium sulfate, iron sulfide, iron oxides or carbonate and various other silicates, phosphates and oxides. In general, the term scale applies to any compound that is insoluble or partly soluble in water in conditions that may be found in oil wells.

When designing an ESP application it is convenient to obtain from the customer or operator a well fluid analysis. This typically comes in the form of a gas analysis and a water analysis. A hydrocarbon analysis may also be available.

If complete, water analysis includes, apart from a list of cations and anions with their respective concentrations, a scale tendency analysis. The latter is a graph indicating precipitation tendencies for specific salts at various temperatures. By looking at the temperatures expected to be found in the pump inside and out and motor and seal housing surfaces, it is possible to determine if there is likely to be a scale problem for the specific installation planned. The fluid analysis may be good for most of the wells in any specific field, and thus can be used in most if not all applications in the reservoir. However, if any oilfield draws production from more than one reservoir, or if the reservoir is large and shows trends in fluid composition, more fluid tests may be required.

If the fluid test is good for the whole field, it is important to understand that not all of the ESP units that will be installed will operate in identical conditions, so temperatures may have to be checked for all cases/wells. For example, some units may be installed below perforations and, even with using motor shrouds or recirculation pumps, motor temperatures may be much higher than in applications set above the perforations.

19.3.4.2 Scale Prevention and Treatment

When conditions warrant it, scale prevention techniques need to be put in place. Some operators wait to see if scale affects performance and/or run life, in which case prevention and treatment may come after the fact.

Prevention and treatment may be the same in most cases. Some prevention can be considered at the early stages of the application, by trying to ensure that the conditions leading to precipitation will not occur. This can entail designing and setting the equipment in such a way that certain triggering temperatures will not be reached, or materials can be selected appropriately. However, the choices for materials in ESP equipment are limited and do not impact scale precipitation. What can be done to prevent to some extent is to use coating materials that do not favor adhesion of scale to equipment surfaces. (See the section on coating.)

The main tool for scale treatment is fighting chemicals with other chemicals. An entire industry is dedicated to scale prevention, whether it is precipitation in surface equipment (not limited to the oil industry) or down in the oil well. Baker Hughes Petrolite, also known as Baker Petrolite and Baker Performance Chemicals (BPC) is the product line and division that is dedicated to this aspect of oil production. Chapter 18 on flow assurance covers this topic in detail.

Batch Treatment Versus Continuous Injection of Chemicals

Different types of scale respond differently to available treatment methods. Chemical treatments require adding chemicals to the produced fluids before they enter the ESP or other artificial lift system. This includes the tubing string, where scale can deposit after exiting the pump and cause plugging that can affect ESP operation.

The common and most cost-effective way of treating a well is pouring the chemical after proper dilution down the casing annulus, which is sometimes referred to as the back side. The problem with this type of application is locating the chemical where it is most needed. Depending on the specific gravity of the chemical solution and the produced fluids, the mixing effect may not be adequate to ensure a good coverage of the surfaces. Another problem with this is the chemical not reaching the bottom of the motor (so the motor, the hottest component and in most cases the most likely to be covered with a layer of scale, does not get the treatment).

This chemical addition may be done as batch treatment on a regular basis or in continuous mode. If done in batches, the treatment is better for cleaning out the scale or other deposition, but the chemical is pumped away and the ESP unit is subject to scaling up again until the next treatment is applied. Continuous treatment is an improvement, but does not meet the requirement of correctly spotting the chemical everywhere it is required.

Injecting Chemical With a Capillary Tube

This method of treatment is also quite common, but not always accepted because of the increased cost. However, there are abundant case histories showing staggering run

life improvements with this optimized treatment (doubling and tripling run life days). The added costs involve the actual cost of the capillary tubes (typically 3/8 in., with 0.049 in. wall thickness stainless steel capillary tubes), the additional care and time to install in the field, and the need for an additional spooler truck to feed the cap tube into the well. On certain occasions, more than one cap tube has been installed simultaneously, making the install procedure even more complex and costly.

Capillary tubes have often been included in the cable construction, thus negating the need for an additional spooler truck at installation time, and making the whole process faster. However, some field service technicians do not welcome the additional work of breaking out the capillary tube from the cable and sometimes having to splice the tube, a process that requires additional hardware. When the capillary tube needs to reach the bottom of the motor (not always possible when running in a tight fit, but may require running a smaller series motor if the scaling issue is serious), a section of bare cap tube will have to be added to the tube running with the cable.

Some cable manufacturers have installed cap tubes inside the main cable construction, as seen in **Fig. 19.33**. The problem with this is getting access to the cap tube, which means cutting open the cable jacket and exposing the individual leads' insulation material to the downhole environment and weakening the cable. Baker Hughes developed and patented the idea of adding the capillary tube to existing cable by adding an additional layer of ARMOR™ coating (**Fig. 19.34**). Although this increases the cost, it provides a number of benefits:

- Access to the tube without opening the base cable.
- The cap tube does not interfere with the layout of the cable leads, which in a round cable is an equilateral triangle that balances the magnetic fields of the individual leads and cancels the effect of the fields on the other leads, which causes load (amperage) imbalance.
- The additional layer of armor protects the cap tube from installation (scraping) damage.
- The size of the cap tube ceases to be of importance.
- Multiple capillary cap tubes can be added to the base cable with the Baker Hughes patented concept.
- Better inventory management, as base cable can be modified to add the cap tube when required.

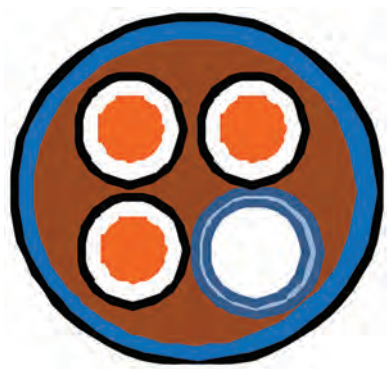

Fig. 19.33—Round cable with built-in cap tube.

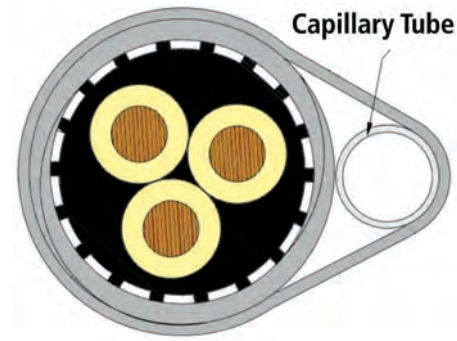

Fig. 19.34—Baker Hughes patent for cap tube cable.

The first two benefits are moot when constructing the cap tube into a flat cable, but the other benefits are in effect. In both cases, the second spooler truck is not required.

Multiple capillaries are added when treatments are simultaneously used for scale, corrosion, and/or other chemical issues. Sometimes additional cap tubes are used for other purposes such as providing air pressure for operating downhole tools. **Table 19.9** shows typical cap tube sizes with recommended pressure ratings.

When operating at high temperatures, take into consideration the de-rating factors for pressure ratings. For example, at temperatures in the order of 400°F, stainless steel tubing, AISI304 and AISI316, must be de-rated by 0.93 and 0.96 respectively. Copper, at only 200°F, must be de-rated by a factor of 0.80.

In certain cases, the chemicals involved for the treatment of even extremely harsh environments may warrant use of special materials in the cap tube. **Table 19.10** shows material recommendations including temperature limitations.

Of all the materials in this table, stainless steel (AISI 304 and AISI 316 are the most common types) and Monel® 400 are most likely used. However, Table 19.10 is useful in situations where a particular material may not be available

Table 19.9—Suggested allowable pressure for seamless stainless steel tubing.

Wall Thickness	0.028	0.035	0.049	0.065	0.083	0.095	0.109	0.12
1/8″ 0.1250″	8500	10900						
1/4″ 0.2500″	4000	5100	7500	10200				
3/8″ 0.3750″		3300	4800	6500				
1/2″ 0.5000″		2600	3700	5100	6700			
3/4″ 0.7500″			2400	3300	4200	4900	5800	
1″ 1.0000″				2400	3100	3600	4200	4700

Table 19.10—Tubing materials and general applications.

Tubing Material	General Application	Recomm. Temp. Range
Stainless Steel	High pressure, high temperature, generally corrosive media	-425°F to 1,200°F -255°C to 605°C
Carbon Steel	High pressure, high temperature oil, air, some specialty chemicals	-20°F to 800°F -29°C to 425°C
Copper	Low temperature, low pressure water, oil, and air	-40°F to 400°F -40°C to 205°C
Aluminum	Low temperature, low pressure water, oil, air, some specialty chemicals	-40°F to 400°F -40°C to 205°C
Monel 400	Recommended for sour gas, marine, and general chemical processing applications	-325°F to 800°F -198°C to 425°C
Alloy C276	Excellent corrosion resistance to oxidizing and reducing media and resistance to localized corrosion attacks	-325°F to 1,000°F -198°C to 535°C
Alloy 600	High temperature applications with generally corrosive media	-205°F to 1,200°F -130°C to 650°C
Titanium	Resistant to many environments such as sea water and salt conditions	-75°F to 600°F -59°C to 315°C

but substitutions are. ESP applications typically encounter temperatures in the middle ranges indicated in the table. So it is unlikely that temperature will be an issue when using capillaries with ESP installations.

When using capillary tubes, provide the operators and the field service technicians with all information regarding proper support for the operation. This includes installing and pulling instructions and how to manage the chemical injection process with input from the chemical treatment vendor. This also must include a process for handling short-term and long-term equipment shutdowns, with a view to preventing corrosion and/or cap tube plugging.

Recirculation Pump and Capillary Tubes

When using recirculation pumps, the tube used for the recirculation of fluid to the bottom of the motor is typically made up of multiple cap tubes. Most of the US uses a recirculation tube made up of three 3/8-in. cap tubes welded together and includes solid bars between them to provide mechanical strength and protection. The tubes are flattened to present a lower profile and allow for installation of larger motors in tighter casings.

The tube cross-section area is small, so it can become critical when any kind of deposition takes place inside the tubes. The gradual plugging of these tubes is quickly manifested by the increase in motor temperature as cooling deteriorates.

When scale or other deposition plugging occurs in the recirculation tube, it is possible to spot the chemical treatment in the tubes and allow these chemicals to protect the tubes, the motor, and the pump as they eventually migrate to the main pump intake. Although the chemical can be injected near the pump intake or below the motor directly, the concentration can be better managed by injecting straight into the recirculation head on top of the recirculation pump section

Table 19.11—Volume (Gal.) of fluid per 1,000 ft. of tubing.

	0.028	0.035	0.049	0.065	0.083	0.095	0.109	0.12
1/8″ 0.1250″	0.19	0.12						
1/4″ 0.2500″	1.54	1.32	0.94	0.59				
3/8″ 0.3750″		3.80	3.13	2.45				
1/2″ 0.5000″		7.54	6.59	5.59	4.55			
3/4″ 0.7500″			17.34	15.68	13.92	12.79	11.55	
1″ 1.0000″				30.88	28.38	26.77	24.95	23.57

(**Fig. 19.35**). This method is good for providing a discharge point for the chemical injection capillary tube.

19.3.4.3 Asphaltenes

Asphaltene exists in crude oil as dispersion of very small platelets (~ 35 Å). They are made up of the heaviest and largest molecules found in a hydrocarbon mixture, thus are most common in heavier crudes (low API gravity).

The platelets are held together by chemicals that form what is known as a micelle. As long as the micelles remain stable, asphaltenes do not readily precipitate. Certain chemical or physical interactions cause the micelles to break up. Then the particles agglomerate and start to stick together (flocculate), forming ever-larger particles and sticking to surrounding surfaces.

Asphaltenes display a preference for attaching themselves to bare metal surfaces. When the process starts, the asphaltene-impregnated surface tends to attract more particles more rapidly. Asphaltenes differ from paraffin in being insoluble in some common solvents such as kerosene, diesel, etc.

Fig. 19.35—Modified recirculation pump head, for cap tube insertion.

Asphaltenes also differ from paraffin in the complexity of their molecular makeup. **Fig. 19.36** shows a typical, very complex, molecular structure for a type of asphaltene, whereas paraffins are aliphatic, linear molecules. Methane is considered to be a paraffin, the lowest in molecular weight, as all paraffins follow the C_nH_{2n+2} formula. Average molecular weights for asphaltenes vary from around 1,000 to the millions.

This type of deposition is a problem with a high cost to handle anywhere from the vicinity of the wellbore region in the reservoir all the way to refinery feedstock pipelines.

Precipitation Mechanisms

- CO_2 (outgassing and pH shift)
- Acid treatments
- Turbulence, particularly mixing crude oil streams
- Changes in chemical composition that upset micelles
- Long-term crude oil storage

Asphaltenes will precipitate (flocculate) when certain chemical proportions are reached in the crude. Resin content in the mixture tends to prevent flocculation so a high resin/asphaltene ratio favors keeping asphaltenes from flocculating. Resins are usually heavy organic acids. **Fig. 19.37** illustrates the asphaltene phase equilibrium. Asphaltene stability also is compromised by pressure changes and shear forces in the fluid.

Effect of Asphaltene Deposition on ESPs

The impact of asphaltenes on ESP systems can be summarized in two words: plugging and heat.

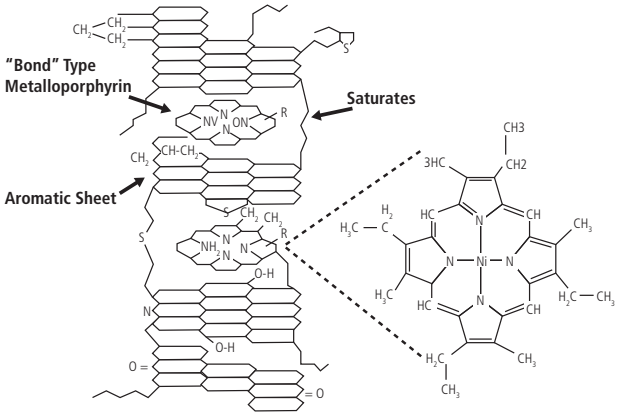

Fig. 19.36—Asphaltene molecule.

Pump: As flocculation occurs at the pump intake and within the flow paths of the pump stages, the particles stick to the rough metal surfaces and start building up almost exponentially, as the first thin coating seems to better attract further deposition. Buildup continues until the flow paths in the stages are blocked completely. This also has been observed at the pump intake and discharge (**Fig. 19.38**). As buildup occurs, the pump will start operating out of range, and the pump stages will wear in downthrust. When the pump plugs up completely or just partially, flow past the motor and seal may not be enough to maintain proper cooling. A proper underload setting may prevent a burned motor, but production may not be restored by chemical treatment, especially when the plug is complete. Using an intake screen can be risky as it may plug up in a very short time, due both to the small openings and to the pressure drop across the screen. Large wire mesh screens have been used at times in place of the standard perforated sheet metal screens, when they are absolutely necessary due to solids.

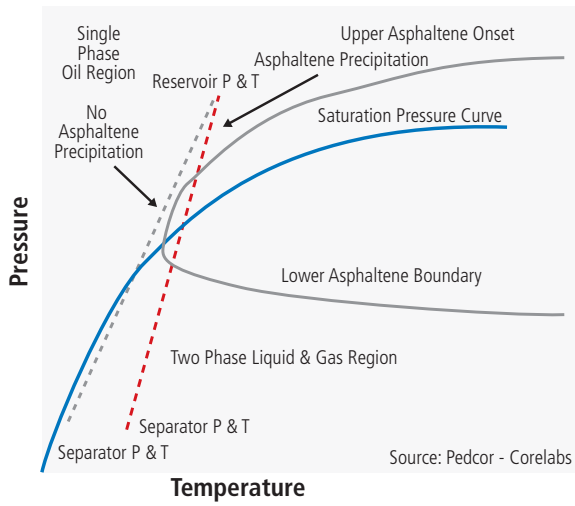

Fig. 19.37—Asphaltene phase equilibrium.

Motor and Seal: Both the motor and seal typically fit tightly in the casing or liner. When this happens there is a pressure drop in the reduced annular space that, compounded with the heat generated in both these components, will favor deposition of asphaltenes. The motor will start to get hot as heat cannot be dissipated normally by the well fluid passing by. This heat can lead to failure from electrical burns or from loss of lubrication in the rotor bearings unless a sensor is included that can trip the unit due to high internal temperature. If buildup is sufficient, it also will affect flow to the pump and cause operation in downthrust. The seal also can be affected in its normal operation. Apart from deposition causing a loss of heat transfer, the expansion capabilities will be reduced and eventually can be completely lost if the asphaltene covers the ports used for pressure and expansion compensation. When a bag is used in the top chamber, the area surrounding the bag also may be filled with asphaltene, thus preventing the normal expansion and contraction of the bag. If expansion and contraction is compromised, the motor and seal assembly will see vacuum conditions when cooling (motor shut down/cycling) and may draw in well fluids from sealed joints.

Cable: The motor lead cable and pothead are particularly sensitive to heat. When the pump and/or seal gets hot, the motor lead cable, which is in close contact with the housings, may also overheat. The motor lead cable tends to run much hotter than the main power cable, as it has a smaller gauge. Overheating is not only limited to the close contact with the housings but also is affected by asphaltene deposition around the pothead and parts of the motor lead cable itself. This prevents heat dissipation, exacerbating the problem.

Fig. 19.38—Asphaltene plugging in pump.

Prevention and Remediation

Due to asphaltene solubility being very low, the best way to combat this problem is to prevent precipitation in the first place. It is very hard to remove once present.

If the operator encountering asphaltene problems is willing to start from scratch, analyze the fluids (heavy hydrocarbons) to understand the deposition mechanism. Laboratory work and statistical modeling can allow for construction of the heavy organics deposition envelope (HODE). Such an analysis benefits the operator in finding up-front solutions to the problem. For example, laboratory testing has demonstrated that if the crude oil contains enough resin concentration, the resins are absorbed by the asphaltene micelles (forming colloids) and no amount of fluid perturbation will cause the asphaltenes to flocculate and form depositions on metallic surfaces.

However, in most cases, such finesse, or such luck as to have enough resin in the fluid, is hard to come by and chemistry must contribute to the solution.

Production method changes are the first approach to controlling asphaltene flocculation, but these techniques usually mean reducing mechanical shear, an unlikely approach if using ESPs, or minimizing pressure drops, also impossible if well production is to be optimized.

The next approach involves attacking the flocculation mechanism by making it hard for the flocculated particles to stick to the surfaces. In our ESP world, this means using coatings to increase the slickness of the surfaces and simultaneously covering the metal substrate. (See the section on coating.)

Although asphaltenes are referred to as insoluble in most solvents, these are mostly aliphatic (linear carbon chain) solvents. The use of aromatic solvents such as toluene and xylene has been found to be effective both in precipitation prevention and in remediation or cleaning out for asphaltene deposition.

The asphaltene problem in the ESP unit is well handled by slick coatings, which can be applied not only on the individual pump stages but also on the surface of other system components.

19.3.5 Coatings

A number of coatings have been tested over the years and new ones are occasionally added as new vendors offer new ideas or similar solutions for a coating already tested.

Coatings have been suggested as solutions for a variety of situations, such as:

- Abrasion
- Corrosion
- Scale deposition
- Paraffin and asphaltene deposition
- Efficiency enhancement

Some coatings have been able to solve more than one of the situations indicated above. Some have been better at one or the other with just a minor change in the composition or technique for application onto the substrate material, which in most cases has been the Ni-Resist Type I metallurgy.

19.3.5.1 Fluorocarbon-Based Coatings

Based on a fluorocarbon chemical composition (similar to polytetrafluoroethylene or PTFE, most commonly used as a coating for cookware), these coatings are applied by a process similar to spray painting and can penetrate the stage vane openings and cover the entire flow path. The painted stage is then placed in an oven and heated to a temperature sufficient to cure the PTFE-based coat and allow it to firmly adhere to the metallic substrate. The coating formulation and heat-treating process are proprietary to the vendors who apply these coats for Baker Hughes.

ARMOR I

This fluoropolymer coating is used mostly for its non-stick characteristics, making it the choice coating for applications with scale and/or paraffins and asphaltenes. The coating is resistant to a number of organic and inorganic compounds and is capable of withstanding temperatures up to 500°F (260°C) in continuous use.

19.3.5.2 Metallic Bond Coatings

Abrasion protection has been a driver for testing a number of coatings and heat treatment for the pump stages. Having achieved extremely satisfactory results with the Baker Hughes AR bearing family of products (ARS, ARM, AR 1:1, SSP, SND, SHD, SSD, and SXD), the wear focus shifts to the stage material itself, as the bearings outlive the base stage material.

Tungsten Carbide

This coating is tungsten carbide material, applied by the high-velocity oxygen fueled (HVOF) process, also known as flame spray.

It provides a very hard surface but the process by which it is applied presents a large disadvantage. The coating only is applied properly in areas where there is line-of-sight (~ 45° maximum application angle), i.e., it cannot be placed in the internal flow areas of the pump stages.

This coating has showed very good results in areas where there is three-body erosion.

ARMOR X

To date this nickel boride based coating appears to be the most cost-effective solution to abrasive wear (cost versus wear resistance), with the tungsten carbide coating being another option if the customer should require one.

This coating currently is being recommended for applications where the additional cost is well compensated by improved run life results such as in offshore applications and other costly well interventions.

The electroless nickel boride coating exhibited an increased wear resistance, compared to the standard stage, when subjected to the accelerated abrasive environment of the slurry loop. In the case of the diffuser bore and the impeller skirt, there was a dramatic difference with respect to abrasive resistance of the coated versus the non-coated stage.

The standard coating thickness for ARMOR X coating is 4 mil. To avoid pump rotational interference and stack out, the stages that will be coated this way have to be pre-machined to remove material, thus achieving standard dimensions after the coating has been applied. Both the required pre-machining and the coating itself, make ARMOR X coating an expensive solution. Tests are currently being carried out to some extent and more are planned to determine the value of a 1 mil and a ½ mil coating, both of which will not require the pre-machining and will be much more cost effective.

The nickel boride coating, as well as other abrasion resistant coatings (implemented or not implemented to date), is intended to be supplemental to the existing AR pump lines and not intended to replace the tungsten carbide bushing/sleeve sets used in the AR stages. The abrasion resistant coatings are to be used with the existing AR designs.

19.4 Temperature

Temperature affects ESP equipment in many ways, but the most common issue lies with the motor, as insulation life is affected by high temperature. However, in certain conditions, temperature may affect other components as well, as in any part of the system that includes elastomers.

Temperature issues are of two main types:

- Those arising from the reservoir/well temperature (bottomhole temperature or BHT) being high
- Those caused by heat generated by the ESP unit itself.

19.4.1 Natural Reservoir Temperature

When looking at reservoirs around the world, depth alone is not a good indication as to what to expect regarding the temperature at the bottom of a producing well. The thickness of the earth's crust has an enormous impact on reservoir temperature. For example, in the Permian Basin, where the earth's crust is relatively thick, a reservoir located at a depth of 10,000 ft. may only have a bottomhole temperature of 175°F. However, when looking at temperatures in the Bakken formation in North Dakota at the same depths, the temperature will be in the order of 240°F. Reservoirs in other parts of the world at similar depths can exceed 300°F.

These different geographical areas all have different geothermal gradients, the rate that temperature increases with depth (**Fig. 19.39**). The thermal gradient in a large geographical area can present local changes, as the earth's crust has inverted hills and valleys. In some relatively small area there may be an outcrop of magma, particularly in areas with active volcanism. The Rocky Mountains in northwest Wyoming is an area slated to be sitting above a super volcano that erupted ages ago and could potentially do so again.

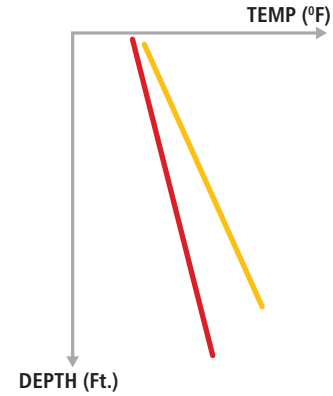

Fig. 19.39—Earth's thermal gradient.

For different geographical areas of the world, the geothermal gradient typically varies between 1.2 to 1.8°F/100 ft.

Knowing the geothermal gradient can help to determine the bottomhole temperature of a well or field that is planned for ESP production but has not yet been drilled.

19.4.2 Heat Generated by Electrical Submersible Pump Equipment

Heat is generated by the flow of electricity and by friction. Thus the main cause of heat generation is the ESP motor, which converts electrical energy to mechanical rotation. As the conversion process involves strong magnetic fields, heat being generated in the motor is found by losses in the electrical circuit inside the motor (i2R losses); losses due to magnetic induction in unintended components of the motor (Eddy current losses); and friction losses. All of these generate heat. The motor is designed to keep all these losses at a minimum. However, to get an overall idea of what these losses represent, consider the motor's overall efficiency, which is in the order of 87%. This means 13% of all power provided to the motor is lost as unwanted heat. Some very minor amounts of energy are lost as sound, vibration, etc. If an ESP motor is rated at 400 HP, this is power output of 87% of the power supplied to the motor. So the original power supplied to the motor in the form of electricity is 400/.87 = 459.77 HP, i.e., 59.77 HP is lost. This is equivalent to a little over 152,000 BTU.h of heat. This heat is removed by the produced fluid flowing by the motor, with some of it warming the motor before the heat generated and heat removed are balanced out. The balance is altered by the fluid rate and characteristics, with water having a higher specific heat (capacity to remove heat) than oil, which in turn is higher than that for gas.

The motor and the seal section, which are in open contact internally, share the same oil. Thus the temperature in the seal section will be similar to the motor temperature. In the bottom of the seal, where the thrust bearing is located, there will be additional temperature rise due to the friction in the bearing.

19.4.3 Heat Generated during Abnormal Operating Conditions

The paragraphs above refer to the best and/or design conditions, where the generated heat is taken into consideration and based on information drawn from AutographPC software, the standard or special materials can be selected to handle the temperatures that are expected in the system.

However, many situations cause overall heating in the ESP downhole unit and/or local heating and hot spots.

Improperly loaded motor. The best efficiency point of the ESP motor is obtained when it is approximately 100% loaded. If a motor is operated at a lower load requirement, the current going through the motor will be reduced and the motor will usually operate slightly cooler. However, further and further away from the optimal load (100%) the efficiency of the motor will be reduced and will generate more heat per HP, even though the overall heat output will be reduced. Depending on the bottomhole temperature of a given well and the load on a motor, application engineers may use underloaded motors to prevent temperatures from going too high. A properly de-rated motor is one in which HP, voltage, and amperage have been changed to preserve optimum electromechanical conditions in the motor frame. A properly de-rated motor achieves the temperature objective while maintaining good efficiency.

An overloaded motor will do the opposite. As the motor is loaded further, the amperage rises and the i2R losses increase, while at the same time magnetic losses increase and more heat is generated. The result is an increase in heat output and, therefore, motor temperature. The induction motor's characteristics allow it to put out increasing amounts of power as the load increases, easily beyond design/nameplate limitations, to the point that the motor will burn up at some point unless a device is used to limit the power output by shutting down the power supply to the motor. The application must take into consideration any type of change in the fluid or operating conditions that may make the power requirement increase unexpectedly, such as a change in fluid specific gravity, friction, etc.

To manage temperature issues in a motor and in the supply cable, select the motor with the highest voltage rating for a given power output, as this will ensure that the default current is the smallest for the given application. For low horsepower applications such as found in the later phases of shale wells' production, special motors are being built (and others may be required) to provide high voltage options for low horsepower requirement.

Overloading cables. The main power cable string and the motor lead cable may be overloaded if not sized properly. Although the first consequence of an overloaded cable can be a burnt cable string if the temperature rating of the cable insulation is not correct (i.e., picking a low temp cable with a plastic such as polypropylene ethylene or PPE) insulation, there will also be an unnecessary power loss that

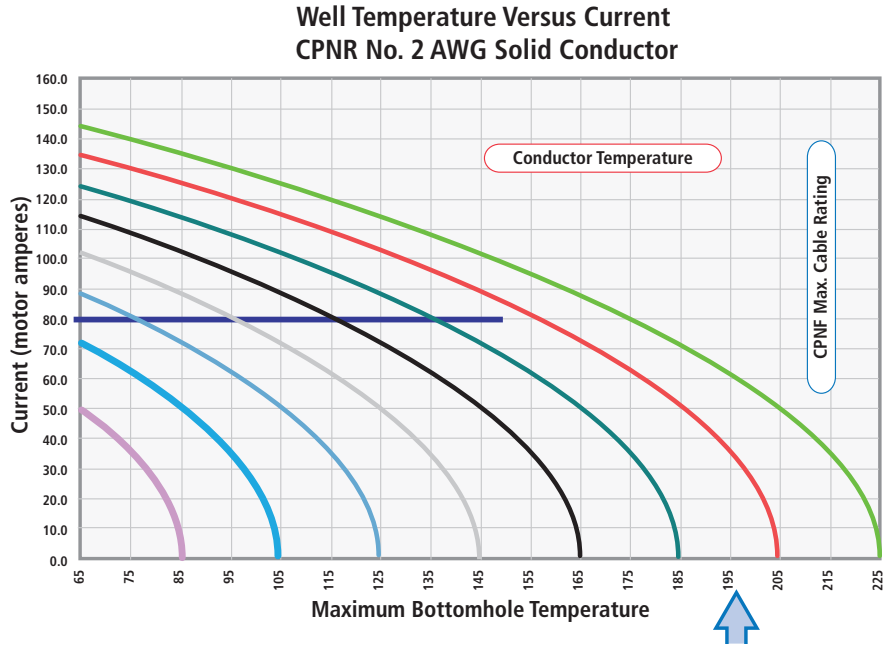

Fig. 19.40—Ampacity curve for #2AWG CPNR cable.

can translate to a very large amount of wasted dollars and additional heat in the system, although most of this heat will dissipate upward and away from the downhole equipment. Standard practice is to keep design voltage drop below 30V/1,000 ft. of cable. AutographPC software does all cable sizing, including calculations for power loss. As mentioned above, a high voltage motor will have low amperage, thus benefiting cable sizing. The smaller the cable that can be used efficiently, the happier the operator will be as cable is usually the most expensive component of the ESP system given the current high prices of copper.

Fig. 19.40 shows a typical example of what is known as an ampacity curve. This gives an idea of the heat generated and dissipated in a typical ESP cable. These curves differ according to conductor size and the insulation and jacket material surrounding the conductor (example is for No. 2 AWG solid copper conductor with polypropylene insulation and nitrile jacket, built in round configuration) and allow for conductor surface temperature calculations based on the motor amperage and the well bottomhole temperature. In the example provided by the intersecting dark and light blue lines, a current of 80 amps and a bottomhole temperature of 140°F gives rise to a conductor surface temperature of 195°F. An application engineer might be tempted to select a low-temperature insulation for this application but it would be much safer to pick ethylene propylene diene monomer (EPDM) instead. As for selecting a motor lead extension, choose the highest cable temperature rating possible, as the motor lead extension may be subjected to moments of very high temperature if the pump runs dry for any period of time (see next section).

Operating the Pump in a Gassy Environment without Proper Underload Protection. The pump and motor (also the seal and pothead and sensor, if in use) are constantly being cooled by the well fluid that is being pumped. Even though the fluid may be relatively hot, the components of the ESP system are running hotter and yielding heat to the fluid as it goes by. If the pump gas locks, the surface controls normally sense this condition and shut in the ESP unit. If the underload is not set properly, is not activated, or does not work at all, the motor will continue to operate without fluid going by and the pump will run dry. Needless to say, all the components in the system will quickly overheat and suffer severe thermal damage. Setting the underload limit may be simple and usually is done after the pump is running with a somewhat stable current reading. A value between 10% and 25% below this stable current is normally all it takes to safely detect when gas is causing a gas locked pump. However, the application engineer plays a part in the correct sizing of the motor to ensure that these settings are even possible. Induction type electric motors, the type used with ESPs, have a minimum current produced by the magnetization of the rotors to turn the motor. By virtue of this characteristic of induction motors, it is easy to establish a minimum (no-load) motor amperage.

To make sure there is room for the underload to activate, the motor selected for the job must not be so large as to be operating with normally loaded amperage that is too close to the no-load current. To be safe, the running load should be a minimum of 50% of nameplate.

In our industry it is a common practice to re-rate and de-rate motors based on operating temperature and often also due to inventory restrictions. De-rating a motor to a smaller horsepower value, by reducing nameplate volts and amps does not proportionally de-rate the minimum magnetization current. Once the ESP is assembled and run in the well, there is also a no-load condition for the ESP assembly when it is turning without a load, that is, when not pumping fluid to the surface. This no-load condition is almost identical to the condition in which it will operate when pumping gas. Although a gas locked pump is not normally full of gas as most of the upper stages still contain liquid and is holding the fluid column in the tubing string, it is not performing the same amount of work. Another situation, in which the pump is not doing quite the same work but is still loaded, is when there is excessive head on the pump (as may occur if a well valve is closed while the pump is running) so the pump is holding the column of fluid but also generating pressure at the wellhead.

The underload must operate in all of these conditions. The application engineer must ensure that the normal load on the motor is not too close to these values, or there is no room for a proper field setting to protect the downhole unit. The final setting of the underload is the responsibility of the installing field technician.

Effect of Running in Unloaded Condition. If no fluid is going past the motor to cool it, the heat developed will continuously increase the temperature of the motor until a new heat transfer balance is reached, unfortunately at a temperature that damages the motor. The high temperature reduces the viscosity of the motor oil, with possible consequences to bearing lubrication that can result in excessive bearing wear or even a bearing locking up completely. This also affects the insulation materials, causing them to age prematurely or even fail completely, in which case the motor burns, usually in the main coils, coil end turns, or in the lead wires going up to the motor insulation block. In a tandem motor, motor-to-motor leads may burn.

However, not all no-flow conditions cause a motor burn. The motor generates less heat when in the underloaded condition. If the downhole temperature is low enough or if some gas is circulating by the motor, a heat transfer balance may be reached in conditions that do not permanently damage the motor.

The pump is also at risk of damage in a situation in which no fluid goes through the pump. The pump stages are agitating the fluid continuously without this fluid being changed out or exiting the pump and being replaced by a cooler fluid from the well. The pump bearings (NiResist or tungsten carbide sleeves and maybe downthrust washers) also are heating from friction and not being properly cooled. Thus this fluid and the bearings keep warming until they reach some heat transfer equilibrium. The heat generated in the pump depends on the type of fluid, the speed at which the pump is rotating, and the pump construction (floater, SND, SSD, etc.). It is amazing how much heat can be generated in the pump, sometimes more than in the motor. Viscosity is a big factor, although in most electric submersible pump applications, viscosity is low, usually between about 1 and 3 Cp.

Apart from causing damage to the pump bearings, the pump can get so hot that it will damage the motor lead cable that is strapped to it. In extreme conditions, motor lead cables with lead jackets have had the lead melt and collect in the armor and in a pool around the pothead.

Indications of heat in the pump can go from brittle (cooked) downthrust washers around 400°F to the washers disappearing completely and heat checking can be observed in tungsten carbide sleeves. Tungsten carbide sleeves can be damaged by the extreme heat caused by running dry in the lower stages of the pump that has gas locked. Most of the stages are still generating head to support the fluid column in the tubing string. The end result is that bearings crack or flake and pieces run through the other pump stages and/or bite into the pump shaft, causing the shaft to wear and break.

Low Well Production. Heat starts causing a problem long before a well is pumped off or gas locked. The mere loss of production in a well (loss of productivity over time and/or due to wellbore damage) can start reducing the flow around the motor to the point that the temperature of the motor rises ever so slowly as the problem increases. The surface controls of the ESP system can be set to shut the unit down when the amperage is close to a no-load condition or when the temperature exceeds a preset limit (provided the proper sensor has been installed with the system). In these cases, the problem usually affects the motor before the pump if the condition is steady such as low flow with or without gas, but if with gas, not enough to gas lock the pump.

No load conditions must be solved by shutting down the unit or if the issue is a gas lock/gas slug condition slowing down the unit until the gas slug is cleared. Working the ESP system with a gradual loss of production should be a planned situation in shale plays, where the drop in production is inevitable with time. If the ESP system is to be successful in a shale play application, it must be able to handle low-flow regimes, and usually with abundant gas production.

19.5 Well Depth

Well depth is a feature of the well related to the depth at which the oil-bearing formations are found. These formations may evolve geographically in a horizontal plane where they start out shallow and gradually sink over distance to where the same formation may be found even at the surface in a state or county and be found at a depth of thousands of feet a few hundred miles away. An example of this is the Bakken shale that can be found at depths in the order of 5,000 ft. in Canada (Manitoba and Saskatchewan) but at depths exceeding 10,000 ft. in northern US in North Dakota and Montana. Well depth can create difficulties for ESP installations.

If the formation is over-pressurized and/or has high productivity, it may not be necessary to draw the fluid down significantly to achieve good production. There may be very serious reasons not to draw down too strongly as the pressure drop in the well and in the surrounding reservoir volume may have consequences such as water coning, sand influx, fracturing sand, and fracture collapse.

However, over time, reservoirs start losing their energy and it may become necessary to draw fluid levels down very deeply to achieve economic production.

When this is the case, have a good casing size that has the capability of putting enough jewelry downhole to get the job done.

Problems occur when a deep well has a casing of small diameter because a large amount of horsepower may be required to drive a long pump with many stages to achieve the desired production. When this happens, limitations with motor size, shaft horsepower ratings, or even pressure limitations in the housings, especially the pump housing near the top of the pump are encountered. Another issue is cable size, as it affects voltage drop and thus the voltage at the motor terminals. If the voltage drop is too large it will reduce the motor torque capacity. The ESP unit may not be able to start, especially if it is worn or there is sand accumulation in the pump.

19.6 Production Decline (Depletion)

Production decline is typically seen in all oil and gas wells, but the difference with the unconventional, particularly shale plays, is the speed at which decline takes place. As mentioned earlier, the fracturing process opens a small reservoir within a reservoir, called the stimulated reservoir volume (SRV). This volume is quickly emptied, although the fracturing network allows for the filling process to continue but at a slow pace, thus reducing the productivity of any given well.

This poses a challenge for ESPs, as centrifugal pumps operate effectively and efficiently within a limited range, albeit some better than others. When decline is very quick, it is hard to find the right pump or even a combination of two pumps that will fit the production profile adequately, as the production range may extend way beyond the normal pump range within a period of time that is usually much shorter than the expected life of the equipment.

The challenge has to be met with the right combination or a new type of pump yet undeveloped that may provide satisfactory performance.

Experience so far in the shale plays, particularly in the Bakken shale in North Dakota, where Baker Hughes has a large number of ESPs in operation, has been that ESPs are used only in the initial phase of production. Then, after production declines, operators choose to use rod pumps or gas lift and plunger pump combinations.

If the ESP is to become the artificial lift system of choice, find a pump with a wider operating range and a pump tough enough to handle the production of fracturing sand and survive frequent gas slugs. The latter also will be a requirement for the rest of the ESP equipment such as motor, seal, and cable, as the issue with slugs becomes one of high operating temperatures.

Selecting the right motor for the application also is a challenge. If the right pump is selected it provides a wide range of operation and the horsepower requirement drops significantly as the production rate drops, even though the pump efficiency declines as it operates further and further out of its optimum range. The most common practice is that of re-rating a specific motor frame (number of rotors/ horsepower rating) for the initial part of the production cycle and then gradually de-rating as horsepower requirement diminishes.

19.7 Oil Producing Unconventional Plays in the US: Electrical Submersible Pump Experience

This section covers the unconventional plays in the US that are produced with artificial lift and have significant use of ESPs.

Baker Hughes has installed many ESPs in the Bakken, Niobrara, and Eagle Ford shales and also in the Mississippi Chat. Canada also has had experience with ESP installations in the much shallower Bakken and in the Cardium shale. Results have been good, but most operators perceive ESPs to be a good choice for an artificial lift system when production rates are high and then look to rod pumps for lower rates and even for the long haul, after the ESP unit has drawn the reservoir down significantly. Baker Hughes is working diligently to change that perception and is developing better equipment and techniques for achieving a better run life and operational efficiency though not necessarily energy efficiency. The Flex 3.2 pump has made some inroads in this respect. In some deep applications where rods tend to fail frequently, the Flex 3.2 has put ESPs in the forefront again.

While Baker Hughes is working with ESP applications, operators are working on such critical issues with significant cost impact as reservoir characterization, resulting in decisions for well direction, toe-up or toe-down configuration, and the amount of fracturing stages to implement. Other choices, such as the bit type and fracturing proppant, also have a large impact on the time to complete the well and ensuing production efficiencies.

It is a requirement to keep track of ESP performance on a daily (or close to) basis to watch the evolution of the wells (quick depletion) and to anticipate any problems with the unit in the well. The use of remote supervision technology has been instrumental in this process. The necessary equipment must be implemented at the start of any ESP installation in any unconventional oil play well.

There is occasionally news of new unconventional plays or extensions of existing plays, and it may take a while before the dust settles on the subject of gas and/or liquids-rich unconventional/shale plays. What is learned in the US, unquestionably the country with the most knowledge and experience regarding unconventional plays, also will have a significant bearing on production from similar formations on a worldwide scale.

19.8 Gas Handling Theory

This section discusses the problems associated with gas and how such problems could affect the performance of ESP systems. Some solutions are presented on how to handle such situations.

19.8.1 What Is Gas and Where Does It Come From?

Gas evolved along with oil over geological time, as a result of the pressure cooking of biological matter (tiny organisms and/or vegetation) that accumulated along with other rocky sediments (detritus) and got buried over time under thousands of feet of rock. Depending on the type of sediment (organic and inorganic) and other factors, different types of rock were formed. The layers of rock that accumulated or were cracked, overturned, and/or mixed by volcanism, ended up with different configurations that vary with distance along the surface of our planet. Some porous rocks contained biological material that developed into gas, and others developed into liquid hydrocarbons. Although there are fields where only gas can be found, generally there is a mixture of both. When this happens, gas being the lighter phase, is typically found at the top with oil below. If water has migrated into this particular type of rock, it underlies the other two, being the heaviest of them all.

The gas is made up of the lighter hydrocarbons, mostly methane, but ethane, propane, and butane, and sometimes slightly heavier hydrocarbons can be found in decreasing amounts. Other gases that may be present in the mix are hydrogen, nitrogen, hydrogen sulphide (H_2S), and carbon dioxide (CO_2).

A substantial part of the gas found with oil will be dissolved in the oil, regardless of whether there is a separate purely gaseous phase.

So, where does gas come from? The answer has been given above. However, to better understand how it affects oil production, more explanation is needed to learn more about reservoir types and gas and oil behavior.

Reservoirs produce oil naturally (flowing wells) when the pressure in the hydrocarbon-bearing rock formation is high enough to push the fluid up the well to the surface. As pressure drops over the lifetime of a well/reservoir, an artificial method is required to produce liquids to the surface. This method can affect the whole reservoir such as injecting fluids to raise/maintain pressure or individual wells through artificial lift methods.

There are three types of reservoirs: gas cap drive, solution gas drive, and water drive.

Gas Cap Drive: A gas cap is defined above the liquid phases in the reservoir. **Fig. 19.41** shows what this would look like, though the formation is not a big cave or hole, as the graphic seems to indicate. Rather, all this occurs in the porous space inside the rocks. The gas is a compressible fluid and will readily expand as liquid is drawn from below it. Thus pressure is maintained for a long time while the gas cap is decompressing. At some point gas may migrate into the wellbore, or, as time goes by, the liquid fluid level will drop until the gas/liquid interface reaches the wellbore perforations. Gas production will increase dramatically at this point.

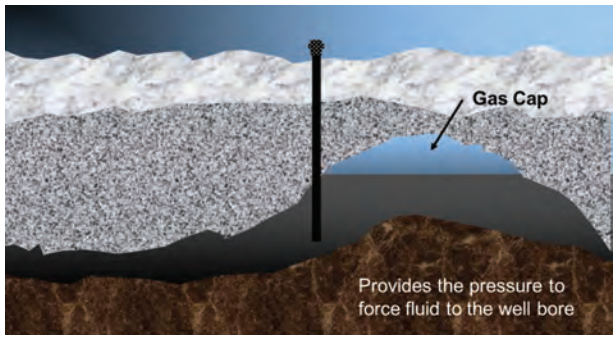

Fig. 19.41—A typical gas cap drive.

Pressure drops, well productivity drops, and the gas-to-oil ratio produced (GOR) increases quickly. Water cut, which is the percentage of water in the oil, may increase gradually, but water may not even be present in some rare cases.

Solution Gas Drive: The gas dissolved in the oil expands slightly as pressure drops, providing a momentary mechanism for maintaining pressure. However, this volume change is small.

At some point in the reservoir life-cycle, gas starts breaking out of the oil. This occurs when the pressure in the reservoir reaches what is known as bubble point pressure, which is the pressure at which gas dissolved in oil will start forming small bubbles, thus releasing the dissolved gas. This mechanism can help drive the reservoir energy to produce a reservoir.

Although the reservoir may remain above bubble point pressure (BPP), pressure falling in the well as it is being produced will usually fall below BPP and gas will be released in the well, thus affecting production. The effect will be positive or beneficial as it breaks out in the tubing string, progressively lowering the specific gravity of the fluid in the column and making the fluid lighter, thus helping existing pressure to move the fluid to the surface. However, if the well is being produced with some method of artificial lift, the effect may be negative as the free gas may affect the producing mechanism. This is the case particularly with ESPs.

Water Drive: A water layer, subjacent to the oil and gas layers, is connected to a larger source of water such as a larger reservoir, sea, ocean, etc., and provides pressure to the oilfield reservoir. In the case of water drives, reservoir pressure is maintained at a stable rate over a long period of time. Oil and gas are produced and eventually run out after which most of the reservoir rock is filled with water.

19.8.1.1 Bubble Point Pressure

As mentioned above, reservoirs usually contain oil, gas, and water, in varying proportions. In most cases, a recently discovered reservoir will have a high reservoir pressure, enough to keep the gas phase dissolved in the oil and maybe a small portion in the water. As pressure falls over time as a result of production, pressure in the reservoir may come down so far as to reach BPP. This pressure is the point at which the first bubble of gas will come out of the oil. For example, it breaks out of solution. This will usually change the production characteristics of the reservoir or field as the gas slows the flow of the fluids inside the reservoir rock.

Regardless of reservoir pressure issues, the conditions in a well will be far more dynamic. When a well is drilled and perforated, the pressure at the perforations is generally very close to the reservoir pressure and is called the well's static bottomhole pressure, the pressure in static conditions. As the well is produced the pressure in the well will start falling and obeys some form of characteristic curve (the well productivity index). This index may be linear in most cases. If the pressure in the reservoir or in the area surrounding the well is below BPP, the function will be known as the Vogel curve. As pressure is drawn down in the well, it will likely rapidly approach and go below it, thus releasing gas. The further pressure is drawn below BPP, the larger the volume of fluid will be to produce the same volume of liquid (oil and water).

19.8.2 Why Is Gas a Problem for Electrical Submersible Pumps?

Centrifugal pumps generate lift by rotating the pumped fluid at high revolutions and converting the rotational energy into potential energy. Centrifugal pumps were designed to pump liquids, which are basically incompressible, and thus the rotating equipment (the pump stage impeller) imparting energy to the fluid, operates effectively and somewhat efficiently. Centrifugal pump efficiency is not high when

compared to positive displacement pumps, due to friction and recirculation losses in the impeller and diffuser. If a compressible component or fraction is added to the fluid, the pumping process will deteriorate.

The presence of gas in a centrifugal pump has several adverse effects, as follows:

Head reduction due to volumetric increase. The increased volume throughput, when adding the free gas component, moves the operating point of the pump to the right of the gradually descending head curve (**Fig. 19.42**). Thus more stages will be required to provide the necessary lift.

Gas blocking. This phenomenon occurs in the impeller of the pump. Gas bubbles in the fluid tend to separate and accumulate in the low-pressure area of the flow path (**Fig. 19.43**) behind the impeller vanes. They form a gas pocket that eventually interferes with the flow by blocking part of the area of the flow path. Depending on the amount of gas going through the pump, this condition may stabilize although there is a dynamic and constant transfer of fluid of both phases at the interface of the two. Or it can worsen as conditions change over time.

At some point the pump may start surging. Surging occurs when the deterioration of pump performance leads to a slowing of the fluid coming into the pump. As this happens, gas at the intake tends to separate a little better by natural separation and a denser fluid with a higher proportion of liquids enters the impeller. This improves the pump's performance, and the rate into the pump increases, fluid velocity increases, natural separation worsens, and the cycle repeats over and over. A sign that this is happening is the change in the power drawn by the ESP motor, which translates to fluctuations in the amperage. These fluctuations are usually read or charted electronically or on paper.

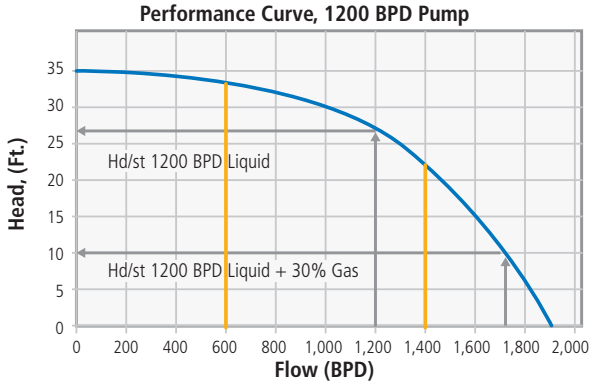

Fig. 19.42—Increased fluid volume through the pump due to free gas.

Gas locking. If gas continues to enter the impeller faster than it can be expelled by the rotational forces, it accumulates until a point at which centrifugal forces separate the liquid phase on the impeller outside perimeter from the phase which remains at the center (**Fig. 19.44**). At this point the pump stops moving fluid; the pump cannot generate enough momentum in the gas to move the liquid along. Also, the pump is not generating enough head or pressure to move the liquid column up the tubing string, so no fluid reaches the surface and production ceases altogether. The pump is turning and consuming energy, which converts to heat, potentially damaging the pump and/or the motor and/or the motor lead cable, unless the controls can detect the gas lock condition and shut off the unit.

The pump cannot push the gas the same way it does the liquid. Pump stages develop head, regardless of the fluids specific gravity, this head will be the same. The pressure generated by the pump is a result of that specific gravity. As the specific gravity of the gas, in conditions typically found at the base of the pump, is about 1% of the liquid's specific gravity, the pump would have to turn much faster to generate the same pressure and momentum to displace the liquid (about 10 times faster).

Cavitation. This is not a phenomenon normally associated with ESPs. An exception is considered for horizontal pumping systems (HPS) as will be explained a little further on.

Cavitation normally occurs when a single liquid substance is being pumped or moved in any other way with

Fig. 19.43—Gas blocking.

Fig. 19.44—Gas locking.

rotational equipment. Propellers in large ships and boats can be affected by cavitation. The fluid, water is typical, can evaporate at the lower pressure side of the impeller and the small vapor bubbles then pass onto an area of higher pressure where they collapse again to the liquid phase. This collapse can be very violent although the bubbles are small and cause stresses in the materials to the point that a single bubble collapse may remove material from the surface of the impeller or propeller that is in contact with the bubble when it collapses. When dealing with mixtures of water, oil, and gas, a different phenomenon is occurring, where the gas bubbles compress or get dissolved in the oil and to a much lesser degree, in the water so the associated stresses are nonexistent or minimal.

In horizontal pump applications, the pumped fluid may be water and in some cases pressures may be low to the extent that cavitation may occur and should be prevented whenever possible.

Having looked at the problems caused by gas, the next step is to understand when this will happen and does it affect any and all ESP installations in the same way.

Different stage designs handle gas differently and special stage designs are available to do the job more effectively and efficiently. Another factor is the ability to handle gas in an ESP pump stage as the pressure of the fluid at the intake varies. See the Gas Handling section.

The application engineer faced with a gas problem needs to calculate the free gas at the pump or gas separator intake that will be present at the desired operating conditions. The right equipment to produce the well in the desired conditions will depend on this.

Calculate is probably not the right word to use, as all these operations will be done with software. Baker Hughes application engineers use AutographPC software, our proprietary application simulation software, and will rarely come across other available commercial software packages for ESP sizing.

AutographPC software issue will do all free gas calculations and other volumetric analyses, resulting in rates before and after separation when separation percent is put into the relevant box.

For application engineers and individuals who get involved with equipment sizing, no attempt should be made to manually calculate pump intake conditions when gas is present. Water well calculations are very simple, though.

To get an idea of how the intake conditions are calculated, a process and some gas calculation formulas is shown, based on gas correlations by Standing (1981):

1. Obtain pump intake pressure (PIP) from Vogel's inflow performance relationship (1968):

$$Q_{omax} = \frac{Q_o}{1 - 0.2\left(\frac{P_{wf}}{P_r}\right) - 0.8\left(\frac{P_{wf}}{P_r}\right)^2}$$

2. Calculate gas in solution (Solution gas-to-oil ratio, Rs) at intake conditions:

$$Rs = Yg\left(\frac{PIP(10)^{.0125\,(API)}}{18(10)^{.00091\,(T)}}\right)^{1.20482}$$

where:

PIP—Pump Intake Pressure
Yg—Gas Gravity
API—Oil Gravity, API Degrees
T—Pump Intake Temperature, °F

3. Calculate oil formation volume factor (FVF or Bo) at intake conditions:

$$Bo = .972 + .000147\left(Rs\left(\frac{Yg}{Yo}\right)^{.5} + 1.25\,(T)\right)^{1.175}$$

where:

Rs—Solution Gas-Oil Ratio
Yg—Gas Gravity
Yo—Oil Gravity
T—Pump Intake Temperature, °F

4. Calculate gas formation volume factor (Bg) at intake conditions:

$$Bg = \frac{5.04(Z)(460+T)}{PIP + 14.7} = \frac{BBL}{MSCF}$$

where:

PIP—Pump Intake Pressure (psi)
T—Pump Intake Temperature, °F
Z—Gas Compressibility Factor (to be obtained from Z charts)

5. If the water cut (%) is large and pressure and temperatures are high, it is also convenient to calculate the water formation volume factor, Bw:

$$Bw = (1 + \Delta Vwp)(1 + \Delta Vwt)$$

where ΔVwp and ΔVwt are obtained from the following charts:

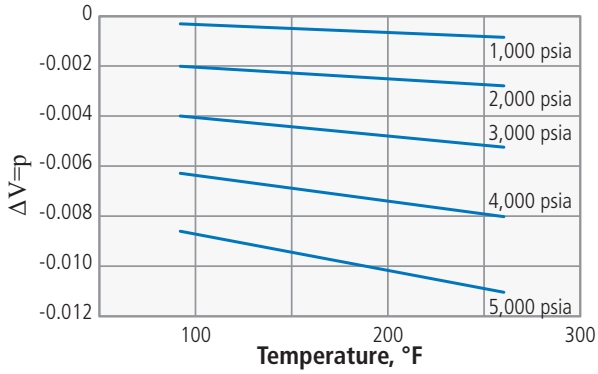

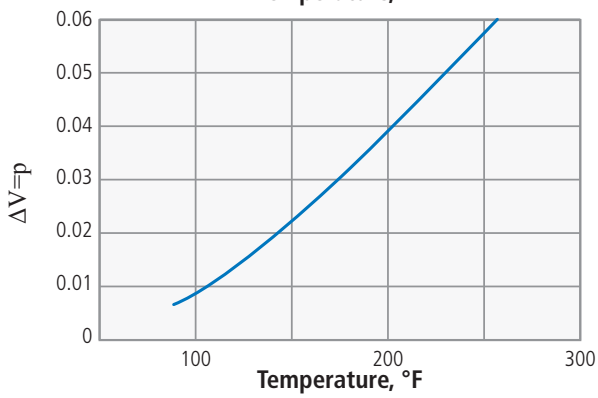

6. The total volume at the pump intake in reservoir barrels per day (RBPD) can now be calculated, per:

$$RBPD = Qo*(1+Bo)+Qw*(1+Bw)+Qo*Bg*(GOR-Rs)$$

7. To calculate the free gas, the final calculation is:

$$Qo*Bg(GOR-Rs)/RBPD$$

The complications involved in this calculation give an idea of the even greater complication of doing the whole ESP sizing by hand. To do so, the following process is required:

- Calculate the reservoir barrels per day as indicated above.
- Using specific gravity data, calculate the mass of the fluid entering the pump.
- Divide mass by volume to obtain the specific gravity of the mixture.
- Using gas lift curves for pressure profiles (as a function of total production rate, oil API gravity, water cut, tubing size, tubing surface pressure and install depth) obtain the required pressure at the pump discharge to move the rate to the surface.
- With the pump discharge pressure, repeat the calculation for reservoir barrels per day, now at pump discharge conditions.
- Repeat the specific gravity calculation at discharge.
- From the intake and discharge conditions, obtain average flow barrels per day through pump and average S.G.
- With the average rate, choose an adequate pump type (series to fit in casing) and obtain the lift per stage from the pump stage performance curve.
- Calculate the fluid level above the pump (FLAP) with intake pressure and intake S.G.
- Calculate the head equivalent for the tubing head pressure (using S.G. at discharge–an approximation)
- Calculate tubing friction from the chart below or using the Hazen–Williams formula.
- Calculate total TDH = Lift requirement (pump setting depth minus FLAP) + friction loss in tubing string and TP (converted to head)
- Divide TDH by Lift per stage at desired rate (RBPD) to obtain the number of stages required.
- From the pump curve, obtain HP/stage at desired rate; multiply by average SG to get minimum motor horsepower requirement.
- The rest of the sizing and design follows the basic procedure for any sizing.

The Rs and formation value calculations can be simplified by using charts (nomographs).

Although the calculations are somewhat simplified by the use of graphs, the purpose of this explanation is to dissuade anyone from doing applications by hand not only because of the lengthy calculations but also because of the errors introduced by averaging data at intake and discharge; calculating pump discharge pressure based on a graph that is an approximation in itself; and the errors of interpretation when using any kind of graph.

AutographPC software calculates all parameters exactly with multiple correlations to choose from if required and calculates fluid volume evolution at every stage. Averaging free gas calculations can be a large error, for example, if free gas volume is zero at discharge conditions, it may have been zero half way up the pump or two stages before discharge. There is no way to know with averaging.

19.8.3 What to Do when There Is Gas

As mentioned earlier in the main text, there are three areas where the application engineer or the operator can work on solutions for producing gassy wells with ESPs:

- Avoid the gas
- Separate the gas
- Handle the gas

Avoid the Gas

Avoiding the gas methods have been covered in the main text and much can be added to better understand the process concept. The other areas have more theory behind the concept.

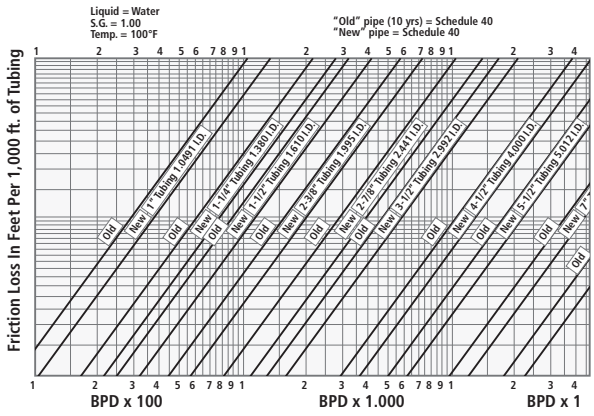

Separate the Gas

When gas cannot be avoided, the second level of action is separation. Although the devices indicated above can arguably also be called separators, there are devices that are considered the true separators. These are mechanical devices attached to the pump usually in lieu of a standard pump intake.

The first separators used in the ESP industry were passive. These took advantage of the same effect that is used in the inverted shroud, and the original reverse flow gas separator was the minimum expression of the inverted shroud.

Reverse Flow Gas Separator

As used in the first ESP applications, this was no more than a lip that the produced fluid had to go over, creating downward path to the pump intake. As indicated for the inverted shroud, the reverse flow separation capability was a function of fluid velocity, obtained from the production rate and casing and pump dimensions. The efficiency of this type of separator was low, estimated to be about 10 to 15% in free gas volume but definitely helpful when total free gas was relatively low. There has been argument in favor of using a lip design intake on all pumps and gas separators to assist in gas separation efficiency for any existing separator type.

Rotary Gas Separator

The original rotary gas separator, as it is known today, in the older DRS, FRS, and GRS models was first patented by Baker Hughes in 1978. The use of a completely closed rotating separation chamber as opposed to an open or paddle type separator chamber ensured a very high separation efficiency of 70 to 90+%, depending on rates and fluid characteristics. Successive improvements to the product, culminating in the GasMaster design not only improved efficiency but also volume throughput, which has been a limiting factor as it causes an internal pressure drop to the point that internal pressure at the gas discharge ports is lower than the annular pressure surrounding the gas separator. At this point, the gas separator discharge ports become an additional set of intake ports and affording 0% separation efficiency. See **Fig. 19.45**.

The design improvements focused on reducing pressure drop at the intake, through the shaft bearing support and at the diverter/gas discharge section. Applications in which the total gas separator throughput is exceeded usually result in production at the surface being lower than the rate suggested in the design (AutographPC software).

The hardest part of designing an application with gas production that requires the use of a gas separator is to

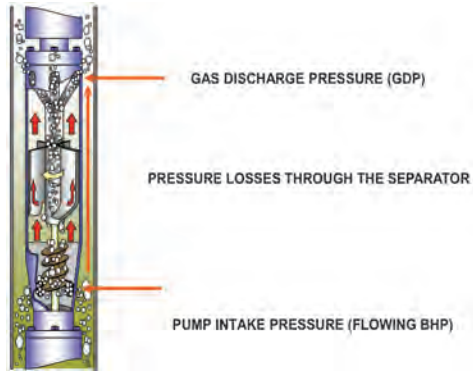

Fig. 19.45—A rotary gas separator.

understand what separation efficiency can be achieved. Not to be ignored is the natural separation effect that will occur in the albeit small annular space between the casing and the gas separator. AutographPC software allows the application engineer to determine what this fraction will be. The no-gas separator option must be selected in the well screen and the correlation is looked up in the Tools drop down menu. The natural separation can be added to the expected gas separator efficiency or the gas can be removed from the total gas-to-oil ratio (GOR) or gas-to-liquid ratio (GLR) entered in the screen. However, natural gas separation will only occur in conjunction with the use of a gas separator if there is ample room between the gas separator and the casing ID. Otherwise, reverse flow from the gas separator discharge will negate the natural separation. See **Fig. 19.46.**

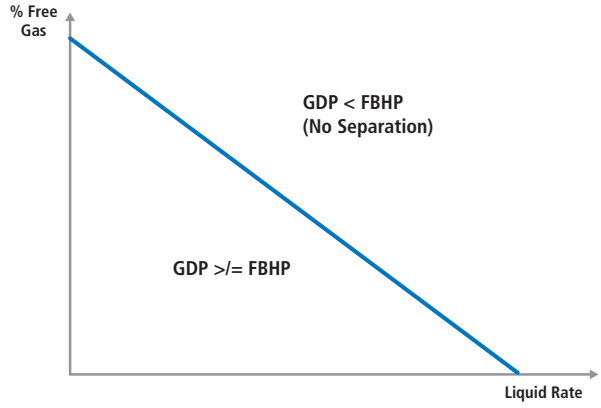

Fig. 19.46—A typical gas separator performance curve.

There is discussion as to the interpretation of the gas separator performance curve. The line or curve that defines the separator's performance is the 100% separation line, which means the line assumes that there is insufficient separation above the line but 100% separation below. Below the line an area of liquid and free gas proportion remains below the total volume that the separator can handle. Although this is a very simplified explanation of the true workings of the gas separator, the system can almost be considered to be self-adjusting. **Fig. 19.47** illustrates a typical operating point that is well below the 100% line and, therefore, 100% separation. The true separation is not 100%, but the amount of gas that goes through and into the pump does not seriously affect the ESP system performance. Fig. 19.52 illustrates the comparative trend when the operating point is just outside of the gas separation envelope.

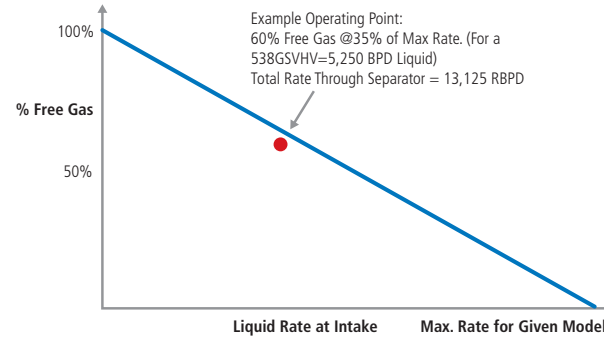

Fig. 19.47—Operating point within the gas separation envelope.

In **Fig. 19.48**, the point is slightly above the separation line. What occurs at this point is that the gas is not properly separated and some of the gas enters the pump. The pump ingests enough gas to cause performance deterioration. As this happens, the produced rate drops and the operation point is displaced to the left until it intersects with the 100% efficiency or capable separation line. Pump performance is no longer affected, and the system continues to operate in a stable manner.

This is a simplification of the real process in the gas separator. As the pundits will be quick to admit, gas separation and gas handling by ESPs is a complex subject

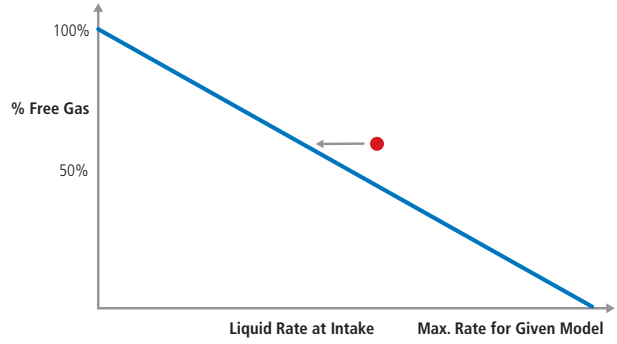

Fig. 19.48—Operating point just outside of the gas separation envelope.

that is only just now beginning to be understood. Every opportunity for new and different testing brings up more answers and more questions.

When Baker Hughes acquired the closed gas test loop and completed design of the new separator, testing started in earnest. If the pump attempts to produce more fluid than the separator can provide, the separator will not have enough pressure to expel the gas through the exit ports. When this occurs, all of the gas entering the separator will be passed directly into the pump. Fig. 19.48 shows an example of a single test.

As the inlet gas volume increases, there is some fluctuation in performance but pressure does not fall until the free gas reaches a point (56% in this example) where the separator is overwhelmed and pump performance is seen to deteriorate (performance points all gather together, not going anywhere). Free gas percentage is increasing but the curve is falling back as the liquid rate into the separator is dropping.

After adding more test results (**Fig. 19.49**), an interesting performance phenomenon became apparent. A diagonal line in the graph of free gas % versus liquid volume started forming and indicated a boundary. It divides the graph into two sections: the area above the line where the unit is unable to perform and the area below where the unit performs without pump degradation.

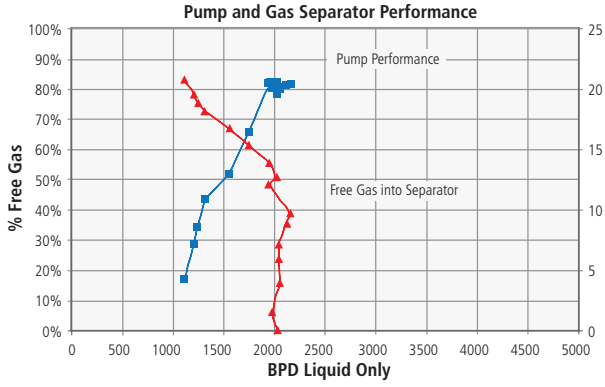

Fig. 19.49—Pump and gas separator performance test.

The performance boundary is practically linear and closely matches the liquid-only performance of the fluid impeller (**Fig. 19.50**). In Fig. 19.48, Fig. 19.49, **Fig. 19.50**, **Fig. 19.51**, and **Fig. 19.52**, the red represents a combination of liquid rate plus gas as a percentage. The blue represents performance (production) readings taken at the text pump.

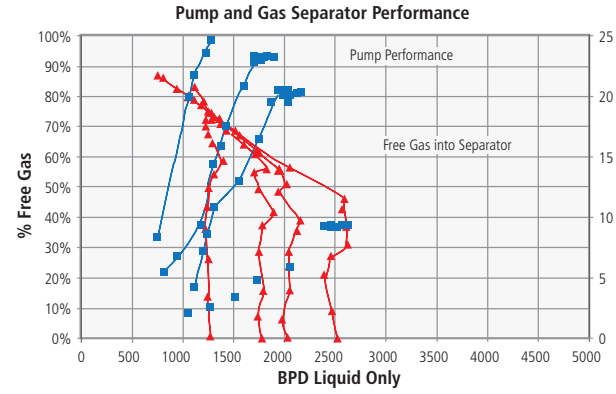

Fig. 19.50—Pump and gas separator performance tests with changing conditions.

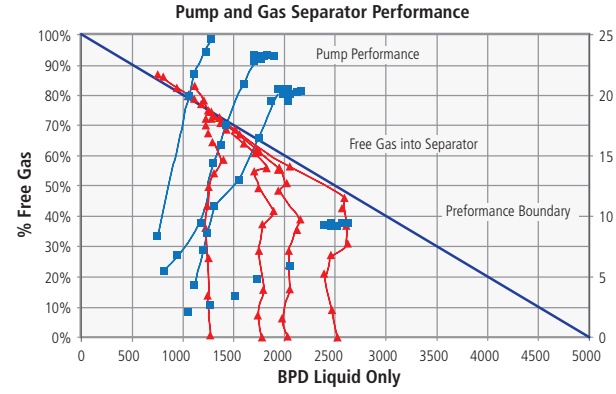

Fig. 19.51—Pump and gas separator tests with added trendline.

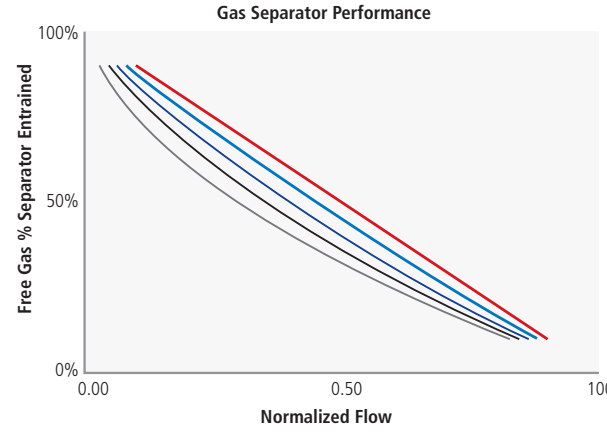

Fig. 19.52—Viscosity effect on free gas separator entrained versus normalized flow.

Although the performance curve or line for the separators is considered to be the 100% separation boundary, this is not altogether true. However, another assumption for this line is that the fluid viscosity is low (< 5 cp). For higher viscosities separation becomes more difficult and a family of descending curves is assumed to represent decreasing efficiency with rising viscosity (Fig. 19.51).

As a rule, vortex separators should not be used when viscosity rises above 5 cp for any reason, as the viscous liquid will not readily create a vortex. Viscous crudes in shale plays have not been seen to this day, but the future is unknown. When viscosity exceeds the stated limit, use a rotary chamber, as this forces the centrifugal separation of the two phases.

Tandem Rotary Gas Separators

There is some discussion regarding the advantage (or not) of using a tandem gas separator. Based on the discussion above, some gas does enter the pump and affects pump performance. By using a tandem separator, a little additional separation is achieved in the second stage, and pump performance is affected less. Proof of this has been observed in the field with older type separators when a single separator, which allowed some gas into the pump, showed evidence of this in the amp chart. The chart displayed the typical gassy curve, a wide band of varying amperage readings. When a tandem separator was installed in its place, the chart showed a straighter, cleaner line, evidence that less gas was entering the pump.

There are obviously situations in which the pump is started and there is so much gas that the initial operating point shoots well above the gas separation curve or line. In these cases, the pump may not able to get primed and there can be no self-adjustment. In other cases, gas slugs may appear from time to time. In these cases the gas separator will no longer have the liquid phase to separate from and be overwhelmed by the gas, consequently the pump will gas lock.

Gas Separators and Hybrid Separation

Gas separators can be installed with ESPs setting them above the perforations or they can be used below perforations, in which case the separation is aided by action of setting below. In these cases a shroud is used to ensure proper motor cooling. Shrouds can be hung by means of a hanger clamp installed between the separator intake and the gas discharge ports, this allows the separator to work as designed. However, when this is the case, the fluid coming down from the perforations toward the bottom of the shroud will drag some gas down with it. It is, therefore, necessary to understand the application inasmuch as having an idea as to how much gas will be drawn down with the liquid and how much room there will be in the annular space for the separated gas to rise again. Nevertheless, an advantage can be obtained with this arrangement apart from the fact that some gas will likely get by. The gas separator acts as a beater or churning device that tends to make the gas bubbles smaller. As mentioned earlier, smaller gas bubbles contribute to making the fluid more pumpable.

Gas Separators in Horizontal Wells

Gas separators will not work very well or not as well in a horizontal position. In the vertical well, the separated gas exits the ports and rises quickly up the annulus. In a horizontal position, a large part of the gas that exits the ports may be drawn into the intake again. In this case, the separation efficiency is reduced, of course, but there will be the added advantage of the processed bubble sizes.

Natural Separation and Gas Separators in Inclined Wells

When the well has an inclined section that meets the requirements for an ESP installation (sufficiently straight section) this is highly desirable for handling gas (Fig. 19.52). Small to medium amounts of free gas will tend to hug the upper section of the casing due to gravity, provided there is no serious turbulence, a function of rate and the length of the straight section, mostly. This can aid pump intake with natural separation. Use of a gas-avoiding type intake also is beneficial in an inclined section of the well.

If the gas is excessive for a standard or a gas avoiding intake, a gas separator works well as a rising motion will carry the gas that exists for the separator ports and the free gas going into the separator will be reduced in any case. As the angle increases, the gas recirculation from the exit ports to the intake tends to increase as well.

Lateral Setting of the Pump/Separator

Setting the ESP unit in a large casing has been beneficial for gas handling (**Fig. 19.53**). This is intuitively so, as a larger area around the unit means more room for the free gas bubbles to rise unimpeded, i.e., without being drawn into the pump intake.

Fig. 19.53—Separation in inclined wells.

Handling Free Gas with the Electric Submersible Pump

As stated previously, there are numerous ways in which free gas affects centrifugal pump performance. Once known how much free gas will be at pump intake conditions, steps must be taken to ensure the ESP system will work regardless.

Practical guidelines that have been around for many years indicate that stage geometry affects the gas handling capability. A radial stage has a poor capacity for handling free gas. However, as the stage design transitions toward the mixed flow design and further to a turbine style stage, gas handling can improve significantly.

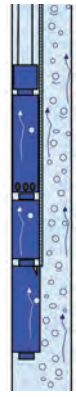

Fig. 19.54—Improved natural separation in a large casing.

Fig. 19.55 shows only the transition from a radial stage to a typical ESP mixed flow stage for 400 and (old) 513 series pumps. **Fig. 19.56** shows the transition all the way to a propeller type impeller. Associated specific speeds are included, where specific speed is defined as revolutions per minute to produce 1 gpm at 1 ft. of head with a particular impeller design, as in the following equation:

where:

$$N_s = \frac{n\sqrt{Q}}{H^{0.75}}$$

Ns—Specific speed (dimensionless)
N—Rev per minute
Q—Capacity (gpm)
H—Head (ft.)

In the past, it was believed that radial stages could handle up to 10% free gas into the pump and mixed flow could handle 15 to 18% free gas. This still holds somewhat true, but other factors can change these limits drastically.

Gas is typically three orders of magnitude lighter (specific gravity) than a typical liquid. This ratio changes as pressure is increased and the gas phase is compressed so that at higher pump intake pressures the difference shrinks and the fluids become manageable by the centrifugal pump. For example, at a pump intake pressure of 350 to 400 psi, the difference may be two orders of magnitude and at about 1,500 psi, the liquid phase is only about 10 times as dense as the gas phase.

This phenomenon and the impact on electric submersible pump operation were studied by Turpin and Dunbar in the 1970s. They came up with correlations (Turpin et al. 1986) to mathematically express their theories.

A simplified adaptation of Turpin's conclusions is a curve (shown as a diffuse dividing line) defining an operating range with liquid plus gas that will be handled well by an ESP and a range in which the ESP will likely gas lock. The

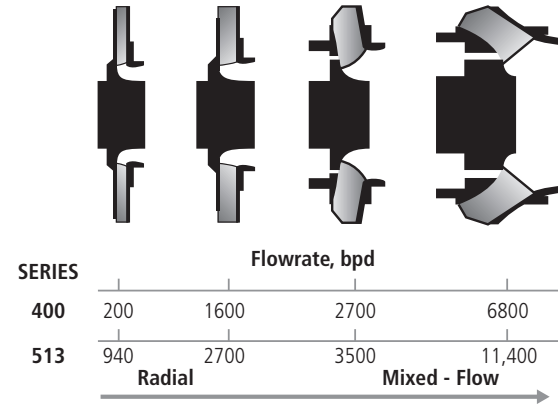

Fig. 19.55—Impeller geometry versus flow rate, including typical rates for 400 and 500 series pumps.

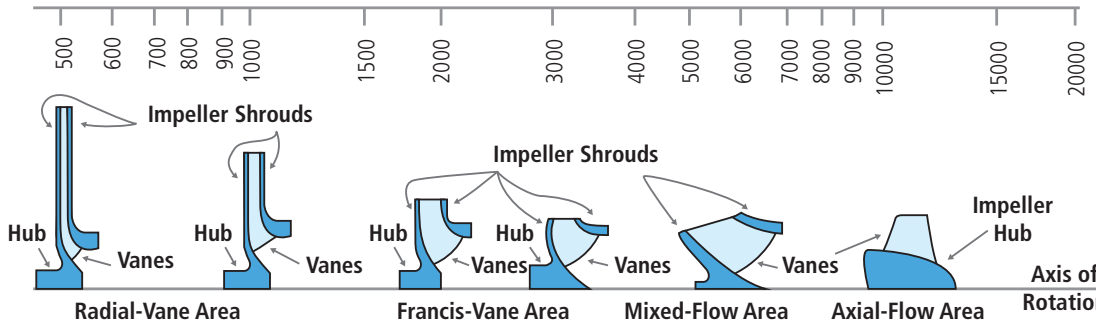

Fig. 19.56—Impeller geometry and specific speeds. (After Hydraulics Institute Standards.)

line in between is not clear as it depends widely on fluid and pump stage characteristics. See **Fig. 19.57**.

The importance is emphasized of looking at these correlations when articulating at an application that will produce gas. There are occasions when the intake pressure may remain high for many reasons (operator preference, water coning risk, etc.) and gas, although prevalent, may be so compressed that no action need be taken (no special equipment needs to be supplied) to handle it adequately. Fortunately for application engineers AutographPC software has a Turpin screen that shows the position of the operating point.

A different issue when dealing with gas is bubble size, as it relates to the gas arriving at the pump intake. Bubble size depends on a number of things, such as fluid properties (liquid and gas), fluid velocity and turbulence, perforation geometry, etc. Large bubbles cause a greater disruption in flow and pumping capability than smaller bubbles. An extremely large bubble is a gas slug. A slug can be so large that is may take minutes to pass by the pump. This causes the pump to gas lock because there is no liquid phase at all for the pump to bite into. No tool or device can help handle the gas slug as it goes though the pump. The only way to defend against a gas slug is to find a device to avoid it. On the other side of the spectrum, bubble sizes can be so small as to be perceived to be nonexistent, and the well fluid is handled by the pump as if it were fully homogenized, resulting in what appears to be a low-density liquid.

Modern technology focuses on ways to design centrifugal pump stages that can handle higher amounts of free gas and/or means to make the fluid entering the pump stage more pumpable.

Thus gas handling stages were designed with artifacts to prevent the buildup of gas bubbles in the low pressure side of the impeller vane such as the Baker Hughes multivane (MVP) pump stage or turbine type designs (high-specific speed) such as the gas insurance stage (GIN pump). Other pumps in the industry have resorted to other devices to achieve the same end.

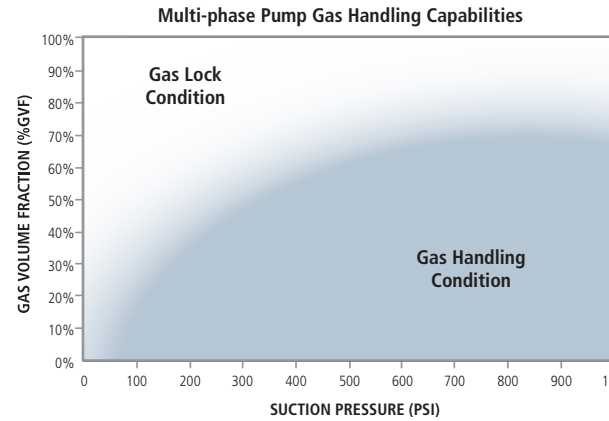

Fig. 19.57—Effect of pump intake pressure on free gas handling capability.

19.9 Conclusion

Like conventional fields, unconventional resources such as shale, coalbed methane, and heavy oil require artificial lift methods to achieve higher volumes of hydrocarbon and other fluids at the surface. When drilling a well, the aim is to achieve the highest possible net present value from the well. In the pursuit of greater productivity, many challenges can impact the performance and applicability of the potential lift method. High gas and solid contents, high temperature, well design and trajectory, production decline, and variable flow regimes are some of the main factors that would leave an operator with serious challenges, making production management of the asset significantly complex especially in potentially tight economic margins associated with shale plays.

Considering such complexity, it makes sense to leverage capabilities of ESP systems not only to handle all the problems and challenges cited but also to extend their run life at

reduced costs. Current lift technologies have the capabilities to address these challenges. As more horizontal wells are drilled in shale plays, many operators need to identify strategies that will work best to cost-effectively maximize their production. Hence, there is a tremendous opportunity for use of this technology in the market. Selecting the most attractive and effective artificial lift strategy requires a unique solution aimed at improving the cost/benefit ratio and monitoring the production events at the same time. Experience in US shale plays, as demonstrated in this chapter, shows success in increased recovery by using FLEXPump technology. The lessons learned help the operator tailor the design and performance of our systems for critical well applications.

19.11 References

API RP 11S3. ***Recommended Practice for Electrical Submersible Pump Installations***, second edition. 1999. Washington, DC: API.

ASTM-E11. ***Standard Specification for Wire Cloth and Sieves for Testing Purposes.*** ASTM International. http://dx.doi.org/10.1520/E0011-09.

HPDI database. http://www.didesktop.com.

Marquez, R. and Prado, M.G. 2003. A New Correlation for Predicting Natural Separation Efficiency. Southwestern Petroleum Short Course, April 2003, Lubbock, Texas.

Simmons & Company International. 2011. U.S. Liquids-Focused Threshold Economics. ***Energy Industry Research.*** 25 August.

Standing, M.B. 1981. ***Volumetric and Phase Behavior of Oil Field Hydrocarbon Systems***, 9th edition. Dallas, Society of Petroleum Engineers.

Turpin, J.L., Lea, J.F., and Bearden, J.L. 1986. Gas-Liquid through Centrifugal Pumps–Correlation of Data. ***Proc.***, Third International Symposium. Texas A&M University. 13–20 May. College Station, Texas.

Vogel, J.V. 1968. Inflow Performance Relationships for Solution-Gas Drive Wells. ***J Pet Technol***, **20** (1): 83–92. SPE 1476-PA. http://dx.doi.org/10.2118/1476-PA.

This page intentionally left blank

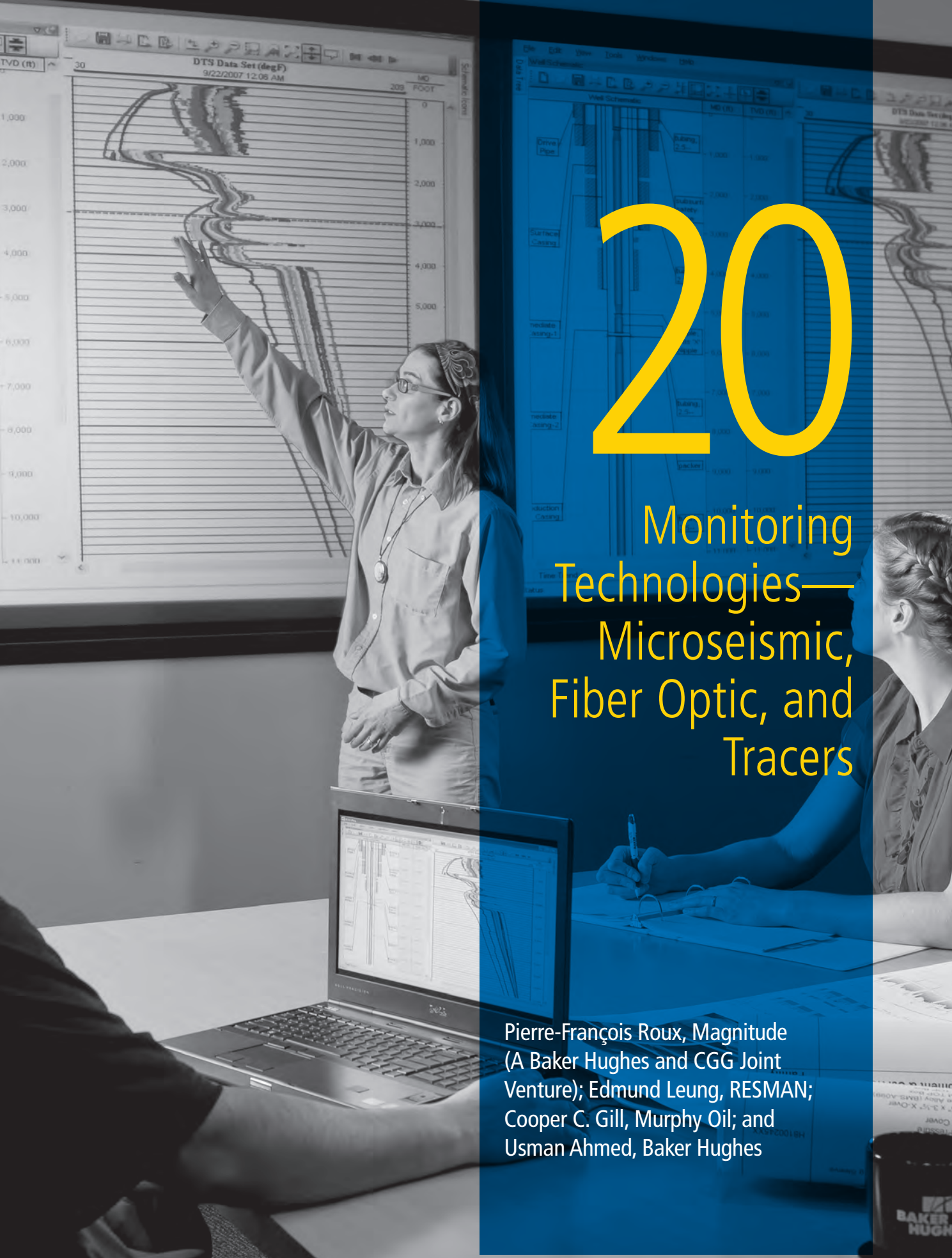

20

Monitoring Technologies—Microseismic, Fiber Optic, and Tracers

Pierre-François Roux, Magnitude (A Baker Hughes and CGG Joint Venture); Edmund Leung, RESMAN; Cooper C. Gill, Murphy Oil; and Usman Ahmed, Baker Hughes

This page intentionally left blank

Chapter 20: Monitoring Technologies—Microseismic, Fiber Optic, and Tracers

20.1 Introduction to Monitoring Technologies

Traditionally, hydraulic stimulation treatments were assessed using their pressure response during and post treatment (Economides, Nolte, and Ahmed 1998). Although robust, these methods are based on the interpretation of pressure curves that have limited resolution of the inverse problem of characterizing fractures. It is desirable to add other engineering tools that can help understanding the behavior of the stimulation, both during and after the treatment has been undertaken. It would be beneficial to gather information away from the wellbore. Microseismic monitoring, permanent downhole inflow tracer monitoring technology, and fiber optic monitoring can constrain the outcomes of stimulation and compare it to the modeled fracture. In the following sections each of the three techniques is discussed with field application case studies (Ahmed et al. 2015).

20.2 Background: About Microseismic

Microseismic diagnosis of hydraulically induced fractures appeared in the 1970s in the context of enhanced geothermal systems (EGS) (Evans et al. 1999) for a review of enhanced geothermal systems (EGS) or reservoir stimulation (Raleigh et al. 1972). Subsequent industrial applications were first associated with mining-related activity (Gibowicz and Kijko 1994). Reservoir impoundment induced seismic activity drew the attention of seismologists as it was shown to potentially generate large magnitude events. For example, a magnitude 6.3 earthquake struck India during the filling of the Koyna reservoir (Gupta 1985). Microseismic monitoring has been extensively developed over the last decade for monitoring unconventional reservoirs stimulation. Commercial applications started to emerge in the late 1990s and early 2000s (Maxwell et al. 2000; Warpinski et al. 1995; Phillips et al. 1998). Microseismic may foster too-high expectations in its users. Microseismic can provide needed, and important, information about the outcome of the treatment.

The term microseismic is probably misused because it (theoretically) designates earthquakes whose magnitude is lower than 3 (Bohnhoff et al. 2010) or, in terms of radiated energy, lower than 1.0. Most microseismic activity recorded during stimulation is lower than 0.

Microseismic monitoring encompasses many different geoscience fields including seismology and geophysics (from which stem most of the concepts), geomechanics (including but not limited to, elastic and brittle deformation of rocks), and reservoir engineering. This chapter attempts to cover each of these fields through the prism of fracture diagnostics and stimulation-induced seismicity, with a list of seminal references emphasizing the background of microseismic monitoring. This section is limited to the application of microseismic compared to other techniques. Details of technology foundation can be found elsewhere (Maxwell 2014).

20.2.1 Seismological Background

Microseismic monitoring in its entirety is standard seismology specifically applied to sources of a much smaller size than what is usually considered in conventional seismology. It is, therefore, based on the same principles regarding wave propagation and source characterization. Although we provide a brief overview of the theories behind microseismic monitoring, the reader is referred to seminal textbooks, including Aki and Richards (2001), Lay and Wallace (1995), and Stein and Wysession (2002). The equations given in the following section are solely provided to show the connection between the different physical terms (medium's mechanical parameters, stress, strain, and displacement to name a few).

20.2.1.1. Wave Equation and Wave Types

Wave propagation in an elastic, linear, isotropic medium is governed by the elastodynamics equation. It combines the stress-strain (static) elastic relation (given here in the case of an elastic, linear, possibly inhomogeneous and isotropic medium) given as:

$$\sigma = \lambda.\mathrm{tr}\varepsilon\ 1+2\ \mu\varepsilon \qquad \textbf{(Eq. 20.1)}$$

and the equation of motion (second Newton's law):

$$\nabla\sigma + f = \rho\ddot{u} \qquad \textbf{(Eq. 20.2)}$$

where σ is the stress tensor, ε the strain tensor, **f** represents body forces (such as the gravitation of the Earth), **u** is the

displacement (at position **x** and time ***t***, both being omitted from the notation for the sake of simplicity), (λ, μ) are the Lamé parameters (also spatially varying), and ρ is the medium's density. Combining these two equations and rearranging terms yields the elastodynamic wave equation, which describes the acceleration of solid particles under the action of a force (Aki and Richards 2001):

$$\rho\ddot{u} = f + (\lambda + 2\mu)\ \nabla(\nabla.u) - \mu\,\nabla \times (\nabla \times u) \qquad \textbf{(Eq. 20.3)}$$

If we replace the volume force ***f*** with a unit impulse at time $t=\tau$ and location $x=x_0$ in the *n*-direction (whose normal vector is $\hat{x}$) then the displacement field is the elastodynamic Green function denoted $G(x,t;x_0,\tau)$. It necessarily satisfies the vector wave equation (once more omitting the $(x,t;x_0,\tau)$ for the sake of simplicity):

$$\rho\frac{\partial^2}{\partial t^2}\boldsymbol{G} = \delta(x - x_0)\,\delta(t - \tau)\,\hat{x}_n + (\lambda + 2\mu)\ \nabla(\nabla.G) - \mu\ \nabla\times(\nabla\times G) \qquad \textbf{(Eq. 20.4)}$$

Note that the Green tensor G is a matrix whose components are the G_{in}, corresponding to the *i* th component of the displacement for a force applied in the n-direction.

Using Helmholtz decomposition of the displacement vector field into a (curl-free) scalar potential and a (divergence-free) vector potential (φ and ψ, respectively):

$$u = \nabla\Phi + \nabla \times \psi \qquad \textbf{(Eq. 20.5)}$$

It is possible to solve the elastodynamic equation separately for the two potentials (Lamé's theorem). Because physically, curl-free implies there is no shearing motion (but there is a change in volume), the first component of *u*, $\Delta\Phi$, is called the ***P-wave component***. By contrast, the second component ($\Delta\times\psi$) is called the S-wave component. Divergence-free implies no change in volume. Therefore, the P-wave is compressional and generates a ground motion that is parallel to the wave direction (**Fig. 20.1**). On the other hand, the shear wave is a transverse wave with two different polarizations: SH and SV (horizontal and vertical, respectively). ***P*** and ***S*** waves are solutions of the wave equation and can both be decomposed in near-field and far-field solutions (spherical and plane waves, respectively). Their amplitude decreases as 1/*r*, where *r* is the distance travelled from the source.

Because the elastodynamic equation depends on the medium's physical parameters, namely λ, μ, and ρ, each of these waves propagates at a velocity that varies according to the mechanical parameters involved in the elastodynamic equation. The P- and S-wave velocities (traditionally symbolized as α and β, respectively) can be expressed as:

$$\alpha = \sqrt{\frac{\lambda + 2\mu}{\rho}} \qquad \beta = \sqrt{\frac{\mu}{\rho}} \qquad \textbf{(Eq. 20.6)}$$

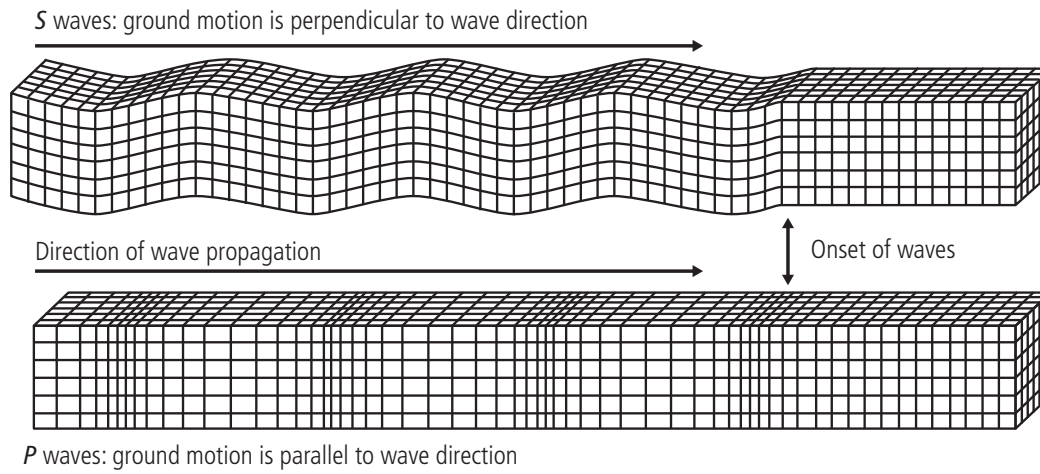

Fig. 20.1—Displacement field for P and S (plane) waves with respect to the wave propagation direction. The P wave involves a displacement parallel to the direction of propagation and involves a volume change, while both S wave polarizations generate a displacement perpendicular to the direction of propagation. (Stein and Wysession 2002.)

The parameters involved in these velocities, and, therefore, the velocities are all functions of the position in the medium where the propagation occurs.

Interactions of body waves near the surface give rise to surface waves: P-SV waves will generate Rayleigh waves, while SH-SH interactions will generate Love waves. The latter are caused by SH waves trapped near the surface. In general, the surface waves have much larger amplitude than the so-called body waves. Their formal expression shows that their amplitude decreases as

$$1/\sqrt{r} \qquad \textbf{(Eq. 20.7)}$$

with r being the distance from the source. Their respective propagation velocities are a much more complex phenomenon to describe and fall beyond the scope of this work.

20.2.1.2 Earthquake Parameterization

In general, earthquakes are parameterized based on their spatial coordinates and their origin time (i.e., the time at which the rupture process is initiated) also termed focal time. To this traditional set of parameters can be added so-called source parameter describing the rupture process itself. This includes focal mechanism (see 20.2.3), magnitude, seismic energy, seismic moment, stress drop, and source-time function.

- **Seismic energy:** Only a (small) portion of the released strain energy is emitted as seismic waves. The remaining strain energy is radiated as heat or through non-elastic processes.
- **Magnitude scale:** The measure of the size of an earthquake. There are many different magnitude scales depending on how it is determined: local magnitude (Richter 1935) surface waves magnitude (Gutenberg 1945a) body-waves magnitude, (Gutenberg 1945b) duration magnitude (Lee et al. 1972), and last but not the least, the moment magnitude (Hanks and Kanamori 1979). The latter is commonly used in the microseismic industry. It is, however, worth noting that each of these scales implies one or several hypotheses and/or approximation that are often overlooked. For instance, the moment magnitude assumes a constant stress-drop of 10^{-4} of the shear-modulus of the fracture under scrutiny, which has been shown to apply to crustal earthquakes and remains unknown as far as hydraulic fracturing induced earthquakes go.
- **Seismic moment:** The ensemble of force couples giving rise to a shear rupture with no torque and constituting the seismic moment tensor.
- **Stress drop:** The difference between the initial, pre-seismic shear stress and the final, post-seismic shear stress.
- **Source time function:** The time variation of the fault motion. In general, it characterizes the time evolution of the body forces involved in the elastodynamic equation; it can thus be viewed as the time dependent part of the seismic moment. The resulting Fourier transform is generally termed as the source spectrum and can be used in conjunction with seismic source models to determine some of the fracture/fault parameters (length, ruptured surface, and so on).

20.2.1.3 Source Characterization: The Moment Tensor

The previous equation and solutions have been written in the general case of a volume force $\boldsymbol{f}$. We now replace the volume force by a (set of) force(s) representing the source mechanism. Because most earthquakes are caused by shear faulting, it is convenient to describe the source as a pair of force couples or moments, constituting the "double-couple" (or DC) source mechanism (Burridge and Knopoff 1964). In order to account for the "*non-shear*" rupture type (such as tensile rupture, linear vector dipoles, isotropic volume changes, or compensated linear vector dipoles), non-DC components are added to the general DC description of earthquakes (Julian et al. 1998; Miller et al. 1998).

Source mechanisms are classically represented by second-order tensors, termed seismic moment tensors. They are a convenient way to mathematically represent source mechanisms, because they are related to the Green functions and the (far-field) displacements through a convolution:

$$u_n = M_{pq} * G_{np,q} \qquad \textbf{(Eq. 20.8)}$$

where $G_{np,q}$ is the derivative along the qth dimension of the Green function and M_{pq} is any of the nine components of the seismic moment tensor. From this equation it appears that the seismic moment tensor contains information on both the source radiation pattern and the magnitude of a seismic event. When solely considering shear rupture on a plane, M is symmetric—i.e., does not induce torque on the plane. It is, however, possible to describe DC and non-DC source mechanisms with the seismic moment tensor. A convenient way to do so is to decompose it as the sum of an isotropic source, a DC and a compensated linear vector (Knopoff and Randall 1970; Jost and Herrmann 1989):

$$M = M^{ISO} + M^{DC} + M^{CLVD}$$
$$M = M^{ISO} + M^{*} \qquad \textbf{(Eq. 20.9)}$$

And M^* is termed deviatoric moment and is the sum of the DC and the CLVD (compensated linear-vector dipole) components.

Fig. 20.2 displays the principal force systems corresponding to this decomposition. Note that CLVD, first introduced by Knopoff and Randall (1970), can be (non-uniquely) physically explained by a combination of a tensile failure and a fluid injection (see Fig. 20.2, right). When dealing with DC only sources, the problem is often parameterized using the fracture or fault plane parameters (azimuth, dip, and strike, usually denoted Φ, δ, and λ, respectively (**Fig. 20.3**). Vavryčuk (2001) proposed to define the general moment tensor in percentages:

$$P_{ISO}^{\%} = \frac{1tr(M)}{3|m_3|} .100$$

$$P_{CLVD}^{\%} = 2|\varepsilon|\,(100 - |P_{ISO}^{\%}|) \qquad \text{(Eq. 20.10)}$$

$$P_{DC}^{\%} = 100 - |P_{ISO}^{\%}| - |P_{CLVD}^{\%}|$$

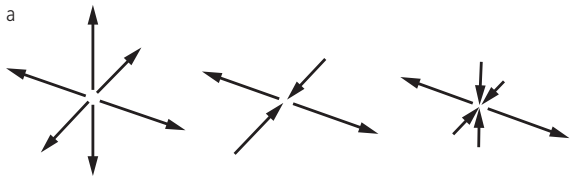

Fig. 20.2—Equivalent source type used in the decomposition of the moment tensor. From left to right: isotropic, double-couple, and compensated linear vector. (Adapted from Julian et al. 1998.)

where m_3 is that eigenvalue of M that has the maximum value and ε is defined as $\varepsilon = -\frac{M_{|min|}}{|M_{max}|}$, with $M^*_{|min|}$ and $M^*_{|max|}$ are the eigenvalues of deviatoric moment M^* with the minimum and maximum values, respectively (Vavryčuk 2001).

Focal mechanisms are traditionally represented by plotting the polarities' distribution on the focal sphere (which is an imaginary sphere surrounding the earthquake focus). This type of representation is being widely used for DCs, but is not always suitable for more complex sources. Riedesel and Jordan (1989) have proposed an alternative way of representing focal mechanisms using the so-called source-type plots and containing information on source orientation as well as source type. Hudson et al. (1989) have also proposed a plot in which the sole source type is represented—noting that most, if not all, source representations solely contain information on the orientation (**Fig. 20.4**).

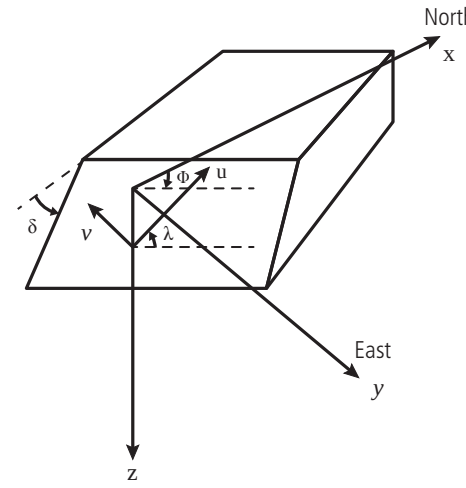

Fig. 20.3—Fault parameters (see text for details). Fractures can be represented by three geometric parameters: strike, dip, and rake. (Jost and Herrmann 1989.)

20.2.1.4 Types of (Micro-) Earthquakes: Induced Versus Triggered

When dealing with human-related seismic activity, it is common to distinguish induced from triggered seismicity. McGarr and Simpson (1997) proposed the following definition: the term "induced seismicity" applies to seismicity that results "from a substantial change in crustal stress or pore pressure from its ambient state," while the term "triggered seismicity" describes "a situation for which the crust is sufficiently close to failure state due to natural tectonic processes that only a small change in either stress or pore pressure stimulates earthquakes" (McGarr and Simpson 1997).

The distinction in the previous paragraph is, however, somewhat loose, as pointed out by Talwani (2000), because it does not account for the stress shadowing or enhancement that necessarily goes with the activation of a fracture. In other words, it is hard if not impossible to certify that the so-called "triggered" earthquakes would occur or not at some point in time without the influence of the underground industrial activity. Conversely, Grasso and Sornette (1998) show that small perturbations can also induce a large seismic activity thanks to several diverse mechanisms (direct loading effects—elastic and poroelastic—or coupled poroelastic effects). Furthermore the above definition assumes that there is a tectonic process in place and that the deformation rate is sufficiently high to generate earthquakes.

We would, therefore, recommend using the terms triggered and/or induced with caution.

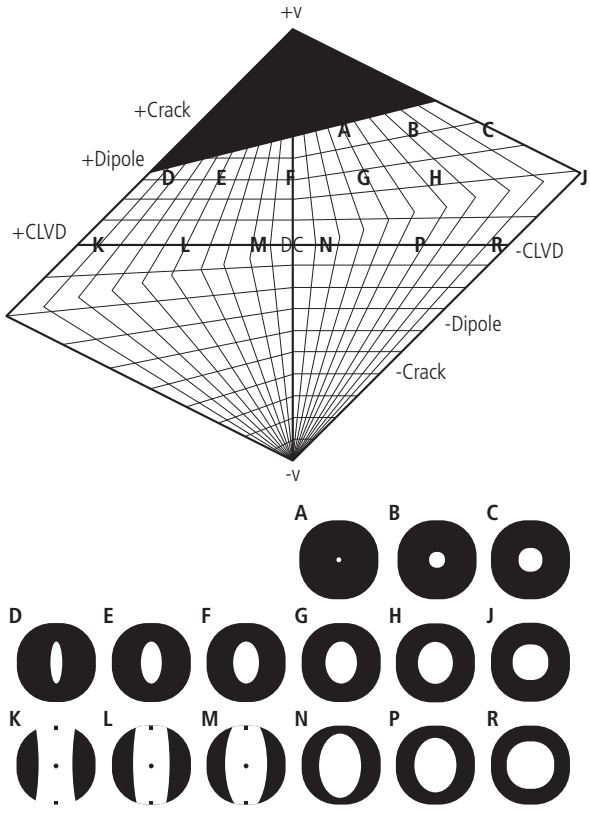

Fig. 20.4—Source type plot as proposed by Hudson et al. (1989). The link between focal mechanisms and their corresponding position on the source type diagram is materialized with letters. (Modified from Julian et al. 1998.)

20.2.2 Acquisition Designs

Because the understanding of the microseismic activity generated by the stimulation goes through the recording of its byproducts, namely the waves it produces, it is necessary to devise tools that are able to pick the corresponding nanometer scale (and sometime smaller) displacement velocities. Because these displacements are very small, it is necessary to use highly sensitive, low-noise sensors. As a matter of fact, the noise remains the main problem when using microseismic monitoring. Noise can be divided into three main categories:

- Digitization noise; i.e., the error made when converting an analogic value into its numerical counterpart. Nowadays, thanks to 24+ bits ADCs (analog-to-digital converters), this error is negligible.
- Self-noise, which is thermal noise generated by the electronics of the acquisition system. It is frequency dependent, because the acquisition device itself has a frequency dependent sensitivity.
- Seismic noise, which is mostly, if not exclusively, generated by sources at the surface of the Earth, and consists mostly of surface waves. It is, by far, the highest contributor to noise in most places.

Increasing the sensitivity and ADCs resolution will help to decipher the second term (self-noise) in the noise sources breakdown. Seismic noise, on the other hand, can be decreased either through processing, or simply by avoiding areas where seismic noise may be high. The best—and as such, the initial—way of avoiding surface noise is by using downhole tools. More recently, thanks to acquisition and processing advances, surface or near-surface arrays are commonly used, providing extra information on the source as the overall coverage is increased compared to a single borehole acquisition.

20.2.2.1 Downhole Monitoring

Downhole geophones tools are the historical means used to monitor microseismic activity generated by hydraulic stimulation (or any other human-related activity potentially generating a seismic activity). These tools were derived from vertical seismic profiling (VSP), usually deployed in wells through wireline services. Borehole seismic acquisition was introduced in the 1970s and was a natural extension of the original wireline-logging industry introduced as early as 1927. This acquisition method has been extensively used in hot dry rock reservoirs (Pine and Batchelor 1984), and later on applied to hydraulic fracture monitoring (Warpinsky et al. 1995).

Downhole tools are typically composed of several geophones or hydrophones. The overall tool string is clamped onto the borehole wall (or casing) to maximize coupling between the tools and the formation. Geophones tools are able to measure all three directions (two horizontal and one vertical geophone) and when coupled with hydrophones are termed 4C sensors. When downloaded in the borehole with wireline, the orientation of the sensors is unknown and has to be calibrated with surface sources. It is also possible to install the tools in horizontal sections of a well through the use of a wireline tractor. In this specific case, horizontality and verticality are ensured by a gimbal.

20.2.2.2 Surface Monitoring

Advances in both seismic acquisition and array seismology (Rost and Garnero 2004) have pushed forward the use of surface-based monitoring networks. First applications of (passive) reservoir monitoring for hazard mitigation purposes date back to the 1970s (Raleigh et al. 1976; Grasso and Wittlinger 1990). These early applications used either regional

networks or dedicated, local seismological networks. The development of crystalline rocks stimulation (enhanced geothermal stimulation) has similarly promoted the use of surface networks for fracture monitoring, because the events are usually sufficiently large to be picked up with a sparse surface network. More recently, dense surface networks have been successfully used for the monitoring of hydraulic stimulation of (unconventional) oil and gas reservoirs. The main challenge for surface arrays to be used in such a context is to cope with the noise associated with human-related activities, drastically reducing the overall sensitivity of the network to small seismic events. Increasing the number of receiving stations (i.e., increasing the stack order) allows the noise to be greatly attenuated while preserving the desired signal.

At first, and thanks to the experience in seismic acquisition in the oil and gas industry, the use of dense, rectangular networks (so-called "grids"—see Lakings et al. 2006) has been advocated. Their density and large aperture provide the best solution for surface microseismic monitoring. However, they are faced with acquisition costs, as well as surface permitting and deployment constraints. Radial networks centered on the stimulated wellhead and composed of a dozen arms were then proposed to attenuate the noise generated by the stimulation equipment. Such a radial geometry also allows for a systematic coverage of the focal sphere. This acquisition design is not well suited to several, spatially distributed sources of noise because they may severely decrease the number of usable arms in the processing. Concomitantly, sparse surface networks remain a solution in use by the industry. Recently, an alternative to dense grids has been offered through "patch array" (Pandolfi et al. 2013). Such a design is somewhat similar to the "button patch," a seismic survey design invented in the 1990s (see, e.g., Galbraith 1994). Patch array boils down to a dense network chopped down into several mini-arrays (each array being a 150m x 150m polygon).

20.2.2.3 Shallow Buried Arrays

Shallow-buried arrays (hereafter SBA) are a solution that has been proposed since the early 2000s for permanent monitoring purposes. SBA consists of geophones vertical arrays that are buried at a few tens of meters, down to a few hundreds. These arrays are generally composed of a few levels—typically three or four, equipped with 3C sensors. In practice, a SBA network is pretty sparse, that is, a station every few hundreds of meters, that covers large surface area. This sparseness, in turn, makes it sensitive mostly to large enough magnitude events, as the channel count is rather small.

Because receiver arrays are buried, they can be used on a permanent basis, or simply to repeat microseismic surveys in the case of multi-pad stimulations or refractures.

20.2.3 Microseismic Data Processing

This section addresses the various types of data processing involved with microseismic imaging, including reducing seismic noise to enhance processing, techniques for managing limitations, velocity modeling, event detection and timing, and locations methodologies to use with microseismic.

20.2.3.1 Pre-Processing Denoising

As is the case for conventional seismic imaging, it is customary (and sometimes mandatory) to apply pre-processing to the raw microseismic data. One of the main objectives—if not the sole objective of pre-processing—is to reduce the noise in the raw data and, therefore, to enhance processing capabilities (detection, location, and characterization of microseismic events). Describing existing denoising procedures and techniques is, of course, beyond the scope of the present work. We will only point the reader to the main denoising techniques commonly used in either downhole or surface acquisition.

Most of the seismic noise stems from surface sources such as pumps, roads, factories, and so on. These surface waves directly affect surface networks and indirectly downhole tools as they are transmitted through tube waves propagating in the casing or the brine in which the tools lie. Such noise will have its own, specific propagation characteristics and frequency content and, therefore, be dealt with using popular transforms such as frequency-wave number (Capon 1969) or radon (Durrani and Bisset 1984). Yet these techniques assume that the noise is unaliased and there is no scattering of the surface waves. Approaches using prediction-subtraction methodologies (Wang et al. 2009; Le Meur et al. 2010) or seismic interferometry (Halliday et al. 2010) are able to at least partially overcome the two aforementioned limitations. These prediction-subtraction methodologies can be applied either to downhole or surface monitoring, provided that it is possible to either numerically simulate the noise or reconstruct appropriately the propagation function between the noise source and the receivers.

20.2.3.2 Velocity Modeling

The first ***sine qua non*** condition to correctly characterize microseismicity is to properly account for the propagation of the waves from the source to the receivers. As seen

previously in this chapter, the elastodynamic equation (which governs the propagation) depends on the medium characteristics through mechanical parameters, which, when combined together, yield the body wave propagation velocities α and β for P- and S-waves, respectively. The propagation can be fully accounted for if the velocity spatial distribution is known. In turn, events location resolution is very much dependent on the information available about the propagation, simply because a faster medium will tend to put events closer than they are (and vice-versa). The process to determine this distribution is based on the measurement of waves parameters (such as arrival time, amplitude, and so on) and is described as seismic tomography. This is an inverse problem, that is, we try to infer a vast number of parameters through the comparison of a theoretical solution that was obtained with an actual measurement. The theoretical solution is termed forward modeling, and is generally a simplified version (in that approximations are made) of the elastodynamic equation, and thus reduces computational efforts.

Seismic tomography is an ill-conditioned geophysical problem, and, as such, it is a difficult task to complete. Following Thurber and Ritsema (2007), there are the four main underlying reasons that address the ill condition of tomographic problems:

- There can be a huge number of parameters to inverse: the subsoil is divided into cells in which the properties are assumed to be constant (**Fig. 20.5**). The higher the desired spatial resolution, the larger the number of parameters there are to search for.
- Because there are more parameters to inverse than there are available data, the problem is underdetermined, resulting in an infinite number of models that can explain a dataset. The best way to cope with the underdetermination aspects of this problem is to add constraints to the problem, therefore ensuring that solutions will be physically acceptable.
- Sampling of the underground by seismic waves is uneven.
- The forward modeling tends to over-simplify the actual physics of wave propagation and the medium itself, thus reducing the overall accuracy of the resolution.

In the specific case of microseismic monitoring, one has generally a good prior idea of the medium between the hypocentral region and the receivers thanks to seismic imaging and/or sonic logging. Velocity calibration is generally undertaken using perforation shots or string shots, both shot at the well location and of known coordinates and initial

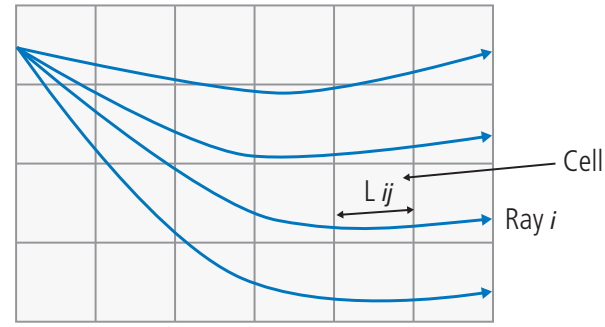

Fig. 20.5—Tomographic inversion is usually done by dividing the medium cells of constant velocity that are resolved through tomographic inversion. (Thurber and Ritsema 2007.)

time. However, because the required spatial accuracy is of the order of a few meters, the resolution of the tomographic images has to be relatively high. Typically, the velocity volume is first derived from the sonic logs (and is, as such, a 1D model) and then multiplied by a constant value for the calibration shots' found positions to match the theoretical ones. There are only a handful of studies dealing with a more complex approach to velocity calibration in the context of microseismic monitoring. Warpinski et al. (2005) proposes a linearized inversion of the arrival times measured on the perforation shots; yet Bardainne and Gaucher (2010) pointed out that linearization of the wave equation can trap the inversion in local minima, especially when the cost-function (i.e., the function that compares the measured data with the calculated data using the forward model) is nonlinear. Bardainne and Gaucher include the polarization of the waves as an additional input data and solve a nonlinear problem through high-frequency approximation of the elastodynamic equation (so-called eikonal; see Podvin and Lecomte 1991) as forward modeling. More recently, Grechka and Yaskevich (2013) have included anisotropy into the velocity model, and use both perforation and microseismic events to solve the inverse problem. Events' locations are then part of the inverse problem as initially proposed by Zhang and Thurber (2003) (the so-called double-difference) and used in microseismic location in an oil and gas context by Zhang et al. (2009) or Charléty et al. (2006) in an EGS context.

20.2.3.3 Detection and Timing of Events

Because the origin time for the microseismic events is part of the unknown parameters, data is inherently recorded continuously. It is, therefore, very important to discretize the data into so-called events (or candidates) that can be analyzed on a one-to-one basis. This discretization process is traditionally termed detection. Depending on the signal-to-noise ratio, several detection methodologies can be used (Withers et al. 1998).

High signal-to-noise events are typically detected using energy transients, such as the well-known STA/LTA (Allen 1978), which stands for short term average/long term average. STA/LTA algorithms compute an envelope function of the signal in two sliding windows of different sizes, the shorter window providing a measure of the instantaneous deviation while the larger window yields an estimate of the background noise.

Several envelope functions have been proposed in the literature to enhance energy transient-based algorithms capabilities toward low signal-to-noise events. There also exist detection techniques that rely on frequency transient (Goforth and Herron 1981; Gledhill 1985), polarization (Cichowicz 1993), neural networks (Dai and MacBeth 1995), autoregressive models (Bai and Kennett 2000), wavelet transforms, and correlation.

As will be explained later in this chapter, an event's location and origin time can be deduced from the accurate pick of the arrival time—i.e., the time at which a ballistic wave reaches a seismic station. The most obvious method to accurately measure an arrival time is the observation, analysis, and handpicking the wave by a skilled operator. Automatic algorithms have been devised early on to help observatories' seismologists to cope with a large number of events and phases arrival required to accurately locate and characterize earthquakes (Baer and Kradolfer 1987; Earle and Shearer 1994). The seismic industry has also brought its contribution through first break automatic picking. (Sabbione and Velis 2010.) The majority of these techniques will provide arrival times for as many phases as possible, possibly including false positives.

20.2.3.4 Correlation Techniques

Using cross-correlation to detect and potentially characterize an earthquake (or any kind of event) has been a longstanding technique in seismology. As a matter of fact, the most effective method of detecting a (known) signal buried inside noise is to correlate the time-series with a waveform template—a so-called matched-filter. Anstey (1964) provided a very comprehensive review of correlation techniques, and demonstrated the detection of a synthetic signal buried in noise through cross-correlation. Yet, cross-correlation detectors have received little attention in the seismology community because of their high sensitivity to the form of the master event used (which depends on both the source mechanism and the propagation). The deployment of seismic arrays (Rost and Thomas 2002) for compliance with the deep Earth imaging and Comprehensive Test Ban Treaty (CTBT) has revived the use of cross-correlation detectors, thanks to the high coherence of a given signal across the array, and the search for repeating, low-magnitude events such as nuclear test explosions (Gibbons and Ringdal 2006).

There are several ways to alleviate the dependence on the template's waveforms—if this is desired. A template event brings both the source and propagation into the equation: $S(x,t)=M(t)*G(x,\tau;x_0,\tau)*\mathrm{R}$, where $S(x,t)$ is the signal recorded at location x and time t, M is the time dependent source term (moment tensor), and R is the receiver impulse response. Getting rid of the source term, for instance, gives access to the Green's functions, and can potentially detect any other event sufficiently close to it. Such an approach is often used in fracture monitoring. Perforation shots (assuming they are pure explosions) can be understood as a convolution between an impulse source and the Green's function.

Cross-correlation can also be used in phase picking (i.e., arrival time assessment) on seismic arrays, by taking advantage of the coherency of the arrivals across the sensors. Automatic or manual picks can be refined automatically (Rowe et al. 2002), or a few precise manual picks can be used to select the remainder of the sensors within the array.

20.2.4 Location Methodologies

20.2.4.1 Conventional Travel-Time and Azimuth Inversion

The determination of hypocentral coordinates and origin time is a longstanding problem in earthquake seismology. Considering that each earthquake's location is a four-parameters vector (x_h,y_h,z_h,t_0, representing spatial coordinates and origin time, respectively), the problem of finding its components using an m-dimensioned vector of data (travel times, wave's polarization, amplitude, and so on) is an ***inverse problem***. A trial-and-error type of methodology is typically used to compute the distance between a theoretical data vector calculated from a trial parameter vector and the actual measured data vector. The smaller the distance is, the closer you are to the solution. This vector difference is termed ***residuals***. The choice of a definition for a distance function (also termed ***cost function*** in the literature) depends on the problem at hand, but the L2 norm (Euclidean distance) is standard—it constitutes the so-called ***least-squares*** inversion. If the dataset is limited to arrival times ($t_k=t_0+T_k$, where t_k is the k-th arrival time, t_0 is the unknown origin time, and T_k is the k-th travel time), the classical solution to the location problem was first proposed as early

as 1910 (Geiger 1910) through the linearization of the nonlinear relationship between travel times and hypocentral coordinates and origin times. Considering an initial solution so as to calculate theoretical travel times:

$$\frac{\partial T_k}{\partial x}\Delta x + \frac{\partial T_k}{\partial y}\Delta y + \frac{\partial T_k}{\partial z}\Delta z + \Delta t_0 = r_k \quad \textbf{(Eq. 20.11)}$$

where T_k is the k-th travel time $k \in [[1;m]]$, r_k is the travel time residual for a trial parameter vector (x,y,z,t_0), and the Δs are perturbations to the initial solution. The relationship between the perturbations and the residuals is linear and can be solved by a series of steps and iterated to convergence.

The above equation demonstrates that it is necessary to model the travel times T_k to compare them to the measures. The complexity of this ***forward problem*** can vary greatly from homogeneous velocity models to complex 3D models with anisotropy through idealized tabular models for which analytical solutions are available. The introduction of other data such as wave polarization (Magotra et al. 1987), amplitude (Battaglia and Aki 2003), and so on may also complicate the cost-function.

20.2.4.2 Migration-Based Techniques

Seismic arrays have introduced ***delay-and-stack*** methods early on in global seismology (Rost and Thomas 2002). These delay-and-stack techniques use the facts that the signal is coherent from one station to another, and the signal can be coherently summed across the array. If delays are expressed as functions of the source's position, it then becomes possible to locate events (and event-detect them) through delay-and-stack. This is strictly equivalent to the exploration industry's migration, in which CDP reflections are back-projected at their spatial position (**Fig. 20.6**). Migration is typically undertaken by discretizing the parameter space (i.e., the source spatial region) in a dense grid. Each grid point is used as a test source, and corresponding lag-times are computed and applied to each trace of the array. They are then summed together through envelope, energy, or coherence functions (semblance stack; Neidell and Taner 1971), because there may exist phase differences due to the source's radiation diagram (Drew et al. 2005; Rebel et al. 2011). Note that migration methods can be used with either downhole (Bardainne et al. 2009; Rentsch et al. 2007) or surface arrays (Duncan 2005).

Although surface arrays processing sequences use almost exclusively the P-wave, it is possible to apply migration techniques to any type of phase. However, because

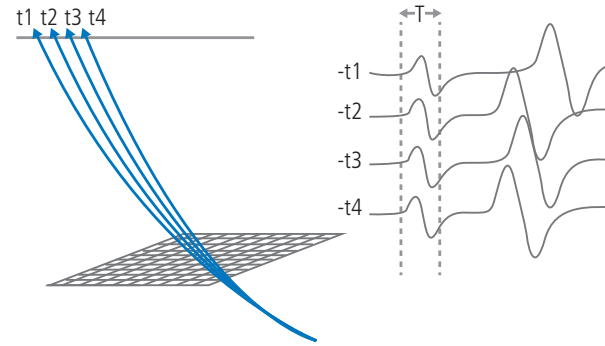

Fig. 20.6—Migration technique: The volume surrounding the sources of microseismic events is divided into cells. Each cell's corner is considered as a potential source location from which travel times are calculated. The corresponding move-out is then applied to each trace (t1, t2…) and stacked together. (Thomas et al. 1999.)

theoretical travel times have to be computed, it is necessary to have both P- and S-wave velocity models to account for the latter. Yet, using the S-wave has proved to drastically increase the resolution for depth (Gomberg et al. 1990).

20.2.4.3 Full-Waveform Back-Propagation

Migration techniques back-propagate energy onto diffracting points using a handful of phases (using main body-wave phases whenever possible) and solely using travel times from the test sources' location to perform a single-phased delay-and-sum operation. Provided that the entire seismogram contains all the information about source location, characteristics, and n the propagation, it is obvious that using the full waveform to perform the back-propagation should be beneficial. Back propagation of wavefields has been inferred in a series of seminal papers by M. Fink and his team (Fink 1992; Wu et al. 1992). This back-propagation approach has been applied to global seismology to image the rupture of large earthquakes (Larmat et al. 2006). Applications to smaller scale seismology, such as microseismic monitoring, have been studied from a purely quantitative standpoint (Artman et al. 2010), or within the rigorous framework of Bayesian inversion (Xuan and Sava 2010).

20.2.4.4 Relative (Re-)Location

At the root of relative location are earthquakes doublets; i.e., pairs of earthquakes with very similar waveforms. In the early 1980s, several authors attempted to study these doublets, and to use them to infer changes in the crust (Fremont and Poupinet 1987, Got and Fréchet 1993).

Later on, authors introduced the notion of earthquakes multiplets, which are several earthquakes with very similar waveforms (see, for instance, Got et al.1994). These clusters of earthquake events are usually generated at several locations on the fault plane, and relocating them all relative to the others allows a drastic increase in the resolution of their spatial distribution. This technique has supported the identification of small-scale structure on the fault plane through methodologies known as relative relocation [when starting with a catalogue of already located events; Deichmann and Garcia-Fernandez (1992)], double-difference location (Waldhauser and Ellsworth 2000) or double-difference tomography (H. Zhang and Thurber 2003), in which events are relocated and the velocity model is updated at the same time. These methodologies have been applied to microseismic monitoring for oil and gas applications only recently (Li et al. 2013; H. Zhang et al. 2009; Poliannikov et al. 2012). These works, in addition to their historical predecessors, stress the advantages of using relative over absolute information. In essence, all of these developments rely on the observation that similar close-by earthquakes have almost identical travel times—i.e., the propagation of their respective waves are quasi-identical (**Fig. 20.7**). As pointed out by Wolfe (2002), such travel-time differences will account for strong event's position dependent velocity heterogeneities at a local scale—i.e., between nearby events, but this bias cannot be reduced in the relative locations between earthquakes that are spaced far apart.

Since cross-correlations can be seen as a differential operation, because, for each lag time, the correlation is the summed phase difference, and scaled to the product of amplitudes. It becomes clear that correlating the detected events (or the raw data stream) with a known template, in its most simple expression, is locating relative to it, although the travel-time differences are not expressed explicitly. Based on Wolfe's comment (Wolfe 2002), the further each detected event is from the template, the lower the resolution on its location will be.

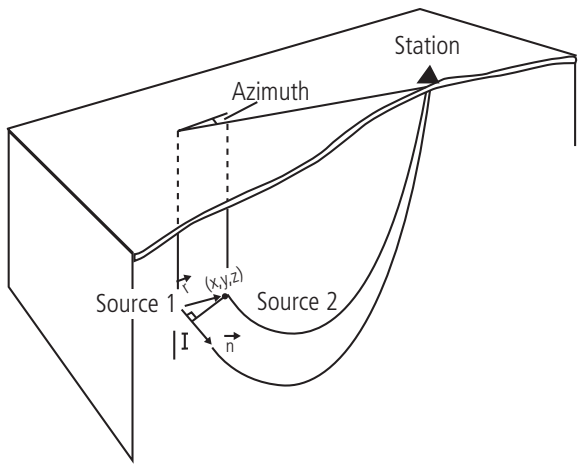

Fig. 20.7—Schematics for the relative location of two sources. Each source's rays share a common path down to a volume surrounding the two sources; the further from each other the sources are, the larger the relative error. (Adapted from Fréchet 1985.)

20.2.4.5 Source Mechanism Inversion and Magnitude Calculation

While there are several types of magnitudes, the source mechanism shall be uniquely defined—provided that the so-called "full moment tensor," i.e., double-couple and non-double-couple components are determined. As discussed earlier, the moment tensor is related to the measured displacement velocity by the convolutional operation $S(\mathbf{x},t)=M(t)*G(x,t;x_0,\tau)*R$, where $S(\mathbf{x},t)$ is the signal recorded at location $\mathbf{x}$ and time t, M is the time dependent source term (moment tensor), G is the Green's function (propagation term depending on the source spatio-temporal location and the receiver's location), and R is the receiver impulse response. Retrieving $M(t)$ is therefore an inverse problem, provided that the propagation term G and the receiver response are both known. Furthermore, the previous relationship shows that for the moment tensor to be determined, the source location must be known as well. Following Godano (2009), there are three methodologies to invert for the moment tensor (**Fig. 20.8**):

- Inversion of the polarization of the waves used (P- and/or S-waves first arrivals)
- Inversion of the amplitude
- Inversion of the full-waveform

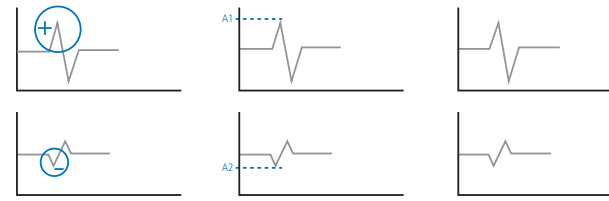

Fig. 20.8—Moment tensor inversion types (see text for details). From left to right: sign only, amplitude, and full waveform. (Godano 2009.)

The convolutional relation may be simplified if either the moment tensor is considered independent of time (i.e., split into a source time function and a time-independent tensor), or when the moment tensor is transformed into the Fourier domain. The relation between observed displacements and

moment tensor components then becomes simpler and can be written in the traditional form as: $d=G(m)$, where $\boldsymbol{d}$ is the n-dimensional data vector (containing the n observed amplitudes), G is the Green's functions (or in the inverse theory terminology, the kernel of the problem), and m is the vector containing the k parameters of the moment tensor (k being 6 in the case of a DC source, or 9 in the general case). This relationship may even become linear, depending on the parameterization of the problem.

Although amplitude inversion is the most used method, because it provides enough information to infer the focal mechanism and its nodal planes, the amplitude inversion can be limited in the sense of amount of data available. The inverse problem would need to have at least six or nine amplitudes to invert so that it remains determined; yet, because of noise and non-modeled velocity structure, the data space needs to be highly overdetermined. Full waveform inversion of moment tensor (Kawakatsu and Montagner 2008, Song and Nafi Toksöz 2011) can also be employed for the moment tensor determination, but it is generally limited to the lower-end of the spectrum because a short-wavelength propagation is hard to achieve with current propagation modelers. Last, but not the least, methods exist in which both the location and the moment tensor of the event are jointly determined (see, e.g., Auger et al. 2006; Vera Rodriguez et al. 2012).

Estimating magnitudes remains challenging especially in the context of low SNR signals. Care must be taken to preserve the amplitude of each recorded trace, as well as to properly recover the propagation effects by including elastic and anelastic attenuations, plus a radiation diagram if the event is close (as is the case for microseismic monitoring, as opposed to teleseismic, and even regional, seismicity). In addition, the proper selection of a magnitude scale with respect to the problem may also influence dramatically the range of estimated magnitudes (Shemeta and Anderson 2010). Moment magnitude remains the principal choice in the oil and gas microseismic monitoring industry, although it is the most difficult to assess properly (quality of the moment tensor inverted, radiation diagram estimation, the phase used to estimate the moment tensor, and so on). Magnitude can also be estimated through amplitude variations (as is the case with the so-called local magnitude, M_L), should the radiation diagram be impossible to infer (single downhole tool).

20.2.5 Understanding the Physical Processes behind the Microseismic Cloud

We have shown in the previous sections that (micro-) earthquakes could be parameterized using their spatiotemporal coordinates, as well as their sources' characteristics (so-called general moment tensor, discussed earlier in this chapter). It is, however, critical to establish the link between these parameters, on the one hand, and the physics of the hydraulic fracturing, on the other hand. Several parameters are traditionally used in the earthquake seismology community and are presented in the following sections. Using these descriptive attributes, we can then infer how the microseismic activity ties in with the geomechanical behavior of the fracturing.

20.2.5.1 Source Mechanisms and Their Relationship to Geomechanical Behavior

In this section, we discuss the background concepts based in geomechanics, including physics, brittle deformation, and microseismic; concepts used to understand the complexities involved with hydraulic fractures and deriving production models; and microseismic monitoring related to events, locations, and time sequences.

20.2.5.1.1 Geomechanical Concepts: Understanding the Physics behind the Dots

During hydraulic fracturing, the fractures induce two changes in the reservoir as they are created and propagate away from the wellbore:

- The stress field is perturbed because of the (elastic) deformation of the rocks surrounding the fracture as it opens.
- The pore pressure changes because of fluid leakoff from the main fractures into the rock matrix and/or through pre-existing fractures crossing the path of the fractures.

Indeed, rocks have natural weakness features (such as bedding planes, natural fractures, and so on) in which both of the above mechanisms will generate shear stresses, possibly resulting in shear slippages on the planes. When the shear stress applied onto the weak plane becomes larger than its friction coefficient (resistance to shear stress, μ), the fracture plane slips over an area A and with a displacement $\boldsymbol{d}$ at a speed large enough to emit seismic waves. Naturally, the type of slippage (from pure shear to tensile) depends on the fracture orientation (Barton, Zoback, and Moos 1995; Fischer and Guest 2011), with respect to the orientations and magnitude of the principal stress (**Fig. 20.9** and **Fig. 20.10**).

As pointed out by Sileny et al. (2008, 2009), their observations of tensile ruptures indicate that ruptures are seldom, if ever, due to the main fracture opening. As a matter of fact, the fracture tips area—where the fracture propagation occurs (as first theorized by Griffith, 1921)—is likely to be too small to generate micro-earthquakes with a magnitude large enough to be measurable, even with a nearby downhole array. However, and as explained by Fischer and Guest (2011), the orientation and magnitude of principal effective stresses may very well induce a tensile component on the (pre-existing) weakness planes. Based on these observations, we can understand that the microseismicity induced by fracturing acts as a proxy for the main hydraulic fracture and that a fraction of this microseismic activity is in direct connection to it, thus, playing a role in the overall permeability increase. The amount of such an increase due to natural fractures is, however, highly dependent on the play—from naturally highly fractured reservoirs to more ductile reservoirs.

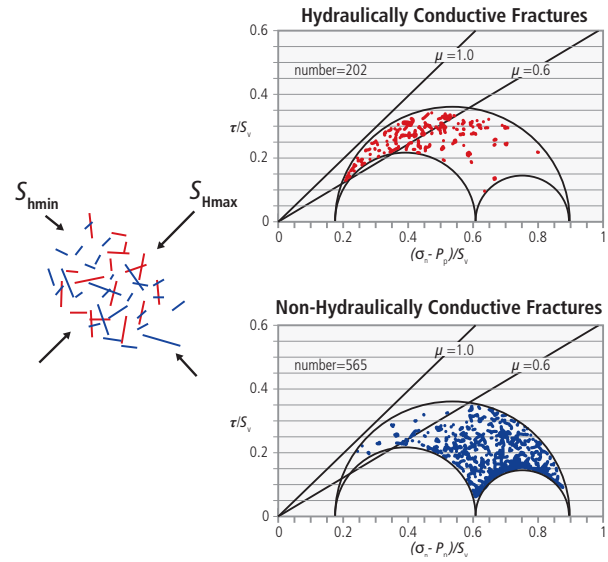

Fig. 20.9—Depending on the relative orientation of the principal stresses' natural weakness planes will be activated when a change in normal stress is applied (as, e.g., stress field modifications and/or pore pressure changes). (Adapted from (Barton et al. 1995, Zoback 2010.)

20.2.5.1.2 Relating Brittle Deformation to Microseismic Parameters

The energy input into the reservoir system through hydraulic fracturing is tremendous when compared to the energy released through microseismic activity. Yet, as pointed out previously, the microseismic cloud can serve as a proxy to estimate the main fracture's characteristics, provided that any stress-induced earthquakes that can possibly occur away from the fracture can be separated from the remainder of the cluster. Combining the measurements made using microseismicity with other measurements (from tiltmeters, pressure curves, production, well testing, fracturing models and so on) can, therefore, narrow down the estimates of the fracture's geometry (Cipolla and Wright 2000).

Several attempts have been made to try to relate microseismic parameters to the increase in connectivity between the reservoir and the wellbore. Among these efforts, the stimulated reservoir volume (SRV) concept, introduced early on by Fisher

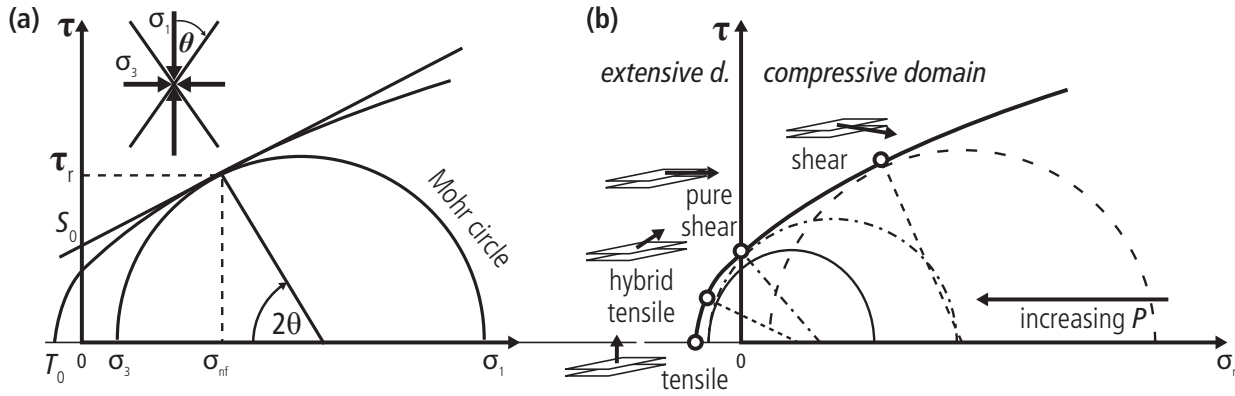

Fig. 20.10—First (a) is the principle of Mohr circle, showing the locus of shear (τ) and normal (σ_n) stresses upon a plane whose orientation makes an angle θ with the principal stress, σ_1. Next, (b) depending on the orientation of the fracture plane and the stress state (magnitude of principal stresses), the rupture type ranges from pure tensile to shear, with a combination of the two mechanisms in- between. (Modified from Fischer and Guest 2011.)

et al. (2004), accounts for the complexities in the description of hydraulic fractures in the Barnett shale. The SRV concept has been used afterward, as a means to derive production models, and has been extended to other plays (Detring and Williams-Stroud 2013; Detring and Williams-Stroud 2012). However, this concept has been shown to poorly represent the production in some instances (Moos et al. 2011). Other authors have tried to associate the microseismically derived parameters (fracture dip and strike, and ruptured area) with discrete fracture networks (DFN). This is assuming that natural fractures contribute extensively to the increase in reservoir-wellbore connectivity. In addition, the seismological understanding associated with source's size are somewhat less understood and tend to be very model dependent (Snoke et al. 1983; Beresnev 2001). The concept of natural facture contribution has been shown to be very plausible in some cases (Fisher et al. 2002, Barton et al. 1995; McClure, Horne, and Keeton 2013), which includes—but is not limited to—crystalline formations. Other authors have measured the conductivity of the fractures through time showing a steep decrease in conductivity caused by recrystallization and healing of the fracture gouge (Stoddart et al. 2012).

20.2.5.2 Event Locations and Time Sequence

The primary application of microseismic monitoring is the capability to map the events that are close enough to the main fracture to assess the fracture's geometry. Ever since monitoring has been used during fracturing operations, the resolution in time and space has dramatically increased. This, in turn, has allowed the events to be mapped alongside with the fracture model as the stimulation goes on. It is, however, important to be able to separate the microseismic activity due to stress-changes (which may act far away from the main fracture; see Nagel et al. 2013) from the microseismic activity related to the fracture itself. Such analysis usually considers both temporal and spatial distributions—so called *r-t* plots, and compares them with hydraulic diffusivity (Hummel and Shapiro 2012), or in a simpler yet practical approach, the hydraulic front based on fracture models (PKN, GDN, radial, **Fig. 20.11**; Economides and Nolte, 2000 for a comprehensive review of existing fracture models).

20.2.5.3 Statistical Description

Understanding the physics of the brittle deformation is a traditional approach used in earthquake seismology. This approach takes a broad view as opposed to evaluating events individually. The goal is to find models that reproduce the overall behavior of seismicity, regardless of small-scale rupture physics.

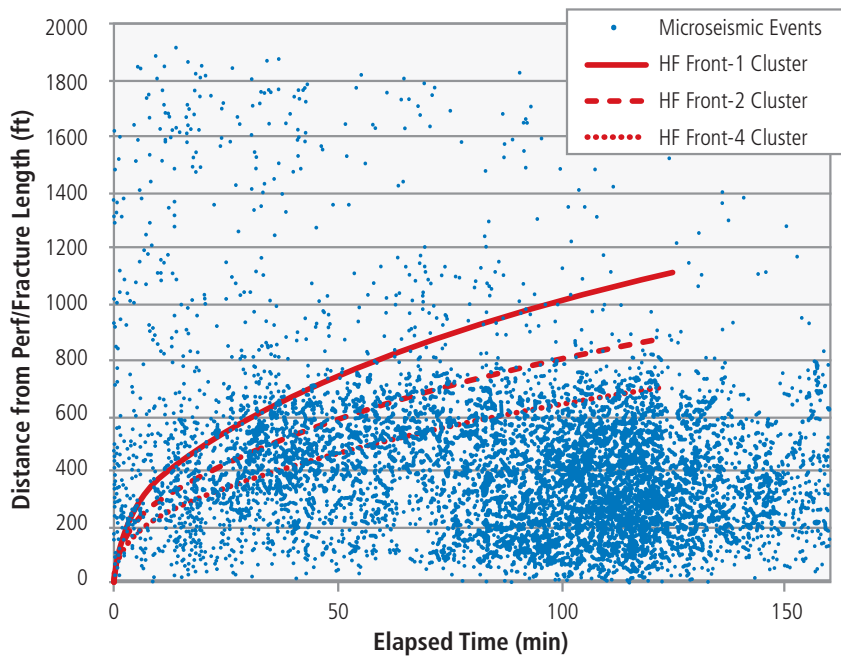

Fig. 20.11—Example of the comparison of a microseismic catalog with a hydraulic front propagation. Events located 2000 ft. away from the wellbore at time 0 are unlikely to be connected with the fluid-front propagation.

20.2.5.3.1 Gutenberg–Richter Relation (Magnitude-Frequency) and *b*-value

A general observation of earthquake size distribution is that large earthquakes are less frequent than small earthquakes. Such a simple statement is quantitatively validated by the Gutenberg–Richter (G-R) relation (Gutenberg and Richter 1944 and1949). The G-R relation describes the number of events expected of each magnitude (or size) in a given area:

$$logN(M)=a-bM \qquad \textbf{(Eq. 20.12)}$$

where a and b are constants and $N(M)$ is the number of earthquakes of magnitude M or greater. **Fig. 20.12** shows an example of the empirical G-R relation at a very large spatial scale (whole Earth) and over a long period of time (almost a century). Fig. 20.12 shows a striking linearity for a catalog encompassing such large space and time scales.

The *b*-value in the G-R relationship has been shown to be consistently nearly 1 at a global scale. However, at smaller space and time scales, the *b*-value can vary significantly from 0.3 to 2 (Utsu 2002, Ogata and Katsura 1993). The main conclusion from these observations is that fracture and fault networks are fractal over a wide (but finite) range of scales. In other words, whatever the scale (from centimeter-scale laboratory experiments to plural-kilometric scale faults in the Earth's crust), the frequency-to-magnitude distribution remains valid. It is, however, difficult, if not impossible, to measure all of these different scales using a single measurement tool or method; each "tool," such as a global network, local network, laboratory measurements, and so on, is limited in the range of magnitude (or energy) that it can measure. The magnitude below which the entire seismic activity is no longer recovered is termed magnitude of completeness (mc) and is dependent on both the sensitivity of the network used and on the ambient seismic noise. Its importance, although sometimes overlooked, is central in the correct interpretation of the seismicity that is generated by the stimulation (Woessner and Wiemer 2005; Williams and Le Calvez 2012).

When following these assertions, it's not surprising to notice that the microseismic activity observed during hydraulic stimulation shows a similar behavior; i.e., the frequency-to-magnitude plot is log-linear. Furthermore, *b*-value variations give insights on how the population of large events relative to smaller ones evolves through space and time (Grob and Van Der Baan 2011).

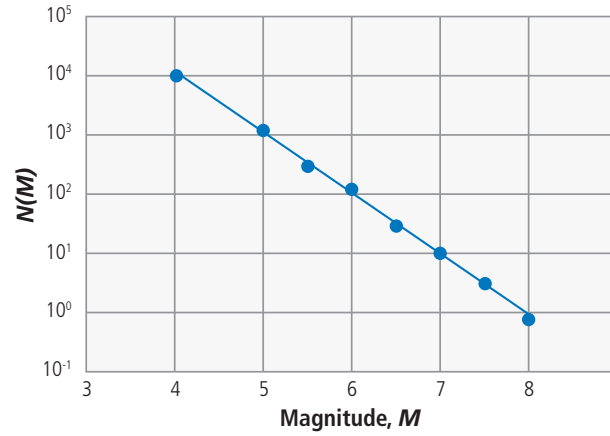

Fig. 20.12—Magnitude-frequency relationships for earthquakes around the world from 1904 to 1980. *N(M)* is the number of events (per year) with a magnitude greater or equal to M. (Kanamori and Brodsky 2004.)

20.2.5.3.2 D-Value

The D-value is a mean value used to measure the "damage" localization and corresponds to the spatial correlation dimension of damage based on the correlation integral method (Grassberger and Procaccia 1983):

$$C(r) = \frac{2}{N(N-1)} N(R > r) \qquad \textbf{(Eq. 20.13)}$$

where N is the total number of events, $N(R>r)$ is the number of pairs of events separated by a distance smaller than r. Should this spatial correlation exhibit a power law; i.e., $C(r) \sim r^D$, the events population is said to be fractal with a dimension D. In general, D is a non-integer value ranging from 0 to 3 and higher. A single point would have a zero D-value, a line 1, a plane 2, and a sphere 3. The D-value therefore allows the spatial structure of the microseismic cloud to be characterized by a single parameter that can be time-dependent. Surprisingly, the D-value is seldom if ever used in the industry (see Grob and van der Baan 2011).

20.2.6 Current and Future Developments

20.2.6.1 Integration with Other Measurements

These past few years, the oil and gas geophysical industry has been leaning toward multi-physics integration (for instance, "seismic imaging is indeed progressively and jointly analyzed with potential methods"). Microseismic monitoring doesn't conflict with this trend. It is becoming

obvious that other measurements can help to better constrain the information that the industry wants to gather from microseismic monitoring. Early on, experts have stated that coupling passive seismic monitoring with other measurements (such as from tiltmeters, radioactive tracers, or temperature logs) and reservoir engineering (well testing, production, or modeling) would help the industry gain a better understanding of hydraulic fracturing and improve treatment designs (Cipolla and Wright 2000). Yet, such integration has remained low despite efforts made by operators (Lowe et al. 2013). As advocated by Cipolla and Wright (2000) and Fisher et al. (2004), the most common, coupled measurements remain passive seismic and tiltmeters, either from the surface or from downhole.

On the other hand, there are a number of other measurements that could—and should—be considered in fracture diagnostics and stimulation monitoring. Here are only a few examples to demonstrate this statement and to leave room for further integration efforts: pre- and post-stimulation seismic survey (Willis et al. 2007), electro-seismology (Mahardika et al. 2012), distributed temperature and acoustic sensing (Molenaar and Cox 2013), and even satellite interferometry in some instances (Bourne et al. 2006). Refer to the next section for a review of tracers and associated tracer technologies.

20.2.6.2 Emerging Sensors

As discussed earlier, several acquisition designs are available. The basis for the presented acquisition schemes lies in the sensing device itself. The most common sensors are S-wave geophones (velocimeters). Many different sensors exist, including accelerometers and hydrophones that could also be used in the context of microseismic monitoring. Consider digital accelerometers that are typically used for strong-motion measurements (Clinton and Heaton 2002; Iwan et al. 1985), which allow a simplified field-manipulation. This is because digital sensors are easier to work with at the acquisition stage, and can integrate with other digital measurements, such as GPS positioning.

Distributed acoustic sensing remains the most promising sensor for both downhole and surface microseismic monitoring. So far, it has been shown to be useful in active monitoring (Mateeva et al. 2013; Kiyashchenko et al. 2013); however, its poor (lateral) sensitivity remains an obstacle for microseismic applications (Grandi Karam et al. 2013). The low cost and ease of deploying an optical fiber in a well—possibly, the treated well—makes digital acoustic sensing a very interesting development for the future of microseismic monitoring.

20.2.7 Case Study: The Information Carried Out by Microseismic Monitoring of a Stimulation in the Upper Devonian of West Virginia

A comprehensive study, encompassing several types of measurements, was carried out in an Upper Devonian shale gas reservoir in West Virginia (Huron formation; Moos et al. 2011). Among the tools used in this study, a downhole microseismic monitoring array was deployed in a horizontal well and used throughout the stimulation (**Fig. 20.13**). This study provided a good example of how to use the microseismically derived information (locations, magnitudes, and moment tensors) to understand the outcome of the fracturing and, ultimately, to provide an estimate of the future production potential.

Overall, 972 events were detected and located on 9 stages (Fig. 20.13 and **Fig. 20.14**) by using the procedure described in Bardainne et al. (2009). Focal mechanisms have been determined for those events with a high signal to noise ratio and that have large enough body-wave amplitude when following the methodology described by Godano et al. (2009) and Godano et al. (2010) (Fig. 20.14). The located microseismic clouds show different behaviors depending on which stage the cloud corresponds to. As an example, stages near the toe of the well show a larger microseismic count than those at the heel of the well. Overall, the clusters are all oriented perpendicular to the wellbore, as expected.

Fractures and stress orientations have been inferred from wellbore breakout and image/acoustic log analysis and the corresponding trends are shown on **Fig. 20.15**. The blue-outlined diagram represents the stress orientation as inferred from the wellbore breakout and geomechanical analysis. The red one shows the fractures orientation deduced from the log analysis.

Comparison with the orientation of the microseismic clouds tends to show that the clusters are oriented parallel to the natural fractures orientation rather than the maximum horizontal stress (Fig. 20.15). Although the location uncertainty can be invoked to explain such behavior, this is especially true because there is little difference in orientation between stress and fractures.

Interestingly, the events count is poorly correlated with the production data measured a year after the stimulation on a stage-by-stage basis (Moos et al. 2011). On the other hand, they report a positive correlation between the fracture frequency and the production logs. Zhang et al. (2014)

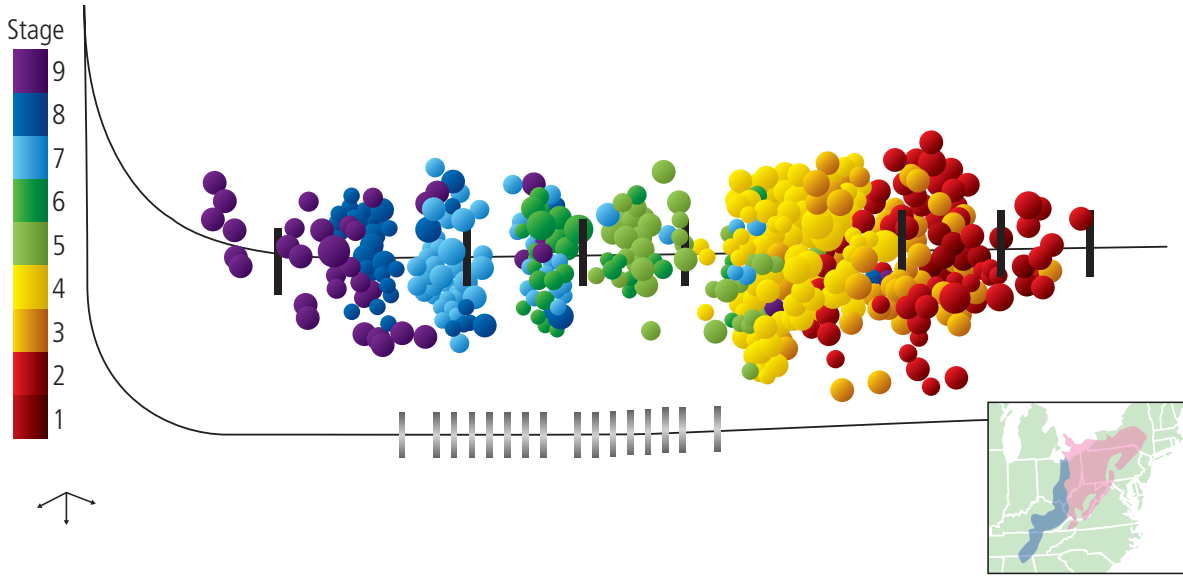

Fig. 20.13—Side view of the wells addressed in the studies of Moos et al. (2011) and Zhang et al. (2014): treatment well (top) and the observation well (bottom). Events are color-coded by stage. The gray bars in the observation well denote the sensors location, while the blue bars in the treatment well are the sleeve locations.

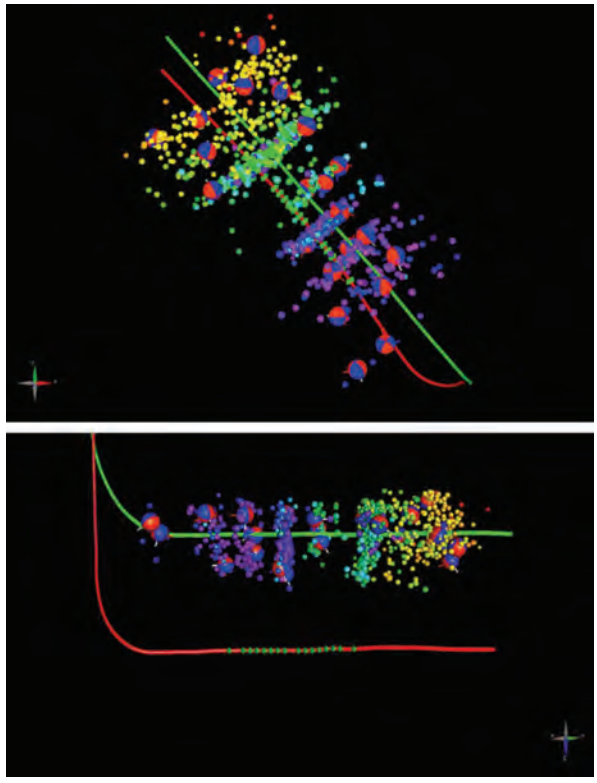

Fig. 20.14—(Top) map view and (bottom) depth view show the detected and located microseismic activity. Moment tensors of selected events are also plotted. Early (toe) stages show larger microseismic clusters. Refer to Fig. 20.13.

proposed to use a proxy for the released energy by brittle deformation (i.e., the cumulative scalar moment) instead of the sole event count to predict productivity of each stage from microseismic monitoring.

In addition, by properly estimating the magnitude of completeness (minimum magnitude below which the microseismic activity is no longer measured properly by the monitoring networks, but only retrieved partially), they extended the Gutenberg–Richter curve's reach toward the low magnitude-end and managed to (statistically) account for small events that remained undetected by the monitoring array. Doing so, they managed to achieve a higher correlation between a microseismic-derived parameter—the cumulative scalar moment—and the production log (**Fig. 20.16**).

20.3 Fiber Optic Monitoring

We start this section introducing the topic of fiber optic monitoring, followed by a discussion of distributed temperature sensors (DTS) and distributed acoustic sensors (DAS) and how they are applied toward hydraulic fracturing monitoring in conjunction with integration with completion. Such integration and application is illustrated via case study. Application of the fiber optic technology and how it is associated with production logging is also discussed. In addition, we will address the evaluation of the effectiveness of the hydraulic fracture treatments.

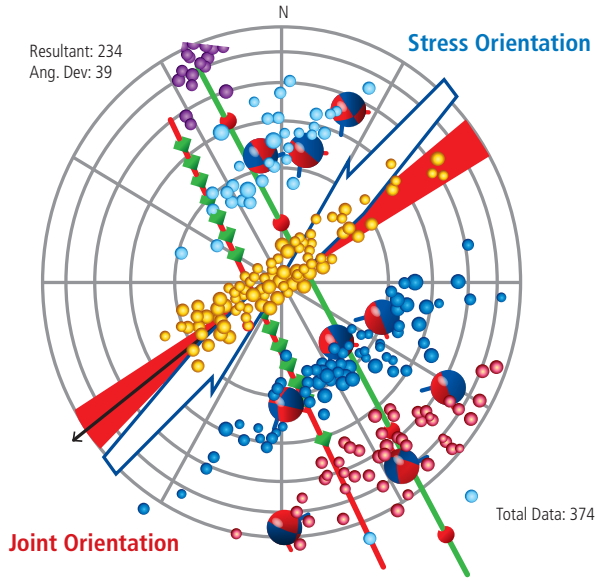

Fig. 20.15—Comparison of the fracture strike inferred from microseismicity (both cloud's orientation and fault plane solutions) and wellbore breakout and natural fracture analysis. (Moos et al. 2011.)

20.3.1 Fiber Optic Monitoring

The development of fiber optics for downhole sensing is rooted in the need to survey long lengths of wellbore without the installation of discrete sensing elements. Fiber optic technology was originally developed for telecommunications applications, but has now been adapted and optimized for the downhole environment. Installing fiber optics into a downhole application requires that the fiber be housed inside a protective 1/4-in. tubing that acts to isolate external pressure and eliminate contact with downhole fluids. A second 1/8-in. internal metal tube is housed within the 1/4-in. line to isolate fiber optic lines from any external stress and strain that can be applied to the cable (**Fig. 20.17**). Optical properties of the fiber are sensitive to strain and can drastically affect measurements if a cable is not properly designed. A non-metallic layer between the 1/4-in. and 1/8-in. tubes also helps to prevent the transfer of strain to the fibers. High temperature applications can initiate fiber optic failure due to hydrogen diffusion into the silica of the glass called hydrogen darkening. Thixotropic gel inside the 1/8-in. tube acts to scavenge free hydrogen within the cable and to prevent hydrogen darkening. In certain applications, an encapsulation is needed for the cable to survive installation or abrasion from fluid flow. Selecting of encapsulation material must consider downhole temperature, fluid chemistry, and cable exposure.

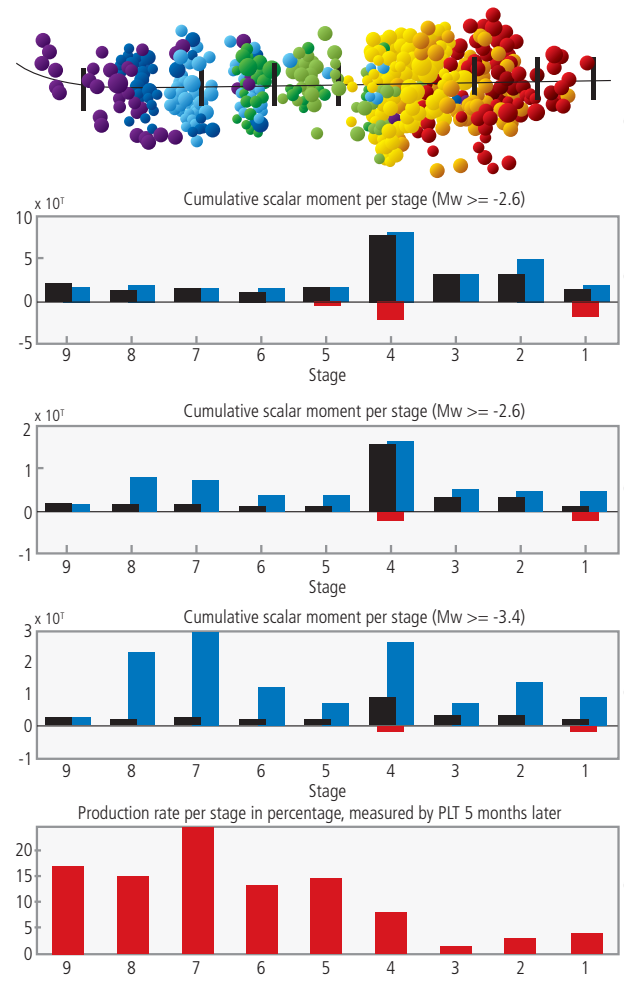

Fig. 20.16—Comparison of (a) the events count (represented as microseismic clouds), (b) cumulative scalar moments with different magnitude of completeness (b, c and d), and stage-wise production logs (e). The lower the magnitude of completeness, the higher the correlation between the microseismic-derived parameter and the production. (Zhang et al. 2014.)

Fiber optic measurements allow for three distinct measurement types to be made with similar fiber optic configurations, depending on the measurement of interest (**Fig. 20.18**). Early applications in downhole environments were for the use of discrete measurements at a single point; i.e., pressure and temperature sensors. The next measurement type is distributed sensors, in which the entire fiber acts as a continuous sensor with no need for discrete sensors, which is used in distributed temperature and distributed acoustic sensing. This topic is covered in more depth later. Typically, a measurement is output continuously along the length of the fiber at a set spatial resolution. Discrete distributed sensors are the multiplex of discrete

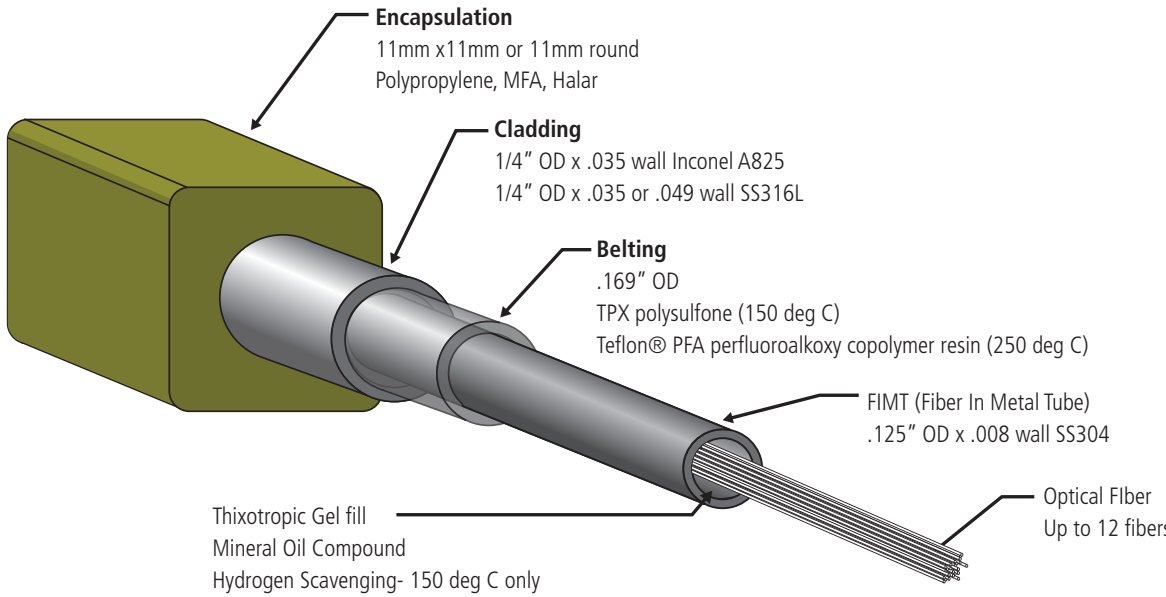

Fig. 20.17—Fiber optic cable cutaway view showing encapsulation and cladding around optical fiber.

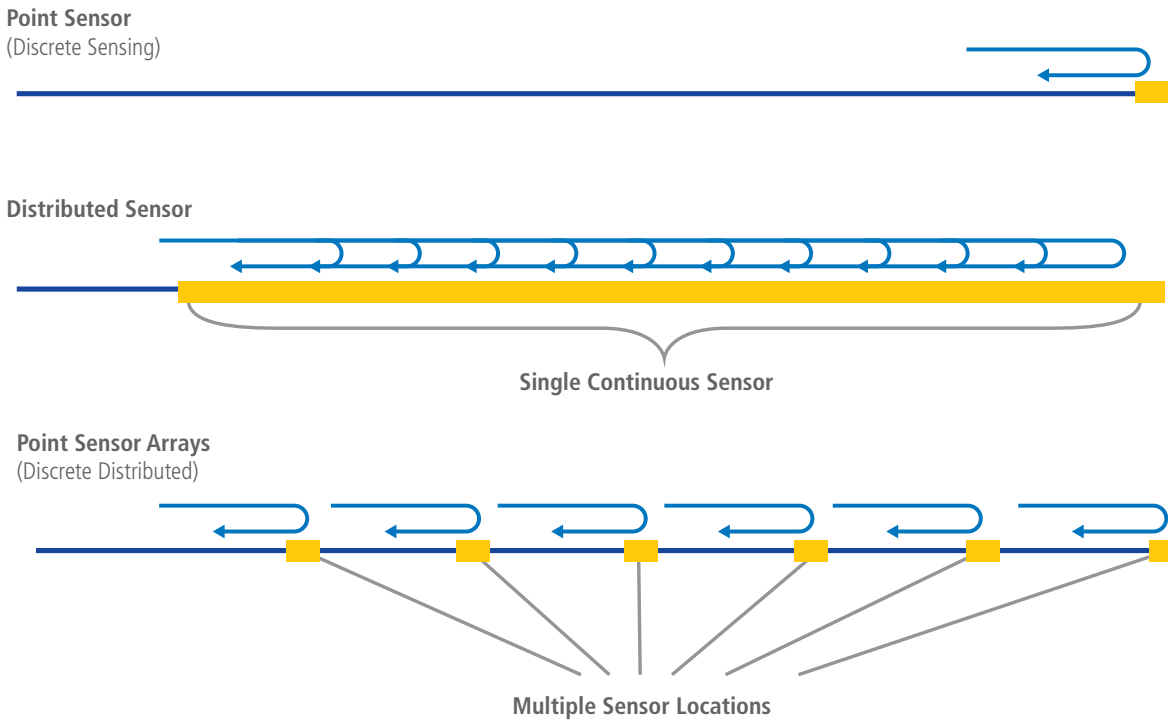

Fig. 20.18—Fiber optic measurement types. (From Molenaar et al. 2012.)

sensors along an individual fiber and typically numbering on the order of several thousand sensors. This technology is used in strain monitoring systems for well compaction and integrity monitoring systems.

20.3.2 Distributed Temperature Sensing

Distributed temperature sensing (DTS) is a fiber optic measurement technique that allows for a continuous temperature measurement along the length of a fiber at lengths of up to 30 kilometers. When a laser pulses light through a fiber optic line, small amounts of light are backscattered to a receiver. The backscattered light returns at the launched wavelength, called a ***Rayleigh band*** (**Fig. 20.19**). At wavelengths just above and below the launched wavelengths, the Stokes and anti-Stokes band are reflected and their ratio is linearly related to temperature. Analysis of the Stokes-to-anti-Stokes ratio, and measuring the two-way travel time to associate depth, allows for a continuous temperature profile measurements.

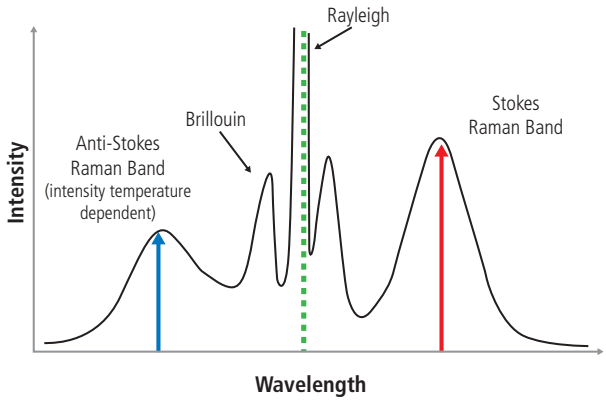

Fig. 20.19—Raman back scattering.

20.3.3 Distributed Acoustic Sensing

Distributed acoustic sensing is a new measurement technique that allows for simultaneous sound measurement across long lengths of a fiber optic line. Acoustic signals are detected by a laser pulsing at a high frequency, and then by analyzing the light that returns to a photo detector. A small fraction of the light is scattered back to the detector at the original wavelength of the laser pulse called ***Rayleigh backscatter***. Using interferometry, very small changes in the backscatter (caused by vibrations) can be measured continuously for up to 50 kilometers at 20 kHz bandwidth (**Fig. 20.20**).

20.3.4 Hydraulic Fracture Monitoring

Integration of a fiber optic monitor into a hydraulic fracture completion offers two distinct challenges: the installation of cable into an open hole with direct contact with formation, and the challenge of the monitor surviving the highly abrasive slurry that can flow as high as 100 barrels per minute. To address these challenges, a system of cable protection has been developed, as well as best practices created for drilling and completing the well to limit the risk of cable damage.

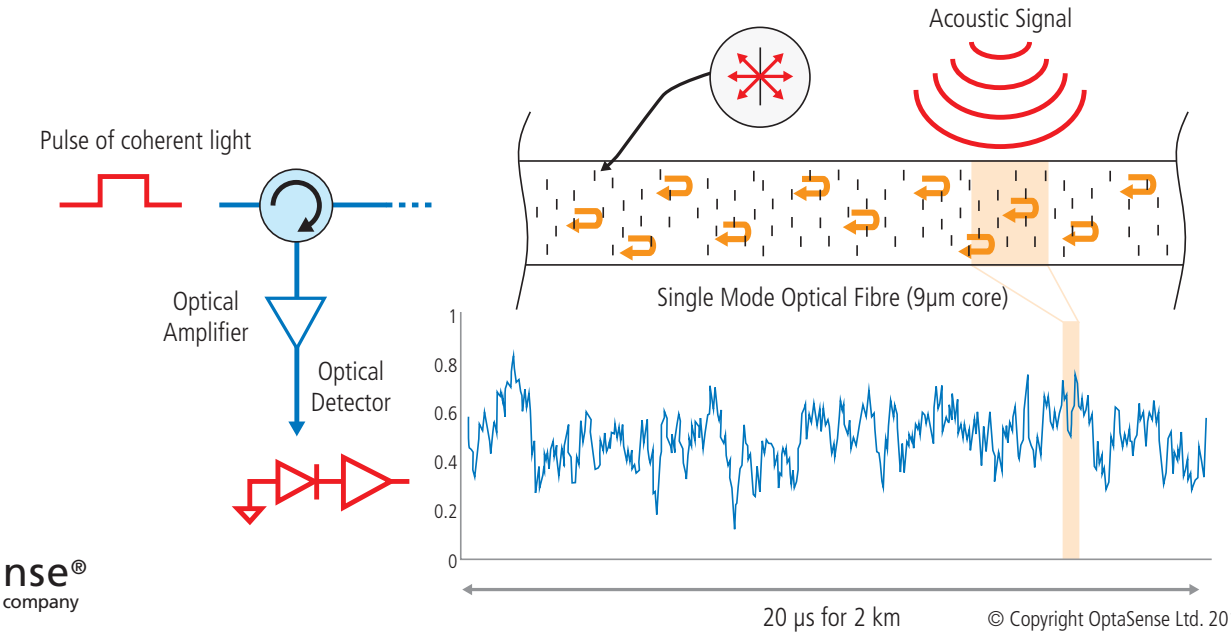

Fig. 20.20—Rayleigh backscatter physics. (Courtesy of Optisense.)

Cable design must be optimized for installation in the openhole formation by selecting an encapsulation material that is suitable for downhole chemistry and temperatures. The encapsulation provides rigid protection in the event of any direct impact with the cable, while also reducing frictional drag as the casing and monitoring cable are run across the formation. Operator experience has shown failure during hydraulic fracturing treatment to be the most common failure mode in casing conveyed systems (Bateman et al. 2013). New encapsulation material with low abrasion loss has shown a doubling of cable durability in lab tests designed to simulate fluid velocities during treatment. Early field trials have shown promising results (Bateman et al. 2013).

Integrating the cable with the completion will first require all the completions to feature casing-to-the-surface as a way to convey instrumented cables (**Fig. 20.21**). Field experience has shown that metal protectors should be used at every coupling to protect the cable from direct impact with the formation at every coupling upset. For openhole completions with swellable packers, provisions must be made to allow for control line bypass through the elastomer. To maintain equivalent packer pressure, an increase in swellable element length is necessary. Plug and perforate completions require blast protectors to be located at each perforation for additional cable protection. In addition, perforation design must be changed to 0° phasing to accommodate instrument cable in the completion. The orientation of the cable is first determined using a magnet flux-logging tool to identify the azimuth of the cable. Perforations are then performed using oriented perforating 120°–180° away from the cable azimuth.

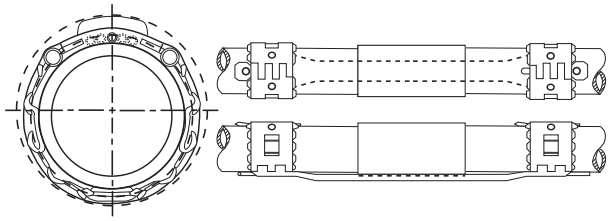

Fig. 20.21—Completion integration. (Courtesy of Forum Energy Technologies, Miguel Ortega.)

Data collection during hydraulic fracturing operations consists of a single truck onsite with appropriate DTS and digital acoustic sensing surface systems. Pumping data for pressure, flow rates, and proppant concentration are fed from the data van to the monitoring truck. Using the surface-provided data and downhole acoustic measurements, the flow rate can be calculated for each perforation (or sleeve) in a multistage completion. Liquid and proppant placement can be calculated in real time, providing the possibility for real-time treatment optimization to control limited entry performance (**Fig. 20.22**). Acoustic and temperature data can also identify loss of zonal isolation due to plug failure or breakdown in cement sheath integrity. Collection of fracture monitoring data allows for diagnosing completion and stimulation design and its effectiveness in heterogeneous formations (**Fig. 20.23**). Multistage completions allow for comparison of multiple completion configurations with sufficient sample size to evaluate stimulation effectiveness.

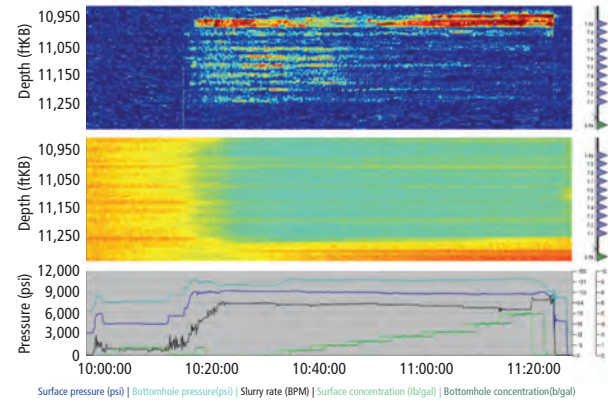

Fig. 20.22—Real-time data collection with fiber optics. (Courtesy of OptaSense 2013.)

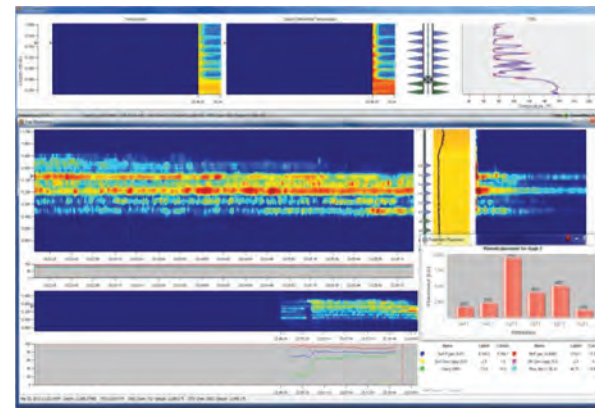

Fig. 20.23—Digital acoustic sensing data indicates limited entry failure mid-stage. (Courtesy of OptaSense 2013.)

20.3.5 Production Logging

Casing a conveyed fiber optic installation remains a post-stimulation activity to allow production logging to be performed without well intervention being necessary. This allows insight into the long-term flow behavior of unconventional wells and the identification of low-productivity intervals. Using DTS

measurements, a geologic wellbore model can be constructed to calculate thermal profiles due to Joule–Thompson induced temperature changes (**Fig. 20.24**). Digital acoustic sensing measurements can also be used to detect acoustic energy while fluid flows through perforations and enters the wellbore.

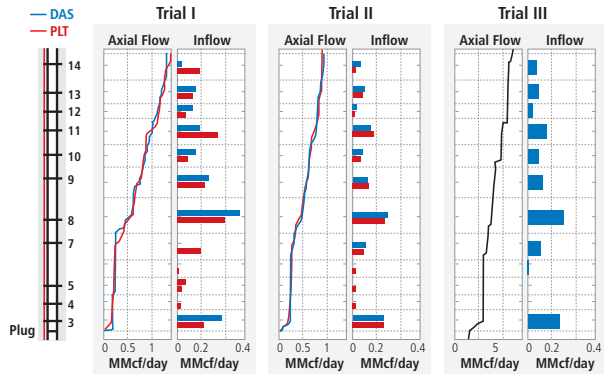

Fig. 20.24—Digital acoustic sensing and tiltmeters and production logging analysis. (Van Der Horst et al. 2013.)

20.3.6 Concluding Remarks

Reservoir engineering tools alone are not capable of constraining the interpretations for complex framework of fracture and subsurface models. Additional microseismic and downhole monitoring techniques are required to scale down the space production-related measurement range and to provide enhanced near-well and far-field heterogeneity for shale characteristics. These techniques can help operators in adjusting the subsequent completion and production planning, and even in ongoing operations. In addition, these surveillance techniques, although new, have shown promising results in numerous field studies since their introduction to the industry. These practices also provide the geoscience team with a valuable, qualitative way to gauge the interpretation methodologies, and an in-depth, quantitative measure to build a continuous profile of acoustic properties. When complemented with each other and other numerical techniques, microseismic and downhole monitoring techniques can reduce the uncertainty for fracture geometry, actual stimulated reservoir volume, connectivity between fractures and wellbores, and production contribution from different fracture stages, all of which can be done without the need for wellbore intervention and the associated risks.

20.4 Permanent Downhole Inflow Tracer Monitoring Technology

Production and reservoir surveillance is the key reason for using permanent downhole inflow tracer monitoring technology. This technology also provides a way to estimate the effectiveness of the induced hydraulic fracture treatment. Here, we first introduce the concept of tracer surveillance and then follow that concept with the challenges associated with inflow monitoring. Next, we discuss the numerical and flow-loop models and the associated interpretation of the data along with how these methods pertain to the surveillance. Chemical methods and sensors are also discussed followed by a multistage case study. This section concludes by addressing how the inflow tracer monitoring technology fits with microseismic and fiber-optic-related methods. Fiber optic methods are discussed in the next major section in detail.

20.4.1 Introduction to Tracer Surveillance

Tracer technology offers a powerful means for conducting production and reservoir surveillance, which is both operationally simple to deploy and cost effective. In terms of reservoir surveillance, an inert and low adsorption tracer is injected into water or gas injection wells, while the tracer's breakthrough time and concentration are monitored in one or more production wells (**Fig. 20.25**). Such tests not only provide an understanding of the preferential flow paths between injectors and production wells, they also provide a method of understanding reservoir connectivity, verifying suspected flow barriers, characterizing flood patterns, and analyzing the effects of volumetric sweep efficiency. The technique is well documented and has been practiced for many decades, as summarized by Du and Guan (2005).

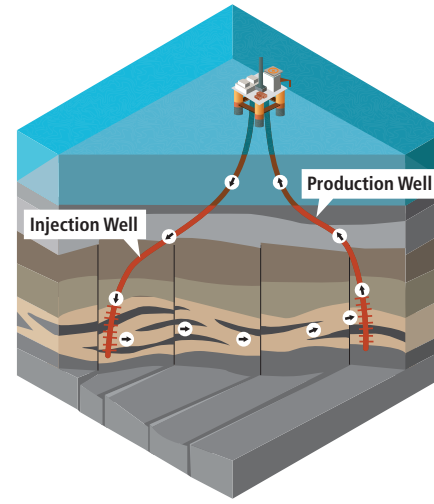

Fig. 20.25—Inter-well tracing between an injection and production well to understand reservoir connectivity between multiple wells. (Courtesy of RESTRACK™.)

Partitioning inter-well tracer tests (PITTs) is a more recent development in tracer technology that can quantify the remaining oil outside the near well region, and access field potential for EOR. Partitioning and ordinary tracers are injected into injectors and sampled at the producers. The partitioning tracer will lag behind the ordinary tracer; this time lag is directly related to the oil saturation in the inter-well reservoir volume. Finding partitioning tracers that survive the harsh temperature, chemical, and microbiological conditions present in petroleum reservoirs is challenging. However, reliable oil-water partitioning tracers suitable for use in oil-reservoir PITT applications were recently developed and field-tested, which now allow measurement of remaining oil saturation in inter-well regions (Viig et al. 2012).

Production surveillance has been practiced widely, and, coupled with single well tracer testing, used successfully to estimate residual oil saturation. Essentially, the operation requires injecting a slug of tracer, which has the property of dissolving to form a second tracer due to hydrolysis while the production well is shut in. The secondary tracer has a different partitioning between oil and water, and this property effects the arrival time of the two tracers allowing residual oil saturations to be estimated. More details can be found in the literature and its field application (Sheely 1978). However, in complex wells and reservoirs, the single-well chemical tracer tests may be challenging to interpret. In such cases, interpretation may require modeling using tracer simulators that can handle chemical reactions as well as its transport (Huseby et al. 2012).

A more recent development with single-well tracer technology is to install unique chemical tracers that are embedded into porous polymers, and place them in selected locations along the lower completion. This means that unique tracers can be installed in the completion to provide a permanent monitoring system. The tracers that are placed at different production intervals will help answer key reservoir management questions such as:

- Which zones or compartments are producing?
- What is the relative contribution from each zone?
- Where is water breakthrough occurring?

The primary purpose of this type of tracer is to characterize inflow performance along production wells. This unique chemical tracer is used for what is more often described as "inflow tracing." Over the last few years, inflow tracing has become widely deployed to monitor conventional reservoirs that are either especially suited to use complex well completions, or in offshore environments where alternative reservoir monitoring techniques are logistically impossible or prohibitively expensive. There are some early adopters using this approach in the unconventional onshore plays as well. The inflow tracers are soluble in either oil or water phases and, therefore, are an alternative to wireline-conveyed production logging tools without the need of intervention. The focus of the remaining is on the application of inflow tracers for monitoring production wells in unconventional reservoirs, particularly in single-trip, multistage fracturing operations.

20.4.2 The Inflow Monitoring Surveillance Challenge

Well surveillance is a key requirement for optimizing the production and ultimate recovery of hydrocarbon reservoirs. It is through monitoring and analyzing how existing wells produce that future wells and their completions can be correctly designed, and reservoir drainage and injection strategies can be fine tuned.

Traditionally, many easily accessible technological solutions have been available for well surveillance. Downhole pressure and temperature gauges for taking samples downhole or at the surface, plus microseismic, tiltmeters, and production logging (PLT) can provide a wealth of information for interpretation that can reveal most of a well's unknowns. For example, you can discover which zones produced oil, gas, and water, how much of each was produced from each zone, whether the zones were isolated from each other, and so on. More recent developments such as fiber-optic sensors simply add to the mix that can sense temperature cooling and sound as noted in the earlier section.

Over the last decade, one key development has complicated past practices in unconventional reservoirs, especially in the popularity of multistage fracturing horizontal wells. The industry quickly recognized that flow regimes along such completions are highly complex, with the three phases mixing in previously unrecorded modes, and water getting trapped in sumps along the way, which could block production along the well. It is important to characterize stage contributions to production, particularly the mid to toe compartments. Sophisticated tiltmeters and production logging tools could help operators answer these questions, but physically deploying wireline tools along very long horizontal sections poses a challenge, even with tractors.

Reliable telemetry from obtaining downhole measurements to the surface is usually through electronic means, and requires power and data transmission cables. In this

context, inflow tracers can provide an alternative method. This tracer technology utilizes the well's production as the telemetry conduit to transport the signal to the sampling point. Therefore, tracer technology is a viable alternative as permanent monitoring technology of choice for well surveillance in today's unconventional field developments, and it is a risk-free solution from both planning and deployment perspectives.

20.4.3 Inflow Tracer Monitoring

Inflow tracer monitoring comprises proprietary chemical tracers that are embedded in polymers and readily inserted into virtually any completion hardware. The tracers are released when oil or water come into contact with the polymer. There are over 100 separate and identifiable tracers for oil and water detection, which is particularly important in commingled production facilities Judiciously placing tracers along a well's production interval and then collecting and analyzing samples any time during the life of the well can answer key reservoir management questions.

Because fluid flow in a producing well provides the communication channel for the chemical tracers, you could argue that this technology when fully reliable and effective could eliminate the need for electrical, fiber-optic, or any other type of connectivity between the surface and downhole. All that is required is the capability to insert the polymer into the completion and then to take samples at the surface. Using inflow tracer monitoring can simplify the operation logistically. Samples may be taken anywhere from the wellhead to a topside facility, offshore or onshore, and can be used to service multiple wells.

Laboratory analysis of the inflow tracer monitoring samples yields tracer concentrations that can be detected in the parts-per-trillion levels. The subsequent inflow interpretation will address all phases in a well's life such as cleanup and water breakthrough, and can provide zonal inflow contributions. For example, toe-to-heel contributions can be accessed from a horizontal well, either qualitatively or in single-phase conditions, quantitatively. Multiphase quantification is not currently possible, but it is an area under research. The inflow tracer operations cycle is illustrated in **Fig. 20.26**.

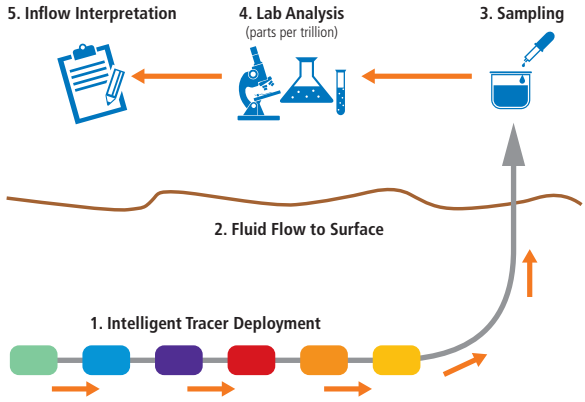

Fig. 20.26—Inflow monitoring operations. (Courtesy of RESMAN.)

20.4.4 Inflow Tracer Interpretation: Well Surveillance Deliverables

The well-surveillance deliverables using inflow tracer technology fall into four main categories:

- Initial well cleanup
- Relative flow contribution and quantitative interpretation
- Steady-state monitoring and water breakthrough
- Well monitoring

Each of these topics is expanded upon in this section.

20.4.4.1 Initial Well Cleanup

The initial production of a producing well is normally associated with chaotic flow and the gradual build-up of well productivity. During this campaign, the unique inflow tracers from different sections of the well will yield quantitative estimates of zonal contributions. This answers questions definitely such as "the toe of a horizontal completion is contributing to production." In this phase, the produced fluid needs to be sampled regularly (every half hour or every hour) until flow stabilizes.

20.4.4.2 Relative Flow Contribution—Quantitative Interpretation

When the flow stabilizes (and also later during the life of the well), inflow tracers can yield quantitative estimates of zonal production. The reliability of the estimate depends on production remaining as predominantly single-phase and each producing zone being isolated from others.

For this application, the well must be shutin for a period of time, typically six or more hours, to allow the build-up of the tracer adjacent to each producing zone. When the well is put back on production, each zone's accumulation of tracer, called a tracer shot, produces a transient shot that can be detected at the surface and interpreted to give relative zonal

contributions. Detecting and interpreting transient requires rapid and precisely timed sampling.

20.4.4.3 Steady-State Monitoring and Water Breakthrough

Another key application of inflow tracer technology is made possible by the longevity of tracers to monitor the long-term behavior of the wells, so-called ***steady-state monitoring***. The main interest is detecting water breakthrough. Another application is analyzing trends in tracer concentrations from different producing zones. Again, this is an application that works best when each producing zone is isolated from others.

During steady-state monitoring, samples are taken over the life of the well, typically at every week to a month intervals, or more frequently if production appears to change. The life of a tracer is more or less indefinite until the tracer system is exposed to its target fluid, at which point, it starts to release. Water tracers remain dormant during initial oil production, and only become active when water breaks through.

A prerequisite for steady-state monitoring is to establish a concentration baseline prior to any particular event, such as water breakthrough, for later comparison with subsequent samples and analysis.

20.4.4.4 Well Integrity Monitoring

Inflow tracers also provide insight into various aspects of well integrity. For example, horizontal wells installed with multiple fracturing sleeves are ideal to know which compartment is producing water, and, subsequently, where to intervene in the offending zones. Other common well integrity questions such as, "has the ball unseated when the well starts production," "how effective is the fracturing job in each compartment," and "has the fracturing deteriorated over time due to closure" can be answered with inflow tracer technology.

20.4.5 The Permanent Downhole Chemical Sensor

20.4.5.1 The Polymer-Tracer System

More than 100 separate identifiable chemical tracers are attracted to oil and water. This means that multiple zones can be instrumented and tracked individually for both oil and water influx. Water tracers work in any salinity and oil tracers work in oil as heavy as 11° API gravity.

Longevity of the polymer-tracer systems is a key design requirement. Well surveillance should continue the entire lifetime of the well, and is a focus for research and development. The average lifetime is three years for oil tracers and one year for water tracers, when the tracers are exposed to their respective fluids. However, it should be noted that until a polymer-tracer system is exposed to its target fluid, the tracer remains dormant and uncompromised. Currently, longevity of more than three-years' surveillance has been demonstrated in the field.

20.4.5.2 Designing the Job

The first step(s) in designing any chemical sensor is to provide background about the field and the wells and to gather details about the completion hardware for the well, and to determine specifics about the cleanup and the fluids likely to be produced.

Next, a deployment strategy to meet the operator's objectives is designed. Where should tracers be located in the completion string? How should the tracers be placed to optimally expose them to the target fluid, either inside the completion string or in an annular deployment? These decisions are crucial for the creation of interpretable tracer responses.

After the deployment strategy is developed, the next step is to design polymer-tracer systems compatible with the given well conditions. For example, the operator can extrapolate the likely fluids to be encountered, including completion fluids, stimulation fluids, and corrosion inhibitors that may deliver long-term performance at the expected well temperature. An important factor in the design is to estimate the maximum likely flow rate at the sampling point, because this largely determines the dilution of the tracer and the capability to detect tracer during subsequent analysis. Polymer-tracer systems are used for most well conditions and temperatures up to 170°C (335°F). The polymer systems have also proved to be mechanically robust during the life of the well.

First, we will need to decide how many tracers, for both oil and water will be installed. Second, decide exactly where the tracers should be placed in the completion. Finally, the polymer-tracer system size and length must be tailored to fit the completion hardware being used, whether the placement is central or in the annulus. Oil and water tracer systems can be placed in the same screen or can be separated.

20.4.5.3 Deployment, Sampling, and Analysis

The deployment of this technology is simple in the sense that no service personnel are required at the wellsite or production facilities, saving unnecessary expense. Wellsite personnel are not needed because the polymer-tracer systems are designed upfront and inserted at the completion service company's yard before the hardware is transported to the well and run in hole.

Samples can be taken at the wellhead, production platform, FPSO (floating production, storage, and offloading system), or onshore as is the case for unconventional reservoirs. Ideally, the sample should be collected as close to the wellhead as possible, but the tracer design is robust enough to allow sampling, even after the separator. As each sample is taken, it is important to record the total flow rate at the sampling point. Samples are taken at ambient conditions, and 300 ml is the standard quantity required for subsequent analysis, although smaller volumes may be sufficient in some cases. Currently, samples are dispatched to a laboratory to detect tracer content.

The number and timing of samples depends on the application. Timing can be critical where simulation is required to predict where the tracer shot will arrive at the sampling point. For cleanup monitoring, up to 100 samples may be taken, of which approximately 30 will be selected for analysis. For quantitative inflow analysis, 30 to 40 samples are required to catch each transient, which means that the exact timing is particularly critical. Steady-state monitoring requires a sample every week to once a month.

The laboratory analysis comprises sample preparation and a series of chromatographic and spectroscopic measurements to identify the presence or absence of each individual tracer deployed in the well. Typically, concentrations are in the "parts per trillion" range, so great care is required to ensure reliable and interpretable results. Analysis and interpretation follow.

20.4.6 Inflow Interpretation

Every well has a unique production history. Inflow tracers captured during flowback sampling can provide unique signatures that are then used for interpretation to characterize inflow along different production intervals along a well. The qualitative interpretations for cleanup and water breakthrough are primarily a matter of correlating the concentration of tracers in the samples to the zones where the tracers are placed, and then deducing the most likely production scenario. Cleanup monitoring requires frequent sampling when the well is first put on production, while water breakthrough and steady-state monitoring require long-term sampling every few days to a month.

20.4.6.1 Quantitative Modeling

This section introduces the fundamentals for a new, patented tracer flowback interpretation method that enables zonal contributions to be estimated from the transient flush-out characteristics of tracer shots from different completion types. The well requires a shut-in to create a stationary accumulation of tracer downhole, called a tracer shot, and then it is flowed back so the tracer shots can be detected at the surface.

20.4.6.2 The Flush-Out Model

The *Technical Bulletin 2, The Flush-Out Model, Quantifying Reservoir Inflow Contribution with RESMAN's Flush-Out Model*, describes the proprietary mathematical technique that allows modeling the transient response of tracer concentrations that are generated during a well start-up. The model is based on the rate of change in tracer concentration as a function of cumulative production (RESMAN 2014). The transport of tracers in the well and pipe can be described as a time-space, convection-diffusion problem

$$\frac{\partial c}{\partial t} = D \cdot \frac{\partial^2 c}{\partial x^2} - V \cdot \frac{\partial c}{\partial x} \qquad \textbf{(Eq. 20.14)}$$

where the diffusivity D includes both turbulent and molecular diffusion. V is the mean velocity of the transporting fluid while c is the tracer concentration. This equation describes the dispersion process of the tracers as they migrate to surface. Tracer accumulations that are formed downhole will be dispersed out into gradually larger fluid volumes while migrating to the sampling point. An understanding of this process is crucial to calculating inflow profiles from tracer flowback concentrations. The following is a description of how the problem in **Eq. 20.12** relates to a fracturing port and sliding sleeve and how the equation can be simplified so it is more easily solved. The tracer transport caused by fluid inflow into a fracturing port and sliding sleeve is illustrated in **Fig. 20.27**.

If the well is shut in, the continuous release of tracers leads to an accumulation of tracer molecules in the fluids surrounding the tracer systems. Note that the tracer concentration along the void will, after just a few hours of shut-in time, be significantly higher than the concentration in the same location when production flow was carrying

away the tracer material continuously. Therefore the tracer concentration in the void space will be dominated by the accumulation and be evenly mixed in and around the vicinity of the tracer carrier itself. This accumulated cloud of tracer material will be referred to as a tracer shot.

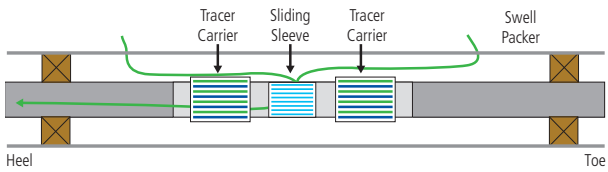

Fig. 20.27—One multistage compartment illustrating two pup joints (tracer carriers) installed on either side of the fracturing port/sliding sleeve. The lines illustrate the flow path taken from the reservoir into the completion.

The production is then restarted and the tracer shot flush out through the fracturing port will be dependent on the flow rate through the completion component that is illustrated in Fig 20.27. High flow rates flush out the shot faster than a lower rate will. A model of an ideal case could be set up assuming proportionality between the zonal inflow and the fracturing valve rates, ideal mixing in the annular void, and axially homogeneous tracer concentration fields.

If these assumptions hold, Eq. 20.12 could be dramatically simplified into a first-order differential equation with the following solution:

$$c(t) = c\,(0) \cdot e^{-f(q_{zone})t} + c_{direct} \qquad \textbf{(Eq. 20.15)}$$

where $c(0)$ is the initial concentration given by characteristics of the tracer system release rate and the shut-in time (and not by zonal production rate), and C_{direct} is the tracer concentration during steady-state flow. The function $f(q_{zone})$ needs to be known for quantitative estimates. The tracer flux through the fracturing valve will, with these assumptions, follow the concentration in the drainage area of the tracer carrier, and be dependent on the zonal rate. A plot of the tracer flux through the nozzle at two different rates is given in **Fig. 20.28**. Note that since the same amount of tracer is flushed out in the two cases, the area under the two curves is the same.

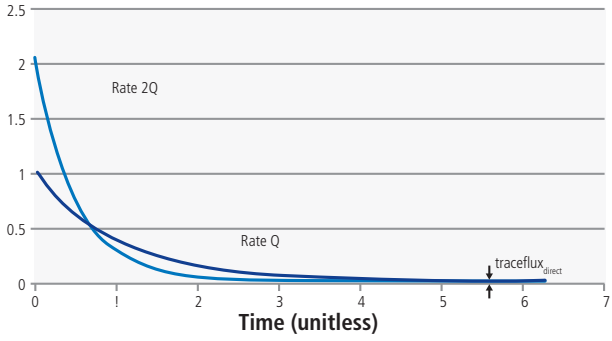

Fig. 20.28—Tracer flux from a joint during steady-state flow for two different flow rates. (Montes et al. 2013.)

The exponential decay function is very well observed in field data from hundreds of flowbacks from oil production wells. This exponential flush-out law forms a basis model for the history matching and the estimation of zonal contribution.

20.4.6.3 Tracer Transport Modeling Tool

In order to simulate the advection and diffusion of the tracer shots, a simulator is required to mimic the convection of initial tracer shots through the well and to compute the time series for the concentration of the tracer clouds at the pipe system outlet. The well proxy can be represented as a general converging network with one outlet to surface. The network and all the production points must be specified. Furthermore, the production in each production point and the initial size and position of each tracer shot needs to be specified. Based on this input, the simulator performs the following tasks:

- The pipe velocity everywhere in the pipe system is computed, since the production in each production point is specified.
- Each initial tracer cloud is advected and diffused to the outlet.
- The tracer concentration at the outlet is computed as a function of time for each tracer cloud.
- The tracer shots are advected and diffused using a semi-analytical method: for each time segment, each cloud is integrated using this solution and the local velocities.

The advantage of this semi-analytical approach is that it provides simulation efficiency and no numerical dispersion, which is the main disadvantage in standard numerical schemes.

20.4.6.4 Model-Based Inflow Tracer Quantitative Workflow

Zonal flow rates can be estimated by using history-matching models that replicate the tracer signal responses from flowbacks. From a history-matched model, an estimate of the zonal contributions can be derived with a workflow process illustrated in **Fig. 20.29** (Montes et al. 2013).

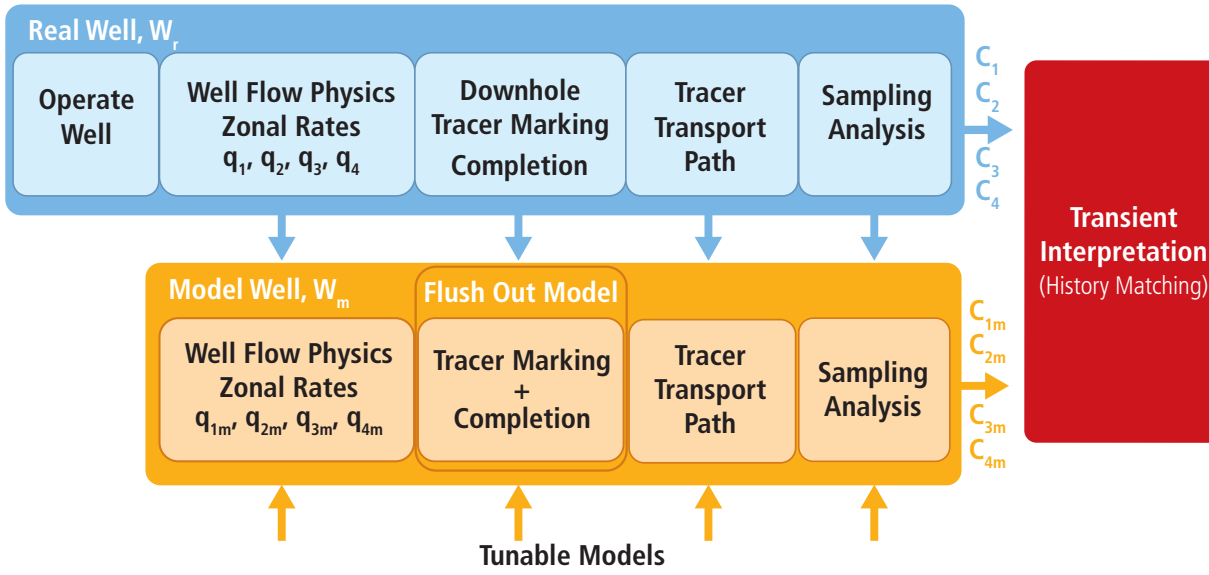

Fig. 20.29—Interpretation workflow to generate quantitative estimates using tuned models. (Montes et al. 2013.)

The major steps of the quantitative workflow are as follows:

1. Model and simulate the responses with equal relative production contribution from each zone, and compare with field data.
2. Tune the models to obtain a better fit.
3. Repeat tuning until optimal fit is achieved.
4. Estimate relative zonal contributions from the Well Flow Model, q_{1m}, q_{2m}, q_{3m}, q_{4m}.

20.4.6.5 Flow Loop Flush-Out Model Verification

As described in the previous section, the exponential-like behavior has been observed from many flow backs, but has since been corroborated experimentally for single-phase flow. The experiments were conducted in a specially designed flow loop that can be retrofitted with almost any completion joint that can be completed in a producing well (**Fig. 20.30**). The decline behavior was measured and documented for a wide variety of well flow rates, different completion components, and shut-in periods.

Gathering a substantial amount of experimental data was necessary to understand, in detail, the relationship between decline rate, inflow, and other key parameters, and to build predictive mathematical models. An exponential behavior has been observed in flow loop experiments, which corresponds closely to what is seen from flowbacks that verify the original flush-out model, which was originally empirically derived. This understanding has proved essential in designing every tracer deployment today that is based on the patented flush-out model, as described above.

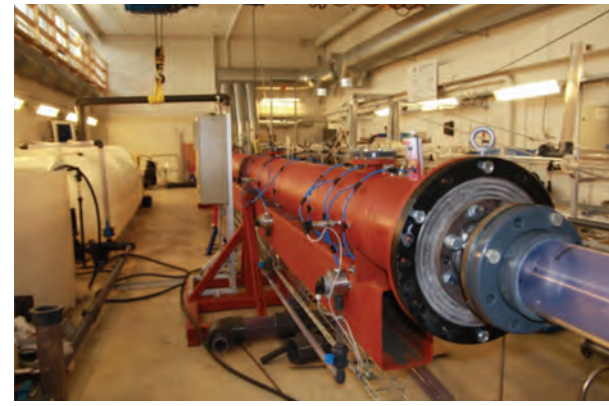

Fig. 20.30—Flow used to verify the flush-out model in different completion components. (Courtesy of RESMAN.)

20.4.7 Multistage Fracturing Case Study

A case study was conducted to gather information about multistage fracturing using tracers in multistage wells. This section discusses the results of the study.

20.4.7.1 Introduction

For the study, unique inflow tracers were installed in a horizontal multistage fracturing well using a drop-ball operation. The well was completed with 8 fracturing stages where a total of 16 unique oil and water tracers were installed. One pair of unique tracers was used in each of the eight fracturing stages. The tracer pairs (oil and water tracer) were installed in outward-vented tracer carriers blank base pipe with a slotted jacket on either side of the fracturing port. A total of eight of these identical compartments were configured from heel to toe. The horizontal production interval was approximately 4000 ft. MD in length in a 6-1/8-in. open hole.

20.4.7.2 Monitoring Objectives

The primary objective for the study was to monitor the oil and water inflow with inflow oil and water tracers. The operator was directed to monitor and document the following:

- Confirm flow was occurring from each zone, by evaluating the following:
  - Did the ball remain seated (i.e., did not unseat)?
  - Was the fracture job effective?
- Assess relative inflow distribution.
- Identify the locations of water breakthrough, if any.

20.4.7.3 The Monitoring Sensors

The inflow tracers are designed to release the related tracers with a trigger that is activated by the corresponding target fluid; oil triggers the oil tracer release, and water triggers the water tracer release. The tracer release rate is independent of fluid velocity. The release changes with the varying degree of target fluid contact. In other words, water tracer systems are dormant while not in contact with a water phase (i.e., during single-phase oil production). Sixteen unique oil and water tracers were installed in the well across eight tracer carriers to protect the polymers when run in-hole. The carrier consists of a blank base pipe with 24 axial rods that hold the polymers in place and a slotted jacket that exposes it to annular fluid flow only (**Fig. 20.31**).This configuration is often described as an *externally vented or outward-vented carrier.*

The oil and water tracer rods (see the rectangular cross section for an illustration) were evenly distributed around the circumference of the blank base pipe, which was held in place by axial wires, and protected by a slotted jacket. A picture of the tracer carrier assembly is shown in **Fig. 20.32**.

Fig. 20.32—Oil and water tracer rods (top) installed between blank base pipe and slotted jacket (bottom, with labeling) of the externally vented tracer carrier.

20.4.7.4 Multistage Fracturing Completion Configuration

Each of the eight compartments consists of a fracturing port, tracer carrier (placed on both sides of the port), and is isolated by swell packers (Fig. 20.27). Each compartment has a separate, unique oil and water tracer; two identical carriers are installed to cover inflow from both sides. Four unique tracer pairs (oil and water) installed in two carriers each (eight carriers in total) are monitoring the eight inflow ports.

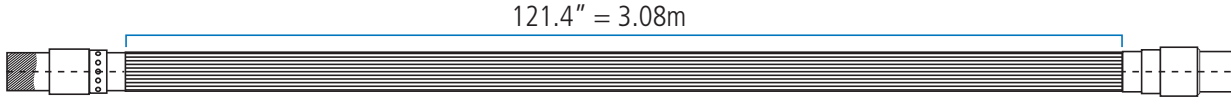

Fig. 20.31—Slotted base pipe used for the tracer carrier with ~3.1 meters' installation length.

20.4.7.5 Tracer Transient Analysis

A transient sampling program is prepared because quantification was a monitoring objective. In such campaigns, the change is in the production rate; for example in cleanup, restarts, and ramp ups. These variations may go down to as little as a five-minute scale. Sampling is prepared using a tracer-transport-modeling tool (as described above) that can predict the peak arrival of each tracer based on the well completion geometry and flow rates for oil, water, and gas. In this particular case study, after a 36-hour shut-in, a total of 65 samples were captured where 35 were analyzed in the lab for tracer content.

20.4.7.6 Restart Tracer Responses

All oil tracers were clearly detected in the sample bottles, which is clear evidence that there was hydraulic connectivity of oil with every stage in the well. The flush-out model described above utilized data from the tracer concentration decay following the arrival peak, which fit the measured concentrations quite closely. The outcome, the model decay factor k, represents the flow velocity; per compartment from each fracturing sleeve and cumulative local velocity for toe tracer OS-5. The *k*-values are normalized to the strongest compartment contributor, which in this particular restart was the OS-6 tracer. The presented volume rate dependent *k*-values are therefore normalized to $k_{OS-6} = 1.00$. For instance, the rate from the compartment with the OS-7 tracer is 74% of the rate from the compartment with the OS-6 tracer. The flush-out model fits are illustrated with good agreement with the measured concentrations from the restart in **Fig. 20.33**.

Based on the above model fits, the distribution of production from the fracturing compartments is summarized in **Fig. 20.34**. The summary consists of the total production data from all eight fracturing compartments, and the percentage presented is the relative contribution per stage. The three compartments in the toe end of the well indicate the most prolific contributors to the production relative to the other compartments. In general, the data show that the heel-to-mid compartments are contributing half of those near the toe, which provided important insight to inflow understanding of each fractured compartment.

20.4.8 Conclusion and Integration with Other Measurements

Inflow tracers can be an effective measurement to verify and monitor completion effectiveness, which can reduce the uncertainty of well productivity, and optimize stimulation designs and completion strategies. Because of the verification and monitoring aspects, inflow tracers can provide qualitative information about which stage is contributing to production and the relative

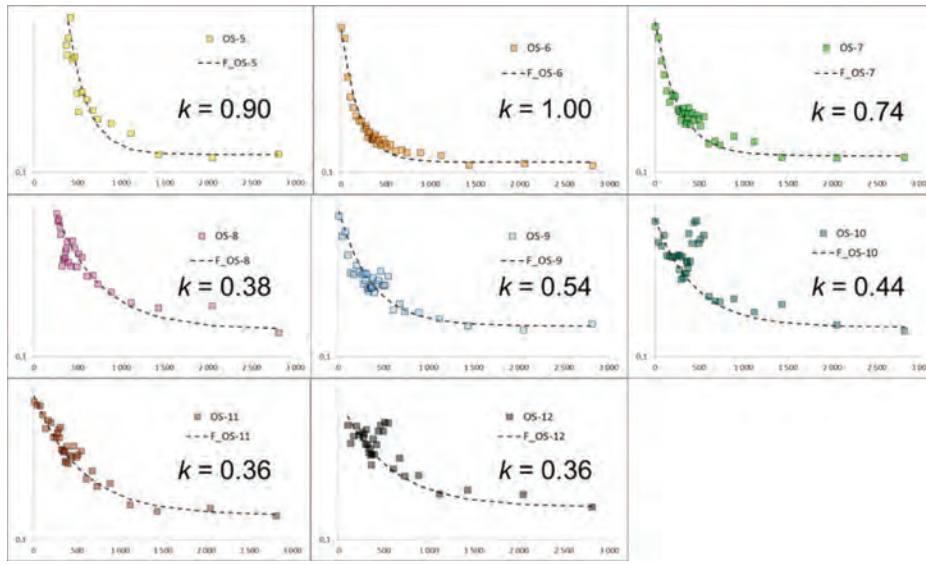

Fig. 20.33—Flush-out model fit with corresponding volume rate dependent k-factor. OS-6 yields the highest value for k and hence the strongest production contribution; all normalized to k OS-6 + 1.00. The y-axis is the tracer concentration (ng/ml), and the x-axis is the cumulative production (bbl). (Courtesy of RESMAN.)

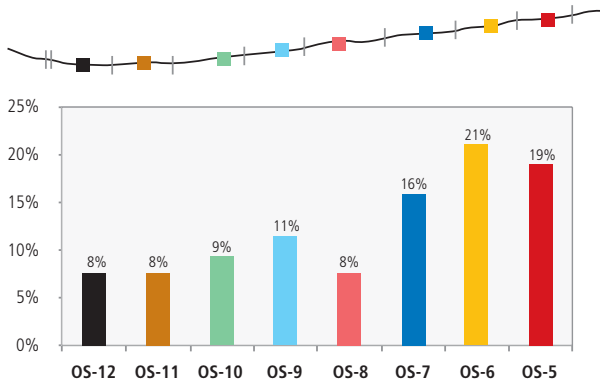

Fig. 20.34—Fracturing sleeve compartment inflow distribution. (Courtesy of RESMAN.)

flow contributions. In addition, knowing where water breakthrough is occurring allows the operator to take remedial action. Another benefit is to use the information to update reservoir models when water breakthrough events occur. Utilizing other measurements, such as microseismic, for example, can assist in characterizing the size of the fracture, and tiltmeters can monitor fracture treatment and measure deformation due to fracturing.

Utilizing different measurements and their associated interpretation methods requires advanced data integration techniques to characterize the near wellbore and are reservoir-critical in improving forecasting ability. Inflow tracers are one of numerous—but critical—measurement technologies that can improve the understanding of reservoir characterization, completion quality, and completion efficiency. This is especially true of monitoring each compartment in long, horizontal multistage fracturing completions, if a holistic approach is taken.

20.5 Conclusion

Unconventional resource plays in both shale oil and shale gas are a to characterize due to the relatively new issues that these reservoirs present to an operator. From a monitoring and surveillance perspective, unconventional resources have these characteristics in common: very low porosity and permeability, primary networks created by hydraulic fracturing (which also activates or communicates with the complex secondary natural fracture networks), high-stress regimes, and low-flow rates.

However, operators can adopt some strategies to offset some of the issues. Cipolla et al. (2011) suggested that effective appraisal and development phases can quickly and reliably determine a well's productivity—if a measure of the three following factors is available:

- Reservoir quality, which is the measure of productivity from a combination of petrophysical parameters.
- Completion quality, which measures the potential for initiating a fracture based on geomechanical parameters required for stimulation design.
- Completion effectiveness, which measures the connectivity between the reservoir, the wellbore, and the stimulation coverage of the producing intervals. In particular, being able to effectively design the fracture stages, assess their geometries (i.e., width and lengths), and monitor the depletion (or deterioration) of the hydraulic fractures over time.

These past few years, the oil and gas geophysical industry has been leaning toward multiphysics integration (for instance, "Seismic imaging is indeed progressively and jointly analyzed with potential methods"). Microseismic monitoring doesn't conflict with this trend. Other measurements can help to better constrain the information that the industry wants to gather from microseismic monitoring. Early on, experts have stated that coupling passive seismic monitoring with other measurements (such as from tiltmeters, radioactive or chemical tracers, temperature logs) and reservoir engineering (well and production testing, near wellbore and reservoir modeling) would help the industry gain a better understanding of hydraulic fracturing and improve treatment designs (Cipolla and Wright 2000). Yet, such integration has remained low despite efforts made by operators (Lowe et al. 2014). As advocated by Cipolla and Wright (2000) and Fisher et al. (2002), the most common, coupled measurements remain passive seismic and tiltmeters, either from the surface or from downhole.

Conversely, other measurements could—and should—be considered in fracture diagnostics and stimulation monitoring. Here are a few examples to demonstrate this statement and to leave room for further integration efforts: pre- and post-stimulation seismic survey (Willis et al. 2007); electro-seismology (Mahardika et al. 2012); distributed temperature and acoustic sensing (Molenaar and Cox 2013); and satellite interferometry in some instances (Bourne et al. 2006). Refer to the next section for a review of tracers and associated tracer technologies.

As discussed earlier, several acquisition designs are available, each of which has pros and cons. In general, the basis for all of the presented acquisition schemes lies in the

sensing device; the most common sensors are geophones (velocimeters). Yet, many different sensors exist, such as accelerometers and hydrophones that could also be used in the context of microseismic monitoring. In particular, consider digital accelerometers that are typically used for strong-motion measurements (Clinton and Heaton 2002; Iwan et al. 1985), which do allow a simplified field-manipulation, because digital sensors are easier to work with at the acquisition stage and can integrate with other digital measurements, such as GPS positioning.

Distributed acoustic sensing remains the most promising sensor for both downhole and surface microseismic monitoring. So far, it has been shown to be useful in active monitoring (Mateeva et al. 2013; Kiyashchenko et al. 2013); however, its poor (lateral) sensitivity remains an obstacle for microseismic applications (Grandi Karam et al. 2013). The low cost and ease of deploying an optical fiber in a well—possibly, the treated well—makes digital acoustic sensing a very interesting development for the future of microseismic monitoring. Having said so, one should recognize that with the complicated completion systems that are evolving one should carefully plan any monitoring system that requires cables to communicate downhole to surface.

Inflow tracers can be an effective measurement to verify, monitor completion effectiveness with no potential completion installation risk (from not having required cables) that can reduce the uncertainty of well productivity and optimize stimulation designs and completion strategies. Because of the verification and monitoring aspects, inflow tracers can provide qualitative information about which stage is contributing to production and the relative flow contributions. Knowing where water breakthrough is occurring allows the operator to take remedial action. Another benefit is to use the information to update reservoir models when water breakthrough events occur. Utilizing other measurements, such as microseismic, for example, can assist in characterizing the size of the fracture, and tiltmeters can monitor fracture treatment and measure deformation due to fracturing.

The three monitoring techniques discussed illustrate that each has its own unique properties along with the associated advantages and limitations. Plus, thoughtful integration of the various techniques can provide superior and better results. Both microseismic and inter-well tracer techniques investigate away from the wellbore and into the reservoir while fiber optic and inflow tracer techniques concentrate mostly in or near wellbore. Though microseismic and inter-well tracer focus away from the wellbore, there are still differences between the two techniques. Tracer techniques are typically associated with flow path within the reservoir. Microseismic techniques typically cover rocks that show a slippage or failure and that could easily be beyond the reservoir in question. The uniqueness of the answers from using the microseismic approach is mainly dependent on the assumptions made with the rock velocity and the associated focal methodology. The tracer inflow monitoring technique also has its own limitations associated with quantitative methods only being valid for single-phase flow, presently. The fiber optic technique only focuses on, and near, the wellbore. Each technique has its arena of contribution. Therefore, the user should be cognizant of these parameters and use them either independently or in combination, determined by the project needs.

20.6 References

Ahmed, U., Roux, P.-F., Leu, E., and Gill, C. Hydraulic Fracturing Monitoring Technologies: Microseismic, Fiber Optic, and Tracers and Their Integration. ***HFJ***, 2 (1), January 2015. 40–60.

Aki, K. and Richards, P.G. 2001. ***Quantitative Seismology***. ed. J. Ellis. University Science Book.

Allen, R.V. 1978. Automatic Earthquake Recognition and Timing from Single Traces. ***Bull. of the Seismological Society of America***, **68** (5): 1521–1532.

Anstey, N.A. 1964. Correlation Techniques—a Review. ***Geophysical Prospecting***, **12** (4): 355–382. http://dx.doi.org/10.1111/j.1365-2478.1964.tb01911.x.

Artman, B., Podladtchikov, I., and Witten, B. 2010. Source Location Using Time-Reverse Imaging. ***Geophysical Prospecting***, **58** (5): 861–873. http://dx.doi.org/10.1111/j.1365-2478.2010.00911.x.

Bateman, L., Molenaar, M.M., and Brown, M.D. 2013. Lessons Learned from Shell's History of Casing Conveyed Fiber Optic Deployment. Paper SPE 167211 presented at the SPE Unconventional Resources Conference. Calgary, Alberta, Canada. 5–7 November. http://dx.doi.org/10.2118/167211-MS.

Baer, M. and Kradolfer, U. 1987. An Automatic Phase Picker for Local and Teleseismic Events. ***Bull. of the Seismological Society of America***, **77**: 1437–1445.

Bai, C. and Kennett, B.L.N. 2000. Automatic Phase-Detection and Identification by Full Use of a Single Three-Component Broadband Seismogram. *Bull. of the Seismological Society of America*, **90** (1): 187–198. http://dx.doi.org/10.1785/0119990070.

Bardainne, T. and Gaucher, E. 2010. Constrained Tomography of Realistic Velocity Models in Microseismic Monitoring Using Calibration Shots. *Geophysical Prospecting*, **58** (5): 725–914. http://dx.doi.org/10.1111/j.1365- 2478.2010.00912.

Bardainne, T., Gaucher, E., Cerda, F., et al. 2009. Comparison of Picking-Based and Waveform-Based Location Methods of Microseismic Events: Application to a Fracturing Job. Paper SEG-2009-1547 presented at the 79th SEG Annual Meeting. Houston, Texas. 25–30 October.

Barton, C.A., Zoback, M.D., and Moos, D. 1995. Fluid Flow along Potentially Active Faults in Crystalline Rock. *Geology*, **23** (8) (August 1): 683.http://dx.doi. org/10.1130/0091-7613(1995)023<0683:FFAPAF>2.3. CO;2.

Battaglia, J. and Aki, K. 2003. Location of Seismic Events and Eruptive Fissures on the Piton de La Fournaise Volcano Using Seismic Amplitudes. *Journal of Geophysical Research*, **108** (B8): 2364. http://dx.doi.org/10.1029/2002JB002193.

Beresnev, I.A. (2001). What We Can and Cannot Learn about Earthquake Sources from the Spectra of Seismic Waves, *Bulletin of the Seismological Society of America*, 91 (2): 397–400

Bohnhoff, M., Dresen, G., Ellsworth, W.L., et al. 2010. Passive Seismic Monitoring of Natural and Induced Earthquakes: Case Studies, Future Directions and Socio-Economic Relevance. In *New Frontiers in Integrated Solid Earth Sciences*, ed. S. Cloetingh and Jorg Negendank. Dordrecht: Springer Netherlands. http://dx.doi.org/10.1007/978-90-481-2737-5.

Bourne, S.J., Maron, K., Oates, S.J., et al. 2006. Monitoring Reservoir Deformation on Land–Evidence for Fault Re-Activation from Microseismic, InSAR, and GPS Data. Paper presented at the 68th EAGE Conference and Exhibition. Vienna, Austria. 12 June.

Burridge, R. and Knopoff, L. 1964. Body Force Equivalents for Seismic Dislocations. *Bull. of the Seismological Society of America*, **54** (6A): 1875–1888.

Capon, J. 1969. High-Resolution Frequency-Wavenumber Spectrum Analysis. Proc., *IEEE* **57** (8): 1408–1418.

Charlety, J., Cuenot, N., Dorbath, C., et al. 2006. Tomographic Study of the Seismic Velocity at the Soultz-Sous-For.ts EGS/ HDR Site. *Geothermics*, **35** (5-6): 532–543. http://dx.doi.org/10.1016/j.geothermics.2006.10.002.

Cichowicz, A. 1993. An Automatic S-Phase Picker. *Bull. of the Seismological Society of America*, **83** (1): 180–189.

Cipolla, C.L. and C.A. Wright. 2000. State-of-the-Art in Hydraulic Fracture Diagnostics. Paper SPE 64434 presented at the SPE Asia Pacific Oil and Gas Conference and Exhibition. Brisbane, Australia. 16–18 October. http:// dx.doi.org/10.2118/64434-MS.

Cipolla, C.L., Lewis, R.E., Maxwell, S.C., et al. 2011. Appraising Unconventional Resource Plays: Separating Reservoir Quality from Completion Effectiveness. Paper IPTC-14677-MS presented at the International Petroleum Technology Conference. Bangkok, Thailand. 15-17 November. http://dx.doi.org/10.2523/14677-MS.

Clinton, J. F. and Heaton, T.H. 2002. Potential Advantages of a Strong-Motion Velocity Meter over a Strong-Motion Accelerometer. *Seismological Research Letters*, **73** (3): 332–342. http://dx.doi.org/10.1785/gssrl.73.3.33.

Dai, H. and MacBeth, C. 1995. Automatic Picking of Seismic Arrivals in Local Earthquake Data Using an Artificial Neural Network. *Geophysical Journal International*, **120**: 758–774.

Deichmann, N. and Garcia-Fernandez, M. 1992. Rupture Geometry from High-Precision Relative Hypocentre Locations of Microearthquake Clusters. *Geophysical Journal International*, **110**: 501–517.

Detring, J.P. and Williams-Stroud, S. 2012. Using Microseismicity to Understand Subsurface Fracture Systems and Increase the Effectiveness of Completions: Eagle Ford Shale, TX. In AAPG Annual Meeting.

Detring, J. and Williams-Strouds, S. 2013. The Use of Microseismicity to Understand Subsurface-Fracture Systems and to Increase the Effectiveness of Completions: Eagle Ford Shale, Texas. *SPE Reservoir Evaluation & Engineering* **16** (4): 456–460. SPE 162845-PA. http://dx.doi. org/10.2118/162845-PA.

Drew, J.E., Leslie, H.D., Armstrong, P.N., et al. 2005. Automated Microseismic Event Detection and Location by Continuous Spatial Mapping. Paper SPP 95513 presented at the SPE Annual Technical Conference and Exhibition. Dallas, Texas. 9–12 October. http://dx.doi.org/10.2118/95513-MS.

Du, Y. and Guan, L. 2005. Interwell Tracer Tests: Lessons Learnt from Past Field Studies. Paper SPE 93140 presented at the SPE Asia Pacific Oil and Gas Conference and Exhibition. Jakarta, Indonesia. 5–7 April. http://dx.doi.org/10.2118/93140-MS.

Duncan, P.M. 2005. Is There a Future for Passive Seismic? *First Break*, **23**: 111–115.

Durrani, T. S. and Bisset, D. 1984. The Radon Transform and Its Properties. *Geophysics*, 49 (8): 1180–1187. http:// dx.doi.org/10.1190/1.1441747.

Earle, P.S. and Shearer, P.M. 1994. Characterization of Global Seismograms Using an Automatic-Picking Algorithm. *Bull. of the Seismological Society of America*, **84** (2): 366–376.

Economides, M.J., Nolte, K.G., and Ahmed, U. 1998. *Reservoir Stimulation*, New York, NY: John Wiley & Sons. Inc.

Emmanuel, A., D'Auria, L., Martini, M., et al. 2006. Real-Time Monitoring and Massive Inversion of Source Parameters of Very Long Period Seismic Signals: An Application to Stromboli Volcano, Italy. *Geophysical Research Letters*, **33** (4): L04301. http://dx.doi.org/10.1029/2005GL024703.

Evans, K.F., Cornet, F.H., Hashida, T., et al. 1999. Stress and Rock Mechanics Issues of Relevance to HDR/HWR Engineered Geothermal Systems: Review of Developments during the Past 15 Years. *Geothermics*, **28** (4-5): 455–474. http://dx.doi.org/10.1016/S0375-6505(99)00023-1.

Felix, W. and Ellsworth, W.L. 2000. A Double-Difference Earthquake Location Algorithm: Method and Application to the Northern Hayward Fault, California. *Bull. of the Seismological Society of America*, **90** (6): 1353–1368.

Fink, M. 1992. Time Reversal of Ultrasonic Fields - Part I: Basic Principles. *IEEE Transactions on Ultrasonics, Ferroelectrics, and Frequency Control*, **39** (5): 555.

Fischer, T. and Guest, A. 2011. Shear and Tensile Earthquakes Caused by Fluid Injection. *Geophysical Research Letters*, **38** (5): L05307. http://dx.doi.org/10.1029/2010GL045447.

Fisher, M.K., Heinze, J.R., Harris, C.D., et al. 2004. Optimizing Horizontal Completion Techniques in the Barnett Shale Using Microseismic Fracture Mapping. Paper SPE presented at the SPE Annual Technical Conference and Exhibition. Houston, Texas. 26–29 September. http://dx.doi. org/10.2118/90051-MS.

Fisher, M.K., Wright, C.A., Davidson, B.M., et al. 2002. Integrating Fracture Mapping Technologies to Optimize Stimulations in the Barnett Shale. Paper SPE 77441 presented at the SPE Annual Technical Conference and Exhibition. San Antonio, Texas. 29 September–2 October. http://dx.doi.org/10.2118/77441-MS.

Frechet, J. 1985. Sismogenesis and seismic doublets (Sismogenese et Doublets Sismiques). PhD dissertation, Univerist. de Grenoble (June 1985).

Fremont, M.J. and Poupinet, G. 1987. Temporal Variation of Body-Wave Attenuation Using Earthquake Doublets. *Geophysical Journal of the Royal Astronomical Society*, **90**: 503–520.

Galbraith, M. 1994. 3-D Survey Design by Computer. *Exploration Geophysics*, **25** (2): 7177. http://dx.doi. org/10.1017/EG994071.

Geiger, L. 1910. In the Event of an Earthquake Arrival (Herbsetimmung Bei Erdbeben Aus Den Ankunfzeiten), *K. Gessell. Wiss. Goett.* 4: 331–349.

Gibbons, S.J., and Ringdal, F. 2006. The Detection of Low. Magnitude Seismic Events Using Array-Based Waveform Correlation. *Geophysical Journal International*, **165** (1): 149–166. http://dx.doi.org/10.1111/j.1365- 246X.2006.02865.x.

Gibowicz, S.J. and Kijko, A. 1994. *An Introduction to Mining Seismology*. 1st edition. Academic Press.

Gledhill, K.R. 1985. An Earthquake Detector Employing Frequency Domain Techniques. *Bull. of the Seismological Society of America*, **75** (6): 1827–1835.

Godano, M. 2009. Theoretical study on the calculation of focal mechanisms in a reservoir and its application to the seismicity of the saline Vauvert (etude Theorique Sur Le Calcul Des M.canismes Au Foyer Dans Un Reservoir et Application. La Sismicite de La Saline de Vauvert). Nice Sophia Antipolis. These de doctorat, Universite de Nice-Sophia Antipolis, 9 (July 2009).

Godano, M., Gaucher, E., Bardainne, T., et al. 2010. Assessment of Focal Mechanisms of Microseismic Events Computed from Two Three-Component Receivers: Application to the Arkema-Vauvert Field (France). *Geophysical Prospecting*, **58**: 775–790. http://dx.doi. org/10.1111/j.1365-2478.2010.00906.x.

Godano, M., Regnier, M., Deschamps, A., et al. 2009. Focal Mechanisms from Sparse Observations by Nonlinear Inversion of Amplitudes: Method and Tests on Synthetic and Real Data. *Bull. of the Seismological Society of America*, **99** (4): 2243–2264. http://dx.doi. org/10.1785/0120080210.

Goforth, T. and Herrin, E. 1981. An Automatic Seismic Signal Detection Algorithm Based on the Walsh Transform. *Bull. of the Seismological Society of America*, **71** (4): 1351–1360.

Gomberg, J.S., Shedlock, K.M., and Roecker, S.W. 1990. The Effect of S-Wave Arrival Times on the Accuracy of Hypocenter Estimation. *Bull. of the Seismological Society of America,* **80** (6): 1605–1628.

Got, J. and Frechet, J. 1993. Origins of Amplitude Variations in Seismic Doublets: Source or Attenuation Process? *Geophysical Journal International*, **114**: 325–340. http://dx.doi.org/10.1111/j.1365-246x.1993.tb03921.x.

Got, J., Frechet, J., and Klein, F.W. 1994. Deep Fault Plane Geometry Inferred from Multiplet Relative. *Journal of Geophysical Research*, **99** (B8): 15375–15386. http:// dx.doi.org/10.1029/94JB00577.

Grandi Karam, S., Webster, P., Hornman, K., et al. 2013. Microseismic Applications Using Digital Acoustic Sensing. In Fourth Passive Seismic Workshop.

Grassberger, P. and Procaccia, I. 1983. Measuring the Strangeness of Strange Attractors. ed. Brian R. Hunt, Tien-Yien Li, Judy A. Kennedy, and Helena E. Nusse. *Physica*, **9**: 189–208. http://dx.doi.org/10.1007/978-0-387-21830- 4_12.

Grasso, J.R. and Sornette, D. 1998. Testing Self-Organized Criticality by Induced Seismicity. *Journal of Geophysical Research*, **103** (B12): 29,965–29,987.

Grasso, J.-R. and G. Wittlinger. 1990. Ten Years of Seismic Monitoring over a Gas Field. *Bull. of the Seismological Society of America*, **80** (2): 450–473.

Grechka, V. and S. Yaskevich. 2013. Inversion of Microseismic Data for Triclinic Velocity Models. *Geophysical Prospecting*, **61** (6): 1159–1170. http://dx.doi.org/10.1111/1365- 2478.12042.

Griffith, A.A. 1921. The Phenomena of Rupture and Flow in Solids. *Phil. Trans. R. Soc. Lond. A*, 221: 163–198.

Grob, M. and Baan, M.V.D. 2011. Inferring in-Situ Stress Changes by Statistical Analysis of Microseismic Event Characteristics. *The Leading Edge*, **30** (11): 1296–1301.

Gupta, H.K. 1985. The Present Status of Reservoir Induced Seismicity Investigations with Special Emphasis on Koyna Earthquakes. *Tectonophysics*, **118** (3-4): 257–279. http://dx.doi.org/10.1016/0040-1951(85)90125-8.

Gutenberg, B. 1945a. Amplitudes of Surface Waves and Magnitudes of Shallow Earthquakes. *Bull. of the Seismological Society of America*, **35** (1): 3–12.

Gutenberg, B. 1945b. Amplitudes of P, PP, and S and Magnitude of Shallow Earthquakes. *Bull. of the Seismological Society of America*, **35** (2): 57–69.

Gutenberg, B. and Richter, C.F. 1944. Frequency of Earthquakes in California. *Bull. of the Seismological Society of America*: 32–35.

Gutenberg, B. and Richter, C.F. 1949. *Seismicity of the Earth and Associated Phenomena*. Princeton: Princeton University Press.

Halliday, D.F., Curtis, A., Vermeer, P., et al. 2010. Interferometric Ground-Roll Removal: Attenuation of Scattered Surface Waves in Single-Sensor Data. *Geophysics*, **75** (2): SA15–SA25. http://dx.doi.org/10.1190/1.3360948.

Hanks, T.C. and Kanamori, H. 1979. A Moment Magnitude Scale. *Journal of Geophysical Research*, **84** (B5): 2348–2350.

Hummel, N. and Shapiro, S.A. 2012. Microseismic Estimates of Hydraulic Diffusivity in Case of Non-Linear Fluid-Rock Interaction. *Geophysical Journal International*, **188**: 1441–1453. http://dx.doi.org/10.1111/j.1365246X.2011.05346.x.

Hummel, N. 2013. Nonlinear Diffusion-Based Interpretation of Induced Microseismicity: A Barnett Shale Hydraulic Fracturing Case Study. *Geophysics*, **78** (5): B211–B226. http://dx.doi.org/10.1190/GEO2012-0242.1.

Huseby, O., Sagen, J., and Dugstad, 2012. Single Well Chemical Tracer Tests—Fast and Accurate Simulations. Paper SPE 155608 presented at the SPE EOR conference at Oil and Gas West Asia. Muscat, Oman. 16–18 April. http://dx.doi. org/10.2118/155608-MS.

Iwan, W.D., Moser, M.A., and Peng, C.-Y. 1985. Some Observations on Strong-Motion Earthquake Measurement Using a Digital Accelerograph. *Bull. of the Seismological Society of America*, **75** (5): 1225–1246.

Jost, M.L. and Herrmann, R.B. 1989. A Student's Guide to and Review of Moment Tensors. *Seismological Research Letters*, **60** (2).

Julian, B.R., Miller, A.D., and Foulger, G.R. 1998. Non-Double-Couple Earthquakes 1. Theory. *Reviews of Geophysics*, **36** (4): 525–549.

Kawakatsu, H. and Montagner, J. 2008. Time-Reversal Seismic-Source Imaging and Moment-Tensor Inversion. *Geophysical Journal International*, **175** (2): 686–688. http://dx.doi.org/10.1111/j.1365-246X.2008.03926.x.

Kiyashchenko, D., Lopez, J., Berlang, W., et al. 2013. Steam-Injection Monitoring in South Oman–from Single-Pattern. *The Leading Edge*, **32** (10): 1246–1256. http://dx.doi.org/10.1190/tle32101246.1.

Knopoff, L. and Randall, M.J. 1970. The Compensated Linear-Vector Dipole: A Possible Mechanism for Deep Earthquakes. *Journal of Geophysical Research*, **75** (26): 4957–4963.

Lakings, J.D., Duncan, P.M., Neale, C., et al. 2006. Surface Based Microseismic Monitoring of a Hydraulic Fracture Well Stimulation in the Barnett Shale. Paper SEG-2006-605 presented at the SEG Annual Meeting. New Orleans, Louisiana. 1–6 October.

Larmat, C.S., Montagner, J.P., Fink, M., et al. 2006. Time-Reversal Imaging of Seismic Sources and Application to the Great Sumatra Earthquake. *Geophysical Research Letters*, **33** (L19312). http://dx.doi.org/10.1029/2006GL026336.

Lay, T. and Wallace, T.C. 1995. *Modern Global Seismology*. Edited by T. Lay and T.C. Wallace. Academic Press.

Le Meur, D., Benjamin, Twigger, L., et al. 2010. Adaptive Attenuation of Surface-Wave Noise. *First Break*, **28** (September): 83–88.

Lee, W.H.K., Bennett, R.E., and Meagher, K.L. 1972. A Method of Estimating Magnitude of Local Earthquakes from Signal Duration. *U.S. Geol. Surv.*, Menlo Park, California.

Li, J., Zhang, H., Rodi, W. L., et al. 2013. Joint Microseismic Location and Anisotropic Tomography Using Differential Arrival Times and Differential Backazimuths. *Geophysical Journal International*, **195** (3): 1917–1931. http://dx.doi.org/10.1093/gji/ggt358.

Lowe, T., Potts, M., and Wood, D. 2013. A Case History of Comprehensive Hydraulic Fracturing Monitoring in the Cana Woodford. Paper SPE 166295 presented at the SPE Annual Technical Conference and Exhibition. New Orleans, Louisiana. 30 September–2 October. http:dx.doi.org/10.2118/166295-MS.

Magotra, N., Ahmed, N., and Chael, E. 1987. Seismic Event Detection and Source Location Using Single-Station (three-Component) Data. *Bull. of the Seismological Society of America*, **77** (3): 958–971.

Mahardika, H., Revil, A., and Jardani, A. 2012. Waveform Joint Inversion of Seismograms and Electrograms for Moment Tensor Characterization of Fracking Events. *Geophysics*, **77** (5): ID23–ID39. http://dx.doi.org/10.1190/geo2012/0019.1.

Mateeva, A., Lopez, J., Mestayer, J., et al. P. 2013. Distributed Acoustic Sensing for Reservoir Monitoring with VSP. *The Leading Edge*, **32** (10): 1278–1283. http://dx.doi.org/1190-tle.32101278.1.

Maxwell, S.C. 2014. Microseismic Imaging of Hydraulic Fracturing Improved Engineering of Unconventional Shale Reservoirs. SEG Distinguished Instructor Series No. 17.

Maxwell, S.C., Urbancic, T.I., and Falls, S.D. 2000. Real-Time Microseismic Mapping of Hydraulic Fractures in Carthage, Texas. Paper SEG-2000-1449 presented at the 2000 SEG Annual Meeting. Calgary, Canada. 6–11 August.

McClure, M. and Horne, R. 2013, E.D. Is Pure Shear Stimulation Always the Mechanism of Stimulation in EGS? Proc., 38th Workshop on Geothermal Reservoir Engineering. Stanford, California.

McGarr, A. and Simpson, A. 1997. Keynote Lecture: A Broad Look at Induced and Triggered Seismicity, Rockbursts and Seismicity in Mines. Proc.,4th International Symposium on Rockbursts and Seismicity in Mines, ed. Gibowicz, S.J., and Lasocki, S., 385–396. A.A. Balkema, Rotterdam.

Miller, D,. Foulger, G.R., and Julian, B.R. 1998. Non-Double Couple Earthquakes 2. Observations. *Reviews of Geophysics*, **36** (4): 525–549. http://dx.doi.org/10.1029/98RG00716.

Molenaar, M.M. and Cox, B.E. 2013. Field Cases of Hydraulic Fracture Stimulation Diagnostics Using Fiber Optic Distributed Acoustic Sensing (DAS) Measurements and Analyses. Paper SPE 164030 presented at the SPE Middle East Unconventional Gas Conference and Exhibition. Muscat, Oman. 28–30 January. http://dx.doi. org/10.2118/164030-MS.

Montes, A., Nyhavn, F., Oftedal, G., et al. 2013. Application of Inflow Well Tracers for Permanent Reservoir Monitoring in North Amethyst Subsea Tieback ICD Wells in Canada. Paper SPE 167463 presented at the SPE Middle East Intelligent Energy Conference and Exhibition. Dubai, UAE. 28–30 October. http://dx.doi.org/10.2118/167463-MS.

Moos, D., Vassilellis, G., Cade, R., et al. 2011. Predicting Shale Reservoir Response to Stimulation: The Mallory 145 Multiwell Project. Paper SPE 145849 presented at the SPE Annual Technical Conference and Exhibition. 30 Denver, Colorado. October–2 November. http://dx.doi.org/10.2118/145849-MS.

Nagel, N.B., Sanchez-Nagel, M.A., Zhang, F., et al. 2013. Coupled Numerical Evaluations of the Geomechanical Interactions between a Hydraulic Fracture Stimulation and a Natural Fracture System in Shale Formations. *Rock Mechanics and Rock Engineering*, **46** (3): 581–609. http://dx.doi.org/10.1007/s00603-013-0391-x.

Neidell, N.S. and M.T. Taner. 1971. Semblance and Other Coherency Measures for Multichannel Data. *Geophysics*, **36** (3): 482–497.

Ogata, Y. and K. Katsura. 1993. Analysis of Temporal and Spatial Heterogeneity of Magnitude Frequency Distribution Inferred from Earthquake Catalogues. *Geophysical Journal International*, **113**: 727–738.

OptaSense 2013. An introduction to fibre-optic Distributed Acoustic Sensing and its impact on IOR and EOR, http://730926bc1eaea1361e79-997641d029b6764b67dd905fd3aab10c.r8.cf2.rackcdn.com/5-%20OptaSense.pdf (accessed June 2014).

Pandolfi, D., Rebel, E., Chambefort, M., et al. 2013. New Design and Advanced Processing for Frac Jobs Monitoring. Presented at the EAGE Fourth Passive Seismic Workshop. Amsterdam, Netherlands. 17 March.

Phillips, W.S., Fairbanks, T.D., Rutledge, J.T., et al. 1998. Induced Microearthquake Patterns and Oil-Producing Fracture Systems in the Austin Chalk. *Tectonophysics*, **289**: 153–169.

Pine, R.J. and Batchelor, A.S. 1984. Downward Migration of Shearing in Jointed Rock during Hydraulic Injections. *International Journal of Rock Mechanics and Mining Sciences & Geomechanics*, **21** (5): 249–263. http://dx.doi.org/10.1016/0148-9062(84)92681-0.

Podvin, P. and Lecomte, I. 1991. Finite Difference Computation of Travel Times in Very Contrasted Velocity Models: A Massively Parallel Approach and Its Associated Tools. *Geophysical Journal International*, **105** (1): 271–284. http://dx.doi.org/10.1111/j.1365-246x.1991.tb03461.x.

Poliannikov, O.V., Malcolm, A.E., Prange, M., et al. 2012. Checking up on the Neighbors: Quantifying Uncertainty in Relative Event Location. *The Leading Edge*, **31** (12): 1490–1494.

Raleigh, C.B., Healy, J.H., and Bredehoeft, J.D. 1976. An Experiment in Earthquake Control at Rangely, Colorado. *Science*, **191** (4233): 1230–1237. http://dx.doi.org/10.1126/science.191.4233.1230.

Raleigh, C.B., Healy, J.H., and Bredehoeft, J.D. 1972. Faulting and Crustal Stress at Rangely , Colorado. *Flow and Fracture of Rocks*, **16**: 275–284. http://dx.doi.org/10.1029/GM016p0275.

Rebel, E., Richard, A., Meunier, J., et al. 2011.Real-Time Detection of Microseismic Events Using Surface Array. Presented at the EAGE Third Passive Seismic Workshop. Athens, Greece.

Rentsch, S., Buske, S., Luth, S., et al. 2007. Fast Location of Seismicity: A Migration-Type Approach with Application to Hydraulic-Fracturing Data. *Geophysics*, **72** (1): S33–S40.

RESMAN 2014. Flush Out Model. Technical Bulletin 2. May 2014. http://www.resman.no/knowledge/pdf/RESMAN-TB2-Flush-Out-Model.pdf (accessed June 2014).

Richter, C.F. 1935. An Instrumental Earthquake Magnitude Scale. *Bull. of the Seismological Society of America*, **25** (1): 1–32.

Riedesel, M.A. and Jordan, T.H. 1989. Display and Assessment of Seismic Moment Tensors. *Bull. of the Seismological Society of America*, **79** (1): 85–100.

Rost, S. and Garnero, E.J. 2004. Array Seismology Advances Research into Earth's Interior. ***Array Seismology Advances Research into Earth's Interior***, **85** (32): 305–306.

Rost, S. and Thomas, C. 2002. Array Seismology: Methods and Applications. ***Reviews of Geophysics***, **40** (3): 1008. http://dx.doi.org/10.1029/2000RG000100.

Rowe, C.A., Aster, R.C., Borchers, B., et al. 2002. An Automatic, Adaptive Algorithm for Refining Phase Picks in Large Seismic Data Sets. ***Bull. of the Seismological Society of America***, **92** (5): 1660–1674.

Sabbione, J.I., and Velis, D. 2010. Automatic First-Breaks Picking: New Strategies and Algorithms. ***Geophysics***, **75** (4): V67–V76. http://dx.doi.org/10.1190/1.3463703.

Sheely, C.Q. 1978. Description of Field Tests To Determine Residual Oil Saturation by Single-Well Tracer Method. ***J. Pet. Tech***. **30** (2): 194–202. SPE-5840-PA. http://dx.doi. org/10.2118/5840-PA.

Shemeta, J., and Anderson, P. 2010. It's a Matter of Size: Magnitude and Moment Estimates for Microseismic Data. ***The Leading Edge***, **29** (3): 296–302.

Sileny, J., Eisner, L., Hill, D.P., et al. 2008. Non-Double-Couple Mechanisms of Microearthquakes Induced by Hydraulic Fracturing. Proc., 70th EAGE Conference and Exhibition. Rome, Italy. 9 June.

Sileny, J., Hill, D.P., Eisner, L., et al. 2009. Non-Double-Couple Mechanisms of Microearthquakes Induced by Hydraulic Fracturing. ***Journal of Geophysical Research***, **114** (B08307): 1–15. http://dx.doi.org/10.1029/2008JB005987.

Simpson, David W. 1976. Seismicity Changes Associated with Reservoir Loading. ***Engineering Geology***, **10** (2-4): 123–150. http://dx.doi.org/10.1016/0013-7952(76)90016-8.

Snoke, J.A., Linde, A.T., and Sacks, I.S. 1983. Apparent Stress: An Estimate of the Stress Drop. ***Bulletin of the Seismological Society of America***. 73 (2), 339–348

Song, F. and Toksöz, M.N. 2011. Full-Waveform Based Complete Moment Tensor Inversion and Source Parameter Estimation from Downhole Microseismic Data for Hydrofracture Monitoring. ***Geophysics***, **76** (6): WC101–WC114.

Stein, S. and Wysession, M.E. 2002. ***An Introduction to Seismology, Earthquakes, and Earth Structure***. Wiley-Blackwell.

Stoddard, T., McLennan, J., and Moore, J. 2012. Residual Conductivity of a Bauxite-Propped Geothermal System—Influence of Self-Propping, Time and Closure Stress. Paper ARMA 12-605 presented at the 46th US Rock Mechanics/Geomechanic Symposium. 24–27 June 2012. Chicago Illinois.

Talwani, P. 2000. Seismogenic Properties of the Crust Inferred from Recent Studies of Reservoir-Induced Seismicity–Application to Koyna. ***Current Science***, **79** (9): 1327–1333.

Thurber, C. and Ritsema, J. 2007. Theory and Observations–Seismic Tomography and Inverse Methods. In ***Treatise on Geophysics***, 323–354.

Utsu, T. 2002. Statistical Features of Seismicity. In ***International Handbook of Earthquake and Engineering Seismology***, Part A, ed. W.H. Lee, San Diego: Academic Press. 719–732.

Van Der Horst, J., Godfrey, A., Ridge, A., et al. 2013. Fibre Optic Sensing for Improved Wellbore Surveillance. Paper IPTC-16873 presented at the International Petroleum Technology Conference. Beijing, China. 26–28 March. http://dx.doi.org/10.2523/167211-MS.

Vavrycuk, V. 2001. Inversion for Parameters of Tensile Earthquakes. ***Journal of Geophysical Research***, **106** (B8): 16,339–16,355.

Vera Rodriguez, I., Sacchi, M., and Gu, Y.J. 2012. Simultaneous Recovery of Origin Time, Hypocentre Location and Seismic Moment Tensor Using Sparse Representation Theory. ***Geophysical Journal International***, **188** (3): 1188–1202. http://dx.doi.org/10.1111/j.1365-246X.2011.05323.x.

Viig, S.O., Juilla, H., Renouf, P., et al. 2013. Application of a New Class of Chemical Tracers to Measure Oil Saturation in Partitioning Interwell Tracer Tests. Paper SPE 164059 presented at the SPE International Symposium on Oilfield Chemistry. The Woodlands, Texas. 8–10 April. http://dx.doi. org/10.2118/164059-MS.

Wang, J., Tilmann, F., White, R.S., et al. 2009. Application of Frequency-Dependent Multichannel Wiener Filters to Detect Events in 2D Three-Component Seismometer Arrays. ***Geophysics***, **74** (6): V133–V141. http://dx.doi.org/10.1190/1.3256282.

Warpinski, N.R., Engler, B. P., Young, C. J., et al. 1995. Microseismic Mapping of Hydraulic Fractures Using Multi-Level Wireline Receivers. Paper SPE 30507 presented at the SPE Annual Technical Conference and Exhibition. Dallas, Texas. 22–25 October. http://dx.doi.org/10.2118/30507-MS.

Warpinski, N.R., Sullivan, R.B., Uhl, J., et al. 2005. Improved Microseismic Fracture Mapping Using Perforation Timing Measurements for Velocity Calibration. *SPE Journal* **10** (1): 14–23. http://dx.doi.org/10.2118/84488-PA.

Williams, M.J. and Calvez, J.L. 2012. Reconstructing Frequency-Magnitude Statistics from Detection Limited Microseismic Data. *Geophysical Prospecting*, (2005): 1–19. http://dx.doi.org/10.1111/j.1365-2478.2012.01097.x.

Willis, M.E., Burns, D.R., Lu, R., et al. 2007. Fracture Quality from Integrating Time-Lapse VSP and Microseismic Data. *The Leading Edge* **26** (9): 1198–1202.

Withers, M., Aster, R., Young, C., et al. 1998. A Comparison of Select Trigger Algorithms for Automated Global Seismic Phase and Event Detection. *Bull. of the Seismological Society of America*, **88** (1): 95–106.

Woessner, J. and Wiemer, S. 2005. Assessing the Quality of Earthquake Catalogues: Estimating the Magnitude of Completeness and Its Uncertainty. *Bull. of the Seismological Society of America*, **95** (2): 684–698. http://dx.doi.org/10.1785/0120040007.

Wolfe, C.J. 2002. On the Mathematics of Using Difference Operators to Relocate Earthquakes. *Bull. of the Seismological Society of America*, **92** (8): 2879–2892.

Wu, F., Thomas, J., and Fink, M. 1992. Time Reversal of Ultrasonic Fields–Part II: Experimental Results. *IEEE Transactions on Ultrasonics, Ferroelectrics, and Frequency Control*, **39** (5): 567.

Xuan, R., and Sava, P. 2010. Probabilistic Microearthquake Location for Reservoir Monitoring. *Geophysics*, **75** (3): MA9– MA26. http://dx.doi.org/10.1190/1.3417757.

Zhang, H., Sarkar, S., Toksöz, M.N., et al. 2009. Passive Seismic Tomography Using Induced Seismicity at a Petroleum Field in Oman. *Geophysics*, **74** (6): WCB57–WCB69. http://dx.doi.org/10.1190/1.3253059.

Zhang, H., and Thurber, C. H. 2003. Double-Difference Tomography: The Method and Its Application to the Hayward Fault, California. *Bull. of the Seismological Society of America*, **93** (5): 1875–1889.

Zhang, X., Holland, M., Van Der Zee, W., et al. 2014. Microseismic Estimates of Stimulated Rock Volume Using a Detection- Range Bias Correction: Theory and Case Study. Paper SPE 168580 presented at the SPE Hydraulic Fracturing Technology Conference. The Woodlands, Texas. 4–6 February.

21

Rejuvenating Unconventional Resources

Robert Kennedy, Baker Hughes; Iman Oraki Kohshour, University of Alaska Fairbanks; Usman Ahmed, Baker Hughes

This page intentionally left blank

Chapter 21: Rejuvenating Unconventional Resources

21.1 Introduction

Restimulation (refracturing) is the most effective method of rejuvenation to restore productivity to declining shale wells, while enhanced shale oil recovery (ESOR) is an emerging technology being studied for several basins. Both the refracturing concept and the practice have been around for some time; the focus in this chapter is on modern refracturing. The ESOR discussion is primarily focused on the US.

21.2 The Potential Refracturing Market for North American and United States Shale Wells

There are more than 180,000 completed shale wells in the US, and the industry is drilling an additional 18,000 shale wells per year (EIA, 2014). The majority of US shale gas wells (as well as the liquids play wells in the Eagle Ford shale and emerging Utica shale play) have been completed using the cased hole, plug-and-perforate method of completion (also called plug-and-perf in the industry). Operators are familiar with this method, because it is a carryover from fracturing practices used with earlier vertical tight gas wells in the US Rocky Mountains. The plug-and-perforate method uses cement to isolate the annulus between the openhole and the steel pipe, perforations divert the fracturing fluid into the wellbore at the desired location, and composite fracturing plugs provide isolation from the stages below. The plug-and-perforate method is flexible, allows multiple perforation clusters as fracturing entry points, and involves minimal downhole wellbore equipment.

Table 21.1 shows a breakdown of the horizontal shale oil and gas wells in major plays in major US shale and tight plays. The information in this table defines the potential refracturing market in the US. In summary, of mid-2014, there are 37,036 horizontal shale gas wells and 24,998 horizontal shale oil wells that are deemed possible candidates for refracturing. Of those total wells, 62,024 (77%) have original completion types of cased hole, plug-and-perf; 14,202 (23%) have original completion types of openhole packers and fracture sleeves (like the Baker Hughes FracPoint™). Based on current gas prices, the near-term market opportunities appear to be with the liquids plays. Economics are discussed later in this chapter.

Coil tubing-activated methods of completion are relatively new in the US, and a limited number of shale wells have been completed using these systems. Wells completed

Table 21.1—Potential refracturing market—Horizontal oil and gas wells in major US plays. [Source: Table developed with information from Information Handling Services (IHS)]

Shale Play	Gas Wells	Oil Wells	Completion	Vert Wells	Tot. Wells
Barnett	14,199	0	PNP	5,005	19,204
Fayetteville	5,405	0	PNP	65	5,470
Woodford	1,565	748	PNP	304	2,617
Marcellus	6,999	10	PNP	2,462	9,471
Haynesville	3,278	0	PNP	75	3,353
Eagle Ford	3,487	7,173	PNP	56	10,716
Utica	291	179	PNP	107	577
Niobrara	0	3,594	OH	1,969	5,563
Bakken (Tight Oil)	0	10,336	9,420 OH 916–PNP	248	10,584
Mississippi Lime (Tight Oil)	341	2,587	2,023–PNP 905–OH	8	2,936
Granite Wash (Tight Gas/Oil)	1,471	361	1,549–PNP 283–OH	3,602	5,434
Total US Major	37,036	24,988		13,901	75,925

using this method can also be considered as an emerging refracturing market.

Refracturing methods for the openhole completion types used in the Bakken and Niobrara will be more complex than refracturing cased-hole (plug-and-perf) wells. The expandable liner (cladding) method of isolation for refracturing (with only a limited number of jobs having been conducted) appears to be one of the few methods of effectively isolating these openhole completions. The expandable liner method is discussed later in this chapter. The typical refracturing method used with cladding isolation is plug-and-perforate.

In the US in 2014, only a few wells were refractured. According to the IHS database, only 530 wells have been refractured since 2000. Vincent (2010 and 2011), Craig et al. (2012), Martin and Rylance (2010), Cipolla (2006), and King (2010) all discuss refracturing in their papers. Vincent has studied refracturing extensively.

21.3 Initial Fracturing Wellbore Completion Types

Three types of completions have proved to be the most effective and efficient in the North American shale plays. These completions are plug-and-perforate, ball-activated systems (such as the Baker Hughes FracPoint™ system), and coiled tubing-activated systems (such as the Baker Hughes OptiPort™ and OptiFrac™ systems). Although these systems have been described in Chapter 16: Multistage Completion Systems in Unconventionals, they are briefly reviewed here. The plug-and-perforate (PNP) method uses cement to isolate the annulus between the openhole and the steel pipe, perforations divert the fracturing fluid into the wellbore at the desired location, and composite fracturing plugs provide through-tubing isolation from the stages below.

Ball-activated completions systems (BACS), such as FracPoint™, were originally designed to provide multistage isolation in openhole operations. Openhole packers isolate the annulus between the openhole and the liner, and ball-activated fracturing sleeves divert the fracture and isolate individual stages. The fracturing sleeves contain a ball seat that corresponds to a fracturing ball that will open the sleeve. The openhole packer can be a hydraulic-set or fluid-activated. Both types of packers provide isolation in the openhole well, just different setting mechanisms.

The coiled tubing-activated completion system (CTACS) enables multistage hydraulic fracturing by using CT to isolate individual stages. Coiled tubing-activated fracturing sleeves can be used to provide the path for the fracturing fluid to enter the selected portion of the formation and a CT packer that is used to isolate through tubing from the stages below. Baker Hughes OptiPort™ is a CTACS fracturing sleeve that is a pressure-balanced sleeve. Setting a CT packer between these two pressure ports and applying annular pressure opens the intended sleeve. Fracturing operations are conducted through the annulus between the coil tubing and casing.

The OptiFrac SJ™ completion system is a CTACS system that uses a sand jet perforator (SJP) to create the diversion path for the fracturing fluid and uses either a CT packer or a sand plug (through tubing) to isolate the fractured interval from the next set of perforations to be fractured. A sand plug is a special mixture of fluid and proppant that is designed to intentionally create a screen-out. When the sand plug reaches the injection point, it cannot pass into the formation and causes a screen-out that will isolate that stage during the next stage fracture. A cleanup run is necessary to remove the sand plugs when the fracturing job is complete. Fracturing operations are conducted through the coil tubing.

21.4 Reasons to Refracture

There are primarily two reasons to refracture:

1. Open and connect new reservoir rock to the existing stimulated reservoir via new set(s) of opening(s) from the wellbore.

2. Revitalize initial fracture treatments that were either unsuccessful or have failed over a period of time.

The first reason is justified when it is noted that the existing fracture stages are not effectively draining the surrounding and adjoining areas. Chapter 20 discusses some of the techniques used to identify the potential unstimulated zones. At times, these stage locations are planned but not stimulated on the first go around pass for many reasons, including lack of upfront capital expenditure. In the event the refracture stages were preplanned, the completion methods were appropriately chosen to facilitate reentry as illustrated in the previous section. In this regard, caution needs to be exercised when refracturing a virgin location. While discussing stress shadowing, Nagel and Sanchez-Nagel (2001) noted: "Each created hydraulic fracture alters the stress field around it.

When hydraulic fractures are placed close enough together, the well-known stress shadow effect occurs in which subsequent fractures are affected by the stress field from the previous fractures."

If the new or added perforated and fracture stages are closer than about 100 ft., the refracturing treatment will probably follow the old stress pattern and refracture into the original perforations. This will not be new rock being stimulated but the old, partially depleted rock. Hence, it is important that proper attention is paid to such completion design.

The second type of refracturing can be divided into four different types depending on the reason the refracture is required (modified from Vincent, 2011).

1. Refracture the existing perforations with the original fracturing design. This is often done because it is believed that the fractures plugged, lost conductivity, or because some perforation clusters may not have been effectively fractured with the initial fracture design. In this case, refracturing existing perforations might actually crack new rock. Plus, as mentioned earlier, there is the potential of propping the top half of the fracture network.

2. Refracture the existing perforations with different fracturing fluid or proppant. That is, using slickwater when the original fluid was gelled fracture fluid, or because it is believed that the proppant was crushed or embedded, or because some of the fractures may not have been effectively fractured initially.

3. Refracture the existing perforations after a number of years of production (because the stress regime along lateral has reversed, and refracturing will actually crack new rock).

4. Refracture by adding stages to the existing fractures (because of incomplete lateral coverage, obviously cracking new rock).

Each created hydraulic fracture alters the stress field around it. When hydraulic fractures are placed close enough together, the well-known stress shadow effect occurs in which subsequent fractures are affected by the stress field from the previous fractures.

If the new or added perforated and fracture stages are closer than about 100 ft., the refracturing treatment will actually follow the old stress pattern and refracture into the original perforations. This will not be new rock, but the old, partially depleted rock.

21.5 Why Initial Fracture Treatments Are Either Unsuccessful or Fail Over Time

Unfortunately, operators log or survey the horizontal lateral open holes in only 8 to 10% of shale wells (EIA, 2014). When fractured shale wells perform poorly, the reason cannot always be ascertained from available production data or even offset well production. Thus identifying the perforated clusters that are responsible for the poor production cannot readily be determined.

Running production logging tools (PLTs) may be able to provide information about which, or how many, of the perforation clusters or stages are producing. However, this is instantaneous information; it cannot provide details as to why the wells are performing poorly. PLTs and other cased-hole logging tools are discussed later in this chapter. Based on information from PLTs run in horizontal laterals in shale wells, the following anecdotal information published in industry literature includes the following statements:

- Unconventional wells in the US that do not reach their production targets: 70% (Hart E&R, 2012).
- Shale well fracturing stages that are ineffective: 40%.
- Shale well fracturing stages that are producing any fluid: 60%

Again, the real question is why such limited success. In attempting to answer the question why only 40% to 60% of fracturing stages are contributing to the production, a listing is provided why fracturing is initially unsuccessful and why fractures fail over time.

21.5.1 Why Initial Fracturing May Be Unsuccessful

The following are some of the reasons why the initial hydraulic fracture stages and cluster perforations are unsuccessful:

- Inadequate reservoir quality and limited hydrocarbons in the area (along the lateral) such as lower TOC, lower porosity, and lower pressure.
- Poor reservoir quality along the horizontal lateral where fracture stages were placed.
- Unfavorable mineralogy, i.e., more pliable clay and less brittle material, such as siliceous or carbonate rock.

- Existing high-stress regime that prohibits a fracture from being initiated and, therefore, not propagated in the intended location.
- No (or limited) natural fractures located near enough to the stage to generate a complex fracture network to facilitate hydrocarbons to flow into the wellbore.
- Fractures possibly encountering a geohazard (such as a fault or water zone).
- With five or more perforation clusters per stage, it is plausible that many clusters were never fractured at all. In other words, the fracturing fluid and slurry went to the point (perforation cluster) of least resistance and fractured only a few of the clusters.
- Ineffective isolation, which could result in fracturing the adjacent stage again.
- Lack of information to assist in designing the fracturing treatment and stage placement.

21.5.2 Why Fractures Fail Over Time

Even if a fracture stage or cluster is placed properly to begin with, it can still fail over time. There are a number of reasons for failure, listed next:

- Fractures close, or plug, or degrade with time.
- Proppants were crushed or embedded, or flowed back.
- Improper initial fracturing fluid used.
- Reorientation of stress field around the well after the well was produced for a period of time.
- Proppants settling in the bottom portion of the fracture.

21.6 Why Refracturing Is Successful

Vincent (2010) provided examples of economic failures in attempted refractures stating that restimulation methods may be unsuccessful for many different reasons, including:

- Poor reservoir quality
- Limited reserves in restricted drainage area
- Low reservoir pressure prohibiting cleanup
- Selection of undesirable candidates
- Poor mechanical integrity or undesirable perforations
- Formation damage induced by refracturing fluids
- A combination of the above.

All of the same reasons could easily apply as to why initial fracturing has been unsuccessful (with possibly only half of the fracturing stages producing anything at all). Therefore, we can readily see that this list is very similar to the list shown previously in Section 21.4 .

Vincent (2010) also provided a list of the reasons why refractures were successful.

Improved stimulation techniques:

- Enlarged fracture geometry, enhanced reservoir contact
- More lateral coverage in horizontal wells or initiation of more transverse fractures
- Increased fracture conductivity compared to initial fractures
- Use of more suitable fracturing fluids
- Increased conductivity in previously unpropped or inadequately propped portions of fracture

Restoration of fracture conductivity lost due to:

- Proppant embedment
- Cyclic stress
- Proppant degradation
- Gel damage
- Scale, asphaltenes, and fines plugging
- Reorientation of stress field and contact with new rock
- Re-energizing natural fractures

New data also suggests that there might be a reason for the success of refractures, especially when the same fracturing stages are being reopened. With the bottom half of the complex fracture geometry being propped during the first time around, the re-fractures are now prone to prop the top half of the complex fracture network.

21.7 Refracturing Procedures

There are primarily four steps to the refracturing process:

1. Cleaning out the well is absolutely required. Consider running production logging tools (PLT) while the well is still producing.

2. Survey and inspect the casing to assess condition (this can partly assist in selecting the isolation method for the refracturing process).

3. Run the necessary cased hole log(s) to provide information to assist in the refracturing treatment design and placement.

4. Design and conduct the refracturing.

21.7.1 Wellbore Cleanouts

Vincent (2010) interviewed three different unidentified operators in the Bakken and obtained the following information about cleanouts used with refracturing. Results of the interviews are listed in the following bullets:

- Can recover more than 300,000 lbs of fracturing sand! This is enough sand to fill 15,000 ft. of a 6-in. hole. The volume of sand recovered from specific wells has exceeded 50% of the initial volume of fracturing sand.
- Some wells initially stimulated with sand have been cleaned out multiple times and still continuously produce sand into the wellbore.
- Superior refracturing production improvement and success ratios have been observed following pre-refracturing cleanouts.
- Cleanouts for multilaterals can cost as much as $500,000, which is similar to the cost of the subsequent refracturing (multilaterals only applicable to the Bakken).
- Pre-refracturing cleanouts of wells treated with ceramic have rarely returned much ceramic proppant.

Note: The previous information is representative of the Bakken, and may not be applicable for wells in other shale plays, especially when the stress regime is quite different.

Before conducting a cleanout, consider running a production log (PLT) while the well is still producing. PLTs can provide information about whether or not a perforation cluster is producing any fluid.

Well cleanout before refracturing is strongly recommended by a number of authors including Rahim et al. (2013), Vincent (2011), and XTO (ExxonMobil) Energy (from a presentation at the NDPC Annual Meeting, 26 September 2011). A Baker Hughes recommended practice for refracturing is that a well cleanout should be required for all refractured wells, no matter what the selected method is for refracturing. In addition, pulling the well tubing and any packers is required as part of the cleanout process.

Coiled tubing (CT) is recommended as the most effective and economic method for cleanup. This only requires the use of a 2-in. coil; a larger diameter is not needed.

A typical well cleanout is estimated to cost from $60,000 to $100,000 using coil tubing. Total spread cost (including day rate) for a CT unit runs from $50,000 to $65,000 per day as of mid-2014. Maximum depth for 2 3/8 in. = 20,000 to 25,000 ft.; maximum depth for 2 7/8 in. CT = 14,000 to 16,000 ft.

Total spread cost (including day rate of $28,000 as of March 2014) for a drilling rig (capable of drilling horizontals with rotary steerable equipment) is $40,000 to $50,000 per day. Usually a workover rig is also used for cleanout of wells, and the day rate is much less than that of a drilling rig.

21.7.2 Inspecting the Casing

A simple casing inspection log will provide information about the condition of the wellbore casing. The findings of the inspection can assist in the selection of the appropriate refracturing method. The casing inspection tool can provide information about which types of isolation or refracturing techniques should be considered. Finding an extensively damaged and/or corroded casing could tip the decision in favor of abandoning refracturing the well. In industry literature, it has been noted that some relatively new wells in the Eagle Ford have been found to have casing damage as a result of the curve and horizontal lateral sitting in mud on the low side of the hole (where a cement job was possibly ineffective). Such damage might prevent implementation of any refracturing process.

21.7.3 Running Necessary Cased Hole Logs

Cased hole logs should be considered in order to gather information for use in design of the refracturing treatment and the placement of stages. Two types of cased hole logs can provide this information. First, a log such as the RPM™ or Kinetix™ (lithology, qualitative TOC, porosity, and saturations) and Star™ (natural fracture information) could be used. The RPM™ or Kinetix™ log was designed to be run as LWT (logging while tripping). Second, Baker's XMAC-F1™ log can be run in open or cased holes to gather information about stress profile; however, conveyance would have to be by tractor or coil tubing and tool size restrictions need to be considered. The risk of these types of logging operations is considered justified at this time (when it was not for a newly drilled well). Information provided by these, or similar, tools is critical to assist in determining optimum placement of the fracturing stages along the lateral for a successful refracture. Due to the size and functionality, any, or all, of these tools may have to be modified or redesigned. Also, the deployment (conveyance method) will require wireline with tractor, coil tubing, pump down, or other. And sensor methods need to be considered (including wired connections with CT, fiber optics, or other new options).

As of late 2014, there were three types of tool connections (wired) for data readout that can be employed with CT. These are ELine, TeleCoil™ (instrumented BHA for CT), and

memory mode. The difference between ELine and the TeleCoil methods is that ELine has only a limited number of sensors.

21.7.4 Designing and Conducting the Refracture

21.7.4.1 Refracturing

Various methods of isolation, refracturing equipment, and methods are discussed next.

21.7.4.2 Isolation

Generally, refractures are ineffective unless the perforation clusters of each stage can be temporarily isolated, so that the energy of the subsequent fracturing stage can be directed specifically to another area along wellbore (Allison et al. 2011). For the case of adding all new perforations, the existing perforations must be permanently isolated, and each new cluster or stage must also be temporarily isolated, just as in reperforating or refracturing the same intervals. The following methods of isolation have been deployed. Permanent or temporary isolation techniques fall into two broad areas: mechanical or chemical, cement or other, as described next.

21.7.4.2.1 Mechanical

- Drillable composite plugs (temporary)
- Separation packers (temporary and retrievable for multi-use)
- Expandable liner—cladding (permanent)
- Retrievable multiset packer and diverters (temporary)

21.7.4.2.2 Chemical, Cement, or Other

- Chemical gel squeezes (temporary or permanent)
- Diverters (temporary)
- Cement squeezes (permanent)
- Emerging (permanent and temporary)

21.7.4.2.3 Mechanical Isolation Methods Discussion—Advantages, Disadvantages, and Costs

Drillable composite plugs are currently used for initial shale well fracturing when the plug-and-perforate method is used with cased hole completions. This is a temporary isolation method and is not applicable for permanently isolating existing perforations to perforate in different locations along the wellbore.

Advantages

- Plugs are readily available.
- Procedures are familiar to operators.
- Plugs can be set using wireline.
- Plugs can be drilled out in a very short time (Baker's QUICKDrill™ plugs can be drilled out in a matter of one- half-hour per plug. Plus PlugLift™ drill out fluid expedites the process).
- Cost is reasonable.

Disadvantages

- Rig required to mill out the plugs from well.
- The casing condition in the refractured well may have bad spots.
- Ensuring if damage would occur if cladding method used.
- Estimated costs.
- Usually included in plug-and-perforate fracturing costs.

The new Baker Hughes SHADOW™ Fracturing Plug was not considered in this evaluation because it was conducted near the end of 2013. SHADOW™ Fracturing Plugs can be used to avoid a millout. These plugs have a large diameter and have flow through capability, so they can be left in the well and produced through. SHADOW™ Fracturing Plugs are used in combination with the IN-Tallic™ Disintegrating Fracturing Balls.

21.7.4.3 Separation Packers

Separation packers (or straddle packers) can be used for either retrievable or permanent isolation. The permanent straddle packers have not been considered because of the impractical aspect of having part of the lateral blocked off from access to refracture. However, straddle packers have been used quite successfully in other CT operations. Originally, one of the intended uses of the Baker Hughes FracPoint™ completion system was for refracturing wells with initial plug-and-perforate completions in cased hole. The packers of FracPoint™ could have been used to permanently isolate (mechanically) the existing perforations in a well. Then or before this was run, new perforations could be added. The actual procedure of just how this was to be accomplished was never really developed as a recommended procedure. And, of course, this is not being widely considered due to the complex array of downhole equipment that would have to be run into the well.

21.7.4.4 Chemical and Cement Mechanical Isolation Methods Discussion

Chemical gel squeezes have only been briefly addressed. So far, it has been determined that drill-in fluids, like

PerFlow™, cannot hold integrity when subjected to 10,000 psi fracturing pressure. Also, discussions with Baker Hughes Water Management Group for Conformance concluded that other gels or chemicals, which are being used by water shut offs, cannot be used as permanent isolation material. If an appropriate gel can be identified, it will become the only other viable method (aside from cladding) to permanently isolate existing perforations in order to perforate in new locations.

Cement squeezes are not being strongly considered at this time. Historically, cement squeezes, even in conventional wells, have been somewhat problematic with only a few sets of perforations. For the Eagle Ford case (discussed later), some 75 individual sets of perforations would have to be squeezed off. The success rate for achieving this is probably low, and costs can be high. Generally it is not believed that cement is an acceptable or effective isolation method for this purpose.

Diverters and diversion products are discussed briefly (later) under the Multiset Retrievable Packer option.

Emerging isolation methods, including Liquid Casing and modified GeoFoam, are essentially in the embryonic stages of consideration for development.

21.7.5 Wellbore Refracturing Equipment and Procedures

The following equipment and procedures have been studied and considered for conducting refracturing using mechanical isolation methods.

21.7.5.1 Expandable Liner Cladding System

Expandables have been under study by Baker Hughes' North America geomarket for the past two years. This expandable liner allows the failed area of casing (or open perforations) to be sealed off, providing high-burst and collapse pressure ratings (**Fig. 21.1**). The expandable liner is expanded from bottom to top with a hydraulic running tool at the toe.

When the anchor at the toe of the liner is hydraulically set, the fixed expansion cone can then be pulled mechanically through the remaining patch with the work string to finish the expansion process. The hydraulic running tool can be actuated at any time during the process. This system can be used to permanently isolate existing perforations or fracturing sleeves, which creates pressure integrity throughout the wellbore. With wellbore isolation achieved, new perforations can be added at different locations along the wellbore, and plug and perforation fracturing operations can commence. Expandable liners can be deployed with either stick pipe (workover rig) or they can be deployed using coiled tubing.

Advantages

- It is developed technology.
- Handles any casing size.
- Has pressure integrity, seals, and multiple seals.
- Cover entire liner, not just perforations
- Has large ID (3.4 in. for 4.5-in. casing).
- High performance tubulars, thicker wall, specifically designed to accommodate higher temperatures and fracturing pressures.
- Successfully tested connections in up to 45° per 100 ft. of deviation.
- Can be placed either in neutral or compression mode with the running tool before the top packer and anchor is set.

Disadvantages

- Needs continued field testing to refine procedures for different configurations.
- Must have a rig on location.
- Expandable liner has limited field testing. In one installation, the expandable liner was run to cover fracturing sleeves to allow the wellbore to be refractured using the plug-and-perforate method.

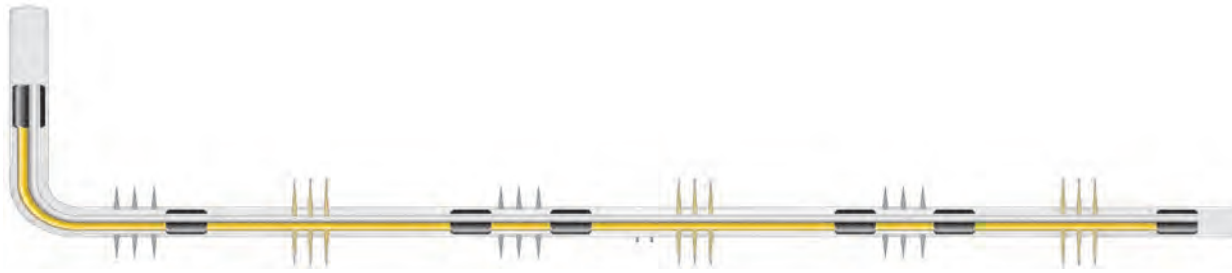

Fig. 21.1—Typical expandable liner downhole configuration.

- Here only part of the 4,500-ft. lateral could be covered by the cladding before the work string (provided by the operator) parted and the expanding tool was stuck in the hole.
- Perforations need to be placed in between the existing fracturing sleeves.

Note: The second installation was successful. A 1,000-ft. expandable liner was deployed in the lateral section across milled out fracturing sleeves to allow the operator to perforate between the existing fracture sleeves in the initial completion.

Estimated Costs

- $833M + 4 days' rig time X $40,000 per day = $160M—total = $993M (9,000 ft. cladding quote for operator). The cleanout quote is $83M plus rig at $60M with a total of $143M. (Quote based on rig and stick pipe.)
- $450M including rig cost (4,500 ft. cladding quote for operator).
- Eagle Ford oil well—15,600 TMD, 5,500 ft. Lateral—cladding cost = $550M to $607M = Avg. $580M. (Estimate based on average between two operator quotes.)
- Barnett gas well—11, 600 ft. TMD, 3,500 ft. Lateral—cladding cost = $350M. (Estimate based on operator quote.)

21.7.5.2 Retrievable (Multiset) Packer with Diverters

The retrievable, multiset-packer-with-diverters method is already under development by Baker Hughes. The process and system would employ coiled tubing with a multiset packer to isolate a single perforation cluster from open perforation clusters above (previously discussed), and diversion materials pumped at the conclusion of each individual cluster stage to sequentially isolate the newly refractured clusters below. This is a temporary isolation method and is not applicable for permanently isolating existing perforations in order to perforate in different locations along wellbore. Further development of this method is required, but only to select the best multiset packer and diverting agent. Currently the Baker LitePlug™ (a 50-50 mixture of LiteProp™ and sand) is strongly being considered as the preferred diverter, but others also continue to be evaluated. The method of using "straddle packers" (mentioned previously) is closely akin to the multiset packer method. The straddle packer method has some of the same advantages and disadvantages as the multiset packer.

Advantages

- Use of CT would reduce pumping rates versus initial fractures through stick pipe. This would require less HHP (at surface) to treat and thus reduce costs.
- Smaller treatment fluid and proppant volumes, thus reduced costs.
- Higher probability of obtaining a more effective fracturing due to single perforation cluster treatment rather than multiple cluster (3-to-10) treatments of initial fractures.
- This system would be very efficient.
- Does not require a rig and CT already on location after cleanout.
- Can recover from screen-out without tripping to surface.

Disadvantages

- Requires development of new or modified tools—a reliable multiset packer that can be set, released, moved, and reset multiple times without risk of becoming stuck due to wellbore debris.
- Selecting or design of diverters. Being considered are sand and degradable particulates, viscous gels, and deforming and disintegrating balls.
- Procedure and smaller, specific treatment designs need to be developed before implementation of this method.

Estimated Costs

- Only minor tool costs are to be added to refracturing cost. Assuming this will be is offset by the reduced fracturing costs gained by this process. Therefore, use the previous normal refracturing costs above for:
  - Eagle Ford oil well—15,600 TMD, 5,500 ft. Lateral-refracturing = $176 M for stage 1 + 152 per M Stage x 14 Stages + 150 M—CT, Plugs, perforations = $2.46 MM
  - Barnett gas well—11, 600 ft. TMD, 3,500 ft. Lateral–refracturing = $151 M per stage 1st + 138 M per stage x 7 stages + 150 M—CT, plugs, perforations = $1.27 MM Total

21.7.5.3 Baker OptiFrac™ Coil Tubing-Assisted Fracturing System

The Baker OptiFrac™ coil tubing-assisted fracturing system has three different options (as discussed in Chapter 16). All options involve annular fracturing and abrasive perforating, but different applications with different isolation methods. However, all of the methods only provide temporary isolation, and OptiFrac™ is not applicable for permanently isolating

existing perforations in order to perforate in different locations along the wellbore. This refracturing method could be used in conjunction with a permanent isolation option such as cladding. However, if this were the case, a better option would be to use plug-and-perforate rather than OptiFrac™. Advantages and disadvantages and costs (using cladding as the permanent isolation method) are included in this chapter for completeness.

Advantages

- Coiled tubing does not have to be removed from the well during pumping, which increases the speed of treatment.
- Jetting creates clean, large holes with no debris in the perforation tunnel and low near wellbore tortuosity.
- Allows hydraulic fractures to propagate at significantly lower pressures.
- Can recover from screen-out without tripping to surface.
- Can treat any number of zones, typically 3-to-6 per day.

Disadvantages

- This tool was designed for conducting original fracturing of a well. When refracturing through the annulus all perforations above (previously discussed) the working point must be permanently isolated and able to handle full fracture pressure (10,000 psi). If the wellbore is in this posture, it is more effective just to conduct a normal plug-and-perforate operation.
- Added cost of permanently isolating existing perforations with method, such as cladding (discussed next).
- Number of tool redresses. Version 2 tools being refined (SureSet™).
- Required setting force limits achievable depth.
- Limited number of jobs performed in US (all of which have been original fractures).

Estimated Costs

- Isolation of existing perforations using cladding:
- Eagle Ford oil well—cladding cost = $580M
- Barnett gas well—cladding cost = $350M
- Refracturing costs:
  - Eagle Ford oil well—15,600 TMD, 5,500 ft. Lateral—refracturing = $176 M per stage1 + 152 M per stage x 14 stages + 150 M—CT, plugs, perforations = $2.46 MM
  - Barnett gas well—11, 600 ft. TMD, 3,500 ft. Lateral—refracturing = $151 M per stage 1st + 138 M per stage x 7 stages + 150 M—CT, plugs, perforations = $1.27 MM Total

21.8 Refracturing Candidate Selection

Candidate selection of refracturing wells is not considered in detail in this chapter. Several SPE papers have addressed selection methods in regard to the second type of well as mentioned in Section 21.4 The following address the topic very specifically:

- Sinha and Ramakrishnan (2011). "A Novel Screening Method for Selection of Horizontal Refracturing Candidates in Shale Gas Reservoirs."
- Moore and Ramakrishnan (2006). "Restimulation: Candidate Selection Methodologies and Treatment Optimization."
- Roussel and Sharma (2011). "Selecting Candidate Wells for Refracturing Using Production Data."
- Martin and Rylance (2010). "Hydraulic Fracturing Makes the Difference: New Life for Old Fields."
- Craig et al. (2012). "Barnett Shale Horizontal Restimulations: A Case Study of 13 Wells."

King (2010), Rahim et al. (2013), Besler et al. (2007), and Vincent (2010 and 2011) also discuss the well selection topic. Selection criteria can be dependent on operator objectives, and also varies with each different shale play and the refracturing method. It is also recognized that choosing a candidate well also dictates the equipment and treatment used to refracture the candidate well.

Although we believe that the operator is best positioned to be able to conduct the refracture candidate selection process, Baker Hughes has also undertaken a study of refracturing well selection criteria. We have identified and developed two different methods for selecting candidate wells. The MAX–Monte Carlo method develops a score for each potential candidate by ranking some 80 data points of information. Wells with the higher scores compared to other wells in the same general area of a play are the better candidates for refracturing. A separate economic analysis is conducted to determine operator economics for each candidate well. A second method for candidate selection is called the RFID (refracture candidate Identification) method. RFID identifies wells that are either poor performers (production) or better performers compared to other nearby wells. Refracture performance predictions can be made based on the model's production profile, which is determined from other wells that

have already been refractured. This method also includes an economic evaluation to determine operator economics for each candidate well.

21.9 The Economics of Refracturing

These example economic cases and results reflect the "operator's economics before tax." A typical shale gas and shale oil well was selected and used for all economic evaluations.

21.9.1 Well Design, Completion, Refracturing, and Costs

The shale oil well selected was from the oil window of the Eagle Ford shale. Well design, completion, refracturing, and costs are shown next:

- Depth (TVD) at 9,400 ft.
- Lateral Length at 5,500 ft. (Max MTD = 15,600 ft.—includes 700 ft. for curve)
- Completion is cased hole with 5 ½-in. production string
- Fracturing design includes 15 stages with 5 perforation clusters per stage = 75 perforation clusters per well.
- Costs for well and refracturing:
  - Total cost of well = $7.0 MM
  - Drilling cost = $7.0MM x 0.40 = $2.8 MM
  - Side tracking = $2.8 MM x 0.75 = $2.1 MM + $2.46 MM (refracturing) = $4.56 MM
  - Refracturing = $176 M per Stage1 + 152 M per stage x 14 stages + 150 M—CT, Plugs, perforations = $2.46 MM. (Does not include some customer costs, i.e., water.) This refracturing cost is based on a recent service company quote for an Eagle Ford well made in the later part of 2013.

The shale gas well selected was from the Barnett shale. Well design, completion, refracturing, and costs are shown next:

- Depth (TVD)—7, 400 ft.
- Lateral Length—3,500 ft. (Max MTD = 11,600 ft.—includes 700 ft. for Curve)
- Completion—cased hole with 4 ½-in. production string
- Fracturing Design—8 stages with 5 perforation clusters per stage = 40 perforation clusters per well
- Costs for well and refracturing:
  - Total cost of well = $3.5 MM
  - Drilling cost = $3.5MM x 0.45 = $1.6 MM
  - Side tracking = $1.6 MM x 0.75 = $1.2 MM + $1.27 MM (refracturing) = $2.47 MM
  - Refracturing = $151 M per Stage1 + 138 M per Stage x 7 Stages + 150 M—CT, plugs, perforations = $1.27 MM. (Does not include some customer costs, i.e., water.) This recent service company quote for a Barnett well was made in the later part of 2013.

It should be noted that fracturing costs across the US (third quarter 2014) are significantly lower and range from $80,000 to $90,000 per fracture stage, depending on the specific shale play.

21.9.1.1 Sidetrack the Well: Advantages, Disadvantages, and Costs

Estimates for sidetracking both the typical oil well and gas well cases were developed (see the details in the previous bullets). It was concluded that these are the maximum costs that an operator would consider for any of the various option methods to refracture the well. With respect to refracturing, some operators have a maximum budgeted cost for a refracturing. One operator has said their budget (roughly half the cost of the original completed well cost) is $3.0 MM for Eagle Ford and $4.0 MM for the Bakken. Although consideration of a sidetrack was only done for cost purposes (economics were also calculated), advantages and disadvantages are listed next.

Advantages

- Reduced cost versus new well.
- Results in a new wellbore and completion equipment in which to conduct newly designed fracturing.
- Allows characterizing of the new lateral—natural fractures, reservoir quality, TOC, porosity, mineralogy (advanced mud logging and cuttings analysis).

Disadvantages

- Reduced hole size
- Location of new lateral versus original (may not be equal)

- Reduced total recovery (well partially depleted)
- Lease constraints
- Risk factor for losing the entire well is higher than drilling total new well

Costs

- Detailed previously—sidetrack and refracturing
- Oil well—$2.1 MM (ST) + $2.46 MM (Refracturing) = $4.56 MM Total
- Gas well—$1.2 MM (ST) + $1.27 MM (Refracturing) = $2.47 MM Total

21.9.1.2.4 Refracturing Economics Discussion

A number of economic cases were run to show the value for the three primarily isolation and refracturing methods that have been identified as currently available or near market offerings from Baker Hughes:

1. Cladding.

2. Retrievable multiset packer and diverters. The straddle packer method has similar results.

3. OptiFrac™.

Cases were run for each method for the two typical wells—Eagle Ford shale oil well and the Barnett shale gas well. Sensitivity tests were run for each case by varying the refracturing design and attaining the original initial productivity (IP) of the well and also for attaining only 60% of the IP of the original well. These economic evaluations were run to calculate an Operator's Before Tax Economic Parameters of Payout, ROI, and NPV10. Costs used for each method were developed and discussed earlier in this document. Flat product prices used in the model were $100 per bbl for oil and $3.50 per Mcf for gas. All cases were run in early 2014.

The IPs for the Eagle Ford (600 BOPD–360 BOPD at 60%) and the Barnett (2.1 MMcfd–1.26 MMcfd at 60%) were obtained by data mining to determine the mean IP for all wells completed in the last three years as of 2014 in each play. The investment costs used in the economic analyses were developed earlier and are summarized in **Table 21.2**.

Table 21.3 shows the result of the economic calculations, i.e., operator economics (value) before tax. Economics are definitely favorable for all shale oil cases and options:

- IPs that match initial IPs
- IPs that attain only 60% of initial IPs
- All payouts less than six months
- Excellent return on investment (ROI)
- Good expected recoveries (ER), and expected ultimate recoveries (EUR)
- Very respectable net present value (NPV10)
- Economics are most favorable for the multiset packer option
- Even the sidetrack and refracturing case yield acceptable economics

Table 21.2—Summary of operator and customer investment costs.

Eagle Ford Oil		Cost — Customer Investment, $ Millions		
Method	**Clean Out**	**Isolation Option**	**Refrac**	**Total, $ Millions**
Cladding	0.100	0.580	2.460	3.140
Multiset Pkr	0.100	No Additional	2.460	2.560
OptiFrac	0.100	No Additional	2.460	2.560
Side Track	2.100	ST Cost	2.460	4.560
Barnett Gas		**Cost — Customer Investment, $ Millions**		
Cladding	0.100	0.350	1.270	1.720
Multiset Pkr	0.100	No Additional	1.270	1.370
OptiFrac	0.100	No Additional	1.270	1.370
Side Track	1.200	ST Cost	1.270	2.470

Table 21.3—Summary of operator and customer economic results.

Eagle Ford								
Method	**Initial Potential**	**PO, Yr**	**ROI, % 5Yr**	**ROI, % 20Yr**	**ER, MBO 5Yr**	**EUR, MBO 20Yr**	**NPV10, 5Yr, $MM**	**NPV10, 20Yr, $MM**
Cladding	600 BOPD (Orig)	3 mo	360	568	220	441	11.3	17.8
Multiset Pkr	600 BOPD (Orig)	2 mo	464	719	220	441	11.9	18.4
OptiFrac	600 BOPD (Orig)	3 mo	360	568	220	441	11.3	17.8
Sidetrack	600 BOPD (Orig)	5 mo	217	360	220	441	9.9	16.4
Cladding	360 BOPD (60%)	6 mo	176	301	132	264	5.5	9.4
Multiset Pkr	360 BOPD (60%)	4+ mo	238	391	132	264	6.1	10.0
OptiFrac	360 BOPD (60%)	6 mo	176	301	132	264	5.5	9.4
Sidetrack	360 BOPD (60%)	12 mo	90	176	132	264	4.1	8.0
Eagle Ford								
Cladding	2.1 MMcfd (Orig)	5	-3	38	1	2	-0.05	0.66
Multiset Pkr	2.1 MMcfd (Orig)	3	22	74	1	2	0.3	1.01
OptiFrac	2.1 MMcfd (Orig)	5	-3	38	1	2	-0.05	0.66
Sidetrack	2.1 MMcfd (Orig)	25	-32	-4	1	2	-0.80	-0.09
Cladding	1.26 MMcfd (60%)	25	-42	-17	0.6	1.2	-0.72	-0.29
Multiset Pkr	1.26 MMcfd (60%)	16	-27	4	0.6	1.2	-0.37	0.06
OptiFrac	1.26 MMcfd (60%)	25	-42	-17	0.6	1.2	-0.72	-0.29
Sidetrack	1.26 MMcfd (60%)	25	-59	-42	0.6	1.2	-1.47	-1.04

All of the shale gas cases and options are uneconomic; only the multiset packer option was marginally economic, paying out in three years with an EUR approaching that of a new well. The primary reason for the uneconomic shale gas options is the current (late 2014) low gas price.

21.10 Refracture Case Histories

Fanguy (2009) states that the first refracture of a horizontal well involving Baker was conducted in 2008 and used the FracPoint™ system. It was a refracture of a well originally completed in openhole (barefoot) in the Edwards Lime, Texas tight gas reservoir. The procedure included reaming the horizontal open hole, installing a 3.5 in., 9.3 ppf, 4-stage multi-zone fracture completion system (a very early FracPoint™), and the refracturing the well (no details could be found on the actual fracturing treatment). The results of the refracturing were actually quite good with an increased producing rate of the well by threefold from 500 Mcfd to 2.5 MMcfd (see **Fig. 21.2**).

In 2009, another refracturing took place for a vertical cased hole well in the Wilcox of south Texas, also a tight gas reservoir, where the packers (of FracPoint™) were used to permanently isolate existing perforations. The refracture was unsuccessful because the operator believed the zones were more depleted

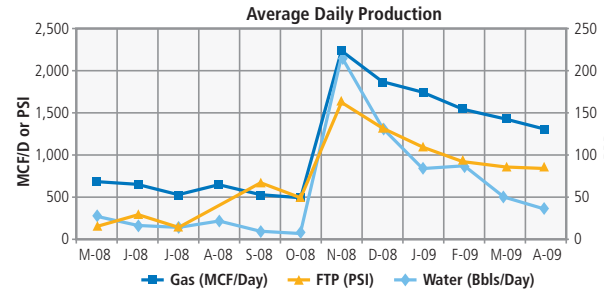

Fig. 21.2—Production plot of the horizontal refracturing in the Edwards Lime tight gas (performed by Baker).

than originally anticipated (see **Fig. 21.3**). This was a good example of lessons learned.

Production rates from refracturing have matched, or sometimes exceeded, those from the original fracturing. **Fig. 21.4** is a Barnett refracture (vertical well) done with slickwater and compared to the original gel fracturing (Cipolla 2006). Note that the decline profile was flattened after the refracturing.

XTO (ExxonMobil Subsidiary) conducted 70 refracturing operations in the Bakken. A production plot for one of these efforts is shown in **Fig. 21.5**. The production rate in this well was returned to a near-original IP, and the decline rate was flattened.

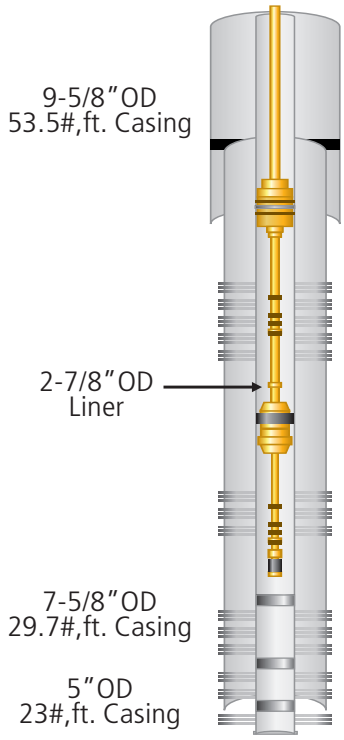

September - October 2009

- Re-Perforated, zones between 12576 ft.-12,694 ft.
- Installed multi-zone fracture completion system size: 435-281
- Fractured two zones: 12576 ft.-12,694 ft. and 13,144 ft.-13,300 ft.
- Installed production tubing and chemical injection system
  Placed well on production
- Well did not respond to fracture treatment

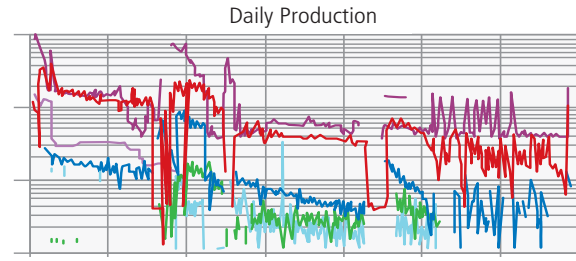

Fig. 21.3—Baker Hughes vertical well refracturing in Wilcox tight gas.

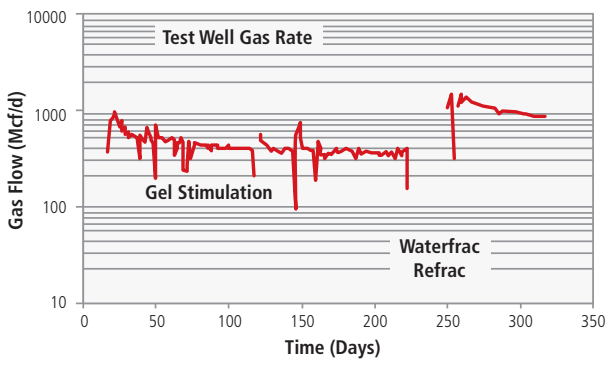

Fig. 21.4—Refracturing of Barnett shale well with slickwater. (From Cipolla 2006.)

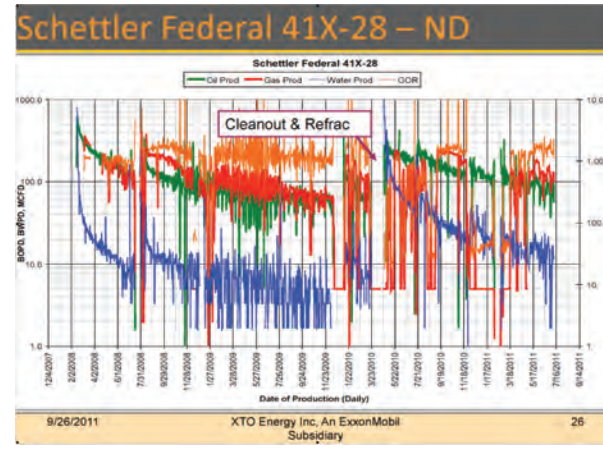

Fig. 21.5—Production plot from a refractured horizontal well in the Bakken. (From XTO Energy 2011.)

XTO had several key lessons learned from the 70-well refracturing project in the Bakken (XTO report 2011):

- Refracturing appears economically and operationally effective.
- The best refracturing techniques are often versatile.
- The exact mechanism of added production is still unclear.
- Good wells make good refracture candidates.
- Cleanouts before refracturing make a huge difference in the success rate.
- There is documented history of success refracturing wells with original inefficient completions.
- Ample opportunity exists for further development of refracturing techniques.

It should be noted that the age of the 70 wells was from 2 to 3 years.

21.11 Recommendations for Refracturing

The following recommendations are suggested based on the case studies and the experiences discussed in this chapter:

- Use a set of selection criteria for different plays, for different types of refracturing equipment, and for procedures or Baker Hughes' MAX or RFID selection criteria methods.
- Use the Four Step Refracturing Procedure discussed earlier.
- Select the applicable refracturing type and equipment and procedure as the following:
  - Use the expandable liner on refractures requiring isolation of existing perforations.
  - Use the multiset packer with diverter or straddle packer system for refracturing of PNP completions.
  - Determine the best, most effective cased hole logs to run to evaluate the horizontal wellbore for each refracturing case (probably the RPM™ and Star™).
  - Use xFractor (MFrac™ and MShale™ Fracturing Simulators) to design the refracturing treatment.

21.12 Concluding Remarks about Refractures

In general, refracturing can re-establish good connectivity with the reservoir. It may secure new reservoir volume, and bypass near-wellbore damage. This process results in restoration and increases in production rates, potentially flattening the original decline profile, and extending the productive life of the well. Potential economic effects are increased NPV and accelerated cash flow.

The three refracturing Isolation methods that are either close to market, or already on the market, are the expandable liner, the multiset packer with diverters, and the straddle packer methods. Operator economics for refracturing shale oil wells are favorable for the expandable liner and the multiset packer with diverters (and the similar straddle packer method).

Operator economics for refracturing shale gas wells are not favorable for any refracturing method, primarily due to low gas prices. In the international market where the gas prices are attractive, we expect operator economics to become favorable.

The following Baker Hughes (or similar) services are recommended:

- Baker Hughes Coil Tubing Services for cleanouts and TeleCoil™ where applicable.
- The Baker Hughes Shale Value Model can be used to calculate the before tax operator economics for the case.
- Baker Hughes Pressure Pumping Services and Wireline Services to refracture the well.

21.13 ESOR–Enhanced Shale Oil Recovery

Despite extensive research and development of unconventional resources over the last few years, ultimate recoveries from shale oil reservoirs are barely 5 to 10% of the original oil-in-place under natural depletion (Hoffman 2012, Xu and Hoffman 2013, Wan et al. 2013a and 2013b, Gamadi et al. 2013, Zanganeh et al. 2014). With these low recovery rates, a significant volume of oil will remain in the formation, substantially reducing the overall economic value of the project. On the other hand, a review of production data from shale oil plays reveals a continuous declining trend in production levels. For instance, consider the Eagle Ford shale play in south Texas, which has an estimated 7 to10 billion bbls oil in place. The total legacy oil production in this play is declining at a rate close to 114,000 bpd as of July 2014 (**Fig. 21.6**) (EIA 2014). If the declining trend continues with no actions or technological innovations to optimize production, a significant number of these wells may have to be shut down due to economic limitations, as infill-drilling operations will not compensate for the aggregate production decline rates. Refracturing, as discussed early in the chapter, can rejuvenate the declining production; however, this still does not address the small recovery factor of these wells. Therefore, plans to avoid these consequences are strongly advised in the development phase of shale oil plays. A growing body of research examines the potential application of injecting CO_2 as an EOR agent in liquid-rich shale formations to evaluate changes in recovery rates. In this section, we look at literature and a case study that is presented at the end of this chapter.

The refracturing technique (discussed earlier) and the ESOR method (discussed here) both provide a common platform for rejuvenating shale assets, even though they are principally and operationally different. They can both be applied to arrest production decline in oil wells and maximize oil recovery in a given play, while ESOR has the potential to additionally increase the recovery factor by sweeping the bypassed oil. Refracturing practices are designed to improve reservoir response to an initial fracture treatment. Under such a scenario, reservoir performance can soon (within a few months) be judged and reflected in the production response. The goal of EOR CO_2 injection, however, is to provide additional pressure support into the matrix to swell the residing remaining oil and achieve higher ultimate incremental recovery in the long-term (a few years) via enhanced sweep efficiency. For both these techniques to work, success depends on knowing the formation characteristics, complexity of the fracture network, and operational constraints present in each given well.

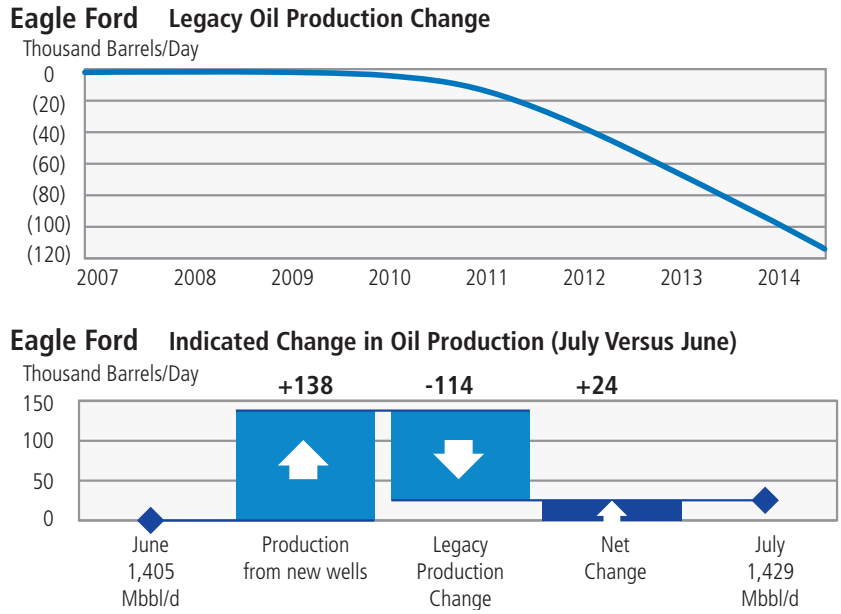

Fig. 21.6—Eagle Ford legacy and oil production change. (From EIA 2014.)

Despite the nanodarcy permeability of shale plays, thermodynamic (displacement and mobilization of hydrocarbon) and kinetic (speed of recovery, breakthrough time) features associated with a miscible EOR injection process could facilitate the transport of a higher volume of oil from a tight matrix to the natural and induced fracture-wellbore system and achieve increased recovery rates from the wells. Shoaib and Hoffman (2009) evaluated the potential benefits of miscible CO_2 injection in the Elm Coulee field under different scenarios (varying the injection rate, the location of each injection well, and the degree of heterogeneity). A solvent model was built to evaluate the benefits gained by injecting CO_2 into the reservoir. The modeled reservoir area, only a sector of the Elm Coulee field, is a 2 mile by 2 mile area divided into 53 grid blocks 200 ft. long in the X and Y directions, and 8 grid blocks 3 ft. thick in the Z direction. The reservoir depth is 7,500 ft. and the model assumes a homogenous porosity of 7.5%. A constant horizontal permeability of 0.01 md (note the scale of the permeability) was used in the model. A minimum miscibility pressure of 3,100 psi was used in the solvent model. Oil displacement is mainly due to miscible injection by CO_2, as the reservoir pressure does not fall below the bubble point pressure. The recovery factor ranged between 19 and 21% for the various scenarios. Comparison of the results shows that continuous gas injection is more suitable for increasing oil recovery than cyclic injection.

Wang and others (2010) numerically investigated the potential of a number of EOR methods, including pure CO_2 injection and enriched CO_2 injection (with CH_4 or N_2) in the Middle Bakken formation of the Williston Basin. They concluded that continuous CO_2 injection gives better recovery and cumulative production than cyclic injection. Though heterogeneity of the formation is important, the results in this study indicate that changes in the porosity and permeability of the formation layers do not substantially impact recovery and cumulative production. In another numerical CO_2 "huff and puff" study performed by Mohanty and others (2013), simulation results from CO_2 injection into the Bakken formation showed that heterogeneity introduced into the formation could result in significant differences in oil recovery. It was concluded that deep transport of CO_2 into the formation closely depends on the heterogeneous structure of the formation and its extent around the wellbore. Mohanty and others (2013) also considered running cases with different shut-in times and concluded that a shorter waiting duration (soak time) resulted in a higher oil recovery, due to a higher number of CO_2 cycles in a period of time. However, a shorter shut-in time resulted in a higher consumption of CO_2 per barrels of oil produced. The longer waiting duration allowed the injected CO_2 slug more time to mix better with the oil, reducing its density. It is also worth noting that Wang and others' (2010) results indicated that mixing the injection solvent with hydrocarbon or nitrogen significantly reduced the required amount of

CO_2 without significantly affecting the desirable increase in production and recovery.

Dong and Hoffman (2013) showed that continuous CO_2 injections can double the recovery rate from 15% of primary production to 30% in the Sanish field, North Dakota.

Wan and others (2013a) conducted a numerical cyclic gas injection study on the Eagle Ford fractured shale oil reservoir, using a single horizontal well with 10 stages of transverse hydraulic fractures to evaluate the EOR response. Their model assumed homogeneous and isotropic properties from published data for the Eagle Ford shale (Bazan et al. 2010), and consisted of two wells in the boundary of a grid model of 200 ft. (x) × 1000 ft. (y) × 200 ft. (z). The initial reservoir pressure for the field was set at 6,425 psi. The permeability and porosity for this shale reservoir were defined as 100 nd and 6%, respectively. Their results showed an increase in recovery factor from 6.62% to about 25% when 30 cycles of 1000-day CO_2 were injected. Later that year, Wan and others (2013b) updated their previous numerical model (Wan et al. 2013a) to account for the presence of natural fractures. Their updated model, which included planar hydraulic fractures, considered orthogonal natural fractures with a fracture network size of 2,000 × 1,000 ft. and a uniform conductivity of 4 md per ft. in the natural fractures inside SRV. It investigated several factors, including the impact of fracture network spacing (for both created and natural fractures), fracture network conductivity, stress-dependent fracture conductivity, and matrix fracture transfer shape factor on the performance of EOR. They concluded that fracture network spacing is the predominating factor and plays a more important role than fracture network conductivity in enhancing oil recovery. It should be noted that their work did not consider the effect of complex natural fracture systems and only considered orthogonal natural fractures with identical properties such as geometric shape, spacing, aperture, and conductivity. In reality, it is obvious that these parameters are much more random, as the result of tectonic events and the in-situ stress state of the reservoir.

For a fracture spacing of 200 ft., their simulation reports a 45% of recovery factor for 40 years of injection. Based on these published outputs, it can be seen that a properly designed injection pattern with an optimum EOR scheme could increase oil recovery significantly.

Defining and executing an EOR project involves high financial risks and uncertainties in field development planning, careful analysis and laboratory tests are required before embarking on field implementations. Teklu and others (2013) used two reservoir compositions (synthetic oil and Bakken oil) and conducted a study to determine MMP (minimum miscibility pressure) with CO_2 and a mixture of CO_2 and CH_4 in unconventional reservoirs. They utilized a multiple mixing cell algorithm (MMC) (Ahmadi and Johns 2008), and corrected the existing correlations used for conventional reservoirs by applying a sensitivity analysis on important parameters such as the effect of capillary pressure and critical properties, determining the shift values from thermodynamic equilibrium and capillary pressure. The results indicated that MMP could be reduced by up to 600 psi for pore diameters less than 3 nm because of capillary property shift. Their results did not show any significant impact on MMP from capillary pressure. The availability of CO_2 and the cost of its transportation to the site is another topic, which is outside the scope of this chapter.

21.14 Case Study

A simulation study completed at the University of Alaska Fairbanks, Department of Petroleum Engineering, was conducted to investigate the effects of EOR CO_2 injection and matrix permeability on the performance of the EOR CO_2 process. The project was funded by the Alaska Department of Natural Resources. Under the proposed pattern in this study, production and injection were performed through a series of completion stages along a single lateral (**Fig. 21.7** and **Fig. 21.8**). This technique may not be simple operationally, but could offer a great benefit in recovery efficiency. In a recent survey conducted by SPE at a shale gas production conference (Zoback 2012), 70%-to-85% of the participants responded positively to a need for a new drilling and completion strategy in shale reservoirs. The focus of the proposed scheme is to increase sweep efficiency and oil recovery by defining optimum

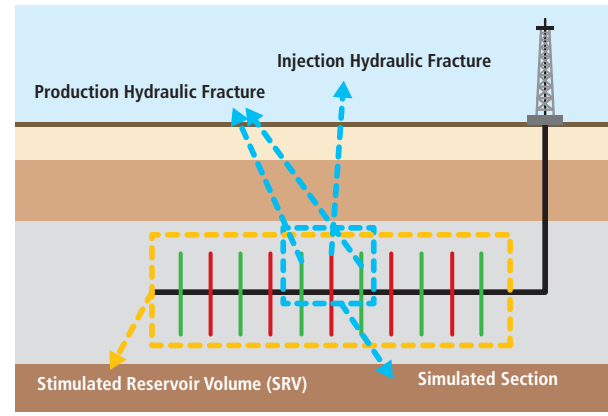

Fig. 21.7—Single lateral completion pattern for EOR scheme. (Modified after Zanganeh et al. 2014.)

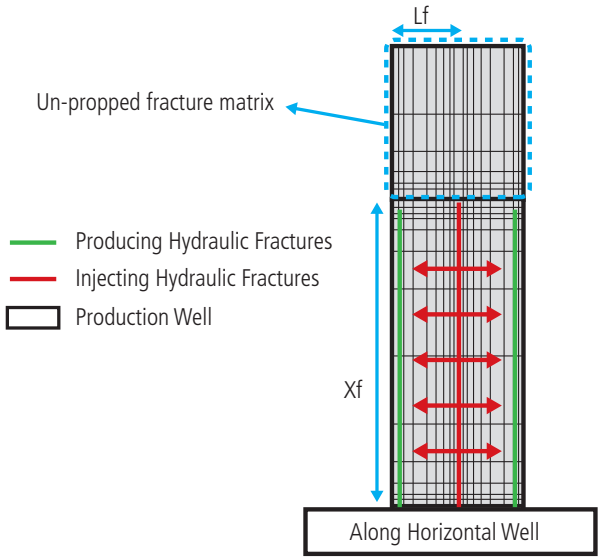

Fig. 21.8—Top view of simulation grid model. (From Kohshour et al. 2014, unpublished.)

hydraulic fracture arrangements and well placements. A 5 × 3 × 11 grid with a total of 16,000 cells (with the properties previously defined) (Zanganeh et al. 2014) (**Table 21.4** and **Table 21.5**) was created and refined to incorporate 3 stages of hydraulic fractures. A simulation model was built in a reservoir simulator (CMG) and considered for potential numerical investigations. In order to take advantage of the thermodynamic properties of CO_2, in this case, the CO_2 was not injected until the reservoir average pressure dropped to the minimum miscibility pressure (MMP) (around year 2023). When the average reservoir pressure dropped to 3,500 psi, which is the estimated MMP, the middle producing hydraulic fracture was converted to act as an injection fracture, injecting CO_2 at a bottomhole injection pressure of 4,000 psi. The results of the simulation for one hundred years are shown in **Fig. 21.9**. Compared to the natural depletion recovery factor of 18.5% for one hundred years, injecting CO_2 has given an oil recovery factor of about 27.5% for fracture spacing of 75 ft. and matrix permeability of 200 nd. Closer fracture spacing increases the pressure gradient and helps displace oil. This can indicate better sweep efficiency. The matrix permeability severely affects the oil recovery outputs during CO_2 injection. The results indicate a recovery factor of about 43.5% when matrix permeability was increased to 500 nd. As matrix permeability decreases, the effectiveness of CO_2 injection also decreases, but its associated recovery remains higher than primary depletion recovery.

Table 21.4—Parameters used in the simulation model. Referenced values have been used from Zanganeh et al. (2014), Orangi et al. (2011), Chaudhary (2011), Honarpour et al. (2012).

Parameter	Value
Matrix porosity (Φ)	0.06
Matrix permeability ($K_{i,j,k}$), nd	200 (base case)
Formation thickness, ft.	200
Depth to top formation, ft.	9,000
Initial reservoir pressure, psia	6,490
Reservoir rock compressibility	5 x 10^{-6} (base case)
Minimum bottomhole flowing pressure, psia	1,000 (base case)
Maximum surface liquid rate, STB	550
Fracture spacing, ft.	75 (base case)
Shut-in time after fracturing treatment, hours	24
Shut-in time after fracturing treatment, hours	24

Table 21.5—Other rock and fluid parameters used in the simulation model. Referenced values have been used by Chaudhary 2011.

Parameter	Value
Reservoir temperature, °F	250
Bubble point pressure for oil, psia	2,398
Solution gas oil ratio*, SCF per STB	1,000
° API for oil	42
Under-saturated oil compressibility, psi-1	1 x 10^{-5}
Gas specific gravity	0.8

The only case where primary depletion recovery outperformed CO_2 EOR is when matrix permeability was the lowest (50 nd) and fracture spacing was the highest (100 ft.). It is clear that in this case, converting the middle hydraulic fracture to a CO_2 injector had negative effects on production and reduced the recovery by a factor of 2.33 (Fig. 21.9).

21.15 EOR Concluding Remarks

Innovative techniques in completion and production schemes are needed to increase the operational efficiency and recovery factor in unconventional shale wells.

Numerous studies suggest the value that could be achieved by utilizing the concept of EOR into shale formations.

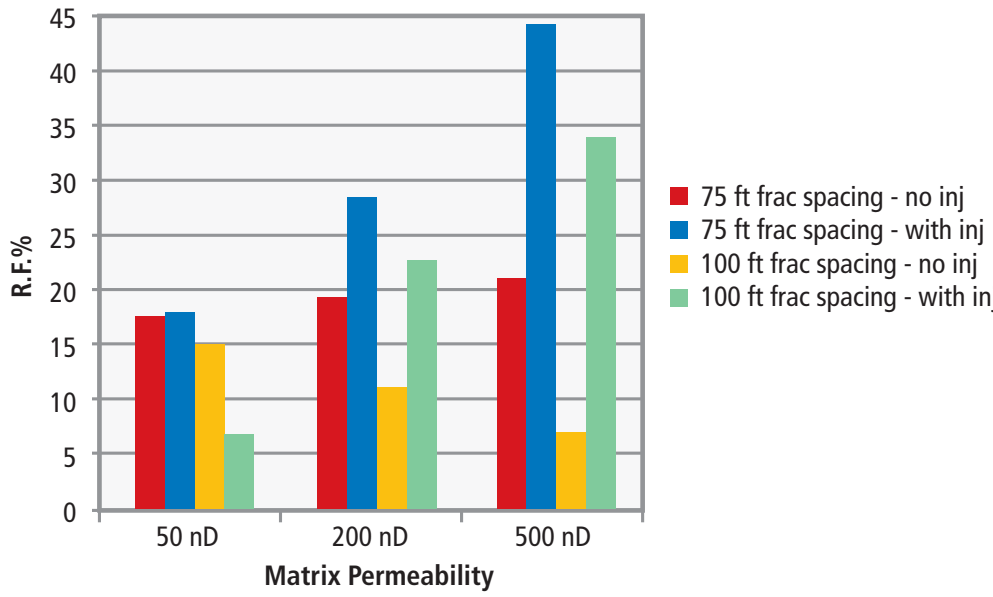

Fig. 21.9—Comparison of oil recovery factor for primary deletion (no injection) and EOR continuous CO_2 injection for different fracture spacing and matrix permeabilities. (From Kohshour et al. 2014, unpublished.)

However, there are a significant number of questions about how the mechanism would work in nanodarcy (nd) formations. Since defining an EOR project involves high financial risks and uncertainties in field development planning, careful analysis and laboratory tests are required before embarking on field implementations including the initial pilot projects. Our understanding of the dynamic effects of the process such as pressure diffusion, and flow mechanics must be further advanced.

More extensive work must be performed to improve our analytical and numerical models suitable for complex fractured horizontal wells, including non-traditional physical and thermodynamic behavior (such as Fick diffusion, the Klinkenberg effect, desorption, shale and water interactions, confinement effects in the PVT, etc.). We need to support ongoing research efforts done by universities and service providers to evaluate the feasibility of these techniques and to accommodate the required level of detail and complexity in reservoir models. For realistic compositional reservoir simulation studies, specific laboratory data such as core flooding performance, MMP measurements, and PVT modeling are essential to set up accurate models and evaluate the long-term benefits of these resources. It is critical to start thinking about these methods now. It took us years to understand EOR in conventional reservoirs and implement it successfully. Small improvements in the recovery of unconventional resources could yield millions of barrels of incremental oil, securing long-term productivity of a well and the associated basins.

As much of the research is yet in the evaluation phase, it is difficult to know which physical effects are relevant and important to design and production. The question is, assuming availability of injection fluid, is CO_2 EOR economically viable? How can we overcome the conformance in the context of existing completion configurations? What will be the optimum development pattern? Data will give us more insights. The ultra-low permeability nature of shale oil formations causes a very long lifespan of unconventional resources, which makes their economic planning highly dependent on finding innovative ways to minimize costs and produce more oil in a given timeframe.

21.16 References

Ahmadi, K. and Johns, R.T. 2008. Multiple Mixing-Cell Method for MMP Calculations. Paper SPE 116823 presented at the SPE Annual Technical Conference and Exhibition. Denver, Colorado. September 21–24. http://dx.doi.org/10.2118/116823-MS.

Allison, D.B., Curry, S.S., and Todd, B.L. 2011. Restimulation of Wells Using Biodegradable Particulates as Temporary Diverting Agents. Paper SPE 149221 presented at the Canadian Unconventional Resources Conference. Calgary, Alberta, Canada. 15–17 November. http://dx.doi.org/10.2118/149221-MS.

Bazan, L.W., Larkin, S.D., Lattibeaudiere, M.G., et al. 2010. Improving Production in the Eagle Ford Shale with Fracture Modeling, Increased Conductivity and Optimized Stage and Cluster Spacing Along the Horizontal Wellbore. Paper SPE 138425 presented at the SPE Tight Gas Completions Conference. San Antonio, Texas. 2–3 November. http://dx.doi.org/10.2118/138425-MS.

Besler, M.R., Steele, J.W., Egan, T., and et al. 2007. Improving Well Productivity and Profitability in the Bakken–A Summary of Our Experiences Drilling, Stimulating, and Operating Horizontal Wells. Paper SPE 110679 presented at the SPE Annual Technical Conference and Exhibition. Anaheim, California. 11–14 November. http://dx.doi.org/10.2118/110679-MS.

Chaudhary, A.S. 2011. Shale Oil Production Performance from a Stimulated Reservoir Volume. MS thesis, Texas A&M University, College Station, Texas. (August 2011).

Cipolla, C.L. 2006. Truth about Hydraulic Fracturing–It's More Complicated Than We Would Like to Admit. Paper SPE 108817 based on a speech presented as a Distinguished Lecture during the 2005–2006 season.

Craig, M.S., Wendte, S.S., and Buchwalter. J.L. 2012. Barnett Shale Horizontal Restimulations: A Case Study of 13 Wells. Paper SPE 154669 presented at the SPE Americas Unconventional Resources Conference. Pittsburgh, Pennsylvania. 5–7 June. http://dx.doi.org/10.2118/154669-MS.

Dong, C. and Hoffman, B.T. 2012. Modeling Gas Injection into Shale Oil Reservoirs in the Sanish Field, North Dakota. SPE paper 168827 presented at the Unconventional Resource Technology Conference. 12–14 August. Denver, Colorado. http://dx.doi.org/10.2118/168827-MS.

EIA. US Energy Information Agency, Eagle Ford Drilling Productivity Report, http://www.eia.gov/petroleum/drilling/pdf/eagleford.pdf (accessed July 2014).

Fanguy, D.J. 2009, Multizone Completion System Enables Primary and Refracture Applications. Abstract SPE 125284 presented at the 2009 SPE Tight Gas Completion Conference, San Antonio, Texas, 15–17 June.

Gamadi, T.D., Sheng, J.J., and Soliman, M.Y. 2013. An Experimental Study of Cyclic Gas Injection to Improve Shale Oil Recover. Paper SPE 166334 presented at the Annual Technical Conference and Exhibition. New Orleans, Louisiana. 30 September–2 October. http://dx.doi.org/10.2118/166334-MS.

Hoffman. B.T. 2012. Comparison of Various Gases for Enhanced Recovery from Shale Oil Reservoirs. Paper SPE 154329 presented at the SPE IOR Symposium. Tulsa, Oklahoma. 14–18 April. http://dx.doi.org/10.2118/154329-MS.

Honarpour, M.M., Nagarajan, N., R., Orangi, A., et al. 2012. Characterization of Critical Fluid, Rock, and Rock-Fluid Properties-Impact on Reservoir Performance of Liquid-Rich Shales. Paper SPE 158042 presented at SPE Annual Technical Conference and Exhibition, San Antonio, Texas. http://dx.doi.org/10.2118/158042-MS.

King, G.E. 2010. Thirty Years of Gas Shale Fracturing: What Have We Learned? Paper SPE 133456 presented at the SPE Annual Technical Conference and Exhibition. Florence, Italy. 19–22 September. http://dx.doi.org/10.2118/133456-MS.

Martin, A.N. and Rylance, M. 2010. Hydraulic Fracturing Makes the Difference: New Life for Old Fields. Paper SPE 127743 presented at the North Africa Technical Conference and Exhibition. Cairo, Egypt. 14–17 February. http://dx.doi.org/10.2118/127743-MS.

Mohanty, K.K., Chen, C., and Balhoff, M.T. 2013. Effect of Reservoir Heterogeneity on Improved Shale Oil Recovery by CO Huff-n-Puff. Paper SPE 164553 presented at the SPE Unconventional Resources Conference. The Woodlands, Texas. 10–12 April. http://dx.doi.org/10.2118/164553-MS.

Moore, L.P. and Ramakrishnan, H. 2006. Restimulation: Candidate Selection Methodologies and Treatment Optimization. Paper SPE 102681 presented at the SPE Annual Technical Conference and Exhibition. San Antonio, Texas. 24–27 September. http://dx.doi.org/10.2118/102681-MS.

Nagel, N.B. and Sanchez-Nagel, M. 2011. Stress Shadowing and Microseismic Events: A Numerical Evaluation. Paper SPE 147363 presented at the SPE Annual Technical Conference and Exhibition. Denver, Colorado. 30 October–2 November. http://dx.doi.org/10.2118/147363-MS.

Oraki Kohshour, I., Ahmadi, A., and Hanks, C. 2014. Enhancing Oil Recovery of Shale Oils by CO2 injection. Funded project by Alaska Department of Natural Resources (DNR), conducted at the University of Alaska Fairbanks, Unpublished.

Orangi, A., Nagarajan, N.R., Honarpour, M.M., et al. 2011. Unconventional Shale Oil and Gas-Condensate Reservoir Production, Impact of Rock, Fluid, and Hydraulic Fractures. Paper SPE 140536 presented at the SPE Hydraulic Fracturing Technology Conference and Exhibition. The Woodlands, Texas. 24–26 January. http://dx.doi.org/10.2118/140536-MS.

Rahim, Z., Al-Anazi, H. Waspada, D., and et al. 2013. Comprehensive Reservoir Assessment and Refracturing Improve Saudi Arabian Gas Well Deliverability. Paper SPE 164453 presented at the SPE Middle East Oil and Gas Show and Conference. Manama, Bahrain. 10–13 March. http://dx.doi.org/10.2118/164453-MS.

Roussel, N.P. and Sharma, M.M. 2011. Selecting Candidate Wells for Refracturing Using Production Data. Paper SPE 146103 presented at the SPE Annual Technical Conference and Exhibition. Denver, Colorado. 30 Ocober–2 November. http://dx.doi.org/10.2118/146103-MS.

Sinha, S. and Ramakrishnan, H. 2011. A Novel Screening Method for Selection of Horizontal Refracturing Candidates in Shale Gas Reservoirs. Paper SPE 144032 presented at the North American Unconventional Gas Conference and Exhibition. The Woodlands, Texas. 14–16 June. http://dx.doi.org/10.2118/144032-MS.

Teklu, T.W., Alharthy, N., Kazemi, H., et al. 2013.Minimum Miscibility Pressure in Conventional and Unconventional Reservoirs. Paper SPE 168825 presented at the Unconventional Resource Technology Conference. Denver, Colorado. 12–14 August. http://dx.doi.org/10.2118/168865-MS.

Vincent, M.C. 2010. Refracs: Why Do They Work, and Why Do They Fail in 100 Published Field Studies. Paper SPE 134330 presented at the SPE Annual Technical Conference and Exhibition. Florence, Italy. 19–22 September. http://dx.doi.org/10.2118/134330-MS.

Vincent, M.C. 2011. Restimulation of Unconventional Reservoirs: When Are Refracs Beneficial?. *J. Cdn. Pet. Tech.* **50** (5): 36–52. SPE 136757. http://dx.doi.org/10.2118/136757-PA.

Wan, T., Sheng, J.J., and Soliman, M.Y. 2013a. Evaluate EOR Potential in Fractured Shale Oil Reservoirs by Cyclic Gas Injection. Paper SPE 168880/URTeC 1611383 presented at the Unconventional Resources Technology Conference. Denver, Colorado. 12–14 August. http://dx.doi.org/10.2118/168880-MS.

Wan, T., Sheng, J., and Soliman, M.Y. 2013b. Evaluation of the EOR Potential in Shale Oil Reservoirs by Cyclic Gas Injection. Paper SPWLA-D-12-00119 presented at the SPWLA 54th Annual Logging Symposium. New Orleans, Louisiana. 22–26 June.

Wang, X., Luo, P., Er, V., and Huang, S. 2010. Assessment of CO2 Flooding Potential for Bakken Formation, Saskatchewan. Paper SPE 137728 presented at the Canadian Unconventional Resources and International Petroleum Conference. Calgary, Canada.19–21 October. http://dx.doi.org/10.2118/137728-MS.

Xu, T. and Hoffman, B.T. 2013. Hydraulic Fracture Orientation for Miscible Gas Injection EOR in Unconventional Oil Reservoirs. Paper SPE 168774 / URTeC 1580226 presented at the Unconventional Resources Technology Conference. Denver, Colorado. 12–14 August. http://dx.doi.org/10.2118/168774-MS.

Zanganeh, B., Ahmadi, M., and Obadareh, A. 2014. Proper Inclusion of Hydraulic Fracture and Unpropped Zone Conductivity and Fracturing Fluid Flowback in Single Shale Oil Well Simulation. Paper SPE 169511 presented at the SPE Western North American and Rocky Mountain Joint Regional Meeting. Denver, Colorado. 17–18 April. http://dx.doi.org/10.2118/169511-MS.

Zoback, M. 2012. Producing Natural Gas from Shale–Opportunities and Challenges of a Major New Energy Source, Shale Gas 101. Stanford University. http://gcep.stanford.edu/pdfs/2wh9Q1Alh3q2zMOQRKD4MQ/MarkZoback_ShaleGas101.pdf (accessed July 2014).

XTO Energy. 2011. Bakken Refracs. NDPC Annual Meeting. 26 September. http://www.ndoil.org/image/cache/Bakken_Refracs.pdf (accessed June 2014).

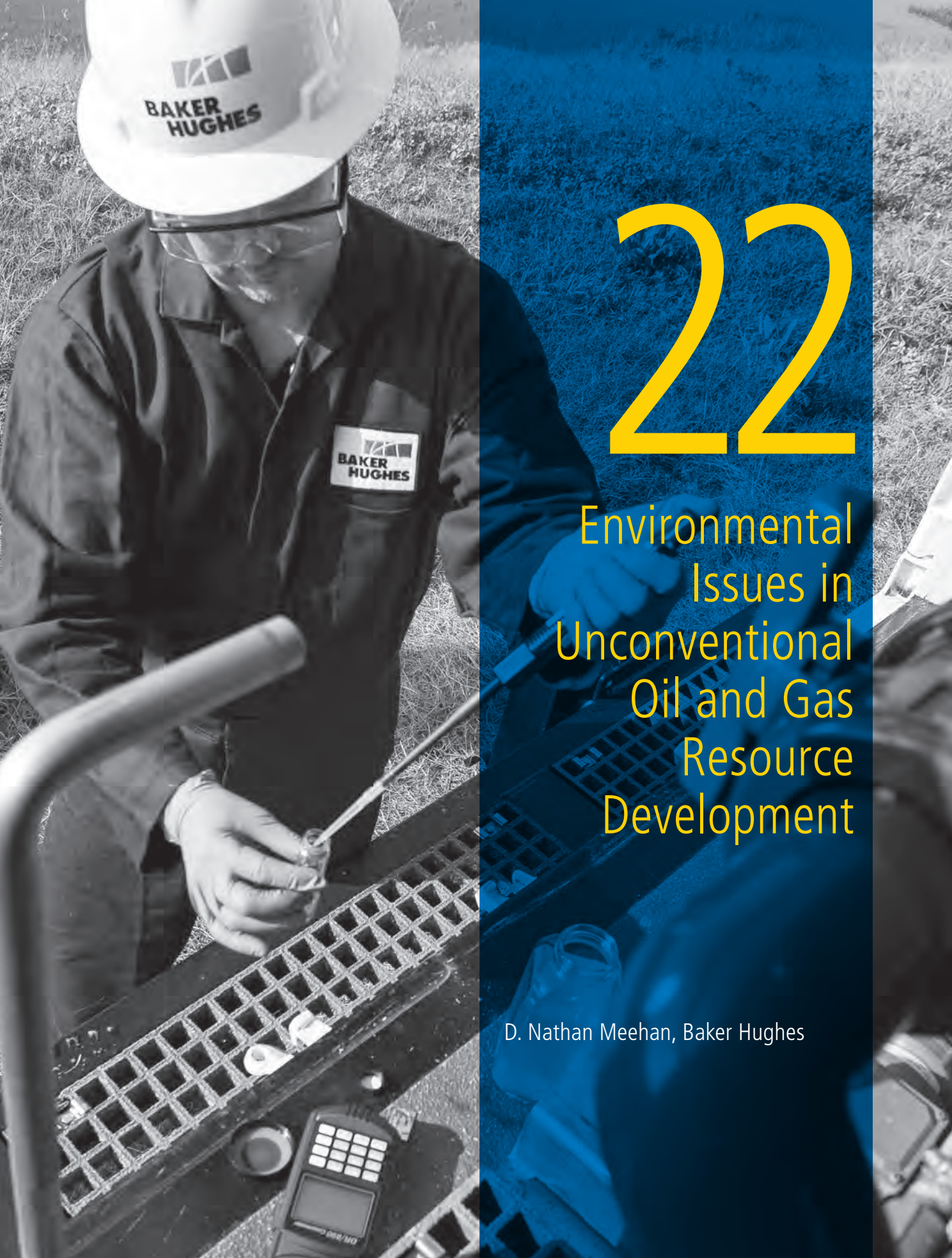

22

Environmental Issues in Unconventional Oil and Gas Resource Development

D. Nathan Meehan, Baker Hughes

This page intentionally left blank

Chapter 22: Environmental Issues in Unconventional Oil and Gas Resource Development

"You don't get your social license by going to a government ministry and making an application or simply paying a fee… It requires far more than money to truly become part of the communities in which you operate."

Pierre Lassonde,
President of Newmont Mining Corporation

22.1 Introduction

The shale revolution in North America has completely changed the visibility of oil and gas operations throughout the world. Shale development is attractive for most countries because it can increase domestic supply (with the potential for exports) and displace the use of coal or liquid hydrocarbons. The liquid hydrocarbons produced in unconventional plays are valued like conventional oil. The economic impact (such as job creation, capital expenditures, and revenues to the state) provides positive benefits. There are potential effects on the environment that are examined in this chapter.

Although hydraulic fracturing is just one aspect of shale exploration, development, and production that has the potential for environmental consequences, hydraulic fracturing (or "fracking" as its detractors refer to it) has become a focal point for activists' protests and government actions. This chapter discusses the social license to operate, the environmental consequences of oil and gas activity (which includes hydraulic fracturing), ways to mitigate environmental damage, and current US federal and state regulatory activities.

22.2 Social License to Operate

The first part of the discussion about environmental issues related to unconventional activities covers a topic that is rarely discussed in technical books: a social license to operate (SLO). However, the target audience for this book includes asset team members operating unconventional activities around the world, to which the topic is unmistakably important. Without a SLO, technical and financial decisions may be irrelevant. Without maintaining the SLO, ongoing production and project profitability are endangered. The primary risks to the social license to operate are environmental impacts from activities, the perception of those impacts, and effective, open communications with a broadly defined community.

Thomson and Boutilier (2011) developed a model of the social license to operate based on studies of mining activities and the surrounding communities. The social license to operate is essentially the perception of a company and its activities based primarily on the affected communities. For shale development activities, this should be expanded to include those who believe that they may be affected whether directly or indirectly and this discussion refers to community in a broad sense. A graphical depiction of their model (**Fig. 22.1**) shows four levels of the social license to operate hierarchy. The lowest (withheld/withdrawn) is currently the de facto status in several US states including New York and many countries (e.g., Germany and France) with significant unconventional resource potential. Much of the opposition to such activity specifically targets hydraulic fracturing. Some of this opposition arises from a 2010 film entitled ***Gasland*** that purports to show environmental damage from oil and gas operations and blames their actions for a host of environmentally damaging activities. The film is controversial and has numerous flaws debated elsewhere. The result of the withheld social license to operate doesn't always mean oil and gas activities are immediately shut down; however, this lowest level of social license to operate generated protests, boycotts, shareholder resentment, and legal actions, along with the potential for violence or sabotage. Another consequence of a very low level of social license is increased regulatory scrutiny, which often results in the removal of the formal license to operate.

The next highest level of social license to operate is acceptance/tolerance. The model shows that moving from withheld to acceptance implies that activities pass the "legitimacy" boundary. Acceptance brings continued examination of activities, involvement of external groups, and the need for improved communication and relationships. Community acceptance should not be confused with approval or support, which is the next level in the social license to operate hierarchy. Approval implies that oil and gas development activities are viewed with some sense of pride and that a level of trust has been developed. Approval is often accompanied by a positive economic effect for the community, but this benefit is insufficient to pass the "credibility" boundary to go from acceptance to approval. At the approval stage, the community implies that communications are truthful and effective, and that they comply with acceptable practices and long-term engagement.

The highest level of social license to operate is psychological identification and implies the trust of the community. At this level, the community has gone beyond cooperating and is identifying positively with the operating company and its activities. There is both technical and social credibility, which implies a very high quality of relationship. There are oil and gas communities who are at the acceptance and approval levels of social license to operate and some areas of psychological identification.

Gaining and maintaining high social license to operate levels doesn't happen because of a series of transactions, but rather as a result of the long-term performance and quality of relationships. It is unlikely that the most ardent opponents of oil and gas activities will ever be convinced of the legitimacy of oil and gas activities. However, effective communications, community involvement, and safe, environmentally sound activities will convince most communities of the legitimacy and credibility of activities. In the following discussions of environmental risks, challenges to the social license to operate will be reviewed.

22.3 Environmental Issues in Unconventional Activities

The potential environmental impacts from unconventional activities include those from well construction activities and those from production activities. Potential issues include:

- Release of greenhouse gases into the atmosphere, particularly vented methane.
- Pollution of surface water associated with disposal of produced water or from spills.
- Air and noise pollution associated with transportation to and from the wellsite.
- Road damage and accidents associated with transportation to and from the wellsite.
- Damage (visual, erosion, loss of habitat, loss of vegetation) associated with the well pads and related production and transportation activities.
- Potentially greater footprint than conventional hydrocarbon extraction activities.
- Surface spills of produced liquid hydrocarbons, hydraulic fracturing treating fluids, drilling mud, or other materials in well construction, corrosion chemicals, or byproducts from other production activities.
- Hydrocarbon migration behind the pipe from either the productive zone, or another hydrocarbon bearing zone, to a usable water zone (either potable or useful for agriculture). This is a potentially hazardous behind-pipe migration event.
- Migration of any fluids from one zone to another. This is a broader category, which includes potentially innocuous events.
- Subsurface seismic (microseismic) events.
- Use of large amounts of water in the hydraulic fracturing process.
- Naturally occurring radioactive materials (NORMs) brought to the surface in production activities or in recovered downhole equipment.
- Disruption of communities.

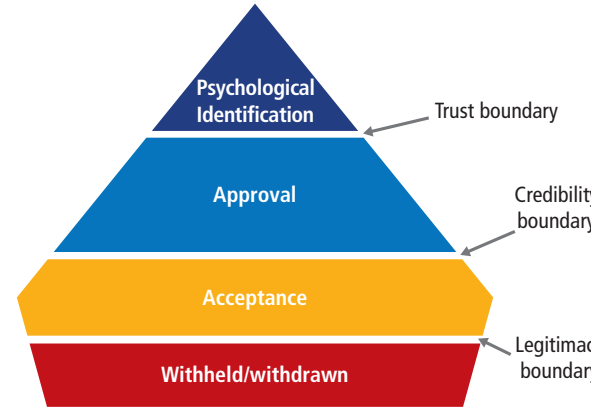

Fig. 22.1—Pyramid model of the Social License to Operate (Thomson and Boutilier 2011).

Some of these concerns are either minor or substantially not present. All of the concerns can be mitigated or eliminated through the application of best practices in the industry. While this chapter doesn't address the issues that are primarily the same as with conventional oil and gas production, those unique to unconventional activities will be addressed. Some major differences between most conventional hydrocarbon extraction activities and unconventional resources are the total area affected, the magnitude of hydraulic fracturing operations, and the total number of wells involved. Unconventional resources typically cover very large areas and are developed with horizontal wells containing from 20 to more than 50 stages. A typical tight gas sand play might only have a few stages; therefore, the total volumes of injected materials are usually smaller than in unconventional treatments. This requires the transportation of significantly greater volumes of sand (or other proppant) to the location and requires significant volumes of water.

22.3.1 Greenhouse Gas Issues

Few environmental issues have gathered more attention in the last few decades than the effects of greenhouse gases on global climate. It is undisputed that CO_2 emissions associated with human activities have increased steadily over a long period. There remains some debate on precisely how much these emissions (along with other greenhouses gases) have—or will—impact the climate. This discussion is outside the scope of this book. There remains a larger debate about precisely what should be done to mitigate the impact of such greenhouse gases.

The United States was not a signatory to the Kyoto Protocol, which sets goals for the reduction of greenhouse gases. However, even without participation in the Kyoto Protocol, total CO_2 emissions in the US have decreased substantially. Increased natural gas production has played a significant role in these reductions, primarily by displacing coal-fired power plants, and this shows a typical annual change where increased natural gas has displaced coal use (**Fig. 22.2**). There is also a slight increase in wind turbine generation that fails to offset the decrease in hydroelectric power.

North American CO_2 emissions continue to drop while the rest of the world, in aggregate, continues to increase CO_2 significantly (**Fig. 22.3**). China is the biggest source of increased CO_2 emissions. Global CO_2 emissions increased by 2845 million metric tons from 2007 to 2011; China's growth in CO_2 emissions represented 84% of this growth.

China continues to expand the use of coal; however, coal usage is on the rise in many other places, particularly in Europe. Germany continues to shut down old, coal-fired power plants and open or expand more modern ones. This trend will accelerate as they shut down nuclear plants and because they have restricted hydraulic fracturing for conventional, as well as unconventional, activity.

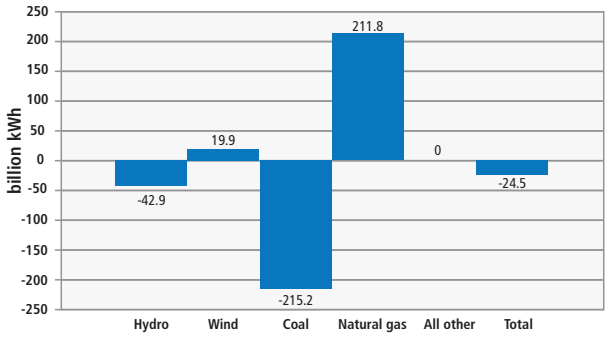

Fig. 22.2—Changes in US fuel sources for electrical power generation. (Source: Energy Information Administration 2013.)

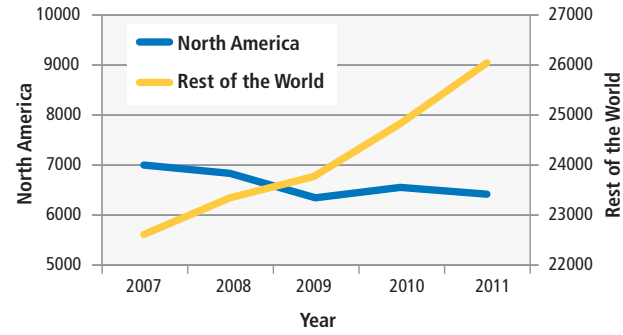

Fig. 22.3—Total carbon dioxide emissions from energy consumption, million metric tons. (Source: Energy Information Administration Statistics.)

There is little doubt that unconventional activity has had a large net positive impact on greenhouse gas emissions in the US. Greenhouse gas emissions from the well construction and production processes are comparable to those of conventional oil and gas production and smaller than that of LNG. The use of shale gas produces less than half of the greenhouse gases of typical coals for electric power generation. For all uses of natural gas, the well construction and production processes generate a tiny fraction of the CO_2 emitted when the fuel is consumed.

Fugitive emissions and venting of methane has a more serious potential impact, because methane is believed to have a larger impact on climate change than comparable volumes of CO_2. Methane venting in conjunction with oil production should be minimized with a goal to make venting of methane as low as reasonably practicable (ALARP). Reduced emission completions should become a standard practice. However, EPA estimates of methane emissions have been dramatically lowered from prior estimates. In spite of dramatic increases in oil and natural gas production and oil drilling, methane emissions have in fact dropped substantially as shown in **Fig. 22.4**.

22.3.2 Air and Surface Effects

Industry best practices include minimizing the total surface footprint by drilling multiple wells from single pads, reusing produced fluids, operating wells to minimize community impact, and eliminating unnecessary wells and well fracturing stages. The use of dual fuel (natural gas and diesel) pumps during hydraulic fracturing (such as the Baker Hughes Rhino™ Bifuel pumps) can reduce diesel usage up to 70%. This carries a corresponding reduction in nitrogen oxides, particulates, and carbon monoxide. Such pumps also reduce flaring of low-pressure methane by using nonsalable gas diverted to storage for reuse rather than being vented.

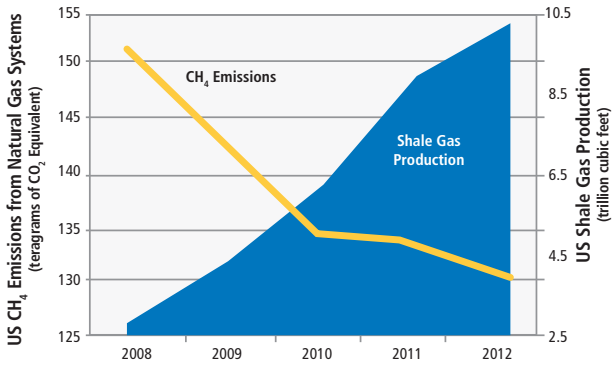

Fig. 22.4—Trends in US CH_4 emission and shale production. (Source: Energy in Depth from data by EIA, EPA.)

The elimination of surface spills is another best practice that can be improved by proper fluid handling practices and effective corrosion treatment. Innovative "green chemistry" permits much more environmentally acceptable corrosion inhibitors that also reduce overall chemical demands. Proper fluid handling practices are also simplified by pad drilling and production.

A Cambridge University study compared an unconventional pad drilling project with wind turbines and solar panels that would deliver comparable amounts of energy over a twenty-year period. In terms of land area and visual intrusion, the unconventional project is the most attractive option (shaded cells in **Table 22.1**). In terms of truck movements, the unconventional project has the smallest impact if water for hydraulic fracturing is piped in; otherwise it could be the largest impact.

Pad drilling results in a significant number of nearly adjacent wellheads. While this generally reduces surface impact and footprint per well, some wells are artificially lifted with sucker rod pumps that have a relatively large and visible surface-pumping unit. As many as a dozen of these wellheads in close proximity is visually unappealing. Technical issues require relatively frequent work to repair or replace downhole sucker rod pumps. The use of electric submergible pumps (ESPs) can reduce the surface impact, accelerate production, and improve lease economics. The Baker Hughes FLEXPump™ series electrical submersible pumps (ESPs) have a very wide operating range, and provide operators with the operational flexibility required in dynamic well conditions to minimize ESP system change outs and nonproductive time, while at the same time reducing operating expenses. These pumps enable the ProductionWave™ production solution that often has lower HSE impact than sucker rod pump alternatives.

Table 22.1—Comparison of impact of unconventional gas development with wind and solar projects. (After Mackay 2014.)

	Shale Gas Pad	Wind Farm	Solar Park
Required Infrastructure	10 wells	87 turbines, 174 MW capacity	1,520,000 panels, 380 MW capacity
Energy delivered over 25 years	9.5 TWh (chemical)	31 (electric)	39 (electric)
Number of tall things	1 drilling rig	87 turbines	None
Height, feet	85	328	8
Land area occupied by hardware, foundations, or access roads, acres	5	89	761
Land area of the whole facility, acres	5	3,583	2,283
Area from which the facility can be seen acres	190	12,850-17,000	2,283
Truck movements	2,900-20,000	7,800	3,800 (or 7,600)

22.3.3 Behind Pipe Migration

Behind pipe migration of fluids (natural gas, oil, or salt water) is most successfully minimized by effective primary cementing of the casing. Proper design of cementing jobs is a conventional practice and can be improved by such techniques as Baker Hughes SealBond™ cement spacer system to mitigate lost-circulation issues. Beyond proper design and execution, assessment of the cement bonding can be made with the Baker Hughes Acoustic Cement Bond Log. This tool provides a valuable source of data pertaining to the effectiveness of the cement sheath surrounding the casing. This data is obtained by evaluating the effect of the casing, the cement sheath, and the formation on the acoustic wave emanating from an acoustic cement bond log instrument. The amplitude curve of the reflected acoustic wave is at its maximum in an unsupported casing and minimum in those sections in which the cement is well bonded to the casing and the formation. In addition, production logging tools and/or distributed temperature surveys allow the operator to monitor the efficacy of the well over the lifetime of the well.

22.3.4 Seismic Activity

Some people have pointed to seismic activity near oil and gas developments in an effort to raise an alarm about increased earthquakes with the potential for surface damage as a result of unconventional activity. This is a complex topic that is often oversimplified by industry detractors and proponents. The term "earthquake" is used both to describe the sudden slip of a fault and the resulting ground shaking and results of radiated seismic energy. Most fault slippage results in surface energy below detection levels; however, large events range from noticeable vibrations to major property damage and/or fatalities.

Current earthquake frequency (ranked by intensity) has changed very little over time, even with the industry's increased reliance on hydraulic fracturing production methods over the last decade (**Fig. 22.5** and **Fig. 22.6**). However, there have been a number of individual seismic events that may have been related to oil and gas production activity. Most scientific enquiries have indicated that long-term wastewater injection (rather than hydraulic fracturing) is a potential contributor to earthquake activity, and that increases are primarily in the very small earthquakes that are generally not felt at the surface. However, larger tremors have been linked to wastewater injection and a few to hydraulic fracturing. The volume of water disposed of into injection wells vastly exceeds even the largest unconventional well hydraulic fracture treatment.

In Oklahoma, there are about 10,000 injection wells, of which about 4,400 are used to dispose of "waste" water. Waste water describes both saline brines produced in association with oil and gas production and hydraulic fracture flowback water that is not reinjected. The majority of Oklahoma's injection wells are associated with waterflooding or EOR projects. Typically, these projects are injecting fluids into a formation capable of producing oil at pressures below the initial reservoir pressure. Little evidence of significant induced seismicity is associated with these types of wells. The wastewater injection wells are widely distributed across the state (refer to **Fig. 22.7**) and are correlated with areas of increased seismicity (Walsh III and Zoback 2015). The increases in seismicity follow five- to tenfold increases in the rate of wastewater injection. Wastewater injection is principally into the Arbuckle formation, a saline aquifer overlying brittle basement rock.

Seismic activity is also generated during hydraulic fracturing. Tensile failure of hydraulic fractures generates very little seismic energy. However, shear events near the created hydraulic

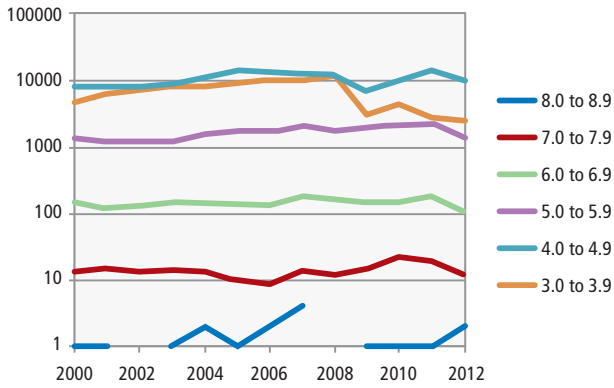

Fig. 22.5—Number of earthquakes worldwide from 2000 to 2012. (Source: USGS.)

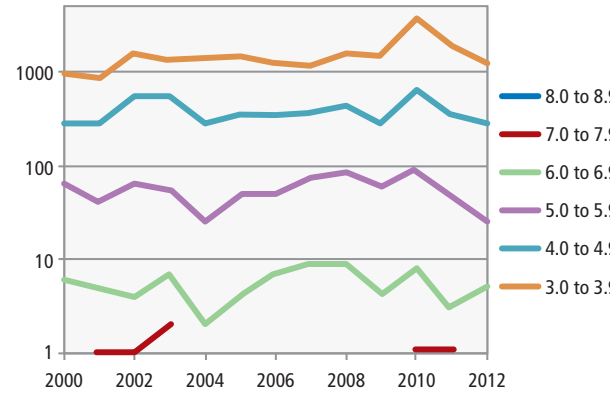

Fig. 22.6—Number of earthquakes in the US from 2000 to 2012. Scales are in Richter magnitude. (Source: USGS.)

fracture can be measured. VSFusion™ (a joint venture of Baker Hughes Inc. and CGG, Inc., a geotechnical engineering firm) measures and interprets this microseismicity. The Richter magnitude scale is a mathematical measure of earthquake energy; each integer increase represents a tenfold increase in energy. For example, a 3.0 earthquake would represent only 1% of the energy of a 5.0 earthquake. The vast majority of microseismic events measured range from less than -3.0 to -1.0 on the Richter scale. For example, a -2.0 event would be 1/100,000th of a 3.0 earthquake. At these levels, these events pose no danger to life or property. Most efforts to even detect them from the surface are challenging.

Injection wells should be sited at locations designed to minimize the risk of damage from earthquakes. Best practices need to be developed and implemented to minimize the potential for damaging induced seismicity. Long-term measurements of microseismic activity near injection wells can be undertaken in populated areas if there is a significant potential for damage from earthquakes. Recycling produced or previously injected water can decrease the likelihood of such damage.

22.3.5 Reducing the Number of Wells to Develop the Resource

The performance of unconventional wells is highly variable. Some operators believe that large statistical variations in the production rates and recoveries from unconventional wells are inevitable and unavoidable. This belief leads to a commitment to "factory drilling" practices, in which hundreds of nearly identical wells are drilled with a focus on reducing well costs. Pad drilling is an important part of this development, because it reduces surface costs and enables reductions in drilling, evaluation, completion, stimulation, and production costs. However, even in commercially

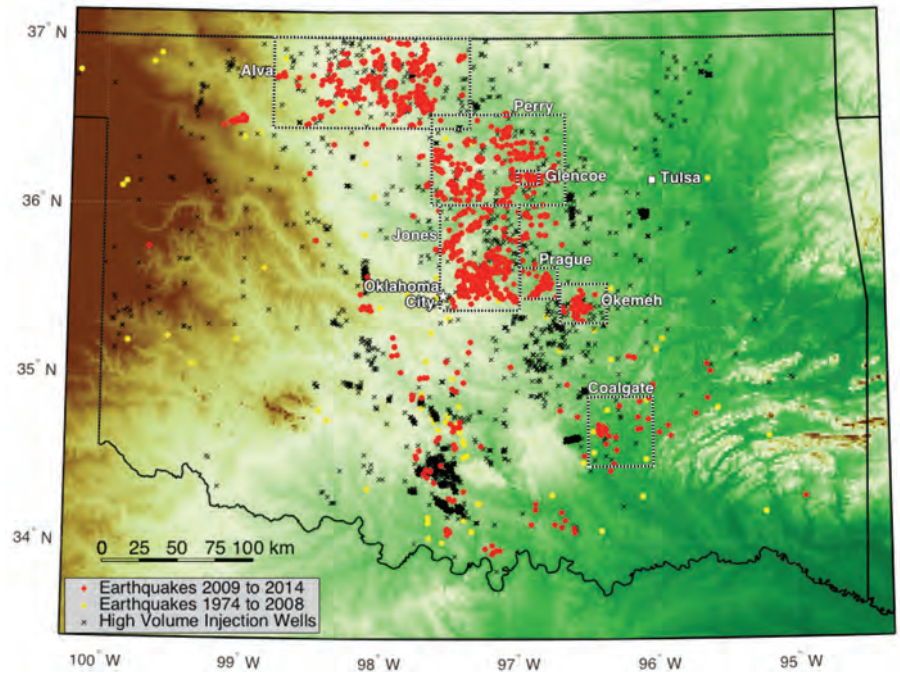

Fig. 22.7—Oklahoma injection wells. (Source: Oklahoma Corporation Commission, 2013.)

attractive unconventional plays, 25% to 40% of all wells drilled are uneconomical. Integrating surface seismic measurements, advanced petrophysics and geomechanics, and reservoir engineering into an integrated model can help operators to identify the most productive areas and eliminate the drilling of sub-economic wells. This can dramatically lower environmental impacts while improving economics.

22.3.6 Regulatory Issues

Investigations, rulemakings, legislative proposals, lawsuits, and an endless array of articles, films, books, and blogs have drawn substantial attention to environmental issues. The public initially struggled to understand the key players in the narrative (especially the technology) and remains skeptical of the energy industry's role and motivations. The federal and state governments have also labored to "read into" their emerging roles as regulator and enforcer while trying to regain public credibility as defenders of science. Now, as the story enters its seventh, eighth, or maybe tenth season, the roles and responsibilities are clearer and the narrative may be smoothing out.

The next section reviews key federal and state developments that may shape the years ahead. Section 22.4.3 focuses on the particular challenge of water management, where operational and technological advances are poised to overcome regulatory constraints and other limitations.

22.4 Outlook on Federal and State Developments

22.4.1 Federal Developments

In this section, we review the developments in the federal outlook, which include developments related to drinking water, diesel use in hydraulic fracturing, proposed regulations for hydraulic fracturing on public land by the US Bureau of Land Management (BLM), the new Clean Water Act, and the Toxic Substances Control Act.

22.4.1.1 EPA Hydraulic Fracturing Study

The Environmental Protection Agency (EPA) continues to work on its study of the relationship between hydraulic fracturing and drinking water resources. EPA's investigation is focused on identifying possible exposure pathways and hazards, as well as assessing the potential risks to drinking water resources from hydraulic fracturing. EPA spent much of 2013 collecting more data to support the study, hosting technical roundtables, meeting with the Science Advisory Board, and extending the time period during which stakeholders could submit to the Agency relevant technical documents and studies. EPA anticipates releasing a preliminary report toward the end of 2014. However, in June 2013, an EPA official indicated that the public would not see a final report until 2016.

While the results of EPA's study remain uncertain, it seems likely that any risk of impact to drinking water would be tied to the typical issues experienced by traditional oil and gas operations. For example, issues such as surface spills, poor cementing, or other well-integrity issues are not related to the migration of hydraulic fracturing fluids from induced fractures through naturally occurring faults into aquifers used for drinking water. To date, several EPA officials have publicly stated that there are no proven cases where the hydraulic fracturing process has resulted in contamination of aquifers or drinking water supplies.

22.4.1.2 EPA Diesel Guidance

In September 2013, it was reported that the White House Office of Management and Budget (OMB) had received EPA's final Underground Injection Control (UIC) Program permitting guidance for diesel use in hydraulic fracturing operations. While industry has repeatedly indicated that diesel is typically no longer used in hydraulic fracturing treatments, some members of Congress have called this into question, citing instances of diesel use reported to FracFocus.org. Based on that information, some in Congress are requesting that OMB expedite its review of the final guidance.

While the broad definition of diesel in this context may theoretically cover more operations, it appears that diesel is now so rarely used that the final guidance will have much less impact than it might have had a decade ago. From a policy perspective, the existence of the diesel guidance indicates EPA's belief that any hydraulic fracturing operations that use diesel should first be permitted under the EPA's UIC Program. While EPA is aware that wells have been hydraulic fractured with diesel since the amendments to the Safe Drinking Water Act by the Energy Policy Act of 2005, the agency has not indicated any plans to undertake retroactive enforcement actions.

22.4.1.3 Bureau of Land Management: Hydraulic Fracturing Rule

In 2013, the BLM reissued a proposed rule applicable to hydraulic fracturing on federal and tribal lands. According to the BLM, its proposed rule would include the minimum standards for drilling on federal land. While the comment period for the BLM's rule officially closed in August 2013, several Congressional hearings held since that time have seen additional comments made by members of Congress and representatives from state governments that question the need for another layer of regulation on top of states' regulations for oil and gas operations. It is not clear when BLM will issue a final rule; however, it is likely that we will see additional Congressional hearings where BLM officials will be questioned about the utility of this rule. In EPA's letter to the National Resources Defense Counsel (NRDC) on 14 January 2014, the agency indicated that it was working with BLM to develop this rule.

22.4.1.4 New Clean Water Act Effluent Limitation Guidelines

EPA has indicated that it will issue a proposed rule to revise the current Clean Water Act wastewater regulations in order to better control discharges from shale gas extraction activities. The federal Clean Water Act authorizes EPA to promulgate water-quality and technology-based effluent limitations. Technology-based effluent limitations are based on currently available technologies for controlling industrial wastewater discharges and are implemented by states that are authorized to administer the Clean Water Act's National Pollutant Discharge Elimination System (NPDES) permit program, or by EPA if a state is not authorized. The effluent guidelines are incorporated into permits issued under the NPDES permit program.

EPA decided to amend the Effluent Limitation Guidelines Program Plan for the Oil and Gas Extraction Point Source Category under Title 40 CFR Part 435, based on the significant increase in unconventional wastewater tied to the rapid expansion of unconventional oil and gas operations. EPA has noted that the treatment technologies employed by private centralized waste treatment facilities (CWTs) that might treat unconventional wastewater "…are not designed to treat high levels of total dissolved solids (TDS), naturally occurring radioactive materials (NORMs), or high levels of metals." EPA has also indicated that the pollutants found in unconventional wastewater are not getting adequate treatment by CWTs and that there are rising concerns of pass-through or interference at the publicly owned treatment works (POTWs) that accept CWT discharges.

22.4.1.5 Toxic Substances Control Act

In response to petitions regarding data reporting of chemical substances and health and safety under the Toxic Substances Control Act (TSCA) of 1976 from several non-governmental organizations (NGOs), the EPA has initiated a rulemaking proceeding under TSCA Sections 8(a) and 8(d). The rulemaking proceeding is in the pre-proposal stage, and the EPA indicates that they will actively engage the public and stakeholders in the design and scope of the reporting requirements. The EPA projects that it will issue an Advance Notice of Proposed Rulemaking under the aforementioned sections in TSCA.

22.4.2 Developments by the States

Over the last five years, states with significant shale resources have reviewed and revised their oil and gas regulatory programs to address the rapid expansion of exploration and production activities. While the primary regulatory updates have focused on the addition of chemical disclosure provisions, several states have also updated rules applicable to waste treatment, setbacks, and well integrity. In 2014 and beyond, states will be tackling some of the more novel issues associated with development of shale gas resources. The following section describes recent trends in state regulatory developments.

22.4.2.1 Air Emissions

In November 2013, the state of Colorado released new rules aimed at reducing methane emissions from oil and gas operations. Colorado's proposal is the first of its kind that would regulate the detection and reduction of methane, which is a potent greenhouse gas. In a regulatory package aimed at fully adopting EPA's recently finalized New Source Performance Standard (NSPS) OOOO, the Colorado Air Pollution Control Division included revisions to Regulation No. 7 that would establish controls and requirements for oil and natural gas operations that exceed the requirements in the NSPS OOOO.

Generally, the proposed revisions to Regulation No. 7 would "…increase control requirements and improve capture efficiency requirements for oil and gas storage tanks; minimize fugitive emissions of hydrocarbons [including but not limited to volatile organic compounds (VOCs) and methane] from leaking components at compressor stations and well production facilities; minimize venting and flaring at new and modified oil and gas wells; and expand control requirements for pneumatic devices" Colorado contemplates that there will be some overlap between the different requirements of NSPS OOOO and Regulation Number 7 but that the requirements "secure different emissions reductions." Industry has estimated that the cost of the new [state] rules could be up to $80 million per year. Moving forward into 2014, we could see additional states enact similar rules—as well as legal challenges—to a state's authority to enact such rules.

22.4.2.2 NORM and Waste Management

In March 2011, EPA sent a letter to the Pennsylvania Department of Environmental Protection (PADEP) expressing concern over reports that wastewater from Marcellus shale operations contained "…variable and sometimes high concentrations of materials that may present a threat to human health and aquatic environment, including radionuclides, organic chemicals, metals and total dissolved solids." EPA announced in the letter that it had specific concerns regarding the concentrations of radionuclides in the effluent from the wastewater treatment plants and that it would be reopen the NPDES permits of POTWs and centralized waste treatment facilities that were then accepting gas drilling wastewater for treatment. Shortly thereafter, on 19 April 2011, PADEP requested that Marcellus shale operators voluntarily cease delivering wastewater to 15 wastewater treatment plants in the state.

Produced water and drill cuttings from Marcellus shale wells may have high levels of NORM. Recent reports and studies have claimed high levels of NORM in public landfills and in streams that receive discharges from wastewater treatment facilities. In January 2013, PADEP announced it would be studying the levels of NORM in materials associated with oil and gas drilling. PADEP's study is expected to be completed in 2014. In November 2013, the Marcellus Shale Coalition and the Pennsylvania Independent Oil and Gas Association announced they would undertake an oil and gas-related NORM study as well.

If NORM levels in oil and gas wastewater reach a certain threshold, the wastewater must be transported and disposed of in accordance with more stringent federal and state laws. The events in Pennsylvania have led most operators in the state to either ship wastewater out of state or to implement an aggressive water treatment and recycling program. Moving forward, expect states to be more actively involved in these issues.

22.4.2.3 Abandoned Well Mapping and Downhole Communication

An interesting well-integrity issue that will be worth following is whether states increase their efforts to track downhole communication between hydraulic fracturing operations and nearby active or abandoned wells. Concerned about whether current hydraulic fracturing operations could cause pollution by altering or affecting an orphaned or abandoned well, Pennsylvania has proposed new regulations that would require operators to identify and monitor orphaned and abandoned wells.

Specifically, operators would be required to locate orphaned and abandoned wells "…within 1,000 feet measured horizontally from the vertical well bore and 1,000 feet

measured from the surface above the entire length of a horizontal well bore." In order to identify the location of these wells, operators would be required to review the state's database of orphaned and abandoned wells, review farm line maps, and submit a questionnaire to nearby landowners. When an abandoned well is identified, the operator would be required to submit a plat to the state showing the location and GPS coordinates of the orphaned or abandoned wells.

Beyond the identification requirement, under proposed Section 78.73, operators would be required to visually monitor the orphaned or abandoned wells during hydraulic fracturing, immediately notify the state of any changes, and take the necessary action to prevent pollution associated with discharges from those wells. Finally, if an operator "alters" an orphaned or abandoned well, that operator must properly plug the altered well. Pennsylvania has estimated the cost for these new requirements at $2,000 per well, which seems low and may not account for the costs of plugging an affected well.

22.4.3 Water: Managing, Sourcing, Treating, and Innovating

22.4.3.1 Water Management and Sourcing

Water management and sourcing presents challenges and opportunities for operators around the US and the globe. Issues with regulations for water use and disposal, water storage, and either finding sources of water or creating ways to use less water, are of utmost importance to any company involved in unconventional development.

22.4.3.1.1 Water Management Challenges

There are many challenges and opportunities for upstream companies operating in the various shale plays across the US. The challenges, some of which are described previously, generally come in the form of legal and regulatory developments that place restrictions on operations. However, these regulatory developments can lead to opportunities as companies seek new ways to push technological advances forward. One area where this dynamic is playing out is life-cycle water management.

On the front end are limitations to availability, transportation, and fresh water storage used in hydraulic fracturing operations. On the back end, companies are seeing additional restrictions on the management of wastewater after hydraulic fracturing, including requirements related to storage, transportation, treatment, and ultimate disposal. These challenges, some of which are unique to unconventional operations, are pushing the industry to develop solutions that save money and reduce impacts on the environment. The remainder of this paper will focus on the dynamic between regulatory drivers and industry-provided solutions in the specific context of water management.

22.4.3.1.2 Water Sourcing Challenges

Water is a crucial part of hydraulic fracturing operations, and water sourcing in particular presents numerous challenges due to plain and simple regional availability, regulatory constraints, and a lack of infrastructure. However, through innovation and a variety of technological advances companies are meeting this challenge head on by introducing new approaches to field development and hydraulic fracturing techniques that require less water.

Water sourcing is increasingly becoming an issue for companies engaged in development of shale resources. Many states now require that an operator provide a detailed water use plan before they issue a drilling permit. Additionally, interstate compact commissions, including the Susquehanna River Basin Commission (SRBC) and the Delaware River Basin Commission (DRBC), require that operators first look to "impaired" waters for their water supply. Water challenges are often unique to the shale play where operations are proposed. In the dryer shale plays, like the Eagle Ford shale of Texas, surface water supplies are limited. Groundwater supplies may be available; however, oil and gas operators increasingly find themselves in competition with industrial and municipal consumers for that water source.

In the Marcellus shale play, precipitation and local geology is such that fresh water is readily available. Water-related restrictions in the Marcellus shale are, therefore, tied to obtaining regulatory approval for withdrawal from a given water source and the proximity of that water source to a proposed well. Even if a surface water body, such as a river or a lake, is available for sourcing fresh water, transportation of that fresh water to a well pad over long distances can be costly.

One traditional solution to local water availability is the construction of man-made fresh water ponds or impoundments in proximity to the well. While fresh water impoundments can reduce transportation costs, there are regulatory hurdles to overcome. Logistically, when constructing a pond for a single well or a centralized impoundment that supplies fresh water for several wells, one thing remains consistent: the best physical location for such an impoundment typically coincides with "jurisdictional" surface water features,

such as streams and wetlands, which introduces additional legal and regulatory hurdles.

Under the federal Clean Water Act, a permit is required before conducting any work in streams or wetlands. The problem: streams don't always look like babbling brooks and wetlands don't always have cattails. This can lead to issues with both federal and state regulators if there are unauthorized impacts to a jurisdictional feature during construction of a fresh water impoundment. Beyond regulatory requirements tied to wetland features, states typically have laws applicable to dam safety. State dam safety laws often require preapproval and permits, and they set restrictions on the height and capacity of man-made impoundments.

Not all man-made freshwater impoundments resemble ponds. Operators are now using large aboveground storage tanks to store fresh water, and in some instances to store flowback water. These large non-traditional oil and gas structures have triggered new regulatory restrictions in states like Colorado, Ohio, and Pennsylvania.

22.4.3.1.3 Water Sourcing Innovation

With increased oil and gas development on the horizon and increased competition for fresh water supplies, operators are exploring new operational practices and technological advances to reduce the need for fresh water in hydraulic fracturing operations.

From an operational standpoint, a technique that is more efficient in terms of water management (and that is becoming more common) is the use of multiwell pads with shared water storage. The concept here is simple: operators can build one well pad with multiple wells and one large fresh water impoundment versus constructing multiple distributed well pads, each with its own impoundment and permitting requirements. The use of multiwell pads has benefits beyond the convenience of a centralized impoundment: it also minimizes surface disturbance and can minimize traffic on local roads.

Depending on the success of certain legislative and regulatory developments, another innovation that could improve water sourcing is the use of non-fresh water sources, such as acid mine drainage, in hydraulic fracturing operations. Acid mine drainage (AMD) is acidic water that is formed when water drains over, or through, sulfur-bearing minerals and is exposed to oxidizing conditions. AMD can be generated in the coal mining process; therefore, states with a long history of coal mining, such as West Virginia and Pennsylvania, have widespread AMD problems. AMD is a major cause of stream degradation in Pennsylvania and has been described as one of the most significant environmental problems associated with the mining industry in the US.

The need for water in hydraulic fracturing operations and the widespread environmental problems caused by AMD have presented what some may argue is a win-win situation. Specifically, if AMD is causing widespread pollution in states with significant shale resources, an ideal situation would be for operators to take that degraded AMD water, treat it, and then use it in hydraulic fracturing operations. This would directly minimize a significant source of fresh water pollution from mining, and, at the same time, reduce the need for fresh water sources for use in hydraulic fracturing operations.

In 2011, a Pennsylvania state commission, the Marcellus Advisory Commission, issued a report recommending that Pennsylvania "…encourage the use of non-freshwater sources where technically feasible and environmentally beneficial… [and] provide operators with immunity from environmental liability for the use of acid mine drainage water from abandoned mine pools would encourage operators to reduce their use of freshwater sources for water utilization, as well as reduce the amount of acid mine water draining into local streams."

In November 2011, Pennsylvania State Senator Richard A. Kasunic (R–32nd District), introduced Senate Bill (SB) 1346, which was intended to amend Pennsylvania's Title 27 (Environment Good Samaritan Act | Environmental Resources) of the Pennsylvania Consolidated Statutes, providing for use of mine drainage water. This act was intended to limit the liability of entities choosing to utilize acid mine water for hydraulic fracturing of oil or gas wells. The 2 October 2012, Pennsylvania publication Senate Appropriations Committee Fiscal Note provided the following summary of the bill:

> *The bill provides that a landowner or mine operator who allows for the withdrawal of acid mine water, or a natural gas operator who withdraws the water, to hydraulically fracture a well, to not be deemed to assume legal responsibility or to incur liability with respect to cost, injury, or damage that arise from the use of the acid mine water, including any injury or damage suffered by a downstream riparian landowner.*

SB 411, the next iteration of Pennsylvania's AMD bill, passed a crucial appropriations vote in January 2014. The bill appears to have the momentum to carry it through the state

legislature. A similar bill has been introduced in the West Virginia Senate.

22.4.3.2 Water Treatment

Unconventional oil and gas operations that involve hydraulic fracturing use larger quantities of water than conventional operations. Water treatment and disposal with unconventional development creates challenges that range far beyond 20th century conventional oil and gas drilling and production. The industry has been pushed to find new solutions to new problems, which has encouraged innovation in methods and solutions.

22.4.3.2.1 Wastewater Treatment Challenges

Unconventional oil and gas operations that involve hydraulic fracturing use larger quantities of water than conventional operations. Historically, oil and gas wastewater would be disposed of via a Class II Underground Injection Control (UIC) well, disposal at a local wastewater treatment facility, and in some instances, road spreading. The quantity of fresh water used in unconventional wells means that operators are also likely to see more flowback than in a conventional well. Additionally, the wastewater that flows back, or is produced, often has some unique characteristics that pose certain challenges to operators. The quantity and quality of the unconventional oil and gas wastewater stream present unique disposal challenges.

Disposal via Class II UIC wells is limited by the availability of the appropriate geology and the time needed to obtain the necessary permit from the state or the regional EPA office, which is the case in Pennsylvania. Costs associated with waste injection are also on the rise, with a 2010 estimate of $0.05 per barrel up to $0.20 per barrel for "out of region" waste.

Induced seismicity is another complication that is gaining attention over the past few years. What started as allegations in Youngstown, Ohio, was confirmed by the state regulators and resulted in the first state regulations applicable to oil and gas disposal wells in relation to induced seismicity. Since that time, there have been increasing reports of induced seismicity linked to disposal of unconventional wastewater in Class II UIC wells. The US Geological Survey (USGS) is currently working with EPA and the Department of Energy to better understand induced seismicity and even map occurrences.

Disposal of unconventional wastewater via traditional means can also be difficult because of its unique chemical make-up. Until recently, oil and gas wastewater could be disposed of at local publicly owned treatment works (POTWs). Another option is privately owned centralized waste treatment (CWT) facilities, which often treat oil and gas wastewater, and then ship it for discharge via a POTW.

As noted previously, wastewater from shale gas wells can be high in NORM, and may exhibit high concentrations of total dissolved solids (salts), organic chemicals, inorganic chemicals, and metals. As mentioned previously, EPA and Pennsylvania coordinated in 2011 to stop POTWs from accepting for treatment wastewater from unconventional wells in the Marcellus shale play. As of early 2014, POTWs in the state of Pennsylvania are still not accepting unconventional wastewater. Some have speculated that disposal of unconventional wastewater at POTWs could be barred nationwide in the future. This has led many operators in the state to start recycling. Additionally, PADEP is currently undertaking a study of oil and gas NORM in Marcellus shale oil and gas wastes.

As referenced previously in this section, EPA has indicated that it intends to provide additional controls on pollutant discharges from the unconventional oil and gas extraction industry, by issuing new standards under the Clean Water Act for oil and gas wastewater discharges from POTWs. EPA continues to collect and analyze data in that effort and confirmed that this was a priority for the agency in its January 2014 letter to NRDC.

22.4.3.2.2 Water Treatment Innovations

As with water sourcing, the industry has shown innovative creativity in the face of regulatory, environmental, and cost challenges associated with unconventional oil and gas wastewater. Whether through the development and distribution of "greener" chemistry chemicals via new treatments that require less water, thereby reducing wastewater, or by adopting recycling programs, we can expect a wider distribution of industry answers to the challenges that come with treatment and disposal of unconventional wastewater.

22.4.3.2.3 Cleaner and Greener Chemicals

Inevitably, the chemicals used in a hydraulic fracturing treatment play a significant role in the contents of the flowback and produced water. Considering this, the use of "greener" chemicals in a treatment can have a positive effect, not only on the front end, but also on the character of the wastewater that is generated. By developing and using

chemicals that degrade quickly, there is less risk to aquatic environments, reduced potential risks when a spill does occur, and increased safety for workers handling the chemicals. Industry is rapidly moving forward with green chemical innovations, and has even developed processes to determine best performing green chemicals for a specific well.

22.4.3.2.4 Treatments Requiring Less Water

While not necessarily a new treatment, fracturing using foam as the carrier fluid may gain popularity if conditions for its use are favorable. In cases where the bottomhole pressure is low or if a reduction in the amount of liquid introduced to the reservoir is favored, a foam-based fracturing treatment may be warranted. Foam fracturing treatment systems may contain nitrogen, carbon dioxide, or a combination of both gases, in place of traditionally used water-based fluid systems. Foam fracturing treatments can reduce the amount of liquids introduced to a reservoir, as up to 80% of the liquids can be replaced with gas.

22.4.3.2.5 Recycling Programs and Water Reuse

Another area where industry is pushing forward, often beyond state regulatory requirements, is in recycling unconventional wastewater in shale plays where disposal options are limited and sourcing fresh water is either difficult or expensive. Recycling not only provides an answer to the disposal question but also helps reduce an operator's fresh-water-sourcing requirements. The quantity of recycled flowback water that a company uses on its next hydraulic fracturing directly offsets the need for fresh water.

Trends in the use of recycling water include using both recycled flowback and produced water, either as all, or part of, a fracturing treatment. Industry has developed methods for centralizing recycling treatment and storage facilities to deliver water to multiple wells or locations efficiently. Additional treatments such as the Baker Hughes H2PrO services can service water through a variety of applications that can be completed at the jobsite to allow for efficient reuse of water. An operator in the Permian has opted to not only recycle water, but also to use brackish water in lieu of fresh water. The H2prO Water Management Services use proven treatment technologies designed to conserve water, reduce transportation and disposal costs, and ensure compliance with regulations. The mobile treatment units eliminate the need for costly permanent equipment that may not be ideal for every application.

22.4.3.2.6 Savings Realized by Reducing the Number of Hydraulic Fracturing Stages

Production logs in unconventional wells allow operators to identify how much oil, gas, and water production is occurring along the horizontal lateral. These tools are somewhat expensive and difficult to deploy in horizontal wells (compared to vertical wells) because they need to reach the bottom of a horizontal lateral that might extend 5,000 to 10,000 feet without the aid of gravity. Although only a small fraction of unconventional wells have production log data, data from the available logs suggest that many of the hydraulic fracturing treatments along a horizontal wellbore are ineffective, producing little, if any, hydrocarbons. Many operators utilize a kind of "geometric" spacing; for example, one fracture stage every 250 feet. More advanced approaches are available that require additional formation evaluation and geomechanical analysis to identify the optimal locations of each fracture stage. Such advanced placement of hydraulic fracture stages is sometimes referred to as "surgical" and is referenced further in Chapter 8, Chapter 16, and Chapter 17. This optimization not only reduces costs, but also significantly reduces the water usage along with corresponding emissions.

22.5 Acknowledgment

The author would like to thank Kevin A. Ewing and Micheal Weller from Bracewell & Giuliani LLP.

22.6 References

Baker Hughes Reservoir Blog, 2014, Environmental Outlook for Shale Gas Development Recent Challenges and Advances in Water Management, http://blogs.bakerhughes.com/reservoir/2014/05/07/environmental-outlook-for-shale-gas-development-recent-challenges-and-advances-in-water-management-part-iviv-water-management-challenges-continued/ (accessed August 16, 2014).

Baker Hughes Reservoir Blog Environmental Outlook for Shale: http://blogs.bakerhughes.com/reservoir/2014/05/07/environmental-outlook-for-shale-gas-development-recent-challenges-and-advances-in-water-management-part-iviv-water-management-challenges-continued/ (accessed August 16, 2014).

Draft Rule for Hydraulic Fracturing on Public and Indian Lands, May 15, 2013, US Dept. of the Interior, Bureau of Land Management, http://www.blm.gov/wo/st/en/info/newsroom/2013/may/nr_05_16_2013.html

EIA–US Energy Information Administration Statistics, http://www.eia.gov/cfapps/ipdbproject/iedindex3.cfm?tid=90&pid=44&aid=8 (accessed April 2014).

EIA–US Energy Information Administration. 2013. Monthly Energy Review, DOE/EIA-0035, http://www.eia.gov/totalenergy/data/monthly/archive/00351309.pdf (accessed April 2014).

Energy in Depth Infographic, September 2014, Methane Leaks and Fracturing, Myths vs. Facts, http://energyindepth.org/wp-content/uploads/2014/09/EID_MethaneMvF.pdf (accessed October 2014).

EPA amendment report for Oil and Gas Extraction Point Source is available at: http://www.epa.gov/region6/6en/w/offshore/effluentguidelines-dec-16-1996.pdf (accessed August 23, 2014).

From the State of Colorado, 2013. Memorandum of Notice to Colorado Air Quality Control Commission, Revisions to Regulation Number 7. November 15.

From The Pennsylvania Bulletin. 2013. Subchapter C. ENVIRONMENTAL PROTECTION PERFORMANCE STANDARDS. http://www.pabulletin.com/secure/data/vol43/43-50/2362a.html (accessed August 17, 2014).

Kondash, A. J., Warner, N. R., Lahav, O., et al. 2013. Radium and Barium Removal through Blending Hydraulic Fracturing Fluids with Acid Mine Drainage. ***J. Environ. Sci. Tech.***, AI. DOI: http://dx.doi.org/10.1021/es403852h.

Letter to the Pennsylvania Department of Environmental Protection, 2011. The Environmental Protection Agency, http://www.epa.gov/region03/marcellus_shale/PADEP_Marcellus_Shale_030711.pdf (accessed April 18, 2014).

Mackay, D. 2014. Shale Gas in Perspective. Sustainable Energy - Without the Hot Air, 12 August 2014, http://withouthotair.blogspot.com/2014/08/shale-gas-in-perspective.html (retrieved October 2014).

Oklahoma Corporation Commission Edited on March 4, 2013, https://www.google.com/fusiontables/DataSource?docid=12bTEuHusn2ywZwiGYTTwHQhVvnEP_dM3mrZZpeM#rows:id=1 (accessed October 2014).

Report of the Governor's Marcellus Shale Advisory Commission. Pennsylvania Environmental Council. August 2011, http://files.dep.state.pa.us/publicparticipation/marcellusshaleadvisorycommission/marcellusshaleadvisoryportalfiles/msac_final_report.pdf (accessed August 2014).

State of Colorado, 2013. Memorandum of Notice to Colorado Air Quality Control Commission, Revisions to Regulation Number 7. November 15, http://www.colorado.gov/cs/Satellite?blobcol=urldata&blobheadername1=Content-Disposition&blobheadername2=Content-Type&blobheadervalue1=inline%3B+filename%3D%22Regulation+Number+7%3A++Memorandum+of+Notice+(8+pages)

Walsh III, F.R. and Zoback, M.D., 2015, Wastewater Injection and Triggered Earthquakes in Oklahoma, Proc. of the National Academy of Sciences, 2015.

This page intentionally left blank

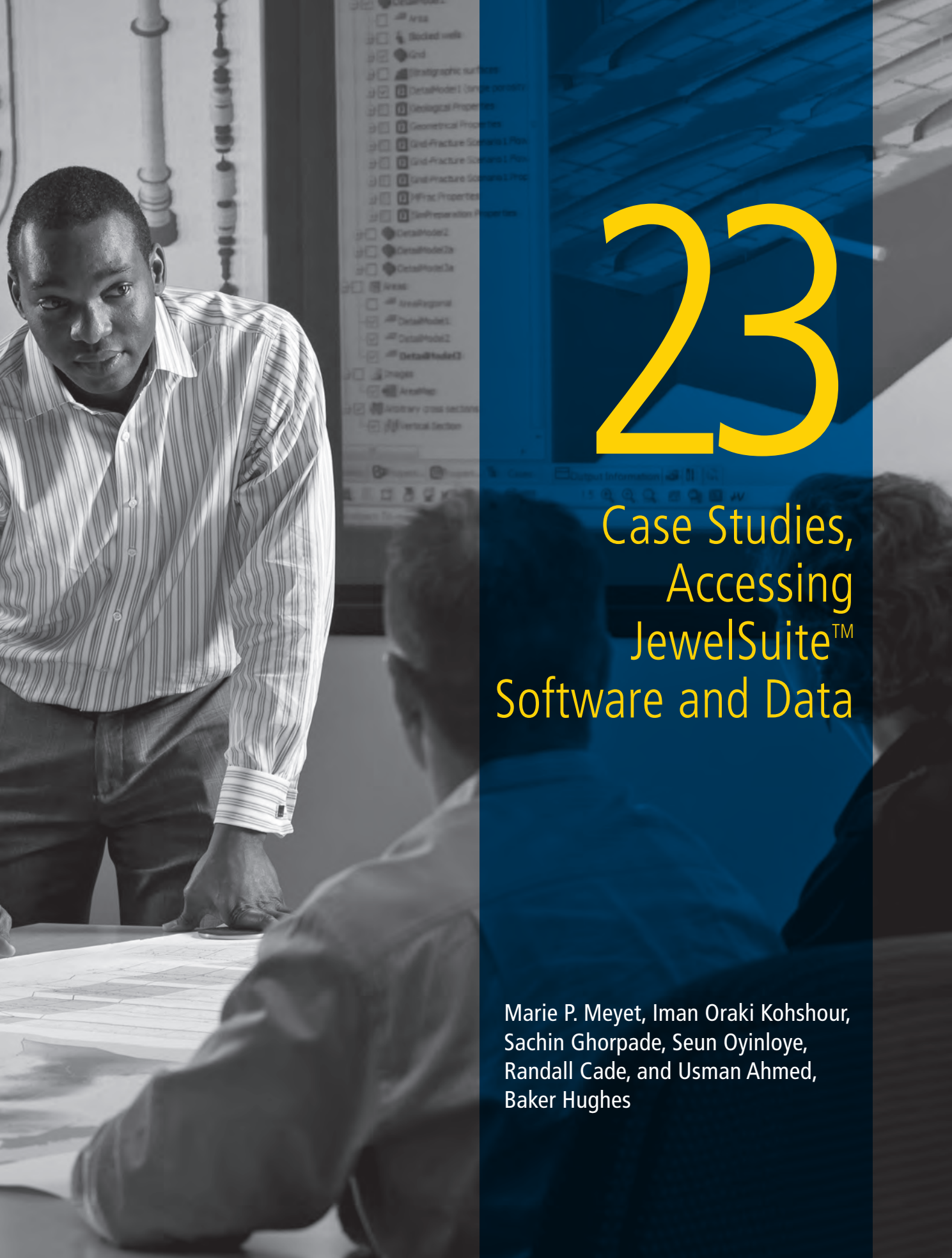

23

Case Studies, Accessing JewelSuite™ Software and Data

Marie P. Meyet, Iman Oraki Kohshour, Sachin Ghorpade, Seun Oyinloye, Randall Cade, and Usman Ahmed, Baker Hughes

This page intentionally left blank

Chapter 23: Case Studies, Accessing JewelSuite™ Software and Data

23.1 Introduction

Subsurface modeling of unconventional resources is essential to evaluate these resources. Whether you have a limited amount of data with a number of wells already drilled and are planning to place your next well, but not sure if the potential production gain would justify the operation costs or you have an abundant amount of data with massive number of poor to intermediate wells and want to optimize your completion design and production, in all of these or many other specific geoscience and engineering cases.

Wellbore stability, sweet spot identification wells and hydraulic fracture stages, and economic hydrocarbon delivery are shared goals and among the most important factors in all drilling, completion, and production aspects of unconventional plays. These workflows have proven successful in many unconventional projects throughout North America. The economic success in North America unconventional exploitation and development has spurred exploratory drilling in China, Argentina, Saudi Arabia, South Africa, Australia, and parts of Europe, and have even attracted interests in North Africa, Colombia, Mexico, and India.

Workflows can be used to drive the exploration and appraisal phases of unconventional resource development for any specific geologic areas globally. **Fig. 23.1** shows how the various data sources are integrated and handled in this software suite starting from seismic interpretation, geomechanical-based reservoir characterization all the way to reservoir simulation and production forecasting. The success of this approach depends on using a multi-disciplinary and integrated team to shorten communication lines and thus optimize the field development.

JewelSuite provides users with an opportunity for a comprehensive view of the subsurface complexity and if and when needed our geoscientists show them the added value that can be generated based on geological measurements and scientific models.

In this chapter, we present case studies from three shale plays in the United States. All three plays are heterogeneous with completion complexity and uncertainty in EUR. In each case, the reader is provided with brief information about the play and the project objectives. The reader is also provided with access to a JewelSuite license to see and practice the software in person. The cases are populated with the pre-loaded datasets and the user is free to change the model inputs and play with the model. These case studies are only for training and information purposes and any misuse will void the license privilege.

23.2 Software Access

Please send the following information to the email address at ReservoirSoftwareSupport@bakerhughes.com to receive the login information along with the guidelines to access to JewelSuite software.

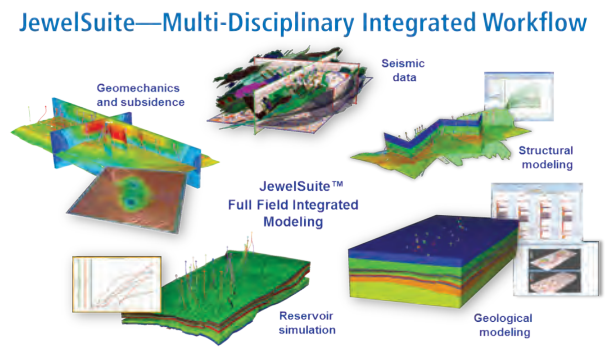

Fig. 23.1—Conceptual representation of unconventional integrated workflow.

After registration, the user has two months' unlimited access to the software. During this period, if there are any software- or license-related questions or issues, contact ReservoirSoftwareSupport@bakerhughes.com.

FULL NAME

COMPANY NAME AND ADDRESS

EMAIL

PHONE NUMBER

If the person and organization are outside the United States and Canada, after contacting the above email, you will receive a software license agreement (a PDF file also created from the information provided above) that needs to be signed before a license can be issued and access can be granted.

The procedure for using the software is straightforward; however, we have provided brief navigation guidance to explain the general workflow used for modeling the three cases from three major shale plays in North America. The case studies files with the saved data are stored in the FTP location. The address to the FTP location will be sent to the users via the same email. If one wants to have a complete understanding of different parts of the software program and be able to build and run an integrated earth model consisting of geological, geophysical, and geomechanical models as well as economics evaluations and to statically and dynamically connect multiple applications under the same platform, provisions are there to provide both in-house and client-office based training courses of Baker Hughes software suites taught by professionals with years of reservoir modeling and industry experience. The workflow for shale evaluation and modeling is illustrated in **Fig. 23.2** (Vassilellis et al. 2011). The workflow (referred to as Shale Engineering Model) can be scaled down to an individual well or scaled up for a basin study.

If the user has a special interest in any of the JewelSuite workflow areas then it is recommended that the local Baker Hughes office or any JewelSuite Support office be contacted. The support team will be glad to organize a customized training based on the area of interest.

23.2.1 The Workflow (Marcellus Case Study)

The Marcellus play is estimated to contain over 140 trillion cubic feet (Tcf) of recoverable natural gas ranging in depth from 4,000 to 12,000 ft. with a formation thickness of about 800 ft. in eastern Pennsylvania thinning to the west. It is the largest natural gas play in the United States. A simulation sector of the play was built based on the Shale Engineering Workflow and designed to investigate the impact of completion design and forecast well performance.

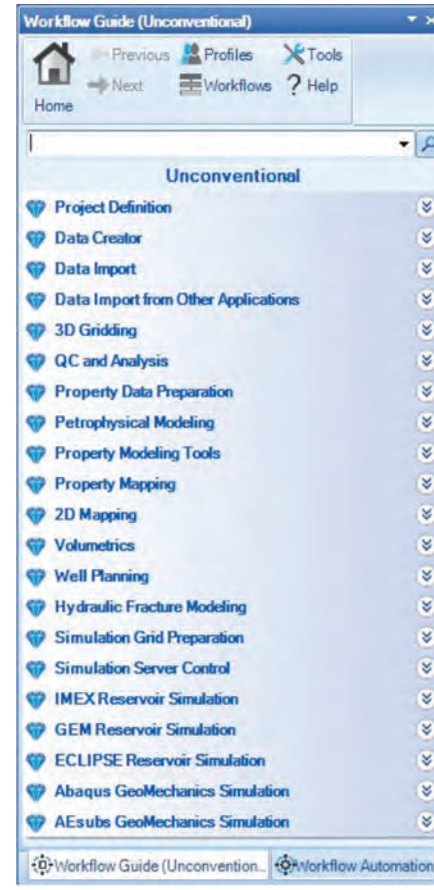

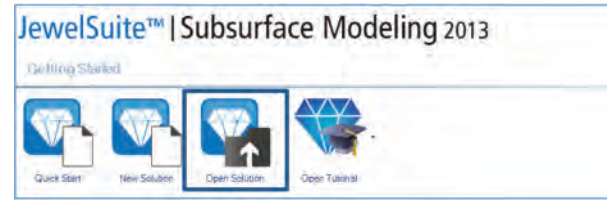

This workflow is provided to show a sector simulation of tight reservoirs in JewelSuite. For practical purposes, we use the Marcellus case study to walk the reader through the model and part of the workflow. When JewelSuite is opened, Marcellus case is to be selected (**Marcellus_B_JG-5.jewel**).

When the model is open, the workflow panel guide can be seen on the left side of the screen. This is also referred to as

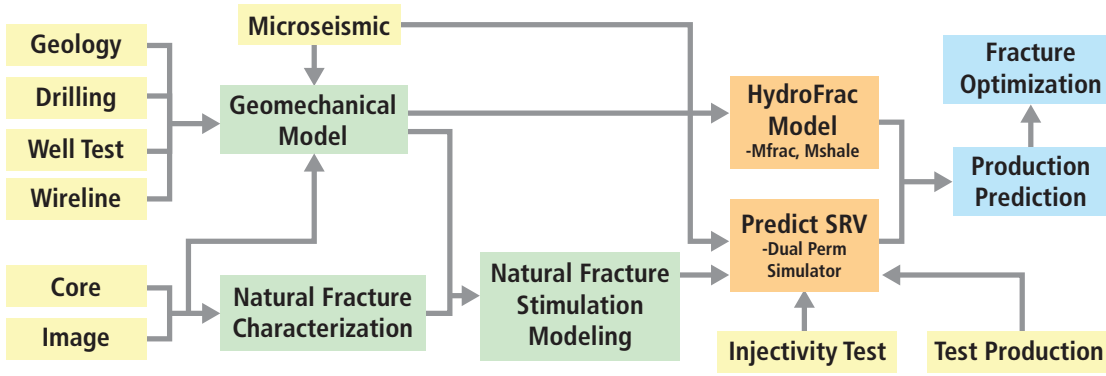

Fig. 23.2—Shale Engineering Workflow for modeling unconventional reservoirs.

the Home tab and contains all the steps and components for a comprehensive modeling of one's project. Since in this case, we have an existing set of the data, the data have already been created and imported into the program. The import data can be 2D and 3D grids, 3D mesh properties, grid properties, seismic, polylines, area data, well design, well tops, well logs, and reservoir simulation. **Please note that the model has been already executed and the user does not need to execute and run the model again, unless the user wants to make some changes to the model and see the outcome. This following procedure would help the user perform the adjustment to properties and execution**.

A. In order to create a modeling area, one needs to define an area (3D area specifying the lateral and vertical grid dimension) to be used throughout the reservoir simulation process. This requires going to Tools. Click on Model Area Definition.

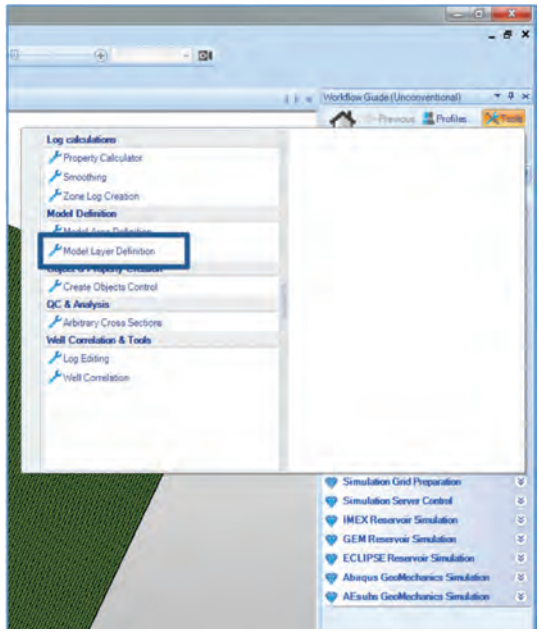

B. Click Create in step 1.

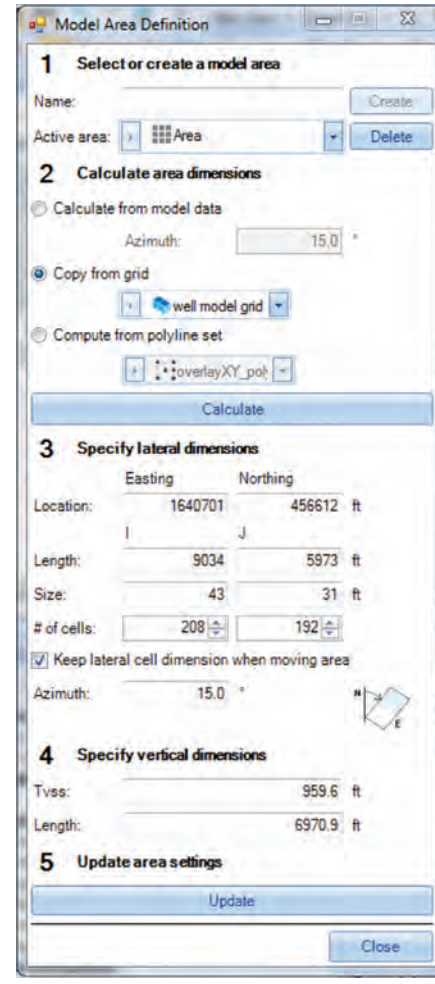

C. Select Copy from grid, and select well model grid in step 2

D. Click Calculate and then close. The area is shown as below.

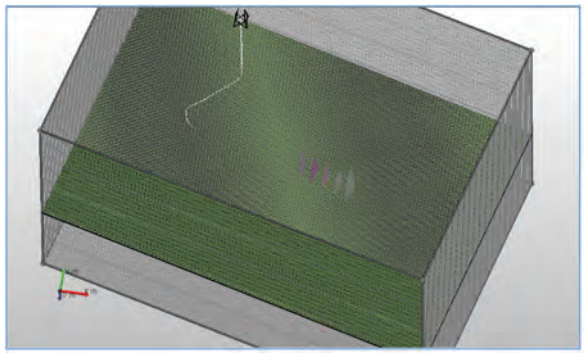

After the area is created, one will need to create a vertical grid so that it can be used for property modeling.

E. Right click on well model grid under Solution Explorer. Select Create a copy. Name the new grid as well model grid copy.

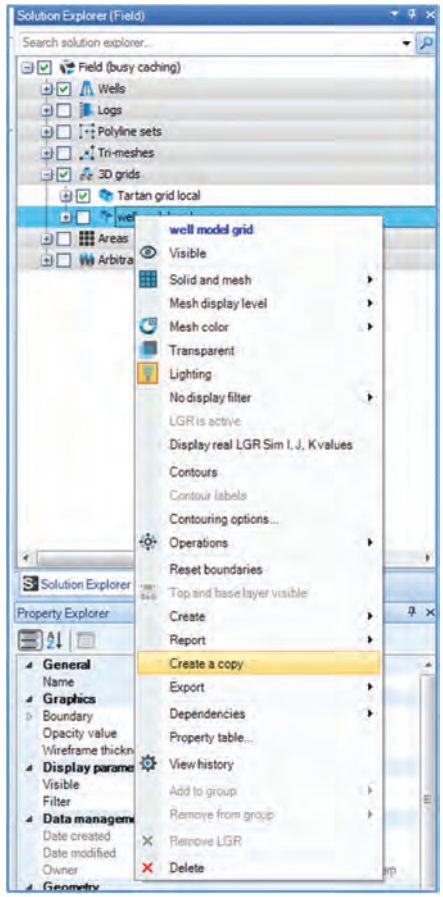

F. Go to workflow panel, select 3D Gridding, select Jewel Gridding.

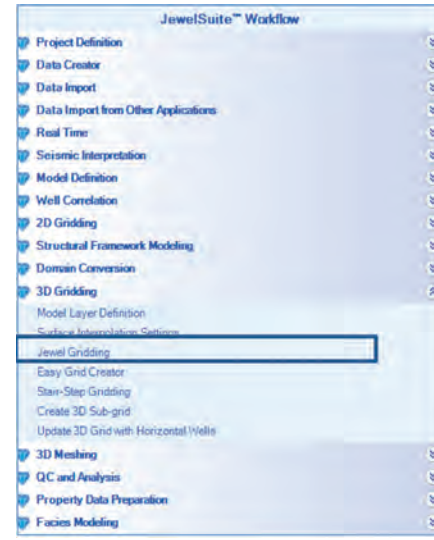

Step 1: Click Existing and select "well model grip copy"

Step 2: Click Open model layer definition panel

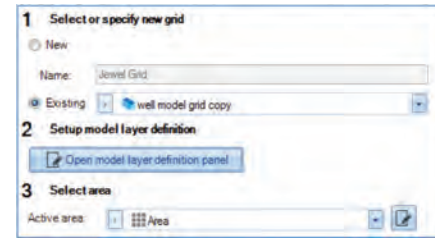

Step 3: Click on Open Model Layer Definition panel

Step 4: Select Reservoir_1.

Step 5: Enter 20 internal layers. Click Close.

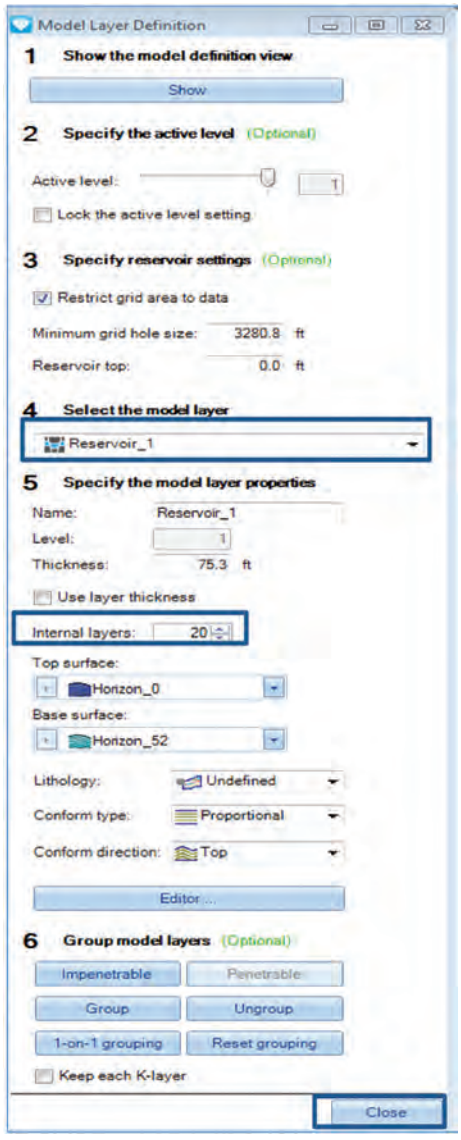

Step 6: Click Execute to regenerate the grid.

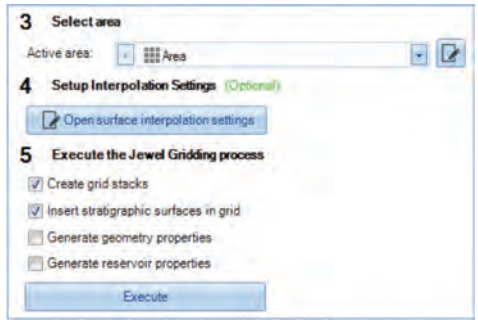

After this step is done, click Yes in the pop-up window.

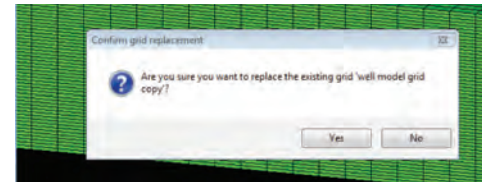

G. Go to **Workflow Panel > Property Mapping> Property Mapping.**

Step 1: Select well model grid

Step 2: Select well model grid copy

Mapping method: XYZ

Step 3: Select all Imported properties.

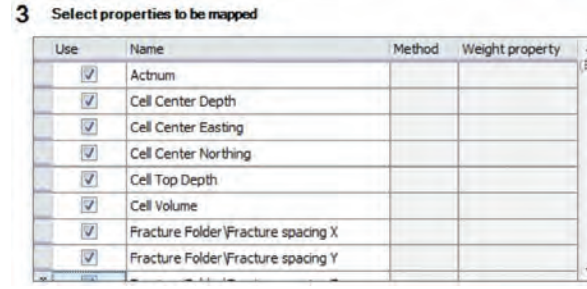

Step 4: Click Execute

Please also note that the units are in Fields (Degrees and Meters). The user can change the unit settings by going to **Tools > Options** and clicking the Unit System tab and choosing the units.

H. Well Data

Go to **Wells> Views > Wellbore View> States**

i. Select Well 1 as wellbore name

ii. Start date: 11/1/2011

iii. End date: 9/1/2013

iv. Type: Producer

v. Status: Existing

vi. Phase: Gas

vii. Condition: Surface

Then, go to the Perforation tab. The user can enter or import perforation data.

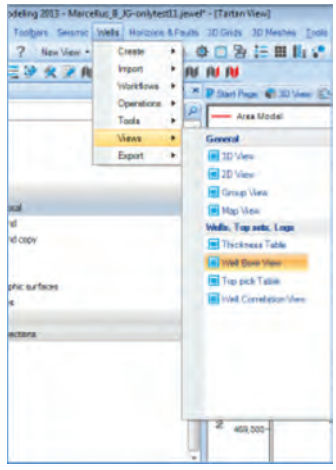

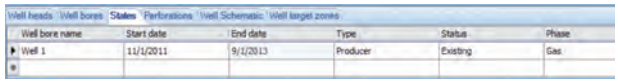

The user can also copy and paste perforation data from the file perf trial.csv. Alternatively, the user can go to **Data import workflow > Well Data > Select the file perf trial.csv > Under Description, select Well Bore PERFORATION Files > Click OK**

Select the appropriate import column then **Click next > Click Finish.**

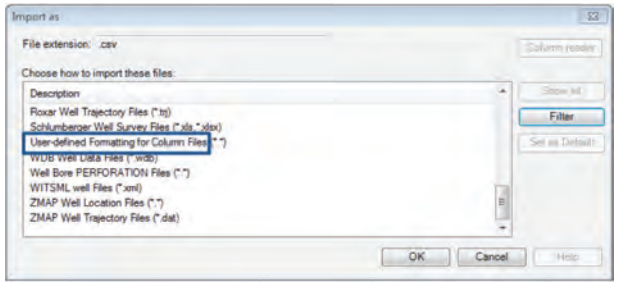

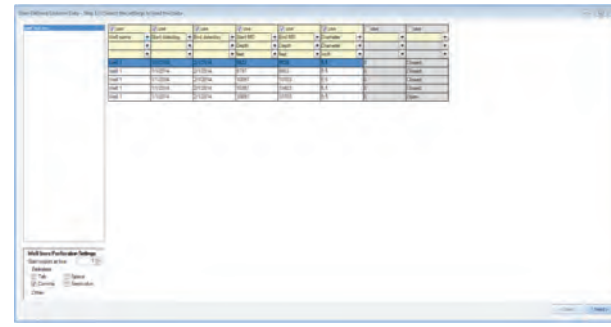

Then, Go to well target zones

Select Well Target Zone under second column

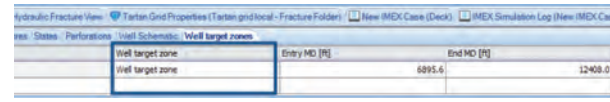

I. Creating Tartan Grid

The Tartan View is a 2D view that allows the user to inspect and edit the grid cell size distribution in the lateral directions. Go to **Hydraulic Fracture Modeling Workflow** on **left panel > Create Fracture Definition**

Section 1: Enter "Fracture Definition" in **name field > Click Create**

Section 2: Click new area icon

1. Click Create
2. Copy from grid "well model grid." Click Calculate, then Close

Select Area of Fracture Definition

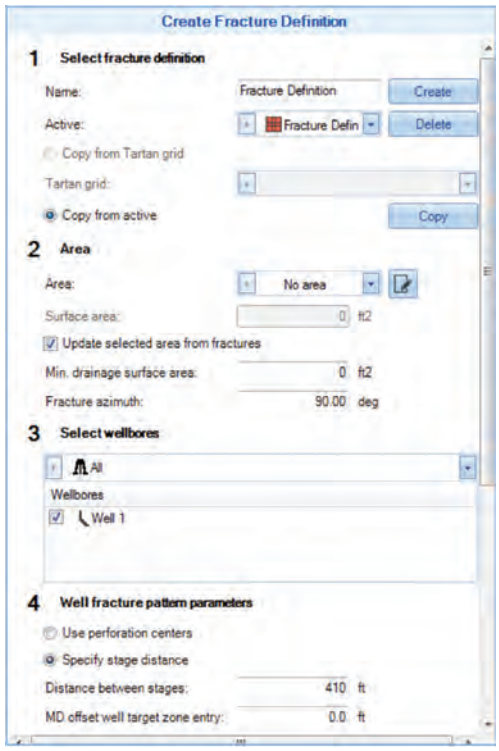

Section 3: Select well of interest: Well 1

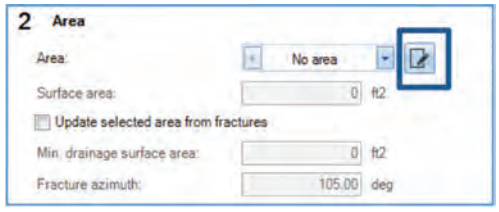

Section 4: For an existing well with perforation data, select "Use perforation center" otherwise, click on Specify stage distance

1. Select "Use Perforation centers"
2. Check Replace existing fractures

Section 5: Enter the following fracture properties according to MFrac outputs

3. Half Length: 250 ft.
4. Height: 1640 ft.

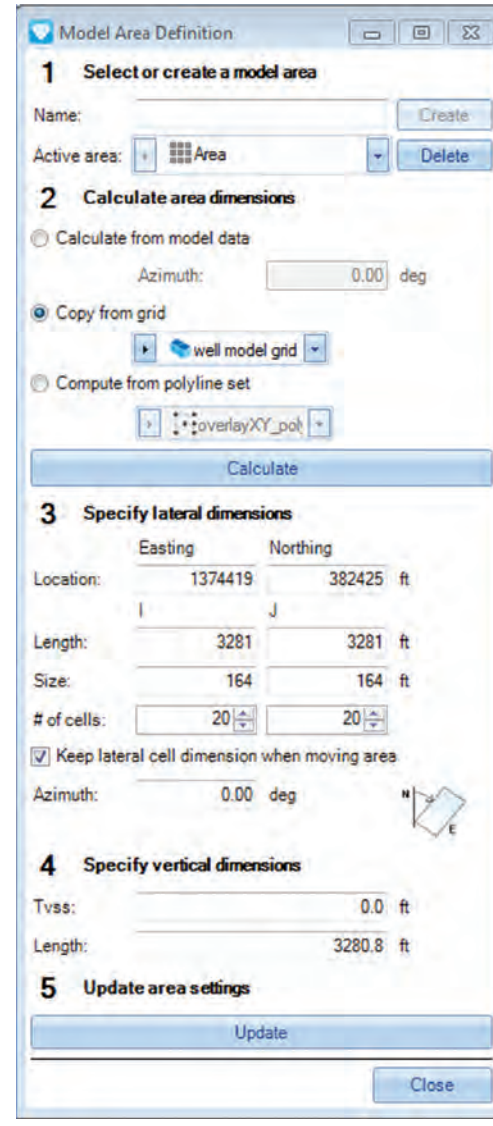

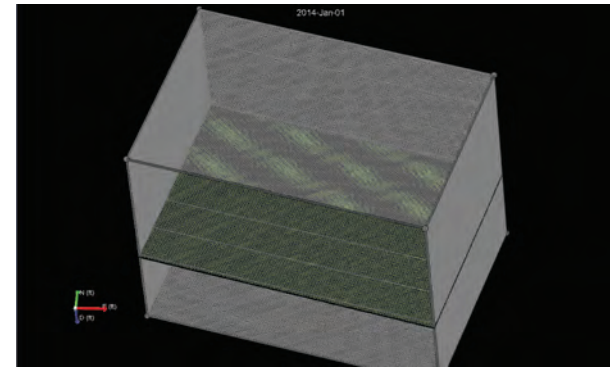

5. Width: 0.039 in (default)
6. Permeability: 10000 mD

7. SRV width: 200 ft. (**Table 23.1**) This value represents the

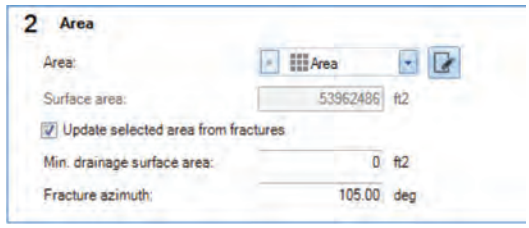

width of the area around the hydraulic fractures in which natural fractures are supposed to contribute to reservoir flow. It can be estimated from microseismic, image logs, modeled DFN if available. If none are available, the rule of thumb is 1/3 of fracture length. User can import microseismic and Mfrac data in this step.

Click on "Edit" and make sure that the following values are entered:

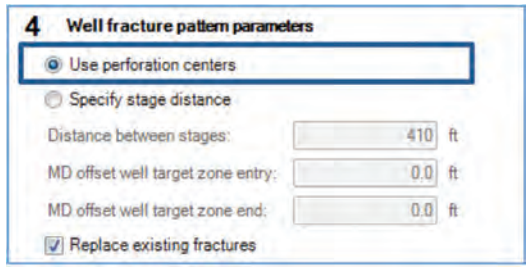

Table 23.1—The properties of natural fractures in the Marcellus example.

Type	Use	Fracture spacing (ft)	Width (in)	Permeability (md)
Primary XZ (explicit)	SRV	100.0	0.039	100.0
Primary YZ (explicit)	SRV	100.0	0.039	100.0
Secondary (implicit)	SRV	10.0	0.039	100.0

Next, click Run. After the run, enter 2 ft. and 100 ft. as min and max perpendicular to wellbore cell sizes. Increasing size factor of 2. Enter 200 ft. and 500 ft. as min and max parallel to wellbore cell sizes. Increasing size factor of 5.

Next, click "Hydraulic Fractures" and make sure that the following values (**Table 23.2**) are entered.

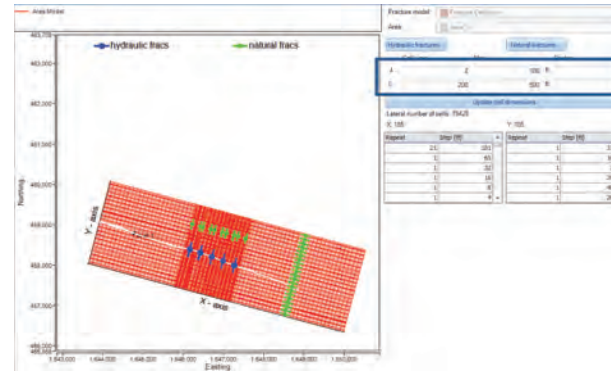

Table 23.2—The properties of hydraulic fractures in the Marcellus example.

Hydraulic fracture stage#	MD (ft)	SRV width (ft)	Half length (ft)	Height (ft)	Width (in)	Perme-ability (md)
1	9525.0	200.0	250.0	1640.4	0.039	10000.0
2	9800.0	200.0	250.0	1640.4	0.039	10000.0
3	10100.0	200.0	250.0	1640.4	0.039	10000.0
4	10400.0	200.0	250.0	1640.4	0.039	10000.0
5	10700.0	200.0	250.0	1640.4	0.039	10000.0

One main assumption here is that the fractures are uniform, although not usually the case but a common assumption in the industry. The Hydraulic Fractures Table can be manually edited to account for the differences in fracture stages, and run sensitivity.

Click Next to create Perforations at Fractures

Section 1: Select Fracture Definition

i. Completion Type: Cased Hole

ii. Perforation properties:

1. Length per stage: 10 ft. (Perf Interval)

2. Wellbore diameter: 7 in (default)

iii. Click Run

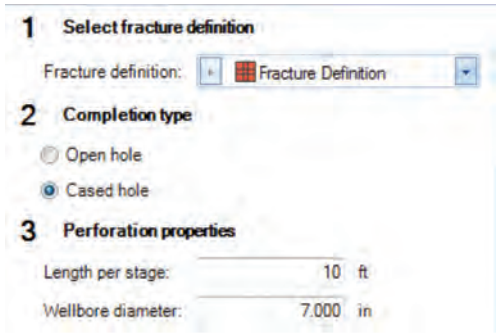

J. Click Next to create Tartan Grid

Section 1: Click New

Section 2: Select Fracture Definition (usually automatically selected)

Section 3: 3D grid cell dimensions is taken from tartan view and populated here. User can edit grid dimensions from either view.

Section 4: Click Use source 3D grid which is the well model grid

Section 5: Select top and bottom surfaces of model

Section 6: Select properties to be mapped to tartan grid (optional). Click Run

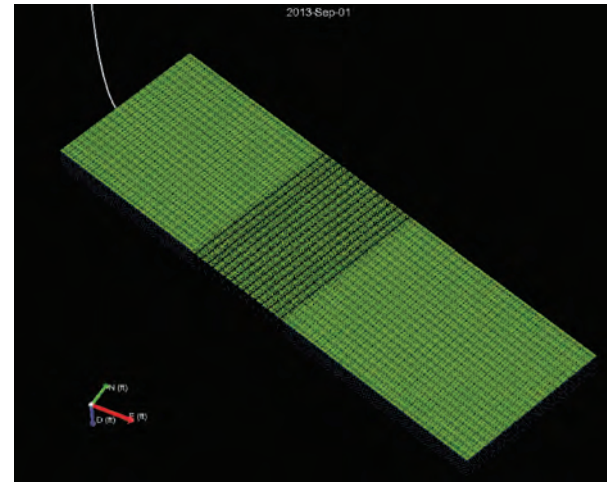

Next, click Next to create Tartan Grid Properties

Section 1: Select created tartan grid "Tartan grid local"

Section 2: Enter folder name as **Fracture Folder** > **Click Enter on keyboard**

Section 3: **Click Dual permeability model** > **click Model explicit hydraulic and natural fractures in fracture-system**

Section 4: Default

Section 5: Select well model grid

Section 6: Do not check "Filter source by property." Click on Specify properties

Enter the values from **Table 23.3** for each property.

Table 23.3—Tartan grid properties for the Marcellus example.

Name	Matrix or Fracture	Constant	Source
Porosity unaffected	Matrix	–	Well model grid copy:\Imported\PHIE_Mapped_Mapped_Mapped_New
Kx unaffected	Matrix	–	Well model grid copy:\Imported\PERMSH\ Mapped_Mapped_Mapped_New
Ky unaffected	Matrix	–	Well model grid copy:\Imported\PERMSH\ Mapped_Mapped_Mapped_New(1)
Kz unaffected	Matrix	–	Well model grid copy:\Imported\PERMSH\ Mapped_Mapped_Mapped_New(1)
NTG unaffected	Matrix	1.0 ratio	–
Porosity unaffected	Fracture	0.1	–
Kx unaffected	Fracture	–	Well model grid copy:\Imported\PERMSH\ Mapped_Mapped_Mapped_New
Kx unaffected	Fracture	–	Well model grid copy:\Imported\PERMSH\ Mapped_Mapped_Mapped_New
Kx unaffected	Fracture	–	Well model grid copy:\Imported\PERMSH\ Mapped_Mapped_Mapped_New
NTG unaffected	Fracture	1.0 ratio	–
Fracture spacing X unaffected	Fracture	100.0 ft	–
Fracture spacing Y unaffected	Matrix	100.0 ft	–
Fracture spacing Z unaffected	Fracture	100.0 ft	–

Please note that each source seen here should be consistent with the properties in the Property Explorer panel. This can be checked by going to Solution Explorer panel. Go to **well model grid copy > properties** and click on each individual property (Kx, Ky, Kz, Porosity) and view its source in the Property Explorer panel.

Click Run.

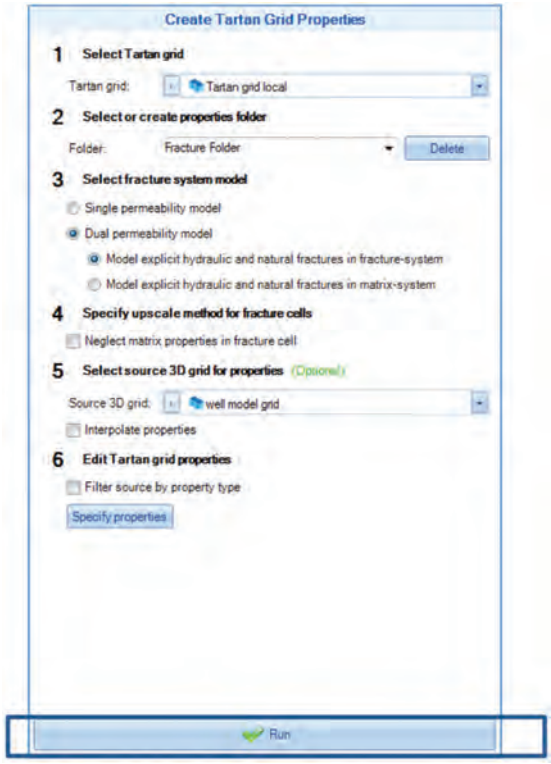

Go to 3D View to see the user's grid. In the Solution Explorer, go to **3D grids > Tartan grid local> Properties> Fracture Geometry.**

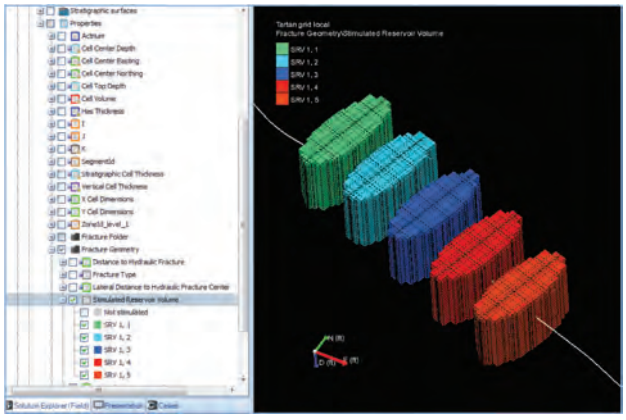

Select Stimulated Reservoir Volume, uncheck "Not stimulated" to see the users' SRV only.

K. Click Next to Create Reservoir Simulation Case

Section 1: Click Create a blank case

1. Select IMEX for simulator
2. New case name: **well model IMEX case > click Create**

Section 2: Tartan grid is selected. Select Fracture Folder as property folder.

Section 3: Click Update simulation case

Click Run

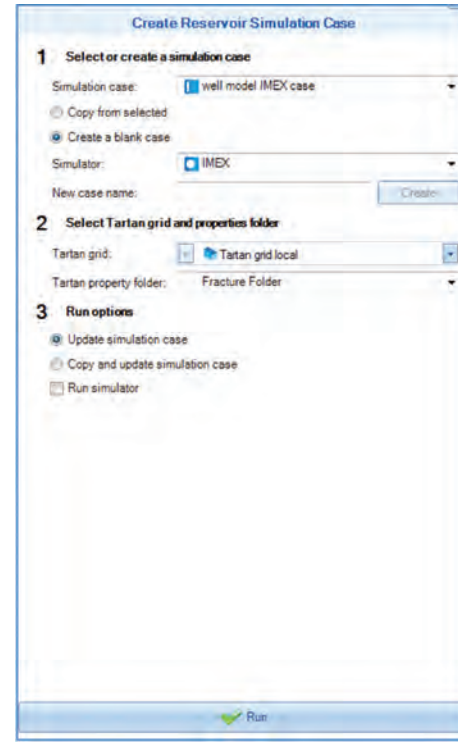

The next step is to establish a simulation case "Well Performance Model." Click Home button.

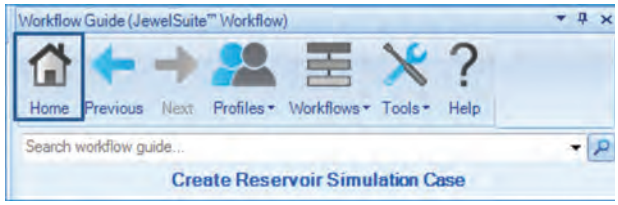

Go to **IMEX Reservoir Simulation** > **Simulation Case**.

Section 1: Simulation is automatically selected

Section 2: Select Tartan grid local as 3D grid

Section 3: Enter 11/1/2011 as Start date

Section 4: Click on Edit Settings

1. General Tab

   Input Data Units: Field

   Output Data Units: Field

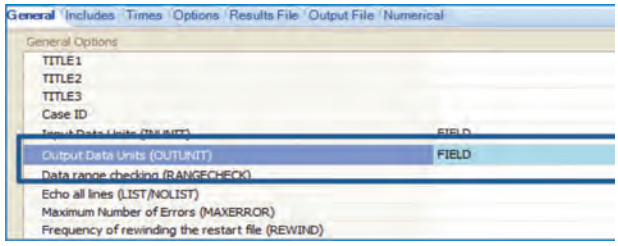

Go to Times tab: Enter 9/01/2013 in the second line. Right click on **Screen > Create Reporting Times > Monthly**

Then, go to Results File tab, and under WSRF, select WSRF Type: WELL, WELL Writing Frequency: TIME. Click OK.Under OUTSRF, select OUTSRF Type: GRID, Grid list (GRID): SG, SW, KRW, KRG, PRES, POROS, PERM, and then click OK.

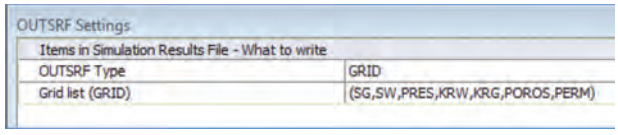

Go back to workflow panel. Click Next to Reservoir Description. After that, click on Edit reservoir. Add CTYPE and RTYPE properties.

CTYPE	Matrix	1.0
CTYPE	Fracture	2.0
RTYPE	Matrix	1.0
RTYPE	Fracture	2.0

The next step is to account for Geomechanical Hysteresis affect.

i. Click on CROCKTYPE tab and Compaction Tables

ii. Enter Model ID 1 (Matrix) in first line

iii. Model ID 2 (Fracture) in second line

iv. Select CROCKTAB from column Type pull-down list for both model IDs

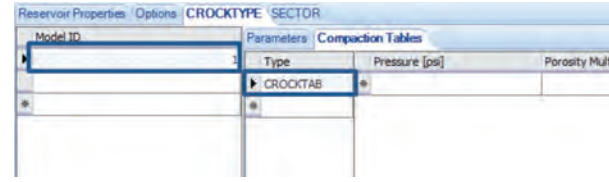

v. Open spreadsheet Fracture hysteresis.xlsx in sheet named GCA.

vi. Enter Input parameter as:

Depth, ft.	6590	1.0
Initial Gradient, psi/ft.	0.58	2.0
Frac Gradient, psi/ft.	0.8	1.0

In the same sheet, Cell J9: Select "Fracture." Go to cmg table sheet, Copy-paste the Loading Path Fracture Hysteresis table in Model ID 2 back in JewelSuite. Copy and paste pressure column of loading path in Model ID 1. Enter 1 at all pressure for Porosity Multiplier, Horizontal Permeability Multiplier Vertical Permeability Multiplier columns. After this step, the Reservoir Description section is completed. The user is cautioned to make sure to quality check the data.

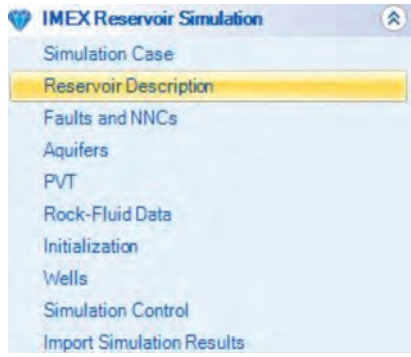

The next procedure for reservoir simulation (including PVT regions, Rock and Fluid, Initialization, validation, and submission) is pretty similar to a typical simulation study and easy to follow and can be found in the JewelSuite user manual. For brevity, it is not included here.

L. View Simulation Results (XY Plots)

Click Window > New View > XY Plot View

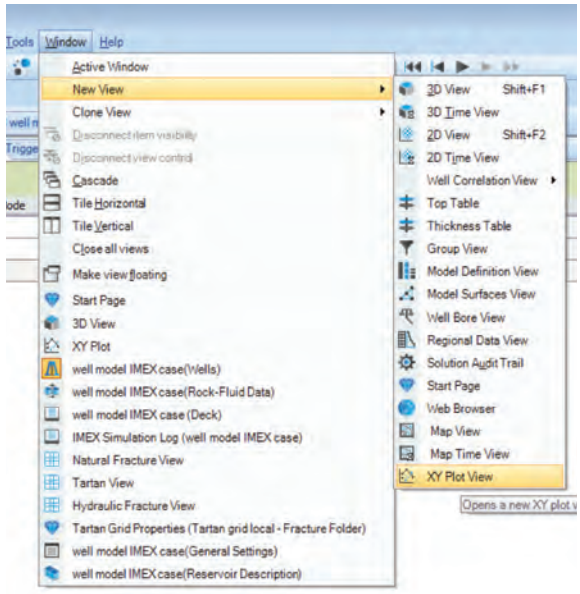

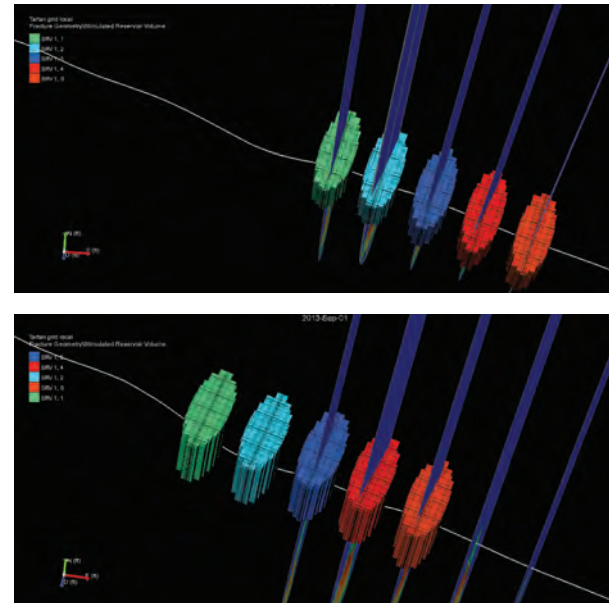

Fig. 23.3—Location of SRV and hydraulic fracture stages in each model. Top: Model A, and bottom: Model B.

Click on tab Manual Data Select and + sign in front of Category: well model IMEX Case. In this example, there are two models, Model A (Marcellus_B_JG-5) that is the base case illustrated thus far, and Model B (Marcellus_B_JG-6). Model B has the same properties, except that the locations of two hydraulic fracture stages are changed to evaluate and observe if such change has any impact on the production from the well. **Fig. 23.3** shows the location and geometries of SRVs with respect to each other for both of the models.

The impact of fracture stage placement on the production is clearly observed in this example (**Fig. 23.4**). Comparison of geometric fractures (model A) versus geologic fracture (model B) shows about 3% increase in cumulative gas produced when placing fractures at geologically more prone locations.

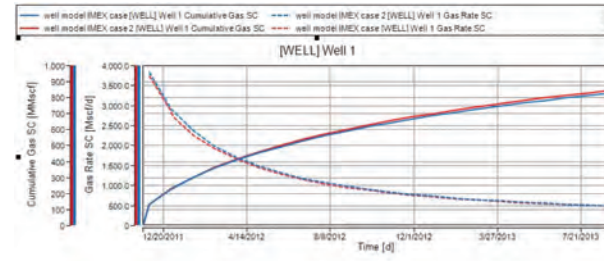

Fig. 23.4—Simulation results for Model A (case 1) and Model B (case 2).

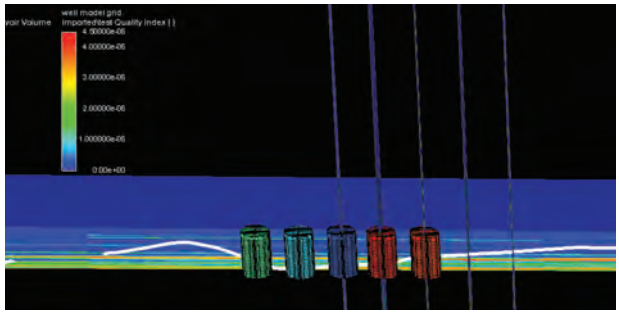

Fig. 23.5—Geologic versus geometric stage placement. Model B is more favorable as it has higher quality index compared with model A.

Fig. 23.5 compares the two models on the same graph. Model A is considered as the base case. It can be seen when the stages are placed at a more geologically favorable section of the wellbore, the production is positively impacted.

Using similar approaches, and for the interpreted matrix and fracture property, an asset team can provide confirmation of geological parameters, optimize the production strategy by determining optimal fracture effective length, fracture spacing, number of wells, well spacing, and assess the sensitivity of each parameter to manage the risks and opportunities.

23.3 Eagle Ford

The Cretaceous Eagle Ford is located between the Austin Chalk and the Buda Limestone at depths ranging from 4,000 ft. to more than 12,000 ft. dropping progressively deeper in the NE direction and in the SE direction. In the SE direction, the hydrocarbon content evolves from oil to gas with abundant condensates to gas only, so ESP applications are viable in the NW section (Fayette, Gonzales, McMullen, and Zavala counties).

The aim of the project was to forecast production for a multistage hydraulically fractured horizontal well for a sector of the Eagle Ford play (**Fig. 23.6**) for three years (01 Jan 2014 to 01 Jan 2017). Here the model is a dual permeability model which is up-scaled horizontally and divided into 22 geologic layers for one to better handle the run time. The sector model can be opened by selecting the solution entitled "Eagle Ford Sector Model.jewel."

The modeling procedure for this case is similar to the procedure for the Marcellus that was followed in the earlier

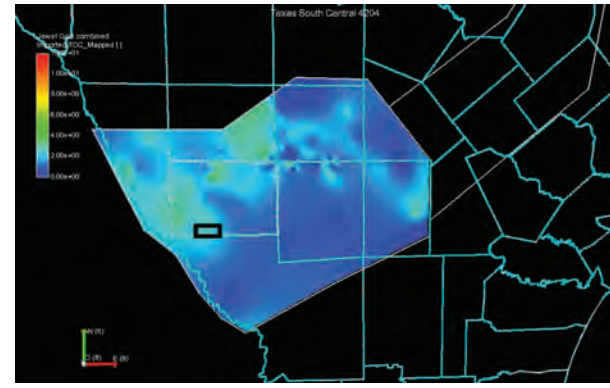

Fig. 23.6—A selected sector for the Eagle Ford shale play project. The map shows the TOC distribution of the Eagle Ford play.

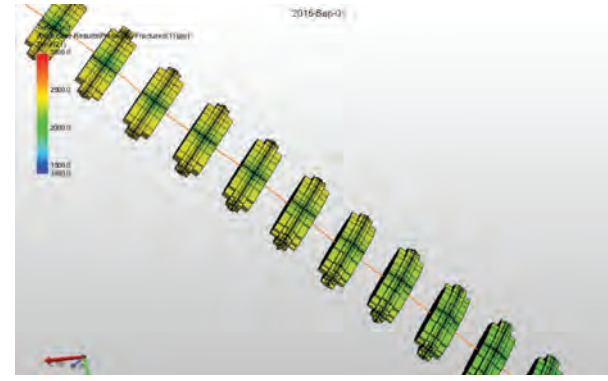

Fig. 23.7—The simulated pressure distribution in each SRV during the simulation time (1 September 2015).

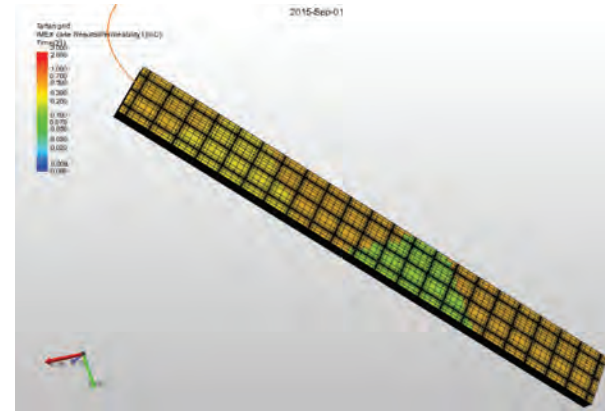

Fig. 23.8—The matrix permeability during the production from the model. (September 1, 2015).

section. The properties of hydraulic fractures, natural fracture and some of the reservoir properties along with their source locations in the model are provided in **Table 23.4, Table 23.5, and Table 23.6**. The fracture tables can be viewed

Table 23.4—The properties of hydraulic fractures in the Eagle Ford example.

Hydraulic fracture stage #	MD (ft)	SRV width (ft)	Half length (ft)	Height (ft)	Width (in)	Permeability (md)
1	8876.0	150.0	200.0	89.0	0.150	1000.0
2	11171.0	150.0	200.0	89.0	0.150	1000.0
3	11426.0	150.0	200.0	89.0	0.150	1000.0
4	11681.0	150.0	200.0	89.0	0.150	1000.0
5	11936.0	150.0	200.0	89.0	0.150	1000.0
6	12191.0	150.0	200.0	89.0	0.150	1000.0
7	12446.0	150.0	200.0	89.0	0.150	1000.0
8	12701.0	150.0	200.0	89.0	0.150	1000.0
9	12956.0	150.0	200.0	89.0	0.150	1000.0
10	13211.0	150.0	200.0	89.0	0.150	1000.0
11	13471.0	150.0	200.0	89.0	0.150	1000.0
12	9131.0	150.0	200.0	89.0	0.150	1000.0
13	13731.0	150.0	200.0	89.0	0.150	1000.0
14	13976.0	150.0	200.0	89.0	0.150	1000.0
15	14227.0	150.0	200.0	89.0	0.150	1000.0
16	9386.0	150.0	200.0	89.0	0.150	1000.0
17	9641.0	150.0	200.0	89.0	0.150	1000.0
18	9896.0	150.0	200.0	89.0	0.150	1000.0
19	10151.0	150.0	200.0	89.0	0.150	1000.0
20	10406.0	150.0	200.0	89.0	0.150	1000.0
21	10661.0	150.0	200.0	89.0	0.150	1000.0
22	10916.0	150.0	200.0	89.0	0.150	1000.0

Table 23.5—The properties of natural fractures in the Eagle Ford example.

Type	Use	Fracture spacing (ft)	Width (in)	Permeability (md)	Width (in)	Permeability (md)
Primary XZ (explicit)	SRV	200.0	0.039	1000.0	0.150	1000.0
Primary YZ (explicit)	SRV	200.0	0.039	1000.0	0.150	1000.0
Secondary (implicit)	SRV	20.0	0.039	1000.0	0.150	1000.0

by going to hydraulic fracture modeling tab, and clicking on either the natural fracture properties, or hydraulic fracture properties. The Edit section for the reservoir properties can be viewed by going to IMEX Reservoir Description, and clicking on the reservoir description section.

Fig. 23.7 shows the schematics of the stimulated reservoir volumes (SRV) with the pressure behavior inside the fractures after the hydraulic fractures and grids have been designed and created. **Fig. 23.8** shows the result of matrix permeability.

Fig. 23.9 shows the production results of cumulative oil and gas and the oil rates after running 3 years of simulation. After three years, about 2,500 Mb of oil and 700 MMscf of gas have been produced.

23.4 Haynesville

Haynesville reservoir is a relatively high-pressure reservoir that sits between the sandstone of the Cotton Valley Group and the limestone of the Smackover formation; where

Table 23.6—The properties of reservoir in the Eagle Ford example.

Name	Matrix or Fracture	Constant	Source	Permeability (md)	Width (in)	Permeability (md)
PERMI	Matrix	–	fracture folder\Kx-MAT	1000.0	0.150	1000.0
PERMJ	Matrix	–	fracture folder\Ky-MAT	1000.0	0.150	1000.0
PERMK	Matrix	–	fracture folder\Kz-MAT	1000.0	0.150	1000.0
POR	Matrix	–	fracture folder\Porosity-MAT			
DIFRAC	–	–	fracture folder\Fracture spacing X			
DJFRAC	–	–	fracture folder\Fracture spacing Y			
DKFRAC	–	–	fracture folder\Fracture spacing Z			
PERMI	Fracture	–	fracture folder\Kx-FRAC			
PERMJ	Fracture	–	fracture folder\Ky-FRAC			
PERMK	Fracture	–	fracture folder\Kz-FRAC			
NETGROSS	Fracture	–	fracture folder\NTG-FRAC			
NRTGROSS	Matrix	–	fracture folder\NTG-MAT			
POR	Fracture	–	fracture folder\Porosity-FRAC			
CTYPE	Matrix	1.0	–			
CTYPE	Fracture	2.0	–			
RTYPE	Matrix	1.0	–			
RTYPE	Fracture	2.0	–			
PB	Matrix	4,000 psi	–			
PB	Fracture	4,000 psi	–			

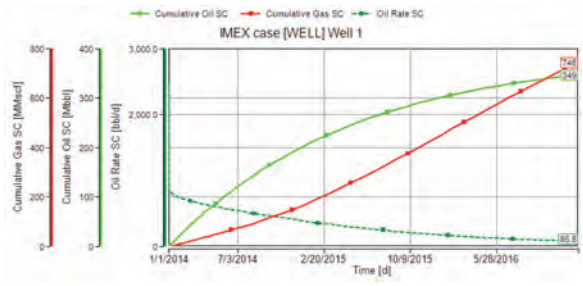

Fig. 23.9—The oil and gas production results from simulation study of Eagle Ford after 3 years.

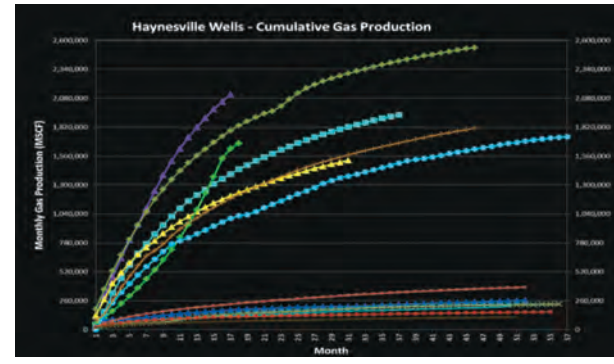

Fig. 23.10—Unproductive wells are at the bottom, but some of the wells in the upper section, while productive, are still sub-economic. At the time of this study (2013), each of these wells, including drilling and completion costs, was approximately $12M each. So, $72M was spent on uneconomic wells, just in this limited area of the reservoir.

usually two formations are targeted, the Bossier and the Haynesville. In this study the lower Haynesville formation is targeted. Integrated reservoir characterization and multi-attribute analysis were the main components of a joint project between Baker Hughes and CGG consortium named as Science Shale Alliance. One aim of this example was to show that variability in cumulative production of wells in the region was a result of random and poor completion strategy. Well log and hard mineralogical information (from Baker Hughes and Robertson, a division of CGG) were used to provide a strong calibration in the seismic inversion process. A multi-attribute analysis allowed the identification of the key reservoir attributes that contribute to the reservoir quality. These attributes included TOC, brittleness, mineralogy, facies, and

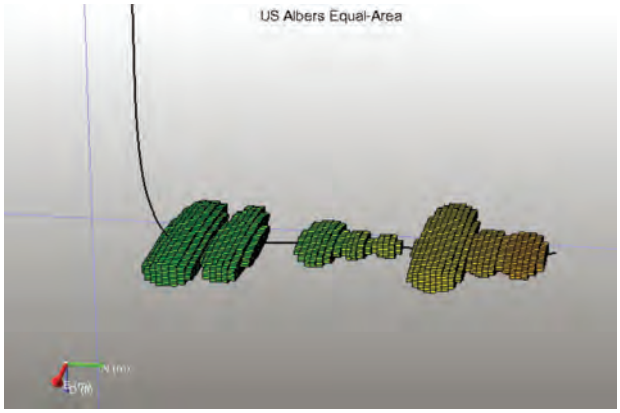

Fig. 23.11—The Stimulated Reservoir Volume for the Haynesville example for one of the wells (Well 3).

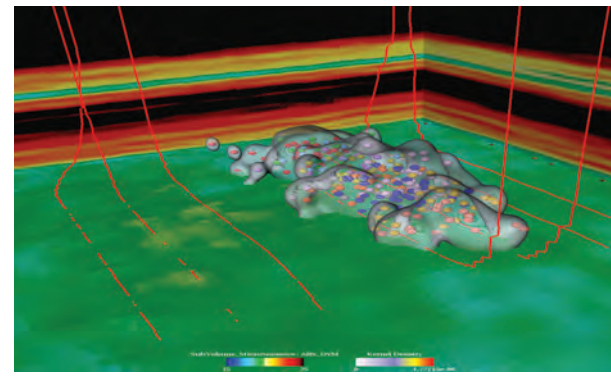

Fig. 23.12—Validation of SRV with the microseismic data for one of the wells (Well 3).

fractures and allowed to model predicted production and thus allowed optimization of the well placement and completion design. The well data was also used within the multi-attribute analysis to provide a robust training dataset for the prediction of reservoir properties into the 3D volume. It was shown that the operator could benefit significantly from the field by optimizing the completion and integrating the results from this study. **Fig. 23.10** shows the variability of production among the wells. The area for this study had 13 producing wells.

To proceed, the user may open the file named "CGGV_URT_Haynesville_Sept 3_Uncropped-Production.jewel." The simulation section of this case study is not provided and left as a practice for the readers and users. The properties of hydraulic fractures, natural fracture, as well as reservoir properties of the model are provided in **Table 23.7, Table 23.8, and Table 23.9**, respectively.

The 3D view of the generated SRV is shown in **Fig. 23.11**. The validation with microseismic data can also be seen in **Fig. 23.12**. As one can see, there is a perfect match between the predicted SRV and the actual microseismic data.

Fig. 23.13 shows the result of rate prediction for one of the wells based on general assumptions of gas prices and well costs. Note that the time at which we reach payback on each well varies from 16 months for Well 3 to almost 4 years for

Table 23.7—The properties of hydraulic fractures in the Haynesville example.

Hydraulic fracture stage #	MD (ft)	SRV width (ft)	Half length (ft)	Height (ft)	Width (in)	Permeability (md)
1	12801.9	800.0	50	200.0	0.022	10000.00
2	12451.6	800.0	50	200.0	0.022	10000.00
3	12075.5	800.0	50	200.0	0.022	10000.00
4	11745.7	800.0	50	200.0	0.022	10000.00
5	15629.6	800.0	50	200.0	0.022	10000.00
6	15279.3	800.0	50	200.0	0.022	10000.00
7	14923.4	800.0	50	200.0	0.022	10000.00
8	14578.1	800.0	50	200.0	0.022	10000.00
9	14209.3	800.0	50	200.0	0.022	10000.00
10	13860.1	800.0	50	200.0	0.022	10000.00
11	13515.7	800.0	50	200.0	0.022	10000.00
12	9131.0	800.0	50	200.0	0.022	10000.00
13	13157.3	800.0	50	200.0	0.022	10000.00

Table 23.8—The properties of natural fractures in the Haynesville example.

Type	Use	Fracture spacing (ft)	Width (in)	Permeability (md)
Primary XZ (explicit)	SRV	100.0	0.039	1000.0
Primary YZ (explicit)	SRV	100.0	0.039	1000.0
Secondary (implicit)	SRV	10.0	0.039	1000.0

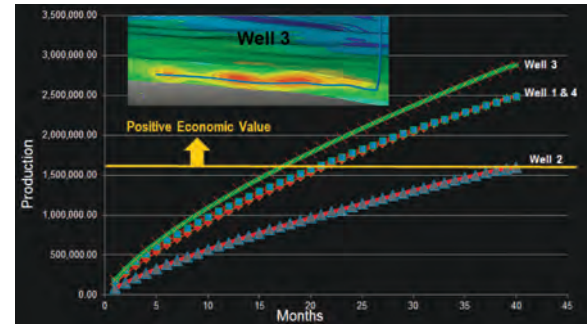

Fig. 23.13—Predicted production based on based on Sweet Spot Well Placement.

well 2. A great lesson for the operator from this study was to avoid spending on uneconomic wells which were drilled based on factory drilling approach and focusing on high grading field while improving production and reducing costs. Examples like this illustrate the joint capabilities of CGG and Baker Hughes and how the combined resource can provide a suite of services that can assist in all the major areas of shale play exploitation—from exploration and appraisal, through field development and rejuvenation (drilling, completions, production, and re-fracturing), along with microseismic to provide validation of completion designs. The combination and integration of technology provides a deeper understanding of the reservoir and potentially helps cut costs, reduce risk, and boost production.

Table 23.9—The properties of reservoir in the Haynesville example.

Name	Matrix or Fracture	Constant	Source
PERMI	Matrix	–	fracture folder\Kx-MAT
PERMJ	Matrix	–	fracture folder\Ky-MAT
PERMK	Matrix	–	fracture folder\Kz-MAT
POR	Matrix	–	fracture folder\Porosity-MAT
DIFRAC	–	–	fracture folder\Fracture spacing X
DJFRAC	–	–	fracture folder\Fracture spacing Y
DKFRAC	–	–	fracture folder\Fracture spacing Z
PERMI	Fracture	–	fracture folder\Kx-FRAC
PERMJ	Fracture	–	fracture folder\Ky-FRAC
PERMK	Fracture	–	fracture folder\Kz-FRAC
NETGROSS	Fracture	–	fracture folder\NTG-FRAC
NRTGROSS	Matrix	–	fracture folder\NTG-MAT
POR	Fracture	–	fracture folder\Porosity-FRAC
CTYPE	Matrix	1.0	–
CTYPE	Fracture	2.0	–
RTYPE	Matrix	1.0	–
RTYPE	Fracture	2.0	–
PB	Matrix	4,000 psi	–
PB	Fracture	4,000 psi	–

23.5 References

JewelSuite User Manual. 2013. JewelSuite™ Subsurface Modeling 2013, Easy–Fast–Accurate.

JewelSuite Subsurface Modeling (Baker Hughes). http://www.bakerhughes.com/products-and-services/reservoirdevelopment-services/reservoir-software/jewelsuite-reservoirmodeling-software (accessed 4 September 2014).

Vassilellis, G. Li, C., and Bust, V.K. et al. 2011. Shale Engineering Application: The MAL-145 Project in West Virginia. Paper CSUG/SPE 146912 presented at the Canadian Unconventional Resources Conference. Calgary, Alberta, Canada. 15–17 November. http://dx.doi.org/10.2118/146912-MS.

Walsh, F. R. and Zoback, M.D. 2-14. Wastewater Injection and Triggered Earthquakes in Oklahoma. (unpublished).

This page intentionally left blank

24

New Considerations and Future Trends in Reservoir Technologies for Unconventional Resources Development

I. Yucel Akkutlu, Texas A&M University

This page intentionally left blank

Chapter 24: New Considerations and Future Trends in Reservoir Technologies for Unconventional Resources Development

Foreword

During the last decade, the North American oil and gas market has seen significant advancement in horizontal well and multistage hydraulic fracturing design and implementation technologies. Yet, many areas still need to be addressed. A prime area that has not been addressed thoroughly is the complexities associated with what is termed as a newly created reservoir. More fundamentally, do we have a clear understanding of the flow behavior of these ultra-tight rocks stimulated with multistage fracturing? The short answer is: no. This chapter explores the complexities of the newly created reservoir, focuses on some of the critical aspects of production, and identifies future trends in shale resource development.

Creation of a reservoir is a new concept for us as engineers. Traditionally, we dealt with reservoirs that were created over geological time in various depositional environments and later charged with hydrocarbons that migrated from a source rock. These accustomed reservoirs are characterized by some fundamental features related to their hydrocarbon storage capacity and fluid transmission ability. According to this traditional view, a unit bulk volume of subsurface formation with low porosity and permeability can hold a limited amount of hydrocarbons in-place. Also, fluids production from the formation can experience a rapid decline and take place at low rates. Although this formation may be considered a reservoir, it may not be a target for the field development. As another example, which is an extreme case, a formation with low porosity and ultra-low permeability, such as the seal rock, cannot be considered a reservoir, although it may contain and transmit some fluids over a long period of time.

Many hydrocarbon-bearing shales were discovered during the early twentieth century and evaluated with this mindset and, thus, were ignored as potential energy resources. Now it is globally recognized that the rapidly evolving horizontal well drilling and hydraulically induced fracturing technologies changed this traditional view and converted these formations into productive reservoirs. These technologies are more affordable day by day and drive the exploration for new discoveries of shale plays.

This renewed interest in exploiting the resource shales led to a remarkable transition. Now reservoir engineers are participating in the reservoir creation process. Drilling a well with a several thousand feet long lateral and multiple-stage fracturing creates a massive stimulated reservoir volume that could be described as a complex wellbore-fracture network and still be identified with the traditional reservoir requirements of decent porosity and permeability.

Reservoir creation is a radical change in petroleum field organization and development. It impacts our normal way of thinking as reservoir engineers. The external boundaries of the created reservoir need to be accounted for in economic recoveries, rather than the geological boundaries. Also, a new generation of key reservoir quantities is in the literature, such as the stimulated or created reservoir volume, the total effective and crushed fracture lengths, the total matrix surface area draining into the wellbore fracture system, etc. How appropriate that the new terminology often is argued by various expert groups. As new reservoir parameters appear and are used more frequently with the shales, we realize that the basic features of the classical reservoir are becoming less meaningful.

As the closing of this book, this chapter addresses these transformations in the resources assessment and development. In parallel, some of the important future trends and considerations in petrophysical characterization and reservoir engineering are covered.

24.1 Kinetics of Hydrocarbon Maturation, Fracture Initiation, and Propagation

In various basins throughout world, the source rocks are over-pressured (in excess of hydrostatic) sedimentary beds undergoing burial at a range of depths suitable for the onset of fractures. The fluid pressures in excess of the least compressive stress in a regional stress field potentially could lead to inelastic behavior and fractures (Hubbert and Willis 1957). The source rock deformation most commonly begins on a much smaller scale, however, at fluid pressures well below the least compressive stress (Handin et al. 1963). These deformations are characterized by microfracture development. Palciauskas and Domenico (1980) argued that the average rate of microfractured zone propagation keeps pace with the rate of sediment burial. There are arguments in literature on the geological time scales pertaining to the

kinetics of hydrocarbon maturation, microfracture initiation, and propagation. These arguments are important to our understanding of the oil and gas migration and accumulation in the source rock.

From a shale oil and gas production point of view, microfractured zones are important because they add to the pore volume—fluid storage. As with hydraulic fracture, microfractured zones create a preferred orientation nearly normal to the least compressive stress. Consequently, regions of high-fluid storativity and directional flow capacity could occur in the hydrocarbon production zone of the resource shale. Identification of these regions and heterogeneous resource shale characterization is an important task that requires integrated studies involving many fields including basin and petroleum systems modeling. Here, the impact of microfractures on production from shale is shown using an apparent permeability approach.

24.2 Stress-Sensitive Microfractured Shale Matrix Permeability

Because of their geometry, microfractures are sensitive to effective stress. Although numerous models previously were proposed to capture the stress dependence of the permeability, we have rather limited choices for microfractured pore-network models (Gangi 1978; Walsh 1981). Kwon et al. (2004) previously showed that Gangi's model could represent the stress-dependent permeability of shale. The model describes an apparent shale permeability k_m as follows:

$$k_m = k_o\left(1-\left(\frac{p_c-\alpha p}{p_1}\right)^m\right)^3 \qquad \text{(Eq. 24.1)}$$

In **Eq. 24.1**, $p_c - \alpha p$ is the effective stress on the microfractured shale matrix. k_0 is the permeability at zero effective stress, i.e., $p_c - \alpha p = 0$. p is the fluid pressure, = often referred to as the pore pressure or reservoir pressure during the production. p_1 is the effective stress when the microfractures are closed completely and when apparent permeability equals to zero. The exponent m is associated with the surface roughness of the inorganic pores. In his original paper, Gangi (1978) considered that the microfracture surfaces could be rough, and he conceptually modeled this roughness as a bed of nails supporting the fracture walls. In the model, m represents a distribution of the height of nails. If the nails' heights are close to uniform with only a few shorter nails, then m is close to unity. If

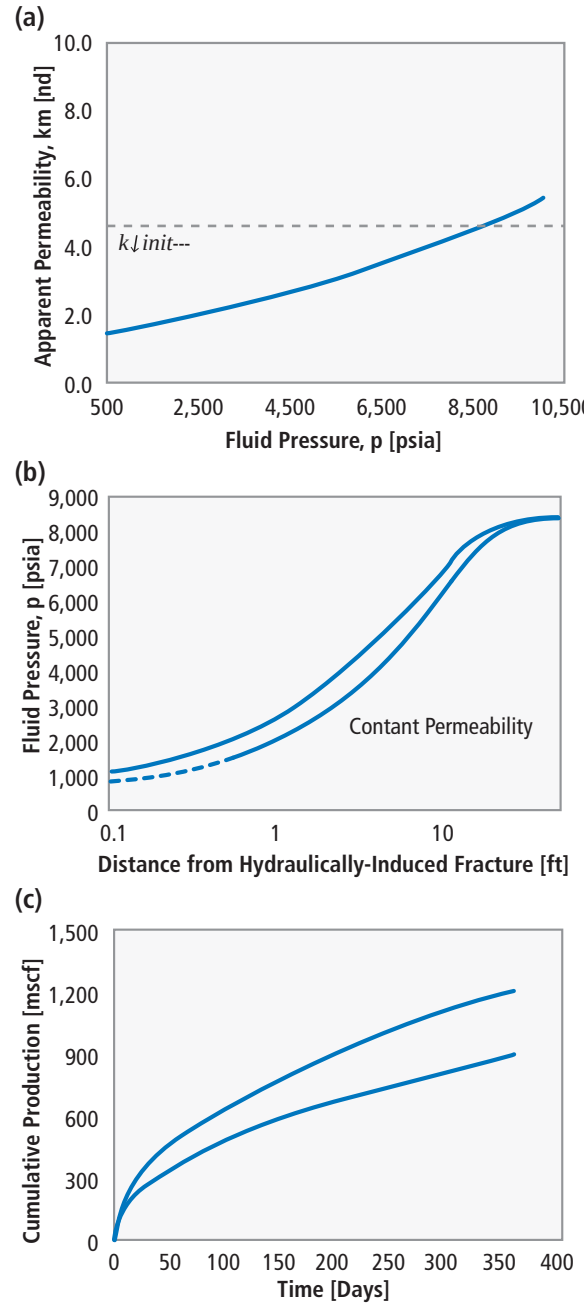

Fig. 24.1—Apparent permeability (a) of a microfractured shale matrix dynamically influences the shale reservoir depletion using a hydraulically induced fracture (b) and cumulative production (c). To demonstrate the influence of the matrix permeability on production, a 1D flow simulation is conducted. A bulk rock volume of 50 ft. x 350 ft. x 30 ft. with a planar hydraulic fracture cell attached at the left side is considered. A producer well is placed in the fracture cell so that the fluid flows from right to left. One year of production is simulated. (Adapted from Wasaki and Akkutlu 2014.)

there is significant variability in the heights, then the surface roughness increases and m takes values close to zero.

Fig. 24.1(a) shows Gangi's permeability model response to fluid production from shale using a nearby hydraulically induced fracture. Note that k_{init} indicates shale permeability at initial reservoir pressure, which is calculated using **Eq. 24.1** with the value of the initial reservoir pressure of 8,350 psi. The apparent shale permeability changes with the fluid pressure due to stress dependence. It decreases with the pressure due to increasing effective stress as the consequence of the aperture of the microfractures closing with the effective stress. The effective stress builds up linearly; hence, the permeability decreases monotonically as the pore pressure is reduced.

Fig. 24.1(b) and **Fig. 24.1(c)** show the numerical simulation of depletion of this microfractured shale matrix and the cumulative recovery during a one-year production. The details of simulation can be found in Wasaki and Akkutlu 2014. Fig. 24.1(b) shows the fluid pressure profile near the induced fracture. Note the retardation experienced during the depletion due to a decrease in the shale matrix permeability. This significantly influences the cumulative gas production because the study predicts a 25.6% reduction in total produced gas amount at yearend. The microfracture sensitivity to the increasing effective stress during production leads to delayed depletion and reduced production.

Because of this, in hydrocarbon producing zones with microfractures, permeability needs to be treated as a dynamical quantity sensitive to the local production conditions. The common industry practice, however, is to treat the shale matrix permeability as a constant or consider its dynamics as part of the stress dependence of the artificially induced hydraulic fractures. One must differentiate that the two media hold their own unique dynamics during the production.

According to this view, one needs to carefully separate the microfractured matrix permeability from the induced-fracture permeability. The microfractured matrix permeability is a direct measure of the formation diffusivity and indicates how fast the pressure transient diffuses away from the induced fractures and how soon the induced fractures begin interfering. The induced-fracture permeability is a measure of how effectively we can produce the fluids.

In our resource shales description, we have considered an important feature although we are far from a complete picture of these prolific rocks. In the next section, other important features are described related to their organic nanoporous nature.

24.3 Resource Shales as Naturally Occurring Nanoporous Materials

In general, shale sediments with the potential for oil and gas recovery are thermally mature and rich in organic matter, also known as kerogen (Wang and Reed 2009; Loucks et al. 2009; Sondergeld et al. 2010; Ambrose et al. 2012). Kerogen often exists as finely dispersed organic phase within the inorganic shale matrix (**Fig. 24.2**). With its nanoscale pore network, kerogen is another important constituent of the shale total pore volume that is related to not only the in-situ generation of hydrocarbon fluids but also to their storage and production (Kang et al. 2011; Akkutlu and Fathi 2012; Wasaki and Akkutlu 2014).

Although they have a relatively small pore volume, the source rocks consist of a dual pore structure, with organic and inorganic (microfracture dominant) pores, contributing to the storage of hydrocarbon fluids. With a significant portion of them at nanoscale with sizes less than 100 nm, the organic pore volumes are not much larger than the fluid molecules they store. Molecular simulations of methane in model pores showed that phase behavior of simple fluids, such as methane in such a small space or under confinement, is different and could lead to various thermodynamic states (Ambrose et al. 2012). Consequently, new phases could develop and co-exist in the pores.

Fig. 24.3 shows simulated methane behavior in an organic pore as part of a methane-rich (dry) shale gas reservoir. The behavior is shown in terms of the fluid density profile obtained from thermodynamic equilibrium molecular simulation in the canonical ensemble, which is also known as NVT ensemble. The estimated fluid pressure at the center

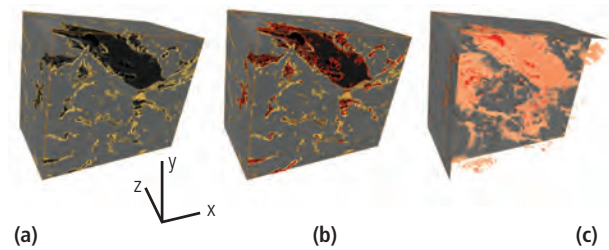

Fig. 24.2—Three-dimensional FIB/SEM segmentations of 300 separate 2D SEM scans generated by our research group. Sample size is 4 μm high, 5 μm wide, and 2.5 μm deep. In (a) yellow outlines the 3D kerogen network; (b) red outlines porosity (in this sample all porosity is found within the kerogen); and (c) in an overlay of a porosity and kerogen 3D network, orange is kerogen, and dark orange depicts porosity within the kerogen. The figure is adapted from Ambrose et al. (2012).

of the pore is 3,043 psi, which is a typical value for various gas shales (Ambrose et al. 2012). Methane shows a distinct density behavior characterized by rapidly damped oscillations that allows us to differentiate the adsorbed fluid by the walls from the bulk or free fluid at the pore center. The discrete density profile on the right exhibits transition layers located between the adsorbed and free methane indicating constant adsorption and release or desorption of the molecules under equilibrium conditions.

Conversely, **Fig. 24.4** shows another numerical methane density profile across a pore. This time the pore is somewhat larger and holds a liquid-gas interface parallel to the wall. Significantly large oscillations in density appear due to presence of the liquid phase and its adsorption by the wall. The oscillations penetrate deeper into the pore space and influence the nearby interface properties on the right. This indicates amplified molecular interactions in the presence of liquid and shows that the liquid is in the stronger wetting phase than the gas. The computed tangential pressures (parallel to the wall), pT, are often two to three orders of magnitude larger than the normal pressure, pN. In addition, the tangential pressures by the wall are one order of magnitude larger compared to those by the interface. These pressures influence the liquid-gas interfacial tension depending on the level of confinement.

The anisotropy in pressure and its influence on the liquid-gas interfacial tension are dependent on several factors. The numerical investigations show that the closest distance from the interface to the walls matters. In **Fig. 24.5**, we show the methane density profile and the pressure (pT-pN) profiles while the thickness of the liquid layer by the wall is decreased; hence, the interface approaches to the wall. The distinct shape of anisotropy across the interface changes in Fig. 24.5 becomes more influenced by the density oscillations caused by the adsorbed liquid.

The methane interface in Fig. 24.4 and Fig. 24.5 is known to have an interfacial tension value 12.88 mN/m in the bulk (Muratov 1982). However, the simulations show that the tension becomes a variable under the confinement (**Fig. 24.6**). It now has values changing between 8 to -0.05 mN/m, depending on the thickness of the liquid layer by the wall. Interestingly, when the thickness becomes too small (toward left on the x-coordinate), we observe a negative tension. The surface tension is typically positive, which indicates that an amount of work is required to increase the interfacial area by one unit. Because any change in a system must be in the direction of decreasing free energy (second law of thermodynamics), a system with positive surface tension shall

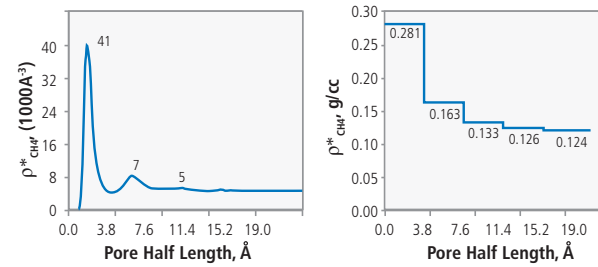

Fig. 24.3—Number density (left) and discrete density (right) profiles are shown for supercritical methane at 176°F (80°C) within a 3.9 nm slit-shape pore with graphite walls. Density values are estimated at each 0.2Å interval for the continuous density profile. Discrete density corresponds to molecular layer density for methane across the pore. The figure is adapted from Ambrose et al. (2012).

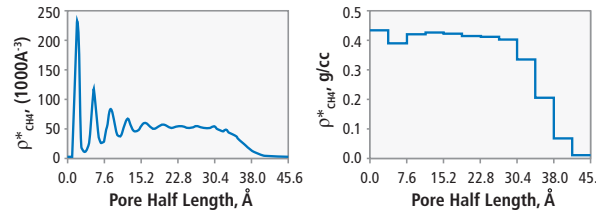

Fig. 24.4—Number density (left) and discrete density (right) profiles are shown for liquid-gas equilibrium in a 9.1 nm slit-shape pore with MgO walls. The liquid-vapor interface is located toward the pore center where the density decreases rapidly. Density values are estimated at each 0.2 Å interval for the continuous density profile. Discrete density corresponds to molecular layer density for methane across the pore.

reduce the interfacial area. For example, the shape of a free water droplet in equilibrium with vapor is a sphere where the area is minimized. On the contrary, the interface dynamics of the resource shale fluids (e.g., phase nucleation and transport) in small pores appears to be different and could be controlled, or fully driven, by the matrix walls.

Fig. 24.3, Fig. 24.4, Fig. 24.5, and Fig. 24.6 indicate that the density of hydrocarbon fluids and pore pressure have a relatively complex structure in small organic pores. Due to lower dimensionality of the pores and strong wall-fluid interactions, fluid storage and transport properties could change under confinement (Akkutlu and Fathi 2012; Fathi and Akkutlu 2013; Rahmani and Akkutlu 2013). In a more general sense, the thermodynamics of hydrocarbon fluids are influenced by the small pores of the shale matrix. This could have significant implications in the economical assessment of shale resources, in particular, during initial hydrocarbons

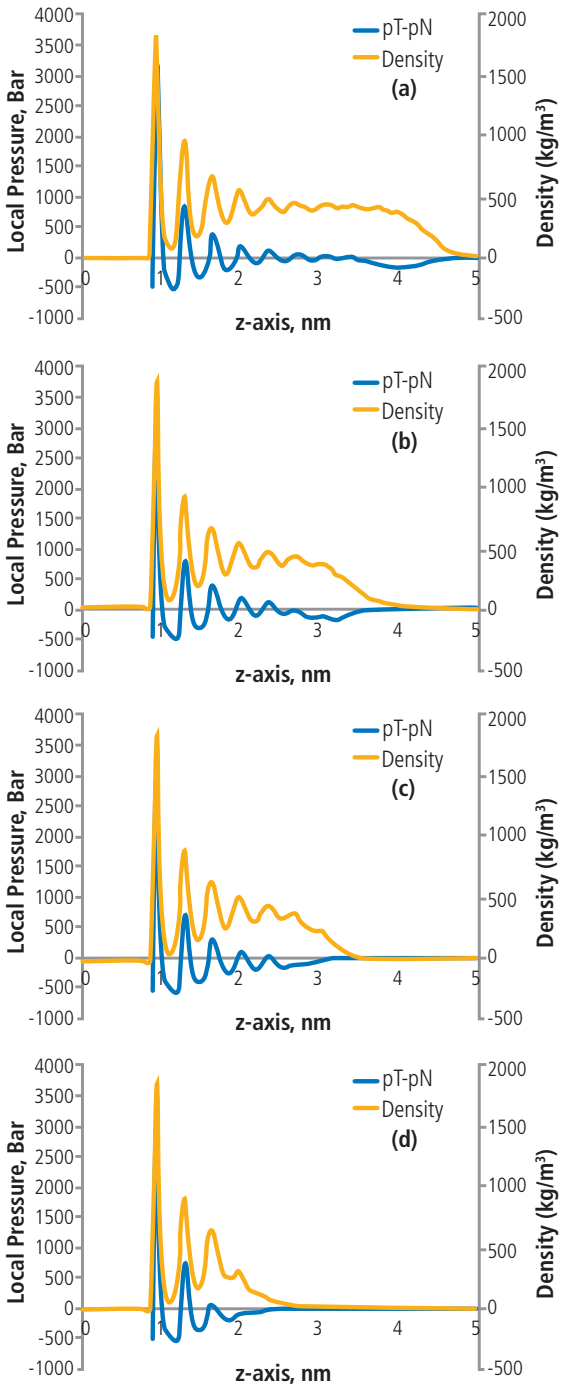

Fig. 24.5—Density and (pT – pN) profiles of methane across the half-length of 8 nm slit-pore when the thickness of the liquid phase is reduced. For clarification, the density and pressure profile are plotted up to z = 5 nm. The figure is adapted from Bui and Akkutlu (2014).

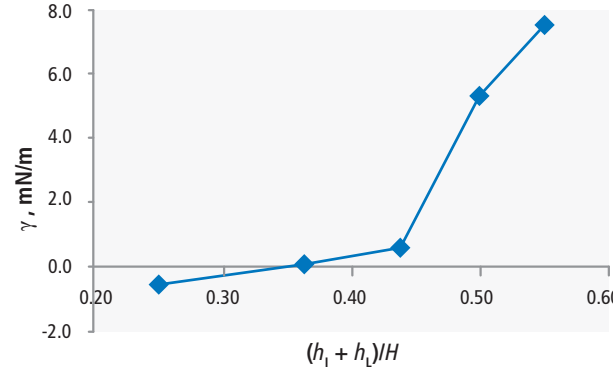

Fig. 24.6—Liquid-gas interfacial tension of methane under confinement as a function of liquid saturation, $(h_I+h_L)/H$. Here, h_I, h_L, and H are the thicknesses of the interface, the liquid phase, and the pore, respectively. The figure is adapted from Bui and Akkutlu (2014).

in-place calculations, and production rate predictions when the fluids in shale matrix are exposed to pressure depletion.

The volumetric calculation based on a water-saturation corrected hydrocarbon pore volume is a difficult task because the hydrocarbon phases inside the small pores have thermodynamic properties that could significantly vary depending on the micro- and mesopore size distribution of the shale matrix. The separation of these phases across the pore size distribution makes flow and molecular transport processes in the pore network complicated. Viscosity, effective permeability, and critical saturations are the fundamental quantities influenced by the distribution of phases and their co-existence under confinement. This raises serious questions on what the producible liquid is and brings in added uncertainties during the prediction of flow in the reservoir.

24.4 From Reservoir Uncertainties to Reservoir Anomalies

In the previous section, we briefly discussed methane behavior in small pores and the co-existence of its liquid and gas phases under confinement. One important consequence of this fundamental level pore-scale observation is that the assessment of gas shales as a resource involves free-phase and adsorbed-phase molecules. Previous work by Ambrose et al. (2012) led to development of a new shale gas in-place calculation based on these molecular-level considerations. Accordingly, during the gas in-place calculations, to properly account for the total and free gas in-place, the shale pore volume occupied by the adsorbed-phase must be determined and subtracted from the total free gas pore volume (**Fig. 24.7**).

Developing new downhole technologies that will predict the volume taken up by the adsorbed phase is an active research area. A future consideration is delineation of the fluids as free and sorbed fluids, as well as separating the phases in the organic nanopores. Currently, we estimate the adsorbed volume by volumetric or gravimetric measurements in the laboratory and using the Langmuir model.

This procedure gives the Langmuir parameters, Gs_L and p_L. The required adsorbed-phase correction on the free gas amount is estimated as follows (Ambrose 2012):

$$G_f = \frac{32.0368}{B_g}\left[\frac{\Phi(1-S_w)}{\rho_b} - \frac{1.318\times10^{-6}\hat{M}}{\rho_s}\left(\frac{G_{sL}p}{p+p_L}\right)\right] \quad \text{(Eq. 24.2)}$$

The volume taken up by the adsorbed phase is represented by the negative term inside the bracket. The volume must be accounted for after the correction for water saturation. This equation is widely used by the unconventional gas industry. However, today we know that there are conditions when it may not work efficiently. First, if the petrophysical and adsorption data are collected poorly, either due to poor analysis and/or alteration of in-situ rock characteristics, any free gas volume correction could be wrong and typically show up as a negative free gas storage capacity. Most of the time this negative anomaly is low and within the bounds of experimental error. However, sometimes we have seen the free gas volume extremely negative and indicative of a real problem.

In post mature shales such as the Marcellus or Haynesville shales, some evidence (production history, logs, etc.) Indicates imbibition of water during coring such that the core is non-representative. Similar problems could occur when the isotherm is inappropriate (i.e., wrong temperature is used, poor laboratory analysis performed, or the samples are contaminated, etc.); the molecular weight/density ratio of the adsorbed phase is not known; or during sample processing aliquots designated for porosity and fluid saturation measurements either imbibe or desiccate moisture.

Isotherm results on multi-component, liquid-rich, bubble-point systems could be non-representative, especially if the bubble point (i.e., the solution gas concentration) is far below the reservoir pressure. During the entire isotherm test, the system at equilibrium is at the bubble point such that the resulting adsorption, which is the sum of the truly adsorbed-phase and the solution gas (i.e., absorbed gas) is too high.

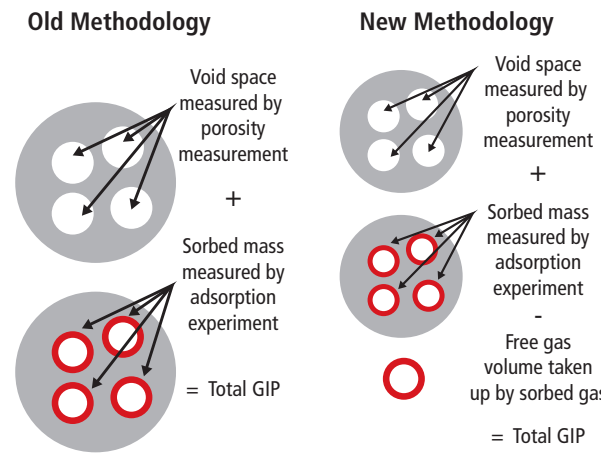

Fig. 24.7—Comparison of the old and new methodologies in predicting shale gas-in-place. For simplicity, oil and water volumes are not shown. The figure is adapted from Ambrose et al. (2012).

Finally, the extremity of reservoir conditions also leads to important confinement effects in the reservoir, which in turn, puts another restriction on the application of our equation. At high pressures, we observe excess amounts of the adsorbed phase that appear as semi-liquid methane on the density profile across the model pore (**Fig. 24.8**). The basic assumption of a single-layer adsorbed phase of the Langmuir theory is not tolerable in this case. Nevertheless, if we persisted in using the Langmuir model to quantify the adsorbed volume, the adsorption measurements under the same subsurface conditions using cores would give extremely large sorption capacity for the sample such that the adsorbed-phase correction would make the free-gas volume, again, negative.

Putting aside the problems related to data collection and measurement errors, this discussion indicates that our volumetric free gas in-place equation has fundamental-level limitations dealing with shale gas reservoirs under extreme reservoir conditions and with liquid-rich shales. This is a serious issue and shows that we do not have suitable tools to assess these shales accurately as a resource.

Revisiting Fig. 24.8, we notice other problems related to our ignorance of the fluid phases existing in the shale matrix. Earlier we referred to the excess amount of adsorbed phase as semi-liquid. During the production, as the pore pressure drops, this high-density methane probably will be released or desorbed and produced as a gas or supercritical fluid. This behavior is fundamentally different than the liquid (oil) behavior occupying the same pore under the same

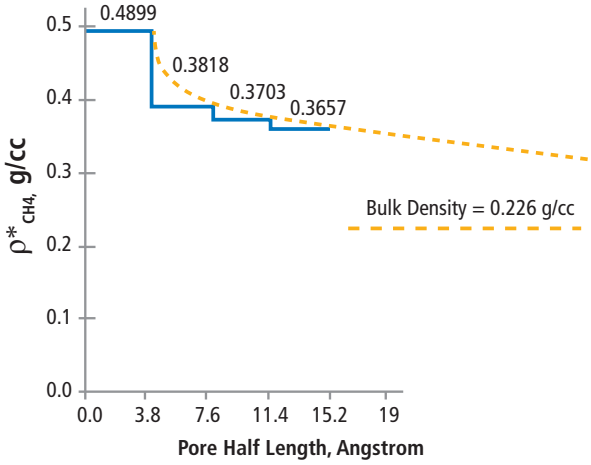

Fig. 24.8—Supercritical methane discrete density profiles across half length of a 4 nm slit pore at 11,000 psi and 340°F (initial Haynesville reservoir conditions). Methane is not observed as free fluid at the center of the pore but rather in a semi-liquid state, the density of which is not too different than the adsorbed phase density. The curve fit indicates that the pore should have been larger than 10 nm for the methane to develop the free state (as in Fig. 24.2) under the initial Haynesville conditions.

conditions. Being the stronger wetting phase and due to its lower mobility, the liquid may not be produced at economical rates (**Fig. 24.9**).

How accurately can we separate and quantify the semi-liquid sorbed phase, which appears to be producible, from the truly liquid phase? The current technologies mainly rely on contrast in physical and transport properties of the fluids, such as density. However, any contrast probably is minimal when we compare the sorbed and liquid phases. Currently it is a difficult task to investigate these phases in the shale matrix.

24.5 Permeability of Organic-Rich Nanoporous Shale with Microfractures

Based on the discussions in the previous section, one can revisit the stress-sensitive permeability model and propose a modification for the presence of fluids in organic rich shale. This model could be based on an approach similar to conventional treatment of the two-phase flow in porous media: each phase follows its own path obeying its own transport mechanisms. Thus, we consider parallel flow of free-gas phase and adsorbed-phase:

$$k_{gas} = k_m + \mu D c_g + \mu D_s \frac{V_{sL}\rho_{grain}B_g}{\varepsilon_{ks}} \frac{p_L}{(p+p_L)^2} \quad \text{(Eq. 24.3)}$$

Details of the derivation of **Eq. 24.3** are in Wasaki and Akkutlu (2014). In the equation, we observe the contributions

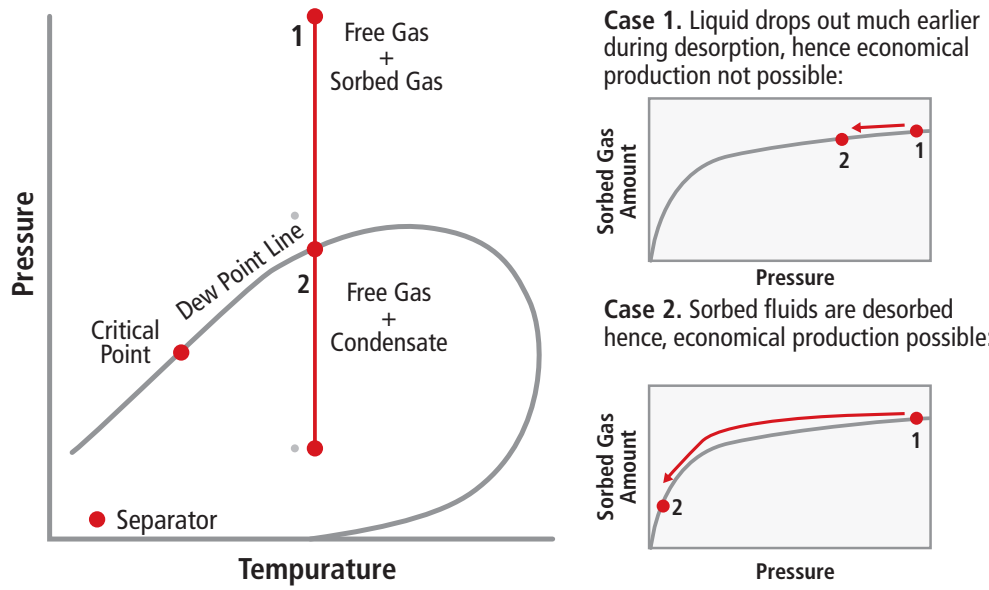

Fig. 24.9—Nanopore size-adjusted phase envelop and the adsorption curve for a retrograde condensate fluid. Currently it is not clear if this fluid would desorb and be produced during the depletion of the reservoir. A similar discussion could be made for shale oil with the initial pressure (point 1) on the left hand side of the critical point.

of several transport mechanisms: km reflects stress-dependent permeability of the microfractured inorganic network as described earlier in Eq. 24.1. The second term includes the contribution of free gas molecular diffusion both in the organic and inorganic pores. The third term includes the contribution of the adsorbed phase transport through the organic pore-network. The last two terms in Eq. 24.3 include deviation from the stress-sensitive Darcy flow.

Eq. 24.3 is derived for gas transport in organic-rich microfractured shale matrix. When the liquid hydrocarbons (oil) is transported, new considerations should come into play. As shown in Fig. 24.4, the solid-liquid interactions associated with the adsorbed liquid molecules in the organic pores are significantly larger in comparison to the natural gas case. This is due to presence of much larger attractive forces by the walls in the presence of liquid. Furthermore, the mobility of free liquid phase is not large either if there is a significant amount in the central portion of the organic pores. Hagen–Poiseuille type flow would be negligible due to the small capillaries. The diffusion in liquid is known to be several orders of magnitude smaller than that in the gas phase. Consequently, the liquid in kerogen is considered limited mobility, in particular, compared to the mobility of gas. The liquid cannot diffuse and cannot be transported on the adsorbed phase. This leaves us with an apparent permeability for liquid as follows:

$$k_{liquid} = k_m \qquad \textbf{(Eq. 24.4)}$$

This behavior of the shale matrix permeability is shown in Fig. 24.1a and in **Fig. 24.10** in the presence of permeability model as described by Eq. 24.3. Again, no molecular transport mechanisms came into play in the case of the liquid. Conversely, the predicted apparent permeability for gas shows a trend similar to that with liquid at high pressure. The molecular transport comes in as a positive effect on permeability as the pore pressure (effective pressure) is decreased (increased) further. Consequently, the permeability reduction rate decreases, reaching a zero rate (a minimum permeability) at around 4,000 psia for the base-case values given by Wasaki and Akkutlu (2014). Interestingly, roughly below 3,000 psia the predicted permeability improves rather dramatically. This increase in permeability indicates that the overall transport is significantly improved even though the microfractures are closed. The improvement in this case is driven by the molecular transport mechanisms, i.e., the diffusion of free and adsorbed molecules. This results in a relatively large difference in the cumulative recovery produced by the induced-fracture when compared to the liquid case.

By comparing the observation to a production from organic-rich shale and based on the numerical results, it

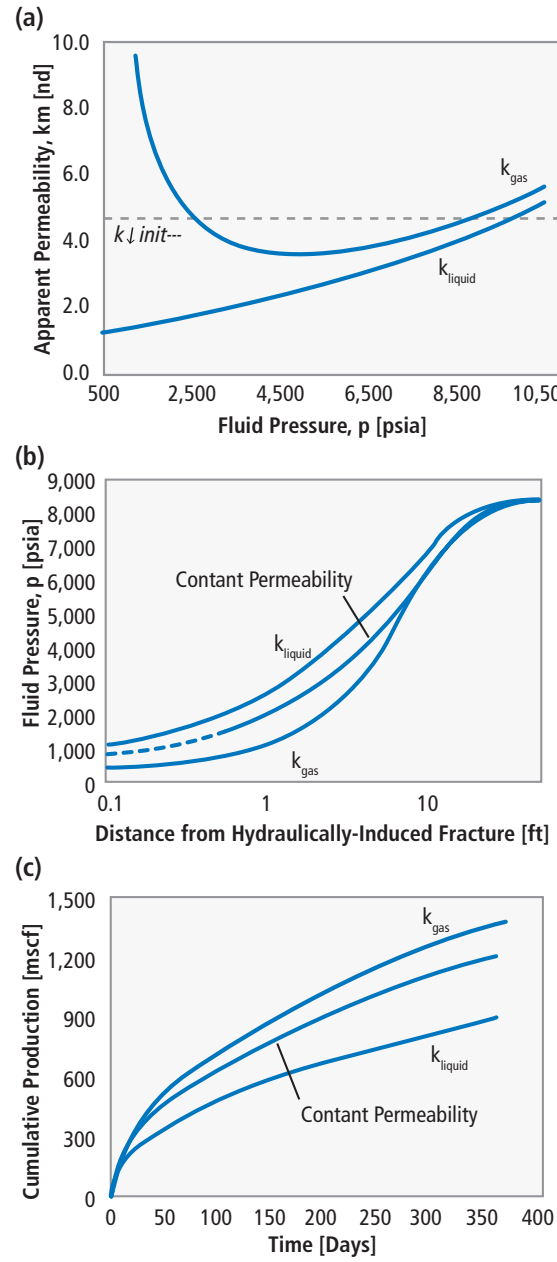

Fig. 24.10—Apparent permeability (a) of an organic-rich nanoporous shale matrix with microfractures dynamically influence the shale reservoir depletion (b) and cumulative production (c).

is expected that the non-Darcian effects are dominating near the fractures, which could appear as improvement in permeability. The flow mechanism shifts to stress-dependent viscous flow away from the fractures. Note that the non-Darcian effects introduced in Eq. 24.3 are different from the so-called slippage effect due to amplified fluid-wall molecular interaction observed at low-fluid pressure.

In the permeability model, this near-fracture improvement is attributed to the free gas and adsorbed gas density gradients in the matrix. Note that the adsorbed gas transport is not the transport of the originally adsorbed fluid that has been desorbed and produced. It is the fluid that is driven by the adsorbed phase gradients near the walls. These effects appear in the reservoir at relatively high-fluid pressures (**Fig. 24.11**).

24.5.1 Pore-Size Effect on Fluid Phase Behavior and Properties

Our recent simulation results indicate that a behavior similar to that with methane in Fig. 24.8 develops in much larger pores at lower pressures when we consider multicomponent fluids. However, for these fluids identifying the phases and their producibility limit is even more difficult to determine in the laboratory. This is because the critical properties of the components change (Singh et al. 2009) and the phase diagram of the fluid mix shifts unpredictably under organic nanopore confinement in the shale matrix.

In the presence of a single-component fluid in a slit-shaped organic nanopore, the interaction of the wall molecules with the fluid molecules becomes a key element to understanding the behavior of that fluid in the pore. These fluids form a certain density profile across the pore (Fig. 24.3). Along the pore walls the interaction between the fluid molecules and wall molecules is the greatest. The fluid molecules are made up of hydrogen and carbons. Carbon, due to its high bonding energy, can easily form strong covalent bonds with other carbons, hence the abundance of carbon chains in nature. When the carbon pore walls come into contact with fluid carbons in the tiny environment of a few nanometers wide, this tendency of the carbons causes the fluid molecules to be attracted and adsorbed onto the pore walls. From this, we can readily predict that longer-chain alkanes, having greater number of carbons in their chain, will be under greater influence of the carbon walls and, therefore, will be adsorbed in greater strength to the walls. As a consequence, if a mixture of different alkane molecules were inside a carbon pore, the longer-chained or heavier alkanes would be those that would occupy the surface along the walls. This often is described as the wall becoming more selective of longer-chain alkanes and will be addressed in later sections of this chapter.

The density profile mentioned above is created as the strong influence along the wall is gradually dampened across the pore. Therefore, the least density of fluid molecules is expected to be in the central portion of the pore (See Fig. 24.3). Such a behavior is completely different from the

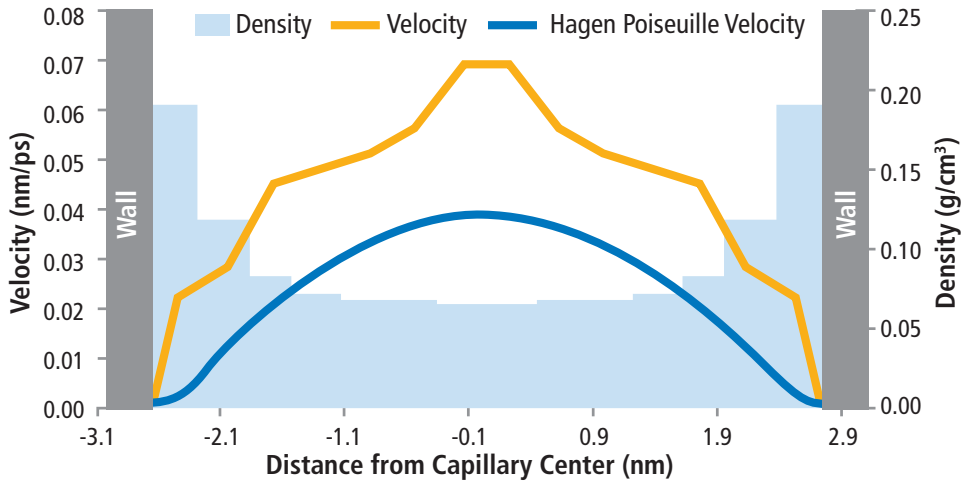

Fig. 24.11—Methane density and velocity profiles under steady-state conditions in a 6-nm diameter and 10-nm length single-wall carbon tube. The average fluid pressure across the tube is 1,687 psia, and the pressure drop across the tube is 50 psia. The figure includes the velocity profile of the equivalent Hagen–Poiseuille flow inside the tube. The figure is adapted from Riewchotisakul (2014).

uniform density profile of the fluid in a bulk state and in larger pores of conventional reservoirs and is, therefore, bound to disrupt the phase behavior and critical properties of the fluid. To investigate this matter, molecular simulations (**Fig. 24.12**) were conducted and found to be in agreement with the initial theory. These findings are reported in our previous work as well as in the works of Singh et al. 2009 (**Fig. 24.13a**). In the same pore size, the phase diagram of a confined longer (heavier) alkane (n-butane) shifts lower than the amount that the lighter (methane). In other words, the phase diagram of confined heavier alkane is more affected because its molecules are under greater influence of the walls.

The effect of pore size on the phase diagram of binary mixtures was studied. Fig. 24.13, shows the phase diagram of a 50% methane and 50% n-butane binary mixture in unconfined (bulk state) and in three confined states (4 nm, 5 nm, and 6 nm). The shift in the phase envelope of the mixture in a 4-nm-wide pore is quite striking. As the pore becomes wider, the phase envelope approaches that of the bulk state mixture. Based on the diagram, it can be predicted that at around 7- to 8-nm pore widths, the confined mixture phase envelope would completely overlap that of the bulk mixture. Therefore, the effects of confinement at these larger pores would disappear and the confined mixture could be treated as bulk mixture. As such, for the remainder of this work, simulations and studies of confinement are conducted in pores of 4-nm widths.

As stated earlier, in addition to pore size, fluid composition in mixtures also plays an important role in its phase behavior in confinement. The role of composition can be demonstrated

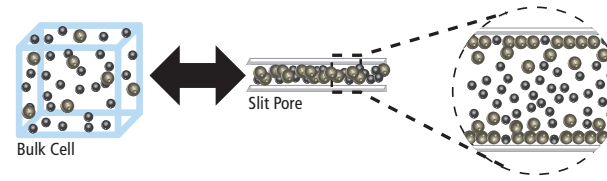

Fig. 24.12—A schematic of the molecular simulation setup used in work by Rahmani and Akkutlu (2013) showing the distribution of molecules at final equilibrium state.

using the same methodology (**Fig. 24.14**). The goal is to study the effect of both the light and heavy alkanes in a binary mixture in confinement first by increasing the composition of the light component (methane), from 50% to 90%, in three different binary mixtures and second, by studying the same three binary mixtures, in which methane is the constant component and ethane, n-butane, and n-octane are the second components of these three mixtures. In Fig. 24.14a, the mixture studied is a binary methane and ethane. On the left, the mixture is equimolar (50% C1 and 50% C2), and on the right, the mixture is 90% methane and 10% ethane. The shift in phase envelope that confinement has caused is not significant even when the methane percentage is increased to 90% (right). Nonetheless, the shift due to increased methane (right) is slightly observable.

The mixture in **Fig. 24.14b** is of methane and n-butane; on the left, equimolar and on the right, 90% methane. The shift in the phase envelope for the equimolar mixture (left) is again almost negligible but is now considerable for the 90% methane case of the mixture (right). The shift for the 90% methane mixture has caused an almost 100K decrease in the critical temperature. Similar to the previous two cases, the binary

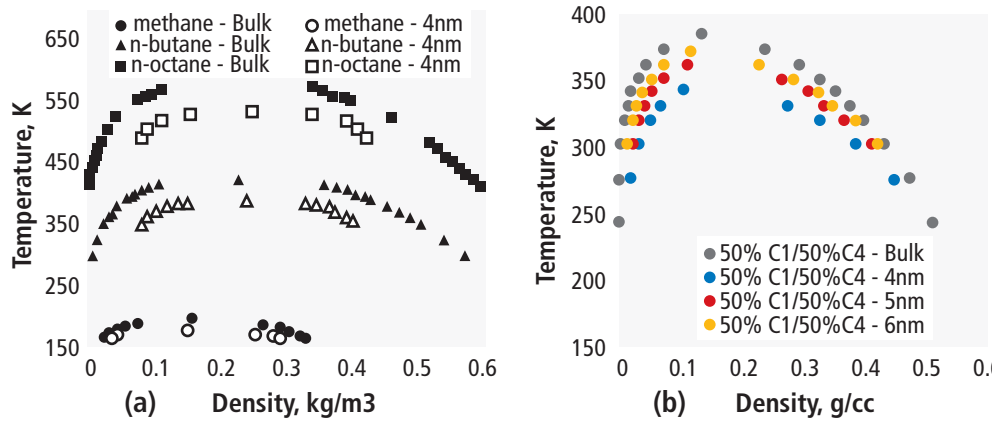

Fig. 24.13—Vapor-liquid coexistence phase envelopes of alkanes used in this work (left) (methane from our previous work; butane and octane from Singh et al. 2009). Vapor-liquid coexistence phase envelopes of a binary 50% methane and 50% n-butane mixture in bulk and confined state (right).

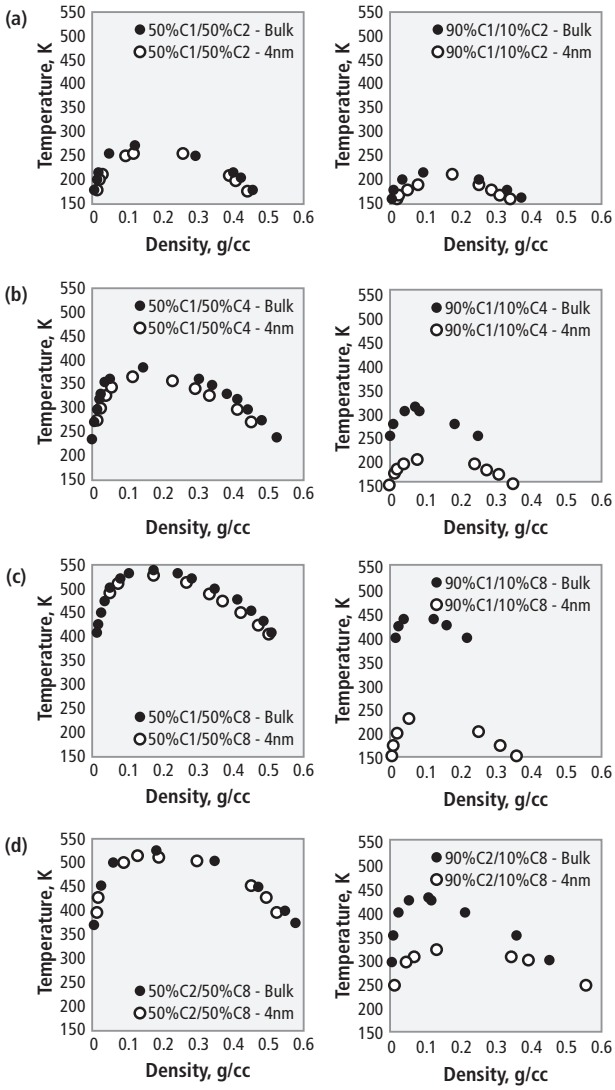

Fig. 24.14—Vapor-liquid coexistence phase envelopes of binary mixtures (a) C_1-C_2, (b) C_1-nC_4, (c) C_1-nC_8, and (d) C_2-nC_8. Left: 50% C_1. Right: 90% C_1.

mixture of methane and n-octane is studied (**Fig. 24.14c**). The shift for the equimolar mixture (left) is again negligible, but the shift for the 90% methane mixture (right) is striking.

Based on these findings, a trend can be detected. At equimolar binary mixtures of methane and longer-chained alkanes, the shifts in phase envelopes due to confinement are insignificant and for all practical purposes, negligible. However, for binary mixtures with a greater percentage of methane, the shifts in the phase envelopes become greater as the second component becomes longer chained and heavier. To investigate whether this finding and trend would hold for any other light component, we followed the same procedure for an ethane and n-octane binary mixture (**Fig. 24.14d**). The equimolar case (left) of this mixture follows the trend. As for the 90% ethane case (right), the envelope shifts, although great, are not as significant as the methane and n-octane binary case.

The reason for the large envelope shift that methane, more than ethane, causes is in part due to its own phase envelope (single-component methane) lying further down at lower temperatures and distant from heavier and longer chained alkanes. Therefore, with the addition of methane to a heavier, longer-chained alkane to form a binary mixture (the main contribution being from 90% methane), the phase envelope of the mixture would shift down from the 100% heavy component toward 100% methane. This downward shift is amplified when the mixture is confined.

We have cases where, for a given pressure path of production, a ternary mixture of model fluid could act as a retrograde condensate or wet gas, depending on the size of the pore where fluid is stored, although the same fluid is an oil in the PVT cell, i.e., the bulk fluid case (**Fig. 24.15**). It is, therefore, reasonable to believe that most of the liquid-producing resource shales have a distribution of phases in the reservoir that is dictated by the micro- and mesopore size distribution of the reservoir rock. In a sense, referring to the oil window or gas window of these formations based on the volume of produced fluids is almost meaningless because the rock could potentially hold all of these phases at the initial conditions or the rock could yield these phases to the fractures in its own unique way as we begin the production (Fig. 24.15).

Unfortunately, we currently do not have a scientific method or an engineering tool to deal with the resource assessment of multicomponent liquid-rich fluids in shale. In the future we, therefore, need to develop a methodological approach for the producing companies to assess their liquid-rich shale as a resource. Any approach should be a novel scientific approach that combines the routine PVT study and petrophysical measurements with advanced-level thermodynamic simulations of multicomponent fluids in pores. This will be done by separating hydrocarbon phases (gas, liquid, supercritical fluid, adsorbed) across the pore size distribution of the shale matrix under the reservoir conditions and then by quantifying producible liquid in terms of pore volume of liquid released and its rate of release.

24.6 Improved Oil Recovery

In Chapter 21 the authors discussed the point of needing the deployment of improved oil recovery techniques for these tight shale rocks. In this chapter we illustrate the areas where we need to concentrate to improve the understanding and bring practicality to the operations.

The section is centered on the importance of a new set of molecular dynamics simulation results in our understanding of microemulsion behavior under nanopore confinement and its application to produce the kerogen oil from the organic-rich shales.

In enhanced oil recovery, the production is influenced by the ability of injected surfactants to adsorb and to modify interfacial tension at different interfaces. As previously demonstrated, surfactant and microemulsion additives enhance the production to a different extent but the mechanisms behind the differences in their action are not fully understood. Recent molecular dynamics simulation shows that the rate of adsorption at a solid surface differs for these two systems and is higher in the case of microemulsion. Furthermore, it shows that the solvent solubilized in microemulsion is transported to the solid surface together with the surfactant. Hence, the kinetics of adsorption could be controlled by designing the chemistry and composition of the self-assembled structure.

The simulation involves an aqueous solution in the presence of oil (heptane) phase. The solution consists of nonionic surfactant dodecylhepta(oxy-ethylene)ether or $C_{12}E_7$ and a solubilized terpene solvent. The presence of solvent inside the micelles causes the trends in adsorption behavior to deviate from those expected for adsorption from micellar surfactant solutions. In the case of solubilized terpene, the swollen micelles adsorb on the surface as one entity (**Fig 24.16**). The

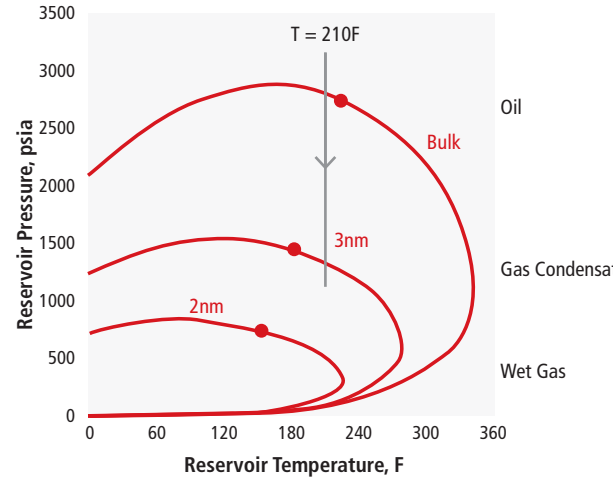

Fig. 24.15—Shifts in phase diagram due to presence of nanopores. The fluid is a mixture of C_1, n-C_4, and n-C_8. The fluid is part of what appears to be an oil reservoir in the conventional sense. It is, however, a gas phase at initial conditions in the nanopores less than 5 nm. Further, this fluid could stay as gas in the smallest pores and yield gas condensates in 3 to 5 nm pores during the production. The figure is adapted from Rahmani and Akkutlu (2013).

delivery of a surfactant to the interface and the associated reduction of the interfacial tension take place at much faster rates controlled by the solvent concentration.

Molecular dynamics simulation also reveals the complex distribution of fluids by the capillary wall. The terpene swollen micelle merges with the film of oil on the wall. The surfactant deposits on the interface between the aqueous phase and the oil, thereby reducing its interfacial tension. Conversely, the solvent originally solubilized in microemulsion droplet penetrates the film of oil (**Fig. 24.17a**). The resulting mixture of oil and solvent has different properties from the oil alone. This indicates a primary difference between the

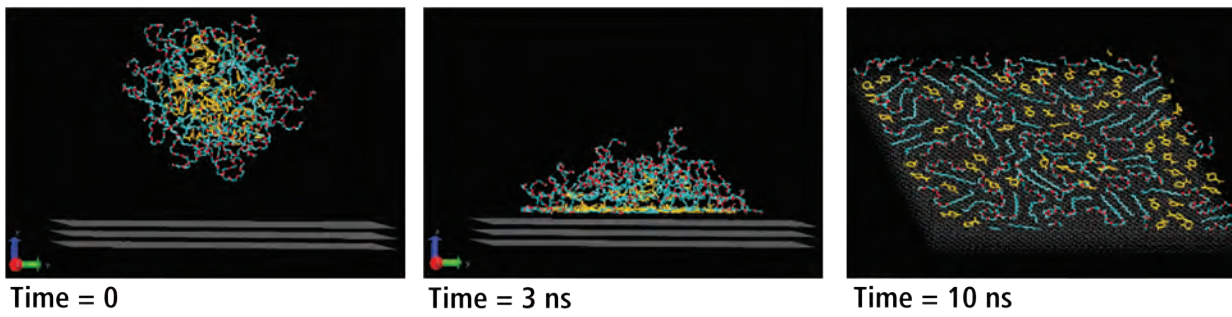

Fig. 24.16—Adsorption of C12E7 micelle containing solubilized terpene solvent on organic wall. From left to right, the snapshots during the simulation are shown. The aqueous phase environment (water molecule) is not shown for clarity in the images. The figure is adapted from Akkutlu et al. (2014).

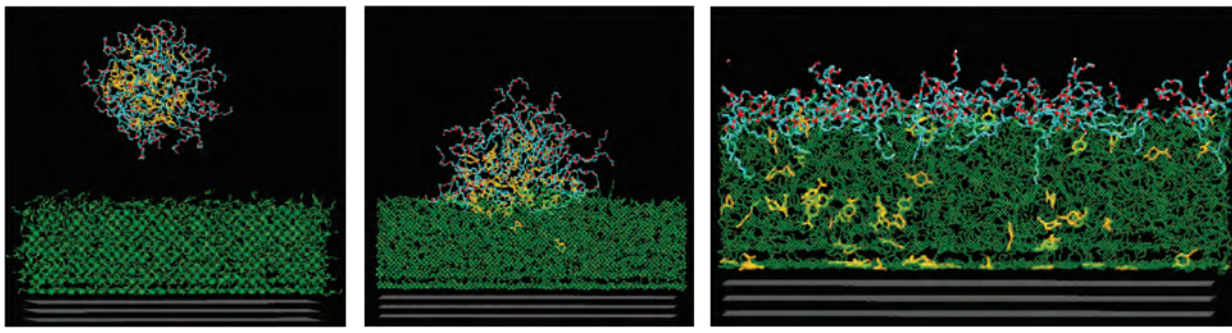

Fig. 24.17a—Adsorption of a microemulsion droplet containing C12E7 surfactant and terpene solvent. From left to right, the snapshots during the simulation are shown. Due to the influence of the organic wall, the solvent molecules penetrate deep into the oil phase (shown as a green film by the wall) and adsorbed on the organic wall.

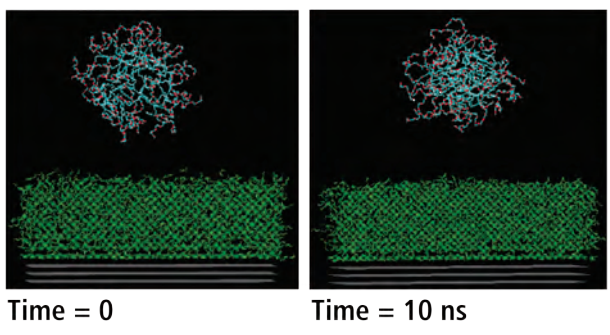

Fig. 24.17b—Simulation of C12E7 micelle near the oil/water interface. From left to right, the snapshots during the simulation are shown. The micelle does not absorb in the absence of terpene solvent. The figure is adapted from Akkutlu et al. (2014). NSTI, http://nsti.org. Reprinted and revised, with permission, from TechConnect World Conference.

mechanism of action between surfactant and a combination of surfactant and solvent. We also observe secondary adsorption of the droplets. For comparison, the same simulation conditions were applied in the case of $C_{12}E_7$ micelles without solvent. As expected by the conventional theory, the whole micelle did not adsorb to the interface (**Fig. 24.17b**).

The molecular simulations indicate the potential of oilfield chemicals to impact future oil recovery from organic-rich shales. When solubilized with terpene, the properties of the oil film changes and the level of its molecular interactions with the walls are modified. These effects are shown in **Fig. 24.18**.

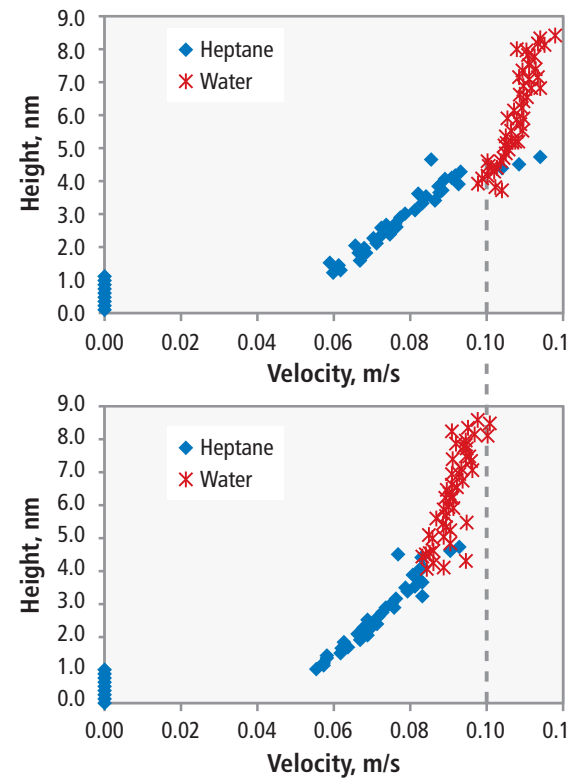

Fig. 24.18—Velocity profiles of water and oil film during laminar flow by organic wall. The profile is obtained using non-equilibrium molecular dynamics simulation applying a constant external force field to the water molecules. The bottom plot includes oil film with with terpene solvent and the surfactants are located at the water oil interface. The figure is adapted from Akkutlu et al. (2014).

24.7 References

Akkutlu, I.Y. and Didar, B.R. 2012. Pore-size Dependence of Fluid Phase Behavior and Properties in Organic-rich Shale Reservoirs. Paper SPE 164099 presented at the SPE International Symposium on Oilfield Chemistry held in the Woodlands, Texas. 8–10 April. http://dx.doi.org/10.2118/164099-MS.

Akkutlu, I.Y., Bui, K., Silas, J., et al. 2014. Molecular Dynamics Simulation of Adsorption from Microemulsions and Surfactant Micellar Solutions at Solid-Liquid and Liquid-Liquid Interfaces. TechConnect World Conference held in Washington, DC, June 15-18.

Akkutlu, I.Y. and Fathi E. 2012. Multi-scale Gas Transport in Shales with Local Kerogen Heterogeneities. *SPE J.*, **17** (4): 1002–1011. SPE 146422-PA. http://dx.doi.org/10.2118/146422-PA.

Allen, M.P. and Tildesley, D.J. 2007. *Computer Simulation of Liquids*. London: Oxford University Press.

Ambrose, R.J., Hartman, R.C., Diaz-Campos, M., et al. 2012. Shale Gas In-Place Calculations Part I - New Pore-scale Considerations. *SPE J.*, **17** (1): 219–229. SPE 131772-PA. DOI: http://dx.doi.org/10.2118/131772-PA.

Atkinson, B. (Editor) *The Compete Essays and Other Writings of Ralph Waldo Emerson*. Hardcover, January 1, 1940.

Bui, K. and Akkutlu, I.Y. 2015. Nanopore Effect on Surface Tension of Methane. *Journal of Molecular Physics*. **113** (22).

Fathi, E. and Akkutlu, I.Y. 2013. Lattice Boltzmann Method for Simulation of Shale Gas Transport in Kerogen. *SPE J.*, **18** (1): 27–37. SPE 146821–PA. http://dx.doi.org/10.2118/146821-PA.

Frenkel, D. and Smit B. 2002. *Understanding Molecular Simulation – From Algorithms to Applications*. San Diego: Academic Press, Computational Science Series.

Handin, J. et al. 1963. Experimental Deformation of Sedimentary Rocks under Confining Pressure: Pore Pressure Tests. *AAPG Bulletin*, **47** (5): 717–755.

Gangi, A.F. 1978. Variation of Whole and Fractured Porous Rock Permeability with Confining Pressure, *International Journal of Rock Mechanics and Mining Sciences and Geomechanics Abstracts*, **15** (5): 249–257. http://dx.doi.org/ 10.1016/0148-9062(78)90957-9.

Hartmann, T. *The Last Hours of Ancient Sunlight*. Mythical Books, a division of Random House, Inc., 1998.

Heller, R. and Zoback, M. 2013. Laboratory Measurements of Matrix Permeability and Slippage Enhanced Permeability in Gas Shales. Paper SPE 168856 presented at the Unconventional Resources Technology Conference, Denver, Colorado. 12–14 August, http://dx.doi.org/10.2118/168856-MS.

Kang S., Fathi, E., Ambrose, R.J. et al. 2011. Carbon Dioxide Storage Capacity of Organic-rich Shales. *SPE J.*, **16** (4): 842–855. SPE 134583-PA. http://dx.doi.org/10.2118/134583-PA.

Kwon, O., Kronenberg, A.K., Gangi, A.F., et al. 2004. Permeability of Illite-bearing shale: 1. Anisotrophy and effects of clay content and loading. *Journal of Geophysical Research-Solid Earth*, **109** (B10): B10205.

Loucks, R.G., Reed, R.M., Ruppel, S.C., et al. 2009. Morphology, Genesis, and Distribution of Nanometer-Scale Pores in Siliceous Mudstones of the Mississippian Barnett Shale. *Journal of Sedimentary Research*, **79**: 848–861. http://dx.doi.org/10.2110/jsr.2009.092.

Muratov, G.N. 1982. Surface Tension of Nitrogen, Oxygen, and Methane Over a Wide Range of Temperature. *Zh. Fiz. Khim*. **56**: 814–817.

Palciauskas, V.V. and Domenico, P.A. 1980. Micro-fracture Development in Compacting Sediments: Relation to Hydrocarbon-Maturation Kinetics. *AAPG Bulletin*, **64** (6): 927–937.

Rahmani Didar, B. and Akkutlu, I.Y. 2012. Pore-size Dependence of Fluid Phase Behavior and Properties in Organic-rich Shale Reservoirs. Paper SPE 164099 presented at the SPE International Symposium on Oilfield Chemistry held in the Woodlands, Texas, USA, 8–10 April. http://dx.doi.org/10.2118/164099-MS.

Singh S. K., Sinha, A., Deo G., et al. 2009. Vapor-liquid phase co-existence, critical properties, and surface tension of confined alkanes. *The Journal of Physical Chemistry C*, **113** (17): 7170–7180.

Sondergeld, C.H., Ambrose, R.J., Rai, C.S. et al. 2010. Micro-Structural Studies of Gas Shales. Paper SPE 131771 presented at the SPE Unconventional Gas Conference, Pittsburg, PA, 23–25 February. http://dx.doi.org/10.2118/131771-MS.

Walsh, J.B. 1981. Effect of Pore Pressure and Confining Pressure on Fracture Permeability, *International Journal of Rock Mechanics and Mining Sciences and Geomechanics Abstracts*, **18** (5): 429–435. http://dx.doi.org/10.1016/0148-9062(81)90006-1.

Wang, F. P. and Reed, R. M. 2009. Pore Networks and Fluid Flow in Gas Shales. Paper SPE 124253 presented at the Annual Technical Conference and Exhibition, SPE, New Orleans, LA, October 4–7. http://dx.doi.org/10.2118/124253-MS.

Wasaki, A. and Akkutlu I.Y. 2014. Organic-rich Shale Permeability. Paper SPE 170830 to be presented during the Annual Technical Conference and Exhibition held in Amsterdam, the Netherlands. http://dx.doi.org/10.2118/170830-MS.

This page intentionally left blank

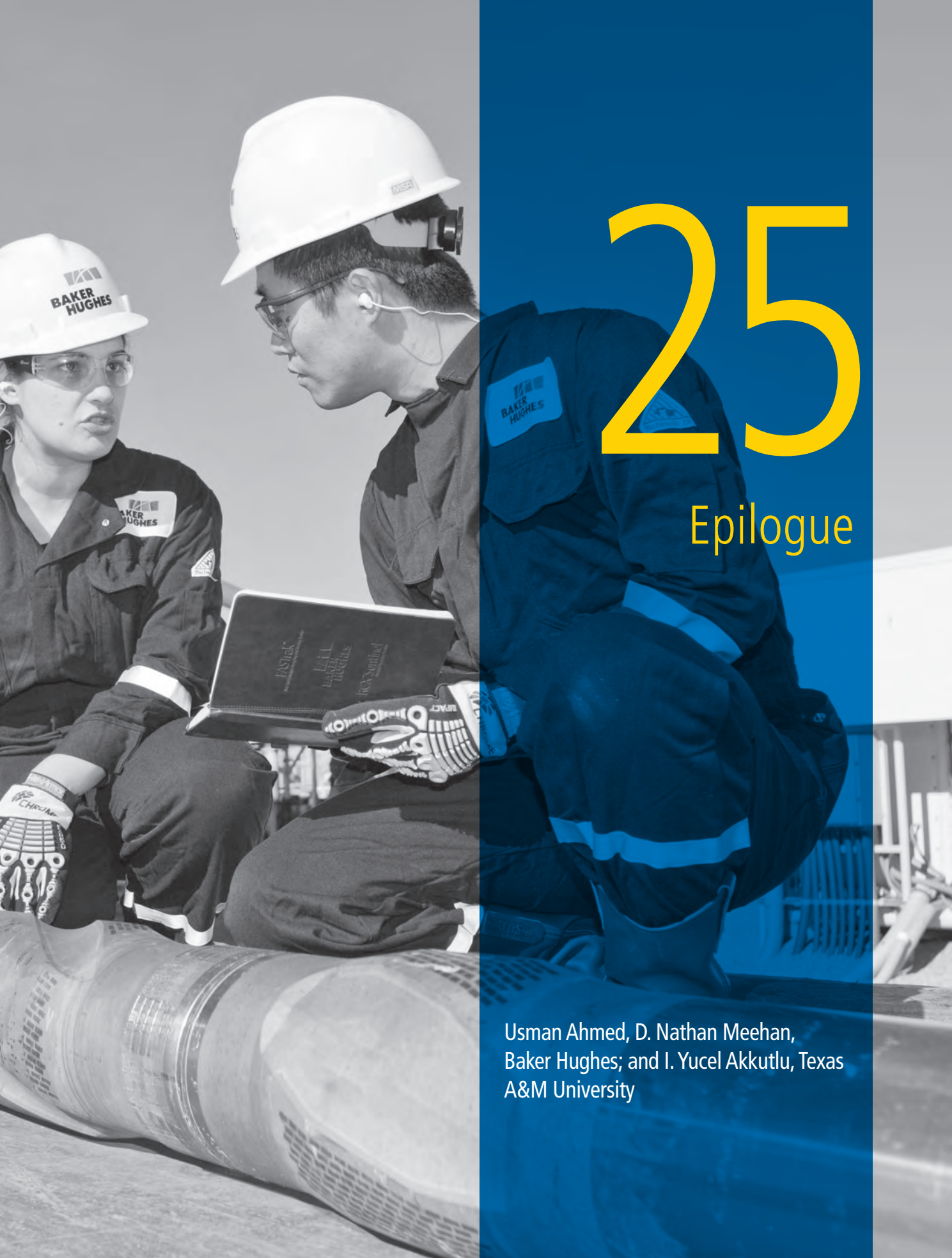

25

Epilogue

Usman Ahmed, D. Nathan Meehan, Baker Hughes; and I. Yucel Akkutlu, Texas A&M University

This page intentionally left blank

Chapter 25: Epilogue

"… And when the profession can no longer evade anomalies that subvert the existing tradition of scientific practice, then begin the extraordinary investigations that lead the profession at last to a new set of commitments, a new basis for the practice of science. The extraordinary episodes in which that shift of professional commitments occurs are the ones known as scientific revolutions [or paradigms shift]."

Thomas S. Kuhn,
The Structure of Scientific Revolutions, 1962

A dramatic increase is being observed in the number of articles related to the unconventional resources, in particular in the area of source rocks—hitherto resource shale or simply shale. Relating the increase in research, publications, and evaluation of field applications directly to the growing interest in the industry could be shortsighted. Our community should exchange views and opinions as to why increasing levels of research associated field application of technology on shale is necessary.

25.1 Nature of Matrix-Fracture Duality

As new reservoir parameters appear, they are used more frequently with the resource shales. In parallel, we experience that the basic features of classic reservoirs are becoming less meaningful. Matrix porosity and fluid saturations, for example, may not be the basic controlling parameters related to the fluid storage. Although they traditionally are not considered so, the shale fractures also can contribute significantly to the fluid storage because their volume is comparable to the tight matrix pore volume. In addition, the resource shales can hold significant volumes of fluids in the matrix in adsorbed and dissolved states. The sorbed fluids are controlled mainly by molecular forces dictated by the fluid-solid and fluid-fluid interactions. They primarily require a large internal matrix surface area not pore volume, high-pore pressure, and suitable pore temperature. Due to the presence of small pores and amplified fluid-wall molecular interactions, confinement effects seem to be influential on the sorbed fluid amounts and the transport.

Conversely, permeability becomes an effective near-fracture quantity reflecting the multiscale complexities of fracturing and proppant placement. We have met geoscientists and engineers working in the industry who are not shy to reduce the act of reservoir creation and the subsequent permeability modification to an act of fracture permeability creation. They argue it is the created fractures and not the created reservoir that make the production possible. Based on this point of view, the matrix practically is impermeable. Therefore, it is not the matrix permeability but the complexity of the created and natural fracture network and its effective conductivity that matters for economic recoveries. Indeed, production involves the fluids residing in the fractures followed by the fluids residing in the matrix. But fluid deliverability of the matrix is so insignificant that one should seriously consider putting another fracture to reach into and unlock those fluids residing in that portion of the matrix. Some also argue that enhanced oil recovery techniques could be deployed if the injected substance can travel through the nanopores.

A much larger group, however, maintains a somewhat more balanced view of the matrix-fracture duality in the created reservoir environment. Fluid storage and transport in the matrix and the associated pressure transient are important for this group, because it is the matrix that holds the fluids and it is the matrix that eventually delivers these fluids into the fractures. According to this view, one needs to separate carefully the matrix permeability from the fracture permeability because the former is a direct measure of formation diffusivity, indicating how fast the pressure transient diffuses away from the hydraulic fractures and how soon the fractures begin interfering. The latter is a measure of how effectively we can produce.

25.2 From Reservoir Uncertainties to Reservoir Anomalies

In spite of the recent advances in the assessment of shale oil and gas resources, technical difficulties remain in characterizing storage and transport properties of the created reservoir volume. The difficulties mainly are due to lack of suitable sampling and measurement techniques. It is hard to work with shale samples because they are fissile and are highly sensitive to changing environment and to the penetrating measurement fluids.

What used to be routine laboratory measurements of porosity, pore size distribution, and permeability are demonstrating to us that shale is in fact an odd rock with anomalous petrophysical behavior. Porosity is a number that varies with the measurement fluid and technique. Pore size distribution is inaccurate and, at best, incomplete. Absolute shale permeability is almost a mysterious quantity that could

vary by orders of magnitude. Under a scanning electron microscope, at sub-micron scale, shale appears as a naturally occurring nanoporous material with diverse mineralogy and complex heterogeneity in local porosity. Due to large contrast in the length scales of observation, it is a real challenge, however, to scale up the SEM images and relate them to the behavior of shale in the laboratory and in the field.

Shale also appears to be a challenging environment pushing the limits of logging tools and inter-well seismic. New measurement procedures and analysis techniques are needed to gain insight into the resource shales and to reduce uncertainties in integration and petrophysical characterization. In the world of microseismic, eliminating or reducing noise is critical and will require deployment of digital accelerometers while adding GPS technology to pinpoint signal positioning.

Measurements and analysis of multiphase flow dynamics in shale is at an infancy stage. The steady-state method of constructing the relative permeability curves requires that the wetting and the non-wetting fluids are injected simultaneously and continuously at some predetermined ratio into the core sample that has been saturated with the wetting-phase. However, it is not clear with shale what the wetting phase is, and it takes an excruciatingly long time to develop a truly multiphase steady-state condition. Conversely, the unsteady-state method requires non-wetting phase injected into a wetting-phase-saturated core at a constant rate. During the injection, the non-wetting phase saturations vary continuously and these saturations typically are computed using the fractional flow theory. The problem with the application of the unsteady-state to the shale samples is that we are not sure if the classic displacement theory is still applicable.

In summary, the relative permeability measurements are not suitable for characterizing the multiphase flow nature of these rocks. Using two- and three-phase relative permeability correlations by adjusting the irreducible or critical fluid saturations seems to be the common practice. However, the validity of these correlations can be questioned.

Difficulties exist in measuring the fracturing ability of shale, i.e., the so-called fracability, during the hydraulic fracturing operation. Fracability is currently a qualitative geomechanical feature of shale indicating how a hydraulic fracture initiates, propagates, and extends into shale matrix; interacts with the natural fractures; and how it establishes a conductive fracture network. The important factors that control fracability of a shale are its mineralogy, geomechanical properties, and in-situ stress field. However, their interrelationship is quite complex and changes from shale play to play. Therefore, our understanding of shale fracability can be considered at a very early stage, making the reservoir creation process challenging during the early development. As lithofacies change in the lateral direction the "fracability" and other potential source rock parameters can be compromised. Diagnostic tools are used in the field to provide information on the fracture geometry, orientation, and performance such as wellbore image logs, microseismic, injection tests, production logging, etc.

Recent investigations on the fluid behavior in nanocapillaries indicate that the fluid properties and other fundamental quantities such as critical properties of the fluid could change under confinement. The related investigations are performed using atomistic modeling and molecular simulations of fluids in capillaries under equilibrium conditions although the nanoscale confinement effects have not yet been shown experimentally under the reservoir conditions. Pore-size dependence of fluid behavior points to an intimate coupling of the fluid and rock through an amplified interaction of the fluid molecules and the pore walls. This could have serious consequences for the laboratory PVT methods we use to characterize the reservoir fluids in the laboratory. It could change the correlations we use in our prediction of the fluids properties during the simulation.

Characterizing the shale fluids is also a challenging task. This primarily is because the reservoir fluids are produced under strong influence of the tight shale matrix. For these fluids identifying the phases (liquid, gas, supercritical fluid, adsorbed, dissolved) in the matrix and identifying their producibility limit currently is not possible because the composition of the produced fluid is different than the compositions of the in-situ phases.

New recombination and redistribution techniques are necessary to convert the well stream fluid composition into the reservoir fluids compositions in the reservoir. These techniques should be developed considering phase change phenomena under the influence of the confinement effects. There are cases where, for a given pressure path of production, a mixture of model fluid could act as a retrograde condensate or wet gas. This depends on the size of the pore where fluid is stored, although the same fluid is an oil in the PVT cell.

We, therefore, believe that most of the liquid-producing resource shales have a distribution of phases in the reservoir that is dictated by the micro- and mesopore size distribution of the matrix. In a sense, referring to the oil window or gas window of the resource shale based on the volume of produced fluids is almost meaningless because fluid is intimately coupled with the rock. The rock potentially could

hold all of these phases at the initial conditions, or it could yield these phases to the fractures in its own unique way as we begin production.

25.3 Reservoir Engineering Discipline in Crisis

Clearly, the computation of transmissibility for unconventional rocks adds complexities. If we extend the discussion to the fluid potential calculations, new intricacies related to capillary pressure estimation would appear as another complexity. These complexities are also the new nonlinearities that we are going to confront in the future for the numerical solutions. They could be significant although they are not well understood. Therefore, they currently introduce uncertainties into a simulation study. In summary, we are missing the first-order physics of unconventional reservoir flow and transport and that the current modeling and simulation approaches are not appropriate for history matching, forward simulation, and optimization of the unconventional resources.

The discussion indicates to us that the created shale reservoir is fundamentally different when compared to the features of the classical reservoirs. It is more complex and less predictable and makes the existing tradition of reservoir engineering practice such as economic evaluation, production forecast, and optimization, potentially unreliable. This explains why the level of research has been on the rise and the number of publications increased. As engineers and geoscientists we learned to work with the reservoir uncertainties, those inherent to complex geology, although we cannot afford to work with the reservoir anomalies. Renewed interest in resource shales, however, forces us to question the basic assumptions, or paradigms, of our classic reservoir engineering theory. These paradigms are what the members of our research community have shared for a while and on which significant scientific progress has been based. In essence, with the interest in resource shales, our discipline has been thrown into a state of crisis.

25.3.1 Is the Crisis Further Complicated by Development-Related Issues and Operational Efficiency?

Waterless hydraulic fracturing jobs, efficient IOR/EOR processes for unconventional resources development, fully automated operations and instrumentations and supercomputing are some of the operational technologies that will need to be addressed in the upcoming decade and more precisely in the ensuing years. From an operational efficiency point of view the industry should be planning the partnership between different sectors and organizations for driving efficiency and cost reduction.

25.3.2 Accepting the Water Challenge and the Way Forward

Most unconventional basins in many countries including the US and China will show that many resource basins are also the drought basins. This has prompted the need for waterless fracturing fluid. Presence of water as a vital fluid for mankind and other creatures on the planet has been long recognized, probably since the beginning of life on the earth. Unfortunately, only 2.5% of the earth's water is fresh water, with 98.8% of that water present in ice and groundwater and the remaining either in rivers, lakes, and the atmosphere (0.3%) or contained within biological bodies and manufactured products (0.003%). With this uneven distribution, water availability and supply is critical in meeting everyday requirements of human life, agriculture, industrial, and municipal uses let alone for hydraulic fracturing purposes. Oil and gas energy and water are closely related to each other. In fact, water has been used by oil and gas industry for many years in processes such as waterflooding to accelerate economic production of conventional resources. The conventional development uses much more water than the shale, the public concerns and environmental arguments have not created any obstacle in their development. One reason for this is that the water that is being used for waterflooding is mostly the produced water from the formation, unlike the unconventional wells where only 20 to 40% of the injected water will flow back and is not readily reuseable. There are also fewer concerns about the total dissolved solid (TDS) content of the produced water or the composition of the produced water, so the treatment costs are at minimum. On the other hand, due to the sensitivity and interactions of the shale rocks with the injected fluid and variation of shale characteristics in different plays, the type and content of the injected water is of vital importance to consider in designing the hydraulic fracturing fluid. The water used in hydraulic fracturing processes must be engineered to have certain quality and standards to allow addition of certain additives (for example, friction reducer for overcoming tubular fiction pressure) to maintain high performance of the fluid.

Water conservationists, have already lined up against fracturing companies. According to EPA, between 60 to 140 billion gallons of water were used in 2010 in the US for hydraulic fracturing. As recently as 2012, about 95% of all fractures in the US was done with water. With the shortage of water, and the need to sustain and grow the production from unconventional resources, there have been a number

of technologies that have been recently introduced and claim to replace water as a fracturing fluid, while the safety-related issues are still under evaluation.

Technologies such as CO_2-based fracturing fluid or LPG (liquefied petroleum gas, C_3H_8) could meet the water supply challenge in fracturing jobs, however, their development and applicability to the shale formation's characteristics are not fully known yet. Use of energized fracturing fluid is not a new topic in the industry. Addition of CO_2, N_2, or other gases in the form of foams to the base fracturing fluid has been tested to give satisfactory results as far back as the 1980s in a number of case studies in south Texas.

25.3.3 Operational Efficiency

By and large, unconventional resource development business for the E&P operators can be a low margin business. This business process in turn also makes the service providers find ways to reduce cost. This is where the operational efficiency comes into play.

The first wave of operational efficiency that came into the unconventional resources development process was the "factory" style operations. This is where the concept of factory drilling, completion, and stimulation was introduced. A pad with 18 wells, for example, demonstrated significant efficiency gain from the operational side. Following critical evaluation of these operations it became noticeable that in many cases the gains in operational efficiency were coming at the expense of compromised production results due to:

- Glossing over subsurface understanding
- Leading to lower recovery factor and unattained production levels

The focus then appears to shift toward deploying operational efficiency while ensuring that the recovery factor (or improved economics) is also maximized thus making the shale business more profitable even in the low-margin business environment.

The authors believe that a good way to address the issue is to become cost effective instead of low cost. The authors observe that when the focus is shifted from low cost to cost effective the realized estimated ultimate recovery (EUR) improves and the severity of the improvement appears to be dependent on how well the cost effective structure/process was implemented. The basic message here is that if we do not plan to know our reservoir at the earlier stages then we do not know what is working and what is not. Hence the initial cost may be low but paid for dearly by delivering low EUR. Whereas, when one has a good understanding of the subsurface with cost effective spending in the initial stages it can lead to long run significant reduction in cost while ensuring higher EUR.

Once the subsurface picture is reasonably well understood then and only then can one effectively bring in the operational efficiency via the interplay between drilling, completion, and stimulation.

Once one has the process outlined based on the above thought process, the entire operational efficiency can be broken down in three phases:

Phase 1. Exploration and Appraisal

Phase 2. Development, with emphasis on drilling, completions, and stimulation

Phase 3. Production

Each phase may require some specific emphasis for optimized operational outcome and the desired enhanced results.

Exploration and Appraisal: Phase 1. Ensure the understanding of the resource play by clearly defining the subsurface and developing the field development plan (FDP) for efficient development in the second phase. Operational efficiency in exploration and appraisal should focus on cost effective development of the second phase and establishing what is important and what is irrelevant. Such a process may require implementation of "science" with practicality in mind.

Development: Phase 2. In this phase the bulk of operational efficiency is expected to potentially be deployed. Based on one's understanding of the subsurface the concept of "factory" drilling, completion, and stimulation will need to be modified to ensure the optimized EUR. Some of the key items to address include:

- Optimizing spud to flowline timeframe; clearly defining well spacing and wellbore fracturing stage, and cluster locations
- Doing it right the first time through pre-planning and being cost effective at all levels of drilling, completion, and stimulation
- Addressing the supply chain: quality aspect of materials and services while being cost effective and efficient

Deployment of soft skills like time management, internal and external communications, selling prospects and proposals (ideas and concepts), and conflict resolution can help the development phase reach its highest level of success.

Production: Phase 3. With the operational efficiency of drilling, completion, and stimulation in place, it will be time to focus on what the wells could be telling one in terms of production and recovery. In this regard the areas of focus potentially include:

- Deployment of production monitoring and evaluation methods
- Regular communication with drilling, completion, and stimulation departments regarding the assurance of production: "factory operations" versus well/reservoir production performance-based operations with continuous feedback and appraisal throughout the full-field life-cycle
- Optimize production, artificial lift, WOs, chemical treatments, other surveillance, and intervention timeframe

Finally, all the above will need to be part of an integration of economics with risk analysis included.

Finally, the untold Phase 4 is closing the phase loop by documenting what fell through the cracks so that in subsequent operations further improvements can be introduced.

25.4 A Shift in Paradigms on Its Way

During the state of crisis in a discipline, Thomas Kuhn, in his influential book, *The Structure of Scientific Revolution*, claims new ideas and approaches are brought in and tried. Eventually a new paradigm is formed, Kuhn continues, that gains its own new followers in the community, and an intellectual battle takes place between the followers of the new paradigm and the holdouts of the old paradigm. Such a shift in scientific revolution and the associated paradigm shift affect the operation process and efficiency part of the game in a similar fashion.

As a team of researchers, educators, practicing engineers, and geoscientists, it is an exciting time and a unique experience for us to be part of this transition era when the paradigms battle is picking up and the shale revolution is just around the corner. As Thomas Kuhn says, the transition to new paradigms is neither instantaneous nor calm. Instead it involves a protracted set of attacks with empirical data, rhetorical or philosophical arguments, with field application outcomes as a result.

Sometimes the convincing force is time itself and the human toll it takes, Kuhn says, using a quote from Max Planck: "A new scientific truth does not triumph by convincing its opponents and making them see the light, but rather because its opponents eventually die, and a new generation grows up that is familiar with it."

This page intentionally left blank

Terms and Definitions

This page intentionally left blank

Terms and Definitions

1P: Proved reserves.

2P: Proved plus probable reserve.

3P: Proved, probable plus possible reserves.

5D interpolation: an algorithm based on Fourier transform that improves signal processing of pre-stack data.

Abandonment pressure: minimum average reservoir pressure at which the continued well operation is not feasible at an economic rate and the wells have to be abandoned.

Acid mine drainage (AMD): produced water from coal mines.

Acoustic emissions (AE): a sound wave produced by deformation or brittle failure of rocks.

Acoustic impedance: product of acoustic velocity that passes through a rock and the density of the rock.

Adjustable kick off (AKO): segment of drill string located above the drill bit; makes it possible to steer the well through sliding.

Adsorption: adhesion of ions, atoms, or molecules from a liquid, gas, or dissolved solid to a surface.

Advanced cutting evaluation: A Baker Hughes advanced service that provides real-time elemental, compositional, and petrophysical analysis on cuttings for precise formation evaluation.

Advection: A transport mechanism of a substance by a fluid due to the fluid's bulk motion.

Affinity laws: show the relationship between variables in pump performance such as head, volumetric flow rate, power, and shaft speed.

Ampacity: current a conductor can carry continuously without exceeding its temperature rating; a function of cable insulation size, type, and conditions of use.

Amplitude versus angle azimuthal (AVAz): variation in amplitudes with shot-receiver azimuth due to local changes in rock stress and intensity of fracturing.

Amplitude versus offset (AVO): the dependency of the seismic attribute, amplitude, with the distance between the source and receiver (the offset); a technique using seismic data to determine a rock's fluid content, porosity, density, or seismic velocity, shear wave information, fluid indicators (hydrocarbon indications).

Anisotropic shear failure: behavior exposed from a rock under a specific range of confined compressive strength and lamination inclination.

ANNIE: three-parameter anisotropic velocity model for shales.

Apparent shale permeability: parameter used to describe the gas flow in nanopores of shale rocks; is a property of the reservoir rock and depends on gas properties at a certain pressure and temperature.

Archaea: a domain of single-celled microorganisms. These microbes are prokaryotes and have no cell nucleus or membrane-bound organelles.

As low as reasonably practical (ALARP): evaluating a level of practice against time, money, and trouble to develop the best possible plan to continue a safe operation.

Atomic force spectroscopy (AFS): Atomic force microscopy (AFM) or scanning force microscopy (SFM) is a high-resolution type of scanning probe microscopy. AFS has resolutions on the order of fractions of a nanometer, more than 1,000 times better than the optical diffraction limit.

Authority for expenditure (AFE): cost-estimate report prepared by the operator as a final step in well planning prior to the start of the drilling operation.

AutographPC™: Baker Hughes software that is the artificial lift industry's most comprehensive and user-friendly system design and application simulation tool.

AutoTrak™: advanced field-proven RSS drilling tool by Baker Hughes offering precise steering with maximum exposure to the reservoir sweet spot and high build-up rates.

aXcelerate™: a Baker Hughes advanced drilling automation service that delivers high-resolution downhole picture in real time helping users make better decisions during reservoir navigation operations.

Azimuthal resistivity: deep-reading measurement to accurately land and navigate a horizontal well along the

target formation. Baker Hughes AziTrak™ deep azimuthal resistivity measurement tool detects reservoir boundaries and offers accurate formation evaluation to reduce wellbore positioning uncertainty.

Backscattered electron (BSE): interaction of the electron beam with atoms in the targeted material.

Ball-activated completions systems (BACS): reduces frictional forces; facilitates a more efficient fracturing of each zone within the wellbore.

Ball-drop systems: a completion system activated by a ball passing through a downhole device.

Balling: an undesirable event when cuttings stick to the bit surface in water-reactive formations resulting in low rate of penetration and bit life.

Barret–Joyner–Halenda (BJH): a method that uses adsorption isotherms to calculate pore size distribution in a rock.

Basis of design (BoD): engineering set of statements and documentations that provide the key requirements and system performance under those requirements.

Beef: bedding-parallel natural fractures.

BEP: point on a pump's performance curve that corresponds to the highest efficiency.

Biocide: a protective chemical and additive used in drilling fluid to kill bacteria and control their growth.

Biot poroelastic coefficient: a poroelastic constant used to transmit the internal fluid pressure to the rock matrix.

Bitumen: a dense and extremely viscous form of petroleum; referred to as tar because of its appearance, odor, and color.

Boosting: a machine-learning algorithm for reducing bias in supervised learning.

Boyle's law: an experimental gas law that describes how the gas pressure tends to decrease as the gas volume increases.

Break-out: a stress-induced enlargement in the wellbore area caused by preferential rock failure in the wellbore; is used to determine stress orientation in wells for geomechanical modeling.

Breakdown pressure: the pressure required to initiate a fracture in the rock.

Brinnel hardness (BH): characterizes the resistance of the rock to scratch by penetration of an indentor.

Brittleness indicator from mineralogy (BIM): brittleness indicator derived from the rock's mineral composition.

Brittleness: a material property that indicates how the rock will break without significant deformation when subjected to external stress.

Broad ion beam (BIB): an ion milling method used to map shale porosity.

Brunauer–Emmett–Teller (BET): a theory that explains the physical adsorption of gas molecules on a solid surface; the basis for an analysis technique to measure the specific surface area of a material.

Bubble point: the point in the pressure depletion at which the first bubble of gas comes out of the solution.

Bulk density: mass of the bulk particles divided by the total volume of the material.

Bulk modulus: the ratio of the hydrostatic stress to the volumetric strain under hydrostatic loading.

Button patch: type of acquisition in which the receivers are placed in button configurations.

Canister desorption: test used to measure the amount of gas released as a function of time from the core samples.

Canonical ensemble: the statistical ensemble used to represent the possible states of a mechanical system that is in thermal equilibrium with a heat bath.

Capillary suction time testing (CST): a fluid compatibility test used to study how clays and shales react with filter cakes and different brines.

Carmhograph Wosthoff apparatus: a tool that estimates the organic content of the rocks by removing carbonates (CO_2) through acid treatment and subsequently heating the samples to high temperatures.

Casing collar locator (CCL): a tool used in downhole operations such as perforating to control the depth.

Cathodoluminescene (CL): a phenomenon resulting from interaction of beam electrons with outer-shell electrons in a crystal.

Cement wiper plug: A plug used to wipe tubulars and reduce cement contamination during a cement job.

CemVision™: Baker Hughes advanced fluid displacement 3D simulator software that offers a better understanding of the fluid contamination risks.

Centrilift: the industry leader of ESP systems and a major component of Baker Hughes solutions in critical well applications.

Chemical squeeze: an inhibition treatment that injects scale inhibitor chemical into the formation.

Circumferential Borehole Imaging Log™ (CBIL™): a Baker Hughes service that offers high-resolution borehole acoustic images in difficult conditions.

Cladding: a permanent isolation method used in refracturing.

Cleat system: micropores or natural fractures in coalbed methane.

Cluster analysis: grouping a set so that objects in the same group (cluster) are more similar to each other than to those in other clusters.

Coalbed methane (CBM): natural gas contained in coal deposits.

Coefficient of determination (R2): an indicator of the fit of data points to a statistical model.

Cohesive strength (So): bonding strength between constituent particles of a rock.

Coiled tubing-activated completion system (CTACS): used in multistage hydraulic fracturing.

Cold finger: test to measure the temperature at which paraffin precipitates in oil solutions.

Common depth point (CDP): a seismic data acquisition method in which a series of tracers are acquired to reflect from the same subsurface midpoint.

Common midpoint (CMP): a seismic data acquisition method in which a series of tracers are acquired to reflect from the same subsurface midpoint.

Compensated linear vector dipole (CLVD): a possible earthquake mechanism and one of the three components of a full moment tensor that can be used to describe volumetric strain in a crack opening or crack closure and to identify the volumetric failure of events in formation rocks.

Compensated neutron (CN): tool used to acquire neuron porosity data. The Baker Hughes tool, Nautilus Ultra CN™, is used to withstand extreme pressure and temperature.

Compressional wave slowness (DTC): reciprocal of compressional velocity.

Compressive strength: capacity of a material to withstand compressive loads.

Computer tomography (CT) core scanning: an X-ray method of rock characterization that takes cross section and longitudinal scans of the whole core; provides information about heterogeneity and properties of the core system.

Computer tomography (CT) sliding sleeve systems: coiled tubing-activated completions system use CT to achieve multistage isolation through two primary methods: use a sand jet perforator or CT-activated sleeves to access the hydraulic fracture stages in the formation.

Confining stress: the pressure simultaneously exerted equally to a material in two opposite directions.

Conodant Alteration Index (CAI): estimates the maximum temperature reached by a sedimentary rock by using the thermal alteration of conodont fossils.

Consistometer: a device to measure consistency or flow characteristics of a viscous or plastic substance.

Continuous deposits: hydrocarbon accumulations that are not significantly affected by hydrodynamic influences.

Correlation coefficient: a measurement of the degree to which predictor and target variables are related.

Corrosion resistant alloys (CRA): materials used to minimize corrosion.

Cost oil: amount of production on an annual basis applied by an operator to recover expenses under the production sharing contract.

Critical strain limit (CSL): a strain limit beyond which the start of sand production from an openhole completion or perforation occurs.

Critically stressed fractures: a set of fractures that would favorably fail in shear under present day stress field of the formation rocks.

Cross-dipole logs: type of logs recorded by dipole receivers used to determine shear anisotropy.

De-watering process: production of water from coalbed methane matrix.

Dean Stark: a thermal distillation and solvent extraction method performed in laboratories to measure the fluid saturation in a core sample.

Decision trees: a support tool using a tree-like graph to model decisions and possible consequences.

Deep shear wave imaging (DSWI): an evaluation method for characterization of fractured systems, geologic boundaries, sub-seismic faults, and discontinuity around the wellbore and into the reservoir; can offer insights about heterogeneity of the shale systems.

Depth of cut control (Doc): a technology used for polycrystalline diamond compact bits to reduce torque.

Desorption isotherms: the increase in amount of gas being released as the pressure is reduced; used in a Langmuir isotherm plot, which is a plot of adsorbed gas quantity versus the pressure.

Desorption: a substance is released from or through a surface.

Deviatory loading: axial direction of the loading.

Differential horizontal stress ratio (DHSR): the differential ratio of the maximum and minimum horizontal stresses.

Differential sticking: a condition when the drill pipe becomes stuck and pushed by the wellbore pressure against the wall.

Diffusion: the random scattering of particles due to kinetic energy of the particles that is affected by viscosity, density, and temperature.

Discrete fracture network (DFN): an approach in modeling fracture geometries that incorporates the discrete fractures as the central component of fluid flow within the system.

Distributed acoustic sensing (DAS): a permanent fiber optic monitoring tool providing real-time observation of acoustic measurements over the well interval.

Distributed temperature sensing (DTS): a permanent fiber optic monitoring tool providing real-time observation of temperature around the well and along the well interval.

Dogleg severity (DLS): total angular inclination and azimuth in the wellbore in 3D space, calculated over a standard length.

Domestic market obligation (DMO): a correction operation in seismic processing workflow that is used to transform the normal move-out (NMO) corrected data to zero-offset.

Double crystal diffractometer (DCD): an X-ray scattering instrument used for small-angle X-ray neutron scattering (SANS) and ultra-small angle neutron scattering (USANS) techniques performed to characterize pore structure and connectivity studies.

Downhole straddle packer: tool used to shut off zone intervals in a series of formations along the well.

Downlinking: surface-to-downhole communication of drilling parameters.

Drill cuttings: rock cuttings brought to the surface during the drilling of oil and gas wells.

Drucker and Prager plasticity failure criterion: a criterion originally developed to deal with soil mechanics, applied to handle wellbore stability problems in the petroleum industry.

Dry microseismic events: events with solely associated change in stress and are unlikely to be in communication with hydraulic fractures or wellbore.

Dual porosity, dual permeability: a model used to show interconnected set of fractures and matrix in which the flow to the wellbore occurs both in matrix and fractures.

Earth Imager: Baker Hughes EARTH Imager™ logging used to acquire high-resolution micro-resistivity images in oil-based mud systems.

EDGAR: electronic data gathering, analysis, and retrieval system on the SEC website.

Effective stress ratio (KESR): a dimensionless parameter used to relate minimum horizontal stress and pore pressure.

Effective stress: the portion of the total stress carried by the rock matrix.

Elastic strain: the distorted material returns to the original shape and size of the material.

Elemental spectroscopy: determination and quantification of elemental concentration and composition of elements within the sample.

Energy dispersive spectroscopy (EDS): an advanced elemental analysis technique used for chemical characterization and compositional evaluation of shales.

Enhanced shale oil recovery (ESOR): the recovery processes that aim to increase the recovery factor by injecting a fluid into the reservoir, and maintaining the reservoir pressure.

Equivalent circulating density (ECD): a pressure management parameter that takes into account the friction pressure of the drilling fluid.

Estimated ultimate recovery (EUR): an estimated quantity of cumulative and economically expected recoverable hydrocarbon from a well or reservoir.

Excluder2000™ sand screen: Baker Hughes sand control screen technology for long horizontal wells, openhole completions, and high flow-rate producing and injecting wells.

Exploratory data analysis: procedure to extract and summarize characteristics of datasets.

Factory drilling: large numbers of nearby wells are drilled in a similar fashion to reduce time-based costs but is done without taking subsurface heterogeneity and detailed drilling planning into account.

Field development plan (FDP): the best plan to develop a field; is formulated based on factors such as technical evaluations, financial risks, environmental impacts, and scalability.

Field emission scanning electron microscopy (FE-SEM) porosity: a high-resolution imaging technique that uses narrow electron beams with high electroenergy to measure the rock porosity.

Final investment decision (FID): key criteria used to manage a company's corporate financial structure and assets.

First Tranche Petroleum (FTP): the oil and gas shared by the parties in the production sharing contract (PSC) before the cost recovery.

FLEXPump™: Baker Hughes efficient and reliable electric submersible pump; designed to maximize the production and ultimate recovery in unconventional resource play wells where production declines significantly over a relatively short period of time.

Foam fracturing treatments: treatments where nitrogen, carbon dioxide, or a combination is used as the fracturing fluid.

Focused ion beam (FIB): an ion milling method to image both meso- and micropores in a mudstone.

Foliation: repetitive layering in metamorphic rocks.

Forced closure method: a technique proposed by Ely (1996) applied to fracture treatments; used to hold the proppant in place between the fracture walls by closing the fracture rapidly and trapping proppants in a uniform distribution.

Formation breakdown pressure: pressure at which rock breaks and the fracture is created; also known as fracture initiation pressure.

Formation Mechanical Logging (FORMEL): a refinement model to enhance rock physical description.

Fracability: describes formations that are likely to produce fracture networks when hydraulically stimulated.

Fracking: a term used by detractors; refers to the hydraulic fracturing operation in the oil and gas industry.

FracPoint™: Baker Hughes field-proven multistage fracturing system.

Fracture aperture: perpendicular spacing between two walls of a fracture.

Fracture closure pressure: pressure needed to initiate opening of a fracture.

Fracture containment: containment of the fracture within the desired zone.

Fracture initiation pressure: pressure at which rock breaks and the fracture is created. Also known as formation breakdown pressure.

Fracture swarm: cluster of fractures close or connecting to each other.

Front end engineering design (FEED): a project-management term that details the project profitability and potential risks; follows the feasibility study; is used to define details and key requirements of the systems involved in the project.

Gas chromatography mass spectrum (GCMS): combination of gas liquid chromatography and mass spectroscopy to study the properties of methane content, carbon dioxide, ethane, propane, butane, pentane, nitrogen, and hexane.

Gas window: the temperature range at which gas is generated and released from the kerogen.

GasMaster™: advanced design gas separator used with Baker Hughes electric submersible pumps.

Gel squeeze: use of a chemical treatment to control the workover operation and provide isolation.

Geochemistry: the branch of chemistry dealing with the specialized reactions of downhole fluids and formations.

GeoFORM™: Baker Hughes patented high-efficiency sand-management system used with Morphic™ shape memory polymer technology to offer total conformance to the borehole.

Geographical information system (GIS): a computer system designed to capture, store, manipulate, and analyze all types of spatial or geographical data.

Geojars: a lab method used to contain the adsorbed gas from the cuttings; is used for gas composition analysis and geochemical studies.

Geomechanics: The study of the mechanics of the earth.

Grain compressibility modulus (Kg): When the rock is empty of fluid; also known as dry rock modulus.

Green chemistry: Use of materials and chemical processes that will prevent pollution and minimize negative environmental impacts.

GRI: a technique developed by the Gas Technology Institute to determine porosity and permeability of rock samples.

Guar: a polymer made from the guar plant; is used in gelation of fracturing fluids.

H2prO™: an environmental friendly water management service offered by Baker Hughes is the industry's most comprehensive solution to reduce health, safety, and environment impact and operational costs.

Hagen–Poiseiulle equation: a physical law that calculates steady-state laminar flow through a cylinder; gives the pressure drop in a fluid flowing through a pipe.

Hardness: the resistance of the rock to scratching by another substance.

HDIL™: Baker Hughes High-definition Induction Log Service™ that accurately measures the true formation resistivity.

Hoek and Brown failure criterion: a nonlinear model used to predict rock failure under tensile stress.

Homoscedasticity: the variance around the regression line is the same for all values of the predictor; also known as homogeneity of variance.

Horizontal transverse isotropy (HTI): HTI anisotropies are found perpendicular to natural fracture planes.

Hot oiling: a thermal method that is based on the circulation of heated oil to dissolve paraffin.

Hot watering: a thermal method based on circulation of heated water to dissolve paraffin.

HSI: horsepower per square inch.

Hydrogen index (HI): indicates un-oxidized hydrogen in the system; equals S2/S1+S2.

Hydrolysis: decomposition of a chemical compound by reacting with water in which water molecules are split into hydrogen cations and hydroxide anions.

Hydrostatic loading: radial direction of the loading.

In-situ stress: the state of the local or principal stresses of tectonic origin found in the reservoir conditions.

IN-Tallic™: features groundbreaking material science technology owned by Baker Hughes. The IN-Tallic™ fracturing balls maintain shape and strength during the fracturing process and disintegrate before or shortly after the well is put on production.

Independent variables: two random variables are independent if they convey no information about each other.

Inductively coupled plasma–optical emission spectroscopy/mass spectrometry (ICP-OES/MS): mass and elemental analysis methods.

Internal friction angle: angle on a graph of shear stress and normal effective stress at which shear failure occurs.

Isotube: a method for analysis of free gas that is used in gas composition analysis and geochemical studies.

IUPAC classification: a pore size classification by the International Union of Applied Chemistry that considers micropores to have width less than 2 nm; mesopores to be between 2 to 50 nm; and macropores to be greater than 50 nm.

Kinetix™: a logging service by Baker Hughes that determines lithology, qualitative total organic carbon (TOC), porosity, and saturations.

Knudsen diffusion: a type of diffusion in nanodarcy formations where pore diameter is smaller than the mean free path of the gas molecules in the system.

Kymera™: Baker Hughes bit that offers superior torque management.

Lamé elastic parameters: two parameters (first Lamé and second Lamé parameter) used in linear elasticity related to bulk modulus and shear modulus of a rock.

Langmuir isotherm: a plot that shows adsorption and desorption of gas as a function of pressure.

LATIDRILL™: Baker Hughes proprietary field-proven, water-based drilling fluid system specially formulated to drill extended lateral sections in unconventional shale plays; a cost-effective solution that outperforms the stability and speed of an oil-based drilling fluid system.

Leak-off test (LOT): the gradual increase of the injection pressure until the fluid leaks off into formation.

Least compressive stress: minimum horizontal stress; one of the in-situ stresses in the formation rocks. Fractures tend to open against this stress direction; therefore, it is a key formation parameter in designing hydraulic fracture models.

LECO: An American Society of Testing and Materials (ASTM) approved tool and method used to analyze carbon content in a rock sample by means of combustion.

Ledging: wellbore quality and smoothness.

Limited entry perforating: a stimulation method of diverting fracturing fluid to multiple zones of interest based on perforation friction pressure.

Linear elastic fracture mechanics (LEFM): the theory of rock mechanics related to linear elasticity (stress proportional to strain) that defines conditions under which the fracture extends in a rock.

Linear variable differential transformers (LVDT): an electromechanical transducer used to measure linear displacement of the material.

Liquid-metal ion sources (LMIS): an ion source that produces high current density ion beams with very small energy spread to enhance the performance of ion beam application systems.

LitePlug™: A Baker Hughes composite sand plug mixture of 50-50 sand and LiteProp™ used in conjunction with retrievable multiple packers.

LiteProp™: An ultra-lightweight proppant by Baker Hughes used in stimulation operations.

Longitudinal fractures: A type of hydraulic fracture configuration that is formed when the horizontal well is drilled in the direction of the maximum horizontal stress.

MaxCOR™: Baker Hughes sidewall coring technology; an efficient coring technology acquiring high-quality 1.5-inch core samples that enables the asset team to accurately describe and evaluate the reservoir.

Maximum horizontal stress (σH): one of the three principal stresses that together with minimum horizontal stress and vertical stress define the stress field of the formation rocks.

Mercury injection capillary pressure (MICP): a plot of capillary pressure data versus the fluid (mercury) saturation used to characterize porosity and matrix permeability distributions in shale reservoirs.

MFrac™: Baker Hughes design and evaluation simulator using 3D fracture geometry and integrated acid fracturing. For real-time and replay fracture simulation, the MFrac simulator works with MView™ for real-time data acquisition and display applications.

Microbial induced corrosion (MIC): a type of corrosion caused by microorganisms such as bacteria.

Microemulsion: clear, thermodynamically stable, isotropic liquid mixtures of oil, water, and surfactant, frequently in combination with a cosurfactant.

Microfrac: a test performed by a downhole wireline straddle packer to determine stress and fracture gradient in a reservoir.

Minifrac: a low-rate injection hydraulic fracture test.

Minimum effective concentration (MEC): The minimum concentration of scale inhibitors that is necessary to inhibit scale formation.

Minimum horizontal compressive stress (σh): one of the three principal stresses that together with maximum horizontal stress and vertical stress define the stress field of the formation rocks; can be calculated using either empirical equations or fracturing data.

Mixed layer illite/smectite (MLIS): a type of swelling clay mixture found in reservoir rocks.

Mode I tensile failure: a type of fracture failure mode that is caused by a load in tension.

Mohr–Coulomb failure criteria: A model used to predict characteristics of a rock behavior failure envelope using shear stress, normal stress, and $\sigma 1$, $\sigma 2$, and $\sigma 3$.

Monte Carlo simulation: Process of running a model many times with random input data selection for each variable.

MReX™ NMR: MR eXplorer™ (MReX™) is an instrument that uses static and pulsed radio frequency magnetic field to make downhole spin-echo magnetic resonance measurements.

MShale™: Baker Hughes 3D discrete fracture network (DFN) simulator; used to predict fracture propagation in fractured and naturally fractured reservoirs and in multiple clusters and complex systems.

Mud invasion: Invasion of mud into formations due to the excessive mud weight higher than the formation pressure.

Mud pulse telemetry: an automation technology in drilling used to communicate with the surface directly controlling drilling operations. Baker Hughes aXcelerate™ is an advanced drilling automation service that delivers high-resolution downhole picture in real time helping users make better decisions during reservoir navigation operations.

Mudrock: a class of fine-grained siliciclastic sedimentary rocks.

Multiset packer: packers designed to work on both openhole and cased hole completions that can be permanent or retrievable.

Multiple linear regression: a linear regression with two or more predictors.

Multivariate analysis: includes all statistical techniques that handle two or more variables of interest.

Navi-Drill™: Baker Hughes in-house manufactured and advanced positive displacement motor (PDM) drilling solution; ideal for directional and horizontal sections; customized to the user's specific needs; can be easily integrated with superior automated drilling systems for improved recovery.

Net pressure: the difference between the pressure in the fracture and the minimum in-situ stress, σmin.

NMR logging: measurement of nuclear magnetic properties such as distribution of T2 amplitude and formation properties such as pore volume and total porosity based on nuclear magnetic resonance technique.

Non-dispersive infrared detection (NDIR): cells that selectively detect and measure the amount of CO_2 produced.

Normal faulted stress regime (NSR): a regime encountered when vertical and minimum horizontal stresses are the largest and smallest stresses, respectively.

Normality: an indicator of whether data can be well modeled by a normal distribution.

Normalized cumulative production: Cumulative production value in which production during well cleanup prior to the well reaching peak production is removed. Peak month becomes month No. 1 and producing months are counted beginning with month No. 1 and proceeding (in this example) to producing month No. 12, then calculating the resulting cumulative production number.

Nuclear magnetic resonance (NMR): A phenomenon by which a nucleus absorbs electromagnetic radiation of a specific frequency in the presence of a strong magnetic field.

NVT: the number of particles (N), system's volume (V), and temperature (T) in a system.

OASIS™: Baker Hughes engineering and consulting drilling service; a proven and highly disciplined drilling plan that can significantly cut drilling costs by reviewing the whole drilling system and providing a detailed analysis of the wellbore environments.

One-way table: A statistical table that shows the observed number or frequency for one categorical variable.

OnTrak™: integrated LWD/MWD system that increases positional certainty and avoids expensive directional remedies when the MWD measurements are combined with near-bit inclination data achieved by X-treme™ motors, which are a series of Baker Hughes downhole drilling motors with shorter power section and shorter radius profile designed for challenging wells that will maximize your ROI by increasing the reservoir exposure and drilling efficiency. Navi-Drill™ motor is an example.

OptiFrac™ SJ: an environmentally friendly technology that uses SJP to create the diversion path for the fracturing fluid and isolate through tubing.

OptiPort™: Baker Hughes multistage fracturing system allowing unlimited number of fracture stimulations with the desired economics and flexibility.

Orthohombic PS™: a more robust and accurate form of velocity analysis below fracture overburdens.

Over-displacement of proppant: injection of clean fluid into the well to remove the residual proppant from the lateral after the treatment is finished.

Overburden: pressure produced by overlying rock layers.

Overpressure: a zone with an abnormally higher hydrostatic pressure at a given depth.

Oxigen Index (OI): equals S3/S1+S2. OI is indicator of gas richness.

P Wave: a portion of seismic wavefield that is compressional and oscillates in the direction parallel to propagation of the wave.

P10: 10% of all the estimates exceed this value.

P50: 50% of all the estimates exceed this value.

P90: 90% of all the estimates exceed this value.

Packoff: a mechanical type of stuck pipe which is developed when circulation is lost or reduced resulting in collapse of cavings around a drillstring.

Pari passu: joint and equal participation of different companies in an operation.

Patch array: a type of acquisition in which the receivers are placed in an array configuration.

Percussion sidewall coring: a type of sidewall coring method to acquire formation samples by utilizing explosive charges into the formation.

PERFFLOW™: a chemical material used as a drill-in completion fluid.

PERFORMAX™: a Baker Hughes fluid solution that is an environmentally friendly water-based fluid comparable to

oil-based mud (OBM) systems, which enhances lubrication for the drill string and the formation face to minimize bit balling and increase the rate of penetration.

Permeameter: an instrument for measuring the absolute permeability of core samples in the lab.

Pinchout: a geologic trap structure condition where a formation has been terminated against another layer of rocks.

Plastic properties: rock mechanical properties under plastic deformation.

Plug and perf: a multistage system that uses cement to isolate the annulus and perforations to breach the liner; was originally used in unconventional plays; is the most common type of multistage completion system.

PLUG-LIFT™: a proprietary drillout chemical product designed by Baker Hughes to remove post-fracture composite plugs.

Poisson's ratio: a measure of the geometric change of shape under uniaxial stress.

Pore pressure: pressure exerted by pore fluid.

Poroelasticity: interaction between pore fluid and rock matrix.

Positive displacement motor (PDM): a downhole motor powered by a circulating fluid without the need of rotating the drill string.

Possible reserves: reserves that cannot be probable but are still significant and have less than a 50% chance of being produced.

Present-day total organic content (TOCpd): is different than the initial state of the TOC prior to generation of oil and gas.

Pressure pulse decay: change in pressure versus time as a result of flow of fluid; a method to calculate the permeability from tight low-permeability formation rocks.

Probable reserves: reserves that are not proven yet but estimated to have a better than 50% chance of being produced.

ProductionWave™: Baker Hughes production solutions that offer a wide range of choices including FLEXPump™ for wells that require artificial lift methods to accelerate the production with better economics and fewer health, safety, and environmental risks for unconventional reservoirs.

Profit oil: the amount of production divided among each participating party under the production-sharing contract after all the expenses and costs have been deducted.

Proppant embedment: embedment of proppants into formations that results in reduced fracture aperture and conductivity.

Proppant: a treated or a man-made sand used in conjunction with hydraulic fracturing fluid to keep the induced fractures open for flow.

Proved undeveloped (PUD): proved reserves that are expected to be recovered from future wells with improved recovery process.

Proven reserves: reserves that have a better than 90% chance of being produced.

Pulsed neutron logging: measures pulse neutron-induced gamma ray counts and spectroscopy with formation and borehole that would give information about reservoir lithology, porosity, and fluid saturations.

PVT cell: a laboratory tool used to study the phase behavior of hydrocarbon fluids and their physical properties.

Pyrobitumen: a type of solid, amorphous organic matter.

Pyrolysis: a geochemical analysis to evaluate the quality, thermal maturity, and potential of the source rock in a system.

Qualified reserve auditors: A person with sufficient background and experience to properly conduct audit exercise of reserve estimation information.

Qualified reserve evaluators: A person with sufficient background and experience to properly exercise prudent professional judgments related to oil and gas reserve evaluations.

Quantitative risk analysis (QRA): a type of Monte Carlo simulation capable of showing distribution of input data and their individual impact on the objective function.

QUICK Drill™: drillable bridge and fracturing plugs designed by Baker Hughes to isolate multiple zones and enabling each zone to be treated independently.

R-T plot: a plot at which microseismic events are plotted with respect to distance from injection well (r) and injection time (t) are used to present additional information about microseismic event quality.

Raman scattering: effect when photons are elastically scattered from an atom or molecule.

RCI™: Baker Hughes Reservoir Characterization Instrument service.

RCX™: Baker Hughes Reservoir Characterization eXplorer used to acquire high-quality data in extreme conditions at up to 395°F and 27,000 psi.

Refracturing: an operation performed on an existing hydraulically fractured well to increase the efficiency of the original hydraulic fracturing process.

Relative hydrocarbon potential (RHP): a parameter derived from Rock-Eval pyrolysis that is S1+S2/TOC to give information about depositional environment.

Reserve booking: resource and reserve volume assets of an oil and gas company.

Retort analysis: a thermal extraction method performed in laboratories in which the fluids are vaporized, condensed, and collected separately.

Reverse faulted stress regime (RSR): a regime encountered when maximum horizontal and vertical stresses are the largest and smallest stresses, respectively.

Rhino™: Baker Hughes Bifuel pumps that reduce diesel fuel consumption and air emissions to the environment without scarifying their horsepower.

RockTest: software developed by Baker Hughes to simulate triaxial core tests.

RockView™: Baker Hughes in-situ mineralogical characterization service that combines geochemical data acquired by SpectraLog™ service and Formation Lithology eXplorer FLeX™ measurements.

Rotary steerable system (RSS): a tool designed to drill directionally with continuous rotation without the need of sliding the motor downhole.

RPM™: Baker Hughes reservoir performance monitor logging platform is a multifunction pulsed neutron reservoir monitoring instrument used in formation evaluation, workover, and production profiling.

S Wave: a portion of seismic wavefield that is shear and oscillates in the direction perpendicular to the propagation of the wave.

S1: In pyrolysis analysis, S1 peak is the amount of hydrocarbon thermally distilled from the rock by heating to about 300°C.

S3: In pyrolysis analysis, S3 peak is the volume of the CO_2 produced.

Sand jet perforator (SJP): a tool designed to perforate casing and cement using abrasive-laden slurry.

Sand-Vac™ Cleanout System: Baker Hughes technology for removing solids and liquids from ultra-low-pressure wellbores that are not treatable with standard circulating methods.

SANS and USANS porosity: small-angle and ultra-small angle neutron scattering techniques performed to characterize pore structure and connectivity.

Sapropel: dark-colored sediments that are rich in organic matter.

Saturate, aromatic, resin, and asphaltene (SARA): a type of analysis performed to characterize crude oil for asphaltene deposition.

Saturation Index (SI): the logarithm of the ratio of the scaling ion activity to the thermodynamic solubility product of a concerned scale in the water.

Scanning transmission electron microscope (STEM): an imaging technique to generate both 2D and pseudo 3D images of the macro-, meso-, and micropores present in mudstones.

Scatterplot matrix: a matrix of scatterplots to assess the relationships between multiple variables simultaneously.

Schmidt plot: used to give information about structural dip of a formation.

Screen-out: when proppants in a fracturing fluid create a bridge across the perforation and are no longer movable, resulting in a sudden and restricted area to fluid flow and an associated rapid increase in the pump pressure.

SealBond™: a technology developed and used by Baker Hughes to enhance the cement bonding and zonal isolation around the wellbore.

SealBond™ Plus: an additive made of all natural-fibrous, granular material which eliminates drilling fluid losses in higher permeability formations.

Sealing fault: a fault that effectively seals a compartment.

Secondary electrons (SE): electrons resulted from ionization process.

Seismic impedance: a product of acoustic velocity that passes through a rock and the density of the rock.

Seismic while drilling (SWD): used where wireline tools are impractical to use or too expensive; is a technology and application the exploration and drilling team can use to gain real-time information about the formation to drill, and to update the reservoir models in real time.

SEM/ESEM imaging: a method that uses an electron beam in a vacuum chamber to image the rock sample.

SEM-FIB tomography: an advanced high-resolution technique for 3D imaging of samples in which the samples are imaged by repetitive use of focused ion beam and focused electron beam.

SHADOW™: a game-changing fracture plug technology by Baker Hughes; used in plug-and-perf completions to maximize efficiency without the need of millout operations.

Shale anisotropy: a directionally dependent property of shale that influences its strength and can be the result of depositional or tectonic processes.

Shale laminations: layering of sedimentary rocks.

Shale oil: can be either an immature oil phase, often called kerogen, or oil in the crocks of pores of a shale rock.

Shale shear stimulation: a stimulation that provides enhanced contact area mainly from existing natural fractures and weakness planes in a shale formation.

Shale spalling: a detrimental effect to proppant pack permeability and well productivity associated with proppant embedment, which is caused by creation of formation fines into the fracture face.

Shale Value Model: a comprehensive economic model developed by Baker Hughes' unconventional resource team.

Shear failure: failure caused by shear stress.

Shear strength (So): an ability of a material to resist sliding and structural failure.

Shear stress: component of a force vector parallel to the cross section of the plane.

Shear wave slowness (DTS): reciprocal of shear velocity.

Sheet flow: flow of slurry on a narrow gap between two fracture faces.

Sidewall coring: a method at which the small cores are taken from a side of the wellbore using percussion and advanced rotary coring tools.

Signal-to-noise ratio (SNR): compares the energy of the background noise with the desired energy of the signal and outputs the result as a ratio.

Simultaneous operations (Simops): a process when multiple operations are being performed parallel.

Single (univariate) linear regression: a statistical process that attempts to find a linear relationship between a predictor (independent) variable and a target (dependent) variable.

Slip region: region of failure around a wellbore.

Sloughing: swelling of shale after interaction with brine or water; can cause borehole enlargement and instability issues.

Sorbed gas: the gas adsorbed on the surface of an organic material.

Source rock analyzer (SRA): the study of source rock maturity and its potential hydrocarbon by monitoring the temperature and petroleum compounds within the rock.

Source rock: a rock that is rich in organic matter.

Special core analysis laboratory (SCAL): techniques performed on core samples to mimic reservoir rock behavior and properties such as capillary pressures, wettability, and relative permeability.

Stabilized Severe Duty (SSD): Baker Hughes enhanced electrical submersible pump (ESP) construction that reduces abrasive wear, decreasing workover expenses and improving reliability.

Stabilized Heavy Duty (SHD): an enhanced electrical submersible pump system by Baker Hughes that provides improved reliability.

Standardized measure of oil and gas (SMOG): discounted future net cash flows relating to the proved oil and gas reserve quantities. It takes into account the price received for selling the oil and gas, the costs of the operations, and the timing of cash flows.

STAR™: Baker Hughes image service used to provide high-resolution resistivity formation images.

Starch: an additive to drilling fluid used to control the fluid loss.

StarTrak™: Baker Hughes high-definition LWD imaging tool offers detailed reservoir characterization, structural classification, and wellbore integrity management in real time.

Stick slip: slip-stick motion of the bottomhole assembly.

StimPlus™: Baker Hughes reservoir flow assurance service used to pump production chemicals deep into the reservoir during the stimulation treatments. It ensures formation fluids are treated before they can cause production flow problems.

Stimulated reservoir volume (SRV): stimulated volume of a reservoir around a hydraulically fractured well.

Stoneley wave: type of surface waves usually generated during sonic logging of a wellbore.

Stress contrast: the difference between stress values of two adjacent zones.

Stress shadow: a change in stress field around a hydraulic fracture from its far field directions.

Strike-slip stress regime (SSR): a regime encountered when maximum and minimum horizontal stresses are the largest and smallest stresses, respectively.

Stuck pipe: a common wellbore stability issue when pipe cannot be moved or rotated.

Sub-irreducible saturation: a condition where the initial water saturation is less than the saturation that would exist typically under prevailing capillary conditions.

SureSet™: a technology that reduces the horsepower and footprint requirements for CT assisted multistage fracturing operations.

Surface logging system (SLS): service consists of analyzing real-time geological data such as lithology, mineralogy, presence of oil, formation gases; helps to improve the drilling efficiency with the ability to predict the drilling events that could jeopardize the well integrity.

Sweet spot: a region of the rock where geochemical, geological, and geomechanical properties have ideal reservoir characteristics for stimulation.

SXD: Baker Hughes patented Stabilized Xtreme Duty pump construction that minimizes abrasive wear and significantly improves the run time.

Synthetic seismogram: the result of forward modeling the seismic response of an input earth model, which is defined in terms of 1D, 2D, or 3D variations in physical properties.

T1: longitudinal relaxation time or decay rate, seconds.

T2: transverse relaxation time or decay rate, seconds.

Talon™ 3D: the Baker Hughes optimized PDC frame designed to improve rate of penetration (ROP), directional control, bit life, and hydraulic efficiency even in low HSI applications encountered in shale play drilling.

Technically recoverable reserve (TTR): the amount of oil or gas producible using current level of technology.

TeleCoil™: Baker Hughes intelligent coil tubing service provides operators with accurate and real-time information about depth, bottomhole assembly (BHA) functionality, and

monitoring the process of the job; eliminates the guess work and assumptions beyond the traditional coiled tubing operations.

Telescoping sleeve: a tool that can be used to increase core recovery by allowing multiple jams during a coring run.

Tensile strength: the force required to pull apart a substance lengthwise.

TERRA-MAX™: Baker Hughes water-based drilling fluid system; a customizable, high-performance drilling system used in low-salinity environments.

Thermal Alteration Index (TAI): indicates the degree of thermal alteration and color variation in kerogens with depth.

Thermal maturity: a measure of the degree of how much the source rock has been exposed to heating during which the kerogen content of the source rock has been transformed to hydrocarbon.

Tight oil: oil contained in petroleum-bearing formations of low permeability, often shale or tight sandstone.

Tmax: temperature at which cracking of kerogen releases the maximum amount of hydrocarbons.

Toe-up: a type of wellbore design in that the landing point is lower than the toe section.

Torque fluctuation (TF): a parameter that limits bit stability and reduces its rate of penetration. Baker Hughes Kymera™ bit offers superior torque management.

Total dissolved solids (TDS): the amount of impurities such as minerals and salts present in drilling and completion fluids.

Total organic content (TOC): the concentration of organic material by weight percent.

Total stress: the summation of pore pressure and the effective stress.

Transformation ratio (TR): the ratio of generated petroleum (S1) to potential yield of petroleum in a source rock (S1+S2).

Transient flow behavior: a flow condition that pressure derivative is a function of both time and location; identified in the pressure interpretation tests to obtain dynamic reservoir data and reservoir characterization.

Transverse fractures: a type of hydraulic fracture configuration that is formed when the horizontal well is drilled perpendicular to the direction of the minimal horizontal stress.

Transversely isotropic (TI): a material that is azimuthally symmetric about a single axis.

Triaxial loading experiment: a type of a laboratory test performed to study the stress-strain relationship and measure static elastic properties of a rock.

Tube blocking test: a lab test performed to determine the dosage and minimum concentration of best inhibitors for a scale inhibition operation.

Turnizontal drilling: a drilling technique with only one surface location but multiple well sites to drill.

Unconfined compressive strength (UCS): used to indicate the strength of the rock sample under loading.

Undercompaction: partial support of rocks by fluid that is unable to escape the rock at a rate required for normal compaction.

Undrained bulk modulus (Ku): the bulk modulus of elasticity under hydrostatic undrained condition. Undrained method is quicker than the drained method in obtaining the strength and rock elastic properties in low-permeability shale samples.

Unit technical cost (UTC): summation of capital and operating costs divided by the barrel of oil produced.

Variable speed drive (VSD): a type of surface electrical control used to optimize pump system performance and efficiency by means of changing power supply frequency.

Variance: a statistical measure of the range of a variable in a dataset.

Vena contracta: an effect resulted when a fluid stream is at its maximum velocity passing through a limited diameter channel (perforation).

Vertical stress (σV): overburden pressure produced by rock layers overlying a measurement point. σV is the maximum

principal stress in normal stress faulting regime, intermediate principal stress in the strike slip stress regime, and least principal stress in reverse stress faulting regime.

Vertical transverse isotropy (VTI): refers to anisotropies that are found perpendicular to horizontal layering.

Vibroseis technology: a vehicle that can provide the seismic source for seismic operation.

Viscoelastic fluids: fluids that exhibit both viscous and elastic characteristics when undergoing deformation.

Viscoelastic surfactants (VES): types of surfactants that exhibit a well-defined hydrophilic head structure with a hydrophobic end that when used as foam in fracturing fluid, minimizes the interfacial tension.

Vision technology: Baker Hughes web-based monitoring system; is a remote collaboration platform used to analyze the operating data and objectives.

Vitrinite Reflectance (%Ro): one of the primary components of coals and most sedimentary kerogens.

Volumetric bulk modulus: prosperity of a material that characterizes resistance of the material to change in volume due to the applied pressure.

VSFusion: a borehole seismic processing and interpretation tool joined venture by CGG and Baker Hughes that is helpful in microseismic monitoring of hydraulic fracturing operations.

Washout: an enlarged area of a wellbore resulted during drilling or circulation.

Water immersion porosity (WIP): a technique used to measure total porosity of shale samples on small rock chips.

Watermelon string mill: a tool used to mill out tight spots in the casing.

Well architecture: measureable variables from well construction, such as azimuth and drift angle.

Wellbore isolation valve (WIV): a cost-saving tool that allows circulation from the completion string to the annulus during wellbore run-in operations.

WellLink VISION™: Baker Hughes web-based monitoring system is a remote collaboration platform used to analyze the operating data and objectives.

Wet microseismic events: Those events associated with a change in pressure likely due to communication with hydraulic fractures or wellbore.

Working interest (WI): A percentage of ownership in an oil and gas lease granting its owner the right to explore, drill, and produce oil and gas from a tract of property.

X-ray diffraction (XRD): a tool to characterize the molecular and chemical structure of a crystal.

X-treme®: series of Baker Hughes downhole drilling motors with shorter power section and shorter radius profile; designed for challenging wells that will maximize the return on investment by increasing the reservoir exposure and drilling efficiency.

XMAC-F1™: Baker Hughes acoustic service that delivers real-time compressional, Stoneley, and slow and fast shear measurements that improve stress profiling, and consequently maximize production by better decision-making.

ZDL™: Baker Hughes Z-density log services.

This page intentionally left blank

Author Biographies

This page intentionally left blank

Author Biographies

Tony Addis is Director for Unconventional Resources (Middle East Asia Pacific) at Baker Hughes. Tony has 29 years of experience in rock mechanics and geomechanical engineering applied to the petroleum industry, and has specialized in drilling optimization and production technology, with 16 years' major operator experience (Shell and BP) working in technology development, technical support, and subsurface asset teams.

Tony has a BSc and PhD from London University and has over 40 technical publications and patents. He is currently based in Dubai, U.A.E.

Usman Ahmed. With more than three decades of petroleum engineering experience, Usman Ahmed is Baker Hughes' Vice President and Chief Reservoir Engineer. He addresses Baker Hughes' reservoir-driven and integrated solution approach to unconventional resources development and reservoir technology in general. Ahmed joined Baker Hughes in 2010 and has previously worked for Schlumberger, TerraTek, and ran his own reservoir and production engineering consulting firm Energy Resources International. He holds a BSc and MSc (both in petroleum engineering) from Texas A&M University. Looked to as a technical and professional industry leader, Ahmed has two patents and is the author and co-author of more than 100 industry papers and textbooks and has been invited to numerous events as keynote speaker and panelist. He is a SPE Distinguished Member and has also been SPE Distinguished Speaker in 2004-2005 and the SPE 2013-2014 Distinguished Speaker on "Unconventional Resources Development."

I. Yucel Akkutlu is associate professor of petroleum engineering at Texas A&M University. He is the holder of the George & Joan Voneiff Development Professorship in Unconventional Resources. He is a chemical engineer and holds a PhD in petroleum engineering from the University of Southern California, Los Angeles, US. His main research interests are fluid flow, heat/mass transport, and reactions in porous media. His work finds applications in reservoir engineering, particularly in the areas of IOR/EOR and unconventional oil and gas recovery. Dr. Akkutlu began his academic career at the University of Alberta in 2004. In 2007, he moved to the University of Oklahoma. He worked on fundamental problems of gas storage and transport in organic-rich shales in the laboratory, in particular the Barnett, and developed the first multiscale reservoir simulation models for shale gas production. He joined the Texas A&M University petroleum engineering faculty in 2013. His current research deals with scaling-up and homogenization of coupled transport (viscous and diffusive) and reaction processes in low-permeability geological formations exhibiting multiscale pore structures.

Akkutlu has numerous publications in peer-reviewed journals and conference proceedings. He has given more than twenty short courses for the industry and numerous invited talks on shale gas production around the world. Akkutlu serves on the Natural Sciences and Engineering Research Council of Canada (NSERC) as a member of the materials and chemical engineering committee. He served on the SPE ATCE Recovery Mechanisms and Flow in Porous Media subcommittee 2007-2010. He is the 2014-15 SPE Distinguished Lecturer and received SPE outstanding service awards in 2008, 2009, and 2010. He is the recipient of the 2014 AIME Rossiter W. Raymond Memorial Award. He received the 2014 TAMU Petroleum Engineering Department Award for Excellence in Teaching.

Antoine Bouziat holds a MSc in numerical geology from the ENSG school in Nancy (University of Lorraine). In 2011, his student work on fault modeling was named by the Society of Petroleum Engineers the winner of the European Student Paper Contest. The same year, Antoine joined CGG as a research geoscientist to develop innovative tools and workflows linking geophysical data with reservoir modeling. Since September 2014, he has been a researcher at the IFPEN center (formerly French Institute of Petroleum) investigating new methodologies for the modeling of sedimentary basins.

Matt W. Bratovich joined Baker Hughes in 2004 and has held several positions until assuming his current assignment as Global Director of Petrophysics working in the Field Development & Production Management Group in the fall of 2014. He has been involved with unconventional resources since 2006 developing shale formation evaluation interpretation

solutions and providing technical assistance and evaluation support internationally, both internally and to Baker Hughes customers.

Prior to joining Baker Hughes he worked with DeGolyer & MacNaughton in Dallas, Texas, as the firm's principal petrophysicist and a vice president in the Middle East/Africa/Europe division. During his tenure at D&M he completed petrophysical studies for projects in the U.S. and over 45 countries worldwide including significant unitization and litigation experience on petrophysical issues. Matt began his career with Shell's Offshore division in New Orleans, Louisiana, working as a petrophysical engineer.

He holds a BS degree in geological engineering from the University of Missouri-Rolla and was awarded an honorary professional degree in geological engineering by that school. He is a registered professional engineer in the state of Texas.

Matt has been active in SPWLA having held several positions on the international board of directors, serving as the president of the society in 2010-2011. He also is a member of the AAPG and SPE.

William (Aaron) Burton is currently Product Line Manager for Multistage Completion Systems, a global group primarily focused on completions tools in shales and similar formations that require multistage hydraulic fracturing. He graduated with a BS degree in mechanical engineering from Mississippi State University. After graduation he joined Baker Hughes as a field engineer trainee for completion tools. During his tenure in operations, he has held the roles of field engineer, operations coordinator, and district engineer. Burton has completed wells and worked in several unconventional plays in North America, including the Bakken, Marcellus, and the Lower Huron. Before taking his current role, he worked as the completions manager for the unconventional resources team, a group focused on unconventional resources from exploration to rejuvenation. He is an active member of the Society of Petroleum Engineers (SPE) and has authored/coauthored several SPE papers. He instructs the unconsolidated formations portion of the SPE course, horizontal completions and the wellbore completions portion of the SPE Course, Unconventional Completions – Wellbore Completions and Fracturing.

Randall Cade started his career with ARCO International in 1983 as a reservoir engineer evaluating and helping to develop fields in several countries. Over the years he has worked both on the service side and operator side of the industry, with projects in the North Sea, Venezuela, Africa, and the Far East, and most recently with unconventionals in North America. Randall is currently with Baker Hughes as Director – Well Solutions, which is part of an initiative launched in 2013 to provide a more integrated approach to service delivery and field development in North America. Prior to that he was manager of the Reservoir Solutions teams in the US. Randall holds a BS in petroleum engineering from the Colorado School of Mines.

Gabino Castillo is the CGG Regional Manager – America Region (GeoConsulting – Seismic Reservoir Characterization) with 15 years of experience in the oil and gas industry. He is a nuclear engineer holding a master's degree in geophysics (Institut Francais du Pétrole), and he also holds a master's degree in computer science.

His experience includes conventional and unconventional reservoir characterization, pre-stack seismic inversion, stochastic inversion, azimuthal inversion, pore pressure prediction, interpretation, pre-stack depth migration, time processing and research and geophysics development.

Kevin Chesser is Chief Petrophysicist of Seismic Reservoir Characterization, in the GeoConsulting group at CGG, based in Houston, Texas. He manages a diverse group of geologists and engineers who are equally committed to seismic petrophysics. Kevin has over 30 years of experience in the upstream oil and gas industry in exploration and development geology, petrophysics, and seismic reservoir characterization. He completed his BSc in geology from Sul Ross State University in 1977 and MSc in geology from the University of Kansas in 1987. Since joining CGG in 2008, Kevin has worked in a variety of unconventional plays including, Barnett, Haynesville, Marcellus, Bakken, and Eagle Ford.

Craig L. Cipolla is Senior Completions Engineering Advisor at HESS. As a senior completions engineering advisor, Craig provides hydraulic fracturing and completions support to HESS business units worldwide. Prior to joining HESS, Craig was chief engineering advisor for Schlumberger-Hydraulic Fracture Monitoring and Optimization, VP of Stimulation Technology for Carbo Ceramics, and VP of Engineering for Pinnacle Technologies. Craig has co-authored over 70 technical papers, was an SPE Distinguished Lecturer on hydraulic fracturing in 2005-2006, and the recipient of the SPE International Completion Optimization and Technology Award in 2013. Craig holds undergraduate degrees in engineering and chemistry from the University of Nevada-Las Vegas and a master's degree in petroleum engineering from the University of Houston.

Dave Cramer is a senior engineering fellow on the ConocoPhillips Global Wells Completions Engineering staff in Houston, TX. He has 37 years of experience in designing, implementing and evaluating well stimulation treatments. Dave has authored 45 papers and is a co-inventor on two U.S. patents. Industry recognitions include the Henry Mattson Technical Achievement Award by the Denver SPE chapter in 1993 and the SPE International Completions Optimization and Technologies Award in 2011. He was an SPE Distinguished Lecturer from 2003-2004 and the SPE Region Director for the US and Canada Rocky Mountain region from 2004-2007. Dave is a registered professional engineer in the state of Colorado.

Brian "BJ" Davis is Manager-Geological Services for Baker Hughes at the Pressure Pumping Technology Center in Tomball, Texas. Since graduating from Texas A&M-Commerce with an earth science/geology degree, Davis has spent 35 years in the petroleum and environmental industries focused on the evaluation of petroleum and geothermal reservoirs through the characterization and laboratory testing of reservoir samples. He is an active member of AAPG, the Houston Geological Society, and SPE. He is the author or co-author of several SPE papers and has served on technical committees for multiple SPE conferences. His background includes research, field operations, quality assurance/quality control, and engineering/sales support. In addition to presentations at AAPG, IOGA, and SPE conferences, he has prepared and presented numerous schools and project summaries to employees and customers. Davis manages the geological team's research and technical support for global product lines such as hydraulic fracturing, acidizing, coiled tubing, cementing, sand control, and remedial well treatment operations. The team provides primary and remedial well stimulation and completion recommendations to both internal and external customers, based upon the results and interpretation of detailed rock/pore network characterization and production materials studies. Davis' areas of interest include understanding the similarities and differences between current mudstone and tight oil plays, defining production and damage mechanisms in both conventional and unconventional reservoirs, and focusing on methodologies to limit production impairment and enhance productivity.

Gregory Devenish is a senior technical advisor with Baker Hughes Drilling Services. Mr. Devenish has global experience in drilling operations management, directional drilling, and drilling optimization and has contributed to various publications in the drilling industry.

Jim Erdle is CMG's vice president for software sales and support for the United States and Latin America. He has 40 years of industry experience, primarily in reservoir and production engineering-related positions within the services and software segments of the E&P industry, since graduating from Penn State with BS and PhD degrees in petroleum engineering in 1971 and 1974. Early in his career Erdle was involved with some of the industry's leading advances in well testing design, monitoring and interpretation technology, including closed chamber and surface pressure readout (SPRO) drill stem testing, production enhancement via NODAL analysis, stimulation treatment design and monitoring techniques, and production surveillance software (The Production Analyst, which was the predecessor to OFM).

Erdle joined CMG in May 1997 and by October of that year had opened CMG's USA office in Houston. Since then he has been responsible for expanding CMG business in the US, in the GCC countries of the Middle East (2003-2008), and since being promoted to vice president in June 2008, in South/Latin America. Erdle has been directly involved

in improvements to CMG's technology, including the workflows available within CMG's products used to build, run, and analyze dynamic reservoir simulation models of unconventional (shale/tight) gas and liquids-rich reservoirs.

Javier A. Franquet is Geomechanics Manager in Global Geoscience and the geomechanics advisor for the unconventional resources products and technology group in Baker Hughes. Javier has accumulated 18 years of applied geoscience and geomechanics consultancy experience in the oil and gas industry. He is recognized as subject matter expert in geomechanics, borehole acoustic and formation stress testing in conventional and unconventional reservoirs, holding over 30 technical publications in SPE, SPWLA, ARMA, ISRM and, SEG.

Javier received two master's degrees, one in petroleum engineering from Texas A&M University and another in reservoir geosciences from IFP School. He worked as a geomechanical researcher at PDVSA's research and technology center in Venezuela before joining Baker Hughes as a senior geoscientist for the Middle East and Asia Pacific, based in Abu Dhabi.

Hans-Christian Freitag is Vice President Integrated Technology at Baker Hughes. Prior to this role, he was VP of Unconventional Resources Eastern Hemisphere from 2012 to 2014, VP Marketing & Business Development from 2010 to 2012 for Baker Hughes. With over 25 years of experience in the industry, Mr. Freitag has held positions in management, sales, service, and applications in various locations, including Senior Log Analyst and Sales Manager in Abu Dhabi, Sales and Business Development Manager for Continental Europe district in Germany, Product Line Manager for Acoustics & Pressure Testing LWD in Houston, Formation Evaluation Manager for Gulf Coast and North America, and Director Marketing – Reservoir Access for Middle East Region in Dubai.

He graduated with bachelor's and master's degrees both in geophysics from the Technische Universität Clausthal (1989), and Technische Universität Berlin (1984), respectively. Mr. Freitag holds a US patent on Apparatus and Method for Mechanical Caliper Measurements During Drilling and Logging-While-Drilling Operations and has numerous publications and presentations to his credit. He is a member of the Society of Petroleum Engineers and his interests include family, travel, and sports.

Sachin Ghorpade is currently working as a Technical Business Development Manager- Reservoir Software based in Houston. Sachin started his career in 2010 as technical sales and support specialist working with various clients around the world supporting reservoir modeling and flow simulation. Throughout his career Sachin has worked in almost all the unconventional basins in the US, supporting clients in building reservoir models integrating data from various scales and domains to help them better understand the reservoir for well planning and fracture placement. Apart from unconventional plays, Sachin also has experience in modeling and flow simulation in the Santos Basin in offshore Brazil, the north Cormorant field in the North Sea, Raagdeep field in Rajasthan, India.

Currently Sachin is involved with supporting the sales and development team with software evaluations, market research for different workflows and functionalities.

Sachin has a MS in petroleum engineering from New Mexico Institute of Mining and Technology and a BS in mechanical engineering from Karnataka University, India. Sachin is an active member of the Society of Petroleum Engineers. He has conducted training at various client locations and presented technology and workflows at numerous industry events.

Cooper Gill has an extensive background in completions and sensor design. He has a bachelor of science in mechanical engineering from the University of Texas and a master's of petroleum engineering from the University of Houston. Mr. Gill is now working as a reservoir engineer at Murphy Oil Corporation in Houston. Previously, and from 2009 to 2014, he worked as Research and Design Engineer in Completions and Productions, Account Manager and Business Development Manager for Intelligent Production Systems at Baker Hughes Incorporated.

Ashish Goel is Senior Technical Support Engineer – Global for Drilling Systems based in Houston, Texas. With a diverse geographic experience in South East Asia, the Middle East, and North America, he has worked to introduce some of the most complex drilling

systems technologies across the globe. He is recognized as a subject matter expert within Baker Hughes for some key LWD technologies and his expertise lies in operations, new product introduction, and product development. He holds a bachelor's in technology from G.B. Pant University, India.

Rajdeep Gupta graduated with a BS degree in drilling technology from the Ambedkar Marathwada University and a MS degree in petroleum technology from the University of Pune in India. He started his career as a drilling engineer with Schlumberger in 2000 in Doha, Qhatar, and has had a variety of global roles and positions since 2005 with Baker Hughes such as technical advisor and applications engineer (global role) in Germany, and tech support engineer – drilling engineering in Saudi Arabia.

He's currently the manager for Unconventional Resources—Drilling Services in Houston. Prior to his current role, he was the product manager for MWD & Telemetry. Rajdeep is a member of the Society of Petroleum Engineers and has been the author and co-author of several SPE papers. His expertise includes directional drilling techniques, single lateral, multi-laterals, ERD, short radius wells, conventional and unconventional resources, deepwater, marketing, business development and technical sales enablement, product line management, MWD & LWD products and services, new product commercialization, PDM process and deliverables, RSS (rotary steerable system), AutoTrak G3, AutoTrak eXpress, AutoTrak-V and AutoTrak Xtreme, advanced drilling services, applications engineering, well engineering and wellbore placement.

Stephen A. Holditch joined the faculty at Texas A&M University in 1976 and retired in January 2013. While on the faculty, he taught both graduate and undergraduate courses and has supervised research in areas involving unconventional gas reservoirs, well completions, well logging and well stimulation, primarily hydraulic fracturing.

Dr. Holditch was the director of the Texas A&M Energy Institute from January 2011–January 2013. From January 2004–January 2012, Dr. Holditch was the head of the Harold Vance Department of Petroleum Engineering. Dr. Holditch is currently a professor emeritus of petroleum engineering.

Dr. Holditch started S.A. Holditch & Associates, Inc. in 1977, which was a full-service petroleum engineering and geologic consulting company. The company specialized in tight gas reservoirs, coalbed methane and shale gas reservoirs. Schlumberger Ltd. purchased the company in 1997, and Dr. Holditch became a Schlumberger fellow. As a fellow, Dr. Holditch was an advisor to the top executives in Schlumberger and represented the company in numerous technical meetings from 1997 to 2004.

Dr. Holditch was the Society of Petroleum Engineers, International (SPE) President 2002, SPE Vice President-Finance and a member of the Board of Directors for the SPE from 1998-2003. In addition he served as a trustee for the American Institute of Mining, Metallurgical, and Petroleum Engineering (AIME) from 1997-1998.

Dr. Holditch has received numerous awards in recognition of his technical achievements and leadership. In 1995, he was elected to the National Academy of Engineering (NAE) and in 1997, to the Russian Academy of Natural Sciences. In 1998, Holditch was elected to the Petroleum Engineering Academy of Distinguished Graduates. He was elected as an SPE and AIME Honorary Member in 2006. In 2010, Dr. Holditch was honored as an Outstanding Graduate of the College of Engineering at Texas A&M University. Dr. Holditch was also the 2011 President of the Academy Medicine, Engineering and Sciences of Texas.

Robert Hurt manages the Geomechanics Group of Applied Reservoir Technology within Baker Hughes Pressure Pumping. He specializes in advanced topics in rock mechanics and hydraulic fracturing, incorporating physical and numerical modeling, dimensional analysis, and scaling. In his current role, he provides technology support for Baker Hughes pressure pumping global operations focused on the design, appraisal, and integration of diagnostics for stimulation treatments in unconventional reservoirs. He is also part of a team working on advanced engineering models for hydraulic fracture design.

Robert L. "Bobby" Kennedy is Manager of Production/Petroleum Engineering of the Unconventional Resources Group of Baker Hughes Inc. in Houston, Texas. He has 38 years of industry experience in production, reservoir engineering, and training and has worked in the US, Egypt, United Kingdom, U.A.E., and Latin America. During his 30 years with Amoco Production

Company he held a number of engineering management positions including Chief Engineer of Amoco U.K., Regional Engineering Manager of the Latin America and Far East Region, Production Manager Amoco UK North Sea, and Manager of Production Training and Technology.

During the last six of his eight years at Baker Hughes, Kennedy has worked exclusively with technologies for unconventional resources. He has been advising customers on unconventional (primarily shale gas/oil and tight gas/oil) technology applications including formation evaluation, reservoir analysis, drilling, completion (including hydraulic fracturing), production, and water management. He has organized and presented seven 5-Day Shale Academies in the US, China, and Latin America; conducted day-long shale and tight gas workshops in Algeria, Hong Kong, Argentina, Colombia, Saudi Arabia, and the US; and organized and conducted over 60 customer symposia on shale gas/oil and tight gas/oil.

Kennedy is the primary author of SPE 160855, "Comparisons and Contrasts of Shale Gas and Tight Gas Developments, North American Experience and Trends," and SPE 162534, "Optimized Shale Resource Development: Proper Placement of Wells and Hydraulic Fracture Stages." He is also the author of a chapter on the Gas Shale Challenges Over the Asset Life Cycle for the book *Fundamentals of Shale Gas Reservoirs* published in 2015 by Curtin University of Australia.

Kennedy is a member of the Society of Petroleum Engineers, where he is a Legion of Honor recipient, and he holds a BS in petroleum engineering from Mississippi State University.

Abbas Khaksar is a global geomechanics advisor, subject matter expert in sand production prediction and sand management with Baker Hughes, Reservoir Development Services. He holds a BSc in mining engineering (1989), a MSc in petroleum geology and geophysics (1994), and a PhD in rock physics (1998), and has 16 years' experience in petroleum geomechanics consultancy having worked on more than 200 consulting studies. From 1989–1992 he worked for Iran's geological survey as a field engineer; in 1999–2000 he was a postdoctoral researcher at the University of Adelaide working on pore pressure prediction and CO_2 sequestration; and from 2000–2005 he worked for Geomechanics International (GMI)-Perth as a geomechanics specialist and later in manager-consulting services in Asia-Pacific. He joined Helix RDS in 2005 as a senior, and later, principal geomechanics specialist and worked in their Perth and London offices until 2009 when Baker Hughes acquired Helix RDS. In 2010-2011 he was the Asia-Pacific geomechanics team leader for Baker Hughes – Reservoir Development Services. Abbas has written in excess of 70 publications in peer-reviewed journals, SPE papers, and many conference presentations. He is a short course presenter in geomechanics and sanding evaluation, workflow and software developer in rock mechanics applications, and has served as a member of technical committees, and as a discussion leader. He has been invited to speak at several workshops organized by SPE and American Rock Mechanics Associations.

Deepak Khatri is the director of cementing operations for North America for Baker Hughes in Houston, Texas. He has a total of eighteen years of industry experience, spread across the Middle East, Europe, Africa, and North America. He has worked primarily in oil well cementing and has specialized in the areas of operations, technical support, design, execution, evaluation of cementing jobs, including, business and training in relation to cementing. He holds a BS in mechanical engineering from Bombay University and a master's in business administration from Oklahoma State University. He has co-authored SPE papers and has published articles for trade shows.

Prior to taking his most recent position, Deepak was director of business development for global onshore cementing for Baker Hughes based out of Houston, Texas.

Bill Knecht is Director of the CORE Team for Unconventional Resources for Baker Hughes. He earned his bachelor of science degrees in geology and petroleum engineering from Texas A&M University. Bill is a "hands on" petroleum engineer with a strong background in vetting opportunities and adding value in drilling and production operations, unconventional resource development, prospect evaluation, and mergers and acquisitions. Bill has over 30 years of engineering and operational experience in most of the major basins in the US. He has focused much of his career on the exploration and development challenges in tight sand and carbonate reservoirs, and over the last 8 years in the major shale and tight oil plays of the US. His diverse corporate background includes start-up E&P companies as well as major international company experience. Previously he has worked and held senior positions with Total, Elf, Norcen Explorer Inc., Amax Oil and Gas, Anadarko, and is a principal in his

own company. Bill joined Gaffney-Cline & Associates in February 2011 as a consultant before joining Baker Hughes RDS as Director – Center of Reservoir Excellence (CORE) Team for Unconventional Resources.

Iman Oraki Kohshour is currently a petroleum engineer intern for Baker Hughes Unconventional Resources business unit in Houston under the direction of Usman Ahmed, Vice President and Chief Reservoir Engineer. Iman's expertise includes unconventional resources, formation damage, and enhanced oil recovery. He has worked as a reservoir engineering specialist at BP in Anchorage and at InPetro Technologies in Houston. He has volunteered with SPE and Energy4Me STEM education and has mentored several undergraduate and graduate students as part of the SPE eMentorship program. In his off time, he enjoys reading about history. He's passionate about the industry and likes the fact that it is constantly evolving.

Iman has a BSc in reservoir engineering from Petroleum University of Technology and a MS degree from the University of Alaska Fairbanks where he is currently a PhD student under the supervision of Dr. Mohabbat Ahmadi. His thesis focused on a particularly challenging and unique topic for a shallow frozen oil reservoir in Alaska, which was a US DOE funded research project and cooperative study with Linc Energy. His work contributed to two SPE conference papers, one journal paper, and one AAPG bulletin paper.

Sergey Kotov is the product line manager for Unconventional Fracturing, Production Enhancement at Baker Hughes. He holds a MS degree in petroleum engineering /oils and gas geology (Russia); he also earned an honors MA degree in linguistics (Russia). Kotov spent 19 years in the oil and gas industry primarily specializing in production enhancement. He started his career in Russia, participating in all aspects of pumping operations in most of the major oil and gas basins from the South to the Arctic Circle. As an application engineer at BJ Services Technology Research Center, he participated in the development of new stimulation technologies. As a senior stimulation specialist, Kotov worked in North Africa. He was involved in many stimulation projects around the world. In recent years Kotov has specialized in unconventional stimulation as a region engineer in the US, senior stimulation advisor/stimulation manager for unconventional resources, and as a product line manager for unconventional fracturing, providing technical expertise and leadership globally.

He is an active member of the SPE. He participated in numerous industry events as a speaker and a panelist. Kotov is an instructor for the "Unconventional Completions and Fracturing" SPE course, he is also a co-author of Baker Hughes Recommended Practices / Data-Driven Solutions for Shale Gas/Oil Analysis and Development, and a co-author and instructor for Baker Hughes Shale Academy.

Julie Kowan is a geoscientist by training and started her career in 2005 at GeoMechanics International (GMI), now a part of the RDS (Reservoir Development Services) group at Baker Hughes. Her primary responsibility is to lead geomechanics consulting projects for the oil and gas industry and using geomechanical modeling to help operators plan their drilling programs and field development. Julie has particular expertise in wellbore stability issues common in unconventional resources. In addition to leading consulting projects, she assists sales efforts, teaches technical training courses, and frequently presents at technical conferences. Julie holds BS and MSc degrees in geology from Rutgers and Brown Universities, respectively.

Vello A. Kuuskraa, President of Advanced Resources International, is internationally recognized for his work in energy economics, supply modeling, and new oil and gas recovery technologies. He has over 40 years of experience with unconventional gas, including gas shales, coalbed methane, and tight gas sands.

Recently Mr. Kuuskraa and the firm completed the World Shale Gas and Shale Oil Resource Assessment for the US Energy Information Administration (EIA). He is the author of the chapter on Unconventional Gas Resources in the *Encyclopedia of Energy*, is a member of the Potential Gas Committee responsible for assessing US natural gas resources, and is the author of over 100 technical papers on energy resources. Mr. Kuuskraa and his firm authored a 3-part series entitled Gas Shale Transformation published in the *Oil and Gas Journal*.

Mr. Kuuskraa is a 2001 recipient of the Ellis Island Medal of Honor that recognizes individuals for exceptional professional and patriotic contributions by America's diverse cultural ancestry. He currently serves on the board

of directors of Southwestern Energy Company (SWN), on the board of directors for Research Partnership to Secure Energy for America (RPSEA), and is a member of the National Petroleum Council. Mr. Kuuskraa holds a MBA, Highest Distinction from The Wharton Graduate School and a BS, applied mathematics/economics from North Carolina State University.

Randy LaFollette is Director, Applied Reservoir Technology, for Baker Hughes Pressure Pumping. Mr. LaFollette holds a BSc degree in geological science from Lehigh University, Bethlehem, Pennsylvania. He has 37 years of experience in the industry. He is active in SPE, HGS, and AAPG, aiding with meeting organization and presenting on various reservoir, completion/stimulation, and data-mining topics. Mr. LaFollette is a subject matter expert for Baker Hughes and leads a team of experts responsible for structuring and implementing laboratory, geospatial, and data-mining studies of stimulation effectiveness linking reservoir quality, well architecture, well completion, and treatments performed to production results.

Edmund Leung is currently Vice President of Well Technology with RESMAN AS leading the flow related interpretation and R&D team, based out of Trondheim in Norway since March 2011. He earned a bachelor's with Honours in Petroleum Engineering from the University of New South Wales in Sydney, Australia, graduating in 1995. He began his career as a Schlumberger reservoir engineering consultant, specializing in well testing, reservoir simulation, data mining, intelligent completion optimization and real-time production surveillance services, and technologies that complement intelligent field implementations. He has held numerous technical, business development positions and management positions throughout his 15-year career with Schlumberger, with assignments in Australia, Indonesia, Malaysia, Kuwait, Saudi Arabia, United States, and United Arab Emirates. Before joining RESMAN AS, Edmund was the Global Reservoir Domain Leader in Schlumberger's Completion and Sand Management Services segment, specializing in sand control, flow control modeling, monitoring and R&D based in Stavanger, Norway. He has authored several SPE papers and is an active discussion leader at SPE ATW's related to sand control and reservoir management themes.

Chi Vinh Ly completed his undergraduate studies in applied physics at Curtin University, Perth, Australia, before completing his master's and PhD in geochemistry at Hiroshima University, Japan. He then returned to Australia to take on various roles in development and commercialization of automated mineralogical technology, and set up and managed the Process Mineralogy department at ALS AMMTEC, providing automated mineralogical services to the minerals, mining, and energy industry in Australia and globally. In 2012 Chi Vinh Ly then joined Robertson to handle the operation and play a leading role in the ongoing development of the RoqSCAN initiative and is a member of the team within CGG helping to further develop the technology and the market, with Baker Hughes, globally.

Lucy Xin Luo is currently Exploration Analyst, Global New Ventures Exploration at ConocoPhillips. Her past experiences include Manager of Data Mining, CORE Unconventional resources, at Baker Hughes from 2011 to 2014, Senior Data Analyst, Z Inc., Contract to EIA, US Department of Energy from 2002 to 2011, and Geologist at CNPC from 1994 to 1998. Lucy has a MS degree in statistics from the University of Central Florida, and another MS degree in geology from Baylor University. She has also a bachelor's degree in geoscience from China University of Petroleum.

Russell Maharidge has a PhD in physics from Rensselaer Polytechnic Institute (1984). He has worked for Sohio (starting in 1984), BP, BJ Services, and now Baker Hughes for 30 years in the O&G industry. He specializes in laboratory testing in the areas of core analysis, formation evaluation, and rock mechanics. He is a member of the Society of Petroleum Engineers, Society of Petrophysicists and Well Log Analysts, and American Rock Mechanics Association.

Tony Martin graduated from Imperial College, London, in 1990 with an honours degree in mechanical engineering and a master's degree in petroleum engineering. After leaving university, he spent 4 years with Halliburton, including 2 years in the North Sea and 2 years in Russia. For the last 20 years Tony

has worked for Baker Hughes in Aberdeen, the Netherlands, Nigeria, Singapore, Indonesia, the US, Italy, and London. During this period he has been extensively involved in cementing, coiled tubing, sand control, acidizing and water control operations, but his main interest and experience has always been in hydraulic fracturing.

Tony is currently Baker Hughes' Reservoir Development Services' Integrated Stimulation Engineering Team Leader, for the Europe-Africa-Russia-Caspian Region He is also a Baker Hughes Subject Matter Expert on hydraulic fracturing and stimulation. In this role, he travels all over the world promoting fracturing and stimulation, and acting as a technical focal point for the company. He is the author or co-author of numerous technical papers and has served on the technical committees for several Society of Petroleum Engineers (SPE) events. He is the author of Baker Hughes' Hydraulic Fracturing Manual and co-editor of ***Modern Fracturing: Enhancing Natural Gas Production***. Tony is a former SPE Distinguished Lecturer and is currently on the SPE Distinguished Lecturer Committee. In 2009 Tony received the SPE South, Central, and East Europe Regional Technical Award for Production Operations.

Tony has been a UK Chartered Engineer since 1997 and is a member of the Institute of Materials, Minerals and Mining.

Rob Mayer is a senior vice president with CGG's GeoConsulting division. He has focused his career on various aspects of seismic reservoir characterization with particular interests in AVO, seismic inversion, and attribute analysis. He has played a key role in the development and refinement of workflows for unconventional resources utilized at CGG. Rob holds a BSc in geology from Trinity University and MBA from the University of Houston.

D. Nathan Meehan has more than 40 years of global experience in reservoir engineering, reserve estimation, hydraulic fracturing and horizontal well expertise. He serves as Senior Executive Advisor to Baker Hughes. Previously he was President of CMG Petroleum Consulting, an independent consultancy; Vice President of Engineering for Occidental Oil & Gas; and General Manager Exploration & Production Services for Union Pacific Resources. Meehan has been elected the 2016 Society of Petroleum (SPE) Engineers President.

Dr. Meehan earned his BSc degree in physics from the Georgia Institute of Technology, his MSc degree in petroleum engineering from the University of Oklahoma, and his PhD degree in petroleum engineering from Stanford University. Dr. Meehan previously served as Chairman of the Board of the CMG Reservoir Simulation Foundation and twice as a director of the Computer Modelling Group, Ltd., as Director of Vanyoganeft Oil Company, Nizhnyvartosk, Russia, as Director of Pinnacle Technologies, Inc., as a director of the Society of Petroleum Engineers, and as a director of JOA Oil & Gas BV. He is an SPE Distinguished Member and the recipient of SPE's Lester C. Uren Award for Distinguished Achievement in Petroleum Engineering, the Degolyer Distinguished Service Medal, and the SPE Public Service Award. He serves on the board of the Georgia Institute of Technology's Strategic Energy Institute, Penn State's and the University of Houston's petroleum engineering departments. He is an appointed member of the Interstate Oil & Gas Compact Commission and widely published author. Dr. Meehan is a licensed professional engineer in four states.

Alfredo Mendez is Director of Business Development, Unconventional Resources Business Unit for Baker Hughes. He is responsible for marketing and developing new business units and services in the Eastern Hemisphere ensuring focus on strategic clients and countries to position new services and technology solutions for maximum market impact. Alfredo has been based and worked in the US, Venezuela, Brazil, and UAE. He has been 17 years in the oil field industry. Unconventional experience starting with tight gas, CBM, and shale projects around the world, shale gas/oil with international focus since 2006. Alfredo has a patent and has authored and co-authored several technical papers in hydraulic fracturing, ultra-deep water sand control, and acid stimulation and coiled tubing. He is currently active in unconventional projects in several US basins, Australia, India, Pakistan, China, Russia, and Saudi Arabia. Alfredo received his bachelor of science in mechanical engineering from Texas Tech University in December 1996. He lives in Dubai with his wife and two kids.

Scott Nelson is Director of Production Enhancement for Baker Hughes supporting worldwide fracturing, acidizing, and sand control operations from the Corporate Pressure Pumping Technology Center located in Tomball, Texas. He has 29 years of industry experience in well construction and completion, primary stimulation, and remedial completion technologies and has

held positions in the areas of treatment engineering, regional engineering, technical account management, engineering management, and R&D product line management. Nelson has a BS degree in petroleum engineering from the University of Oklahoma. He is an active member of the Society of Petroleum Engineers with service on various technical program committees and is also a member of the American Petroleum Institute. He was awarded the Hart's E&P Meritorious Award for Engineering Innovation for work in relative permeability modifiers. He has authored some 20 technical papers, numerous journal articles, and is listed as an inventor on over 30 United States patents, issued and pending.

Marie Meyet is currently Lead Reservoir Engineer – Unconventional Resources Team based in Tomball, Texas. Marie's main responsibility is to conduct reservoir modeling for shale plays as well as data mining. Throughout her career, Marie has been deeply involved with investigating unconventional resources EUR using multiples advanced decline curve analysis technique, a subject on which she co-authored two papers. Marie has spoken at various industry events presenting her work on decline curve analysis in unconventional plays.

Marie began her career in 2011 as a petroleum engineer with Gaffney, Cline & Associates (Baker Hughes). In 2013, she moved to the Reservoir Development Services in Baker Hughes before getting to her new role in 2014. Marie has done short-term assignments in Abu Dhabi (UAE) and Ecuador.

She has a BSc (high distinction) in petroleum engineering from The Pennsylvania State University and is currently pursuing a master's in petroleum reservoir engineering from Texas A&M University. Marie is an active member of the Society of Petroleum Engineers.

Neal Nagel has nearly 30 years of oilfield geomechanics experience having started as a college professor and then with Phillips in the 1980s. He has provided geomechanics consulting since 2009 and geomechanics training since the late 80s. He is a well-known expert in the geomechanics of unconventionals and has given many invited SPE, AAPG, HGS, SEG, and SPWLA presentations in the last several years. Nagel has also authored or coauthored more than 20 technical and journal papers related to unconventionals, including several keynote presentations. He is a past SPE Distinguished Lecturer (2004) and was chief editor of the 2010 SPE Monograph on Solids Injection.

Guy M. Oliver, PhD, is Vice President of CGG's Geoconsulting Group, with overall responsibility for the Robertson US business line.

Based in Houston, Guy's responsibilities include the overall management of company performance; strategy; technical marketing support of sales and business development; and the implementation of quality, health, safety and environment (QHSE) policies. He also guides the business development and strategic efforts of CGG's RoqSCAN™, a step change tool for analyzing drilling cuttings at the wellsite. Guy is also a member of CGG's Geoconsulting Senior Management Team.

Guy began his career with Fugro Robertson (formerly Robertson Research International Ltd.) in 1997 as a sedimentologist. He has extensive project management experience working on a wide range of rock and reservoir basin exploration studies in petroleum provinces worldwide. Guy has served as a director and more recently president of Fugro Robertson between 2004 and 2012, folding three new business lines into the company.

Seun Oyinloye is currently Software Support Manager – Reservoir Software based in Houston, Texas. Seun's main responsibility is to provide consolidation and effective management of Baker Hughes Reservoir Software support function globally. In addition he builds models with clients to demonstrate the strengths of the software, supervises delivery of commercial software training and handles special reservoir modeling projects as required.

Seun began his career in 2005 working in the software support services division in IBM after which he obtained a master's degree in petroleum engineering. Seun joined the JOA Oil & Gas JewelSuite™ team in 2009 as a technical sales engineer after completing his graduate program. In 2011 JewelSuite™ was acquired by Baker Hughes and Seun assumed a new role of reservoir engineering consultant in the new organization and this included support for JewelSuite™ Subsurface Modeling Software, MFrac Suite Hydraulic Fracturing software, and JewelSuite™ Geomechanics Software. He was appointed global

support manager for the RDS Reservoir Software group in January 2014.

He has a BSc (Honors) in chemical engineering from University of Lagos, Nigeria, and an MSc in petroleum engineering from University of Louisiana, Lafayette. Seun specialized in reservoir simulation and wrote a thesis to develop an artificial neural network for the determination of minimum miscibility pressure for candidate south Louisiana reservoirs undergoing flue gas floods. Seun is an active member of the Society of Petroleum Engineers and the American Association of Petroleum Geologists.

Pierre-François Roux is a seismologist by background. He graduated in 2004 from the Paris Pierre et Marie Curie University at the Science and Technology Institute with a specialization in geophysics and geomechanics. He then turned to an academic career and in 2007 he earned a PhD in (micro-) seismology at the ISTerre laboratory, Grenoble, France, on the study of fracturing processes of glacier ice through microseismic monitoring. He then continued as a post-doctoral researcher at two French research institutes working on a variety of topics, ranging from brittle deformation of sea ice through microseismic monitoring to underground nuclear explosions monitoring and characterization using their seismological signature. In 2010 he joined CGG as a research geophysicist in reservoir monitoring, dealing with onshore 4D and microseismic monitoring. He has participated in several projects in the Middle East, Europe, and North America and has international patents on noise attenuation for onshore monitoring. He's now technical business development manager for Magnitude, Baker Hughes/CGG Joint Venture for microseismic monitoring.

Shanna Sambol-Koseoglu, Strategic Marketing Manager for Baker Hughes Reservoir Development Services, has 10 years of marketing experience in the oilfield services industry. She earned her bachelor of liberal arts and social sciences degree in communications from the University of Houston. Since joining Baker Hughes in 2005, she has gained valuable experience in market analytics, strategic planning, and integrated marketing communications. Shanna is a strategic thinker who applies a holistic, marketing approach to understand the voice of the customer, shape product offerings, and unleash untapped opportunity. She has spent most of her career focused on market segments, to understand customer challenges and identify multi-product solutions to overcome those challenges. Recent contributions include the opening of the Dhahran Research and Technology Center and the Shale Technology Symposium in Saudi Arabia—both of which received high recognition for raising awareness on Baker Hughes' life-cycle solutions for unconventional assets. In addition to market segments, Shanna manages strategic marketing efforts for Reservoir Development Services, which includes geoscience, reservoir software, consulting, and field management.

Rawdon Seager is currently Global Director – Quality Assurance based in GCA's western hemisphere headquarters in Houston, Texas. Rawdon's main responsibility is to implement and manage QA programs throughout the GCA group. In addition he provides internal quality assurance for technical projects. Throughout his career, Rawdon has been deeply involved with the proper evaluation and reporting of oil and gas reserves, a subject on which he now provides clients with advice and training. Rawdon has spoken at various industry events as well as presenting in-house and public courses to clients on matters relating to reserve estimation, classification and reporting. He has also provided expert testimony at international arbitrations.

Rawdon began his career in 1972 as a petroleum engineer with Shell International in Malaysia, Brunei, the Netherlands, and Australia. In 1980 he joined Roy M. Huffington Inc. in Indonesia where he became Petroleum Engineering Manager, before joining GCA in 1985 with whom he has held senior positions in the United Kingdom, Singapore, Argentina, Venezuela, and the US.

He has a BSc (Honors) in physics from Bristol University, England, and an MSc (Distinction) in petroleum reservoir engineering from Imperial College, London. Rawdon is an active member of the Society of Petroleum Engineers (and is past-Chairman of the SPE Oil and Gas Reserves Committee), Society of Petroleum Evaluation Engineers, American Association of Petroleum Geologists, UK Energy Institute and is a Chartered Petroleum Engineer in the UK. He is also registered as a European Engineer with FEANI.

Norbert Van De Coevering is currently a senior staff QI geophysicist for Murphy Oil in Houston within the Technology group. He performs, supervises and recommends seismic reservoir characterization and rock physics techniques as well as (re-) processing to the Asset Teams both off- and onshore. Previously he held various positions for 17 years within CGG, lastly being the US manager for CGG's GeoConsulting – Seismic Reservoir Characterization group in Houston. He holds a master's degree in geophysics (Utrecht University, Netherlands). His experience includes shale gas characterization, various seismic inversion techniques, fracture characterization, pore pressure prediction, AVO, shallow hazard studies, 4C/4D feasibility studies, azimuthal seismic attribute analysis, seismic processing and conditioning, multi-component, evaluation-integration of new software, and development-implementation of new workflows. He has published various articles in industry journals.

George D. Vassilellis is Senior Advisor, Reservoir Engineering at Repsol's US Technical Hub at The Woodlands, Texas.

His role is to guide and oversee the implementation of new technologies cooperating directly with the respective business units as a core team member of the Technology Hub. The Hub under the direction of Emad Elrafie has achieved remarkable success in introducing and implementing game changing methods of extraction in unconventional oil plays and particularly in the Mississippi Lime.

George has over 25 years of experience in the international oil and gas industry. His technical contributions in modeling and forecasting performance with unconventional reservoirs has been recognized in the industry and particularly when it comes to coupling reservoir performance with geomechanics. Other specialties include heavy oil, EOR, field development. He has extensive experience in property evaluation, economics, and strategic planning.

Previously he was a senior manager with Gaffney, Cline & Associates (GCA) which was acquired by Baker Hughes in 2008. George has been a key technical contributor at Baker Hughes where he was named a shale engineering/reservoir subject matter expert and he also served as a senior technical advisor for EOR and field development. Before that he was with SI International (presently MHA Petroleum Consultants) in California and before that with Richardson Operating Company, an independent based in Denver, Colorado.

George graduated from Aristotle University, Thessaloniki, Greece, with a bachelor of science in geology and completed his master's of science in petroleum engineering from the Colorado School of Mines. He is a registered professional engineer in Texas and California.

George has authored several technical articles and has been a member of the Society of Petroleum Engineers for more than 20 years, serving in many roles and at various events. He is also a member of AAPG and an honorary life member of the South East Europe Energy Institute.

Alex Vilcinskas is a senior applications engineering advisor for the US Land Artificial Lift group at Baker Hughes. With over 30 years of experience in the industry, Alex has held positions in management, sales, service, engineering, and applications, including 17 years of international assignments. He graduated with a master's degree in industrial engineering from the Buenos Aires Institute of Technology (ITBA). Alex holds four patents related to ESP equipment, and is a member of the Society of Petroleum Engineers.

Simon Voisey is a geophysicist at Apache Corporation in the E & P technology group, Houston, focusing on seismic attribute analysis for reservoir characterization. Previously, Simon spent several years with CGG Hampson-Russell, initially located in London within the software group and then moving to Houston's GeoConsulting services team. Simon studied petroleum geology (MSc) at the University of Aberdeen and University College London.

Frank Walles advices within a team of highly experienced global specialists as projects director within the Global Geoscience group of the Reservoir Development Service (RDS) business unit. He has 34 years of applied unconventional and conventional (multidiscipline) reservoir characterization experience within hydrocarbon exploration and production. Global advisory teams of large independent E&P operators have especially benefitted from his broad scientific experience.

Integrating the most appropriate advanced applied technology applications along with preferred interpretation approaches is a defined expertise. Applying the most cost effective, most rapid acquisition, and highest quality first-order datasets is a value focus that results in improved capital efficiency and improved hydrocarbon assessment and recovery.

Frank's key expertise includes integrated unconventional reservoir characterization and assessment including special optimization toward improved capital efficiency and hydrocarbon production, advanced applied technology approaches integration expert for developing first-order unconventional reservoir characterization datasets, petroleum and inorganic geochemistry specialist of unconventional and conventional systems, integrated process model approaches for prediction of special changes of unconventional reservoir character, optimization of vertical positioning for lateral placement (singular or stacked) within unconventional resource play (URP) targets, custom completion design opportunities corresponding to changes of reservoir characterization within laterals of URP targets, and custom completion fluids that minimize reservoir damage and enhance fluid recovery flow back and hydrocarbon productivity.

Joel Walls is a geophysicist and entrepreneur with extensive experience in the research, development, launch, and sale of advanced technology products and services for the upstream oil and gas industry. He joined Ingrain in 2010 as a director of unconventional technology with responsibility for developing and commercializing services focused on shale and other unconventional reservoirs. Dr. Walls was a co-founder and the first president of the Society of Core Analysts and is a member of multiple additional professional associations. He is the author of many professional publications and holds four US patents in the fields of digital rock properties and seismic reservoir characterization. Dr. Walls holds MS and PhD degrees in geophysics from Stanford University and a BS in physics from Texas A&M University, Commerce.

Dr. Ming Zhong is a senior applied statistician in the Applied Reservoir Technology (ART) team of Baker Hughes Pressure Pumping. Dr. Zhong has a multidisciplinary background and 10 years of experience in conducting data mining and statistical analyses across various fields, including the oil and gas industry, financial services, clinical trials, and statistical genetics. He received his PhD in statistics and his master's in physics from Texas A&M University, BS in physics from University of Science & Technology of China.

This page intentionally left blank

Petroleum Engineering

UNCONVENTIONAL OIL AND GAS RESOURCES

EXPLOITATION AND DEVELOPMENT

"… a valuable reference tool and guide. … This text provides insight into current methods and workflows, and aids further investigations into emerging areas of unconventional resources."

—Dr. Raymond Johnson, Jr., Senior Lecturer, University of Queensland, and Adjunct Associate Professor, University of Adelaide, Australia

"If you are in this business, you need to have this book. If you are considering this business, you could stumble without this book. It should be required reading at any university with programs in petroleum science. … In my judgment, if you could only have one book on this topic, this is it."

—Dr. Raymond Levey, Director, Energy and Geoscience Institute, University of Utah, Salt Lake City, USA

Unconventional Oil and Gas Resources: Exploitation and Development provides a comprehensive understanding of the latest advances in the exploitation and development of unconventional resources. With an emphasis on shale, this book:

- Addresses all aspects of the exploitation and development process, from data mining and accounting to drilling, completion, stimulation, production, and environmental issues
- Offers in-depth coverage of sub-surface measurements (geological, geophysical, petrophysical, geochemical, and geomechanical) and their interpretation
- Discusses the use of microseismic, fiber optic, and tracer reservoir monitoring technologies and JewelSuite™ reservoir modeling software
- Presents the viewpoints of internationally respected experts and researchers from leading exploration and production (E&P) companies and academic institutions
- Explores future trends in reservoir technologies for unconventional resources development

Unconventional Oil and Gas Resources: Exploitation and Development aids geologists, geophysicists, petrophysicists, geomechanic specialists, and drilling, completion, stimulation, production, and reservoir engineers in the environmentally safe exploitation and development of unconventional resources like shale.

BAKER HUGHES

CRC Press
Taylor & Francis Group
an informa business
www.crcpress.com

6000 Broken Sound Parkway, NW
Suite 300, Boca Raton, FL 33487
711 Third Avenue
New York, NY 10017
2 Park Square, Milton Park
Abingdon, Oxon OX14 4RN, UK

K28652

ISBN: 978-1-4987-5940-3
90000
9 781498 759403